ISSN 0971-4570

IASTA BULLETIN

Vol. 20 DECEMBER 2012 No. 1 & 2

SPECIAL ISSUE

Proceedings of

IASTA-2012 Conference

(December 11-13, 2012)

- Aerosol Characterization
- Aerosol Fundamentals: Physics and Chemistry
- Aerosol Instrumentation
- Aerosol Remote Sensing
- Aerosol Climate Effects
- Nuclear and Radioactive Aerosols
- Aerosols in Health and Agriculture

Indian Aerosol Science and Technology Association
Bhabha Atomic Research Centre
Mumbai – 400 085, India

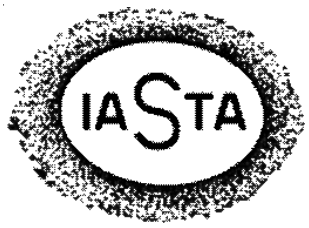

IASTA-2012

Conference of
Indian Aerosol Science and Technology Association

at

Fortune Select Exotica, Vashi, Navi Mumbai

(December 11-13, 2012)

Sponsored By

Board of Research in Nuclear Sciences
Atomic Energy Regulatory Board
Defense Research and Development Organization
Ministry of Earth Sciences
Indian Space Research Organization
Uranium Corporation of India Ltd.

Co-Sponsored by

Alfatech Services, New Delhi

Hosted By

Indian Aerosol Science and Technology Association
C/o Environmental Assessment Division
Bhabha Atomic Research Centre
Mumbai- 400 085, India

IASTA Bulletin – 2012

Proceeding of the IASTA-2012 conference

December -2012

Printed by
Perfect prints
22/23, Jyoti Industrial Estate
Nooribaba Darga Road
Thane 400 601, INDIA
Tel. : 2534 1291

Editorial ...

Recognising the need for research on impact of aerosols in several critical areas pertaining to climate change, public health and agriculture, several integrated national programmes have been initiated. Such programmes bring together the researchers working in common areas thus enhancing the research capabilities of the individual institutes. In the context of global climate change, the role of black carbon aerosols, which is a component of atmospheric aerosols, has gained utmost importance due to its high absorption characteristics which affects radiative forcing. This calls for studies on quantification of its various regional sources such as bio-fuels, bio-mass burning, diesel engines combustion of coal etc. A yet emerging sub-discipline is the nanoparticle science and technology with applications in microelectronics, space research, medicine and environment. The research in this area is significantly different from classical areas of aerosol research. The differences lie not only in the formation mechanisms but also in the potential applications. This topic is fast catching up in the national institutes and several specific centres for nanoparticle science and technology have emerged with opportunities for collaboration with internationally-famed institutes.

This bulletin is a compendium of such related works presented by the researchers during the three day deliberations under the aegis of the conference organized by Indian Aerosol Science and Technology Association (IASTA) during December 2012. A healthy sign has been the participation of a large number of young researchers and students from several national institutes, universities and colleges. The wide spread in the areas of aerosol research is brought out clearly in this bulletin indicative of the fact that the impact of aerosols is well recognized. The invited talks by well-experienced researchers have tried to focus on some important aspects which would be beneficial for all participants and readers.

It is hoped that the conference will result in national collaborations on various fields of aerosol science and technology. This is an opportunity for the young researchers to interact with their peers and gain deeper insights into the evolving regimes of the subject. IASTA is happy that it has been able to provide such a forum for the past several years wherein various institutes working towards diverse applications of aerosol science have come under a cover to establish long-standing research collaborations.

On behalf of the Organising Committee and the Technical Programme Committee, I wish the participants a very fruitful stay at Mumbai during this conference!

B.K. Sapra
Convenor, IASTA-2012

IASTA-2012

Patrons

1. Dr R K Sinha, (Director, BARC and Chairman AEC)
2. Dr U C Mishra, Ex Director HS&EG, BARC
3. Dr Pratim Biswas,Chairman, Dept of Energy, WUStL

National Organizing Committee

1. Dr A K Ghosh, Dir. HS&EG, BARC
2. Dr S S Bajaj, Chairman, AERB
3. Dr D N Sharma, Assoc. Dir HS&EG, BARC
4. Mr S G Markandeya, Controller BARC
5. Dr Y S Mayya, Head RPAD, BARC
6. Dr P C S Devara, President IASTA
7. Dr A Jayaraman, Director NARL, Gadanki
8. Dr M M Sarin, PRL Ahmedabad
9. Dr R S Patil, IIT, Mumbai
10. Dr P V N Nair, Ex. BARC

Technical Programme Committee

1. Dr B.K. Sapra, BARC, Mumbai (Convenor)
2. Dr Chandra Venkataraman, IIT Mumbai (Co-Convenor)
3. Dr. S.N. Tripathi, IIT Kanpur (Co-Convenor)
4. Dr R Baskaran, IGCAR, Kalpakkam
5. Dr Sanjay K Ghosh, BI, Kolkata
6. Dr G GPandit, BARC, Mumbai
7. Dr R M Tripathi, BARC, Mumbai
8. Dr A Vinod Kumar, BARC, Mumbai
9. Dr Tarun Gupta, IIT Kanpur
10. Dr P E Raj, IITM , Pune
11. Dr P S P Rao, IITM Pune
12. Mr S Anand, BARC, Mumbai
13. Mr Arshad Khan, BARC, Mumbai

Local organizing Committee

1. Mr Arshad Khan, BARC, Mumabi (Convener)
2. Mr Manish Joshi, BARC, Mumbai
3. Mr B K Sahoo, BARC, Mumbai
4. Dr Rosaline Mishra, BARC, Mumbai
5. Mr S Anand, BARC, Mumbai
6. Mr Sanjay Singh, BARC, Mumbai
7. Mr Tanmoy Das, BARC, Mumbai
8. Mr Sandeep Kanse, BARC, Mumbai
9. Mr Tarun Agrawal, BARC, Mumbai
10. Ms Rajeswari P Rout, BARC, Mumbai
11. Ms Rama Prajith, BARC, Mumbai
12. Mr Jitendra Gaware, BARC, Mumbai
13. Ms Pallavi Khandare, BARC, Mumbai
14. Mr Jalaluddin Shriamirullah, BARC,Mumbai
15. Ms Amruta M Koli, BARC, Mumbai

CONTENTS

AEROSOL FUNDAMENTALS: PHYSICS AND CHEMISTRY

AEROSOL INSTRUMENTATION

AEROSOL REMOTE SENSING

AEROSOL CLIMATE EFFECT

NUCLEAR AND RADIOACTIVE AEROSOLS

AEROSOLS IN HEALTH AND AGRICULTURE

AEROSOL RADIATIVE FORCING

IASTA2012/IT-1

ATMOSPHERIC CARBONACEOUS AEROSOLS FROM INDO-GANGETIC PLAIN: SOURCES, CHARACTERISTICS AND TEMPORAL VARIABILITY

M. M. SARIN

Physical Research Laboratory, Ahmedabad, 380 009, India

In the present-day scenario of growing anthropogenic activities, carbonaceous aerosols contribute significantly (20 to 70%) to the total atmospheric load of particulate matter and are, thus, considered to be of immense potential in influencing the Earth's radiation budget and climate on a regional scale. In order to understand the climatic perturbations, aerosol radiative forcing not only requires quantitative assessment but needs to be evaluated in terms of atmospheric chemical constituents and their sources. In addition, formation of secondary organic aerosols is being increasingly recognized as an important process in contributing to the air-pollution and poor visibility in the urban atmosphere. The divergence of absorbing and scattering properties of carbonaceous aerosols assumes particular importance in the polluted regions of the Indo-Gangetic Plain (IGP). During the wintertime, prevalence of agricultural-waste burning, fossil fuel combustion and wood-fuel for domestic heating result in enormous amount of organic carbon (OC) and elemental carbon (EC) that modify the total particulate carbon content of the atmosphere. It is, thus, essential to study the atmospheric concentrations of carbonaceous species (EC, OC and WSOC), their mixing state and absorption properties on a regional scale.

The mass concentrations of OC, EC, WSOC and ÓPAHs exhibit large spatio-temporal variability in the IGP. This is attributed to seasonally varying anthropogenic emissions, their source strength, long-range atmospheric transport of chemical constituents, boundary layer dynamics and secondary aerosol formation. Based on diagnostic ratios [OC/EC, K^+/OC and ÓPAHs/EC], biomass burning emission (post-harvest agricultural-waste burning) is documented as a major source of carbonaceous aerosols in the IGP. The cross-plot of PAH isomers {FLA/(FLA+PYR), BaP/(BaP+B[b,j,k]FLA and IcdP/(IcdP+BghiP)} also reaffirms the dominant impact of biomass burning emissions. In the lower atmosphere, alteration of carbonaceous aerosols from hydrophilic to hydrophobic state (with relative humidity changes) is of significant interest in making the surface of soot particles more polar, which increases their efficiency to act as cloud condensation nuclei (CCN). Furthermore, highly acidic environment (due to sulphate and nitrate aerosols) in the IGP may significantly alter the morphological features of soot particles (EC). Therefore, optical properties of aerosols assessed from the scattering coefficient and widely used for the determination of single scattering albedo need re-evaluation for the radiative impact assessment due to aerosols.

IASTA2012/IT-2

ISSUES IN NANOPARTICLE MEASUREMENTS

B. K. SAPRA

Radiological Physics & Advisory Division
Bhabha Atomic Research Centre
Mumbai

In the past few years, studies involving ultrafine/ nanoparticle aerosols (with geometric diameters less than 100 nm) have gained momentum. Their generation, control, measurement, dynamics and fate aretopics of the research requiring immediate attention. The modern age technology has provided aerosol researchers with advanced instruments for nanoparticle generation (Electro hydrodynamic atomizer, hot wire generator) as well as their measurements (condensation particle counter, mobility particle sizers, electrical impactor, aerosol electrometers). A lot of data is being generated and interpreted using one or more of these devices in several laboratory, regional and multi-institutional studies. Several of these studies being undertaken are targeted towards estimating the potential hazard of nanoparticles. The correctness of the produced data and validity of the subsequent analysis are crucial to the estimation of the hazard. This talk is focused on issues related to nanoparticle concentration measurements, particularly in reference to condensation particle counter (CPC) and scanning mobility particle sizer (SMPS). It is important to formulate and adhere to protocols for using these devices. The most important issues which can lead to discrepancies, specially between measurements made by two different systems, albeit working on the same principle,are - counting logic for the CPC, concentration based responses, incorporation of slip correction factor, ion-aerosol attachment coefficients, charge-size distribution, charge neutralization efficiencies, transfer functions and the inversion routines for obtaining the aerosol size distribution. All these issues have been discussed in the literature; however, technical harmonization of measurement protocols should be followed in any laboratory using these instruments. In addition; the role of calibration, effect of inaccuracies of aerosol and sheath flow, changes with respect to differences in sample and sheath air drying also play a critical role in using these instruments, efficiently. Since, large scale field studies involving aerosol nanoparticles focused on climate effects and other aspects sometimes involve CPCs and SMPSs of different age and make; the inter-comparison exercises can provide additional valuable information assisting the measurement protocols. The talk discusses some aspects related to the harmonization of nanoparticle concentration measurements using two most widely used SMPSs. The reasons for the concentration dependent responses and the effect of aerosol and sheath air drying will be discussed. The talk concludes providing key points which should be taken care of while using CPCs and SMPSs for correct measurements.

IASTA2012/IT-3

REMOTE SENSING OF AEROSOLS AND RELATED PARAMETERS: PRESENT STATUS AND FUTURE NEEDS

A. JAYARAMAN

National Atmospheric Research Laboratory
Gadanki - 517112, AP

Recent years have seen significant progress in remote-sensing of aerosol parameters both from ground and from space. There have been progress in establishing sun-photometer network both within the country and globally to obtain columnar aerosol optical depth fields. There are satellite-borne instruments such as MODIS capable of providing global distribution of selected aerosol properties, albeit their limitation in getting reliable data over regions of high surface albedo. The Cloud-Aerosol Lidar and Infrared Pathfinder Satellite Observation (CALIPSO) satellite overcomes this problem to some extent by using "active remote sensing technique" with a laser on-board despite its limitation in detecting aerosols below thick clouds. However, if one asks a question, whether the currently available tools are sufficient to address all issues related to aerosols, the answer is a dismal 'no'. The two major issues related to aerosols are, environment and health related and second, the role of aerosols in climate change by modifying cloud microphysics. For studying aerosol cloud interactions, there are experiments for example, on board aircrafts which do in situ sampling of aerosols and cloud properties. But, obviously they are highly limited in space and time and are very specific to the prevailing meteorological condition and hence there is limitation in applying the findings to a larger scale. At the National Atmospheric Research Laboratory (NARL) efforts are on way to remotely sense the aerosol and cloud properties using a combination of optical and radio remote sensing techniques. A few sample results from the existing systems and the plan for the future will be presented and discussed.

IASTA2012/IT-4

SPORADIC ENVIRONMENTAL INTERVENTIONS AND AIR POLLUTION REDISTRIBUTION: IMPLICATIONS FOR CLIMATE AND HEALTH (SEARCH)

NARESH KUMAR

Associate Professor, Department of Epidemiology and Public Health,
University of Miami, Miami, FL 33136.
Email: nkumar@med.miami.edu; web: web.ccs.miami.edu/~nkumar

This preliminary session provides insight into how sporadic environmental interventions can lead to air pollution redistribution, which has important implications for local climate change and health? The session will also demonstrate how high resolution satellite data fromMODrate resolution Imaging Spectroradiometer (MODIS) can be used to investigate shortand long-term changes in air pollution and radiative forcing. Delhi became an exemplary city by instituting radical environmental interventions to improve air quality. However, areas outside Delhi (but adjacent to Delhi's border) did not institute the similar interventions. Using high resolution satellite data from MODIS, Landsat TM and *in-situ* monitored air pollution data, we examine spatial (re)distribution of air pollution. A comparison of multi-resolution satellite data suggests that we can detect anthropogenic aerosols at 2km spatial resolution, which otherwise cannot be detected using the 10km NASA's aerosol optical depth (AOD) products. The central parts of Delhi experienced an improvement in air quality and decline in AOD after the interventions. But areas bordering Delhi experienced a significant deterioration in air quality after the interventions. This will have important implications for radiative forcing and public health in areas outside Delhi. This research further suggests that air pollution is likely to (re)distribute in the absence of uniform policy interventions. We plan to retrieve daily AOD at 2km spatial resolution from 2000 to 2012 for the Indian sub-continent and make these data available to researchers through our website by August 2013. This is likely to support research on air pollution, local climate change and public health in several other cities in India.

AEROSOL CHARACTERIZATION

UNDERSTANDING FINE PARTICULATE EMISSIONS FROM INDIAN MOSQUITO COILS

DEEPANJAN MAJUMDAR [a,*], JITESHWARI SAHU [b], ANURADHA CHINTADA [b]

[a] Air Pollution Control Division, National Environmental Engineering Research Institute, Nehru Marg, Nagpur - 440020, India

[b] Department of Biotechnology, Kalyan P.G. College, Bhilai Nagar, Pt. Ravishankar Shukla University Raipur, Chhattisgarh, India

E mail: d_majumdar@neeri.res.in/joy_ensc@yahoo.com

Keywords: MOSQUITO COILS, EMISSION RATE, TOXICITY

INTRODUCTION

Mosquito coils are used worldwide for protection against mosquitoes (Yap, 1985; Yap *et al.*, 2000). Mosquito coils are usually burnt indoors for at least several months a year. Pyrethrin is the most common active ingredient used in the mosquito coils, accounting for about 0.3-0.4% of coil mass (Lukwa and Chandiwana, 1998). Lee and Wang (2006) have estimated and found appreciable amount of particulates and gases like CO, NO, NO_2, CH_4, NMHC, formaldehyde and acetaldehyde in coil smoke. They reported $PM_{2.5}$ emission factors of 20.3-47.8 and PM_{10} emission factors of 15.9-50.8 mg/g coil. Liu *et al.*, (2003) reported $PM_{2.5}$ emission factors of 32-70 mg/g coil. Chang and Lin (1998) have found that the gas phase of mosquito coil smoke contains carbonyl compounds (e.g. formaldehyde and acetaldehyde) that could produce strong irritating effects on the upper respiratory tract. Epidemiologic studies have shown that long-term exposure to mosquito coil smoke can induce asthma and persistent wheeze in children (Azizi and Henry, 1991; Fagbule and Ekanem, 1994). Toxicologic effects of mosquito coil smoke on rats include focal deciliation of the tracheal epithelium, metaplasia of epithelial cells, and morphologic alteration of the alveolar macrophages (Liu and Sun, 1988; Liu and Wong, 1987).

Mosquito coils are a major source of indoor fine particulates and very little scientific information is available on emission of particulates including the rate and emission factors of fine particulates from Indian mosquito coils. The present study was undertaken with the objective of estimating particulate matter ($PM_{0.2\text{-}1}$, $PM_{0.2\text{-}2.5}$ and $PM_{0.2\text{-}5.0}$) emission rate and emission factors of Indian mosquito coils.

MATERIALS AND METHODS

Seven brands of mosquito coils (designated as M1-M7), which are commonly marketed in India were tested in this study. Their ingredients are summarized in Table 1 as per the specifications printed on the coil boxes. The coils were tested for their burning time, burning rate and ash generation quantity. Subsequently, an experiment was conducted in a test chamber (0.0689 m^3 volume), maintained at about 26$\pm$2^oC and 35$\pm$3% RH, to study particulate matter ($PM_{0.2\text{-}1}$, $PM_{0.2\text{-}2.5}$ and $PM_{0.2\text{-}5.0}$) emissions from the coils. The basic experimental design has been reported earlier by Liu *et al.*, (2003) but minor modifications had been incorporated in this experimental set-up for the present study. During each experimental run, a mosquito coil was lit on its metal stand and placed inside the chamber. Ambient air was introduced into the chamber through a particulate filter fitted inlet at a back end of the smouldering coil at a constant flow of 1.35 l/min to support combustion and eviction of the

smoke from an outlet fitted at the other end in the chamber. The experimental chamber was thus maintained at a slightly positive pressure. Air was driven out of the combustion chamber at an average flow rate of about 10 ml/min through a delivery tube into a dilution chamber which was kept at 7x dilution by delivering air after particle filtration via delivery pumps kept outside. Thus the dilution chamber was also kept under a positive pressure to prevent infiltration of air from outside. A pressure release vent was installed in the dilution chamber for venting out extra pressure, if any.

A single-compartment mass balance model was used to describe the whole combustion process and to determine the emission rate as described by Liu *et al.,* (2003). Basic assumptions for this model are a) background concentration of the analyte is zero; b) pollutant concentrations are homogeneous within the chamber; and c) emission rate and decay rate of the pollutants remain constant throughout the entire experimental run. The relationship between the pollutant concentration C (mg/m^3) and the emission rate P (mg/h) can be expressed as:

$$C = P/Vk \ (1- e^{-kt}) \text{ (when } 0 \leq t \leq T) \quad (1)$$

where, C= steady-state concentration of the analyte in side chamber in mg/m^3; P= emission rate of the analyte in mg/h; V= volume of the chamber in m^3; k is the total removal rate of analyte in hr^{-1}; t is time in hour. Coil burning was started at t = 0 and extinguished at t = T.

When the concentration of the pollutant is stabilized inside the chamber i.e. it reaches a steady state, equation 1 can be re-written as:

$$C = P/Vk \quad (2)$$

Therefore, the emission rate P (mg/h) could be easily obtained using steady-state concentration (C), pollutant removal rate (k), and the volume of the chamber (V). To determine particulate removal rate k, real time particle mass concentration in the chamber during the postburning period is needed for the calculation (Liu *et al.*, 2003). An aerosol spectrometer was used to determine real time particulate mass concentration (mg/m^3) in the size ranges of 0.2-1.0, 0.2-2.5 and 0.2-5 μm during coil burning as well as the postburning period at a regular time interval of 1 minute. The linear regression slope of ln (C) (steady state concentration) against t was the total removal rate of particulate matter in the chamber (Liu *et al.,* 2003).

An aerosol spectrometer (model 1.109, GRIMM, Germany) was used to measure particle mass concentration in the size ranges 0.2-1.0, 0.2-2.5 and 0.2-5.0 μm. The analyzer was allowed to take measurements throughout the burning period and the postburning period, until the particulate readings fell back to the background level. Emission factor of the mosquito coils were calculated by dividing emission rate of particulates per hour (mg/h) by amount of coil (g) burnt in the same time and the emission factor thus was calculated in milligram of particulate emission per gram of coil burnt (mg/g).

RESULTS AND DISCUSSION

The experiment on the burning characteristics of the coils revealed that each mosquito coils had a different burning duration than the other and most of the full coils burnt for about 5-6 hours except MC5, which burnt for lower than 5 hours. The MC7 coil (marketed as a low smoke coil), being longer and having more material, burnt for an exceptionally higher time of 14 hours and 38 minutes. All the coils, except MC7, had similar burning rate ranging between 2.02 and 2.58 g/h but had widely variable ash content, ranging from 3.91 to 11.08% (w/w). Burning rate of the low smoke coil was lower (1.47 g/h) than all other, implying that by allowing lesser material being burnt per unit

Name/ Code	Toxicity Code	Active Ingredient	Reported Composition	Reported Burning Time (h)	Mean Coil wt. (g)
MC1	Yellow	d-trans allethrin	d-trans allethrin (0.1% w/w), Other ingredients (99.9% w/w)	8 h	13.04
MC2	Yellow	d-trans allethrin	d-trans allethrin (0.1% w/w), Wood flour (52.9% w/w), Coconut shell powder (35.00% w/w), Binder starch (12.0% w/w)	8 h	12.58
MC3	Green	Transfluthrin	Transfluthrin A.l. (0.03% w/w), Other adjuvands (99.97% w/w)	8 h	11.69
MC4	Yellow	d-trans allethrin	d-trans allethrin (0.1% w/w), Wood flour (52.90% w/w), Coconut shell powder (35.00% w/w), Binder starch (12.00% w/w)	8 h	13.05
MC5	Yellow	d-trans allethrin	d-trans allethrin (0.1% w/w), Wood Flour (45.0% w/w), Coconut Shell Powder (35.0% w/w), Binder starch (12.00% w/w), Dye (Malachite Green, 7.90% w/w)	8 h	12.8
MC6	Blue	Allethrin	Allethrin (0.2% w/w), Wood flour (80.0% w/w), Pine charcoal (7.3% w/w), Starch (12.0% w/w), Dye (0.5% w/w)	8 h	12.44
MC7	Blue	Prallethrin	Prallethrin (0.05% w/w), Smouldering Agent (Potassium Nitrate, 5.0% w/w), Preservative (Sodium Benzoate, 0.3% w/w), Binders (Guar Gum, 3.0% w/w; Starch, 3.0% w/w), Emulsifiers [Anionic & Non ionic blend {UNITOX-3, 0.05% w/w (Alkyl aryl sulphonate and polyoxy ethylene ether blend)}], Carriers (Clay dust, 10.0% w/w, Calcite dust, 10.0% w/w, Wood flour, 15.0% w/w, charcoal QS, 53.15% w/w)	12 h	21.44

Table 1. Characteristics of select mosquito coils

Av. coil weight burnt (g)	Av. burning Time (min)	Av. weight of Ash (g) [a]	Burning time for full coil in chamber (min., extrapolated)	Av. burning rate (g/min)	Av. burning rate (g/h) [a]	Av. ash (%)
2.1985	55.5	0.139	329 min (5 h 29 min)	0.039	2.34	6.32
2.3525	68	0.151	364 min (6 h 4 min)	0.034	2.04	6.42
2.3645	68.5	0.262	339 min (5 h 39 min)	0.035	2.1	11.08
2.1855	63.5	0.144	379 min (6 h 19 min)	0.034	2.04	6.59
2.3195	54	0.182	298 min (4 h 58 min)	0.042	2.52	7.85
2.325	69.5	0.091	372 min (6 h 12 min)	0.033	1.98	3.91
2.283	93.5	0.253	878 min (14 h 38 min)	0.024	1.44	11.08

[a] values are presented as mean±SD

Table 2. Average burning characteristics of mosquito coil pieces inside the simulation chamber

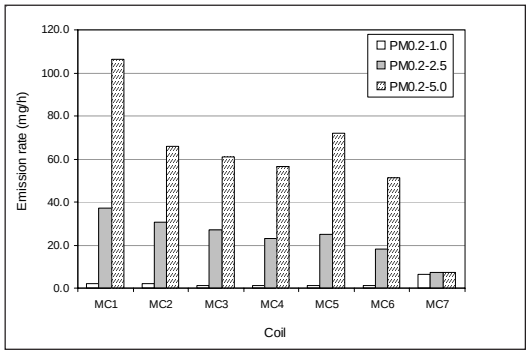

Figure1. Emission rate (mg/h) of particulate matter from select mosquito coils

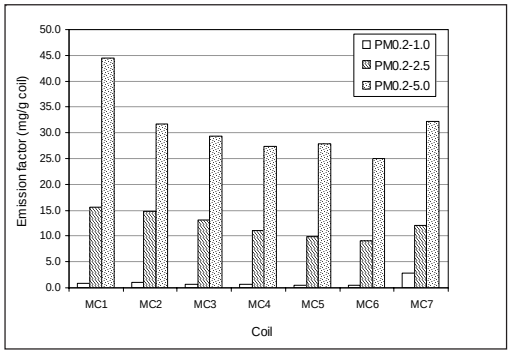

Figure 2. Emission factor (mg/g) of particulate matter from select mosquito coils

Coil	Ratio	Percent Share	Ratio	Percent Share	Ratio	Percent Share
	$PM_{1}/PM_{2.5}$	$PM_{1}/PM_{2.5}*100$	$PM_{2.5}/PM_{5}*100$	$PM_{2.5}/PM_{5}*100$	$PM_{1}/PM_{5}*100$	$PM_{1}/PM_{5}*100$
MC1	0.059	5.9	0.35	35	0.021	2.06
MC2	0.066	6.6	0.465	46.5	0.031	3.08
MC3	0.052	5.2	0.444	44.4	0.023	2.3
MC4	0.057	5.7	0.404	40.4	0.023	2.29
MC5	0.053	5.3	0.352	35.2	0.019	1.85
MC6	0.057	5.7	0.356	35.6	0.02	2.03
MC7	0.878	87.8	0.998	99.8	0.876	87.64

Table 3. Ratio and percent share of emission rates for select mosquito coils calculated as $PM_{0.2\text{-}1}/PM_{0.2\text{-}2.5}$, $PM_{0.2\text{-}1}/PM_{0.2\text{-}5}$ and $PM_{0.2\text{-}2.5}/PM_{0.2\text{-}5}$

time it burnt for much longer time. But, ash percent in MC7 was much higher than all other coils except MC3, probably due to the presence of clay and calcite dust in this particular type of coils (Table 1) which ended up in the ash.

Emission rates of $PM_{0.2-1}$, $PM_{0.2-2.5}$ and $PM_{0.2-5}$ from different coils are presented in Fig. 1. Emission rate of $PM_{0.2-1}$ varied between 1.0-6.3 mg/h and interestingly, the highest rate was obtained from the low-smoke coil (MC7), implying that it had higher emission rate of the finer particles than others. But, $PM_{0.2-2.5}$ emission rate was much lesser (7.2 mg/h) in low-smoke coil than all other coils that ranged from 18.2-37.3 mg/h. Emission rate of $PM_{0.2-5}$ from the low-smoke coil was only slightly higher than its $PM_{0.2-2.5}$ emission rate, implying that there was negligible emission of PM in between 2.5 and 5 micron (μm) size range from MC7. PM_5 emission for other coils ranged from 51.2-106.4 mg/h. Overall, the low smoke coil generated much lower amount of particulates up to 5 μm range than other coils, underlying it's slow smoking character. But, it's particulate emission within 1 μm range was higher than others.

When $PM_1/PM_{2.5}$ and $P_{2.5}/PM_5$ ratios and their corresponding percent share were calculated (Table 3), it showed that share of PM_1 emission was about 87.8% of $PM_{2.5}$ fraction and $PM_{2.5}$ had a share of 99.8% in PM_5 emissions in emissions from the low smoke coil. This indicated that low smoke coil emissions consisted of much more proportion of finer particulates. On the other hand, normal coils had PM_1 share of about 5-7% in $PM_{2.5}$ fraction. For these coils, about half of the total PM emissions were below 2.5 micron size range. Different types of organic fillers (base materials) used for making the coils could be the main reason of the differences obtained in particulate emission rates.

Emission factor of $PM_{0.2-1}$, $PM_{0.2-2.5}$ and $PM_{0.2-5.0}$ varied between 0.5-2.9, 9-15.6 and 25-44.5 mg/g coil and the highest factor for $PM_{0.2-1.0}$ was of the low smoke coil MC7, implying that from human health perspective, it may be more harmful than other coils. But, its $PM_{2.5}$ emission factor (12.1 mg/g coil) was comparable to several of the other coils ranging from 9.0-15.6 mg/g coil. Similarly, emission factor of PM_5 from the low smoke coil MC7 (32.2 mg/g) was also comparable with other coils ranging from 25-44.5 mg/g (Fig. 2).

SUMMARY AND CONCLUSIONS

- Different mosquito coils had variable burning time and none of the coils except MC7 could exceed 6.3 hrs burning time for the full coil. MC7 being longer and having more material, burnt for 14 hours and 38 minutes.
- All the coils, except MC7 (marketed as a low smoke coil), had similar burning rate of 2.02-2.58 g/h but variable ash content, ranging from 3.91 to 11.08%.
- Burning rate of the low smoke coil was lower (1.44 g/h) than all others implying that by allowing lesser material being burnt per unit time it emitted lesser smoke per unit time. But, ash percent in MC7 was much higher than all other coils except MC3.
- Emission rate of $PM_{0.2-1}$ varied between 1-6.3 mg/h and interestingly, the highest rate was obtained from the low smoke coil. But, its $PM_{0.2-2.5}$ emission was much lesser (7.2 mg/h) than all other normal coils, ranging from 18.2-37.3 mg/h. $PM_{0.2-5}$ emission for normal coils ranged from 51.2-106.4 mg/h.

- When $PM_{0.2\text{-}1}/PM_{0.2\text{-}2.5}$ and $P_{0.2\text{-}2.5}/PM_{0.2\text{-}5}$ ratios and their corresponding percent share were calculated, it showed that most of the emissions (87.8%) of low smoke coil were within 1 micron size and there was little emission of particulates above 2.5 micron.
- Normal coils had only about 5-6% of the PM emissions within 1 micron size. For these coils about half of the PM emission fell below 2.5 micron size range.
- Emission factor of $PM_{0.2\text{-}1}$ varied between 0.5-2.9 mg/g coil and the highest factor was obtained from the low smoke coil. But, its $PM_{0.2\text{-}2.5}$ emission factor (12.1 mg/g coil) was comparable to normal coils ranging from 9.0-15.6 mg/g coil.
- Emission factor of $PM_{0.2\text{-}5}$ from the low smoke coil MC7 (32.2 mg/g) was also comparable with other coils ranging from 25-44.5 mg/g.

ACKNOWLEDGEMENT

The authors acknowledge the constant guidance and encouragement of Director, NEERI and Head, Air Pollution Control Division, NEERI.

REFERENCES

Azizi, B.H.O., Henry, R.L. (1991). The effects of indoor environmental factors on respiratory illness in primary school children in Kuala Lumpur, *Int. J. Epidemiol.*, **20(1)**, pp. 144-149.

Fagbule, D., Ekanem, E.E. (1994). Some environmental risk factors for childhood asthma: a case-control study, *Ann. Trop. Paediatr.*, **14(1)**, pp. 15-19.

Lee, S. C. and Wang, B. (2006). Characteristics of emissions of air pollutants from mosquito coils and candles burning in a large environmental chamber, *Atmos. Environ.*, **40(12)**, pp. 2128-2138.

Liu, W.K., Sun, S.E. (1988). Ultra structural changes of tracheal epithelium and alveolar macrophages of rats exposed to mosquito-coil smoke, *Toxicol. Lett.*, **41**, pp. 145-157.

Liu, W.K., Wong, M.H. (1987). Toxic effects of mosquito coil (a mosquito repellent) smoke on rats, *Toxicol. Lett.*, **39**, pp. 223-239.

Liu, W.L., Zhang, J.F., Hashim, J.H., Jalaludin, J., Hashim, Z. and Goldstein, B.D. (2003). Mosquito coil emissions and health implications, *Environ. Health Perspect.*, **111**, pp. 1454-1460. Lukwa, N. and Chandiwana, S.K. (1998). Efficiency of mosquito coils containing 0.3% and 0.4% pyrethrins against An. Gambiae sensulato mosquitoes, *Cent. Afr. J. Med.*, **44**, pp. 104-107.

Yap, H.H. (1985). Biological control of mosquitoes especially malaria vectors anopheles species. Symposium on research on the mosquito vectors of malaria in Southeast Asia held at the tropical medicine and public health project technical meeting, Kuala Lumpur, Malaysia, *Southeast Asian J. Trop. Med. Public Health*, **16**, pp. 163-172.

Yap, H.H., Lee, Y.W., Zairi, J. (2000). Chemical control of mosquitoes. In: *Mosquitoes and Mosquito-borne Diseases*, Ng, F.S.P., Yong, H.S. (Eds.). Academy of Science, Kuala Lumpur, Malaysia, pp. 197-210.

MOLECULAR CHARACTERIZATION OF DICARBOXYLATE SPECIES IN SUBMICRON (PM_1) AEROSOLS IN CENTRAL INDIA

D. K. DESHMUKH[1], M. K. DEB[1], YING I. TSAI[2], B. K. SEN[1]

[1]School of Studies in Chemistry, Pt. Ravishankar Shukla University, Raipur 492 010, Chhattisgarh, India
[2]Department of Environmental Engineering and Science, Chia Nan University of Pharmacy of Science, 60, Sec, 1, Erh-Jen Road, Jen-Te, Tainan 71710, Taiwan
E mail: dhananjaychem@yahoo.in

Keywords : DICARBOXYLATES, PARTICULATE MATTER

INTRODUCTION

Atmospheric aerosols play an important role in global climate forcing. Aerosol chemical composition is important in quantifying their radiative climate effects by means of absorption and scattering (Ho *et al.*, 2007). Several epidemiological studies have suggested a statistical association between health effect and ambient fine particle concentrations, especially the submicron fraction that can penetrate deep into the alveolar region of the lungs (Hsieh *et al.*, 2007; Pope *et al.*, 2000). Raipur city, the capital of newly formed state "Chhattisgarh", located in the eastern central region of India is one of the polluted cities in India today. Air quality in Raipur city has become a serious concern due to the high mass concentration levels of PM_{10} and $PM_{2.5}$ atmospheric aerosols (Deshmukh *et al.*, 2010) Therefore, aerosol air pollution in Raipur city continues to be a serious problem. The organic species of interest is dicarboxylates (DCs) which are important organics resulting from the marine pathway (Yao *et al.*, 2004), fossil fuel and biomass burning cooking (Wang *et al.*, 2006), forest bio-sources and anthropogenic emissions (Hsieh *et al.*, 2009). Therefore, the main objective of the present study is to determine the mass concentration of submicron aerosols and associated dicarboxylate species in the ambient air of Raipur city, India. Correlation analysis between DCs was also performed to understand the source of dicarboxylate species and the formation of secondary species.

METHODS

Raipur city (22°33' to 21°14' N Latitude and 82°6' to 81°38' E Longitude, ~297 m above sea level) was selected for continuous sampling of aerosols. The sampling site at Raipur (Fig. 1) was located on the roof of the building, School of Studies in Chemistry, Pandit Ravishankar Shukla University at a height of ~15 m above the ground level. The eight-stage cascade impactor aerosol sampler (TE 20-800; Flow rate, 28.3 L min^{-1}) was used for the collection of aerosols. Aerosol sampling was carried out for 24 hrs twice in a week spread over all the major seasons, namely monsoon, winter, spring and summer. Whatman 41 glass filter with diameter of 80 mm was used for the collection of aerosols. Each filters used for the sampling was pre-conditioned and post-conditioned in a controlled environment at 20°C temperature and 40% relative humidity for 24 hrs and weighed using an electronic balance (Sartorius CP225D) with reading precision 10 µg. The filters of the actual samples and field blanks were placed into polyethylene (PE) bottles and kept frozen at 4°C during storage to prevent the loss of DCAs prior to analysis.

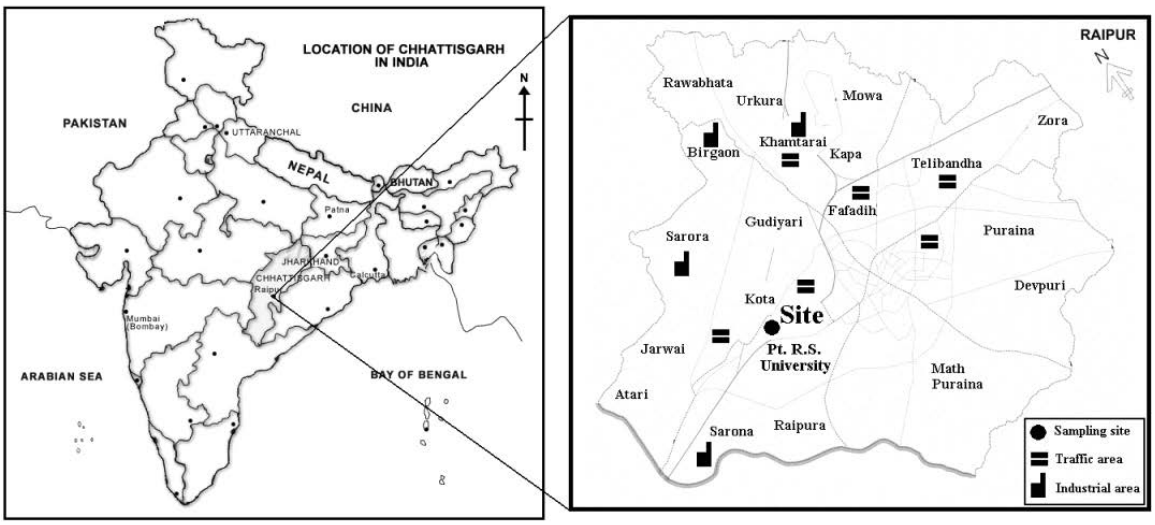

Figure 1. Location of sampling site in Raipur city

One-fourth of sampled filters were placed in PE bottle, 10.0 mL of deionized water (resistivity: 18.0 μΩ cm^{-1} at 25°C, Barnstead) was added and the content was shaken in an unlit refrigerator at 4°C for 90 min to prevent the decomposition of extracted DCs. The liquid was then filtered through a 0.2 μm ester acetate filter and the aqueous filtrate was characterized using ion chromatography (IC). The IC (DX–600, Dionex) was equipped with a gradient pump (Model GP50), an ASRS–Ultra anion self-regenerating suppressor, a conductivity detector (CD25), a Spectra system automated sampler (AS1000) with 2 mL vials and a Teflon injection valve using a 1000 μL sample loop, in combination with an AS11 analytical column (250 mm × 4 mm I.D.), an AG11 guard column (50 mm × 4 mm I.D.), an anion trap column (ATC-3), a 5–100 Mm NaOH gradient and 100% methanol eluent. The flow rate was maintained at 2.0 mL min^{-1} during the dicarboxylates analysis. All reagents were of analytical grade, obtained from Merck and were used without further purification. Detection limit was used to determine the lowest concentration level that can be detected to be statistically different from a blank. Method detection limits (MDLs) were determined from selecting the concentration slightly higher than the low concentration of the standard line. The obtained MDLs were ranged between 0.20 ngm^{-3} for tartarate and1.42 ng $m^{-3}$for oxalate. The overall mean concentrations for field blank samples collected over a year ranged from 0.86 ng m^{-3} for glutarate to 12.70 ng m^{-3} for oxalate. All the data of aerosol mass and dicarboxylates concentrations were corrected with reference to a field blank.

The meteorological data, such as temperature (T, ºC), rainfall (RF, mm), relative humidity (RH, %), wind speed (WS, m/s) and wind direction (WD) were collected during the study period. The ambient temperature in Raipur city started to decrease in October and reached to a minimum of 18.7°C in January 2010 then increased to a maximum of 36.1°C in May 2010. Based on the observed data, in Raipur city monsoon was relatively wet with monthly average of 130.9, 56.7 and 8.5 mm in July, August and September 2009, respectively. The RH in Raipur city was 60% as annual average with the highest monthly average of 86% in August 2009 and the lowest of 29% in April 2010. The annual average of WS was found to be 5.1 m s^{-1}during the study period.

RESULTS AND DISCUSSION

The annual mean concentration of PM_1 aerosols is given in Table 1. The mass concentration of PM_1aerosols ranged from 4.4 to 135.3 µg m^{-3} with an average value of 72.5 µg m^{-3}. High PM_1 aerosols mass concentration in Raipur city could be attributed to the anthropogenic activities which may include high rate of biomass combustion. PM_1 aerosols concentration varies significantly in different season of the year with highest concentration during winter and spring seasons with an average value of 108.4 and 81.4 µg m^{-3}, respectively and lowest concentration during the monsoon and summer seasons with an average value of 42.7 and 48.4 µg m^{-3}, respectively. Winds are relatively calm (2.4 m s^{-1}) during winter season and this prevailing calm conditions favored more stable atmospheric conditions; consequently reducing the dispersion of aerosol particles with increase in anthropogenic activities such as biomass burning and space heating. Lowest concentration observed during monsoon season can be attributed to washout by rainfall and higher humidity which led to reduce re-suspension of soil particles.

Species	Statistics (n = 120)				
	Mean	Standard deviation	Minimum	Maximum	Coefficient of variation
	PM_1 aerosols, µg m^{-3}				
	72.5	12.3	28.8	79.4	0.29
	Dicarboxylate species, ng m^{-3}				
TDCs	281.3 (0.5)[a]	168.9	122.4	628.6	0.6
Oxalate, C_2	205.8 (68.8)[b]	150.7	69.4	498.9	0.73
Malonate, C_3	16.3 (6.6)[b]	9.2	6.1	43.5	0.56
Succinate, C_4	9.0 (3.8)[b]	5.4	1.7	28	0.59
Glutarate, C_5	5.3 (2. 4)[b]	3.9	1.5	18.8	0.74
Adipate, C_6	3.9 (1.8)[b]	2.5	1.5	16.8	0.64
Maleate, M	8.9 (3. 8)[b]	4.2	3.2	29.4	0.47
Fumarate, F	8.4 (3.1)[b]	6.9	2	29.5	0.82
Phthalate, Ph	9.4 (3. 9)[b]	4.5	2	19.8	0.48
Malate, hC_4	7.8 (3.3)[b]	4.6	2.5	26.9	0.59
Tartarate, Ta	6.7 (3.5)[b]	4.1	1.8	18.3	0.62

Table 1.Annual statistics on concentrations of PM_1aerosols and associated dicarboxylate species in Raipur citybetween July 2009 and June 2010

The concentration of total dicarboxylates ranged from 122.4 to 628.6 ngm^{-3} with an average of 281.3 ng m^{-3}. The concentrations of total dicarboxylates accounted for 0.2% to 3.3% with an average of 0.5% of the total PM_1aerosol mass. Oxalate was found as the most abundant dicarboxylate species in PM_1 aerosols ranging from 69.4 to 498.9 ng m^{-3} with an average of 205.8 ng $m^{-3}$and

constituting from 51.6 to 87.3% (68.8%) of all measured dicarboxylates in PM_1 aerosols. Malonate (6.1 to 43.5 ng m^{-3}, average 16.3 ng m^{-3}) was the second most abundant dicarboxylate species accounting for 2.4 to 15.1% with an average of 6.6% of total dicarboxylates analyzed in PM_1 aerosols.

The concentrations of dicarboxylates were higher during winter and spring seasons and lower during summer and monsoon seasons. Dicarboxylate species showed two different seasonal distribution trends. The first group of DCs, including oxalate, glutarate, adipate, maleate, fumarate and tartarate showed maximum concentrations during winter season. While, the second group of DCs including malonate, succinate, phthalate and malate showed maxima during spring season. The different seasonal variations between first and second group of dicarboxylates suggested the difference in the sources or atmospheric processing. Therefore, the different seasonal trends should be caused by a difference in the emission of their precursors of photochemical processing. The lower mixing height, the formation of inversion layer and the less chances of wet deposition can contribute to the accumulation of air pollutants during winter season. All the dicarboxylates showed lower concentrations during monsoon season. The low concentration during monsoon and summer seasons might be related to the low emission strength, the washout effect as well as the partition between gas and particle phase.

The mass concentration ratio of oxalate to succinate ranged between 5.7 and 97.2 with an average of 28.2. Higher oxalate to succinate mass concentration ratio found in this study was attributed to photochemical production of oxalate from succinate within biomass burning plume. The malonate to succinate mass concentration ratio ranged between 1.0 and 3.0 with an average of 2.0. This result suggested that in addition to primary exhaust secondary formation of particulate dicarboxylic acids by photo-oxidation reaction is also possible. This result may suggest that a significant fraction of malonate is secondarily produced in the atmosphere by photochemical degradation of succinate. A good correlation of oxalate and precursor compounds, such as malonate and succinate as well as malate with sulfate concentration would imply secondary production of di-acids through photochemical degradation. A good correlation between oxalate and malonate DCs indicate that these three DCs were emitted from similar type of sources, probably from fossil fuel combustion.

SUMMARY AND CONCLUSIONS

This study reports, for the first time, the molecular distribution of dicarboxylate species associated with PM_1 aerosols in an urban area of eastern central India between July 2009 and June 2010. The annual average mass concentration of PM_1 aerosols varied from 4.4 to 135.3 μg m^{-3} with an average of 72.5 μg m^{-3}. Seasonal cycle showed higher concentration of submicron aerosols during winter and spring seasons and lower concentration during summer and monsoon seasons. The highest concentration observed during winter season can be attributed to low wind speed and low temperature which lead to lower mixing height and poor dispersion conditions coupled with increase in anthropogenic activities such as vehicular emissions, biomass burning, industrial processes and space heating. Molecular distributions of dicarboxylates were characterized by a predominance of oxalate and malonate followed by phthalate and succinate. The concentration of total dicarboxylates ranged from 122.4 to 628.6 ngm^{-3} with an average of 281.3 ng m^{-3}. The concentration of total dicarboxylates accounted for 0.5% of the total PM_1 aerosol mass. The characteristics seasonal variation of dicarboxylates was found in Raipur city which are associated with their sources and photochemical processing. These findings are consistent with seasonal variations of DCs, whose concentrations maximized in winter and spring seasons than summer and monsoon seasons. Malonate to succinate mass concentration ratio may effectively be used to distinguish the relative importance of their primary and secondary sources. This result may suggest that a significant fraction of malonate is secondarily

produced in the atmosphere by photochemical degradation of succinate. A good correlation of oxalate with malonate and succinate indicated that these three DCs were emitted from similar type of sources, probably from fossil fuel combustion.

ACKNOWLEDGEMENT

The authors would like to thank Prof. K.S. Patel, Head of the School of Studies in Chemistry, Pt. Ravishankar Shukla University, Raipur, India, for providing laboratory support. This research was supported partly by the grants of National Science Council of Taiwan NSC 96-2221-E-041-013-MY3 and NSC 99-2221-E-041-014-MY3. The authors also wish to express gratitude to the anonymous reviewers for their valuable comments and suggestions.

REFERENCES

Deshmukh, D.K., Deb, M.K., Tsai Y.I, Mkoma, S.L. (2011).Water soluble ions in $PM_{2.5}$ and PM_{1} aerosols in Durg city, Chhattisgarh, India, *Aerosol Air Qual. Res.***11,** 696.

Deshmukh, D.K., Deb, M.K., Verma, S.K. (2010). Distribution patters of coarse, fine and ultrafine atmospheric aerosol particulate matters in major cities of Chhattisgarh, *Indian J. Environ. Prot.* **30**, 184.

Ho, K.F., Cao, J.J., Lee, S.C., Kawamura, K., Zhang, R. J., Chow, J.C., Watson, J.G. (2007). Dicarboxylic acids, ketocarboxylic acids and dicarbonyls in 14 cities of China, *J. Geophys. Res.* **112**, D22S27, doi: 10.1029/ 2006JD008011.

Hsieh, L.Y., Chen, C.L., Wan, M.W., Tsai, C.H., Tsai, Y.I. (2008). Speciation and temporal characterization of dicarboxylic acids in $PM_{2.5}$ during a PM episode and a period of non-episodic pollution, *Atmos. Environ.* **42**, 6836.

Hsieh, L.Y., Kuo, S.C., Chen, C.L., Tsai, Y.I. (2007). Origin of low molecular weight dicarboxylic acids and their concentration and size distribution variation in suburban aerosol, *Atmos. Environ.* **41**, 6648.

Pope, C.A. (2000). Review: Epidemiology basis for particulate air pollution health standards, *Aerosol Sci. Technol.* **32**, 4.

Wang, G. H., Kawamura, K., Lee, S.C., Ho, K.F., Cao, J.J. (2006).Molecular, seasonal and spatial distribution of organic aerosols from fourteen Chinese cities, *Environ.Sci. Technol.* **40**, 4619.

Yao, X. H., Fang, M., Chan, C.K., Ho, K.F., Lee, S.C. (2004).Characterization of dicarboxylic acids in $PM_{2.5}$ in Hong Kong, *Atmos. Environ.* **38**, 963.

CHARACTERIZATION OF CARBONACEOUS AEROSOLS IN FINE ($PM_{2.5}$) PARTICLES AT AGRA, INDIA

TRIPTI PACHAURI, APARNA SATSANGI, VYOMA SINGLA, ANITA LAKHANI & K. MAHARAJ KUMARI

Department of Chemistry, Faculty of Science, Dayalbagh Educational Institute, Dayalbagh, Agra
E mail: triptiipachauri@yahoo.co.in

Keywords: VOLATILE ORGANIC COMPOUNDS, CARBONACEOUS AEROSOLS

INTRODUCTION

The carbonaceous matter consists of organic carbon (OC) and elemental carbon (EC). Elemental carbon is a primary pollutant emitted from incomplete combustion of fossil fuel and biomass, while OC can be either released directly into the atmosphere from anthropogenic and biogenic sources (primary OC, POC) or formed within the atmosphere through gas – to – particle conversion of volatile organic compounds through photochemical reactions (secondary OC, SOC). Airborne carbonaceous aerosols are largest contributor to fine particles with an aerodynamic diameter smaller than 2.5 μm ($PM_{2.5}$). It is found to be associated with human health problems causing serious respiratory and cardiovascular diseases (Pope *et al.*, 2002) and air quality problems such as visibility reduction.

The high loading of carbonaceous aerosols in fine particles has also been identified as the important factor in climate change, urban haze formation, crop production and atmospheric chemical reactions (Li and Bai, 2009). Thus, in lieu of the importance in recent years, special attention has been drawn on carbonaceous species and studies have been carried out in a large variety of environments worldwide. In India, there are several studies focusing on the field measurements of carbonaceous aerosols in TSP (Ram and Sarin, 2010; Satsangi *et al.*, 2010; Sudhir and Sarin 2008) but the information regarding the chemical composition, concentration, sources and formation mechanism is still limited in India. Therefore, the present work is to quantify the relative contribution of carbonaceous species in $PM_{2.5}$ mass, to identify the possible sources and factors affecting carbonaceous species and to characterize the elemental composition and morphology of individual atmospheric particles using SEM – EDX method.

MATERIALS AND METHODS

The study was carried out at Dayalbagh, an urban site, which is 10 km away from the industrial sector of the Agra (27°102 N, 78°052 E, and 169 m.s.l.). Sampling was performed on the roof of Science Faculty building (8 m above the ground) in the Institute campus. All $PM_{2.5}$ were collected using Fine Particulate Sampler (Envirotech APM 550) operated at a constant flow rate of 16.6 $Lmin^{-1}$ on pre-weighed 47 mm quartz fibre filters (Pallflex, Tissuquartz) for 24 hours from May 2010 to April 2011.

A portion of filter samples (1.5 cm^2) was cut and analyzed for OC and EC by a thermal/optical Carbon Aerosol Analyzer (Sunset Laboratory, Forest Grove, OR) using NIOSH 5040 (National Institute of Occupational Safety and Health) protocol based on Thermal Optical Transmittance (TOT) which is described in detail elsewhere (Birch and Cary, 1996).

Water soluble K^+ was determined by using Dionex ICS 1100 Ion Chromatograph system (Dionex Corp, Sunnyvale, CA). To extract, half of each filter was sonicated for 45 min in 1% HNO_3 and K^+ concentrations was determined by using 20mM Methane Sulfonic Acid as an eluent.

The aerosol samples were analyzed by SEM - EDX at National Institute of Oceanography, Goa. The SEM – EDX analysis was carried out with the help of computer controlled field emission scanning electron microscope SEM (JSM – 5800 LV) equipped with an energy dispersive X – ray system (Oxford 6841). The working conditions were set at an accelerating voltage of 20 kV, a beam current of 40 – 50 μA and the Si (Li) detector 10mm from the samples to be analyzed. X- Ray detection limit is ~0.1%. The EDX analysis was carried out at each analysis point and the elements present were both qualitatively and quantitatively measured.

RESULTS AND DISCUSSION

Concentration levels of $PM_{2.5}$

Mass concentration is the key criteria for the assessment of air quality. At this site, the mass concentrations of $PM_{2.5}$ ranged from 24.6 to 163.6 μg/m^3 while the annual average concentration was found to be 79.7 ± 40.5 μg/m^3. The average daily concentration of PM during the measurement period exceeded the 24 hour National Ambient Air Quality Standard (NAAQS, CPCB 1994; 60 μg/m^3) of India. Higher level of particulate matter at this sampling site may be attributed to the combined impact of climatic conditions and anthropogenic emissions by various local sources such as vehicular exhaust, waste incineration, coal and biomass combustion as well as re-suspended dust.

The seasonal average concentrations of $PM_{2.5}$ was 72.2 ± 7.1 μg/m^3 in summer, 116.6 ± 39.1 μg/m^3 in winter and 39.2± 9.3 μg/m^3 in monsoon, respectively. In winter, $PM_{2.5}$ mass concentration was 1.6 and 2.9 times higher than in summer and monsoon seasons. The levels were found to be slightly elevated during winter season due to different emission sources (increased biomass, coal and fossil fuel combustion) and meteorological conditions. Stable and cold conditions (i.e. less dispersion and low mixing heights) during winter months favors the ambient particles to be remain for longer time in the atmosphere. During summer, local sources in addition to long range transport, especially during dust storm contribute to PM levels while in monsoon, heavy rainfall leads to wet scavenging of aerosol particles.

Concentration of carbonaceous species in $PM_{2.5}$

Seasonally averaged PM mass, TC (Total carbon), OC, EC, OC/EC ratio and TCA in $PM_{2.5}$ and TSP are summarized in Table 1. Seasonally averaged $PM_{2.5}$ mass, TC, OC, EC and OC/EC ratio show strong seasonal variation with the highest concentration in winter followed by summer and monsoon. The average concentration of OC in $PM_{2.5}$ was 36.1 ± 19.1, 20.3 ± 7.1 and 8.0 ± 2.1 μg/m^3 during winter, summer and monsoon respectively. The OC mass concentration during winter season was about 1.7 and 4.5 times higher than summer and monsoon season respectively. However, the EC concentrations were found to be 5.0 ± 1.2, 2.9 ±1.1 and 1.7 ± 1.0 μg/m^3 in $PM_{2.5}$ during winter, summer and monsoon respectively. The results show that during winter, fine particles contribute more than half of OC and EC concentration to total suspended particulate matter. On applying t – test, seasonal variations in OC and EC concentrations was observed to be statistically significant. This may be attributed to different climatic conditions and emissions sources.

Sampling season	Mass ($\mu g/m^3$)	OC ($\mu g/m^3$)	EC ($\mu g/m^3$)	OC/EC	TCA ($\mu g/m^3$)	POC ($\mu g/m^3$)	SOC ($\mu g/m^3$)	SOC/OC (%)
Winter	116.6	36.1	5	7.1	62.7	15.5	20.5	47.5
Summer	72.2	20.3	2.9	6.7	34.1	15.1	5.1	24.5
Monsoon	39.2	8	1.7	5.9	14.5	3.9	4.1	43.9
Annual	79.7	22.8	3.4	6.6	40.1	12	10.8	42.2

Table 1. Average PM mass, TC, OC, EC OC/EC & TCA for $PM_{2.5}$ and TSP during different seasons.

The origin of OC and EC can be evaluated by the relationship between OC and EC (Li and Bai, 2009; Turpin and Huntzicker, 1995). A good OC – EC correlation with correlation coefficient (R) of 0.88, 0.69 and 0.76 for $PM_{2.5}$ were obtained for summer, winter and monsoon respectively. These results indicated the presence of common dominant sources for OC and EC (biomass burning, coal combustion and motor vehicular exhaust) because the relative rates of OC and EC would be proportional to each other. The annual average OC/EC ratio was found to be 6.6 ± 2.8 for $PM_{2.5}$. The ratio is similar to that reported in the literature for biomass burning emissions.

Contribution of carbonaceous species to $PM_{2.5}$

Total carbonaceous aerosol was calculated by the sum of EC and organic matter (OM) which was estimated by multiplying the amount of OC by 1.6 (TCA = 1.6*OC + EC) (Turpin and Lim 2001). The average concentration of TCA was 62.7, 34.1 and 14.5 $\mu g/m^3$ in $PM_{2.5}$ during winter, summer and monsoon season. This indicates that the carbonaceous fraction nearly accounted for about half of $PM_{2.5}$ mass which shows that fine particles are enriched with carbonaceous species. K^+ is generally used as an index of biomass burning due to its release during combustion processes. A significant correlation between water soluble K^+ and OC abundances (R^2 = 0.63) supports that the biomass burning emissions are the main source of carbonaceous species. In the present study, the K^+/EC ratios range from 0.2 to 0.69 with an average value of 0.52. The relatively higher value of K^+/EC ratios indicates biomass burning emissions which contribute carbonaceous particles in the atmosphere. The dominance of biomass burning and agricultural waste burning emissions during winter and summer season was further characterized by SEM/EDX analysis. The morphology of this kind of carbonaceous particle varied from soot chains to complex structures, which depend on fuels, burning conditions and atmospheric processes (Cong *et al.*, 2009). Fig. 1 shows a single carbon particle with nearly spherical morphology dominated by C and O (> 90%).

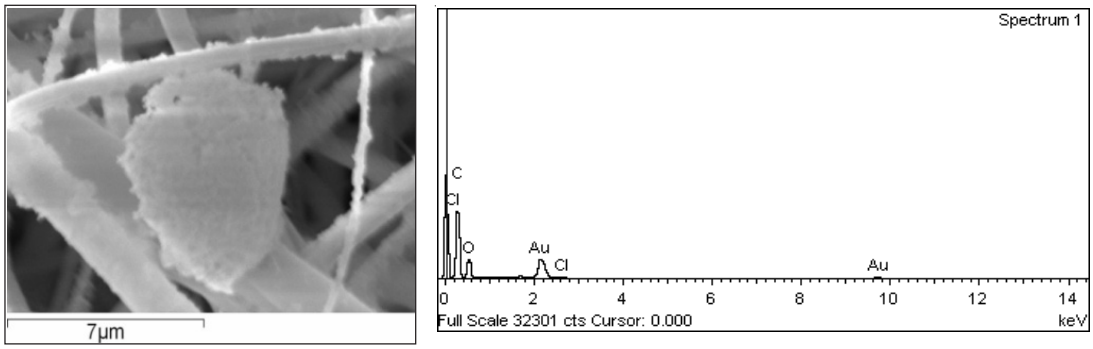

Figure 1. SEM/EDX image of nearly spherical carbonaceous particle

Estimation of secondary organic carbon (SOC)

SOC can be estimated from primary carbonaceous compounds and TOC (total organic carbon) using following equation: SOC = TOC – EC × (OC/EC)pri, where (OC/EC)pri is the ratio for the primary sources contributing to the sample. The primary ratio of OC/EC is usually affected by many factors such as types of emission sources, temporal and spatial variation, ambient temperature etc. Thus, (OC/EC)pri was represented by the observed minimum ratio of (OC/EC)min (Castro *et al.*, 1999). The observed values of (OC/EC) min in this study were 4.7, 2.3 and 3.1 for $PM_{2.5}$ during summer, monsoon and winter respectively.

The seasonal average concentration of SOC in $PM_{2.5}$ samples were 20.5, 5.1 and 4.1 μg/m^3 in winter, summer and monsoon respectively. The results indicated that the SOC concentration in $PM_{2.5}$ samples was 4 times higher in winter than during summer. High SOC concentration might be due to great coal consumption for heating in winter which causes enhanced emissions of primary carbonaceous particles and organic gases which in addition to stagnant meteorological conditions (low mixing layer height) results in SOC precursors stagnation and SOC formation.

REFERENCES

Castro L M, Pio C A, Harrison R M & Smith D J T (1999). Carbonaceous aerosol in urban and rural European atmospheres: Estimation of secondary organic carbon concentrations, *Atmospheric Environment,* **33**, pp. 2771–2781.

Central Pollution Control Board (1994). *National Ambient Air Quality Standards*, New Delhi, India.

Cong Z, Kang S, Dong S, Zhang Y (2009). Individual particle analysis of atmospheric aerosols at Nam Co, Tibetan plateau, *Aerosol Air Quality Research,* **9**, pp. 323- 331.

Li W and Bai Z (2009). Characteristics of organic and elemental carbon in atmospheric fine particles in Tianjin, China, *Particuology* **7**, pp. 432–437.

Pope C A, Burnett R T, Thun M J, Calle E E, Krewski D, Ito K *et al.,* (2002). Lung cancer, cardiopulmonary mortality and long-term exposure to fine particulate air pollution, *Journal of Am Med. Assoc.* **287**, pp. 1132– 41.

Ram K, Sarin, M M, (2010). Spatio-temporal variability in atmospheric abundances of EC, OC and WSOC over Northern India, *Journal of Aerosol Science*, **41**, pp. 88–98.

Satsangi A, Pachauri T, Singla V, Lakhani A, Kumari M K (2010). Carbonaceous aerosols at a suburban site in Indo – Gangetic plain, *Indian Journal of Radio and Space Physics,* **39**, pp. 218 – 222.

Sudheer A K and Sarin, M M (2008). Carbonaceous aerosols in MABL of Bay of Bengal: Influence of continental outflow, *Atmospheric Environment,* **42**, pp. 4089–4100.

Turpin B J and Huntzicker J J (1995). Identification of secondary organic aerosol episodes and quantification of primary and secondary organic aerosol concentrations during SCAQS, *Atmospheric Environment,* **29,** pp. 3527–3544.

Turpin B J, Lim H J (2001). Species contributions to $PM_{2.5}$ mass concentrations: revisiting common assumptions for estimating organic mass, *Aerosol Science and Technology,* **35**, pp. 602–610.

INFLUENCE OF AEROSOL COMPOSITION ON VISIBILITY DEGRADATION: A CASE STUDY FROM MEGA-CITY DELHI

AJIT SINGH* AND SAGNIK DEY

Centre for Atmospheric Sciences, Indian Institute of Technology Delhi,
Hauz Khas, New Delhi – 110016, India.
E mail: ajitsingh528@gmail.com

Keywords: AEROSOL COMPOSITION, VISIBILITY, SENSITIVITY, FOG.

INTRODUCTION

Visibility is an important air quality problem that has drawn attention of the scientific community for long time. Theoretically, visibility is inversely proportional to the total extinction coefficient (b_{ext}) (Koschmieder, 1924**)**, which depends on the aerosol composition, number concentration, trace gas concentration and RH. Visibility may vary within a wide range (from few meters to few hundred km) (Horvath, 1995) depending on the concentration of gaseous pollutants and aerosols and their optical and microphysical properties (Bäumer *et al.*, 2008). Hence, visibility may also be utilized as a proxy for concentration of atmospheric aerosols and trace gases. The presence of gaseous pollutants and aerosols in the atmosphere reduces visibility by directly scattering and absorbing visible radiation. Aerosols also facilitate formation of fog droplets under favourable meteorological conditions and thus contribute to further visibility degradation. The visibility degradation is often hazardous as per the human safety is concerned, particularly in the northern India during the winter season. Previous investigations have demonstrated that visibility degradation is directly related to aerosol number concentration, but a thorough quantitative analysis of influence of aerosol composition on visibility is lacking, particularly in India.

METHODS

The daily horizontal visibility data of Delhi were taken from National Climatic Data Centre of U.S (http://www7.ncdc.noaa.gov/CDO/cdo), which archives visibility data across the world for 30 years (1980-2009). Temperature and dew point temperature reported along with visibility were utilized to derive the RH of each day of observation. However, the columnar aerosol optical depth (AOD) over Delhi is available for the period of 2000-2009 and hence visibility data during this period were only used to constrain the model simulations to examine the sensitivity of visibility to aerosol composition. The analysis has been carried out for four seasons, winter (Dec-Feb), pre-monsoon (Mar-Jun), monsoon (Jul-Sep) and post-monsoon (Oct-Nov). Columnar Rayleigh extinction coefficient at 550 nm wavelength has been calculated following Bodhaine *et al.*, (1999).

OPAC (Optical Properties of Aerosol and Clouds, Hess et al., 1998) model has been used for examining the impacts of aerosol composition on visibility. OPAC utilizes the microphysical properties of various aerosol components from Global Aerosol Data set (Koepke *et al.*, 1997) to calculate composite columnar aerosol spectral optical properties following Mie theory assuming an external mixing state. A new aerosol composition has been defined by choosing five individual aerosol components (insoluble, water-soluble, accumulation and coarse mode dust and soot). Sensitivity of visibility (calculated by converting the columnar b_{ext} to surface b_{ext} using CALIPSO-derived scale heights) in

response to changing number concentrations have been examined. Finally, mean seasonal aerosol composition has been derived by tuning the number concentrations of each individual species constrained by MISR-retrieved spectral AOD following Dey and Tripathi (2008).

Mean VIS_M at 50%, 70%, 80%, 90% and 95% RH are compared with observed visibility without the contribution of gaseous components (Fig. 1). In general, the model captures the RH-dependence of VIS_O reasonably well in the pre-monsoon and post-monsoon seasons because all the points lie very close to 1:1 line. This suggests that the observed visibility degradation can be explained by gaseous and particulate air pollutants using the seasonal aerosol composition derived by the model despite uncertainties in MISR-AOD and aerosol scale height. VIS_M is underestimated by 11-20% relative to VIS_O during the monsoon season, which may result from a combination of factors, such as the uncertainty in the model due to large variability in seasonal aerosol vertical distribution and MISR-retrieved AOD (Dey and Di Girolamo, 2010). The excess attenuation of visible radiation in the winter, which cannot be explained by aerosols and trace gases, is caused by fog droplets. Aerosols contribute ~90% to the observed visibility degradation in non-foggy condition in Delhi, while the relative influence of aerosols on VIS_O decreases at high RH during the winter season in presence of fog. Sensitivity study has been carried out to examine the influence of scale height on VIS_M for the pre-monsoon aerosol composition. We noticed that VIS_M increases (decreases) by ~20% for an increase (decrease) in scale height by 10% for same columnar AOD. This implies that the underestimation of VIS_M during the monsoon season in the closure study (Fig. 1) may be explained by uncertainty in scale height.

VIS_M shows reasonable agreement with VIS_O at 50% and 70% RH in the winter season (Fig. 1). However, notable differences (>20%) are observed at RH between 80% to 95% and the difference in VIS_M and VIS_O increases with increase in RH (Fig. 1). During winter, Delhi experiences fog and fog formation is facilitated at high RH. Fog droplets contribute to additional attenuation of visible radiation. In this season, the relative influence of aerosols on visibility degradation reduces with an increase in RH above 70% during the winter season and varies from 78% at 80% RH to 40% at 95% RH. Larger difference at higher RH is understandable because more fog droplets will form at higher RH relative to lower RH (Quan *et al.*, 2011).

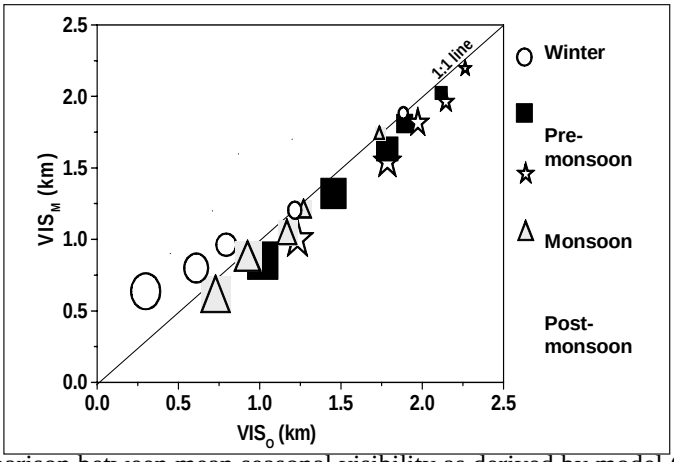

Figure 1. Comparison between mean seasonal visibility as derived by model (VIS_M) and from observations without the influence of gaseous pollutants (VIS_O) at five RH regimes during winter (open circle), pre-monsoon (filled square), monsoon (open star) and post-monsoon (filled triangle) seasons. Smallest size of each symbol represents 50% RH followed by 70%, 80%, 90% and 95% RH in the ascending orders of size.

Further, sensitivity of visibility in response to reduction in mass concentration various components was also examined. Visibility in Delhi is least sensitive to insoluble particles as shown by small changes (0.33±0.3% to 0.56±0.4%) in visibility due to reduction in mass concentration by 10-50%. It is moderately sensitive to accumulation mode and coarse mode dust particles, because visibility improves in the range 1.1±0.6% to 4.8±2% and 1.2±0.1% to 5.6±1.8% respectively in response to large reduction (10%-50%) of mass of accumulation and coarse mode dust particles. On the other hand, reduction in mass of soot and water-soluble particles by 10%-50% leads to an improvement in visibility by 2.4±0.1% to 11.3±1.6% and 4.9±2% to 29±12% respectively. Water-soluble particles have highest relative influence on VIS_M during the post-monsoon season, while soot particles have maximum influence in the winter season.

CONCLUSIONS

Influence of aerosol composition on visibility degradation in megacity Delhi is examined. Results suggest that visibility degradation is primarily attributed to water-soluble and soot particles and hence, controlling these two anthropogenic pollutants will increase the visibility directly and indirectly (through their influence on fog droplet formation). This measure has co-benefits for regional climate and health.

ACKNOWLEDGEMENT

This research is supported by financial grant from DST under Fast Track scheme (SR/FTP/ES-191/2010) operational at IITD (IITD/IRD/RP02509). Visibility data are distributed by National Climatic Data Centre of USA. MISR aerosol data are distributed by the NASA Langley Research Atmospheric Science Data Centre.

REFERENCES

Bäumer, D., Vogel B., Versick S., Rinke R., Mohler O. and Schinaiter M. (2008), Relationship of visibility, aerosol optical thickness and aerosol size distribution in an ageing air mass over South-West Germany, *Atmos. Environ.,* **42,** pp. 989-998.

Bodhaine, B. A., Wood, N. B., Dutton, E. G. and Slusser, J. R. (1999), On Rayleigh optical depth calculations, *J. Atmos. Ocean. Tech., **16**,* pp.1854-1861.

Dey, S. and Di Girolamo, L. (2010), A climatology of aerosol optical and microphysical properties over the Indian subcontinent from 9 years (2000-2008) of Multiangle Imaging SpectroRadiometer (MISR) data, *J. Geophys. Res., **115,*** D15204 doi:10.1029/2009JD013395.

Hess, M., Koepke, P. and Schult, I. (1998), Optical properties of aerosols and clouds: The software package OPAC, *Bull. Amer. Meteor. Soc., **79*** **(5),** pp. 831-842.

Horvath, H. (1995), Estimation of the average visibility in Central Europe, *Atmos. Environ., **29*** **(2)**, pp. 241-246.

Koepke, P., Hess, M., Schult, I. and Shettle, E. P. (1997), Global Aerosol Data Set. MPI Meteorologie Hamburg Report No. **243**, 44.

Koschmieder, H. (1924), Theorie der horizontalen Sichtweite, *Beitr. z. Phys. freien Atm.,* **12**, pp. 33 – 53.

Quan, J., Zhang, Q., He, H., Liu, J., Huang, M. and Jiu, H. (2011), Analysis of the formation of fog and haze in North China Plain (NCP), *Atmos. Chem. Phys., **11,*** pp. 8205-8214.

SPRAY CHARACTERIZATION USING PDIA TECHNIQUE

AMIT PASI*, MEENAKSHI GUPTA, RAJESH RAJORA, SANDEEP DUBEY

Center for Fire Explosive and Environment Safety
Defence Research and Development Organization
Timarpur, Delhi – 110054, India
E-mail: amit2k133@yahoo.com

Keywords: MIST, PDIA, VISI-SIZER SOFTWARE

INTRODUCTION

Water mist based system is being widely used for fire suppression in defence as well as civil sector. The fine water droplets (10-50 μm) that comprise a mist interacts with flames and suppress a fire through different mechanisms, viz., heat absorption, oxygen displacement, radiation attenuation and dilution of the fuel vapor/air mixture. Droplet transport and fire suppression performance depend on atomization and dispersion characteristics of the spray. Different types of atomizers viz. single fluid and twin fluid atomizers are used for generating mist which constitutes a wide range of droplet size distribution. It is important to study the mist generation characteristics in detail to determine the fire suppression performance of a mist system. A typical nozzle which operates on air aspiration principle and generates droplet size in the range of 15- 30 μm using an air pressure in the range of 4-8 bar has been investigated in the present study. Experiments have been conducted to determine volume flux distribution, drop size distribution, average velocity in the horizontal plane at different vertical distances from the atomizer head and spray cone angle. Advance spray particle imaging technique based system, particle/droplet image analyzer (PDIA, Oxford Lasers ,UK) has been used to measure these parameters over the operating range of pressure (4-8 bar). These parameters are used as input parameters for numerical validation of CFD codes used for prediction of fire suppression performance of water mist in enclosed chambers.

EXPERIMENTAL SETUP AND PROCEDURE

The droplet diameter and velocity of droplets were measured with different air pressures using the above mentioned PDIA system. This measurement technique is based on the spatial sampling technique where a collection of drops occupying a given volume is sampled instantaneously. The probe volume is 3.59 x 3.59 mm and 2 mm thick. Measurements were performed at two vertical locations located at 500 and 850 mm from the atomizer and the probe volume located at three location in the horizontal plane, at the centre and at each side of spray. Fig. 1 shows the arrangement that comprises of a traversing system for mounting the atomizer, measurement plane and various PDIA system components. The PDIA system comprises of a pulsed laser source, camera, optics for light transmission and collection, timing device and a computer for image processing. The system uses a backlit-imaging arrangement, where the output from the laser is expanded through a diffuser to break up the coherence of laser light. Image of droplets appear dark on light background which is captured using a CCD digital camera with image resolution of 1008 x 1008 pixels and data rates up to 7500 droplets per

second. A threshold grey-level is set on the image, and an automated algorithm then effectively scans the image, pixel by pixel, and determines the droplets sizes.

PDIA system used can provide spatial and temporal information on droplet size and velocity. It uses a particle tracking technique and time of flight measurement for determining the droplet velocity. For this purpose, the laser light is pulsed twice in one image and the Visi-sizer software (Fig.2) uses correlation technique to measure the distance travelled by particles in two images taken I_1 and I_2 (Fig. 3) at two short interval of time (10 μs~ time between the first and second pulse) to compute the droplet velocity.

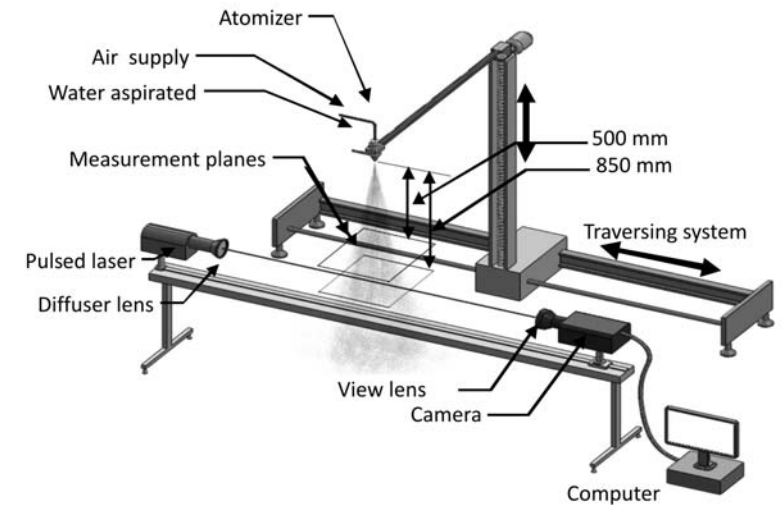

Figure 1. PDIA Schematic

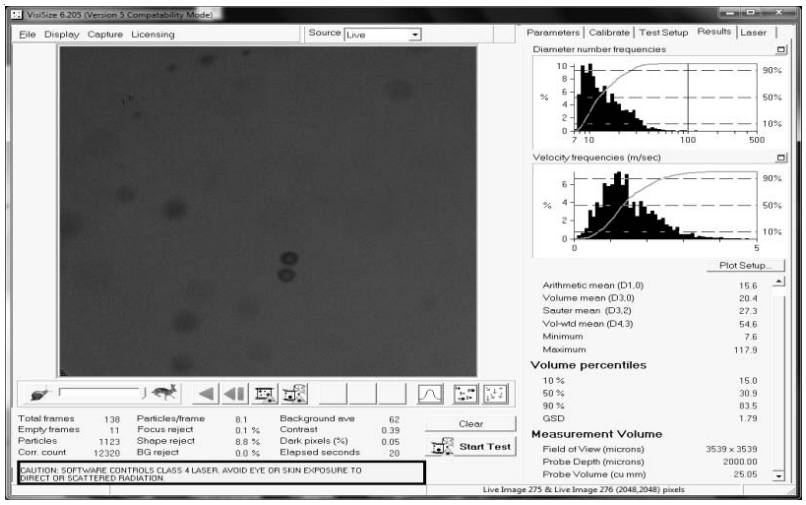

Figure 2. Visi-Sizer

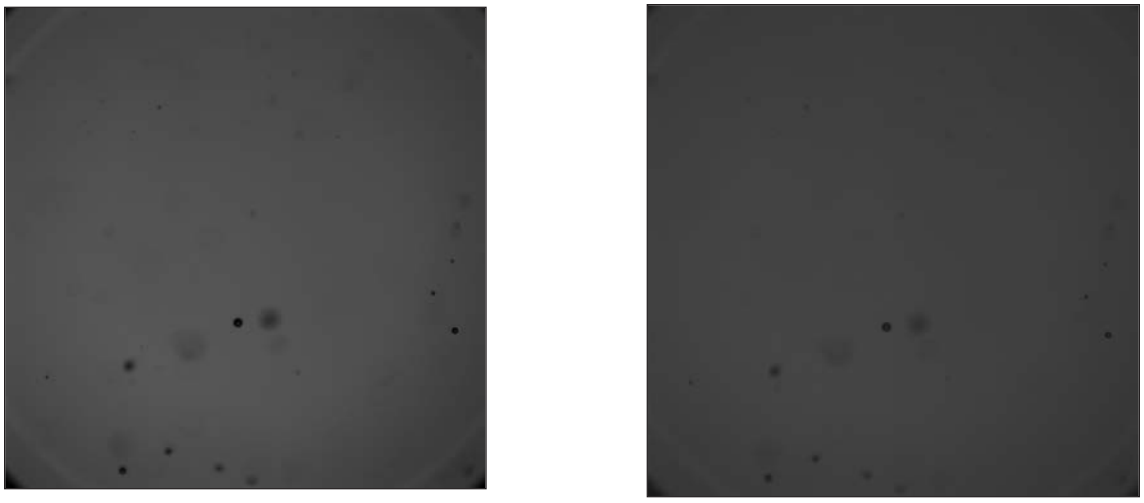

(a) Image I_1 (b) Image I_2

Figure 3. Images taken at short interval of time

RESULTS

At a distance of 500 mm from the exit of atomizer, the D_{v50} decreases from 29.5μm to 26.2 μm with increasing air pressure from 4 to 8 bar and the average droplet velocity increases from 2.2 to 3.2 m/s as measured at the centre of the measurement plane (Fig. 4).

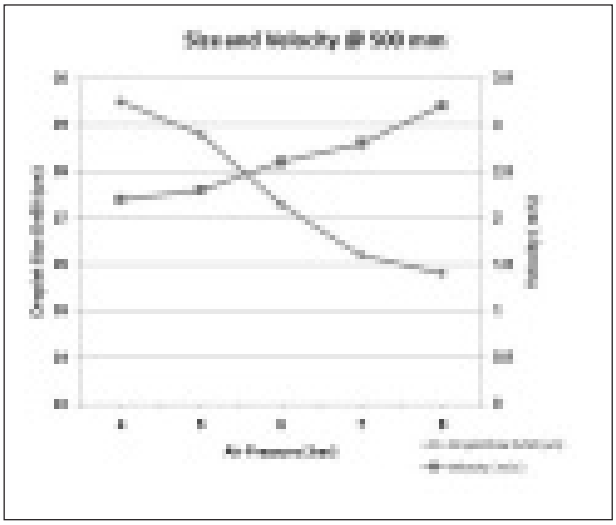

Figure 4. Variation of droplet size with air pressure

At 850mm from the atomizer, the mean droplet diameters decreased from 26.6 μm to 17.7 μm, however, there is no significant change in the average velocity (2.1 to 2.3 m/s). Measurement at different planes in the horizontal plane shows that the droplet sizes are smaller at the sides and velocities are also lower than those at the centre.

AEROSOLS PHYSICAL AND OPTICAL CHARACTERISTICS IN A FREE TROPOSPHERIC ENVIRONMENT: RESULTS FROM LONG-TERM OBSERVATIONS OVER WESTERN TRANS-HIMALAYAS

MUKUNDA M GOGOI, JAI PRAKASH CHAUBEY, SOBHAN KUMAR KOMPALLI, K KRISHNA MOORTHY, S SURESH BABU, MANOJ M R, VIJAYAKUMAR S NAIR AND TUSHAR P PRABHU[1]

Space Physics laboratory, Vikram Sarabhai Space Centre, Trivandrum-695022, India
[1]Indian Institute of Astrophysics, Bangalore, India

Keywords: HIMALAYAN AEROSOLS, AEROSOL OPTICAL DEPTH, BLACK CARBON, TOTAL NUMBER CONCENTRATION

INTRODUCTION

In the recent years, there is a global awareness in the requirement of observational data on aerosol parameters from data-sparse regions with distinct environmental characteristics. In this perspective information on high altitude aerosols assumes importance, and in particular the Himalayas, the world's tallest mountain ranges, have an unequivocal relevance. The searing discussions on the dramatic impacts of black carbon (BC) aerosols on Himalayan glacier retreat, role of enhanced heating by dust (mixed with soot) aerosols in the middle/upper troposphere over northern India and the foothills of the Himalayas and Tibetan Plateau in advancing the monsoon rainfall in early summer, the first observational evidence of elevated atmospheric warming by aerosol absorption and its northward gradients in height and amplitude during ICARB-2006 (Satheesh *et al.*, 2008) and subsequent evidence of the atmosphere heating due to elevated layers of BC at ~ 4.5 km and ~ 8 km (Babu *et al.*, 2011) over central Indian landmass, all point to the necessity of the examination of aerosol characteristics from high-altitude locations over long periods of time. Viewed in the backdrop of this, an aerosol observatory has been set-up at Hanle (32.78°N, 78.96°E, 4520 m amsl) in the western Trans-Himalayas in the premises of the Himalayan Chandra Telescope atop Mt. Saraswati in the Hanle Valley (Moorthy *et al.*, 2011). The characteristics of mass concentration of BC aerosol (M_B), number size distribution (NSD) and total number concentration (N_T) of composite aerosols and columnar spectral AOD are discussed in the present study for the database obtained at Hanle for a period from August 2009 to June 2011.

RESULTS AND DISCUSSION

BC Mass Concentration

The annual variation of monthly mean BC mass concentrations (M_B) in Fig.1 depicts a systematic pattern; with the lowest value in August-September and highest during April-May. The climatological annual mean has been 79.9 ± 32.9 ng m^{-3}. The climatological mean annual variation, not considering the years, (shown by the grey color dotted line in Fig.1) reveals a drastic reduction in the BC concentrations from June, and continuing at a low level until December, while the highest values are seen during March to May. The seasonal mean values (in ng m^{-3}) during the 3-years period are highest (~ 116.9 ± 8.3) during spring (MAM) and lowest (~ 58.7 ± 8.4) in autumn (SON).

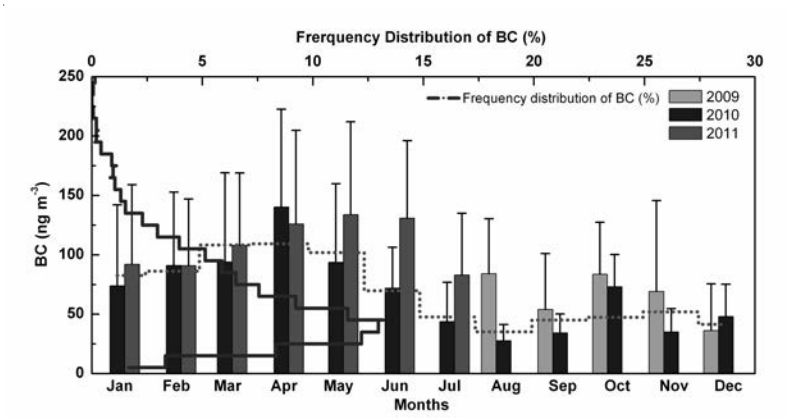

Figure 1. Monthly variation of BC mass concentrations at Hanle. The green (dotted) line shows the variability in the climatological monthly mean values, while the frequency distribution of BC is shown by the brown line

The higher BC abundance during the spring is attributed to the increased vertical transport of effluents, which might have been confined within the very shallow winter boundary layer, due to the increased thermal convection associated with increased solar heating of the mountain surface and the contribution of upslope thermal winds (Babu *et al.*, 2011). During winter (when temperature remains sub-zero), the much shallower boundary layer in the valley region isolate the measurement site from local and regional emissions. With the advent of spring, the increased convection leads to the deepening, eventually breaking up of the surface layer as the season advances, flushing up particles to be lofted and dispersed spatially by the prevailing winds. The seasonal variation of BC at Hanle is also attributed to the regional meteorology. During summer, air-mass trajectories arriving from the northeastern locations of Hanle (across China/ Tibet) show significant contribution; while during spring, westerly air-masses (from West Asia and North Africa) contribute mainly to the significant increase in BC. However, the effect of long-range transport is more efficient during spring, because in summer regional washout of aerosols also become significant. Even though westerly advection is seen during autumn, the lower replenishment after the summer washout coupled with the lower thermal convection (October onwards, temperatures become subzero as solar elevation decreases) leads to the lowest seasonal mean values of BC. On the other hand, the increase in the local domestic anthropogenic activities such as burning of wood, dry animal-dung for warming the interior during winter nights along with confinement by the shallow ABL might lead to the gradual increase in BC from autumn to winter.

Total Number Concentrations (N_T)

Monthly mean values of total number concentrations and geometric mean diameter (of the size distribution) of the composite aerosols are shown in Fig. 2 (4-months in 2009 and 8-months in 2010) and thus is representative of spring, summer and part of the autumn seasons. In general, the concentration lies below 2000 cm^{-3}; the highest monthly mean being ~ 1500 cm^{-3} in October 2010 and the lowest (~ 628 cm^{-3}) in May 2010. It is interesting to note that this pattern is nearly opposite to that of BC, which showed lowest concentration in October and highest in April-May. The frequency distribution of daily total N_T is also highly skewed, with > 48% of the values lying in the range 1000-1400 cm^{-3} and only in <11% of cases, the N_T > 2000 cm^{-3}. The monthly mean values of the geometric mean diameter (GMD, G_d, Fig. 2) ranged from 50 nm to 85 nm; with the highest value in

May 2010 and the lowest value in Dec 2010. In general, the annual variation of G_d depict an opposite pattern to that of N_T, indicating that large increase in the number concentration is associated with a large increase in the abundance of nucleation and Aitken mode particles arising from frequent new particle formation from precursors under the favorable conditions of enhanced humidity and abundance of UV radiation availability (Moorthy *et al.*, 2011).

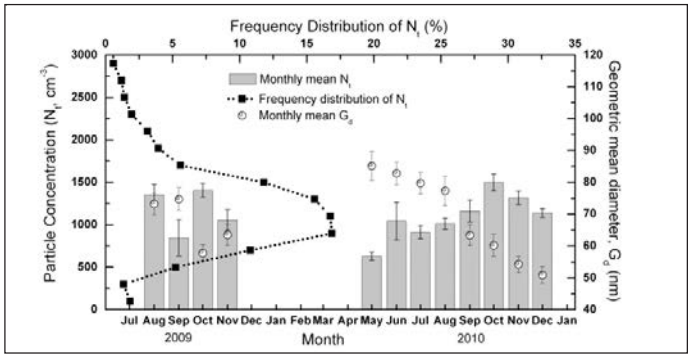

Figure 2. Monthly variation of total number concentrations (N_t), Geometric mean diameter (G_d) and frequency distribution of N_t at Hanle

Columnar Characteristics: Spectral AOD

Despite being quite low, the spectral AOD over Hanle varied significantly in short (within a week) and long (seasonal) time scales; with values being very close to the uncertainty limits of the instrument (0.02 – 0.03) at the near IR wavelengths in autumn and winter seasons to moderately high values of ~ 0.16 at 500 nm during spring/ summer and a little higher at the lower wavelengths. The temporal variations of the monthly mean AOD at 500 nm is shown in Fig. 3, where the vertical bars through the mean are the standard errors. It indicates that the values of AOD at 500 nm varied between ~ 0.05 ± 0.004 and 0.16 ± 0.03. The frequency of occurrences of AOD (at 500 nm) during the measurement period (Fig. 3) shows again highly skewed distribution, with > 78% of values lying below 0.1 and with the mode at ~ 0.05, indicating, in general, low aerosol loading, which is logical to expect at this high altitude. Frequency of occurrence of higher AODs are less, and only in 9% of the cases AOD was > 0.11.

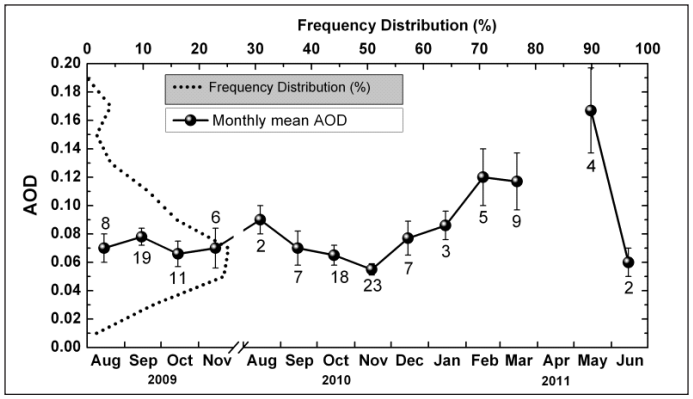

Figure 3. Temporal variation of monthly mean AOD at 500 nm, along with the frequency of occurrences of AOD at 500 nm. The numbers indicate the total number of AOD data points in estimating the monthly mean values.

VERTICAL PROFILES OF EXTINCTION COEFFICIENTS

The extinction profiles from the Cloud-Aerosol LIDAR with Orthogonal Polarization (CALIOP) on-board CALIPSO satellite (Winker *et al.*, 2003) have been examined and the mean extinction profiles were estimated from the datasets (day and night 5 km aerosol profile, version-3) obtained in the 1°x1° geographic grid centred at Hanle, for each season during the measurement period of 2009 and 2010. Interestingly, prominent elevated layers of enhanced aerosol extinction are seen during winter and spring (Fig. 4), at altitudes around 6-7 km. It is evident from the analysis of HYSPLIT trajectory clusters that the sole advection from west Asian land masses (at different altitude levels of transport) during winter and spring might be leading to the increased concentrations of fine mode aerosols at elevated levels. During summer, the west Asian contribution decreases significantly and builds up gradually again in autumn with increased contribution from west Asia. This led to a small peak at 7 km altitude during autumn season.

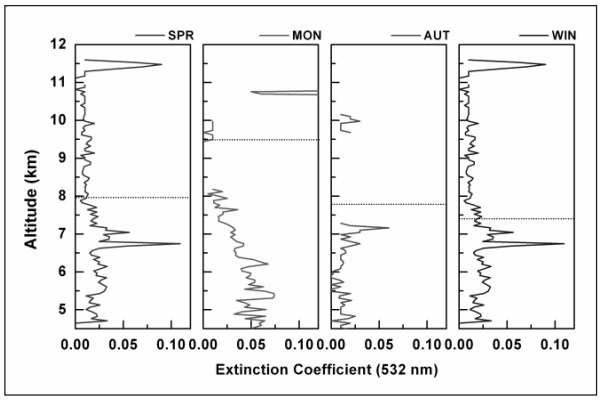

Figure 4. Vertical profiles of aerosol extinction coefficients at 532 nm at different seasons. The mean values are obtained from the 1°x1° spatially resolved CALIPSO profiles (5 km aerosol profile, version-3), centered at Hanle. The horizontal line shows the seasonal mean values of cloud top heights

CONCLUSIONS

The study of physical and optical properties of aerosols over the free-tropospheric locations at Hanle revealed the followings:

i. Monthly mean BC mass concentration varied from a 28 ng m^{-3} to a high value of 140 ng m^{-3} with an annual mean of 80 ng m^{-3} and standard deviation of 32 ng m^{-3}. Seasonally highest BC concentration was obtained in the spring (116.9 ± 8.3) and the lowest (58.7 ± 8.4) in autumn from the climatologically averaged monthly mean data.

ii. The monthly mean total number concentrations ranged from 628 cm^{-3} to 1500 cm^{-3} with a mean value of 1114.2 ± 72.9 cm^{-3}.

iii. The daily mean values of AOD were, in general, very low with a mean for the measurement period as ~ 0.08 and a standard deviation of 0.03 at 500 nm.

iv. The vertical distribution of extinction coefficients, obtained from CALIPSO data, indicated the presence of elevated aerosol layers during winter and spring

ACKNOWLEDGEMENT

This work is carried out under the ARFI Project of ISRO-GBP. We acknowledge NOAA ARL for the provision of the HYSPLIT. CALIPSO data are obtained from LaRC Atmospheric Sciences Data Center (ASDC) through their website at http://eosweb.larc.nasa.gov/.

REFERENCES

Babu, S. S., Jai Prakash Chaubey, K. Krishna Moorthy, Mukunda M. Gogoi, Sobhan Kumar Kompalli, V. Sreekanth, S. P. Bagare, Bhuvan C. Bhatt, Vinod K. Gaur, Tushar P. Prabhu, and N. S. Singh. (2011). High altitude (4520 m amsl) measurements of black carbon aerosols over western trans-Himalayas: Seasonal heterogeneity and source apportionment, *J. Geophys. Res.*, **116**, D24201, doi:10.1029/2011JD016722.

Moorthy, K. K., V. Sreekanth, Jai Prakash Chaubey, Mukunda M. Gogoi, S. Suresh Babu, Sobhan Kumar Kompalli, S. P. Bagare, Bhuvan C. Bhatt, Vinod K. Gaur, T. P. Prabhu, and N. S. Singh (2011). Fine and ultrafine particles at a near–free tropospheric environment over the high altitude station Hanle in the Trans Himalaya: New particle formation and size distribution, *J. Geophys. Res.*, **116**, D20212, doi:10.1029/2011JD016343.

Satheesh, S. K., K. Krishna Moorthy, S. Suresh Babu, V. Vinoj, and C. B. S. Dutt (2008). Climate implications of large warming by elevated aerosol over India, *Geophys. Res. Lett.*, **35**, L19809, doi:10.1029/2008GL034944.

Winker, D. M., J. R. Pelon, and M. P. McCormick (2003). The CALIPSO mission: Spaceborne lidar for bservation of aerosols and clouds, in *Lidar Remote Sensing for Industry and Environment Monitoring III*, edited by U. Singh, T. Itabe, and Z. Liu, Proc. SPIE Int. Soc. Opt. Eng., **4893**, pp. 1–11.

CHEMICAL CHRACTERIZATION OF SIZE SEPARATED AEROSOLS OVER TWO HIGH ALTITUDE STATIONS IN SOUTH WESTERN INDIA

M.P.RAJU[1], P.D.SAFAI[1], P.S.ALHAT[2], P.S.P.RAO[1] AND P.C.S. DEVARA[1]

[1] Indian Institute of Tropical Meteorology, Pune

[2] Department of Environmental Sciences, University of Pune

Keywords: AEROSOL AND SPM

INTRODUCTION

Aerosols are defined as a relatively stable dispersion of solid/liquid particles in a gas, with particle diameters in the range of 0.001 to 100 μm. Atmospheric aerosol plays a major role in global issues, such as hydrological cycle, climate forcing and the general chemistry of earth atmosphere systems (Ramanathan *et al.*, 2001). Aerosol size distribution and chemical composition are essential to study their impact on global radiation budget and atmospheric chemistry. Ground based observations of atmospheric aerosols from urban locations in this region are more (Khemani, 1989; Momin *et al.*, 1999; Safai *et al.*, 2005). However, those from less polluted high altitude locations are scarce. In this study we present the chemistry of size separated aerosols, collected using a nine- stage cascade sampler from two high altitute stations in SW part of India i.e., Sinhagad and Mahabaleshwar, during winter 2011.

LOCATION OF SAMPLING SITES

Sinhagad (18° 212 N, 73° 452 E 1350 M amsl)

Sinhagad is a historical fort in the Western Ghat region of India. This fort is situated about 100 km away from Arabian Sea and 40 km by road, to the southwest of Pune city. The top of the hill is flat terrain with an area of about 0.5 sq. km. The only noticeable local source of pollution is wood burning, mainly for cooking. Sinhagad being a tourist spot, vehicular activity like cars, jeeps and two-wheelers is occasional. Aerosol sampling was carried out in the complex of a Micro Wave Tower building owned by Bharat Sanchar Nigam Limited (BSNL), Government of India. This site is away from any major anthropogenic activity.

Mahabaleshwar (17° 582 N, 73° 432 E 1438 m amsl)

Mahabaleshwar, one of the famous tourist spots in Maharashtra is situated in the Western Ghat region of India. Mahabaleshwar is about 120 Km from Pune city with vast terrain of area 150 Km^2 bound by valleys on all sides and receiving good amount of rain fall during the season. Aerosol observations were conducted near the Wilson/Sunrise Point. The main source of pollution is by vehicular emissions, local transport station (Bus Stop) and city market which is nearer to the experimental site.

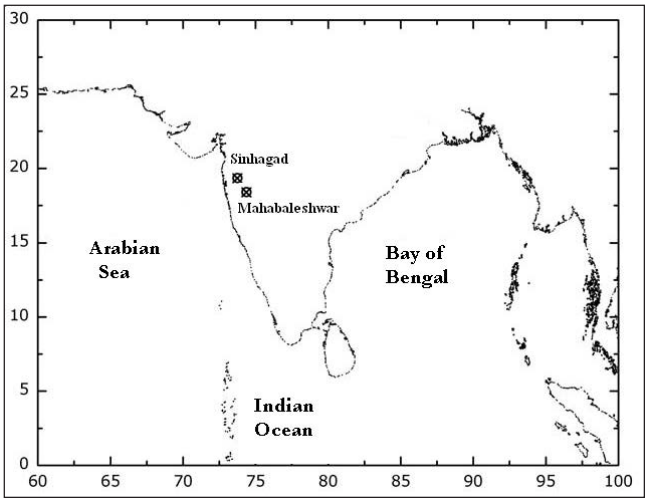

Figure 1. Locations of sampling site (Sinhagad and Mahabaleshwar)

RESULTS AND DISCUSSION

MASS SIZE DISTRIBUTION OF AEROSOLS AT SINHAGAD AND MAHABALESHWAR

Aerosols showed bimodal distribution at both Sinhagad and Mahabaleshwar during the winter season of 2011 as shown in Fig. 2. There was a peak, each in fine ($r < 1$ μm) and coarse ($r > 1$ μm) size modes. However, coarse size peak was dominant at both the locations. At Mahabaleshwar, coarse mode showed more dominance (62%) than at Sinhagad (54%) indicating more influence of natural sources like soil and sea which is obvious due to less anthropogenic activities. Total concentration of Suspended Particulate Matter (SPM) was almost comparable at both Sinhagad (271μg/m^3) and Mahabaleshwar (289 μg/m^3).

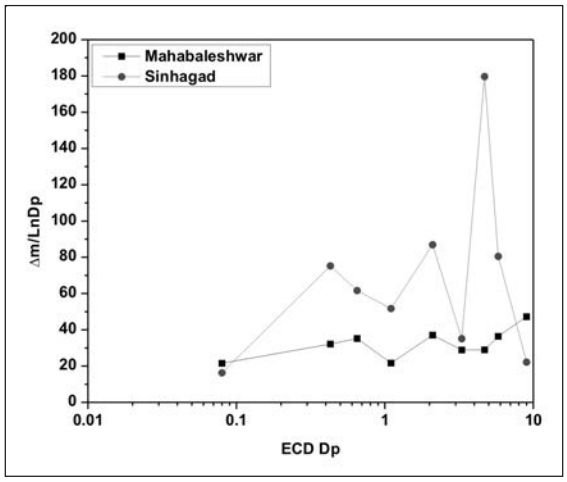

Figure 2. Mass size distribution of aerosols at Sinhagad and Mahabaleshwar during winter 2011

As seen from Fig.3, particles in the nucleation mode ($r < 0.1$μm) showed concentration of 27.4 μg/m^3 at Sinhagad and at Mahabaleshwar they showed about concentration of 21.5 μg/m^3. Whereas, particles in accumulation mode (0.1 μm < r < 1.0 μm) showed concentration of 97 and 88.9 μg/m^3,

respectively at Sinhagad and Mahabaleshwar. Concentration of coarse size particles (r >1.0μm) was maximum at both Sinhagad (147.1μg/m^3) and Mahabaleshwar (178.5 μg/m^3).

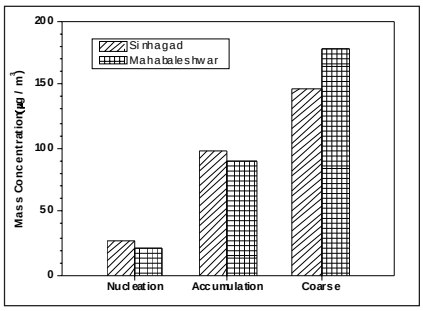

Figure 3. Concentration of aerosols in different size modes at Sinhagadand Mahabaleshwar during winter 2011.

Fig. 4 shows the percentage contribution of different size modes to the SPM. At Sinhagad, particles in the nucleation mode contributed about 10 % to total SPM whereas, at Mahabaleshwar, these particles contributed about 7.5%. Accumulation size particles contributed about 36 % and 31 % to SPM at Sinhagad and Mahabaleshwar, respectively. Maximum contribution to SPM was from coarse size particles i.e. about 54 % and 62 %, respectively at Sinhagad and Mahabaleshwar.

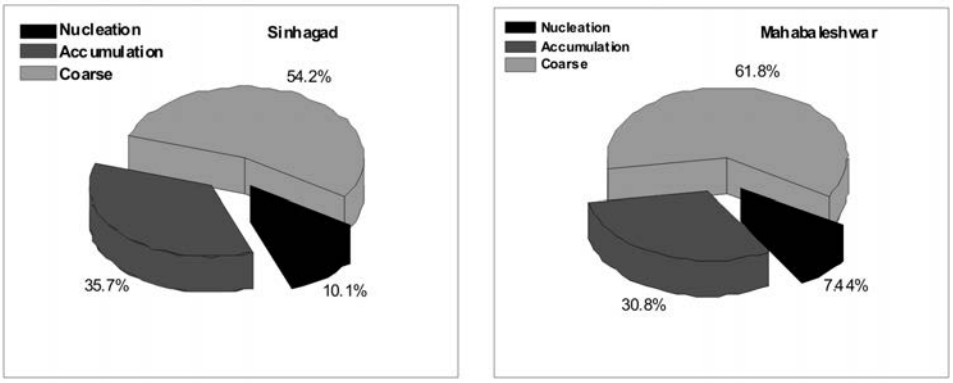

Figure 4. Percentage Contribution of aerosols in different size modes at Sinhagad and Mahabaleshwar during winter 2011.

CONTRIBUTION FROM DIFFERENT SOURCES TO THE CHEMICAL COMPONENTS OF SIZE SEPARATED AEROSOLS

Chemical composition of size separated aerosols at Sinhagad and Mahabaleshwar showed dominance of natural aerosols (from soil and sea) for Na, Cl, Ca Mg and F whereas, anthropogenic aerosols contributed more to SO_4, NO_3, NH_4, and K. The source categorization of aerosols was carried out from their chemical composition using a method described by Safai et al (2010). From (Fig. 5), it was observed that at Sinhagad and Mahabaleshwar, marine source contributed maximum (52 and 67 % respectively). Crustal source contributed about 15 and 14 % respectively at Sinhagad and Mahabaleshwar. Whereas anthropogenic source contributed 33 and 19 %, respectively at Sinhagad and Mahabaleshwar.

This feature indicates the dominance of anthropogenic activities at Sinhagad especially, vehicular emissions from tourist vehicles. Also biomass burning activity for agricultural or domestic purposes

in the nearby surroundings could be equally important. In addition, the contribution of anthropogenic aerosols was more as the observations were conducted during winter. The prevailing meteorological conditions during this season such as low wind speeds and low mixing heights giving rise to low ventilation coefficients account for less dispersal of fine size particles (which are generally secondary aerosols like SO_4, NO_3, NH_4, K). Therefore not only the availability of potential sources but the prevailing meteorology also is vital for the fate of aerosols and their chemical nature at any location.

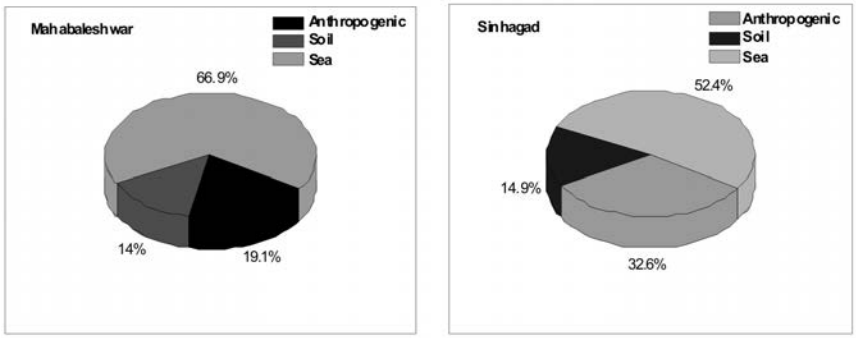

Figure 5. Percentage contributions of different sources to aerosol composition at Sinhagad and Mahabaleshwar.

CONCLUSIONS

Aerosols showed bimodal size distribution at both Sinhagad and Mahabaleshwar with a peak, each in fine and coarse size modes indicating presence of both natural as well as anthropogenic aerosols. Mass concentrations of aerosol were dominent in coarse mode at Mahabaleshwar than at Sinhagad where as in fine and accumulation mode mass concentration of aerosol was dominent at Sinhagad than at Mahabaleshwar. At both the locations, marine source contributed maximum mainly due to proximity to Arabian Sea. Anthropogenic sources contributed more at Sinhagad which can be attributed to more tourist and other human activities. In addition, the prevailing meteorological conditions during winter were conducive for significant contribution from anthropogenic sources at both locations, especially at Sinhagad.

REFERENCES

Khemani, L.T. (1989). Physical and chemical characteristics of atmospheric aerosols. In: Cheremisinoff, P.N. Air Pollution Control, *Encyclopedia of Environmental Control Technology* **Vol. 2**, Gulf Publishing Co., USA, pp. 401–452.

Momin, G. A., Rao, P.S.P., Safai, P.D., Ali, K., Naik, M.S. and Pillai, A.G. (1999). Atmospheric aerosol characteristic studies at Pune and Thiruvananthapuram during INDOEX programme—1998, *Current Science*, **76**, pp. 985–989.

Ramanathan, V. *et al.* (2001). J. *Geophys. Res.*, **106(D22)**, pp. 28,371–28,398.

Safai P.D., Budhavant, K. B., Rao, P.S.P., Ali, K. and Sinha, A. (2010). Source characterization for aerosol constituents and changing roles of calcium and ammonium aerosols in the neutralization of aerosol acidity at a semi-urban site in SW India, *Atmospheric Research*, **98**, pp. 78–88.

Safai, P.D, Rao, P.S.P., Momin, G.A., Ali, K., Chate, D.M., Praveen, P.S. and Devara, P.C.S. (2005). Variation in the chemistry of aerosols in two different winter seasons at Pune and Sinhagad, India, *Aerosol and Air Quality* **5/1**, pp. 115–126.

INTER-ANNUAL AND INTRA-SEASONAL BEHAVIOR OF FINE PARTICULATES ($PM_{2.5}$) FOR DELHI, INDIA

S. TIWARI[1], P. PRAGYA[2]. B P SINGH[3], A. K. SRIVASTAVA[1], D. S. BISHT[1], R K SINGH[3], V. UPADHYAY[2] AND MANOJ K SRIVASTAVA[3]

[1]Indian Institute of Tropical Meteorology, New Delhi Branch, India
[2]S. C. P. G. College, Ballia, India
[3]Department of Geophysics, Banaras Hindu University, Varanasi, India
Email: mksriv@gmail.com

Keywords: $PM_{2.5}$, ANNUAL BEHAVIOUR, INDO-GANGETIC PLAIN

INTRODUCTION

Aerosols interact with earth energy budget and impact human health (Dey *et al.*, 2004; Pandithurai *et al.*, 2008; Singh *et al.*, 2005; Srivastava *et al.*, 2010). Among these particles, fine particles ($PM_{2.5}$) have received special attention due to their potential impacts on human health (Anderson *et al.*, 1992; Dockery and Pope, 1994; Wang *et al.*, 2003), since they have longer residence times and posses relatively large surface to volume ratio which helps higher proportion of persistent organic compounds (Jaenicke, 1984). Approximately, one-third of population at Delhi is suffering from respiratory disorders, caused due to air pollution (Kandlikar and Ramachandran, 2000). $PM^{2.5}$ is also associated with visibility degradation associated with haze (Milne *et al.*, 1982), which causes possible road accidents.

Industrial and population growth, increased transportation system, burning of fossil fuel, high rate of urbanizations and migrations are identified as major causes of concern for air-quality (Bishoi *et al.*, 2009; Goyal and Sindhanta, 2003; Kumar and Foster, 2007) for the fourth most polluted and the seventh most populous metropolis in the world, Delhi. The main sources of fine particles ($PM_{2.5}$) have been identified as the combustion of fossil fuels from automobiles, construction equipments (mobile sources), furnaces and power plants (stationary sources) (Faiz *et al.*, 1992; Madronich, 2006).

In order to investigate the annual behaviour of $PM_{2.5}$ for the duration 2007 to 2009, data has been obtained from Central Pollution Control Board (CPCB). Corresponding weather parameters have been collected from India Meteorological Department. The $PM_{2.5}$ measurements have been carried out under National Ambient Air Quality Monitoring Network (NAAQMN). Monitoring station at Delhi is situated at Income Tax Office (I.T.O.) intersection since 1990s. I. T. O. intersection is one of the heavy traffic intersections in Delhi.

SAMPLING SITE

Delhi is situated between 28°212 17 to 28°532 latitude and 76°202 373 to 77°202 373 longitude (218 m asl), at around 160 km away in south from the southern part of Himalayas. Delhi is bounded by the Thar-Desert of Rajasthan in the West, plains of central India in the South and Indo-Gangetic Plains (IGP) in the East. It experiences variable weather conditions during the annual cycle, e.g. from hot and humid weather in summer to cold and dry weather during winter. The prevailing wind throughout the year is easterly, northerly and north-westerly, and it is strongest during summer.

Apart from such swings of weather during the annual cycle, the entire northern part of India, especially the IGP, experiences a thick foggy conditions during winter and show low boundary layer height. During such conditions, pollutants could not be dispersed or mix with free troposphere and cause poor visibility and high levels of pollutants in the lower atmosphere. The weather during winter amalgamated with low temperature along with northerly and north-westerly wind, rich in pollutants. During monsoon season, however, the wind is mostly easterly and south-easterly.

TEMPORAL VARIABILITY OF MASS $PM_{2.5}$ CONCENTRATIONS

Day to day variability of $PM_{2.5}$ mass concentrations (Fig. 1) from January 2007 to December 2009 shows the mean concentration as 111.4±73.3μg m^{-3} ranging between 12 μg m^{-3} (August 18, 2009) to 357 μg m^{-3} (January 8, 2007), substantially higher than the 40 μg m^{-3} limit of Indian National Ambient Air Quality Standards. Approximately 69% of $PM_{2.5}$ samples have exceeded the 24-h limit of NAAQS $PM_{2.5}$ standard of 60μg m^{-3}.

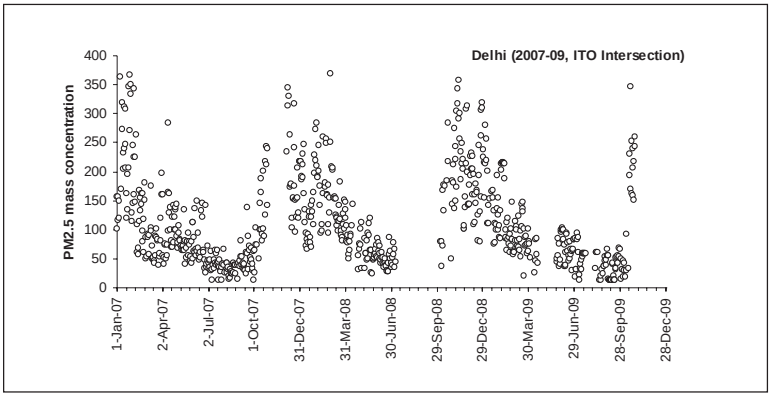

Figure 1. PM2.5 mass concentration for a busy traffic intersection during 2007-09

Recent increase in the number of diesel cars and diesel light trucks along with non-exhaust particles originate from wear and corrosion of road pavements, vehicle components, and particles originating in surroundings as well as industrial processes, increasing construction activities, loss of vegetation, and thermal power plants, Badarpur, Indraprastha, and Rajghat with the total electricity generation capacity of 1,087 MWs, appear to be the cause of higher level of observed $PM_{2.5}$ mass concentration. Furthermore, during these years especially, Delhi witnessed massive dust due to continuous constructional activities as preparation of Commonwealth Games.

Based on the observations, yearly and monthly mean concentration of mass concentrations of $PM_{2.5}$ during 2007 to 2009 (Fig. 2) shows the higher range of particulate concentration during January, April, May, June, and December months of 2007, and February, March, July and September months of 2008. During 2009, however, only the months of August and November show the higher particulate concentrations. The year-wise highest concentrations is observed during 2008 (135.44±77μg m^{-3}), followed by 2007 (107.3±88μg m^{-3}) and 2009 (87.1μg m^{-3}). These large inter-annual variations are found to be associated with synoptic meteorological changes. Seasonally, variation of mean mass concentrations shows highest values during post monsoon (159.1±77μg $m^{-3)}$, followed by winter (153.4±63ì g μg m^{-3}), pre-monsoon (70.0±26μg m^{-3}) and monsoon (42.77±17μg m^{-3}). $PM_{2.5}$ concentrations during monsoon were nearly equal to the National Ambient Air Quality (NAAQ) standard, but seriously higher during post monsoon and winter (4 times) and summer (2 times). High

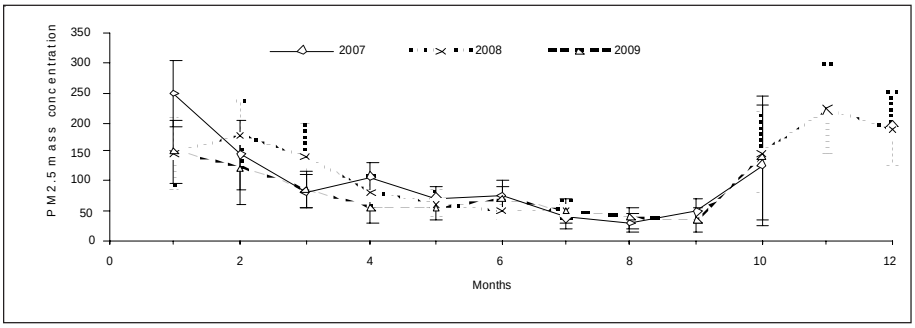

Figure 2. Mean monthly mass concentration of $PM^{2.5}$ for 2007, 2008 and 2009

range of mass concentrations of $PM_{2.5}$ during post-monsoon and winter may be related to particle generation due to fire cracking during Deepawali festival (Attri *et al.*, 2001; Barman *et al.*, 2009; Singh *et al.*, 2003; Tiwari *et al.*, 2012), which is generally celebrated in the last week of October or in the first week of November in the northern part of India. Such elevated level of particulates has also been reported by Bach *et al.*, (1975) caused due to fireworks on various global events (Wang *et al.*, 2007; Wehner *et al.*, 2000) due to fireworks on lantern day. Minimum level of particulates observed during monsoon is related to the washout effect (Tiwari *et al.*, 2011).

Temperature, relative humidity, wind speed, rainfall and mixing height play crucial role in dispersion, transportation and accumulation of the atmospheric pollutants. In order to understand the annual behavior of particles, the climate of Delhi is discussed herewith in brief. During winter Delhi climate is characterized by low relative humidity, low solar heating of land and low ventilation coefficients. The combination of these parameters results in less dispersion of aerosols, which leads to increase in the concentrations of fine particulate matter in Delhi atmosphere. The long range transport of fine particles plays crucial role during post-monsoon season (Srivastava *et al.*, 2009; Tiwari *et al.*, 2010). Clearing agricultural land after harvesting the rice by burning the agricultural waste during post-monsoon is a common practice in large agricultural surroundings of Delhi, and the smoke generated out of burning reaches Delhi atmosphere to contribute substantially the smog formation and increment in PM and ozone level concentration on a regional level (Awasthi *et al.*, 2011; Badrinath *et al.*, 2006; NASA, 2008). They found that the concentration of fine particulate matter was increased substantially (78%) during post–monsoon (October–November) due to burning of crop residue with the maxima (100 to 147μg/m^3) in 2009. Therefore, the significantly high concentrations of fine size aerosols observed over Delhi for considered years have larger influence of certain anthropogenic activities related to agriculture during the winter season (Tiwari *et al.*, 2011). In addition to this, Delhi's low night time temperature during the winter (~2°C) and indoors and outdoors heating of bio fuels for heating purpose are accomplished with small coal-burning boilers, stoves, open burning of leaves and woods (Ali *et al.*, 2004). Overall, the level of $PM_{2.5}$ in Delhi is comparable to Beijing, China (115μg m^{-3}, He et al., 2001) and to the wintertime in California's San Joaquin Valley, USA (138 μg m^{-3}, Watson *et al.*, 2002), and higher to the Belgrade City (75μg m^{-3}). The values reported here (111.4μg m^{-3}) are, however, lower than the previously reported values (171ì g $m^{-3,}$ Khillare *et al.*, 2008) during 2004, which can be attributed due to introduction of metro-rail and use of CNG for public transport in Delhi (Kathuria, 2005).

Frequency distribution of $PM_{2.5}$ over Delhi during study period, divided into nine categories of 40 μg m^{-3} interval within NAAQS limit of 0 to 360 μg m^{-3} show that $PM_{2.5}$ concentration is skewed toward higher to lower concentration in respect of corresponding spectrum except 0-40μg m^{-3} (15%). The

highest contribution was 30% (40-80 μg m^{-3}), followed by 17% (80-120 μg m^{-3}), 14% (120-160 μg m^{-3}), 10% (160-200 μg m^{-3}), 9% (200-240 μg m^{-3}), 3% (240-280 μg m^{-3}), 2% (280-320 μg m^{-3}) and 1% (320-360 μg m^{-3}). $PM_{2.5}$ mass concentrations were higher (85%) than the national ambient air quality standard limits, however 30% samples were in between 40-80 μg m^{-3} range, which is indicating the environment of Delhi is more dangerous for health point of view due to high loadings of fine particles into the atmosphere. This feature is basically due to anthropogenic emissions and climatic conditions of Delhi.

CONCLUSIONS

Mass concentrations of $PM_{2.5}$ were collected during three consecutive years over Delhi at a busy traffic intersection, I.T.O., for 2007 till 2010. The data were analyzed for inter-annual and intra-seasonal variations of $PM_{2.5}$. The city of Delhi is found to be heavily loaded with fine particulate matter ($PM_{2.5}$) showing mean mass concentration of 111.4±73.3 μg m^{-3} (range: 12 μg m^{-3} to 357 μg m^{-3}), which is substantially higher and far in excess of recommended annual averages of Indian National Ambient Air Quality standards. Approximately 69% samples of $PM_{2.5}$ mass were exceeded of 24-h NAAQS $PM_{2.5}$ standard (40 μg m^{-3}) and 85% samples were higher than the annual NAAQS (60 μg m^{-3}). Most of the samples were population existed between 40-80 μg m^{-3} (30%) ranges and indicates that the environment of Delhi is vulnerable for human health. Significant negative correlations is found for $PM_{2.5}$ and temperature (-0.72) as well as for wind speed (-0.53). On the basis of the study, it is concluded that this interplay of meteorological variables with pollution plays a key role in assessing the impact of pollution. The seasonal variations of $PM^{2.5}$ show that the maximum pollution levels occur during post-monsoon, followed by winter, summer and monsoon.

ACKNOWLEDGEMENT

The authors gratefully thank Prof. B. N. Goswami, Director, IITM, Pune and for his encouragement and moral support for preparing this manuscript. Authors MKS and BPS are thankful to ISRO-ARFI program for support. Authors also thank to Central Pollution Control Board for data provision.

REFERENCES

Ali K., Momin, G. A., Tiwari, S., Safai, P. D., Chate, D. M. and Rao, P. S. P. (2004). Fog and precipitation chemistry at Delhi, North India, *Atmosph. Environ.*, **38**, 4215.

Anderson, W. P., Reid, C. M. and Jennings, G. L., (1992). Pet ownership and risk factors for cardiovascular disease, Med J Australia, **157**, 298.

Attri, Arun K., Kumar, Ujjwal, Jain, V. K. (2001). Formation of ozone by fireworks, *Nature*, **411**, 1015.

Awasthi *et al.*, (2011). Study of size and mass distribution of particulate matter due to crop residue burning with seasonal variation in rural area of Punjab, India, *J. Environ. Monit.*, **13**, pp. 1073-1081.

Bach *et al.*, (1975). Fireworks pollution and health, *Intern. J. Environ. Studies*, **7**, 183.

Badrinath, K.V.S., Kiranchand, T.R. and Krishna, P. V. (2006). Agriculture crop burning in the Indo-Gangetic plains-a study using IRS-P6AWiFS satellite data, *Curr. Sci.*, **91(8)**, 1085.

Barman, S.C., Singh, R, Negi, M.P.S., Bhargava, S.K. (2009). Fine particles (PM2.5) in ambient air of Lucknow city due to fireworks on Diwali festival, *J. Environ. Biol.*, **30 (5)**, pp. 625-632.

Bishoi, B., Amit, P. and Jain, V.K. (2009). A Comparative Study of Air Quality Index Based on Factor Analysis and US-EPA Methods for an Urban Environment, *Aerosol and Air Quality Res.*, **9**, 1.

Dey, S., Tripathi, S. N. and Singh, R. P. (2004). Influence of dust storm on the aerosol optical properties over Indo-Gangetic basin, *J. Geophys. Res.*, **109**, D20211.

Dockery, D.W. and Pope, C.A. (1994). Acute respiratory effects of particulate air pollution, *Annual Rev. Pub. Health.*, **15**, 107.

Faiz, A., Weaver, C., Sinha, K., Walsh, M. and Carbajo, J. (1992). Air pollution from motor vehicles: Issues and options for developing countries (pp. 280), The World Bank, Washington- DC.

Goyal, P. and Sidhartha (2003). Present Scenario of Air Quality in Delhi: a case study of CNG implementation, *Atmosph. Environ.* , **37**, 5423.

Jaenicke, R. (1984) Protein Folding and Protein Association, *Angewandte Chemie International (Edition in English)*, **23(6)**, 395.

Kandlikar, M., and Ramachandran, G. (2000). The causes and consequences of particulate air pollution in urban India: a synthesis of the science, *Annual Rev Energy Environment*, **25**, 629.

Kathuria, V. (2005). Impact of CNG on Delhi's Air Pollution, *Economic and Political Weekly*, **40**, 1907.

Khillare, P.S., Agarwal, T. and Shridhar, V. (2008). Impact of CNG implementation on PAHs concentration in the ambient air of Delhi: A comparative assessment of pre- and post-CNG scenario, *Environ. Monit. Assess.* , **147**, 223.

Kumar, A. and Foster, T.C. (2007). Shift in Induction Mechanisms Underlies an Age- Dependent Increase in DHPG-Induced Synaptic Depression at CA3–CA1 Synapses, *J. Neur.*, **98**, 2729.

Madronich, S. (2006). Chemical evolution of gaseous air pollutants downwind of tropical megacities: Mexico City case study, *Atmos. Environ.*, **40**, 6012.

Milne, J. W., Roberts, D. B., Walk, S. J. and William, D. J. (1982). Sources of Sydney brown haze, In: The Urban Atmosphere Sydney, A case Study, CSIRO, Australia.

NASA (National Aeronautics and Space Administration) Top Science (2008). Exploration and Discovery Stories of 2008.

Pandithurai, G., Dipu, S., Dani, K.K., Tiwari, S., Bisht, D.S., Devara, P.C.S. and Pinker, R.T. (2008). Aerosol radiative forcing during dust events over New Delhi, India, *J. Geophys. Res.*, **113**, 1-13, D13209.

Tiwari, S., Chate, D. M., Srivastava, M. K., Safai, P. D., Srivastava, A. K., Bisht, D. S., Padmanabhamurty, B. (2012). Statistical evaluation of PM10 and distribution of PM1, PM2.5, and PM10 in ambient air due to extreme fireworks episodes (Diwali festivals) in megacity Delhi, *Nat. Hazards*, DOI: 10.1007/s11069-011-9931-4.

Singh, R.P., Dey, S., and Holben, B. (2003). Aerosol behavior in Kanpur during Diwali festival, *Current Sci*, **84 (10)**, 1302.

Singh, S., Nath, S., Kohli, R., and Singh, R., (2005). Aerosol over Delhi during pre-monsoon months: Characteristics and effect on surface radiative forcing, *Geophys. Res. Lett.*, **32**, L13808.

Srivastava, A.K. and Tripathi, S.N., (2010). Numerical study for production of space charge within the stratiform cloud, *J. Earth Sys. Sci.*, **119**, 627.

Wang, Y. X., Lee, C. H., Tiep, S., Yu, R.T. , Ham, J. *et al.*, (2003). Peroxisome-proliferator-activated receptor delta activates fat metabolism to prevent obesity. *Cell.*, **113**. 159.

Wang, Y., G. Zhuang, Ch. Xu and An, Z. (2007). The air pollution caused by the burning of fireworks during the lantern festival in Beijing, China, *Atmosph. Environ.*, **41**, 417.

Wehner, B., Wiedensohler, A., Heintzenberg, J. (2000). Submicrometer aerosol size distributions and mass concentration of the millennium fireworks 2000 in Leipzig, Germany. *J. of Aerosol Science*, **31**, 1489.

CHEMICAL CHARACTERIZATION OF ATMOSPHERIC OUTFLOW TO THE BAY OF BENGAL

BIKKINA SRINIVAS AND M. M. SARIN

Physical Research Laboratory, Ahmedabad- 380 009, India

Keywords: AEROSOLS, BAY OF BENGAL, CONTINENTAL IMPACT, CHEMICAL COMPOSITION

INTRODUCTION

The densely populated regions of south and south-east Asia are undergoing rapid industrialization leading to enhanced emissions and a variety of air pollutants injected into the atmosphere, making these regions climatically sensitive in the global perspective (Lawrence and Lelieveld, 2010; Novakov *et al.,* 2000; Ramanathan *et al.*, 2001). These pollutants serve as an ideal substrate for various heterogeneous phase chemical reactions occurring in the atmosphere; thus, leading to changes in their surface properties (from hydrophobic to hydrophilic), size-distribution and the life-time (Andreae and Crutzen, 1997; Dentener *et al.*, 1996; Ravishankara, 1997). All these factors have led to a large degree of uncertainty in estimating the aerosol forcing on climate change (IPCC 2001). This assessment is further constrained due to inadequate ground-based data on chemical composition of aerosols and their physical properties from different environment (from urban and remote marine regions) (IPCC, 2007). In this context, the Bay of Bengal (northern limb of the Indian Ocean), confined by the land area from three sides, is ideally located to study the impact of continental outflow during the short span of four months (Jan-April). In this study, our primary objective is to assess the impact of continental outflow (emissions from biomass burning and fossil-fuel combustion), occurring during the late NE-monsoon (January-April), on the chemistry of marine atmospheric boundary layer (MABL) over the Bay of Bengal. During rest of the year (during SW- and NE-monsoon), the atmosphere is relatively clean over this oceanic region.

METHOD

Ambient aerosols, $PM_{2.5}$ (N = 31) and PM_{10} (N = 33), were collected onboard ORV Sagar Kanya during 27th December 2008 - 28th January 2009 and PM_{10} (N = 23) during March-April 2006 along the cruise tracks depicted in Fig.1. The relevant details regarding sampling protocol and meteorological parameters are described in our earlier publications. Briefly, aerosol samples were collected on tissuquartz filters (20 x 25 cm^2 size, PALLGELMAN) with high-volume samplers (typical flow rate: 1.08-1.13 m^3 min^{-1}) procured from Thermo-Anderson (USA). Each sample was collected over a time period ranging from 20 to 22 hrs when ship was cruising at a speed of ~10 knots/hr, thus, avoiding the contamination from ship's exhaust. After sampling, filters were packed in zip-lock bags and preserved in the deep-freezer (at ca. -19 $^{\circ}$C) until their analysis. The mass concentrations of PM_{10} and $PM_{2.5}$ samples were ascertained gravimetrically by weighing the full filters (with a precision of 0.1 mg) before and after the sampling. Prior to their weighing, all filters were conditioned at a relative humidity of 40 ± 5 % and temperature of 23 ± 1°C for 10-12 hrs.

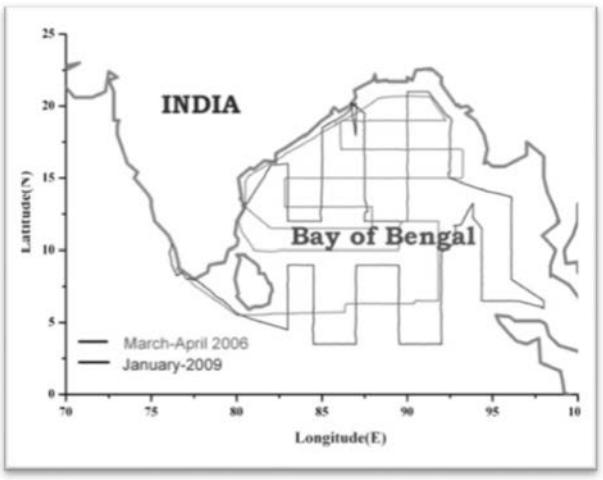

Figure 1. Cruise tracks undertaken in the Bay of Bengal during the continental outflow (January-April).

For all chemical analysis, aerosol samples were handled under the clean laminar flow bench (class-100). A portion of the aerosol filter was extracted with Mill-Q water and analyzed for water soluble inorganic constituents (Na^+ , NH_4^+ , K^+, Mg^{2+}, Ca^{2+}, Cl^-, NO_3^- and SO_4^{2-}) and were analyzed on Dionex–500 Ion Chromatograph. Another portion of filter was digested in distilled HF and HNO_3 by Microwave digestion system (~ 100 bar; Temp: 210^{o}C). The crustal elements (Al, Fe, Ca and Mg) were measured in these acid extracts using ICP-AES. In addition, Elemental Carbon (EC) and Organic Carbon (OC) were also measured on sunset EC-OC analyzer using NIOSH (National Institute for Occupational Safety and Health protocol (Birch and Cary, 1996). Along with the samples, procedural filter blanks were analyzed and mass concentrations were suitably corrected for blanks. For relevant analytical details reference is made to our earlier publications (Kumar *et al.*, 2010; Rengarajan *et al.*, 2007; Srinivas *et al.*, 2011a; Srinivas *et al.*, 2011b; Sudheer and Sarin, 2008).

RESULTS AND DISCUSSION

Air Mass Back Trajectory analysis

In order to identify the potential sources that are contributing to the aerosol chemical composition over the Bay of Bengal, we have computed 7-day air-mass back trajectories (AMBT) by using NOAA Air Resource Laboratory HYSPLIT-Model (GADS data set) at three different arrival heights (100m, 500m and 1000m). The back-trajectory analyses suggest the dominance of air-masses from the Indo-Gangetic Plain (referred as IGP-outflow; Fig. 2) during the initial period of the cruise (27th December 2008 to 10th January 2009). During later part of the cruise (i.e. in south Bay of Bengal), majority of air-masses over the south Bay of Bengal originated from south-east Asia (referred as SEA-outflow; Fig. 2). The AMBTs computed at an arrival height of 1000 m., during March-April'06, show their origin from Thar and Arabian Deserts and subsequently pass over the Indo-Gangetic Plain before entering into the Bay of Bengal. In this study, we have characterized these air-masses during *Winter* (January 2009) and *Spring-intermonsoon* (March-April 2006) based on diagnostic ratios of chemical constituents. A temporal shift in the wind regimes from Desert regions shows characteristic differences in the composition of mineral dust.

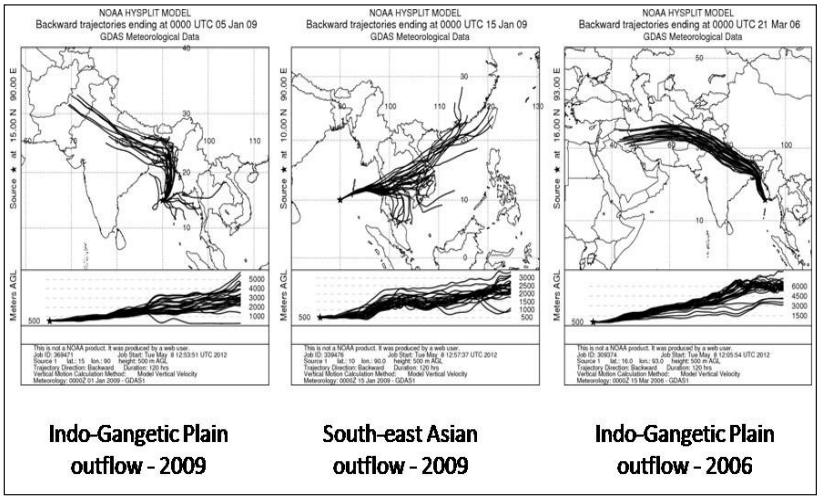

Figure 2. Air mass back trajectory cluster for the sampling days over the Bay of Bengal during January 2009 (IGP- & SEA-outflow) and March-April 2006 (IGP-outflow).

Mass Closure

Mass concentrations were estimated from the measured constituents in aerosol samples and compared with the gravimetrically obtained PM_{10} and TSP mass concentrations. In the present study, particulate mass concentration (PM_x) in aerosols is calculated as follows.

PM_X = Mineral dust + Sea Salt + Anthropogenic water-soluble ions (ANTH) + Particulate Organic Matter (POM) + EC

$$= (Al \times 12.5) + (Cl^- + 1.47 \times Na^+) + (NH_4^+ + NO_3^- + nss\text{-}SO_4^{2-} + nss\text{-}K^+) + (1.6 \times OC) + EC$$

Here X = 2.5 or 10 respectively.

The relative contribution of chemical species to average particulate mass for aerosols collected from the IGP- and SEA-outflow over the Bay of Bengal during January'09 (this study) and March-April'06 (Kumar et al., 2008) were shown as pie diagrams (*Figure 3*). The anthropogenic components constitute the significant fraction during *Winter* and *Spring-intermonsoon*. The anthropogenic fraction of water-soluble inorganic ionic constituents (ANTH) account for near about 35 % in aerosols sampled from the IGP- and SEA-outflow over the Bay region during *Winter* and *Spring-intermonsoon*. Likewise, the fractional contribution of organic matter to particulate mass is significantly high ($P < 0.05$) during *Winter* (IGP-outflow: ~ 24 %; SEA-outflow: ~ 16 %) compared to that in *Spring-intermonsoon* (IGP-outflow: ~11 %). In contrast, concentration of mineral dust during *Spring-intermonsoon* (~ 50 %) is relatively high as compared to that in *Winter* cruise (i.e., ~36 and 25 % for IGP- and SEA-outflow, respectively). On an average, elemental carbon accounts for near about 4 % during *Winter* (IGP: ~ 5 %; SEA: ~ 4 %) and 2 % in *Spring-intermonsoon*. Surprisingly, the sea-salts contribution is of comparable magnitude in the IGP-outflow sampled during both seasons. However, relatively high concentrations were observed during SEA-outflow over the Bay of Bengal (~ 16 %) during *Winter* cruise.

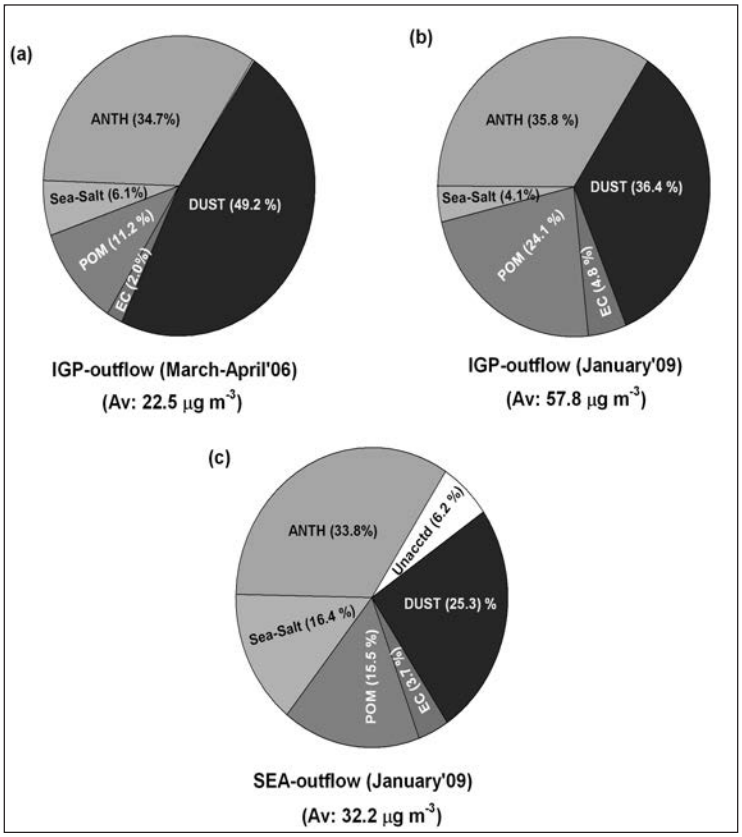

Figure 3. Percentage contribution of anthropogenic water-soluble inorganic constituents (ANTH = NO_3^- + nss-SO_4^{2-}+NH_4^+), mineral dust (Al*12.5), Sea-Salt, particulate organic matter and EC to the particulate (PM_{10}) mass in air masses sampled from the IGP- and SEA-outflow during January'09; and from the IGP-outflow during March-April'06.

CONCLUSIONS

The present study encompasses chemical characterization of water-soluble ionic species, mineral dust, sea-salts and carbonaceous species in ambient aerosols (with regard to their abundances, sources, size-distribution and spatio-temporal variability), collected over the Bay of Bengal during *Winter* (January'09) and *Spring-intermonsoon* (March-April'06). Significant differences were observed between the two sampling seasons with relatively high concentration of anthropogenic constituents (nss-SO_4^{2-}, NH_4^+, NO_3^-, nss-K^+, EC and OC) observed during the *Winter* cruise as compared to that for *Spring-intermonsoon* suggests their dominance during the former sampling period. Sea-Salts contribution towards mass loading is relatively low compared to that from anthropogenic constituents and mineral dust during *Winter* and *Spring-intermonsoon*. On average, mineral dust accounts for ~30 and 50 % of particulate mass during *Winter* and *Spring-intermonsoon*; respectively with distinctly differ in terms of their source. The alluvial soil from the Indo-Gangetic Plain is major source of mineral dust during *Winter* whereas the transport from the desert regions (eg: Thar, Arab etc.,) is a significant contributor of aerosols to the MABL.

ACKNOWLEDGEMENT

The present work is funded by ISRO-Geosphere Biosphere Programme (GBP). We thank Drs. C.B.S. Dutt and K. Krishnamurthy for their logistic support and help during the field campaign.

REFERENCES

Andreae, M. O., Crutzen, P. J.(1997). *Science* **276**, 1052.

Birch, M. E., Cary, R. A. (1996). *Aerosol Science and Technology,* **25**, 221.

Dentener, F. J., Carmichael, G. R., Zhang, Y., Lelieveld, J., Crutzen, P. J. *J.* (1996). *Geophys. Res.*, **101**, 22869

Kumar, A., Sarin, M. M., Srinivas, B. (2010), Marine Chemistry 121, 167.

Lawrence, M. G., Lelieveld, J., (2010). *Atmos. Chem. Phys.* ,**10**, 11017.

Novakov *T. et al.*, (2000). *Geophys. Res. Lett.*, **27**, 4061.

Ramanathan, V., Crutzen, P. J., Kiehl, J. T., Rosenfeld, D., (2001). *Science,* **294**, 2119.

Ravishankara, A. R. (1997). *Science* **276**, 1058.

Rengarajan, R., Sarin, M. M., Sudheer, A. K. (2007) *J. Geophys. Res.* **112**, D21307.

Srinivas, *et al.* (2011). *Marine Chemistry* , **127**, 170.

Srinivas, B., Sarin, M. M., Kumar, A. (2011), *Biogeochemistry,DOI 10.1007/s10533-011-9680-1*.

Sudheer, A. K., Sarin, M. M. (2008). *Atmospheric Environment* **42**, 4089.

CONTINUOUS MEASUREMENTS WITH HIGH TIME RESOLUTION OF SEMI-VOLATILE COMPONENTS IN THE ATMOSPHERIC AEROSOL

M. PESCH[1], H. GRIMM[1], T. KÜLZ[1], M. RICHTER[1]

[1]Grimm Aerosol Technik GmbH & Co. KG, 83404 Ainring, Germany

Keywords: ATMOSPHERIC AEROSOL, INSTRUMENT DEVELOPMENT, PM_{10} $PM_{2.5}$ PM_1, SVC

INTRODUCTION

EU limit and guideline values for the protection of human health (DIRECTIVE 2008/50/EG) demand a continuous monitoring of the atmospharic aerosol, more precisely its fine dust fraction PM10 and PM2.5. The tresholds are being exceeded in many areas in Europe, primarily in congested urban areas, where many people are affected. Fine dust is rated harmful to health which therefore strongly needs action to be taken, in order to minimize this exposure.

The EU regulates, when exceeding the set limit and guideline values, to develop clean air plans, in which efficient reduction strategies have to be enlisted. These plans are based upon cause analysis, which assigns certain dust exposure to certain sources.

For monitoring the thresholds, many measuring technologies proved well, whereas in the past years especially the optical measuring technology gained in importance. The optical detection of the aerosol enables a non-contact, continuous, and temporally high resolved measurement of the aerosols in real-time, where next to the PM fractions also particle size as well as particle counts can be determined.

A significant part (up to 60% of the particle mass) of the atmospheric aerosol is determined by semi-volatile components (SVC), which varies depending on location and season. This meaningful fraction of the SVC impedes the exact determination of the aerosol mass: The volatile components get lost, when heating the aerosol while sampling, e.g. when using a heated sampling probe for drying the sample, or when dust clogged filters remain several days without cooling inside the sampler.

Thus it is important to determine the volatile fraction of the aerosol for two reasons: On the one hand this fraction is very helpful for the source identification of the dust, because different sources create different SVC fractions, and on the other hand it is very important to measure the SVC for comparing the results of different fine dust measuring devices, which reveal the difference in their losses of SVC while measuring.

Thus the gas-particle-conversion from nitrogen oxides to nitrates and ammonium compounds, or the condensation from gaseous emitted carbon hydrides leads to organic aerosols.

METHODS

The company Grimm Aerosol Technik GmbH & Co. KG developed a compact, mobile, and highly efficient measuring instrument, which enables the continuous determination of the volatile fraction within the atmospheric aerosol. This device is in possession of two sampling probes with complementary characteristics:

One probe dries the particles by a nafion membrane in such a way, that no volatile aerosols get lost, while in the other probe the aerosol can be heated to a temperature of up to 300 °C. The aerosol is alternating being sucked through the sampling probes and subsequently analyzed inside the same optical chamber. This means, that in one interval all aerosol are analyzed and in the other one only the thermically stabilized aerosols. Forming this difference of both intervals, a determination of the volatile fraction is possible. There the volatile components are classified simultaneously into 31 size channels from 250 nm up to 32 µm, as well as a simultaneous detection of the PM_{10}, $PM_{2.5}$, and PM_{1} fractions (fig. 1).

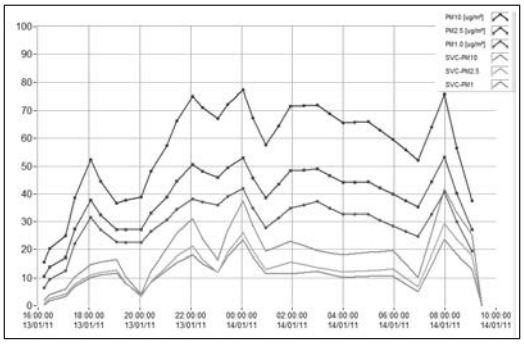

Figure 1. Temporal course of the PM fractions and its volatile components at 100°C

The temporal resolution is 6 seconds. By limiting the size channels, measurements can be executed at 1 Hz, which enables the application of the Eddy-Correlation calculation for determination of aerosol flows.

CONCLUSIONS

Measurements at different locations prove the high temporal and spatial variability of the volatile aerosol components, and moreover provide valuable indication for the causes of fine dust exposure as well as a better understanding of the aerosol formation within the lower atmosphere.

REFERENCE

REGULATION 2008/50/EG OF THE EUROPEAN PARLIAMENT AND THE COUNCIL for air quality and clean air for Europe

STABLE CARBON AND NITROGEN ISOTOPIC COMPOSITION OF HIMALAYAN AEROSOLS

PRASHANT HEGDE

Space Physics Laboratory, Vikram Sarabhai Space Centre, Trivandrum

Keywords: HIMALAYAN AEROSOL, SOURCE CHARACTERIZATION, STABLE ISOTOPES.

INTRODUCTION

Carbonaceous aerosols that comprise elemental carbon (EC) and organic carbon (OC) have large impacts on human health and radiation budget in the atmosphere. Stable carbon isotopic compositions ($\delta^{13}C$) of total carbon (TC) are very useful for investigating sources and the long range atmospheric transport of organic aerosols. Recently, it has been found that a depletion of $\delta^{13}C$ in the Northern Hemispheric aerosols relative to the Southern Hemispheric aerosols is due to an enhanced contribution of anthropogenic carbon in the Northern Hemisphere.

The atmospheric aerosol Nitrogen (N) contains both inorganic (NH_4^+ and NO_3^-) and organic N. They are produced in atmosphere by several processes. The determination of the isotope ratios ($\delta^{15}N$) are helpful in assessing the origin of aerosol N, because the isotope ratios of particular atmospheric species depend on the sources and are modified by chemical and physical processes in the atmosphere.

EXPERIMENTAL

The atmospheric aerosol samples were collected using a high volume air sampler from Nainital (2006-07). Measurements of total carbon (TC) and total nitrogen (TN) were made by an elemental analyzer (EA) (Carlo Erba, NA 1500). Stable carbon and nitrogen isotope ($\delta^{13}C$ and $\delta^{15}N$) analysis were conducted using the EA combined to an isotope ratio mass spectrometer (irMS, Finnigan MAT Delta Plus). A part of the filter paper (diameter of 1.8 cm^2) was cut using a circular cutter and packed by using a tin cup and made in to a round shape ball. Then, the sample was introduced into the EA and subsequently oxidized at 1020 ºC in a combustion column that is packed with chromium (III) oxide. The combustion column emitted nitrogen oxides were converted to molecular nitrogen (N2) at 650 ºC in a reduction column which is packed with metallic copper. By using a gas chromatograph (GC) in line with the EA, the derived N_2 and carbon dioxide (CO_2) were separated and measured from a thermal conductivity detector. By using an interface (ThermoQuest, ConFlo II), a part of the same CO_2 was then introduced to the irMS. From the standard isotopic conversion equation the carbon isotopic composition ($\delta^{13}C$) relative to the Pee Dee Belemnite (PDB) standard was estimated.

$$\delta 13C(‰) = \left[\frac{[(13C/12C)sample]}{[((13C/12C)standard)]} - 1 \right] \times 1000$$

Known amounts of acetanilide were used as standard (external calibration) to calculate mass concentrations of TC, TN and $\delta^{13}C$ of TC ($\delta^{13}CTC$) as well as $\delta^{15}N$ of TN. Total five ranges of standards (0.2 - 0.6 mg of acetanilide) were prepared and measured by the EA-irMS. Acetanilide has

a δ^{13}CTC of 27.26 ‰. Field blank corrections were also made for the mass concentrations and δ^{13}CTC values reported here by applying isotope mass balance equations. The TC and TN blank levels of mass concentrations were 1.5% and 1.0% of the measured concentrations, respectively. The triplicate analyses of the filter sample reveal analytical errors for TC and TN mass concentrations were 2.0 % and 4.0 %, respectively.

RESULTS

The temporal variations of Total Carbon, SO_4^{2-}, K^+ and δ13C in aerosol samples from Nainital are shown in Fig. 1. The annual average TC concentrations over Nainital (13.7 ± 8.4 μg m^{-3}) were comparable to many Indian cities, but significantly higher than European urban background sites. ä^{13}C values of TC in summer aerosols were slightly lower (-26 ± 1.1 ‰) than those of winter season (-24 ± 0.89 ‰). TN concentrations during winter period were on average 0.77 ± 0.34 μg m^{-3} and 0.59 ± 0.26 μg m^{-3} for day and night, respectively (Figure 2). During summertime the concentration of TN was almost doubled the winter value (1.71 ± 0.79 μg m^{-3} and 1.55 ± 0.61 μg m^{-3} for day and night, respectively). During winter δ^{15}N values were regularly higher (24.0 ± 1.6 ‰ and 24.6 ± 1.5 ‰ for day and night, respectively) than those in summer (17.0 ± 3.7 ‰ and 16.3 ± 2.0 ‰ for day and night, respectively). As compared to winter, the smaller ä^{13}C and δ^{15}N values as well as stable carbon isotopic ratios of dicarboxylic acids during summer season indicate the entrainment of more fresh aerosols in the sampling site. Weak correlation between δ^{13}C of C_2 to C_4 diacids and WSOC/OC ratios suggests that effect of photochemical aging on stable carbon isotopic composition of diacids during atmospheric transport seems to be insignificant (Hegde and Kawamura, 2012). This, instead, indicates the contribution of more fresh aerosols during summer. On the contrary, the opposite trend was observed for winter. Annual average ratios of δ^{13}C of TC and δ^{15}N of TN indicate considerable contribution from C_4 plants (e.g., sugar-cane, maize) during winter and C_3 plants (e.g., wheat, rice etc.) during summer, respectively.

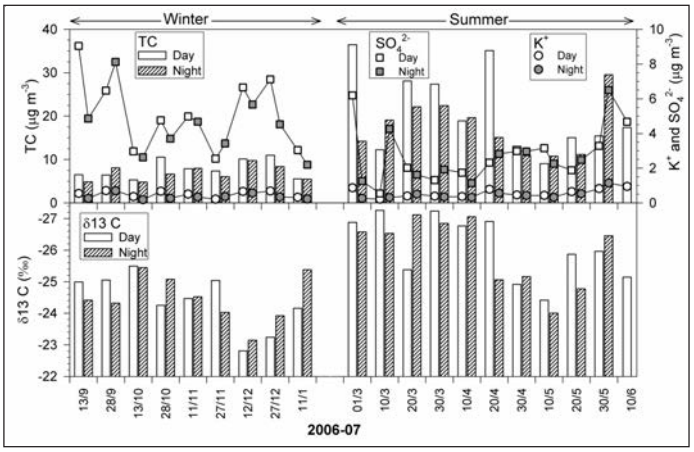

Figure 1. Temporal variations of Total Carbon (TC), SO_4^{2-}, K^+ and δ13C in aerosol samples from Nainital, India.

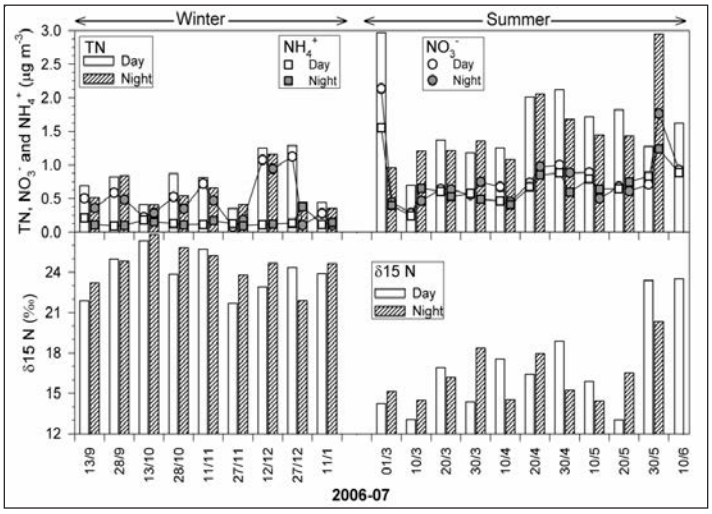

Figure 2. Temporal variations of Total Nitrogen (TN), NH_4^+, NO_3^- and $\delta^{15}N$ in aerosol samples from Nainital, India

For the winter months the observation site remains above the boundary layer and represents a free tropospheric site. Conversely, the boundary layer height increases during summer months and the observation site will be well within the boundary layer. The pollutants of northwestern Indian origin are readily transported towards the central Himalayas due to high wind, elevated temperature, and supplementary convection during summer season. The data sets reported from this study could serve as baseline observation of carbonaceous aerosols for northern part of the Indian subcontinent, which could contribute to regional climate and air quality models.

REFERENCES

Hegde, P. and Kawamura, K. (2012). Seasonal variations of water-soluble organic carbon, dicarboxylicacids, ketoacids, and α-dicarbonyls in central Himalayan aerosols, *Atmospheric Chemistry and Physics* ,**12**, pp. 6645–6665.

DISTRIBUTION OF PARTICULATE MATTER, CO AND NOx AT A SEMI URBAN SITE OF UDAIPUR IN RAJASTHAN, INDIA

RAVI YADAV[1], S.N.A. JAAFFREY [1], L.K. SAHU[2], G. BEIG[3]

[1] Department of Physics Mohanlal Sukhadia University, Udaipur-313001 India
[2] Physical Research Laboratory, Ahmedabad- 380009 India
[3] Indian Institute of Tropical Meteorology, Pune - 411008 India

Keywords: METHANE, PM, NMHCS, TROPOSPHERE, SEASON, AEROSOL.

INTRODUCTION

Anthropogenic emissions of aerosols and trace gases in Asia are increasing because of rapid economic growth and urban development (Ohara, *et al.*, 2007; Zhang, *et al.*, 2009). In addition to natural sources, aerosols are emitted primarily by incomplete combustion. Ozone is one of the secondary pollutants whose high concentration is harmful for humans and plants (e.g. Finnan, *et al.*, 1997). Photochemical ozone production takes place by photo oxidation of CH_4, CO and NMHCs in the presence of sufficient amount of NOx. The tropical troposphere is the region of biogenic and pyrogenic emissions of trace gases, including NMHCs, which react with high OH radical concentration and thus making it the most active photo chemical region of the atmosphere (e.g. Andrae and Crutzen, 1997). Atmospheric particles constitute one of the main factors of urban air pollution and one of the hotspots in international global change study (Houghton, *et al.*, 2001). It is recognized that particles in urban air are responsible for serious health effects (Harrison, *et al.*, 2000). The atmospheric abundance of BC comprises mainly fine particles, including ~90% fraction of PM2.5, which can be harmful to human health in polluted regions. Simultaneous measurements of surface ozone and its precursor gases over this region are lacking. A project Modeling Atmospheric pollutants and networking (MAPAN) is undergoing by the Indian Institute of Tropical Meteorology, Ministry of Earth Science. Measurement at Mohanlal Sukhadia University, Udaipur is key network of this project for the measurements of ozone and its precursor gases. We present here the results of NOx, CO, CH_4, TNMHC and PM 2.5/10 based on measurements made in Udaipur. These measurements will not only help to study the semi urban air quality but will also be useful in studying the changes in the chemical composition of the regional atmosphere.

METHODS

For this study we have installed analyzers for detection of the ambient level concentrations of various aerosols and trace gases. The site is located in the campus of Mohanlal Sukhadia University, Udaipur (24.58^o N, 73.68^o E 598 msl) in the southern Rajasthan. Indian Institute of Tropical Meteorology, Pune (Autonomous under Ministry of Earth Sciences, Govt. of India) has established a MAPAN project under the MOU with Mohanlal Sukhadia University Udaipur. Under project has BETA Attenuation Monitoring (BAM) 1020 for taking data for PM_{10} & $PM_{2.5}$

The annual variability of particulate matter show strong variability. Emissions are mainly local and impact of long range transport could be seen annual variations. Both PM_{10} and $PM_{2.5}$ attain higher levels during autumn/winter seasons as they get transported through NE wind flow from the polluted regions. Also in winter months, the pollutants, emitted from various anthropogenic and natural

sources, are trapped in the boundary layer due to frequent temperature inversions, while in the summer months this polluted air mixes well with clean air causing dilution of the pollutants.

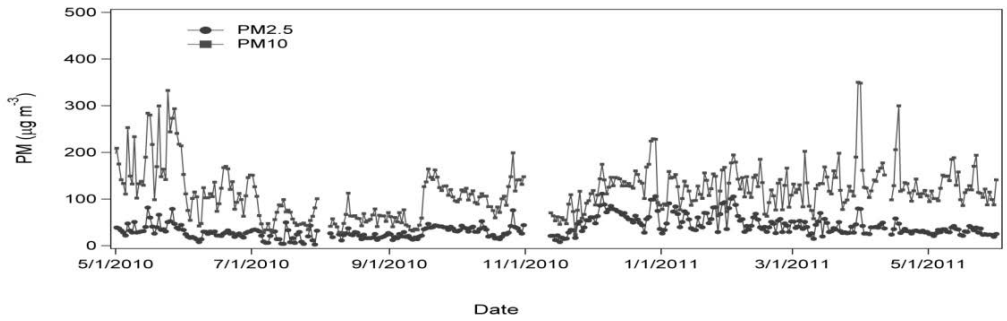

Figure 1. Time series variations of PM_{10} and $PM_{2.5}$ at Udaipur.

As shown in Fig. 2, the mixing ratios of CO and NOx attain higher levels during autumn/winter seasons as they get transported through northeasterly wind flow from the polluted regions. Differences in the levels of CO and NOx during different months are larger during morning and late evening/ night hours as compared to noontime. During afternoon hours, when CO and NOx get depleted by OH chemistry, the seasonal difference in the levels of these species is found to be much less.

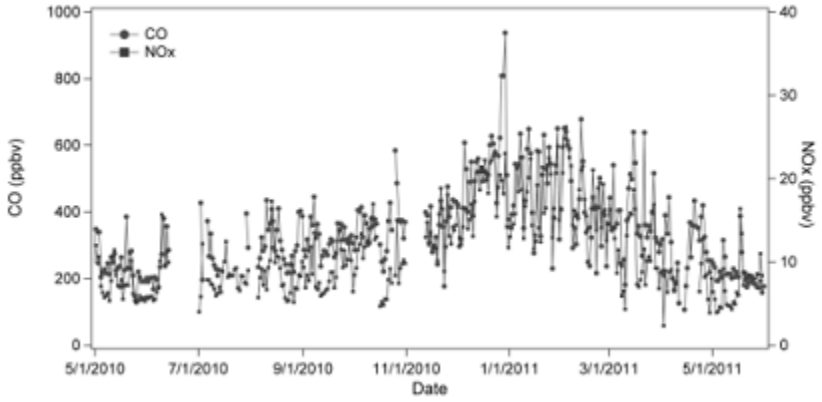

Figure 2. Time series variations of CO and NOx at Udaipur.

The levels of PM 2.5 and PM 10 were found to be lower in the summer season compared to the winter season. The morning and evening peaks in all species coincide with the peak traffics in Udaipur city. In the night hours of winter season, because of shallow planetary layer (PBL) pollutants are trapped near the surface.

CONCLUSIONS

Simultaneous surface measurements of Particulate Matter (PM_{10} and $PM_{2.5}$), total non methane hydrocarbons (TNMHCs), ozone (O_3), carbon monoxide (CO), oxides of nitrogen ($NOx=NO+NO_2$), and methane (CH_4) were conducted during the year 2010-2011 at a tropical semi urban site of Udaipur in western India. We have analyzed the data to investigate the causes of both short (diurnal) and long term (seasonal) variations observed in the concentrations of aerosols and gaseous species.

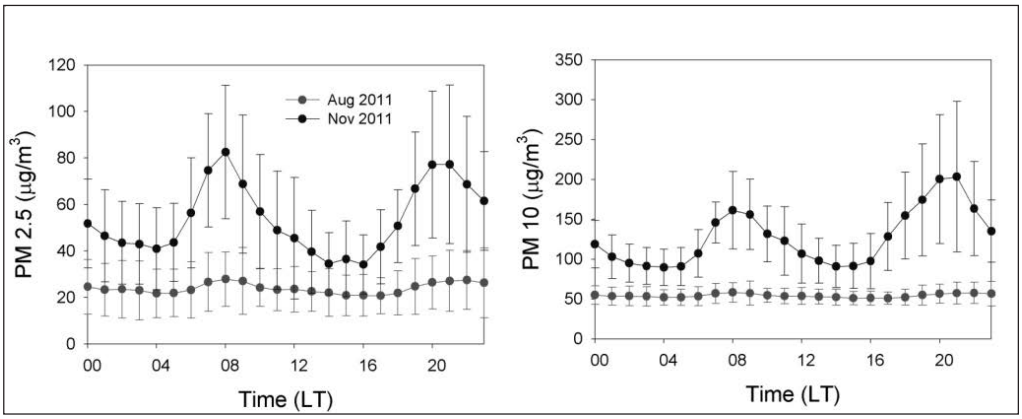

Figure 3. Diurnal variations of PM_{10} and $PM_{2.5}$ at Udaipur.

The diurnal patterns of PM concentrations and mixing ratios of precursors exhibit two peaks, one in the early morning hours and other during the late evening hours with lowest in the afternoon. Their levels were highest during late winter and lowest during the summer monsoon. Analysis of meteorological data suggests that the diurnal patterns of these species were mainly controlled by the variations in planetary boundary layer (PBL) depth and local emissions. On the other hand, the seasonality in these species is expected to be governed by the long-range transport associated mainly with the summer and winter monsoon circulations over the Indian subcontinent.

ACKNOWLEDGEMENTS

We thank MAPAN (Modeling Atmospheric Pollution and networking) programme for supporting our study and we also thank G.Beig (Indian Institute of Tropical Meteorology, Pune) for providing the data through MAPAN Programme. And thanks to L.K. Sahu (Physical Research Laboratory) for their support scientific purpose and data analysis.

REFERENCES

Andreae, M.O., Crutzen, P.J. (1997). Atmospheric aerosols: bio-geochemical sources and role in atmospheric chemistry, *Science*, **276**, pp.1052-1058.

Finnan, J.M., Burke, J. I., Jones, M.B. (1997). An evaluation of indices that describe the impact of ozone on the yield of spring wheat (Triticum aestivum L.), *Atmospheric Environment*, **31**, pp. 2685-2693.

Harrison, R. M., Yin, J. (2000). Particulate matter in the atmosphere: which particle properties are important for its effects on health, *The sci. Total Environ.* , **249**, pp. 85-101.

Houghton, J. T., Ding, Y., Griggs, D. J. (2001). IPCC (Intergovern-mental panel on climate change), climate change 2001: The scientific Basis.

Aerosols, their Direct and Indirect Effects, London, *Cambridge University Press*, pp. 289-348.

Ohara, T., Akimoto, H., Kurokawa, J., Horii, N., Yamaji, K., Yan, X., Hayasaka, T. (2007). An Asian emission inventory of anthropogenic emission sources for the period 1980-2020, *Atmos. Chem. Phys. Discuss*., pp. 6843-6902.

FINE AND ULTRAFINE AEROSOLS OVER EASTERN HIMALAYA, INDIA

A. ADAK[1], A, CHATTERJEE[1,2], S.K. GHOSH[2] AND S. RAHA[1,2]

[1]Environmental Sciences Section, Bose Institute, Kolkata – 700 054, India
[2]Center for Astroparticle Physics and Space Science, Bose Institute,
Salt Lake, Kolkata – 700 091, India

Keywords: ULTRAFINE AEROSOLS, NUCLEATION, HIMALAYA, DARJEELING

INTRODUCTION

The study of atmospheric aerosols especially fine and ultrafine mode is gaining importance in scientific community as numerous studies have demonstrated their association with health-related problems and climate changes. Further, the study of aerosol over Himalayan region is of paramount interest as the ecology of the Himalaya is under serious threat from various forms of pollutants (Bostrom, 2002).

The fine mode aerosols (<2.5 μm) can be classified as accumulation mode (< 1 μm), Aitken mode (0.1–0.01ìm) and nucleation mode (0.01–0.001μm) (Satheesh *et al.*, 2004). Nucleation, Aitken and accumulation mode particles could be collectively called ultra fine particles. These fine and ultra fine particles penetrate into lungs and produce many respiratory problems. Although various studies have been carried out on the characterization of total fine mode aerosols, the size segregated fine mode aerosol characteristics specially the formation of ultra fine particles through nucleation of their gaseous precursors is not well documented in India especially over eastern Himlayan region. New particle formation is a complex process that depends on the nature of gaseous precursor species, which differ according to the environment; on meteorological factors such as UV-radiation, temperature, and relative humidity; and on boundary layer dynamics.

The present study has been carried out over a high altitude hill station, Darjeeling at eastern Himalaya in India on a long-term characterization of fine and ultra fine particles. This has been performed during two important seasons, premonsoon and winter, over three consecutive years 2008, 2009 and 2010. The seasonal and diurnal variations of fine and ultra fine aerosols have been performed for three years with the objectives that 1) how the local anthropogenic activities (mainly biomass burning and tourist activities) contribute to the loading of fine mode aerosols, 2) how the long-range transport is efficient for the enhancement of ultrafine (accumulation mode) aerosols mainly during premonsoon and 3) what are the controlling factors for the formation of ultrafine particles (nucleation and Aitken mode) over this high altitude eastern Himalayan region

METHODS

For the measurement of aerosol number distribution, a portable optical particle counter (Aerosol Spectrometer, Grimm Series 1.108, Germany) was used. Particle concentration is measured in an optical size range of 0.30–20 μm in 15 channels and with concentration range of 1–2,000,000 particles/ lit for count distribution mode. We have not studied aerosol concentrations for all the size ranges (for all channels in the instrument) but we have studied aerosol concentrations of the size below 2.0 ìm as our study was mainly focused on fine and ultra-fine particles. Thus we have studied aerosol concentrations of three different size modes namely i) nucleation cum aitken mode, ii) accumulation

mode and iii) fine mode for our study. Aerosols of size less than 0.32 μm or 320 nm have been considered as nucleation cum aitken mode. It was the first and the lowest channel of the instrument. The particles of size 0.32 – 1.0 μm have been considered as accumulation mode and the particles of size 1.0 – 2.0 μm have been considered as fine mode. Thus the first two modes (up to 1.0 μm) collectively were considered as ultra fine aerosols. Nucleation cum aitken mode aerosol concentration has been designated as PM_{Nu+At}, accumulation mode aerosol concentration has been designated as PM_{Ac} and fine mode aerosol concentration has been designated as PM_{F} in this study.

RESULTS AND DISCUSSION

The ultrafine particles (nucleation cum aitken mode plus accumulation mode; 0-1.0 μm) showed higher concentrations during premonsoon compared to winter over the years 2008, 2009 and 2010. On the other hand, the fine mode aerosol (1.0 – 2.0 μm) concentrations were found to be comparable during premonsoon and winter. The ultrafine aerosol concentration over Darjeeling at eastern Himalaya was found to be much higher than the other Himalayan stations in India and Nepal and also than the several high altitude stations in Europe.

The nucleation cum aitken mode aerosol (0 – 0.32 μm) formation over Darjeeling was governed by several micro-meteorological parameters. The sunny and non-cloudy days with lower relative humidity and higher solar radiative fluxes were found to favour whereas the cloudy days were found to inhibit the formation of these particles. The initiation of the formation of these particles was observed during 0900 – 1000 hours LT over the study period.

The accumulation mode aerosols (0.32 – 1.0 μm) were mainly the long-range transported aerosols from distant sources. During premonsoon, the sharp diurnal variation of accumulation mode particles was observed with the peak during late morning till late afternoon. High wind speed favored the loading of these particles in the atmosphere by up-slope valley wind. Along with these particles, the up-slope valley wind might have carried precursor gases necessary for the nucleation mode particle formation, but finally the formation depended on the meteorological conditions.

Fine mode aerosols were mainly the locally generated anthropogenic aerosols. During premonsoon, these particles were emitted mainly from the vehicular sources (due to tourist influx in premonsoon, being peak tourist season) and during winter, these particles were emitted mainly from the biomass burning. The diurnal variation of fine mode aerosols showed two prominent peaks during peak office hours in morning and evening. In addition to this, the minimum concentration during afternoon and slightly higher night-time concentrations during winter were due to the thermodynamic conditions and the dynamics of the planetary boundary layer.

Overall, our study provides the first long-term analysis of fine and ultrafine aerosol concentrations which could be used to validate the predictions of regional and global aerosol models. The study will also help to better understand its implication on aerosol dispersion, because particle size distributions bear a fingerprint of the related source and removal processes.

REFERENCES

Bostrom, N. (2002). Existential Risks: Analyzing human extinction scenario and related hazards, *J. Evol. Tech.,* **9(4.7)**, pp. 1–30.

Satheesh, S. K., Moorthy, K. K. and Srinivasan, J. (2004). Introduction to aerosols and impacts on atmosphere: Basic concepts, ISRO-GBP Scientific Report; SR 05, pp. 1–100.

CHEMICAL AND MORPHOLOGICAL ANALYSES OF ATMOSPHERIC AEROSOLS (PM_5) OVER A SEMI-ARID ZONE OF WESTERN INDIA (RAJASTHAN)

RAJESH AGNIHOTRI, SUMIT K. MISHRA, PAWAN YADAV, RASHMI, SUKHVIR SINGH, M.V.S.N. PRASAD AND B.C. ARYA

CSIR-National Physical Laboratory
K.S. Krishnan Marg, New Delhi, 110012, India
E mail: rajagni9@gmail.com

Keywords: $PM_{5,}$ MINERAL DUST AEROSOLS, CHEMICAL COMPOSITION, HEMATITE.

INTRODUCTION

Mineral dust particles are known to influence the radiation budgets, and thus climate, mainly by back scattering and absorbing incoming and outgoing radiation (Sokolik *et al.*, 2001). These particles are produced by aeolian erosion mainly in the arid and semi-arid regions of the world. A direct forcing due to mineral dust particles is of the order of ±0.5 W m^{-2}. However, quantification of the magnitude of warming or cooling remains open due to significant variability of the atmospheric dust burden as well as lack of representative data for the spatial and temporal distribution of the dust chemical composition. Many modeling studies also point to the uncertainties accountable to lack of physico-chemical properties of mineral dust, as a limiting factor in estimating their climatic impact (Myhre and Stordal, 2001).

In India, the Thar Desert of Rajasthan is known to be a major source of mineral dust influencing optical/ raditaive properties of the atmosphere extending over entire Indo-Gangetic Plain (IGP). Additionally, chemical composition of mineral dust especially hematite fraction can significantly influence optical properties (such as single scattering albedo, asymmetry factor) (Mishra & Tripathi, 2008). State capital of Rajasthan, the *Pink city* is surrounded by several old forts situated on medium scale barren mountains such as Amber, Jaigarh, Nahargarh of varying altitude ranging from 500-1000m from ground level. Besides these, Jaipur industrial area is situated in the vicinity of Kukas hills (at height ~800m from ground). This makes Jaipur an ideal locale to sample atmospheric particles at varying altitudes in order to investigate chemical and physical characteristics of mineral dust particles originating from the Thar Desert. To accomplish this aim, we collected atmospheric particles with aerodynamic size <5μm (PM_5) and a few bulk particles (TSP) from seven sites of Jaipur (in the vicinity of Thar Desert) at varying altitude, during late winters of 2012 and carried detailed chemical and physical characterization at bulk as well as individual particle level. Though bulk chemical compositions of the particles were found broadly in consistence with that of individual particles, our detailed analyses revealed several interesting features of mineral dust particles over Jaipur (Rajasthan). For example, PM_5 particles over Kukas Hill area (at ~800 meter above ground level (MAGL)) showed maximal mineral dust characteristics compared to that of other sites, with highest Fe mass fractions.

METHODOLOGY

To collect ambient mineral dust aerosols at varying altitude in the vicinity of Thar Desert region, we conducted a field trip of Jaipur from 19-25 February, 2012. Using low volume air sampler (APM 801; *Envirotech*) with typical air flow rate ~1.5 liter per minute (LPM), atmospheric PM_5 particles (and a few bulk particles also; TSPs) were collected on pre-weighed Teflon and glass-fiber filters (37 mm and 25 mm, respectively) for investigating chemical composition of particles. However, for examining individual particle morphology and chemical composition, particles were collected on pure Tin substrates (~1×1 mm^2), placed on Teflon/GF filters. Using Scanning Electron Microscope equipped with Energy Dispersive X -ray (SEM-EDX) facility of NPL, individual particles were imaged and chemical compositions were assessed using EDX. Bulk chemical compositions of PM_5 particles were determined using X ray fluorescence (XRF) technique at NPL. $PM_{5.0}$ mass concentrations of particles were determined by weighing Teflon filters after collection and before carrying out to any analysis.

RESULTS

PM_5 mass concentrations show large variations ranging from 34.72 (over lower Jaigarh, near Amber fort) to 499.82 $\mu g.m^{-3}$ (near Makarana mining area, Rajasthan) (Fig. 1a). Using measured elemental data, and converting them into their oxides, we also estimated portion of total mass accounted by elemental oxides. Particles over Kukas hill area show maximum mass fraction accounted by measured elemental oxides while particles sampled near Makarana mining area showed minimum accountable portion by elemental oxides. Thus, particles over Kukas Hill area seem to show maximal mineral dust characteristics compared to that of other sites. Figure 1b shows distribution of measured elemental mass concentrations at all the sites. In general, common elements found in atmospheric particles over all the sites are Si, Al, Cr, Fe, however, maximum variability was shown by Fe. Presence of significant amount of Cr in ambient PM_5 particles over almost all the sampled sites is also noteworthy (Fig. 1b). This is because; enriched Cr in high dust episodes over IGP (Kanpur) has been inferred to be of Oman origin (Chinnam *et al.*, 2006).

Individual particle images reveal occurrence of highly non-spherical particles rich in Si, Al, Fe, Ca and Mg, that supports the dominance of mineral background dust component in ambient PM_5 at all the sites, in general. Anthropogenic elements such as Cu, S, C, Ag and Pb were observed only over main city (Jaipur Birla Temple; 26.893°N, 75.816°E; at ~10 MAGL). Figure 2a shows distribution of elemental mass fractions of particles over Kukas hill, with highest Fe mass fractions (~43%). Particles over Kukas NH-8 (highway connecting Jaipur to Delhi; at ground level) were also found to be rich in Fe. Finding of Fe rich mineral dust over Kukas hill and surrounding area is of significant importance as Fe is a key element (in form of hematite; Fe_2O_3) for incoming solar (visible) energy absorption and thus heating the atmosphere (Lafon *et al.*, 2006). Likewise, chemical composition of ambient PM5 particles at bulk as well as individual particle level were measured at all sites. In addition, using SEM images of individual particles, key morphological parameters (*e.g.* Aspect ratio; AR, Circulatory parameter; CIR) were also measured, and geometrical size distributions of the particles were generated for each site.

IMPLICATIONS

Generated region-specific chemical and physical database of ambient aerosols from dust source region is highly useful to better estimate optical constants of mineral dust (governing optical/ radiative

properties) and assessing long range transport of dust aerosols and to identify origin of dust storms that are frequent during pre-monsoon season in northern India.

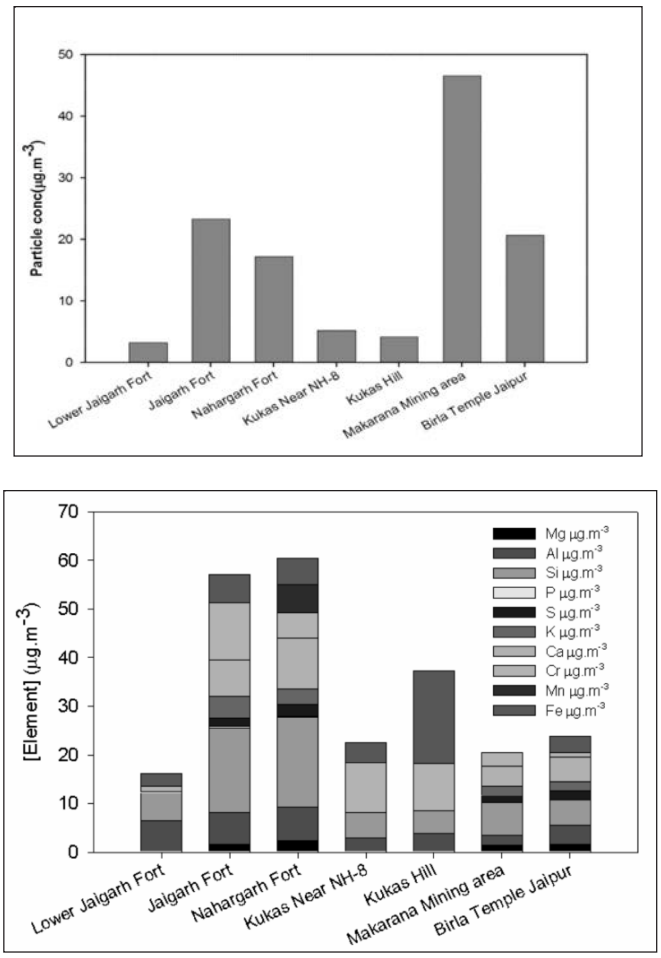

Figure 1**.** (a) Spatial variability of particle mass concentrations over all the sites. (b) Variability in measured elemental concentrations in PM_5 particles for all sites, as determined by XRF analyses.

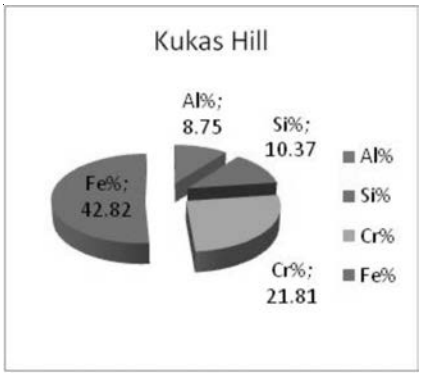

(c) *Individual aerosol particles over Kukas Hill, Jaipur*

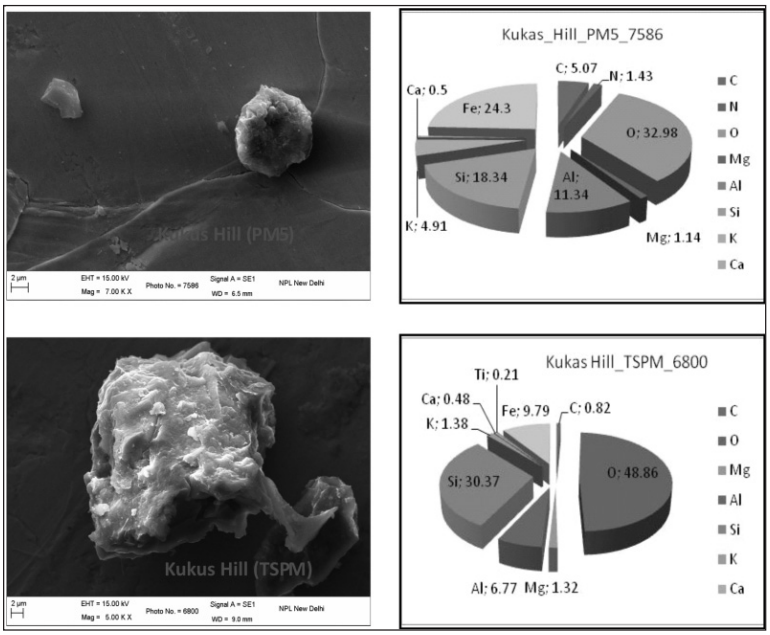

Figure 2**.** (a) Distribution of elements in PM_5 particles over Kukas Hill on bulk level (as determined by XRF) showing highest Fe mass fraction. (b) SEM images of individual aerosol particles (of PM_5 as well as TSPM) over Kukas Hill (Jaipur) and chemical compositions as determined by spot EDX.

ACKNOWLEDGEMENT

The authors are thankful to Director NPL, Prof. R C Budhani for his consistent support to the ongoing work.

REFERENCES

Chinnam, N., Dey, S., Tripathi, S. N., and Sharma, M. (2006). Dust events in Kanpur, northern India: Chemical evidence for source and implications to radiative forcing, *Geophys. Res. Lett.*, **33**, L08803.

Lafon, S., Sokolik, I. N., Rajot, J. L., Caquineau, S., and Gaudichet, A. (2006). Characterization of iron oxides in mineral dust aerosols: Implications for light absorption, *J. Geophys. Res.*, **111**, D21207.

Mishra, S. K. and Tripathi, S. N. (2008). Modeling optical properties of mineral dust over the Indian Desert, *J. Geophys. Res.*, **113**, D23201, 19.

Myhre, G. and Stordal, F. (2001). Global sensitivity experiments of the radiative forcing due to mineral aerosols, *J. Geophys. Res.*, **106**.

Sokolik, I. N., Winker, D. M., Bergametti, G., Gillette, D. A., Carmichael, G., Kaufman, Y. J., Gomes, L., Schuetz, L., and Penner, J. E. (2001). Introduction to special section: Outstanding problems in quantifying the radiative impacts of mineral dust, *J. Geophys. Res.*, **106**, pp. 18,015–18,027.

TIME-SIZE-SOURCE CHARACTERIZATION OF AEROSOLS OVER AN URBAN SITE IN WESTERN GHATS

SUMIT KUMAR[1], K. VIJAYAKUMAR[2] AND P.C.S. DEVARA[2]

[1] Atmospheric Sciences Program, Michigan Technological University, Houghton, MI, USA
[2]Indian Institute of Tropical Meteorology, Pune - 411008, India
E mail: devara@tropmet.res.in

Keywords: AEROSOL SIZE DISTRIBUTION, HYGROSCOPIC GROWTH, COAGULATION, SUN/SKY RADIOMETER

INTRODUCTION

Aerosols exhibit a large spatial and temporal variability and this feature, along with their short lifetimes and mixing processes, is a key reason for the uncertainty in their climatic effect. The optical properties of aerosols, which determine their climatic effects, depend on size distribution, chemical composition and the chemical processes that mix different constituents. Globally, the dominant aerosol types are smoke from biomass burning, mineral dust, aerosols from urban/industrial sources and marine aerosols.

Urban/industrial environments are places where most of the anthropogenic activities are centered and in turn they provide a natural laboratory to study the evolution of aerosols with time. Also, the local meteorology and long-range transport play an important role in enhancing or altering their effects. Long- term observations are a way to discern the aerosols behavior in detail. By this, one can differentiate the background levels as well as the changing levels of aerosols. The present study is about aerosol size distribution and it's intra-annual to seasonal variation, including effect of air.

Size distribution together with optical and radiative properties of aerosols is important for assessing their direct and indirect effects on earth-atmosphere radiation balance. In this paper, we study the columnar aerosol optical properties over Pune with a focus on aerosol volume size distribution (AVSD), which helps understanding local aerosol properties, variation, hygroscopic growth and coagulation. Long-term ground-based passive remote sensing measurements from 2004 to 2011 have been performed using a sun-sky radiometer.

RESULTS AND DISCUSSION

In this section, the aerosol size distribution parameter is analysed in order to characterize their timeseries and representative mean statistical values.

Aerosol Volume Size Distribution

To illustrate the main features and the values of the AVSD, the monthly averaged values for the entire dataset (2004-2010) have been calculated, from the daily mean values. The detailed and specific examples of the AVSD behaviour under different situations related with low and high turbidity conditions are presented. In Fig. 1 the mean AVSD value for every month is shown together with a table of the monthly mean of AOD at 440 nm and α. A bimodal structure is observed. The fine- and coarse-modes can be separated by a radius of ~ 0.6 μm.

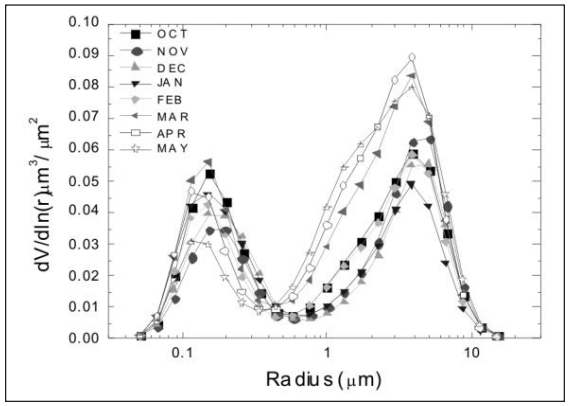

Figure 1. Multiannual monthly average of aerosol volume size distribution.

First of all the high variability of coarse-mode concentration stands out, as well as the predominance of the coarse mode concentration for the premonsoon months (March through May). This issue is related to the frequency of sea salt and desert dust intrusions, as shown by trajectory analysis presented by Kumar *et al*. (2001). It is found that the marine and desert dust episodes are more frequent in premonsoon months. Also the Angstrom exponent values (Table 1) are found to be low for premonsoon months than other seasons, corroborating the fact that atmosphere during the same period is influenced by bigger size particles. Whereas, both fine- and coarse-modes are predominant during the post-monsoon and winter months. The month-to-month differences are small for fine-mode relative to coarse-mode.

Month	$AOD_{440\ nm}$	Álfa
Oct	0.50	1.21
Nov	0.43	1.23
Dec	0.48	1.29
Jan	0.50	1.34
Feb	0.45	1.25
Mar	0.58	1.15
Apr	0.50	0.99
May	0.41	0.77

Table 1. Multiannual monthly average of AOD and Angstrom exponent (α).

Fig. 2 shows the average size distribution for each year (2004-2011) [Fig. 2 (a)] and also the size distribution for each seasonally, averaging the daily distributions of the year (October 2004 - December 2011) [Fig 2(b)]. From Fig. 2 (a) (b) shows more coarse aerosols are dominated over this experimental site. During monsoon months, the higher coarse-mode particles are dominated compared to other seasons, because of sea salt and desert dust intrusions.

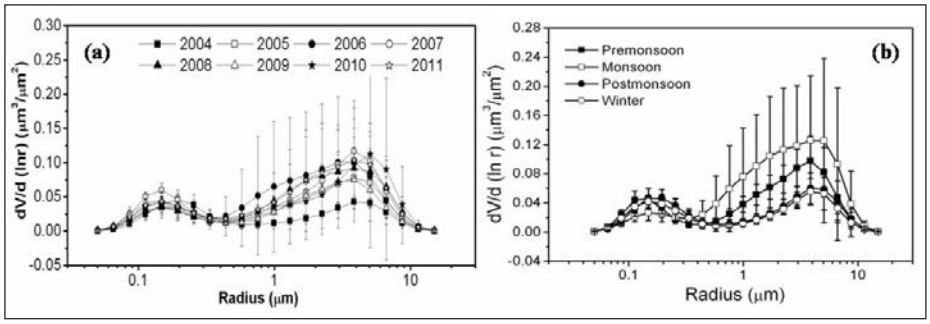

Figure 2. Mean aerosol size distributions obtained by (a) Yearly averaging the monthly distributions. (b) Seasonally averaging the daily distributions.

Aerosol Volume Concentration

Fig. 3 depicts the monthly average behaviour of total, coarse- and fine-mode aerosol volume concentration with AOD (440 nm). A first look shows the different behaviour from one another, and although in general the highest concentration is found in the premonsoon months, also a few relative maxima appear in post monsoon months. This graph confirms the enhanced contribution of coarse-mode to total AOD over Pune during premonsoon months relative to other seasons. A back trajectory analysis together with a study conducted by (Safai *et al.*, 2010; 2012) confirms the increase in concentration of marine origin and desert dust aerosol particle to AOD.

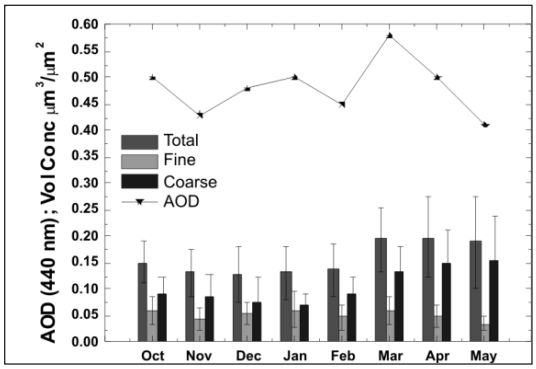

Figure 3. Multiannual monthly avareg of the aerosol volume concentration total, coarse and fine mode (vertical bars indicate standard devviation). The solid line represents the monthly avarage values of AOD at 440 nm.

CONCLUSIONS

A bimodal size distribution, with a pronounced seasonality, is found with the fine-mode centering at ~0.2ìm and coarse-mode centering at ~3ìm, respectively. The fine- and coarse-mode particles contribute nearly 30% and 60% fraction, respectively, in composing local aerosols. Inter-comparison of AVSD during different years shows slight increase in both fine- and coarse-mode aerosol concentrations. The seasonal variability in coarse-mode particles is found to be more as compared to that of fine-mode particles with maximum during pre-monsoon season; due to changes in circulation, land-surface and long-range transport processes. The inter-annual variability in Ångström exponent (á) reveals a decreasing pattern, from October through May, exhibiting a seasonal dependence. The relationship between á and AOD suggests that the experimental location is characterized by different

types of aerosol loading contributed by regional air mass. More works combining laboratory, sampling and modelling methods would help to understand the aerosol hygroscopic growth and coagulation.

ACKNOWLEDGEMENTS

The authors are grateful to the AERONET for their valuable support. One of the authors (KV) acknowledges the financial support, in the form of Research Fellowship, from the ISRO-GBP-ARFI Project. Thanks are also due to the Director, IITM for encouraging the study.

REFERENCES

Kumar S.,Devara P.C.S., Dani K.K ,Sonbawne S.M. and Saha S.K. (2011). Sun-sky radiometer–derived column-integrated aerosol optical and physical properties over a tropical urban station during 2004-2009, *Journal of Geophysical Research* **116**, doi:10.1029/2010JD014944.

Kumar, S., Devara, P.C.S. and Manoj, M.G. (2012). Multi-site characterization of tropical aerosols: Implications for regional radiative forcing, *Atmospheric Research* **106**, pp. 71-85.

Safai, P.D., Budhavant, K.B., Rao, P.S.P., Ali, K. and Sinha, A. (2010). Source characterization for aerosol constituents and changing roles of calcium and ammonium aerosols in the neutralization of aerosol acidity at a semi-urban site in SW India, *Atmospheric Research* **98**, pp. 78–88.

Safai, P.D., Raju M.P., Maheskumar R.S., Kulkarni J.R., Rao P.S.P. and Devara P.C.S. (2012). Vertical profiles of black carbon aerosols over the urban locations in South India, *Science of Total Environment* **431**, pp. 323-331.

ASSESSMENT OF PARTICULATE MATTER (PM_{10}) AND CHARACTERISATION OF ALLIED MAJOR CHEMICAL COMPONENTS OF MUMBAI CITY, INDIA

ABHAYSINH SALUNKHE#*, INDRANI GUPTA#, SUGANDHA SHETYE*
AND RAKESH KUMAR#

National Environmental Engineering Research Institute, CSIR, Worli, Mumbai –400 018, India.
* K.J.Somaiya College of Science and Commerce, Vidyanagar, Vidyvihar Mumbai-400 077
E mail: abhay.salunkhe@rediffmail.com, i_gupta@neeri.res.in,
sudhashetye@gmail.com, r_kumar@neeri.res.in

Keywords: HEAVY METAL, ENRICHMENT FACTOR, PCA, CLUSTER ANALYSIS

INTRODUCTION

Particulate Matter in recent past has been considered one of the most potent pollutants with regard to its impact on human health. PM with aerodynamic diameter less than 10 µm (PM_{10}) has been shown to be associated with increases in mortality *(*Schwartz *et al.*, 1996). In addition, many researchers, scientists have observed higher rates of hospitalizations, emergency room visits and doctors visits for respiratory illnesses like asthma or cardiovascular diseases during times of high PM concentrations (Kuo *et al.* 2002). The present study examines the qualitative contribution of local emission sources contributing to aerosol mass. The objectives of the study were as (a) Evaluation PM_{10} levels in Mumbai with different land use pattern (b) Chemical characterization of the different chemical components (such as Heavy metals, water soluble inorganic ionic and carbonaceous species) associated with the collected PM_{10} mass (c) Source distribution of PM_{10} using statistical tools such as factor and cluster analysis for these sites.

STUDY AREA, ANALYTICAL METHODOLOGY

In the present study, PM_{10} was measured at Colaba was designated as Control site, Dadar as Kerb cum commercial site**,** Khar as residential site and Mahul as industrial site during Summer, post monsoon and winter season of 2007-2008. PM_{10} was collected to represent 24hrs sample using a glass fiber filter (8X10"pall life science GF/A) with the help of Envirotech Respirable dust Sampler (Model APM460NL). The concentrations of 11 metals in collected samples were determined by Inductive Coupled Plasma Atomic Emission Spectroscopy (ICP-AES) (Compendium Method IO 3.4, 3.1).Small portion (47mm) of exposed filter papers were subjected to extraction using ultra pure distilled water in ultrasonic bath for 60 minutes followed by the syringe filtration. Samples were then analyzed on Ion chromatograph (Dionex Corp. Model-ICS3000) (CARB SOP-064)**.** For water soluble carbonaceous species analysis, same water extract was analyzed for Total carbon (TC) and Inorganic carbon (IC) in terms of soluble Carbonate and Bicarbonate using TOC Analyzer (TOC-V CSH/ CSN, Shimadzu, Japan, Karthikeyan et al.,2005). Here TC was considered as Water soluble Total carbon (WSTC) and IC as Water soluble inorganic carbon (WSIC).Therefore Water Soluble Organic Carbon (WSOC) was calculated by subtracting the total carbon from inorganic carbon.

STATISTICAL ANALYSIS

Principal component analysis (PCA) and cluster analysis (CA) are the most common multivariate statistical methods used in atmospheric deposition studies to explore associations and origins of

trace elements and air pollutants (Ragosta *et al.*, 2008). PCA was applied to the characterization data of PM_{10} concentrations using Varimax rotated method in SPSS statistical software. Based on the matrix of principle component loading for each element, the sources were determined. The hierarchical CA was conduced to identify relatively homogeneous groups of variables, before CA, the variables were standardized by means of Z-scores; and then Euclidean distances for similarities in the variables were calculated.

RESULTS AND DISCUSSION

From three seasons average, the highest concentration of PM_{10} was (191 μg/m^3) observed at industrial site and lowest at control site (120 μg/m^3) (Table 1). The average values at all the four sites exceeded the CPCB National Ambient Air Quality standards. During winter, the exceedance was found to be 100% for Dadar, Khar and Mahul; whereas it was 88% for Colaba.

Total percentages of anion in PM_{10} were 19, 14, 13, and 12% at Colaba, Dadar, Khar and Mahul respectively, whereas percentage of cations was 6% at Colaba and 5% each at other sites. Formation of Secondary Organic Aerosols (SOA) is the major source for WSOC. WSOC particles are part of OC fractions that are directly emitted from sources such as fossil fuel combustion, biomass burning, industrial emissions, along with the natural source such as soil (Zhang *et al.* 2008). Soil is enriched with Organic Matter (OM) such as Humic Acid and Fulvic acids. They are also termed as HULIS i.e. Humic like Substances (Graber *et al.* 2006).

	Colaba		Dadar		Khar		Mahul	
	Average	**Std.dev**	**Average**	**Std.dev**	**Average**	**Std.dev**	**Average**	**Std.dev**
PM_{10}	120	71	157	62	178	103	191	67
Cr	0.018	0.02	0.033	0.037	0.027	0.021	0.04	0.031
Cu	0.037	0.034	0.069	0.027	0.077	0.043	0.078	0.03
Cd	0.04	0.035	0.048	0.04	0.052	0.044	0.058	0.045
Co	0.027	0.016	0.029	0.017	0.038	0.014	0.042	0.011
Fe	2.145	2.053	3.633	2.569	3.649	2.451	4.092	2.315
Mn	0.109	0.056	0.143	0.056	0.146	0.052	0.168	0.05
Ni	0.033	0.025	0.038	0.019	0.026	0.016	0.039	0.023
Pb	0.454	0.389	0.481	0.383	0.601	0.507	0.741	0.573
Zn	1.515	1.04	1.748	1.327	1.806	1.326	2.457	2.135
F^-	0.159	0.504	0.171	0.288	0.052	0.048	0.086	0.05
Cl^-	3.546	3.876	3.944	1.704	3.322	2.099	3.71	1.105
SO_4^{-2}	10.27	4.462	9.969	5.128	11.219	7.16	10.931	5.501
NO_3^-	6.374	4.081	9.032	5.817	7.88	5.575	8.222	5.226
PO_4^{-2}	0.06	0.092	0.041	0.062	—	—	0.054	0.084
Na^+	1.718	0.763	1.427	0.642	1.714	0.976	1.616	0.656
NH_4^+	1.924	1.742	2.698	2.07	1.752	2.161	2.671	2.358
K^+	0.679	0.685	0.947	0.561	0.796	0.777	1.055	0.894
Mg^{+2}	0.196	0.157	0.315	0.088	0.305	0.094	0.327	0.128
Ca^{+2}	1.654	1.222	2.785	1.185	1.017	1.318	3.003	1.604
WSTC	5.776	2.945	6.966	2.953	8.956	4.647	7.287	3.253
WSIC	1.131	0.512	1.688	0.575	1.91	0.775	1.887	0.528
WSOC	4.646	3.099	5.279	3.155	7.046	4.502	5.4	3.54

** Less Count Indicates Parameters was not detected at particular season Note*: All Concentrations in μg/m^3

Table 1: Seasonal Average of PM_{10} mass and its Chemical Composition at 4 sites

In winter highest concentration of Cd was observed at Khar (0.101 μg/m^3), which may be due to wind dispersion from Dharavi where small scale industries such as scrap and smelting industries are operating. Cd content in PM_{10} was higher during post monsoon sampling at Mahul station. Cr was higher at Mahul as compared to other sites during winter (0.054 μg/m^3) and post-monsoon (0.058 μg/m^3). During winter, highest Cu concentrations was observed at Khar (0.116μg/m^3) followed by Mahul (0.103 μg/m^3), Dadar (0.078μg/m^3) and Colaba (0.055μg/m^3). From the average seasonal concentration of Co it can be observed that Highest concentration of Co in post-monsoon and winter at Mahul was 0.041, and 0.043 μg/m^3 and next highest at Khar 0.031, 0.044 μg/m^3. Mn concentrations observed in winter were, Mahul (0.166 μg/m^3), Khar (0.146 μg/m^3), Dadar (0.143 μg/m^3) and Colaba (0.109 μg/m^3). Fe emission was higher at Dadar site (5.485 μg/m^3) during winter and at Mahul (5.181μg/m^3) during post monsoon. Highest values of Ni were observed during post-monsoon at Mahul, Colaba, Dadar and Khar were 0.068, 0.059, 0.055 and 0.041 μg/m^3 correspondingly. Most of the time, the concentrations exceeded the NAQM standard at all sites. Lead during winter it is highest at Khar (1.090 μg/m^3) followed by Mahul (1.085 μg/m^3). Mahul showed high values of Zn during post monsoon (2.046μg/m^3) and winter (4.056μg/m^3).

ENRICHMENT FACTOR (EF) ANALYSIS

EF analysis is one of the most popular receptor techniques in data analysis of particulate matter (Feng *et al.*, 2009*;* Huang *et al*., 2010*;* Kothai *et al.*, 2009). If the EF of an element close to 1, it suggests that atmospheric particulate matters are emitted mainly from soil or weathered rocks. The element with EF less than 1 was Mn which is mainly from natural sources. EF value of Pb shows that even after implementation of Pb free fuel in Mumbai, there is still enrichment of Pb in atmospheric PM. The probable source for this could be the presence of Pb in the road side soil, which gets dispersed in air by the mechanical chain of re suspension of soil. To some extent, trash burning activity and fuel adulteration in vehicles could be responsible for Pb emission in air. Metals like Pb and Cd are considered relatively volatile metals and because they are mainly transported through the atmosphere, they have been termed as Atmophile Elements**.** EF values of Zn are found to be 684 at Colaba, 311 at Khar, 292 at Mahul and 271 at Dadar. Likewise EF of Cu was higher at Colaba (246) followed by Khar (70), Dadar (55) and Mahul (54). High enrichment of Zn and Cu could be due to the heavy duty diesel vehicles. Cobalt (Co) metal is the tracer of industrial emission which shows moderate enrichment in PM_{10}. Highest value is observed at Colaba (28); and lowest at Dadar (14).

CONCLUSIONS

Mass concentration of PM_{10} shows very high values at all location in all season. From the enrichment analysis, it is marked that high enrichment of metals is almost at all sites, the reason for this could be the effect of meteorology and trans-boundary movement of pollutants. Geographically, Colaba is located in the downwind direction of Mahul, wind carry all the pollutants resulting into the high enrichment of these metals at Colaba along with some localized sources of emission. Multivariate statistical analysis was used to analyze the elemental data obtained from four sites in Mumbai. At all four location common sources identified were Vegetative burning, secondary aerosol, break ware, Residual oil combustion, smelting, Natural soil, Vehicles tyres wear- road dust and marine aerosol. Findings indicate that most of the sites were dominated by local sources based on activities in the vicinity of the sampling locations. Overall action plan preparation will need to concentrate on local sources as priority, as reduction of these source strengths, will give maximum benefit in terms of lower exposure from air pollution.

Site	Sources Identified by PCA	Sources Identified by CA
Colaba Control site	Vegetative burning, Sec. Aerosol, Residual Oil Combustion, Smelting, Oil Combustion, vehicle tier ware, Marine Aerosol, Re- suspension of Road dust	Marine Aerosol, Residual Oil Combustion, Coal Combustion, Vehicular Emission, Biomass Burning and secondary aerosol, Soil/Road Dust
Dadar Kerb cum commercial site	Road Dust, Vehicular Emission, Sec. Aerosol, Biomass Burning, Wear and Tear of Vehicle Tyres, Heavy Fuel Oil, Brake Wear, Concrete Dust	Marine Aerosol, Concrete Dust, Break Ware and Traffic, Heavy Fuel Oil, Coal, Biomass Burning, Sec.Aerosol, Road Dust
Khar Residential Site	Coal burning, Smelting, Sec. Aerosol, Biomass Burning, Vehicular Emission, Road Dust, Marine Aerosol	Marine aerosol, Concrete dust, Vegetative burning, Coal burning, Vehicle ware, Sec.Aerosol, Motor Vehicle
Mahul Industrial Site	Motor Vehicles, Vegetative Burning, Paved Road Dust, Concrete, Marine Aerosol, Traffic and brake wear	Smelting, Vegetative Burning, Paved Road Dust, Vehicles

REFERENCES

1:1 U.S. Environmental Protection Agency, (1998a). National Air Quality and Emissions Trends Report, 1997. EPA 454/R-98-016, December.

CARB SOP-064-California Environmental Protection Agency Air resource Board, SOP MLD 064 Standard Operating Procedure for the Analysis of Anions and Cations in $PM_{2.5}$ Speciation Sample By Ion Chromatography.

Compendium Method IO – 3.4, (June 1999). Determination of metals in ambient particulate matter using Inductively Coupled Plasma (ICP) Spectroscopy, Compendium of Methods for the determination of Inorganic Compounds in Ambient Air, Center for Environmental Research Information, US EPA.

Compendium Method IO – 3.1, (June 1999). Selection, Preparation and Extraction of filter material. Compendium of Methods for the determination of Inorganic Compounds in Ambient Air, Center for Environmental Research Information, US EPA.

Feng, X. D., Dang, Z., Huang, W. L. and Yang, C. (2009). Chemical Speciation of Fine Particle Bound Trace Metals, *International Journal of Environmental Science and Technology*, **6 (3)**, pp. 337-346.

Graber, E. and Rudich, Y. (2006). Atmospheric HULIS: How Humic-like are they? A Comprehensive and Critical Review, *Atmospheric Chemistry Physic.*, **6**, pp. 729–753.

Huang, L., Wang, K., Yuan, C. S., and Wang, G. (2010). Study on the Seasonal Variation and Source Apportionment of PM_{10} in Harbin, China, *Aerosol and Air Quality Research*, **10**, pp. 86–93.

Karthikeyan, S. and Balasubramanian, R. (2005). Rapid Extraction of Water Soluble Organic Compound from Airborne Particulate Matter, *Journal of Analytical Sciences*, **21**, pp. 1505-1508.

Kothai, P., Prathibha, P., Saradhi, I. V., Pandit, G. G. and Puranik, V.D. (2009). Characterization of Atmospheric Particulate Matter Using PIXE Technique, *International Journal of Environmental Science and Engineering*,

Kuo, H.W., Lai, J. S., Lee, M. C., Tai, R.C. (2002). Respiratory effects of air pollutants among asthmatics in central Taiwan, *Arch Environ Health*, **57**, pp.194–200.

Ragosta, M., Caggiano, R., Macchiato, M., Sabia, S., Trippetta, S. (2008). Trace elements in daily collected aerosol: level characterization and source identification in a four-year study, *Atmospheric Research*, **89**, pp. 206–217.

Schwartz, J., Dockery, D.W., Neas, L.M.(1996). Is daily mortality associated specifically with fine particles? *Journal of Air and Waste Management Association*, **46**, pp. 927–939.

Zhang Y., Quraishi, T. and Jay Schauer, J. (2008). Daily Variations in Sources of Carbonaceous Aerosol in Lahore, Pakistan during a High Pollution Spring Episode, *Air Quality Research*, **8**, 2, pp. 130-146.

SOURCE APPORTIONMENT OF PM_{10} AT AN INDUSTRIAL TOWN OF MAHARASHTRA, TARAPUR, INDIA

P. KOTHAI, SUNIL BHALKE, R.C. BHANGARE, S.K. SAHU, I.V. SARADHI, G.G. PANDIT AND V.D. PURANIK

Environmental Assessment Division, Bhabha Atomic Research Centre,
Trombay, Mumbai – 400 085, India

Keywords: PM10, SOURCE APPORTIONMENT, FA-MLR

INTRODUCTION

The air pollution resulting from rapid industrialization and urbanization has prompted increased attention to its influence on the global atmospheric environment (Kulshreshta *et al.*, 2001). Over the past 20 years, epidemiological studies have demonstrated that ambient particulate pollution is associated with mortality and morbidity. Elevated concentrations of particulate matter impact health, and the magnitude of the health impacts are strongly dependent on particle size and composition. Urbanisation is an index of transformation from traditional rural economies to modern industrial one and the subsequent increase in particulate emission. Even though megacities will play a significant role in India's urban future, patterns of growth suggest that most of India's urbanisation will take place in smaller cities and towns. The application of effective abatement strategies to reduce PM levels is only possible when the emission sources have been uniquely identified and characterized (Viana *et al.*, 2006). The dominant approaches to the identification and the quantitative apportionment of the sources of particulate matter in the atmosphere are the multivariate methods or various receptor modeling techniques such as Factor Analysis – Multiple Linear Regression (FA-MLR) and Positive Matrix Factorization (PMF). In the present study particulate matter of size fraction $d \approx 10\mu m$ were collected at Tarapur and the possible sources of contribution were identified and apportioned using FA-MLR receptor model technique.

METHODS

The sampling site Tarapur is a census town located at 17.7 ^{o}N and 75.47 ^{o}E in the Indian state of Maharashtra near at a distance of about 45km north of Mumbai. Tarapur inhouses one of the major industrial estates of Maharashtra Industrial Development Corporation (MIDC) named as Tarapur Industrial Estate situated at a distance of approximately 12km from the sampling point, which comprise large percentage of chemical and pharmaceutical manufacturing units, steel plants, textile plants, Glass, rubber and some plastic manufacturing industries. The sampling was carried out using a High Volume Sampler (HVS–410, Envirotech). Particulate Matter was collected on pre– desiccated glass fibre filters. Acid digestion, required for the metal determination by Atomic Absorption Spectrometry (AAS), was carried out using HNO_3 and Perchloric acid. Subsequently samples were analysed for various trace metals using AAS.

Principal component analysis (PCA) is one of the receptor model technique builds on the variability of the PM components (Trace Metals) at the receptor site and seeks to determine the matrices A and S in the equation $C = A \times S$, where C represents the concentrations of the various Particulate Matter components, S the source contributions and A the source profiles. A Varimax normalised rotation is

applied to maximise (or minimise) the values of the loading factors of each compound analysed in relation to each rotated principal component. Quantification of the source contributions is then performed by multi-linear regression analysis (MLRA), using absolute score factors as source tracers.

RESULTS

Annual arithmetic mean concentration and standard deviation of PM_{10} observed at Tarapur is 59.9 $\mu g/m^3$ and 20.7 $\mu g/m^3$ respectively. The highest concentration at the study place is found to be 117.9 $\mu g/m^3$ during the month of January, and the lowest concentration was about 32.7 $\mu g/m^3$ observed in the month of July. Mass concentrations of PM_{10} fraction, obtained in four seasonal campaigns during 2007/2008 show significant variations with high concentrations during winter season.

Varimax based FA was performed to identify the major contributing sources in the study area (Kothai *et al.*, 2011). Sensitivity analysis was carried out prior to FA application on the entire data set. Extraordinarily high or low concentration values were not observed in any individual samples and hence all the 14 elements analyzed were included in the FA study. The lowest eigen value for the factors extracted was restricted to 1.0. Six sources were resolved using the above mentioned receptor technique. The first component was loaded with Ca, Fe, Mg and Mn representing this as crustal originated source. The second component found to be with high loadings of As and Se, which are the signature elements of thermal power plants. The third factor identified was marine source with the maximum loadings of Na and K. Industrial sources were resolved into three main sources such as textile, rubber and steel with high loadings of Cu-Pb, Co-Zn and Cr-Fe-Ni respectively. The details of factor loadings are presented in table 1. Further, the percentage contribution of each source was estimated by following Multiple Linear Regression technique based on Absolute Principal Component Analysis method described by Thurston and Sprunger, (1985). The study showed major contribution of PM, 17-18% from natural sources such as crustal and marine emissions. Second highest contribution of 12% was estimated as due to thermal power plant. The detailed contributions by different sources are presented in Fig. 1.

Element	Crustal	Thermal	Marine	Textile pigment	Rubber	Steel	communality
As	0.194	**0.949**	0.071	0.076	0.07	0.169	0.983
Ca	**0.85**	0.199	0.157	0.191	0.197	0.261	0.93
Co	0.263	0.089	0.228	0.221	**0.88**	0.147	0.973
Cr	0.39	0.194	0.204	0.229	0.15	**0.808**	0.958
Cu	0.338	0.058	0.163	**0.863**	0.236	0.154	0.967
Fe	**0.851**	0.201	0.2	0.308	0.175	**0.512**	0.976
K	0.279	0.054	**0.861**	0.137	0.274	0.216	0.963
Mg	**0.792**	0.197	0.292	0.281	0.226	0.168	0.91
Mn	**0.802**	0.216	0.3	0.234	0.149	0.261	0.925
Na	0.37	0.118	**0.764**	0.228	0.359	0.208	0.957
Ni	0.386	0.321	0.354	0.225	0.196	**0.684**	0.934
Pb	0.391	0.188	0.213	**0.764**	0.269	0.257	0.955
Se	0.21	**0.95**	0.066	0.092	0.089	0.112	0.98
Zn	0.194	0.127	0.479	0.27	**0.758**	0.128	0.947
% Var	62.81	11.97	7.77	5.67	4.2	2.94	Total= 95.360

Table 1. Principal Component Analysis with varimax rotation for PM10

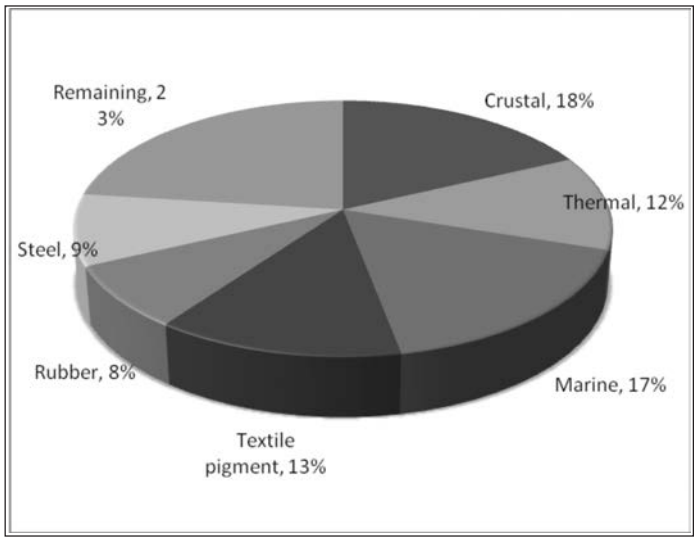

Figure 1. Source apportionment of PM10 sources using FA-MLR technique.

CONCLUSIONS

In the present work chemical characterisation and source apportionment of PM10 at an industrial town, Tarapur, has been performed. Factor Analysis technique was used to determine the main particulate matter sources at the study area. Six major sources resolved by the receptor model technique are crustal, marine, thermal power plant, textile, rubber and steel plant emissions with the percentage contribution of 18, 17,12,3,8 and 9 respectively.

REFERENCES

Kothai, P., Saradhi, I.V., Pandit, G.G., Markwitz, A. and Puranik, V. D. (2011). Chemical Characterization and Source Identification of Particulate Matter at an Urban Site of Navi Mumbai, India, Aerosol and Air Quality Research, **11**, 560.

Kulshrestha, U.C., Jain, Monika, Sekar, R., Vairamani, M., Sarkar, A. K. and Parashar, D. C. (2001). Chemical Characteristics and Source Apportionment of Aerosols over Indian Ocean during INDOEX-1999, Current *Science*, **(Supplement) 80**, 180.

Thurston, G. D. and Spengler, J.D. (1985). A quantitative assessment of source contributions to inhalable particulate matter pollution in metropolitan Boston, *Atmos. Environ.*,**19**, 9.

Viana, M., Querol, X., Alastuey, A., Gil, J.I., and Menendez. M. (2006). Identification of PM Sources by Principal Component Analysis (PCA) Coupled with Wind Direction data, *Chemosphere*, **65**, 2411.

CHEMICAL CHARACTERISTICS OF SUMMER AEROSOLS OVER THE COASTAL ANTARCTICA

P.S.P. RAO[1], K. B. BUDHAVANT [2], AND P. D. SAFAI[1]

[1]Indian Institute of Tropical Meteorology, Pune, India
[2]Vishwakarma Institute of Technology, Pune, India

Keywords: ANTARCTIC AEROSOLS, PM_{10} AND $PM_{2.5}$, CHEMICAL COMPOSITION, LONG RANGE TRANSPORT

INTRODUCTION

Atmospheric aerosols play a significant role in the understanding of both global and regional climate effects. These include their number concentration, mass, size, chemical composition, aerodynamic and optical properties. The chemical composition of aerosols is the manifestation of the chemical state of the atmosphere at any place. In fact, the study of the chemical constituents of aerosols helps in assessing the causes behind acidic/alkaline nature of the aerosols (Safai *et al.*, 2010). Antarctica is one of the cleanest places on earth and therefore the observation over this region gives a great opportunity to study properties of aerosols, which are not influenced by anthropogenic activities (Shaw, 1998, Asmi *et al.*, 2010). Therefore a better understanding of Antarctic aerosols gives us an idea of the impact of human activities on atmospheric aerosols. In the present study, an effort has been made to estimate the chemical characteristics of aerosols in both fine ($PM_{2.5}$) and coarse (PM_{10}) sizes over the coastal Antarctica during 29th Indian Antarctic Expedition (summer 2009-10).

SAMPLING AND ANALYSIS

PM_{10} and $PM_{2.5}$ Aerosol samples were collected during 12 December 2009 to 4 February 2010 at LH using an air sampler (Envirotech Pvt. Ltd., India). Twenty samples (ten each of PM_{10} and $PM_{2.5}$) at about 48 hours sampling period for each sample, were collected. Also three PM_{10} samples were collected over Indian Ocean during the cruise period. Samples were collected on the front side of the uppermost deck (30 m above sea level) of the ship to avoid any contamination from sea spray and ship's exhaust. Filter papers used for the collection of PM_{10} and $PM_{2.5}$ were Whatman- 40 and Teflon Micro Fibre (2 ìm PTFE) filters, respectively.

All the $PM_{2.5}$ and PM_{10} filter samples were extracted for water and acid soluble components by using deionised water and diluted HCl, respectively, using a standard Soxhalet extractor. The major and trace metals i.e., Na, K, Ca, Mg, Fe, Al, Sr, Sb, Zn, Mn, Cu and Pb were determined by using Atomic Absorption Spectrometer (AAS) and major anions i.e., Cl, SO_4 and NO_3 were measured by using Ion Chromatograph. NH_4 was measured by the colorimetric method using UV- visible spectrophotometer.

RESULTS AND DISCUSSION

Chemical Composition of aerosols

The mean total mass concentrations of PM_{10} and $PM_{2.5}$ along with their chemical constituents over the Indian Ocean and Coastal Antarctica are shown in Table 1.

Element / Radical	PM_{10} (Ind. Ocean)	PM_{10} (Ant. Coast)	$PM_{2.5}$ (Ant. Coast)	($PM_{10"2.5}$) Ant. Coast
Mass (μg/m^3)	13.4 ±5.28	5.13 ±1.46	4.30 ±1.54	0.83
Na	2933 ±1090	279 ±148	138 ±50.7	141
K	220 ±136	21.4 ±12.0	8.4 ±5.85	13
Ca	290 ±142	93.3 ±52.3	20.3 ±12.8	73.1
Mg	342 ±251	44.8 ±19.5	12.0 ±8.6	29.7
NH_4	290 ±142	142 ±68.1	99.6 ±48.3	42.3
Cl	5426 ±2135	538 ±305	261 ±86.2	276
NO_3	70.1 ±56.8	30.1 ±26.1	10.5 ±4.11	19.6
SO_4	1371 ±579	321 ±157	250 ±102	70.2
Nss SO_4	1004 ±393	286 ±146	233 ±109	53.1
Fe	188 ±99	96.8 ±61.7	45.2 ±12.4	51.6
Al	177 ±75	79.7 ±38.5	27.2 ±13.7	52.5
Cu	9.02 ±5.8	2.19 ±0.53	1.28 ±1.23	0.91
Mn	12.7 ±8.8	4.08 ±2.66	2.77 ±0.80	1.31
Zn	18.8 ±13.3	9.04 ±4.30	5.51 ±8.32	3.53
Sb	17.5 ±13.3	16.7 ±6.14	11.8 ±6.33	4.92
Sr	0.72 ±0.31	0.39 ±0.21	0.25 ±0.10	0.14
Pb	0.58 ±0.19	0.26 ±0.18	0.12 ±0.10	0.14
*NH_4/nss SO_4	0.77	1.52	1.12	-

* Equivalent ratio of NH_4^+/nss SO_4, Ind.- Indian, Ant.- Antarctic

Table 1. Average chemical Composition of aerosols (ng/m^3) over the Coastal Antarctica during summer 2009-10

The average concentration for PM_{10} over Indian Ocean was found to be 13.4 μg m^{-3}and that over coastal Antarctica was 5.13 μg m^{-3} indicating the impact of marine sources, especially sea salt over the Indian Ocean. Over the Antarctica coast, the concentration of $PM_{2.5}$ was 4.30 μg m^{-3}. The difference between the concentrations in PM_{10} and those in $PM_{2.5}$, i.e., $PM_{10-2.5}$ is the actual contribution of the coarse fraction. All the ionic concentrations in PM_{10} were found to be less over Antarctica coast than over Indian Ocean indicating the atmosphere is more pristine over Antarctica than over Indian Ocean. The concentrations of Sea salt and crustal originated components (i.e., Na, Cl, K, Ca, Mg, Fe and Al) were found to be high in coarse aerosols than in fine aerosols. High concentration of NO_3^- in coarse ($PM_{10-2.5}$) size at Antarctic coast indicates its presence in $NaNO_3$ (salt) form rather than acidic i.e HNO_3 form. The anthropogenically originated components (SO_4, NH_4, Sr, Sb, Zn, Mn, Cu and Pb) were higher in fine size than in coarse size aerosols.

The concentrations of nssSO_4 and NH_4 were higher in fine size i.e in $PM_{2.5}$ (332.6 ng/m^3) than in coarse ($PM_{10"}PM_{2.5}$) size (95.4 ng/m^3) over the Antarctic coast, where as over the Indian Ocean contribution of these two constituents in PM_{10} was 1294 ng/m^3 which is nearly three times higher than that over coastal Antarctica (428 ng/m^3). This indicates that the anthropogenic contribution is

three times less over Antarctica than over Indian Ocean possibly due to the proximity of Indian Ocean with anthropogenic sources of Northern Hemisphere. Among the trace metals, Al, Fe and Sb were found to be high than the other metallic components i.e, Cu, Mn, Zn, Sr and Pb which also indicates the low anthropogenic pollution over Antarctica.

The percentage contributions of ionic components to the total ions in PM_{10} over the Indian Ocean and at coastal Antarctica location (LH) are shown in Fig. 1.

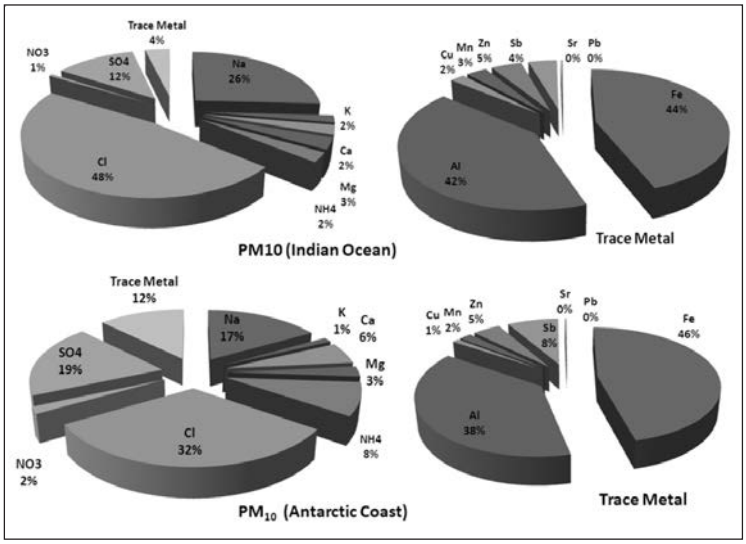

Figure 1. Percentage contribution of ionic species to the total measured ions in PM_{10} over Indian Ocean and Antarctic coast

Contribution of marine components i.e. Na, Cl and Mg were dominant over Indian Ocean (77%) than over coastal Antarctica (52%). Sea spray is generated by the wind stress on the ocean surface. Over the Antarctic coast, for coarse particles ($PM_{10"}PM_{2.5}$), among all the ions, Cl (42%) showed maximum concentration followed by Na, Ca, SO_4, NH_4, Mg, NO_3, and K (2%). Similarly for fine particles ($PM_{2.5}$), Cl (33%) showed maximum concentration followed by SO_4 (31%), Na, NH_4, Ca, Mg, NO_3 and K.

The NH_4/nss-SO_4 ratio of 1.12 in $PM_{2.5}$ over Antarctica indicates that the NH_4 and SO_4 ions were in the form of NH_4SO_4. It was observed that about 73 % contribution of SO_4 aerosols was from anthropogenic sources and 27 % from marine source over the Indian Ocean. In coastal Antarctica, only 8 % of SO_4 aerosols were observed from marine source and 92% from anthropogenic sources. This significant excess sulphate over the coastal Antarctic may mainly be due to oxidation of dimethyl sulphide (DMS) produced from the oceans due to biogenic process and partly due to long range transport.

CONCLUSIONS

Concentrations of both fine ($PM_{2.5}$) and coarse (PM_{10}) aerosols were very low at coastal Antarctic station. Na and Cl were the major ionic constituents of aerosols. Concentrations of trace metals were very low indicating less anthropogenic activity over this region. NH_4 and SO_4 were in the form of $(NH_4)_2SO_4$. Neutralization of acidity of aerosols was mainly due to NH_4 and Ca however the acidity

was not completely neutralized by them and both fine and coarse aerosols showed acidic nature. Overall it is evident that the coastal Antarctica represents one of the least polluted environments on the Earth.

ACKNOWLEDGMENTS

Authors are grateful to the Director, IITM, Pune, India for the support and encouragement given to undertake this work. Thanks are also due to the National Centre for Antarctic and Ocean Research (NCAOR) and Ministry of Earth Sciences (MoES) for giving opportunity to participate in the 29th Indian Antarctic Expedition.

REFERENCES

Asmi, E., Frey, A., Virkkula, A., Ehn, M., Manninen, H.E., Timonen, H., Tolonen-Kivimaki, O., Aurela, M., Hillamo, R., Kulmala, M. (2010). Hygroscopicity and chemical composition of Antarctic sub-micrometre aerosol particles and observations of new particle formation, Atmos. Chem. Phys. **10**, pp. 4253–4271.

Safai, P.D., Budhavant, K.B., Rao, P.S.P., Ali, K., Sinha, A. (2010). Source characterization for aerosol constituents and changing roles of calcium and ammonium aerosols in the neutralization of aerosol acidity at a semi-urban site in SW India, Atmos. Res., **98**, pp. 78-88.

Shaw, G.E. (1998). Antarctic aerosols: a review, Reviews of Geophys.,**26**, pp. 89-112.

MULTI-POLLUTANT EMISSIONS INVENTORY FOR THE RESIDENTIAL SECTOR IN INDIA

P. SADAVARTE[1], A. PANDEY[1], C. VENKATARAMAN[1,2]

[1]Department of Chemical Engineering, Indian Institute of Technology Bombay, Powai, Mumbai-400076.

[2]Centre of Excellence in Climate Studies, Indian Institute of Technology Bombay, Powai, Mumbai-400076.

Keywords: EMISSION INVENTORY, RESIDENTIAL COOKING, AEROSOLS, GHGS, OZONE PRECURSORS

BACKGROUND AND MOTIVATION

Emission inventories are an important tool to quantify pollutants from energy sources for climate and air-quality assessment and modeling. The total impact or mitigation potential related to a given sector or source, requires treatment of the emitted basket of multiple pollutants, which could affect both air-quality and climate. The highest level of detail (IPCC guidelines, 2006), Tier 3, prescribes incorporation of fuel consumption data at individual facility level, for area sources, or sources which are numerous like residential, with specific details in combustion technology. Previous studies for India, have addressed only specific pollutants, i.e. aerosols and aerosol precursors (Reddy and Venkataraman, 2002, Habib *et al*., 2004), trace gases (Garg *et al*., 2006), using different energy-use assumptions, typically with a low to medium level of technology detail.

The residential sector is a large source of biofuel consumption in India. Particularly, biofuel is used extensively for cooking in rural areas, using traditional cookstoves which are often highly polluting (Venkataraman *et al*., 2010). The household combustion of biofuels causes indoor air pollution associated with chronic respiratory ailments and lung cancer in women and children (Ezzati, 2004). In addition, the use of kerosene wick-lamps for lighting also causes significant emission of pollutants. Therefore, this work attempts incorporation of detailed sector specific information to estimate emissions of multiple pollutants of relevance to both climate and air quality, from cooking and lighting in the Indian residential sector.

METHODOLOGY

Fuel consumption data for cooking is calculated using a bottom up approach (see Fig. 1), by estimating end use energy consumption for cooking.

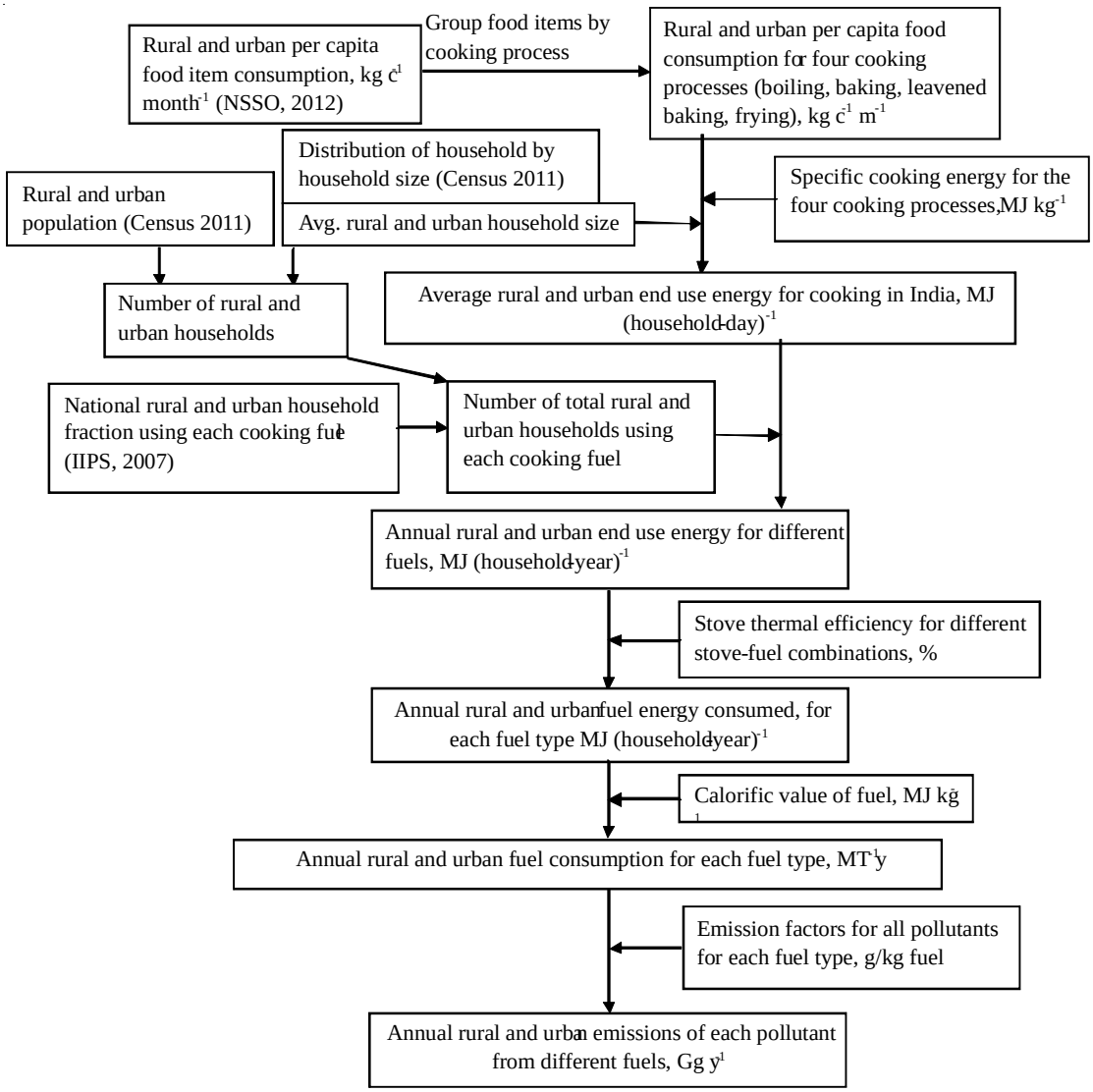

Figure 1. Methodology for emissions estimate from residential cooking.

The food items reported in consumption data from NSSO, (2012) are regrouped based on the primary cooking process used for their preparation, to calculate end use energy consumption by applying process specific cooking energy. An average household size of 5 is used for rural and urban areas (estimated size was: rural-4.93 and urban-4.61). It was observed that the efficiency and emission characteristics of the various combustion technologies (stove types) used for a fuel do not differ significantly. They are therefore, replaced with a single *representative* baseline technology (weighted average of device efficiency for all the major technologies is used). Appropriate emission factors are selected/derived according to the fuel and technology characteristics.

State wise rural and urban fraction of households with electricity which also use kerosene The amount of kerosene used for lighting is estimated from fraction of households using kerosene primarily, total number of households and fraction of electrical load shedding in both rural and urban regions (Fig. 2).

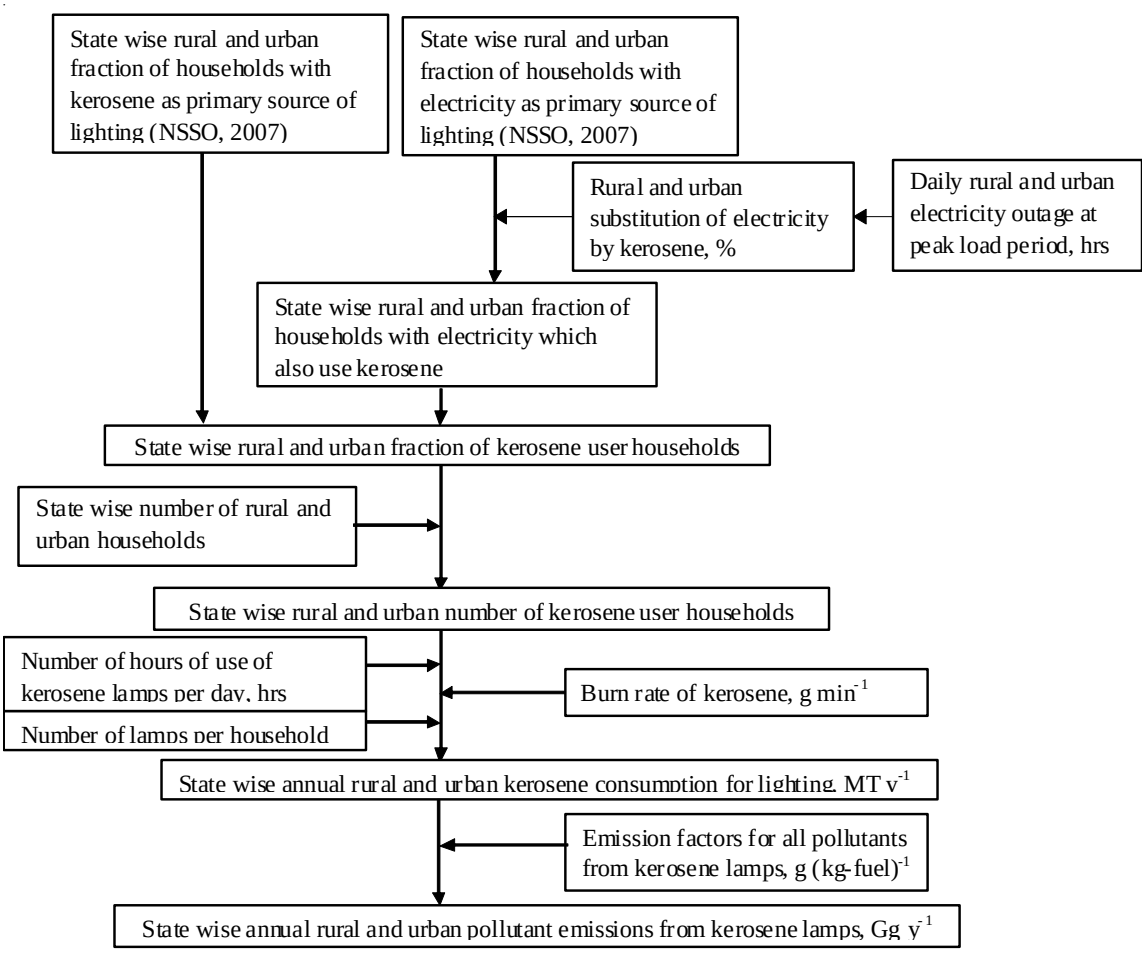

Figure 2. Methodology for emissions estimate from residential kerosene lighting.

Assumptions for number of lamps per household and their daily usage are made from our impression of household lighting requirement and evening load shedding data respectively. Measured burn rate and emission factors depicting the combustion technology for kerosene lamps are used.

PRELIMINARY RESULTS

Preliminary results relate to emissions for the year 2010, using the most recently available activity data (Figure 3), from residential cooking. Wood combustion in traditional baseline biofuel stoves is the largest contributor to emissions of all pollutants, except for SO_2, which is emitted by the fossil fuels (LPG, kerosene and coal) used for cooking.

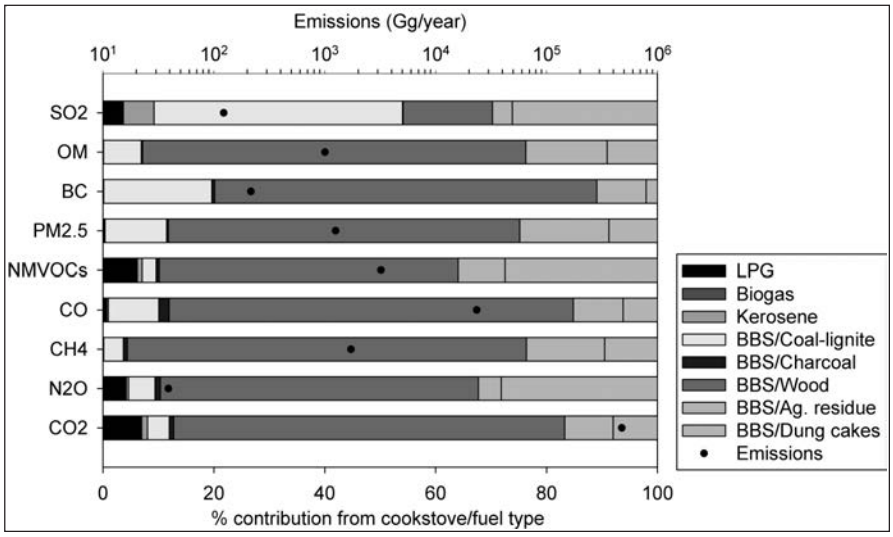

Figure 3. Indian emissions of aerosols, GHGs, ozone precursors for 2010, from residential cooking.

These emissions will be disaggregated further at state level and district level using population as the proxy and spatially distributed at fine resolution of 25km × 25km. Further analysis will be done by comparing different types of stoves and their contributions. Emissions from lighting activities will also be presented and discussed.

REFERENCES

Ezzati, M, Lopez, A.D., Rodgers, A,, Murray, C.J. (2004). Comparative quantification of health risks: The global and regional burden of disease attributable to selected major risk factors, Geneva: World Health Organization.

Garg, A., Shukla, P. R., and Kapshe, M. (2006). The sectoral trends of multi-gas emissions inventory of India, *Atmospheric Environment*, **40**, pp. 4608-4620.

Habib, G., Venkataraman, C., Shrivastava, M., Banerjee, R., Stehr, J. W., and Dickerson, R. R. (2004). New methodology for estimating biofuel consumption for cooking: Atmospheric emissions of black carbon and sulfur dioxide from India, *Global Biogeochemical Cycles*, **18**, doi: 10.1029/2003gb002157.

IPCC (Intergovernmental Panel on Climate Change) (2006), IPCC Guidelines for National Greenhouse gas Inventories, Vol2: Energy, Authors: Garg, A., Kazunari, K., Pulles, T.

Reddy, M. S., and Venkataraman, C. (2002a). Inventory of aerosol and sulphur dioxide emissions from India: I - Fossil fuel combustion, *Atmospheric Environment*, **36**, pp.677-697.

Smith KR (2000). National burden of disease in India from indoor air pollution. *Proc Natl Acad Sci USA*, **97**, pp. 13286–93.

Venkataraman, C., Sagar, A.D., Habib, G., Lam, N., Smith, K.R. (2010). The Indian National Initiative for Advanced Biomass Cookstoves: The benefits of clean combustion, *Energy for Sustainable Development*, **14**, pp. 63–72.

SURFACE OZONE LOSS: INTERACTION WITH POLYCYLIC AROMATIC HYDROCARBONS

VYOMA SINGLA, TRIPTI PACHAURI, JITENDRA DUBEY, APARNA SATSANGI, K. MAHARAJ KUMARI AND ANITA LAKHANI

Department of Chemistry, Dayalbagh Educational Institute,
Dayalbagh, Agra – 282110, India.
E-mail: anita.lakhani01@gmail.com

Keywords: OZONE LOSS, PAH, GAS-PARTICLE PARTITIONING, OZONOLYSIS

INTRODUCTION

The role of particulate matter in the atmosphere has elicited a great deal of recent interest due to the possible influence of heterogeneous interactions on the balance of trace gas species in the atmosphere. In the lower atmosphere, both organic and inorganic surface coatings of the particles can influence ozone interactions with aerosol (Usher, *et al.* 2003; Bonasoni, *et al.* 2004). Among organic species, particulate polycyclic aromatic hydrocarbons (PAHs) are known to possibly cause O_3 degradation. PAHs are present both in the vapour and particulate phases, especially aerosols with an aerodynamic diameter less than 2 μm. Low molecular weight PAHs tend to be more concentrated in the vapour phase, while the ones with higher molecular weight are often associated with particulates. They are introduced into the environment through natural and anthropogenic preocesses inolving incomplete combustion. The major natural sources of PAHs includes volcanic eruptions and forest and prairie fires while the anthropogenic sources include automobile exhaust and tire degradation; industrial emissions from catalytic cracking; air blowing of asphalt; coal combustion; tobacco smoking; domestic heating emissions from coal, oil, gas and wood; refuse incineration and biomass burning (Manoli, *et al.* 2000). In urban areas, automobile exhaust acts as one of the important source of PAHs and approximately 90% of PAH emissions are estimated from anthropogenic sources typically including the combustion of fossil fuels, industrial processes, and domestic heating systems (Rogge, *et al.*, 1993a; 1993b). These emissions comprises of both gas and particulate phase PAHs, where the latter reacts with O_3 rapidly and causes subsequent degradation. To understand the interactions between aerosol and photochemical oxidants in the ambient air of Agra, the effect of aerosols on tropospheric chemistry was studied with the focus on ozone loss by interaction with polycyclic aromatic hydrocarbons.

METHODS

The study was carried out at Dayalbagh, an urban site, which is 10 km away from the industrial sector of the Agra (27°102 N, 78°052 E, and 169 m.s.l.). Sampling was performed on the roof of Science Faculty building (8 m above the ground) in the Institute campus. Sampling for PAH was conducted over a period of 48-72 hr at an average flow rate of 1.2 m^3 min^{-1} on pre-desiccated and pre-weighed glass fibre filters (Whatman, EPM 2000) using a high volume sampler (HVS, Envirotech APM 430) ensuring sufficient collection of material to be within the detection limits. The filters were extracted thrice with aliquots of 50 ml HPLC grade dichloromethane (DCM) (Merck) by ultrasonication for 1 h. The samples were then filtered through Whatman filter paper. The extract

thus obtained was subjected to undergo cleanup process. The extract was loaded on the top of the column (10 cm x 1.0 cm i.d.) slurry packed with silica gel (Fluka 230 mesh). The column was eluted with DCM to give a fraction enriched with PAH. The PAH containing fraction was concentrated to 1.5 ml using Buchi rotary evaporator. The extract was stored in a Teflon vial at a low temperature until analysis of PAHs.PAHs were analyzed in the splitless mode using a temperature gradient program by Gas Chromagraph, GC-17A (Shimadzu 17AATF, version 3.0) equipped with a FID detector and capillary column (25 m length, 0.3 mm internal diameter: BP) with dimethyl polysiloxane as stationary phase. The GC was calibrated with a standard solution of 16 PAH compounds (Supelco EPA 610 PAH mixture).

RESULTS

Concentrations of O_3 and NO_2

Nitrogen dioxide has been regarded as one of the main traffic related air pollutant and a precursor to the formation of photochemical smog and ground level ozone (Finlayson Pitts and Pitts, 2000). Ozone on the other hand is a reactive atmospheric pollutant that plays role in the photochemical reaction in the troposphere. It is formed through a series of complex photohcmeical reactions among NOx and VOC in the presence of heat and sunlight (Pudasainee, *et al.* 2006).The concentration of O_3 varied from 47.3 µg m^{-3} to 103.3 µg m^{-3} with an average concentration of 76.8 ± 14.0 µg m^{-3}. The maximum concentrations of O_3 were observed in summer followed by winter with the minimum concentrations in monsoon. The maximum concentration in summer is attributed to higher in-situ photochemical formation through photolysis of NO_2 in presence of solar radiation. Comparatively higher O_3concentrations observed in winter might be due to build up of O_3 precursors as a result of low temperature. NO_2 concentration varied from as low as 12.8 µg m^{-3} to as high as 32.2 µg m^{-3} with the average concentration of 23.6 ± 4.6 µg m^{-3}. At this site, vehicular emissions serves as the main source of NO_2.

Concentrations of PAH

Table 1 gives the geometric mean concentration and standard deviation of TSPM, TPAH and individual PAH during the sampling period. Long sampling time was required to determine atmospheric PAH due to the fact that volatilization and/or chemical and physical transformations can lead to underestimated PAH concentrations. As expected, the more volatile compounds like Nap, Acy and Ace were generally not detected in most of the samples or were detected in very low concentrations. The concentration of BbF+BkF (66.2 ng m^{-3}) was found to be maximum followed by DbA+IP (45.2 ng m^{-3}) and BaP (42.8 ng m^{-3}). The TSPM and PAH concentration presented a large variability during the sampling period probably attributable to meteorological variations and thus showed a positively skewed distribution. Hence, mean concentrations of Total Suspended Particulate Matter (TSPM), individual PAH and TPAH (i.e. sum of all determined PAH in each sample) have been presented as their geometric means.

PAH	Mean Concentration (n=50)
Nap	4.2 ± 1.0
Acy	6.2 ± 1.3
Ace	2.7 ± 1.4
Flu	6.2 ± 4.5
Phen	3.9 ± 1.9
Anth	1.2 ± 2.3
Fla	2.1 ± 1.7
Pyr	0.9 ± 1.4
BaA+Chy	24.5 ± 4.5
BbF+BkF	66.2 ± 2.9
BaP	42.8 ± 3.0
DbA+IP	45.2 ± 4.9
BghiP	27.9 ± 2.6
TSPM (μg m^{-3})	368 ± 1.5
TPAH (ng m^{-3})	151.8 ± 3.4

Table 1: Mean PAH (ng m^{-3}), TPAH (ng m^{-3}) and TSPM (μg m^{-3}) concentration

Interactions between O_3, NO_2 and PAH

Pearson correlation was used to study the interaction between O_3, NO_2 and PAHs. NO_2 was found to have a strong positive correlation (R^2=0.71) with total particulate PAH concentration (Fig. 1). This positive correlation may be attributed to similar emission sources (vehicular combustion) of NO_2 and PAHs. NO_2 is mainly produced by the oxidation of NO, which is mostly originated from vehicular emissions. Further the correlation of NO_2 with individual PAHs was also investigated. The correlations obtained showed that NO_2 exhibited strong positive correlation with most of the PAHs (Table 2). To mention a few, NO_2 displayed strong positive correlation with BaP (r=0.90), Phen (r-0.92) and moderate correlation with Acy (r=0.79), Chy (r=0.82), BghIP (r=0.86), Fla (r=0.81) and BkF (r=0.80). BaP, Phen, BghIP, Acy and Chy are the mostly emitted from combustion sources and vehicular fuels whereas Fla and BkF are the source signatures of heavy duty diesel vehicles. Hence the role of emissons form vehicular and combustion activities plays a major role and the positive correlation confirms the co-emission of PAHs and NO_2 at this site. The results observed were found to be consistent with the studies reported by Park et al., 2002 and Yasmin et al., 2008. Besides this, the particulate PAHs present in the atmoshere could be expected to undergo nitration in presence of NO_2 to form nitro-PAHs. Based on the strong positive correlations obtained, nitration of PAHs seems to play no role in the present study.

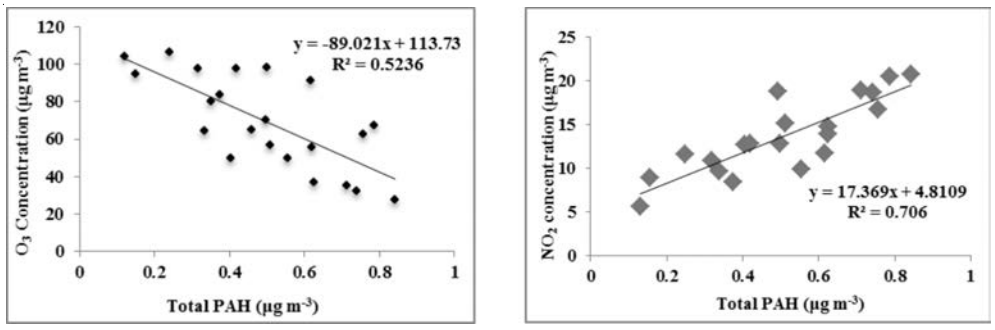

Figure 1: Correlation between PAH, O_3 and NO_2

Similar correlation was performed with photochemical oxidant, O_3. O_3 was found to exhibit good negative correlation with total particulate PAH (R^2=0.52) as also reported by Park, *et al.* 2002 and Yasmin, *et al.* 2008. This negative correlation could be explained by gas-particle partioning. The fomation of O_3 takes place under high ambient temperature and high solar radiation intensity conditions. This formation is further enhanced with enhancement of ambient temperature and solar radiation intensity. Under such conditions, PAHs present in the atmosphere might undergo gas-particle partitioning. The gas particle partitioning of PAH under high temperature and solar radaition intensity would be expected to favour conversion of particulate PAH to gaseous phase PAH thorugh evaporation mechanism. Hence we observed negative relationship between O_3 and total particuate PAH.

Further O_3 also showed good negative correlation with individual particulate PAHs. Unlike NO_2, O_3 correlation with PAH tends to be selective. shows selective BaP (r = -0.62) and BghIP (r = -0.60) showed significant negative correlation with ozone. Besides this, the moderate negative correlations were also observed between ozone and Chy (r = -0.42), BaA (r = -0.50), Pyr (r = -0.52), Anth (r = -0.40) and Phen (r = -0.70). BbF (r = -0.58) and BkF (r = 0.47), a pair of isomers shows unexpected correlation. Being isomers with similar physical properties, they are expected to react in a similar fashion with respect to gas-particle shift and hence should exhibit similar negative correlation. Here BbF shows a negative correlation with ozone while Bkf displays a positive correlation. Hence the selective behaviour of PAHs was observed not to hold good and therefore we can say that gas-particle partitioning might not be the only reason the negative correlation between O_3 and PAH.

Another plausible reason for the negative correlation might be ozonolysis of PAHs under suitable atmospheric conditions. The ozonolysis of PAHs in the atmosphere yields oxy-PAHs (Finlayson Pitts and Pitts, 2000). Under high temperature and high solar radiation intensity conditions, higher ozone formed could possible enhance the ozonolysis reaction and hence the degradation of particulate PAHs and resulting in a negative correlation between O_3 and PAHs.

Study on ozonolysis of 5 individual PAHs (Pyr, Flu, BaA, BeP, BaP) collected on glass fibre filters by Pitts et al., 1986 reported BaP, BaA and Pyr to be most potent and reactive among the 5 PAHs species considered. BaP and BaA were observed to significantly more reactiive than BeP at an ambient ozone concentration varying from 50-300 ppb. Similarly significant conversion of PAHs at an ambient ozone concentration of 100 ppb was observed by Van Vaeck and Van Cauwenberghe, 1984 while studying the decay of five PAHs viz. BaP, BgP, Ind, BeP and BkF in diesel particles and reported BaP and BgP to be most reactive PAH. Similar observations were also reported by Yasmin, *et al.* 2008. Overall such studies suggests the possible degradation of particulate PAHs in the presence of sufficient concentration of ambient ozone. Therefore the ozonolysis of PAHs at this site holds responsible for the negative correlation between ozone and PAH.

PAH	O_3	NO_2
Acy	0.33	0.79
Ace	0.52	0.47
Flu	0.54	0.46
Phen	-0.70	0.92
Anth	-0.40	0.63
Fla	0.50	0.81
Pyr	-0.52	0.63
BaA	-0/50	0.56
Chy	-0.42	0.82
BbF	-0.59	0.51
BkF	0.48	0.80
BaP	-0.62	0.90
BghIP	-0.60	0.86

Table 2: Pearson Correlation between Particulate PAH, O_3 and NO_2

CONCLUSIONS

The negative correlation (r=-0.72) observed between PAHs and $O_3$was attributed to ozonolysis of PAHs under suitable atmospheric conditions. The ozonolysis of PAHs in the atmosphere yields oxy-PAHs (Pitts, *et al.* 1986) and hence causes O_3 loss.

ACKNOWLEDGEMENT

Authors gratefully acknowledge the financial support for this work which is provided by ISRO-GBP under AT-CTM project.

REFERENCES

Bonasoni, et al. (2004). Aerosol-ozone correlations during dust transport episodes, *Atmospheric Chemistry and Physics*, **4**, pp. 1201–1215.

Finlayson-Pitts, B.J. and Pitts Jr., J. N. (2000). Chemistry of the Upper and Lower Atmosphere, Academic Press: San Diego, CA.

Finlayson Pitts, B.J. and Pitts, J.N. (1986). Fundamentals and Experimental Techniques, *Atmospheric Chemistry*, 1097.

Manoli, E., Samara, C., Konstantinou, I. and Albanis, T. (2000). Polycyclic aromatic hydrocarbons in the bulk precipitation and surface waters of Northern Greece, Chemos., **41**, pp. 1845-1855.

Park, S. S., Kim, Y. J. and Kang, C. H. (2002). Atmospheric polycyclic aromatic hydrocarbons in Seoul, Korea. Atmospheric Environment, **36**, pp. 2917-2924.

Pudasainee, et al. (2006). Ground level ozone concentrations and its association with NOx and meteorological parameters in Kathmandu valley, Nepal, *Atmospheric Environment*, **40(40)**, pp. 8081-8087.

Rogge, W. F., Hildemann, L., Mazurek. M. A., Cass, G. R., and Simoneit, B.R.T. (1993b). Sources of fine organic aerosol: 3. Road dust, tire debris and organometallic brake lining dust: roads as sources and sinks, *Environment Science and Technology*, **27**, pp. 1892-1904.

Rogge, W. F., Hildemann, L., Mazurek, M. A., Cass, G.R., and Simoneit, B. R. T. (1993b). Sources of fine organic aerosol: 2. Non-catalyst and catalyst-equipped automobiles and heavy duty diesel trucks, *Environment Science and Technology*, **27**, pp. 636-651.

Usher, C.R., Michel, A.E., and Grassian, V. H. (2003). Reactions on mineral dust, *Chem. Rev.*, *103*, pp. 4883–4939.

Vaeck, L. Van and Cauwenberghe, K. Van. (1984). Conversion of polycyclic aromatic hydrocarbons on diesel particulate matter upon exposure to PPM levels of ozone, *Atmospheric Environment*, **18**, pp. 323-328.

Yasmin, W. F. T, Takeda, K. and Sakugawa, H. (2008). Exploring the correlation of particulate PAHs, sulphur dioxide, nitrogen dioxide and ozone, a preliminary study, *Water Air Soil Pollution*, **194**, pp. 5-12.

A CASE STUDY OF AEROSOL BLACK CARBON AND AEROSOL OPTICAL DEPTH DURING WINTER OVER A TROPICAL INLAND STATION – RANCHI (23.42N, 85.33E AND 650M ABOVE MSL)

KUMARI LIPI[1], MANOJ KUMAR[1], S. SURESHBABU[2] AND N C MAHANTI[1]

[1]Dept. -Applied Mathematics, BIT Mesra,Ranchi-835215,Jharkhand,India
[2]Space Physics Laboratory ,Vikram Sarabhai Space,CentreThiruvananthapuram- 695 022,India

Keywords: BLACK CARBON, AOD

INTRODUCTION

Aerosols have been identified as the major source of uncertainty in the present day climate studies (Intergovernmental panel on Climate Change (IPCC), 2007). Lack of adequate observational data, coupled with poor understanding of the spatiotemporal and vertical distribution of aerosol properties has been identified as the major cause for the uncertainty. Aerosol modulates Earth's radiation balance directly by scattering and by absorbing incoming radiation. In addition to their effect on radiation, they also serve as cloud condensation nuclei and thereby influence the number and size distribution of cloud droplets. This process can change cloud radiative properties, cloud lifetime, and precipitation properties, thus indirectly affecting the climate.

LOCATION AND GENERAL METEOROLOGY OF THE SAMPLING SITE

The sampling site selected for the present work was Department of Applied Mathematics, Birla Institute of Technolgy, Mesra, Ranchi, which is located in the Northern India. It is 23.42N, 85.33E and 650m MSL.The Instrument used for continuous measurement of BC mass concentration was Aethalometer (AE-31), which is developed by Magee Scientific, USA. Measurements of BC mass concentration were mainly based on the aerosol light absoption.BC from the ambient air accumulated on a quartz fiber tape. The measurement of BC concentration is taken at seven wavelengths 370,470,520,590,660,880 and 950nm.The measurement of the attenuation of light beam was linearly proportional to the amount of BC deposited on filter stripe. The Instrument was operated at the time base of 5 minute with a flow rate 4 LPM. Effect of meteorological parameters like temperature and relative humidity, data collected through 32m meteorological tower.

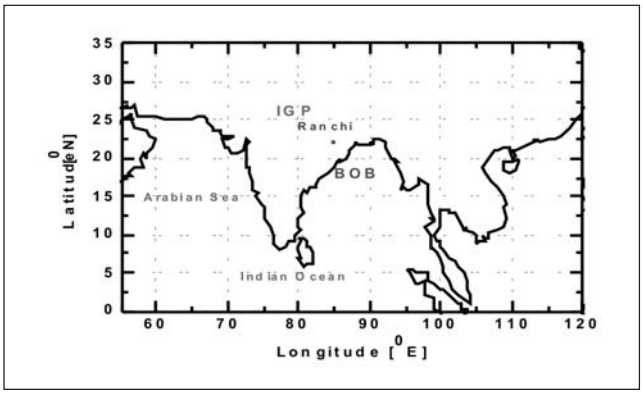

Figure 1. Map of Indian subcontinent showing the observational site – Ranchi

RESULTS AND DISCUSSION

The monthly variation of black carbon is presented in Fig. 2. Average monthly BC concentration varied between 1.1 to 8.1 µg/m³. The monthly variation results showed higher concentration during winter as compared to monsoon. This may be due to the decrease of the average temperature which causes the decrease in wind speed in turn resulted in low transport of the black carbon because of low dispersion. In 2010 and 2011 highest monthly average was found in month of January.

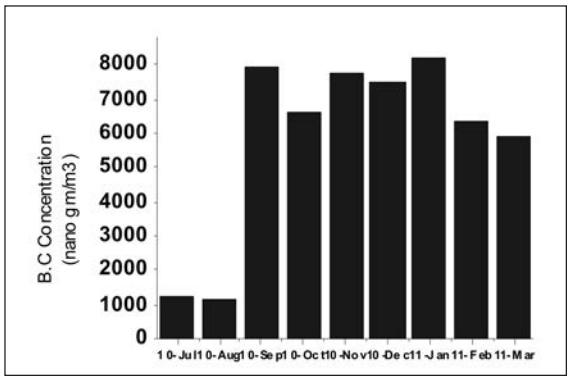

Figure 2. Monthly average variation of black carbon aerosol during July-10 to March-11

Location	Period	BC concentration (µg/m³.)
Ranchi	July10 to March-2011	1.0-18(Daily average),1.1-8.1(Monthly average)
Varanasi	Oct -08 to March-2010	2-40(Daily average),3.6-25.4(Monthly average)
Trivandrum	20 Feb.05 to 16 March 05	0.3-6
Hyderabad	Jan to July 2003	0.5-68(dry season),0.5-45 (wet season)
Kanpur	Dec.2004	6-20
Pune	Jan.05 to Dec.05	4.1(average)
Anantapur	Jan-08 to Dec.09	2.74±0.63(annual average)
Northern BoB close to India	Oct.2003	1.8±1.6
Shillong	2008	~5(annual Mean)
Hanle in Himalaya	Aug.-Dec.2009	.06(Mean)
Dehradun	2007-2009	4.39(Mean)
Mohal-Kullu(H.P)	July09-March2010	2.7-8(Monthly mean)

Source- Scientific Progress Report-2010(ARFI & ICARB)

Table1. Stations/regions of India along with their average value of BC concentration

CONCLUSIONS

1. Average BC concentration in Ranchi region is significantly higher as compared to BC concentration reported from other location of India.

2. BC showed well defined diurnal variations. This is due to local factors and boundary layer dynamics.

3. High BC concentration was observed when the humidity of air was and high and vice versa.

4. Average BC Concentration in Ranchi region is significantly large fractuation in winter season (December) as compared temporal variation on that time.

5. The aerosol number concentration and AOD measurements would be helps us to find the role of boundary layer dynamics in the above typical temporal and monthly variations of BC at BIT Mesra, Ranchi site. Moreover, it is proposed to study the impact of aerosols and trace gases on the biodiversity dynamics in and around Ranchi and other parts of Northern India.

6. Winter season that may cause adverse effect to the agricultural crops and also to the human health. Increased aerosol loading may likely affect the rainfall which is responsible for the observed drought conditions over the Indian subcontinent. Detailed analysis of AOD, crop yields and rainfall data are required to understand the impact of increasing aerosol loading over the Northern India.

ACKNOWLEDGEMENT

The authors express sincere gratitude to Birla Institute of Technology, Mesra, Ranchi for allowing working in its premises and providing the facilities and necessary data to main author.

CHARACTERIZATION AND MORPHOLOGICAL ANALYSIS OF PARTICULATE MATTER IN ALLAHABAD LOCATED IN CENTRAL INDIA

RAJESH KUSHWAHA, HIMANSHU LAL, NABA HAZARIKA AND ARUN SRIVASTAVA

School of Environmental Sciences, Jawaharlal Nehru University
New Delhi-110067, India

Keywords: PARTICULATE MATTER, PARTICULATE MORPHOLOGY, SIZE FRACTION, METALS, SEM-EDX, ALLAHABAD

INTRODUCTION

Particle- solid or liquid dispersed in gaseous medium; present in air is termed as aerosol (Reist, 1933; Vincent *et al.*, 1989). Atmospheric aerosol consists of particle of both natural and anthropogenic origins. It is now well established that the elements from natural sources are generally found in the coarse particle whereas elements emitted from anthropogenic activities are associated with fine particles (Seinfeld,1986). Most importantly, the particle size distribution of aerosols is vital for an accurate and reliable assessment of their impact on human health (Fernandez *et al.*, 1994). This is due to the degree of respiratory penetration retention, which is a direct function of the aerodynamic diameter of these particles. It has been found that particles >30 μm in aerodynamic diameter have a low probability of entering the nasal passage of humans. Particles with diameter >5 μm are usually filtered in the nose. Particles with <1-2 μm diameter predominantly get deposited in the alveolar region of the lung during normal breathing (Epstein, 1975; Mc Cornace, 1971; McCormac, 1971). Particle size distribution is also an important input in models dealing with climate change studies, as radiative forcing of short wave and long wave radiation critically depend on size distribution (Bryson *et al.*, 1967). In addition, particle size characteristic of aerosol also affects cloud physics (Hayhood *et al.*, 1997; Muller *et al.*, 1999). Airborne particulate matter and metal in particulate matter have been associated with both short-term and long-term adverse health effects including chronic respiratory disease, heart disease, lung cancer, and damage to the other organ (Allen *et al.*, 2001; Costa and Dreher, 1997; Lingard *et al.*, 2005; Niu *et al.*, 2008; Rasmussen, 2004; Vincent *et al.*, 2001; Williams and Wheelar, 2007). In Indian context, very few comprehensive studies using SEM-EDX have been conducted, except for two studies in which Srivastava and Jain (2007a; 2009) used SEM for the morphological analysis of pollutants inside an indoor and outdoor environment of Delhi. Other studies were done by Taneja *et al.* 2011etc. In the present study an application of elemental composition, morphology and particle density of aerosols determined by SEM-EDX techniques have been used, with respect to different sizes of particulate matter.

MATERIALS AND METHODS

Study area

The district of Allahabad is centrally located in Uttar Pradesh and lies between $24^0 47'$ N and $25^0 47'$ N latitude and $81^0 9'$ E and $82^0 21'$ E longitude. The maximum length from east to west is about 117 km and breath from north to south about 101 km. The entire area of the city is about 7254 sq km. Allahabad enjoys different seasons which are winter season, summer, and monsoon. The average temperature is 15.25^0 and 8^0C respectively winters extend from November to January. Summer

season extends from half of June to September, where temperature shows a steep fall of 5.5^{0}C to 8.0^{0}C. The sampling size segregated aerosol was done from December 2011 to February 2012 at urban site which is directly affected by traffic emissions and other residential sites including public schools, colleges. Rural site is situated approximately 35 km away from main city. Open fields, agricultural farm, use of cow dung cake as fuels and a few brick kilns characterize the vicinity of the rural site.

Sampling and analysis

Sampling was done in Urban and Rural area of Allahabad shown in Fig. 1. The samples collected for $PM_{<1}$, PM_1, $PM_{2.5}$ and PM_{10} μm^{-3} were from the roof of buildings at urban and rural sites in Allahabad. Size segregated aerosol samples were collected with Dekati PM Sampler, which runs at a constant flow are of 30 LPM for 24 hrs. It has a portable Anderson impactor for the sampling of $PM_{<1}$, PM_1, $PM_{2.5}$ and PM_{10} . The particles were collected on 47 mm diameter GA/F glass filter paper for $PM_{<1}$ and PM_1; $PM_{2.5}$ and PM_{10} were collected on 25 mm diameter GA/F glass filter paper. Filter papers were weighed twice before and after sampling using four-digit balance (Sartorius model - GD 603) with sensitivity of ± 0.1 mg. Before weighing the samples were equilibrated in desiccators at 20-30˚C and relative humidity of 30-40% in humidity controlled room for 24 hrs. Particulate matter mass was determined gravimetrically by subtracting the initial average mass of the blank filter from the final average of the sampled filter dividing by air volume passed through sampler.

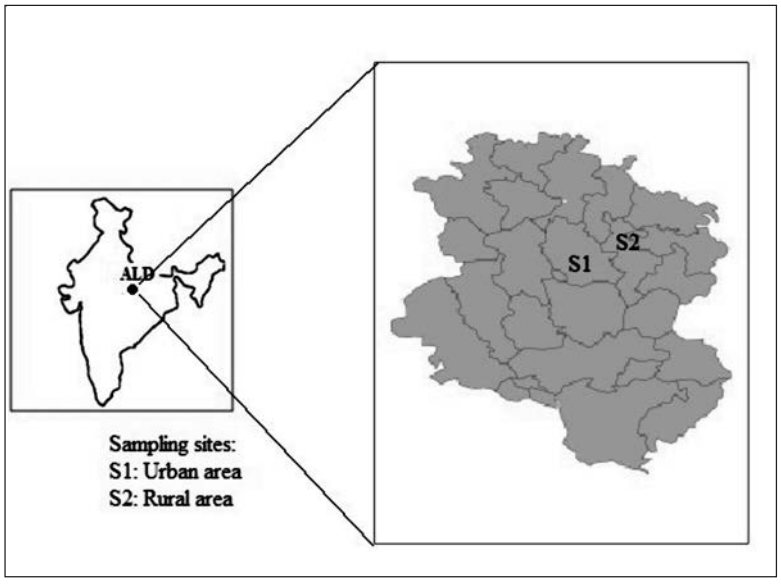

Figure 1. Sampling site (not to scale)

SEM-EDX measurement

The samples (dry filter papers) were cut in 1 mm^2 size out of the main filter (Xie *et al.* 2005). A very thin film of gold and palladium (Au-Pd) were deposited on the surface of the samples to make them electrically conductive using vacuum coating unit. This very fine coating was done through the evaporation of Au-Pd plate under the inert atmosphere (argon environment). These samples were mounted on electron microprobes stubs. The SEM-EDX analyses were carried out with the help of computer controlled filed emission SEM (Carl Zeiss EVO 40, Germany) equipped with a EDX-

Detector system, (Bruker-X-Flash – 4010). In the present investigation, the SEM was used in its most common mode the emissive mode. Energy used at 20K.

CONCLUSIONS

The SEM-EDX technique was used to characterize the size segregated particulate matters at Urban and Rural site in Allahabad in India. The SEM micrographs inferred that the particulate matter of urban site was different in shapes, sizes and morphology from rural site. EDX spectra of size segregated particulate matter showed the elemental composition of individual particles and indicated two main groups i.e. O, Si rich particles, Al, Na, Ca, C, Mg, Fe, Ti, K rich particles on the basis of their percentage contribution in $PM_{<1}$, PM_1, $PM_{2.5}$ and PM_{10} . The $PM_{<1}$ constitute O, Si (97.28), Zn, Na, Al, K, Ca, and Ti (2.72), PM_1 constitute O, Si (98.36), Al, K, Ca, Fe, Mg, Na, Cl (1.63), $PM_{2.5}$ μm^{-3} O, Si (97.53), Ca, Al, Fe, Mg, K (2.47), and PM_{10} constitute O, Si (97.18), Na, Al, Ca, K, Ti (2.83) at rural site whereas at urban site, $PM_{<1}$, constitute O, Si (98.74), Al, Zn, K, Ca, Ti (1.36), PM_1, constitute, O, C (98.91), Al, Na, Ca, Fe (1.09), $PM_{2.5}$ constitute O, Si (97.74), Al, Na, Ca, K, Fe, Zn, Mg, Ti (2.26) and PM_{10} O, Si (96.45), Na, Al, Zn, Ca, K, Fe, Ti and Mg (3.49) respectively. SEM-EDX technique used in this study is capable to provide valuable information on the morphology and elemental composition of the collected samples.

ACKNOWLEDGEMENT

Authors deeply acknowledge University Grant Commission (UGC) for fellowship, Government of India, New Delhi. We are also thankful Miss Pooja Singh, for helpful suggestion during the course of this work.

REFERENCES

Adams, H. S., Nieuwenhuijsen, M. J., Colvile, R. N., McMullen, M.A.S. and Khandelwal, P. (2001). Fine particle ($PM_{2.5}$) personal exposure levels in transport microenvironments, London, UK, *The Science of the Total Environment*, **279**, pp. 29-44.

Allen, A.G., Nemitz, E., Shi, J.P., Harrison, R.M. and Greenwood, J.C. (2001). Size distribution of trace metals in atmospheric aerosols in the United Kingdom, *Atmos. Environ.*, **35**, pp. 4581-4591.

Baryson, R.A. and Baerreis, D.A. (1967). Possibilities of major climatic modification and their implications: Northwest India, a case study, *Bull. Am. Soc.*, **48**, pp. 136-142.

Cao,J.J., Lee, S.C., Zheng, X.D., Ho, K.F., Zhang, X.Y., Gue, H. (2003). Characterization of dust storms to Hong Kong in April 1998, *Water, Air and Soil Pollution*: **3(2)**, pp. 213-229.

Esposito, F., Pavere, G. and Serio, C. (2001). A preliminary study on the correlation between TOMS aerosol index and ground-based measured aerosol optical depth, *Atmospheric Environment*, **35**, pp. 5093-5098.

Fernandez, A. J., Ternero, M., Barragan, F.J., and Jimenez, J.C. (1999). Sources characterisation of airborne particle in Seveille (Spain) by multivariate statistical analysis, *I. Dojoras*, **103 (4)**, pp. 261-273.

Fernandez, A.Z., Turner, M., Barragan, F.J., Jimenez, J.C., (2000). An approach to characterization of source of urban airborne particle through heavy metal speciation, *Chemosphere*, 2, pp. 123-136.

Haywood, J.M. and Ramaswamy V. (1998). Global sensitivity studies of the direct radiative forcing due to anthropogenic sulphate and black carbon aerosol, *Journal of Geophysical Research*, **103(D3),** pp. 6043-6058.

Li, M., Frette, T. and Wilkinson, D. (2001). Particle size distribution determination from spectral extinction using neural network, *Industrial & Engineering Chemistry Research*, **40**, pp. 4615-4622.

Marcazzan, G. M., Vaccaro, A., Valli, G. and Vecchi, R. (2001). Characterisation of PM_{10} and $PM_{2.5}$ particulate matter in the ambient air of Milan (Italy), Atmospheric *environment*, **35**, pp. 4639-4650.

Mc Cornac, B. H. (1971). Introduction to the Scientific Study of Atmospheric Pollution, Reide Dordrent, Holland.

Muller, D., Wandinger, U., and Ansmann, A. (1999). Microphysical particle parameters from extinction and backscatter lidar data by inversion with regularization theory, *Applied Optics*, **38**, pp. 1981-1999.

Murry, F., McGranahan, G., Kuylenstierna, J.C.I. (2001). Assessing health effects of air pollution in developing countries, *Water, Air and Soil Pollution*, **130 (1-4),** pp. 1799-1804.

Pipal, A.S., Kulshtrstha, A., Tajeja, A. (2011). Characterization and morphological analysis of airborne $PM_{2.5}$ and PM_{10} in Agra located in north central India, *Atmospheric environment*, **48,** pp. 3621-3630.

Rasmussen *et al.*, (2007). Monitoring personal, indoor, and outdoor exposures to metals in airborne particulate matter: Risk of contamination during sampling, handling and analysis, *Atmospheric environment*, **41**, pp. 5897-5907.

Reist, P.C. (1933). Introduction to aerosol sciences, Macmillan publishing company New York.

Seinfeld, J.H. (1986). Atmospheric Chemistry and Physics of Air Pollution, John Wiley, New York, P.

Srivastava, A. and Jain, V.K. (2007a). Seasonal trends in coarse and fine particle sources in Delhi by the chemical mass balance receptor model, *J. Hazard. Mater*, **144**, pp. 283–291.

Vincent, J. H. (1989). Aerosol Sampling: Sciences and Practice, *John Wiley and Sons, Chichester,* **390**.

Williams et al., (2008). Personal coarse particulate matter exposure in an adult cohort, *Atmospheric Environment*, **42**, pp. 6743-6748.

Xie, R. K., Seip, H. M., Leinum, J. R., Winje, T and Xiao, J. S., (2005). Chemical characterization of individual particles (PM10) from ambient air in Guiyang City, China, *Sci. Total Environ.*, **343,** pp. 261– 272.

SCATTERING PROPERTIES OF SURFACE AEROSOLS OVER SEMI-ARID REGION IN THE SOUTHERN INDIA

S.MD. ARAFATH[1], K. RAMA GOPAL[1*], R.R. REDDY[1], A.P. LINGASWAMY[1], K. UMADEVI[1], S. PAVAN KUMARI[1], N. SIVAKUMAR REDDY[1], G. BALAKRISHNAIAH [1,2], B. SURESH KUMAR REDDY[1,3], K. RAGHAVENDRA KUMAR[1,4], Y. NAZEER AHAMMED [5,] P. ABDUL AZEEM[6] AND S. SURESH BABU[7]

[1] Aerosol & Atmospheric Research Laboratory, Department of Physics, Sri Krishnadevaraya University, Anantapur 515 003, Andhra Pradesh, India

[2] Institute of Environmental Engineering, National Chiao Tung University, Taiwan.

[3] Institute of Low Temperature Science, Hokkaido University, Japan.

[4] School of Chemistry and Physics, University of KwaZulu-Natal, Westville Campus, Durban 4000, South Africa

[5] Atmospheric Science Laboratory, Department of Physics, Yogi Vemana University, Kadapa 516 003, Andhra Pradesh, India

[6]Department of Physics, National Institute of Technology (NIT), Warangal

[7] Space Physics Laboratory, Vikram Sarabhai Space Centre, Trivandrum – 695 022, India

Keywords: AEROSOL SCATTERING PROPERTIES, SCATTERING COEFFICIENT, ANGSTROM EXPONENT.

INTRODUCTION

Light optical properties of atmospheric aerosol particles are vital importance in estimating the radiative forcing of climate and also in global radiation budget studies **(**Muller, 2011**),** and human health hazard by pollution exposure (White and Roberts, 1997). Aerosols perturb the radiation balance of the Earth directly through scattering and absorbing solar radiation, and indirectly by acting as condensation nuclei in cloud (CCN) formation, thus affecting the optical properties and lifetimes of clouds **(**Rosenfeld, 1999**)**. The effect of direct aerosol radiative forcing may currently have an influence of potentially the same magnitude but in the opposite direction as greenhouse gas forcing (IPCC2007). The aerosol light scattering coefficient, an extensive optical property, can yield crucial information about the aerosol size distribution.

The local radiative forcing will depend up on the local atmospheric column burden of a particular anthropogenic aerosol species in the atmosphere. Atmospheric aerosols in the accumulation mode are efficient scatterers of solar radiation because their size is of the same order as the wavelength of radiation. If the magnitude of aerosol forcing is at the low end of the uncertainty range, aerosols are negating only a small fraction of the greenhouse forcing. However, if the aerosol forcing is at the high end of the uncertainty range, aerosols could be negating virtually all of the present greenhouse forcing. This has great implications on empirical inferences of climate model accuracy and requires that the uncertainty in aerosol forcing be greatly reduced. This demonstrates a cooling of the Earth-Atmosphere- System by aerosols, as extra solar radiation is reflected back to space. Aerosol associated reductions of the downward solar radiation at the Earth's surface are larger.

In this work, we presented the results relating to scattering properties of atmospheric aerosols such as total scattering, back scattering coefficients and Angstrom exponent. These results are obtained

from TSI Model 3563 three wavelength integrating nephelometer during the period Jan- Dec 2011. The diurnal and monthly variations of scattering properties of atmospheric aerosols have been studied and analyzed. The factors responsible for the effect of the aerosol scattering coefficients (total/back) and Angstrom exponent are due to the pollutants which are from long range transport and local anthropogenic factors.

EXPERMENTAL METHODOLOGY

Near real time continuous measurements of aerosols scattering properties are recorded using a TSI Model 3563 three wavelength integrating nephelometer during Jan-Dec 2011 in a semi arid region, Anantapur (14.62^0 N, 77.65^0 E, 331m asl) located in southern India. It is geographically situated on the boundary of a semi-arid and rain shadow region. The continental conditions prevailing at this site are responsible for large seasonal temperature differences, providing hot summers (March–May) and cool winters (December–February). Most of the rainfall occurs during the monsoon (southwest monsoon; June–September) and post monsoon (northeast monsoon; October and November). Within a 50 km radius, this region is surrounded by a number of cement plants, lime kilns, slab polishing and brick making units. These industries, the national highways (NH 7 and NH 205) and the town area are situated in the north to southwest side of the sampling site. Calibration of the nephelometer by using CO_2 as span gas while zero measurements and adjustment are performed once in a week by using internally filtered particle free air. The instrument was located on the top floor of the building (12m) with the sample inlets. The flow through the inlet is maintained at 120 LPM and at s time base of 5min, so that scattering coefficients estimated are available for every 5min, on all the days and also round the clock.

RESULTS AND DISCUSSION

DIURNAL VARIATION

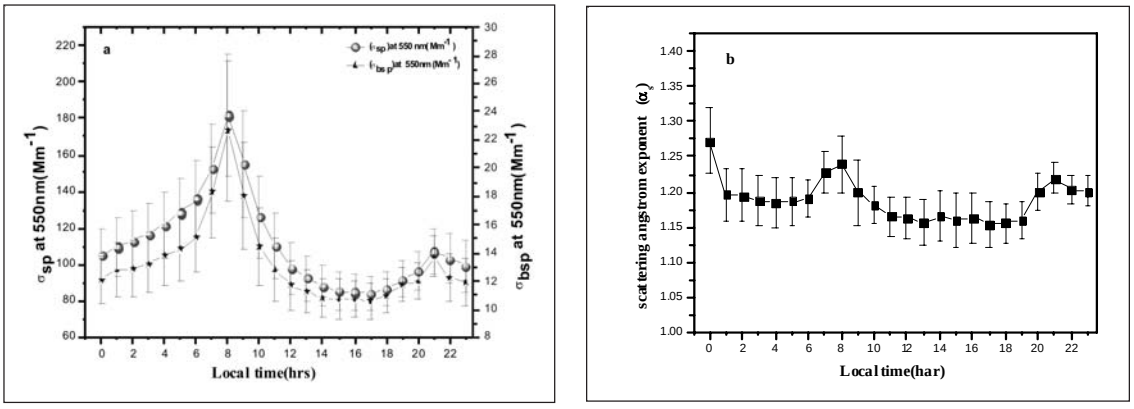

Figure 1 (a). shows temporal variation of Scattering coefficient($5\emptyset ß_{sp}$) at 550nm, and Back scattering coefficient($5\emptyset ß_{bsp}$) at 550nm, (b). diurnal variation of Angstrom exponent($\alpha._s$) The vertical bars represent standard errors from the mean of observation

Fig. 1 (a) and (b) illustrates the diurnal cycles observed for the total scattering coefficient, back scattering coefficient and Angstrom exponent, respectively during the entire study period. For all diurnal variation of the parameters, two maxima and one minima are observed within a day, and the vertical bar lines represents the standard error calculated for the all observations. Evident diurnal

variation can be found for all of those variables, during the diurnal cycle of the boundary layer height and also local emission. The diurnal cycle of the scattering ($5Øß_{sp}$) and back scattering ($5Øß_{bsp}$) followed same pattern. Primary peak (181.6±33.82Mm^{-1} for $5Øß_{sp}$; 22.6±4.9Mm^{-1} for $5Øß_{bsp)}$ observed during the morning around 7:00 to 9:00 LT due to the morning hours local anthropogenic activities increase and also the traffic density may be more just before the increase of the boundary layer height. As well as second peak found at late night(20:00-22:00 hr) which is less than that of morning peak since particle emission are accumulated in shallow nocturnal boundary layer. Minimum values (84.03±9.7Mm^{-1} for $5Øß_{sp}$; 10.56±1.2Mm^{-1} for $5Øß_{bsp}$) appeared in the afternoon hours 14:00 to 16:00 LT this is due to dilution effect of the increasing boundary layer height and drastic reduction of local anthropogenic activities. Figure 1 (b) represents the diurnal variation of Angstrom exponent which gives an idea of the size of the particles involved in this phenomenon. The Angstrom exponent slowly decreases to minimum at 12:00 LT hour which stays constant till around 20:00 LT, and then slowly increases again.

MONTHLY VARIATION

The seasonal variability is mainly due to the prevailing meteorological conditions in their respective seasons. The monthly or seasonal variation of σ_{sp}^{550nm} and Angstrom exponents are shown in Figures 2. (a) and (b). High and low σ_{sp}^{550nm} values are observed in the months of December and September respectively. The maximum σ_{sp}^{550nm} (average ±standard error) is observed (158.3±12.2Mm^{-1}) in the month of December and it is due to the boundary layer subsidence and the result of the confinement of aerosols. This type of boundary layer dynamics is due to the surface temperature variations and which could be the reason for the maximum scattering coefficient observed in winter months. The air mass pathway observed at the site during winter is from northeast direction and which result in bringing mostly the continental air and leading to enhanced anthropogenic component (Kumar *et al.*, 2011). In the month of January, the maximum Angstrom exponent values are observed which corresponds the fine mode domination. From March to May dispersion of aerosol is high owing to the large ventilation coefficient which is a product of mixing height and local wind speed, and therefore the surface concentrations are relatively low compared to winter months. We found low values of $ó_{sp}^{550nm}$ (average ±standard error) (41.3±2.4Mm^{-1}) in the month of September, which is due to south-westerly winds rich with marine air mass, prevail over this region.

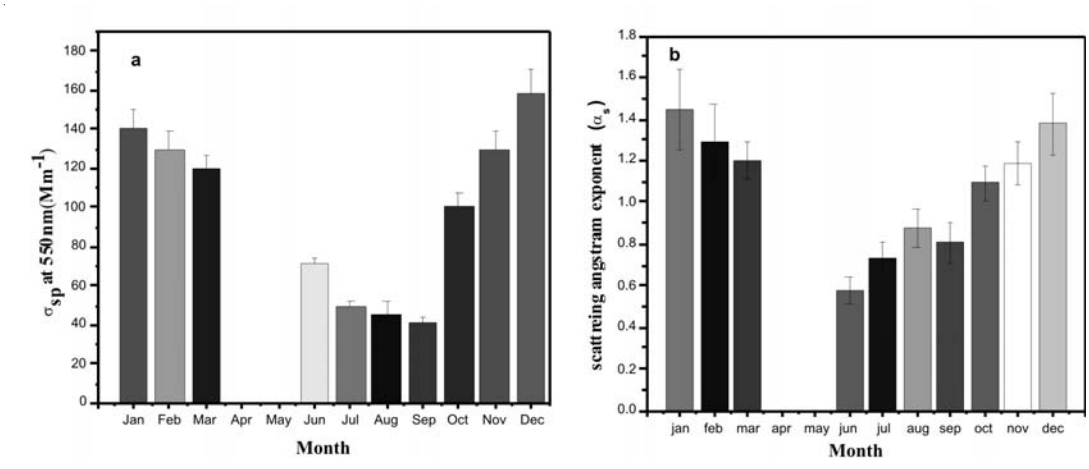

Figure 2. (a)Variation of monthly averages of observed scattering coefficient ($5Øß_{sp}$) at 550nm, (β) Monthly variation of scattering angstrom exponent (α_s) for study period Jan- Dec 2011 over Anantapur

ACKNOWLEDGEMENTS

The authors are indebted to Indian Space Research Organization (ISRO), Bangalore for carrying out this work through its Geosphere Biosphere Programme (GBP) under Aerosol Radiative Forcing over India (ARFI) project**.** One of the authors (RRR) wishes to express his thanks to UGC, New Delhi for providing UGC-BSR Faculty Fellow ship during which part of the work was done.

REFERENCES

Intergovernmental Panel on Climate Change, Climate Change; The Scientific Basis. Contribution of Working Group I to the Fourth Assessment Report of the Intergovernmental Panel on Climate Change, edited by, Solomon.,S. (2007). (Cambridge University Press, Cambridge, UK.).

Kumar. K. R., Narasimhulu, K., Balakrishnaiah, G., Suresh Kumar Reddy, B., Rama Gopal, K., Reddy, R. R., Satheesh, S. K., Krishna Moorthy, K. and Suresh Babu, S. (2011). Characterization of aerosol black carbon over a tropical semi-arid regionof Anantapur, India, *J. Atmos Environment*, **100**, 12.

Muller, T., Laborde, M., Kassell, G. and Wiedensohler A. (2011). Design and performance of a three-wavelength LED-based total scatter and backscatter integrating nephelometer, *J. Atmos. Meas. Tech.*, **4**, pp. 1291.

Rosenfeld, D. (1999). TRMM observed first direct evidence of smoke from forest fires inhibiting rainfall, *Geophys. Res. Lett.*, **26(20)**, pp. 3105.

White, W.H. and Roberts, P. T (1977). Nature and origins of visibility-reducing aerosols in Los-Angeles air basin, J. *Atmos. Environ.*, **11**, pp. 803.

DIURNAL AND SEASONAL VARIATION OF BLACK CARBON, SIZE PARAMETER AS MASS CONCENTRATION OF SURFACE AEROSOLS OVER ANANTAPUR, A SEMI-ARID REGION

S.PAVAN KUMARI[1], K. RAMA GOPAL[1*], R.R. REDDY[1], S.MD. ARAFATH[1] A.P. LINGASWAMY[1], K. UMADEVI[1], N. SIVAKUMAR REDDY[1], G. BALAKRISHNAIAH [1,2], B. SURESH KUMAR REDDY[1,3], K. RAGHAVENDRA KUMAR[1,4], Y. NAZEER AHAMMED [5] P. ABDUL AZEEM[6] AND S. SURESH BABU[7]

[1] Aerosol & Atmospheric Research Laboratory, Department of Physics, Sri Krishnadevaraya University, Anantapur 515 003, Andhra Pradesh, India
[2] Institute of Environmental Engineering, National Chiao Tung University, Taiwan.
[3] Institute of Low Temperature Science, Hokkaido University, Japan.
[4] School of Chemistry and Physics, University of KwaZulu-Natal, Westville Campus, Durban 4000, South Africa
[5] Atmospheric Science Laboratory, Department of Physics, Yogi Vemana University, Kadapa 516 003, Andhra Pradesh, India
[6]Department of Physics, National Institute of Technology (NIT), Warangal
[7] Space Physics Laboratory, Vikram Sarabhai Space Centre, Trivandrum – 695 022

Keywords: BLACK CARBON AEROSOLS, ACCUMULATION MODE, COARSE MODE, TOTAL MASS CONCENTRATION.

INTRODUCTION

Aerosols have a significant regional and global effects on climate, which is opposite in sign to that of the greenhouse gases. Aerosols plays a crucial role in radiation balance of the earth and there by modify the global climate, i.e. the direct and indirect effect of aerosols produces large uncertainty in the prediction of climate change (IPCC,2007). In direct forcing mechanism involved in aerosols, aerosols reflected back to space and thus cooling the planet. In indirect forcing involves, aerosols particles acting as a cloud condensation nuclei. The dynamics of aerosol number density, their production process, the size transformation and lifetime are influenced by the aerosol size distribution. By acting as a cloud condensation nuclei, aerosols modify the macrostructure of clouds (Ramakrishna *et al.*, 2003). The aerosol black carbon (BC), the by product of all incomplete combustion process, is mostly of anthropogenic origin. The chief sources of BC are burning of biomass and fossil fuels, automobile exhaust, aircraft emissions and forest fires. Atmospheric BC directly accounts for the reduction in incoming short wave solar Radiation, leading to the heating of atmosphere. Because of strong absorption over a wide range of wavelengths, BC contributes significantly to atmospheric warming (Jacobson, 2001).

In the present study provides an account of diurnal and seasonal variation of BC concentration and size segregated total mass concentration over a Semi- arid region of Anantapur.

METHODOLOGY AND DATASETS

Simultaneous measurements of BC mass concentration (M_b) and size segregated total aerosol mass concentration were carried out using Aethalometer (AE-21 Magee Scientific, USA) and 10 channel Quartz Crystal Microbalance (PC-2 of California Measurements Inc., USA) respectively. AE-21

measures BC mass concentrations at two wavelengths 370 and 880 nm. The measurements are made from an altitude of about 12 m above the ground using its inlet tube and pump. The BC mass concentrations are estimated using the optical method of measurement of the attenuation of a beam of light transmitted through the sample collected on a filter, which is proportional to the amount of BC mass loading in the filter deposit. Aethalometer was operated with a flow rate of 3 $lmin^{-1}$ at a time resolution of 5 min, round the clock. The BC measured at 880 nm wavelength is considered to represent a true measure of BC in the atmosphere as at this wavelength BC is the principal absorber of light while the other aerosol components have negligible absorption at this wavelength. The measured location is a suburban and semi-arid station and is dominated by local sources, mainly anthropogenic. As at 880 nm the major absorbing species is BC, in this work. The raw data from Quartz Crystal Microbalance (QCM) was used to measure both total mass concentration (M_t) and mass size distribution (m_{ci}) of aerosol size range 0.05 to 25 μm over 10 size bins. It operated at a flow rate of 0.24 $lmin^{-1}$ and sampling was done at nearly hourly intervals, manually round the clock , with the sampling duration of 6 min, when the ambient RH<75%.

RESULTS AND DISCUSSION

THE DIURNAL VARIATION OF BLACK CARBON MASS CONCENTRATION

Fig. 1 shows that diurnal variation of black carbon aerosols for different seasons at semi-arid region Anantapur during Jan-Dec 2011. There is a gradual build up of BC in the morning and a sharp peak occur between 7:00 and 9:00 hrs almost one hour after sunrise and a broad nocturnal peak from 19:00 to 21:00 hrs.

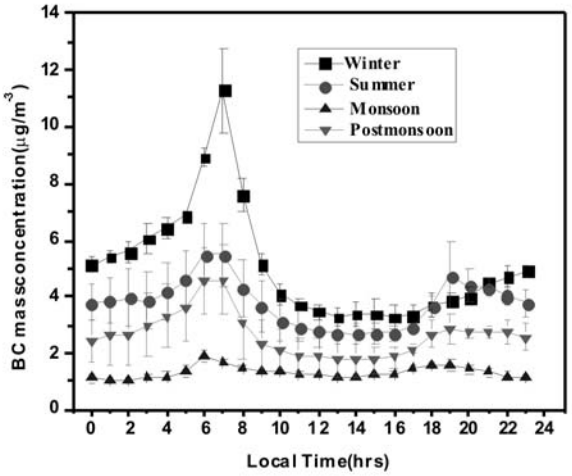

Figure1. Diurnal variation of BC mass concentration for the year 2011 observed at Anantapur.

(Vertical lines refer standard deviations)

BC concentration decreases substantially and the diurnal minimum is attained in the afternoon hours (14:00-16:00hrs). The morning peak in BC arises from the combined effects of fumigation effect in the boundary layer, which brings in aerosols from the nocturnal residual layer shortly after the sunrise and build up of local anthropogenic activities in the urban area (stull, 1998). Low values of BC during afternoon hours have been attributed to the dispersion of aerosols, due to increase in boundary layer height in addition to the low traffic density.

Seasonal variations of BC suggest large concentrations during the winter (5.09±0.37 μg/m^3) due to biomass burning (i.e. burning of agricultural wastes, and forest fires) and low during the monsoon season (1.33±0.12μg/m^3) due to rain out and washout to the pollutant particles.

THE DIURNAL AND SEASONAL VARIATIONS OF AEROSOL MASS CONCENTRATIONS IN DIFFERENT SIZE REGIMES

The QCM is operated every week on Wednesday systematically and the total number of days in a year will be around 49. Diurnal and seasonal variations of accumulation (M_a), coarse mode (M_c) and total mass concentrations (M_t) have been shown in Fig. 2. The vertical bars over the points represent the standard deviation of the mean.

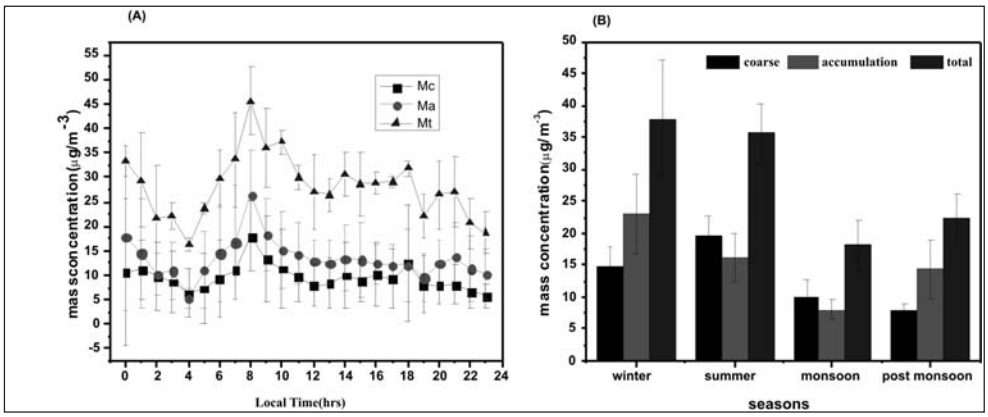

Figure 2. (A) diurnal, (B) seasonal variations of coarse (M_c), accumulation (M_a) mode and total mass (M_t) concentrations for the year 2011 observed at Anantapur. The vertical lines refer standard deviations.

Diurnal variation of M_c, M_a and M_t showed a primary peak at 3:00 LT then a sharp increase secondary peak at 8:00 LT, followed by increase in18:00 LT. Enhancement in aerosol mass concentration during morning hours has been attributed to the increase in vehicular traffic and related human activities in the study area. As night advances there have been a reduction in the anthropogenic and rural activities leading to reduction in aerosol generation. In the early morning hours aerosols closer to the surface are lost by sedimentation, which results in decrease in aerosol concentrations. The solar heating of land during the day increases convective activity leading to increase in boundary layer height, because of this at noon hours the concentration decreases due to faster dispersion of aerosols. In general solar radiative forcing is reduced by evening and the boundary layer height decreases which results in increasing particle concentrations in the evening hours. Similar observations have been reported in other regions over India (Parameswaran *et al.*, 1997; Pillai *et al.*, 2001). The highest concentrations of M_c, M_a and M_t are 17.9, 26.3 and 45.4 μg/m^3 respectively.

The seasonal variations of mass concentrations showed that the total aerosol mass concentration has been observed to be high during the winter (37.9μg/m^3) which plays an important role in heating and lifting the loose soil with association of wind speed and low during the monsoon period (18 μg/m^3), at that period the sky is generally overcast and it decreases the solar insulation and reduces the mass concentrations. Also during rainy season, some of the pollutants are washed out. The coarse mode particles observed are high during the summer (19.4 g/m^3) and low in the post monsoon season (7.9 μg/m^3). But accumulation mode particles are found to be high during the winter season

(23μg/m^3) and low during the monsoon season (8 μg/m^3). Examination the variation of aerosol it is seen that accumulation contribution to the total mass concentration is quite significant.

ACKNOWLEDGEMENTS

The authors wish to thank the Indian Space Research Organization (ISRO), Bangalore for carrying out this work through its Geosphere Biosphere Programme (GBP) under ARFI project. The authors are grateful to Dr. P.P.N. Rao, Program director and Dr. K.Krishna Moorthy, Director, SPL, Trivendrum, IGBP, Bangalore. One of the authors (RRR) wishes to express his thanks to UGC, New Delhi for providing UGC BSR Faculty Fellowship during which part of the was done.

REFERENCES

Intergovernmental Panel on Climate Change, Summary for policymakers, in Climate Change (2007). The Physical Science Basis. Contribution of Working Group I to the Fourth Assessment Report of the Intergovernmental Panel on Climate Change, edited by S.Solomon et al., pp. 129-234, Cambridge Univ. Press, New York.

Jacobson, M. Z. (2001). Strong radiative heating due to the mixing state of black carbon in atmospheric aerosols, *Nature*, **409(6821)**, pp. 695-697.

Parameswaran K. et al.,(1998). Seasonal and long term variations of aerosol content in the atmospheric mixing region of a tropical station on the Arabian Sea-coast, *J. Atmos. Sol. Terr. Phys.* ,**60**, pp.17–25.

Ramakrishna, R. R., Madhavi, L. K., Badarinath, K.V.S, Ramakrishna Rao, T.V., Nazeer Ahammed, Y., Rama Gopal, K. and Abdul Azeem, P.(2003). Studies on Aerosol Optical Properties over Urban and Semi-arid environments of Hyderabad and Anantapur, *J. Quant.Spectrosc. Radiat. Transf.*, ***78***, pp. 257-268.

Stull, R.B. (1998). An introduction to Boundary Layer Meteorology, Kluwer Academic Publishers, Dordrecht.

COARSE & FINE PARTICLES MEASUREMENTS IN DIFFERENT INDOOR WORKING ENVIRONMENTS OF AGRA CITY

DAVID D MASSEY[1], MAHIMA HABIL[1] &AJAY TANEJA[2]

[1]Department of Chemistry, St John's College Agra-282002
[2]Departmen of Chemistry, Dr. B.R.A. University, Agra-282002
E mail: davidmassey22@gmail.com, ataneja5@hotmail.com

Keywords: COARSE AND FINE PARTICLES, MASS AND NUMBER CHARACTERIZATION, FULL DAY VARIATION, INDOOR AIR QUALITY

INTRODUCTION

The last few decades have seen major changes in the home and work environments. Public concern over indoor air quality (IAQ) has increased dramatically in recent years, as hundreds of pollutants from various indoor and outdoor sources have been identified in indoor environments, depending on the operations and activities that occur within the environment (Brown *et al.*, 2012). These air pollutants have been associated with adverse health effects that have significant socioeconomic impact (Harrison *et al.*, 1997). Most of the people in India spend 80-90% of their time indoors, where exposure to majority of air pollutants is quite different from those of outdoors (Taneja *et al.*, 2008 and Massey *et al.*, 2009). Therefore the understanding of how indoor air pollutants affect the human health is of great importance. Exposure to airborne particles and specifically to its fine fractions ($PM_{2.5}$, PM with d <2.5 μm in aerodynamic diameter) is of particular importance as these particles have a higher probability of penetration into the deeper parts of the respiratory tract including trachea, bronchi, bronchioles and alveoli (Brick *et al.*, 1997) and also contain higher levels of trace elements and toxins (Ando *et al.*, 1996). Particles deposited in these areas are removed more slowly from the body and thus, have more opportunities to impair healthy cells and tissues (Miller, 1999).These problems are intimately bound up with modern lifestyles and at the same time require the urgent attention and action of many different parts of society as huge commitments which, are currently being made for the future in the absence of a coherent urban environment policy framework (WHO, 2002). Environmental awareness rises with the affluence of Indian people as more people are seeking higher living standards and a better living environment (Massey *et al.*, 2012). Thus the development of sound environmental policy requires both scientific information about the linkages between pollutant emissions and human health effects and value judgments about the importance of these effects relative to other social concerns. Thus detailed investigations of the size and number of particulate matter are important for elucidating the possible particulate toxicity. Present study aims in deriving the relationships between coarse and fine particles in offices and other commercial buildings of the city. The objective of this study will be to pinpoint the integrated actions essential to reduce the particulate pollution. These should be implemented to other towns and cities of India where some type of situation occurs that can benefit health, quality of life and the economy.

METHODOLOGY

Site Description

Agra, the city of Taj (27°10'N, 78°02'E) is located in the central part of northern India, about 204 km of south of Delhi in the Indian state of Uttar Pradesh. The city, situated on the west bank of the

river Yamuna 169 m above sea level, is known world over as home to a wonder of the world, the Taj Mahal. A part of the great northern Indian plains, Agra has a tropical climate. The climate during summer is hot and dry with the temperature ranging from 32°C to 48°C. In winter the temperature ranges from 3.5°C to 30.5°C.The downward wind is south-southeast 29% and northeast 6% of the time in summer, and it is west-northwest 9.4% and north-northwest 11.8% of the time in winter. Agra has about 1,400,000 total population and the population density is about 19,246 persons per sq km (ORG, office of the registrar New Delhi, India: Ministry of Home Affairs, 2003). In the present study real time series data for mass and number of PM was monitored in indoor environment of three different location (two shops , two shopping malls or commercial buildings and two offices) in different regions of Agra city (Fig. 1).

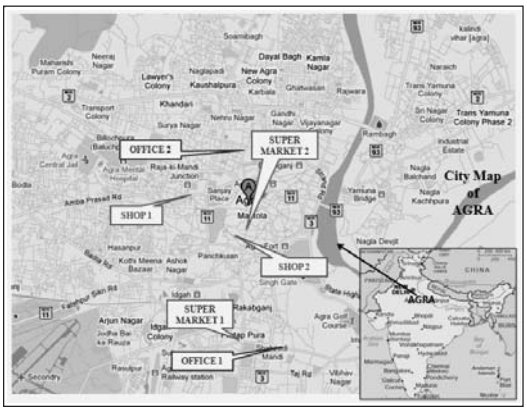

Figure 1 Map of Agra city showing different sampling sites.

Sample Collection

A campaign study was conducted from September to November 2011 to determine mass and number concentration of PM_{10}, $PM_{5.0}$, $PM_{2.5}$, $PM_{1.0}$, $PM_{0.5}$ & $PM_{0.25}$ in indoors of three different microenvironments (i.e. commercial centers, shops and offices) in different locations of Agra city. Grimm 31-Channel Portable Aerosol Spectrometer model No.1.109 was selected for the monitoring of particulate matter, which runs at a flow rate of 1.2 L/min ± 5% constant with controller for continuous measurement during the sampling period. It can give mass in μg m^{-3} and number in particles/m^3. Particles are collected close by the analyzer from a dedicated 5 cm long vertical sampling head (no sampling tubes and therefore no particle loss).

RESULT AND DISCUSSIONS

Particulate Mass

A total of twelve samples per month (i.e. six for mass concentration and six for number concentration) for PM_{10}, $PM_{5.0}$, $PM_{2.5}$, $PM_{1.0}$, $PM_{0.5}$ & $PM_{0.25}$ were collected from three different indoor microenvironments. Fig. 2 a & b gives the statistical summary of particulate mass and number concentrations during the total sampling days. During the campaign study the mean PM_{10}, $PM_{5.0}$, $PM_{2.5}$, $PM_{1.0}$, $PM_{0.5}$ & $PM_{0.25}$ mass concentration and standard deviation (SD) was 324.17±46.70 μg/m^3, 270.27±42.66 μg/m^3, 223.41±48.19 μg/m^3, 137.47±23.43 μg/m^3, 99.84±20.39 μg/m^3 & 52.34±11.45 μg/m^3 at supermarket sites, 324.57±47.13 μg/m^3, 271.30±40.63 μg/m^3, 225.44±49.79 μg/m^3, 137.89±23.86 μg/m^3, 99.41±20.72 & 53.07±11.36 μg/m^3 at shop sites and 327.00±47.03 μg/m^3, 272.98±40.03 μg/m^3, 227.44±50.54 μg/m^3, 139.17±23.75 μg/m^3, 101.33±20.75 μg/m^3 & 56.13±11.58 μg/m^3 at office sites.

Particulate Number

For number concentrations, mean PM_{10}, $PM_{5.0}$, $PM_{2.5}$, $PM_{1.0}$, $PM_{0.5}$ & $PM_{0.25}$ was 564050±91578.43 Particles/L, 320394±39385.52 Particles/L, 193678±17880.25 Particles/L, 174101±23865 Particles/L, 158428±29089.22 Particles/L & 73378±22638 Particles/L at supermarket sites, 589882±98489.67 Particles/L, 349888±39072.42 Particles/L, 206648±25422.77 Particles/L, 181495±24131.06 Particles/L, 166050±28853.73 Particles/L & 77619±22858.65 Particles/L at shop sites and 622352±77730.91 Particles/L, 352319±38052.23 Particles/L, 232186±35323.51 Particles/L, 193769±28899.68 Particles/L, 178172±24245.03 Particles/L & 85121±24879.46 Particles/L at office sites.

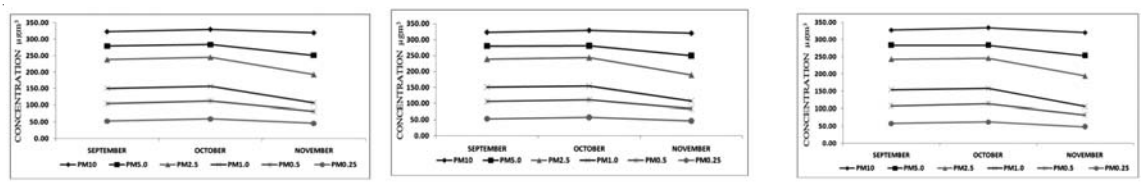

A. Supermarkets B. Shops C. Offices

Figure 2 a. Mass concentration of PM_{10}, $PM_{5.0}$, $PM_{2.5}$, $PM_{1.0}$, $PM_{0.5}$ & $PM_{0.25}$ at supermarkets, shops and offices.

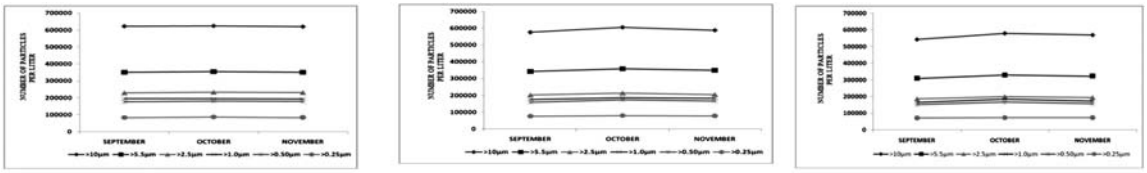

A. Supermarkets B. Shops C. Offices

Figure 2 b. Number concentration of PM_{10}, $PM_{5.0}$, $PM_{2.5}$, $PM_{1.0}$, $PM_{0.5}$ & $PM_{0.25}$ at supermarkets, shops and offices from September 2011 to November 2011.

On comparing with the standards given by WHO guidelines (24 hours mean = 25 µg/m^3, 50 µg/m^3 for $PM_{2.5}$ and PM_{10}), $PM_{2.5}$ exceeded 9 times and PM_{10} exceeded 6.5 times in all the indoor microenvironment (i.e. supermarkets, shops and offices). On comparing with NAAQS standards (24 hours mean = 60 µg/m^3, 100 µg/m^3 for $PM_{2.5}$ and PM_{10}), $PM_{2.5}$ exceeded 3.7 times and PM_{10} exceeded 5.4 times at all the sites. PM concentrations were found in similar trend at the three types of the microenvironment. However, the mass and number concentration trends were comparatively higher for all the particle sizes in the offices followed by shops and supermarkets. The higher concentrations in the offices are due to particle resuspension from vacuum cleaning, sweeping, low air exchange rate or the movements of office workers (Corsi *et al.*, 2008; Kemp *et al.*, 1998). PM concentrations are also greatly affected in the offices by the use of printers and multi-task devices (Massey *et al.*, 2011). During the campaign study a slight increase was notice in the PM concentrations during month of October in comparison to September and November.

Full Day Variation

The average diurnal trend of particulate mass and number concentrations during the study period monitored continuously throughout the day and night in indoors at the supermarket, shop and office sites is given in fig. 3 a & b. Full-day variation means monitoring of particulate pollutant around the clock (24h), covers all the indoor activities taking place in a day. The highest mass and number concentration peaks are observed during the morning hours from 9:00 to 10:00 AM and

late in the evening hours from 18:00 to 19:00 PM. These occurrence times of maximum concentrations of the particulate are due to re-suspension generated by traffic and other human activities, as these sites are mostly adjacent to busy traffic roads of the city (Figure 1a). As a result concentrations reaches maximum during the peak rush hours in the morning and evening (Harrison *et al.,* 1997). Whereas, the low concentrations of all the particles are observed between the 3:00 to 4:00 AM early in the morning hours. While during the working hours low concentrations were reported between 14:00 to 15:00 PM late in the afternoon hours at all the sampling sites. The mass and number concentrations for all the particulate sizes showed the similar kind of trends in all the sampling sites during the sampling duration.

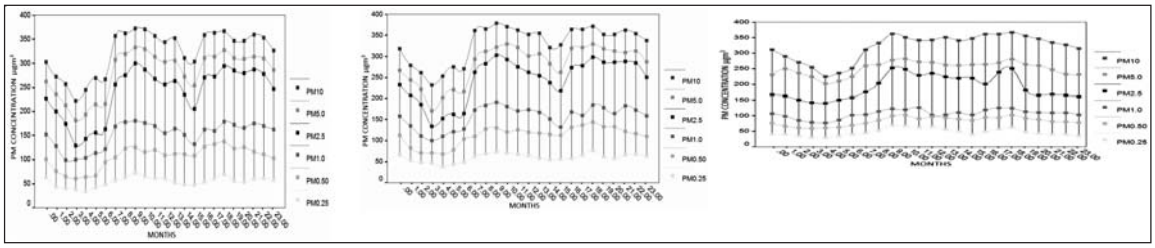

A. Supermarkets B. Shops C. Offices

Figure 3 a. Full Day variation in μgm^{-3} in different indoor microenvironment.

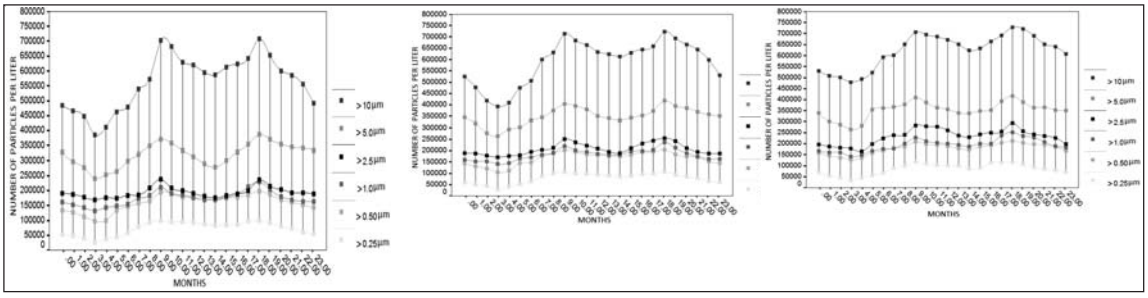

A. Supermarkets B. Shops C. Offices

Figure 3 b. Full Day variation in Particles/L in different indoor microenvironment

CONCLUSION

The results of the particulate measurements given here, gives an overview how adverse the condition may be in our working environment. We found that air quality at the working sites is greatly affected by particulate pollutant especially by fine particles. Our measurements on comparison with National Ambient Air Quality Standard were 3 to 5 times higher and with WHO they were 6 to 9 times higher for coarse and fine particles. Therefore based on the results of this study, the PM especially the fine particles should be concerned in view of annual human exposure. In future a more detailed study on personal exposure, chemical characterization and model based exposure assessment is required to understand the human exposures and health risks.

ACKNOWLEDGEMENT

The authors like to thank CSIR (Council of Science and Industrial Research) Project No: 8/109 (0010)/2011-EMR-I for funding this prject.

REFERENCES

Brown, K.W., Sarnat, J. A., Koutrakis, P. (2012). Concentration of $PM_{2.5}$ mass and components in residential and non-residential indoor microenvironment: The source and composition of particulate exposure study, *Journal of Exposure Science and Environmental Epidemiology*, **22**, pp. 161-172.

Harrison, R.M., Deacon, A.R., Jones, M.R., and Appleby, R. S. (1997). Sources and processes affecting concentrations of PM_{10} and $PM_{2.5}$ particulate matter in Birmingham (UK), *Atmospheric Environment*, **31**, pp. 4103–4117.

Taneja, A, Saini, R, Masih, A. (2008). Indoor air quality of houses located in the urban environment of Agra, India, *Ann New York Academy of Sciences,* 1140, pp. 228-245.

Massey, D., Masih, J., Kulshrestha, A., Mahima, H., & Taneja, A. (2009). Indoor/Outdoor relationship of fine particulate less than 2.5μm ($PM_{2.5}$) in residential homes located in central Indian region, *Building and Environment*, **44**, pp. 2037-2045.

Brick, M., Luciani, A., Formignani, M. (1997). Atmospheric aerosol in an urban area-measurements of TSP and PM_{10} standards and pulmonary deposition assessments, *Atmospheric Environment*, **31**, pp. 3659–65.

Ando, M., Katagiri, K., Tamura, K., Tamamoto, S., Matsumo, M., Li, Y. (1996). Indoor and outdoor air pollution in Tokyo and Beijing super cities, *Atmospheric Environment*, **30(5)**, pp. 695–702.

Miller, F.J. (1999). Dosimetry of particles: critical factors having risk assessment implications, *Inhale. Toxicology*, **12**, pp. 389-395.

WHO, 2002. The World Health Report, World Health Organization, http://www.who.int/whr/2002/en.

Massey, D., Kulshrestha, A., Masih, J., , Taneja, A. (2012). Seasonal trends of PM_{10}, $PM_{5.0}$, $PM_{2.5}$ & $PM_{1.0}$ in indoor and outdoor environments of residential homes located in North-Central India, *Building and Environment*, **47**, pp. 223-231.

Corsi, R.L., Siegel, J.A., Chiang, C. (2008). Particle resuspension during the use of vacuum cleaners on residential carpet, *Journal of Occupational and Environmental Hygiene*, **5**, pp. 232-238.

Kemp, P.C., Dingle, P., Neumeister, H.G. (1998). Particulate matter intervention study: a causal factor of building-related symptoms in an older building, *Indoor Air*, **8**, 153-171**.**

Massey, D., & Taneja, A. (2011). Emission and Formation of Fine Particles from Hardcopy Devices: The cause of Indoor Air Pollution in new InTect Publishers book project under the title of. Monitoring, Control and Effects of Air Pollution, *In-Tech Publication*, ISBN: 978-953-307-204-3.

PROPERTIES OF ATMOSPHERIC AEROSOLS IN SOUTH INDIAN REGION: CHARACTERISTICS OF PARTICLE NUMBER SIZE DISTRIBUTION FROM A CONTINENTAL RURAL SITE

SHIKA S.[1], C. PÖHLKER[2], M.N.S. SUMAN[3], H. GADHAVI[3], A. JAYARAMAN[3], R. RAVIKRISHNA[4], S. M. SHIVANAGENDRA[1], U. PÖSCHL[2], AND S. S. GUNTHE[1]

[1]EWRE Division, Dept. of Civil Engineering, Indian Institute of Technology Madras, Chennai-36, India,

[2]Max Planck Institute for Chemistry, Biogeochemistry Department, Hahn-Meitner-Weg 1, Mainz, Germany,

[3]National Atmospheric Research Laboratory, Gadanki, India,

[4]Dept. of Chemical Engineering, Indian Institute of Technology Madras, Chennai-36, India

E mail: shikasuren@gmail.com

Keywords: AEROSOL, NUMBER SIZE DISTRIBUTION

INTRODUCTION

Atmospheric aerosols have wide variations in size, concentration and chemical composition. To understand the effects of aerosols on climate and health, measurements of chemical and physical properties of aerosols, mainly size distributions and concentrations are indispensable. The lack of proper representation of aerosol data from different anthropogenic and natural sources in climate models, due to limited measurements, causes largest uncertainty in the current understanding of the climate change. The paucity of such observations and studies, mainly of aerosol size distributions, over India is highly contradictory to its global relevance as a major source of aerosol particles due to high temporal and spatial variability and consequent role in radiation budget, cloud formation and precipitation, and human health.

METHODS

As a part of investigating the aerosol size distributions over continental Indian region, Phase-I of measurements was initiated at the contrasting environmental and seasonal conditions in south Indian region. For the purpose two sampling sites were chosen in the south Indian region viz., National Atmospheric Research Laboratory (NARL; 13.5^0 N, 79.2^0 E, 336.5 m AMSL) at Gadanki and Indian Institute of Technology Madras, Chennai (IITM; 13.08N, 80.27, 6m AMSL). The main objective of the study was analysing the particle number size distribution, with size varying from 5.12 -34000 nm at contrasting environmental conditions using scanning mobility particle analyser (SMPS) with a scanning time of 5 minutes

RESULTS AND CONCLUSION

The preliminary one month of data analysis from Gadanki, for the month of May showed that the aerosol size distribution was bimodal with modal diameter of 83.09 nm in Aitken mode and 171.16 nm in Accumulation mode. The total aerosol concentration was ~4822 cm^{-3}, which indicates that Gadanki represents the typical rural characteristics based on the similar range of particle concentration observed at other rural locations. The total night-time aerosol number concentration was found to be higher when compared with daytime concentration as shown in Fig. 1. The modal

diameter, however, was similar during day and night-time, which indicates that the sources of aerosols during day and night time might be similar.

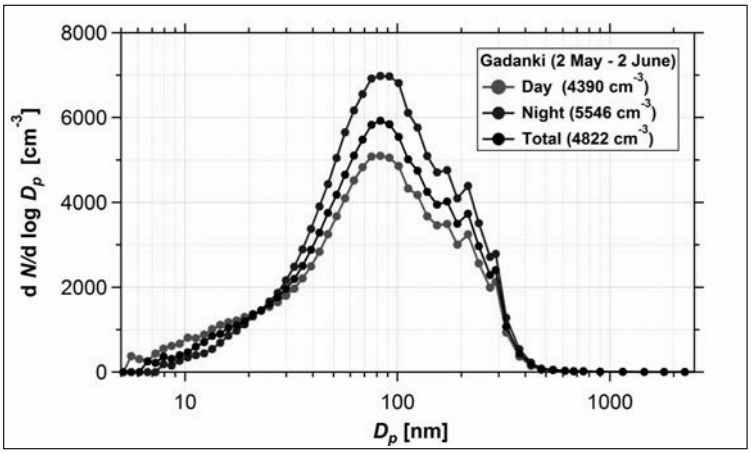

Figure 1. Average (black), daytime (grey), and night-time (dark) aerosol number size distribution averaged over the month of May-2012 measured at Gadanki using a Wide Range Aerosol Spectrometer (WRAS).

It also appeared that seemingly a new particle formation event took place during 0900 hr on 7th May.2012 to 0830 hr on 8th May.2012. as shown in Fig. 2.

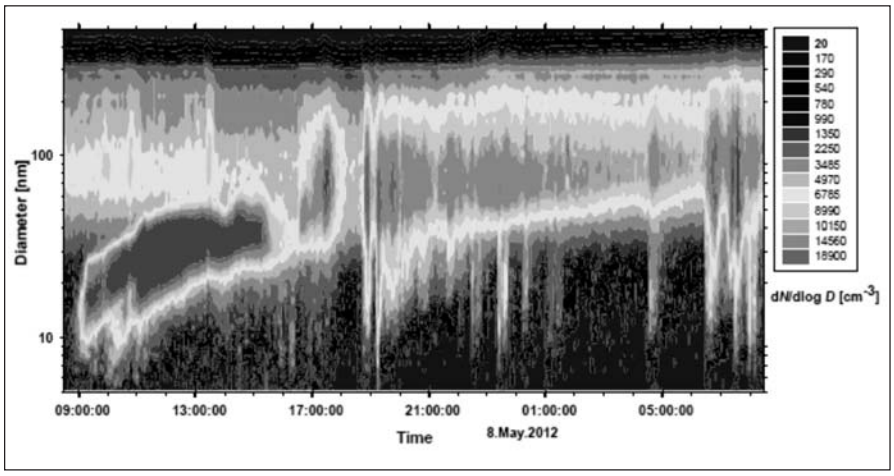

Figure 2. A contour plot depicting the aerosol number size distribution plotted against the time from 07/05 0830 hr to 08/05 0830 hrs. A distinct banana shape in the plot is representative of typical new particle formation event.

During this time the modal diameter showed an increase at the rate of 130% hr^{-1} starting from 15 nm till 109 nm. The further detailed findings regarding the size distribution measurements will be presented.

ACKNOWLEDGEMENTS

Authors would like to thank Rohit J. for support to carry out the measurements at Gadanki. SSG acknowledges the support from IC&SR, IIT Madras for the support under new faculty seed grant (project number CIE/11-12/560/NFSC/SAC)

TEMPORAL VARIATIONS OF AEROSOL CHARACTERISTICS OVER PATIALA, PUNJAB, INDIA

DEEPTI SHARMA, ATINDERPAL SINGH AND DARSHAN SINGH

Physics Department
PunjabiUniversity Patiala-147002
E mail: dsjphy@yahoo.com

Keywords : AOD, ANGSTROM COEFFICIENTS

INTRODUCTION

Aerosols perturb the global climate both directly and indirectly and give rise to radiative forcing (Charlson *et al.,* 1992). They affect the climate directly by both scattering and absorption of solar radiation, while indirectly by acting as cloud condensation nuclei (CCN) and modifying the microphysical properties of clouds (Ramachandran *et al.,* 2008).Patiala (lat; 30.33^0N, long. 76.4^0 E, 249m a.s.l) is situated in the northwest part of Indo-Gangetic plain where significant seasonal variations in AOD, aerosol mass concentration and their optical properties are expected due to increased anthropogenic activities.The climate of the study region is divided in to four seasons viz. winter (December-March), pre-monsoon (April-June), monsoon (July-September) and post-monsoon (October-November).Severe fog, haze and smog occur during winter and westerly or north-westerly winds prevail throughout this season. Dust storms are frequent during pre-monsoon (PrM) due to south-westerly winds that carry the coarse dust particles from the Thar Desert (*Sikka,* 1997). Total rainfall of ~750 mm occurs over Punjab mostly during the monsoon season. During post-monsoon season, mostly dry weather conditions prevail and vast clouds of smoke engulfs the Punjab state due to biomass burning resulting in dim sun shining.The present paper highlights the monthly and seasonal variations in the aerosols physical and optical characteristics during the years 2009-2010.

OBSERVATIONS AND RESULTS

Aerosol Optical Depth

Aerosol optical depth (AOD) measurements are made at 380, 440, 500, 675, 870 nm using a MICROTOPS II sun photometer of Solar Light Company, USA (Porter *et al.,* 2001). Fig. 1 (a-d) shows the seasonal variation of AOD during the study period (2009-2010). The mean spectral AOD is minimum during winter (0.3-0.8) and maximum during PoM (0.3-1.2) season. During PrM season AOD at longer wavelengths is high as compared to that during other seasons due to the dominance of the coarse dust particles while it is highest at shorter wavelengths during PoM season due to the emission of submicron black carbon aerosols due toburning of paddy residue. The monthly averaged value of AOD_{500} shows high values ($AOD_{500} > 0.53$) in the months of January, May, October and November for the years 2009 and 2010 (Fig. 2a) attributing to high aerosol loading during these months. The high AOD during months of October - November is due to post-harvest burning of paddy residue in the fields and during January month may be attributed to bio-fuel and fossil fuel burning. In the month of May, coarse mode particles are loaded in the atmosphere over the study area due to the frequent dust storms originating from Thar Desert (*Sikka,* 1997).

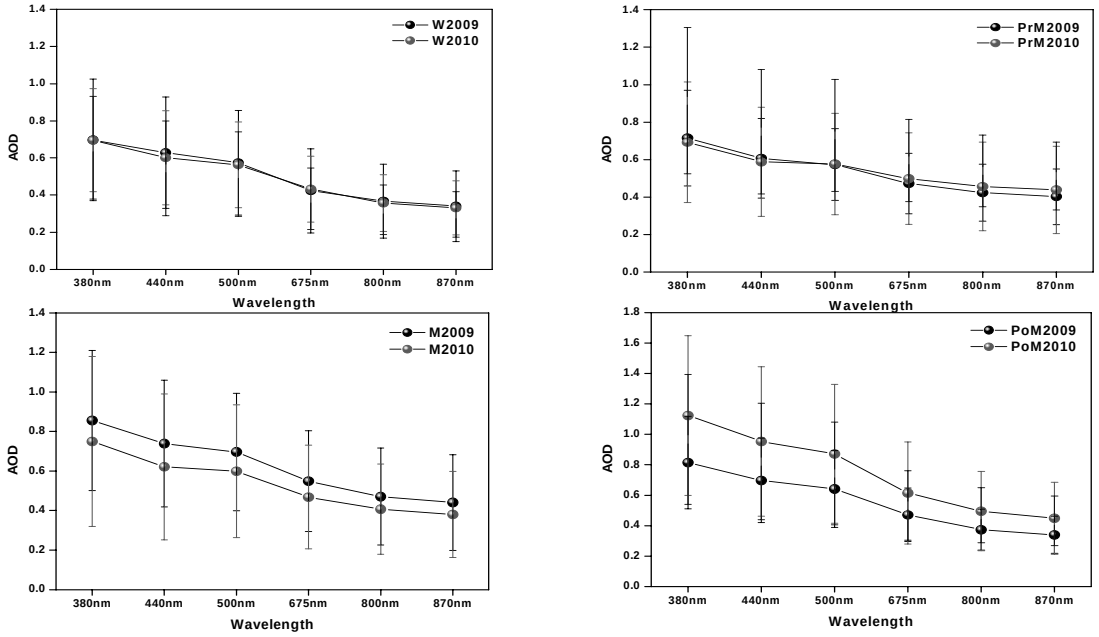

Figure 1 (a-d). Seasonal variation of spectral AOD during 2009-2010.

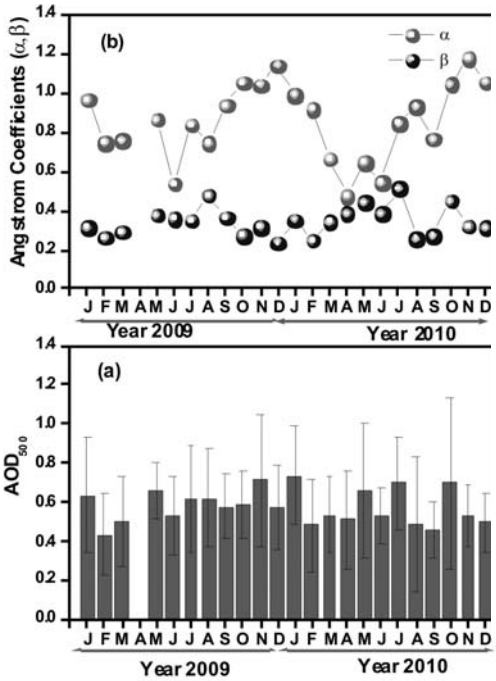

Figure 2 (a-b). Monthly variation of (a) AOD_{500} and (b) angstrom coefficients (á, â) during 2009-2010.

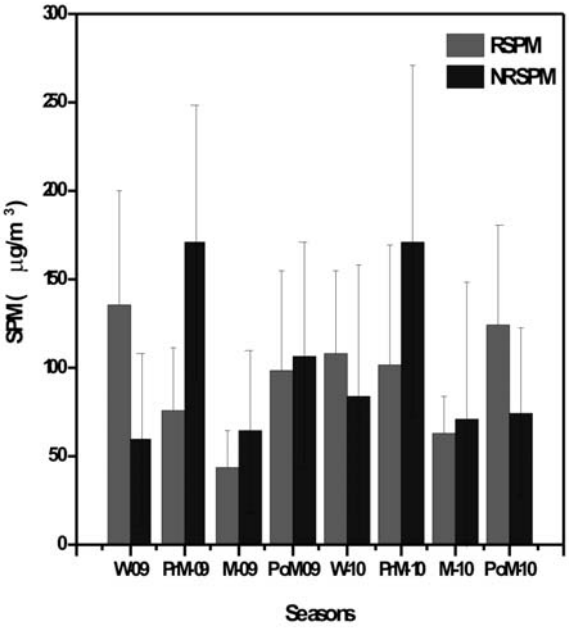

Figure 3. Seasonal variation of RSPM and NRSPM during 2009-2010.

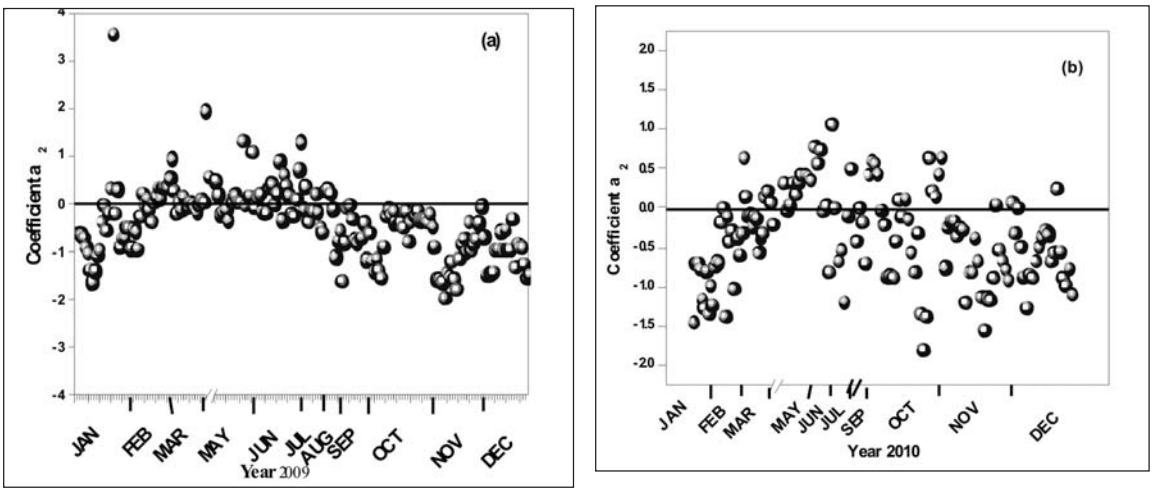

Figure 4. Scatter plot of coefficient $a_2$versus AOD_{500} during the study period (2009-2010).

Angstrom coefficients

Angstrom parameter á that indicate the aerosol size distribution is computed from a linear fit of log (AOD) versus log (wavelength) according to Angstrom relation (*Angstrom*, 1964)

$$\tau = \beta\ \lambda^{-\alpha} \qquad (1)$$

where â is turbidity coefficient and á is wavelength exponent. Fig. 2b shows the monthly variation of angstrom coefficients (α, β) during the study period. It is clear from the figure that during both the years (2009-2010) the angstrom exponent á is high (0.92-1.18) during the months of October to February and decreases thereafterand becomes minimum (0.47-0.86) during the months of April to June. High values of á during post-monsoon and winter are attributed to emissions of fine mode particles due to biomass burning during Oct & Nov and bio-fuel as well as fossil fuel burning during winter. But on the other hand, loading of coarse mode particles due to dust storm events during the months of April to June is responsible for low á values during these months. However, turbidity parameter β is high during PrM as well as PoM season showing high aerosol loading but it is minimum in winter for both the years under study.

Suspended particulate matter (spm)

Particle mass concentration measurements were made with HVS, Envirotech make(Model; APM460 DXm) that separates the fine and coarse particles viz. RSPM (PM_{10}) and NRSPM(Non Respirable Suspended Particulate Matter, > PM_{10}). Seasonal variations of RSPM and NRSPM are shown in Figure 3.Mass concentration of RSPM islow (~43-102 µgm/m^3) during PrMfollowed by monsoon season and high (~97-123µgm/m^3) during PoM followed by winter seasons whereas NRSPM is high (~171µgm/m^3)during PrM seasonduring both the years.

Coefficient a_2

The Ångström relation is related to Junge's power law (*Junge, 1955*) as;

$$\frac{dN}{d(lnr)} = cr^{-v} \qquad (2)$$

where, dN is the number concentration of the particles with radii between r and r+dr and c and í are fitting parameters. Dubovik *et al*. (2002) found that the retrieved size distribution of aerosols does not follow Junge's power law but they exhibit a bimodal distribution. The departure of this relationship introduces curvature into the $\ln\tau_\lambda$ versus $\ln\lambda$ relationship and the second order polynomial fit to versus is in good agreement with measured AOD (Eck *et al.,* 1999). The second order polynomial equation is given by;

$$\ln\tau_\lambda = a_2\ln\lambda^2 + a_1\ln\lambda + a_0 \qquad (3)$$

where, coefficient a_2 accounts for curvature and its negative value indicates that the aerosol-size distribution is dominated by fine mode particles and positive value of curvature indicates the dominance of coarse mode particles (Eck *et al*., 1999).

Fig. 4 (a-b) shows the scatter plot of coefficient a_2 versus AOD_{500} during the study period. It is clear from the figure that during both the years coefficient a_2 has negative values during PoM and winter season whereas it has positive values during PrM season. This conform to our finding that fine mode particles are abundant during PoM and winter season and coarse mode particles during PrM season.

CONCLUSIONS

Mean monthly spectral AOD shows significant seasonal variations during both the years of study. PoM and winter seasons are dominated by fine particles but coarse particles dominate during PrM season. Dust storms and biomass burning has significant effect on the spectral AOD variations over Patiala. Angstrom parameters and SPM also exhibit significant seasonal variations over the period of study. During both the years, coefficient a_2 shows negative value during PoM and winter season and positive values during PrM season**.**

ACKNOWLEDGEMENT

Present work has been carried out under ISRO-GBP (ARFI) project. Financial help rendered by ISRO is highly acknowledged. The meteorological data for Patiala Station provided by IMD is highly acknowledged.

REFERENCES

Angstrom, A. (1964). The parametersof atmospheric turbidity, *Tellus* , **16,** pp. 64-75.

Charlson, R. J., Schwartz, S. E., Hales, J. M., Cess, R. D., Coakley, J. A., Hansen, J. E., and Hoffmann, D. J. (1992). Climate forcing by anthropogenic aerosols, *Science*, **255**, pp. 423-430.

Dubovik, O., Holben, B. N., Eck, T. F., Smirnov, A., Kaufman, Y. J., King, M. D., Tanre, D., and Slutsker, I. (2002).Variability of absorption and optical properties of key aerosol types observed in worldwide locations, *Journal of Geophysical Research* ,**105**, pp. 9791–9806.

Eck, T. F., Holben, B. N., Reid, J. S., Dubovic, O., Smirnov, A., O'Neil, N. T, Slutsker, I., and Kinne, S. (1999). Wavelength dependence of the optical depth of biomass burning, urban, and desert dust aerosols, *Journal of Geophysical Research*, **104**, pp. 31,333–31,349.

Junge, C. E. (1955). The size distribution and aging of natural aerosols as determined from electrical and optical measurements in the atmosphere, *Journal of Meteorology*, **12**, pp. 13–25.

Ramachandran, S. and Cherian, R. (2008). Regional and seasonal variations in aerosol optical characteristicsand their frequency distributions over India during 2001–2005, *J. Geophys.Res.*,**113**, Article ID D08207.

Sikka, D. R. (1997). Desert climate and its dynamics, *Current Sciences*, **72 (1)**, pp. 35-46.

Porter, J. N., Miller, M., Pietras, C., and Mottel, C. (2001). Ship based sunphotometer measurements using Microtops Sun Photometers, *Journal of Atmospheric and Oceanic Technology*, **18 (5)**, pp. 765-774.

CHARACTERIZATION OF CARBONACEOUS AEROSOLS IN AMBIENT AIR OVER KADAPA, ANDHRA PRADESH

G.R. BEGAM, C.V. VACHASPATI, K. REDDY AND Y.N. AHAMMED

Atmospheric Science Laboratory, Department of Physics, Yogi Vemana University, Kadapa.
E-mail:ynahammed@gmail.com

Keywords: CARBONACEOUS AEROSOLS, ABSORPTION COEFFICIENT, ABSORPTION ANGSTROM EXPONENT

INTRODUCTION

Atmospheric carbonaceous aerosol is one of the important constituents of ambient particulate matter and is inert in the atmosphere as a result of its chemical structure and also due to its predominant sub-micron size. Recent modeling and field studies indicate that aerosol light absorption in an important component of climate forcing. For instance, the direct radiative forcing of light-absorbing aerosols may be greater than that of methane and equal to about one third of that of carbon dioxide (Jacobson, 2001). These carbonaceous aerosols are either present as organic carbon (OC), which is mainly volatile and/or reactive in a heated air stream, or as elemental carbon (EC), which is non-volatile and non-reactive, or as carbonate in the ambient air. The characterization of carbonaceous particles is a very active field, especially with respect to its effects on human health and atmospheric radiative properties, and interaction with clouds (Weingartner *et al.*, 2003). Mainly due to the presence of EC, ambient particulate material appears black when collected on a filter. Therefore, black carbon (BC) is defined as the fraction of carbonaceous aerosol absorbing light over a broad region of the visible spectrum, and is measured by determining the attenuation of light transmitted through the sample. Accurate information on BC is essential for the predictions of the radiative forcing caused by Black Carbon aerosols. Relatively small changes in the BC input data can change the radiative forcing from positive to negative. In view of this, surface measurement of Black Carbon (BC) has been made over Kadapa (14.47 ºN; 78.82 ºE; 138 m asl) using Portable Model AE 42-7 Aethalometer since May, 2011 as a part of Indian Space Research Organization-Geosphere Biosphere Programme's Aerosol Radiative Forcing over India (ARFI) Project. This is the simultaneous measurement of optical absorption of aerosols at seven different wavelengths (370, 470, 520, 590, 660, 880 and 950 nm). Data collected for a period of one year has been analysed to infer carbonaceous aerosol characteristics at Kadapa.

OBSERVATIONAL SITE AND EXPERIMENTAL SETUP

Kadapa is situated in the central part of Andhra Pradesh is located 8 km south of the penna river and is surrounded by the Nallamala and the palakonda hill on three sides. Kadapa is located at 14.47 °N and 78.82 °E at an elevation of about 138 meters. Kadapa has a tropical climate and the weather conditions are generally hot. Summers months are more hot and humid and monsoon season brings substantial rain to the area. Winters are comparatively milder and the temperatures are lower after the onset of the monsoons. Summer season is from March to May. During this time temperatures range from a minimum of 34°C and can rise up to a maximum of 44°C. Humidity is around 75% during the summer months. Monsoon season brings good amount of rainfall to the place and

temperatures are lower. Kadapa gets rainfall from both the South West Monsoon as well as the North East Monsoon. June to October is usually the monsoon. Winter season starts from the month of December and lasts till February. During this season temperatures range from a maximum of 25°C and can rise up to a maximum of 35°C. Humidity is much lower during the winter season. HYSPLIT model, 5-day back-trajectory analysis revealed different pathway clusters for advection of aerosols in different seasons.

Figure1. Observed site

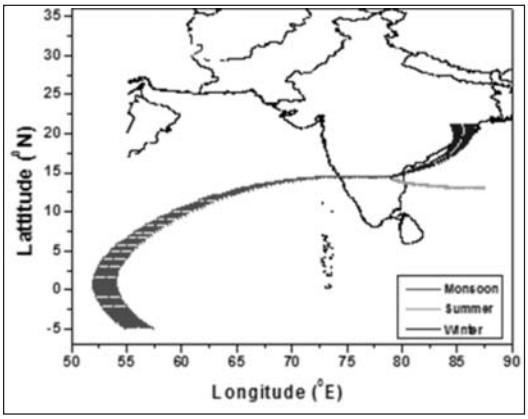

Figure2. The trajectory clusters arriving at the measurement site during different seasons.

Continuous observation on Black Carbon (BC) aerosols have been carried out by using an Aethalometer (Magee Sci. Inc., USA, Model AE-42-7) since April, 2011. In this method, atmospheric air is pumped through an inlet at the desired flow rate (about 4 LPM in present studies), which impinges on a quartz micro fibre strip. A light beam from a high-intensity LED lamp is transmitted through the sample deposit on the filter strip at desired wavelength. This attenuation is sensitive only to the amount of carbon in the sampled air. It is insensitive to any amounts of extractable organic carbon, or other aerosol species that frequently contribute substantially to the total aerosol mass, yet are not optically absorbing. The result implies that black carbon is the only aerosol species that is optically absorbing in the visible spectrum, and that a measurement of visible light absorption may be interpreted directly in terms of a mass of BC. Dust has an absorption cross-section that is smaller than that of BC by a factor of from 100 to 1000. Thus, if the amount of dust is 100 to 1000 times greater than that of BC, a comparable optical absorption may be produced. This can only be resolved by chemical analysis of the filter sample. As we know black carbon species have strong optical absorbance in the visible portion of the spectrum, but the illumination wavelength becomes shorter, the absorption cross-section of the six-member graphitic carbon rings increases as the photon frequency increases. Thus, the 'specific attenuation' at blue-violet wavelength of 400 nm is expected to be twice that for illumination in the near-infrared at 880 nm, as used for the standard 'BC' measurement. At wavelength shorter than 400 nm, certain classes of organic compounds (such as polycyclic aromatic hydrocarbons and also certain compounds present in tobacco smoke and fresh diesel exhaust) start to show strong UV absorbance. AE-42-7 Aethalometer uses seven different wavelength LEDs like 370, 470, 520, 590, 660, 880 and 950 nm for monitoring of Black Carbon and other Carbon compounds present in ambient air.

RESULTS AND DISCUSSION

During the measurement period concentrations were found maximum during winter (Dec. and Jan.), followed by those in the post-monsoon (Oct. and Nov.). Minimum concentration was observed in the monsoon (June, July, Aug. and Sep.) months. In fact, average concentration in winter (3500ng/ m^3) and post-monsoon (2400 ng/m^3) were three times more than that in monsoon period (600ng/ m^3).The average BC concentration at Kadapa during May, 2011 to May, 2012 was 1906 ng/m^3, which is good comparison with those reported for other ural stations like Nainital (1360 ng/m^3), Sinhabad (1500 ng/m^3) and Anantapur (1970 ng/m^3). Whereas, this value is much less as compared to that reported at urban locations like Delhi (17900 ng/m^3), Kanpur (6000-20000 ng/m^3), Mumbai (12500 ng/m^3), Hyderabad (45000 ng/m^3) etc.

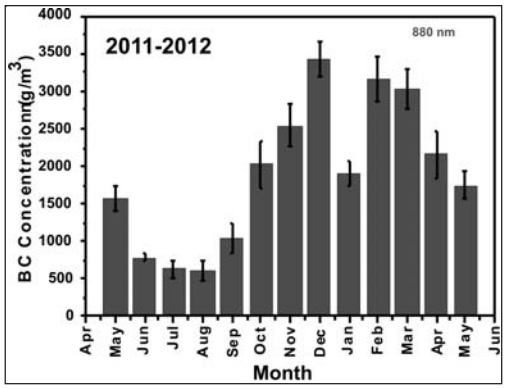

Figure 3. Monthly variation of average BC concentration.

Coen *et al.* (2010) and Weingartner, (2003) correction algorithms are chosen for the present study and the absorption coefficient has been estimated from the Aethalometer data in all wavelengths.

Absorption coefficient, σ_{abs} = BC x 14625 x 10^{-3} / (λ x C x R) in Mm^{-1}

Where BC is the mass concentration in ng m^{-3} and λ is the wavelength in nm. The values of C and R are 2.14 and 1, respectively. The spectral as well as monthly variations of absorption coefficient along with their standard deviations for 12 months are shown in Fig. 4 and Fig. 5. We observed the monthly mean values of σ_{abs} peaks in the months of December, 2011, February, 2012 & March, 2012 while the minima during June, July & August months of 2011 at all the wavelengths. It is also observed that the absorption coefficient decreases with the increase of the wavelengths in all months in our measurement period.

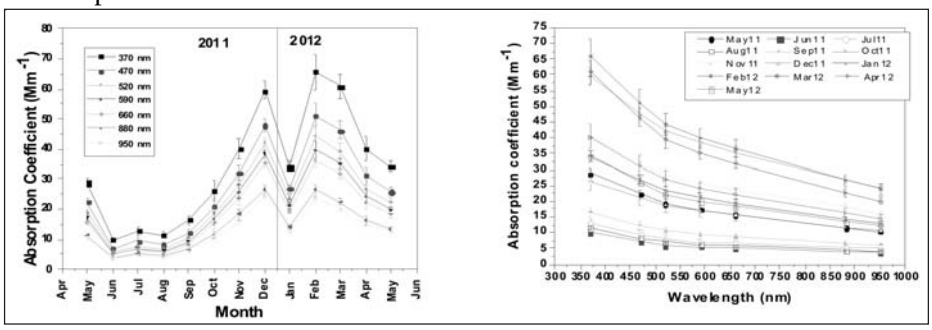

Figure 4. Monthly variation of average σ_{abs} Figure 5. Monthly spectral variation of average σ_{abs}

Following the approach of previous investigators (Thomas W. Kirchstetter *et al.*, 2004 and Schnaiter *et al.*, 2006), the dependence of aerosol light absorption on wavelength was parameterized using a power law relationship:

$$\sigma_{abs} = K \cdot \lambda^{-\alpha}$$

where σ_{abs} is the spectrally dependent mass absorption coefficient, K a constant, λ the light wavelength, and α the absorption Angstrom exponent. Thus the value of α is a measure of the strength of the spectral variation in aerosol light absorption. We show in Fig. 6 that α value is greater than 1.0 during all the months except October, November & December in 2011, which approximates the reasonably moderate spectral dependence of the biomass burning aerosols. α values less than 1.0 describes well the weak spectral dependence of the motor vehicle aerosols.

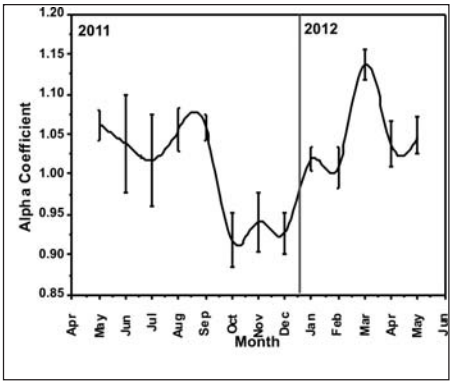

Figure 6. Monthly variation of average α_{abs}

ACKNOWLEDGEMENTS

Authors are thankful to ISRO - GBP for their financial assistance in the form of Research project under ARFI Network stations. G. Reshma Begam also thankful to DST for awarding JRF under INSPIRE Programme.

REFERENCES

Collaud Coen *et al.* (2010). Minimizing light absorption measurement artifacts of the Aethalometer: evaluation of five correction algorithms, *Atmos. Meas. Tech.*, **3**, pp. 457-474.

Jacobson, M.Z. (2001). Strong radiative heating due to the mixing state of black carbon in the atmospheric aerosols, *Nature*, **409**, pp. 695-697.

Schnaiter, M., Gimmier, M., Liamas, I., Linke, C., Jager, C. and Mutschke, H. (2006). Strong spectral dependence of light absorption by organic carbon particles formed by propane combustion, *Atmos. Chem. Phys. Discuss*,**6**, pp. 1841-1866.

Thomas W. Kirchstetter, Novakov, T. and Peter V. Hobbs (2004). Evidence that the spectral dependence of light absorption by aerosol is affected by organic carbon, *J. Geophys. Res.*, **109**, D21208.

Weingartner, E., Saathoff, H., Schnaiter, M., Streit, N., Bitnar, B. and Baltensperger, U. (2003). Absorption of light by soot particles: determination of the absorption coefficient by means of aethalometers, *Aerosol Science*, **34**, pp. 1445-1463.

PHYSICAL, OPTICAL, MORPHOLOGICAL, AND CHEMICAL STUDY OF DUST CHARACTERISTICS OVER THE INDO-GANGETIC BASIN

AMIT MISRA[1], ABHISHEK GAUR[1], DEEPIKA BHATTU[1], SUBHASISH GHOSH[1], ANUBHAV KUMAR DWIVEDI[1], ROSALIN DALAI[1],DEBAJYOTI PAUL[1], TARUN GUPTA[1], SUMIT KUMAR MISHRA[2], SUKHVIR SINGH[2],ELLSWORTH J. WELTON[3]AND SACHCHIDANAND TRIPATHI[1]

[1]Department of Civil Engineering, Indian Institute of Technology, Kanpur, India 208016
[2]National Physical Laboratory, New Delhi, India 110012
[3]NASA/Goddard Space Flight Center, Greenbelt, MD, USA
E mail: snt@iitk.ac.in

Keywords: AEROSOL, DUST, INDO-GANGETIC BASIN

INTRODUCTION

Dust has a large contribution to the overall aerosol climatology over the Indo-Gangetic Basin during the period April to June. Severe dust storms also occur during this period which affects the local air quality as well as climate (Dey *et al.*, 2004). Dust can be either transported from far-off desert regions or be of local origin. In the former case, mixing with anthropogenic aerosols modifies the properties of dust. In spite of studies carried out over the region, large uncertainty remains in dust properties characterization.

A four month long (April to July 2011) campaign mode study is carried outfor dust characterization over the Indo-Gangetic basin. The measurement location is Kanpur (26.52^0N, 80.23^0E), India.The overall objectives are to characterize the optical, physical, chemical, mineralogical, and morphological properties of dust, to study its mixing with anthropogenic aerosols, the variability in dust optical properties due to transport and mixing with pollution, and to identify proxies for dust and burning events based on chemical composition of aerosols (Formenti *et al.*, 2011).

METHOD

A variety of in-situ, remote sensing, and analytical techniquesare employed to measure various dust properties. Classification of aerosol types among various categories like Continental, Polluted Dust, Burning, and Dust is made on the basis of dust properties.

RESULTS AND CONCLUSION

Variation in Aerosol Optical Depth (AOD) at 500 nm during April to Juneis observed to be from 0.2 to 1.2 (Fig. 1). Classification of aerosol types among various categories like Continental, Polluted Dust, Burning, and Dust is made. For aerosols associated with Burning events, bimodal distribution is observed in the observed size distribution, whereas Polluted Dust and Dust cases show tri-modal distributions.Backtrajectory analysis shows NW Indian desert region and Nepal as the primary sources of Dust and Burning generated aerosols, respectively. Different particle shapes, e.g. platelets, parallelepiped, and rhombic, are observed in the SEM images. Presence of clay minerals, carbonates, bio-aerosols, and particles rich in C, Ca, O, and Cu, Si are confirmed. Ion analysis (Na^+, NH^{4+}, K^+, Ca^{2+}, Mg^{2+}, Cl^-, NO_3^-, SO_4^{2-}) show SO_4^{2-} dominating the $PM_{2.5}$ (5.97±2.87 μg/m^3) and PM_{10}

(7.04±4.39 μg/m^3) samples. XRF analyses of 17 aerosol samples and 11 blanks for each $PM_{2.5}$ and PM_{10}show the presence of Al, Ti, Fe, Ca, Mg, and K in PM_{10} samples collected on dust dominated days, and high S content in $PM_{2.5}$ for burning events. Characteristically higher Ca/Fe ratio and high K/Al ratio are observed for dust and burning events, respectively.

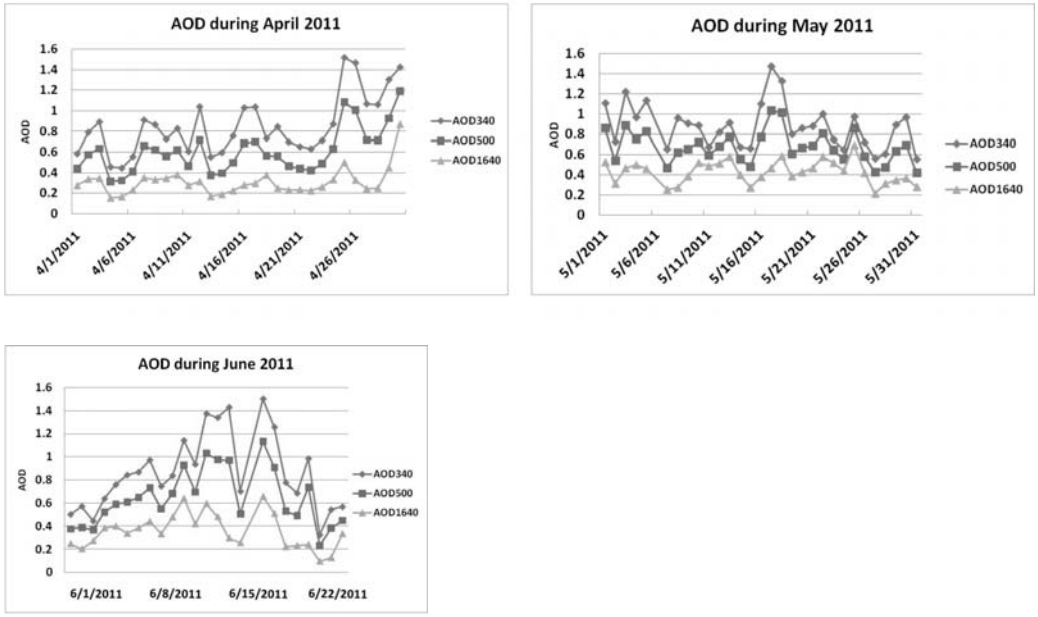

Figure 1.Variation in Aerosol Optical Depth at three representative wavelengths during April, May and June 2011.

ACKNOWLEDGEMENT

This work is supported by Department of Science and Technology under the CTCZ program.

REFERENCES

Dey, S., Tripathi, S. N., Singh, R. P. and Holben, B. (2004). Influence of dust storm on the aerosol parameters over the Indo-Gangetic basin, *J. Geophys.Res.*, **109**, D20211.

Formenti, P., Schütz, L., Balkanski, Y., Desboeufs, K., Ebert, M., Kandler, K., Petzold, A., Scheuvens, D., Weinbruch, S., Zhang, D. (2011). Recent progress in understanding physical and chemical properties of African and Asian mineral dust, *Atmos. Chem. Phys*., **11**, pp. 8231-8256.

TEMPORAL CHARACTERISTICS OF PARTICULATES, BLACK CARBON AND TRACE GASES OVER DIBRUGARH, NORTH-EAST INDIA

C.BHARALI, B. PATHAK, G. KALITA AND P. K. BHUYAN

Centre for Atmospheric Studies
Dibrugarh University, Dibrugarh, Assam-786004

Keywords: TRACE GAS, PARTICULATES, PCA, BLACK CARBON

INTRODUCTION

The atmospheric aerosols along with green house gases are one of the principal internal agents of climate change (Kaufman *et al*., 2002). Apart from direct and indirect effect on climate, aerosol particles are found to influence the abundance and distribution of atmospheric trace gases by heterogeneous chemical reactions and other multiphase processes. Due to its irregular agglomerate structure soot or black carbon (BC) aerosol offers a large surface for interactions with reactive trace gases like ozone. Laboratory studies and model results indicated a possible effect of soot surface reactions on the nitrogen partitioning in the troposphere (Hauglustaine *et al*., 1997; Rogarski*et al*., 1997) and tropospheric ozone concentrations (Bekki *et al*., 1997). Also BC accounts for most of the light absorption by atmospheric aerosols and is, therefore, of crucial importance for the direct radiative effect of aerosols on climate. Black carbon and trace gases likecarbon monoxide (CO), nitrogen oxide (NO) are emitted from the same sources like vehicular emission, biomass burning etc. Since NO is still the best indicator for the vicinity of road traffic, it can be stated that BC is more directly linked with the local traffic (IBGE-BIM Report, 2010). Therefore, understanding the relationship between particulates (PM) including BC and trace gases like ozone, CO, NOx can help in improving BC emission inventories and the evaluation of global and regional climate forcing effects.

In the present study an attempt has been made to analyze characteristics of particulates, BC and gaseous pollutants and look for common patterns and relationship among them over Dibrugarh (27.3ºN, 94.6ºE, 111 m amsl), a continental location in north-east India.In terms of human activity Dibrugarh is an urban location but with low population density and without heavy industrialization.

INSTRUMENTATION AND DATA

Continuous ground-based measurements of particulate matter and BC concentrations and trace gas mixing ratios have been carried out at Dibrugarh (27.3ÚN, 94.6ÚE and 111 m amsl) located in North-East India. Surface level PM concentrations are measured using a QCM. BC concentrations are being measured by a seven channel Aethalometer (model AE 31-ER from Magee Scientific) which is based on the principle of optical attenuation. The instrument measures attenuation of light beam at seven different wavelengths, viz., 370, 470, 520, 590, 660, 880 and 950 nm among which the observation at 880 nm wavelength is considered standard for BC measurement. The Ozone analyzer (*TeledyneModel T400*) based on UV-photometric technique and CO analyzer (*TeledyneModel* T300) based on IR-photometric technique have been used for surface Ozone and CO analysis. For surface NO_2 analysis NO_X analyzer (*TeledyneModel* T200) is used, which is based on the principle that the reaction of NO with O_3 results in electronically excited NO_2 molecules,

which releases their excess energy by emitting a photon and dropping to a lower energy level. Here the characteristics luminescence that produced is linearly proportional to the NO concentration.

Simultaneous measurements of BC, O_3, CO, SO_2 and NOxfrom 1st to 15th October, 2012 are utilized in the study.

RESULTS AND DISCUSSION

TEMPORAL VARIABILITY OF NEAR SURFACE AEROSOL CONCENTRATIONS AND TRACE GASES

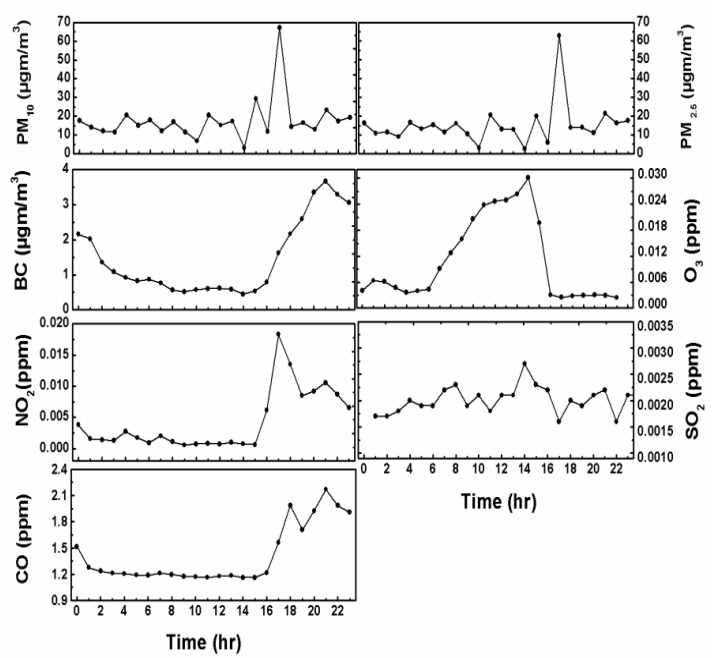

Figure 1. Diurnal variation of PM_{10} $PM_{2.5}$, BC and the trace gases O_3, NO_2, SO_2 and CO for a representative day in post-monsoon season.

In Fig. 1 the diurnal variation of PMs (i.e., PM_{10} and $PM_{2.5}$), BC and the trace gases O_3, CO,SO_2 and $NO_2$are shown for a clear day (14th October, 2012) in post-monsoon.There is a peak in PMs,NO_2 and CO concentrations at around 1700hrs, which may be due to a sudden rise in vehicular traffic.The diurnal variations of NO_2, CO andBC show a primary peak level during night time 1900-2200 hrs (local time), a less prominent secondary maximum in the morning hours between 0500-0800 hrs. Minimum concentrations have been observed in the daytime between 1000-1600 hrs. Diurnal variation of BC and the other two trace gasesis mainly governed by the diurnal evolution of atmospheric boundary layer (ABL), which remain low during morning hours, then gradually deepens to its peak by the noon time and starts decreasing in the evening (Krishnan and Kunhikrishan, 2004). Later in the evening and throughout the night, on the other hand, the radiative cooling of the ground surface results in the suppression or weakening of turbulent mixing and consequently in the collapse of the ABL depth. This results in the confinement of aerosols and a consequent increase in its concentration during early night period. After reaching a peak level, the concentrations decrease gradually due to reduction in anthropogenic activities.The minimum level of CO and NO_2during noon hours is associated with high level of O_3 as large amounts of precursors (like CO, NO*x*, etc.) are needed for O_3 production. Theatmospheric abundance of CO also affects the tropospheric O_3,

depending on the NOxconcentration (Crutzen, *et al.*, 1985). Ideally, in ambient air, the correlation between BC and CO depends onseveral factors such as i) wet and dry deposition, ii) vertical mixing and convection, iii) longrange transport, iv) reaction of CO with OH radical, and v) secondary emissions of CO throughthe oxidation of anthropogenic and biogenic VOCs and methane (Hudman, *et al*.,2008). Again the photolysis of NOx in the troposphere leads to the formation of O_3. The regional distribution is strongly controlled by the local emissions, while in the mid troposphere and upper troposphere it is mainly associated with the long range transport. The O_3 concentration starts to increase just after sunrise and attains peak level during afternoon hours (around 1400 LT), which then gradually decreases. This is directly associated with the photochemical reactions involving the solar radiation and precursor gases like CO, methane and VOCs in presence of NO_X. The night time minimum can be attributed to titration by NO. The variation of mixing ratio of surface O_3 is well correlated with its precursor gases such as CO and NOx. The production of O_3 in the troposphere is mainly controlled by the oxidation of CH_4, CO and hydrocarbons in the presence of NOx (Crutzen, 1974). SO_2 peaks at around 1400hrs and in the evening hours between 1800-2100hrs. As SO_2 is formed by the oxidation of sulfur present in diesel fuels, vehicular emissions from the highway running through the university campus may contribute to the observed high value of SO_2.

Seasonally, PM-s, BC, SO_2, NO_2 and CO exhibit similar seasonal variability with maximum in winter and minimum level in monsoon.This may be attributed to reduced boundary layer height and less rainfall during winter months and the minimum in monsoon months is associated with sufficient wet removal processes. Ozone is maximum during pre-monsoon months due to intense solar radiation and minimum in winter due to reduced intensity and duration of solar radiation.

ASSESSMENT OF AEROSOL-TRACE GAS INTERACTION USING PCA

PCA is used to analyze the relationship between pollution sources and PM, BC and trace gases (O_3, CO, NO_2 and SO_2). The highest contribution (50.47%) to PC1 is from CO, BC and NO_2, all being strongly associated with vehicular emission (Table 1). This is also clear from the good correlations between CO, BC and NO_2 as shown in Table 2. This result also confirms that NO_2, CO and BC are emitted from same sources. NO_2 and CO are the most important precursors for the production of ozone and their higher levels indicate that ozone production is significant over Dibrugarh. PC2 is loaded with particulate matters (27.11%) which are also emitted from vehicles. BC contributes 17.86% to PC3, which is the primary constituent of vehicular exhaust. PC4 indicates the presence of sulphur in diesel fuel with 2.79% contribution from SO_2.

Variables	PC1	PC2	PC3	PC4
PM10	0.1764	0.6824	-0.0116	0.019
PM2.5	0.2016	0.6678	0.0118	0.122
NO2	0.4995	-0.0409	-0.1813	-0.294
O3	-0.3739	0.17	-0.5282	-0.7137
SO2	0.1439	-0.1027	-0.8253	0.5281
CO	0.5084	-0.163	-0.0459	-0.3014
BC	0.5097	-0.1439	0.0684	-0.1388
variances%	50.4667	27.1104	17.8636	2.7892

Table 1. PCA results for BC, PM and Trace gases

	PM10	PM2.5	NO2	O3	SO2	CO	BC
PM10	1	**0.98**	0.26	-0.01	-0.03	0.1	0.13
PM2.5		1	0.29	-0.07	-0.03	0.15	0.18
NO2			1	-0.52	0.41	**0.91**	**0.87**
O3				1	0.25	-0.65	-0.74
SO2					1	0.31	0.21
CO						1	**0.97**
BC							1

Table 2. Correlation Coefficients of particulate matters, BC and trace gases

CONCLUSION

The diurnal variation of particulate matter, black carbon and traces gases O_3, CO and NO_2 over Dibrugarh and their interrelationship using PCA is studied. Good interrelationship among them has been observed indicating their origination from same sources.

ACKNOWLEDGEMENTS

The work is carried out with support from the ISRO-GBP-ATCTM and ARFI projects. C Bharali and B Pathak are indebted to ISRO-GBP for providing them fellowship and associateship respectively.

REFERENCES

Bekki, S. J. (1997). On the Possible Role of Aircraft-Generated Soot in the Middle Latitude Ozone Depletion, *Geophys.Res*, **102,** 10751.

Crutzen, P. J. (1974). Photochemical reactions initiated by and influencing ozone in unpolluted tropospheric air, *Tellus*, **26**, pp. 47–57.

Crutzen, *et al.* (1985). Tropospheric chemical composition measurements in Brazil during the dry season, *Journal of Atmospheric Chemistry*, **2**, pp. 233–256.

Hauglustaine, D. A., Ridley, B. A., Solomon, S., Hess, P. G., and Madronich, S. (1996). HNO_3/ NO_xratio in the remote troposphere During MLOPEX 2: Evidence for nitric acid reduction on carbonaceous aerosols?*Geophys. Res. Lett*. ,**23,** pp**.** 2609-2612.

Hudman, *et al*. (2008). Biogenic vs. anthropogenic sources of CO over the United States.*Geophys. Res. Lett*. , **35**, L04801, doi:10.1029/2007GL032393, 2008

Kaufman, Y. J., Tanre, D. and Boucher, O. (2002).A satellite view of aerosols in the climate system, Nature,**419**, pp. 215–223.

Krishan, P. and Kunhikrishan, P. K. (2004). Temporal variations of ventilation coefficient at a tropical Indian station using UHF wind profiler, *curr. Sci*., **86** (3), pp. 447-451.

Rogarski, C. A., Golden, D. M. and Williams, L. R. (1997).Reactive uptake and hydration experiments on amorphous carbon treated with NO_2, SO_2, O_3, HNO_3 and H_2SO_4,*Geophys. Res. Let*t. **24,** pp. 381-384.

PHYSICAL AND CHEMICAL PROPERTIES OF ATMOSPHERIC AEROSOLS AT MAHABUBNAGAR DURING CAIPEEX-IGOC-2011

D. S. BISHT[1], S. TIWARI[1], A. K. SRIVASTAVA[1], K. K. DANI[2] AND MANOJ K. SRIVASTAVA[3]

[1]Indian Institute of Tropical Meteorology (Branch), Prof Ramnath Vij Marg, New Delhi, India
[2]Indian Institute of Tropical Meteorology, Dr Homi Bhabha Road, Pashan, Pune, India
[3]Department of Geophysics, Banaras Hindu University, Varanasi, India
E-mail: dsbisht@tropmet.res.in

Key words: ION-CHROMATOGRAPH, ATMOSPHERIC AEROSOLS , CAIPEEX

INTRODUCTION

To understand the pathways of aerosol–cloud interaction through which this might be achieved, a national experiment named Cloud Aerosol Interaction and Precipitation Enhancement Experiment (CAIPEEX), an Integrated Ground Observational Campaign (IGOC) was conducted by Indian Institute of Tropical Meteorology, Pune under Ministry of Earth Sciences at Mahabubnagar (a rural environment in Andhra Pradesh), during the period from July-October 2011. During campaign, coarse (PM_{10}) and fine ($PM_{2.5}$) mode aerosol samples were collected on 24hrs basis using medium volume sampler (APM-550 Envirotech Pvt. Ltd.). These samples were analyzed for elemental and organic carbon (EC and OC) using OC-EC analyzer (Sunset, USA) and ionic species (water soluble components such as F^-, Cl^-, SO_4^{2-}, NO_3^-, Na^+, K^+, $Ca^{2+}$and Mg^{2+}) by Ion-chromatograph (DIONEX-2000). The preliminary results are given below.

SAMPLING AND ANALYSIS

PM_{10} and $PM_{2.5}$ aerosol sampling by off line method were conducted inside the campus of the Jaiprakash Narayan College of Engineering, Mahabubnagar, (16.44^0N, 77.59^0E) which is 180Km south from Hyderabad, Andhra Pradesh during July to October 2011, on the top of the building (~15m above the ground level). Sampling of aerosols were carried out using single stage Fine Particulate aerosol sampler, which provides information about aerosol mass concentrations of sizes up to 10μm and < 2.5μm, respectively. Both aerosol samples were collected on Whatman Quartz filter papers of the size 46.2 mm using APM 550 sampler (Envirotech Pvt. Ltd., India).

Exposed filter papers of $PM_{2.5}$& PM_{10} were analyzed for the mass concentrations of OC and EC by semi-continuous thermal/optical carbon analyzer (Sunset Laboratory Inc. Model 4L) using NIOSH 5040 (National Institute for Occupational Safety and Health) (Na, 2004) protocol**.** Briefly, an aliquot of sample filter (2.1cm2) is stepwise heated in a furnace up to 840^0C in a non-oxidizing atmosphere (100% He); furnace is then cooled to 550^0C and filter is stepwise heated to 850^0C in an oxidizing atmosphere (90% He, 10% O2), during each temperature step, evolved carbon is converted to methane and detected by a flame ionization detector. A calibration is performed at the end of each analysis by introducing a known amount of methane gas into the oven and measuring its constant response. Also, the major chemical species such as anions (F^-, Cl^-, SO_4^{2-} and NO_3^-) and cations (Na^+, K^+, $Ca^{2+}$and Mg^{2+}) were quantitatively determined by Ion Chromatograph (DIONEX- 2000, USA). The analytical column IonPac- AS15 with micro-membrane suppressor ASRS ultra II 2mm,

38 mM Potassium Hydroxide and the IonPac-CS17 column with micro-membrane suppressor CSRS ultra II 2mm, 6 mM methyl sulfonic acid as eluents and triple distilled water as regenerator were used for anion and cations, respectively. The details of the chemical analysis procedure are discussed by Tiwari *et al.*, (2010).

RESULTS AND DISCUSSION

The average concentration of OC was about 14µg m^{-3} and 9µg m^{-3}, while the EC was about 2.1 µg m^{-3} and 1.5µg m^{-3} in PM_{10} and $PM_{2.5}$ respectively (Fig. 1). The ratio of OC/EC in both PM_{10} and $PM_{2.5}$ was found to be ~7, which indicates the dominance secondary aerosols over the station. Higher concentration of carbonaceous aerosol species (OC and EC) over study site is due to emission from vehicular exhaust, biomass and fossil fuels burning, wood burning which is used during the cooking period.

The mean mass concentration of PM_{10} and $PM_{2.5}$ were found to be about 68±14µg $m^{"3}$ varied from 48 to 97µgm$^{"3}$ and 50±10µgm$^{"3}$ varied from 29 to 74µgm$^{"3}$, respectively during the entire measurement periods. These concentrations were approximately equal to the standards stipulated by National Ambient Air Quality Standards (NAAQS, 2005) for PM_{10} (60µg $m^{"3}$) and $PM_{2.5}$ (40µg $m^{"3}$). The ratio of $PM_{2.5}$/ PM_{10} varied between 0.60 and 0.76, which indicates the dominance of coarse mode particle in this area over study period. The mean level of aerosol (PM_{10}) pollution is approximately seven times larger than World Health Organization (WHO) guidelines. As per WHO air quality guidelines, aerosol levels should be less than 10µg m^{-3} of air. The mean $PM_{2.5}$ (50µgm^{-3}) mass concentrations were considerably higher (more than three times) than the United States National Ambient Air Quality $PM_{2.5}$ annual standard (15µg m^{-3}) (U.S. EPA, 1997).

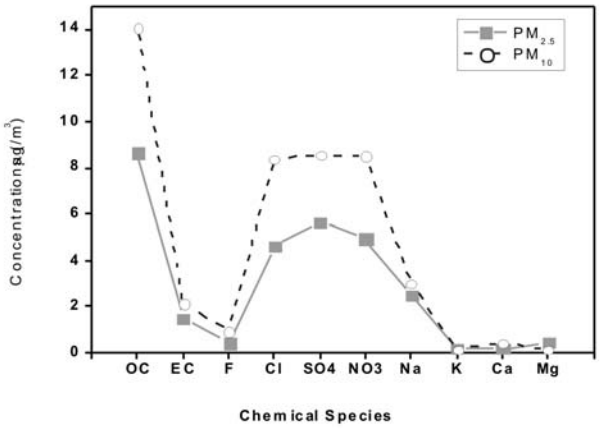

Figure 1. Concentrations of different ionic species in PM_{10} and $PM_{2.5}$

Also, Fig. 1 shows the concentrations of ionic species in the aerosol of PM_{10} and $PM_{2.5.}$ The ions such as F^-, K^+, $Ca^{2+}$and Mg^{2+} were found very low concentrations in both fine and coarse mode particles however Cl^-, SO_4^{2-}, NO_3^-, and Na^+ were higher concentrations over study period. It is clearly indicating that SO_4^{2-} is the highest concentrations in both the aerosol samples among the other ions, which varied from 2.49 to 13.70ìg m^{-3} in $PM_{2.5}$ with a mean concentration of 5.67(±2.97)µg m^{-3} however, in $PM_{10,}$ it was varied between 2.26µgm-3 to 18.08µgm-3 with a mean concentration

of 8.56(±4.15)μg m^{-3}. The details results and its source identification will be discussed during the conference.

ACKNOWLEDGEMENTS

The authors express their gratitude to Prof. B. N. Goswami, Director, Indian Institute of Tropical Meteorology for inspiration. The CAIPEEX-IGOC program was fully funded by the Ministry of Earth Sciences, Govt. of India.

REFERENCES

NAAQS (2005). National Ambient Air Quality Standards (NAAQS), http://cpcb.nic.in/oldwegion/environmental%2520standards/default-environment-standards.html

Na, K., Sawant, A.A., Song, C., Cocker, D.R. (2004). Primary and secondary carbonaceous species in the atmosphere of Western Riverside County, California, *Atmos. Environ.*, **38**, pp. 1345–1355.

Tiwari, S., Srivastava, A. K., Bisht, D. S., Bano, T., Singh, S., Behura, S., Srivastava, M. K., Chate, D. M., Padmanabhamurty, P. (2010). Black carbon and chemical characteristics of PM_{10} and $PM_{2.5}$ at an urban site of North India, *J. Atmos. Chem.*, **62**, pp. 193-209.

U S EPA. (1997). National Ambient Air Quality Standards for Particulate Matter: Final Rule. Federal Register, **62**, pp. 38651–38701.

CHEMICAL EVIDENCES OF ATMOSPHERIC PROCESSING OF AMBIENT AEROSOLS: IMPLICATIONS

NEERAJ RASTOGI

Geosciences Division, Physical Research Laboratory,
Navrangpura, Ahmedabad- 380 009, India

Keywords: PARTICLE-INTO-LIQUID SAMPLER, INORGANIC IONS, WATER-SOLUBLE ORGANIC CARBON

INTRODUCTION

Atmospheric particles and gases from megacities are increasing in unprecedented way. They have significant potential to impact natural atmospheric chemistry and alter the effects of airborne species on air quality, ecosystem, and climate on scale ranging from local to regional and up to global. Emissions of primary aerosol particles are compounded by the emissions of high levels of secondary aerosol precursors resulting in the production of large amounts of secondary aerosols during atmospheric transport. Chemical processing during aging further modify their physicochemical characteristics. Atmospheric chemical processing includes but not limited to secondary formation of inorganic and organic aerosols via multi-phase chemistry, condensation of volatile species at the surface of pre-existing particles and subsequent oxidation, change in solubility of insoluble species, and so on. As case studies, chemical evidences for secondary inorganic and organic aerosol formation, and acid neutralization by mineral dust and sea-salts, are presented.

EXPERIMENT

Long-term sampling of bulk-aerosols was carried out onto a tissuquartz filters using high volume sampler over Ahmedabad. These samples were assayed for the variety of chemical species including water-soluble inorganic cations and anions, carbonaceous aerosols (organic, elemental and carbonate carbon), and acid-soluble mineral dust (details given in Rastogi and Sarin 2005a, 2009). Major inorganic ions and water-soluble organic carbon (WSOC) were measured semi-continuously using particle-into-liquid sampler (PILS) coupled to ion chromatograph and total carbon analyzer (TOC) over Atlanta, USA (details are given in Rastogi *et al.* 2011).

RESULTS AND DISCUSSION

At Ahmedabad, the mineral dust component varied in the range 16–220 μg m^{-3} (Avg: 88, sd: 42); and contributed to 69 ± 5% of the TSP (range: 43–273 μg m^{-3}, Avg: 125, sd: 49) throughout the year, whereas contribution from anthropogenic and sea-salts emissions exhibited noticeable variability depending on changing meteorological conditions. Free sulfate and nitrate were found to be reacting with mineral dust (carbonates of Ca and Mg) over Ahmedabad, inferred based on anti-correlation between estimated acidity and measured alkalinity of aerosols (Rastogi and Sarin 2006). Acid neutralization by mineral dust over study region was also reflected in the form of alkaline nature of rainwater (pH range: 5.2 to 8.2, Avg: 6.8 ± 5, n= 91), despite having high concentration of acidic species in rainwater studied over the period of three years at Ahmedabad. Over the marine boundary layer of Bay of Bengal, almost quantitative chloride depletion from sea-salts was observed as a result of reactions between acidic species and sea-salts (Sarin *et al.* 2010).

Ambient aerosol NO_3^- concentrations over Atlanta usually varied between 0.05 to 2 μg m^{-3} but, increased as high as up to ~10 μg m^{-3} on particular evening, and high concentration lasted for ~12 hrs (Fig. 1). It was found to be related to favorable ambient temperature and relative humidity (low temperature-high humidity condition) (Rastogi *et al.*, 2011). Diurnal variability of WSOC over Atlanta peaks in afternoon, suggesting photochemistry play important secondary organic aerosol formation.

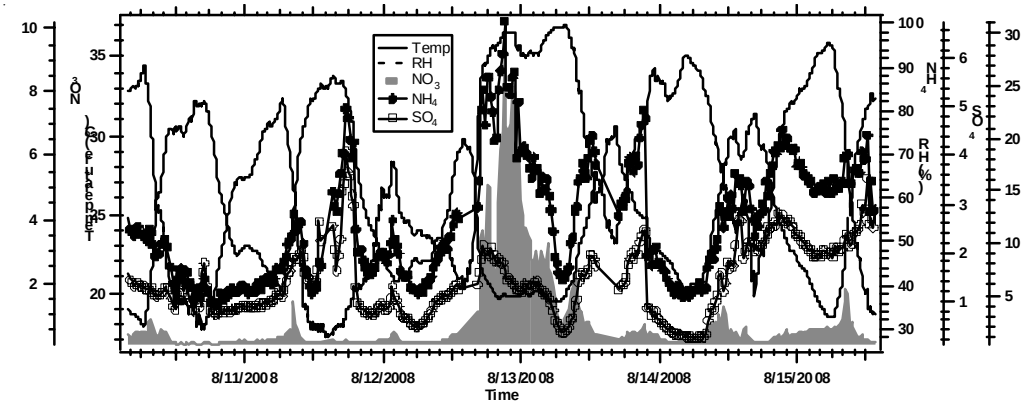

Figure 1. Temporal variability in NO_3^-, NH_4^+, SO_4^{2-} (μg m^{-3}) along with temperature and relative humidity over Atlanta (Figure reproduced from Rastogi *et al.*, 2011)

IMPLICATIONS

Acid neutralization by mineral dust may change the surface property of mineral dust from hydrophobic to hydrophilic, change the optical properties of mineral dust and thus, affects their capability to act as cloud condensation nuclei (CCN) and their radiative effects. It may also considerably reduce the number concentration of acidic species, shift their size distribution from fine to coarse mode and thus, change their residence time. Understanding the secondary aerosol formation is important to predict and model the aerosol composition and transport over regional and global areas.

REFERENCES

Rastogi, N., Zhang, X., Edgerton, E. S., Ingall, E., and Weber, R. J. (2011). Filterable water-soluble organic nitrogen in fine particles over the southeastern USA during summer, *Atmospheric Environment* ,**45**, pp. 6040-6047.

Sarin, M. M., Kumar, A., Srinivas, B., Sudheer, A. K., and Rastogi, N. (2010). Anthropogenic sulphate aerosols and large Cl-deficit in marine atmospheric boundary layer of tropical Bay of Bengal, *Journal of Atmospheric Chemistry,* **66**, pp.1-10.

Rastogi, N. and Sarin, M. M. (2009). Quantitative chemical composition and characteristics of aerosols over western India: One year record of temporal variability, *Atmospheric Environment* , **43**, pp. 3481-3488.

Rastogi, N. and Sarin, M. M. (2006). Chemistry of aerosols over a semi-arid region: Evidence for acid uptake by mineral dust, *Geophysical Research Letters*, **33**, L23815.

Rastogi, N. and Sarin, M. M. (2005). Long-term characterization of ionic species in aerosols from urban and high altitude sites in western India: Role of mineral dust and anthropogenic sources, *Atmospheric Environment,* **39**, pp. 5541-5554.

STUDY OF ATMOSPHERIC BLACK CARBON AEROSOLS OVER WESTERN INDIAN TROPICAL SITES DURING DIWALI FESTIVAL

B.M.VYAS[1], VIMAL SARASWAT[1, 2] AND CHHAGAN LAL[1]

[1]Department of Physics, M. L. Sukhadia University, Udaipur– 313001, India.
[2]Department of Basic Sciences, Pacific College of Engineering, Udaipur– 313003, India.

Keywords: ATMOSPHERIC BLACK CARBON AEROSOLS, ANTHROPOGENIC ACTIVITY, AIR POLLUTION, DIWALI FESTIVAL

INTRODUCTION

Atmospheric aerosols produced due to a wide range of global natural phenomena such as forest fire, dust storms and oceanic waves as well as with a large number of regional and local anthropogenic activities such as burning of fossil-fuel, industrial waste, automobiles, home furnaces, etc. Besides such manmade activities, specific intensive fire ignition and crack work activities also have ample potential to alter air quality and regional climate (Parashar *et al.*, 2005). Such anthropogenic aerosols activities occur during a certain celebration of festival period like Diwali festival in India, Lass Fallas in Spain, Lantern festival in Beijing, New year celebration all around the worldwide and other major similar ceremonies (Badarinath *et al.*, 2004; Drewnick *et al.*, 2006; Eck *et al.*, 1998; Mandal *et al.*, 1997; Novakov *et al.*, 2000; Vecchi *et al.*, 2007; Wang *et al.*, 2007).

The Indian major festival like Diwali is mainly celebrated across the whole Indian Subcontinent in the span of a few days of either October or November of every year. During such specific events, the large number of anthropogenic activities like bursting of firecrackers& sparkles, burning of bio-gases and residues of waste agricultural crop materials etc., take place over Indian urban and rural sites(Badarinath *et al.*, 2009; Sharma *et al.*, 2010). In recent years,the considerable attentions onthe impacts of firework activities on short-term perturbation in air pollutant levels and its chemical compositions have been given by several researchers during Indian festival Diwali, New-Year and other celebrations over India and other parts of the globe (Attri *et al.*, 2001; Barman *et al.*, 2008; Ravindra *et al.*, 2003;; Thakur *et al.*, 2010; Vyas & Saraswat, 2012). Their main findings suggested that in such occasions, exceptionally high emission levels of several air pollutants (i.e., different trace toxic metals present in various sizes of Suspended Particulate Matters), air toxic gases,aerosols optical depth and chemical matters reported above the prescribed limit of their National Ambient Air Quality Standard levels. These extensive findings have established the fact that the injections of these hazardous materials are responsible for accumulation of air pollutants and aerosols in the Earth's atmosphere for short duration. Hence, these events have become unusual extra sources of acute short-term air pollution episodes (Ganguly, 2009; Khaiwal *et al*., 2003; Kulshrestha *et al.*, 2004; Singh *et al.*, 2010).

The variations in the Black Carbon Mass Concentrations (BCMC) during Diwali over few Indian cities were reported by some group members at Trivandrum, Bangalore and Ahmedabad. Their studies showed the evidence ofsubstantial amounts of increase in BCM Cover Trivandrum (Babu & Moorthy, 2001), Bangalore (Nair *et al.*, 2010) and Ahmedabad (Ramachandran & Rajesh, 2007)during Diwali. However, such studies have given preliminary evidence about an increase of BC in Diwali only over urban sites. These efforts have created a lot of motivation to perform the detailed

investigation on the spectral diurnal behavior of BCMC from UV to IR range andtheir association with the meteorological parameters around the four days of Diwali as well as a normal day's trend.

In view of the above perspectives, the analysis of simultaneous observations of BCMC at 370,590 and 950nm over two close sites, located in the Western Indian region, have been presented in this paper during the Diwali days and normal day period of year 2009 and 2010. These two close tropical sites are specially chosen based on their different population density and geographical environment.Udaipur (24.6°N, 73.7°E, 580m AMSL) is region of large anthropogenic activities concerned with high populations of more than one million and semi arid zone. Another is Jaisalmer (27°N, 70°E, 221m AMSL) having small anthropogenic activities due to its lower population (less than two lacs), less industrial activity and TharDesert arid region. An attempt has also been made to correlate these extra perturbations in BC aerosols level with other plausible meteorological parameters like Wind Speed (WS, m/sec) and Planetary Boundary Layer Height (PBL, meter) etc., during Diwali days and normal day period.

EXPERIMENTAL INSTRUMENTATION AND DATA ANALYSIS

The regular measurements of BCMC from UV to IR ranges are being carried out at both stations by the well known near real time instrument i.e., Aethalometer(Model AE-31, Magee Scientific, USA) under the ARFI ISRO-GBP project. To infer the effect of Diwali on BCMC on different wavelengths 370,590 & 950 nm and its associated influence due to meteorological & boundary layer parameters and vice versa,special observations about BCMC on Diwali day period (Diwali, before and after the day of Diwali) were recorded for five minute interval, which are further averaged at regular interval of 15 minutes.

To compare the Diwali day period results to those of normal days, special round the clock observations of the Diwali as well as of before and after the Diwali day were taken along with normal days before the 10 days of Diwali occasion. The diurnal behavior of the BC parameter on Diwali festival period as well as the average normal day period has shown in Fig. 1. The corresponding variations of the several meteorological parameters over the Diwali day period as well as the normal day period have also plotted and shown in Fig. 2.The normal as well as Diwali days are shown by the red and black color lines, respectively.

RESULTS AND DISCUSSION

1. Fig. 1(a) and 1(c) show the mean diurnal hourly variation in BCMC at three specific wavelengths over Jaisalmer on Diwali as well as normal day period during 2009 and 2010, respectively. It is evident from the first look to these figures that the diurnal behavior of BCMC has always exhibited primary peak from late evening hour to night hours and another secondary peak around sunrise hours during both normal as well as Diwali days. But there is a substantial amount of increasing the maximum BC value of the order of 2.5 times more than from the normal day period of BCMC during the late evening to night hours. The corresponding timings coincide with Diwali firing activity hours.While in morning hours, no appreciable change in BCMC is seen during Diwali as compared to the normal day period. It is also noticed that more significant change in BCMCis seen at the UV range in comparison to IR range of BCMC, which is further showing the evidence of the high emission level of organic BC aerosols of UV range.

2. The average diurnal variation of BCMC at different wavelengths over Udaipur are shown for Diwali as well as the normal day period for both years 2009 and 2010 in Fig. 1(b) and 1(d),

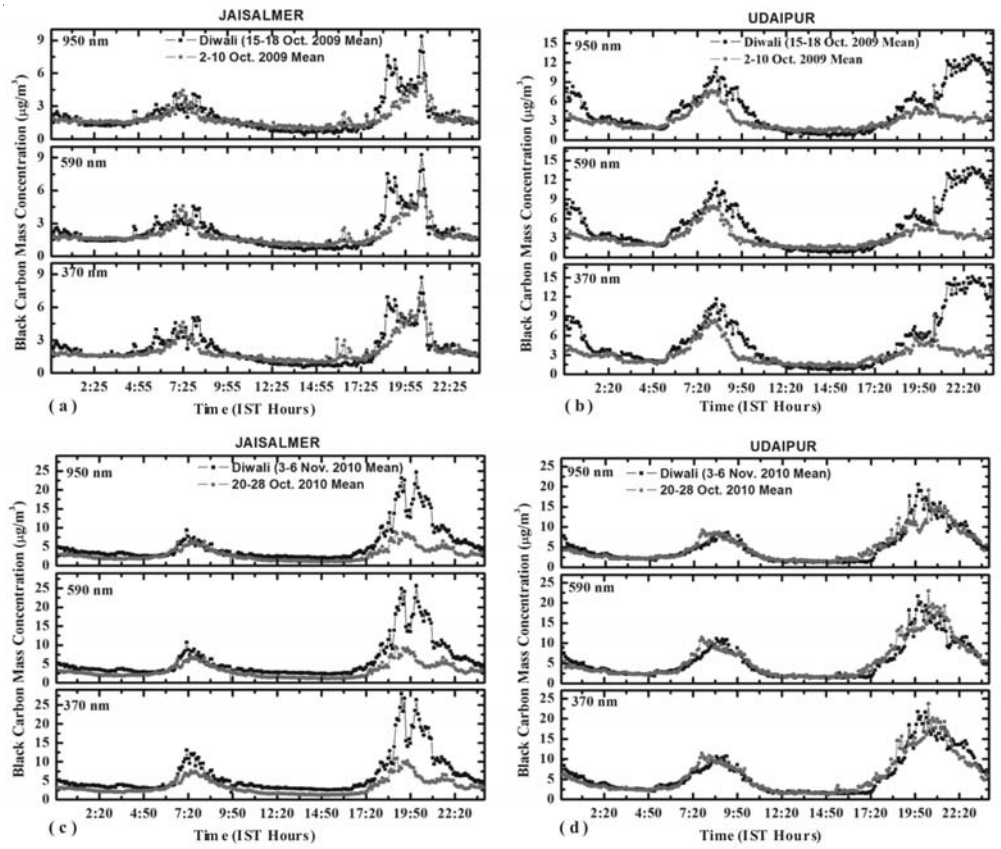

Figure1.Diurnal variation of BC Mass Concentration at different wavelengths during Diwali as well as normal days over Jaisalmer and Udaipur

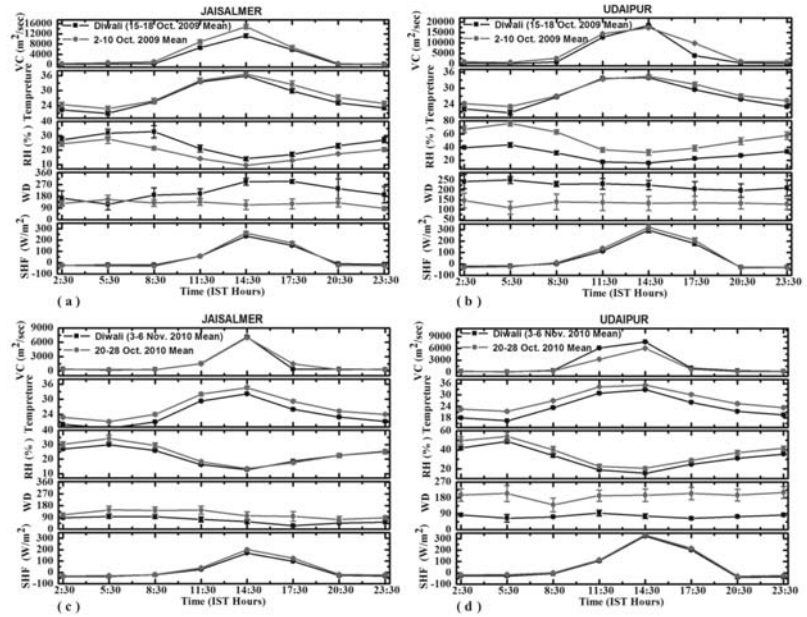

Figure2.Diurnal variation of meteorological parameters during Diwali as well as normal days over Jaisalmer and Udaipur.

respectively. It is observed that large changes in peak value of BCMC are also seen about 2.5 more than from their corresponding change in the normal day period inlate evening hours. However, in Udaipur, the influence in BCMC value during Diwali festival is clearly seen for longer duration, which is further extended from late evening to midnight hours. Here, a significant change in BCMC of 1.5 times more than their control day trend valueis also noticed in the morning hours. Influence in magnitude of BC during Diwali is also associated with lower value of both temperature and Ventilation Coefficient (VC), which implying the high air pollution level in the Diwali day period as compared to the normal day behavior.The diurnal variation Relative Humidity (RH) and Sensible Heat Radiation Fluxes do not show any change inthe Diwali period from control day behavior, however, there is an appreciable change in diurnal variation of wind direction during the Diwali period from the normal day period, which may seem to be another possible cause for altering the amplitude of diurnal oscillation in BCMC during Diwali festival.

CONCLUSIONS

The substantial amount in change in maximum value of BCMC about 2.5 times more is found during the late evening to night hours along with the most prominent change in BCMC value of UV range i.e., at shorter wavelength over both the places during Diwali occasion. The duration of primarypeaks of BCMCvalues is further extended from late evening to midnight hours at Udaipur only.Influence on BCMC magnitude due to Diwali days during the morning hours is also portrayed over Udaipur, which is not seen over Jaisalmer. Such unusual perturbation in BCMC can be seen in terms of cooling the Earth's surface and decreasing the VC values or increasing the air pollution level over both locations.

ACKNOWLEDGEMENTS

This study was fully financially supported and carried out as a part of Aerosols Radiative Forcing over India (ARFI) project network of ISRO-GBP Project.The authors would also like to express their sincere indebtedness with gratitude to Prof. K. Krishna Moorthy, Director, SPL, VSSC, Trivandruam as well as thanks to Dr. S. Suresh Babu, ARFI Project Manager, SPL, VSSC for providing all around academic and moral support to carry out the present study.

REFERENCES

Attri, A.K., U. Kumar and V.K. Jain (2001).Formation of Ozone by Fireworks, *Nature*, **411**, 1015, doi: 10.1038/35082634.

Babu, S.S. and K.K. Moorthy (2001). Anthropogenic impact on aerosol black carbon mass concentration at a tropical coastal station: A case study, *Curr. Sci.* ,**81**, pp. 1208-1214.

Badarinath, K.V.S et al. (2004). Characterization of aerosols from biomass burning- A case study from Mizoram (Northeast), India, *Chemosphere,* **54**,pp. 167-175.

Badarinath, K.V.S., Kharol, S.K., Sharma, A.R.and Prasad, K.V. (2009). Analysis of aerosol and carbon monoxide characteristics over Arabian Sea during crop residue burning period in the Indo-Gangetic Plains using multi- satellite remote sensing datasets, *Journal of Atmos. & Solar – Terr. Phys.,* **71**, pp. 1267-1276.

Barman, S.C., Singh, R., Negiand, M.P.S. , Bhargava, S.K. (2008). Ambient air quality of Lucknow City (India) during use of fireworks on Diwali Festival, *Environ Monit Asses.,* **137**, pp. 495-504.

Drewnick, F., Hings, S.S., Curtius, J., Eerdekens, G. and Williams, J. (2006). Measurement of fine particulate and gas-phase species during the New Year's fireworks 2005 in Mainz, Germany, *Atmospheric Environment* , **40**, pp. 4316-4327.

Eck, T.F., Holben, B.N., Slutsker, I. and Setzer, A. (1998). Measurements of irradiance attenuation and estimation of aerosol single scattering albedo for biomass burning aerosols in Amazonia, *J. Geophys. Res.*, **103**, pp. 31,865-31,878.

Ganguly, N. (2009). Surface ozone pollution during the festival of Diwali, New Delhi, India, *e-Journal Earth Science India*, **2**, pp. 224-229.

Khaiwal, R., Suman, M. and Kaushik, C.P. (2003). Short term variation in air quality associated with firework events: A case study, *J. Environmental Monitoring* , **5**, pp. 260-264.

Kulshrestha, U.C., Rao, T.N., Azhaguvel, S. and Kulshrestha, M.J. (2004). Emissions and Accumulation of Metals in the Atmosphere Due to Crackers and Sparkles During Diwali Festival in India, *Atmos. Environ.*, **38**, pp. 4421-4425.

Mandal, R., Sen, B.K. and Sen, S. (1997). Impact of fireworks on our environment, *Indian Journal of Environmental Protection*, **17**,pp. 850-853.

Nair, A.V., Mohan Kumar, K. and Satheesh, S.K. (2010). Measurements of Aerosols Black Carbon at an Urban Site in Southern India, *Bull. IASTA*, pp. 463-465.

Novakov, T. *et al.* (2000). Origin of carbonaceous aerosols over the tropical Indian Ocean: Biomass burning or fossil fuels? *Geophys. Res. Lett.*, **27**, pp. 4061-4064.

Parashar, D. C., Gadi, R., Mandal, T.K. and Mitra, A.P. (2005). Carbonaceous aerosols emission from India , *Atmospheric Environment*, **39**, pp. 7861-7871.

Ramachandran, S. and Rajesh, T.A. (2007). Black carbon aerosols mass concentration over Ahmedabad, an urban location in western India: Comparison with urban site in Asia, Europe, Canada, and the United States, *J. Geophys. Res.*, **112**, D0621.

Ravindra, K., Mor, S. and Kaushik, C.P. (2003). Short-term variation in air quality associated with fireworks events: a case study, *Journal of Environmental Monitoring*, **5**, pp. 260-264.

Sharma, A.R., Kharol, S. K. , Badarinath, K.V.S. and Singh, D. (2010). Impact of agriculture crop residue burning on atmospheric aerosol loading- a study over Punjab State, India, *Ann. Geophys.*, **28**, pp. 367-379.

Singh, S., Soni, K., Bano, T., Tanwar, R.S., Nath, S. and Arya, B.C. (2010). Clear-sky direct aerosol radiative forcing variation over mega-city Delhi, *Ann. Geophys.*, **28**, pp. 1157-1166.

Thakur, B. *et al.* (2010). Air pollution from fireworks during festival of lights (Deepawali) in Howrah, India- a case study, *Atmosfera*, **23**, pp. 347-365.

Vecchi, R. *et al.* (2007). The impact of fireworks on airborne particles, *Atmospheric* Environment, **42**, pp. 1121-1132.

Vyas, B.M. and Saraswat, V. (2012). Studies of Atmospheric Aerosol's parameters during Pre-Diwali to Post–Diwali festival period over Indian Semi Arid Station i.e., Udaipur, *Applied Physics* Research, **4(2)**, pp. 40-55.

Wang, Y., Zhuang, G., Xu, C. and An, Z. (2007). The air pollution caused by the burning of fireworks during the lantern festival in Beijing, *Atmospheric Environment*, **41**, pp. 417-431.

CHARACTERIZATIONS OF PARTICULATE MATTER ASSOCIATED TRACE METALS AND ITS MORPHOLOGICAL STUDY IN PUNE

SUMAN YADAV, AMRUTA P. KODRE AND P. GURSUMEERAN SATSANGI

Department of Chemistry, University of Pune, Pune – 411 007
E mail: pgsatsangi@chem.unipune.ac.in

Keywords: PM CHARACTERIZATION, TRACE METALS, TOXICITY, MORPHOLOGY

INTRODUCTION

The particulates may include a wide range of chemical species, ranging from metals to organic and inorganic compounds (Tsai and Cheng, 2004; Park and Kim, 2005). Among the inorganic compounds, most important one are the trace metals. Metals are ubiquitous in the environment and its presence occurs in both natural and anthropogenic sources (Kulshrestha *et al.*, 2010; Shah and Shaheen, 2010). As trace metals associated with particles are nonvolatile in nature, they are less prone to chemical transformation and remain in the form as they are emitted, even though they tend to undergo long range atmospheric transport (Morawska and Zhang, 2002). Particulate heavy metals can have severe toxic and carcinogenic effects on humans when inhaled in higher concentration. Beside the concentration of metals, the morphology of atmospheric particles is also important due to effect of the particle shape on their radiative (as climate effect) (Adachi *et al.*, 2010) and chemical properties (as health effect) (Ghio and Devlin, 2001). Thus, the aim of the present study is to evaluate the chemical composition of particles in terms of metals along with their morphological studies.

EXPERIMENTAL

Measurements of PM_{10} were conducted (July –Sept., 2011) on the roof of Chemistry Department, University of Pune, building about ~12 m above the ground. 24 hr PM_{10} samples were collected on 47 mm diameter glass fiber filter papers with particulate sampler (Mini Vol TAS, USA). For the concentrations of total metal, after water analysis, the same filter was digested with an acid mixture in 10 ml analytical grade (Merck) HNO_3 and kept on a hot plate at the temperature of 40–60°C for 90 min. This solution was diluted up to 25ml with Milli-Q water and stored in clean polypropylene bottles. Analysis for 17 metals was done on Inductively Coupled Plasma (ICP-AES) (ARCOS, Spectro, Germany) regularly within two months of extraction. For the morphological study of PM_{10}, samples (dry filter papers) were randomly cut in 1 cm^2 size out of the main filter and analysed through SEM-EDX (JEOL JSM-6330F, JEOL Ltd., Akishima, Tokyo, Japan).

RESULTS AND DISCUSSION

The average mass concentration of PM_{10} is 73.2 ± 20.3 μg m^{-3} which is less than the NAAQS standard (100 μg m^{-3}). The average concentration of metals ranged from 0.06 μg m^{-3} to 3.4 μg m^{-3}. The results for the total mean concentrations of individual metals specify Ni as the most abundant metallic element (3.49 μg m^{-3}) followed by Al> Fe > Cr > Co > Cu > Zn > Cd > Mn > Pb and Sr.

Enrichment factors (EFs) for the mean concentration of trace elements in PM_{10} are calculated using Fe as a reference element (Table 1). The EF sequence is as; Ni> Co> Cr> Cu> Zn> Sr> Mn> Al. According to the degree of enrichment, the elements are grouped as follows: Ni, Co, Cr, Cu and Zn elements with a toxic character, are highly enriched (EF>100) confirming that anthropogenic sources prevail over natural inputs for these elements; Sr (23.7) and Mn (11.3) are intermediately enriched (EF between 10 and 100); probably attributed to both natural and anthropogenic sources.

Metals		**PM_{10}**	**Cu**	**Zn**	**Co**	**Cr**	**Ni**
Mean (ìg m^{-3})	73.2	0.62	0.55	1.08	1.51	3.49	
EF	-	215	180	887	404	2262	
Metals	**Sr**	**Cd**	**Mn**	**Al**	**Fe**	**Pb**	
Mean (ìg m^{-3})	0.068	0.49	0.27	2.02	1.96	0.07	
EF	23	-	11	1.3	1	-	

Table1. Mean concentration of PM_{10} and metals along with EF values

EF values around 1 were found for Al and Fe suggesting mainly crustal origin. The highly enriched elements are generally volatile elements, primarily emitted from high temperature processes (e.g. fossil fuel combustion and smelting), and these elements are usually associated with small and medium sized aerosol particles and can be transported to remote areas. Thus, EF for Ni was the highest (2262); EF for Cr (404) which are considered to be the toxic metals. Cr, Cd, Ni and Pb are known to be carcinogenic metals and excess cancer risk of these four metals has been calculated among the 12 metals investigated in this study. According to the EPA guidelines of carcinogenic risk assessment, the excess cancer risk can be obtained through the multiplication of environmental concentration and unit risk (for Cr = 1.2×10^{-2} $(\mu g\ m^{-3})^{-1}$, Cd = 1.8×10^{-3} $(\mu g\ m^{-3})^{-1}$ and Ni = 2.4×10^{-4} $(\mu g\ m^{-3})^{-1}$) (US EPA, 2005). From the calculation it was found that Cr had the highest excessive cancer risk followed by Cd and Ni.

Atmospheric PM_{10} sampled are analyzed with SEM-EDX analysis with the aim to identify their shape and origin. In present study, shapes of the particles are as rectangle, cubes, rough rectangle and spherical and an agglomerates types. Related to the chemical composition and morphology, the analyzed particles are classified into the most abundant groups such as soot, Si-rich particles (aluminosilicates) and fly ash, sulfates, metal-rich (fly ash) and biological particles. Soot is present as agglomerates of many fine spherical primary particles. This kind of aggregate has an irregular morphology of various shapes. C-rich particles are mainly resulting from the vehicular traffic as site is very near to source. This kind of particles usually contains metals which are presented in Fig. 1.

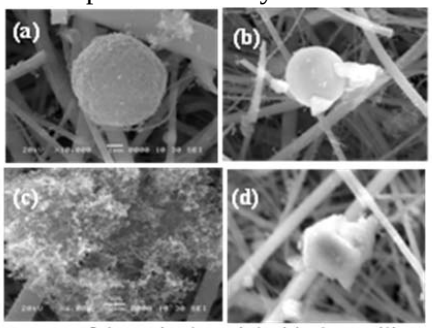

Fig. 1: SEM of deposited particle (a) alumosilicateparticle (soil) (b) fly ash (c)) soot agglomeration (f) Sodium salt

CONCLUSIONS

The average mass concentration of PM_{10} is ranging from 13.8 μg m^{-3} to 111 μg m^{-3} (Avg =73.2 μg m^{-3}) which is less than the NAAQS standard (100 μg m^{-3}). The average concentration of metals ranged from 0.06μg m^{-3} to 3.4 μg m^{-3} with Ni as highest metal in concentration. Enrichment factor values for Ni, Co, Cr, Cu and Zn elements were found to be high (EF>100) confirming their anthropogenic sources; Al and Fe suggesting a mainly crustal origin with their low EF value (EF = 1). Excess cancer risk was found to be highest for Cr followed by Cd and Ni. SEM study illustrated that shapes of particles as rectangle, cubes, irregular and spherical and an agglomerates. On the basis of SEM determination, the chemical composition particles were grouped as soot, Si-rich particles (aluminosilicates) and fly ash, sulfates, metal-rich (fly ash) and biological particles.

ACKNOWLEDGEMENTS

Authors wish to thank Department of Science and Technology (DST No. SR/FTP/ES-91/2009), New Delhi and BCUD, Pune for financial assistance. Authors also express their gratitude to Head, Department of Chemistry, University of Pune for his encouragement. Further, authors acknowledge SAIF IIT– Mumbai for sample analysis on ICP.

REFERENCES

Adachi, K., Chung ,S. H. and Buseck, P.R. (2010). Shapes of soot aerosol particles and implications for their effects on climate, *J. of Geophysical Research,* **115** (D15206).

Ghio A.J. and Devlin R.B. (2001). Inflammatory lung injury after bronchial instillation of air pollution particles, *Am. J. Respir. Crit. Care Med*., **164**, 704.

Kulshrestha A., Satsangi P.G., Masih J, Taneja A. (2009). Metal concentration of $PM_{2.5}$ and PM_{10} particles and seasonal variations in urban and rural environment of Agra, India, *Science of the Total Environment*, **407,** 6196.

Morawska L and Zhang J. (2002). Combustion sources of particles.1. Health relevance and source signatures, *Chemosphere*, **49**, 1045.

Park, S.S., Kim, Y.J. (2005). Source contributions to fine particulate matter in an urban atmosphere, *Chemosphere*, **59**, 217.

Shah, M.H. and Shaheen, N. (2010). Seasonal behaviours in elemental composition of atmospheric aerosols collected in Islamabad, Pakistan, *Atmospheric Research,* **95**, 210.

Tsai, Y.I., Cheng, M.T., 2004. Characterization of chemical species in atmospheric aerosols in a metropolitan basin, *Chemosphere*, **54**, 1171.

US EPA (2005). Guidelines for carcinogen risk assessment and supplemental guidance for assessing susceptibility from early-life exposure to carcinogens. Guidelines for carcinogen risk assessment, EPA/630/P-03/001f, 2005. Research and development, National Center for Environmental Assessment.

SIZE-SEGREGATED AEROSOLS DURING DIWALI FESTIVAL EPISODE IN RURAL AREA OFCHHATTISGARH, INDIA

JAYANT NIRMALKAR[1]and MANAS KANTI DEB[1]

[1]School of Studies in Chemistry, Pt. RavishankarShukla University,
Raipur 492 010, Chhattisgarh, India

E mail: j_nirmalkar@yahoo.com

Keywords: DIWALI FESTIVAL, $PM_{2.5-10}$, PM_1

INTRODUCTION

In past few decades there has been considerable research study in the field of atmospheric pollution and its properties. Biomass burning is the common ritual in the Asian communities both in indoor and outdoor premises. It is essential to compute the influence of anthropogenic emission on the aerosol burden, both globally and regionally, and both in term of mass and number due to the effect of aerosol in the climate and air quality (Ward *et al*., 2006; Thakur and Deb, 2000). PM is described as combination of solid and liquid particle in the air (Engling *et al*., 2009; Mohanraj and Azeez, 2004). PM is combination of inorganic and organic substances, present everywhere in air and produced from both anthropogenic and natural sources (Kundu *et al*., 2010; K. Hungershoefer *et al*., 2007). PM_{10}, also called as respirable suspended particle matter (RSPM) is defined as the particle having the aerodynamic diameter of less than 10 µm. RSPM is a combination of submicron (Size range less than 0.1 µm), fine (0.7–0.1 µm) and coarse (1"10 µm) particles (Thornburg *et al.* 2009).PM is allied with serious human health risk, together with increased risks of morbidity and mortality due to respiratory illness, cardio–vascular disease and cancer. Association between long term exposures to fine-particulate has most strongly and consistently been associated with adverse cardiovascular and pulmonary health effect (Samet *et al*., 1999). A number of studies have been already done by many researchers in different areas in all over the world.Aerosol particles have complicated and diverse influences on regional and global climate impact. The present work aims at the observation of variations in size-segregate particulate matters levels during pre-Diwali, Diwali and post-Diwali festival episode in a rural area of Chhattisgarh, India in PM_1 and $PM_{2.5–10}$ size fraction.

EXPERIMENTAL SECTION

The ambient aerosol samples were collected in rural site of Chhattisgarh, India. Rajim sampling station (20Ú 59´ N 81Ú 55´E), located in Chhattisgarh, is believed to be a famous religious place due the confluence of three river (i.e. Mahanadi, Pairee and Sodbhadra) and is known as *Triveni Sangam*. The Rajim is about 45 km away from Raipur city. The sampling site is situated at an altitude of 281 meter above sea level.

The collection of size-segregated aerosols was performed at Rajim sampling site at the terrace of a double-storied building at an altitude of about 15 meters above the ground level using eight-stage cascade impactor sampler (Modal TE 20"800 Tisch Air Pollution Monitoring Equipment USA) with 28.3 actual L/min. average flow rate. The initial and final flow rate was checked by dry gas meter (Model 12393959, Invensys (TM) Purchased by Thermo Fisher Scientific) and flow rate

was found to be within ±1% L/min.The cut off diameters of the different stage of Andersen sampler are stage 0: 10 to 9.0, stage 1: 9.0 to 5.8, stage 2: 5.8 to 4.4, stage 3: 4.4 to 2.5, stage 4: 2.5 to 2.1, stage 5: 2.1 to 1.0 stage 6: 1.0 to 0.7 and stage 7: 0.7 to 0.4. During pre-Diwali, Diwali and post-Diwali aerosol samples were collected for 24 h, continuously in the month of October and November 2011. Aerosol particle were collected on 80mm glass fiber filters (Whatmann 41).

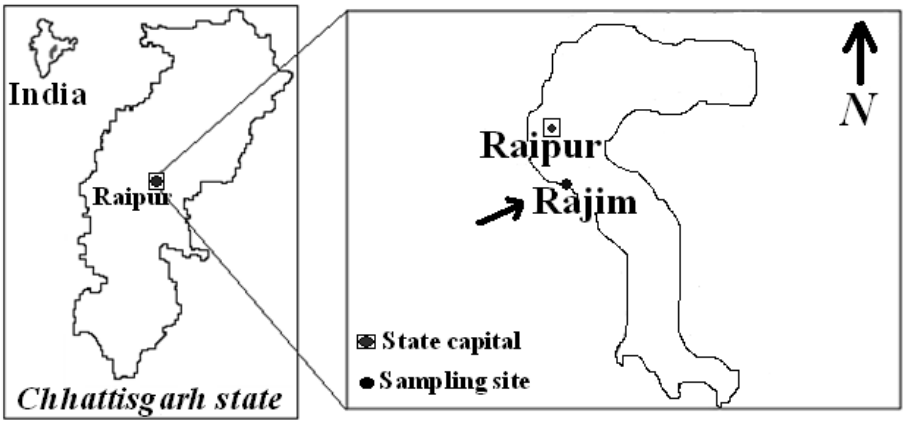

Figure1. Sampling site at India

The mass concentration of size-segregated aerosols was determined by the gravimetric analysis. The filters were placed in desiccators for ~24 hrs before and after the sampling to remove the absorbed water and weighed in a controlled environment chamber, after taking the filters out of the desiccators, using an analytical balance (Sartorius, Model CP225D) with a reading precision of 10 µg. Each of the filters including backup filter was analyzed gravimetrically by taking proper care in order to prevent minute deviation in weight measurements. Two of the most important factors to consider massconcentration measurement are variation of weight with temperature (T) and relative humidity (RH). Thus, the filters were first conditioned for ~24 hrs at 20°C and 40% RH. All weight measurements were repeated three times to ensure reliability and readings were accepted when the difference was not exceeding above 5 ì g. To ensure the quality of data, field blanks were also collected.The gravimetric mass (µg) was calculated by subtracting the weight of the filter after sampling from that of the prior sampling and the concentration (µg/m^3) was determined by dividing the aerosol mass by total volume of air sampled (m^3). After the gravimetric analysis, the loaded filters and field blanks were placed in clean polyethylene (PE) bottles and stored in a refrigerator at about ~4°C to prevent the loss of volatile or semi-volatile species from the sample filters. The mass concentration of the sampled filters obtained was corrected for field blank values.

RESULTS AND DISCUSSION

Mass concentrations of size-segregated PMs i.e., $PM_{2.5–10}$ and PM_1 during pre-Diwali, Diwali and post-Diwali period are given in Table 1. As shown in Table 1, $PM_{2.5–10}$ concentrations ranged from 71.2 to 77.7 µg/m^3 (avg. 74.2±3.0 µg/m^3) during pre-Diwali, from 155.4 to 166.8 µg/m^3 (avg. 160.1±4.9 µg/m^3) during Diwali, and 180.0 to 191.0 µg/m^3 (avg. 185.8±5.0 µg/m^3) during post-Diwali period, respectively. Similarly, PM_1 concentration varied from 34.9 to 74.0 µg/m^3 (avg. 45.6±16.2 µg/m^3) during pre-Diwali, from 199.0 to 234.7 µg/m^3 (avg. 209.7±14.8 µg/m^3) during Diwali, and from 50.6 to 65.6 µg/m^3 (avg. 57.9±7.0 µg/m^3) during post-Diwali period, respectively.Higher a concentration of PM_1 was reported during Diwali period was due to the burning of huge amount of fire-crackers (Vecchi *et al*., 2008; Deshmukh *et al.*, 2011). In Delhi City, India,

a study conducted by Tiwari *et al*. (2011) also found higher concentrations of PM_1 size fraction during-Diwali festival period due to the extreme fire-crackers burning (Tiwari *et al*., 2011). However, the concentration of coarse fraction ($PM_{2.5–10}$) was found during post-Diwali period, which was due to the crop harvesting events (Deshmukh *et al.*, 2012).During post-Diwali period concentration of $PM_1$was found to be lower due to low biomass burning and absence of any other particulate initiating activity in study site where as the high concentration of $PM_{2.5-10}$ was due to resuspension of dust particles by cropharvesting. But during pre-Diwali period concentration of PM_1 was higher due to high biomass and waste burning (during the preparation of Diwali festival). (Ravendra *et al.*, 2003; Majumdar *et al.*, 2011)

Study period	N[c]	$PM_{2.5–10}$ (μg/m^3)	PM_1 (μg/m^3)
		Mean±Stdev[a]	Mean±Stdev[a]
		Range (CV)[b]	Range (CV)[b]
Pre-Diwali	5	74.2±3.071.2"77.7 (0.04)	45.6±16.234.9"74.0 (0.36)
Diwali	5	160.1±4.9155.4"166.8 (0.03)	209.6±14.8199.0"234.7 (0.07)
Post-Diwali	5	185.8±5.0180.0"191.0 (0.03)	57.9±7.050.6"65.6 (0.12)
Total	15	140±58.474.2"185.8 (0.36)	114.2±69.345.6"209.6 (0.61)

[a]Standard deviation; [b]Coefficient of variation (SD/Mean) and [c]Number of sample

Table1.Mass concentration of size segregated aerosols

CONCLUSIONS

This study documents PM exposure of spectators to outdoor fire cracker burning displays. The data reported in this study represent the result of 15 days operation (during pre-Diwali, during-Diwali and post-Diwali) of size-segregated PM measurement in the rural area of Chhattisgarh, India.Short-period average concentration of $PM_{2.5\%10}$ and PM_1 during-Diwali festival were 160.1±4.9 and 209.6 μg/m^3, respectively.These temporal variations in PM_{10} are due to emission from fire cracker burning during festival.Due to high penetrating power of PM_1 are very harmful to respiratory and cardiovascular diseases as a result of extreme fire cracker burning in Chhattisgarh, India during-Diwali festival. Therefore, it is recommended that some effective control measures should be implemented in order to reduce fire cracker burning during-Diwalifestival.

ACKNOWLEDGEMENTS

The authors would like to thanksHead, School of Studies in Chemistry, Pt. Ravishankar University Raipur, India for providing laboratory support.

REFERENCES

Deshmukh, D.K. , Deb, M.K. , Suzuki, Y. and Kouvarakis, G.N. (2011). Water-Soluble Ionic Composition of $PM_{2.5–10}$ and $PM_{2.5}$ Aerosols in the Lower Troposphere of an Industrial City Raipur, the Eastern Central India,*Air Quality, Atmosphere & Health*, doi:10.1007/s11869-011-0149-0.

Deshmukh, D.K., Tsai, Y.I., Deb, M.K. and Mkoma, S.L. (2012). Characteristics of Dicarboxylate Associated with Inorganic Ions in Urban PM_{10} Aerosol in Eastern Central India, *Aerosol and Air Quality Research* doi:10.4209/aaqr.2011.10.0160.

Engling, G., Lee, J.J., Tsai, Y.W., Lung, S.C.C. and Chan C.C.K.C.Y. (2009). Size-Resolved Anhydrosugar Composition in Smoke Aerosol from Controlled Field Burning of Rice Straw, *Aerosol Science and technology* **43,**662.

Hungershofer, K. , Zeromskiene, K. , Iinuma, Y. ,Helas, G., Trentmann, J. , Trautmann, T. ,Parmar, R. S. , Wiedensohler, A. , Andreae, M. O. and Schmid, O. (2007). Modelling the Optical Properties of Fresh Biomass Burning Aerosol Produced in a Smoke Chamber: Results from the EFEU campaign,*Atmospheric Chemistry and Physics Discussions* ,**4,**12657.

Kundu, S., Kawamuraa, K., Andreae, T.W., Hoffer, A. and Andreae, M.O. (2010). Diurnal Variation in the Water-Soluble Inorganic Ions, Organic Carbon and Isotopic Compositions of Total Carbon and Nitrogen in Biomass Burning Aerosols from the LBA-SMOCC Campaign in Rondônia, Brazil, *Aerosol Science* , **41,** 118.

Mohanraj, R., Azeez, P.A. and Priscilla, T. (2004). Heavy Metals in Airborne Particulate Matter of Urban Coimbatore, *Archives of Environmental Contamination and Toxicology*, **47**,162.

Majumdar, D., and Nema, P. (2011).Assesment of fine particle number profile in fugitive emission from firecrackers, *Journal of Scientific and Industrial Research*, **70,** 225.

Peng, G., Wang, X., Wu, Z., Wang, Z., Yang, L., Zhong, L. and Chen, D. (2011).Characteristics of Particulate Matter Pollution in the Pearl River Delta Region, China: an Observational–Based Analysis of Two Monitoring Sites, *J. Environ. Monit.* , **13,** 1927.

Ravindra K, Mor S, Kaushik CP. (2003). Short-term variation in air quality associated with firework events: A case study, *J. Environ. Monit*., **5**, 260.

Simoneit, B.R.T., Schauer, J.J., Nolte, C.G., Oros, D.R., Elias, V.O., Fraser, M.P., Rogge, W.F. and Cass, G.R. (1999). Levoglucosan, a Tracer for Cellulose in Biomass Burning and Atmospheric Particles, *Atmospheric Environment*, **33,** 173.

Thakur, M. and Deb, M.K. (2000). Lead Level in the Airborne Dust Particulates of an Urban City of Central India, *Journal of Environmental Monitoring & Assessment*, **62,**305.

Thornburg, J., Rodes, C.E., Lawless, P.A. and Williams, R. (2009). Spatial and Temporal Variability of Outdoor Coarse Particulate Matter Mass Concentrations Measured with a New Coarse Particle Sampler During the Detroit Exposure and Aerosol Research Study, *Atmospheric Environment* , **43,**4251.

Tiwari, S., Chata, D.M., Srivastava, M. K., Safai, P.D.,Srivastava, A. K., Bisht, D. S., and Padmanabhamurty, B. (2011). Statistical evaluation of PM_{10} and distribution of PM_{1}, $PM_{2.5}$ and PM_{10} in ambient air due to extreme fireworks episodes (Deepawali festivals) in megacity Delhi, *Naturals Hazards* , **61,**521.

Vecchi, R., Bernardoni, V., Cricchio, D., Alessandro A. D., Fermo, P., Lucarelli Franco, Nava S., Piazzalunga, A. and Valli., G. (2007).The impact of fireworks on airborne particles, *Atmospheric Environment* ,**42,**1121.

Ward, T.J., Hamilton R.F.Jr., Dixon, R.W., Paulsen, M. and Simpson, C.D (2006). Characteristic and Evaluation of Smoke Tracers in PM: Result from the 2003 Montana wildfire season, *Atmospheric Environment*, **40,** 7005.

CHARACTERISATION OF AEROSOLS PHYSICAL AND OPTICAL PROPERTIES AND THEIR INFLUENCE ON SOLAR RADIATION DURING A HAZY AND A RELATIVELY CLEAR DAY - A CASE STUDY OVER HYDERABAD

SUBIN JOSE AND BISWADIP GHARAI

Atmosphere and Ocean Sciences Group (AOSG),Earth & Climate Science Area (ECSA)
National Remote Sensing Centre (NRSC), Indian Space Research Organisation (ISRO)
Department of Space, Govt. of India, Balanagar, Hyderabad-500 037,India

Key words: ABSORPTION, SCATTERING COEFFICIENT, DDR, SSA, VISIBILITY, ARF

INTRODUCTION

Aerosol haze normally enhances the aerosol loading and thereby reduces the transmission of solar radiation. In the present study attempt were made to characterise the physical and optical properties of aerosol during a hazy (29th March, 2012) and a relatively clear day (19th March,2012) and their role in modifying solar radiation over an urban region Hyderabad. A reduction of 14.65% of solar irradiance has been observed on 29th March compared to a relatively clear day on 19th March. Study revealed that day average columnar aerosol has almost doubled on hazy day and the Ångström co**e**fficient also showed a sharp increase in comparison to clear day suggested the abundance of fine mode aerosols. The high concentration of fine mode aerosols had modified the diffuse to direct ratio (DDR), which was reflected in the enhancement of columnar AOD value on 29th March compared to clear day. The absorption coefficient calculated using the in situ measurement on Black Carbon (BC) attenuation showed a little difference of about 9 Mm^{-1} between the hazy and clear day at 880nm. On the contrary a large difference of scattering coefficients of about 150Mm^{-1} observed between two contrasting days suggested that scattering phenomenon was predominant on hazy day compared to clear day. The average Single Scattering Albedo (SSA) at 550nm showed an increase of its value from 0.75 to 0.87 in hazy day, which could be attributed as dominance of scattering aerosols. About 29% reduction of visibility estimated on 29th March compared to a relatively clear day on 19th March. Nocturnal observations using boundary layer Lidar on 29th March also showed pronounced aerosol-rich layer extending from ground up to ~1.5 -2 Km height, while no such characteristic feature was observed on 19th March. The ground based aerosol properties were then fed to radiative transfer model SBDART to evaluate the aerosol radiative forcing (ARF) on the hazy day. A large negative surface forcing was observed during hazy days in comparison to a relatively clear day on 19th March, 2012.

METHODS

In situ measurement were carried out at the premises of National Remote Sensing Centre (NRSC), Hyderabad on a hazy day and a relatively clear day to study the physical and optical properties of aerosols and their influence on solar radiation during the two contrasting days. Aerosols optical Depth (AOD) was measured by MICROTOPS-II and the spectral variations of AOD and the Ångström coefficients for two contrasting days (19th & 29th March,2012) are shown in fig. 1. Solar irradiance was measured by Pyranometer CMP11 (Campbell Scientific, Inc.) in the spectrum range of 285 nm-2800 nm to analyse the solar irradiance variations during a hazy and a relatively clear day.

The different spectral bands of Multi-Filter Rotating Shadow-Band Radiometer (MFRSR) has been analysed to investigate the diffuse-to-direct- beam irradiance ratio (DDR) separately for a clear and a haze day.

Absorbing black carbon measurements were carried out using seven channels Aethalometer (model AE31,Magee Scientific, USA). Aethalometer uses quartz fiber filter tape through which air is passed for a fixed amount of time (5 minutes) with a selected constant flow rate (~3 LPM). Due to deposition of aerosols on fiber tape, light is attenuated through the tape, which is measured by Aethalometer at seven wavelengths (370nm, 470nm, 520nm, 660nm, 880nm and 950nm). In a nearly unloaded condition, fiber filter causes multiple scattering, which in turn enhanced the light absorption. As the filter load is increased, optical path in the Aethalometer filter decreases, which underestimates the measured signals. This effect is termed as "shadowing effect", which causes Aethalometer attenuation measurement significantly different from the real. Hence to calculate true absorption coefficient, two corrections were made suggested by Weingartneret *et al.*,2003; (1) multiple scattering caused by unloaded filter (2) attenuation corrections required due to gradual accumulation of particles on the filter and thereby change of fraction of scattered light (shadowing effect).

Aerosol light scattering was measured by well calibrated Nephelometer (TSI 3563) at three wavelengths (450nm,550nm and 700nm). It detects scattering properties by measuring light scattered by the aerosol and subtracting light scattered by the gas, the walls of the instrument and the background noise in the detector. The effect of angular nonidealities of Nephelometer data has been corrected following Anderson and Orgen,1998.

Absorption and scattering coefficients thus calculated has been used to derive major aerosols parameters like single scattering albedo (SSA), asymmetry parameters separately for a hazy and a clear day. In situ measurements and its derived aerosols optical parameters were then fed to the Santa Barbara DISORT Atmospheric Radiative Transfer model (SBDART) developed by Ricchiazzi *et al.* (1998) to derive aerosol radiative forcing in short wave region (0.2-4ì m) as shown in figure-2.

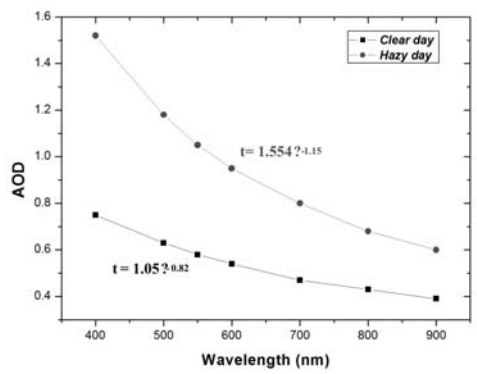

Figure-1 Spectral variation of Aerosol Optical Depth (AOD) on clear day (19th March,2012) and a hazy day (29th March,2012)

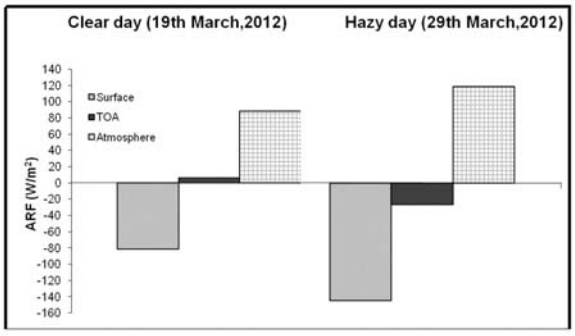

Figure-2 Aerosol Radiative Forcing (ARF) during clear and hazy day.

CONCLUSIONS

In this study we investigated the aerosol optical properties using Aethalometer, Nephelometer, in conjunction with Pyranometer and MFRSR at the urban region, Hyderabad, India during a hazy and clear day. The results of the study suggest that

- Solar irradiance reduced to 14.65% on hazy day.
- Day average columnar aerosol showed doubled the value on hazy day and the Ångström coefficient also showed a sharp increase in comparison to clear day suggested the abundance of fine mode particles.
- A greater magnitude of scattering coefficients enhancement has been observed in comparison to absorption coefficient on hazy day (29th March,2012). It indicates the presence of large scattering aerosols on hazy day which in turn reflects in the enhancement of SSA value from 0.75 to 0.87 on hazy day compare to clear day.
- It has been observed that at the same solar zenith angle (40^{0}), DDR has also increased to 1.8 times at 496.6nm spectral band indicating the presence of large number of scattering particles on 29th March,2012.
- Night time Lidar observations showed pronounced aerosol-rich layer extending from ground up to ~2 Km height on hazy day (29th March,2012), while no such characteristic feature was observed on 19th March.
- About 29% reduction of visibility estimated on 29th March compared to a relatively clear day on 19th March.
- The hazy day are characterised by large negative surface forcing value (~140w/m^{2}) in comparision to relatively clear day (~-81w/m^{2}) as enhanced aerosols on hazy day obstruct the incoming solar irradiance.
- The study is based on only two days of measurements and hence conclusions may not be generalised.

ACKNOWLEDGEMENTS

The authors thank Director, NRSC; Deputy Director (ECSA) for necessary help at various stages of this work and ISRO-GBP, ARFI for funding the project. We are also thankful to Dr. Vijay Kumar Nair, Scientist, SPL for his technical suggestions and Dr.Bhavani Kumar of NARL for providing the boundary layer LIDAR system.

REFERENCES

Ricchiazzi, P., Yang, S., Gautier, C., and Sowle, D (1998). SBDART: A Research and Teaching Software Tool for Plane-Parallel Radiative Transfer in the Earth's Atmosphere, *Bull. Am. Meteorol. Soc.*,**79**, 2101.

Theodore L. Anderson and John A. Ogren (1998). Determining Aerosol Radiative Properties Using the TSI 3563 Integrating Nephelometer, *Aerosol Science and Technology*, **29**,1, 57.

Weingartner, E., Saathoff, H., Schnaiter, M., Streit, N., Bitnar, B., Baltensperger, U. (2003). Absorption of Light by Soot Particles: Determination of the Absorption Coefficient by Means of Aethalometers, *J. Aerosol Sci.*, **34**, 1445.

CHEMICAL PROPERTIES OF AEROSOLS OVER GADANKI (13.48º N, 79.18º E)

K. RENUKA[1], ABHIJIT CHATTERJEE[2], H. GADHAVI[1], A. JAYARAMAN[1] AND S. V. B. RAO[3]

[1]National Atmospheric Research Laboratory, Gadanki, 517 112, A. P., India.
[2]Environmental Sciences Section, Bose Institute, Kolkata, India.
[3]Dept. of Physics, Sri Venkateswara University, Tirupati, 517 502, A. P., India.

INTRODUCTION

Aerosols are the tiny solid or liquid particle suspended into the atmosphere. They have adverse health effects and climate effects in the atmosphere. The direct effect includes the interaction of aerosols with solar radiation directly by scattering and absorption, and in-direct effects include the interaction of aerosols with clouds by acting as cloud condensation nuclei. Scattering type of aerosols cools the atmosphere whereas absorbing type of aerosols warms the atmosphere, also absorbing type of aerosols increases the stability of the atmosphere, there by suppressing the convection activity. These aerosols are highly variable on spatial and temporal scales. Hygroscopic nature of aerosols is important for deciding whether they will act as cloud condensation nuclei (CCN) which in turn depends on the chemical nature of the aerosol. Chemical characteristics of aerosols depend on the sources of aerosol. Hence there is a need of investigation of chemical composition of aerosols over the globe.

National Atmospheric Research Laboratory, Gadanki, Andhra Pradesh has a dedicated climate observatory named Indian Climate Observatory Network (ICON) for climate studies. The observations of aerosol, trace-gases and radiation are made since 2010. $PM_{2.5}$ particles are collected using a sampler and wet scavenged aerosol samples (rain-water) on terrace of this observatory.

METHODS

Rain-water samples are collected into a two litre jar with 22 cm diameter funnel kept in gauze kind of arrangement. Rain water samples are collected on 24 hour basis. Thymol is added to the samples to prevent biological formation in the water. The collected samples are analysed to know the ionic species present in the sample, which are scavenged by rain, using Advanced Ion-chromatograph (Metrohm IC-861), located at Bose-Institute, Kolkata.

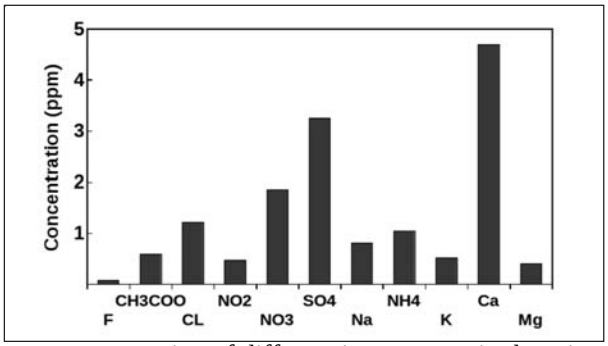

Figure 1. Average concentration of different ions present in the rain water samples (18 samples collected from october 2010 to April 2011)

$PM_{2.5}$ samples are collected on Teflon filters using Fine Particulate Sampler (Envirotech APM -550) on 3 days basis. Two filters are used for each collection for day and night separately. The filters are used to kept in desiccator before sampling for 24 hours for moisture removal and weighed (W1) before sampling, also the weight (W2) is taken after the sampling. From these two weights the concentration [(W2-W2)/V] has been calculated.

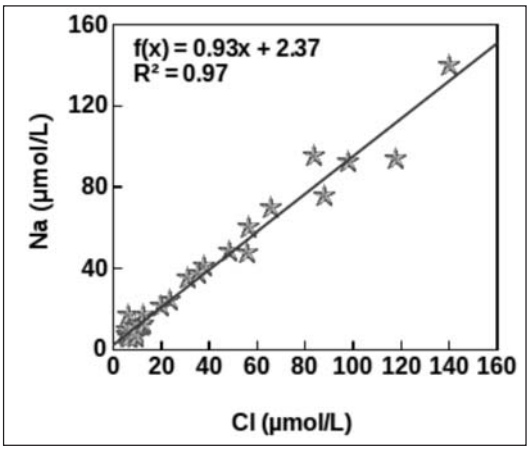

Figure 2. Correlation between Na and Cl ions present in the rain water samples

RESULTS AND DISCUSSIONS

Fig. 1 shows the total ionic concentrations (units - ppm) from all the samples during the study period for different ions. Among all the cations and anions Ca^+ ion is the major contribution (37 %) for the total ions present in the samples. High amount of Ca^+ indicates the dominance of crustal source for aerosol possibly lifted from surface by wind. Sulphate ionic concentration is also high compared to other species. Sulphate is having both sea-salt and non sea-salt contribution. Fig. 2 shows the scatter plot between Na^+ and Cl^- ions present in the samples, the regression coefficient is 0.97 which represents a strong positive correlation between them. This indicates that there is significant contribution of sea-salt aerosols over Gadanki during the observation period. Na^+ and Cl^- constitutes 15 % mass of total aerosol mass in rain-water. Fig. 3 and Fig. 4 show monthly accumulated ion concentrations for different anions and cations (units – mg/L). January month is having very less amount of rain as well as less amount of ions present in the sample, this is possibly because of low wind speed which results in less aloft of crustal aerosols and less transportation of aerosols from long distance.

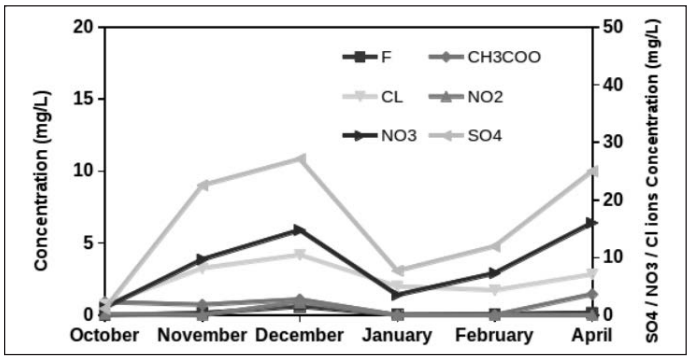

Figure 3. Monthly accumulated anion concentrations

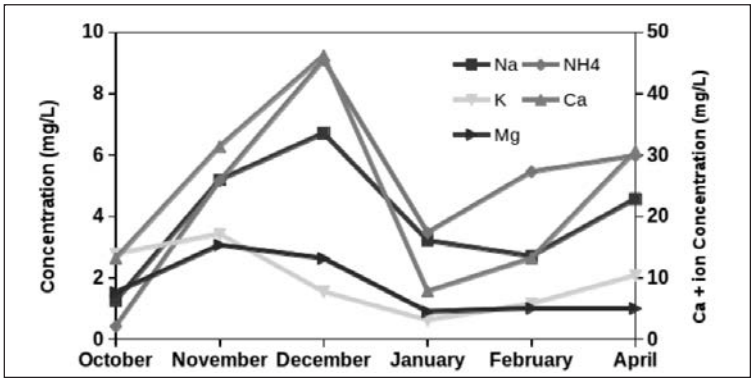

Figure 4: Monthly accumulated cation concentrations

Fig. 5 shows the mass concentration of $PM_{2.5}$ samples collected during 2011 for day time and night time. On average, the aerosol concentration is 30.7 μg/m^3. Aerosol concentration is high during night time this is because of lower boundary layer height and low wind speed whereas day time concentration is less because of dilution of pollutants in increased boundary layer height and increased wind speed. The day time average concentration is 27.6 μg/m^3 and night time concentration is 33.8 μg/m^3.

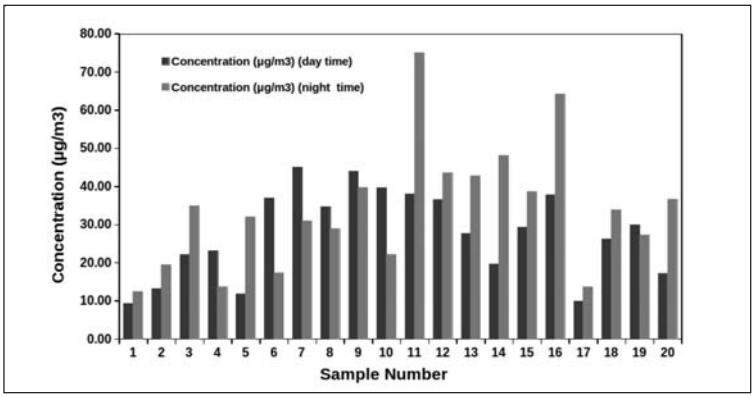

Figure 5: PM2.5 concentration collected over Gadanki for day and night times separately (20 samples for day time and 20 samples for night time)

CONCLUSIONS

1. We found high amount of Calcium ion in wet scavenged aerosol samples. Hence, crustal aerosols are predominant over Gadanki.
2. NaCl contributes nearly 15% of total mass of aerosols in rain samples.
3. Ionic composition of anions and cations are followed the wind speed pattern observed over Gadanki for the study period. Which indicates that the mineral aerosols are lifted by the winds into the atmosphere and is less during January.
4. The mass concentration of $PM_{2.5}$ observed over Gadanki is 30.7 μg/m^3.

CHEMICAL CHARACTERIZATIONS OF PARTICULATE MATTER IN PUNE

AMRUTA P. KODRE, SUMAN YADAV, P.S.P. RAO[1] AND
P. GURSUMEERAN SATSANGI

Department of Chemistry, University of Pune, Pune – 411 007
[1]Indian Institute of Tropical Meteorology, Pashan, Pune – 411 007
E mail: pgsatsangi@chem.unipune.ac.in

Keywords: PM CHARACTERIZATION, ANIONS, CATIONS AND ALKALINE

INTRODUCTION

Rapid urbanization and industrialization led to increase in air pollution level of cities worldwide. Changing of socioeconomic conditions and modern lifestyle, change the number games and ultimately aggravates pollution (AAQ, 2011). Urban air pollution problems are aggravated by meteorological and topographical factors that often accumulate pollutants in the city and prevent proper dispersion and dilution. Thus, the awareness of air pollution has led to numerous studies on the chemical composition of ambient PM and the determination of pollution sources. Accumulation of these pollutants in the air adversely affects the air quality, health of living beings including human and environment (Schleicher *et al.*, 2011). Both gaseous pollutants and atmospheric PM contribute the deterioration of air quality (Parmar *et al.*, 2001). Thus, the present study has made an attempt in chemical characterization of PM in Pune University.

EXPERIMENTAL

Measurements of particulate matter (PM) were conducted (Jan. –April, 2012) on the roof of Chemistry Department, University of Pune, building about ~12 m above the ground. 24 hr PM_{10} and $PM_{2.5}$ samples were collected with particulate sampler (Mini Vol TAS, USA). The mass of PM was determined by the difference in weights before and after sampling. For the analysis of water soluble fraction, the filters were extracted by ultrasonic bath in 50 ml Mili-Q water for 1h. One part was refrigerated and used for the analysis of ions of F^-, Cl^-, NO_3^-, SO_4^{2-} and NH_4^+ and the other part was acidified with HNO for the analysis of ions of Na^+, K^+, Ca^{2+} and Mg^{2+}. Major inorganic anions (F^-, Cl^-, NO_3^- and SO_4^{2-}) were analysed by ion chromatography (Dionex 100). The cations were determined by ICP-AES (ARCOS, Spectro, Germany). NH_4^+ was determined colorimetrically using indophenol blue method.

RESULTS AND DISCUSSION

The average mass for PM_{10} and $PM_{2.5}$ were 125 μg m^{-3} and 84.49 μg m^{-3}, respectively in the month of Jan. to April. The ratio of $PM_{2.5}$ to PM_{10} is ranging from 0.23 to1.43 (average = 0.67) which indicates that PM_{10} consists of 67% of $PM_{2.5}$. The present data was compared with the Indian Standard (PM_{10} =100 μg m^{-3} and $PM_{2.5}$ = 60 μg m^{-3}), which is almost 25% higher for PM_{10} and 40% higher for $PM_{2.5}$ than the reported standard values. Higher concentration of particulate matter indicates that more efforts should be taken to control particulate matter in Pune.

Ions	PM_{10}	$PM_{2.5}$	Ions	PM_{10}	$PM_{2.5}$
Cl^-	5.1 ± 0.83 -143.6	3.21± 1.2 -90.4	Ca^{2+}	1.14 ± 0.3 -57.1	**0.26 ± 0.12 (13.0**
NO_3^-	7.4 ± 5.7 -119.5	6.9 ± 8.2 -111.1	Mg^{2+}	0.09 ± 0.01 -7.31	**0.02 ± 0.02 -1.59**
SO_4^{2-}	6.28 ± 1.8 -130.8	5.8 ± 2.0 -119.9	Na^+	10.1 ± 0.47 -438.6	**8.77 ± 0.2 -381.5**
NH_4^+	4.7 ± 1.0 -261.7	3.95± 10.6 -219.2	K^+	13.2 ± 5.5 -339.5	**4.08 ± 3.6 -93.4**

Values in parenthesis indicate concentration in neq m^{-3}

Table 1. Ionic concentration (µg m^{-3}) of PM_{10} and $PM_{2.5}$ in Pune

The pH of PM_{10} and $PM_{2.5}$ was ranged from 5.7 to 6.2 (Avg. = 6.03) with a blank value of 5.74. The components of soluble particulate matter include F^-, Cl^- NO_3^-, SO_4^{2-}, Na^+, K^+, Ca^{2+}, Mg^{2+} and NH_4^+. Table 1 presented the measured mean concentrations of these particulate matters and the percentage of each PM to the total soluble PM mass. The trend for the mean water soluble ionic concentration in PM_{10} was $K^+ > Na^+ > NO_3^- > SO_4^{2-} > Cl^- > NH_4^+ > Ca^{2+} > F^- > Mg^{2+}$, while in $PM_{2.5}$ was $Na^+ > NO_3^- > SO_4^{2-} > K^+ > NH_4^+ > Cl^- > Ca^{2+} > Mg^{2+} > F^-$. The concentration of total water soluble ionic concentration ranged from 0.087 µg m^{-3} to 13.2 µg m^{-3} with an average of 5.37 ± 4.4 µg m^{-3} for PM_{10}, whereas in $PM_{2.5}$ it was ranged from 0.01 µg m^{-3} to 8.77 µg m^{-3} with an average of 3.65 ± 3.15 µg m^{-3}. Out of the total PM_{10} and $PM_{2.5}$, 62% and 66% are unanalyzed components. The unanalyzed residues are likely to be silicates, phosphates, trace metals, organic and elemental carbon. In anions, higher concentrations of SO_4^{2-} and NO_3^- are found to be higher. Among the anions, in both PM_{10} and $PM_{2.5}$, SO_4^{2-} and NO_3^- concentrations were found to be higher (Table 1). SO_4^{2-} is major constituent of PM comprising ~15% in both the fraction. At this site particulate sulphate may be formed through oxidation of SO_2 (emitted from the vehicular emissions) through the homogeneous and heterogeneous reactions on the surface of basic soil particles. The present site is nearby a busy road therefore sufficient amount of NO_x is present due to vehicular emissions. Particulate NO_3 may thus be formed by the absorption and subsequent reaction of NO_2 on the soil particles. Particulate ammonium originate by reaction of NH_3 vapours with acidic gases such as H_2SO_4, HNO_3 and HCl or ammonia vapour may react or condense on an acidic particle surface of anthropogenic origin. The stability of the products NH_4NO_3, $(NH_4)_2SO_4$ and NH_4Cl are different and depend on temperature and relative humidity. $(NH_4)_2SO_4$ is most stable while NH_4Cl is most volatile, Dentener and Crutzen (1994). From the Table 1, it is noted the NH_4 concentrations are approximately twice than the NO_3^- concentration and SO_4^{2-} concentration (PM_{10} = 130.8 neq m^{-3} and $PM_{2.5}$ = 119.8 neq m^{-3}). However, higher concentration of NH_4^+ can be from both NH_4NO_3 and $(NH_4)_2SO_4$. The ratio of NO_3^-/NH_4^+ can be calculated by;

$NO_3^-/NH_4^+ = (AN + SN)/AN + AS)$

where AN is NH_4NO_3; SN is $NaNO_3$ and AS is $(NH_4)_2SO_4$. If AS is greater than SN, the ratio of NO_3^-/NH_4^+ is generally smaller than 1.0 or if AS is lower than SN the ratio of NO_3^-/NH_4^+ is higher than 1.0. In present study, the observed ratios were 1.23 for PM_{10} and 1.21 for $PM_{2.5}$, which is greater than 1, indicating that the concentration of $NaNO_3$ formed from the heterogeneous reaction, play an important role in the present site. Among the cations, Na^+ shows the highest concentration

in both fractions. Ca^{2+} and Mg^{2+}concentrations were found to be 57.1 neq m^{-3} and 7.36 neq m^{-3} for PM_{10} while 13.0 neq m^{-3} and 1.59 neq m^{-3} for $PM_{2.5}$. Ca^{2+} originates as $CaCO_3$ and $CaSO_4.2H_2O$ from soil while Mg^{2+} is present in sufficient amount in soil as dolomite ($CaMg(CO_2)_2$ and illite [$K(AlMg)_3SiAl_{10}(OH)$] (Pitts and Pitts, 1986). Compared to the previous studies conducted in IITM, Pune, concentration of Ca^{2+} and Mg^{2+} is very low in present study. Lower concentration of Ca^{2+} and Mg^{2+} in both PM_{10} and $PM_{2.5}$ are might be due to the insoluble carbonates, bicarbonates and silicates. Similar results have been found at Ahmedabad and Agra (Rastogi and Sarin, 2005; Parmar *et al.*, 2001) in India.

CONCLUSIONS

The present study deals with physical and chemical characteristics of particulate matter (PM_{10} and $PM_{2.5}$) in Pune University during Jan to April 2012. The results show that the anthropogenic activities, especially biomass burning, vehicle emission and natural sources such as soil derived particles have dominated effect on particulate matter concentration. In present study, the observed NO_3^-/ NH_4^+ ratios were 1.23 for PM_{10} and 1.21 for $PM_{2.5}$, which is greater than 1, indicating that the concentration of $NaNO_3$ formed from the heterogeneous reaction. The alkaline pH (Avg. = 6.03) and higher cation by anion ratio (mean =2.5 for PM_{10} and 2.3 for $PM_{2.5}$) indicates that particulate matter of present site (i.e. Pune University) was in alkaline in nature.

ACKNOWLEDGEMENTS

Authors wish to thank Department of Science and Technology (DST No. SR/FTP/ES-91/2009), New Delhi and BCUD, Pune for financial assistance. Authors also express their gratitude to Head, Department of Chemistry, University of Pune for his encouragement. Further, authors acknowledge IIT, SAIF – Mumbai for sample analysis on ICP.

REFERENCES

AAQ (Assessment of Ambient Air Quality) of Lucknow City During Pre-Monsoon, 2011.

Dentener, F.J., Charmichael, G.R., Zhang, Y., Leliveld, J., Crutzen, P.J. (1996). Role of mineral aerosols as a reactive surface in the global troposphere, *J. Geophys. Res.* ,**101**, pp. 22869-22889.

Parmar *et al.* (2001). *Atmospheric environ.* , **35**, pp. 693-702.

Pitts, B.J., Pitts Jr., J.N. (1986). *Atmospheric chemistry, fundamentals and elemental techniques*. Wiley New York.

Rastogi, N., Sarin, M.M. (2005). Long term characterisation if ionic species in aerosols from urban and high altitude sites in western India: role of mineral dust and antropogenis soures, *Atmospheric Environment*, **43**, pp. 5541-5554.

Safai, P.D., Rao, P.S.P., Momin, G.A., Ali, K., Chate, D. M., Praveen, P.S., and Devara, P. C. S. (2005). Variation in the Chemistry of Aerosols in two Different Winter Seasons at Pune and Sinhagad, India, *Aerosol and Air Quality Research*, **5/1**, pp. 115 - 126.

Schleicher, N. J. , Norra S., Chai F., Chen Y., Wang S., Cen K., Yu Y., Stüben D. (2011). Temporal variability of trace metal Mobility of urban particulate matter from Beijing - A contribution to health impact assessments of aerosols, *Atmos. Environ.*, **45**, 7248-7265.

VARIATION OF SURFACE MICRO PHYSICAL PROPERTIES OF AEROSOLS OVER A RURAL SITE IN SOUTH INDIA

M. N. SAI SUMAN [1], HARISH GADHAVI [1], A. JAYARAMAN [1]

[1] ARTG, National Atmospheric Research Laboratory, Gadanki, 517 112 India.
E mail: sumankasyap@gmail.com

Keywords: AEROSOL, NUMBER SIZE DISTRIBUTION

INTRODUCTION

Study of optical and micro physical properties of aerosols is very important for air quality maintenance and climate of the earth. Particles of diameter 2.5 μm ($PM_{2.5}$) or less can easily reach lungs and could have disastrous effects on health. $PM_{2.5}$ particles are also very efficient in scattering the sun-light and affect Earth's radiation budget. Aerosols act as cloud condensation nuclei and help in the formation of clouds. Certain non hygroscopic aerosols like black carbon can interact with the clouds and change the cloud albedo. With an aim to study long term variations of micro physical properties of aerosols at the surface, observations of size distribution of aerosols over Gadanki (13.456^{O} N, 79.18^{O} E) are carried out since October 2008. Gadanki is a rural location in South India. The experimental site Gadanki experiences both monsoons namely south west (June to August) and north east (October to December) and the air mass associated with these monsoons are entirely different and could give raise to aerosols with varying size and chemical composition. The biomass burning activities in pre monsoon (March to May) with co allocated forest fires is also a major source for absorbing aerosols over this study site. It would be possible to get the information about the type of aerosol by studying the size distribution of it. An attempt has been made to study the surface and columnar size distribution of aerosols at the study site for a period of almost 3 years.

METHODOLOGY

The observations of number size distribution are carried out using an aerodynamic particle sizer (Model: 3321, TSI Inc, USA). The instrument measures the size distribution in 52 bins for size range from 0.5 μm to 19.8 μm. The instrument uses measurements of time of flight of aerosol to travel for known distance and under known acceleration to estimate aerodynamic diameter of the particles. The overall uncertainty in the sizing of the particles can be underestimated upto 5% or overestimated by 10% if the density of the particles are taken less than 0.9 g/cc or greater than 1.1 g/cc respectively. For the current study to estimate the mass concentration we have assumed particle density to be 1g/cc.

RESULTS AND DISCUSSION

The seasonal variations of the number size distribution and mass size distribution of the surface aerosols are shown in the Fig. 1 and 2. Mass concentration of sub micron particles (particles less than 1 μm dia) is maximum during winter (DJF) and minimum during south west monsoon season (JJAS). In case of super micron size aerosols (particles > 1 μm), maximum mass concentration is during south west monsoon season and minimum during north east monsoon season. Fig. 3 represents the time series of the daily mean mass concentration for PM_1, $PM_{2.5}$ and PM_{10}. The data gaps in

white space indicate the period where the instrument was having some technical problem. All the modes show high seasonal variation indicating the effect of the dynamics of the atmosphere such as the variation of boundary layer height and the seasonal changes of the meteorological parameters like the wind speed, relative humidity and temperature. The possible effects of meteorology and the boundary layer height on the variation of aerosol parameters will be briefly discussed at the time of presentation.

CONCLUSIONS

Study of long term variations of microphysical properties has been carried out at a rural site in south India. The aerosol size distribution and the particulate matter (PM) modes (PM_1, $PM_{2.5}$ and PM_{10}) show high seasonal variation indicating The effects of the dynamics of the atmosphere such as the variation of boundary layer and the variations of the meteorological parameter such as windspeed, relative humidity and temperature. The surface mass concentrations of $PM_{2.5}$ and PM_{10} are well under the limits of NAAQ (National Ambient Air Quality, India) which are 60 µg/m^3 for PM2.5 and 100 µg/m^3 for PM10.

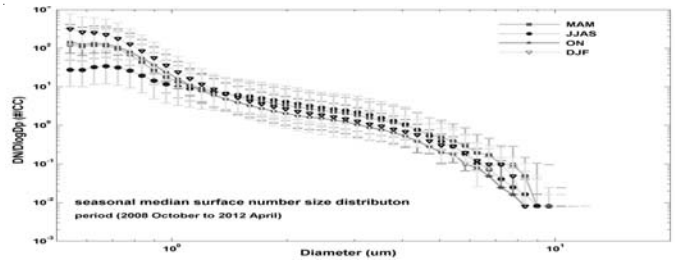

Figure 1. Seasonal variations of surface number size distributions. The points describe the median values with first quartile and third quartile being the error bar.

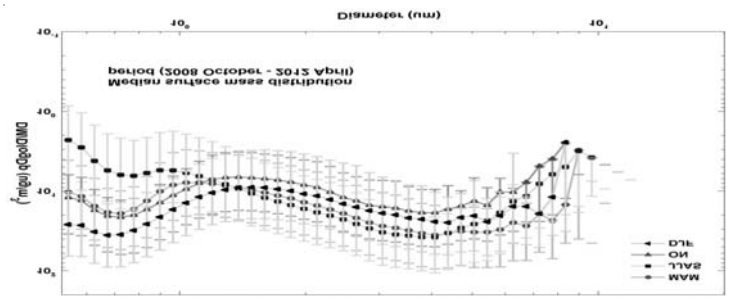

Figure 2. Seasonal variations of surface mass size distributions. The points describe the median values with first quartile and third quartile being the error bar.

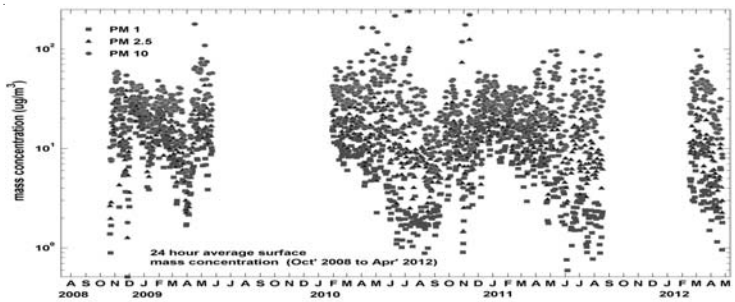

Figure 3. Time series of the 24 hour average mass concentration. The pink squares represent the PM_1, the blue triangles represent the $PM_{2.5}$ and the green circles represent the PM_{10}.

DIURNAL VARIATION OF WATER-SOLUBLE CONSTITUENTS IN AMBIENT AEROSOLS AT AHMEDABAD

A. K. SUDHEER, R. RENGARAJAN, Y. M. ASLAM, DIPJYOTI DEKA, B. R. BHUSHAN, S. K. SINGH

Physical Research Laboratory, Navrangpura, Ahmedabad, 380009, India
Email: sudheer@prl.res.in, rajan@prl.res.in

Keywords: SECONDARY AEROSOLS, DIURNAL VARIABILITY, WATER-SOLUBLE IONIC SPECIES, $PM_{2.5}$

INTRODUCTION

Atmospheric aerosols influence regional and global climate significantly (IPCC, 2007) and have adverse effect on human health. Understanding their sources, formation and transformation processes and temporal evolution is important to assess their environmental impact. Water-soluble constituents are dominant component of fine particulate matter in ambient air and known for their direct and indirect effect on climate forcing. Secondary aerosols, produced from their predecessor gases by chemical and physical processes in atmosphere occurring on time scales of few hours are a major source of the soluble constituents. Their composition exhibits large spatial variability as well as seasonal differences. Studies on aerosol chemical composition with real-time measurement in order to understand such processes are limited from Indian region. The primary focus of this study is to identify factors controlling abundances of various aerosol constituents in an urban environment. In order to study the diurnal variations of these constituents, we have measured water-soluble ionic composition of fine particulate matter with a time resolution of one hour during winter and summer seasons at Ahmedabad.

METHODS

Ionic constituents of $PM_{2.5}$ were measured using Ambient Ion Monitor (AIM) system during winter as well as summer at Ahmedabad, a typical urban location situated in a semi-arid region in India with proximity to desert regions from the north. AIM is equipped with steam jet aerosol collector (SJAC) for collection and extraction of aerosol particles with deionized water with a time resolution of one hour (Khlystov *et al*., 1995). Two ion chromatographs are simultaneously used to measure major cations (Na^+, NH_4^+, K^+, Mg^{2+} and Ca^{2+}) and anions (Cl^-, NO_3^- and SO_4^{2-}). The interfering gaseous constituents like NH_3, SO_2 and NO_x are removed from the air stream before entering into SJAC using a parallel plate diffusion denuder. Deionized water used as denuder solution is also analyzed for cations and anions in order to determine the gaseous constituents. While sampling, ion chromatographs were frequently calibrated and comparison with conventional filter based measurements was performed for some of the constituents to maintain the quality control and establish the collection efficiency. Elemental carbon and organic carbon content were measured in the samples collected on quartz filters using EC-OC analyzer.

RESULTS AND DISCUSSION

Typical diurnal variations of measured constituents during winter as well as summer are shown in Fig. 1. Among the water-soluble ionic species, NO_3^-, SO_4^{2-} and NH_4^+ show distinctly different diurnal variation compared to Ca^{2+} and Mg^{2+}. The former constituents are generally produced by secondary processes through photochemical oxidation mechanism. The observed differences are due to changes

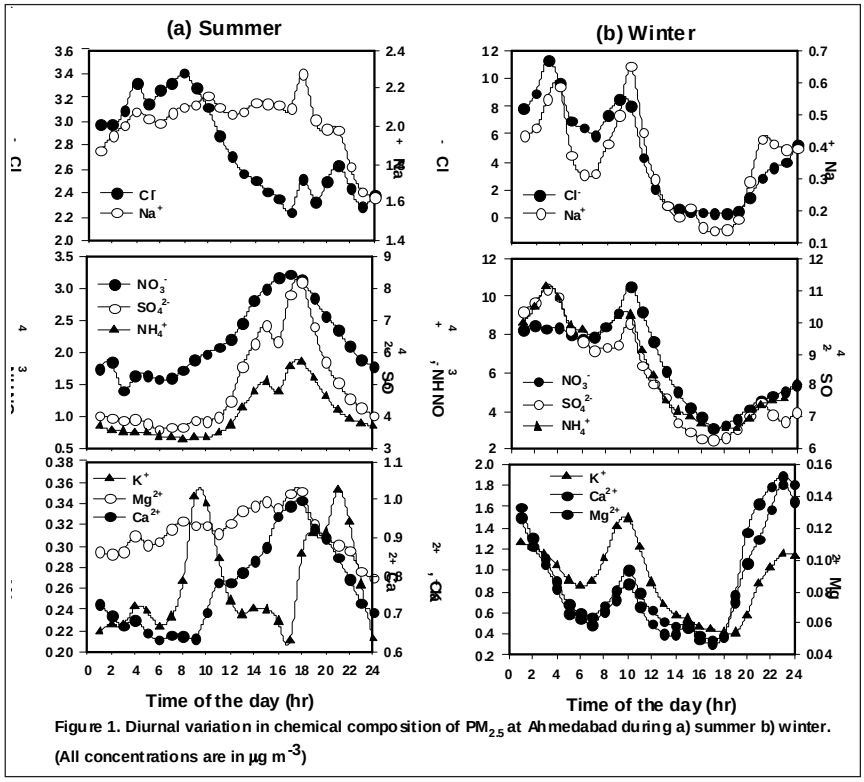

Figure 1. Diurnal variation in chemical composition of $PM_{2.5}$ at Ahmedabad during a) summer b) winter. (All concentrations are in μg m^{-3})

1. Among the water-soluble ionic species, NO_3^-, SO_4^{2-} and NH_4^+ show distinctly different diurnal variation compared to Ca^{2+} and Mg^{2+}. The former constituents are generally produced by secondary processes through photochemical oxidation mechanism. The observed differences are due to changes inemission, formation processes, transport and transformation processes along with boundary layer changes. There is a conspicuous difference between winter and summer diurnal trend. For example, secondary species exhibit minimum concentrations during post-noon hours during winter but it reaches maximum during summer period. Oxidation processes are expected to be high during day time, which increase the concentration of these constituents even though boundary layer dynamics tend to dilute it. Detailed analysis of chemical composition along with local meteorological parameters is made in order to elucidate the chemical processes leading to formation and evolution of ambient aerosols.

REFERENCES

IPCC (2007). Intergovernmental Panel on Climate Change, Third Assessment Report. (Cambridge University Press, Cambridge, U.K.).

Khlystov, A., Wyers, G. P., Slanina, J. (1995). The steam-jet aerosol collector, Atmos. *Environ.*, **29**, pp. 2229-2234.

MORPHOLOGICAL CHARACTERIZATION OF AEROSOLS AT A SUBURBAN SITE IN INDIA

ASHOK JANGID[1] AND RANJIT KUMAR[2]

[1]Department of Physics and Computer Science, Faculty of Science
[2]Department of Chemistry, Technical College,
Dayalbagh Educational Institute (Deemed University), Dayalbagh, Agra-5(India).
E-mail: ashjangid@gmail.com/rkschem@rediffmail.com

INTRODUCTION

One of the most basic and useful indicators for judging the degree of air pollution is the level of total suspended particulates (TSP) (Momin *et al.*, 1999). Atmospheric particulates play an important role in radiative forcing and climate change. In addition, they are responsible for visibility impairment and have significant implications for human health. Particulates are also associated with acid deposition and, therefore, effects on terrestrial and aquatic ecosystems. There are a number of properties of particles which are important to their role in atmospheric processes. These include their number concentration, their mass, size, and chemical composition and aerodynamic and optical properties and biological properties. Understanding of physical properties of aerosol is of fundamental importance. Physical properties includes mass, number, size, and shape of aerosols.Of these, size and shape is one of the most important properties it not only reflects the nature of the source of the particles, but also relates to their health effects (Bates *et al.*, 1966) and to their aesthetic and climatic effects via their light scattering properties.

In the present study physical characterization of aerosols has been carried at Dayalbagh, Agra a suburban site in indo-Gangetic plain.

METHODS

Aerosol samples were collected at Dayalbagh, a suburban sites in India using High Volme Sampler. PM_{10} and $PM_{2.5}$ samples were collected using glass fibre filter paper and PTFE filter paper, respectively as a collecting surface. To compute the aerosol load the difference in mass of the filter paper before the sampling and after the sampling were divided by total air volume collected. To analyse the shape and size of the collected aerosol partciles over Agra, scanning electron microscopic analysis were carriedout using JEOL, Japan. The samples (dry fuilter papers) were randomly cut nin $1mm^2$ size out of the main filter and a very thin film of gold was deposited on the surface of the samples to make it conductive under inert environment.

The concentration of PM_{10} and $PM_{2.5}$ are 180.8 and 125.4 μg m^{-3}, respectively. The load of PM_{10} and $PM_{2.5}$ are higher than NAAQS value. SEM anaysis reveals particles of different shape viz., spherical, rounded, traingle, elongated etc. Round shapes were common. Round and elongated particles were dominant in the sample.

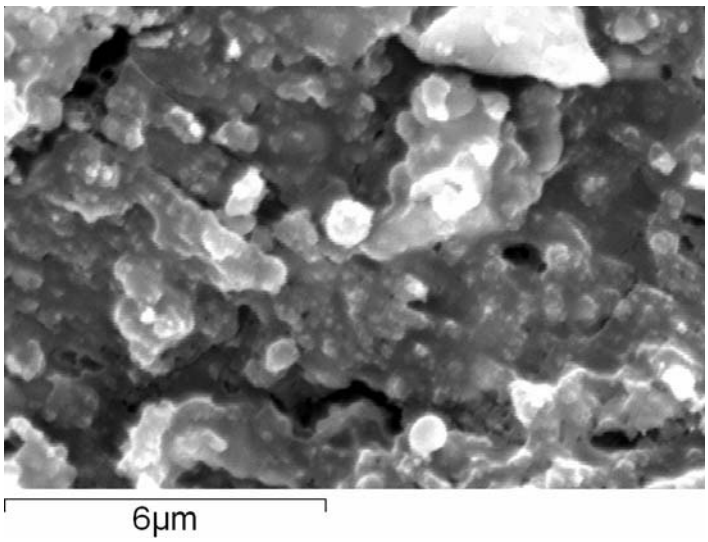

Figure 1. Scanning electron micrograph of $PM_{2.5}$ at x10,000.

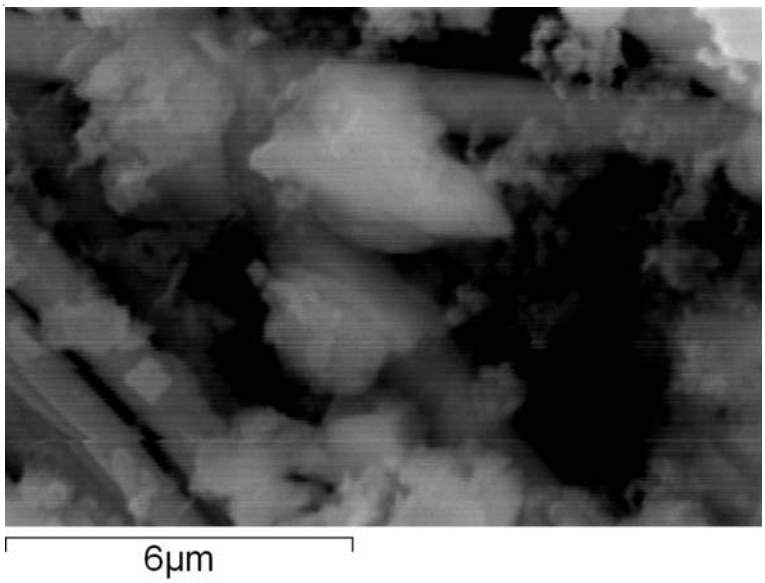

Figure 2. Scanning electron micrograph of PM_{10} at x10,000.

CONCLUSION

The airborne particulate matter contains a mixture of pollutants and their shape and size are enormous. Some are rounded, oval, and cylindrical and some are platelate types.

ACKNOWLEDGEMENT

Authors are grateful to Dr. M. Shyam Prasad, Chief Scientist and Mr. Arif, In-charge, SEM instrument, NIO, Goa. This work is supported by Department of Science and Technology, Govt. of India, New Delhi

SEASONAL VARIATION OF CARBONACEOUS AEROSOLS AT AN URBAN REGION (KOLKATA) IN EAST INDIA

SUDHA DAS KHAN[1], DEBRAJ DUTTA[2], SOUMENDRA NATH BHANJA[3] AND SHUBHA VERMA[2]

[1]Department of Infrastructure Design and Management, Indian Institute of Technology Kharagpur, Kharagpur-721302, India
[2]Department of Civil Engineering, Indian Institute of Technology Kharagpur, Kharagpur-721302, India
[3]Department of Geology and Geophysics, Indian Institute of Technology Kharagpur, Kharagpur-721302, India

Keywords: CARBONACEOUS AEROSOLS, ORGANIC CARBON, BLACK CARBON

INTRODUCTION

Aerosols are fine solid particles or liquid droplets originating from natural or anthropogenic activities. Aerosols are coming from incomplete combustion of any kind of firing such as natural forest fire, volcanic eruption, fossil fuel burning, bio fuel burning, industrial activity, bio mass burning etc. These human made aerosols have a very significant effect on climate change through scattering and absorption of solar radiation through a variety of complex radiative and microphysical processes (*Ramanathan et al, 2001*). Carbonaceous aerosols (CA) are composed of light-scattering organic carbon (OC) and light absorbing black carbon (BC) (Allan Chen *et al.,* 2004). The co-emission ratio of BC to OC varies by fuel type, combustion efficiency, and the extent of emissions control (Bahner *et al.*). Generally BC is formed in much larger amounts than OC in case of fossil fuel burning, bio-fuel burning whereas OC is formed more in case of biomass burning (Bahner *et al.*).

CA has two types of effect on climate- direct effect and indirect effect (Allan Chen *et al.,* 2004). Scattering and absorption property of carbon aerosols are considered as Direct Effect (Allan Chen *et al.,* 2004). OC scatters light back to the space and causes cooling (Ramanathan *et al.,* 2001).BC absorbs solar wave length coming to the earth and also absorbs the radiation reflected from earth surface. It decreases the amount of reflected radiation at the top-of-the-atmosphere and also reduces the amount of solar radiation reaching to the earth (Ramanathan *et al.,* 2001). Here BC acts as a positive top of the atmosphere aerosol forcing. In case of indirect effect, reflectivity of cloud changes due to the presence of CA (OC and BC) which makes cloud more shiner (Allan Chen *et al.,* 2004). It is also a cooling effect.

Kolkata is the second largest city of India (http: //www.kolkataonline.in/about/Profile/index.asp). It is the second largest metropolis in south Asia and is one of the worst polluted cities in the world (Ghose *et al.,* 2004). Increasing urban populations and increased concentration of industry, domestic heating (in temperate climates), cooking, refuse burning and automobile traffic in and around Kolkata city have resulted in severe air pollution. In this scenario, long term measurement of OC and BC may have fruitful impact on characterizing aerosols as well as on air pollution management.

METHODS

We carry out measurements of carbonaceous aerosols using an aerosol sampler (fabricated at the Indian Institute of Technology Kharagpur) at the campus of Indian Institute of Technology Kharagpur Extension Centre (22.57 N, 88.42 E) from November 2010 to May 2011. The aerosol sampler is operated at a flow rate of 9.0 to 10.5 liters per minute. The sampler consists of two stacked filter units (SFU). Nuclepore and quartz filters are placed on filter holders located on one of the two SFU. Ambient air loaded with suspended particulate matters enters through an inlet pipe. The air stream passes through those two filter papers and particulate matters are deposited on the filters. Quartz filters are prefired at 8000C for 8 hours before analysis to remove any OC fractions present within it. The measurement is carried out once a week for a period of 2 hours. After that the filter papers are collected, preserved, packed and sent for analysis at National Physical Laboratory (NPL, Delhi). The filters containing samples are analyzed using an OC and BC analyzer (Desert Research Institute, USA).

CONCLUSIONS

Fig. 1 shows the monthly mean graph of OC and BC along with OC/BC ratios during the study period. During that period, OC value is found to be 13.6 to 46.33 μg/m^3, with a maximum value seen during month of Nov'2010 (31.02 μg/m^3). But we got a significant value in Mar'2011 (24.74 μg/m^3) also. In case of BC, it's value is found to be 3.12 to 10.98 μg/m^3, with a maximum value seen in month of Dec'2010 (7.62 μg/m^3). BC value is almost same from Nov'2010 to Mar'2011(7.28 μg/m^3 to 7.62 μg/m^3). It has a relatively low value in Apr'2011 (4.92 μg/m^3) and May'2011 (4.19 μg/m^3).

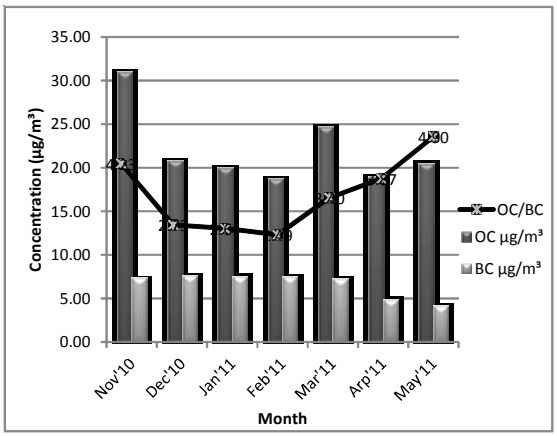

Figure 1. Variation in BC and OC concentration

Fig. 2 shows the seasonal variation of OC and BC during study period. We have divided the study period in two seasons- winter (Nov. to Feb.) and summer (Mar. to May) as per the regional meteorological considerations. Seasonal mean curve shows distinct inter-seasonal anthropogenic influence of biomass burning. OC and BC values are higher in winter season than in summer season. This might be because in winter there is increased bio-mass burning by urban slum dwellers to keep warm. The possible source of CA can be said through the analysis of OC/BC ratios. From Sandradewi *et al.* (2008), it is reported that OC/BC is 7.3 for wood-fuel burning, 1.1 for vehicular emissions. In a recent study, it has reported that OC/BC is 6.6 for biomass burning, 12 for long range transport, 3.3 for secondary organic carbon and 0.71 is for traffic emissions (Saarikoski *et al.*, 2008).

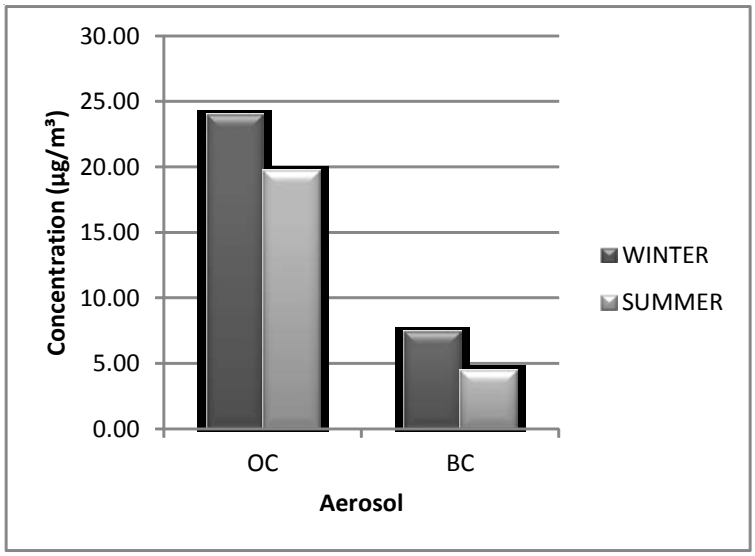

Figure 2. Seasonal variation in BC, OC concentration

In Kolkata, maximum value of OC/BC is 4.9 (4.23 second highest). So we can say that the main source of CA present in Kolkata is biomass burning.

ACKNOWLEDGEMENT

We are very much thankful to Dr. Tuhin Kumar Mandal and Dr. Sudhir Kumar Sharma, scientist at Radio and Atmospheric Sciences Division in National Physical Laboratory, Delhi for his kind help in doing BC/OC analysis.

REFERENCES

Allan Chen (2004). Carbonaceous Aerosols and Climate Change: How Researchers Proved That Black Carbon is a Significant Force in the Atmosphere (A. Science beat)

Ghose, M.K., Paul, R., Banerjee, S.K. (2004). Assessment of the impacts of vehicular emissions on urban air quality and its management in Indian context: the case of Kolkata (Calcutta), *J. Environmental Science and* Policy,7, pp. 345– 351.

Bahner, *et al.* (2000). Use of Black Carbon and Organic Carbon Inventories for Projections and Mitigation Analysis, Prepared for U.S. Environmental Protection Agency

Ramanathan, V., Crutzen, P. J. , Kiehl, J. T. and Rosenfeld, D. (2001). Aerosols, Climate, and the Hydrological Cycle, *J. science's Compass* **, 294**.

Saarikoski,S. *et al.*(2008).Sources of organic carbon in fine particulate matter in northern European urban air, *Atmospheric Chemistry and Physics*, **8,** pp. 6281–6295

Sandradewi *et al.*(2008). A study of wood burning and traffic aerosols in an Alpine valley using a multi-wavelength Aethalometer, *Atmospheric Environment*, **42**, pp. 101–112.

IDENTIFY METALS AS SOURCE MARKER FOR OPEN-WASTE BURNING AEROSOLS

S. KUMAR, S.G. AGGARWAL, R.K. SAXENA, P.K. GUPTA

CSIR-National Physical Laboratory, New Delhi, 110012, India

E mail: aggarwalsg@nplindia.org

Keywords: AEROSOL CHARACTERIZATION, WASTE BURNING, METAL MARKERS, ICP-HRMS

INTRODUCTION

Tracing of aerosol sources is an important task helpful for making control strategy, and for climate change study. However, it is a difficult job as aerosols have several sources, involve in complex atmospheric processing, degradation and removal processes. Several approaches have been used for this task, e.g., models, which are based on the input of chemical species; stable- and radio-isotope compositions of certain species; chemical markers in which trace metals are the better options because they persist in atmosphere until the life of a particle. For example, K, Pb and Hg, Fe, and Ca are used for biomass, coal burning, soil crust, and dust aerosol tracing, respectively (Aggarwal and Kawamura, 2009; Wang *et al.*, 2010).

Open-waste burning has recently been believed to be a considerable source of aerosols in several megacities in India and China (Kawamura and Pavuluri, 2010) including Maxico city (Hodzic *et al.*, 2012). The detailed chemistry of the emissions from waste burning has not been available and the degree to which these emissions affect air quality in urban regions of the developing world is rarely studied (Christian *et al.*, 2010). Most garbage burning occurs in close proximity to people, despite the knowledge that garbage burning is a major source of some hazardous air toxics such as polyaromatic hydrocarbons (PAHs), dioxins (Costner, 2005, 2006) and toxic metals like antimony (Tian *et al.*, 2012) and lead (Zhang *et al.*, 2009).

Delhi, the national capital of India is the largest metropolis by area and the second largest by population (~16.7 million). Delhi city is surrounded by rapidly urbanizing/industrializing locales (e.g., Ghaziabad, Gurgoan). Together with these areas the whole region is commonly known as National Capital Region (NCR). Delhi- NCR reported several folds high aerosol mass loadings than that defined in National Ambient Air Quality Standards (NAAQS), especially in winter season (Miyazaki *et al.*, 2009). In New Delhi, open burning of garbage from road side, shops and homes, garden waste and other biomass are the common practices. Sometimes it is just to dispose of the waste, but in the severe winter, it is one of the easily available refuges to get over cold for many people in the megacity. Common materials in these trashes are plastics, polythene bags, paper waste, clothes, tyres etc. These common materials form a major chunk of waste too. Such wastes are mainly dumped at three working landfill sites in Delhi, namely Okhla (South Delhi), Bhalswa (North Delhi) and Ghazipur (East Delhi).

To better understand the waste burning source contribution in aerosols in New Delhi, we have conducted aerosol sampling at 2 landfill sites (Okhla and Bhalswa) and in proximity (within 1 km

distance) of Okhla site. Aerosol filter samples were acid digested in microwave digestion system and analyzed using inductively coupled plasma - high resolution mass spectrometry (ICP-HRMS) for the determination of metals. The metals, e.g., Sn, Sb and As those are found almost negligible in remote aerosols, are maximized in these waste burning aerosols. Sample collected in other location of New Delhi (i.e., at National Physical Laboratory, NPL) also shows a considerable presence of these metals in particles. Preliminary studies of these metals suggested that these metals, especially Sn can be used as marker for tracing the open waste burning sources of aerosols.

METHODS

We have collected aerosol particles on Quartz filters (pre-baked at 450 ºC at least for 6 h) using low-volume handy sampler (Envirotech Instruments Pvt. Ltd., India) and high-volume sampler (Vayubodhan Upkaran Pvt. Ltd., India) at landfill sites (Okhla and Bhalswa), nearby Okhla site (rooftop of ESI hospital) and on rooftop of NPL during November - December 2011. Samples were collected down winds at fire breaking places of landfill sites. Handy samplers (with a flow rate of ~2 lpm) were placed at a height of ~2 metre above the ground level. High-volume air sampler run at a flow rate of ~1000 lpm at the landfill site about 30 meters away from the fire breaking location, Fig. 1. Similarly, high-volume sampler was used for sample collection on the rooftop (at ~ 20 meter of height from ground level) of ESI hospital and NPL. Sampling details are summarised in Table 1. The information about landfill sites has given in table 1 of Chakraborty *et al.* (2011). Total 8 numbers of samples and 4 field blank samples from different sites were considered in this work. Filter samples were conditioned before and after sampling in a desiccator for gravimetric mass determination (however in this paper, we are not discussing mass concentration). Samples were stored in a refrigerator until analysis.

Figure 1. Sampling at Okhla landfill site.

Location/site	Date of sampling	Sampler type	Number of samples considered in this study
Okhla	15/11/2011, 17/12/2011	Handy sampler	02
Okhla	17/12/2011	High-volume sampler	01
Bhalswa	17/11/2011	Handy sampler	01
Nearby site (ESI hospital, Okhla)	06/12/2011, 09/12/2011	High-volume sampler	02
NPL rooftop	19/12/2011, 20/12/2011	High-volume sampler	02

Table 1. Sampling sites and sampling details.

For analysis purpose, samples were acid digested using microwave assisted digestion system (Berghof, Germany). A piece of filter was taken in Teflon digestion vessels, then 5 ml HNO_3 (sub-boiled) and 2 ml H_2O_2 (ulta-pure) were added, and digestion (under 25 bar pressure and 200 ^oC for 30 minutes) was performed. Digested samples were transferred to polythene bottles. Solution was finally filtered and diluted as per the requirement of the instrumental analysis. These samples were analyzed for some specific metals using ICP-HRMS (Attom, Nu Instruments Ltd., UK). Standard solutions traceable to SI units were used for the calibration purpose.

The objective of this study was to identify the chemical tracers for open-waste burning aerosols. Therefore, aerosol sampling was conducted at landfill waste burning sites at Okhla and Bhalswa and for a comparison, at ESI hospital (within a close proximity of Okhla site) and a far location, NPL. The dump site height of both the landfill sites was about 30-40 meters. As per the data from Municipal Corporation of Delhi (2008), on an average, the compostable matter in municipal solid waste (MSW) of Delhi ranged within 55±20% with rest of the fraction as non-compostable material. Out of the non-compostable materials, recyclable materials (mainly polythene, plastic materials, foam, paper, packing and packaging materials, metals, cloths etc.) amounts to 20-30% while rest are inert material like construction and demolition waste, excavated soil, silt etc. Personal observation of the landfills gave an impression of typical household and demolition wastes and also the biomass generated from pruning of trees forming a good chunk of the whole mass. Plastics and polythene bags were by far the most abundant material present noticeable in the household wastes (Fig. 1). One other noticeable observation was that the fires which keep breaking out now and then or which keep on smouldering are mainly on the slopes where the soil and construction waste added for compaction are not much effective or eroded by wind and air easily.

In urban aerosols, abundant metals observed are Al, Fe, Zn, Pb, Ti, etc. (Wang *et al.*, 2010). All these metals have considerable multiple sources, e.g., soil crust, dust, industrial, traffic, and coal burning, etc. Therefore, it is not a good choice to select such metals for tracing the waste burning aerosols specifically. We focus to identify metals in open-waste burning aerosols, which should have not been reported from other sources in urban aerosols or at least other source contribution for the metal should not be significant. Fig. 2 shows the concentration of As, Cd, Sb and Sn determined in the samples. Tin followed by Sb are found to be dominant in all the samples collected from different sites. These metals are peaked in landfill site samples followed by samples collected at NPL which are well mixed urban aerosols (traffic, biomass and waste burning, and industrial influences). Although the ESI hospital is located at very close proximity of Okhla site, because of the elevated height of nearby waste burning site, it was observed that the ESI hospital site is not much affect by smoke plumes from the burning site. Unlike the case studied in the central Mexico where emission factor (g/kg fuel) of Sb (0.00212 - 0.01872) has reported to be slightly higher than Sn (0.00199 - 0.00410) in garbage burning emissions, we observed abundant concentrations of Sn in all the samples. The ratios of Sn to Sb waste burning aerosols (landfill sites and ESI hospital) are calculated to be ~ 3 or higher, whereas in NPL aerosols, these ratios are found to be less than 2. This lower value is possibly due to other sources of Sb, e.g., traffic activity (from brake wear) as reported in Bukowiecki *et al.* (2009).

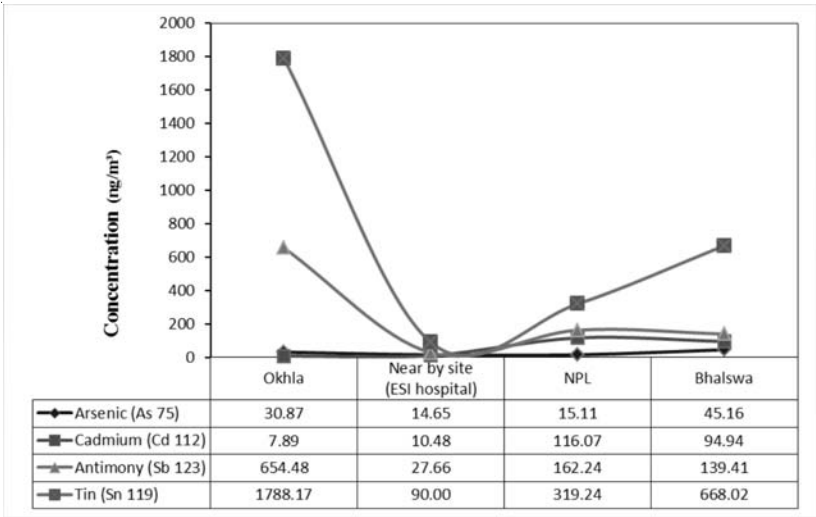

Figure 2. Metal concentrations (blank corrected) at three sampling sites.

CONCLUSIONS

Open-waste burning has been recognised as considerable source of organic aersols. Despite this, a specific chemical marker has not been clearly defined for estimation of waste burning emission contribution in aerosol burden, especially in meagcities. Our resulsts suggeste that Sn can be used as potential metal marker for open-waste (which generally has a large composite of plastics and polythene bags) burning aerosol sources. Tin is used in the manufacturing processes of plastic and related material. Future study can be taken up for the eastimation of aerosol loading due to open-waste burning practices using Sn concentration and ratio of Sn with other species in aerosols.

ACKNOWLEDGEMENTS

We appreciate the help of Bighnaraj Sarangi, Monojit Chakraborty, Khem Singh and other group members of Analytical Chemistry (SASD7.01.04) in field sampling and related work. We thank the staff members of Bhalswa and Okhla and nearby site (ESI hospital, Okhla) who assisted us to carry out the sampling work. Prof. R. C. Budhani, Director - NPL is acknowledged for his encouragements and all support.

REFERENCES

Aggarwal, S. G. and Kawamura, K. (2009). Carbonaceous and inorganic composition in long-range transported aerosols over northern Japan: Implication for aging of water-soluble organic fraction, *Atmos. Environ.* ,**43**, pp. 2532-2540.

Bukowiecki, N. et al. (2009). Real-world emission factors for antimony and other brake wear related trace elements: Size-segregated values for light and heavy duty vehicles, *Environ. Sci. Technol.*, **43**, pp. 8072-8078.

Chakraborty, M., Sharma, C., Pandey, J., Singh, N. and Gupta, P.K. (2011). Methane emission estimation from landfills in Delhi: A comparative assessment of different methodologies, *Atmos. Environ.*, **45**, pp.7135 -7142

Christian, T. J., Yokelson, R. J., Cárdenas, B., Molina, L. T., Engling, G. and Hsu, S. C. (2010). Trace gas and particle emissions from domestic and industrial biofuel use and garbage burning in central Mexico, *Atmos. Chem. Phys.*, **10**, pp. 565–584

Costner, P. (2005). Estimating Releases and Prioritizing Sources in the Context of the Stockholm Convention: Dioxin Emission Factors for Forest Fires, Grassland and Moor Fires, Open Burning of Agricultural Residues, Open Burning of Domestic Waste, Landfill and Dump Fires. *The International POPs Elimination Project*, (Mexico), 40.

Costner, P. (2006). Update of Dioxin Emission Factors for Forest Fires, Grassland and Moor Fires, Open Burning of Agricultural Residues, Open Burning of DomesticWaste, Landfills and Dump Fires. *International POPs Elimination Network*, (Mexico), 13.

Hodzic, A., Wiedinmyer, C., Salcedo, D. and Jimenez, J. L. (2012). Impact of trash burning on air quality in Mexico city, *Environ. Sci. Tech.* , **46**, pp. 4950–4957.

Kawamura, K. and Pavuluri, C. M. (2010). New Directions: Need for better understanding of plastic waste

burning as inferred from high abundance of terephthalic acid in South Asian aerosols, *Atmos. Enviro*, **44**, pp. 5320–5321.

Miyazaki, Y., Aggarwal, S. G., Singh, K., Gupta, P. K. and Kawamura, K. (2009). Dicarboxylic acids and water-soluble organic carbon in aerosols in New Delhi, India, in winter: Characteristics and formation processes, *J. Geophys. Res.*, **114**, D1920.

Tian, H. *et al*. (2012). Anthropogenic atmospheric emissions of antimony and its spatial distribution characteristics in China, *Environ. Sci. Technol.* ,**46**, pp. 3973"3980.

Wang, G., Xie, M., Hu, S., Gao, S., Tachibana E. and Kawamura K. (2010). Dicarboxylic acids, metals and isotopic compositions of C and N in atmospheric aerosols from inland China: implications for dust and coal burning emission and secondary aerosol formation, *Atmos. Chem. Phys.*, **10**, pp. 6087-6096.

Zhang, Y., Wanga, X., Chen, H., Yang, X., Chen, J. and Allen J. O. (2009). Source apportionment of lead-containing aerosol particles in Shanghai using single particle mass spectrometry, *Chemosphere*, **74**,pp. 501–507.

FORMATION OF NH_4^+ AEROSOLS AND ITS COEXISTENCE WITH GASEOUS NH_3 AT JNU, NEW DELHI

S. SINGH AND U. C. KULSHRESTHA

School of Environmental Sciences
Jawaharlal Nehru University, New Delhi 110067 India.

Keywords: REACTIVE NITROGEN, GASEOUS NH_3, PARTICULATE NH_4^+, GAS TO PARTICLE CONVERSION

INTRODUCTION

Very recently, atmospheric ammonia (NH_3) has been a topic of increasing interest among atmospheric scientists. It affects human health, visibility, earth radiation budget and climate change (Barthelmie and Pryor, 1998). Ammonia is a dominant basic species of atmosphere and prefers to react with acidic species such as sulphuric acid, nitric acid and hydrochloric acid etc. in the atmosphere resulting in the formation of compounds such as ammonium sulphate, ammonium nitrate and ammonium chloride etc. Most of these exist as submicron size range aerosols. The neutralization reactions of ammonia give rise to fine particulates through gas-to-particle conversion process (Lemmetty *et al.*, 2007; Kulshrestha et al., 2009) which has put NH_3 under regulation. According to recent NAAQS published by CBCB, the prescribed limit of annual average of ambient NH_3 is 100 µg m^{-3}.

Ammonia (NH_3) and ammonium (NH_4^+) are important atmospheric reactive nitrogen species (NHx). It has been realized that the increased deposition of NHx may lead to changes in plant community (Sutton *et al*., 1998; Kulshrestha and Kulshrestha, 2007). Also, deposition of NHx to the sensitive ecosystems can lead to serious ecological consequences such as eutrophication and soil infertility. Such changes may prevail in the regions having high ammonia emissions due to intensive livestock and agriculture (Buijsman *et al*., 1987; Demmers *et al*., 1999).

N as gaseous ammonia (NH_3-N) has partitioning with particulate phase (NH_4^+-N) because NH_3 is converted to NH_4^+. The formation of NH_4^+ aerosols from NH_3 depends on several factors such as strength of pollution sources of gaseous ammonia in the vicinity of a site, humidity, temperature and wind speed etc. This study reports the abundance and distribution of gaseous ammonia (NH_3) and particulate ammonium (NH_4^+) at JNU site which is located in south of Delhi city representing urban background characteristics of the site.

METHODS

Sampling was carried out at the building of School of Environmental Science (SES), Jawaharlal Nehru University, New Delhi. JNU campus lies in extreme South of Delhi having mini forest area in its surroundings. The campus is located away from any industrial activities.

Gaseous NH_3 samples were collected by aspiration of air through dilute sulphuric acid (20 ml) in a standard impinger at a flow rate 1 LPM. The resultant ammonium ion was determined by Indo phenols blue method. Particulate NH_4^+ was collected on a filter (dia= 47 mm) placed upstream of the impinger.

CONCLUSION

Gaseous NH_3 varied from 9.8 to 63.8 µg/m^3 with an average of 29.4 µg/m^3. Particulate NH_4^+ varied from 1.4 to 39.4 µg/m^3 with an average of 15.6 µg/m^3. As shown in Fig. 1, NH_4^+ represented 35 % fraction of total NH_x (NH_4^+ + NH_3). The percent fraction of NH_4^+ at JNU was noticed higher than the values at Agra (18.8 %) and Yokahama, Japan (30%) as reported by Singh *et al*. (2001) and Yamamoto *et al.*(1988) respectively. The significant concentration of NH_3 and NH_4^+ can be attributed to various sources and activities taking place in the surroundings, vegetation cover, land use patterns and meteorological factors.

The range of NH_3 concentration of our study is very similar to the ranges reported for other Indian sites but slightly higher than the values reported in the temperate region. This indicated that factors affecting ambient levels of NH_3 and NH_4^+ in two different geographical regions need to be investigated thoroughly in order to highlight the role of sources and atmospheric chemistry.

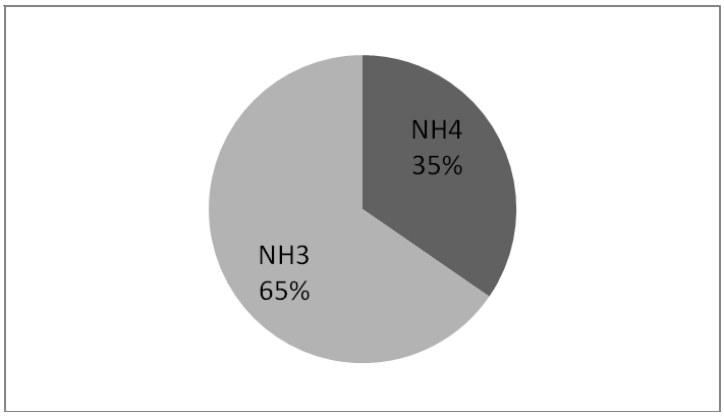

Figure 1. Percent fraction of NH_4^+ in total NHx (NH_4^+ + NH_3).

ACKNOWLEDGEMENTS

Authors are thankful to DST and JNU for providing financial assistance through PURSE CBF. Help of CSIR is also acknowledged for awarding Junior research fellowship to Saumya Singh.

REFERENCES

Barthelmie, R. J., Pryor, S. C. (1998). Implications of Ammonia Emissions for Fine Aerosol Formation and Visibility Impairment–A Case Study from the Lower Fraser Valley, British Columbia, *Atmos. Environ.* ,**32**, pp. 345-352.

Buijisman, E., Mass, H. F. M. and Asman, W. A. H. (1987). Anthropogenic ammonia emission in Europe, *Amos. Environ.* ,**21(5),** pp. 1009-1022.

Demmer *et al.* (1999). Ammonia emissions from two mechanically ventilated UK livestock buildings, *Atmos. Environ.*, **33**, pp. 217-227.

Kapoor, R. K., Singh, G., and Tiwari, S. (1992). Ammonia Concentration Vis-à-vis Meteorological Conditions at Delhi, India, *Atmos. Res.*, ***28***, pp. 1-9

Kulshrestha, U. C. and Kulshrestha, M. J. (2007). Reactive N species in air, precipitation and soil and their role in nutrient cycling in south-central India, Nitrogen 2007 Conf., Bahia (Brazil) October 1-5.

Kulshrestha *et al.* (2009). Secondary aerosol formation and identification of regional source locations by PSCF analysis in the Indo-Gangetic region of India, *J. Atmos. Chem.*, **63(1)**, 33-47.

Lemmetty, M., Vehkamäki, H., Virtanen, A., Kulmala, M., and Keskinen, J. (2007). Homogeneous Ternary H2SO4–NH3–H2O Nucleation and Diesel Exhaust: A Classical Approach, *Aerosol Air Qual. Res.* , **10**, pp. 119–124.

Singh, *et al.* (2001). Multiphase Measurement of Atmospheric Ammonia, *Chemosphere-Global Change Sci.* **3**, pp. 107-116.

Sutton, M. A., Burkhardt, J. K., Guerin, D., Nemitz, E., and Fowler, D. (1998). Development of Resistance Models to Describe Measurements of Bi-directional Ammonia-surface Exchange, *Atmos. Environ.* ,**32**, pp. 473-480.

Yamamoto *et al.* (1988). Seasonal variation of atmospheric ammonia and particulate ammonium concentrations in the urban atmosphere of Yokohama over a 5-year period, *Atmos. Environ.*, **22**, pp. 2621-2623.

CHEMISTRY OF SNOWFALL IN RELATION TO AIR MASS TRAJECTORY AT NAINITAL SITE IN HIMALAYAN REGION

BABLU KUMAR, YASHPAL MEENA, ANKUSH CHAUHAN, SUDHA SINGH, GYAN PRAKASH GUPTA AND U C KULSHRESTHA

School of Environmental Sciences, Jawaharlal Nehru University
New Delhi 110067 INDIA
E mail: umeshkulshrestha@yahoo.in

Keywords: SNOWFALL CHEMISTRY, CRUSTAL INFLUENCE, ANTHROPOGENIC INFLUENCES, AIR MASS TRAJECTORY, TOURIST ACTIVITIES.

INTRODUCTION

Gaseous and particulate pollutants emitted by various sources in the atmosphere are significantly removed by wet deposition processes (Kulshrestha *et al.*, 2009; Pandis and Seinfeld, 1990). Snow is one of the most effective wet removal process which scavenges pollutants via in-cloud and below cloud scavenging process. Hence, the chemical composition of snowfall acts an indicator of the air quality of the region.

A rapid growth of industrialization and urbanization in India is responsible for large emissions of air pollutants adversely affecting the remote areas too. Sensitive ecosystem of Himalayan ranges is also not the exception in this regard. Increasing tourist activities have also resulted in increased emission of various gaseous and particulate pollutants. These pollutants are responsible for altering the atmospheric composition around these remote hills. Signatures of these activities are trapped in various forms of atmospheric depositions which can easily be revealed by the chemical characterization of snowfall. Hence, chemical characterization of snow is necessary in order to understand the sources, transport and scavenging of pollutants. Despite its great importance, with the increasing human perturbation, very limited studies have been reported so far on snow chemistry in Indian region. The present study is an effort to fulfill this gap. This study reports chemical characteristics of snowfall and air mass trajectory at Nainital which is located in Kumauon region of Himalayas.

EXPERIMENTAL

Nainital is a town in the Indian state of Uttarakhand located at 29.38°N 79.45°E, at an altitude of 1,938 meters above sea level. Snow samples were collected in a plastic tray during winter season of 2010-12 at Nainital. The collected snow was transferred to 125 ml storage bottles followed by the addition of thymol as a biocide for preservation. Samples were analyzed for pH and EC. pH and EC were measured using Aqua lytic SensoDirect pH110 and Aqua lytic SensoDirect CD21 model respectively. Further ionic composition of snow was determined by Ion Chromatography (Metrohm883 Basic IC plus model).

CONCLUSION

Results indicated that Nainital snowmelt had very high concentrations of anthropogenic as well as crustal components. The average pH of snowmelts was recorded as 6.9 which was more alkaline

with reference to natural pH of cloud water (pH-5.6). The order of concentration of ions was Ca^{+2} > Mg^{+2} > $SO_4^{—}$> NH_4^+ > NO_3^-~ Na^+>Cl^- > K^+> F^-. The higher pH could be related to very high concentration of Ca^{+2} and Mg^{+2}. Similarly, the concentrations of SO_4^{-2} and NO_3^- were recorded very high indicating significant influence of fossil fuel and biomass combustion in Himalayan region. Air mass trajectory analysis revealed significant influence of local sources. It is interesting to note that in spite of high concentrations of SO_4^{-2} and NO_3^-, the pH was recorded very high. This feature is similar to rain water characteristics reported in Indian region (Kulshrestha *et al.*, 2005).

REFERENCES

Kulshrestha, *et al.* (2005). Review of precipitation monitoring studies in India a search for regional patterns, *Atmospheric Environment* ,**39**, pp. 7403-7419.

Kulshrestha *et al.* (2009). Real-time wet scavenging of major chemical constituents of aerosols and role of rain intensity in Indian region, *Atmospheric Environment,* **43,** pp. 5123-5127.

Pandis, S. N., Seinfeld, J. H. (1990). On the interaction between equilibration processes and wet or dry deposition, *Atmospheric Environment,* **24,** pp. 2313–2327.

INTER-COMPARISON STUDY BETWEEN SURFACE O_3, NO_X, AEROSOL AND BC CONCENTRATIONS OVER ANANTAPUR (INDIA)

A.P. LINGASWAMY[1], K. RAMA GOPAL[1], R.R. REDDY[1], S.MD. ARAFATH[1], K. UMADEVI[1], S. PAVAN KUMARI[1], N. SIVAKUMAR REDDY[1],

G. BALAKRISHNAIAH [1,2], B. SURESH KUMAR REDDY[1,3], K. RAGHAVENDRA KUMAR[1,4], Y. NAZEER AHAMMED [5]AND SHYAM LAL[6]

[1] Aerosol & Atmospheric Research Laboratory, Department of Physics, Sri Krishnadevaraya University, Anantapur 515 055, Andhra Pradesh, India
[2] Institute of Environmental Engineering, National Chiao Tung University, No. 1001, University Road, Hsinchu 300, Taiwan
[3] Institute of Low Temperature Science, Hokkaido University, Sapporo 060 0819, Japan
[4] School of Chemistry and Physics, University of KwaZulu-Natal, Westville Campus, Durban 4000, South Africa
[5] Atmospheric Science Laboratory, Department of Physics, Yogi Vemana University, Kadapa 516 003, Andhra Pradesh, India
[6] Space and Atmospheric Sciences Division, Physical Research Laboratory, Ahmedabad 380 009, Gujarat, India
E mail: krgverma@yahoo.com

INTRODUCTION

Ozone (O_3) is a natural compound present in different layers of atmosphere. In the troposphere, it is involved in several atmospheric physical and chemical processes. For instance, Tropospheric ozone is a major greenhouse gas in the troposphere and plays an important role in determining the oxidation capacity of the atmosphere as a photo chemical precursor of OH radicals (Brasseur, *et al.*, 1999). Its concentration in any given area is the result of the combination of formation, transport, destruction and deposition. Their sources include: (i) photochemical reactions involving its precursors (volatile organic compounds and nitrogen oxides) with natural or anthropogenic origin; (ii) downward transport from stratosphere; (iii) long-range transport (intercontinental) of ozone from distant pollutant sources (Reddy, *et al.*, 2011).

An abundance fraction of aerosols is part of the natural components of the Earth's atmosphere and harmful to human health and contributes to visibility degradation when present in high amounts (Leitao, *et al.*, 2010). Aerosols present in the atmosphere interact with radiation and affect the atmospheric trace gases. The change of aerosol concentration has an important impact on the surface ozone concentration and oxides of nitrogen. Li, *et al.* (2005) have been reported that the presence of black carbon aerosols resulted, decrease in ground level O_3 in the Houstan area. Reddy, *et al.* (2010) have been reported that there is a clear anti correlation existed between aerosol mass concentration and Surface O_3. Moreover high aerosol concentration can increase the NO_x concentration in Megacity Plumes in spring over the north western Pacific by reducing its photolytic loss (Tang, *et al.*, 2003).

Anantapur is a very dry continental rain shadow region of Andhra Pradesh in Southern India, is a non-industrialized, medium-sized city with a population of ~5 Lakhs inhabitants. Within 50 km radius, this region is surrounded by a number of cement plants, lime kilns, slab polishing and

brick making units. These industries, the national highways (NH 7 and NH 205) and the town area are situated in the north to southwest side of the sampling site. In this study mainly exposed that mean diurnal and monthly variations of surface O_3, NO_x along with total aerosol mass and black carbon mass (BC) for the total study period, January-July 2011. And also multi-regression analysis of Mt and BC with Surface O_3 was analyzed.

INSTRUMENTATION

Surface ozone was measured by using an analyzer (O_3 41M; Environment S.A, France) based on absorption of Ultraviolet (UV) radiation at 253.7 nm by ozone molecules. NO_X is measured continuously by using an ambient analyzer (model APNA-370, HORIBA, and Germany). The APNA-370 uses a combination of the dual cross flow modulation type chemiluminescence principle and the reference calculation method. For black carbon measurements, Magee Scientific Aethalometer (model AE-21) was used. The ten channel Quartz crystal microbalance impactor was used to measure total aerosol concentration. Ten wavelength Multi Wavelength Radiometer (MWR) was used to measure Aerosol Optical Depth (AOD) during the study period.

RESULT AND DISCUSSION

DIURNAL VARIATION OF SURFACE O_3, NO_X, AEROSOL (MT) AND BC MASS CONCENTRATIONS

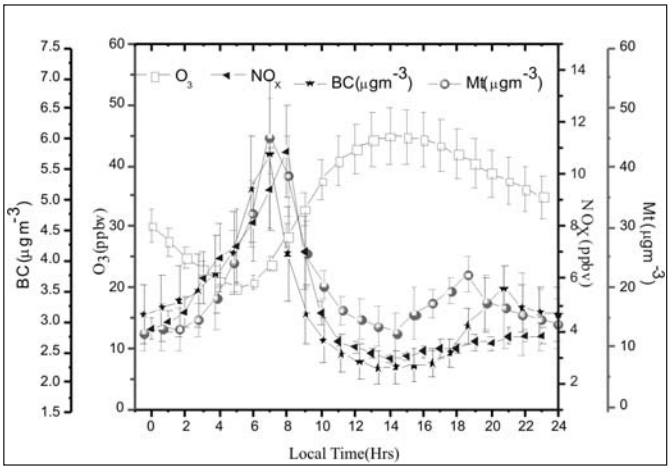

Figure 1. Mean diurnal variations of surface O_3, NO_X, aerosol (Mt) and BC concentrations over Anantapur during study period January-December 2011.

The mean diurnal variations of surface O_3, NO_x, Aerosol (Mt) and BC concentrations were observed at measurement site during the study period are shown in Fig. 1. The vertical bars denote the $\pm 1\sigma$ standard deviation. The diurnal variation of surface O_3 shows a minimum at before sunrise and concur with solar radiation attain maximum at noon time and after gradually decreasing due to titration effect. And boundary layer also plays an important role on a diurnal scale of O_3 and its precursors. Whereas NO_x has opposite trend to O_3 maximum values during morning and late evening hours and low values during noon hours. The surface aerosol (BC and aerosol) mass variations are same of NO_x variation and opposite to O_3 variations.

The diurnal variation of O_3 at this measurement site are characterized by high concentration during the day time and low concentration during the early morning hours and late evening hours for entire study period. The minimum O_3 concentration of about (19±1.6 ppbv) is noticed during the early morning around (08:00 hrs). From onwards O_3 concentration starts increasing and attains maximum value (45 ±2.6 ppbv) during (14:00-16:00 hrs). It decreases rapidly after peak until evening, maintains low values during night hours due to the absence of photolysis of NO_2 and continuous loss of O_3 by NO_X. Similar results are also shown in rural site Gadanki rural site in southern India (Naja and Lal, 2002). The maximum peak during the afternoon time mainly from oxidation of natural and anthropogenic emission of hydrocarbons, carbon monoxide (CO), methane (CH_4) by hydroxyl radical in the presence of NO_X and VOC (Seinfeld and Pandis, 1928).

The diurnal cycle of NO_X shows that maximum peak (11±0.9 ppbv) is present during early morning hours (08:00-09:00 hrs) and late evening hours (18:00-20:00 hrs) and minimum (2.1±0.2 ppbv) is present during afternoon time (16:00 hrs). The morning peak is higher in magnitude than the late evening peak. O_3 showed low values when NO_X had highest concentration during early morning hours. During early morning hours NO values are abruptly increase from motor vehicles and industrial activities. The newly emitted NO react with O_3 without solar radiation forms NO_2 and reducing O_3 concentration.

$$NO_2 + h\nu = NO + O \quad (1)$$

$$O + O_2 + M = O_3 + M \quad (2)$$

$$O_3 + NO = NO_2 + O_2 \quad (3)$$

Where M represents a molecule (N_2 or O_2) absorbs excess vibrational energy and forms stable O_3. Surface ozone shows peak values when NO_X had the lowest concentration during after noon time. During this period, NO_X accumulations were not significant because of more NO_X photochemical consumption and increased dilution as the height of the boundary layer increases.

The diurnal variation of black carbon concentration (BC) and total aerosol concentration shows that maximum peak is present during early morning hours, due to biomass burning and vehicle emissions, after onwards slowly decreases and attains minimum values at (14:00-16:00 hrs). Furthermore attains another peak during (18:00 – 22:00 hrs), at this time increasing vehicle emissions and more stable atmospheric conditions are responsible for presence of second peak. During the afternoon period aerosols shows less concentration due to the boundary layer height should reach a maximum and additional venting of the boundary layer convection. The fig.1 clearly shows that O_3 had low values when aerosol concentration maximum. This strongly suggests that high aerosol concentration should show impact on trace gases budget. High aerosol concentration significantly affects chemical oxidation process, especially through photo-dissociation (Li, *et al.*, 2005). This generally happens at early morning hours, this characterized by windless condition and less stratified boundary layer. If an ozone molecule collides with an active site on the surface of carbon sample, one of its oxygen atoms gets adsorbed while the resultant oxygen molecule is liberated. The adsorbed oxygen atom can then combine with another adsorbed oxygen atom to form oxygen molecule. The reaction causes ozone depletion in the atmosphere (Fendel, *et al.*, 1995). The authors are found that the O_3 concentration was very sensitive to aerosol loading over measurement site. Similar results are also shown in (Bian, *et al.*, 2007).

MULTI-REGRESSION ANALYSIS OF SURFACE O_3 WITH MT AND BC MASS CONCENTRATIONS

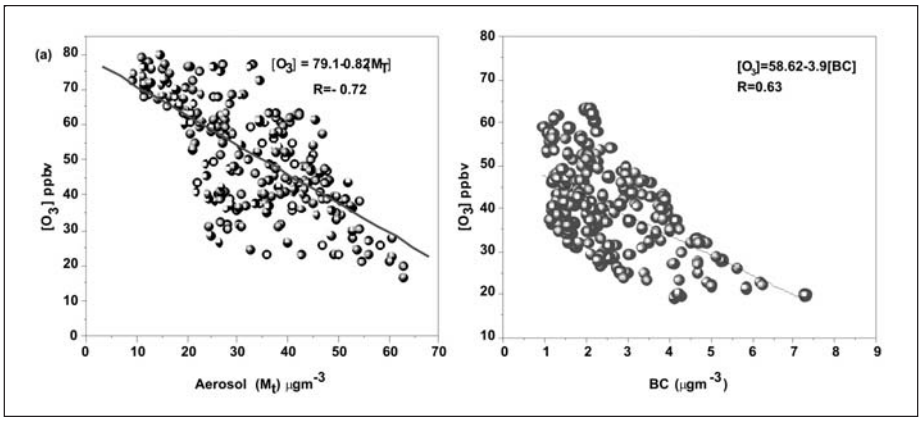

Figure 2. Multi-regression analysis of Surface O_3 with aerosol (Mt) and BC mass concentrations during study **period**

The authors have made an attempt to study the correlation among total aerosol concentration and black carbon aerosols with surface ozone (see Fig. 2). The results suggest an inverse relation among Mt and BC with surface ozone was found to be correlation coefficient (R) of 0.72, 0.63 res. The slope between the black carbon aerosols and surface ozone has been found to be – 3.9 suggesting that an increase of 1 $\mu g/m^3$ black carbon aerosol mass concentration causes a reduction of 3.9 $/m^3$ in surface ozone concentration. Moreover, it is clearly depicted from figure1 that that positive relation between aerosol concentration and oxides of nitrogen (NO_x). The results estimated that aerosols can increase the NO_x concentration by reducing the photolytic loss over the measurement site. Similar results are also shown in (Tang, *et al.*, 2003).

ACKNOWLEDGEMENTS

The authors wish to thank the Indian Space Research Organization (ISRO), Bangalore for carrying out this work through its Geosphere Biosphere Programme (GBP) under ARFI project. The authors are grateful to Dr. P.P.N. Rao, Program director, IGBP. One of the authors (RRR) wishes to express his thanks to UGC, New Delhi for providing UGC BSR Faculty Fellowship during which part of the was done.

REFERENCES

Bian, H., Han, S., Tie, X., Sun, M., Liu, A. (2007). Evidence of impacts of aerosols on surface ozone concentration in Tianjin, China, *Atmospheric Environment*, **41**, pp. 4672-4681.

Brasseur, G.P., Orlando, J. J., Tyndall, G.S., (1999). Atmospheric Chemistry and Global Change, **13**, Oxford Univ. Press, New York, pp. 465–486.

Chand, D., Lal, S., (2004). High ozone at rural site in India, *Atmos. Chem. Phys. Discuss.*, **4**, pp. 3359–3380.

Fendel, W., Matter, D., Burtscher, H. and Schmidt-Ott, A. (1995). Interaction between Carbon or Iron Aerosol Particulates and Ozone, *Atmos. Environ.*, **29**, pp. 967–973.

Leitao, J., Richter, A., Vrekoussis, M., kokhanovsky, A., Zhang, Q.J., Beekmann, M., and Burrrows, J.P. (2010). On the improvement of NO2 sattellite retrievals – aerosol impact on the air mass factors, *Atmospheric Measurement Technique*, **3**, pp. 475-493.

Li, G., Zhang, R., Fan, J., Tie, X. (2005). Impact of black carbon aerosol on photolysis frequencies and ozone in the Houston area, *J. Geophys. Res.*, **110**, D23206.

Naja, M. and Lal, S. (2002). Surface Ozone and Precursor Gases at Gadanki (13.5°N, 79.2°E), a Tropical Rural Site in India, *J. Geophys. Res.*, **107**, 4197.

Reddy, B.S.K., Kumar, K.R., Balakrishnaiah, G., Gopal, K.R., Reddy, R.R., Narasimhulu, K., Ahammed, Y.N., Reddy, L.S.S. and Lal, S. (2010). Observational Studies on the Variations in Surface Ozone Concentrations at Anantapur in Southern India, *Atmos. Res*. , **98**, pp. 125–139.

Reddy, B.S.K., Reddy, L.S.S., Cao, J.J., Kumar, K.R., Balakrishnaiah, G., Gopal, K.R., Reddy, R.R., Narasimhulu, K., Lal, S., and Ahammed, Y.N. (2011). Simultaneous measurements of surface ozone at two sites over the southern Asia: a comparative study, *Aerosol Air Qualit*. , **11**, pp. 895-902

Tang, Y., Carmichael, G.R., Uno, I., Woo, J.H., Kurata, G., Lefer, B., Shetter, R.E., Huang, H., Anderson, B., Avery, M.A., Clarke, A. (2003). Impacts of aerosols and clouds photolysis frequencies and photochemistry during TRACE- P: 2, doi: 10.1029/2002 JD 003100.

ROLE OF AMBIENT AMMONIA IN THE FORMATION OF SECONDARY AEROSOL OVER NATIONAL CAPITAL REGION OF DELHI

MANISH KUMAR[1,2], ROHTASH[1,] N.C. GUPTA[2], H. PATHAK[3], M. SAXENA[1], SARASWATI[1], T.K. MANDAL[1] AND S.K. SHARMA[1]

[1]CSIR-National Physical Laboratory, Dr. K S Krishnan Road, New Delhi-110 012, India
[2]Guru Govind Singh Indraprastha University, Dwarka, New Delhi-110075, India
[3]Environmental Sciences Division, Indian Agricultural Research Institute, New Delhi-110 012, India
E mail: rosiga.vansh86@gmail.com

Keywords: MIXING RATIO, WSIC, PM_{10}

INTRODUCTION

NH_3 is an important atmospheric pollutant that plays an important role in several air pollution problems and affects the soil, water system as well as climate. It is a highly reactive gas that has important effects on atmospheric chemistry and sensitive terrestrial or aquatic ecosystems arises from both natural and anthropogenic sources. Anthropogenic sources of atmospheric NH_3 are agricultural practices, livestock establishment, roadside vehicles and industrial activities (Sutton, *et al*., 2000; Sharma, *et al*., 2010) along with natural sources like forest fire and losses from soil under native vegetation.It has been considered up to 1995 that the contribution of vehicles (non-agricultural) to NH_3 emissions is negligible (Sutton, *et al*., 1995). But, recent studies show that NH_3 concentration in urban environments has also increased due to over reduction of NO compounds in catalytic converters in automobiles exhaust and industrial power station emission abatement technology (Sutton, *et al*., 2000). NH_3 is a vehicle exhaust species and is an unregulated byproduct of three way catalytic converters over reducing NO when reducing agents are present. Hydrogen produced in the water-gas shift reaction ($CO + H_2O$ '! $CO_2 + H_2$) could be a major contributor to NH_3 formation through overall reaction of $2NO + 2CO + 3H_2$ '! $2NH_3 + 2CO_2$ or $2NO + 5H_2$ '! $2NH_3 + 2H_2O$ (Gandhi and Shelef. 1991). Road side measurements in UK, in USA and Europe have shown strong links between NH_3 emission and traffic. The studies indicated that petrol engine vehicles constitute a major source of urban NH_3.

There have been a number of studies of NH_3 emissions reported from remote, rural, urban and suburban sites in the world. However, limited studies on NH_3 emissions in India are available. In the present study, the mixing ratios of ambient ammonia (NH_3 and NH_4^+) were estimated during winter and summer seasons of 2012 at 12 locations of NCR of Delhi to study the distribution and day-to-day variation of ambient NH_3 and its role of formation of secondary aerosol.

METHODOLOGY

Mixing ratio of ambient NH_3 and NO_x ($NO+NO_2$) were mesaured at National Physical Laboratory (NPL), New Delhi and 11other locations of NCR of Delhi alongwith PM_{10} during January to June 2012 (Table 1). NH_3 and NO_x were measured continuously over various locations of NCR using NH_3-analyzer (Model: CLD 88CYp, M/s. ECO Physics AG, Switzerland) operating on chemiluminescence method (Sharma, *et al.*, 2010). PM_{10} samples were also collected simultaneously (24 h basis) using Particle Sampler (APM 460NL, Make: M/s. Envirotech, India) at 5 locations of

NCR during January to June 2012. The water soluble inorganic ionic components (WSIC) of PM_{10} were estimated using chromatography techniques.Meteorological parameters (temperature, RH, wind direction and wind speed etc) were also measured to correlate the role of ambient NH_3 in the formation of secondary aerosol.

Locations	Type	Sampling Duration
New Delhi		
NPL, New Delhi	Traffic and Agriculture	January to June, 2012
Rohini, New Delhi	Traffic	13-14 October, 2011
IARI, New Delhi	Agriculture	9-15 February and 6-9 March, 2012
CRRI, New Delhi	Traffic and Industry	13-15 April, 2012
NEERI, New Delhi	Traffic and Industry	16-19 April, 2012
Haryana		
Faridabad	Traffic	16-17 April, 2012
Rewari	Traffic	27 January, 2012
Rohtak	Traffic	28-29 January, 2012
Jhajjar	Agriculture	27-28 January, 2012
Uttar Pradesh		
Ghaziabad	Agriculture and Industry	21-25 April, 2012
Gautam Buddh Nagar	Traffic	24-26 February, 2012
Meerut	Traffic and Agriculture	26-27, April, 2012

Table 1. The sampling locations and duration over NCR of Delhi.

RESULTS AND DISCUSSIONS

The mixing ratio of ambient NH_3 over different locations of NCR is summarized in Table 2. The average mixing ratio of ambient NH_3 over NCR was recorded as 21.2±1.5ppb with significant day (17.5±1.2ppb) and night (21.6±1.9ppb) variation. The maximum average mixing ratio of ambient NH_3 was recorded at Naraina industrial area (28.8±3.0 ppb) followed by IARI, New Delhi (27.5±2.1 ppb) and Meerut (26.2±1.4 ppb). The minimum average mixing ratio of ambient NH_3 was recorded (6.4±1.2 ppb) at CSIR-HRD Centre, Ghaziabad (Uttar Pradesh) which is a semi urban area (Table 2). Other observational sites of NCR like IARI, New Delhi; HRD, Ghaziabad and Jhajjar are generally surrounded by agricultural activities where the inorganic fertilizers are used for growing the crops. The mixing ratios of ambient NH_3 were recorded > 20 ppb at such sites except Ghaziabad (6.4±1.2 ppb). The sampling sites over the NCR are mostly surrounded by road side traffic, agricultural activities and industries. As a local influence the major sources of ambient NH_3 over the region are may be the huge road side traffic followed by agricultural activities, biomass burning and industries etc.

Sites	Mixing Ratio (ppb)				
	Minimum	Maximum	Day	Night	Average
Delhi					
NPL, New Delhi	1.03	90.72	22.2±8.3	21.7±5.2	22.0±6.7
Rohini, New Delhi	1.71	51.12	18.1±0.7	-	18.1±0.7
IARI, New Delhi	3.87	64.06	23.4±2.0	31.6±2.2	27.5±2.1
CRRI, New Delhi	4.27	47.11	21.7±0.8	27.8±0.7	24.7±0.7
NEERI, New Delhi	0.89	65.50	26.7±2.9	30.9±3.6	28.8±3.0
Haryana					
Faridabad	2.71	49.11	22.8±0.4	25.7±3.8	23.8±0.9
Rewari	3.91	29.72	19.5±1.4	-	19.5±1.4
Rohtak	0.93	43.84	21.7±1.0	23.7±1.8	22.8±1.1
Jhajjar	1.10	38.12	-	24.5±3.6	24.5±3.6
Uttar Pradesh					
Ghaziabad	0.71	25.62	5.9±1.0	6.9±1.50	6.4±1.2
Gautam Buddh Nagar	0.82	26.19	10.8±0.5	10.5±0.9	10.6±0.7
Meerut	1.62	52.53	21.9±2.1	30.4±1.0	26.2±1.4
Overall Average	**2.05**	**44.81**	**17.5±1.2**	**21.6±1.9**	**21.2±1.5**

Table 2. Mixing ratio of ambient NH_3 over NCR of Delhi.

The mixing ratio of NO_x over different locations of NCR of Delhi is summarized in Table 3. The average mixing ratio of ambient NO_x over NCR was recorded 34.1±1.7 ppb with significant day (31.1±1.7 ppb) and night (38.3±1.7 ppb) variation. The highest average mixing ratio was recorded (45.7±1.2 ppb) at Rohini with a range of 2.83 to 89.94 ppb, whereas the minimum average mixing ratio was recorded at Rewari (16.2±1.2 ppb) with a range of 5.52 to 46.91 ppb.

Sites	Mixing Ratio (ppb)				
	Minimum	Maximum	Day	Night	Average
Delhi					
Winter	1.95	85.51	28.4±9.5	27.6±9.4	28.0±9.5
Rohini, New Delhi	2.83	89.94	45.7±1.2	-	45.7±1.2
IARI, New Delhi	3.35	71.16	37.2±2.4	48.1±2.7	42.6±2.6
CRRI, New Delhi	3.38	65.98	34.1±1.4	42.0±0.8	38.1±1.1
NEERI, New Delhi	5.62	85.21	36.3±3.7	43.3±2.7	39.8±3.2
Haryana					
Faridabad	3.63	66.41	35.9±1.7	39.8±1.2	37.9±1.5
Rewari	5.52	46.91	16.2±1.2	-	16.2±1.2
Rohtak	2.74	71.02	24.5±2.1	39.3±0.9	34.2±1.6
Jhajjar	9.32	40.64	-	27.2±1.9	27.2±1.9
Uttar Pradesh					
Ghaziabad	1.65	46.41	25.9±0.8	33.2±1.1	29.5±1.0
Gautam Buddh Nagar	2.83	50.83	25.2±0.9	38.6±1.4	32.1±1.2
Meerut	3.61	96.54	30.3±1.2	33.9±2.5	32.1±1.8
Overall Average	**4.04**	**66.45**	**31.1±1.7**	**38.3±1.7**	**34.1±1.7**

Table 3. Mixing ratio of ambient NO_x over NCR of Delhi.

The correlation of ambient NH_3 with NO_x were estimated for each locations of NCR and non-significant positive correlation were recorded at most of the locations except the sites that is influenced by agrcultural activitites. The computed NO_x/NH_3 ratios are > 1 at all the locations except Rewari indicates the possibility that roadside vehicles may be of one of the source of ambient NH_3 at these locations. Similar results were reported by several researchers (Gandhi and Shelef. 1991, Sutton, *et al*., 2000).NH_3 is also a motor vehicle exhaust species and is an unregulated by-product of three way catalytic converters over reducing NO when reducing agents are present. Hydrogen produced in the water-gas shift reaction ($CO + H_2O$ '! $CO_2 + H_2$) could be a major contributor to NH_3 formation through overall reaction of $2NO + 2CO + 3H_2$ '! $2NH_3 + 2CO_2$ or $2NO + 5H_2$ '! $2NH_3 + 2H_2O$ (Gandhi and Shelef, 1991). In the urban area road side vehicle exhaust is the major source of ambient NH_3. In the present study we also observed the similar type of observation over the various locations of NCR of Delhi where huge number of road side vehicles emits NO_x, CO and NH_3 gases in the atmosphere.

PM_{10} samples were collected at 5 sites (NPL, New Delhi; IARI, New Delhi; CRRI, New Delhi; HRD, Ghaziabad and NEERI, New Delhi) of NCR during trace gases campaign and analyzed for water solible inorganic ionic components (WSIC). The concentration of PM_{10} were recorded as 199.3 ± 27.1, 258.3 ± 66.2, 280.5 ± 36.5, 227.1 ± 26.1 and 331.2 ± 42.6 µg m^{-3}at NPL, New Delhi; IARI, New Delhi; CRRI, New Delhi; HRD, Ghaziabad and NEERI, New Delhi, respectively. The concentration of WSIC (Na^+, NH_4^+, Ca^{2+}, K^+, Mg^{2+}, SO_4^{2-}, Cl^- and NO_3^- etc) of PM_{10} collected at these locations are are given in (Table 4). A significant correlation of SO_4^{2-}& NO_3^- with NH_4^+ and SO_4^{2-}& NO_3^- with NH_3 over these locations indicates the formation of secondary aerosol during the study period (Sharma, *et al*., 2012).

WSIC	**NPL**	**IARI**	**CRRI**	**Ghaziabad**	**NEERI**
Mass	199.3±27.1	258.3±66.2	280.5±36.5	227.1±26.1	331.2±42.6
Na^+	5.91±1.62	6.38±2.61	6.61±3.22	9.24±3.32	2.56±1.-2
K^+	2.80±0.41	1.69±0.23	4.33±2.02	6.00±2.53	1.77±0.42
Mg^{2+}	0.82±0.11	0.47±0.11	1.57±0.61	1.09±1.25	1.19±0.51
Ca^{2+}	11.14±2.62	6.88±3.25	7.98±3.32	12.74±3.92	11.86±3.65
NH_4^+	13.40±3.72	11.68±3.21	2.26±0.63	4.68±1.61	1.58±0.23
SO_4^{2-}	12.52±1.41	8.89±3.37	9.23±2.69	11.83±3.85	8.19±4.02
NO_3^-	10.91±3.90	2.10±0.53	3.07±1.32	5.07±1.62	2.65±1.69
Cl^-	6.73±1.92	4.48±1.25	12.95±3.55	10.47±4.24	6.80±3.22

Table 4. WSIC(µg m^{-3})of PM_{10} of NCR of Delhi.

Possible local sources of the atmospheric NH_3 andNO_x are identified analyzing the surface wind direction at observation site during the study period (at NPL). Maximum magnitude of NH_3 mixing ratio recorded from the NW direction during winter (Fig.1). The episodic high speed wind from the NW direction may be attributed to the higher mixing ratio of NH_3 from the NW direction during winter and summer. The average wind speed from the NW direction during winter and summer recorded as 3.5 $ms^{-1}$and 4.7 ms^{-1} respectively. These indicate that the NH_3 was transported from

nearby area, as the atmospheric lifetime of NH_3 (30-40%) is only few hours. Application of inorganic N fertilizers in the large agricultural field located in NW direction of the observational site may be the major source of ambient NH_3. Similar observations also reported by other researchers from different parts of the world (Sakuri, *et al*., 2003; Whitehead, *et al*., 2007). Wind rose of NO_x mixing ratio indicates higher mixing ratio from the NW direction during winter whereas NW, NE and SE directions during summer seasons. Higher NO_x mixing ratio from the NE and SE direction indicates that the major source of NO is the road traffic, which is about 100 to 200 m away from the observational site. However, the major mixing ratio of NO_x from NW direction may be attributed to the agricultural field.

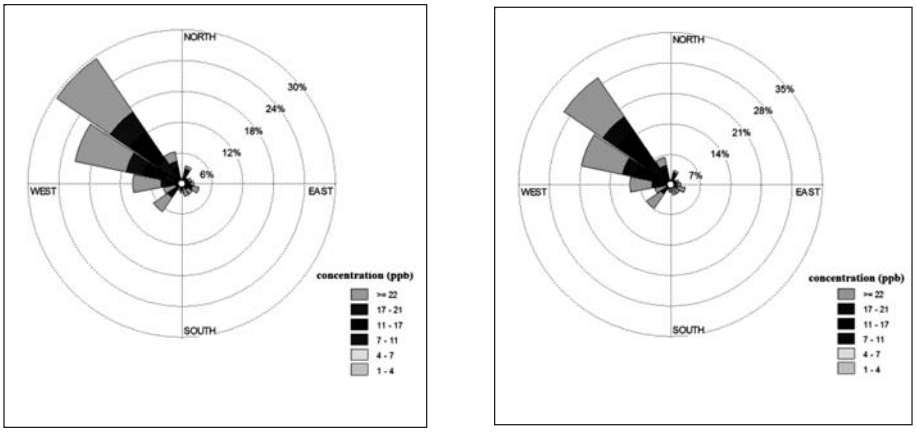

Figure1. Mixing ratios of NH_3 and NO_x with wind direction

CONCLUSIONS

Ambient NH_3 mixing ratio shows large variation from 0.89 ppb to 90.72 ppb, with an average value of 21.2 ± 1.5 ppb over NCR. Present analysis suggests that traffic could be one of the major sources of ambient NH_3 in winter and summer over urban areas NCR of Delhi. Positive correlations of NH_3 with other pollutants (NO_x and CO), which might have originated from transport sector in urban station and surface wind direction supports the above hypothesis. The ionic concentration of NH_4^+, SO_4^{2-},$NO_3^-$and ratio of $NH_4^+/SO_4^{-2}$and NH_4^+/NO_3^-indicate the formationof secondary aerosolat the study sites. However, detail study is needed on long term basis to develop a better scenario.

ACKNOWLEDGEMENTS

Authors are thankful to Director and Head, RASD, CSIR-National Physical Laboratory, New Delhi, India for their constant encouragement and support. Authors acknowledge Department of Science and Technology, New Delhi for financial support of this study.

REFERENCES

Baek, B. H. and Aneja, V. P. (2004). Measurement and analysis of the relation between ammonia, acid gases and fine particles in eastern North Carolina, *J. Air and Waste Management Association*, **54**, pp. 623-633.

Gandhi, H.S. & Shelef, M. (1991). Effect of sulphur on noble metal automotive catalysts. *Applied Catalyst*, **77**, pp.175-186.

Sakuri, T, Fujita, S. I., Hayami, H. & Furuhashi, N. (2003). A case study of high ammonium concentration in the nighttime by means of modeling analysis in the Kanto region of Japan, *Atmos. Environ.,* **37**, pp. 4461 – 4465.

Sharma, *et al.* (2010). Study on concentration of ambient NH_3 and interactions with some other ambient trace gases, *Environ. Monit. & Asses.*,**162**, pp. 225-235.

Sharma, *et al.* (2012). Study on water soluble ionic composition of PM_{10} and trace gases over Bay of Bengal during W_ICARB campaign, *Meteo. Atmos. Phys*., **118**, pp. 37-51.

Sutton, M. A, Dragostis, U., Tang, Y. S. and Flower, D. (2000). Ammonia emissions from non-agricultural sources in the UK, *Atmos. Environ*., **34**, pp. 855-869.

Sutton, M.A., Place, C.J., Eagar, M., Fowler, D., and Smith, R. L. (1995). Assessment of the magnitude of ammonia emissions in the United Kingdom, *Atmosp. Environ.*, **29**, pp.1393-1411.

Whitehead, J. D, Longley, I. D., and Gallagher, M. W. (2007). Seasonal and diurnal variation in atmospheric ammonia in an urban environment measures using a quantum cascade laser absorption spectrophotometer, *Water Air and Soil Pollution*, **183**, pp. 317 – 329.

VARIATIONS IN MASS CONCENTRATION OF THE PM_{10}, $PM_{2.5}$ AND PM_1 DURING PRE-MONSOON AND MONSOON SEASON

P.Y. AJMAL, S.K. SAHU, R.C. BHANGARE, M.TIWARI, G.G. PANDIT AND V.D. PURANIK

Environmental Assessment Division, Bhabha Atomic Research Centre, Trombay, Mumbai – 400 085, India
e-mail: ggp@barc.gov.in

Keywords: PARTICULATE MATTER, PRECIPITATION SCAVANGING, MASS CONCENTRATION, PM_{10}, $PM_{2.5}$, PM_1

INTRODUCTION

PM plays pivotal role in the climate change, cloud dynamics, health impact, fog formation and visibility through a variety of atmospheric processes. High concentrations in the PM_{10}, $PM_{2.5}$ and PM_1 can cause human health problems, related to both short-term and long-term exposure to these particles. As a consequence of epidemiological studies on health effects of particulate matter (PM) many studies on various aspects of PM have been conducted during the past decade. Generally epidemiological studies indicate that particularly the fine particle fractions have considerable impact on human health. Therefore many of the researchers are focusing on fine particles—$PM_{2.5}$ and perhaps even PM_1 —thus underlining the need for better information about these fractions. With the rapid urbanization and corresponding increase in the traffic and energy consumption, there has been growing evidence that ambient concentration levels of $PM_{2.5}$and PM_1 are also high in metropolitan cities. The major source of PM_{10}, $PM_{2.5}$and PM_1 are referred as windblown dust, secondary aerosol, coal combustion, traffic exhausts and biomass burning, etc (Sahu et. al., 2004). Furthermore, $PM_{2.5}$and PM_1 remain air-borne through nonlinear processes for days-to-weeks during monsoon months as washout processes are least efficient for cleansing particles in these size bins. Since background number concentrations of PM_{10}, $PM_{2.5}$and PM_1 particles are very high in megacities their formation and removal processes by rainfall are not clearly understood. Aerosol distributions presented by taking seasonal or annual simple averages of data can suppress the peaks owing to local effects and also by variations with rain scavenging over very short durations. Therefore, time series distributions of PM_{10}, $PM_{2.5}$and PM_1 can be presented by performing running mean on raw data in order to address environmental and rain scavenging processes in those size regimes.

The main aim of this paper is to present the analyses of the temporal variations of the PM_1, $PM_{2.5}$and PM_{10} fractions in pre-monsoon and during monsoon. The mass concentrations of PM_{10}, $PM_{2.5}$ and PM_1 have been measured continuously at Mumbai for days-to-weeks period in a month during March–August, 2012. Running mean variations for 1440 minutes in the PM_{10}, $PM_{2.5}$ and PM_1 concentration during the monsoon and the pre monsoon period are presented. Differential behavior of PM_{10} as compared to $PM_{2.5}$ or PM_1 for washout patterns is discussed to understand removal mechanisms in these size regimes.

MATERIALS AND METHODS

The sampling of aerosols for this study was carried out at about 15 m above the ground level, on the rooftop of a building. The area is primarily a residential area, and no large pollutant source exists nearby which could have influenced the sampling site directly. The GRIMM Ambient Dust Monitor, Model 365 (OPC, GRIMM Inc.) is a portable particle analyzer and is specifically designed for PM_{10}, $PM_{2.5}$ and PM_{1} ambient air analysis using dual technology consisting of both optical and gravimetrical analysis. This technology enables the Model 1.108 to make precise cut off diameters for all three PM sizes. This system allows collecting all three PM fractions simultaneously without changing sampling heads. Coarse particles (PM_{10}) and fine particulates ($PM_{2.5}$ and PM_{1}) have been monitored with the GRIMM particles sampler. The GRIMM particle counter was operated continuously during April 2012 to July 2012. A constant flow rate ~1.2 L/min is maintained throughout the measurements. The GRIMM particles measuring system is equipped with GRIMM 1174 Software for data acquisition. It was set to collect data at 1 minute intervals and store them in memory to be downloaded to a PC and analyzed further.

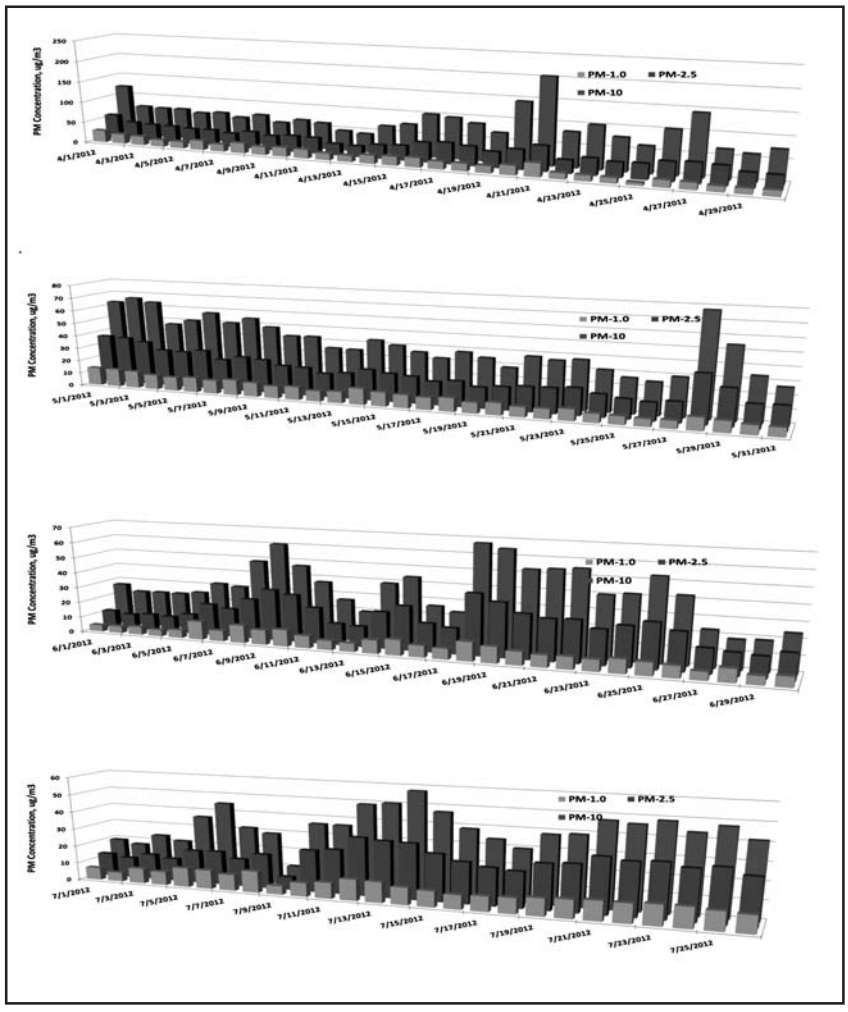

Figure 1. Month wise daily average concentration of PM_{10}, $PM_{2.5}$ and PM_{1}

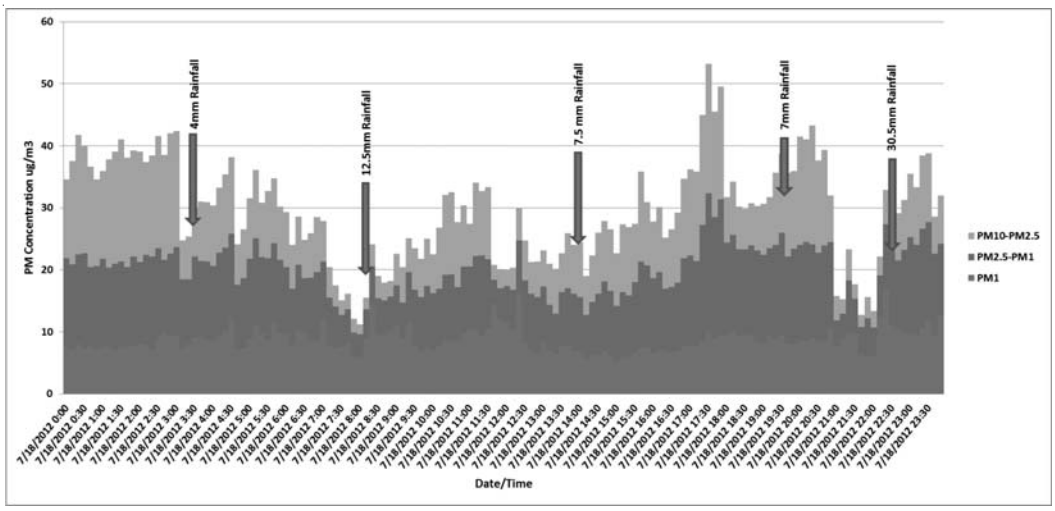

Figure 2. Variation of PM10, PM2.5 and PM1 particulate concentration during a typical rainy day in July, 2012

RESULT AND DISCUSSIONS

The pre-monsoon monitoring of particulate matter was carried out during march-april and monsoon monitoring was carried out during June-July. Figure 1 depicts daily averages for PM_{10}, $PM_{2.5}$ and PM_1 for the month of April to July. Average atmospheric concentrations for PM_{10} during April were varying from 144.2 to 43.8µg/m^3 while those of $PM_{2.5}$ and PM_1 were between 59.0 to 25.3 and 31.6 to 6.3µg/m^3 respectively. Average PM_{10} concentration during the month of May were between 77.5 and 24.9 µg/m^3 and $PM_{2.5}$ and PM_1 concentrations varied between 39.1 to 9.71 and 12.2 to 4.13µg/m^3 respectively. Average particulate concentrations are lower during monsoon due to precipitation wash-out. Variations in PM_{10}, $PM_{2.5}$ and PM_1 display distinct monsoon months' peaks which are attributed upon impositions of aerosols with splashing of raindrops on the Earth surface (Chate et. al, 1993). The PM_{10}/ $PM_{2.5}$ ratios during the sampling period were varying between 1.3 to 3.14 while PM_{10}/PM_1 and $PM_{2.5}$/PM_1 were found to be varying between 2.2 to 9.93 and 1.4 to 5.62.

Good correlation between the concentrations of PM_{10} and $PM_{2.5}$ was observed (R^2=0.839) may be due to overlapping source profiles. Correlation was also observed between $PM_{2.5}$ and PM_1 (R^2=0.72). But the correlation between PM_{10} and PM_1 was not found to be that significant (R^2=0.61).

$PM_{2.5}$ and PM_1 particles falls in the accumulation size bins and thus they are air-borne for days-to-weeks even during monsoon months as washout processes are least efficient for cleansing these particles. Also, background number concentrations of PM_{10}, $PM_{2.5}$ and PM_1 particles are very high in Mumbai in turn their washout patterns by rainfall are not clearly understood. To understand washout processes, a typical rain scavenging patterns for $_{PM1}$, $PM_{2.5}$ and PM_{10} were studied during the month of July. Figure 2 shows the variation of concentration of particulate matter on a typical rainy day in the month of July for measured rainfall rates of 4, 7, 7.5, 12.5 and 30.5 mm/h. The figure illustrates the precipitation mostly affect the coarse fraction as there were significant drop in the PM_{10} concentration during each rainfall event during the day. The PM_1 concentration was virtually unaffected which shows the precipitation scavenging in insignificant for the fine particulates

regime. Since large mass fractions of $_{PM1}$ and $PM_{2.5}$ particles resides in the accumulation mode, they are too large to have sufficient Brownian diffusivity and too small to get collected effectively by falling raindrops due to inertial impaction mechanism (Seinfeld and Pandis, 1998). As significant fractions of mass concentrations of PM_{10} particles are in the size range of coarser mode, they are effectively washed out by rain over 1 hour due to their inertia higher than that of PM_1 or $PM_{2.5}$ particles.

REFERENCES

Chate, D.M. and Kamra, A.K. (1993). Charge Separation Associated with Splashing of Water Drops on Solid Surfaces, *Atmos. Res.*, **29**, pp. 115–128.

Sahu S.K, Pandit G.G, Sadasivan S. (2004) Precipitation scavenging of polycyclic aromatic hydrocarbons in Mumbai, India, *Science of Total Environment*, **318(1-3)**, pp. 245-9.

Seinfeld, J.H. and Pandis, S.N. (1998). Atmospheric Chemistry and Physics, A Wiley-Inter Science Publication, John Wiley & Sons, Inc, New York.

ELEMENTAL CHARACTERIZATION OF AIRBORNE PARTICULATE MATTER DURING DUST STORM EVENT IN MUMBAI

I.V. SARADHI, P. SANDEEP, G.G. PANDIT AND V.D. PURANIK

Environmental Assessment Division
Bhabha Atomic Research Centre, Mumbai – 400085 India

Keywords: DUST STORM, PARTICULATE MATTER, ENRICHMENT FACTOR ANALYSIS

INTRODUCTION

Dust storm events are defined as the natural events with substantial airborne particulate matter concentrations usually occur in arid, semi arid or desert areas and primarily resulting from low vegetation cover and strong surface winds (Shahsavani *et al.*, 2012). Several studies have shown that the dust storm events result in large scale transport of dusts globally (Lee *et al.*, 2010, Mamane *et al.*, 2008). On 21st March, 2012 Mumbai witnessed a dust storm that completely covered the atmosphere of the city reducing the visibility to less than 1 Km. In order to understand the effect of dust storm on the environment of Mumbai Respirable Suspended Particulate Matter (RSPM) samples are collected before, during and after the dust storm and chemical composition of air particulate matter has been carried out.

MATERIALS AND METHODS

For collection of particulate matter Gent air particulate sampler is used. The Respirable Suspended Particulate Matter (Particulate matter of size <10μm) is collected on 47 mm dia nucleopore polycarbonate filters. The average flow rate of the sampler is 16 lpm and each sample is collected for a period of 24 h. Sampling has been carried out at a height of 15 m above the ground on the terrace of a building at Trombay, Mumbai. The particulate samples are collected on 12th, 15th, 19th, 21st, 22nd, 26th and 29th March, 2012. The particulate load on the filter is measured by gravimetry using a Mettler balance with 10μg sensitivity.

Elemental characterization of particulate matter collected on nuclepore polycarbonate filters has been carried out using Xenemetrix make Energy Dispersive X-Ray Fluorescence spectrometer (EDXRF) having 400W Rh (Rhodium) anode X-ray tube as an excitation source. The instrument has eight secondary targets Viz., Si, Ti, Fe, Ge, Mo, Sn, Zr and Gd. The detector is cryogenically cooled Lithium drifted Silicon with 7μm Be window and resolution of 131eV at Mn Kα. The instrument was calibrated using pure thin film standards (Micromatter-XRF Calibration standards).

ENRICHMENT FACTOR ANALYSIS

Enrichment factor (EF) analysis technique is widely used to identify the anthropogenic source of metallic elements and it is generally applied to show the degree of enrichment of a given element compared to the relative abundance of that element in crustal material or sea salt. In the current study crustal EF's are calculated with Al as reference element. The reference elemental concentrations of soil used are the average background values of soil in Mumbai (Mahadevan, 1986). The crustal enrichment factor for each element is calculated using the following equation.

$$EF_i = \frac{(C_i / C_j)_{air}}{(C_i / C_j)_{crust}} \quad (1)$$

where EF_i is the enrichment factor of species i, j is a reference element for crustal material, $(C_i/C_j)_{air}$ is the ratio of concentration of species i to species j in the aerosol sample and $(C_i/C_j)_{crust}$ is the ratio of concentration of species i to species j in the soil.

RESULTS AND DISCUSSION

ELEMENTAL COMPOSITION

The average elemental composition of PM_{10} before, during and after dust storm is presented in Table 1. As shown in the table the elemental concentrations during non-dust storm periods are much lower than the concentrations during dust storm period. Seventeen elements have been analyzed in PM_{10} samples collected between March, 12 to 29, 2012. The concentration levels of many elements analyzed suddenly increased during dust storm period on 21st March, 2012 and gradually reached normal levels of Mumbai by 29th March, 2012. Of these the concentrations of soil originated species (viz., Al, Fe, Si etc) increased remarkably during dust storm period. The anthropogenic species (S, Zn and Pb etc) did not show much difference between dust storm period and non dust storm period. However the concentration levels of V, Cr and Ni which are from industrial origin have also shown an increase during dust storm period. In order to study the percentage increase in elemental concentrations during dust storm on 21st March, 2012 the ratio of the concentration of element during dust storm (i.e. 21st March, 2012) to the average elemental concentration before dust storm has been estimated. Fig. 1 shows the ratio of concentration of each element during dust storm to the corresponding elemental concentration before dust storm. As shown in fig. 1 the ratio of Cl, K, Ca, Mn, Fe are more than 5 while the ratios of Mg, Al, Si, Ti, V, Cr and Ni are between 3 to 5. These ratios clearly indicate the significant contribution of crustal (Ca, Mg, Al, Si, Mn, Fe, Ti) and marine (Cl, Br) derived elements compared to anthropogenic elements. Significant increase in contribution from Cl during dust storm indicates the contribution of sea salt to particulate matter. However, the ratios of S, Zn, Pb remain unchanged indicating contribution from the local sources for these elements.

ENRICHMENT FACTOR ANALYSIS

The elements analyzed in the samples can be divided into three major groups: earth crust elements or soil derived elements, marine and anthropogenic elements. Crustal enrichment factors for each element are calculated using equation 1 with Al as reference element. Table 2 shows the crustal enrichment factors for the elements of PM_{10}. As given in table 2 the EF values during dust storm for crustal derived elements (Mg, K, Ca, Mn and Fe) are less indicating larger contribution from crustal derived sources. However the EF value of Ca is 18 and 17 on 21st and 22nd March, 2012 respectively indicating marginal enrichment during dust storm period compared to non-dust storm period. The dusts from the Middle Eastern Region are known to be richer in Ca and Mg (Shahsavani *et al.*, 2012). The marginal enrichment observed in Ca could be due to the contribution of dust from this region. However, it should be further confirmed by the wind trajectory plots during that period using various models (e.g., HYSPLIT). The enrichment factors for other elements viz., Zn, Br and Pb are much higher indicating contribution from sources other than crustal origin. The enrichment factor values calculated are comparable with the study carried out by Kothai *et al.* 2011, at a similar sampling site in Mumbai.

CONCLUSION

The elemental composition of air particulate matter during dust storm period and non-dust storm period shows increased contribution from soil and marine derived elements during dust storm event. Enrichment factor analysis also indicates crustal contribution during dust storm event. High values of Ca and Mg during dust storm period and the increased contribution from marine derived elements (Cl) indicates that the dust storm could have come from the Middle Eastern Region.

Element*	Average before Dust Storm	During Dust Storm	Average After Dust Storm
Mg	1.07	6.5	1.37
Al	4.7	14.48	4.05
Si	10.6	42.71	12.18
S	3.5	3.03	3.29
Cl	0.67	3.71	0.96
K	1.61	8.9	2.36
Ca	4.35	29.82	6.52
Ti	0.57	2.84	0.85
V	0.03	0.15	0.05
Cr	0.02	0.06	0.04
Mn	0.12	0.65	0.18
Fe	6.31	34.04	9.88
Ni	0.02	0.06	0.04
Cu	0.05	0.09	0.05
Zn	0.65	0.57	0.5
Br	0.04	0.08	0.04
Pb	0.24	0.21	0.18

*-All values in $\mu g/m^3$

Table 1. Elemental Composition of PM_{10} on different sampling periods

	Mg	K	Ca	Cr	Mn	Fe	Cu	Zn	Br	Pb
12-Mar-12	2.9	9.1	13.7	1.9	2.9	3.0	7.9	383.6	156.1	178.8
14-Mar-12	2.1	11.4	12.0	2.4	3.0	3.0	9.9	765.1	214.8	282.9
19-Mar-12	1.4	3.4	5.6	1.1	1.0	1.1	4.1	218.1	49.4	59.1
21-Mar-12	3.6	10.8	18.8	1.3	3.1	3.2	3.6	100.2	34.1	36.8
22-Mar-12	3.8	11.5	17.2	3.3	3.9	3.9	7.8	294.9	66.7	101.2
24-Mar-12	2.3	11.7	13.3	4.7	3.8	3.8	10.7	549.0	188.6	204.7
27-Mar-12	3.2	9.4	14.8	2.4	2.7	3.1	5.8	321.0	84.2	118.4
29-Mar-12	3.0	8.2	11.7	1.2	2.0	2.6	4.2	144.3	98.9	48.7

Table 2. Crustal Enrichment Factors for the Elements

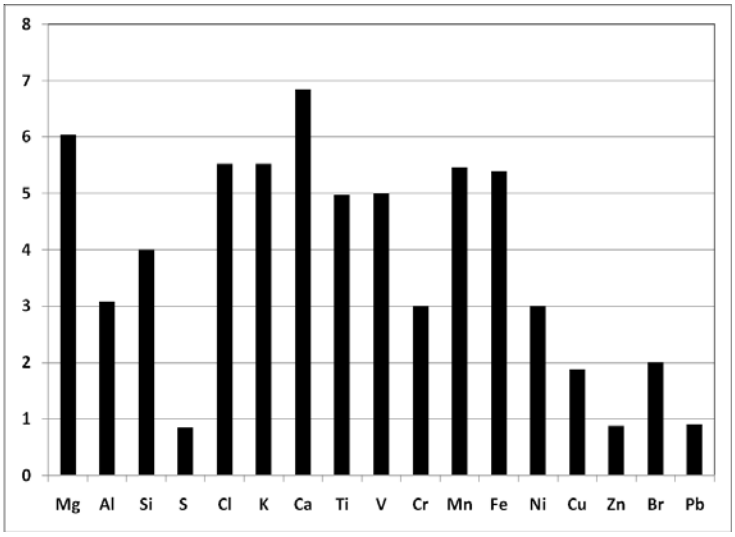

Figure1. Ratios of elements in PM_{10} between non-dust storm period and dust storm period

REFERENCES

Kothai P., Saradhi, I.V., Pandit, G.G., Markwitz, A., Puranik, V. D. (2011). Chemical Characterization and Source Identification of Particulate Matter at an Urban Site of Navi Mumbai, India, *Aerosol and Air Quality Research*, **11**, pp. 560-569.

Lee Y.C., Yang, Xun, Wenig, Mark (2010). Transport of dusts from East Asian and non-East Asian sources to Hong Kong during dust storm related events 1996-2007, *Atmospheric Environment*, **44**, pp. 3728-3738.

Mahadevan T.N. (1986). Studies on aerosol size distribution and chemical composition in urban, rural and marine environment and their deposition through precipitation, Ph.D Thesis, University of Mumbai, 321-322.

Mamane Y., Perrino, Cinzia, Yossef, Osnat, Catrambone, Maria (2008). Source characterization of fine and coarse particles at the East Mediterranean coast, *Atmospheric Environment*, **42**, pp. 6114-6130.

Shahsavani *et al*. (2012). The evaluation of PM_{10}, $PM_{2.5}$ and PM_{1} concentrations during the middle eastern dust (MED) events in Ahvaz, Iran from April through September, 2010, *Journal of Arid Environments*, **77**, pp.72-83.

AEROSOL FUNDAMENTALS: PHYSICS AND CHEMISTRY

ABSORPTION ENHANCEMENT OF POLYDISPERSE AEROSOLS UNDER VARYING HYGROSCOPIC CONDITIONS

P.M. SHAMJAD[1], S.N. TRIPATHI[1], S.G. AGGARWAL[2], S.K. MISHRA[2], MANISH JOSHI[3], ARSHAD KHAN[3], B.K. SAPRA[3], KIRPA RAM[4]

[1]Department of Civil Engineering, Indian Institute of Technology, Kanpur, India
[2]CSIR, National Physical Laboratory, New Delhi, India
[3]Radiological Physics & Advisory Division, Bhabha Atomic Research Centre, Mumbai, India
[4]Department of Earth and Planetary Science, Graduate School of Science, University of Tokyo, Japan

Keywords: AEROSOL MIXING STATE, HYGROSCOPIC GROWTH, CORE-SHELL STRUCTURE, ENHANCED ABSORPTION.

INTRODUCTION

Impact of aerosols on climate usually classified as direct effect, semi-direct effect and indirect effect. Significant uncertainties are introduced in to the estimation of these effects due to its dependence on aerosol size, hygroscopicity, morphology, mixing state, refractive index, and solubility. Out of different aerosol species present in atmosphere, Black Carbon (BC) has great importance due to its highly absorbing nature (Jacobson, 2001). The estimation of radiative impact of BC strongly depends on the accurate measurement of its absorption coefficient(β_{abs}), mass concentration and its mixing state. Mixing of BC with other inorganic species induce change in optical properties. Internal mixing of BC (homogeneous or a core-shell structure) show more realistic absorption estimates as compared to external mixing models in which BC particles co-exist with other particles in a physically separated manner (Bond, Habib *et al.* 2006). Absorption by BC increases when BC particles are mixed and/or coated with other less absorbing materials, which are hygroscopic in nature.This enhanced absorption in a core-shell structure is because of the focusing effect of coated materials (shell) which act as a lens (Fuller, 1995; Fuller, Malm, *et al.* 1999).

In this study we calculated the hygroscopic growth of aerosols during winter season over an urban site (Kanpur) in the Indo-Gangetic Plane (IGP) and there by explain the enhancement in BC absorption coefficient observed for the same period. From the hygroscopic growth factor (g_{exp}) calculated we derived a model to predict the chemical composition of particles during the experimental period. An Aethalometer is used to quantify the BC mass and one single wavelength Photoacoustic Soot Spectrometer (PASS-1) is used to calculate the absorption and scattering coefficients.

Absorption and scattering coefficients are derived using a core-shell assumption based on Mie theory. These derived optical parameters are compared with observed values and the closure is found to be very close. The estimated optical properties agree within 7% for absorption coefficient and 30% for scattering coefficient (β_{scat})with that of measured values. The enhancement of absorption is found to vary according to the thickness of the shell and BC mass, with a maximum of 2.3 for a shell thickness of 18 nm for the particles.

METHODS

To quantify the hygroscopic growth of particles, a laboratory experiment were setup using two scanning mobility particle sizers (SMPSs) operating in parallel for 5 days in winter season of February 2011. A schematic diagram of the experimental setup is given at Fig. 1. One SMPS (TSI-model 3696) measures the ambient size distribution while other SMPS (Grimm-model no: 5.403) has a dryer attached to its inlet to remove the water content from the atmospheric aerosols there by measuring dry size distribution. The ratio of mode diameters of the ambient distribution to that of dry distribution is reported as g_{exp}. An internal mixing of BC with a core-shell structure is assumed to be present during the winter season over Kanpur and the refractive index of core and shell is calculated using volume mixing rule. The core is assumed as a mixture of all species (BC, WISOC, WSOC, $(NH_4)_2SO_4$ and NH_4NO_3) in dry state and shell as a mixture of soluble species (WSOC, and) with water content. Using this hygroscopic growth factor (i.e. Zdanovskii-Stokes-Robinson (ZSR) approach), a model has been developed to predict the chemical composition of particles. A flow chart depicting the steps to derive the volume fractions of each selected species is shown in Fig. 2.

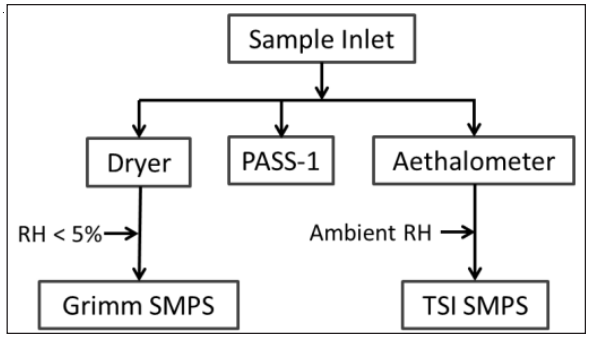

Figure 1. Experimental Setup

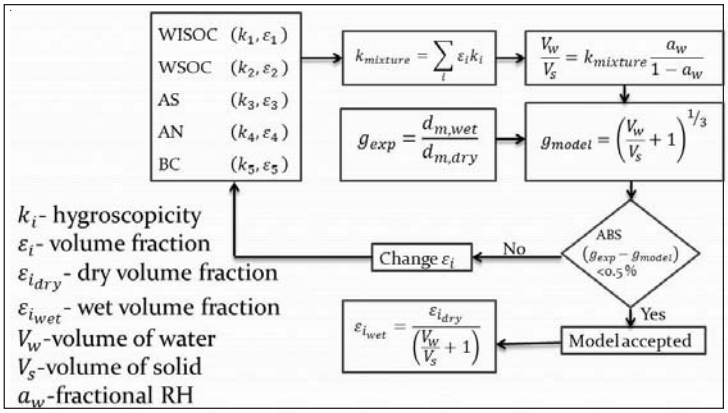

Figure 2. ZSR approach

Observed parameters such as size distribution, radii of core and shell, and their refractive indices are used to calculate the optical parameters of aerosol using Mie theory (Toon and Ackerman, 1981). These optical parameters show good agreement with. Enhancement in absorption (γ) due to hygroscopic growth is also calculated from Mie Theory. Fig. 3 shows the variation in ã as a function of BC mass fraction and shell thickness. This figure shows a clear trend of increase in ã values as shell thickness increases for a constant BC mass fraction. While a maximum ã of 2.3 is observed for the shell thickness of 18 nm, the lowest ã of 1.035 corresponds to very thin coating (2 nm).

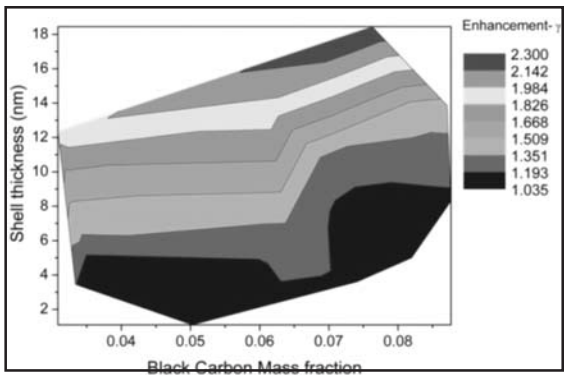

Figure 3. Absorption enhancement as a function of BC mass fraction and shell thickness. Each color shows range of absorption enhancement.

CONCLUSIONS

Coating of soluble material over black carbon can significantly increase the absorption depending upon the thickness of the coating and type of coating material. High RH conditions and the presence of hygroscopic materials are very much favorable for forming such coatings. Knowledge of easily measurable hygroscopic growth factors can be effectively used to identify the volume fractions of different species present in the ambient aerosol. Using this information in conjunction with the size distribution data, an effective optical closure can be performed to match the experimental optical parameters.

ACKNOWLEDGEMENTS

The present work is supported by a grant under Board of Research in Nuclear Sciences, Department of Atomic Energy.

REFERENCES

Bond, T. C., Habib, G. *et al.* (2006). Limitations in the enhancement of visible light absorption due to mixing state, *Journal of Geophysical Research-Atmospheres*, **111**(D20).
Fuller, K. A. (1995). Scattering and absorption cross sections of compounded spheres containing arbitrarily located spherical inhomogeneities, *J. Opt. Soc. Am. A*, **12**, pp. 893-904.
Fuller, K. A., Malm, W. C. *et al.* (1999). Effects of mixing on extinction by carbonaceous particles, *Journal of Geophysical Research-Atmospheres*, **104**(D13), pp.15941-15954.
Jacobson, M. Z. (2001). Strong radiative heating due to the mixing state of black carbon in atmospheric aerosols, *Nature*, **409**(6821), pp. 695-697.
Toon, O. B. and Ackerman T. P. (1981). Algorithms for the calculation of scattering by stratified spheres, *Applied Optics*, **20**(20), pp. 3657-3660.

STUDY OF ION-AEROSOL NEAR-CLOUD MECHANISM TO EXPLAIN COSMIC RAY -CLOUD -CLIMATE CONUNDRUM

A. RAWAL[1], S.N. TRIPATHI[1], M. MICHAEL[1], A.K. SRIVASTAVA[2]

[1]Department of Civil Engineering, Indian Institute of Technology, Kanpur, India
[2]Indian Institute of Tropical Meteorology, Pune (New Delhi Branch)

Keywords: AEROSOL CHARGING, CLOUD FORMATION, DROPLET GROWTH, GCR FLUX.

INTRODUCTION

Satellite data have shown very close correlation between GCR (Galactic Cosmic Rays) flux and fraction of low altitude cloud in earth's atmosphere (Gray *et al.*, 2010). GCR flux is one of the major sources for the production of ions in the lower troposphere. Recent studies have shown that ions coagulate to form electrically charged particles and these particles grow to become cloud droplets (Tinsley *et al.*, 2000). Aerosol particles can be charged by the attachment of ions and electrons. Aerosol-cloud interactions can be enhanced as the collision efficiency between a particle and a water droplet increases if the particle is electrically charged (Tripathi *et al.*, 2006).

This study is to create a computational model, which can quantify how the GCR flux affect aerosol and cloud microphysics, which subsequently changes radiative properties in cloud. A coupled ion-aerosol-cloud global electrical model is developed. A model for droplet growth in cloud is also developed. All these models are used together to study impact of GCR flux and effect of electric charging on cloud droplet formation.

METHODS

To study the effect of GCR flux and cloud charging separate models are developed for each phenomenon and then coupled. First model is to calculate conductivity and ionic concentration in the altitude range of 0-45 km (M. Michael *et al.*, 2008). In this model ion balance equations are used and all attachment coefficients are calculated. Second model is to calculate electric field and charge distribution within the cloud (Srivastava and Tripathi 2010; Zhou *et al.*, 2007). In this model ion balance equations and Poisson's equation are used. Third model developed is cloud droplet growth model to analyze growth of particle to droplet (Jacobson 1999; Nenes *et al.*, 2001). In this model cloud parcel model is used with conservation of water and mass in cloud. And growth of particle is governed by super-saturation of cloud. Fourth model developed is collision efficiency model to calculate scavenging rate of charged particles by droplets (Tinsley *et al.*, 2000). In this model forces due to image charge, gravitation, thermophoratic force, difusophoratic force and inertia are considered in motion of particle and droplet. Then probability of collision occurrence is calculated. All the four models are coupled with a model which calculates cloud height from calculation of dew point and temperature profile. In the coupled model height of the cloud, boundary conditions of the cloud, growth of droplet inside the cloud, electrification and scavenging of the particles are simulated simultaneously.

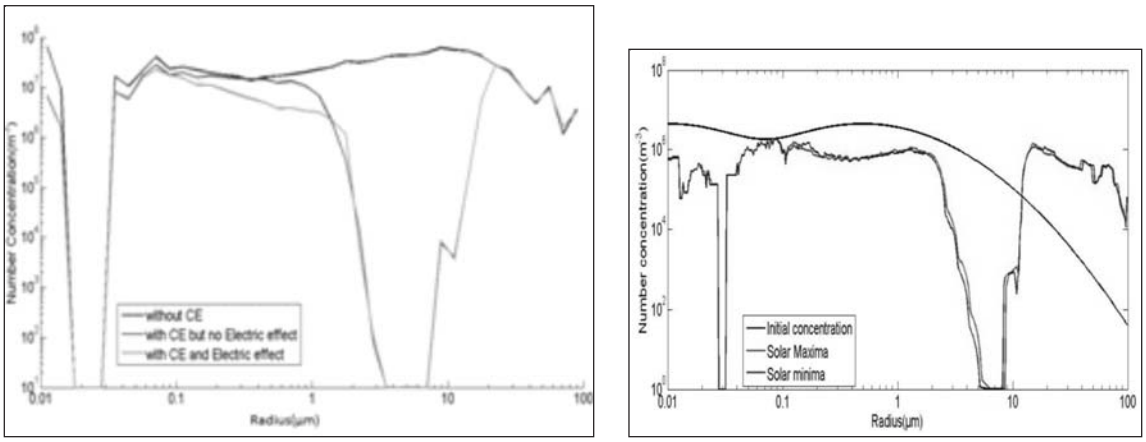

Figure 1. Particle size distribution within cloud (a) Comparison of particle distribution for effect of electric field and collision efficiency, (b) Comparison of particle distribution for two extreme GCR conditions during solar maxima and solar minima

CONCLUSIONS

There is significant effect of electric charging on the droplet concentration within the cloud. Charging of aerosol increases the scavenging of particle which affects ice nucleation. There is no significant change in CCN distribution for solar maxima and minima. Implication of result is that variation of GCR flux does not affect CCN particle distribution. And microphysical process within the cloud might not be the cause of correlation between GCR flux and fraction of low altitude clouds.

ACKNOWLEDGEMENTS

The present work is supported by a grant from Ministry of Earth Science.

REFERENCES

Nenes, A., Ghan, S., Abdul-Razzak, H., Chuang P. Y., Seinfeld J. H. (2001). Kinetic limitations on cloud droplet formation and impact on cloud albedo, *Tellus*, **53B**, pp. 133–149.

Jacobson, M. Z. (1999). Fundamentals of atmospheric modeling, Cambridge University Press.

Gray, L. J. *et al.* (2010). Solar influences on climate, *Rev. Geophys.*, **48**, RG4001

Michael, Marykutty, and Tripathi, S. N. (2008). Effect of charging of aerosol in the lower atmosphere of Mars, Planetary and Space Sciences, DOI:10.1016/J.PSS-2513.07.030.

Srivastava, A. K., and Tripathi, S. N. (2010). Numerical Study for Production of Space Charge within the Stratiform Cloud. *JESS*, **109(5)**, pp. 627-638.

Tinsley *et. al.*, (2000). Effects of image charge on the scavenging of aerosol particles by cloud droplets, and on droplet charging and possible ice nucleation processes. *J. Atmos. Sci.*, **57**, pp. 2118-2134

Zhou, L. and Tinsley, B. A. (2007). The production of space charge at the boundaries of layer clouds. *J. Geophys. Res.*, **112**, D11203.

EXAMINATION OF NEW PARTICLE FORMATION MECHANISMS IN A TROPICAL URBAN ENVIRONMENT

VIJAY P. KANAWADE[1*], SACHCHIDA N. TRIPATHI[1], ALOK S. GAUTAM[2], DEVENDRAA K. SIINGH[2], A. K. KAMRA[2], ATUL K. SRIVASTAVA[3]

[1]Center for Environmental Science & Engineering, Indian Institute of Technology, Kanpur, India
[2]Indian Institute of Tropical Meteorology, Dr. Homi Bhabha Marg, Pune, India
[3]Indian Institute of Tropical Meteorology (Branch), Prof. RamnathVij Marg, New Delhi, India

Key words: ION INDUCED NUCLEATION, HYSPLIT

INTRODUCTION

New particle formation (NPF) has been observed globally at the Earth's surface (Kulmala *et al.*, 2004), which can have climatic effects via cloud condensation nuclei (CCN) activation.While such NPF events have been widely reported globally; the observations of NPF in a tropical urban environment are very limited.

METHODS

During the pre-monsoon (March-May) season of 2012, we carried out first comprehensive observation of ion and aerosol properties at the Indian Institute of Tropical Meteorology (IITM), Pune, India. These include particle number-size distributions in the diameter range of 4–750 nm from two sets of scanning mobility particle sizers (SMPS) in combination with butanol condensation particle counter (CPC, TSI 3775), ion number-size distribution in the diameter range of 0.5–40 nm from neutral air-ion spectrometer (NAIS), radon/thoron concentrations using a radon/thoron monitor (RTM 2200), together with sulfur dioxide (SO_2) and meteorological parameters. We have used an aerosol microphysical box model (Kanawade and Tripathi, 2006), incorporated with ioninduced nucleation (IIN) (Modgil *et al.*, 2004) and binary homogeneous nucleation (BHN) (Vehkamaki *et al.*, 2002) parameterizations, to investigate the mechanisms responsible for observed NPF. Additionally, particle growth and nucleation inverse model (PARGAN) (Verheggen and Mozurkewich, 2006) was also used to calculate particle growth rates (GR) and nucleation rates (J_1) from the measured particle number-size distributions.

RESULTS AND CONCLUSION

Fig. 1 depicts contour plot of particle size distributions measured on April 17, 2012. The particle size distributions displayed a burst of small particles and a sustained growth in the size and in N_{20} concentrations, (2–18) × 10^3 cm^{-3}. The condensational sink (CS_{total}) does not appear to be decreasing at the onset of nucleation, suggesting that particles were not formed locally. We observed such particle bursts frequently during the pre-monsoon season followed by significant growth over several hours (31% out of 69 days).The HYSPLIT back trajectory, NPF start time and box model simulations further led us to believe that particle nucleation occurred somewhere else in the anthropogenic plume, containing high SO_2 concentrations. The calculated averaged GR and J_1 were found to be 5.5±3.21 nm $h^{-1}$and 6.8±5.13 $cm^{-3}s^{-1}$, respectively, within observed ranges at other urban sites worldwide. NPF events were mainly associated with low relative humidity, high calculated H_2SO_4 proxy, high ionization rate, and low wind speed. Our key finding is that IIN could explain only up to

30% of the observed NPF whereas BHN failed to explain NPF at all for observed environmental conditions. The other underlying mechanisms (ternary homogeneous nucleation, THN, with ammonia or amines or organics) for observed NPF were not possible to examine and future studies are required to reveal the other likely contributing mechanisms.

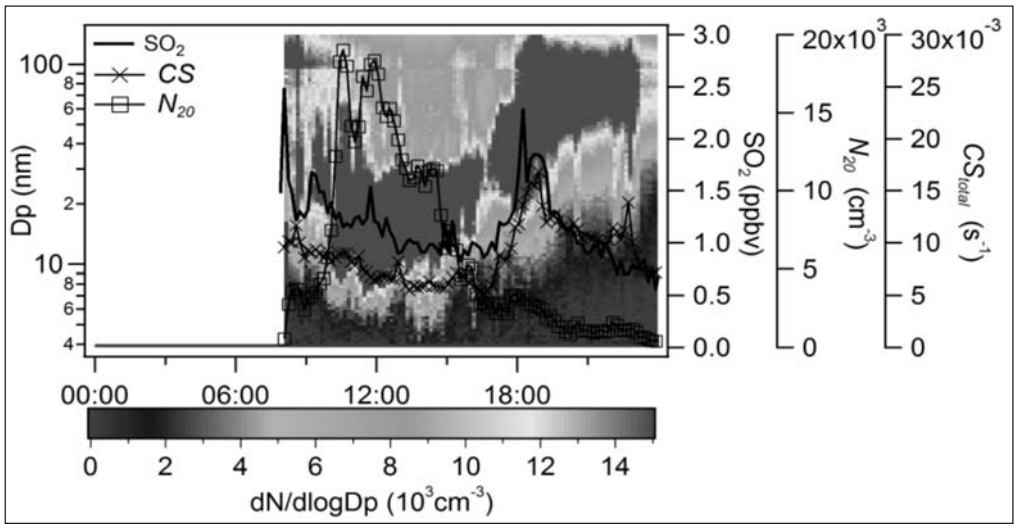

Figure 1. Particle size distributions in the size range from 4–140 nm measured on April 17, 2012 at IITM, Pune. The N_{20}concentrations (particles of diameter 3–20 nm) (line connected by open square), SO_2 (solid line) and condensational sink (line connected by asterisk) are also shown.

REFERENCES

Kanawade, V. P. and Tripathi, S. N. (2006). Evidence for the role of ion-induced particle formation during an atmospheric nucleation event observed in TOPSE, *J. Geophys. Res.,* **111**, D02209.

Kulmala, M., Vehkamaki, H., Petaja, T., dal Maso, M., Lauri, A., Kerminen, V. M., Birmili,W. H., McMurry, P. H. (2004). Formation and growth rates of ultrafine atmospheric particles: A review of observations, *J. Aerosol Sci.*, **35**, 143–176.

Modgil, M. S., Kumar, S., Tripathi, S. N., and Lovejoy, E. R. (2005). A parameterization of ion-induced nucleation of sulfuric acid and water for atmospheric conditions, J. *Geophys. Res.*,**110**, D19205.

Vehkamaki, H., Kulmala, M., Napari, I., Lehtinen, E. J., Timmreck, C., Noppel, M., and Laaksonen, A. (2002). An improved parameterization for sulfuric acid-water nucleation rates for tropospheric and tratospheric conditions, *J. Geophys. Res.*, **107**, pp. 24347–24358.

Verheggen, B., Mozurkewich, M. (2006). An inverse modeling procedure to determine particle growth and nucleation rates from measured aerosol size distributions, *Atmos. Chem. Phys.*, **6**, pp. 2927-2942.

STABLE FOG GENERATION AND STUDY OF THE EFFECTS OF DIFFERENT PHYSICOCHEMICAL PARAMETERS OF CLOUD CONDENSATION NUCLEI (CCN) ON FOG MICROPHYSICAL PROPERTIES AND DISSIPATION USING AN EXISTING LABORATORY SCALE FOG GENERATION FACILITY

A. CHAKRABORTY, T. GUPTA and S.N.TRIPATHI

Indian Institute of Technology Kanpur, Department of Civil Engineering
Kanpur, UP – 208016, India
E mail: cabhi@iitk.ac.in

Keywords: FOG STABILITY; CCN, HYGROSCOPIC, DISSIPATION

INTRODUCTION

Kanpur is located in Indo-Gangetic plane and every year experiences severe fog episodes during winter months which results in serious disruption of daily life and transportation. Very little is known about the cause and mechanism which results in such severe and persistent fog. The IIT Kanpur Fog chamber facility (Singh *et al*., 2011) has been conceptualized and built indigenously to study the fog formation and dissipation under various environmental conditions. Fog was generated using different cloud condensation nuclei (CCN) and it has been observed that fog microphysical properties like droplets concentration, size distribution depends on the nature of the CCN. Fog stability was achieved by creating equilibrium between droplet lost via settling and formation of new droplets. Higher number of CCN resulted in higher number of relatively smaller fog droplets. Fog stability and dissipation also depends on CCN properties; Fog generated from very hygroscopic CCN seems to dissipate faster where as fog generated from less hygroscopic and light absorbing carbon nanotube (CNT) CCN was reported to be very persistent (Banerjee *et al.,* 2012). The results of this study will help us in better understanding of the causes behind formation and persistence of fog in this region.

METHODS

FOG GENERATION

Initially, the chamber was cooled by a closed loop circulation of Isopropyl alcohol from the chiller to flow through the annular walls of the chamber to maintain the desired temperature (3.5°C-5.5°C). Two outlets provided at the bottom of the chamber were opened to maintain atmospheric pressure inside the chamber. After the desired temperature was reached, moist air was poured inside it through two adjacent pipes under high pressure through spray nozzles. Next, CCN were injected inside the fog chamber. Different types of aerosol like NaCl, graphite, ambient air were employed. Steam was generated by a 20 L pressure cooker and wet aerosols were generated through a wet aerosol generator (TSI, Model 3079) at different flow rates. Wet aerosols were dispersed through the nozzles attached to parallel tubes placed on the upper end of the chamber. Dry aerosol generator was used for dispersing dry aerosols into the chamber with high velocity with an injector nozzle connected to one side of the upper annular wall of the chamber to carry and disperse the aerosols uniformly. Relative humidity and temperature inside the chamber was continuously monitored through a small humidity and temperature transmitter (HMT, Vaisala model 337).

CCN AND DROPLET SIZE DISTRIBUTION

Measurement of particle (CCN) size distribution was carried out using Scanning Mobility Particle Sizer (SMPS, TSI Model 3936). Fog droplet size distribution from 3 μm to 50 μm was measured by Cloud Combination Probe (CCP) of Droplet Measurement Technology (DMT).

RESULTS

CCN physicochemical properties have a significant effect on fog microphysical parameters. Higher number of CCN resulted in relatively smaller and higher number of fog droplets where as lower number of CCN produced bigger droplets and smaller number of fog droplets; since same amount of moisture is distributed among higher number of CCNas indicated by almost same liquid water content (LWC) for both the cases. Although the difference in droplet diameter is not that significant may be due to continuous availability of moisture but droplet concentration was very different for different CCN flow rates due to difference in number of CCN. Fog became stable almost 20 minutes after the vapour and CCNwere first introduced inside the chamber. This may be due to the fact that immediately after the vapour input, temperature inside the chamber increased and took some time to stabilize. Fog generated from NaCl as CCN dissipates quickly may be because of formation of very large droplets due to its hygroscopic nature.

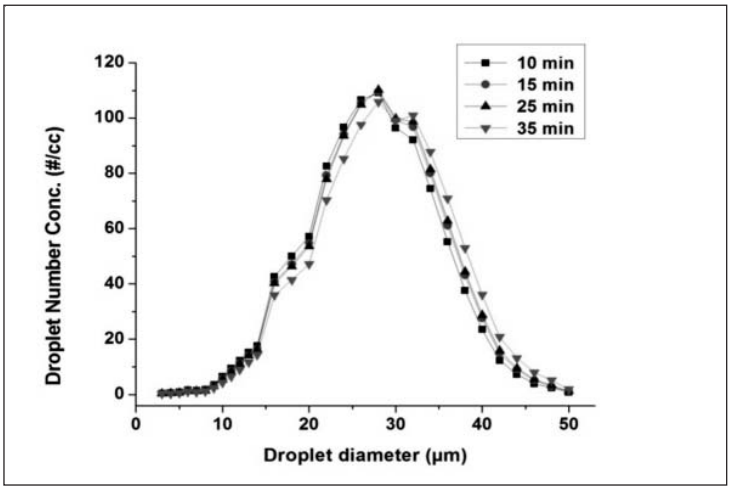

Figure 1. Fog droplet size distribution generated using NaCl as CCN at 150 L/h

CCN	Flow rate (L/h)	Number of CCN particles entering into Fog chamber (#/min)	Average droplet diameter (μm)	Droplet number conc. (#/cc)	LWC (g/m^3)
NaCl	100	5.11×10^{10}	33.10 ± 0.41	970±56	0.125±0.010
NaCl	150	7.19×10^{11}	32.08 ± 0.57	1036±36	0.126±0.012

Table 1. Different CCN and Fog microphysical parameters

ACKNOWLEDGEMENT

This work is supported through a grant from the Board of Research in Nuclear Science.

REFERENCES

Banerjee, S., Tripathi, S.N., Das, U., R., Raju, J., Nilesh, *et al.* (2012). Enhanced persistence of fog under illumination for carbon nanotube fog condensation nuclei, *Journal of Applied Physics*, **112**, 024901.

Singh,V.P. , Gupta, T., Tripathi, S.N., Jariwala, C., Das, U. (2011). Experimental Study of the Effects of Environmental and Fog Condensation Nuclei Parameters on the Rate of Fog Formation and Dissipation Using a New Laboratory Scale Fog Generation Facility, *Aerosol and Air Quality Research*, **11**, pp. 140–154.

SIZE RESOLVED CLOUD CONDENSATION NUCLEI (CCN) ACTIVATION OF AEROSOLS IN KANPUR, INDIA

DEEPIKA BHATTU, S.N. TRIPATHI

Department of Civil Engineering, Indian Institute of Technology, Kanpur, India
E-mail: deepikab@iitk.ac.in

Keywords: CLOUD CONDENSATION NUCLEI, HETEROGENEITY, HYGROSCOPICITY PARAMETER, SUPERSATURATION.

INTRODUCTION

Aerosol particles that have ability to form cloud dropletsare known as Cloud Condensation Nuclei (CCN). Total concentration of CCN is a function of both critical supersaturation (SS) and critical diameter (D_c),which further depends on aerosol dry particle diameter and chemical composition (Frank *et al.*, 2006).TheCCN particlesare link between cloud microphysical properties such as cloud droplet number concentration and size distribution, and physicochemical properties of aerosols, like bulk density, molecular weight of species and their dissociation property (Patidar *et al.*, 2012).They affect the cloud optical properties by modifying the cloud coverage area and precipitation rate due to elevated concentrations (Rose *et al.*, 2010). Most studies to date have shown the combined effect of both particle size and its compositionin polydisperse CCN sampling. To decouplethe effect of size and chemical composition, various researchers have carried out size-resolved CCN studies. In this wayone canunderstand the relative importance of most crucial parameters such as, number concentration, particle size, chemical composition, hygroscopicity and mixing state on CCN predictability (Frank *et al.*, 2006; Rose *et al.*, 2010). Earlier such measurements were done only to study activation properties of lab generated aerosols such as $(NH_4)_2SO_4$ and NaCl, where chemical composition and mixing state is already known (Frank, 2006). In order to represent local pollution levels and long range transport, which varies both spatially and temporally, ambient size-resolved studies are required. To our knowledge, no size resolved CCN measurements have been reported from India.

The main objective of ourstudy is to characterize the hygroscopicity parameter of aerosols as a function of two independent variables, dry particle diameter and water vapour supersaturation based on calculated activation diameter using Kohler model during different seasons i.e. spring and summer, over ahighly polluted urban site, Kanpur, India. Two different approaches which involve inversion of CCN data and fitting of measured CCN efficiency spectra using cumulative Gaussian distribution function (CDF), respectively were followed to calculate the activation diameter (D_a) at different supersaturations. Effects of multiple charged particles and DMA transfer functionhave also been accounted for.

METHODS

The Calibration set up and procedure employed in this study is same as that of Patidar *et al.* (2012). Size-resolved CCN activation (CCN/CN) curve is obtained by running Cloud Condensation Nuclei counter (CCNc, DMT CCN-100) and Condensation Particle Counter (CPC, TSI 3075) in parallel to Differential Mobility Sizer (DMA, TSI 3085) for 9 days in Feb-Mar, 2012 (Spring) and 18 days in

May-June, 2012 (Summer). For each CCN measurement cycle, size selected dry particles ranging from 20 nm – 300 nm were provided 5 different supersaturation levels (SS=0.2% - 1.2%). Two measurement cycles were completed in a day and the integration time for each measurement data point was 60 sec. Particle size distribution is also measured in the middle of sampling period of each supersaturation of measurement cycle (after every 15–17 minutes). Other measurements were also done with instruments namely Vaisala RH sensor, Condensation Particle Counter (CPC, TSI 3076), Aerodynamic Particle Sizer (APS, TSI), Optical Particle Counter (OPC, Grimm) and Photo Acoustic Soot Spectrometer (PASS, DMT).

First approach involves a model given by Petters *et al.* 2007 to calculate the activation or critical diameter by the inversion of measured CCN activation spectra accounting effect of multiple charged particles and DMA transfer function.This model assumes that the particles are internally mixed i.e. composition do not vary with size. Second approach used in this study to calculate activation diameter is to do 3-parameter CDFfit of measured CCN activation spectra (Rose *et al.*, 2010) after correcting it for multiply charged particles and DMA transfer function (Frank *et al.*, 2006). The best fit parameters such as MAF, D_a and σ_a/D_a are used to explain the internal properties of the CCN active particles like mixing state and heterogeneity.

Fig. 1 shows the averaged CCN activation spectra at SS = 0.2% - 1.2%. This figure shows that the mid-point activation diameter decreases as supersaturation increases. These values are greater than the lab generated pure Ammonium Sulfate aerosol particles at same supersaturation conditions. Also at higher SS (SS=1.2%), the activation spectra does notapproach unity, which suggests that all aerosol particles above the mid-point activation diameter are not fully CCN active.

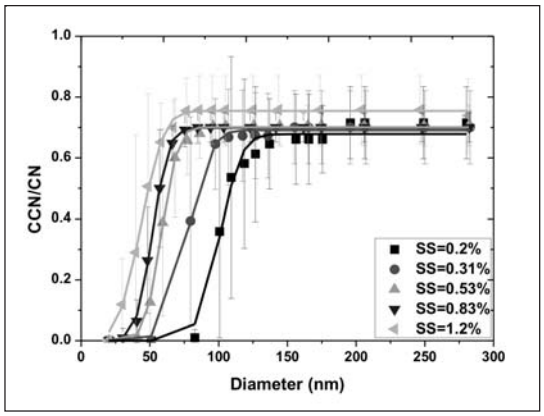

Figure 1. Averaged CCN activation spectra at SS=0.2%-1.2% for summer (May-June), 2012. The data points are obtained by calculating the median value of CDF fits to all measured spectra and the error bars are the difference of upper and lower quartile and the solid lines are CDF fit to the data points.

CONCLUSIONS

In this study we presented size resolved CCN measurements in highly polluted urban site, Kanpur. Such studies help in understanding the relative significance of aerosol particle number concentration, size, composition and hygroscopicity which all are the major factors affecting the CCN concentration temporally and spatially. These size resolved measurements provide more information about aerosol particles by separating two factors, i.e. size and chemical composition which is required for better

prediction of CCN through various models like GCM and WRF-Chem, which need a simplified aerosol composition as a function of size and their mixing state, which cannot be obtained from the widely used polydisperse CCN sampling.

REFERENCES

Frank, G. P., Dusek, U., and Andreae, M. O. (2006). Technical note: A method for measuring size-resolved CCN in the atmosphere, *Atmos. Chem. Phys. Discuss.*, **6**, pp. 4879–4895.

Patidar, V., Tripathi, S. N., Bharti, P. K., and Gupta, T. (2012). First Surface Measurement of Cloud Condensation Nuclei over Kanpur, IGP: Role of Long Range Transport, *Aerosol Science and Technology*, **46**, pp. 973-982.

Petters, M. D., Prenni, A. J., Kreidenweis, S. M., DeMott, P. J. (2007). On Measuring the Critical Diameter of Cloud Condensation Nuclei Using Mobility Selected Aerosol, *Aerosol Science and Technology*, **41(10)**, 907-913.

Rose, D., Nowak, A., Achtert, P., Wiedensohler, A., Hu, M., Shao,M., Zhang, Y., Andreae, M. O., and Poschl, U. (2010). Cloud condensation nuclei in polluted air and biomass burning smoke near themega-city Guangzhou, China - Part 1: Size-resolved measurements and implications for the modeling of aerosol particle hygroscopicity and CCN activity, *Atmos. Chem. Phys.*, **10**, pp. 3365–3383.

MODELING SECONDARY ORGANIC AEROSOL DURING FOGGY AND NONFOGGY EPISODE

D. S. KAUL, S. N. TRIPATHI, T. GUPTA

E mail: snt@iitk.ac.in, tarun@iitk.ac.in
Department of Civil Engineering, Indian Institute of Technology
Kanpur, India

INTRODUCTION

The organic aerosols which are directly emitted are referred to as primary organic aerosol (POA). Globally, 20 % of the total organic aerosol mass is POA. The aerosol produced by chemical photo-oxidation in the atmosphere is referred to as secondary organic aerosols (SOA). SOA is produced by both gas to particle partitioning mechanism and aqueous phase mechanism. In the gas to particle partitioning mechanism, VOCs directly emitted from the anthropogenic and natural sources are photo-oxidized by oxidant such as O3 and OH radical and semi volatile organic compounds are produced which then condense over the pre-existing aerosols (Odum *et al.,* 1997). In the aqueous mechanism such as in the fogs and clouds, VOCs are scavenged and dissolved into the droplets. Subsequent reaction and oxidation of dissolved VOCs by dissolved oxidants inside the fog droplets produces more oxygenated organic compounds compared to those produced from gas to particles mechanism. As these fog droplets evaporate, the oxygenated compounds are left behind and condense over the particles (Ervens *et al.,* 2011). The direct SOA estimate is complicated due to numerous organic compounds involved in the SOA formation. Thus, numerous indirect methods, for example elemental carbon (EC) tracer method have come up and are widely used to estimate SOA. The modeled SOA with a chemical transport model (WRF-CHEM) and the same estimated by the indirect methods (Kaul *et al.*, 2011) will be compared and possible chemistry involved in the SOA formation during foggy and non-foggy episodes will be investigated.

METHODS

Particulate matter (PM_1) samples on filters were collected and were analyzed for chemical composition. Elemental carbon-organic carbon (EC-OC) analyzer was used to measure organic and elemental carbon on the collected filters. EC tracer method was used to estimate secondary organic aerosol (Kaul *et al.,* 2011). A chemical transport model (WRF-CHEM) has been used to model SOA. The modeled SOA has been evaluated against the estimated SOA from the EC tracer method.

RESULTS AND CONCLUSIONS

The enhanced SOA formation through aqueous phase mechanism was observed over this region during foggy episodes (Kaul *et al.*, 2011). Foggy episode was considerably loaded with organic and inorganic species. The biomass generated aerosols were also scavenged by the fog droplets. A chemical transport model (WRF-CHEM) has been used to evaluate the indirectly estimated SOA under both dry and wet (foggy) conditions. More details regarding simulation and findings will be presented at the conference.

ACKNOWLEDGEMENT

We thank Jai Prakash, Rajmal Jat, Abhishek Gaur and Soumabha Chakroborty for their help in the field experiment.

REFERENCES

Odum, J. R., Jungkamp, T. P. W., Griffin, R. J., Flagan, R. C., and Seinfield, J. H. (1997). The atmospheric aerosol forming potential of whole gasoline vapor, *Science*, **276**, pp. 96-99

Ervens, B., Turpin, B. J., and Weber, R. J. (2011). Secondary organic aerosol formation in cloud droplets and aqueous particles (aqSOA): a review of laboratory, field and model studies, *Atmos. Chem. Phys.*, **11**,pp. 11069-11102.

Kaul, D. S., Gupta, T., Tripathi, S. N., Tare, V., Collett, J. L. (2011). Secondary organic aerosol: a comparison between foggy and nonfoggy days, *Environ. Sci. Tech.*, **45**, pp. 7307-7313

Kaul, D. S., Gupta, T., Tripathi, S. N. (2012). Chemical and microphysical properties of the aerosol during foggy and nonfoggy episodes: a relationship between organic and inorganic content of the aerosol, *Atmos. Chem. Phys. Discuss.* , **12**, doi:10.5194/acpd-12-14483-2012, 2012

A PRELIMINARY STUDY OF AEROSOL-LAND- ATMOSPHERE INTERACTIONS DURING INDIAN SUMMER MONSOON USING REGIONAL CLIMATE MODEL

ABHISHEK LODH, RAMESH RAGHAVA, SUBODH SINGH AND KARANJIT SINGH

Centre for Atmospheric Sciences, Indian Institute of Technology Delhi, HauzKhas,
New Delhi-110016, India
E mail: abhishek.lodh@gmail.com

Key words**:** SOIL MOISTURE, BATS, EVAPOTRANSPIRATION AND AEROSOLS

INTRODUCTION

SOIL–MOISTURE PRECIPITATION FEEDBACK

Drier soil leads to absorption of less solar radiation and enhanced longwave radiation results in weakening of evapotranspiration. Consequently, more of the available surface energy is devoted to sensible heat (SH) flux rather than latent heat (LH) flux, and the Bowen ratio (SH/LH) is high. These factors lead to less moist static energy of the air in the boundary layer over dry soils compared to over wet soils. Arid and semi-arid regions and/or the transitional climatic zones lying between wet and dry climates are **soil-moisture limited regions** where soil moisture strongly constrains evapotranspiration variability and thus resulting feedbacks to the atmosphere. The feedback parameter λ(soil moisture, precipitation) represents the fraction of precipitation change attributed to variations in monthly soil moisture.

$$\lambda = \frac{\rho[s(t-\tau), p(t)]}{\rho[s(t-\tau), s(t)]} \qquad (1)$$

where λ measures the instantaneous feedback of *s* on *a* at time t (Notaro, *et al.* 2008), *s* (soil moisture) is a slowly varying quantity, *p* (precipitation) is a faster moving atmospheric variable, τ = 1 month is the time period of soil-moisture memory and ρ is correlation.

EXPERIMENTAL DESIGN

The Regional Climate model RegCM4.0 is used in the present study as it has meritoriously simulated Indian summer monsoon circulation features and rainfall. The physical parameterizations employed in the control simulations include the radiative transfer package of the NCAR Community Climate Model version 3 (CCM3, Kiehl, *et al.* 1996), the boundary layer scheme by Holtslag *et al.* (1990) and the cumulus cloud scheme of Grell (1993) with Fritsch and Chappell (1980) closure, subex moisture flux scheme by Pal, *et al.* (2000) and Ocean flux scheme by Zeng *et al.* (1998). The chosen configuration results in the most realistic representation of summer monsoon hydro climate. RegCM4.0 was run at approximately 50-km horizontal resolution with Normal Mercator map projection with 18 vertical levels in the atmosphere (sigma coordinate) and model domain is from 40°E-130°E, 0°-40°N to include all the significant geographical features of the South-Asian Monsoon region. The time step of model integration is 60 seconds. The lateral and lower boundary conditions for ground temperature (T_g), surface pressure (p_s), sea surface temperature (SST) (except for soil moisture) were provided by the National Centers for Environmental Prediction, NCEP-DOE AMIP-

II Reanalysis (R-2) (Kanamitsu, *et al.* 2002) 6-hourly data and Reynolds weekly sea surface temperature (SST) (Reynolds et al. 2002) respectively. For the present study, four consecutive (2000-2003) years of Indian southwest monsoon season has been chosen. The model is run from 00GMT of 1st January to 24 GMT of 31stDecember, for all the four years from 2000-2003. The two sensitivity experiments to include the aerosol usage in the model are named as AER00D1andAER11D1. The AER00D1 experiments are with no aerosol, with DUST whereas AER11D1 are experiments which include anthropogenic, biomass, SO2, BC, OC with DUST. The representation of dust emission processes in the dust model depends on the wind conditions, the soil characteristics and the particle size. The numbers of tracers used in the sensitivity experiments are ten and the optical aerosol scheme allows aerosol feedbacks on radiative thermodynamic and dynamic fields. Out of the years chosen in context of Indian summer monsoon (ISM), the year 2000 is a normal *+LA NIÑA*, 2001 and 2003 are normal years and 2002 is drought+ *EL NIÑO*.

RESULTS

The correlation between temperature (T_g) and evapotranspiration (E), ρ (E, T) has been used as diagnostic for soil moisture-temperature coupling. Fig.1 shows that regions of negatively high correlation (red coloured) are regions of soil moisture-limited evapotranspiration and hence, regions of moisture sink at the earth's surface and strong soil moisture-temperature coupling (soil moisture control) whereas regions of positively high correlation (green coloured) are energy-limited evapotranspiration regions and hence, low soil moisture-temperature coupling (atmospheric control) (Seneviratne, *et al.* 2010). Over the regions of negative correlation between evapotranspiration and temperature, when solar radiation falls on the surface, the moisture of the soil evaporates resulting in release of latent heat. This release of latent heat results in cooling of the air, consequently the temperature decreases. Thus, over the regions of negative correlation between evapotranspiration and temperature when evapotranspiration increases temperature decreasesand correspondingly the Bowen's ratio is low, resulting in a boundary layer that is shallow and unstable.But over the regions of positive correlation between evapotranspiration and temperature, the external forcings dominate the local atmosphere conditions such that the temperature cooling due to latent heat release is nullified. Hence, we conclude that over regions of negative correlation land impacts atmosphere and vice-versa atmosphere impacts land over regions of positive correlation between evapotranspiration and temperature.

As aerosols impact the global radiation hence, correlation between global radiation (R_g) and evapotranspiration (E), ρ (R_g, T) has been used as an added diagnostic studying its impact. Thus, aerosols affect soil moisture-temperature coupling by impacting the ground temperature as they cool the earth's surface (Lau, *et al.* 2006). Comparing figure 2(b), 3(b) with 2(a), 3(a) clearly reveals that extent of spatial domain of negative correlation decreases. This shows how aerosols affect global radiation and simultaneously the feedback. But, IGP and NWP are still the dominant regions of feedback between soil moisture and precipitation affected by aerosols. This observation is also corroborated by fig. 4 that feedback primarily exists over CI, IGP.

The temporal analysis, based on sensitivity experiments (AER00D1 and AER11D1), reveals that over IGP and NWP the aerosol induced feedback between precipitation and soil moisture decreases from corresponding CONTROL experiment. The time series plot of correlation, ρ(E,T) between evapotranspiration (mm/day) and temperature (K), and soil moisture precipitation feedback, λ(SM, P) from 2000 -2003 over CI,IGP and NWP is shown in fig. 5 and 6 respectively. Though fig. 5 does not reveal the effect of aerosol loading on feedback but fig. 6 clearly reveals that feedback value

decreases in the AER11D1 sensitivity experiment. The increasing load of black carbon anthropogenic sources in the IGP region results in cooling of the earth's surface, as a result ground temperature decreases and hence, feedback value decreases.

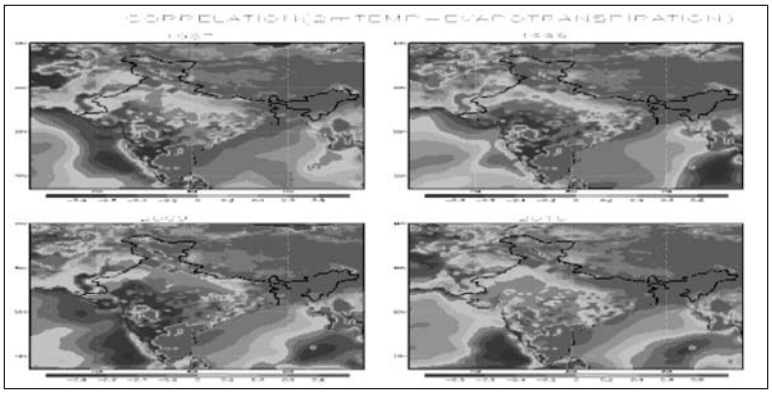

Figure 1. Model (CONTROL) variation of correlation, ρ (E, T) between evapotranspiration (mm/ day) and temperature (K), (May – September) from 2000-2003.

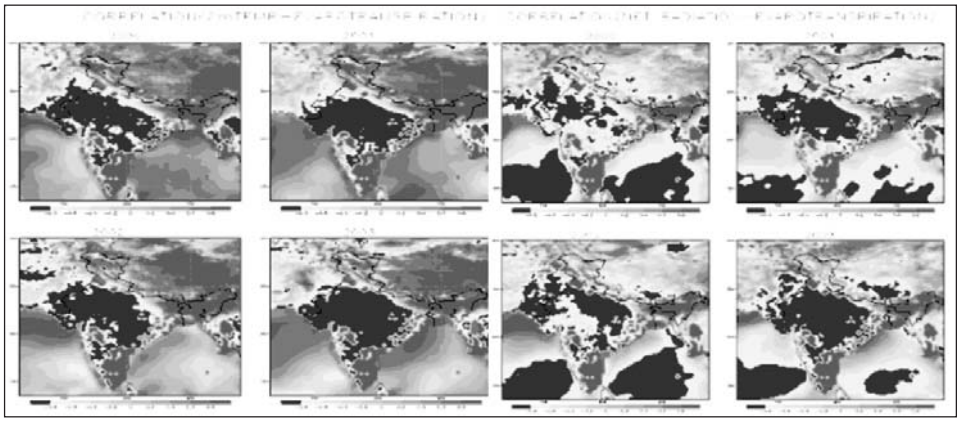

Figure 2 (a). Model(AER00D1) seasonal variation of correlation, (E, T) between evapotranspiration (mm/ day) and temperature (K)&**2(b)**correlation, ρ (Rg, T) between evapotranspiration (mm/day) and temperature (K), (May – September) from 2000-2003, from aerosol sensitivity run AER00D1.

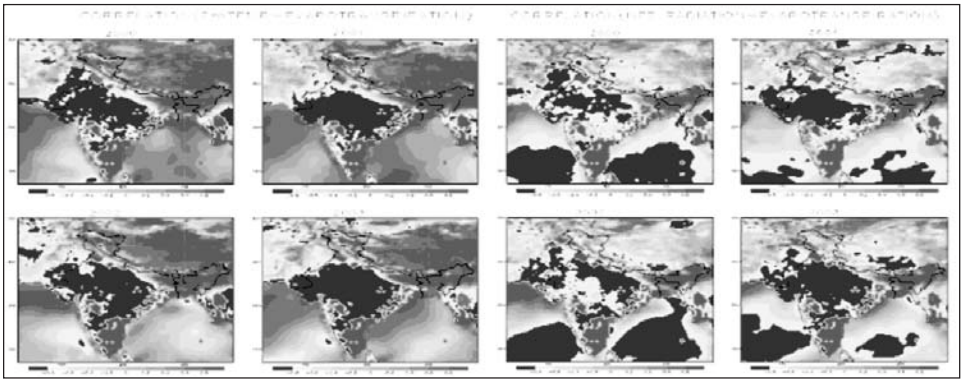

Figure 3 (a). Model (AER11D1) seasonal variation of correlation, ρ (E, T) between evapotranspiration (mm/ day) and temperature (K) &3(b) correlation, ρ (Rg, T) between evapotranspiration (mm/day) and temperature (K), (May – September) from 2000-2003, from aerosol sensitivity run AER11D1.

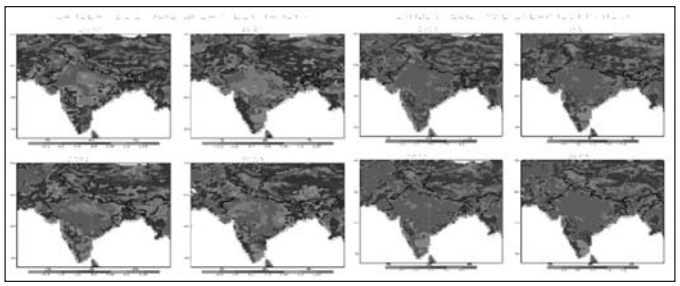

Figure 4(a). Model (AER00D1) seasonal variation (May – September) from 2000-2003 of feedback parameter,λ(SM,P) between soil-moisture (mm) and precipitation(mm/day) from aerosol sensitivity run AER00D1 &4(b)AER11D1.

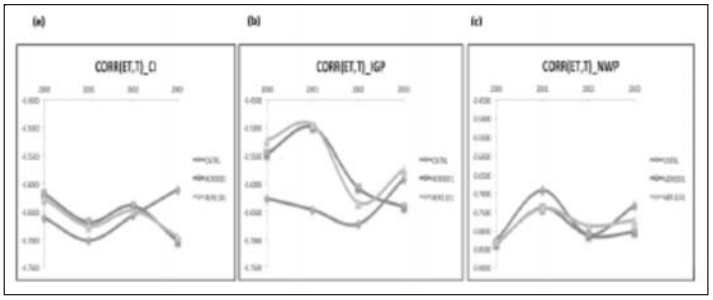

Figure 5.Time series plot of correlation, ρ (E, T) between evapotranspiration (mm/day) and temperature (K) from 2000 -2003 over (a) Central India (b) Indo-Gangetic plains and (c) Northwestern province.

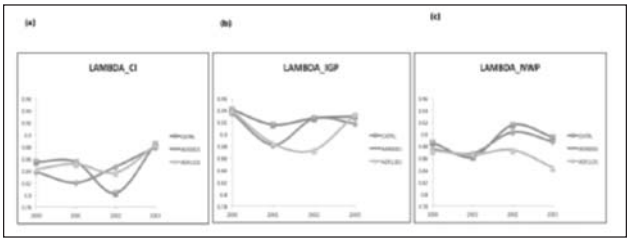

Figure 6.Time series plot of soil moisture precipitation feedback,λ(SM, P) from 2000 -2003 over (a) Central India (b) Indo-Gangetic plains and (c) Northwesternprovince.

ACKNOWLEDGMENTS

We are thankful to Abdus Salam International Centre for Theoretical Physics, Trieste, Italy for making available the model codes of RegCM4.0 for this study. We also thank National Center for Environmental Prediction/ National Center for Atmospheric Research (NCEP/NCAR) for providing high-resolution meteorological datasets.

REFERENCES

Lau, K. M., Kim, M. K. and Kim, K. M. (2006). *Climate Dynamics*, **26** (7-8), pp. 855-864.
Notaro, M. (2008). Statistical identification of global hot spots in soil moisture feedbacks among IPCC AR4 models, *J. Geophys. Res.*, **113**, D09101.
Seneviratne, S. I., Corti, T., Davin, E. L., Hirschi, M, Jaeger, E. B., Lehner, I., Orlowsky, B., Teuling, A. J. (2010). Soil moisture-climate interactions in a changing climate: A review. *Earth Science Review.*

STUDY OF ELECTROHYDRODYNAMIC ATOMIZATION OF A FLUID

P.SHUKLA[1], P.K.PANIGRAHI[2], KOUSHIK DUTTA[1], YASHWANTH REDDY[1]

[1] Department of Mechanical Engineering, Indian Institute of Technology (BHU), Varanasi- 2210 05
[2] Department of Mechanical Engineering, Indian Institute of Technology, Kanpur – 2080 16

Keywords: ELECTROHYDRODYNAMIC ATOMIZATION, ELECTROSPRAY, CONE-JET MODE

INTRODUCTION

A liquid surface subjected to an electric field beyond a certain threshold point breaks up into fine droplets depending upon a host of factors like the applied hydrostatic pressure gradient, voltage and properties of the fluid like electrical conductivity and surface tension (Tang and Gomez 1996, Castellanos 1991). Different modes of operation are available depending on the above mentioned factors. These include dripping, micro dripping, spindle mode, cone-jet mode and multi cone-jet mode. These have been studied in detail by Cloupeau & Prunet – Foch (1989). Researchers have tried to find out the range of the physical properties than allow for a cone-jet mode of operation Smith (1986). In the present work, the cone–jet mode of liquid breakup has been experimentally studied by varying the conductivity of the atomizing liquid in three steps- 1.08, 10.8 and 100.8 μS/cm. The experiments have been carried out at different deposition distances. The voltages at which the cone-jet mode is initiated and terminates have been measured. The current carried by the liquid droplets at these regimes has been measured as also the size of droplets generated. This has been studied by earlier researchers F.de la Mora, and several others. A comparative study has been made of the effect of electrical conductivity on these parameters. It is observed that the electrical conductivity of the liquid has a significant effect on the droplet size generated. The droplet size is found to decrease significantly with increased conductivity while the voltage and current show a marginal increase.

EXPERIMENTAL SYSTEM AND METHODS

A syringe infusion pump (Make- Cole Parmer) is used to provide flow rate of Ethylene Glycol (EG) from 0.1 ml/hr to 5.5 ml/hr. The liquid is pumped through a capillary of outer diameter 24 AWG, (inner diameter - 0.311 mm). A high potential difference is generated between the tip of the capillary and a grounded metallic electrode placed at a distance called the deposition distance. This High Voltage DC supply is maintained by a Spellman 60 W power supply. The current carried by the liquid droplets is measured through a Keithley 6485 picoammeter. The other fluid properties like electrical conductivity, viscosity and surface tension are measured using a Eutech conductivity meter, Brookfield Viscometer and Kruss Tensiometer respectively. The conductivity of pure ethylene glycol is measured to be 1.086μS/cm. It is increases in two steps of one order of magnitude (by a factor of 10) by adding HCl. The droplets generated are made to pass through a slit in the grounded metallic electrode and are collected over a non polar immiscible mineral oil. The droplets are photographed using a CCD camera attached to a stereo microscope and are sized using a software program.

EXPERIMENTAL RESULTS AND DISCUSSIONS

Electrohydrodynamic systems can be classified as electroquasistatic systems where the observation time is much greater than electromagnetic wave transit time. The cone-jet mode appears beyond a critical value of the applied voltage V_A and continues till V_B beyond which it shifts to multi cone-jet mode in lower flow rate region and enters the region of kink instability for higher flow rates. As shown in Fig. 1, the initiation of cone-jet mode is referred to as point A and its termination as point B. The readings shown are for a deposition distance of 25 mm. The cone-jet mode appears above a critical value of the applied voltage and continues till beyond which it shifts to multi cone-jet mode for lower flow rates and kink instability mode for higher flow rates. This transition from the cone-jet mode to other modes is characterized by a surge in the current shown by the picoammeter. It is observed that the voltage values are practically insensitive to change in flow rate as far as initiation and termination of the cone-jet mode is concerned. The current variation with flow rate is plotted in Fig. 2. There is a gradual increase in the current carried by the droplets with increasing flow rate though the increase is more marked for the termination zone of the cone-jet. The variation of droplet size with flow rate is shown in Fig. 3. It is observed that there is a slight decrease in the droplet size as the applied voltage is increased from to . For a low flow rate of 0.1 ml/hr, the droplet size is about 6 microns and as the flow rate increases the droplet size increases to about 25 microns for a higher flow rate of 5.5 ml/hr. The effect of increased electrical conductivity on the voltage for the initiation of the cone-jet mode is shown in Fig. 4. It is observed that a higher conductivity leads to a higher voltage for the initiation of the cone-jet. However, the voltage appears to be a weak function of flow rate. The profile of current with flow rate is depicted in Fig. 5. Here too, the current increases with increased conductivity of the liquid though the current appears to be a stronger function of flow rate. The most marked effect of enhanced conductivity is on the droplet size and this phenomenon is seen in Fig. 6. The data for 100.8μS/cm conductivity are missing below a flow rate of 2.5 ml/hr because the droplet sizes produced were very small and difficult to be measured by the microscope. It is observed that increased conductivity enhances the tendency to produce finer droplets. This result proves that if one were to control the size of droplets produced by electrospray, then modification of the electrical conductivity of the fluid provides an easy way to accomplish this.

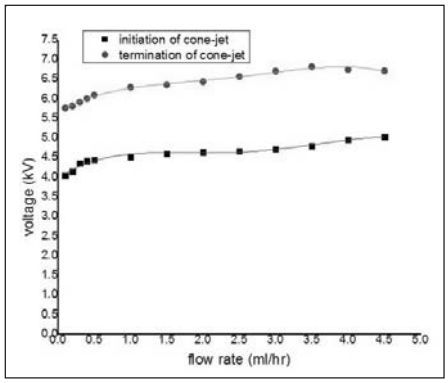

Figure 1. Voltage profile with flow rate variation.

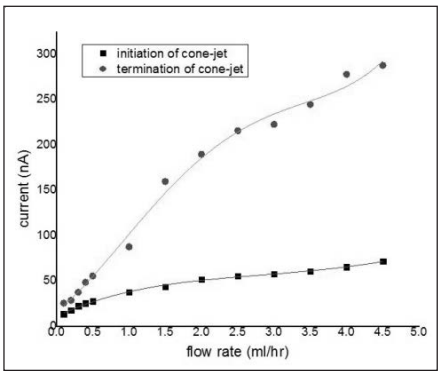

Figure 2. Current profile with flow rate variation.

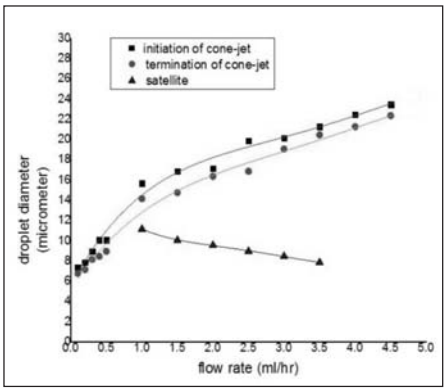

Figure 3. Droplet dispersity with flow rate variation

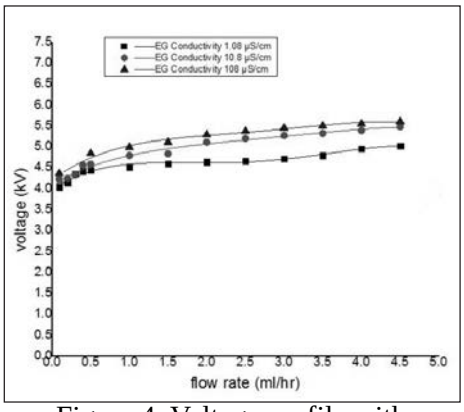

Figure 4. Voltage profile with conductivity variation.

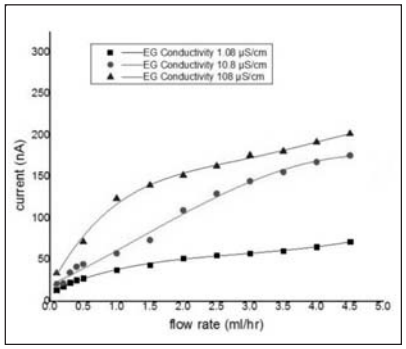

Figure 5. Current profile with conductivity variation.

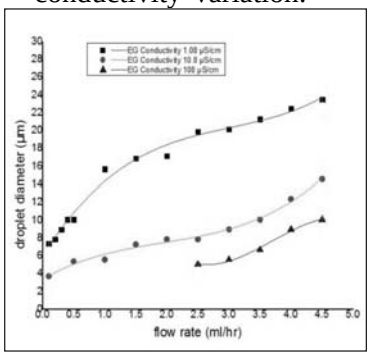

Figure 6. Droplet dispersity with conductivity variation.

CONCLUSIONS

The onset and the region of stability of the cone-jet mode is a strong function of the electric field existing between the electrodes. It is observed that the flow rate plays a crucial role in determining the droplet diameter generated. Increase in electrical conductivity if found to drastically reduce the size of droplets generated.

ACKNOWLEDGEMENTS

This research work has been funded by a grant SR/S3/MERC-0126/2009 provided by the Department of Science & Technology, Govt. of India.

REFERENCES

Tang, K. and Gomez,A. (1996). Monodisperse electrosprays of low conductivity liquids in cone-jet mode, *J. Colloid and interface science*, **184**, pp. 500-511.

Castellanos, A. (1991). Coulomb- driven convection in Electrohydrodynamics, *IEEE Transactions on Electrical Insulation*, **26(6)**, pp.1201-15.

Cloupeau, M.and Prunet- Foch, B. (1989). Electrostatic spraying of liquids in cone jet mode, *J. Electrostatics*, ***22***, pp.135-159.

Smith, D.P.H. (1986). The Electrohydrodynamic Atomization of Liquids. *IEEE Transactions on Industry Applications*, **1A-22(3)**, pp. 527-35.

STUDY OF COAGULATION OF DISPERSING AEROSOL SYSTEMS

S. ANAND[1], MANISH JOSHI[2] AND Y. S. MAYYA[2]

[1]Health Physics Division, [2]Radiological Physics & Advisory Division,
Bhabha Atomic Research Centre, Mumbai - 400 085.

Keywords: COAGULATION, DISPERSION, SURVIVAL FRACTION

INTRODUCTION

The key to predicting the effects of aerosols on air quality and climate change, and health effects lies in improving our understanding of key processes, in long-term monitoring, and in improved predictive capabilities through models. Aerosol effects are complicated because of variation in sources, particle sizes, chemical compositions, and dynamic evolutionary characteristics. In view of these, considerable interest has grown in understanding the evolution of particle size, number and composition of aerosol particles from various natural and anthropogenic sources in recent years. Usually aerosol emissions from multiple sources occur in a highly inhomogeneous manner being distributed randomly in time and space. Freshly emitted aerosols near the emission source undergo evolution due to various aerosol microphysical processes and their number concentrations are reduced to background levels rapidly in the atmosphere due to large atmospheric dilution. The near source characteristics, be it number or mass emission factors, provide only indices of potential for effects, and the actual effects are more closely related to the characteristics of emitted particles which ultimately persist in the atmosphere and their subsequent interaction with background aerosols. Thus, along with near source characterization, it is equally important to estimate its far field consequence, namely, contribution to particle number loading factors to aerosol background. Since direct measurements of far field contributions from a given source are hugely difficult due to enormous atmospheric dilutions, it should essentially rely on model estimates. Furthermore, the problem of understanding the evolution lies in the fact that one cannot easily perform experiments with real-world conditions in order to understand how it behaves if certain parameters of the system are changed. Hence, approximate analytical solutions and numerical computer simulations are needed to quantify the effective contribution of emission sources to background aerosols. These solutions (simple formulae) are proposed as modifiers of the emission factors, and hence they are called as 'source term modifiers'. They provide an important analysis tool in the study of coagulation of dispersing aerosols in the atmosphere at early time scale or near the emission sources.

The present work aims at developing analytical and numerical models, and their solutions to estimate the fraction of particles that persist in the atmosphere to form background aerosols. Coagulation is an important growth process for the aerosol particles in a high-concentration system. It occurs when two particles collide and stick together, reducing the number concentration but conserving the mass concentration of particles in the atmosphere. Simulating coagulation in a model is important, since if coagulation is neglected, erroneously large aerosol number concentrations will be predicted. Even if the total aerosol mass concentration in a model is correct, the mass concentration will be spread among too many particles. The condensation/evaporation processes, being number conserving, are

beyond the scope of this study. Hence, in the present study, the combined action of coagulation and dispersion is investigated through suitable microphysical models.

The combined action of coagulation and dispersion reduces the total particle number concentration significantly in a high concentrated release of aerosol particles near the source. The fraction of particles surviving the coagulation in the puff or plume is termed as 'survival fraction'. The survival fraction for various release scenarios is obtained in this study by solving the coagulation-dispersion equation using analytical and numerical techniques. The following specific objectives are attempted in this study:

1. Obtaining simpler expressions or approximations for the survival fraction for puff and plume releases, and
2. Estimation of important metrics like total number concentration, average particle size, etc., in the case of continuous volumetric releases.

METHODS

Although a large number of studies are available on aerosol coagulation as well as dispersion/ diffusion taken separately, the joint problem has received far less attention. Furthermore, most of the work on the Smoluchowski coagulation equation has been concerned with the time dependent spatially homogeneous situation. The present study, however, introduces the spatial heterogeneity in the system to account for the dispersion/diffusion process. This renders the problem difficult for obtaining the solutions both numerically and analytically. The primary processes considered in the present study are (i) coagulation, and (ii) atmospheric dispersion. The present study explicitly postulates diffusion as the mechanistic basis of dispersion and allows for spatial gradients.

The study problem is formulated by considering simultaneous action of these two processes by constructing coagulation-dispersion equation which is a second order non-linear integro-differential equation. To overcome the difficulty of handling dispersion along with coagulation, due to the non-linearity introduced by the latter process in the model, certain approximations are made either at the level of formulating the equation itself or at the level of developing solutions. However, the numerical solutions (Prakash *et al.*, 2003) to these models are obtained without any approximations, and hence they are considered as the exact solutions for these models.

Using these models, analytical approximate formulae for the survival fraction are obtained for the puff and plume releases. In some cases where the analytical approximations are difficult, the numerical solutions are fitted to obtain the survival fraction formula. In the case of continuous volumetric release, asymptotic analytical solutions for the total number concentration and average particle size are obtained using the two-species coagulation model. The temporal evolution of the particle number concentration and its size distribution are obtained from the numerical solutions.

RESULTS AND DISCUSSION

For puff releases, the analytical solutions have been obtained for constant and free-molecular coagulation kernels by combining prescribed diffusion approximation with Laplace transforms and scaling theory, respectively. These yield a simple formula for survival fraction ($F(t)$) which combines the variables of the problem in to a single parameter A as shown below:

$$F(t) = \frac{1}{[1+A\,\mu(t)]^{(1/(1-\alpha))}} \qquad (1)$$

where, $\mu(t) = 1 - \frac{1}{\sqrt{1+4Dt/b_0^2}}$, and $A = \frac{R\phi_0^{\alpha} N_0^{1-\alpha}(1-\alpha)}{2(2\pi)^{3/2} D b_0}$. For constant coagulation kernel, *?* = 0, and *R* = *K*/2; for free-molecular kernel, *?* = 1/6, and $R = 6\sqrt{kT/\rho}$. *D* is the particle diffusion coefficient, b_0 is the initial puff width, N_0 is the initial total number concentration, and *K* is the constant coagulation coefficient. It may be noted that the quantity *A* captures all the basic parameters of the problem in a single expression.

This analytical approximation is further improved by taking a closer look at the formulation and the solution procedure. The new solution approach consists of constructing moment equations from the Fourier transformed equation for the evolution of number concentration and variance of the spatial extension of puff in terms of either time or downstream distance. The original diffusion-coagulation equation is then reduced to a simpler coupled set of ordinary differential equations. These equations capture the essential elements of the coagulation-dispersion problem and carry information on the important variables such as the particle number concentrations and puff dimensions. Although still nonlinear, these equations are solved relatively more easily since redundant space and size variables have already been eliminated. Analytical solutions are obtained for special cases; when this is not feasible, numerical solutions are generated in terms of the relevant combination of dimensionless parameters.

The puff model, applicable to instantaneous releases is solved within a 3-D, spherically symmetric framework. An asymptotic analytical formula is obtained for the number survival fraction for a puff of initial width (b_0) consisting of (N_0) particles as,

$$F(\infty) = \frac{1}{[1+(5A/4)]^{4/5}} \tag{2}$$

where, *A* is the parameter defined above. The present solution (4/5th law) is seen to agree closely with the exact numerical solution of the diffusion-coagulation equation even for large values of *A*. The asymptotic survival fraction in the case of plume release (fitted formula for the plume model) is then given by,

$$F(\infty) = \frac{1}{[1+1.32B]^{0.76}} \tag{3}$$

where, $B = \frac{KS_0}{6\sqrt{3}U\sigma_0^{4/3}(C\varepsilon)^{1/3}}$, and *C* is a constant.

In the case of continuous volumetric release, asymptotic analytical solutions for the total number concentration and average particle size are obtained using the two-species model. The simplified model considers coagulation of two species in the system, the first species (A) is the primary nanoparticles emitted continuously by a source and the second one (B) is all the particles other than the first species. In this model, time dependent coagulation coefficient for the heterogeneous coagulation between the two size groups is introduced. The set of equations in this model with the given initial conditions are solved easily using the differential equation solver of the Mathematica (2008). Further, the simplified equation is amenable to asymptotic analysis to obtain large time results. The main advantage of this two-species model is the computation time.

Exact numerical solutions for this case are obtained through suitable modification to the numerical code used for the previous studies, and the simulations are based on the general dynamic equation for the aerosol coagulation process along with a continuous source term. A source term is added to the coagulation equation to account for the continuous particle injection. The numerical model is then suitably modified to take into account the appropriate definitions of the mobility and the area equivalent radii required for the Fuchs kernel for fractal agglomerates. Other aerosol processes like removal by ventilation and deposition are also added in this model. The simulations are carried out with various options like, i) coagulation kernel, ii) source injection rates, iii) fractal nature of the particles, and iv) ventilation removal rates. From these studies, it is found that the rate of coagulation process along with the source injection rate plays important role in determining the aerosol particle characteristics, and the following interesting observations are made. The total particle number concentration reaches a peak value in a short time and then it gradually decreases, even though the source is continuously emitting the particles. The size spectrum at the source is lognormal with single mode, but it evolves to bimodal distribution from a single mode in the injected volume. Numerous possible release conditions are simulated by varying few input parameters like source injection rates, count median diameter, fractal dimension etc.

Further, a comprehensive numerical study of the coagulation process in a well-mixed aerosol chamber with a constant source term of nanoparticles has been carried out to analyze and place into perspective the experimental observations made by Seipenbusch *et al.* (2008) related to the accidental release of nanoparticles into workplace air. When allowing for a fractal nature of particles, the numerical simulation reproduces the salient features of the experimental observations of Seipenbusch *et al.* (2008) such as the peaking effect in the time variation of the total number concentration and formation of a bimodal distribution. The model results are further discussed from the point of view of the aerosol metrics required for toxicological assessment.

Furthermore, an experimental system is designed and assembled for carrying out studies in the case of continuous volumetric releases (Fig. 1). Fig. 2 shows that the theoretical predictions compares well with the experimental results during the initial period (upto 1500 seconds). After this duration, the experimental results show faster decay of total number concentration as compared to simulated results. This may be due to the increase in the coagulation rate. The coagulation rate increases because of the particle growth by vapour condensation (vapour being continuously emitted by the source) in addition to the coagulation. Also, the observed multiple peaks suggest that the nulceation bursts are taking place whenever the vapour concentration reaches above the saturation value in this system. These processes (nucleation and condensation) are not accounted in the present numerical model, and hence the deviation of the predicted values from the experiments in the later part.

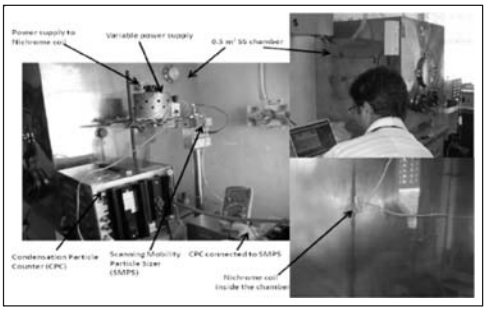

Figure 1. Experimental setup to study the aerosol evolution in a well-stirred chamber

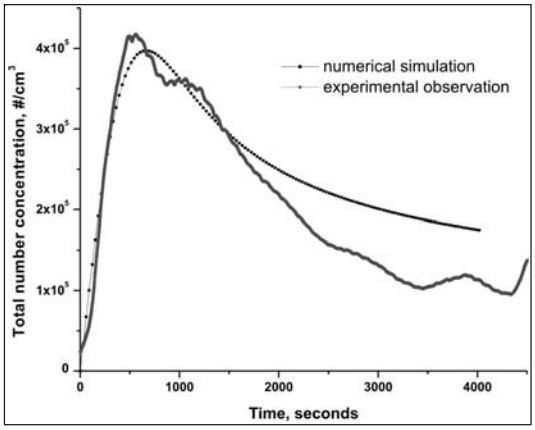

Figure 2. Evolution of total number concentration in the 0.5 m^3 chamber – comparison of experimental results with numerical simulation

CONCLUSIONS

A key question for assessing the impact of anthropogenic aerosols on the environment pertains to the estimation of the fraction of particles that persist in the atmosphere to form background aerosols. Among the various factors that contribute to this, coagulation is an important and numerically the most difficult issue to handle. The study addresses this question by combining coagulation with dispersion and different emissions scenarios to understand the long time and far field behaviour of aerosol size spectra and number concentrations. To this end, numerical and analytical models have been developed for modeling aerosol evolution in the atmosphere, emitted from localized sources under the combined action of coagulation and dispersion. In particular, the study introduces the concept of survival fractions as a means of predicting the atmospheric number loading factors of particles released from localized sources.

For puff emissions, an approximate analytical formula, termed as $4/5^{th}$ law, is obtained for the survival fraction which is in close agreement with accurate numerical solutions. This formula combines the coagulation and diffusion variables into a single parameter and provides a simple estimator of modifier for the source emission factor.

The study addresses the question of plume emissions from localized sources in the presence of atmospheric turbulence. It provides simple scaling relations for the survival fractions and the number loading factors. When the source is intense, it is shown that the atmospheric ultimate number loading factor ($S(\infty)$) is relatively insensitive to the original number emission rate ($\sim S_0^{1/4}$), and the turbulent energy dissipation rate.

The detailed numerical study for the volumetric releases brings forth several important features of coagulation of particles injected continuously into an air space. Fractal dimension, initial particle size, injection rate, and ventilation are identified as key variables that influence the evolution of particle characteristics. An asymptotic law ($t \to \infty$) for the decay of number concentration is derived using a simple analytical model. The numerical approach of integration of the coagulation equation using realistic kernels is computationally quite intensive and requires considerable investment of time to obtain long time results under different parametric scenarios. To obtain asymptotic results, the numerical code has to be run for few hours (>2 hours) in a single core desktop computer

whereas it takes less than a minute to obtain the same results using the simplified two-species model.

Simulations combined with analytical results using simplified model indicate an asymptotic decay of number concentration in the form $N^*\left(t^*\right) \sim t^{*-0.4}$ which is in marked contrast with the well known t^{-1} behavior for systems with a one-time aerosol injection. The above results have implications for an assessment of toxicological risk as well as in planning of safety measures in the context of industrial processing and applications of nanoparticles.

REFERENCES

Prakash, A., Bapat, A.P., & Zachariah, M.R. (2003). A Simple Numerical Algorithm and Software for Solution of Nucleation, Surface Growth, and Coagulation Problems, *Aerosol Science and Technology*, **37**, 892–898.

Seipenbusch, M., Binder, A., Kasper , G. (2008). Temporal distribution of nanoparticle aerosols in workplace exposure, *Annals of Occupation Hygiene*, **52-8**, 707-716.

Wolfram Research, Inc., Mathematica, Version 5.2, Champaign, IL (2005).

ESTIMATION OF AEROSOL PROPERTIES IN FIREBALL PHASE OF THE CLOUD FORMED IN CHEMICAL EXPLOSIONS

B.SREEKANTH[a], S.ANAND[b], Y.S.MAYYA[c]

[a] Radiation Safety Systems Division,
[b] Health Physics Division,
[c] Radiological Physics & Advisory Division,
Bhabha Atomic Research Centre, Trombay, Mumbai 400085, India.

Keywords: AEROSOL AND CHARGE

INTRODUCTION

Most of the existing aerosol transport models predict the aerosol concentration at various receptor locations of interest by using the aerosol characteristics at the release point and atmospheric conditions. Thus the aerosol characteristics at the release point play a significant role in the later simultaneous processes like diffusion, gravitational settling etc which affects the transport of aerosol. Sufficient literature is available for many kinds of aerosol releases, either continuous or instantaneous fashion (ex: vehicular emission), but very little information is available in the open literature for high energetic explosive releases like chemical explosion. The immediate measurement and analysis of the aerosols at the release point i.e. fireball phase in the explosion may be practically impossible due high temperature and pressure of the fireball which creates structural damage and makes the place inaccessible up to few minutes. A theoretical model has been developed to simulate the TNT explosion and to estimates the aerosol characteristics of the fireball formed in the explosion. Using the model instantaneous state parameters of the fireball, total particle number concentration, particle size distribution and average particle size has been estimated for different quantities of the explosives of TNT. This data will be useful for the aerosol transport models for obtaining the more conservative results.

When the detonation of charge (explosive) initiates the exothermic reaction it results in generation of reaction products (gases) which are also called as detonation products. This state at which phase transition takes place i.e. solid to gases is called C-J state; it depends on the type of explosive material and density of the charge. At the instant of generation detonation products are at very high temperature and pressure form a fireball. For example initial temperature and pressure of the detonation products of TNT with 1.5 gm/cm^3 density are at 3400^{o}K and 1.56X10^5 atm respectively (Miller and Jones, 1948). This fireball expands very rapidly to reach the atmospheric conditions; during the expansion the detonation products undergo chemical as well as physical changes simultaneously. The chemical changes are the composition change due to highly reactive nature of the detonation products. The physical changes are nucleation of the condensed vapour i.e. formation of aerosol, particle growth due to inter particle collisions in aerosol i.e. coagulation and dilution of aerosol due to its volume expansion.

This paper describes the development of a theoretical model to simulate the fire ball phase of the air blast of TNT explosive of 1.5 gm/cm^3 density. This model has been formulated by considering all the significant physical and chemical changes of the aerosol formed by the detonation products. A

numerical scheme has been developed by using finite difference method to quantify the aerosol characteristics.

METHODS

Initial conditions for fireball expansion

During the fire ball expansion its temperature reduces rapidly, Miller and Jones (1948) estimated the composition of the fireball of TNT at various temperatures and found that chemical changes occur till temperature reaches 1600°K and corresponding pressure is $4.26X10^3$ atm; afterwards the composition of the fireball is fixed. Since the volume change in the fireball to reach 1600°K is negligible our model uses this temperature as starting value and treats the expansion as adiabatic in nature. It has been observed that out of all the detonation products only elemental Carbon is in particle form and it is estimated that one mole of TNT explosion produces three moles of carbon. It is assumed that at the starting stage all the available elemental carbon is in the form of particles of 1 nm diameter with 1 gm/cc density.

Estimation of the State parameters of aerosol

Since the particle interactions in the aerosol system depends on it's concentration and temperature, which are rapidly changing in the current system, a new scheme has been developed to obtain the time dependent state variable of the system. A spherical uniformly mixed gaseous cloud of radius *R*, mass *M*, temperature *T*, and pressure *p* which expands adiabatically has been considered. The pressure-volume relationship is obtained from the JWL (Jones-Wilkins-Lee) equation while the pressure-volume-temperature relationship is given by Jones and Miller (1948). The **Taylors's** theory (Taylor, 1963) is then applied to obtain the time dependent nature of the equation of state variables under thermal and chemical equilibrium. The following expressions are obtained for the temporal evolution of the equation of state variables:

$$V(t) = \frac{4}{3}\pi R^3(t) \tag{1}$$

where, $R(t)$ is the radius of the expanding fireball with respect to time obtained by numerically solving the Taylor's model. The pressure in the expanding fireball is given by,

$$p(t) = Ae^{-R_1\left(\frac{V(t)}{V_0}\right)} + Be^{-R_2\left(\frac{V(t)}{V_0}\right)} + C\left(\frac{V(t)}{V_0}\right)^{-(\omega+1)} \tag{2}$$

where, A = 371.2 GPa; B = 3.231 GPa; C = 1.045 GPa; R_1 = 4.15; R_2= 0.95; ω = 0.30 are all constants and their values are given for TNT of density 1.5 g/cm^3, and the temporal evolution of the temperature in the expanding puff is given by,

$$T(t) = \frac{1}{R}\left[p(t)\frac{V(t)}{N'} - b_1 p(t) - c_1 p(t)^2 - d_1 p(t)^3\right] \tag{3}$$

where, *N'* is the number of moles at temperature *T* and pressure *p* of the gaseous products of the detonation of 1 mole of explosive. The values of the coefficients for 1.5 g/cm^3 loading density of TNT are b_1 = 25.4, c_1 = -0.104, d_1= 2.33x10^{-4}.

General Dynamic Equation (GDE) of Aerosol interactions

The change in the number density of the particles as a result of the continuing expansion of the cloud is given by, $$\frac{\partial n(u,t)}{\partial t} = \frac{1}{2}\int_0^u K(u',u-u',t)\, n(u',t)\, n(u-u',t)\, du' - n(u,t)\int_0^\infty K(u,u',t)\, n(u',t)\, du' - n(u,t)\frac{d\log V(t)}{dt} \qquad (4)$$

where, $n(u, t)$ be the number of particles with volumes lying between u and $u\,du$ per unit volume of the fluid at time t , $K(u, u',t)$ is the coagulation kernel between the particles of volume u and u' which changes with time mainly due to the change in the atmospheric temperature. The above has been solved numerically by using the nodal method (Prakash *et al.*, 2003) using the inputs obtained in the above section for the volume and temperature transients.

RESULTS AND DISCUSSIONS

TNT explosions of various masses have been simulated to estimate the total particle number concentration, particle size distribution and average particle size. The results for one particular case has been shown in fig 1 which is showing particle size distribution of 2 kg TNT explosive charge.

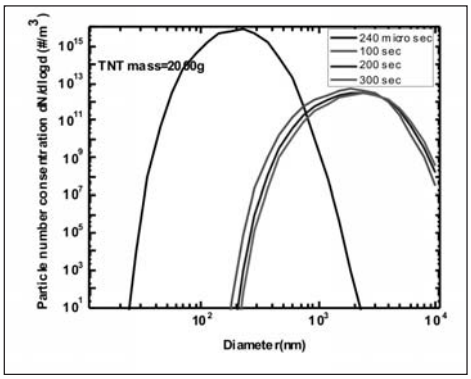

Figure 1. Particle size distribution in the fireball of 2 kg TNT explosion

The estimated time for fireball to reach the atmospheric conditions is 240 ?sec and corresponding volume of the cloud is 1.4 m^3, the particle size distribution at this point shows a mode corresponding to 200 nm of particle diameter. Later we studied the importance of particle growth due to coagulation by fixing the volume of the cloud at this point. The results shows that as the time progress the mode is shifting towards the higher particle size and particle number concentration reduces which is clearly indicating that coagulation playing a significant role in particle size growth.

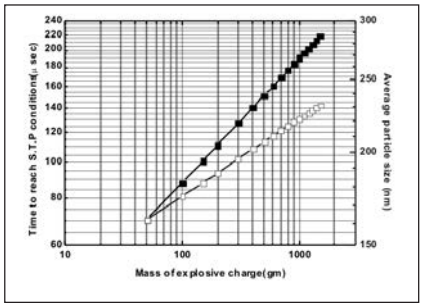

Figure 2. Final average particle size for various explosive masses

We have estimated the average particle size for various masses of TNT explosions and observed that after certain mass even though we increase the mass of explosive the increase in average particle size is very minimum. We have generated fitted expressions for the time to reach the atmospheric conditions and average particle size for a given mass of explosive. They are,

$$D_{avg}\ (\text{nm}) = 107.932\ W^{0.10429} \qquad (5)$$

$$t\ (\text{sec}) = 1.8978 \times 10^{-5}\ W^{0.33394} \qquad (6)$$

CONCLUSION

A numerical model is developed for simulating the early phase evolution of aerosol characteristics due to conventional explosions. The basic aerosol properties like number concentration, particle spectrum, and average particle size has been estimated which serve as an important inputs to the atmospheric aerosol transport models. Parametric study of the model shows that the final average particle size varies as $W^{0.10429}$, indicates the particle size is less sensitive to the explosive mass.

ACKNOWLEDGEMENTS

I wish to express my sincere thanks Dr. D N Sharma, Associate Group Director, Health Safety and Environment Group, Head, Radiation Safety Systems Division, and Dr. K S Pradeepkumar, Head, Emergency Response Systems and Methods Section to provide me the opportunity to carry out this work and for their keen interest in this work. I am heartily thankful to Shri. Probal chaudhury, Radiation Safety Systems Division, for his constant encouragement and support.

REFERENCES

Anand, S. and Mayya, Y. S. (2009). Coagulation in a diffusing Gaussian aerosol puff: Comparison of analytical approximations with numerical solutions, *J. Aerosol Science,* pp. 348-361.

Jones, H. and Miller, A. R. (1948). The Detonation of solid Explosives: The Equilibrium Conditions in the Detonation Wave-Front and the Adiabatic Expansion of the Products of Detonation, *R. Soc. Lond. A,* **194**, pp. 480-507.

Nathans, M. W., Thews, R., Holland, W. D. and Benson, P. A. (1970). Particle Size Distribution in Clouds from Nuclear Airbursts, *J. Geophysical research,* **75**.

Prakash, A., Bapat, A. P., & Zachariah, M. R. (2003). A simple numerical algorithm and software for solution of nucleation, surface growth, and coagulation problems, *Aerosol Science and Technology*, **37**, pp. 892-898.

Taylor, G. J. (1963). Analysis of the Explosion of a Long Cylindrical Bomb Detonated at One End, The Scientific papers of Sir G. J. Taylor, Vol. III, pp. 277, Cambridge University Press, London.

UNDERSTANDING AEROSOL MIXING AND AGING USING PARTICULATE MASS AND CHEMICAL DATA COLLECTED OVER THE LAST FIVE YEARS AT AN URBAN LOCATION

NIKHIL RASTOGI[1], TARUN GUPTA[1,2]

[1]Environmental Engineering and Management Program, Indian Institute of Technology, Kanpur, Uttar Pradesh, India
[2]Department of Civil Engineering, Indian Institute of Technology Kanpur, Uttar Pradesh, India

Keywords: SEASONAL VARIATION, PM2.5, DUST MIXING, MINERAL DUST

INTRODUCTION

Atmospheric particles, emitted from natural or anthropogenic sources, play a very important role in modifying both local and global climate scene attributed primarily to their ability to absorb or scatter light. They are also known for deleterious effects on human health either due to their small size or specific chemical composition or a combination of both.

In a typical urban environment various anthropogenic sources can be broadly identified as Industrial, Commercial, Transport, Domestic, Institutional and Fugitive. Besides these, mineral dust is also an important source. Often it is very difficult to appropriately apportion the resultant ambient aerosol due to the complex interaction of emissions from these listed sources. This makes prioritizing and control of key emission sources more difficult hence these complex interactions need to be understood well.

Mixing of mineral dust with anthropogenic pollutants allows pollutants to be transported to far off places along with them and significantly modifies the elemental signature of mineral dust and makes source apportionment more challenging. During transportation of dust various secondary chemical transformations take place. Mineral dust aging primarily refers to the leaching and slow replacement of water soluble carbonates and bicarbonates by nitrate and sulphate during their sufficiently long residence times in the air parcels transporting them to far off places. Preliminary results from our ongoing study will be presented in the form of a poster presentation. Meteorological data as well as Air Back trajectory data have also been employed to aid our understanding of these complex aerosol mixing as well as aging phenomena.

METHODS

Ambient aerosol measurement and collection followed by gravimetric and chemical speciation in and around Kanpur (a prominent site in the Indo-Gangetic Plains) has been going on for quite some time. Filter based samples of submicron ($PM_{2.5}$) particles have been collected over the last five years inside IIT Kanpur campus (26°50´ N, Longitude: 80°20´ E). They were primarily analysed for ions (NH_4^+, Cl^-, NO_3^- and SO_4^{2-}), trace elements (Ti, V, Cr, Mn, Co, Ni, Cu, Fe, Zn, Pb, Cd, Sr, Ca, Na, K, Mg etc.) and WSOC (water soluble organic carbon) and Elemental Carbon-Organic Carbon (only for a sub-set of data). All necessary precautions were taken for quality control. Seasonal and temporal variation of particulate matter over these last five years will be presented.

RESULTS AND DISCUSSION

Enrichment Factor:

In order to know the origin (anthropogenic or crustal) of trace metal abundances in atmospheric aerosols, average enrichment factors (EF) have been estimated in $PM_{2.5}$ at the monitoring site. EF is the ratio of concentration ratios of element in the aerosol samples normalized to crustal concentrations. It is the first step to know about pollutant sources. Fe is commonly used as crustal source indicator and EFx is calculated by using the equation:

$$EF_x = (C_{xs} / CFe_s) / (Cx_c / CFe_c)$$

Where Cxs and CFes are concentrations of the element x and Fe in samples and Cxc and CFec are that in the average crust (Taylor and McLennan, 1995). This calculation assumes that contribution of anthropogenic Fe is insignificant at this sampling region. If the EF approaches 1, crustal sources are predominant and generally a value > 5 indicates large fraction can be attributed to non-crustal or anthropogenic sources (Wu *et al.*, 2007).

By convention (Zhang *et al.*, 2002), if EFd”10 it is considered to show that element in aerosols has a significant crustal contribution, and hence termed as the non-enriched element. The EF > 10 indicates that element has an important proportion of non-crustal and sources and hence termed as the enriched element (Zhang *et al.*, 2002). In this study, we have used average seawater and earth crustal compositions as references in calculating EFc and EFs.

Ca is used as an indicator element for knowing the extent of crustal dust or natural dust while Cu indicates anthropogenic source of dust (Zhang *et al.*, 2002). So by comparing the Enrichment Factors for these elements over the years we can determine out of Natural and Anthropogenic sources which has been dominant over the years.

We have also studied seasonal variation of Ca and Cu for four seasons namely winters (Dec-Feb), summer (Mar-Jun), monsoon (Jul-Sep) and post monsoon (Oct-Nov). These are shown in Fig 1(a), Fig. 1(b), Fig. 1(c) and Fig. 1(d) respectively. Seasonal variation of enrichment factors for Ca and Cu has been summarized in Table 1.

During summers Ca was less enriched for most of the period (EF<10), so all of Ca was due to crustal origin while Cu had been moderately enriched with EF values in the range of 100-300, so they indicate moderate pollution by anthropogenic sources. High EF values indicate higher pollution. During winters also Ca remained due to Crustal sources only except for a few days (10-12-10, 31-12-10, 10-1-11, 17-1-11, 14-2-11) where it was moderately enriched indicating dominance of anthropogenic sources on those days. Majority of Ca on those days came from anthropogenic sources. The main source of Ca here is soil and road dust hence not much contribution to anthropogenic tracers (Behera and Sharma, 2010).

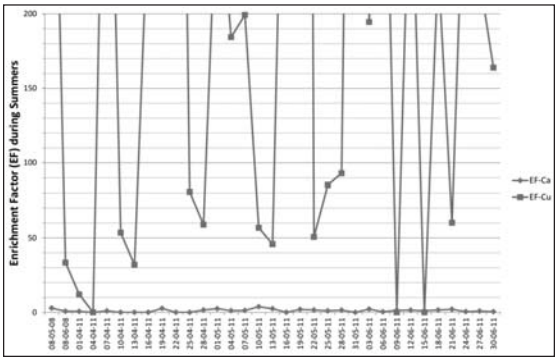

Figure 1(a). Seasonal variation of Enrichment Factors for Summer Season

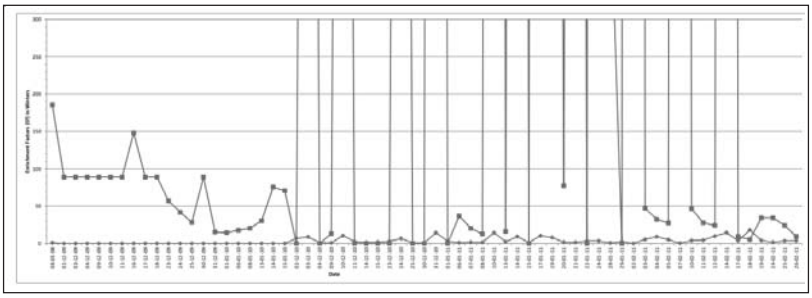

Figure 1(b). Seasonal variation of Enrichment Factors for Winter Season

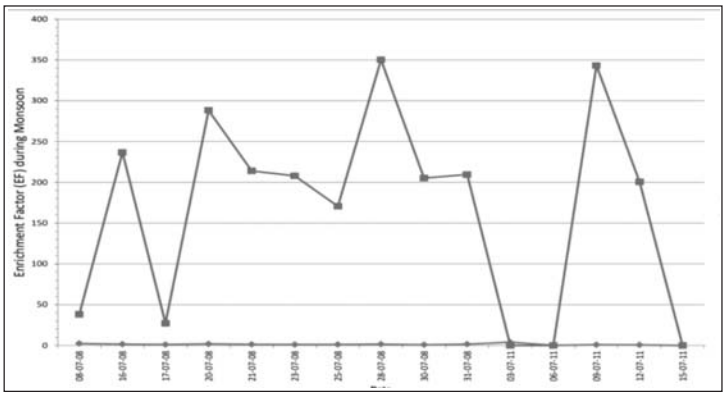

Figure 1(c). Seasonal variation of Enrichment Factors for Monsoon Season

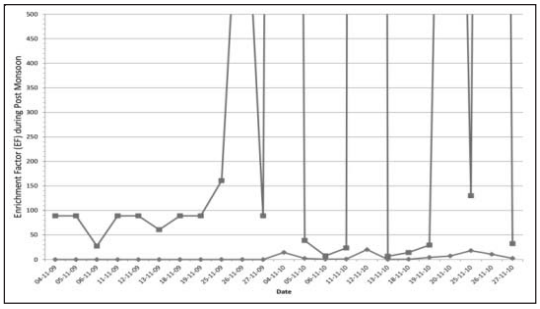

Figure 1(d). Seasonal variation of Enrichment Factors for Post Monsoon Season

The major source of Cu is Thermal Power Plants (Kim and Fergussen, 1994), and as we can see Cu is very high in all the seasons. This is due to Panki thermal power plant located near our sampling site (6 kms from IIT K). Cu has shown exceptionally higher enrichment during post monsoon and winter seasons. This could be attributed to relatively stable atmospheric conditions and lower atmospheric mixing height. Cu is higher in winters than summers as much of the pollutants are dispersed due to high temperature and mixing height is also more during summers. Cu can also originates from wear of engine parts thus vehicular emissions may also contribute to Cu concentrations in the ambient atmosphere. During monsoons we can see relatively clear and pollution free days. Both natural and anthropogenic pollutants are less in concentration. This is mainly due to washing down of dust particles along with precipitation.

Element	**Season**	**Avg. Enrichment Factor Value**	**Std. Dev.**	**Max Value**	**Min Value**
Calcium (Ca)	Summer	1.1602	0.9918	3.7814	0.0000
	Monsoon	1.2739	0.9371	3.8813	0.0000
	Post-Monsoon	3.5612	6.2227	20.2370	0.0000
	Winter	3.2803	4.3126	17.9932	0.0000
Copper (Cu)	Summer	268.4020	380.6113	2056.6319	0.0000
	Monsoon	166.1096	123.1648	350.3030	0.0000
	Post-Monsoon	1500.6317	3916.3533	17279.8434	6.5945
	Winter	1512.2187	3602.5644	17329.8605	0.0000

Table 1. Summary statistics for seasonal enrichment factor variation

Based on the seasonal variation characteristics and the EFs of each species, the elements and ions measured can be divided into crustal, pollutant, mixed, and secondary groups. The crustal group includes elements with enrichment factor less than 10. The pollutant group includes elements with high enrichment factors of the order of 100-1000. Elements which have EF below 100 are in mixed group as they show properties similar to crustal and pollutant group. Sulphate, nitrate and ammonium ions are called secondary species.

CONCLUSIONS

The element concentrations were studied and major pollutant sources identified in preliminary investigations to get a rough insight into extent of pollution. PM2.5 samples were collected in IIT Kanpur over a period of 5 years and analysed for various elements to study their variations and co-relations. The pollutants were high in winter and post monsoon seasons and moderate during summers. There were relatively clearer days during monsoons due to dust settlement by rains. Major source for Ca has been road dust and soil while thermal power plants have been main source of Cu as well as anthropogenic pollutants in and around Kanpur.

REFERENCES

Kumar, A. and Sarin, M. M. (2009). Mineral Aerosols from Western India: Temporal Variability of Coarse and Fine Atmospheric Dust and Elemental Characteristics, Atmos. *Environ*, **43**, pp. 4005–4013.

McLennan, S. (2001). Relationships between the Trace Element Composition of Sedimentary Rocks and Upper Continental Crust. *Geochem. Geophys. Geosyst*., **2**, 1021, doi: 10.1029/2000GC000109.

Behera, Sailesh N. & Sharma, Mukesh (2010). Reconstructing Primary and Secondary Components of PM2.5 Composition for an Urban Atmosphere, *Aerosol Science and Technology*, **44**:11, pp. 983-992.

Wu, Y.S., Fang, G.C., Lee, W.J., Lee, J.F., Chang, C.C. and Lee, C.Z. (2007). A Review of Atmospheric Fine Particulate Matter and its Associated Trace Metal Pollutants in Asian Countries during the Period 1995-2005, *J.Hazard. Mater*., **143,** pp**.** 511–515.

Zhang, X.Y., Arimoto, R., An, Z.S., Chen, T., Zhang, G.Y., Zhu, G.H. and Wang, X.F. (1993). Atmospheric Trace Elements over Source Regions for Chinese Dust: Concentrations, Sources and Atmospheric Deposition on the Loess Plateau, *Atmos. Environ.*, **27,** pp. 2051–2067.

Zhang, J., Wu, Y., Liu, C. L., Shen, Z. B., and Zhang, Y. (2002). Major Components of Aerosols in North China: Desert Region and the Yellow Sea in the Spring and Summer of 1995 and 1996, J. *Atmos. Sci.*, **59,** pp. 1515–1532.

PRELIMINARY EVIDENCE OF THE EFFECT OF VARYING AEROSOL CHEMISTRY ON ITS PHYSICAL BEHAVIOR OVER CENTRAL HIMALAYAS DURING GVAX

SHIVRAJ SAHAI[1*], M. NAJA[1], N. SINGH[1], D.V. PHANIKUMAR[1], U.C. DUMKA[1], ANNE JEFFERSON[2], VIMLESH PANT[3], P. PANT[1], RAM SAGAR[1], S. K. SATHEESH[4], K KRISHNA MOORTHY[5], V. R. KOTAMARTHI[6]

[1]Aryabhatta Research Institute of Observational Sciences, Nainital, India
[2]Earth System Research Laboratory, 0020 National Oceanic & Atmospheric Administration (USA),
[3]Indian Institute of Technology, New Delhi, India.
[4]Indian Institute of Science, Bangalore, India
[5]Space Physics Laboratory, Vikram Sarabhai Space Centre, Thiruvananthapuram, India
[6]Argonne National Laboratory, United States

Keywords: AEROSOL ABSORPTION, AEROSOL SCATTERING, ANGSTROM EXPONENT, SINGLE SCATTERING ALBEDO, CCN.

INTRODUCTION

Limited simultaneous observations of absorption and scattering properties of aerosols over central Himalayas are available for the autumn season. The observations of light absorption, light scattering, aerosol number density (N_{CN}), and cloud condensation nuclei (N_{CCN}) as part of the Regional Aerosol Warming Experiment-Ganges Valley Aerosol Experiment [RAWEx-GVAX; a collaborative experiment between US Dept. of Energy's Atmospheric Radiation Measurement (ARM), Aryabhatta Research Institute of Observational Sciences (ARIES), Indian Space Research Organization (ISRO) and Indian Institute of Science (IISc)] are being used to address the following questions about the aerosols over a Central Himalayan site: (1) How does absorption and scattering coefficients (σ_{ap} and σ_{sp}), N_{CN} and N_{CCN} concentration change? (2) What does the derived values such as hemispheric backscattered fraction (β), single scattering albedo (ω), absorption angstrom exponent ($å_{ap}$) and scattering angstrom exponent ($å_{sp}$) disclose in terms of size and chemical nature of the aerosols. These aerosol properties for the autumn and winter seasons along with the (background) summer monsoon (SM) season over the Manora Peak is used to derive the organic carbon (OC) and black carbon (BC) contents of the aerosols explaining its physical behavior over the site. The study has also been supplemented with satellite observations and back air trajectories to help identifications of emission sources for linkages with aerosol behavior over the study site.

METHODOLOGY

Observational site

In-situ observations are carried out at Manora Peak (29.37°N, 79.45°E, 1958 m amsl) in Nainital district of the Uttarakhand province of India, in the Shivalik range of central Himalayas. The observation site is surrounded by sharply peaking mountains in the north-east and low altitude mountains in the south-west. The site is well below the snowline and is surrounded by thick vegetation cover with almost no industry in Nainital. South of the site, some small scale industries are located in Haldwani (423 m amsl; ~20 km from the site) and Rudrapur (209 m amsl; ~40 km from the site). The plains on the south and south-west are densely populated and include several urban areas like

New Delhi, Kanpur, Lucknow within aerial distance of 200 km (Kumar *et al.*, 2011). On the south-west also lies the nearest magacity Delhi (~235 m amsl; ~225 km from the site). The wind patterns are generally northwesterly during winter and southwesterly during summer/monsoon (Kumar *et al.,* 2011). The prevailing wind patterns in this region are generally westerly and northwesterly during the periods of FBCR fires. Owing to its large elevation this site is mostly above the boundary layer particularly during winter season (Pant *et al.,* 2006). The three seasons of summer monsoon (June, July and August), autumn (September, October and November) and winter (December) show distinct variation in precipitation, temperature, relative humidity (RH in %), vapour pressure and wind patterns. The autumn season experience predominantly north westerly winds, which is important consideration for studying the atmospheric characteristics over the site during the study period.

Measurements and methods

The measurements were carried out using ARM's Aerosol Observing System (AOS), a suite of in-situ surface instruments for measurement of multiple aerosol properties starting from June 2011 through March 2012. A 3-wavelength Particle Soot Absorption Photometer (PSAP; 470, 528 and 660 nm; Model Radiance Research-3λ) was used to measure the particle absorption coefficient (σ_{ap}). A 3-wavelength nephelometer (450, 550, and 700 nm; TSI Model 3563) was used to measure total angular scattering (σ_{sp}) and hemispheric backscattering (β). A Condensation Nuclei Counter (TSI; Model 3010) was used measures the total number concentration (N_{cn}) of condensation particles of diameter in the size range of 10 nm to 3 ìm. A Single-column Cloud Condensation Nuclei Counter (CCNC; DMT Model 1), that measures cloud droplet concentration (size 1 ìm to 10 ìm) was used for CCN measurements. The primary optical measurements are those of the aerosol absorption and scattering coefficients as a function of particle size and radiation wavelength and cloud condensation nuclei (CCN) measurements. Additional measurements include those of the particle number concentration (N_{cn}). These measurements are used for calculating aerosol derived parameters viz Back scatter fraction (β), single scattering albedo (ω), absorption angstrom exponent ($å_{ap}$) and scattering angstrom exponent ($å_{sp}$) in the present work. Aerosol elemental carbon (EC), organic carbon (OC) and organic matter (OM) have been derived from the measured aerosol physical parameters as described elsewhere (Sahai *et al.,* 2012).

RESULTS

σ_{ap} and σ_{sp} recorded significant rise with σ_{sp} dominating during the autumn and winter seasons as contrast to the SM, which is also supported by the single scattering albedo (ω) over the site (Fig. 1). Lower β support lesser contribution of small aerosols, whereas, lower $å_{sp}$ supports higher contribution of larger (accumulation size) aerosols during the autumn (Fig. 1). The $å_{ap}$ changes show a shift in the aerosol contents from predominantly BC during SM to that of OC during the autumn and winter seasons (Fig. 1). The seasonal variation in the correlation (coefficients) between ω and $å_{ap}$ and between ω and $å_{sp}$, showed almost no dependence of ω on $å_{ap}$ and $å_{sp}$ during autumn, representing dominance of secondary aerosols over the site during the season. This autumn-time typicality also coincided with raised aerosol organic matter content, giving a possible cause for perturbed aerosol characteristics over the site during the autumn season. The satellite (MODIS, Collection 5) fire-count results show occurrence of major crop residue burning during the same period in the Punjab region of Indian-sub continent (Sahai *et al.*, 2012). Further, the back air trajectories (using NOAA Hysplit 5 Model) showed that the central Himalayan site received air masses predominantly from over the same Punjab region during the autumn season, suggesting a strong possibility of the crop

residue burning in Punjab during the autumn season to cause organic enrichment of the aerosols over the Central Himalayan site during the autumn season.

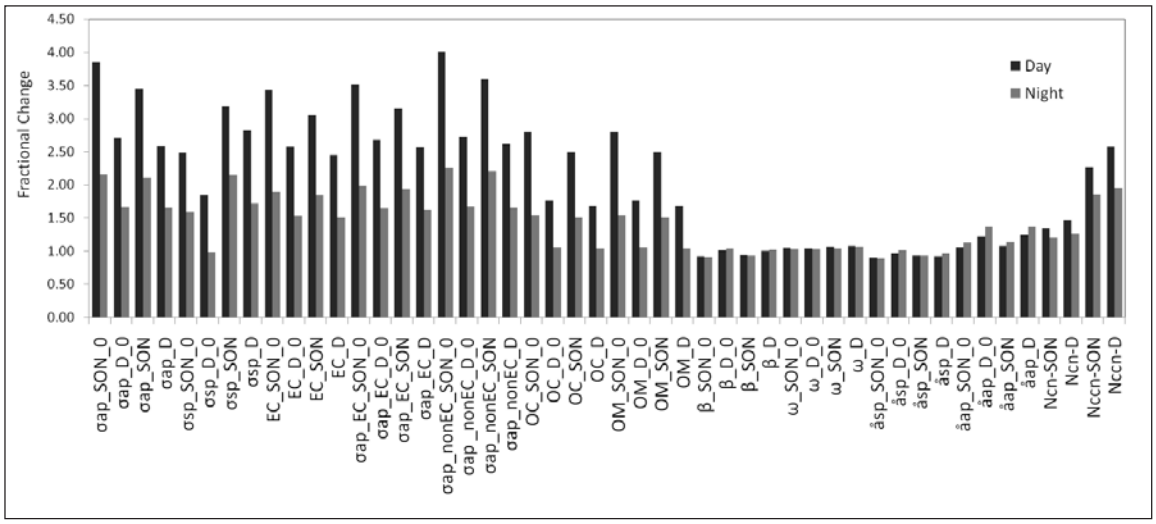

Figure 1. Seasonal fractional change observed in various aerosol properties during autumn (SON) and winter (D) as compared to the summer-monsoon (SM) season during the day-time and night-time.

ACKNOWLEDGEMENTS

This work has been carried out as part of the Regional Aerosol Warming Experiment-Ganges Valley Aerosol Experiment (RAWEX-GVAX) in joint collaborations among Atmospheric Radiation measurement [ARM; Department of Energy (US)], Indian Institute of Science (IISc, India), Indian Space Research Organization (ISRO, India) and ARIES (India). We thank all the personal who helped in logistics and making the observations successful.

REFERENCES

Kumar, R., Naja, M., Satheesh, S. K., Ojha, N., Joshi, H., Sarangi, T., Pant, P., Dumka, U. C., Hegde, P., and Venkatramani, S. (2011). Influences of springtime northern Indian biomass burning over the central Hymalayas, *J. Geophys. Res.*, **116**, D19302.

Pant, P *et al.*(2006). Aerosol characteristics at a high-altitude location in central Himalayas: Optical properties and radiative forcing, *J. Geophys. Res.*, **111**, D17206.

Sahai, S. et al. Evidence of perturbed aerosol physico-chemistry over Central Himalayas caused by post-harvest biomass burning in Punjab region during autumn season, Personal Communication (under review).

ESTIMATION OF ELECTRICAL CONDUCTIVITY FOR THE REGION 8 – 32 KM

KAMSALI NAGARAJA[1], S.D. PAWAR[2], P. MURUGAVEL[2]
V. GOPALAKRISHNAN[2]

[1]Department of Physics, Bangalore University, Bangalore 560 056
[2]Indian Institute of Tropical Meteorology, Pahsan, Pune – 411 008
Email: kamsalinagaraj@bub.ernet.in

Keywords: AEROSOLS, CONDUCTIVITY, STRATOSPHERE, MODEL STUDIES.

INTRODUCTION

Ion-aerosol interaction studies are important in atmospheric research for the better understanding of the electrical state of the atmosphere as related to aerosols over the region. The stratospheric ion conductivity is sensitive to the presence of aerosols and thus, aerosol loading on the stratosphere has a bearing on the corresponding electrical conductivity. The aerosols alter stratospheric conductivity by either converting highly mobile small ions into less mobile aerosol ions through ion-aerosol attachment β or neutralizing small ions through the aerosol ion-small ion recombination α_s. Another process which makes ion-aerosol attachment rate faster is the recombination between aerosol and aerosol with coefficient α_a. Variation of conductivity is primarily governed by the corresponding mobility of small ions and coefficients are dependent on size distribution of aerosols (Nagaraja *et al.*, 2006). Using these as input to the model, the electrical conductivity of the stratosphere is computed and presented.

EXPERIMENTAL METHODOLOGY

Ion-aerosol Model

The ion-aerosol model used in this study is shown in Fig.1, whereas the details of this model for surface level conductivity near to the earth's surface under enhanced aerosol conditions is described by Nagaraja *et al.* (2009) and variation of small ions by Nagaraja *et al.* (2011). The two types of β for the attachment of positive and negative ions with the neutral aerosols are considered to be equal. Similarly, the two types of α_s are also assumed to be equal in the present study, although these two types of α_s are known to be slightly different. It is found that the results of this study are not altered by this assumption.

The steady state small ion and aerosol ion densities are given by the basic equations as:

$$q - \alpha_i N_{\pm}^2 - \beta Z N_{\pm} - \alpha_s N_{\pm} A_{\pm} = 0 \qquad (1)$$

$$\beta Z N_{\pm} - \alpha_s N_{\pm} A_{\pm} - \alpha_a A_{\pm}^2 = 0 \qquad (2)$$

where q is cosmic ray ion production rate, α_i is ion-ion recombination coefficient, $N_{\pm}$ and $A_{\pm}$ are concentrations of positive or negative molecular and aerosol ions, respectively.

Steady state molecular ion density N_o in absence of aerosols is:

$$N_0 = \left[\frac{q}{\alpha_i}\right]^{\frac{1}{2}} \tag{3}$$

Fractional depletion (η) of small ions due aerosols are:

$$\eta = \frac{A_{\pm}}{N_0} = \frac{N_0 - N_{\pm}}{N_0} \tag{4}$$

Solving equations (1) and (2) simultaneously and using equations (3) and (4), one can write the expressions for βZ and α_s as:

$$\beta Z = N_0 \eta \left\{\frac{\alpha_i(2-\eta) + \alpha_a \eta}{2(1-\eta)}\right\} \tag{5}$$

$$\alpha_s = \left\{\frac{\alpha_i(2-\eta) - \alpha_a \eta}{2(1-\eta)}\right\} \tag{6}$$

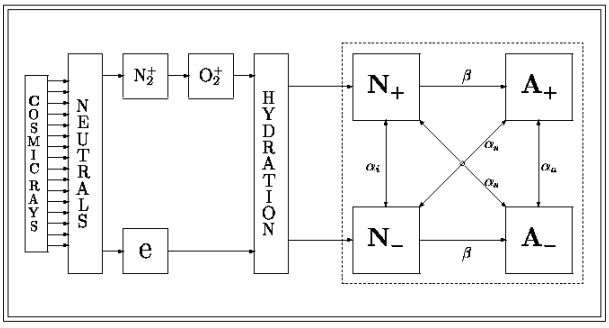

Figure 1. Simplified ion-aerosol model used in this study for the stratospheric region.

The conductivities σ_o and $\sigma_{\pm}$ of the stratosphere at any altitude in the absence and presence of aerosols, respectively, are given by:

$$\sigma_0 = N_0 e b_{\pm} \quad and \quad \sigma_{\pm} = (1-\eta)\sigma_0 \tag{7}$$

where e is elementary charge, $b_{\pm}$ is molecular ion mobility and is given by (Meyerott *et al.*, 1980):

$$b_{\pm} = \frac{b_0 P_0 T}{T_0 P} \tag{8}$$

where T and P are, respectively, the temperature and pressure at the altitude of interest. The parameters b_o, P_o and T_o refer to their respective values at sea level.

Methodology

Modelling of the stratospheric conductivity shown schematically in Fig. 1 requires a knowledge of recombination coefficients α_i, α_a and α_s. Parametric formulae for α_i have been used in the stratospheric model studies (Smith and Adams, 1982) and α_i is found to be height dependent, varying from about 4×10^{-6} to 5×10^{-8} cm^3s^{-1} in the height range of 10-60 km (Srinivas and Prasad, 1993, Srinivas *et al.*, 2001). For singly charged aerosols, the relative magnitudes of α_a and α_s are such that $\alpha_a \leq \alpha_s \leq \alpha_i$ (Hoppel, 1985). Several difficulties encountered in the modelling of stratospheric conductivity using background aerosols, where large values of α_a and α_s are used in the model and this problem was overcome by analytically determining α_a or α_s for an assumed background aerosols. However, the results of this study showing $\alpha_s \geq \alpha_i$ is to be interpreted in view of multiple charging of aerosols. Initially, with a suitable assumed value of α_a, value of η is computed from Eq. (5). Then the value of α_s is computed by using Eq. (6). It is noted that, in this step, α_s becomes negative if the assumed value of α_a is unrealistically large. In the present computations $\alpha_a = 10^{-7}$ cm^3s^{-1} is found to be suitable. From the values of η obtained from Eq. (5), the values of $N_\pm$ and hence $\sigma_\pm$ were computed, and computations were repeated for various assumed effective sizes r.

RESULTS AND DISCUSSIONS

The conductivity-profiles were computed for different r = 0.001, 0.004, 0.008, 0.02, 0.06, 0.1, 0.4 and 0.8 μm, however, the profiles for r = 0.001 – 0.02, 0.1, 0.4 and 0.8 μm only shown in figures for clarity. The input parameters such as ionization rate and aerosol concentration are plotted in Fig. 2. As one moves upward, ionization drops and aerosol concentration has structured profile and it obtained from Rosen *et al.* (1985). The model computed small ion concentrations for various assumed values of r are shown in Fig. 3. The fluctuations in aerosols cause similar fluctuations in corresponding small ions only for larger r values. It is noted that the reduction in conductivity by aerosols is because of the ion depletion due to ion-aerosol attachment and aerosol ion-small ion recombination. In computation, it is observed that at all heights $\alpha_s \geq \alpha_i$. Thus, the aerosol ion-small ion recombination is seen to be very important in the studies of ion depletion due to aerosols, particularly, under enhanced aerosol condition. The coefficient, α_s, is dependent on the aerosol size distribution as well as on the small ion mobility. Thus, the relatively smaller fluctuations of α_s with respect to Z at lower altitudes as compared to those at higher heights are due to the relatively smaller ionic mobilities at lower altitudes. It is evident that the ion depletion levels are directly reflected in the α_s values at any height. Hence, it is clear that, rather than variations in aerosols, the variations in α_s represent the possible reduction and/or variations in the atmospheric ion concentration due to the presence of aerosols.

The model predicted $\sigma_\pm$-profiles is shown in Fig. 4. It may be observed that the fluctuations in aerosol values do not cause any considerable fluctuations in the measured $\sigma_\pm$-profiles, particularly, at lower heights. However, an examination of Z and model $\sigma_\pm$-profiles reveals that the anti-correlation

between Z and model $\sigma_{\pm}$ is apparent only for larger r values, and is very small for r = 0.001 – 0.02 μm. Further, the sensitivity of the model $\sigma_{\pm}$-profiles in Figure 4 to the variations of Z is large at higher altitudes. The model predicted conductivity profiles for $r < 0.1$ μm agree well with the $\sigma_{\pm}$-profile of Rosen *et al*. (1985). The model computed conductivity values agrees well with experimental values at greater heights.

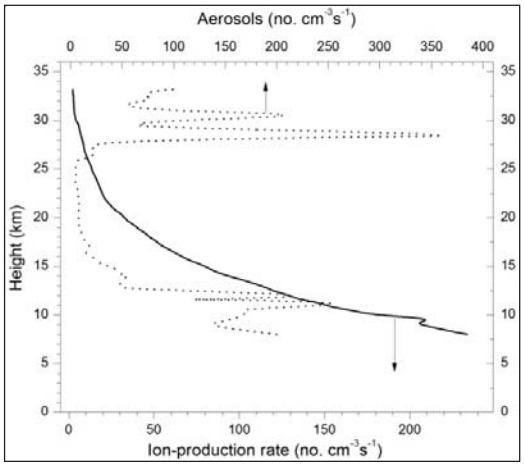

Figure 2. Profiles of input Z and ion-production rate

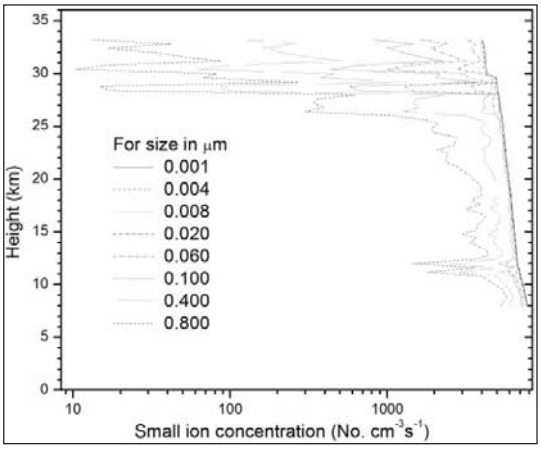

Figure 3. Profiles of small ion concentration

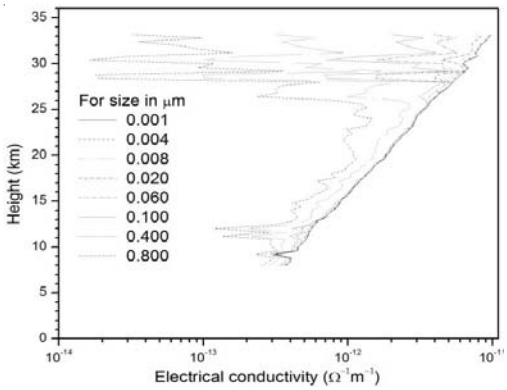

Figure 4. Profiles of model predicted electrical conductivity for stratosphere.

SUMMARY

Ionic conductivity of the stratosphere is one of the important parameters for understanding the electrical state of the region. This parameter is sensitive to the presence of aerosols and thus, aerosol loading on the stratosphere has a bearing on the conductivity. Preliminary efforts were made to study the behaviour of stratospheric ion conductivity and its variation under enhanced aerosol conditions by making use of an Ion-aerosol model. The aerosol ion-small ion recombination coefficient obtained from the model determines the extent to which aerosols can alter the conductivity of the stratosphere. This necessitates the requirement of experimental measurements of attachment and

recombination coefficient along with simultaneously measured aerosol density to have the proper information on electrical conductivity of the region.

REFERENCES

Hoppel, W.A. (1985). Ion-aerosol attachment coefficients, ion depletion, and the charge distribution on aerosols, *J. Geophys. Res.* , **90**, pp. 5917-5923.

Meyerott, R.E., Reagan, J. B., and Joiner, R.G. (1980). The mobility and concentration of ions and the ionic conductivity in the lower stratosphere, J. *Geophys. Res.,* **85**, pp. 1273-1278.

Nagaraja, K., Prasad, B.S.N., Srinivas, N., and Madhava, M.S. (2006). Electrical conductivity near the Earth's surface: Ion – aerosol model, J. *Atmos. Solar Terr. Phys.* , **68**, pp. 757-768.

Nagaraja, Kamsali, Datta, Jayati and Prasad, B.S.N. (2009). Measurement and Modeling the Atmospheric Electrical conductivity for monitoring the Air pollution, *J. Adv. Space Res*., **44**, pp. 1078-1087,

Nagaraja Kamsali, Pawar, S.D., Murugavel, P., Gopalakrishnan, V. (2011). Estimation of Small ion concentration near the Earth's surface, *J. Atmos. Solar Terr. Phys.,* **73**, pp. 2345-2351.

Rosen, J.M., Hofmann, D.J., and Gringel, W. (1980). Measurement of Ion mobility to 30 km, J. *Geophys.Res.* **90**, pp. 5876-5884.

Smith, D., and Adams, N.G. (1982). Ionic recombination in the stratosphere, *Geophys. Res. Lett.* ,**9**, pp.1085-1087.

Srinivas, N., Prasad, B.S.N., and Nagaraja, K. (2001). An ion-aerosol model study for the stratospheric conductivity under enhanced aerosol condition, *Indian J. Radio Space Phys.* , **30**, pp. 31-35.

Srinivas, N., and Prasad, B.S.N. (1993). Seasonal and latitudinal variations of stratospheric small ion density and conductivity, Indian *Radio Space Phys.* , **22**, pp. 122-127.

AEROSOL TRANSPORT THROUGH CRACKS

ARSHAD KHAN, AMRUTA KOLI, PALLAVI KOTHALKAR, MANISH JOSHI,
B K SAHOO AND B K SAPRA

Radiological Physics and Advisory Division
Bhabha Atomic Research Centre
Mumbai – 400 085, India

Keywords: CRACK, DEPOSITION, CONTAINMENT

Containment system is an engineered safety feature, which act as the last barrier to meet the requirement of containing radioactivity. Importance of the containment integrity under severe accidents was exemplified during TMI-2 reactor accident of 1979 when the intact containment resulted in negligible radiological consequences to the external environment. The containment is likely to develop extensive cracking under severe accident loading conditions. It is important to know its structural and leak-tightness performance in terms of air leakage rate and escape of aerosols under severe accidents to factor it in accident management strategies. Aerosol deposition in these cracks could be due to sedimentation, Brownian diffusion or inertial impact. Dominance of any specific deposition process would depend on particle size composition of aerosols and air flow characteristics. Thus subject of air leakage and aerosol escape through cracked concrete containment continues to be active area of research due to its importance with regard to nuclear safety. To understand the aerosol transport through cracks simulated cracks have been designed and experiments have been carried out.

Experiments have been carried out using ambient room aerosols as test particles. Two geometries of cracks with parallel straight channel and another suffering single bend were used or this study. Room aerosols were allowed to enter through the crack and the number concentrations of particles entering and leaving the crack channel were recorded by using Grimm Scanning Mobility Particle Sizer (9.8 nm-870 nm). Fig. 1 below shows the variation in % capture of particles as a function of particle size.

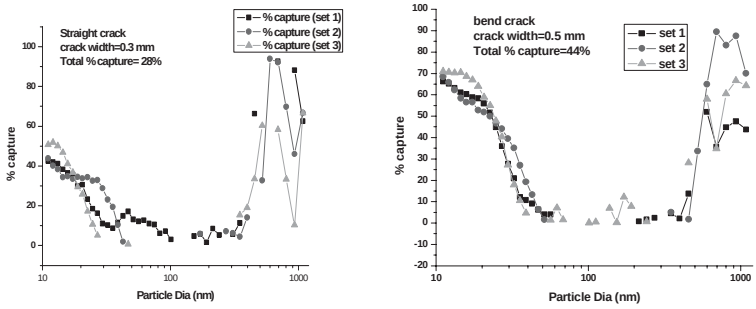

Figure 1. Variation in % capture of particles in the crack with particle size

It could be clearly seen from the figures that the total % capture is found to be higher in case of bend crack as compared to the straight crack. For both crack geometries, deposition mechanisms are found to be weak for particle sizes from 40 nm to 400 nm as compared to the other smaller and larger particle size groups.

AEROSOL MEASUREMENTS USING SCANNING MOBILITY PARTICLE SIZERS: WHAT SHOULD BE KNOWN?

MANISH JOSHI, ARSHAD KHAN, B K SAPRA, S N TRIPATHI, Y S MAYYA

Radiological Physics & Advisory Division
Bhabha Atomic Research Centre
Mumbai – 400 085, India

Keywords: CPC, SMPS, HARMONIZATION

In past few years, the significance of using number concentration measurements with or in place of conventional mass measurements (PM limits) is being discussed. For aerosols, Condensation Particle Counter (CPC) for number concentration and Scanning Mobility Particle Sizer (SMPS) for size distribution are widely used, including ultrafine range measurements. Therefore, an obvious but important part of aerosol research is to understand these systems and their usage protocols. There are several key factors which influence performance and consequent data interpretation of these systems. For example, CPC counting logic, SMPS neutralizer role, SMPS data inversion etc. are some issues which are often neglected while using these devices for aerosol measurements. The discussion of sub-systems (or components) of SMPS helps to validate and evolve measurement protocols, for normal conditions as well as other relevant conditions for Indian context such as high humidity etc. Key points such as recently developed protocols, ISO requirements etc. should be known or understood/validated before using SMPS for measurement and its data for interpretation. In addition, field studies (particularly targeting climate effect studies) involve CPCs and SMPSs of different make. However, concentration dependent responses were observed in the past studies. There is a need to focus on harmonizing the differences between two SMPSs of different make observed worldwide for different conditions. In the present work, we carried out experiments with ambient (low concentration) as well as laboratory controlled (high concentration) for the similar device condition involving SMPS of GRIMM & TSI make. It was observed that the concentration differences between these devices increased with aerosol concentration. CPCs of these devices matched for low concentration but a large difference was observed at high concentration (Fig. 1a). For high concentration conditions, the shifting of counting logic resulted in CPC differences. Analyzing the inversion routines and other possible differences for these devices, neutralization efficiency of SMPS is an investigating aspect for observed concentration differences (Fig. 1b). The introduction of diffusion dryer in path of one of the SMPS produces a significant change in measured aerosol size. The introduction of sheath air dryer in GRIMM SMPS produced a considerable shift towards the lower size.

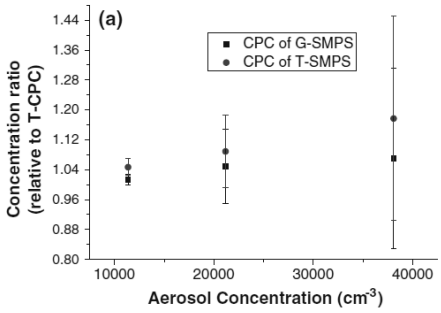

Figure 1a.CPC differences with concentration

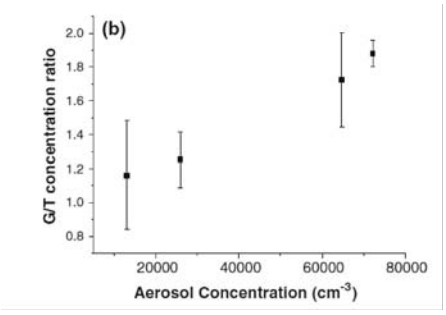

Figure 1b. SMPS differences with concentration

NANOPARTICLE GENERATION FROM AN ELECTRICALLY HEATED NICHROME WIRE: EXPERIMENTS AND THEORY

MANISH JOSHI, B. K. SAPRA, S. ANAND, ARSHAD KHAN, Y. S. MAYYA

Radiological Physics and Advisory Division
Bhabha Atomic Research Centre
Mumbai- 400085, India

Keywords: NANOAEROSOLS, NICHROME, HOT WIRE GENERATOR

Electrically heated hot wire has been used as an aerosol generator for the calibration of particle counters and for coagulation and nucleation studies. The particle number concentrations can be varied by changing applied voltage while mean size can be varied by changing the sampling mode (directly or after evolution in chamber). The generated particles have a near monodisperse size distribution with median in nano size range which is important for calibration of nanoparticle counters. Also, total concentration produced by this technique is one of the viable techniques to study coagulation/nucleation and to develop a calibrator for total particle concentration. Although some nanoparticle generators are commercially available but limited studies exist describing the aerosol emission, characteristics and behavior. Moreover, the behavior of these nanoparticles in a closed chamber can be used as an experimental verification to the recent coagulation/nucleation theories. The objective of this work is to study behavior of nanoaerosols generated from electrically heated nichrome wire. This wire was placed inside a cubical chamber of volume 0.512 m^3 and a small sampling flow (0.3 lpm of Condensation Particle Counter or Scanning Mobility Particle Sizer) was used for extracting the aerosol concentration and size distribution as a function of time in well mixed conditions. The voltage applied to the coil was 8.9 volts. The first measured spectrum of SMPS (after 7 minutes) showed that primary particle spectrum is below the lower detection limit (9.8 nm). The next distribution (after another 7 minutes) showed a secondary peak at 15 nm which can be explained as a result of homogeneous coagulation. Subsequent measurements showed the shifting of secondary peak to higher sizes with a consistent reduction of total concentration (Fig. 1). The temporal evolution of total concentration showed that it increases to a peak value and then decreases steadily. The effect of coagulation as a result of high concentration resulted in a characteristic time to achieve peak for a continuous source conditions. Theoretical predictions for total concentrations matched well with the experimental observation (Fig. 2). However a difference of theoretical predictions and experimental observations was observed after approximately 1500 seconds with faster experimental decay and multiple peaking after first peak.

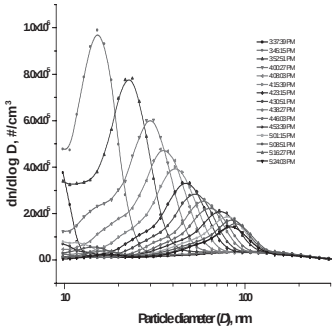

Figure 1. Temporal evolution of spectrum

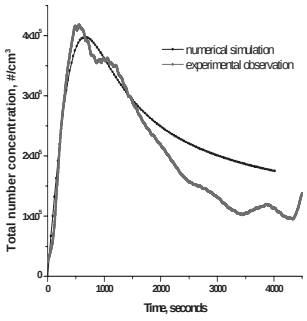

Figure 2. Variation in total concentration

DEPENDENCE OF LIQUID PROPERTIES ON PERFORMANCE OF ELECTROHYDRODYANAMIC ATOMIZATION (EHDA)

SANJAY SINGH[1], ARSHAD KHAN[2], B.K.SAPRA[2], Y.S.MAYYA[2] AND D.N SHARMA[1]

[1]Radiation Safety Systems Division
[2]Radiological Physics and Advisory Division
Bhabha Atomic Research Center, Mumbai- 400 085

Electro-hydrodynamic atomization (EHDA) is based on the principles of liquid jet break-up due electro-hydrodynamic instability (Hartman, *et al.* 2000 and Jaworek and Krupa, 1999). The liquid jet emerges from the tip of a liquid cone which is the modified shape of a drop, due application of high electric filed to the bulk of the liquid. Perhaps the main reason why the technique has caught the attention of the aerosol community is the phenomenal size range of particles that it can produce, from molecular dimensions to hundreds of microns, depending on the liquid flow rate and liquid electrical conductivity.

The cone-jet mode operation of EHDA not only offers the droplet monodispersity, but it is also stable, as apposed most other electrostatic alternatives. The capability of producing monodisperse particles using this technique with relative ease is unmatched by any other aerosols generation scheme especially is nanometric size range. Although the EHDA phenomena have intrigued scientists for over 100 years, but many detailed features of their operation still not fully understood (Fernandez de la Mora, 2007).

Adding to above mentioned studies, we are reporting the size distribution characteristics of EHDA generated aerosols with two different solution, namely Ethylene Glycol and Aqueous solution of sucrose. These two liquids are very different with respect to their viscosity and surface tension. In this study, measurements have been made using scanning mobility particle analyzer (SMPS) after neutralizing the generated particles using Am-241 radioactive source (Maria, *et al.* 2008). It was observed that for both of the liquid the generated particles were in nano-size range. In case of the Ethylene Glycol the mean size was 25.7 nanaometer and in the case of sucrose solution the mean size range was 63.03 nanometers. The geometries standard deviation from Ethylene Glycol particles was 1.72 whereas for sucrose solution the geometries standard was 1.54. A qualitative explanation of this parametric variation of the particles is the formation of secondary droplet due to high viscosity. This has been reported that higher liquid viscosity adds to the formation of secondary droplets and satellites in addition to main jet break-up (Hartman, *et.al* 2000).

REFERENCES

Fernandez de la Mora, J. (2007). The fluid dynamics of Taylor cones, *Annual review of fluid mechanics*, **39,** pp. 217,-242

Jaworek, A., and Krupa, R. (1999). Classification of the modes of EHD spraying, *J. Aerosol Sci.*, **30**, pp. 873-93

Hartman, R. P. A., Brunner, D. J., Camelot, D. M. A., Marijnissen, J. C. M., Scarlett, B. (2000). Jet Break-Up in Electrohydrodynamic Atomization in the Cone-Jet Mode, *J. Aerosol Sci.* , **31(1)**, pp. 65-95.

Maria, *et al.* (2008) M. Vivas, Hontanon Esther, Schmidt-Ott Andreas. Design and evaluation of a low-level (0.24 μCi) radioactive aerosol charger based on ^{241}Am., *J. Aerosol Sci.* , **39**,pp. 191-210.

AEROSOL INSTRUMENTATION

THE "DUAL-SPOT" AETHALOMETER: REAL-TIME DISCRIMINATION OF "BLACK" *VS.* "BROWN" CARBON FOR SOURCE APPORTIONMENT OF FOSSIL FUEL *VS.* BIOMASS COMBUSTION AEROSOLS

G. MOÈNIK [1], L. DRINOVEC [1], P. ZOTTER [2], A.S.H. PRÉVÔT [2], C. RUCKSTUHL [3], J. SCIARE [4], J.-E. PETIT [4], R. SARDA ESTEVE [4], A.D.A. HANSEN [1,5]

[1] Aerosol d.o.o., SI-1000 Ljubljana, Slovenia
[2] Paul Scherrer Institut, CH-5232 Villigen, Switzerland
[3] inNet Monitoring AG, CH- 6460 Altdorf, Switzerland
[4] LSCE CNRS-CEA-IPSL, F-91191 Gif-sur-Yvette, France
[5] Magee Scientific Corp., Berkeley, CA 94704, USA
E mail: Grisa.Mocnik@Aerosol.si

Keywords: BLACK CARBON, SOURCE APPORTIONMENT, OPTICAL PROPERTIES, AEROSOL ABSORPTION

Filter-based measurements of aerosol optical absorption are widely used to determine Black Carbon (BC) concentrations in real time. Measurements at multiple wavelengths (Sandradewi, *et al.*, 2008) can identify the contributions from different combustion sources, separating 'Black Carbon' (BC) from 'Brown Carbon' (BrC). These methods sometimes show non-linearity due to 'loading effects' of increasing aerosol deposit on the filter (Arnott, *et. al.*, 2005; Gundel, *et al.*, 1984; Virkkula, *et al.*, 2007; Weingartner, *et. al.*, 2003). These effects are highly variable and cannot be treated by static algorithms, either in post-processing of the data or fixed in the instrument firmware. A dynamical and auto-adaptive approach is required, in order to capture the details and variability of the aerosol optical properties and allow for accurate real-time source apportionment.

We have developed a new Aethalometer®, Model AE33, in which two parallel sampling channels collect the aerosol simultaneously at different loading rates. Combining the data from the two parallel analyses eliminates the 'loading effect' and yields an accurate measurement of BC together with a dynamical value of the non-linearity parameter which is indicative of aerosol properties. These analyses are performed for multiple optical wavelengths spanning the range from 370 nm to 950 nm and with a time resolution as rapid as 1 second. The results show greatly improved analytical performance for measurement of BC. The instrument is network-ready and is designed for both research and routine monitoring operations.

We present results from the use of this new instrument in urban and rural measurement campaigns in Switzerland, France, Austria, Slovenia and the USA. The data show high sensitivity and time resolution, with a complete absence of loading artifacts. We have developed a real-time application based on a published method (Sandradewi, *et. al.*, 2008) for source apportionment to separate contributions of biomass and fossil fuel combustion to ambient aerosols.

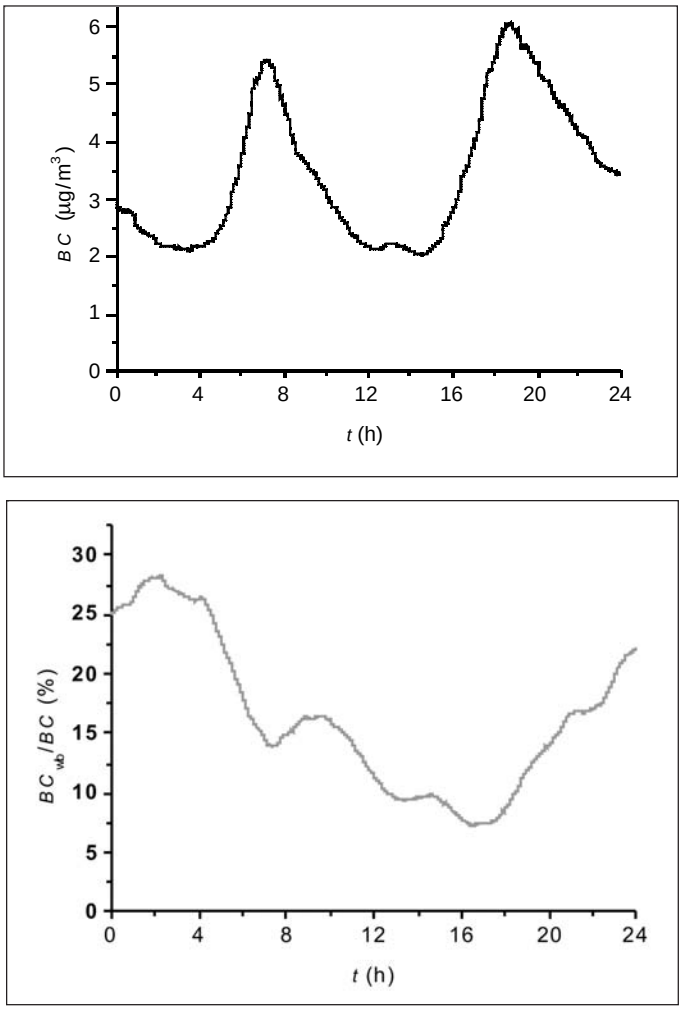

Figure 1. Diurnal Black Carbon concentrations (top) in Klagenfurt (Austria), March 2012, and the fraction apportioned to wood combustion (bottom).

ACKNOWLEDGMENT

The work described herein was co-financed in part by the EUROSTARS grant E!4825 FC Aeth and the Slovenian national grant JR-KROP 3211-11-000519.

REFERENCES

Arnott, W. et al. (2005). *Aerosol Sci. Technol*., **39**, 17-29.

Gundel, L.A., et al. (1984). *Sci. Total Environment*, **36**, 197.

Sandradewi, J. et al. (2008). *Environ. Sci. Technol*., **42**, 3316.

Virkkula, A. et al., (2007). *J. Air & Waste Manage. Assoc*., **57**, 1214.

Weingartner, E., et al. (2003). *J. Aerosol Sci*., **34**, 1445.

A NEW VERSATILE CONDENSATION PARTICLE COUNTER FOR RESEARCH AND ENVIRONMENTAL MONITORING

J. SPIELVOGEL, M. WEISS

Palas® GmbH, Greschbachstr. 3b, 76229 Karlsruhe, Germany

Keywords: NANOPARTICLES, SMPS SIZE DISTRIBUTION, CPC NUMBER CONCENTRATION, ULTRAFINE PARTICLES

INTRODUCTION

Presented is a recently developed condensation particle counter in which the unique, patented way (US 7,543,803 B2) of providing the working fluid for condensation allows the user to change the working fluid from e.g. butanol to isopropanol or water. Within the saturator, the working fluid is moved helically around the flow area of the aerosol leading to a homogeneous contact area. By changing the working fluid but with the same hardware; it is for example possible to conclude on hydrophilic and hydrophobic particles or to study how these properties change during aging of the aerosol. Measurements using this feature were made at a mail distribution center and are presented.

The counting is performed by an optical aerosol spectrometer (sensor) that also measures the size of the droplets that result from the internal condensation process. A researcher can easily monitor changes in this droplet distribution due to different temperature settings, different working fluid or different particle composition in the analyzed aerosol. Selected measurements will be shown.

The modular design of this instrument further allows adapting the sensor to different concentration levels up to single particle counting of concentrations of 10^6 particles/cm^3. This eliminates the need to dilute the aerosol in many cases.

In combination with the universal scanning mobility particle sizer (U-SMPS) two identical CPCs but one operated with butanol, the other with water were monitoring ambient air. Results of this study will be discussed.

THE UF-CPC

Fig. 1 shows the principle of operation of the UF-CPC. The aerosol with nanoparticles enters the UF-CPC at the bottom and first enters the heated evaporation chamber – the saturator. Within the saturator the working fluid is moved helically around the flow area of the aerosol leading to a more homogeneous contact area compared to designs where only one or two walls of the saturator are lined with a porous material that is soaked with the working fluid. Further, the working fluid is circulated continuously from the reservoir to the constantly heated helical U-shaped channel and back to the reservoir with a flow rate that can be adjusted to accommodate different working fluids.

Downstream of the evaporation chamber the aerosol and the saturated carrier gas enter a cooled region - the condenser - in which the working fluid condenses onto the nanoparticles forming droplets of sizes larger than 1 µm. After the condenser the droplets enter the optical sensor. The size of the droplets is analyzed and by counting the droplets the concentration is measured. In contrast to other CPCs the sensor of the UF-CPC uses a patented technology to count particles in single count mode at concentrations up to 10^6 particles/cm^3 without diluting the aerosol.

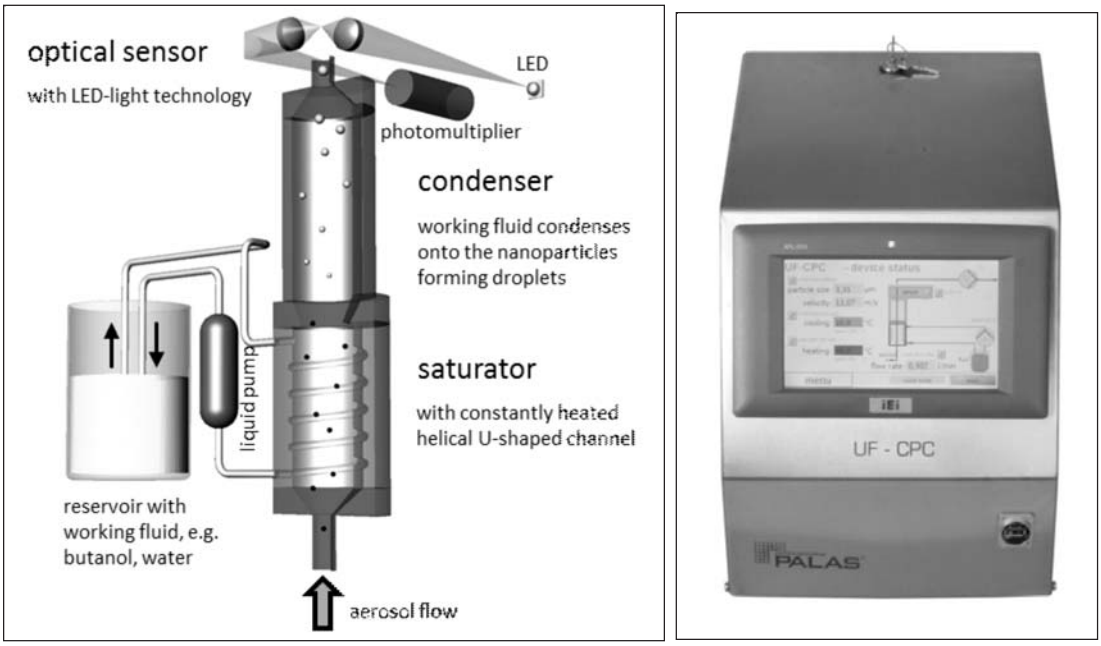

Figure 1. Principle of operation and picture of the universal fluid condensation particle counter (UF-CPC).

PERFORMANCE CHARACTERISTICS

The ISO/CD 27891 "Aerosol particle number concentration – Calibration of condensation particle number counters" describes in detail how a CPC calibration is performed by determining the detection efficiency and its associated uncertainty of the CPC against a traceable reference standard.

The UF-CPC was characterised according to this method by several reputable laboratories (e.g. METAS, IfT Leipzig). Fig. 2 shows the results from the characterisation of the UF-CPC at METAS with combustion aerosol from a miniCAST against a TSI aerosol electrometer 3068B used as reference. As can be seen the d50 was determined to be at 4.5 nm.

At present, a diploma thesis is conducted at Palas® where the performance of the UF-CPC with different working fluids and different materials is studied.

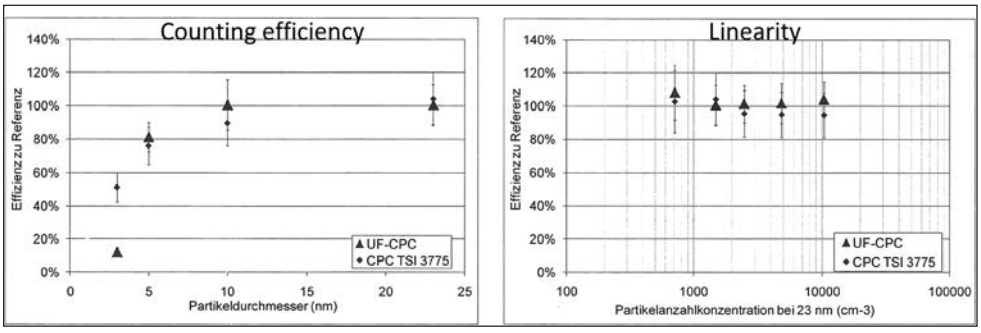

Figure 2. Counting efficiency and linearity (at 23 nm) with butanol as working fluid. Settings: saturator temperature 44°C, condenser temperature 10°C, flow rate 0.5 l/min [Source: METAS Report 235-10285]

DROPLET SIZE DISTRIBUTIONS

As the optical sensor used in the UF-CPC allows a detailed size classification of the droplets, the continuous droplet size distributions are reported to the user. While these distributions in no way allow the deduction of the original particle size, they can be a valuable feedback about the condensation process and can be used to further optimize the condensation (e.g. increase the sensitivity of the UF-CPC by increasing the temperature difference between saturator and condenser).

Fig. 3 and 4 present data that were obtained by measuring the constant output (mean particle diameter 45 nm) of a Palas® DNP 3000 defined nanoparticle generator (Evans, *et. al.*, 2003) and changing the temperatures of the saturator and condenser, then varying the working fluid from butanol to water and repeating the experiment. In fig. 3, the saturator temperature is kept constant at 40°C but the condenser temperature changed from 12°C (dark blue) to 10°C (red). The resulting marginal change in the size distribution of the resulting droplets can be explained that by keeping the saturator temperature constant no change in working fluid vapour is introduced and a change in cooling has little effect on droplet size and number. However, keeping the condenser temperature constant at 10°C but changing the saturator temperature from 40°C (dark blue) to 44°C (green) and to 47°C (blue) leads to a considerable shift in droplet size distribution. Here, the available amount of working fluid vapour is influenced by the temperature change in the saturator and visible in the increasing size of the forming droplets. At the same time a larger “T between saturator and condenser increases the sensitivity of the UF-CPC.

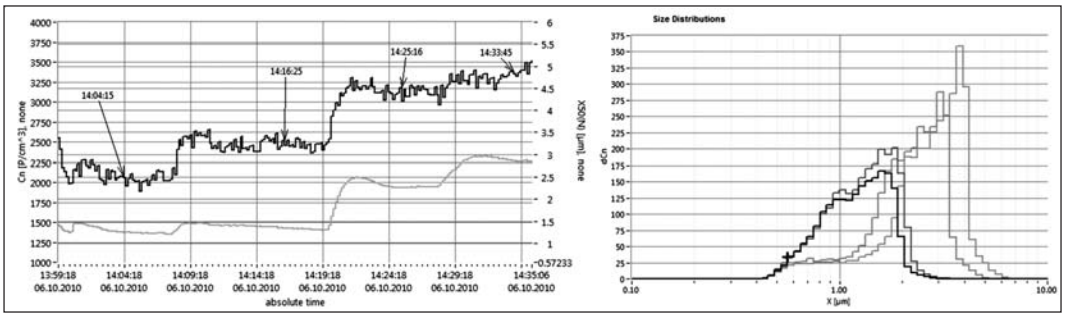

Figure 3. Number concentrations (left) and droplet size distributions (right) for different settings of saturator and condenser temperatures (working fluid butanol).

In fig. 4, the butanol was replaced with water and the experiment repeated with three different settings for the saturator temperature (65°C, 70°C, 75°C). Similar to the experiment with butanol, an increase in saturator temperature resulted in a shift in droplet size distribution to larger particles.

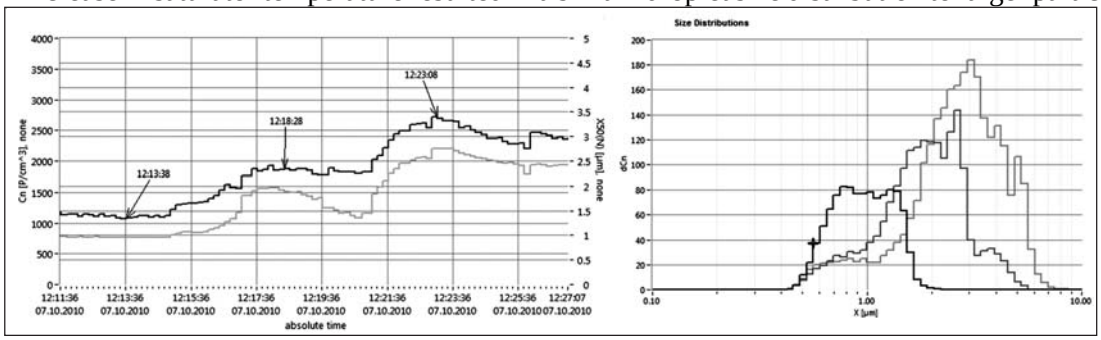

Figure 4. Number concentrations (left) and droplet size distributions (right) for different settings of saturator and condenser temperatures (working fluid water)

MEASUREMENT RESULTS AND DISCUSSION

The following measurement was conducted in an industrial area using two UF-CPCs in parallel, one operated with butanol, the other with water as working fluid. Based on the aerosol composition (fresh aerosol with more hydrophobic components, aged aerosol with lesser) the count ratio changes. It approaches one on Sunday night when no traffic leads to no fresh aerosol, but increases significantly on Monday morning when workers come back to work and park their cars in the parking lot in front of the measurement station.

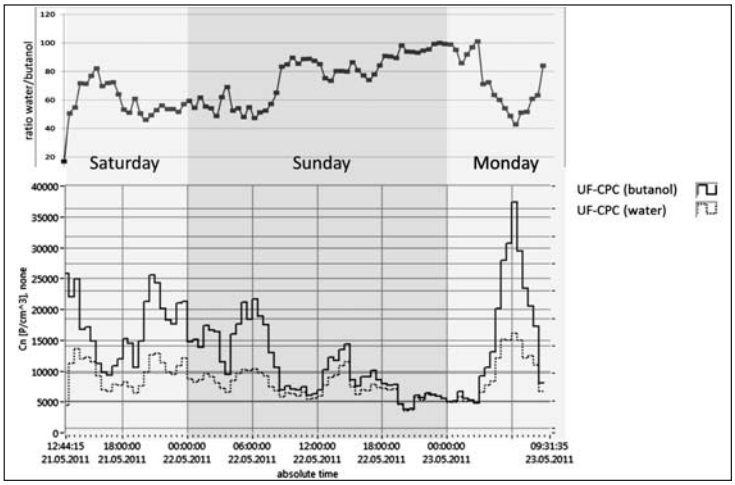

Figure 5. Ambient particle number concentration measurements near a mail distribution center in an industrial area with parallel UF-CPCs (one operated with butanol, one with water).

CONCLUSIONS

The universal fluid condensation particle counter (UF-CPC) presented here offers the scientific community the following key features:

- exchange the working fluid, e.g. butanol, isopropanol, DEHS, etc. and adjust the speed with which the working fluid is provided if necessary.
- obtain real time droplet size distributions as feedback on the condensation process.
- adjust the concentration limit of the counting mode by exchanging the sensor within the unit (one included, second optional)
- count up to 10^6 P/cm^3 in single count mode with live coincidence correction (model UF-CPC 100)

The UF-CPC further features simple operation through a 7" touch panel display with intuitive user interface and limitless integrated network connectivity.

REFERENCES

Evans, D. E., Harrison, R. M., Ayres, J. G. (2003). The generation and characterisation of elemental carbon aerosols for human challenge studies, *Journal of Aerosol Science*, **34**, 1023-1041

ISO/CD 27891. Aerosol particle number concentration – Calibration of condensation particle number countersUS Patent No. US 7,543,803 B2

THE FIDAS® - A NEW CONTINUOUS AMBIENT AIR QUALITY MONITORING SYSTEM THAT ADDITIONALLY REPORTS PARTICLE SIZE AND NUMBER CONCENTRATION

J. SPIELVOGEL, M. WEISS

Palas® GmbH, Greschbachstr. 3b, 76229 Karlsruhe, Germany

Keywords: AMBIENT AEROSOL MONITORING, PM-10, PM-2.5, CONTINUOUS PARTICLE MEASUREMENT

INTRODUCTION

Today's regulation demands that fine dust is continuously monitored and that the mass fractions PM_{10} and $PM_{2.5}$ comply with limit values. These PM-fractions are defined by particle size since the original goal was to mirror the deposition in the human respiratory tract. PM_{10} would thereby correspond to the inhalable fraction whereas $PM_{2.5}$ would correspond to the respiratory fraction.

While the mass concentration can be routinely monitored it however carries little extra information when it comes to possible health effects. Studies suggest that especially small particles that penetrate deeper into the body can lead to high plaque deposits in arteries causing vascular inflammation and atherosclerosis.

In a mass measurement these small particles are not identifiable. We will present a continuous ambient air quality monitoring system that reports all PM-fractions but in addition also particle size and number concentration. Due to its high time resolution of 2 minutes this system also allows monitoring dynamic events or provides useful real-time information for source apportionment.

THE FIDAS® FINE DUST MONITORING SYSTEM

The Fidas® fine dust monitoring and emission system allows the continuous and simultaneous monitoring of PM_1, $PM_{2.5}$, PM_4, PM_{10}, TSP (PM_{tot}) and the particle number concentration, optionally also the particle size distribution (see fig. 1).

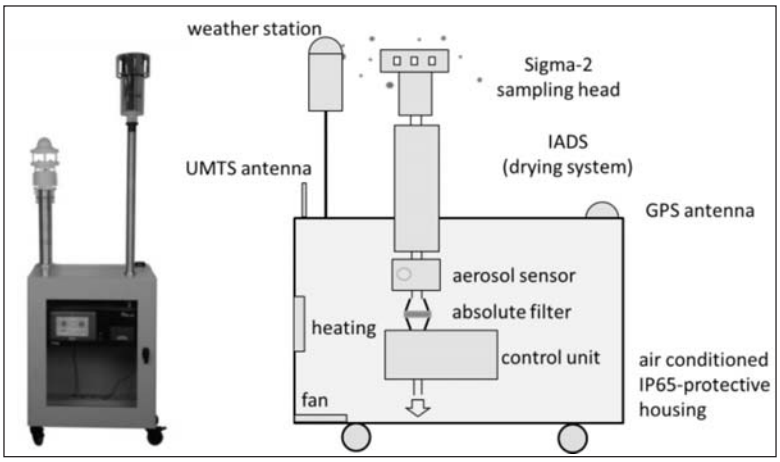

Figure 1. Set up of the Fidas® fine dust monitoring system

The system consists of a Sigma-2 sampling head, which allows also representative measurements in case of strong winds and an Intelligent Aerosol Drying System (IADS), which evaporates volatile elements prevents erroneous classification of particles due to moisture.

The aerosol sensor is an optical aerosol spectrometer, which determines the particle size by means of a scattered light analysis according to Lorenz-Mie. The particles move separately through an optically differentiated measurement volume, which is homogeneously illuminated with white light. Each particle generates a scattered light impulse, detected at an angle of 85° to 95° degrees.

The particle mass – the frequency of occurrence – that is the number concentration is deducted from the number of scattered light impulses. The intensity of the scattered light is a measure for the particle diameter.

The lower detection limit was reduced to 180 nm by using optimized optics, higher light density and improved signal analysis (logarithmic analog digital converter). In this way, smaller particles, which are generated in high amounts during combustion processes, can be reproduced much better (see fig. 2).

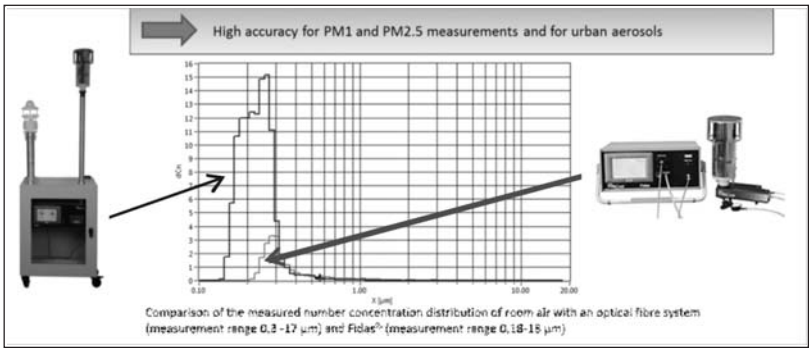

Figure 2. Higher sensitivity with the Fidas® fine dust monitor for particle size 0.18 – 18 µm

The better the classification precision and the resolution capacity of a particle measurement device, the more accurate the particle size distribution can be defined.

In order to be able to convert the measured particle number concentration and particle sizes into a mass concentration, classification accuracy and high resolution are indispensable. The mass is calculated with the data obtained from the particle size distribution and is initially based on spherical particles. Then, the number concentration is weighted separately according to the size of the particle (see fig. 3).

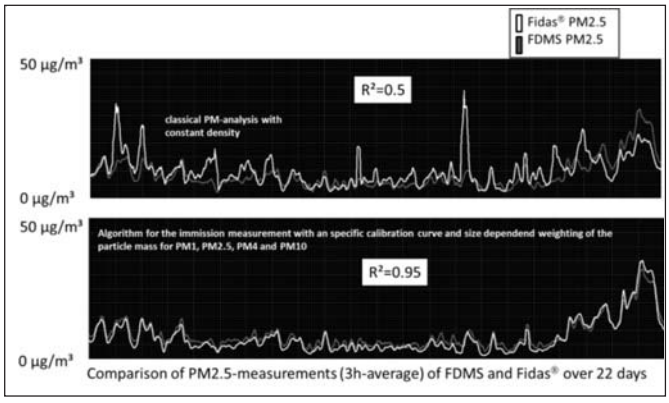

Figure 3. Comparison of algorithms for the conversion of particle size distribution according to mass

Downstream to the optical sensor there is a filter holder for an optional gravimetric validation of the measured data. The control unit offers intuitive handling by means of a big color touch screen. The integrated data logger allows the measured data to be saved and managed. An UMTS antenna enables remote maintenance and data transmission via the internet.

An optional meteorological station records wind direction and speed as well as the amount and kind of rainfall. For the exact location determination by mobile use, a GPS antenna can be integrated.

MEASUREMENT RESULTS

Easter in Vienna

Every year during the night to Easter Sunday, in many cities in Germany and Austria, a clearly higher particulate load can be measured (see fig. 5). This is caused by the Easter Fires, an old custom to chase away, to burn winter.

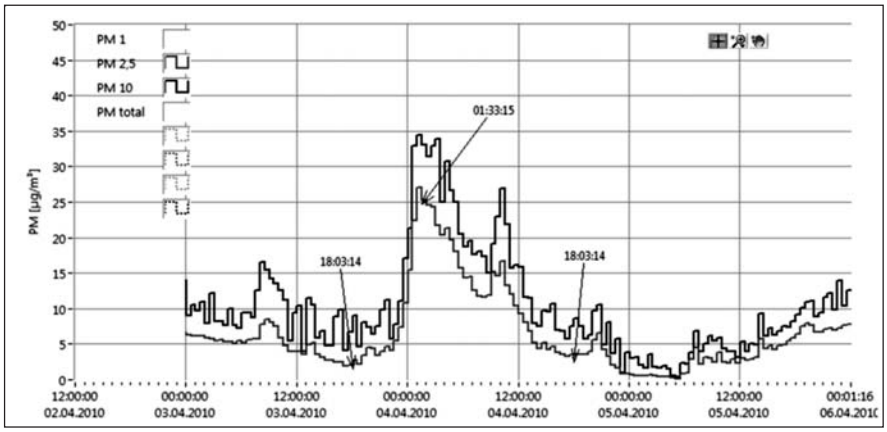

Figure 5. Higher PM-concentration measured in Vienna during the night to Easter Sunday

The generated combustion aerosols contain a high number of small particles (see fig. 6 on the left, max. at ca. 300 nm). In order to be able to simulate the spreading behavior of fine dust, a high time resolution (a resolution of one second is technically feasible with the Fidas® system) as well as the particle size distribution is extremely important, because the physical characteristics of the particle are significant to be able to predict the spreading behavior. From the diameter, we can deduce e.g. the sink rate and from the number concentration, we can deduce the coagulation behavior.

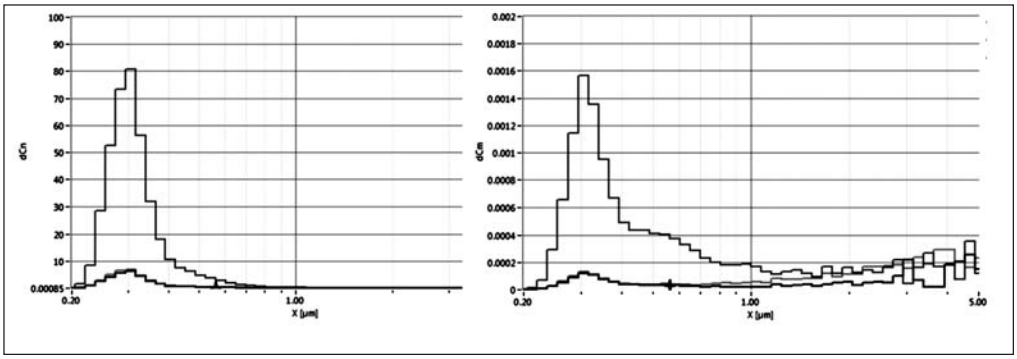

Figure 6. Left, number concentration, right mass concentration of the combustion aerosols generated by the Easter fires

Fog in Lübeck

To enable a detailed record of fog formation, the moisture compensation of the monitoring system located in Lübeck was turned off. In the morning of 22.05.2010, for three hours an increase in the mass concentration could be observed (see fig. 7).

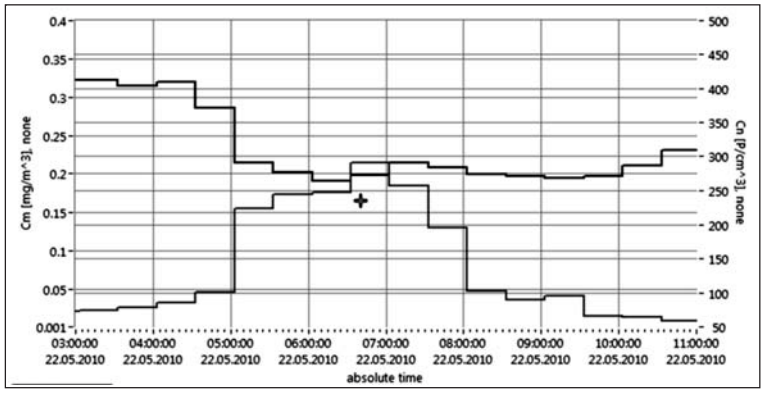

Figure 7. The development of particle mass concentration and particle number concentration during fog measured in Lübeck

Having a more precise look at the particle size distribution, it could be seen that in the size range of ca. 3 to 15 µm, there had been detected one order of magnitude more particles than usually. At the same time, the meteorological sensors showed a high relative humidity and a low air temperature. A look at the weather in the internet confirmed the presence of fog during the measurement.

Fig. 8 shows that during the fog formation, within one hour the size distribution changes dramatically and then, however, stays constant. The fading of the fog, on the contrary, takes much more time, as can be seen in figure 10. Here as well, a high time resolution as well as the particle size information is of extreme importance for the exact simulation of the fog formation process.

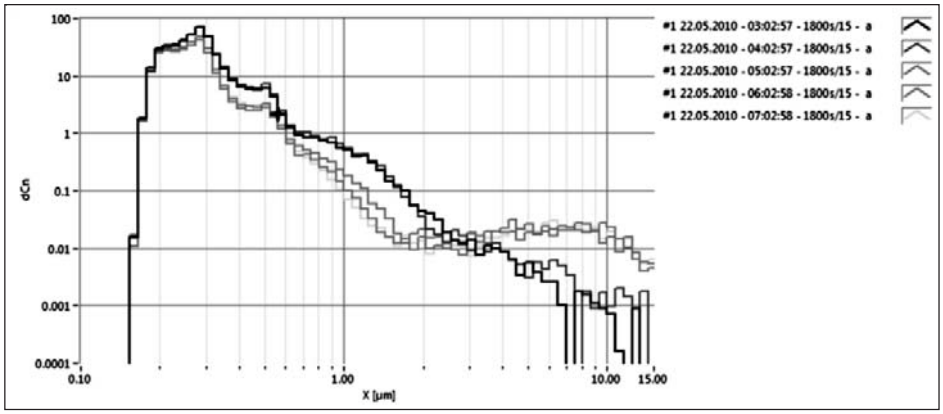

Figure 8. The particle size distribution measured every hour during the fog formation process

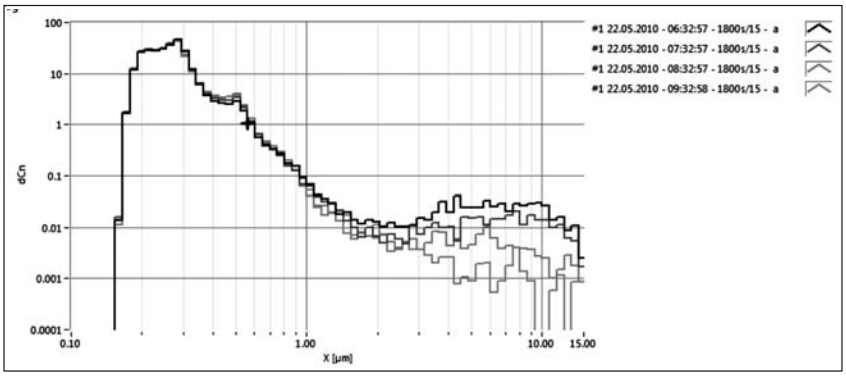

Figure 9. The particle size distribution measured every hour during the fading of the fog

CONCLUSIONS

In this paper, the Fidas® fine dust monitoring system for reliable and time-resolved emission measurements has been presented. In contrast to other methods, the optical light scattering measurement technology allows the continuous measurement of particle number and particle size as well as the simultaneous output of various PM values, such as PM_{10} and $PM_{2.5}$. The examples of the small particles generated by a combustion processes (Easter Fires in Vienna) and the big droplets (fog in Lübeck) have shown how – by means of the additional information on the particle size distribution – the respective underlying formation and dispersion processes can be understood and definitely also be simulated better.

REFERENCES

Report “Fidas® 200 fine dust and immission measurement device, Results of parallel measurements with the reference method and testing the equivalence”, (Müller-BBM, 2012)

Witschger, O., Fabries, J.F. (2005). Particules ultrafines et santé au travail: 1-caractéristiques et effets potentiels sur la santé. Hygiène et sécurité du travail, Cahiers de notes documentaires, *INRS*, **199**, 21-35

DESIGN OF A SMALL, BATTERY-OPERATED NANOPARTICLE SIZER

T. JOHNSON[1], A. ZERRATH[1], J. JOHNSON[1], M. NISHANT[2], B. JAYARAH[2] AND Y.C. KHOO[3]

[1] TSI Incorporated, 500 Cardigan Road, Shoreview, MN 55126, USA
[2] TSI Instruments India Private Limited, 3rd Floor, Sri Sai Heights, #447, 17th Cross, 17th Main, Sector 4, HSR Layout, Bangalore – 560034, India
[3] TSI Instruments Singapore Pte Ltd, 150 Kampong Ampat, #05-05 KA Centre, Singapore 368324

Keywords: NANOPARTICLE, CONCENTRATION, SIZE DISTRIBUTION, EXPOSURE

INTRODUCTION

A small, portable nanoparticle sizer has been developed to provide an affordable method to measure nanoparticle size distributions. The new nanoparticle sizer incorporates a SMPS Spectrometer into a chassis that is <1 cu.ft. The instrument consists of: 1) an inlet cyclone to remove large particles, 2) a cross-flow uni-polar charger to increase nanoparticle transmission efficiency and eliminate logistical issues with radioactive neutralizers, 3) a Radial DMA (RDMA) which is lightweight and compact, 4) an isopropyl based Condensation Particle Counter (CPC) to provide accurate measurements at high and low concentrations using a working fluid acceptable in workplace environments, and 5) the instrument control, analysis and data logging can be done through the instrument touch screen. In addition to nanoparticle size distributions, the instrument can be used to collect second by second concentration data at a single nanoparticle size. If the nanoparticle source of concern generates 50 nm particles, the particle concentration at 50nm can be monitored with 1 second time resolution. Instrument design will be reviewed and performance data including counting efficiency, size resolution and concentration range will be discussed.

INSTRUMENT DESIGN

The new nanoparticle sizer incorporates the five primary components of a Scanning Mobility Particle Sizer (SMPS) Spectrometer into a chassis that is <1 ft^3. Principle design elements include:

1) Inlet cyclone to remove large particles.

2) Unipolar charger (Kaufmann et al., 2000) to increase nanoparticle transmission efficiency and eliminate logistical issues with radioactive neutralizers.

3) Radial Differential Mobility Analyzer (DMA) (Pourprix, 1994) which is lightweight and compact

4) Isopropanol-based Condensation Particle Counter (CPC) to provide accurate measurements at high and low concentrations using a working fluid acceptable in workplace environments

5) Instrument control, analysis and data logging which can be done through the instrument touch screen.

DESIGN DETAILS

- Size distributions are taken every 60 seconds: 45 second up-scan (measured) and 15 second down-scan.
- In addition to nanoparticle size distributions, the instrument can be used to collect second-by-second concentration data at a single mobility diameter with one-second time resolution.
- The instrument's CPC can operate off an internal wick for greater than 6 hours. It should be operated with an external fill bottle for longer term use.
- The instrument is battery powered, and also has a AC power adaptor
- The size distribution can be weighted as number, surface area or mass concentrations.

KEY TECHNICAL FEATURES

- The particle size range covered (10 – 420 nm) matches optimally to the typical exposure in workplace environments not covered by optical particle sizers.
- The inlet cyclone was especially designed to prevent larger particles present in the investigated environments from entering the charger and overlaying the nanoparticle regime as multiple charged particles with smaller apparent electrical mobility diameter.
- The data acquisition and system control is fully integrated to enable the operator to concentrate on their tasks.

Feature	Description
Size Range	10 – 420 nm
Size Channels	13 Channels (fixed)
Concentration Range	de1,000,000 particles/cm^3
Modes of Operation	Scanning (size distribution & number concentration).Single mobility size (number concentration @ fixed size).
Measurement Time	Scanning: 60 seconds (fixed) Single: 1 second (fixed)
Inlet Flow Rate	0.8 L/min
Instrument Run Time	~6 hrs w/o A/C power or external reservoir.3-8 days with A/C power & external reservoir.
Data Storage	On-board (3-8 days continuous operation)USB storage drive option
Communications	USB
Power Requirement	Battery (6 hrs) or AC (100 to 240VAC, 50/60 Hz)

Table 1. Key features of the NanoScan SMPS, TSI model 3910

COMPARISON TO REFERENCE

Scanning Mobility Particle Sizing (SMPS) is the reference technology for online airborne nanoparticle size distribution measurements. The NanoScan SMPS was compared to our high-end reference systems as displayed in following figures.

The NanoScan SMPS is designed to be used to monitor polydisperse aerosols. In addition, fractions of the particle distributions can be monitored in the single channel mode. The polydisperse aerosol is scanned at fixed settings of flows and size range. Its performance is compared to the component SMPS system, TSI model series 3936, as shown exemplary in Figure 1 and Figure 2.

Working Fluid: Isopropyl alcohol is used as a working fluid instead of butyl alcohol (frequently used in component SMPS systems) or water (which requires significantly more power consumption). NanoScan is a portable instrument that has an easily removable wick that may result in some dripping of the working fluid. Isopropyl is less toxic and has significantly less odour than butyl alcohol. Isopropyl alcohol does absorb water at a higher rate than butyl alcohol but the removable wick in the NanoScan SMPS provides an easy way to dry out the wick.

Unipolar versus Bipolar charger: Bipolar charging is accomplished either with a radioactive source (which has significant regulatory issues) or with a soft x-ray source (which has larger size and higher power consumption). NanoScan SMPS has a unipolar charger, which improves the counting statistics for nanoparticles. There is decreased size resolution (due to multiple charging) and a small amount of under-reporting of concentration at the larger particle sizes compared to a component SMPS.

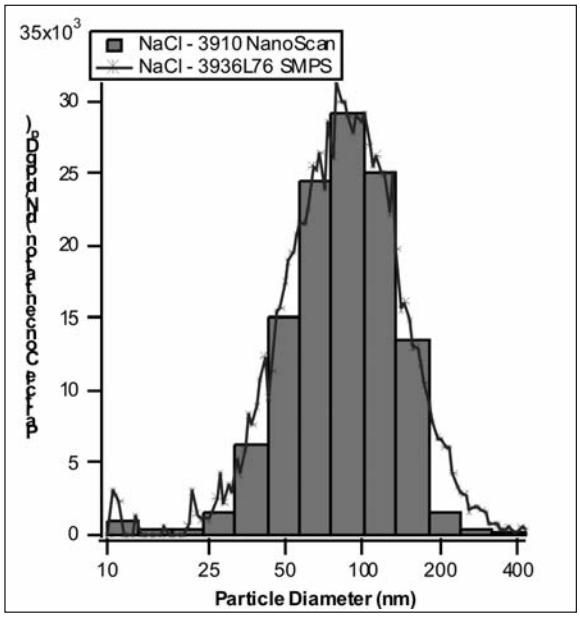

Electrical Mobility Diameter (nm)

Figure 1. Polydisperse NaCl aerosol with peak concentrations around 100 nm. The blue line represents the high-resolving SMPS system data. Both systems are in agreement.

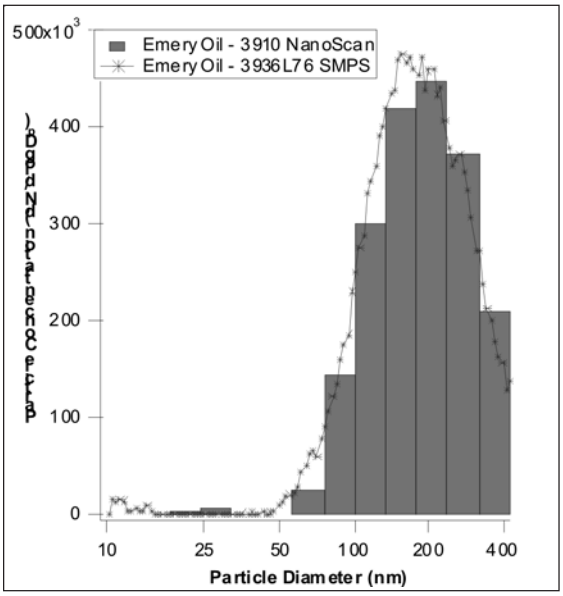

Figure 2. Polydisperse oil aerosol with peak concentrations around 200 nm. The blue line represents the high-resolving SMPS system data. Both systems are in agreement.

Figure 1 is simulating a polydisperse aerosol similar to most common indoor air. Evaluating exposure to nanoparticles in workplace environments for example usually requires a background measurement, which would show similar distributions as, displayed. The NanoScan results match very well with the reference SMPS concerning total number concentration, mode and width of the distribution.

In Figure 2 the NanoScan SMPS was challenged with a polydisperse size distribution of a different type of aerosol (nebulized emery oil) shifted to larger diameters. In the example of workplace environments this could be compared to a simulation of exposure to larger sized aerosol, for example while large amounts of powders are filled in a bag. The NanoScan results match well with the reference SMPS.

Two NanoScan systems were compared with regards to total number concentration of an aerosol in parallel with a reference condensation particle counter, TSI model 3776. Total number concentrations agree within ±5% for these two units under test.

INDOOR AIR QUALITY

Indoor air aerosol is often tested under various aspects, e.g. for organic volatiles, particle mass and number concentrations. Various local sources can contribute to the chemical composition as well as particle sizes and number concentrations. Size distributions are usually determined using optical particle counters, covering the size range typically from 300 nm to 10 µm. In parallel condensation particle counters are frequently used determining total number concentrations typically from 10 nm to >1 µm. The combination of the two techniques indicates the fraction from 10 nm to 300 nm. Having an optical particle counter and a NanoScan SMPS measuring in the same place reveals a higher level of information as visualized in Figure 3. The room air monitored was mixed with combustion aerosol from alcohol burners used to keep a lunch buffet warm, as well as a artificial source of large particles nebulized by a portable aerosol generator (TSI model 8026). The distribution measured was compared to the background room air measured before. The peak around 30 nm

resulted from the combustion aerosol. The nebulized aerosol raised the particle concentrations in the range from 300 nm to 2 μm.

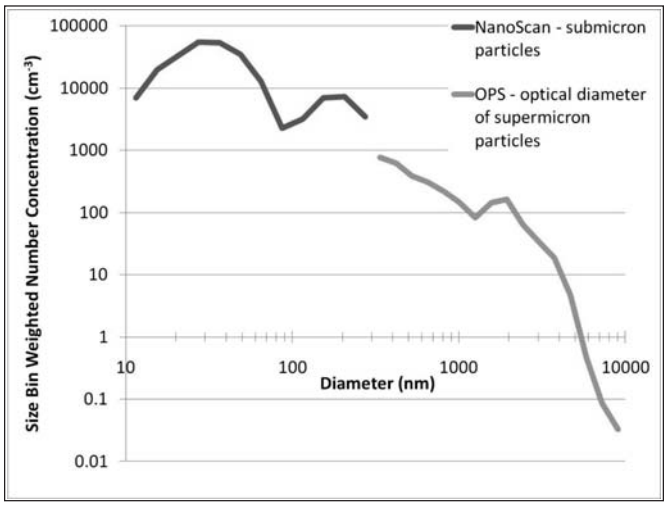

Figure 3. Indoor air quality example: A mixture of combustion aerosol in room air with a local source of supermicron particles. The blue distribution is from the NanoScan SMPS and the green distribution is from the Optical Particle Sizer (TSI model 3330). The data is not corrected for merging electrical-mobility (from NanoScan) and optical equivalent diameter (from OPS).

REFERENCES

Kaufman, Stanley L and Dorman, Frank D., (2000) US Patent 6,544,484.
Pourprix, M. (1994) French Patent No 94 06273.

HTDMA SYSTEM FOR FIELD AND LABORATORY USE

FRANCISCO J. ROMAY, KEUNG S. WOO AND BENJAMIN Y. H. LIU

MSP Corporation, 5910 Rice Creek Parkway, Suite 300, Shoreview, MN 55126, USA

Keywords: HUMIDITY CONDITIONING, TANDEM DIFFERENTIAL MOBILITY ANALYZER, AEROSOL HYGROSCOPICITY

A Humidified Tandem Differential Mobility Analyzer (e.g. HTDMA) has been developed to measure aerosol hygroscopicity in the 10-93% relative humidity range, with high accuracy and stability. A HTDMA data fitting program based on the DMA log-normal transfer function (Stolzenburg and McMurry, 2008) has also been developed to largely reduce the time needed for data analysis.

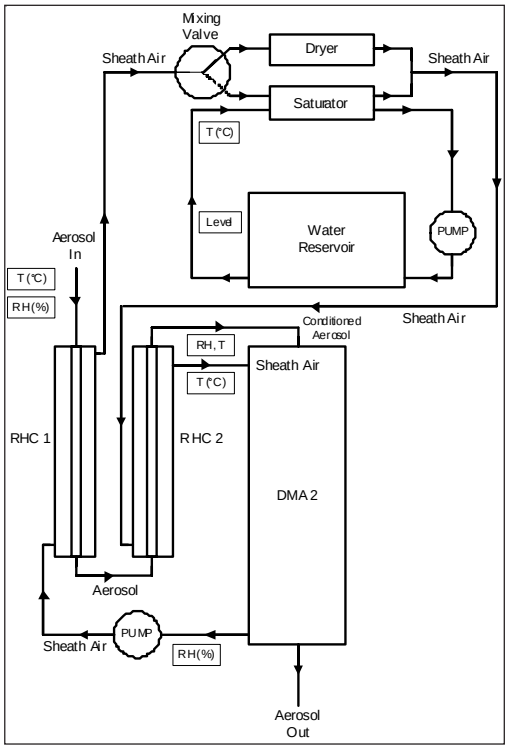

Figure 1. Schematic Diagram of Humidity Conditioner for DMA 2

In the HTDMA, the RH of the recirculated DMA sheath air is achieved by accurately controlled mixing of the calculated fractions of dry and water-saturated air by a fast, automatic switching valve (Johnson *et al.*, 2008). The RH is controllable up to 93%, just below the typical detection limit of a chilled-mirror dew-point sensor combined with an accurate temperature sensor (i.e. RTD). The aerosol sample RH is equilibrated in two Nafion® membrane tubes to ensure that it is at the same RH as that of the DMA sheath air (Fig. 1). A thermally conductive block is used to equilibrate the sample temperature with the surrounding environment, largely reducing the risk of condensation and improving instrument stability. Temperature and RH are monitored and/or controlled by a programmable logic controller (PLC). The closed-loop control for RH initially uses a capacitive RH

sensor as the feedback signal to reduce the oscillations, and then it switches to the chilled-mirror dew point sensor to attain greater accuracy of the controlled relative humidity. The RH response of the HTDMA system is reasonably fast (e.g. 2 to 3 minutes) and stable once the set point is reached, as shown in Fig. 2.

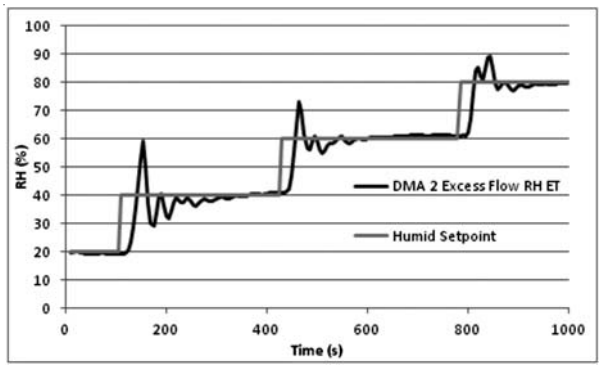

Figure 2. Response of the RH Controller

The hygroscopic growth of 100-nm monodisperse sodium chloride particles has been measured with this HTDMA. An atomizer was used to generate the NaCl aerosol, which was then dried (e.g. RH < 10%), charge-neutralized in a non-radioactive electrical ionizer, and mobility-classified by the first DMA of the system. The monodisperse NaCl aerosol was then conditioned to different values of relative humidity, and the corresponding mobility-size distributions were measured by the second DMA/CPC operated in the voltage-scanning mode. The experimentally obtained growth factor for the NaCl particles agreed very well with the theoretical prediction as shown in Fig. 3.

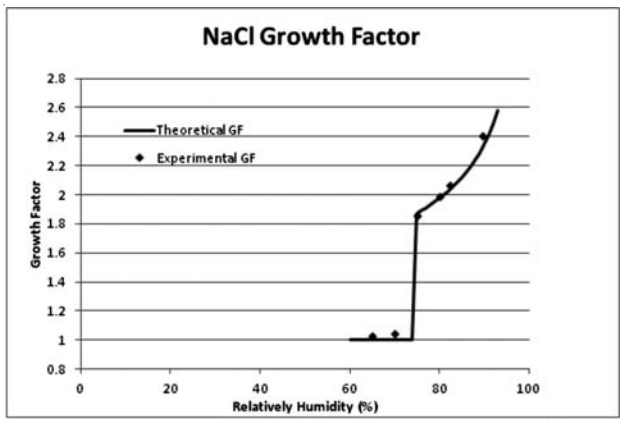

Figure 3. NaCl Growth Factor measured by the HTDMA system

REFERENCES

Johnson, G. R., Fletcher, C., Meyer, N., Modini, R. and Ristovski, Z. D. (2008). A robust, portable H-TDMA for field use, *Journal of Aerosol Sci.*, **39(10)**, 850–861.

Stolzenburg, M. R. and McMurry, P. H. (2008). Equations Governing Single and Tandem DMA Configurations and a New Lognormal Approximation to the Transfer Function, *Aerosol Sci. Technol.*, **42**, 421–432.

COMPREHENSIVE MEASUREMENT OF ATMOSPHERIC AEROSOLS WITH A WIDE RANGE AEROSOL SPECTROMETER

M. PESCH[1], L. LECK[2] AND H. GRIMM[3]

[1]GRIMM Aerosol Technik GmbH & Co. KG, Dorfstrasse 9, D-83404 Ainring, Bayern, Germany

Keywords: ATMOSPHERIC AEROSOLS, WIDE RANGE AEROSOL SPECTROMETER, PARTICLE SIZE DISTRIBUTION

INTRODUCTION

Measurement of aerosol size distribution plays an important role in the atmospheric aerosol investigations, such as particle source apportionment, effect of atmospheric aerosols on human health and the climate and so on. Nowadays people pay more and more attention to the airborne nanoparticles due to higher particle number concentration and larger surface area, i.e. airborne nanoparticles have higher concentration of adsorbed or condensed toxic material per unit mass. In this study, a wide range aerosol spectrometer (WRAS, Grimm Aerosol Technik, Germany) was applied for comprehensive aerosol measurements of atmospheric aerosols.

METHODS

This WRAS system consists of a scanning mobility particle sizer with condensation particle counter (SMPS+C) and an optical aerosol spectrometer (OPC), as illustrated in Fig.1, including a sampling probe with a Nafion dryer inside and optional meteorological sensors for measuring ambient air temperature and relative humidity.

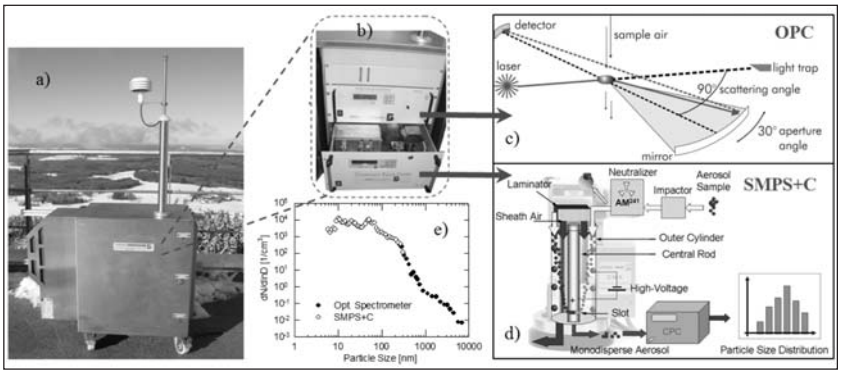

Figure 1. a) WRAS system mounted in a stand-alone stainless steel outdoor housing; b) configuration of the WRAS system; c) Measurement principle of the GRIMM OPC; d) Measurement principle of the GRIMM SMPS+C; e) Particle size distribution measured with the WRAS system.

The GRIMM OPC works on the basis of the light-scattering technology for single particle counts. As shown in Fig.1c, a semiconductor laser serves as the light source. The signal scattered from the particle passing the laser beam is collected at ca. 90° by a mirror and transferred to a recipient-diode. The detected signals are further analyzed and classified in multi channels. With this spectrometer one can measure the particle size distribution in the size range of 250 nm – 32 µm.

The GRIMM SMPS+C includes a condensation particle counter (CPC) and a differential mobility analyzer (DMA), as shown in Fig.1d.

During the measurement larger particles, which would complicate the data analysis, are removed firstly by an impactor at the inlet of the DMA, and then fine and ultrafine particles are classified with a DMA after they pass through a bipolar charger (Neutralizer Am241), which establishes a well defined charge distribution of the particles. The classification (i.e. the selection of a well defined fraction from a broad size distribution) occurs in the electrostatic field in the annulus between inner and outer electrodes of the DMA. Only particles of a certain size or mobility reach a narrow slit at the bottom of the inner electrode and are measured with a CPC. A size distribution in the size range of 5.5nm - 350nm can be obtained by changing the DMA voltage stepwise.

These two datasets from the OPC and SMPS+C are automatically synchronized and combined using the GRIMM software, as displayed in Fig.1e. Thus, this WRAS system allows the measurement of wide range particle size distributions from 5.5 nm to 32 µm. Fig. 2 shows a particle size distribution measured at the Meteorological Observatory Hohenpeissenberg, Germany.

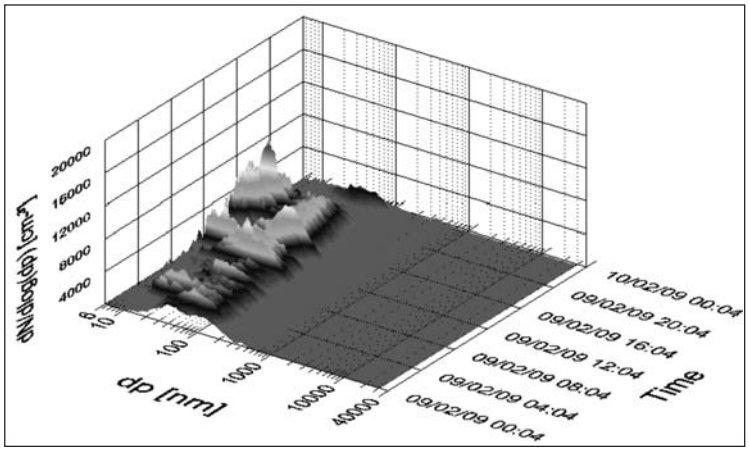

Figure 2. Results of the size distributions of atmospheric aerosols continuously measured at the Meteorological Observatory Hohenpeissenberg, Germany.

CONCLUSIONS

Numerous continuous measurements of particle size distribution indicate the time variation of airborne particles from various sources, like rush hour, traffic emissions, power plants out of the measurement site, and organic components due to photochemical reactions. Furthermore, combination with meteorological data and gas concentrations will also help study the transport and mixing processes of atmospheric aerosols.

CALIBRATION OF SUNPHOTOMETER AT MT ABU, RAJASTHAN, INDIA

SHAILENDRA S. SRIVASTAVA[A], HELISH SHARMA[C], YOGDEEP DESAI[A], B. KARTIKEYAN[A], N. K. VYAS[B]

a Space Applications Centre, ISRO, Ahmedabad-380015, India
b Scientist (retired) of Space Applications Centre, ISRO, Ahmedabad,
c Indian Institute of Technology Delhi, Delhi
E mail : sss.isro@gmail.com

Keywords: AEROSOL, AOT

INTRODUCTION

Aerosols affect the remote sensing measurements. Aerosol model/concentration is among the most important parameters in the top of the atmosphere radiance computations, which is our concern in calibration/validation of the Indian Remote Sensing (IRS) optical sensors through vicarious method (Thome, *et al*., 1997). Five quantities viz. aerosol mass concentration, particle size distribution, chemical & physical composition of the aerosol (providing index of refraction), particle shape & relative humidity establishes the relation between light scattering and aerosol properties (Covert, *et al*., 1972). Mathematically, spectral variation of the aerosol optical thickness (AOT) is used to derive these quantities (King, *et al*., 1978). Typically, a multi-wavelength Sunphotometer is used to measure aerosol optical thicknesses in narrow spectral bands. These bands are kept away from molecular atmospheric absorption lines (Shaw, 1983). These devices measure the direct Sun radiation. The detectors and filters used in these devices deteriorate with time and due to their use in extreme temperatures like of desert and glaciers, and demands frequent calibration for reliable measurements.

This paper discusses the calibration of a ten year old five channel Sunphotometer using Langley method, and its validation using the other well calibrated Sunphotometer. There are four common spectral bands in the instruments viz., 380nm, 500nm, 675nm, and 870nm. Calibration exercise was performed at high altitude site Mt Abu, Rajasthan, India. It also discusses the viability of other methods, which may be utilized for this purpose. Comparisons of spectral optical thicknesses from the synchronous measurements of both the Sunphotometers show an acceptable agreement in the clear atmosphere case (AOT~0.2) in band-870nm (within 14%), while the differences are large in the case of band-500nm & band-675 (within 19%), and in the case of band-380nm (~32%). Langley plot calibration method is found to be the most feasible method, if applied carefully in the very clear atmospheric conditions.

INSTRUMENTS USED IN THE CALIBRATION EXERCISE

Two handheld Sunphotometers (Microtops®, manufactured by Solar Light Inc., USA) were used in this study. One of them, which is ten year old is to be calibrated, and is configured to measure direct Sun radiation in five channels viz., 380nm, 440nm, 500nm, 675nm and 870nm with 2.4 nm (FWHM) band pass filters. And, the other is a well calibrated recent instrument (2012 make), which is taken as a standard reference for validation, configured with 380nm, 500nm, 675nm and 870nm, and 1020nm with the same bandwidth of 2.4nm (FWHM[1]). Pressure and temperature are also measured through in-built transducers, which are used in the molecular optical thickness calculations. These instruments have an uncertainty of ~ 0.02 in AOT measurements.

THE BASIC PHYSICS-PRINCIPLE

The guiding principle of Sunphotometer is the Beer-Bouger-Lambert's law. It describes the radiation passing from an atmosphere (plane parallel strictly (Brookes, 2008)).

$$I_\lambda = I_0 e^{-\tau./\cos(\theta)} \quad (1)$$

Where, ô is columnar optical thickness and è is the solar zenith angle (secant of which is also known as relative air mass). I_0 is the top of the atmosphere intensity, which is diminished to $I_{\ddot{e}}$, by the scattering and absorption by the molecules and aerosols in the atmosphere. The plane parallel assumption is true for higher altitude measurements, where local time changing drifts in atmospheric transmissions may be assumed to be negligible (Schmid and Wehrli, 1994).

METHODOLOGY

These Sunphotometers use an aerosol optical thickness calibration coefficient (AOT-CC) for each of the five channels. These represent the natural logarithm of the top of the atmosphere signal in millivolts (User guide, Microtops).

Langley method is traditionally used for Sunphotometer calibration, in which measurements are taken over a range of air masses on a clear day. Though, there are other methods, which were exercised for its calibration, for example: calibration using standard irradiance lamp (Schmid and Wehrli, 1994), general method of Forgan (1994), method of Lee, *et al*. (2010) etc.

Measurements were made at high altitude site Mt Abu (24.64ÚN, 72.77ÚE, and 1762m msl), Rajasthan for a period of consecutive 5 days in January 2012. The measurement timings were shortly after sunrise, this choice of time period gives a fast variation in airmass. It is assumed that, the atmosphere did not change with time (time of measurements ~ 2 hrs). The data collected as a function of time is represented as a Langley plots.

RESULTS

Following langley plots (Fig.1) shows the variation of the logarithm of the measured signal (in mV) with the airmass (i.e., the secant of the solar zenith angle).

Extrapolating the linear fit to this dataset to abscissa equal to zero provided the calibration coefficients. Following table shows the AOT calibration coefficients:

	AOT-CC-380nm		AOT-CC-440nm	AOT-CC-500nm		AOT-CC-675nm	AOT-CC-870nm
Old	6.383	5.535	6.221	7.149	6.923		
New	6.262	5.429	6.046	7.041	6.841		

Table 1. Aerosol Optical Thickness Calibration coefficients

New calibration coefficients were applied. Comparison of the spectral aerosol optical thicknesses with the calibrated instrument shows acceptable agreement (Figure 2) in band-870nm (within 14%), while the differences are large in the case of band-500nm & band-675 (within 19%), and worse in the case of band-380nm (~32%).

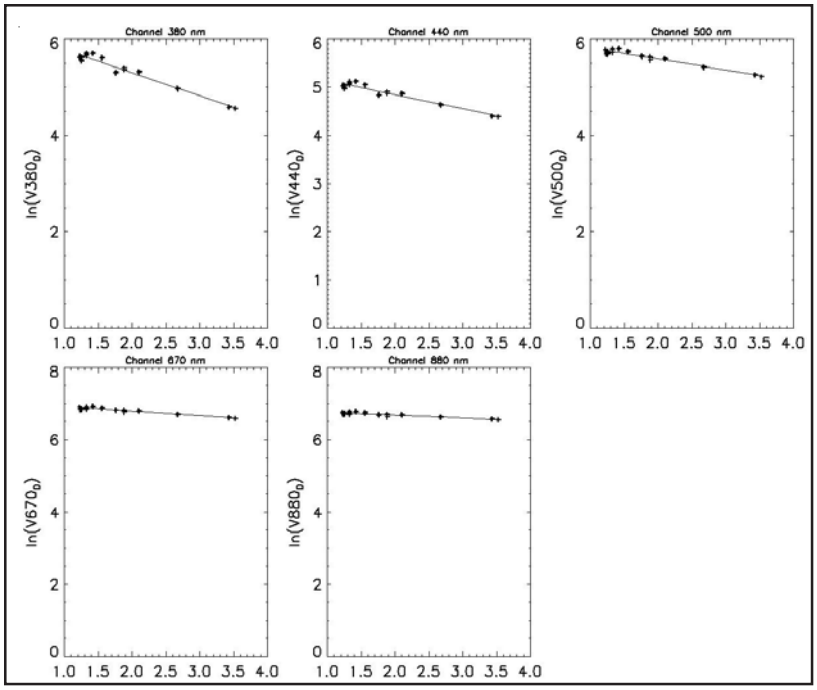

Figure 1 Langley plots for the different channels of the Sunphotometer, X-axis is the airmass (secant of the solar zenith angle) and Y-axis is the logarithm of the Sunphotometer measure signal in mV. Coefficients of determination (R^2) were 0.949, 0.916, 0.916, 0.871, and 0.791 respectively (from left to right).

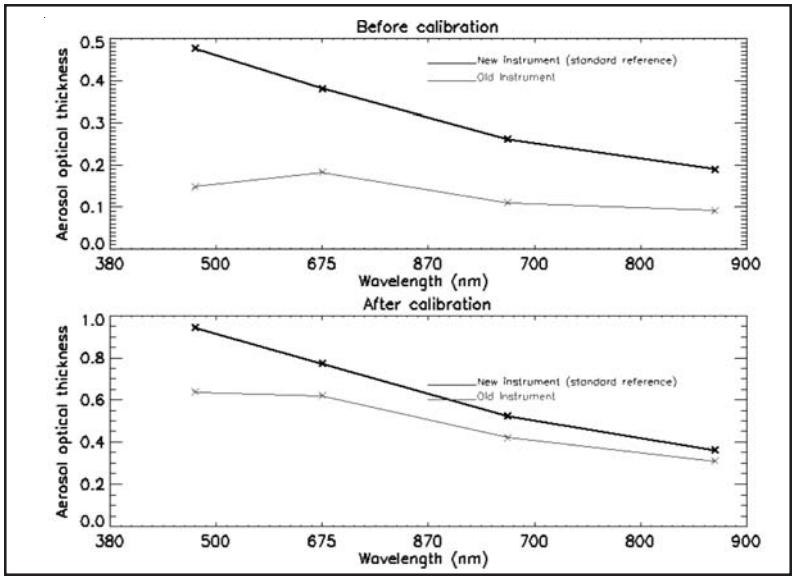

Figure 2 Comparison of Aerosol optical thickness measurements from both the instruments (before and after the calibration through Langley plot technique).

This large difference may be mainly contributed to the deterioration of the filters of the old instruments for these channels and needs replacements.

CONCLUSIONS

Langley technique has improved the calibration to a very good level, as in case of band-870nm, it has improved from the disagreement of 51% to an agreement of 14%. This method does not require any other equipment for its execution. For example, for lab calibration, one needs a standard source like integrating sphere. Hence, it can be safely said, that Langley method is the most feasible method, if applied carefully in the very clear atmospheric conditions.

ACKNOWLEDGEMENTS

Authors thank Shri, A S Kirankumar, Director, SAC, Ahmedabad for encouragement during the course of this work. We also wish to acknowledge Shri, Santanu Chowdhury, Deputy Director, SIPA and Shri, B Gopalkrishna, Group Director, SPDCG/SIPA for their continuous support and useful advice during the progress of this work. Authors wish to acknowledge Dr. S. G. Prabhu Matondkar of National Institute of Ocenography, Goa for his technical help and useful discussions. Authors also wish to thank Dr. K. N. Babu, CVD/MPSG/EPSA, SAC and Sri, Vaibhav Malhotra, IAQD/ SPDCG/SIPA for their full cooperation and technical discussions.

REFERENCES

Brooks, David R. (2008), Bringing the Sun down to earth, designing inexpensive instruments for monitoring the atmosphere, Springer Publication.

Covert, D. S., Charison, R.J. and Ahlquist, N.C. (1972). A study of the relationship of chemical composition and humidity to light scattering by aerosols, *Journal of Applied Meteorology,* **11**, pp. 968-976,

Forgan, Bruce W. (1994). General method for calibrating Sun photometers, *Applied Optics,* **33**, No. 21, pp. 4841-4850.

King, *et al.* (1978). Aerosol size distributions obtained by inversion of spectral optical depth measurements, *Journal of the Atmospheric Sciences*, **35**, pp. 2153-2167.

Lee, *et al. (2010).* Aerosol optical depth measurements in eastern China and a new calibration method, *Journal of Geophysical Research,* **115**, D00K11.

Rollin, E.M., An introduction to the use of Sun-photometry for the atmospheric correction of airborne sensor data, NERC EPFS, Department of Geography, University of Southampton, web – www.soton.ac.uk/~epfs.

Schmid, Beat, and Wehrli, Christoph (1994). High precision calibration of a Sunphotometer using Langley plots performed at Jungfraujoch (3580 m) and standard irradiance lamps, *IEEE Xplore*, pp. 2314-2316, 0-7803-1497-2/94.

Shaw, Glenn E. (1983). Sun photometry, Bulletin *American Meteorological Society*, **64**, No. 1, pp. 4-10.

Thome, K.J., Crowther, B. G., Biggar, S.F. (1997). Reflectance and Irradiance based calibration of Landsat-5 thematic mapper, *Canadian Journal of Remote Sensing,* **23**, No. 4, pp. 309-317.

User's guide Microtops II, Sunphotometer version 5.5, Solar Light Company, Inc.

IMPLEMENTATION OF RF NETWORK LINKAGE FOR AEROSOL SAMPLING SYSTEM

N. GOPALA KRISHNAN, V. SUBRAMANIAN, R. BASKARAN AND B. VENKATRAMAN

Radiological Impact Analysis Section, RSD, EIRSG, IGCAR

Keywords: AEROSOLS, SODIUM COOLED FAST REACTOR

INTRODUCTION

One of the important safety studies of Sodium Cooled Fast Reactor (SFR) is related to characterization of sodium burns and produces large amount of aerosols. These aerosols would get released through various ducts of Steam Generator Building (SGB) and dispersed in the atmosphere. Sodium aerosols assume various chemical species and the immediate manifestation of sodium aerosols is sodium hydroxide aerosols. In the postulated event of secondary loop leak, hot liquid sodium upon contact with atmosphere, is highly corrosive and produce severe health hazards to humans (TLV is 2 mg/ m^3). Hence it is essential to study the dispersion characteristics and ground level concentration of dispersed sodium aerosols along with its chemical composition reaching various locations in the downwind direction. Towards this, a collaborative study is planned with Fast Reactor Technology Group, IGCAR to burn the sodium in open atmosphere and determination of sodium aerosol characteristics that are dispersed in the downwind direction upto 1.5 km distance (distance of the site boundary). To accomplish the task, several sampling instruments like filter paper sampling system, chemical speciation system, high volume samplers, bag samplers, particle counters etc. will be deployed upto 1.5 km distance from the burning site. There are about 60 sampling stations identified for placing the above instruments. When more numbers of samplers are deployed, it needs to have synchronized operation among them to obtain co-related data (In our case, the first task is to start all the sampling units at a time). Synchronization between samplers could be obtained by various means. One method is by using real time clock (RTC) in each sampling unit and triggers the samplers with respect to the RTC. But it requires synchronization among the RTCs of all the sampling units and it is also very important to receive the on-line status of the samplers. Implementing RF control is the choice to simultaneously trigger, acquire and visualize the status of all the samplers from a control node. This article deals with a ZigBee based wireless network implementation for the sampling systems.

DESCRIPTION

The block diagram of a networked sampling system is shown in Fig.1. It is divided into five parts.

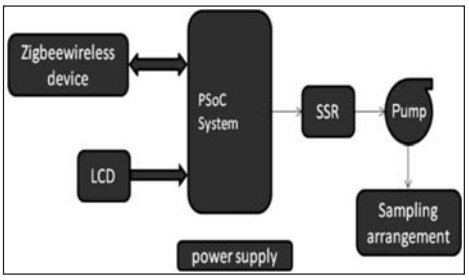

Figure 1. Block diagram of the sampling system

Part 1 consists of sampling manifold (filter paper head / liquid sampler) coupled with pump. Part 2 consists of Solid State Relay to switch on and switch off the pump. Part 3 consists of PSoC controller. This is the heart of the sampling system. The control of the components and communication protocols are implemented with a PSoC controller. An LCD display interfaced with PSoC will indicate the status of the process. The fourth part is ZigBee RF module which enables RF linking with control node. The fifth part is the power supply source. A brief content of the system building blocks and control node are described below:

PSoC™ (Programmable System on Chip)

The PSoC™ family consists of many mixed Signal Array with On-Chip Controller devices. These devices are designed to replace multiple traditional MCU-based system components with one, low cost single-chip programmable device. PSoC devices include configurable blocks of analog and digital logics, as well as programmable interconnects. This architecture allows the user to create customized peripheral configurations that match the requirements of each individual application.

The ZigBee RF device

ZigBee is wireless communication protocol, based on IEEE802.15.4 standard for personal area networks. It is low cost, low power RF device suitable for embedded applications. It uses unlicensed band of 2.4GHz (worldwide), with sixteen channels. Its channel access mode is CSMA-CA (carrier sense, multiple access/collision avoidance). The ZigBee devices consist of three modules viz. (i) Co-coordinator, (ii) Router, and (iii) End device. The Co-coordinator creates and manages the network. The Router communicates data between two devices separated by distance. The End device is a node where applications are implemented like control and collection of data.

Control Node

The Control Node is a laptop computer and a ZigBee RF device. The control node programs are written in LabVIEW 7.1 software. The screen shot of the control panel is shown in Fig.2.

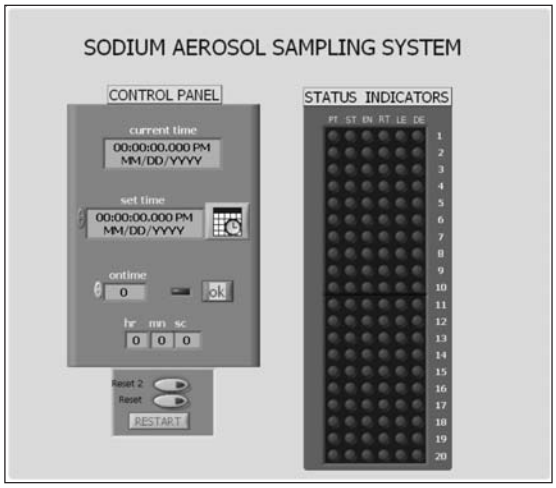

Figure 2. LabVIEW GUI for control node

As stated earlier, the first step in the programming is to synchronize the program control with RTC of the computer. Once live time is synchronized in the program, the other parameters incorporated with the program are (i) starting time and (ii) the duration of the sampling. These parameters are to

be given as the input by the user and they are set from the dials provided in the Graphical User Interface (GUI). On pressing the confirmation key the set parameters are encapsulated and broadcasted from the control node to the samplers' nodes by means of RF devices attached on both ends (one at the control node and the others at the sampling systems i.e. it can be one to many). The PSoC controller in the sampling systems decodes the encapsulated information and operates the sampler accordingly. The most important part of the networking is live information of status of the sampling system. To get this task, programming has been done such that, coordinator of the control node sends the query commands to the samplers sequentially to know the status of the samplers. The status of samplers are acquired back by the control node and displayed on the GUI as soft LED indications. During the polling of samplers, the status LEDs is refreshed with the current status of the sampler.

The status indicator in the control panel has been devised as a matrix with 6 columns and as many as rows equal to that of number of sampling systems. The six parameters described on the columns, about sampling systems at the GUI, to indicate (i)Waiting to start sampling, (ii) Sampling started, (iii) Sampling has completed, (iv) Reset state, (v) Link error and (vi) Re-send status. Waiting to start sampling ('PT') is 'on' duringcount-down period to start the sampling system. The sampling started indication ('ST') glows when the sampling process started by issuing command from PSoC control circuit in each sampler to put on the pump. This is an indication of successful triggering of the samplers. The end of sampling is indicated by 'EN' status indicator. If RF communication fails due to any reason then the link error ('LE') status indicator glows. The 'DE 'status indicator is due to data send error, which glows when there is a failure in delivery of time data to the sampler and the sampler is not started. This may occur when power failure occurs in the local sampling system. Once it is corrected, the control node attempts to initiate the sampler by re-sending the time data automatically, synchronizes the clock with real time clock and system will be put-on. Also when there is a power supply failure during the sampling and consequently if it is corrected, then control node automatically starts the sampling system and run it till the complete duration of the sampling period. The reset key in the GUI is provided to terminate the sampling process intermittently when required.

TESTING

The photograph of the control node and Aerosol Sampling System is shown in Fig. 3. The RF linked aerosol sampling system was tested upto 100m distance in the area near to lab.

Figure 3. Photograph of the control node and the sampler system

The control node program is loaded in a laptop computer and attached with the ZigBee module. The operating parameters are set in the GUI of the control node and the samplers are triggered and various status conditions are tested. The link error was generated by putting off the power supply in some sampler nodes. By restoring the power, the particular samplers are reinitiated by the control node with the operating parameters derived from the current time of the control node.

SUMMARY

The important task in this type of field study is virtual instrumentation and mesh communication. The task is accomplished with ZigBee mesh network and LabVIEW design platform. The successful operation of the aerosol sampling system has been demonstrated. The testing of sampler for long range communication is under progress.

REFERENCES

www.cypress.com/?id=1353

www.digi.com/de/products/wireless/zigbee-mesh/xbee-zb-module#overview

ftp://ftp1.digi.com/support/documentation/90000976_F.pdf

LabVIEW™ User Manual

A NEW DEVICE FOR FAST MEASUREMENTS OF NANOPARTICLE SIZE DISTRIBUTIONS

M. PESCH[1], H. GRIMM[2], L. LECK[3] AND M. RICHTER[4]

[1]GRIMM Aerosol Technik GmbH & Co. KG, Dorfstrasse 9, D-83404 Ainring, Bayern, Germany

Keywords: NANOPARTICLE SIZE DISTRIBUTIONS, FAST AEROSOL PARTICLE EMISSION SPECTROMETER, AUTOMOTIVE, DIFFERENTIAL MOBILITY ANALYZER

INTRODUCTION

Grimm has re-engineered the Fast Aerosol Particle Emission Spectrometer (FAPES) for fast measurements of nanoparticle size distributions in the range of 6.3 – 474 nm. The instrument comprises an integrated hot diluter and is particularly designed for measurements of combustion particles and for automotive applications.

METHODS

The FAPES system has three unique features (Fig. 1). Firstly, it employs a strong bipolar charger (241-Am á-emitter) for establishing a well defined equilibrium charge distribution. Unlike for unipolar chargers, even the larger particles feature a low apportion of multiple charged particles and the different size fractions have well distinguishable mobilities. These two features are the base for an accurate reconstruction of the particle size distribution.

Secondly, the charged particles are classified with twelve individual Differential Mobility Analyzers (DMAs) of Vienna type design operated in parallel. The signal of each size channel originates from a single DMA and corresponds thus to a well defined and narrow size range. This well proven principle of size classification makes the FAPES a reference for fast particle sizers. Unlike for SMPS systems, each DMA voltage is kept constant and thus the sampling frequency is no longer limited by the scan-time for the DMA voltage. The 12 DMA voltages cover the broad range of 5 to 10000 V and the voltages of adjacent DMAs differ by a factor two to ease the correction of remaining multiple charged particles.

Thirdly, the detection of particles is accomplished with twelve Faraday Cup Electrometers (FCEs), one FCE for each DMA, and spatially separated from the mobility analyzing section. Therefore, the detected currents are unaffected from any variations of the high voltage and the FCEs feature a very low noise level. Due to the rinse air, the FCEs have a fast response time of T10-90 = 200 ms, which is the base of the fast overall response time of the FAPES (T10-90 = 0.7 s). The use of rinse air has a second advantage, namely to prevent contaminations on the isolation of the detection electrodes and thus leakage currents. In other products for fast measurements of nanoparticle size distributions, leakage currents between electrodes can degrade the size resolution in the course of the measurements, and cleaning of the surfaces is required. Such leakage current can be a major problem particularly for the measurement of engine exhaust because the soot particles are conducting. The FCE signals are insensitive to mechanical shocks and vibration.

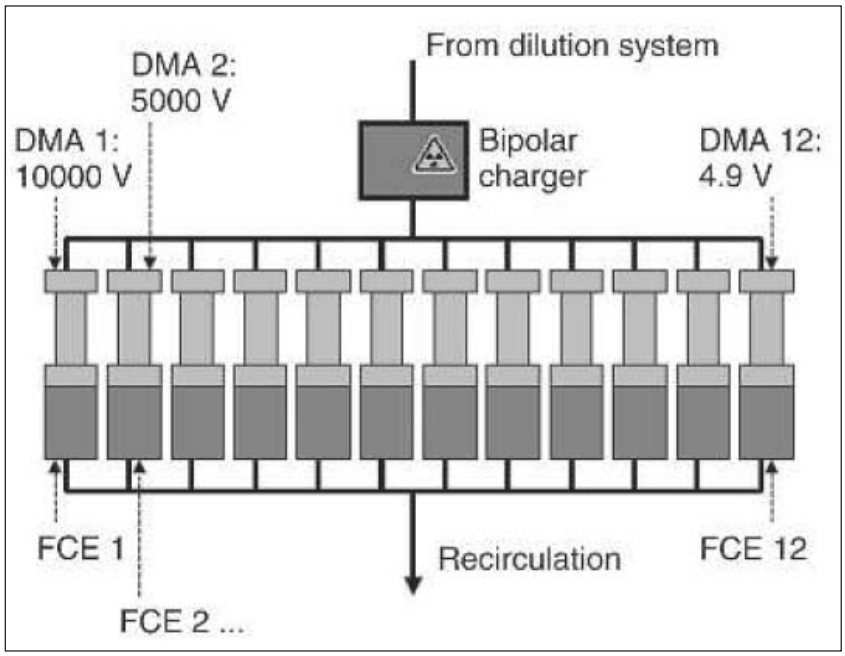

Figure 1. Principle of the FAPES

The concept of the sampling system is too "freeze" the state of the particles in the exhaust gas and to stabilize their condition for the analysis. This is achieved with a special integrated sample conditioning system with a heated dilution (temperature up to 500°C) right after the sample inlet. The diluter uses recycled sample air to achieve a variable dilution ratio of 1:5.7 – 1:40 in 7 steps. The recycled sample air is filtered, dried, and purified from organic gases with active carbon.

CONCLUSIONS

The main application of FAPES is measuring the particle size distributions in engine exhaust gas with high time resolution. As particle formation is connected to the fuel combustion process, such investigations can be used to optimize the efficiency of car engines. Moreover, they may assist the achievement of compliance with the new EURO5/6 regulations, which include a limit for particle number concentrations emitted by diesel and gas engines. The system is, however, also suitable for the fast measurements of size distributions at other applications. Monitoring the size of engineered nanoparticles in airborne state, nucleation events in industrial processes, or measurements in turbine exhaust are just examples.

NEW PORTABLE DEVICE FOR HIGH TIME RESOLVED MEASUREMENTS OF PARTICLE SIZE DISTRIBUTIONS

MARKUS PESCH, HANS GRIMM, DANIEL HUHN, MATTHIAS RICHTER

Grimm Aerosol Technik GmbH & Co. KG, 83404 Ainring, Germany
Keywords: aerosol instruments, Nano particles, particle size distributions, work place measurements
E mail: mp@grimm-aerosol.com

Measurements of particle size distributions for Nano particles and particles in the µ-meter size range generally requires a combination of separated devices as SMPS and optical particle counters (OPC) or aerodynamic particle sizers (APS). The company GRIMM developed in the frame of the EU founded Project NANODEVICE a new compact and portable (pre)-prototype that consists of an optical and electrical sensor in one device. It allows a wide range of particle size detection between approx. 10 nm and 20 µm with over 30 size channels with a time resolution of one complete scan of only 1 minute. Thus very short-lived as well as highly time-varying particle sources can be examined. Fig. 1 shows the new prototype.

Figure 1. New prototype for particle size distributions

The measured values of the two sensors are combined internally by a special electronics and firmware, such that the user receives measurements, which do not differ from the output of a single sensor in the nature and structure. The calculation of the derived measures as particle surfaces and particle volumes is done online and the output as data telegram is send via the interfaces Bluetooth or RS232. Special control software was developed, which allows full operation with a small Netbook. Fig. 2 shows a typical measurement example.

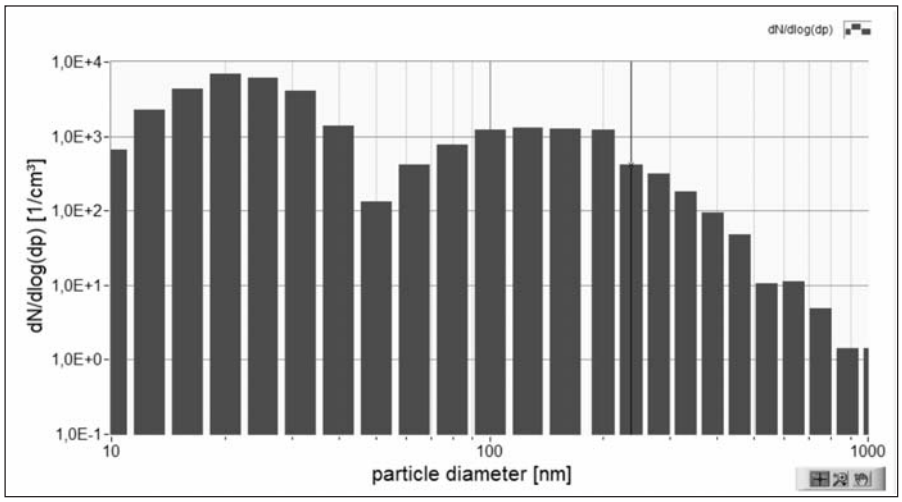

Figure 2. Measurement example

The optical module is a newly designed particle spectrometer, which detects each individual particle and classifies its size accordingly (single particle counting).

A powerful laser diode is used as a light source. An internal monitor diode monitors the power of the laser diode and keeps it constant. A pin diode generates the detection signal, which turned out to be the best compromise between reliability and performance. The number of particles is determined by the number of stray light pulses per period, the particle size determines the amplitude of the scattered light. These measurements require a precisely controlled flow rate which is determined continuously via aperture and pressure sensors.

The electrical module consists of three main components, the unipolar corona charger, a precipitation electrode and a Faraday Cup Electrometer (FCE). Once the aerosol particles (each single particle) are counted by the optical sensor and classified, they go through a short tube connected directly to the electrical sensor. Here all Nanoparticles can be reliably detected. Initially the particles are charged unipolar (negatively) in the electric sensor with a negative corona charge. Then the particles go into a collecting electrode, where they are separated according to their electrical mobility. A portion of the aerosol stream passes through the collecting electrode and is recorded in the Faraday Cup Electrometer (FCE). Based on the current measured at the FCE, the volume flow, the geometry of the sensor and the charge efficiency of the particles, the size of the particles can be determined. The electrical sensor offers the possibility to determine the number of particles of a size distribution of particles similar to the optical sensor: A change of the electrode voltage in 10 steps classifies the particle size between 10 nm to approximately 300 nm in 10 classes.

When measuring particles humidity plays an important role. On the one hand, increased air humidity leads to a swelling of particles, which alters their diameter, on the other hand charges of particles change with air humidity. In addition, the determination of currents with an FCE is very sensitive to moisture and cause changes in the offset. To ensure reliable operation at varying humidity levels and to permit very high humidity (up to 90%), an internal drying cycle was designed. The FCE is continuously purged with dry air, dried through a cartridge filled with silica gel.

They calibration and validation is based on parallel SMPS measurements with latex particles of different sizes.

AEROSOL REMOTE SENSING

HETEROGENEITY IN THE VERTICAL DISTRIBUTION OF AEROSOLS OVER DIBRUGARH

B. PATHAK AND P. K. BHUYAN

Centre for Atmospheric Studies, Dibrugarh University, Dibrugarh-786004, Assam, India

Keywords: LIDAR, AEROSOL, EXTINCTION COEFFICIENT, DEPOLARIZATION RATIO

INTRODUCTION

Atmospheric aerosols play an important role in the global climate system and introduce large uncertainties in climate modelling (IPCC, 2001).Assessments of aerosol models have to date focused primarily on comparing estimates of column integrated aerosol optical depth (AOD) with satellite retrievals and/or ground-based measurements of AOD. However, AOD alone does not provide enough information to resolve several specific model deficiencies. The lack of a climatological database to characterize the vertical distributions of aerosols has hampered efforts to evaluate and consequently improve such models. The verticaldistribution of aerosols assumes significance while addressingthe radiative impact due to aerosols (Satheesh, *et al*., 2009). However, it is difficult to characterize aerosol extinction since few data sets provide extinction profiles with ample spatial and temporal coverage. In the Indian subcontinent information on vertical distribution of aerosol was initiated at Pune by Devara, *et al*., (2002) using groundbased LIDAR. Other studies include those carried out over the south central India, Visakhapatnam and Kharagpur, Hyderabad, Ahmedabad, Near Delhi (Gual Pahari) etc. (Komppula, *et al*., 2010 and references therein). Several investigators across the Indian subcontinent have reported presence of the elevated aerosols layers resulting from the transportation of aerosols from different sources during the pre-monsoon period (March-May) (e.g. Niranjan, *et al*., 2007; Satheesh, *et al*., 2006, 2009; Gautam, *et al*., 2010). Vertical profiling of aerosols assumes further importance in view of the reported elevated heat pump effect and from the point of view of Asian summer monsoon.

In this report the vertical distribution of aerosols over Dibrugarh (27.3ºN, 94.6ºE, 111 m amsl) has been studied in order to further investigate the observed heterogeneity between surface and columnar aerosol properties (Gogoi, *et al*., 2011) and to understand the elevated heat pump effect with respect to the occurrence of the summer monsoon.

METHOD

A dual channel polarization Nd-YAG Micro Pulse LIDAR (MPL) operating at 532 nm (Foretech Systems PTE LTD, Singapore) is being used for the direct observation of the vertical distribution of aerosols. Data for the period Monsoon 2010 to Premonsoon 2012 have been utilized in the present study.

RESULTS AND DISCUSSION

Vertical distribution of aerosols is essential for more accurate knowledge of perturbation induced by aerosols on climate. Typically the vertical aerosol distribution over Dibrugarh is inhomogeneous in nature with variable extinction coefficient values with height and time. Time evolution of extinction coefficient value during 1900-2030 hours for 26 May 2012 is shown in Fig. 1. Though for most of the profiles extinction coefficient is of exponential decay type, in some profiles elevated layers are also

observed. Typical vertical extinction coefficient profiles without and with presence of elevated aerosol layer on two representative days viz. November 3, 2010 and February 27, 2012 respectively are shown in Figure 2 (a) and (b). The extinction profiles showed an increase in extinction from the surface with altitude up to a maximum extinction within the region ~0.8-1.3 km. Similar extinction profiles with gradual increase in extinction coefficient upto mixing layer height have been reported by Ramana and Ramanathan (2006) over island of Hanimaadhoo in Maldives and by Minvielle, *et al*., (2004) over Goa. This peak region above ground level is most likely due to local emissions of pollutants trapped within the boundary layer. On November 3, 2010 (Fig. 2) the extinction profile after peaking within ~0.8-1.3 km

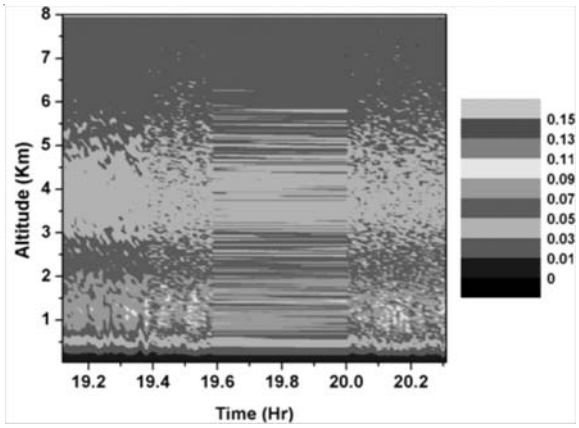

Figure1.Temporal extinction profile during 1900-2030 hours on 26 May 2012.

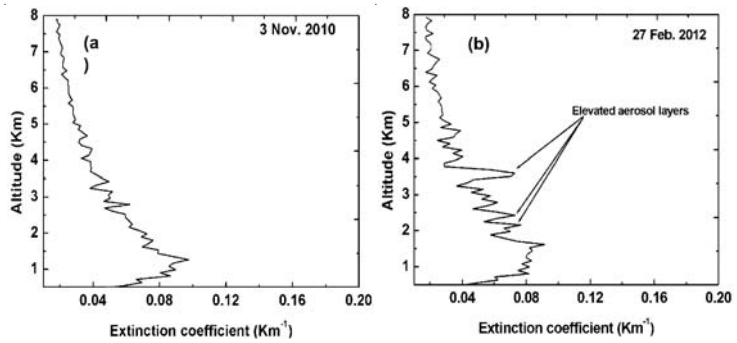

Figure2.Vertical profiles of Extinction coefficient (km^{-1}) for (a) 3 Nov, 2010 and (b) 27 Feb. 2012.

decays exponentially towards higher altitudes. But on February 27, 2012 (Fig. 2b) multiple aerosol layers have been observed at higher altitudes between ~2-4 Km. Since 27 February 2012 is nearly at the onset of pre-monsoon season (March-May), these elevated layers may be associated with the dry convective lifting of pollutants at distant sources and subsequent horizontal upper air long- range transport as well as forest fire taking place in nearby hilly regions, which are maximum during this season (Badarinath, et al. 2004). Such profiles are available for some other days of the pre-monsoon season also. This observation of elevated aerosol layers during the onset of the pre-monsoon season is consistent with the observed aerosol layer within 3-5 km in pre-monsoon season over North-eastern India by Sharma, *et al*. (2009). On the other hand the normal distribution of aerosols in the vertical column (Fig. 2a) is associated with the background aerosol environment in the post-monsoon

(Pathak, *et al*., 2012). The annual variation in extinction coefficient shows maximum within 1-2 km in all the months with highest variability in January and lowest variability in September (Fig. 3).

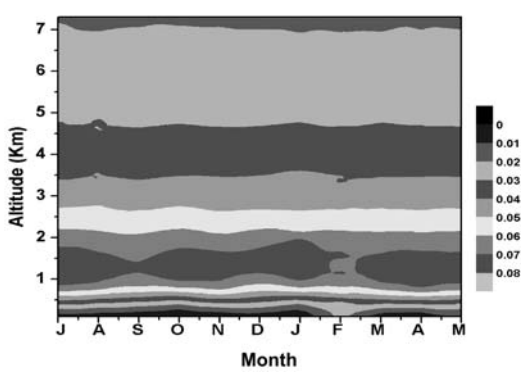

Figure3. Annual variation of extinction coefficient profiles from July-May (data for the month of June is absent).

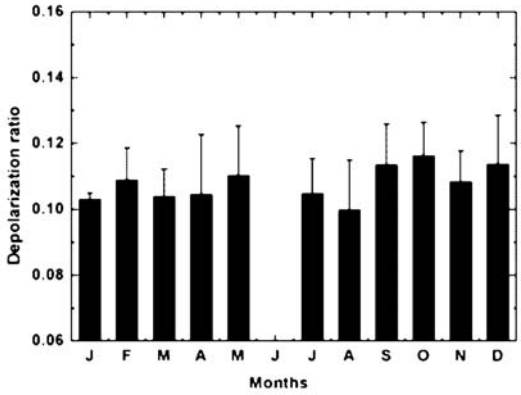

Figure.4. Annual variation of MPL derived depolarization ratio for the period July, 2010-May, 2012.

The Volume Depolarization Ratio (VDR) derived from the extinction coefficient values is a good proxy to distinguish between spherical (e.g. sulfate) and non-spherical (e.g. cloud droplets, dust) aerosols. Higher value of VDR implies greater amount of non-spherical particles in cloud free conditions. The VDR for smoke and pollution aerosols are normally small because of small size of soot particles, although soot particles are non-spherical. Figure. 4 shows that the annual variation of VDR over Dibrugarh derived from MPL for the period July, 2010- May, 2012. The VDR values are below 0.15 throughout the observation period. Gautam et al., (2009) have reported significant amount of dust loading over IGP based on VDR values which is >0.15 during pre-monsoon season. Kharol, *et al*. (2011) have reported the depolarization ratio values of <0.15 over Indo Gangetic Plains and Bay of Bengal due to presence of pollution and fine mode aerosols during winter season. VDR lying within 0.01-0.15 suggests the contribution of local anthropogenic pollution mixed with dust (Gautam, *et al*., 2009). Thus it can be concluded that over Dibrugarh the aerosols present in the atmospheric column are either fine biomass burning aerosols or the anthropogenic pollution.

CONCLUSION

The vertical distribution of aerosols derived from MPL is found to be inhomogeneous with altitude

and time. Seasonal variability in the distribution is prominent with presence of elevated layers occasionally, particularly in winter and pre-monsoon seasons. VDR values <0.15 suggests fine mode aerosol contribution over the location.

ACKNOWLEDGEMENTS

The work was carried out with support from the ISRO-GBP-ARFI project. Binita Pathakis indebted to ISRO for providing her fellowship.

REFERENCES

Badarinath, *et al.* (2004).Characterization of Aerosols from Biomass Burning – A case Study from Mijoram (Northeast) India, *Chemosphere*, **54 (2)**, pp. 167-175.

Devara, P. C. S., Maheskumar, R. S., Raj, P. E., Pandithurai, G., and Dani, K. K. (2002). Recent trends in aerosol climatology and air pollution as inferred from multiyear LIDAR observations over a tropical urban station, *Int. J. Climatol*., **22**, pp. 435–449.

Komppula, *et al.* (2010). One year of Raman-lidar measurements in Gual Pahari EUCAARI site close to New Delhi in India: seasonal characteristics of the aerosol vertical structure, *Atmos. Chem. Phys. Discuss*., **10**, pp. 31123–31151.

Gautam, R. N., Hsu, Christina and Lau, K.M. (2010). Premonsoon aerosol characterization and radiative effects over the IndoGangetic Plains: Implications for regional climate warming, *J. Geophys. Res*,**115**, D17208.

Gogoi et al. (2011). Multi-year investigations of near surface and columnar aerosols over Dibrugarh, north-eastern location of India: Heterogeneity in 845 source impacts, *Atmos. Env*., **45**,pp.1714-1724.

Minvielle et al. (2004). Modelling the transport of aerosols during INDOEX 1999 and comparison with experimental data—1: carbonaceous aerosol distribution, *Atmos.Env.***38**, pp. 1811–1822.

Niranjan, K., Sreekanth, V., Madhavan, B. L. and Krishna Moorthy, K. (2007).Aerosol physical properties and Radiative forcing at the outflow region from the Indo- Gangetic plains during typical clear and hazy periods of wintertime, *J. Geophys. Res*, **34**, L19805.

Pathak, B., Bhuyan, P. K., Gogoi, M. M., Bhuyan, K. (2012).Seasonal heterogeneity in aerosol types over Dibrugarh-North-Eastern India, *Atmos. Env.*,**47**, pp. 307-315.

Ramana, M. V. and Ramanathan, V. (2006). Abrupt transition from natural to anthropogenic aerosol radiative forcing: Observations at the ABC-Maldives Climate Observatory, *J.Geophys. Res*, **111**, D20207.

Satheesh, S. K., Vinoj, V., and Moorthy, K. K. (2006). Vertical distribution of aerosols over an urban continental site in India inferred using a micro pulse LIDAR, *Geophys. Res. Lett.*,**33**, L20816.

Satheesh, S.K., et al.(2009). Vertical structure and horizontal gradients of aerosol extinction coefficients over coastal India inferred from airborne LIDAR measurements during the integrated campaign for aerosol, gases and radiation 41 budget (ICARB) field campaign, *J.Geophys. Res*, **114**, 921 D05204.

Sharma, A. R., Kharol, S.K., Badarinath, K.V.S. (2009).Satellite observations of unusual dust event over north-east India and its relation with meteorological conditions, *J. Atmos. Solar-Terrest.Phy*.,**71**, pp. 2032-2039.

AEROSOL OPTICAL AND RADIATIVE PROPERTIES OVER NORTH-EAST INDIA DERIVED FROM MODIS AND CERES

B. PATHAK, J. BISWAS AND P. K. BHUYAN
Centre for Atmospheric Studies, Dibrugarh University, Dibrugarh 786 004, India

Keywords: AEROSOL, SWARF, MODIS, CERES

INTRODUCTION

The surface reaching solar radiation is a key component of the net radiation balance at the surface determining the regional climate. Since the middle of the twentieth century surface reaching solar radiation has undergone decadal variations in many parts of the world leading to global dimming up to 1990 (Liu, *et al*., 2004; Stanhill and Cohen, 2001) and brightening after 1990 (e.g., Wild *et al*., 2005). However, at few regions continuous dimming is observed (Che *et al*., 2005; Padma Kumari, et al., 2007). It is believed that solar dimming is caused by the aerosols through their direct and indirect effects. Aerosols participate in the Earth's energy budget directly by scattering and absorbing solar radiation (e.g., McCormick and Ludwig, 1967) and indirectly by acting as cloud condensation nuclei and thereby aecting cloud microphysical and radiative properties (e.g., Gunn and Phillips, 1957), with feedbacks to the hydrological cycle (e.g., Lohmann and Feichter, 1997). A significant continued dimming has also been observed over India under all sky conditions (Padma Kumari, *et al*., 2007; Ramanathan, *et al*., 2005), where aerosols and clouds together contributed to the annual trend. Decrease in surface solar radiation may lead to decrease in evaporation and slowdown of the monsoon hydrological cycle (Wild, *et al*., 2005; Ramanathan, *et al*., 2005). This observation of significant decreasing trend of surface reaching solar radiation has important implications on the role of aerosols relative to that of green house gases on the regional monsoon climate especially in the context of observed increasing trend of surface temperatures over the region (Kothawale and Rupa Kumar, 2005). Current global radiative balance estimates attribute to the atmospheric aerosols a negative forcing comparable and opposite to the one of greenhouse gases (e.g. Penner, *et al*., 2001). Due to large uncertainty in global distribution and mixing states of aerosols, knowledge on its direct radiative forcing is limited to a large extent. This is also due to large heterogeneity in aerosol properties and inadequate data from regions of interest. For example, high population density and resultant anthropogenic action in the South and South-east Asia including the Indian subcontinent might greatly contribute to the alteration of earth's radiation budget. As such characterization of atmospheric aerosols from the location like north-eastern part of India, which is unique owing to its unique topography (Gogoi, *et al*., 2011, Pathak, *et al*., 2012) would add up to the knowledge of regional picture of aerosol radiative forcing. Earlier Pathak, *et al*., (2010) have estimated the aerosol radiative forcing over Dibrugarh, but information from only one location is not enough to provide the regional ARF and impact of aerosols on climate.

The present work aims to study the optical properties and hence to assess the radiative impacts of the complex aerosol system over the north-east Indian region using MODIS and CERES satellite observations.

STUDY LOCATION AND DATA

The North Eastern (NE) region stretches between 22°N and 30°N latitude and 88°E and 98°E longitude. The region comprises of the states of Arunachal Pradesh, Assam, Manipur, Nagaland,

Mizoram, Sikkim and Tripura with about 72% area under hilly ecosystems. Rocky surface, alpine vegetation and snowcapped high peaks dominate the physical landscape of this area. The North-East India receives highest rainfall every year during the monsoon (June-September) season. Due to high rainfall the NE region is clothed with diverse and dense vegetation.

The data set utilized includes the Aerosol optical depth (AOD) obtained from the Moderate-Resolution Imaging Spectro-radiometer (MODIS) instruments and the Clouds and the Earth's Radiant Energy System (CERES) derived short wave top of the atmosphere (TOA) radiative flux for the year 2011. The CERES instrument onboard Terra satellite makes broadband radiance measurements (Wielicki, *et al*.,1996) at the TOA, both in the longwave (LW) and shortwave (SW) region. The CERES instrument has three channels – a SW channel for measuring reflected sunlight (0.3 – 5 μm), an infrared (IR) channel (8 –12μm) for measuring Earth-emitted thermal radiation "window" region, and a total channel (0.3 – 200 μm) for total radiation measurement. The well-calibrated radiance measurements are then converted to reflected and emitted fluxes using angular dependence models (e.g., Loeb, *et al.,* 2003).

RESULTS AND DISCUSSION

The Fig. 1 shows the annual variation of average AOD over the NE region (22ºN-30ºN, 88°E-98°E). In general, AOD is highest during the pre-monsoon season (March-May) varying between 0.49±0.28 in April and 0.37±0.25 in March and lowest in the post-monsoon season (October-November) with average value 0.26±0.04. Considerable spatial variability of AOD within the study region is noticeable from the length of the bars representing the standard deviations. This observation is analogous to the observed AODs over Dibrugarh, a location within this region (Gogoi, *et al*., 2009; Pathak, *et al*., 2012).

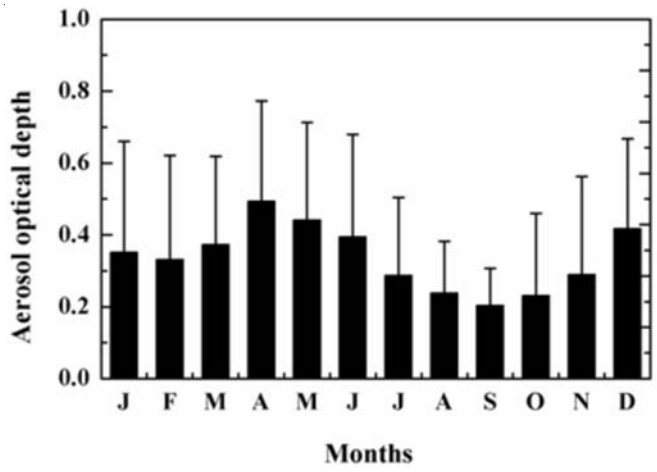

Figure 1.The spatio-temporal variability of mean aerosol optical depth over north-east India.

Higher AOD in pre-monsoon may be attributed to the highest biomass burning taking place in the NE region during March-April which is associated with shifting cultivation practices. Again long range transportation of mineral dust from the arid regions of west Asia and north-west India across the Indo-Gangetic plain (IGP) (Gogoi, *et al*., 2009) is another probable reason for the observed higher AOD in pre-monsoon. This observed highest AOD in pre-monsoon season is very important in the context of the "Elevated Heat Pump Effect" as explained by Lau, *et al*., (2008), which is

based on the enhanced buildup of aerosols over IGP during pre-monsoon season transported from western arid/desert regions such as the Arabian Peninsula and Thar Desert. The lowering of aerosol loading in monsoon is associated with wet removal process. The lowest AOD observed in post-monsoon could be attributed to the combined effect of local meteorological conditions and topography of the region (Gogoi, *et al*., 2011). Aerosol loading starts to build up by end of post- monsoon leading to continued high AODs in winter. Also, scanty rainfall results in longer residence time of aerosols in the atmosphere resulting in comparable high AOD during this season.

The shortwave aerosol radiative forcing (SWARF) in cloud-free sky conditions, is defined as the difference in TOA shortwave fluxes from the CERES in the absence (F_{clr}) and in the presence (F_{aero}) of aerosols (SWARF = F_{clr} - F_{aero}). F_{clr} i.e. flux in zero AOD conditions are derived from the y-intercept of the regression line between all AOD_{MODIS} and TOA CERES SWF for each latitude-longitude grid

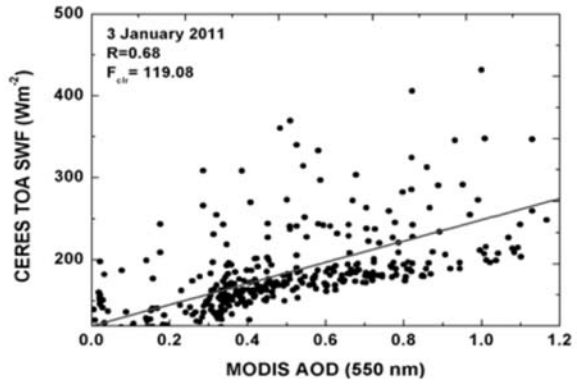

Figure 2. Example of regression between CERES top of atmosphere shortwave fluxes and MODIS AOD (550nm) used to estimate F_{clr} for 3rd January, 2011.

following Patadia, *et al*., (2008). F_{clr} is computed only if number of data points within a grid is >10 and positive correlation exists (r>0.2) between SWF and $AOD_{MODIS.}$ Figure 2 shows an example of regressions used to estimate F_{clr} for 3rd January 2011. Negative slope indicates scattering and positive slope indicates absorption by aerosols. The annual mean F_{clr} varies from ~136 Wm^{-2} in January to 283 Wm^{-2} in July. On the other hand F_{aero} varies between 146 Wm^{-2} in February to 284 Wm^{-2} in June. Thus the regionalaverage instantaneous TOA SWARF varies from~ -37.5 Wm^{-2} in pre-monsoon to ~2.3 Wm^{-2} in post-monsoon season with annual mean ~ -19Wm^{-2}. This observation of seasonal instantaneous TOA SWARF is analogous to the observed diurnal TOA SWARF over Dibrugarh, a location in NE India by Pathak, *et al*., (2010). Patadia, *et al*., (2008) have reported instantaneous flux of -13.05±3.9 Wm^{-2} averaged for the years 2000-2005 over Amazonia. The uncertainty in estimated F_{clr} is found to be 1.8 Wm^{-2} from the maximum uncertainty in MODIS AOD of ±0.05 over land and mean TOA instantaneous aerosol radiative forcing efficiency of -35 $Wm^{-2}\tau^{-1}$. Further uncertainties in SWF that arise from the unfaltering of SW radiances and the radiance to flux conversion using Angular Distribution Model are discussed by Loeb and Kato, (2002).

CONCLUSIONS

The optical properties and radiative impacts of the complex aerosol system over the north-east Indian region have been assessed using MODIS and CERES satellite observations. Large temporal and spatial variability in optical and radiative properties have been observed.

ACKNOWLEDGEMENTS

The work is carried out with support from the ISRO-GBP-ARFI project. Binita Pathak and Jhuma Biswas are indebted to ISRO for providing them fellowships.

REFERENCES

Badarinath, *et al.* (2004).Characterization of Aerosols from Biomass Burning – A case Study from Mijoram (Northeast) India, *Chemosphere*, **54 (2)**, pp. 167-175.

Che, H. Z., et al., (2005). Analysis of 40 years of solar radiation data from China, 1961–2000, *Geophys. Res. Lett.*, **32**, L06803.

Gunn, R. and Phillips, B. (1957). An experimental investigation of the eect of air pollution on the initiation of rain, *J. Meteor.*, **14**, pp. 272-280.

Gogoi, M. M., Moorthy, K. K., Babu, S. S. and Bhuyan, P. K. (2009). Climatology of columnar aerosol properties and the influence of synoptic conditions: Firsttime results from the northeastern region of India, *J. Geophys. Res.*,**114**, D08202.

Gogoi, *et al.*, (2011). Multi-year investigations of near surface and columnar aerosols over Dibrugarh, North-Eastern location of India: Heterogeneity in source impacts, *Atm. Env*., **45**, pp. 1714-1724.

Lau, *et al.*, (2008). The Joint Aerosol-Monsoon Experiment: A new challenge for monsoon climate research, *Bull. Am. Meteorol. Soc*., **89**, pp. 369– 383.

Liu, B., Xu, M., Henderson, M., and Gong, W. (2004). A spatial analysis of pan evaporation trends in China. 1995–2000, *J. Geophys. Res*., **109**, D15102.

Lohmann, U. and Feichter, J. (1997). Impact of sulfate aerosols on albedo and lifetime of clouds: A sensitivity study with the ECHAM4 GCM, *J. Geophys. Res*., **102**, pp. 13 685–13 700.

Loeb, N.G., Manalo-Smith, N., Kato, S., Miller W. F., Gupta, S. K., Minnis, P., and Wielicki, B. A. (2003). Angular distribution models for top-of-atmosphere radiative flux estimation from the Clouds and the Earth's Radiant Energy System instrument on the Tropical Rainfall Measuring Mission satellite. Part I: Methodology, *J. Appl. Meteor.*, **42**, pp. 240–265.

Loeb, N. G., and S. Kato (2002).Top-of-atmosphere direct radiative effect of aerosols over the tropical oceans from the Clouds and the Earth's Radiant Energy System (CERES) satellite instrument, *J. Clim.*, **15**, pp. 1474– 1484.

Kothawale, D. R., and Rupa Kuma, K. (2005).On the recent changes in surface temperature trends over India, *Geophys. Res. Lett.*,**32**, L18714.

McCormick, R., and Ludwig, J. (1967). Climate modication by atmospheric aerosols, *Science*, **156** (3780), pp. 1358-1359.

Padma Kumari, B., A. L. Londhe, S. Daniel, and D. B. Jadhav (2007). Observational evidence of solar dimming: Offsetting surface warming over India, *Geophys. Res. Lett*., **34**, L21810.

Penner, J. E., et al., (2001). Aerosols, their direct effects, in climate change 2001: the scientific basis: Contribution of working Group I to the third Assessment Report of the Intergovernmental Panel on Climate Change, edited J. T. Houghton et al., (Cambridge University Press, New York), **chap. 5**, pp. 291-336.

Pathak, B., Bhuyan, P. K., Gogoi, M. M., Bhuyan, K. (2012). Seasonal heterogeneity in aerosol types over Dibrugarh-North-Eastern India, *Atmos.Environ*. **47**, pp. 307-315.

Pathak, B., Kalita, G., Bhuyan, K., Bhuyan, P. K. and Moorthy, K. K., (2010).Aerosol temporal characteristics and its impact on shortwave radiative forcing at a location in the North East of India, *J. Geophys.Res*., **115**, D19204.

Patadia, F., Gupta, P., Christopher, S. A., and Reid, J. S. (2008).A Multisensor satellite-based assessment of biomass burning aerosol radiative impact over Amazonia, *J. Geophys.Res.*, **113**, D12214.

Stanhill, G., and Cohen, S. (2001). Global dimming: A review of the evidence for a widespread and significant reduction in global radiation with discussion of its probable causes and possible agricultural consequences, *Agric. For. Meteorol*.,**107**, pp. 255–278.

Ramanathan, V., et al. (2005). Atmospheric brown clouds: Impacts on South Asian climate and hydrological cycle, *Proc. Natl. Acad. Sci. U. S. A*., **102**, pp. 5326–5333.

Wild, M., et al., (2005). From dimming to brightening: Decadal changes in surface solar radiation, *Science*, **308**, pp. 847–850.

Wielicki, *et al.* (1996). Clouds and the Earth's Radiant Energy System (CERES): An Earth Observing System Experiment, *Bull. Amer. Meteor. Soc.*, **77**, pp. 853-868.

STUDY OF VERTICAL DISTRIBUTION OF STRATOSPHERIC AEROSOL NUMBER DENSITY

A. VENKATESWARA RAO[a], PRATIBHA B. MANE[a], D. B. JADHAV[b],

a- Department of Physics, Shivaji University, Kolhapur-416 004, Maharashtra state, India.
b- Indian Institute of Tropical Meteorology, Dr. Homi Bhabha Road, Pashan, Pune-411 008, India.

Keywords**:** AEROSOLS, TWILIGHT PHOTOMETER, STRATOSPHERE, TSM.

INTRODUCTION

The stratospheric aerosols are studied by several workers in all over the world (Jadhav, *et al.*, 2000). In the present work aerosol measurements have been carried out at Kolhapur (16°422N, 74°142E) by using newly designed Semiautomatic Twilight Photometer during the period 1 January 2009 to 30 December 2011 to study the vertical distribution of the stratospheric aerosol number density per cm^3 (AND) (Here after aerosol number density per cm^3 is abbreviated as AND). The day to day variability of the vertical distribution of stratospheric AND, monthly and seasonal variations of stratospheric AND have been discussed in the present study. The stratosphere is the layer of the Earth's atmosphere situated about 17 to 50 kilometers above the Earth's surface.

INSTRUMENTATION

The instrument, **semiautomatic**twilight photometer, has been newly designed, developed and tested at IITM, Pune, India. The semiautomatic twilight photometer consists of a simple experimental set up. It comprises of a telescopic lens of diameter 15 cm having a focal length of 35 cm.amd a red glass filter peaking at 670 nm with a half band width of about 50 nm. The red filter of 2cm diameter and an aperture of 0.6 cm diameter are placed at the focal length of convex lens, provides approximately 1^0 field of view [(Aperture diameter/Focal length of lens) X57= (0.6cm/35cm) X 7=0.9771 degree]. A photomultiplier tube (PMT)-9658B is used as a detector. The PMT requires a high voltage i.e. 700Volts and hence a DC-DC converter (Powertex -061081001, High volt unit) with high output voltage is used as a power supply. The output signal (current) of the PMT, used for detecting the light intensity during the twilight period, is of the order of nano to microamperes. The amplitude or strength of this low signal is amplified by using newly designed fast pre-amplifier during this study. The more details regarding the instrument and Fast pre-amplifier were given elsewhere, (Mane *et al.*, 2012).The amplifier output recorded by the digital multimeter, Rishcom-100, having an adapter can store the data automatically for every 10secs in the form of date, time and intensity in Volts.

RESULTS AND DISCUSSION

The day-to-day, monthly and seasonal variability of 'AND' in lower stratosphere

Various types of variability of aerosol loading in terms of AND in between the altitudes 17 to 30 Km (lower stratosphere) are shown in Fig. 1. The figure shows day-to-day variability in lower stratospheric AND from 1 January 2009 to 31 December 2009 for morning observations. In this figure Y-axis represents aerosol loading (Q, calculated by equ.1) and X-axis represents day numbers (i.e. date for each month). The TSM data collection at Kolhapur is generally not possible during ~mid-May to ~mid-October in any year because of the prevailing monsoon conditions (rains and extensive cloud

cover). This being a passive technique, clear sky conditions are preferable for obtaining the vertical profile of aerosols. Thus data coverage is for the period ~mid-October of any year to ~mid-May of the succeeding year.

The aerosol number density was calculated by using an empirical formula derived by actual Lidar observations and Twilight Photometric observations as stated below:

Aerosol number density per dm^3

$$= \text{Antilog}_{10} \{10[\text{`-1/I (dI/dh)'}]-1\} \quad (1)$$

Where 'I' is the observed intensity, 'dI' and 'dh' are the differences in intensities and shadow heights, respectively observed at time't' and (t+dt).

The values of the aerosol loading factor 'Q' have been computed using equation (Jadhav and Londhe, 1992):

$$Q = \sum_{h1}^{h2} Aerosolnumberdensityper\ cubicdecimeter \quad (2)$$

In this equation h_1 and h_2 represents the lower and upper limits of the shadow heights respectively. The method for calculating the height of the earth shadow is given by Shah, (1970).

For studying the seasonal variations, the year is divided into four seasons as follows:
Monsoon or rainy season: Kolhapur city receives abundant rainfall (southwest summer monsoon) from June to September due to its proximity to the Western Ghats.
Post-monsoon season: This is lasting from October to November. These two months are usually cloudless and experience the dry northeast monsoon.
Winter season: Kolhapur experiences winter from December to February. Humidity is low in this season making weather much more pleasant.
Summer or pre-monsoon season: Kolhapur experiences summer from March to May.

The lower stratosphere (altitudes between 17 Km to 30 Km) showed day-to-day variability from October to May with highest aerosol loading (here after abbreviated as Q_1) in the month of March and lowest in the January. In the post-monsoon season the Q_1 started decreasing form mid-October to end of November. In winter the Q_1 started decreasing from early December to the mid-January (11 January 2009). This was the coldest period in the winter having lowest temperature ~14^0C. From 11th January Q_1 values increased up to end of the February. The atmosphere started warming in this period. Aerosol loading was highest in March, with many fluctuations due to frequently observed clouds. In the summer the Q_1 values started decreasing from end of the March through April up to May, at the face of arrival of south-west summer monsoon season. Deviations from this trend in March were observed for clear days in between cloudy days. Cumulous clouds were observed frequently in March 2009. There was no TSM data available after 15 May 2009 due to extensive cloud cover formed by the active phase of the south-west monsoon. The monthly and seasonal variability of AND (Q_1) obtained for very clear days in the present study are very well sound with the aerosol optical depth variations obtained at Mysore by Raju *et al.*(2000). Results got by Jadhav and Londhe, (1992) and Khemani, *et al.* (1985) are also very good agreements with the results of the present study.

This lower stratospheric aerosol loading showed opposite phase relation with that of tropospheric aerosol loading. Upward transport of aerosol from troposphere to stratosphere takes place in the months of January to March; whereas downward transport takes place from April onwards to create privilege conditions for cloud formation process. The observational evidence of this study supported this fact.

The day-to-day, monthly and seasonal variability of aerosol number density in upper stratosphere

Varies types of variability of aerosol loading in terms of AND in between the altitudes 31 to 50 km (upper stratosphere) are shown in the following Fig. 2. The figure show day-to-day variability in upper stratospheric AND from 1 January 2009 to 31 December 2009 for morning observations. The upper stratospheric aerosol loading values were in between ~20-30 particles per cm^3. These values are very much less than that of lower stratospheric aerosol loading; implying decreasing AND with respect to increasing altitude. Upper stratospheric aerosol loading showed day to day variability but there was no specific trend for monthly variability for all the three years. One noticeable point was that for the entire three years upper stratospheric aerosol loading was lowest for the month of February, the period free from strong meteor activities; whereas maximum for the month of December, the period followed by Orionids, Leonids and Geminids activities. Very slight variations were observed in the months of February, March and April, the period of weak meteor showers. The considerable fluctuations were detected in the period of strange meteor activities. The conclusion drown from these observations is that, the upper stratospheric aerosols completely depend on an influx of meteor matter including sporadic asteroidal dust particles and meteor showers. During meteor showers a large amount of dust particles intrude into the mesosphere. These dust particles perturb the middle and upper atmosphere and also contribute to additional scattering in the atmosphere. The observational evidence supported this fact.

Comparison between three year's stratospheric aerosol number density per cubic centimeter

Fig. 3 shows graph of lower stratospheric aerosol loading abbreviated as 'Q_1' plotted against day numbers for all of the three years. Fig. 2 shows graph of upper stratospheric aerosol loading abbreviated as 'Q_2' plotted against day numbers for all of the three years. In these figures Y-axis represents aerosol loading and X-axis represents day numbers (i.e. date for each month). The numbers from 1 to 365 corresponds to dates from 1 January 2009 to 31 December 2009. Similarly the numbers from 366 to 730 represents dates from 1 January 2010 to 31 December 2010. Also the numbers from 731to 1095 stands for dates from 1 January 2011 to 31 December 2011.

The month of January 2011, showed higher aerosol loading than other two years, 2009 and 2010 for lower stratosphere. Both of the remaining two years showed negligible difference. There is ~66% increase in the values of 'Q' in February 2009, showing higher 'Q' than years 2010 and 2011, which showed very small, difference among them. There are top most aerosols loading in the month of March 2009, which then showed sharp decrease in April 2009. The observations ended at 15 May 2009. After that sky was covered with low level clouds. The starting of rainy season (southwest summer monsoon) was prolonged up to end of June for year 2009.

In year 2010, lower stratospheric aerosol loading started decreasing from 7th March and again increased from 28th March onwards. One noticeable feature is that upper stratospheric aerosol loading decreased highly from 28th March onwards. This implies that aerosols perturbed downwards

in this period, could be attributed to increase in lower stratospheric aerosol loading. The aerosol observations ended at 6 May 2010 and the rainfall started near about mid June 2010.

Lower stratospheric loading started decreasing from 12 March 2011 and observations closed after 6th April. The monsoon started very early, near about end of May for the year 2011.

Upper stratospheric aerosol loading showed insignificant difference for three of the years for the months of February, March and beginning of April. The considerable variations were observed after the strong meteor activities of Quadrantids (3rd January), Lyrids (22st April) and Eta Aquariids (6th May) , implying that the dust particles intruded into the mesosphere during meteor showers penetrated downwards causing increase in upper stratospheric aerosol loading. The amount of dust particles added in the atmosphere is not same for every year. Therefore significant deviations were noticed.

Comparison between three year's stratospheric aerosol loadings for the months of October, November and December resulted with unclear outcomes. The lower stratospheric aerosol loading showed many variations for all of the three months due to frequently observed high, medium and low level clouds in this period. On the other hand the strong meteor activities of Orionids (21st October), Leonids (17th November) and Geminids (14th December) revealed significant fluctuations in the upper stratospheric aerosol loadings.

SUMMARY AND CONCLUSIONS

The measurements using the Semiautomatic twilight photometer presented in this paper suggest the following:

1. There is an annual variation in aerosol loading. Its maximum at lower stratospheric levels is observed during March.
2. The lower stratospheric aerosol loading shows seasonal variations and it decreases at the face of arrival of south-west monsoon season.
3. The lower stratospheric aerosol loading showed opposite phase relation with that of tropospheric aerosol loading.
4. The dust particles intruded into the mesosphere during meteor showers penetrate downwards causing increase in upper stratospheric aerosol loading.

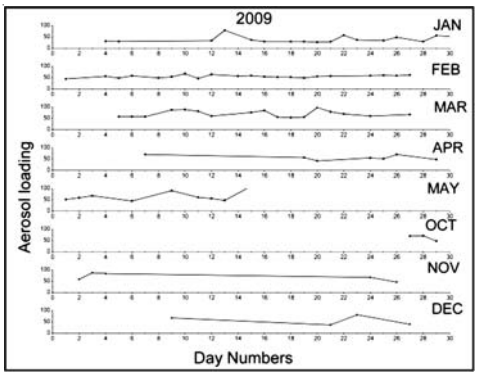

Figure 1.Various types of variability of AND in between the altitudes 17 to 30km (lower stratosphere).

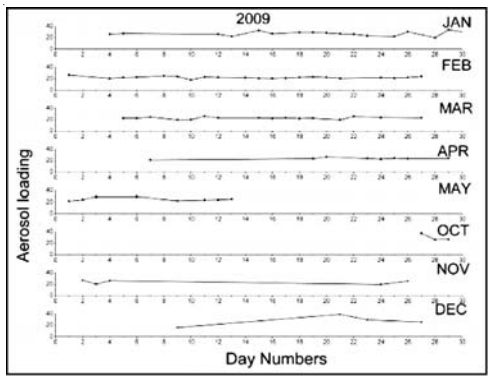

Figure 2. Various types of variability of AND in upper stratosphere (in between the altitudes 31 to 50km).

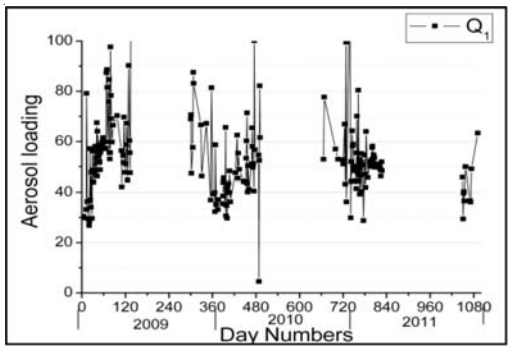

Figure 3.Three years variability of lower stratospheric (17-30 Km) aerosol loading (Q_1).

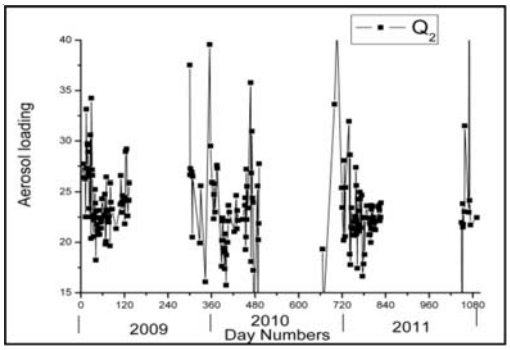

Figure 4. Three years variability of upper Stratospheric (31-50 Km) aerosol loading (Q_5).

ACKNOWLEDGEMENTS

The authors are grateful to the Vice-Chancellor, Shivaji University, Kolhapur, for the encouragement during the course of this work.

REFERENCES

Jadhav, D. B., Padma Kumari, B. & Londhe, A. L. (2000).A review on twilight photometric studies for stratospheric aerosols, *Bulletin of Indian Aerosol Science & Technology Association*, **13**, pp.1–17.

Raju, N. V., Prasad, B. S. N., Narasimhamurthy, B.and Thukarama, M. (2000).Meteorological and anthropogenic influences on the atmospheric aerosol characteristics over a tropical station Mysore (12^0N), *Indian J. Radio & Space Phys*. **29**, pp. 115-126.

Jadhav, D. B. & Londhe A. L. (1992). Study of atmospheric aerosol loading using the twilight method, *J. Aerosol Sci*. **23**, pp. 623-630.

Khemani, *et al.*, (1985). Impact of alkaline particulates on pH of rain water in India, *Water,Air Soil Pollutk* , **25**, pp. 365-376.

Mane, Pratibha B., Jadhav, D. B., Venkateswara Rao, A. (2012). Fast pre-amplifier designed for semiautomatic twilight photometer, *DAVInternational Journal of Science (DAVIJS)***1**, Issue-2, pp. 9-11.

LONG-RANGE TRANSPORT OF AEROSOLS INFERRED FROM GROUND-BASED AND SATELLITE OBSERVATIONS OVER SINHAGAD ($18^0$21' N, $73^0$45' E, 1450 m AMSL)

K. VIJAYAKUMAR[1] AND P.C.S. DEVARA[1]
[1]Indian Institute of Tropical Meteorology, Pune - 411008, India
E mail: devara@tropmet.res.in

Keywords: AEROSOL EXTINCTION AND TRANSPORT, MODIS AND CALIPSO SATELLITES, AEROSOL RADIATIVE FORCING

INTRODUCTION

Biomass burning is an important source of trace gas emission, aerosols and has important effects on atmospheric chemistry and radiation budget. The major sources of biomass burning in India are from shifting cultivation, accidental fires, controlled burning, fire wood burning, burning from agricultural residues, burning due to fire lines etc. Scientific interest in the impact of biomass burning on atmospheric chemistry grew when it became evident that it is an important source of atmospheric pollution (Crutzen and Andreae, 1990) and its products could affect large areas of the world as a consequence of long-range transport (Andreae,1983). Long-range transport is one of the most important factors controlling the spatial and temporal variability of the aerosol concentration. Although a large fraction of aerosols remains in the planetary boundary layer, particularly desert dust plumes and biomass burning plumes may be lifted into the free troposphere and transported over long distances, even between continents. During long-range transport from the source region to the far field, the microphysical, optical and radiative properties of aerosols are modified. The present study focuses on the variations in aerosol properties at high-altitude station, Sinhagad ($18^0$21'N, $73^0$45'E, 1450 m AMSL) during 28 April 2011 – 06 May 2011.

RESULTS AND DISCUSSION

Fig. 1 depicts day-to-day variation in aerosol optical depth (AOD) at 500 nm during 28 April 2011 – 06 May 2011. It can be noticed from the figure that the AOD values are high on 01 May 2011. Fig. 2 shows the variation of AOD at 500 nm on a high aerosol loading day and a normal day. The AOD values were 173% higher on aerosol loading day as compared to that on a normal day. This significant enhancement in AOD, during the study period over the high-altitude region of Sinhagad is attributed to wood burning, which is mainly carried out for cooking and sometimes to clear the forest for agricultural activity. Vehicular exhaust, arising from tourist activity, is another source of pollution at the experimental site.

The nearest CALIPSO pass, available on 28 April 2011, covering central part of the Indian region is shown in Fig. 3. The enhanced aerosol loading seen in CALIPSO data over central Indian region covering the belts between 15.72–27.91 N and 70.58–73.46 E, suggests long-range transport of aerosols from biomass burning in the down-wind direction (Ramanathan, *et al.*, 2007). To identify the sources and to examine how transport paths affect the concentrations of air pollutants over Sinhagad, India, the 5-day back trajectories at 1500, 3000 and 5000 m altitudes from Hybrid Single-Particle Lagrangian Integrated Trajectory (HYSPLIT) model were performed (Fig. 4a). The analysis of backward trajectory suggested that the winds above the boundary layer height (~1.5km) are originating from the biomass burning regions (Fig. 4b).

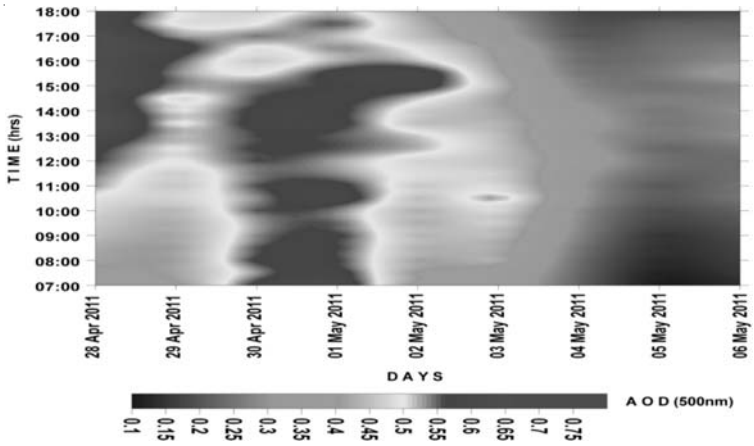

Figure 1.Day-to-day variation of aerosol optical depth at 500 nm during 28 April 2011 - 06 May 2011.

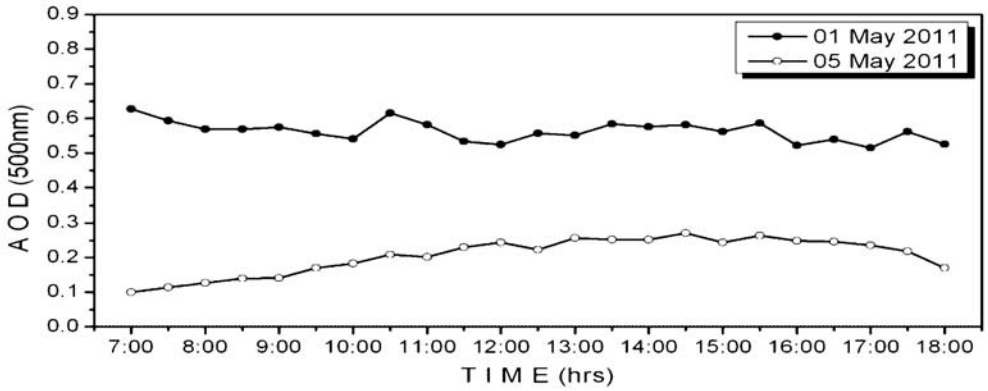

Figure 2. Variation of AOD at 500 nm on high aerosol loading day (01 May 2011) and normal day(05 May 2011).

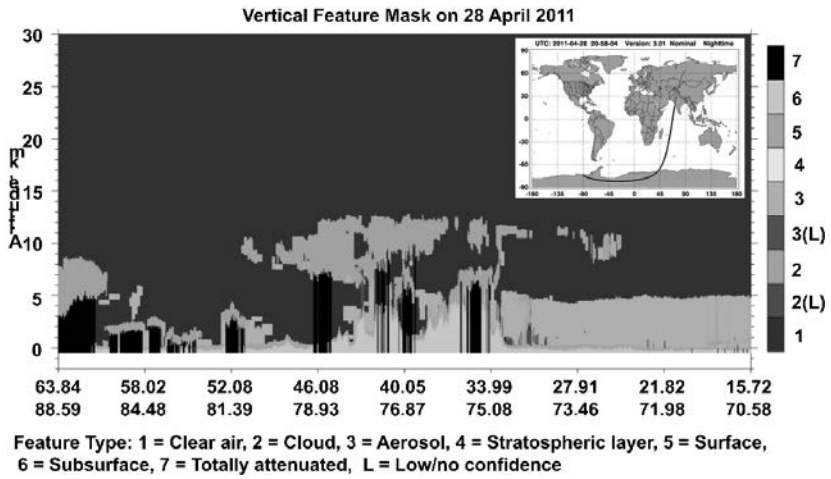

Figure 3. CALIPSO-derived vertical feature mask image of India on 28 April 2011.

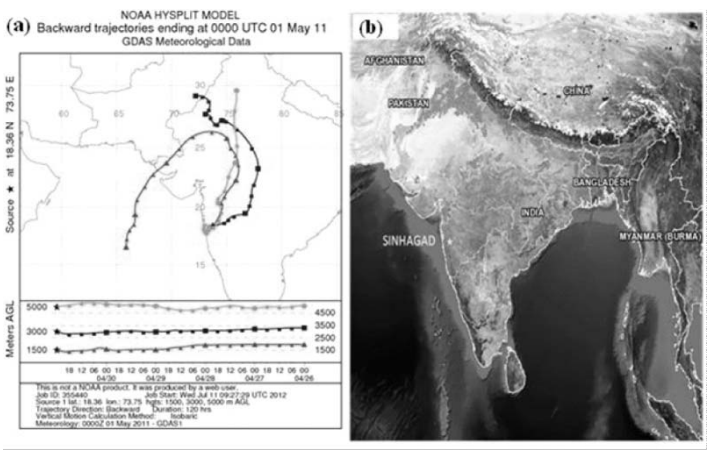

Figure 4. (a) NOAA HYSPLIT 5-day backward trajectories ending at Sinhagad, India on 01 May 2011 and (b) Location map of the study area and MODIS active fire image from 28 April 2011 – 06 May 2011.

Fig. 5 shows scatter plot of the measured normalized SW flux with AOD for Sinhagad during high aerosol loading day and normal day. A straight line could be fitted with a negative slope of about 257, 165 Wm^{-2} per unit AOD for Sinhagad during high aerosol loading day and normal day, respectively. Thus, the decrease in global solar flux with every 0.1 increase in AOD, for SZA<60^0, over Sinhagad came out to be 26 and 17 Wm^{-2}, respectively.

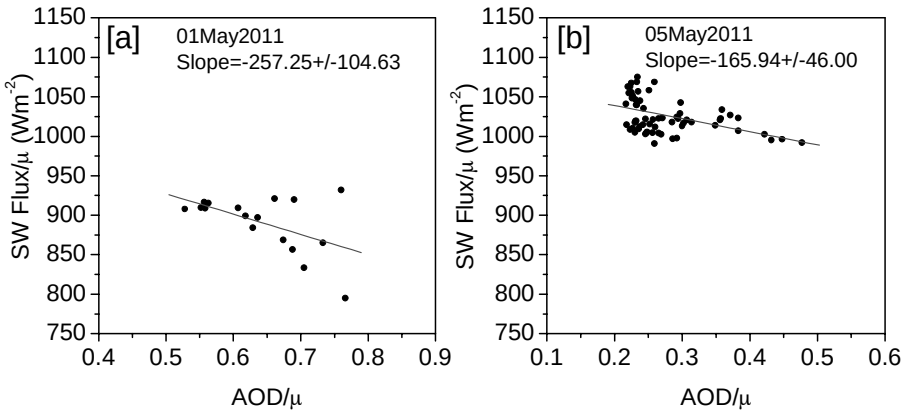

Figure 5.Association between global solar flux and columnar $AOD_{500\,nm}$ normalized for theair mass (1/μ) over Sinhagad during high aerosol loading day [a] and normal day [b]. A linear correlation is obtained by restricting AOD/μ within 0.8.

ACKNOWLEDGEMENTS

This work was supported by the sponsored project, ISRO-GBP-ARFI Program of ISRO, Department of Space, Government of India. One of the authors (KV) acknowledges the financial support, in the form of Research Fellowship, from the ISRO-GBP-ARFI Project. Thanks are also due to the authorities of Bharat Sanchar Nigam Limited (BSNL), Pune, for according permission to carry out the observations and providing necessary help at the experimental site. Finally, we thank the Director, Indian Institute of Tropical Meteorology, Pune for infrastructure support.

REFERENCES

Andreae, M.O. (1983). Soot carbon and excess fine potassium: Long-range transport of combustion-derived aerosols,*Science*, **220**, pp. 1148-1151.

Crutzen, P. J. and Andreae, M. O. (1990). Biomass burning in the tropics: Impact on atmospheric chemistry and biogeochemical cycles, *Science*,**250**, pp. 1669-1678.

Ramanathan, V., Ramana, M. V., Roberts, G., Kim, D., Corrigan, C., Chung, C. and Winker, D. (2007). Warming trends in Asia amplified by brown cloud solar absorption, *Nature*, **448**, pp. 575-578.

SUN-SKY RADIOMETER VIEW OF MULTI-YEAR VARIATIONS IN URBAN AEROSOL CHARACTERISTICS OVER PUNE

P.C.S. DEVARA[1], K. VIJAYAKUMAR[1], SUMIT KUMAR[2], S.M. SONBAWNE[1], S.K. SAHA[1], AND K.K. DANI[1]

[1]Indian Institute of Tropical Meteorology, Pune-411008, India

[2] Atmospheric Sciences Program, Michigan Technological University, Houghton, MI, USA

E mail: devara@tropmet.res.in

Keywords: COLUMNAR AOD, AEROSOL SIZE DISTRIBUTION, AEROSOL TYPES, AEROSOL DIRECT RADIATIVE FORCING.

INTRODUCTION

Atmospheric aerosols are of great importance because of their impact on human health, visibility, continental/maritime ecosystems, Earth‘s climate, hence require dedicated monitoring of their concentration and other properties at both regional and global scales. The importance of aerosol particles for climate forcing is well recognized, but the magnitude of their contribution is uncertain. Aerosols may have an influence of the same magnitude but in the opposite direction as greenhouse gas forcing. This paper focuses on long-term spectral-temporal variations, different types and direct radiative forcing due to aerosols over Pune, a fast growing tropical urban city.

INSTRUMENTATION

The Sun-sky radiometer measurements reported in this paper have been in progress for the past more than eight years at the Indian Institute of Tropical Meteorology (IITM), Pune, India employing a CIMEL Electronique CE-318 instrument as a part of the AERONET global network. This instrument is described in detail in the work of (Holben, *et al.*, 2001) and more details about the site, instrumentation, methodology and error analysis of the data products can be found in Kumar, *et al.* (2011).

DATA ARCHIVAL

The knowledge of daily variations in aerosols and their pre-cursor gases is of primary importance to air quality. Such small-scale variations, many times, help to investigate short-lived episodic events. But the monthly variations over a station or region are useful in order to study the local/regional climatology. The analysis presented here from measurements of spectral direct Sun-sky radiances represents the aerosol optical properties integrated over the entire atmospheric column from the surface to the top of the atmosphere. However, the column-integrated parameters are very useful in the analysis of the radiative forcing effects which these aerosols exert on the regional climate.

It was not possible to operate the radiometer throughout the daytime during the southwest monsoon months of June, July, August, and September due to persistent cloud presence and rain, and even if it was operated, it was only for a small duration or part of the day. The average of such data may not be a true representative of the day‘s average, and hence such data sets have not been considered here. It ultimately resulted in a data gap during these 4 months’ duration in each year of the study period.

RESULTS AND DISCUSSION

Long-Term Variations in Aerosol Optical Depth and Angstrom Parameter

Fig. 1 shows variations in monthly mean $AOD_{440\ nm}$ and Angstrom exponent (440-870 nm) during October 2004 – December 2011. Wide dispersion is evident, indicating large daily variations, especially in December–January and March–April months. The mean AOD for the seven-year period is 0.57. From Fig. 1, higher AOD values are observed during premonsoon months while lower values in winter months.

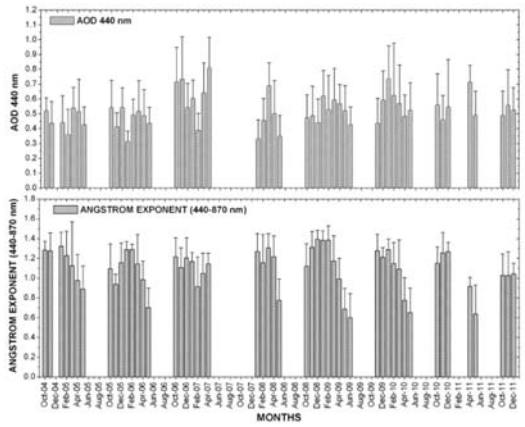

Figure 1. Histograms with standard deviation of AOD at 440 nm and Ångström exponent (440-870 nm).

The spectral variation of AOD can be expressed in the form, $\tau(\lambda) = \beta\lambda^{-\alpha}$, where β and α are Ångström coefficient / exponent which vary widely depending on environmental conditions and aerosol sources and sinks. It is clear from the figure that higher values are observed in winter and lower values in premonsoon months. The decrease in α during premonsoon months is associated with marked shift in the trajectories with air masses originating in March over the Arabian sea and Arabia but shifting westward in April-May to air masses originating primarily over the Arabian sea. Thus the lower values of α in premonsoon months are indicative of increased coarse-mode in the lower atmosphere over this region.

Discrimination of Aerosol Types

In order to characterize the aerosol properties, both AOD and Ångström exponent values have to be used (Holben, *et al.*, 2001) since they both strongly depend on wavelength. The AOD-α patterns have been utilized to describe different aerosol types (e.g., biomass smoke, anthropogenic aerosols, desert dust) at several locations (Kim, *et al.*, 2004). Fig. 2 depicts the density maps of $AOD_{440\ nm}$ versus Ångström exponent (440-870 nm) over the Pune region during 2004-2011. These contour maps were constructed using 0.1 steps for both $AOD_{440\ nm}$ and $\alpha_{440–870\ nm}$ values. In these maps, the rectangle areas denote urban/industrial (UI), clean maritime (CM), desert dust (DD) and mixed type (MT) aerosols, and boundaries of these areas correspond to the selected threshold values of $AOD_{440\ nm}$ and $\alpha_{\ 440\text{-}870\ nm}$. The $AOD_{440\ nm}$ -α plot qualitatively indicates the amount and dimension of the observed aerosols.

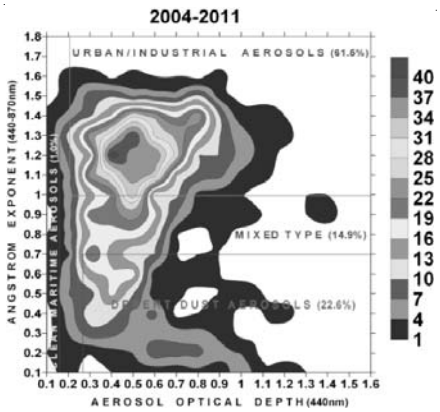

Figure 2. Contour density map of $AOD_{440\ nm}$ versus Ångström exponent (440-870 nm) over the Pune

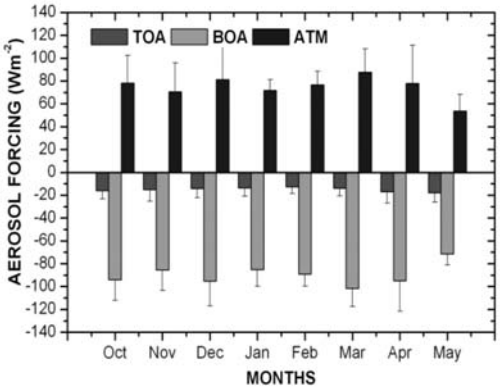

Figure 3 Clear Sky ADRF over Pune at TOA BOA and ATM. regin during 2004-2011.

The above figure shows maximum density area for the pair ($AOD_{440\ nm}$, $\alpha_{440–870\ nm}$) = (0.4, 1.2), indicative of UI aerosols. This clearly indicates the influence of the anthropogenic pollution from the industrialized areas of the Indian west coast, which was found to have a spatial offshore extent of <100 km at the coast and about 61.5% of urban aerosols are dominated over this region compared to clean maritime, desert dust and mixed type of aerosols.

Aerosol Direct Radiative Forcing (ARDF)

Fig. 3 shows average values of radiative forcing over Pune during 2004 to 2011. Radiative forcing calculations have been carried out separately for each month in all years. Large negative surface forcing (more than -60 Wm^{-2}) is observed in all the months. Surface forcing values are higher for premonsoon months comparable to that for winter and postmonsoon months. From figure 3, the very high atmospheric heating (more than 40 Wm^{-2}) persists throughout the year. These interactions between aerosols and solar radiation can be attributed to combination of aerosol properties, surface properties, and geographical parameters (latitude, season).

ACKNOWLEDGEMENTS

The authors are grateful to the AERONET for their valuable constant support. Thanks are also due to the Director, IITM encouraging the study. One of the authors (KV) acknowledges the financial support, in the form of Research Fellowship, from the ISRO-GBP-ARFI Project.

REFERENCES

Holben, *et al.*, (2001).An emerging ground-based aerosol climatology: Aerosol optical depth from AERONET,*Journal of Geophysical Research*, **106**, pp. 12067-12097.

Kim, et al. (2004). Aerosol optical properties over East Asia determined from ground-based sky radiation measurements, *Journal of Geophysical Research*,**109**, doi:10.1029/2003JD003387.

Kumar, *et al.*(2011). Sun-sky radiometer–derived column-integrated aerosol optical and physical properties over a tropical urban station during 2004-2009, *Journal of Geophysical Research*,**116**, doi:10.1029/2010JD014944.

A YEAR ROUND DATASET OF THE AEROSOL PHASE FUNCTION RECORDED AT THE HIGH-ALPINE RESEARCH STATION JUNGFRAUJOCH

M. LABORDE[1], P. ZIEGER[1], T. MUELLER[3], N. BUKOWIECKI[1], G. KASSELL[2], E. WEINGARTNER[1], U. BALTENSPERGER[1]

[1]Paul Scherrer Institute, Laboratory of Atmospheric Chemistry, Villigen, Switzerland.

[2]Ecotech PtyLtd, Knoxfield, VIC, Australia.

[3] Department of Physics, Leibniz Institute for Tropospheric Research , Leipzig, Germany

Keywords: NEPHELOMETER, AEROSOL PHASE FUNCTION

INTRODUCTION

The aerosol phase function is an important parameter for radiative transfer calculations in the Earth's atmosphere. It describes the angular distribution of the light scattered by aerosols and varies with the aerosol size, shape and chemical composition. The phase function of aerosols is needed for many satellite and lidar data retrievals but is often not well known. Based on assumed aerosol properties, calculated phase functions are then used instead of measurements, leading to uncertainties in the data process.

A commercially available polar nephelometer, measuring the aerosol phase function, with a 5°-angular resolution and at three wavelengths was installed for one year at the high-alpine research, on top of the Jungfraujoch, (alt. 3580m) Switzerland.

RESULTS AND DISCUSSION

The high-alpine research station is a unique place to investigate aerosol properties, as it is most of the time in the free troposphere. As a Global Atmosphere Watch (GAW) station, it is equipped with numerous instruments continuously characterizing the chemical and physical properties of the aerosol. Throughout the year, time periods with air masses originating from the free troposphere, from the planetary boundary layer below the station and long-range transported Saharan dust were measured, resulting in a unique dataset. The influence of particle size and chemical composition on the aerosol phase function and on the asymmetry factor is here investigated. The asymmetry factor G is defined as the cosine-weighted average of the phase function, where the phase function is the probability of radiation being scattered in the direction θ and is here calculated according to Mueller et al, 2012 parametrisation (Eq.1) using the Ecotech Polar Nephelometer.

$$G = \frac{\sum_{n}^{N-1}(\sigma_{\theta_i} - \sigma_{\theta_{i+1}})\cos\left(\frac{\theta_i + \theta_{i+1}}{2}\right)}{\sum_{n}^{N-1}(\sigma_{\theta_i} - \sigma_{\theta_{i+1}})} \times 1.7752 - 0.6599 \qquad (1)$$

A clear evidence of a strong influence of the origin of the aerosol on the asymmetry factor was observed with higher asymmetry factor observed during Saharan dust events (SDE<0) that are characterized by highly unspherical particles (Fig.1).

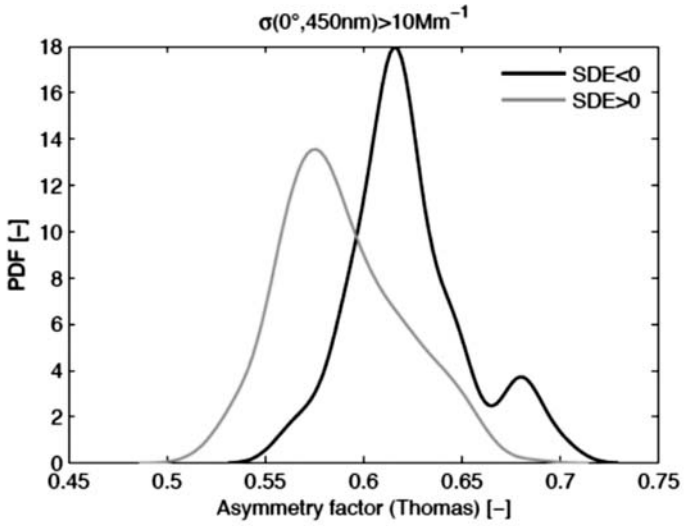

Figure 1. Asymmetry factor probability distribution function observed during Saharan dust event (SDE<0) and outside Saharan dust event (SDE>0).

A comparison between measurements and Mie theory predictions is also here presented, using measurements of various different instruments installed at the research station such as an optical particle counter, a scanning mobility particle sizer, a nephelometer, an aerosol chemical speciation monitor, and a multi-angle absorption photometer.

REFERENCE

Mueller *et al.*, (2012).Scattering Coefficients and Asymmetry Parameters derived from the Polar Nephelometer Aurora 4000, EAC.

DATA ASSIMILATION TO IMPROVE GCM PREDICTIONS USING MISR AOD PRODUCTS

ANKIT BARASKAR, CHANDRA VENKATARAMAN, MANI BHUSHAN
Department of Chemical Engineering, Indian Institute of Technology Bombay,
Powai, Mumbai 400 076, INDIA.

Keywords: AEROSOL, SCATTERING

BACKGROUND AND MOTIVATION

Aerosols in the atmosphere contribute towards backscattering and extinction of radiation, which can be measured either via satellite (MISR, MODIS) or using ground observations (AERONET). Atmospheric models are now being used to predict aerosol concentrations that can be further fed into radiative transfer modules to compute Aerosol Optical Depth (AOD) and radiative forcing. However, considering that there is a large bias between model predictions and observations, the quality of the model data needs to be enhanced. One of the methods to do this is data assimilation using satellite observations and uncertainties. For this we use an algorithm that is a variant of the Kalman filter, namely Optimal Interpolation.

MISR PRODUCTS

MISR (Multi-angle Imaging Spectro-Radiometer) is an imaging tool that is mounted atop a NASA satellite that uses observed top of the atmosphere (TOA) reflectances to derive 'Best Estimate' TOA AODs in four wavelength bands. In addition, it provides uncertainties in AODs for the aforementioned bands. This is the Level 2 Aerosol product that is obtained at a resolution of 17.6 km by 17.6 km (David, *et al.* 2008, Dey, *et al.* 2010)

Moreover, MISR provides particle properties in the form of size and shape optical depth fractions.AODs are provided for three size fractions – small ($r < 0.35\mu m$), medium ($0.35\mu m < r < 0.7\mu m$) and large($r > 0.7\mu m$) as well as two shape fractions – spherical and non-spherical. This additional information can be utilized for either an unconstrained assimilation of the individual fractions or assimilation where the total AOD (small + medium + large or spherical + non-spherical) is kept as a constrained variable. Data assimilation helps improve the quality of the model data by reducing the associated uncertainty, since the resulting uncertainty is smaller than both the model uncertainty and satellite uncertainty.

ALGORITHM DESCRIPTION

Optimal Interpolation is a widely used technique for data assimilation, notable examples being Collins, et al. (2001) who used it for the assimilation of MATCH (Model of Atmospheric Transport and Chemistry) data using AVHRR (Advanced Very High Resolution Radiometers) observations, and Adhikary, et al. (2008) who used MODIS (Moderate Resolution Imaging Spectrometer) datato improve STEM (Sulphur Transport dEposition Model) predictions over the Indian subcontinent and East Asia.

The algorithm is a variant of the Kalman filter approach using predetermined error covariance matrices instead of those computed dynamically, where the model predictions(background, τ_m), the satellite observations(observation, τ_o) and the posterior AOD(analysis, τ_a) is assumed to be the following

$$\tau_a = \tau_m + \boldsymbol{K}(\tau_o - \mathrm{H}\tau_m) \quad (1)$$

Where **K** is the Kalman gain matrix and H is a linear interpolator from the model space to the observation space. Since we scale the satellite observations to the model grid, for us H is an identity matrix (I). The Kalman gain matrix is computed as follows:

$$K = BH^T(HBH^T + O)^{-1} \quad (2)$$

where B and O are error covariance matrices. O and B are calculated as follows

$$O = (f_0\tau_0 + \varepsilon_0)^2 I \quad (3)$$

where I is the corresponding identity matrix, ε_0 is the minimum RMS(root mean square) error of the observation and f_0 is the fractional error in the observation AOD. The mathematical representation of the matrix B in terms of its components is given by

$$B_{ij} = (f_m\tau_m + \varepsilon_m)^2 \exp\left(\frac{-(d_x^2 + d_y^2)}{l_{xy}^2}\right) \quad (4)$$

Here, f_m is the fractional error in the model AOD, ε_m is the minimum RMS error in the model AOD, and d_x, d_y are the horizontal distances along the X and Y axis between model grid points i and j. l_{xy} is the horizontal correlation length scale for errors in model fields. In addition, we also compute the post-assimilation error covariance matrix.

$$P = B - KHB \quad (5)$$

RESULTS AND PROPOSED METHODOLOGY

An ordinary average of values while scaling data from the satellite grid to the model grid leads to loss of information, since all the satellite grid points falling within a model grid 'box'(formed by adjacent pair of lat-lon values) are assigned equal weights. To remedy this, we take a weighted average for the Best Estimate AOD using the inverse of the uncertainty squared as weights wherever the uncertainty value is reported as a nonzero positive number. Thus, if we have AOD values τ_1, τ_2, ...,τ_k with associated uncertainties σ_i (1 d" i d" k), the resulting satellite AOD value for the model grid is calculated as

$$\tau_{resultant} = (\sum_{i=1}^{k} w_i\tau_i)/(\sum_{i=1}^{k} w_i), \text{ where } w_i = 1/ó_i^2 \quad (6)$$

Similarly, the resulting uncertainty is calculated as

$$\sigma^2_{resultant} = \frac{1}{1/\sum_{i=1}^{k} w_i} \quad (7)$$

This study proposes to utilize the MISR AOD in terms of both size and shape fraction for assimilation of ECHAM data in the year 2006 which shall be verified against AERONET ground observations to assess the impact of assimilation on the quality of model data. For the same, we also propose an unconstrained assimilation for the fractional AODs, and have arrived at a mapping between MISR fractional AODS and ECHAM fractional AODs as follows.

The shape fraction mapping is proposed as:

S. No. (1-6) in Table 1 => MISR spherical

S. No. (7) in Table 1 => MISR non-spherical (Since Coarse soluble(no. 6) has Secondary Organic Aerosols, we assume the particles in that particular bin to be spherical). With this proposed mapping, an assimilation of AOD with ECHAM 2006 output will be made. Assimilation of both total AOD and fractional AOD, as unconstrained independent variables, will be undertaken. The paper will evaluate the ability of both assimilation procedures in improving the modelled AOD products, vis-à-vis AERONET measurements.

S. No	ECHAM Mode	Variable Name	Size range(μm)	CorrespondingMISR size Fraction
1	Nucleation Mode	TAU_MODE_NS	R<0.005	Small + Medium(0<r<7)
2	Aitken soluble mode	TAU_MODE_KS	0.005<r<0.05, σ = 1.59	
3	Aitken insoluble	TAU_MODE_KI		
4	Accumulation soluble	TAU_MODE_AS	0.05<r<.5, σ = 1.59	
5	Accumulation insoluble	TAU_MODE_AI		
6	Coarse soluble	TAU_MODE_CS	r > 0.5, σ = 2.0	Large(0.7<r)
7	Coarse insoluble	TAU_MODE_CI		

Table 1. Mapping modelled ECHAM aerosol modes to MISR size fractions

REFERENCES

Adhikary, B., Kulkarni, S., Dallura, A., Tang, Y., Chai, T., Leung, L.R., Qian, Y., Chung, C.E., Ramanathan, V., Carmichael, G.R., (2008). A regional scale chemical transport modeling of Asian aerosols with data assimilation of AOD observations using optimal interpolation technique, *Atmospheric Environment* ,**42**, pp. 8600-8615.

Chung, *et al.*, (2010), Anthropogenic aerosol radiative forcing in Asia derived from regional models with atmospheric and aerosol data assimilation, *Atmos. Chem. Phys.*, doi: 10.5194/acp-10-6007-2010

Collins, W.D., Rasch, P. J., Eaton, B. E., Khattatov, B. V., Lamarque, J. F., Zender, C. S., (2001), Simulating aerosols using a chemical transport model with assimilation of satellite aerosol retrievals: Methodology for INDOEX, *Journal of Geophysical Research-Atmospheres*, **106**, pp. 7313-7336.

David, J. Diner *et al.*, (2008). MISR Level 2 Aerosol Retrieval Algorithm Theoretical Basis

Dey, S. and Girolamo, L. Di (2010). A climatology of aerosol optical and microphysical properties over the Indian subcontinent from 9 years (2000-2008) of Multiangle Imaging Spectroradiometer(MISR) data, *J. Geophys. Res.*,**115**, D15204.

Khattatov, B. V., Lamarque, J.-F., Lyjak, L. V., *et al.* (2000). Assimilation of satellite observations of long-lived chemical speciesin global chemistry transport models, *J. Geophys. Res.*,**105**, pp. 29135–29144.

Park, R. S., Song, C. H., Han, K. M., Park, M. E., Lee, S. S., Kim, S. B., Shimizu, A. (2011). A study on the aerosol optical properties over East Asia using a combination of CMAQ-simulated aerosol optical properties and remote-sensing data via a data assimilation technique, *Atmospheric Chemistry and Physics*,**11**, pp. 12275-12296.

IMPACT OF INTENSE DUST STORM OF MARCH 2012 ON SURFACE REACHING SOLAR RADIATION OVER PUNE

G. HARIKISHAN, B. PADMA KUMARI, AND R. S. MAHESKUMAR
Indian Institute of Tropical Meteorology, Pune 411008, India

INTRODUCTION

Atmospheric aerosols have a significant impact on the radiative and heat balance of the Earth-atmosphere system. Dust aerosols constitute a major fraction of atmospheric aerosols over the globe and play an important role in regulating the global climate (Christopher, et al., 2003). Usually Dust storms are common in the north-western part of the Indian subcontinent. During mid of March 2012, an intense dust storm spanned thousands of kilometers from the Red Sea to Afghanistan, and from the Arabian Peninsula to India. During this period entire India is under the influence of this dust storm. Present study is focussed on the ground based radiative measurements over Pune during this intense dust event of March 2012. The temporal variability of aerosol microphysical properties and the radiative forcing due to aerosols is studied.

DATA AND METHODOLOGY

In the present study, data collected from ground based Multi Filter Rotating Shadowband Radiometer (MFRSR) is used. It measures the total, direct, and diffuse components of shortwave, narrowband irradiance at six wavelengths (415nm, 500nm, 615nm, 670nm, 870nm and 940nm). From these measurements aerosol optical depth, angstrom coefficient and single scattering albedo are derived using retrieval algorithms. Satellite data is also used in support of the ground based observations.

RESULTS AND DISCUSSION

The total radiation and derived aerosol optical depths are in good agreement with the simultaneous measurements of pyranometer and sky radiometer, respectively. The total, direct and diffused radiation and the aerosol optical depths (AOD) at different wave lengths from 15 to 25 March 2012 are shown in Figure 1(a,b). Dip in total as well as direct normal radiation is observed on 22nd and 23rd March. On these days the drop in direct normal and increase in diffused radiation is found to be almost double the normal values. Also the increase in AOD on these two days indicates that Pune was under the influence of the severe dust storm event on 22 and 23 March 2012. MODIS also showed the AOD values in the same range. Dominance of dust up to 3-4 km is observed in CALIPSO profiles. Angstrom exponent derived from MFRSR as well as MODIS show the dominance of coarse mode particles with high scattering efficiency.

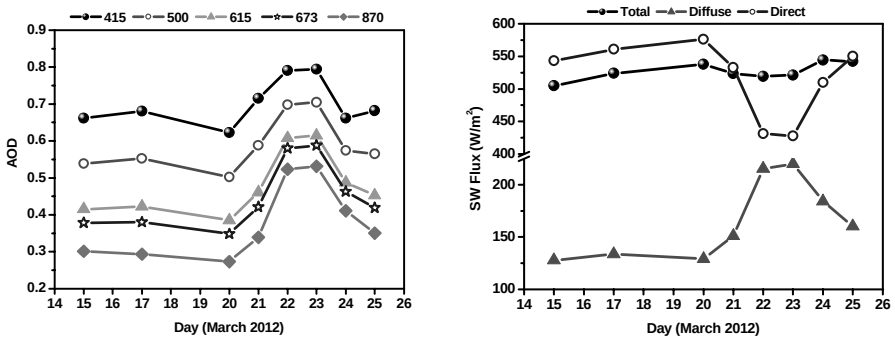

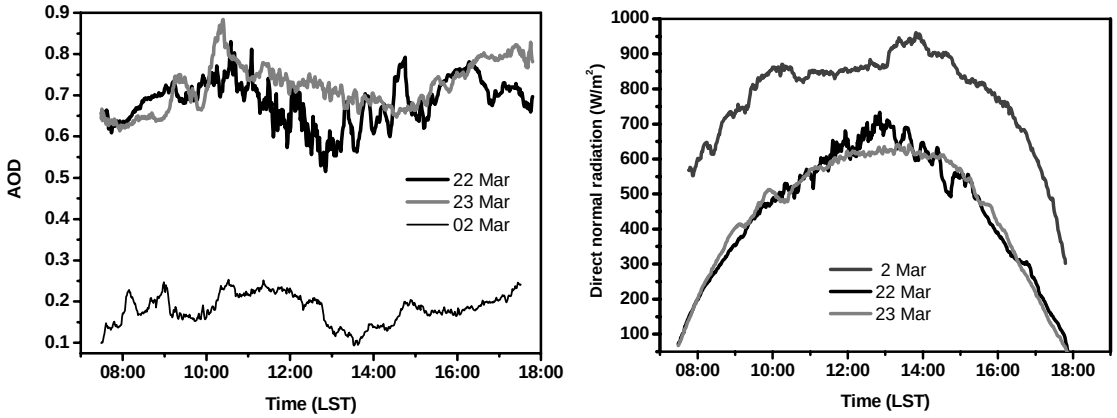

Figure 1. (a) The total, direct and diffused radiation from ground based MFRSR, (b) AOD at different wave lengths, (c) Diurnal variation of direct normal radiation on 22nd and 23rd March are compared with 2nd March, considered as background, and (d) diurnal variation of AOD at 500nm for the same days as shown in figure c.

The diurnal variation of direct normal radiation and AOD for 22nd and 23rd are compared with that of 2nd March, a very clear day and considered as a background profile (Fig. 1 c, d). The estimated radiative forcing for 22nd and 23rd is found to be around 34 W/m^2 against the background 2nd March. Further the diurnal variability in radiative forcing against the AOD will be presented to understand the impact of the dust event on regional scale.

ACKNOWLEDGEMENTS

The authors wish to thank Ministry of Earth Sciences (MoES) and Director IITM.

REFERENCES

Christopher, S. A., Wang, J., Ji, Q. and Tsay, S. C. (2003).Estimation of diurnal shortwave dust aerosol radiative forcing during PRIDE, *Journal of Geophysical Research*, **108**, no. D19, Article ID 8596.

ESTIMATION OF AEROSOL ASYMMETRY PARAMETER FROM SUN/SKY RADIANCE MEASUREMENT AT IAO-HANLE

SHANTIKUMAR SINGH NINGOMBAM, S. P. BAGARE, AND RAJENDRA BAHADUR SINGH
Indian Institute of Astrophysics, Bangalore, 560034

Key words: AEROSOL RADIATIVE FORCING AND SKYRAD.PACK RADIATIVE TRANSFER MODEL

INTRODUCTION

It may be mentioned that contribution of aerosol radiative forcing (ARF) is one of the most important aspects on climate change phenomenon. Absorption and scattering by aerosols can modify the radiative forcing efficiency in the atmosphere. The main parameters to deal with the ARF is to get the proper knowledge of aerosol optical properties, such as the aerosol optical depth, single-scattering albedo and angular distribution of light scattering by aerosols or asymmetry parameter (g). Aerosols are heterogeneous in nature and it varies temporally and spatially. In spite of high temporal and spatial aerosol variability, there are a rather limited number of observations in the high altitude and pristine locations. Such observations are important as they provide a sort of background against the anthropogenic component.

The main objective of the present study is the estimation of aerosol asymmetry parameter (g) for the studies of ARF over the region. The observing station is located at the hilltop of Mt. Saraswati and houses the Indian Astronomical Observatory (IAO), at $32^0 47'$ N and $78^0 58'$ E, and 4500 m amsl. A detailed description of the topography and orography of the site is given by Verma et al., (2010).

METHODOLOGY

A Skyradiometer, Model POM-01L of Prede, Japan was used for the study. The instrument consists of an automatic sun tracker and a spectral scanning radiometer with rain and sun sensors. It measures both direct and diffuse irradiance at five wavelengths from visible to the near-infrared. The data was processed using Version 4.2 of the Skyrad. Pack radiative transfer model [Nakajima, *et al.*, (1996)]. Thereafter, a cloud-screening task was performed following Khatri and Takamura, (2009), in order to remove the cloud-contaminated data.

The angular distribution of aerosols or asymmetry parameter, g is defined as the cosine-weighted average of the scattering angle:

$$g = \frac{1}{2}\int_0^{\pi} cos\theta P(\theta) sin\theta d\theta$$

where, θ is the angle between the incident light and scattering direction, P() is the angular distribution of scattered light (phase function). The values of g can range from -1 for 180 degree backward scattering to +1 for completely forward scattering. Andrews, et al., (2006) have presented various methods of estimating g from a large measurements made from in-situ and remote from surface and aircraft. The median values of g estimated at all the methods for dry atmospheric condition at 550 nm are ranged between 0.55-0.63. Global maps of asymmetry parameter presented by d'Almeida,

et al., (1991) reported a value of g of 0.67 at ambient relative humidity for most of the mid-west and southeast regions of the US. In the present work, g values were estimated by using the Version 4.2 of the Skyrad.Pack radiative transfer code [Nakajima et al., (1996)] at five wavelengths such as 400, 500, 675, 870 and 1020 nm.

RESULTS

Fig. 1 shows the normalized phase function at 500 nm observed on a fully clear sun/sky day, 23 April, 2008. The different lines with color in the figure indicate the time of observation in IST. The figure shows the scattering angles in degree with a logarithmic scale. The Skyrad code estimated the angular distribution of aerosols from 0 to 180 degrees. It is found that normalized phase function varies with time and it approaches a maximum towards the post afternoon. The median values of g observed at Hanle are 0.69, 0.66, 0.67, 0.68, and 0.71 at 400, 500, 675, 870 and 1020 nm respectively during the period January 2008 to December. Fig. 2 (a) shows the spectral variation of g during this one year of study with the standard error lesser than 0.003. The value of g decreases at the visible region and slightly increases in near-infrared region as seen in the figure. Fig. 2 (b) shows the inverse relationship between g at 500 nm with the Angstrom parameter during January-December 2008. It indicates the asymmetry or the forwards scattering efficiency increases as the particle size increases. Aerosol concentration at the high altitude sites in central Himalaya can get enhanced due to long-range transport phenomenon. The prevailing winds over the site are predominantly south-westerly throughout the year. The south-westerly circulation of surface wind apparently enhances the influx of desert aerosols over Hanle, and thereby forming an additional source of aerosols at the site. In our earlier study (Verma, *et al.*, 2010), we have reported the influx of desert aerosols (of Saharan type) towards the observing station Hanle, using HYSPLIT back trajectory analysis. Therefore, it is expected that the site may have different types of air mass apart from those of local origin.

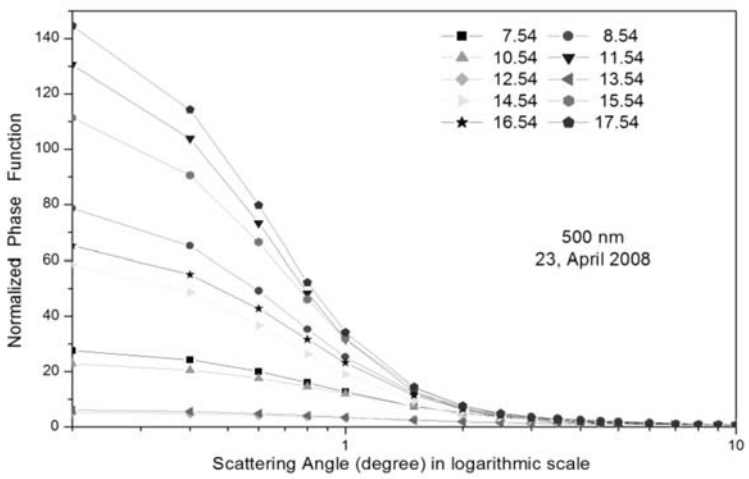

Figure 1.Variation of normalized phase function at 500 nm from different scattering angles during a full clear sky observation on 23, April 2008 at IAO Hanle.

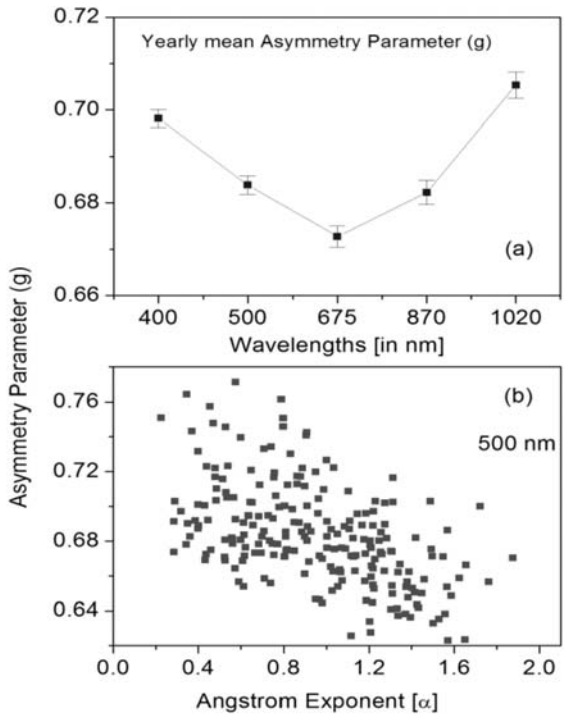

Figure 2. Variation of Asymmetry Parameter, (g) with (a) spectrally and (b) Angstrom Exponent, (á) during January - December 2008.

CONCLUSION

The median values of estimated g values are 0.69, 0.66, 0.67, 0.68, and 0.71 at 400, 500, 675, 870 and 1020 nm, respectively. The value of g decreases around 500 nm and increases towards the near-infrared. The retrieved g parameter is strongly depends on both wavelength and Angstrom parameter.

REFERENCES

Andrews, *et al.*, (2006).Comparison of methods for deriving aerosol asymmetry parameter, *J. Geophy. Res.*, **111**, D05S04..

d'Almeida, G. A., Koepke, P., and Shettle, E. P. (1991). Atmospheric Aerosols: Global Climatology and Radiative Characteristics, (A. Deepak Publishing, Hampton, Va)

Khatri, P., and Takamura, T. (2009).An algorithm to screen cloud-affected data for sky radiometer data analysis, *J. Meteorol Soc. Jpn*., **87**, pp.189-204.

Nakajima, T., Tonna, G., Rao, R., Boi, P., Kaufman, Y., and Holben, B. N. (1996). Use of sky brightness measurements from ground for remote sensing of particulate polydispersions, *App. Opt*.,**35**, pp.2672-2786.

Verma, N., Bagare, S. P., Ningombam, S. S. and Singh, R. B. (2010). Aerosol Optical Properties retrieved using Skyradiometer at hanle in western Himalayas, *J. Atmos. Solar-Terrestrial Phys*., **72**, pp. 115-124.

COMPARISON OF THE ANGSTROM EXPONENT RETRIEVAL IN DIFFERENT SPECTRAL RANGES TO INFER AEROSOL PROPERTIES OVER URBAN POLLUTED LOCATION

G.R. AHER[1], G.V. PAWAR[1], S.D. MORE[2], P.C.S DEVARA[3]
[1] Physics Department Nowrosjee Wadia College, Pune 411 001, India
[2] Department of Atmospheric and Space Sciences, University of Pune, Pune 411 007, India
[3] Indian Institute of Tropical Meteorology, Pashan, Pune 411 008, India
Email: aher.g.r@gmail.com

Keywords: ANGSTROM WAVELENGTH EXPONENT, AEROSOL OPTICAL DEPTH

INTRODUCTION

The Angstrom Wavelength Exponent (á) is a commonly used tool to investigate spectral dependence of aerosol optical depth (AOD) and thereby used to derive basic information on the aerosol size spectra since it is an indicator of the average particle size present in the atmosphere. It is also used to extrapolate AOD throughout the broad spectral rangeand to distinguish different aerosol types (Eck *et al*., 2001; Kalapureddy and Devara, 2008; O'Neill *et al*., 2001). Values of $\alpha > 1$ signifies dominance of fine-mode aerosols of effective radii smaller than 0.5 µm usually associated with urban pollution and biomass/biofuel burning. On the other hand, for $\alpha < 1$, aerosol size spectrum is mainly dominated by coarse-mode aerosols having average particle radii greater than 0.5 µm originating mainly from dust outflows or sea-spray. However, Angstrom Exponent is found to be strongly dependent on the wavelength range used for its estimation. Due to this, curvature is found to be prevalent in the spectral AOD curve paving the way to provide crucial information on aerosol size spectrum (Holben *et al*., 2001; Kaskaoutis *et al.,* 2010; Shuster *et al*., 2006). Analysis of curvature in the spectral AOD curve has been therefore employed to delineate different aerosol components like maritime aerosols, biomass-burning aerosols, and rural and urban aerosols.

In the present work, monthly/seasonal variation of Angstrom Exponent, and curvature of AOD spectral curve is examined to associate the results with the presence of fine-and coarse-mode aerosols over the urban polluted location of Nowrosjee Wadia College (NWC), Pune.

OBSERVATIONAL DETAILS

The data used in the present study has been derived from the comprehensive field campaign carried out at Nowrosjee Wadia College (NWC), Pune ($18^0$31' N, $73^0$55' E, 559 amsl) by operating Microtops II sunphotometer on clear sky, cloudless days during 2008-2011.It consists of AODs at five spectral wavelengths centered at 0.44, 0.5, 0.675, 0.870 and 1.020 µm. The observing season normally spans over Dec-May period.

METHODOLOGY

AODs (τ_λ) at four wavelengths (viz., 0.44, 0.5, 0.675and 0.870 µm) were used to determine Angstrom Exponent (α) using the Angstrom empirical formula given as:

$$\tau_\lambda = \beta\lambda^{-\alpha} \quad (1)$$

The Angstrom wavelength exponent (α) can be calculatedusing the AODs (τ) at two different wavelengths by applying the Volz method:

$$\alpha = -\frac{d\ln\tau}{d\ln\lambda} = -\frac{\ln\left(\frac{\tau_1}{\tau_2}\right)}{\ln\left(\frac{\lambda_1}{\lambda_2}\right)} \quad (2)$$

It is clear from Equation (2) that α is the negative of the slope(or negative of the first derivative) of τ with respect to wavelengthin logarithmic scale. This approach is fully described by Knobelspiesse, *et al.* (2004).

However, application of Angstrom power law over wide wavelength range would lead to significant inaccuracies when aerosol size distribution is multimodal. Under such conditions, a curvature is observed in the AOD spectra which can be determined by fitting a second order polynomial to the plot of τ with respect to wavelengthin logarithmic scale. This yields curvature parameters viz., $á_1$ and α_2 (Eqn. 3) over NWC, Pune.

$$\ln\tau = \alpha_2 (\ln\lambda)^2 + \alpha_1 \ln\lambda + \alpha_0 \quad (3)$$

RESULTS AND DISCUSSION

Aerosol optical depths at 0.5 µm are correlated with short, long and full spectral band á values over the urban polluted observing site NWC, Pune (Fig.1a). It is found that at NWC;$\alpha_{0.4\text{-}0.5}$ exhibit an increasing trend while $\alpha_{0.675\text{-}0.870}$ show a decreasing trend with increasing AODs. Angstrom exponent for the full spectral band (), however, depicts a neutral trend over the site. Kedia and Ramachandran, (2009), reported similar observations over Bay of Bengal and Arabian Sea. However, Kaskaoutis et al., (2006) and Soni, *et al.*, (2011) obtained negative correlation between $\alpha_{0.34\text{-}0.38}$ and 0.5 µm AODs, and positive correlation between $\alpha_{0.67\text{-}0.87}$and 0.5µm AODs. Their observation that $\alpha_{0.34\text{-}0.87}$ remains uncorrelated with 0.5 µm AODs is similar to the present results. These findings including the present one indicate that the increase in turbidity reduces similar increase in AODs at both short and long wavelengths. This implies the presence of a well mixed aerosol type probably having a bi-modal size distribution with similar contributions from fine-and coarse-mode fractions to AOD at all wavelengths. In the present analysis, however it is seen that there is a large spread in á values in short and long wavelength pairs used for its estimation in the AOD range 0.5-0.7.

Fig. 1b reveals the monthly/seasonal variation of Angstrom exponent in the short, long and full spectral band. Over the observing site, a large variation in α is observed when calculated at different wavelength interval. During 2008-10, the value of $\alpha_{0.44\text{-}0.5}$ is higher as compared to corresponding values at the long and full spectral band. However, the variation pattern shows the reversing trend during 2010-11. On an average, ávalues in full spectral band is found to be > 1 indicating the dominance of fine-mode aerosols.

The correlation between $\alpha_{0.44\text{-}0.5}$ and $\alpha_{0.67\text{-}0.87}$ the correlation on the basis of curvature parameter (α_2) is shown in Fig. 3. This analysis helps to identify the dominant mode of aerosols contributing to the aerosol size distributions over NWC, Pune. The curvature parameter values will be less than zero for an atmosphere with higher fine-mode aerosol concentration, while α_2>0 for an atmosphere in which coarse-mode aerosol concentration is high (Kaskaoutis, *et al.*, 2007).

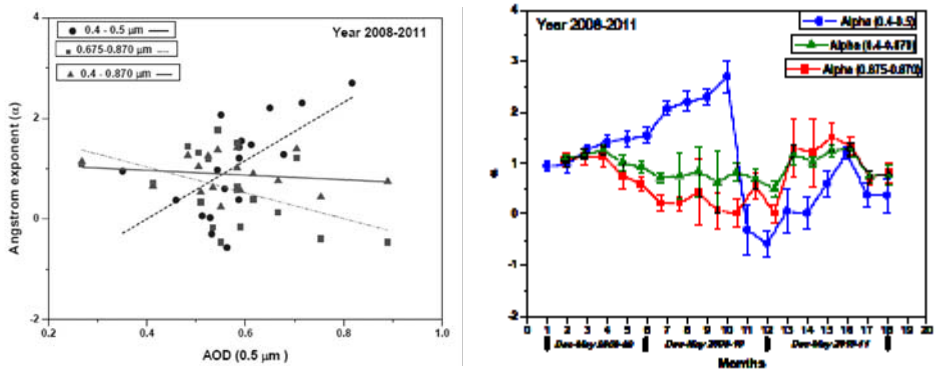

(a) (b)

Figure 1. (a): Monthly mean Angstrom exponent in three wavelength bands versus Monthly mean AOD at 500 nm. (b): Monthly mean variation of Angstrom exponent in three wavelength bands at NWC Pune.

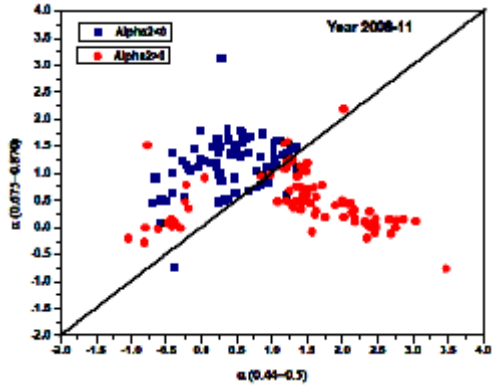

Figure 2. Correlation between $\alpha_{(0.675\text{-}0.870)}$ and $\alpha_{(0.44\text{-}0.5)}$ categorized on the basis of curvature parameter $á_2$

CONCLUSION

The observations that the á values are different in different spectral band indicates the presence of mixed type aerosols over the observing site.

ACKNOWLEDGEMENTS

The present study was supported and funded by the Indian Space Research Organization under the joint programme of ISRO. Authors also thank the Principal, Nowrosjee Wadia College, Pune and Dr. M. M. Andar, Secretary, Modern Education Society, Pune for support and encouragement.

REFERENCES

Eck, T. F., Holben, B. N., Dubovik, O., Smirnov, A., Slutsker, I., Lobert, J. M. and Ramanathan V. (2001).Column-integrated aerosol optical properties over the Maldives during the northeast monsoon for 1998–2000, *J. Geophys.Res*., **106**, pp. 28,555– 28,566.

Holben, B. N., et al. (2001). An emerging ground-based aerosol climatology:Aerosol optical depth from AERONET, *J. Geophys. Res*., **106**, pp. 12,067– 12,097.

Kalapureddy, M. C. R. and Devara, P. C. S. (2008). Characterization of aerosols over oceanic regions around India during pre-monsoon 2006, *Atmos. Environ*., **42**, 6816.

Kaskaoutis, D. G., Kalapureddy, M. C. R., Krishna Moorthy, K., Devara, P. C. S., Nastos, P. T., Kosmopoulos, P. G. and Kambezidis, H. D. (2010). Heterogeneity in pre-monsoon aerosol types over the Arabian Sea deduced from ship-borne measurements of spectral AODs, *Atmos. Chem. Phys.*,**10**, 4893.

Kaskaoutis, D. G., Kambezidis, H. D., Adamopoulos, A. D., and Kassomenos,P. A. (2006b). On the Characterization of Aerosols Using the Ångstr¨omExponent in the Athens Area, *J. Atmos. Sol-Terr. Phys.* **68,** 2147.

Kedia, S., and Ramachandran, S. (2009). Variability in Aerosol Optical and Physical Characteristics Over the Bay of Bengal and the Arabian Sea Deducedfrom Angstrom Exponents, *J. Geophys. Res.*, **114** , D14207.

Soni, *et al.*, (2001). Wavelength Dependence of the Aerosol Angstrom Exponent and Its Implications Over Delhi, India, *Aerosol Science and Technology*, **45**, 1488.

Knobelspiesse, K. D., Pietras, C., Fargion, G. S., Wang, M., Frouin, R., Miller, M. A., Subramaniam, A., and Balch, W. M. (2004). Maritime AerosolOptical Thickness Measured by Handheld Sun Photometers, *Remote Sens. Environ*,**93**, 87.

O'Neill, N. T., Eck, T. F., Holben, B. N., Smirnov A. and Dubovik O. (2001). Bimodal size distribution influences on the variation of Angstrom derivatives in spectral and optical depth space, *J. Geophys. Res*.,**106**, 9787.

Schuster, G. L., Dubovik, O. and Holben B. N. (2006).Angstrom exponent and bimodal aerosol size distributions, *J. Geophys. Res.*,**111**, D07207.

PLANETARY SCALE OSCILLATIONS IN AEROSOL PROPERTIES AT DELHI

S NASEEMA BEEGUM, NEELESH K LODHI, SACHCHIDANAND SINGH
Radio & Atmospheric Sciences Division, National Physical Laboratory, CSIR,
New Delhi-110012
E mail: ssingh@nplindia.org

Keywords: AEROSOL, AOD, OSCILLATIONS, TIME SERIES

INTRODUCTION

Atmosphere can support a wide variety of waves/oscillations from molecular scale to planetary scale. These atmospheric waves are categorized, according to their scale sizes, triggering and restoring as micro-scale, meso-scale, synoptic scale and planetary-scale motions. All these waves being efficient means for the transport of energy and momentum, these would modulate atmospheric trace species including aerosol particles. Making use of this property, aerosols were used as tracers to study how the Earth's atmosphere moves. The atmospheric wave motions/ large scale circulation systems can greatly influence the horizontal and vertical distribution of aerosols.

Here we present a quantitative analysis of the time series of long-term spectral AODs (10 years from 2001 to 2011) using Microtops Sunphotometer at Delhi (28.6º N, 77.3º E, 238 m msl) in the Indo Gangetic Plain, to delineate the contribution due to various periodicities from intra-seasonal to inter-annual time scales.

RESULTS AND DISCUSSION

Time-series of the monthly mean spectral AODs at four wavelengths (340 nm, 500 nm, 870 nm and 1020 nm) has been subjected to wavelet analysis and the resulting spectra are shown in Fig. 1. The figure revealed the presence of periodicities of intra-seasonal (periodicities of ~1-2 months), annual (~ 12 months) and inter-annual time scales (2-3 years). Detailed examination of the periodicities in the meteorological parameters such as wind vectors revealed that the intra-seasonal periodicity of 1-2 months are the eastward propagating Madden Julian Oscillations (MJO), the 12 months periodicity is the well known annual oscillations (AO), and the 2-3 year periodicity is the Quasi-Biennial Oscillations (QBO). Signatures of a periodicity of ~ 4-5 year are also observed in significant amplitude. It is interesting to note the gradual decrease in amplitude of QBO in AOD as wavelengths increases. The percentage contribution of the periodicities have been examined in details by estimating the percentage contribution of these periodicities towards the climatological mean AOD values and is shown in Fig. 2. Among the three periodicities the higher contributions are observed for AO and ISO at all the three wavelengths and the contribution due to these two periodicities are found to increase towards longer wavelengths to reach as high as ~25% for AO at 1020 nm. The highest contribution for QBO is observed at shorter wavelengths (~8% at 340 nm), decreases continuously towards longer wavelengths and the amplitude becomes less significant at 1020 nm. The observed strong QBO, comparable to that of MJO and AO, at 340 nm is an indication of the relatively high amount of fine/accumulation mode aerosols at higher elevations.

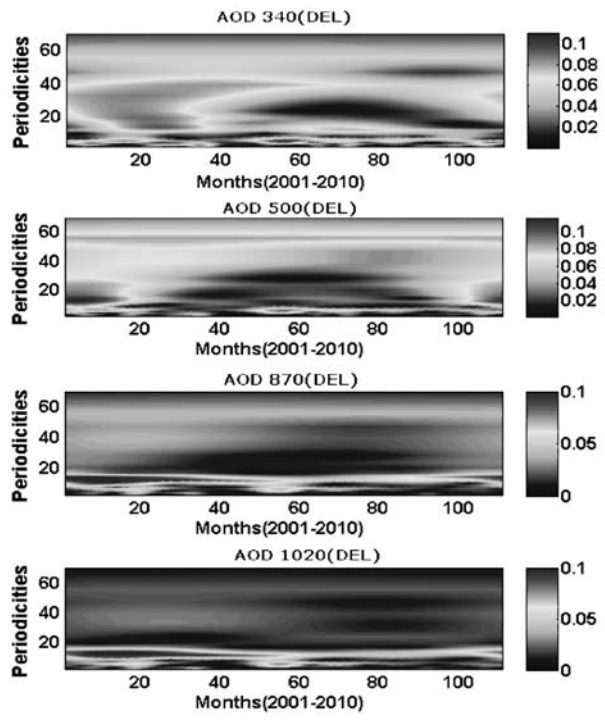

Figure 1. Wavelet spectra of the time series of monthly mean spectral AODs at Delhi

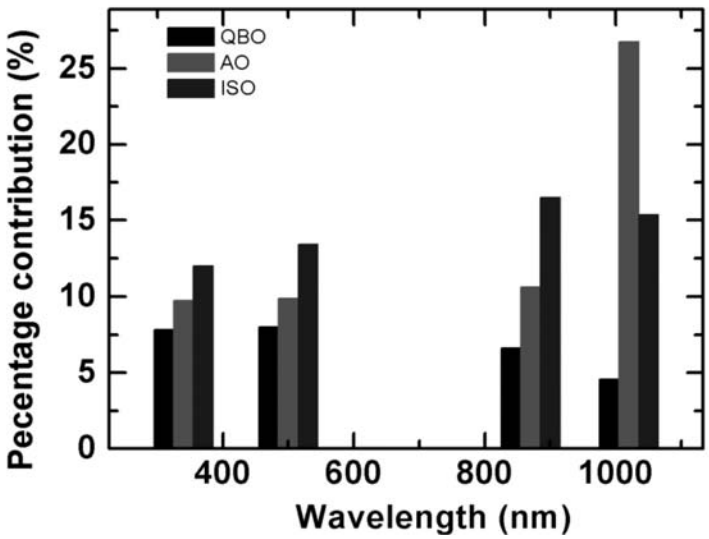

Figure 2. Percentage contribution of the periodicities towards the climatological mean spectral AODs at Delhi

Similar analysis of the wavelet of wind vectors and rainfall revealed the presence of similar periodicities in the meteorological parameters too. While the shorter periodicities in aerosol parameters were strongly correlated with the corresponding oscillations in the near surface meteorological parameters, the inter-annual oscillations were found to be associated with the circulation pattern in

the Upper troposphere/lower stratosphere region.The results signify the role of natural atmospheric motions in producing significant modulations in aerosol distribution, which will have strong implications in not only in Radiative forcing and climate impact assessment but also on reducing the uncertainties in satellite retrieval of various aerosol products.

CONCLUSIONS

Continuous and long-term measurements of Spectral Aerosol Optical Depths (AOD) for a period of 10 years (from 2001 to 2011) at Delhi have been analyzed to delineate the significant modulations by different time scale atmospheric motions or circulations. Wavelet spectra of the time-series data have revealed the presence of three dominant periodicities, the 30 -50 days Madden Julian Oscillation, Annual Oscillations, and Quasi Biennial Oscillations in significant amplitudes. While the shorter periodicities in aerosol parameters were found to be strongly correlated with the corresponding oscillations in the near surface meteorological parameters, the Quasi Biennial Oscillations (QBO) were found to be associated with the circulation pattern in the Upper troposphere/lower stratosphere region.

SEASONAL VARIABILITY IN AEROSOL CHARACTERISTICS AT NEW DELHI USING SUN/SKY RADIOMETER MEASUREMENTS

VIBHUTI YADAV[1, 2], A. K. SRIVASTAVA[2], V. PATHAK[1], D. S. BISHT[2], S. TIWARI[2] AND P. C. S. DEVARA[3]

[1]Department of Civil Engineering, Institute of Engineering and Technology, Lucknow, India
[2]Indian Institute of Tropical Meteorology (Branch), Prof Ramnath Vij Marg, New Delhi, India
[3]Indian Institute of Tropical Meteorology, Dr Homi Bhabha Road, Pashan, Pune, India
E-mail: vibhu_euphoric@yahoo.co.in

INTRODUCTION

Atmospheric aerosols have high temporal and spatial variability due to their different residence time in the atmosphere and the geographical distribution of their emission sources. New Delhi, one of the highly polluted megacities in Asia, is situated in the western part of the Indo Gangetic Basin (IGB). Being situated near to the Thar Desert region, the station is also influenced with desert dust activities, mostly during the pre-monsoon season (Pandithurai, *et al.*, 2008). These dust aerosols, mix with various anthropogenic aerosols, may influence the overall optical properties and the associated radiative characteristics of aerosols (Deepshikha, *et al.*, 2005). Consequently, they may further complicate the satellite retrieval of aerosol characteristics and quantifying the climatic effects (Mishra *et al.*, 2010). Hence, it is important to understand the diurnal and spatial variability of various aerosol characteristics over such regions.

INSTRUMENTATION AND DATA USED

A calibrated sun/sky radiometer (CIMEL, Paris, France) was installed at the Indian Institute of Tropical Meteorology (Branch), New Delhi (28.6^{o}N, 77.2^{o}E) during May 2008 as part of the Aerosol Robotic Network (AERONET) programme by National Aeronautics and Space Administration (NASA), USA to understand the various aerosol characteristics (Holben et al., 1998). The instrument measures direct Sun radiances at eight spectral channels (340, 380, 440, 500, 670, 870, 940 and 1020 nm), where 940 nm channel is used to estimate the columnar water vapor content, and remaining channels are used to retrieve spectral aerosol optical depth (AOD). On the other hand, sky radiance measurements at four spectral bands (440, 670, 870 and 1020 nm) are used to deduce other crucial aerosol optical parameters such as size distribution, single scattering albedo (SSA), asymmetric parameter (AP) etc (Holben, *et al.*, 1998). The data of different AERONET stations get centrally processed at NASA and processed data are available on the AERONET site (http://aeronet.gsfc.nasa.gov/) in three categories: cloud contaminated (level 1.0), cloud screen (level 1.5) and quality assured (level 2.0) (Smirnov, et al., 2000).

In the present study, level 2.0 aerosol optical products derived from sun/sky radiometer for New Delhi were analyzed during the year 2009. Monthly and seasonal variability of aerosols have been studied over the station. Apart from the general characteristics of composite/total aerosols, discrimination of aerosol types/compositions was also done based on the sun/sky radiometer measured aerosol products (Srivastava, *et al.*, 2012) to understand optical and radiative properties of each aerosol type.

RESULTS AND DISCUSSION

The variability in monthly averaged AOD and Angstrom exponent (AE) has been plotted in Fig. 1. The annual average AOD at 500 nm wavelength during the period of present observations is ~0.66±0.10 with the corresponding mean of AE ~0.99±0.26. The average monthly AOD showed maximum value during the months of November (0.95±0.39), August (0.75±0.15) and May (0.70±0.18). The high AODs in May and August are associated with the enhanced contribution from natural desert dust aerosols, frequently transported from the neighboring desert regions whereas high AOD in November is mainly due to anthropogenically-enhanced pollution. The average monthly AE values during these months were found to be (1.27±0.11), (0.50±0.23) and (0.69±0.22) respectively, indicating dominance of fine-mode particles during November and coarse-mode during May and August.

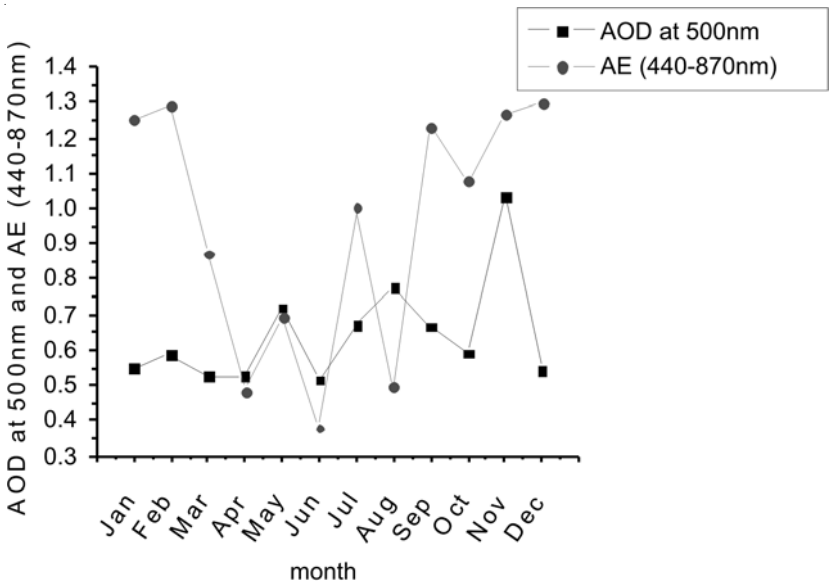

Figure 1. Monthly averaged AOD and AE

The fine- and coarse-mode fractions of aerosol particles have been studied over the station, which exhibit significant contribution of coarse-mode during pre-monsoon/monsoon period and fine-mode during winter/post-monsoon period. Aerosol volume size spectra show bi-modal distributions during all the seasons, with significantly different volume concentrations, and effective radius of aerosols in fine- and coarse-modes. The other aerosol parameters, namely, single scattering albedo (SSA), refractive index and asymmetric parameter were also analyzed and discussed.

The optical properties derived from sun/sky radiometer, associated with the size (i.e. fine-mode fraction; FMF) and radiation absorptivity (i.e. SSA) of aerosols were used to discriminate the possible aerosol types/compositions (e.g. polluted dust; PD, polluted continent; PC, mostly black carbon; MBC and mostly organic carbon; MOC) over the station. The spectral variations in AOD and SSA for each aerosol type are shown in Fig. 2a and 2b, respectively, showing significantly different features. The other optical properties for these aerosol types were also studied. To quantify radiative impacts over the station due to these aerosol types, the associated radiative properties were estimated for individual aerosol types using corresponding optical properties measured by sun/sky radiometer.

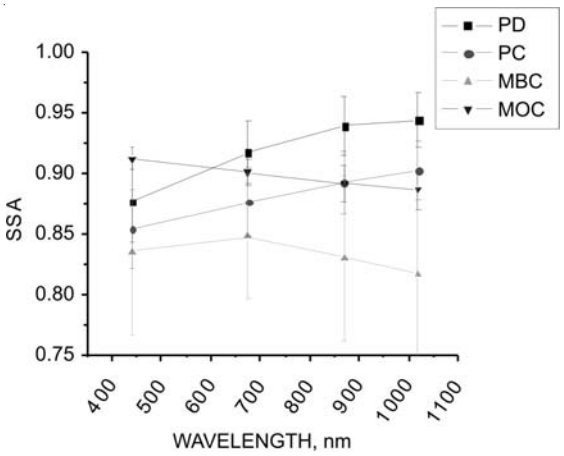

Figure 2(a). Spectral variation in SSA

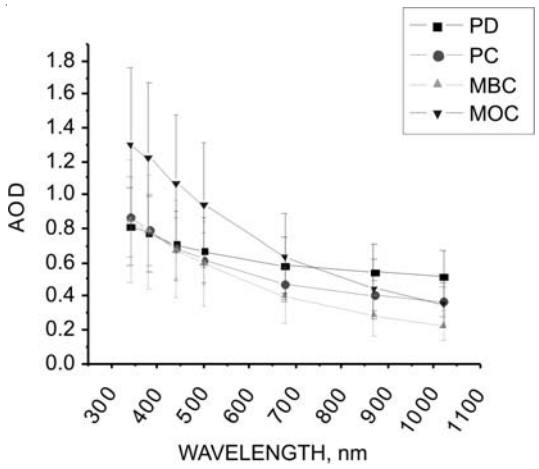

Figure 2(b). Spectral variation in AOD

ACKNOWLEDGEMENTS

Sincere thanks to the Director, IITM, Pune for allowing Vibhuti Yadav to pursue her M. Tech. dissertation work at IITM (Branch), New Delhi. Authors are thankful to B. N. Holben, AERONET group of NASA and PHOTONS French Service d'Observation from LOA/USTL for the deployment of CIMEL sun/sky radiometer at IITM, New Delhi Branch.

REFERENCES

Deepshikha, S. *et al.* (2005).Regional distribution of absorbing efficiency of dust aerosols over India and adjacent continents inferred using satellite remote sensing, *Geophys. Res. Lett.*, **32**, pp. 1–4.

Holben, B. N. *et al.* (1998). AERONET - a federated instrument network and data archive for aerosol characterization, *Remote Sens. Environ.*,**66**, pp. 1–16.

Mishra, S. K. *et al.* (2010). Effects of particle shape, hematite content and semi-external mixing with carbonaceous components on the optical properties of accumulation mode mineral dust, *Atmos. Chem. Phys. Discuss.*, **10**, pp. 1–48.

Pandithurai, G. *et al.* (2008). Aerosol radiative forcing during dust events over New Delhi, India, *J. Geophys. Res.,* **113**, D13209.

Smirnov, A. *et al.*(2000). Cloud screening and quality control algorithms for the AERONET database, *Remote Sens. Environ.,* **73**, pp. 337–349.

Srivastava, A. K. *et al.* (2012). Inferring aerosol types over the Indo-Gangetic Basin from ground based sun-photometer measurements, *Atmos. Res.*, **109-110**, pp. 64–75.

VARIATION OF AEROSOL OPTICAL THICKNESS OVER BANGALORE

KAMSALI NAGARAJA[1], K. CHARAN KUMAR[1], B. MANIKIAM[1], D. JAGADEESHA[2] AND T.S. PRANESHA[3]

[1]Department of Physics, Bangalore University, Bangalore 560 056

[2]Atmospheric Science Programme, ISRO Headquarters, Bangalore 560 094

[3]Department of Physics, BMS College of Engineering, Bangalore 560 019

E mail: kamsalinagaraj@bub.ernet.in

Keywords: AEROSOLS, MODIS, MISR, SATELLITE DATA, RAINFALL.

INTRODUCTION

In South Asia, the atmospheric aerosols have increased significantly in the last few decades due to population growth, energy demand, forest fires, industrial growth, changes in land use/land cover and anthropogenic activities. The effect of increasing atmospheric loading is felt in the region directly and indirectly and also, locally and globally. The recent studies have shown that pollution in the northern parts of India affects the day-to-day life of million people living in India and adjoining regions. The increasing pollution may affect the hydrological cycle, agriculture, climate and weather conditions.

Atmospheric aerosol is a major concern for climate prediction and public health, but global aerosol distributions have only become available in the last decade from dedicated satellite observations (Kahn, *et al.,* 2005) such as MODerate resolution Imaging Spectro-radiometer (MODIS) and Multiangle Imaging Spectro Radiometer (MISR). Despite much progress made recently in using satellite data to derive surface aerosol concentration over land, several challenges exist. The radiance or reflectance data collected by currently operational passive remote sensing instruments for aerosol retrieval are mostly at the atmospheric window channels in the visible spectrum. Therefore, they offer little information on aerosol vertical distribution beyond the retrieval of columnar properties such as aerosol optical thickness (AOT). In the near UV spectrum, the slope of the reflectance is regulated by height-dependent Rayleigh scattering and aerosol absorption, and this relationship can be used to estimate the centroid height of absorbing aerosols. However, such an algorithm requires a priori information on aerosol single scattering albedo to infer AOT, and it lacks sensitivity to changes in lower tropospheric aerosol mass. With very few observational constraints on aerosol vertical distribution, studies to date have had to use chemistry transport models to interpret the 2D satellite information of either AOT or reflectance into the 3D aerosol fields. A common practice so far has been that the simulated aerosol mass at each vertical layer in a model grid box is updated by a scale factor that is the ratio of spatiotemporally-collocated AOT values from the model and the satellite retrieval algorithm. Resultant surface aerosol concentrations generally show better agreement with ground-based counterparts than those obtained without applying the scale factor, highlighting the value of the satellite AOT for the remote sensing of air quality.

In this paper, focus will be mainly on a comprehensive evaluation of Terra and Aqua MODIS spectral aerosol optical thickness, which is the most important parameter from which others can be derived. Another aspect is to study the patterns of aerosol distribution (Wang, *et al.,* 2003) The aerosols scatter and absorb sunlight, and thus can cool or warm the surface and atmosphere leading to the estimation of energy budget, as nucleation centers, aerosols can also change the drop size distribution within clouds, affecting cloud reflectance and lifetime, thereby controlling the microphysics

of clouds, fine particles penetrate lung tissue and affect respiratory function lead to several health problems, even high altitude aerosol plumes affect aircraft which has aviation hazards, also it acts as an index of air pollution, forecasting of weather, dynamics of the earth's atmosphere. In this regard, an effort is made to study the influence of AOT on the atmosphere and on clouds.

METHODOLOGY

The Moderate Resolution Imaging Spectroradiometer (MODIS) instruments on board the Terra and Aqua platforms provide nearly daily global coverage of key atmospheric and land surface parameters. Retrievals of aerosol optical depth (AOD) by MODIS are 25 the most commonly used of any satellite AOD product. Although MODIS is technically a research instrument, its use in operational applications is increasingly widespread. The MODIS Collection 5 aerosol product at 10×10 km^2 resolution from the Terra and Aqua satellites, which are polar-orbiting satellites, cross the equator during the daytime at approximately 1030 and 1330 local time, respectively. Radiance data are acquired by MODIS in 36 spectral bands, spanning 405–14,385 nm wavelengths, which range from the visible (VIS) through the near-infrared (NIR) and midinfrared (MIR) up to the thermal infrared (TIR) regions of the electromagnetic spectrum. They are acquired in one of three spatial resolutions at nadir: 0.25 km (bands 1–2: VIS), 0.5 km (bands 3–7: VIS-MIR), and 1 km (bands 8–36: VIS-TIR). MODIS data are being used operationally to generate a variety of geophysical parameters employed in monitoring the Earth's lands, oceans, and atmosphere.

The quality of the aerosol optical thickness (AOT) data retrieved operationally from the Moderate Resolution Imaging Spectroradiometer (MODIS) sensors aboard the Terra and Aqua satellites for 11-years from 2000 to 2011 were evaluated thoroughly for Bangalore station.

RESULTS AND DISCUSSION

The effect of aerosols on climate has an important role since they alter the radiation balance of the earth-atmosphere system considerable and reduce amount of solar radiation reaching the ground. The spatial and vertical distribution of aerosols and their absorptive and reflective properties also influence atmospheric circulation patterns, cloud formation and hydrological processes. Therefore, monitoring spatial distribution of aerosols and their properties is critical for climate research, and for validating the performance of dust models in higher-resolution mesoscale models(Holben, *et al.*, 2001).

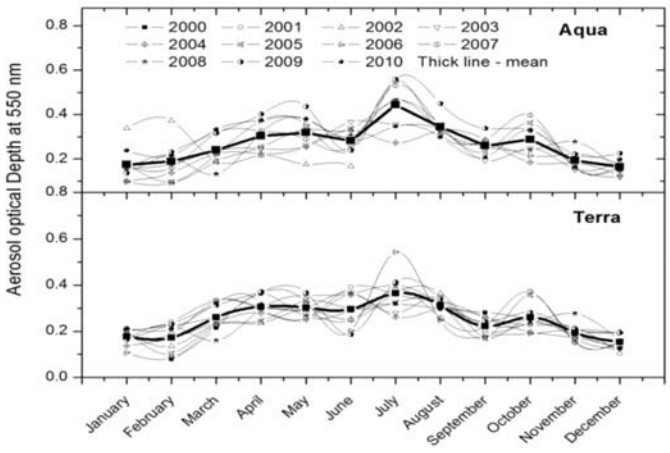

Figure 1.Monthly variation of Aerosol optical depth at 550 nm from Aqua/Terra for the duration from January 2000 to December 2010 for the region 75E-80E and 10N-15N.

The area-averaged time series of Aerosol optical depth at 550 nm from Terra/Aqua for the duration from January 2000 to December 2010 for the region 75E-80E and 10N-15N is shown in Fig. 1. One can observe the maxima in AOTs in July and all the profiles show similar trend. The values show an increasing trend from January to July and then decrease till the end of the year, December. Monthly variations range from 0.165 to 0.443 with a mean of 0.267 ± 0.08 for Aqua, and from 0.154 to 0.365 with a mean of 0.25 ± 0.07 for Terra, respectively. The standard deviation does not exceed 0.1 in all the cases. Monthly variation of Aerosol optical depth for different wavelengths from MISR for the period of 11-years from 2000 to 2010 for the region 75E-80E and 10N-15N is estimated and the AOT varies from 0.221 to 0.371 with a mean of 0.30 for the wavelength 443 nm in blue region, varies from 0.176 to 0.296 with a mean of 0.239 for the wavelength 555 nm in green region, varies from 0.147 to 0.249 with a mean of 0.197 for the wavelength 670 nm in red region and varies from 0.116 to 0.202 with a mean of 0.156 for the wavelength 865 nm in infrared region. Maximum AOT is observed for the shorter wavelength than for the longer wavelengths. In addition, an increase of 52% of AOT is observed for the change in wavelength from blue to green and red to infrared, while a change of 25% observed for the wavelength shift from blue to red or from green to infrared, whereas only 21% changes between red and green.

Fig. 2 depicts the seasonal variation of Aerosol optical depth at 550 nm for Terra and Aqua for the duration of 11-yeaars for the region 75E-80E and 10N-15N. The seasons were classified according the standard convention of India Meteorological Department (IMD), Government of India. Higher concentrations were observed during summer and monsoon seasons compared to winter and post-monsoon seasons. The results obtained here show contradiction to the usually expected behaviour of decrease in AOT due to washout because of precipitation (Singh, *et al.,* 2004). The reason being that, even though the reductions in AOTs exist in monsoon, the transportation of aerosols from other areas and local activities such as vehicular traffic, emissions from industries will lead to enhancement of AOTs (Vinoj, *et al.* 2004) To get clear picture of transport of parcel of air, the trajectories will help in arriving the solution to this problem. In view of this, air mass trajectories from HYPSPLIT during different months covering entire year during 2009 and shows that the wind is coming from northern-west northern part of land to the studied area during winter, from Arabian ocean during summer, from Indian Ocean and Bay of Bengal during monsoon and from Bay of Bengal during post monsoon seasons (Kaskoutis, *et al.*2009).

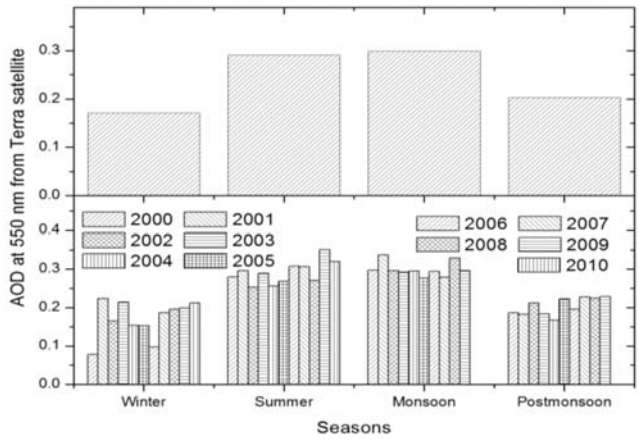

Figure 2. Seasonal variation of Aerosol optical depth at 550 nm from MOD/MYD for the duration of two years from 2000 to 2010 and its mean for 11-years for the region 75E-80E and 10N-15N.

In winter, winds over Indian subcontinent are generally low, exhibiting larger speeds over the oceanic areas. The wind flows mainly from eastern/northeastern directions, may be carrying significant amounts of polluted air masses over the Arabian Sea in certain cases. Fair weather conditions with clear skies exist during winter with continental air masses passing over the region. Low-level inversions in the morning and evening hours, and haze in the morning occur during this period along with the incursion of dry polar continental air in the wake of low-pressure systems. In general, during premonsoon season, the weather over and around India is very hot with a daily maximum temperature around 40 ^{o}C, while the surface winds are mostly gusty, especially over northern AS, northern Indian Ocean (NIO) and Bay of Bengal (BoB). The dust content over northwestern India (Thar Desert) is at its maximum and often dust exposures affect.

CONCLUSION

The area-averaged time series of AOD from Terra/Aqua for the region 75E-80E and 10N-15N is observed and analyzed and is found that AOTs were maxima in July. Monthly variations show mean value of 0.252 and 0.265 for Terra and Aqua respectively. Monthly variation of AOD for different wavelengths from MISR shows a mean of 0.306, 0.240, 0.198 and 0.157 for 443, 555, 670 and 865 nm, respectively. Maximum AOT is observed for the shorter wavelength than for the longer wavelengths. Higher concentrations were observed during summer and monsoon seasons compared to winter and post-monsoon seasons. Aerosol index (AI) is obtained from OMI measures the upwelling radiance in the 270–500 nm bands. It has near daily global coverage with a 2600 km swath width and a spatial resolution of 13x24 km^2 at nadir and 28 x 150 km^2 near the edge. The AI is derived from the difference between the wavelength dependence (354 and 388 nm) of reflected radiation in an atmosphere containing aerosols and a pure molecular atmosphere from Rayleigh scattering. In the UV, absorbing aerosols such as dust and smoke often produce positive AI values.

ACKNOWLEDGMENTS

The aerosol optical depth data is obtained from MODIS and MISR that are available at Atmospheric Sciences Data Center at NASA Langley. Also, the back trajectories for the station are obtained from HYSPLIT and the authors are thankful to the scientific community maintaining the data.

REFERENCES

Wang, *et al.* (2003).Geostationary satellite retrievals of aerosol optical thickness during ACE-Asia, *J. Geophys.Res.*, **108**, D23, 8657.

Kahn, R. A., Gaitley, B. J., Martonchik, J. V., Diner, D. J., Crean, K. A., and Holben, B. (2005). Multiangle Imaging Spectroradiometer (MISR) global aerosol optical depth validation based on 2 years of coincident Aerosol Robotic Network (AERONET) observations, *J. Geophys. Res.*, **110**, D10S04.

Kaskaoutis,*et al.*, (2009), Variations in the aerosol optical properties and types over the tropical urban site of Hyderabad, India, *J. Geophys Res.*, **114**, D22204.

Singh, R. P., Dey, Sagnik, Tripathi, S. N., and Tare, Vinod (2004).Variability of aerosol parameters over Kanpur, northern India, *J. Geophys.Res.*, **109**, D23206.

Vinoj, V., Satheesh, S. K., Babu, S. S., and Krishna Moorthy, K. (2004). Large aerosol optical depths observed at an urban location in southern India associated with rain-deficit summer monsoon season, *Annales.Geophysicae.*,**22**, pp. 3073-3077.

MODEL NEAR SURFACE TEMPERATURE INVERSION IN BOUNDARY LAYER AND THE ROLE OF SUSPENDED PARTICLES

D.DEKA[1], S.NATH[2], K.R.SREENIVAS[3] AND D.K.SINGH[3]

[1]Department of Chemical Engineering, National Institute of Technology Karnataka, Surathakal, Mangalore-575025, India.
[2]Department of Mechanical Engineering, Jadavpur University, Kolkata-700 032, India.
[3]Engineering Mechanical Unit, Jawaharlal Nehru Centre for Advanced Scientific Research, Jakkur, Bangalore-560 064, India.

Keywords: TEMPERATURE MAXIMUM, AEROSOLS, RADIATIVE HEATING, SUB-CLOUD LAYER.

INTRODUCTION

A near surface temperature inversion has been observed in the diurnal sub-cloud layer beneath the mixing layer over the Arabian Sea (Bhat, G. S., 2006; Near-surface temperature inversion over the Arabian Sea due to natural aerosols, Geophys. Res. Lett.). To study this phenomenon in a more controlled manner, similar temperature profile is reproduced in the laboratory using 45 micron graphite particles suspended in water. Results from laboratory experiments will be presented in the conference. Results show that the near-surface radiative heating of suspended particles could lead to the formation of lifted temperature maximum (LT-Maxima) as proposed by Bhat, (2006). Results include the dependence of the LT-Maxima on concentration profile of particles, as it provides the heterogeneity required for the preferential radiative heating causing the temperature inversion. Turbulence in the mixing layer, by determining the distribution of halide-particle concentration over the relevant length scales, plays a key role in the phenomenon. Experimental evidence is presented to support this hypothesis.

RESULTS AND CONCLUSIONS

The expected temperature profile above the bottom surface of the laboratory setup is as shown in fig. 1.

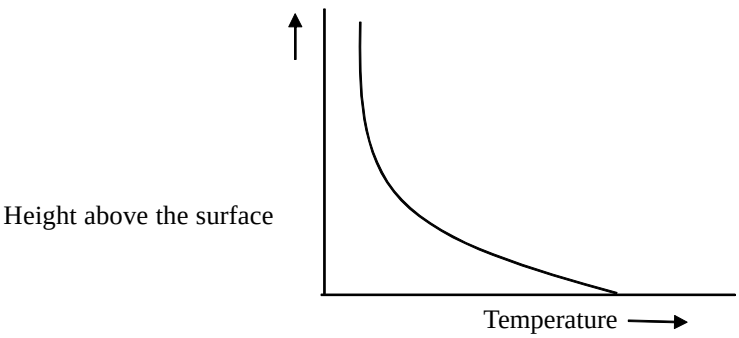

Figure 1

But the experimental result while suspending 2g of graphite particles in the water contained in the setup is as shown in fig. 2.

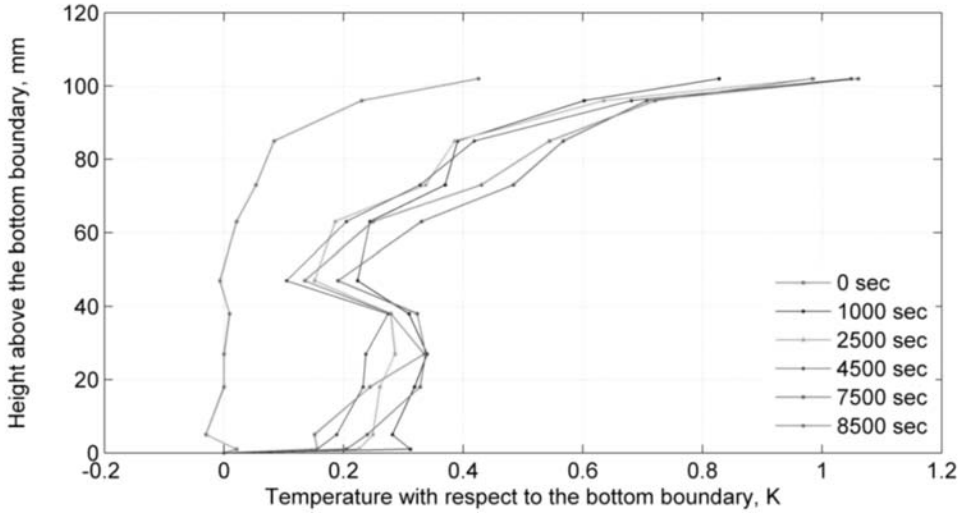

Figure 2

This shows that the temperature first increases and then starts decreasing leading to a certain intensity of lifted temperature maxima. As the amount of suspended particles is increased, the intensity of LT maxima increases, thus proving the fact that the temperature inversion occurs due to the near surface radiative heating of the particles.

ACKNOWLEDGEMENTS

We are really thankful to Ms. Ponnu Lakshmi and Mr. K. N. Singh for their help in the research work.

REFERENCES

Hutchison, J. E. and Richards, R. F. (1999).Effcet of Nongray Gas Radiation on Thermal Stability in Carbon Dioxide, *J. Thermophysics and Heat* Transfer, **13**, 1.

Bhat, G.S. (2006). Near-surface temperature inversion over the Arabian Sea due to natural aerosols, *Geophys. Res. Lett.***33**, 2.

Gille, J and Goody R. M (1964).Convection in a radiating gas, *J. Fluid Mechanics.*

Goody R. M (1956). The influence or radiative transfer on cellular convection, *J. Fluid Mechanics.*

STUDY OF DUST AEROSOL VARIATION DURING NORTHERN WINTER OVER ARABIAN SEA USING SATELLITE DATA

A.ANAND[1, 2], N.SANWLANI[3], M.C.R. KALAPUREDDY[2], P. CHAUHAN[3]

[1] Department of Atmospheric & Space Science, University of Pune, Pune-411007, India.
[2] Indian Institute of Tropical Meteorology, Pashan , Pune-411008, India.
[3] Space Applications Centre, ISRO, Satellite Road, Ahmedabad-380015, India

Keywords: DUST AEROSOL, AOD, ANGSTROM EXPONENT, VISIBILITY.

INTRODUCTION

Dust storm is one of the severe environmental issues. In meteorology, dust storm is a catastrophic atmospheric phenomenon where the violent winds pick up and transport fine particles like dust and silt from the ground, making the air hazy and severely reducing the visibility. Such natural calamity causes serious damage to atmospheric environment, transportation, property, health and subsequently the economy and social development. Therefore it calls forth a great attention and needs to be studied extensively (Kauffman, *et al.* 2002).

DATA AND METHOD

The aim of our study is to utilize satellite data for characterization of special category of aerosols - dust aerosol as satellite sensors provide a useful platform for making observations spread with a wide area coverage with advantage of their short-term and frequent observations (Kaufmann, *et al.* 1997). In this study, MODIS Aqua Level-1B satellite data was used for case study of dust storm events from 20th to 22nd December, 2011. Dust storms are characterized by high Aerosol Optical Depth (AOD), τ_a, lower Angstrom exponent (α) and near zero visibility condition (Sanwlani, *et al.* 2011).

The backscattered radiance data from Earth's surface reaching satellite sensor is processed by a (C language code) scientific algorithm and ENVI 4.4 image processing software to estimate these parameters. Spectral variation of aerosol optical depth (AOD), angstrom exponent (á) and horizontal visibility range of dust aerosols were estimated. Also the comparative study of AOD variation along with angstrom exponent (á) and AOD variation with visibility was plotted. Air mass back-trajectory analysis using online Hybrid Single Particle Lagrangian Integrated Trajectory HYSPLIT *(version 4.0)* model of the National Oceanic and Atmospheric Administration, NOAA was also done to identify possible source regions of aerosols during dust storm.

SUMMARY

The spectral variation of AOD(τ_a,) and Angstrom Exponent (á) characterize the dust particles and their size variation just before start of the dust storm and during the peak of dust storm. From the AOD variation, it is observed that there is increase in AOD from staring date 20th Dec 2011 to 22nd Dec 2011, similarly the concentration of larger particles increases as the Angstrom exponent (á) value decreases. Such increase in aerosol mass concentration noted along with decreasing Angstrom exponent (á) value infers the domination of coarse mode dust particles. Similarly the decline in the visibility was observed to be less than 1 km, noticed during the peak of the dust storm.From the HYSPLIT back trajectory analysis ,it was noticed that this dust event has originated from the

deserts of Afghanistan Pakistan, and dry lake beds of Central Asia traveled over northern Arabian Sea and finally reached towards Oman. The possible cause of the rise of dust storm is change in the wind pattern, and flow of strong northeasterly winds towards the Arabian sea. The area of sea affected is of 500km x 200km ,as the dust event continues for 2 days. The lowest Angstrom exponent (α) value estimated for 555nm was 0.8 and highest AOD (τ_a,)value was estimated for 555nm was 1.8.

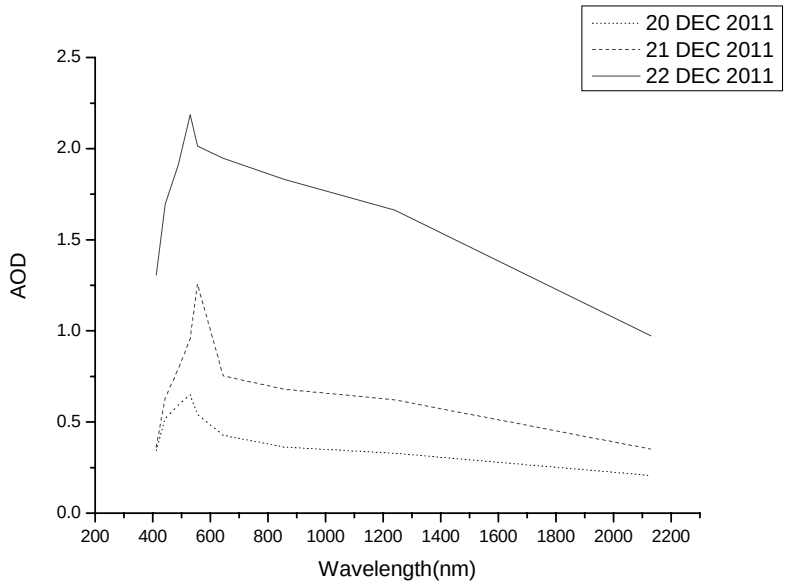

Figure 1. Spectral Variation of AOD on different dust strom days.

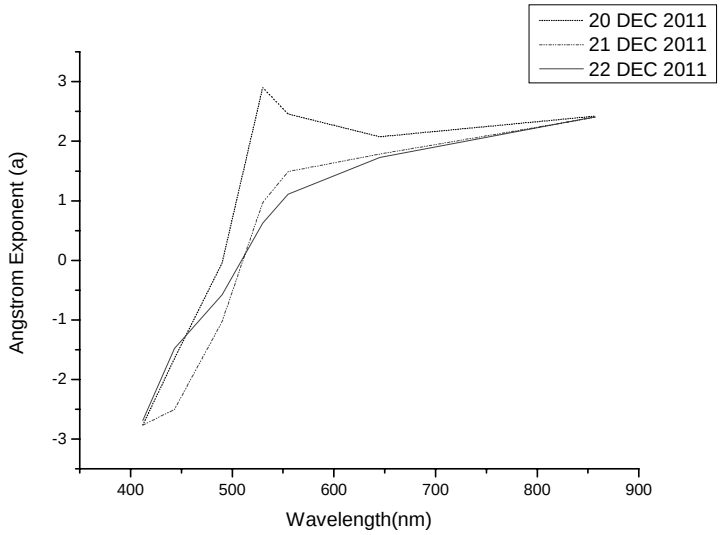

Figure 2. Spectral variation of angstrom exponent (α) on different dust storm days.

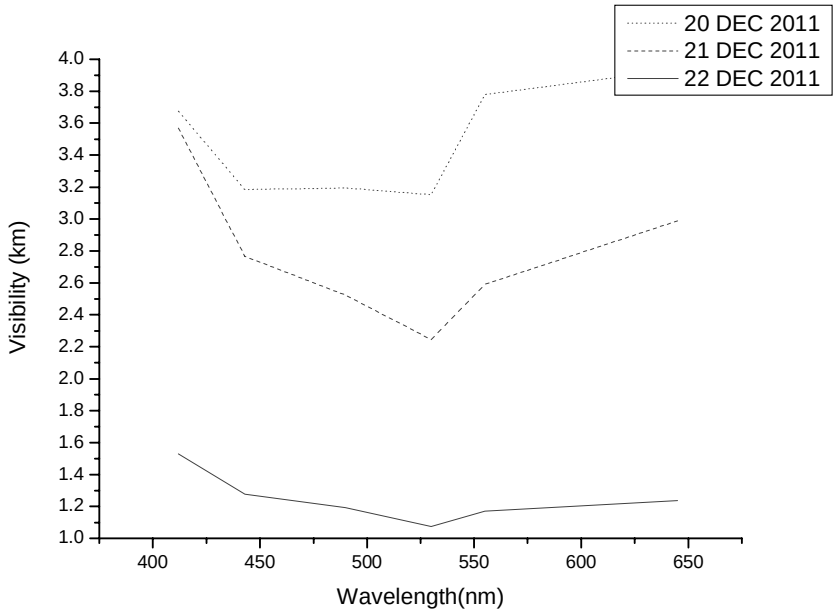

Figure 3.Spectral variation of visibility on different dust storm days.

ACKNOWLEDGEMENTS

I would like to acknowledge Indian Academy of Sciences, Bangalore, Indian National Academy of Sciences, New Delhi and The National Academy of Sciences India, Allahabad; who jointly awarded me the summer research fellowship. I am very grateful to Space Applications Centre (SAC), Indian Space Research Organisation (ISRO), Ahmedabad for providing me logistic support and various facilities like Library and uttermost a research friendly environment . I am also thankful to Dr. P. Pradeep Kumar, HOD, Department of Atmospheric and Space Sciences, University of Pune, for recommending me for this prestigious fellowship.

REFERENCES

Joseph George, (2003). Fundamentals Of Remote Sensing (Universities Press).

Kaufman, Y. J., Tanre, D., Gordon, H. R., Nakajima, T., Lenoble, J., Frouin, R., Grassl, H., Herman, B. M., King, M. D. and Teillet, P. M. (1997). Passive Remote Sensing Of Tropospheric Aerosol and Atmospheric Correction For The Aerosol Effect, *Journal Of Geophysical Research,* **16**, pp. 815–830.

Kaufman Y.J., Tanre, D. and Boucher, O. (2002). A Satellite View Of Aerosols In The Climate System, *Nature* ,**419**, pp. 215–223.

Sanwlani, N., Chauhan, P. and Navalgund, R. R. (2011).Dust Storm Detection and Monitoring Using Multi-Temporal INSAT-3A-CCD Data, *International Journal of Remote Sensing,* **32(19)**, pp. 5527-5539.

STUDY OF VERTICAL DISTRIBUTION OF MESOSPHERIC AEROSOL NUMBER DENSITY

PRATIBHA B. MANE[a], D. B. JADHAV[b], A. VENKATESWARA RAO[a]*

[a]Department of Physics, Shivaji University, Kolhapur-416 004, Maharashtra state, India.
[b]Indian Institute of Tropical Meteorology, Dr. Homi Bhabha Road, Pashan,
Pune-411 008, India.
Email: pratibhabm263@gmail.com

Keywords**:** AEROSOLS, TWILIGHT PHOTOMETER, MESOSPHERE, TSM

INTRODUCTION

Twilight scattering method (TSM) is extensively used by several workers in all over the world to study the vertical distribution of aerosol particles which is a strong function of their sources, sinks and their residence times. All this study is mainly on the stratospheric aerosols.

The mesosphere is the layer of the Earth's atmosphere situated about 50 to 85 kilometers above the Earth's surface. The mesosphere lies above the maximum altitude for aircraft and below the minimum altitude for orbitalspacecraft. It has only been accessed through the use of sounding rockets. Therefore the mesospheric aerosols are least studied.

In the present work an attempt is made to calculate the mesospheric and thermospheric aerosol number density per cubic decimeter(AND) by TSM, for the first time in India. The aerosol measurements have been carried out at Kolhapur (16°422N, 74°142E) by using newly designed Semiautomatic Twilight Photometer during the period 1 January 2009 to 30 December 2011 to study the vertical distribution of the mesospheric and thermospheric aerosol number density per cubic decimeter Here after aerosol number density per dm^3 is abbreviated as 'AND'. The day to day variability of the vertical distribution of mesospheric AND, monthly and three years variations of mesospheric AND have been discussed in the present study.

INSTRUMENTATION

The instrument, semiautomatictwilight photometer, has been newly designed, developed and tested at IITM, Pune, India. The semiautomatic twilight photometer consists of a simple experimental set up. It comprises of a telescopic lens of diameter 15 cm having a focal length of 35 cm.amd a red glass filter peaking at 670 nm with a half band width of about 50 nm. The red filter of 2cm diameter and an aperture of 0.6 cm diameter are placed at the focal length of convex lens, provides approximately 1^0 field of view [(Aperture diameter/Focal length of lens) X57= (0.6cm/35cm) X 7=0.9771 degree]. A photomultiplier tube (PMT)-9658B is used as a detector. The PMT requires a high voltage i.e. 700Volts and hence a DC-DC converter (Powertex -061081001, High volt unit) with high output voltage is used as a power supply. The output signal (current) of the PMT, used for detecting the light intensity during the twilight period, is of the order of nano to microamperes. The amplitude or strength of this low signal is amplified by using newly designed fast pre-amplifier during this study. The more details regarding the instrument and Fast pre-amplifier were given elsewhere, (Mane, *et al.*, 2012).The amplifier output recorded by the digital multimeter, Rishcom-100, having an adapter can store the data automatically for every 10secs in the form of date, time and intensity in Volts.

RESULTS AND DISCUSSION

The day-to-day, monthly, seasonal and annual variability of aerosol number density per dm³ in mesosphere

The aerosol number density over Kolhapur in volcanically quiescent period (3 January 2010-Morning) vary from 185 particles per cm^3 at ~6 Km to about 1 particle per cm^3 at ~44Km. After 45 Km the aerosol number density is less than 1 particle per cm^3. It is inconvenient to say some fraction of particle per cm^3 (i.e. say 0.637 particles per cm^3). So the aerosol number density for the mesosphere is expressed in terms of the aerosol number density per decimeter^3 (AND/ dm^3). Thus, it is convenient to say 637 particles per dm^3 instead of 0.637 particles per cm^3. The aerosol number density in mesosphere vary from 637 particles per dm^3 (~50 Km) to 315 particles per dm^3 (~85 Km) over location Kolhapur (16°422N, 74°142E) in volcanically quiescent period (6 February 2009-Morning).

The values of the aerosol loading factor 'Q' have been computed using equation (Jadhav and Londhe, 1992):

$$Q = \sum_{h1}^{h2} Aerosolnumberdensityper\ cubicdecimeter \qquad (1)$$

In this equation 'h_1' and 'h_2' represents the lower and upper limits of the shadow heights respectively. The method for calculating the height of the earth shadow is given by Shah (1970).

The aerosol number density was calculated by using an empirical formula derived by actual Lidar observations and Twilight Photometric observations as stated below:

Aerosol number density per dm^3

$$= \text{Antilog}_{10} \{10['-1/I\ (dI/dh)']-1\} \qquad (2)$$

Where 'I' is the observed intensity, 'dI' and 'dh' are the differences in intensities and shadow heights, respectively observed at time't' and (t+dt).

Various types of variability of 'Q' are shown in Fig. 1, 2 and 3. Figure-1 shows graph of lower mesospheric aerosol loading abbreviated as 'Q_1' plotted against day numbers for all of the three years. The values of 'Q_1' are calculated for altitude interval between 51 and 65 Kilometers. Figure-2 shows graph of upper mesospheric aerosol loading abbreviated as 'Q_2' plotted against day numbers for all of the three years. The values of 'Q_2' are calculated for altitude interval between 66 and 85 Kilometers. Figure-3 shows graph of lower thermospheric aerosol loading abbreviated as 'Q_3' plotted against day numbers for all of the three years. The values of 'Q_3' are calculated for altitude interval between 85 and 100 Kilometers. In these figures Y-axis represents aerosol loading and X-axis represents day numbers (i.e. date for each month). The numbers from 1 to 365 corresponds to dates from 1 January 2009 to 31 December 2009. Similarly the numbers from 366 to 730 represents dates from 1 January 2010 to 31 December 2010. Also the numbers from 731to 1095 stands for dates from 1 January 2011 to 31 December 2011.The TSM data collection at Kolhapur is generally not possible during ~mid-May to ~mid-October in any year because of the prevailing monsoon conditions (rains and extensive cloud cover). This being a passive technique, clear sky conditions are preferable for obtaining the vertical profile of aerosols. Thus data coverage is for the period ~mid-October of any year to ~mid-May of the succeeding year.

Values of Q_1 are greater than Q_2, implying a decrease of aerosol number density with respect to increasing amplitude. Mesospheric aerosol loading showed day to day variability but there was no specific trend for monthly variability for all the three years. The mesospheric aerosols completely depend on an influx of meteor matter including sporadic asteroidal dust particles and meteor showers, which bring particles of both cemetery and asteroidal origin (Mateshvili, *et al.*, 1998). Mateshvili, *et.al* proved that the meteor material enters in the atmosphere non uniformly (Mateshvili, *et al.*, 1997). The results of our study are in good agreements with earlier workers.

One noticeable point was that for the entire three years mesospheric aerosol loading was lowest for the month of February, the period free from strong meteor activities; whereas maximum for the month of December, the period followed by Orionids, Leonids and Geminids activities. There are so many evidences for the influx of meteoric matter in the mesosphere, which support our study. (Bigg, 1956; Mateshvili, *et al.*, 1998, 1999, 2000).

Three years variability of lower mesospheric (51-65 km), upper mesospheric (66-85 km) and lower thermospheric (86-100 km) aerosol loadings

Comparison between three year's lower mesospheric aerosol loadings for the months of October, November and December resulted with uncertain outcomes. The strong meteor activities of Orionids (21st October), Leonids (17th November) and Geminids (14th December) attributed noticeable fluctuations in the values of 'Q_1'. Lower mesospheric aerosol loading showed unclear difference for three of the years for the months of February, March and beginning of April. The considerable deviations were observed after the strong meteor activities of Quadrantids (3rd January), Lyrids (22st April) and Eta Aquariids (6th May), implying that the dust particles intruded into the upper atmosphere during meteor showers penetrated downwards causing increase in lower mesospheric aerosol loading. One noticeable point was that for the entire three years 'Q_1'was lowest for the month of February, the period free from strong meteor activities; whereas maximum for the months of December and January, the period followed by Orionids, Leonids and Geminids activities. The amount of dust particles added in the atmosphere is not equal for every year. Therefore considerable deviations were noticed. The results of present study revel that the dust particles during strong meteor showers intrude in the Earth's atmosphere below 120 km. These dust particles penetrate the lower atmosphere and also acts as cloud condensation nuclei. Thus middle and upper atmospheric aerosol loadings completely depend on an influx of meteor matter including sporadic asteroidal dust particles and meteor showers, which bring particles of both cemetery and asteroidal origin. The results of our study and earlier workers are supporting this fact.

All the above explanation is applicable for remaining two aerosol loadings viz. 'Q_2', and 'Q_3'. All of these three aerosol loadings from 'Q_1' to 'Q_3' showed in-phase relation with each other.

SUMMARY AND CONCLUSIONS

The measurements using the twilight sounding method presented in this paper suggest the following:

1. The semiautomatic twilight photometer yields a reasonable qualitative picture of the vertical distribution of mesospheric and thermospheric aerosol number density per cubic decimeter (AND/ dm^3).

2. The AND profiles derived by imperial formula matches well with general trend of vertical profiles of aerosols.

3. The mesospheric AND shows lowest values in the quiescent period of meteor activities and highest values following departure of meteor showers.

4. There is no specific annual variation in mesospheric aerosol loading. This is indicative of the no uniformity on an influx of meteor matter.

5. The middle and upper atmospheric aerosol loadings completely depend on an influx of meteor matter including sporadic asteroidal dust particles and meteor showers, which bring particles of both cemetery and asteroidal origin.

6. All of the three aerosol loadings from 'Q_1' to 'Q_3' showed in-phase relation with each other.

7. The main aim of this study is to demonstrate the measurement capabilities offered by semiautomatic twilight photometer and it is the first attempt in India made by the authors to estimate mesospheric and thermospheric aerosol number density per cubic decimeter (AND/ dm^3).

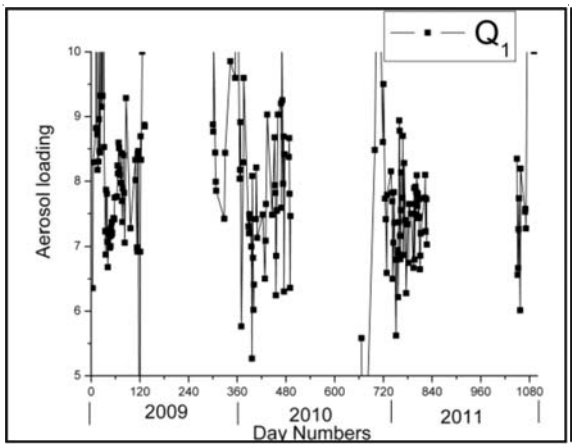

Figure-1: Three years variability of lower mesospheric (51-65 Km) aerosol loading (Q_1)

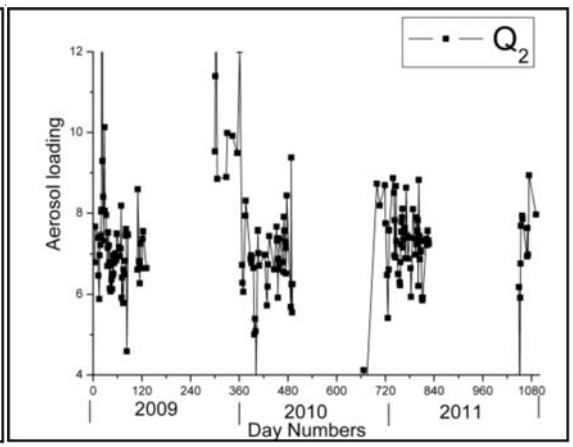

Figure-2: Three years variability of upper mesospheric (66-85 Km) aerosol loading (Q_2)

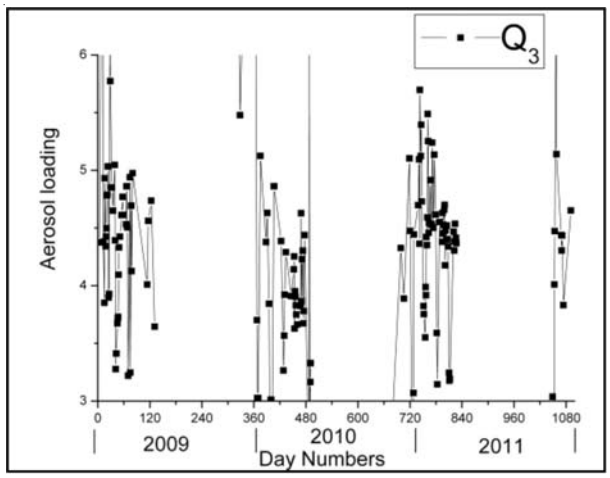

Figure-3: Three years variability of lower Thermospheric (86-100 Km) aerosol loading (Q_3)

ACKNOWLEDGEMENTS

One of the authors (Sou. Pratibha B. Mane) is grateful to the Shivaji University authorities, Kolhapur, for the encouragement during the course of this work.

REFERANCES

Jadhav, D. B. & Londhe, A. L. (1992).Study of atmospheric aerosol loading using the twilight method, *J. Aerosol Sci*., **23**, pp. 623-630.

Mane, Pratibha B., Jadhav, D. B., Venkateswara Rao, A. (2012). Fast pre-amplifier designed for semiautomatic twilight photometer, *DAVInternational Journal of Science (DAVIJS)*, **1**, Issue-2, pp. 9-11.

Mane, Pratibha B., Jadhav, D. B., Venkateswara Rao, A. (2012). Semiautomatic twilight photometer design and working, *International Journal of Scientific and Engineering Research (IJSER)*, **3**, Issue-7, pp. 1-7.

Mateshvili, Iuri, Mateshvili, Giuli, Mateshvili, Nino (1998). Measurement of the vertical aerosol distribution in the middle atmosphere by the twilight sounding method, *J. Aerosol sci*., **29**, No. 10, pp. 1189-1198.

Mateshvili, G. G., Mateshvili, Yu. D., Mateshvili, N. Yu. (1997). Optical observations of ç-Aquarid dust in the Earth æ˚$%a¨ s atmosphere, *Solar System Research*, **31**, pp. 483-488.

Nino Mateshvili, *et al.*, (1999).Vertical distribution of dust particles in the Earth's atmosphere during the 1998 Leonids, *Meteoritics and Planetary Science*, **34**, pp. 969-973.

Nino Mateshvili *et al.*,(2000). Dust particals in the atmosphere during the Leonid meteor showers of 1998 and 1999, *Earth,Moon and Planets*, **82-83**, pp. 489-504.

Bigg, E. K. (1956). The detection of atmospheric dust and temperature inversion twilight scattering, *Journal of Meteorology*, **13**, pp. 262-268.

COMPARATIVE STUDY OF CAIPEEX AIRCRAFT OBSERVATIONS WITH MODIS AND UTILITY OF REANALYSIS DERIVED DATA

G.R.CHINTHALU

Indian Institute of Tropical Meteorology
Dr. Homi Bhabha Road Pashan Pune 411008

Key words: CAIPEEX, break, active, monsoon, reanalysis satellite-derived

INTRODUCTION

The Asian summer monsoon rainfall during June–September plays and important role in the lives of people of Asia by bringing the much needed rainfall to provide relief from scorching hot summer. The health of Indian economy is very much dependent on monsoon rainfall. Due to the behavior of monsoon three different scenarios emerge every year viz. normal about 89 cm of the long term average, below normal and excess monsoon. According to (Sperber and Palmer, 1996) numerical prediction of monsoon variability on all time scales is severely handicapped due to the inability of models to simulate the year to year variability. These deficiencies have been demonstrated clearly in the Atmospheric Model Intercomparison Program (AMIP). The Indian summer monsoon rainfall (ISMR) shows large interannual and intraseasonal variations due to embedded active and break spells, which leads to large scale and localized droughts. The agriculture activities are severely affected during drought monsoon seasons and growth of economy is under major pressure. Drought conditions leads to the deficiency of drinking water food fodder and large scale agricultural unemployment and suffering of the affected people. In order to alleviate such problems many state Governments in India viz. Andhra Pradesh, Karnataka, Maharashtra etc have conducted cloud seeding experiments as an alternative to enhance rainfall during deficient monsoon seasons (CAIPEEX Science plan). Weather modification experiments for rain enhancement were carried on in recent years over different parts of the world for a wide variety of applications such as water resource management, hydroelectric power generation and agriculture for e.g. (Komuscu A.U., 2008).

During the summer monsoon season 2009 a field experiment named CAIPEEX (Cloud aerosol interactions precipitation enhancement experiment) phase –I was conducted over India, to examine the role of aerosols on cloud development, growth and dissipation. The CAIPEEX experiment was mainly conducted along the west coast east coast of India and the monsoon trough zone region. An instrumented air-craft was used to collect in-situ observation of aerosols and cloud microphysical parameters viz. Cloud condensation nuclei (CCN), liquid water content, total water content, temperature, humidity etc. The different instruments onboard aircraft were (CDP) Cloud droplet probe, (CIP) Cloud imaging probe, (CCN) Cloud condensation nuclei counter, LWC probe etc.

DATA AND METHODOLOGY

Daily mean Air craft derived CDPRe, (Cloud droplet effective radius μm), Satellite derived (MODIS) (Cloud droplet effective radius μm), Liquid water content, Aerosol Optical Depth, (NCEP) National centre Environment Prediction derived reanalysis data, such as Winds, Sea surface temperature, Specific humidity and (GPCP) Global Precipitation Climatology Project derived rainfall are analyzed and compared with CAIPEEX aircraft observations collected over Hyderabad and Benguluru during June 2009.

CONCLUSIONS

In this study the CAIPEEX recorded air-craft observation over Hyderabad and Banguluru viz. Cloud droplet effective radius are compared with co-located satellite derived Cloud droplet effective radius. The CAIPEEX- derived CDPRe for break phase varied between 5.6 to 11.7 μm, while during active phase CDPRe varied between 11.7 to 17.0 μm.

The MODIS derived CDPRe in the domain 5°S-25°N and 40°E-100°E was of the order of d" 10 μm during the break phase, and during the active phase for the same domain the CDPRe varied between 15-20 μm. Although the accuracy of air-craft derived data is better than satellite derived CDPRe, It is suggested that with the availability of satellite derived data and reanalysis data products with minimum lag period may help us in taking suitable and more accurate decisions in operational cloud seeding experiments.

ACKNOWLEDGEMENTS

The author is thankful to Prof. B.N.Goswami Director IITM-Pune for his keen interest in the subject and constant encouragement. Thanks are also due to the IITM -2009 CAIPEEX field observing team for collecting valuable data utilized in this study.

REFERENCES

CAIPEEX- Science plan (www.tropmet.res.in)

Komuscu A.U. (2008). An assessment of impact of cloud seeding on local rainfall- A case study of part of the ISKI rain enhancement program conducted in Istanbul, Turkey during 1990-1991, *Weather modification,* pp. 17-27.

Sperber, K. R., and Palmer T. N. (1996). Interannual tropical rainfall variability in general circulation model simulations associated with the Atmospheric Model Intercomparison Project, *J.Climate*, **9**, pp. 259-278.

In-Situ Observations Of Aerosol Properties During RAWEX-GVAX Field Campaign At Nainital

U. C. Dumka[1], Manish Naja[1], Narendra Singh[1], D.V. Phanikumar[1], Ram Sagar[1], S. K. Satheesh[2], K. Krishna Moorthy[3] and V R Kotamarthi[4]

[1]Aryabhatta Research Institute of Observational Sciences (ARIES), Nainital 263129, India
[2]Center for Atmospheric and Oceanic Sciences, India Institute of Observational Sciences, India
[3]Space Physics Laboratory, Vikaram Sarabhai Space Center, Trivandrum, India
[4]Argonne National Laboratory, USA

Keywords: AEROSOL OBSERVING SYSTEM, CLOUD CONDENSATION NUCLEI, SINGLE SCATTERING ALBEDO

Introduction

The Indo-Gangetic Plain (IGP) is one of the largest and most rapidly developing region and encompasses a variety of anthropogenic and biogenic source of pollutants (gaseous and particles). Among the major sources of aerosol, emissions from agricultural-waste and biomass burning dominate during the wintertime (December –February) (Venkataraman, *et al.*, 2005). The transport of mineral aerosol from arid and semi-arid regions of western India, during the summer (April–early June), imparts strong temporal variability in the optical properties of aerosol (Chinnam *et al.*, 2006; Jethva *et al.,* 2005). The measurements of aerosol optical depth (AOD) and absorption aerosol optical depth (AAOD) have characterized IGP as a hotspot for anthropogenic aerosol in south-Asia (Ramanathan *et al.,* 2007). In view of this, a field campaign RAWEX-GVAX (Regional Aerosols Warming Experiment-Ganges Valley Aerosol Experiment) is conducted at a high altitude station in Nainital (29.5^{o} N, 79.5^{o} E; ~1958 m above the mean sea level) under Indo-US collaboration programme to study the optical and microphysical properties of aerosols, cloud-aerosol interaction and its impact on earth's radiation budget. The Aerosol Observing System (AOS) that comprises a set of instruments designed primarily for the continuous measurements of optical and microphysical properties of atmospheric aerosol at the surface was operational. The principal measurements are those of the aerosol absorption and scattering coefficients, backscattered radiation, concentration, cloud condensation nuclei, particle number concentration and particle size distribution as a function of the particle size and radiation wavelength. These measurements are used for calculating the aerosol single scattering albedo (SSA), asymmetry parameter (g) and hygroscopic growth factor and those are used for radiative forcing estimation.

Experiment Details And Data Base

The experimental site (29.5^{o} N, 79.5^{o} E) Manora Peak, Nainital is located in the lower part of central Himalayas at an altitude of ~1958 meter above mean sea level and hence is above the planetary boundary layer for most of the time (Pant *et al.,* 2006). Multiple aerosol sources are prevalent including organics from dense local vegetation, biomass and biofuel burning and fossil fuel combustion as well as dust from long range transport.

The experimental data are considered of scattering and absorption coefficients of aerosols coefficients using the three wavelengths TSI Nephelometer and Particle Soot Absorption Photometer along with the total number concentration of condensation particles (from Condensation Particle Counter;

TSI Model 3010) and Cloud Condensation Nuclei (CCN) concentration (from single column DMT Model 1). The details of measured and derived parameters are given in table 1. The details of the instruments, measurements and data analysis is given elsewhere (Delene *et al.*, 2002; Sheridan *et al.*, 2001).

Instruments	Primary measurements	Derived measurements
TSI model 3563 three wavelength, backscatter/total scattering integrating Nephelometer operated at low (<40%) and variable (~40-90%) relative humidity	Total scattering and hemispheric backscattering coefficients (σ_{sp}&σ_{bsp}) from <1µm and < 10µm particles at blue (0.45), green (0.55) and red (0.70) µm	Hemispheric backscatter fraction, b $=\sigma_{bsp}/\sigma_{sp}$ Scattering Ångström exponents, α_{sp}= $-\log[\sigma_{sp}(\lambda_1)/\sigma_{sp}(\lambda_2)]/\log[\lambda_1/\lambda_2]$ Single scattering albedo, $\omega = \sigma_{sp}/(\sigma_{sp}+\sigma_{ap})$ Submicron scattering fraction, $R_{sp} = \sigma_{sp}(1\text{-}\mu m)/\sigma_{sp}(10\text{-}\mu m)$ Hygroscopic growth factor, f(RH) $= \sigma_{sp}(RH=85\%)/\sigma_{sp}(RH=40\%)$
Radiance Research Particle Soot/Absorption Photometer (PSAP)	Light absorption coefficients (σ_{ap}) from <1 µm &<10 µm particles at blue (0.467), green (0.53) and red (0.66) µm	Single scattering albedo, $\omega = \sigma_{sp}/(\sigma_{sp}+\sigma_{ap})$ Absorption Ångström exponents, α_{ap}= $-\log[\sigma_{ap}(\lambda_1)/\sigma_{ap}(\lambda_2)]/\log[\lambda_1/\lambda_2]$ Submicron absorption fraction, $R_{ap} = \sigma_{ap}(1\text{-}\mu m)/\sigma_{ap}(10\text{-}\mu m)$
Continuous Light Absorption Photometer (CLAP)	Light absorption coefficients (σ_{ap}) from <1 µm &<10 µm particles at blue (0.467), green (0.53) and red (0.66) µm	Single scattering albedo, $\omega = \sigma_{sp}/(\sigma_{sp}+\sigma_{ap})$ Absorption Ångström exponents, α_{ap}= $-\log[\sigma_{ap}(\lambda_1)/\sigma_{ap}(\lambda_2)]/\log[\lambda_1/\lambda_2]$ Submicron absorption fraction, $R_{ap} = \sigma_{ap}(1\text{-}\mu m)/\sigma_{ap}(10\text{-}\mu m)$
TSI model 3010 Condensation Particle Counter (CPC)	Total particle concentration over the range 0.01-3 µm diameter (CN)	None
Cloud Condensation Nuclei Counter (CCN) (Single column Droplet Measurement Technologies)	C oncentrations of cloud condensation nuclei (N_{CCN}) at seven supersaturations between - 0.01 to + 0.75%.	None

Table 1.AOS instruments and their parameters.

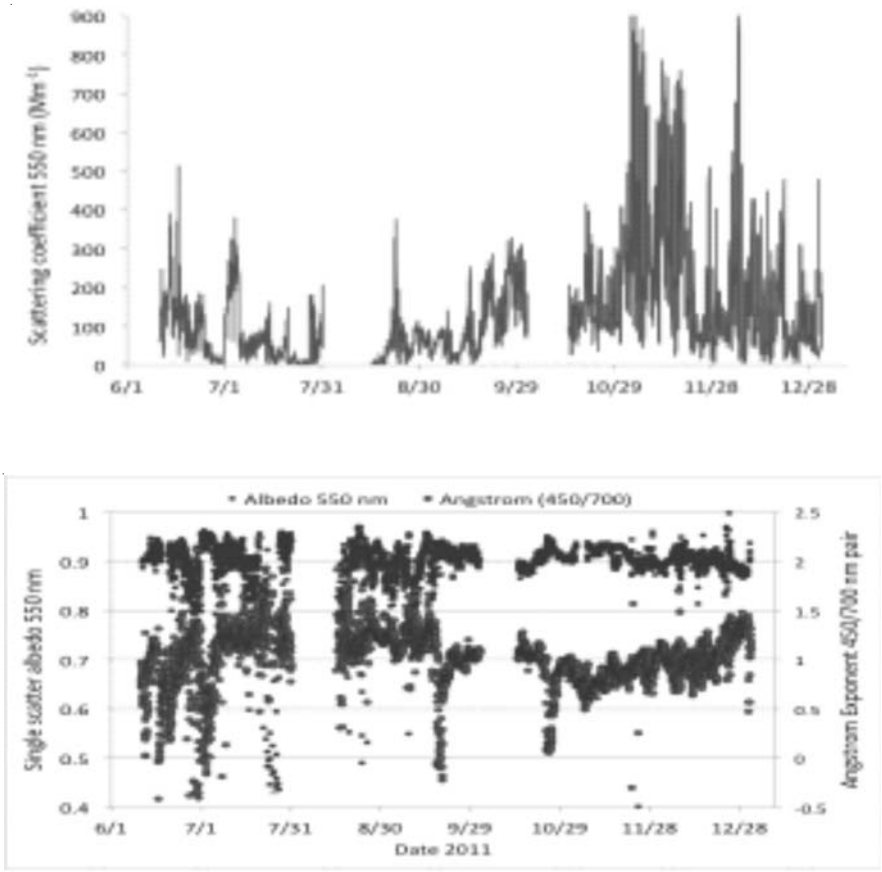

Figure 1. Top panel shows the temporal variation of scattering coefficient at 550 nm and bottom panel shows the temporal variation of single scattering albedo and Ångström exponent between 450 to 700 nm wavelengths.

Results and Discussion

Fig. 1 shows different observed parameters using the aerosol observing system (AOS). Observed scattering coefficient show a large variability during the observational period. Lower values of scattering coefficients are seen during the monsoon seasons and it shows an increasing trend thereafter. It can be noticed that the scattering coefficient shows large variability between the summer monsoon and the post monsoon season, while there is a little variability in the aerosol intensive properties. There are some episodic events, when either large or dark aerosols are present. In general the aerosol over the observational site has a relatively higher single scattering albedo and a low Ångström exponent, which indicates relatively large particles with a low absorption. Also the hygroscopic growth factors which are the ratio of scattering at 85/40% RH are moderate to low and indicate that the aerosol isn't highly oxidized. Detailed analysis will be shown during the presentation.

Conclusion

The major findings are as follows:

1. Near surface aerosol properties measured at ARIES, Nainital shows significant temporal variation during the observation period.

2. Generally the aerosols over the sites are large in size with low absorption.

ACKNOWLEDGEMENT

The author wishes to thank the technical staff of ARM for providing the valuable data. This study is carried out under the RAWEX-GVAX project in collaboration among Department of Energy, U.S., Indian Institute of science, Bangalore, Indian Space Research Organization and ARIES.

REFERENCES:

Chinnam, et al. (2006).*Geophys. Res. Lett.* , **33**, L08803.

Delene, et al. (2002).*J. Atmos. Sci.*,**59**, 1135.

Dumka, U. C. et al. (2008). JAMC.

Jethva, et al. (2005).*J. Geophys. Res*., **110**, D21204.

Pant, et al. (2006). *J. Geophys, Res*.,**111**, D17206.

Ramanathan, et al. (2007).*J. Geophys, Res*.**112**, D22S21.

Sheridan, et al. (2001).*J. Geophys. Res*., **106,** D18, 20735

Venkatraman et al. (2005).*Science*, **307**, pp. 1454–1456

PRE-MONSOON AND POST-MONSOON LONGTERM TRENDS AND VARIABILITY OF AEROSOL OPTICAL DEPTH USING MODIS DATA OVER AN URBAN SITE IN THE INDO-GANGETIC

KIRTI SONI AND TARANNUM BANO

Radio and Atmospheric Sciences Division,
National Physical Laboratory (CSIR), Dr. K.S. Krishnan Road, New Delhi, 110012, India

Keywords: AEROSOL OPTICAL DEPTH, ANGSTROM EXPONENT,MODIS

INTRODUCTION

The atmospheric aerosols affect directly the climate by absorbing and scattering solar radiation. Aerosols also have an indirect effect on the Earth's radiation budget by varying the microphysical properties of clouds, consequently influencing their optical properties and lifetimes (Pereira, *et al.*, 2008). Anthropogenic pollutants increased in the past decades owing to extensive urbanization, industrialization, construction activities, increase in the vehicular pollution and biomass burning etc. Variability in aerosol is one of the most important factors determining the change in the radiative budget of the climate system (Xia, 2011). For that reason, it is essential to study the long term change in Aerosol Optical depth (AOD) and Angstrom Exponent (AE) in order to know the processes involved in the climate change (Streets, *et al*. 2009; Wang, *et al.* 2001; Wild *et al.* 2009; Xia, 2011).The main objective of the present work was to investigate the variability of the satellite measured AOD and AE in recent decades. Monthly averaged MODIS data for 147 months (from March 2000 to May 2012) have been investigated to determine the trend and variabilities in AODs, AE over Delhi.

DATA AND SITE DESCRIPTION

MODIS (MODerate resolution Imaging Spectroradiometer) Terra, level -3 monthly data of Aerosol Optical Depth (AOD) (550nm) and Angstrom Exponent (AE) (470/660nm) have been used in this study over Delhi (28.38 N, 77.10 E; 235m above mean sea level). Delhi is amongst the top 10 for cities with the most poor air quality. In the past two decades, Delhi is expanding speedilysubsequently, demands for transportation, energy generation, construction, waste generation, domestic cooking and heating, and industrial activity grew considerably.In the present paper to observe the trend, the complete data set (from March 2000 to May 2012) has been divided in to two periods, namely Pre-monsoon or summer (April to June) and Post-monsoon or winter (October to January) on the basis of the existing meteorological conditions.

RESULTS AND DISCUSSIONS

The long term average AOD values were found to be 0.798±0.258and 0.675±0.147 for pre-monsoon and post monsoon seasons respectively. AE values were 0.558±0.027, and 0.765±0.117 for pre-monsoon and post monsoon seasons respectively.The post-monsoon season is characterized by higher values of AE i.e., fine mode aerosols particles. The high AE during post-monsoon periods is mainly caused by local meteorological conditions developed over the study area when the boundary layer is low and, because of relatively low wind speed, the ventilation coefficient is also very low, resulting in the accumulation of pollutants and aerosols emitted from vehicular emissions, thermal power plants and industries emission etc. (Soni, *et al.*, 2010). On the other hand, the lowest values

of AE are found in pre-monsoon season owing to frequency in dust activity as Delhi is in the downwind direction of the dust outflows (Gautam ,*et al.*, 2009; Prasad, *et al.*, 2007).Decreasing trend is observed for the pre-monsoon season while increasing trend is observed for post-monsoon season in AOD. On the other hand, increasing trend is observed for AE during both the seasons. An increasing trend in AE during both the seasons is related with increase in fine mode anthropogenic emissions while an increasing trend in AOD is observed during post-monsoon seasons. This was due to the meteorological conditions and human activities (Khillare, *et al.*, 2004).

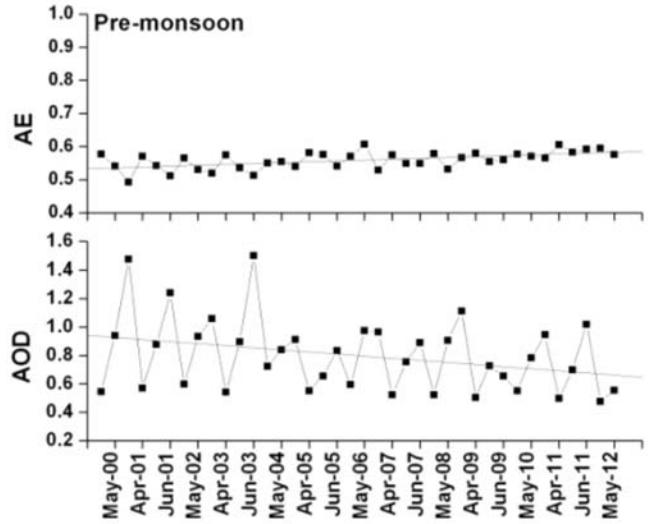

Figure 1.Monthly average variation of AOD and AE during Pre-monsoon season over Delhi (from Mar 2000 to May 2012).

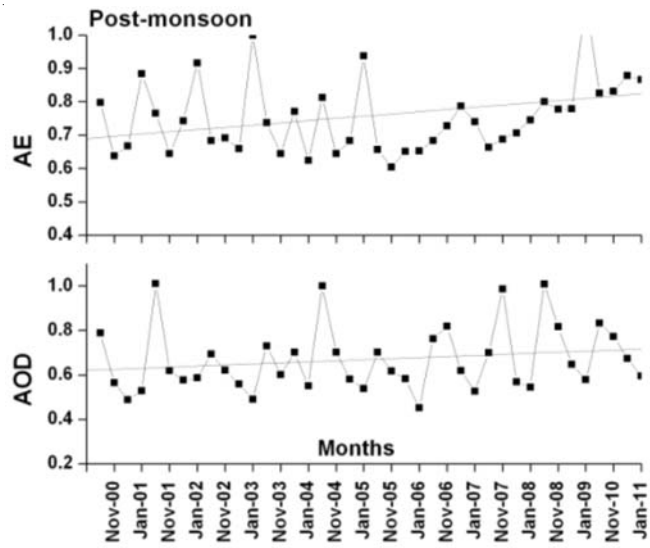

Figure 2.Monthly average variation of AOD and AE during Post-monsoon season over Delhi (from Mar 2000 to May 2012).

SUMMARY

In the present study long term (13-years) MODIS AOD data from Mar 2000 to May 2012 have been analyzed to observe the long term trend and variability's. The analysis of the results suggested that –

- Decreasing trend is observed for the pre-monsoon season while increasing trend is observed for post-monsoon season in AOD.
- Increasing trend is observed for AE during pre-monsoon and post-monsoon seasons.
- Lower values of AE are found in pre-monsoon season whereas higher values are observed during post-monsoon seasons.

ACKNOWLEDGEMENTS

Authors are thankful to NASA's , GIOVANNI and MODIS for making aerosol datasets available for research.

REFERENCES

Khillare, P. S., Balachandran, S., Meena, B. R. (2004). Spatial and temporal variation of heavy metals in atmospheric aerosol of Delhi, *Environmental Monitoring and Assessment*, **90**, pp. 1-21.

Pereira, S., Wagner, F., Silva, A. M. (2008).Scattering properties and mass concentration of local and long-range transported aerosols over the South Western Iberia Peninsula, *Atmos. Environ*, **42**, pp. 7623-7631.

Prasad, A. K., Singh, R. P. (2007). Comparison of MISR-MODIS aerosol optical depth over the Indo-Gangetic basin during the winter and summer seasons (2000–2005), *Remote Sensing of Environment*, **107** ,pp.109–119.

Soni, *et al.* (2010). Variations in single scattering albedo and Angstrom absorption exponent during different seasons at Delhi, India, *Atmospheric Environment*, **44,** pp. 4355–4363.

Gautam , R., Liu, Z., Singh, R. P., and Hsu, N. C. (2009). Two contrasting dust-dominant periods over India observed from MODIS and CALIPSO data, *Geophys. Res. Lett*.,**36,** L06813.

Streets, *et al.* (2009). Anthropogenic and natural contributions to regional trends in aerosol optical depth, 1980–2006, *Journal of Geophysical Research*, **114,** D00D18.

Wang, B., Wang, Y. (1996). Temporal structure of the southern oscillation as revealed by waveform and wavelet analysis, *Journal of Climate*, **9**,pp.1586-1598.

Wild M. (2009). Global dimming and brightening: A review, *Journal of Geophysical Research*, **114**, D00D16.

Xia, X. (2011).Variability of aerosol optical depth and Angstrom wavelength exponent derived from AERONET observations in recent decades, *Environmental Research Letters*, **6**, 044011, pp. 1-9.

AEROSOL CLIMATE EFFECT

INFLUENCE OF EPISODIC DUST EVENTS ON THE AEROSOL OPTICAL PROPERTIES OVER DEHRADUN

PIYUSH PATEL[1], YOGESH KANT[2], AND D. MITRA[2]

[1]Cal-Val Division, Marine, Geo& Planetary Sciences Group (MPSG)
Space Applications Centre, Indian Space Research Organization (ISRO),
[2]Marine & Atmospheric Science Department, Indian Institute of Remote Sensing,
Indian Space Research Organisation (ISRO), Dept. of Space, Govt. of India,
Dehradun- 248001

Keywords : AOD, MODIS

INTRODUCTION

Aerosols are significant contributors to atmospheric extinction and play an important role in atmospheric heating patterns by scattering and absorbing solar radiation.The intergovernmental panel on climate change fourth assessment report (IPCC, 2007) estimate for the global annual radiative forcing of the first indirect effect is -0.7 Wm^{-2} with an uncertainty range of -1.8 to -0.3 Wm^{-2}.Recent studies indicate that the variations in heating pattern affect the monsoon rainfall patterns by modulating cloud processes (Lau et al., 2006). Dehradun (30° 30' N, 78°18' Eand 730 m a.m.s.l.)is situated in the northeast part of Indo-Gangetic plains where significant seasonal variations in AOD, aerosol mass concentration and their optical properties are expected due to increased anthropogenic activities. This region experiences four dominant seasons each year winter (December-March), pre-monsoon (April-June), monsoon (July-September) and post-monsoon (October-November). During pre-monsoon season, air mass carries dust particles by southwesterly winds from Thar Desert (Sikka D.R. 1997) and during post-monsoon season, atmosphere is loaded with black carbon and other fine mode organic particles due to large-scale biomass burning from the Indo-Gangetic plain.

Measurements of AODs by Microtops-II sunphotometer & ozonometer and black carbon (BC) concentration have been carried out over Dehradun during April -May2012. In addition to these observations, satellite derived AOD and Aerosol index (AI) from MODIS- Terra satellite while $NO_2$and Angstrom exponent from OMI Aura satellite wasused. A range of large-scale atmospheric condition was obtained from NCEP reanalysed data and air mass back-trajectories.

RESULTS AND DISCUSSION

The aerosol optical depth over northern parts of the India is found to be higher than over southern parts of India due to the proximity of the region to the source of natural aerosols from the deserts and due to higher growth rate of population, urbanization and industrialization.DuringApril and May, high value of AOD is observed,especially in the month of May due to the impact of episodic dust events, whichare transported from the western desert region. In the present study, the value of AOD was found in the range of 0.20–0.55 during April and 0.40-0.90duringMay 2012 in the 500 nm (figure: 1& 2). More dust episodesare observed in May than in April.For the investigation of dust episodes, the aerosol indexusing MODIS-Terra satellite was studiedon daily basis for April & May. From the analysis, it is observed that AI more than 2.50 depicts the dust episodic events and total six episodic events were observed in the month of May.

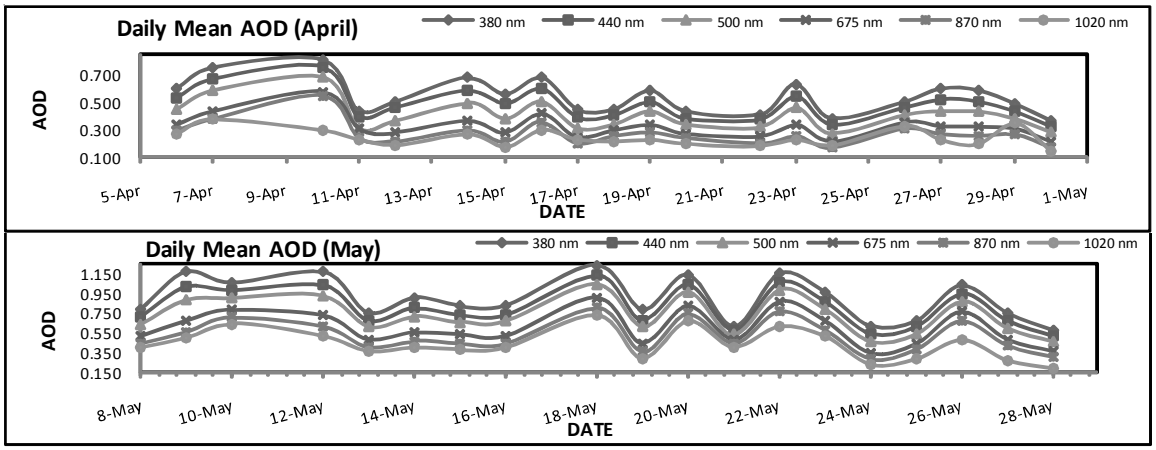

Figure 1 Temporal variations of daily mean AOD in the month of (a) April and (b) May.

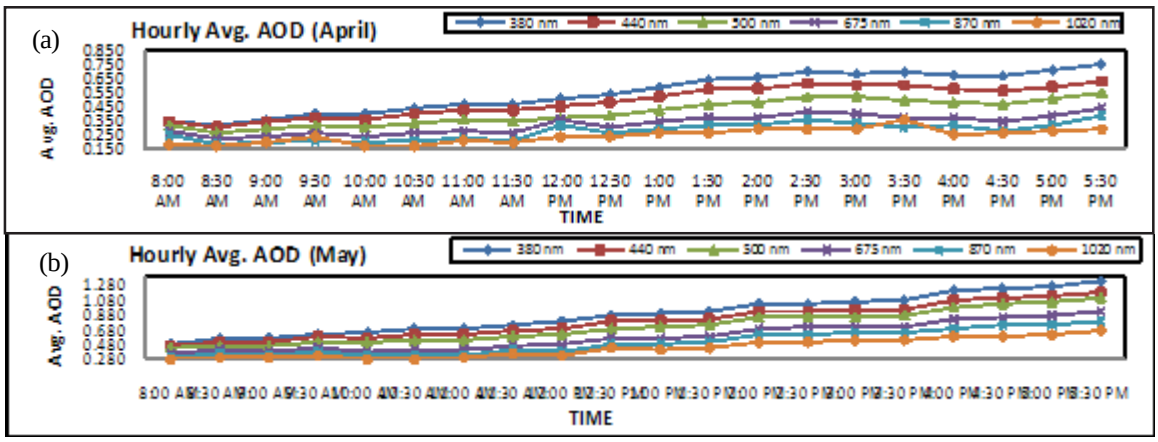

Figure 2 Temporal variations of hourly mean AOD in the month of (a) April and (b) May.

For more detail, investigation of dust episodes,single scattering albedo was derivedusing aerosol absorption coefficient and aerosol scattering coefficient.The single scattering albedo is the ratio between scattering and absorption in the total extinction:

$$\omega = \sigma / (\sigma+\alpha) \qquad (1)$$

where σ is the scattering coefficient and α is the absorption coefficient. To calculate the scattering coefficient at ambient relative humidity, the Kasten–Hanel formula was used:

$$\sigma = \sigma_0(1 - R)^{-\gamma} \qquad (2)$$

where R is relative humidity and γ is the parameter of condensation activity of aerosol particles. The aerosol absorption coefficient was determined from the data on the soot concentration:

$$\alpha = \alpha_m \times 10^{-3} \times M_S \qquad (3)$$

The value of á is the specific cross-section of absorption = 4.61 m^2/g (at the wavelength of 0.53 ìm). According to the results of theoretical calculations for dispersed soot particles as well as according to literature data for many atmospheric situations (Clarke et al. 1987; Gundel et al 1984; and Wolff 1984).Mass concentration of soot M_S and The formulas (1) to (3) allow us to estimate the single scattering albedo. One can reduce Eq. (1) to the obvious form:

$$\omega = [1+ 0.3 \times a_m \times P_S \times (1 - R)^{\gamma}]^{-1} \quad (4)$$

where, $P_S = M_S / M_A$ is the relative content of soot in dry particles, M_A is the concentration of the atmospheric aerosol.Thederived single scattering albedo was found to be in the range of 0.90-0.95during May (more dust events occurrences)thereby indicating more scatteringby the particles present in the atmosphere and in the range 0.86-0.89 during April depictingmore absorbing particles. The high value of single scattering albedo confirms the dominance of dust particles and dust plume during May.Mostly fine mode organic particles like NO_2 are produced by biomass burning, forest fire, etc.For understanding, the impact of forest fires on aerosol optical depth during these months, the satellite derivedaily columnar NO_2 data was investigatedfor March, April & May (figure:3). The observations indicatethe columnar NO_2in the range of 4.6 – 5.0 ($x10^{15}$ molecules/cm^3) and 6.1 - 7.9 ($x10^{15}$ molecules/cm^3) and 5.5 - 6.4($x10^{15}$molecules/cm^3) duringMarch, April and Mayrespectively, which was supported by MODIS active fire data which indicates the forest fire in March was low and it increased in April and further decreased in the month of May.

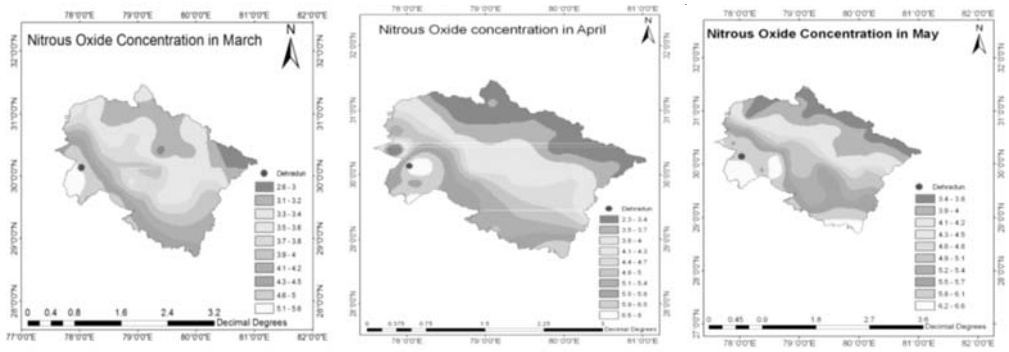

Figure 3: Map of NO_2over UttarakhandRegion during March, April &May 2012.

The NOAA-HYSPLITderived seven-day back trajectoriesat altitudes of 500, 1000 and 3000 meters a.g.l on each day was studied during April &May 2012. The analysis shows that northwesterly winds were prominent over the region during thestudy period at different altitudes attributed to the transport of dust aerosols over the region. The easterly and northeasterly winds were minimum hence theinfluence of forest fire was low over Dehradun thereby less impact on AOD during May.CALIPSO data providing daily global maps of the vertical distribution of aerosols and clouds was also analysed for the month April and May.The CALIPSOderived vertical feature mask image suggested vertically extended aerosol layer (~6 Km) over the region on 11 May 2012 associated with dust events over the region (figure: 4).

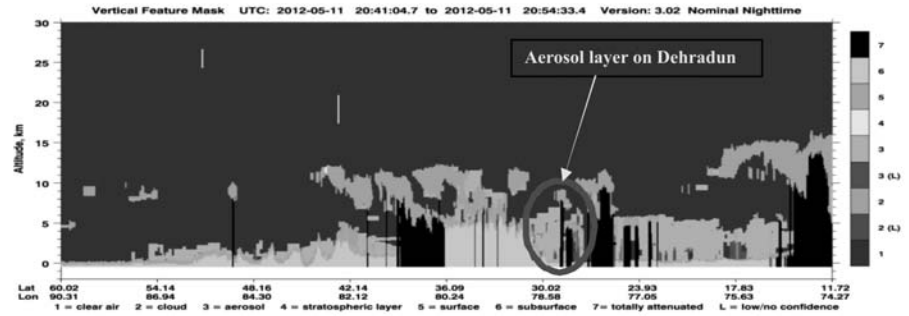

Figure 4: Calipso derived vertical feature mask image showing high aerosol loading over central region of India on 11th May 2012.

For more detailinvestigation, measurement of Angstrom exponent (á) and turbidity (â) constant using ground measurement and fromsatellite, derived Angstrom exponent was used. The Angstrom exponent was found to be in the range of 0.5-1.2 in April and 0.35 – 0.85 in May thatindicatescoarse mode particle distribution in May than in April. The values of turbidity constant was found to be 0.4 - 0.9 in April and 0.65 - 1.30 in May. For focussed understanding of particle type present in the atmosphere, the second order polynomial of Angstrom exponent ($á_2$) was studied (figure: 5). The analysis reveals positive curvature in May meaning the occurrence of coarser particles (dust) in the atmosphere, which is being addedby the dust events during this month.

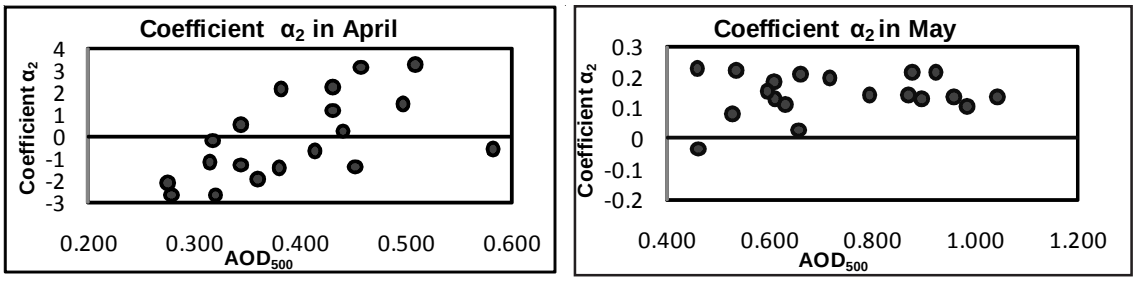

Figure - 5Scatter plot of Second order alpha in the month of April & May

The BC concentration was analyzed using aethalometer during these months and the result reveals that the BC concentration was low in May as compared to April (figure: 6).

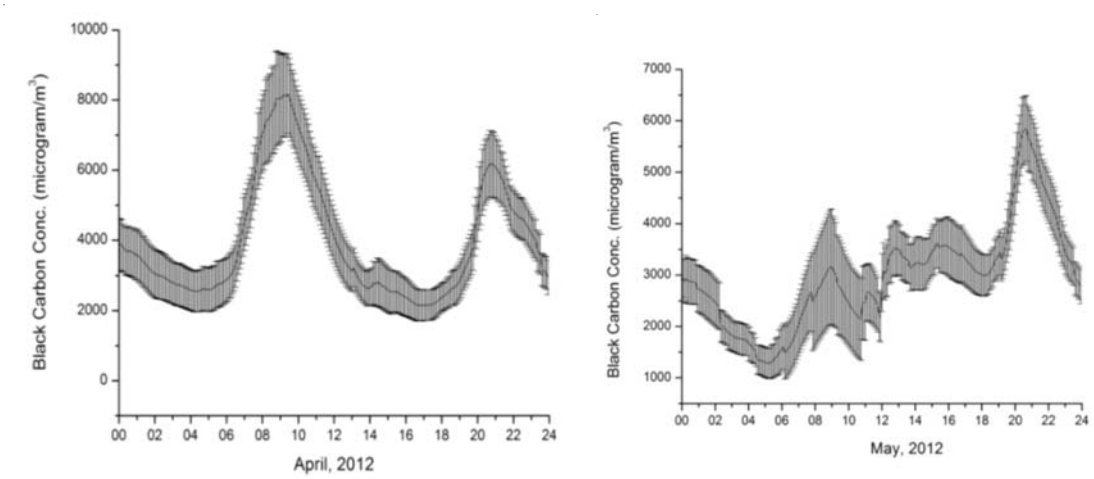

Figure - 6 BC concentration in the month of April & May using aethalometer

The study concludes that, there were dust episodic events in May, which were responsible for the increment of the AOD as compared to April month,and these have been well-observed using ground and satellite optical parameters.

CONCLUSION

Spectral aerosol optical depths (AODs) made at Dehradun in the central Himalayas have revealed the following.

- Significant increase in AOD values up to 1.5 has been observed during the dust storm days.
- The very low values of α and high values of β attributed to the abundance of large-sized particles in the atmosphere.The MODIS and OMI observations justify the dust transport over Dehradun and IGP.
- The SSA values during the intense dust storm days ranged from 0.90 to 0.95 and are wavelength dependent with higher values at longer wavelengths suggesting abundance of more scatter particles (dust particles).
- The value of NO_2 and BC was decreased during the dust period.
- Calipso data also revealed that during the study period more dust & polluted dust aerosols were present in the atmosphere.

STUDY OF MINERAL DUST TRANSPORT OVER THE INDIAN SUBCONTINENT USING REGIONAL CLIMATE MODEL REGCM4.1

S.DAS[1], S.DEY[1] and S.K.DASH[1]

[1]Centre for Atmospheric Sciences, Indian Institute of Technology Delhi, HauzKhas, New Delhi, India – 110016.

Keywords: MINERAL DUST, REGCM4.1, VERTICAL DISTRIBUTION

INTRODUCTION

Large uncertainty still persists in quantifying the climatic effects of aerosols at regional scales (IPCC, 2007). The problem is more critical in the Indian subcontinent due to large uncertainty in emission factors and poor knowledge of the evolution of aerosol characteristics during transport (Ganguly, *et al*., 2009). For example, absorption of solar radiation by mineral dust (purely a natural component) is enhanced as it is transported over the polluted regions (Dey, *et al*., 2008). Data from ground-based radiometers and satellites are not adequate to fully resolve this problem because they can only measure the optical properties of composite aerosols. Rather relative abundance of dust and anthropogenic aerosols can be better quantified by chemical analysis of samples collected on filters. Scarcity of such data in the Indian subcontinent motivated us to utilize a regional climate model to study and understand the space-time distribution of aerosols in this region.

METHODS

We utilized the latest version of the regional climate model RegCM4.1 to simulate the dust aerosol optical depth (τ_d) over the subcontinent for the first time for an entire year 2009. RegCM4.1 is a hydrostatic, sigma vertical coordinate model which has inbuilt aerosol modules for simulating natural aerosols like mineral dust (Zakey, *et al*., 2006) as well as anthropogenic aerosols (Solmon, *et al*., 2006).The model domain covered the Indian subcontinent (5^0N-40^0N, 60^0E-100^0E) with 30 km × 30 km horizontal resolution on 18 vertical levels. The initial and lateral boundary conditions were extracted from the NCEP/NCAR ($2.5^0 \times 2.5^0$) reanalysis data for the atmospheric variables. Land surface processes are represented through Biosphere-Atmosphere Transfer Scheme. The dust scheme in relation to the BATS scheme becomes effective in the model for the cells dominated by desert and semi desert land cover. The dust aerosols are represented by four size bins ranging from 0.1-1.0 μm, 1.0-2.5 μm, 2.5-5.0 μm and 5.0-20 μm. The soil textures are taken from United States Department of Agriculture data set of soil type, texture and other properties.

The model results are first compared with available in-situ observations over the land. The seasonal distributions of τ_d have been examined in view of the synoptic meteorology and model derived vertical distributions of dust is studied during the peak transport season. The year 2009 was chosen because of the availability of Aerosol Robotic Network (AERONET) level 2 data (Holben, *et al*., 1998) at maximum 5 sites viz. Jaipur, New Delhi, Kanpur, Gandhi college(near Ballia), Kharagpur in India(locations shown in figure 2a), which have been used to validate the simulated τ_d(Fig. 1). The seasonal variability of τ_d is well captured by the model close to the dust source region. However, simulated τ_d is underestimated relative to AERONET-retrieved coarse mode optical depth (τ_c), particularly during the pre-monsoon season when the dust transport peaks. This underestimation increases as we move away from the source region as indicated by larger positive intercepts at

Gandhi College and Kharagpur compared to the other three sites.The model does not account for any local sources of dust, viz. construction activities, road dust etc. This may explain the observed differences at stations far away from the source region (i.e. Great Indian Desert), when the relative abundance of transported desert dust is low.

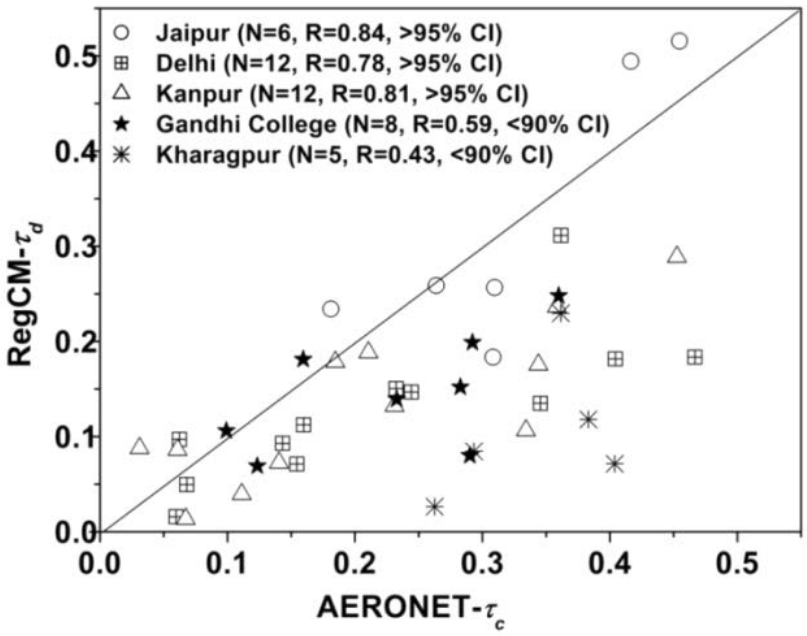

Figure1. Monthly variations of model-simulated τ_d and AERONET-retrieved τ_c at five AERONET stations across the Indo-Gangetic plain.

The seasonal variability of τ_d over the subcontinent is shown in Fig. 2. The Great Indian Desert situated at the north-western region of India is identified as the primary source of dust in the subcontinent by the model as supported by numerous observation based studies (e.g. Sikka, 1997).During the winter season (Figure 2a), τ_d is very low (<0.04) over most parts of the subcontinent. Even over the desert, τ_d is in the range 0.05-0.08, while the high τ_d (~0.1-0.4) in the north of 35^0 N latitude is attributed to the dust emitted from TaklamakanDesert.During the pre-monsoon season, dust emission increases due to high wind speed (Sikka, 1997) over the Great Indian Desert (τ_d>0.3). The dust is then transported over the IGB and Himalayan foothills (Fig. 2b) by strong north-westerly wind above boundary layer.The vertical distributions of τ_d along the transport path taking transect of 1^0x 1^0 grids are averaged over the entire pre-monsoon season and represented as meridional-altitude cross section. Dust particles are mostly transported at 700-850 hPa altitude over the IGB with a reduction in τ_d as it settles down away from the source(Figure 3a).Zonal gradient of vertical distribution of τ_d across the Indian Subcontinent during the pre-monsoon season of peak dust transport (Fig. 3b) clearly demonstrates accumulation of dust over the IGB and Himalayan foothills at ~700hPa altitude. During the monsoon season, τ_d further increases over the source region. Larger τ_d (>0.3) over the Arabian Sea in this season relative to the pre-monsoon season along with a stronger spatial gradient relative to the Bay of Bengal are attributed to transport of dust from the Great Indian Desert and middle-east Asia.Dust load reduces in the post-monsoon season over the entire region and τ_d mostly lies in the range 0.06-0.1.

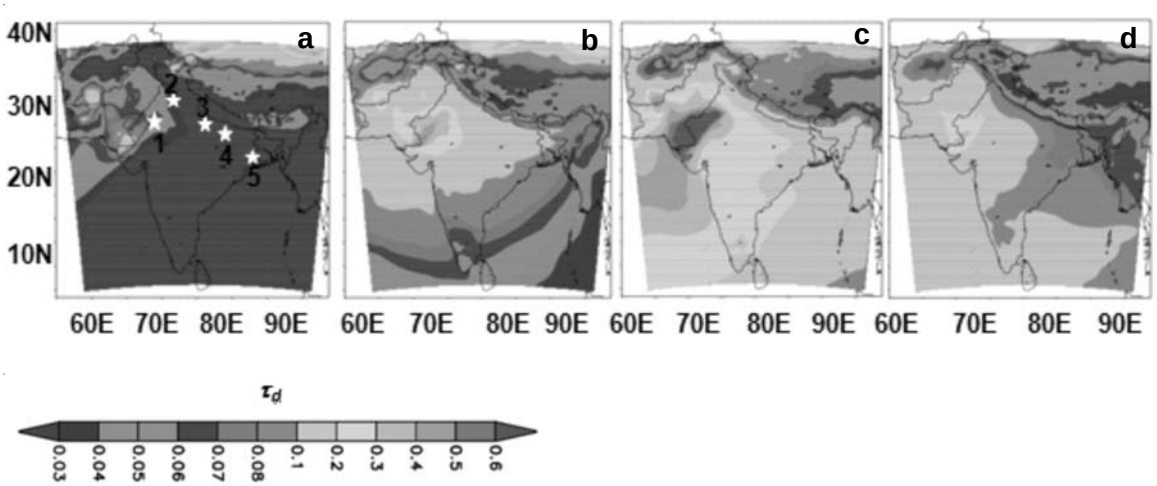

Figure 2. Spatial distributions of model-simulated τ_d over the Indian subcontinent during (a) winter (Jan-Feb), (b) pre-monsoon (Mar-May), (c) monsoon (Jun-Aug) and (d) post-monsoon (Sep-Nov) seasons.

Dust aerosols exerts negative TOA SWDRF except the Great Indian Desert and Himalayan region where the surface albedo is very high. The SWDRF values were highly dominant as compared to the LWDRF leading to a net cooling effect at TOA. The surface SWDRF efficiency (defined as DRF per unit τ_d) varies in the range -50 to -70 W m^{-2} close to the source region and -35 to -50 W m^{-2} away from the source region. Transport and deposition of mineral dust over Himalayan snow may have climatic implications as it may accelerate the glacier melting (Prasad, *et al.,* 2011). Our simulations capture the accumulation of dust over the IGB and Himalayan foothills during the pre-monsoon season. The peak dust concentration at ~700 hPa corresponds well with the peak of the heating rate profiles as reported in Gautam, *et al.* (2010), which further supports the applicability of the model. Large dust load over the ocean may have biogeochemical implications (Moore, *et al.,* 2008), because dust provides nutrients and facilitates phytoplankton bloom.

CONCLUSIONS

Regional climate model RegCM4.1 has been used to simulate the space-time distributions of mineral dust over the Indian subcontinent at 30 km × 30 km resolution for the first time for a whole year. We showed that the model can be applied for studying aerosol characteristics in this region at high spatial scale (as opposed to coarse resolution of global climate models), particularly for the dust. The present study was limited to dust as we wanted to quantify the dust transport over the Indian Subcontinent.The model RegCM4.1 captures the seasonality of dust emission and transport well in the vicinity of source area, while it underestimates τ_d far away from the Great Indian Desert, which may be attributed to local sources not considered by the model (e.g. agricultural activities, transport on rural roads, construction activities etc.).Dust is transported across the IGB in 700-850 hPa altitude range and accumulated against Himalayan foothills at ~700 hPa during the peak transport season (Mar-May).

ACKNOWLEDGEMENTS

The authors acknowledge ICTP for providing the RegCM4.1 Model (http://eforge.escience lab.org/gf/project/regcm). The efforts of PIs and staffs of the AERONET sites used in this study are acknowledged for establishing and maintaining the sites. The first author is thankful to CSIR for providing scholarship to carry out research work in IIT Delhi. NCEP reanalysis data are obtained

from NOAA CIRES Climate Diagnostics Centre. CALIPSO data are downloaded from Atmospheric Science Data Center. The work is partially supported by research grants from DST, Govt. of India under contract SR/FTP/ES-191/2010 and DST/CCP/PR/11/2011 through research projects operational at IIT Delhi (IITD/IRD/RP02509 and IITD/IRD/RP2580).

REFERENCES

Dey, S. and Tripathi, S. N. (2008). Aerosol direct radiative effects over Kanpur in the Indo-Gangetic basin, northern India: Long-term (2001-2005) observations and implications to regional climate, *J. Geophy. Res.*, 113.

Ganguly, *et al.* (2009), Retrieving the composition and concentration of aerosols over the Indo-Gangetic basin using CALIOP and AERONET data, *Geophys. Res. Lett.*,***36*(13)**, pp. 1-5.

Gautam, R., Christina Hsu, N. and Lau, K. M. (2010). Premonsoon aerosol characteristics and radiative effects over the Indo-Gangetic Plains: Implications for regional climate warming, *J. Geophys. Res.*, *115*, D17208, doi:10.1029/2010JD013819.

Holben, B. N. et al. (1998), AERONET-A Federated Instrument Network and Data Archive for Aerosol Characterization, *Rem. Sens. Environ.*, pp. 1-16.

Intergovernmental Panel on Climate Change(IPCC)(2007), *Summary for policymaker of climate change 2007: the physical science basis. Contribution of working group I to the fourth assessment report of intergovernmental panel on climate change*. (Cambridge Univ. Press, Cambridge).

Moore, J. K., and Braucher, O. (2008). Sedimentary and mineral dust sources of dissolved iron to the world ocean, *Biogeosciences*, pp. 631-656.

Prasad, A. K., Elaskary, H. M. and Asrar, G. R. (2011). Melting of Major Glaciers in Himalayas/: Role of Desert Dust and Anthropogenic Aerosols, *Planet Earth*, pp. 90-122.

Sikka, D. R. (1997), Desert climate and its dynamics, *Curr. Sci.*, **72**, pp. 35-46.

Solmon, F., Giorgi, F. and Liousse, C. (2006). Aerosol modelling for regional climate studies: application to anthropogenic particles and evaluation over a European/African domain, *Tellus B*, ***58*(1)**, pp. 51-72.

Zakey, A. S., Solmon, F. and Giorgi, F. (2006). Development and testing of a desert dust module in a regional climate model, *Atmos. Chem. Phys.*,**6,** pp. 4687–4704.

EVALUATION OF THE WRF-CHEM MODEL OVER THE INDIAN DOMAIN: TRACE GASES AND AEROSOLS

MARYKUTTY MICHAEL[1], ARUN YADAV[1], S. N. TRIPATHI[1], AND C. VENKATARAMAN[2]

[1]Department of Civil Engineering, Indian Institute of Technology, Kanpur – 208016, India
[2]Department of Chemical Engineering, Indian Institute of Technology, Mumbai – 400076, India.
Email: mary@iitk.ac.in

Keywords: REGIONAL MODEL, WRF-CHEM, CHEMICAL-TRANSPORT MODEL, BC-PREDICTION.

INTRODUCTION

Though extensive studies have been carried out to understand the distribution of aerosols in the atmosphere and their direct and indirect effects, the assessment of the aerosol climatic impacts are highly uncertain. As the anthropogenic emissions from the Asian countries contribute substantially to the global aerosol loading, the study of the distribution of aerosols over this region has become very important. The evaluation of aerosol properties over the Indian domain during the pre-monsoon season has been addressed in the present study.

The "online" meteorological and chemical transport Weather Research and Forecasting/Chemistry (WRF/Chem) model has been implemented over Indian Subcontinent for three consecutive summers in 2008, 2009 and 2010. The meteorological parameters, trace gases distribution and aerosol properties predicted by the model are compared with the observed data. The agreement between the prediction and the observation are discussed.

METHODS

WRF-chem was developed by National Centre for Atmospheric Research (NCAR) in collaboration with other institutions like NCEP, FSL, AFWA etc. (http://www.wrf-model.org/index.php).The domain of the study is set-up over India. The domain encompasses the region 68° to 99° E and 6° to 37° N. The input geographical data includes the static terrain data like land use, soil type etc. The important meteorological data such as wind velocities, temperature, pressure, soil data, SST etc. are available in the public dataset of National Centre for Environmental Prediction (NCEP). These NCEP FNL (Final) Operational Global Analysis data are available on 1° x 1° grids continuously at every six hours. This product is from the Global Forecast System (GFS) that is operationally run four times a day in near-real time at NCEP. The global emission inventory (RETRO and EDGAR) has been used and are projected for the period of study using the method provided in Ohara*et al.* (2007). The emission rates of SO_2, BC, OC and $PM_{2.5}$ available in the global inventory are replaced with the high resolution emission inventory developed over India for the present study. For example the emission inventory used for SO_2 emissions is shown in fig. 1.

CONCLUSIONS

The model simulated meteorological parameters, trace gases and particulate matter. Predicted mixing ratios of trace gases (Ozone, CO, NOx, and SO_2) are compared with ground based as well as satellite observations over India with specific focus on Indo-Gangetic plain. Simulated aerosol optical depths are in good agreement with those observed at a few ground Aerosol Robotic Network

stations (AERONET). The vertical profiles of Black Carbon have also been compared with observations from aircraft campaign held during summer of 2008 and 2009 resulting in good agreement. This study shows that WRF-Chem model captures many important features of the observations and makes it useful for understanding and predicting regional weather over Indian subcontinent.

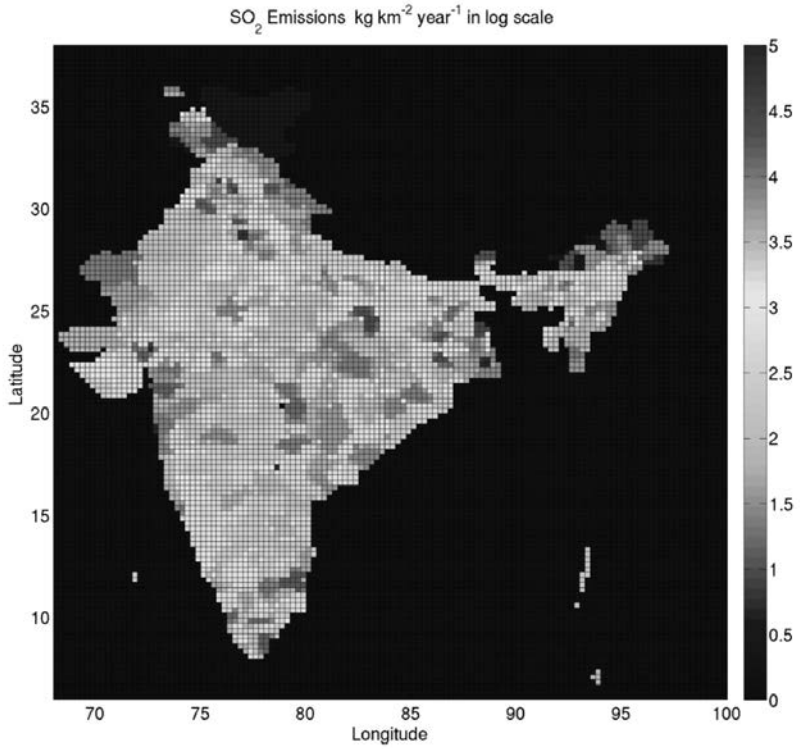

Figure 1. The emission rates of SO_2.

ACKNOWLEDGEMENTS

The author MM was supported by the DST Fast Track fellowship. Part of this work is supported through a grant under Changing Water Cycle program of MoES.

REFERENCES

Ohara, T. et al. (2007). An Asian emission inventory of anthropogenic emission sources for the period 1980–2020, *Atmos. Chem. Phy*., **7**, 4419.

AEROSOL CHARACTERISTICS AT DELHI: MICROPHYSICS AND LONG-TERM TRENDS

NEELESH K LODHI[1], S NASEEMA BEEGUM[1], SACHCHIDANAND SINGH[1], KRISHAN KUMAR[2]

[1] Radio & Atmospheric Sciences Division, National Physical Laboratory, CSIR, New Delhi-110012

[2] School of Environmental Science, Jawaharlal Nehru University, New Delhi-110067

E mail : ssingh@nplindia.org

Keywords : AOD, ANGSTROM WAVELENGTH EXPONENT

INTRODUCTION

Atmospheric aerosols are known to affect the radiative balance of the earth at local, regional and global scale through direct and indirect effects. Over the past few decades, our understanding of direct and indirect radiative effects of aerosols has increased; the uncertainties on their effects on climate are still high. One of the crucial factors contributing to this uncertainty is their large spatio-temporal heterogeneity in the optical and microphysical properties and this necessitates the importance of the continuous monitoring of aerosol parameters in good spatial resolution. Here, we present the climatology of aerosol microphysics, its trends and impact of potential sources based on the long term measurements of spectral aerosols optical Depths (AOD) from December 2001 to February 2011, using Microtops II Sun-photometer from the urban centre Delhi (28.6º N, 77.3º E, 238 m msl) in the western Indo Gangetic Plain (IGP). We have used two Microtops alternately. Both the Microtops are periodically calibrated (once in a year) alternately so that the quality of data is maintained over a long period of time. All calibrations are done by sending the instruments to Mauna Loa where it is calibrated using Langley technique by the manufacturer, Solar Light Company Inc, USA to the NIST (National Institute of Standards and Technology) traceable standards.

RESULTS AND DISCUSSIONS

With a view to examine the seasonal, annual and inter-annual variations, the monthly mean values of spectral AODs and Angstrom parameters were estimated from the time series of the daily mean data. The contour map showing the spectral AOD variations for the entire period of study is shown in Figure 1a. The monthly mean values are in the range of ~0.25 - 1.5 at 500 nm with strong seasonal/annual variations in both spectral AOD as well as in spectral gradient along with a weak but significant inter-annual variability. The seasonal changes in the spectral variation of AOD is clear from the figure with comparatively steeper spectra during winter (December to February)/ post monsoon season with exceptionally flat spectra during summer/monsoon (July to September), associated with the dominance of fine and coarse-mode aerosols during the contrasting seasons respectively. The time series of the monthly mean Angstrom wavelength exponent, α and turbidity parameter β clearly demonstrates this (Figure 1b). Higher value of á (~1.0) is observed during post monsoon/winter seasons and the lower values (<1.0) during summer/monsoon seasons. The turbidity parameter β shows similar variations as that of AOD. The monthly mean climatology of spectral AODs reveal that AODs at 340 and 500 nm depict highest values during October-November (~1.1 at 340 nm), decrease continuously to reach the least values by March (~ 0.77 at 340 nm) and again

increases towards May; whereas at longer wavelengths, AOD shows the least value during February (~0.35 at 1020 nm), increases gradually to reach the highest values by June (~0.75 at 1020 nm) and decreases thereafter. The Angstrom turbidity parameter showed similar variations (both monthly and seasonal) as that of AOD at longer wavelengths with highest aerosol loading during June (summer) and least during February (winter). But, the Angstrom wavelength exponent, á varies between 0.35 and 1.0 as season progresses from summer to winter with an average of ~ 0.75±0.24.

Notwithstanding the consistency in the seasonal pattern of aerosol distribution over the entire period, one can observe some weak but significant trends in AODs. Figure 2 (a, b, c, d, e and f) presents the time series of anomalies in the mean monthly spectral AODs and Angstrom parameters during the study period after deseasonalizing the time series by removing the climatological monthly means from the respective monthly means. The figure shows a decreasing trend in spectral AODs with ~ -0.02/year at 500 nm, increases towards longer wavelengths to reach ~ -0.03/year at 1020 nm. The slopes of the trend line are statistically significant in 95% confidence level. Similar analysis of α, reveals an increasing trend of more or less same magnitude (~ 0.02/year), and the decreasing trend in β (~ -0.03/decade) suggests a gradual decrease in the columnar aerosol loading. This clearly evidences that the trend in aerosol parameters (decrease for AOD and increase for α) is due to the decrease in the concentrations of coarse mode natural aerosols.

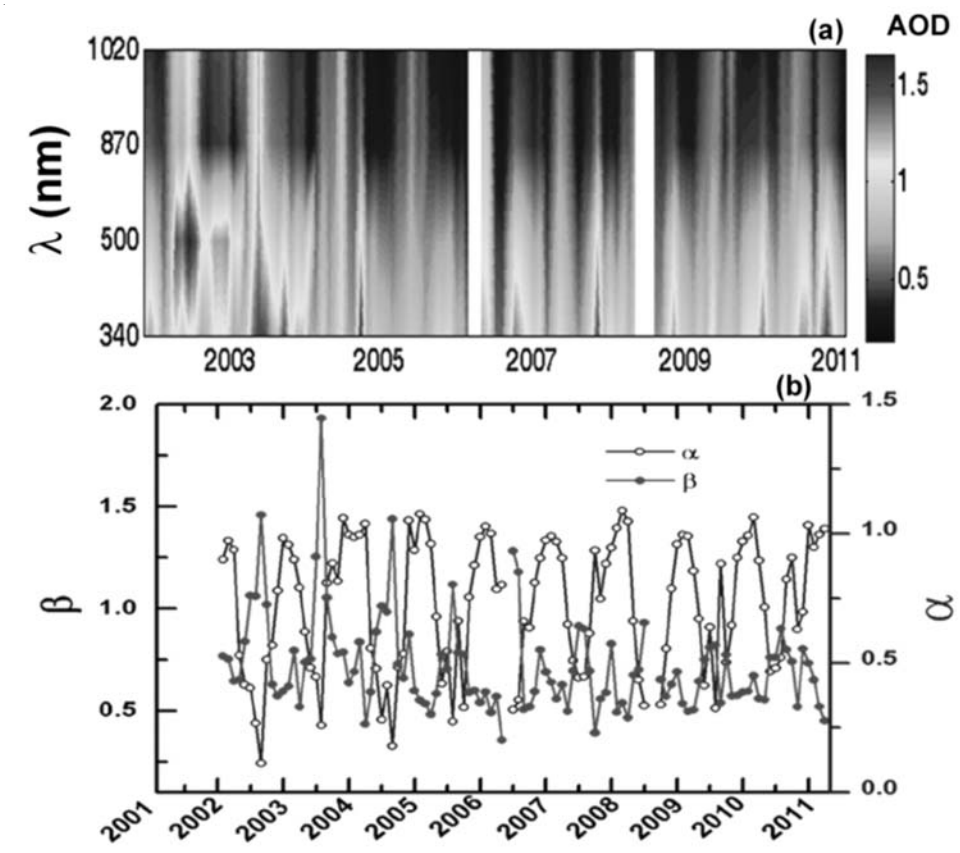

Figure 1: Monthly mean pattern of spectral AOD and Angstrom parameters (a): the contour map showing the spectral variation of AOD (b) time-series of α and β

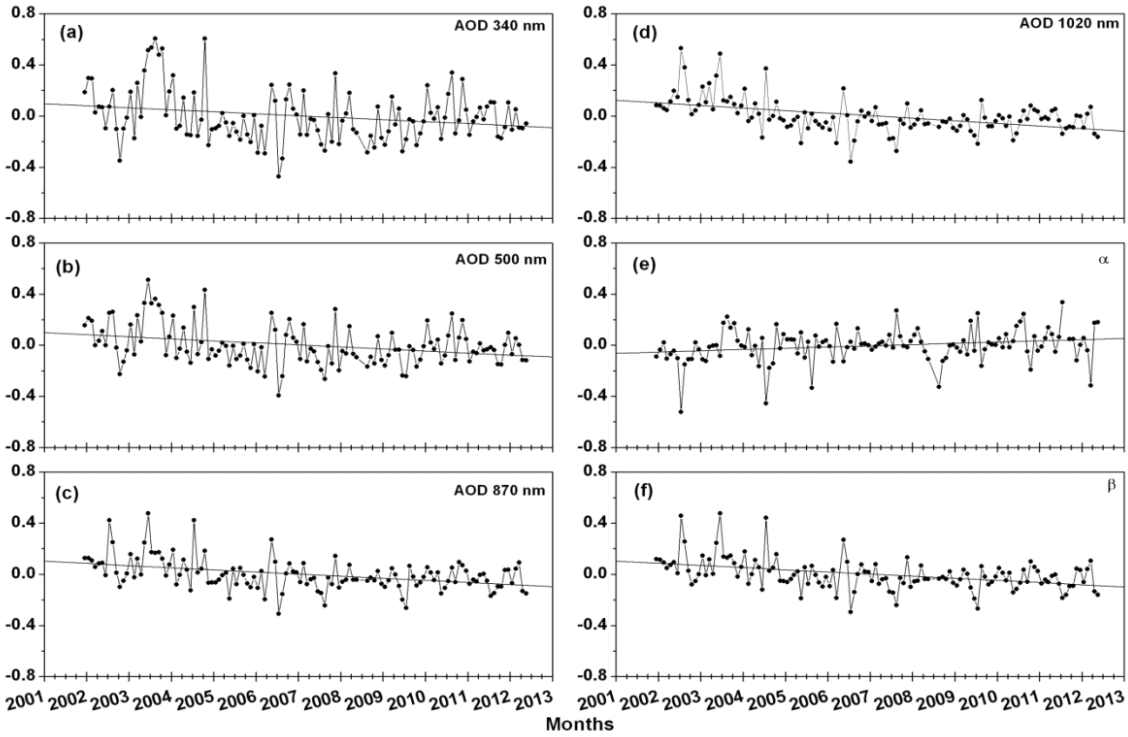

Figure.2: The de-seasonalized pattern of monthly mean spectral AODs (a, b, c and d) and Angstrom parameters (e and f) from December 2001 to May 2012 at Delhi. The solid line represents the trend.

SUMMARY AND CONCLUSIONS

Analysis of the long term measurements of columnar spectral AOD (December 2001 to February 2011) over Delhi, an urban station in the western Indo Gangetic Plain, unveiled certain interesting features. The seasonal variations of spectral AODs and Angstrom parameters are also generally consistent throughout the study period. The monthly mean AOD at shorter wavelengths peaks twice, during June and November, while at longer wavelengths it shows only one peak in June. The Angstrom exponent, α showed a near inverse relationship with a summer low and winter/post monsoon high. The most striking result from the present study at Delhi is the decreasing trend observed in the columnar aerosol loading with a maximum value of -0.03/year at the longer wavelength of 1020 nm and it reduces spectrally towards shorter wavelengths (of -0.02/year at 500 nm). The Concentration Weighted Trajectory Analysis of the 5 day isentropic airmass back trajectories revealed the role of seasonally changing potential advection pathways in modifying the aerosol pattern at the receptor location.

AEROSOL-CLOUD-PRECIPITATION INTERACTION OVER THE INDIAN MONSOON REGION USING CONCURRENT SATELLITE MEASUREMENTS

KAMALIKA SENGUPTA, ARJYA SARKAR AND SAGNIK DEY

Centre for Atmospheric Science, Indian Institute of Technology, New Delhi 110016
Corresponding Author: sagnik@cas.iitd.ac.in

Keywords: AEROSOL-CLOUD INTERACTION

INTRODUCTION

Unravelling the aerosol-cloud-precipitation conundrum continues to be a major challenge in accurately quantifying the anthropogenic climate forcing. The relative vertical distributions of clouds and aerosols, critical in understanding the interaction (Chand *et al.*, 2009), are not well-known in the Indian monsoon region. The influence of aerosols on precipitation through the microphysical link (Sorooshian*et al.*, 2009) needs to be understood in the Indian monsoon region. The past decade has brought to India, 8 normal monsoon years and 3 significant drought years with decadal rainfall seeing a decreasing trend overall. In the present work, precipitation susceptibility has been examined in the Indian monsoon region by using multi-sensor satellite data. In particular, we studied the cloud macrophysical (vertical distribution) and microphysical (effective radius and water path) properties for positive and negative rainfall anomaly to understand the difference in cloud evolution in the two contrasting scenario. The results are interpreted in view of varying aerosol properties. The analysis is carried out for the monsoon season (Jun-Sep) in 11-yr period.

DATA AND METHODOLOGY

The analysis focuses on the 'core monsoon region' that extends from 20^0 to 25^0 N and 70^0 to 88^0 E. The variation of rainfall over the Indian landmass has been shown to be strikingly similar, with a significant correlation coefficient of 0.87, to that over this region (Gadgil, 2003). The results obtained for this core region are then tested for the 6 homogeneous (defined by IMD) rainfall regions of India.

We use TRMM TMI 3 hourly data from 2000-2010 at $0.25^0 \times 0.25^0$ spatial resolution to calculate daily precipitation. For data on Cloud Fraction for the concurrent period, we have used CFbA daily product derived by MISR onboard TERRA spacecraft. This product gives valuable insight to the vertical distribution of clouds at 40 vertical levels upto 20 km at a horizontal resolution of 0.5^0 and vertical resolution of 0.5 km. Aerosol Optical Depth (550 nm) data has been taken from MODIS onboard the same satellite. The daily anomaly for these 11 years has been standardized with respect to the average monthly values. This method has been chosen in order to compensate for the lack of data for a longer time period.

The analysis may be divided into two parts. First, we examine the vertical distribution of clouds for positive and negative rainfall anomaly to understand the possible influence of cloud evolution. Next the relation of precipitation with cloud effective radius and water path was examined to understand the precipitation susceptibility following Sorooshian*et al.*, (2009). Further, the relations of AOD with cloud effective radius and water path are investigated to interpret possible aerosol-cloud-precipitation connection in the Indian monsoon region.

RESULTS

The mean data distribution of aerosols, total cloud fraction and precipitation for contrasting years of normal and deficit rainfall show statistically insignificant differences in the total cloud cover and aerosol optical depth (Fig. 1). A significant difference between the median values of normal and drought periods is observed only in case of precipitation as evident from the distance between the notches in Fig. 1. One notable aspect is the broader range of values for cloud fraction during the drought period as opposed to the small range as well as lesser inter-quartile differences during normal years. This indicates greater positive as well as negative fluctuations in amount of cloud formed in drought years. This led to the question – what factors influence precipitation pattern from similar cloud amount and whether the signal of aerosol-cloud-precipitation can be isolated in the satellite data.

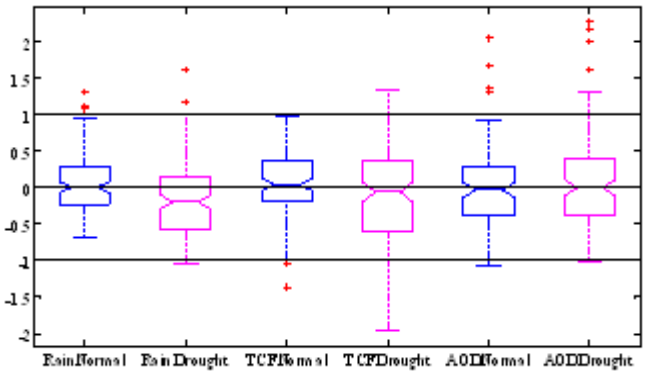

Figure 1. Rainfall, aerosol optical depth (AOD) and total cloud fraction (TCF) anomaly for the region 20N to 25N and 70E to 88E normalised with respect to monthly mean and averaged for 8 normal years and 3 drought years from 2000-2010.

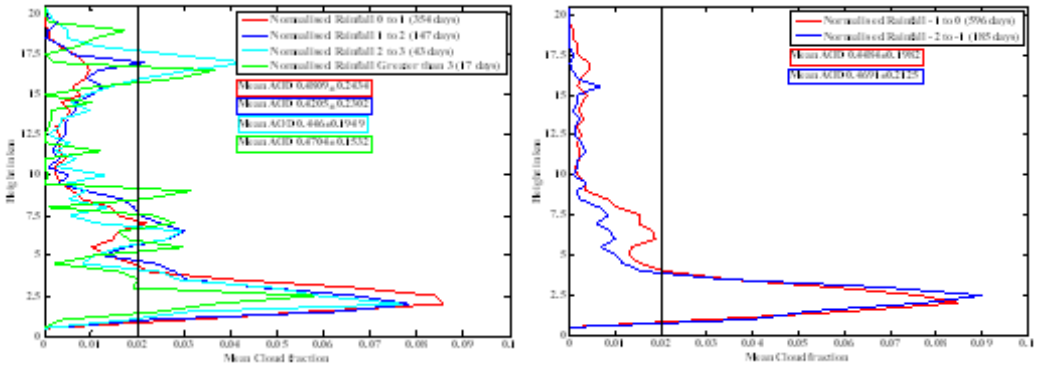

Figure 2. Vertical Distribution of clouds for days having positive rainfall anomaly (left panel) and negative rainfall anomaly (right panel)

Next we generate the mean vertical distribution climatology of clouds for the days of positive and negative rainfall anomaly in the last 11 years. The days have been divided into 6 groups according to the value of normalized rainfall anomaly in ranges of unity starting from -2 to 3 (Fig. 2). On days when the normalised daily rainfall anomaly is negative, the lower levels of the atmosphere happen to house more clouds than during days when rainfall anomaly is positive. This is true for all the days in the eleven year period irrespective of whether the day fell in a normal or drought monsoon year.

The situation reverses at about 4 to 10 km when clouds in excess rainfall days exceed that in deficit rainfall days. It is relevant to note here that 3 km is the maximum height, conventionally associated with low clouds while clouds beyond 6 km are considered to be high clouds. Thus to sum up conventionally, in days of negative rainfall anomaly we find a very large population of low clouds while positive rainfall anomaly days are characterised by lesser lower level clouds and sufficient middle and high cloud fraction. Mean AODs are similar for theses 6 groups, suggesting either a buffering effect of meteorology (Stevens and Feingold, 2009) on cloud formation or more complex microphysical processes that cannot be resolved with the present dataset or both. However, the standard deviation values about the mean suggest that the spread of the values is much more when the anomalies are greater than when it is near zero.

The daily time series of cloud vertical distribution within a single monsoon season reveals association of negative rainfall anomaly with positive cloud anomaly. We examined the relation of rainfall with cloud effective radius (liquid, ice and mixed) in four domains (< 1^{st} quartile, 1^{st} – 2^{nd} quartile, 2^{nd} – 3^{rd} quartile and > 3^{rd} quartile) of water path. Rainfall tends to be sensitive for a certain ranges of effective radius in these domains and unless the threshold is exceeded, positive rainfall anomaly is not obtained. Further, analysis of cloud effective radius in terms of AOD reveals that the effective radius does not show significant changes with an increase of AOD for water clouds, while the relations are significant for ice clouds. The results are analyzed and interpreted in view of the indirect and semi-direct effects, hypothesized for the Indian monsoon region.

CONCLUSIONS

Aerosol-cloud-precipitation interaction has been examined for the Indian core monsoon region by analyzing multi-sensor data. In general, evolutions of mid-level to high clouds are associated with positive rainfall anomaly, while low clouds are associated with negative rainfall anomaly. Cloud effective radius does not show much sensitivity to AOD for low clouds, while the opposite behaviour was observed for high clouds. The results are interpreted in terms of possible remote sensing artefacts and aerosol-cloud interaction.

ACKNOWLEDGEMENT

The authors are thankful to the ministry of Earth Sciences (MoES) for their support in sponsoring this project under the CTCZ programme. We also thank NASA for archiving MISR, MODIS and TRMM data used in the present work.

REFERENCES

Chand, D., Wood R., Anderson T. L., Satheesh S. K., and Charlson R. J. (2009). Satellite-derived direct radiative effect of aerosols dependent on cloud cover, *Nat. Geosci.*, **2**, 181 – 184.

Huang, J., Zhang, C. and Prospero, J. M. (2009). Large-scale effect of aerosols on precipitation in the West African Monsoon region, *Q. J. R. Meteorol. Soc.*, **135**, 581-594.

Koren, I. and Feingold, G. (2011). Aerosol–cloud–precipitation system as a predator-prey problem, *Proc. Natl. Acad. Sci. U. S. A.*, **108**,12,227–12,232, doi:10.1073/pnas.1101777108.

Koren,I., Altaratz,O., Remer,A.L., Feingold, G. Martins,V.J. and Heiblum,H.R. (2012). Aerosol-induced intensification of rain from the tropics to the mid-latitudes, *Nat. Geosci.*,**5**, 118–122.

Parathasarathy, B., Munot, A. A., and Kothawale, D. R. (1994). Droughts over Homogeneous Regions of India: 1871–-1990 (inDrought Network News (1994-2001), Paper 67).

Rajeevan, M., Bhate, J., Kale, J.D. and Lal, B. (2006). High resolution daily gridded rainfall data for the Indian region:Analysis of break and active monsoon spells, *Current Science*, **91**, 3, 296 -306.

Rajeevan, M., Gadgil, Sulochana and Bhate, Jyoti (2008). Active and Break Spells of the Indian Summer Monsoon, NCC Research Report No. **7/2008**, 45 pp.

S. Gadgil. (2003). The Indian monsoon and its variability, *Annu. Rev. Earth Planet. Sci.*, **31**, *pp. 429–467*

Sorooshian, *et al*. (2009). On the precipitation susceptibility of clouds to aerosol perturbations, *Geophys. Res. Lett.*, **36**, L13803.

Stevens, B., and Feingold, G. (2009). Untangling aerosol effects on clouds and precipitation in a buffered system, *Nature*, **461**, 607–613.

ON THE LOW OZONE MIXING RATIO IN THE MARINE BOUNDARY LAYER OF ARABIAN SEA DURING PREMONSOON: EFFECT OF AEROSOLS

LIJI MARY DAVID[1] PRABHA R NAIR[1] AND SUSAN GEORGE K[2]

[1]Space Physics Laboratory, Vikram Sarabhai Space Centre,
Thiruvananthapuram 695 022, India
[2]presently at Ministry of Environment and Forests, New Delhi

Keywords: TROPOSPHERIC O_3, AEROSOLS, MARINE BOUNDARY LAYER

INTRODUCTION

Tropospheric O_3 is produced through photochemical reactions involving CO, CH_4, non-methane hydrocarbons (NMHCs) and volatile organic compounds (VOCs) catalyzed and controlled by NO_x, OH and peroxy radicals. O_3 is destroyed by either dry deposition or photochemical loss mechanisms, the most efficient being the reaction with water vapour. The remote marine boundary layer (MBL) is an ideal place to study the basic processes that drive atmospheric photochemistry and the relationship between free-radical sources and sinks. Advection from the adjoining landmass is a major factor that controls the level of O_3 and precursors in the MBL. The aerosols present in the atmosphere can interact with the incoming solar radiation and alter the photochemical production rates of oxidants in the atmosphere. Apart from providing surfaces on which in situ chemistry can take place leading to production/destruction of O_3, high aerosol loading in the atmosphere reduces the incoming solar radiation required to initiate photochemistry during daytime. Both positive and negative association between aerosols and O_3 have been reported (Castro, *et al.* 2001). Reactive halogens also play a key role in controlling O_3 chemistry. The halogen species present in the marine environment affect O_3 concentration (Ali, *et al.* 2009; Dickerson, *et al.* 1999). However, knowledge on the impact of aerosols on tropospheric oxidant cycle is limited. This is mainly due to the large spatial variability in the physical and chemical nature of aerosols and trace gases. Most of the inference on the inter-dependence of aerosols and trace gases are based on model-based analysis. This paper presents the role of aerosols in modifying the O_3 concentration based on the co-located measurement of aerosol mass loading (M_L) and number density (N) over the Arabian Sea (AS) during the premonsoon period.

EXPERIMENTAL DETAILS AND DATA

As part of Integrated Campaign for Aerosols, gases and Radiation Budget (ICARB), cruise-based measurements of O_3 have been carried out over the AS during the premonsoon months of April-May 2006 using a UV Photometric O_3analyzer (Model 49C, Thermo Electron Corporation, USA). The instrument works on the principle of absorption of UV light by the O_3 molecules at a wavelength of 254 nm. Calibration of the instrument is done using the built-in ozonator (ozone generator) and zero air generator. The instrument has a lower detection limit of 1.0 ppb.

The aerosol measurements were carried out using a high volume sampler (HVS model GH2000 of Graseby Anderson, USA). The HVS was operated at the front end of the ship to collect aerosol samples taking extreme care to avoid contamination from ship exhausts. Pre-conditioned and tare-weighed quartz fibre filters were used as collection substrate and the a M_L (in μg m^{-3}) of air was estimated gravimetrically. These samples were analyzed for various water soluble chemical species

using an ion chromatograph (model DX100 of Dionex, USA). An aerosol spectrometer (model 1.108 of GRIMM, Germany) was also used to measure the number density of near-surface aerosols at regular intervals of time. This instrument is an optical particle counter operating at 15 size channels with cut-off diameters 0.3, 0.4, 0.5, 0.65, 0.8, 1, 1.6, 2, 3, 4, 5, 7.5, 10, 15 and 20 μm and provides size-segregated number density (http:/www.grimm-aerosol.com). In addition to this, an automatic weather station (AWS) operational on the port side and starboard side of the ship recorded the meteorological parameters viz temperature, relative humidity, rainfall, wind speed and wind direction at every 5 minutes.

RESULTS AND DISCUSSIONS

Spatial pattern of O_3 in the MBL of AS

The spatial map of O_3 based on the continuous data collected along the cruise track is shown in Fig. 1. The O_3 mixing ratio over the AS varied in the range ~3-22 ppb with a mean of 13.5±2 ppb. It was comparatively high over the southern AS and regions close to the southern coast. The observed high near the coast is due to the seaward intrusion of pollutants from land. Over the southwest (22-23 April), in the latitude and longitude sectors 14°-18°N and 68°-70.5°E (29, 30 April), andmid-AS (06 May) three regions of low O_3 was seen.

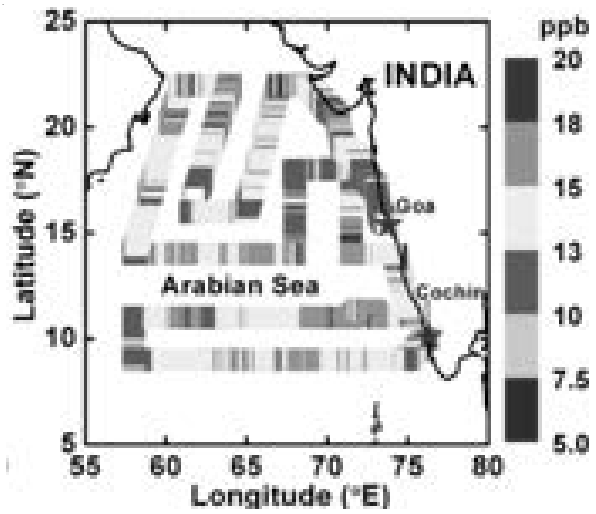

Figure 1. The spatial pattern of O_3 along the cruise track

Effect of aerosol mass loading (M_L) and number density (N) on O_3

O_3 and M_L both showed a more or less similar variation, particularly when the ship was cruising in the southern AS. The low O_3 regions coincided with low M_L regions and where high O_3 mixing ratios were observed, M_L was also high. This suggests that (1) the source regions of both are same and/ or (2) aerosols and O_3 are interdependent. The region of low O_3 over south west and mid AS (shown in Fig. 1) coincides with that of low N. This analysis brings out the association of O_3 with aerosol loading.

In the present cruise, no measurements of halogens were available, but the chemical analysis of aerosols collected over the cruise region showed distinct spatial features of various chemical species. It is seen that regions of low chloride matched with those of low O_3. It is noted that the Cl^-/Na^+ ratio

was low (~1.5-2) compared to that of sea water suggesting that depletion of chloride occurred in this region which can result in the release of Cl in gaseous form. Reaction of O_3 with chlorine species either in gaseous form or on surface of aerosols could be one of the probable causes of the low O_3 observed.

REFERENCES

Ali, *et al.* (2009). Sink mechanism for significantly low level ozone over the Arabian Sea during monsoon, *J. Geophys. Res.*, **114**, D17306.

Castro, T., Madronich, S., Rivale, S., Muhlia, A., Mar, B. (2001). The influence of aerosols on photochemical smog in Mexico City, *Atmos. Environ.*,**33**, pp.1765-1772.

Dickerson, R. R., Rhoads, K. P., Carsey, T. P., Oltmans, S. J., Burrows, J. P., Crutzen, P. J. (1999). Ozone in the remote marine boundary layer: A possible role of halogens, *J. Geophys. Res.*, **104**, pp. 21,385-21,395.

VALIDATION OF AEROSOL PROPERTIES FROM TIGER-z MEASUREMENTS WITH GCM SIMULATIONS, DURING PRE-MONSOON OVER KANPUR

DUDAM BHARATH KUMAR[1*], SUBHA VERMA[2]

[1]Research scholar, [2]Asst. Professor,
Department of Civil Engineering,
Indian Institute of Technology, Kharagpur-721302
E mails: dbharath.iitkgp@gmail.com

Key words**:** INDO- GANGETIC PLAIN, PRE-MONSOON, FIELD CAMPAIGN, SIMULATIONS.

INTRODUCTION

It has been established that the aerosols are the pollutants presence over the atmosphere, influence energy-radiation balance in the climate system. The aerosols influenced by different chemical species contributes aerosol loading. Thus, the transport of aerosols from the source to the receptor is significant phenomena to assess the sensitivity of a global model. It is relevant that the evolution of species based on distinct prevailed meteorological conditions. It is also evident that (*Reddy et al*., 2004) suggested emissions associated with source region contribute to the global burden is considered as source dependent. Numerous aerosol studies have been conducted on pre-monsoon aerosols over the Indo-Gangetic plain, for the last two decades (Dey *et al.*, 2004; Singh *et al* ., 2005; Tripathi*et al*., 2006; Gautam*et al*., 2009, 2011; Giles *et al*., 2011). These studies were examined the aerosol optical properties, while the previous findings of (Singh *et al*., 2005; Gautam *et al*., 2009) demonstrated radiative properties, during the pre-monsoon season over the Kanpur. Altogether offers a collective scope on the examination of aerosols, thus provide an attention to explore the transport of aerosols over the Indo-Gangetic region.

In this regard, it is essential to minimize the discrepancy of aerosols being predicted with the quantitative measurements of the aerosols to fulfil the need of convergence; particularly it is required to attain the stability in the model.Further, we need to focus on several species being presence over the world; contribution of these species to aerosol loading plays an important role in identification of an invisible sector of a shade on the evaluation of atmospheric aerosol system behaviour and consequent changes in meteorological system. Hence,the objectives of this study were four-fold: ((i) to examine the aerosols and its consequent loadings over the study location (Kanpur) using simulated data, (ii) to correlate the aerosol optical depth GCM simulations with the TIGERZ measurements, (iii) to observe the single scattering albedo of aerosols and (iv) to identify the source regions contributing aerosol loadings using back trajectory analysis.

METHODOLOGY

The analysis of this paper based on the observations conducted during the Tiger-z field campaign for the period from 1 May to 12 June 2008 over the Kanpur with a Latitude of 26.51°, Longitude of 80.23° (Giles *et al*., 2011). In order to assess the influence of various source regions on the temporal variations of aerosols measured during the campaign, the methods used in this study include: (1) Prediction of aerosol chemical species composition through aerosol transport simulations is carried out using general circulation model of the Laboratoire de Me´te´orologieDynamique (LMD-ZT

GCM) for INODEX due to the unavailability of simultaneous aerosol chemical measurements for the field campaign and sampling for the overlapped times of INDOEX-IFP, (2) In order to diminish the potential influence of species composition of aerosols on receptor location, we use source region aerosol flux composition from the emission Inventory, and (3) We estimate the predictions of source region contributions to total aerosols and aerosol chemical species, through aerosol transport experiments in the LMD-ZT GCM with region-tagged emissions for overlapping days using the back trajectory analysis. Brief description about the LMD-ZT general circulation reported in recent studies (Reddy *et al*., 2004; Verma *et al*., 2007). The back trajectory is calculated by using NOAA HYSPLIT (Hybrid Single-Particle Lagrangian Integrated Trajectory) (Version 4) model (Draxler *and* Hess, 1998) and grouped for 7 days during pre-monsoon period, on the basis of its origin and traverse over the Kanpur.

RESULTS AND DISCUSSION

Aerosol Optical Depth (AOD)

AOD at 500 nm obtained from measurements during the period between May 1 and June 12 2008, during TIGERZ campaign held at Kanpur, is shown in Fig. 1(a). These measurements data are from Giles*et al*., 2011. In general, monthly mean AODs in May and June are found to be almost equal, with mean values in May and June being 0.65 and 0.68 respectively, and overall mean during the complete period of study being 0.66. The modelled AOD at 550 nm obtained for the days of measurement during the tiger-z campaign through aerosol transport simulations in GCM is shown in Fig. 1. The monthly mean AODs during May and June from GCM are found to be 0.23 and 0.35 respectively, with the overall mean during the period of study being 0.25. On comparing the modelled estimates with those from measurements data, it is seen that mean AODs estimated from GCM during May and June are underestimated by a factor of 2.8 and 1.94 respectively, with the overall factor of model underestimation being 2 to 3 (2.64) times the measurements. It is to be noted that model underestimation has been described by a factor of 2 to 3 during the northeast winter monsoon over the Arabian Sea and Bay of Bengal of the Indian Ocean (Verma, *et al.*, 2007 and 2008; Reddy *et al.*, 2004). It is interesting to be found that few features of high and low AOD values in measured data along with the modelled data, e.g. AOD draw-down in model domain on May 14, May 23, May 28, May 29, and June 12, respectively, while peaked AOD of measured data on May 25 and 26, and June 9, respectively.

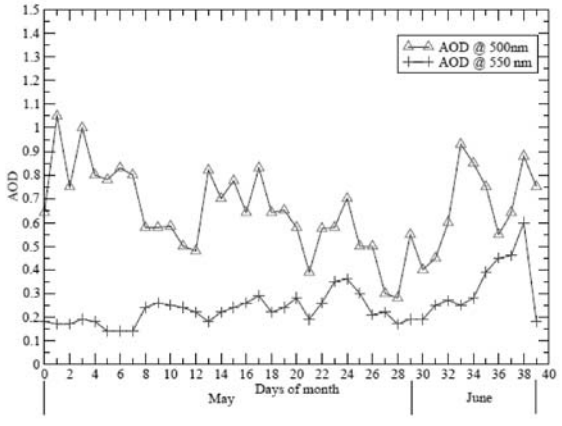

Figure 1. Comparison of AOD measured at 500 nm and AOD modeled at 550 nm for pre-monsoon season during TIGERZ campaign, Kanpur (2008).

Single Scattering Albedo (SSA)

In order to understand the relative contribution of absorbing or scattering aerosols, we also evaluate aerosol SSA obtained from aerosol transport simulations in GCM for the days of tiger-z campaign during May-June period.SSA during days of measurement in May is seen to have large day-to-day variations with their values estimated to be as low as 0.89 on May 27 to as high as 0.955 on May 23, compared to its value in the range 0.93-0.96 in June. Mean SSA during days of measurements in May and June months are estimated to be about 0.925 and 0.965 respectively, thus indicating predominant contribution from absorbing aerosols during May while that from scattering aerosols in June. It is seen from aerosol constituents (discussed above) analysis that features of low or high SSA values are in correspondence with the low or high contributions from sulphate and OM AODs, thus indicating prevalence of transport of these constituents at Kanpur during period of study.

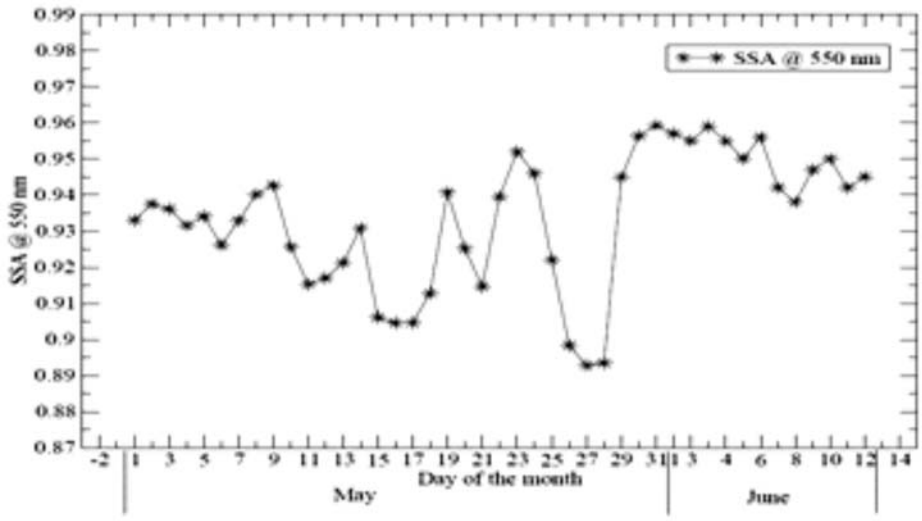

Figure 2. Temporal variation of modeled single scattering albedo over an IGP during pre- monsoon

CONCLUSIONS

The aerosol loadings over the Indo-gangetic plain (IGP) investigated during the pre-monsoon season, with a special focus on emphasizing the aerosol characteristics such as aerosol optical depth (AOD), single scattering albedo (SSA), and mass concentrations using the GCM model. Aerosol constituents enlisted in this paper comprises such as follows

- The aerosol optical depth (AOD) measured from collocated observation during the TIGERZ field campaign found in the range of 0.3-1.05 from May and 0.45-0.95 from June, while simulated columnar optical depth (AOD) predicted using GCM model observed the range as 0.15-0.35 from May while 0.18-0.6 from June.
- Model simulated aerosol optical depth correlated with the AERONET measurements of TIGERZ campaign revealed the discrepancy of GCM model with a factor of ~4, due to the possibility of uncertainty in region-tagged emissions in the model as well as it can be the reason why the mixing of black carbon with the dust occurs over IGP during pre-monsoon from the measurement perspective.

- The absorbing aerosols during pre-monsoon played a significant role on single scattering albedo such as dust followed by black carbon (BC), and the mixer of both dust and the black carbon (BC). The average single scattering albedo (SSA) at 550 nm predicted from model to be ~0.94, with the emphasis on the range to be falls from 0.895-0.95 in May while SSA in the range of 0.96-0.97 in June.
- From the HYSPLIT back trajectory model analysis, and the detailed emphasis on the correlation of mass concentration with the AOD for different source regions (world regions and Indian regions) presented using scatter plot analysis (Figure 8) revealed the Indo-Gangetic plain (IGP) is the main source for the local emissions such as organic carbon (OC), black carbon (BC), and sulfate, while dust and the sea salt (SS) observed to be evolve from the world regions such as mainly Africa west Asia (AFWA) and North west India (NWI), due to the long range transport of the air parcels carrying mineral dust.

Present study suggests the aerosols over the Indo-Gangetic region needs to be characterized in detail as such evaluate the aerosol loadings during all the seasons with the continuous collocated measurements in order to investigate the optical and radiative effects on the climate. Further, it is also important that the source to be identified properly using prolonged studies of source apportionment using local and global emission data, and to be validated through sufficient measured (both temporal and spatial) data over this study location.

REFERENCES

Dey, S., SachchidaNandTripathi, and Ramesh P. Singh (2004). Influence of dust storms on the aerosol optical properties over the Indo-Gangetic basin, *J. Geophysic. Res.*, **109**, D20211.

Draxler, R. R. and Hess, G. D. (1998). An overview of the HYSPLIT-4 modeling system for trajectories, dispersion and deposition, *Aust. Meteorology Mag*., **47**, pp. 295–308.

Giles, M. David, et al., (2011). Aerosol properties over the IndoGangetic Plain: A Mesoscale perspective from the TIGERZ experiment, *J. Geophysic. Res.*,**116**, D18203.

Jethva, H., Satheesh, S. K. and Srinivasan, J. (2005). Seasonal variability of aerosols over the Indo-Gangetic basin, *J. Geophysic. Res.,* **110**, D21204.

Reddy, M. S., and Boucher, O. (2004). Global carbonaceous aerosol transport and assessment of radiative effects in the LMDZ GCM, *J. Geophysic.Res,* **109**, D14202.

Singh, R.P., Dey, Sagnik, Tripathi, S. N. and Tare, Vinod (2004). Variability of aerosol parameters over Kanpur, northern India, *J. Geophysic. Res.,* **109**, D23206.

Tripathi, S. N., *et al.* (2006). Measurements of atmospheric parameters during Indian Space Research Organization Geosphere Biosphere Programme Land Campaign II at a typical location in the Ganga Basin: 1. Physical and optical properties, *J. Geophys. Res.*, **111**, D23209.

Verma, S., Venkataraman, C., Boucher, O. and Ramachandran, S. (2007). Source evaluation of aerosols measured during the Indian Ocean Experiment using combined chemical transport and back trajectory modeling, *J. Geophysic. Res.*, **112**, pp. 0148-0227.

CONTINENTAL INFLUENCE ON AEROSOLS OVER BAY OF BENGAL DURING PRE-MONSOON AND WINTER

ARYASREE S, GIRACH IMRAN ASATAR AND PRABHA R NAIR

Space Physics Laboratory, Vikram Sarabhai Space Centre,
Thiruvananthapuram 695 022, India

Keywords: AEROSOLS, TRANSPORT, CONTINENTAL INFLUENCE

INTRODUCTION

Aerosols in the marine environment have various sources like wind induced sea-spray, biogenic activity, transport from nearby continental regions and even emissions from ships. Due to the large heterogeneity of aerosol properties with respect to space as well as time, regional scale investigations on varying temporal scales are needed to classify and quantify them and to assess their climatic / environmental impacts. With this objective a major campaign -Integrated Campaign for Aerosol gases and Radiation Budget (ICARB)- was undertaken under the Geosphere Biosphere Programme of Indian Space Research Organization (ISRO). Under this programme two major ship cruises were conducted in two different seasons viz. pre-monsoon (May-June2006) and winter (December 08-January 09). Fig. 1 shows the ship tracks over Bay of Bengal (BoB) during these cruises. Several reports are available on the physical and radiative characteristics of aerosols over BoB. But observations on the chemical characteristics are very few.

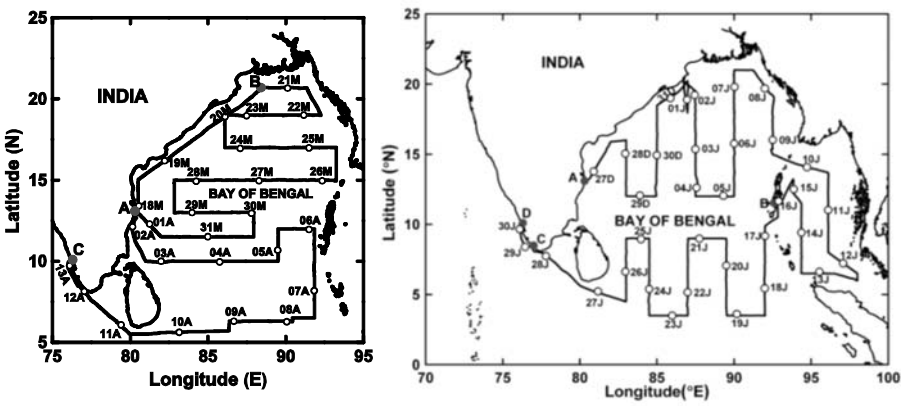

(a) (b)

Figure.1. Cruise track of (a) pre-monsoon cruise (b) winter cruise.

The present study focuses on the continental influence on the marine environment of BoB in terms of the chemical composition of aerosols for two contrasting seasons pre-monsoon and winter.

AIRFLOW PATTERNS

Fig. 2 shows the mean airflow patterns at 925hpa during the pre- monsoon month of March 2006 and the winter period of December 27, 2008- January 29, 2009, obtained from NCEP NCAR reanalysis. During pre-monsoon, the winds are weak over BoB with a weak outflow from Indo-Gangetic Plains (IGP). In winter strong northerly/north easterlies prevail over BoB favouring advection of airmass

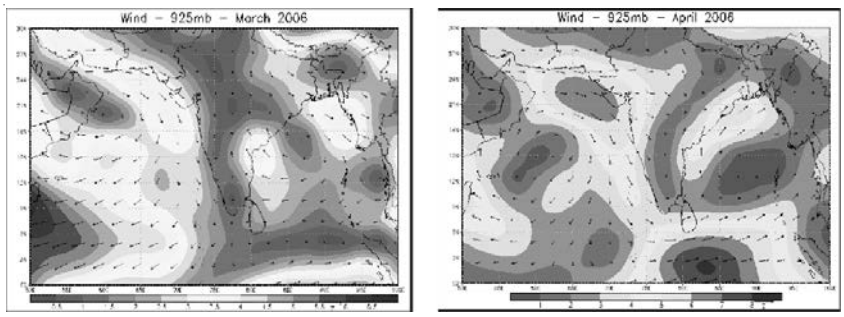

Figure 2. Mean airflow patterns at 925hpa during the pre-monsoon month of March 2006 and the winter 2008-09

EXPERIMENTAL TECHNIQUES

Aerosols samples were collected using a High Volume Sampler (Model GH2000 of Graseby Anderson, USA) on preconditioned and tare weighed quartz fibre substrates during both the cruises. The aerosol mass loading in ($\mu g\ m^{-3}$) is estimated gravimetrically. The sample-laden substrates are chemically analysed using an Ion Chromatograph (DX-120 of Dionex, USA) for identifying and quantifying various water soluble chemical species which include anions of F,Cl,NO_2,NO_3,PO_4 ,SO_4,etc and cations of Na,NH_4, Mg,Ca and K. Details of aerosol sampling and chemical analysis procedure are discussed in earlier publications (George *et al.*,2008; Nair *et al.*, ,2006). In addition, the meteorological parameters were also monitored onboard by an automatic weather station which records the wind speed,wind direction,RH and Temperature at 5 minutes interval.

RESULTS AND DISCUSSIONS

Fig. 3 shows the spatial pattern of aerosol mass loading during the two seasons. Obviously the aerosol mass loading is significantly high during winter. Irrespective of the season, aerosol mass loading exhibits high over north BoB. However, the amplitude and extent of the high is much larger in winter (there is an increase of ~1.5 times). Moreover high mass loading is also seen close to the entire coastal regions during winter. They have intruded into larger oceanic regions in winter compared to pre-monsoon. This indicates the continental influence over the oceanic environment owing to transport. The strong outflow from the IGP is responsible for the high mass loading over north BoB. Unlike the

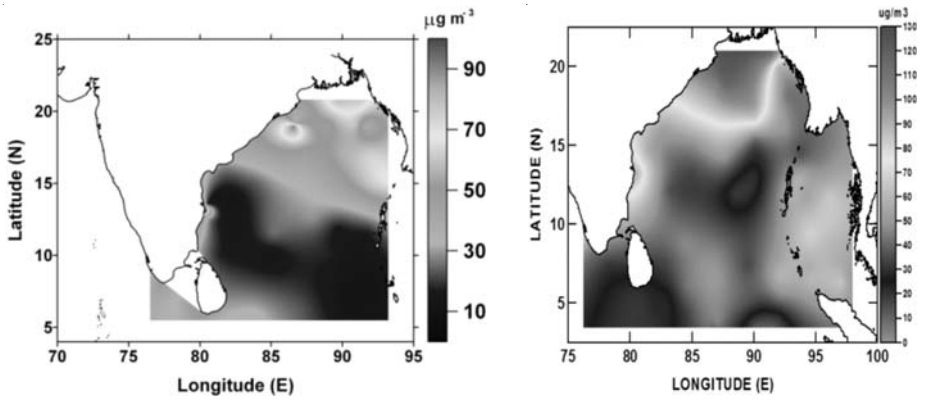

(a) (b)

Figure 3. Aerosol mass loading during (a) premonsoon and (b) winter

Pre-monsoon season, there is high aerosol mass loading over the south/south eastern BoB during winter. Airmass back trajectories reveal that this is caused by transport from East Asian regions. Chemical composition of aerosols also reveal the presence of significant amount of continental species like SO_4, NO_3, Ca, K, etc over north BoB and the coastal regions. Over southern BoB, the oceanic species like Na, Cl and Mg are more prominent. The spatial distribution of various species are analysed in terms of airflow patterns, airmass back trajectories and source regions and potential source function analysis is also attempted.

REFERENCES

George, S.K., Nair, P.R., Parameswaran, K., Jacob, S., Abraham, A., (2008). Seasonal trends in chemical composition of aerosols at a tropical coastal site of India,*Journal of Geophysical Research*, **113**, D16209.

Nair, *et al*. (2006). Chemical composition of aerosols over peninsular India during winter, *Atmos. Environ.*, **40**, 6477-6493.

RELATING MODELED RAINFALL TO ATMOSPHERIC AEROSOL VARIABLES OVER INDIA IN GCM SIMULATIONS WITH IN-SITU REGIONAL AEROSOLS

NITIN PATIL[1], C. VENKATARAMAN[1,2], RIBU CHERIAN[3]

[1]Climate Studies Program, Indian Institute of Technology Bombay, Powai, Mumbai-400076, India.
[2]Department of Chemical Engineering, Indian Institute of Technology Bombay, Powai, Mumbai-400076, India.
[3]Institute for Meteorology, University of Leipzig, Leipzig, Germany.

Keywords: INDIAN SUMMER MONSOON, ECHAM5.5-HAM MODEL, ATMOSPHERIC AEROSOLS

INTRODUCTION

Atmospheric aerosols, which are a mix of both natural and anthropogenic emissions, have been implicated in climate change, including altering the radiation balance in the Earth-atmosphere system, dimming solar radiation reaching the Earth's surface (Padma Kumari and Goswami, 2010) and increasing solar heating of the atmosphere (Forster *et al*.,2007*)*. Further, modeling studies have related increases in absorbing aerosols like black carbon, to decreases in Indian summer monsoon rainfall (Ramanathan*et al*., 2005)and radiative forcing related to change in snow albedo in the Himalaya (Flanner *et al*., 2009).

Possible mechanisms of aerosol influence on precipitation, believed to be uncertain, like Elevated-Heat-Pump (Lau *et al*., 2006) and surface dimming effect (Ramanathan *et al*., 2005). Recently, GCM simulations of precipitation change over India using pre-industrial and present-day aerosols (Cherian *et al*., 2011) indicated a reduction in total and convective rainfall attributed tosuppression of convection by a high negative surface forcing from the aerosol indirect effect. To further understand this perturbation, the present study investigates spatial distributions of deviation in seasonal rainfall (summer monsoon, JJAS) and aerosol variables (in pre-monsoon, MAM and summer monsoon, JJAS).

METHODOLOGY AND DATA SETS

Atmosphericsimulationsweremadewiththe European Centre for Medium-Range Weather Forecasts-Hamburg (ECHAM5.5) GCM (Cherianetal., 2012,inreview) with ahorizontal resolution of T63 (about1.8ox1.8o) and avertical resolution of 31levels (extended from thesurfaceto10hPa) combine dwiththe Hamburg Aerosol Module (HAM, Stieretal.,2005).Dustand seasal temission swerecal culate donline. In the simulation, aerosolglobale missions based on the AER OCOM emission inventory (Denteneretal.,2006) of the year 2000 are combine dwithregional emission invent oriesover India developed by IITB. The combine demission data setwasused forresidential, transport, industry and agricultural residue burning emissionsectors. Precipitation andaeroso loptical properties weres imulated forthe period of five years (2001-2005).

PRELIMINARY RESULTS

The spatial distribution in deviation of seasonal rainfall in JJAS from the five-year mean is calculated for each year (Fig. 1). Also shown is the spatial distribution in deviation of seasonal aerosol optical depth (AOD) in MAM and JJAS for the corresponding year. The spatial distribution addresses the

relationship between the deviation in precipitation with pre-monsoon and monsoon aerosol optical depth. There is significant inter-annual variation in the distribution of rainfall, as evidenced by differences in the maps of rainfall deviation from the 5-y mean (Fig.1, top panel). No consistent trend in was seen in AOD deviation vis-à-vis rainfall deviation. Positive rainfall deviation in eastern India correlated with positive deviation in pre-monsoon and monsoon AOD (2001), while positive rainfall deviation in central (2003) and north-western (2005) regions had a negative correlation (i.e. negative AOD deviation), in the corresponding years. The paper will further assess spatial distributions in other aerosol effects like top-of atmosphere and surface forcing (both direct and indirect) vis-a-vis the spatial distribution of deviation in rainfall patterns to relate the modeled rainfall to atmospheric aerosols variables in GCM simulations, toward understanding mechanisms of aerosol perturbation of rainfall.

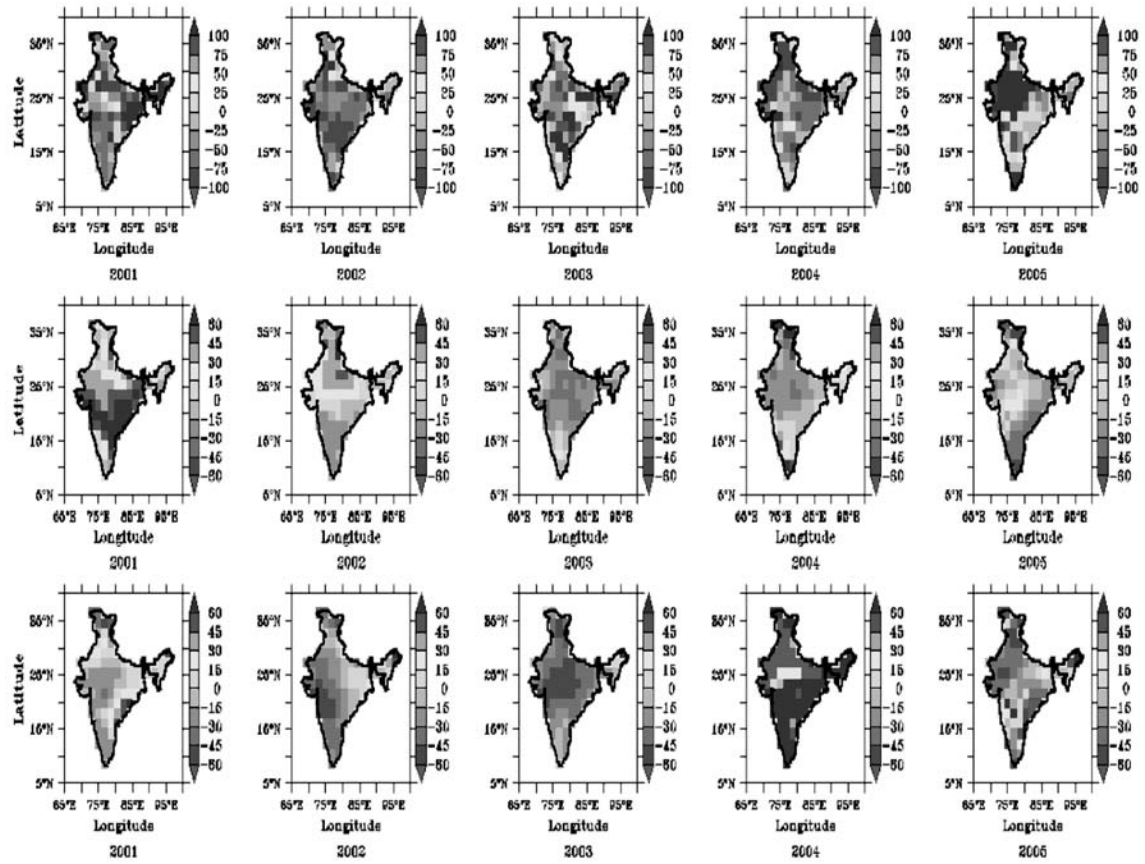

Figure 1. Upper row: Seasonal (JJAS, %) precipitation Middle row: Pre-monsoon (MAM, %) AOD@550nm Lower row: Monsoon (JJAS, %) AOD@550nm deviations from 2001-2005.

REFERENCES

Cherian, R., Venkataraman, C., Ramachandran, S., Quaas, J. and Kedia, S. (2011). Examination of aerosol distributions and radiative effects over the Bay of Bengal and the Arabian Sea region during ICARB using satellite data and a general circulation model, *Atmos. Chem. Phys.*, **12**, pp. 1287–1305.

Cherian, R., Venkataraman, C., Quaas, J. and Ramachandran, S. (2012).GCM simulations of aerosol extinction, atmospheric heating and precipitation changes over India, Under Review.

Dentener, F., et al. (2006). Emissions of primary aerosol and precursor gases in the years 2000 and 1750 prescribed data-sets for AeroCom, *Atmos. Chem. Phys.*, **6**, pp. 4321-4344.

Forster, P., et al. (2007). Changes in atmospheric constituents and in radiative forcing, in Climate Change, *The Physical Science Basis-Contribution of Working Group I to the Fourth Assessment Report of the Intergovernmental Panel on Climate Change*, edited by S. Solomon et al., **chap. 2**, pp. 153–171, Cambridge Univ. Press, Cambridge, U. K.

Flanner, *et al*. (2009). Springtime Warming and Reduced Snow Cover from Carbonaceous Particles, Atmos. Chem. Phys., **9(7)**, pp. 2481-2497, http://www.atmoschem-phys.net/9/2481/2009.

Lau, K. M., Kim, M. K. and Kim, K. M. (2006). Asian summer monsoon anomalies induced by aerosol direct forcing: the role of the Tibetan Plateau, *Climate Dynamics*, ***26*(7-8)**, pp. 855-864.

Padma Kumari, B., and B. N. Goswami (2010). Seminal role of clouds on solar dimming over the Indian monsoon region, *Geophys. Res. Lett.*, **37**, L06703, doi:10.1029/2009GL042133.

Ramanathan, V. *et al.,* (2005). Atmospheric brown clouds: Impacts on South Asian climate and hydrological cycle, *Proc. Natl. Acad. Sci.*, **102 (15)**, 5326-5333, doi:10.1073/pnas.0500656102.

Stier, P., *et al*., (2005). The aerosol-climate model ECHAM5-HAM, *Atmos. Chem. Phys.*,***5***, pp. 1125-1156.

STUDY THE EFFECT OF SOLAR VARIABILITY, AEROSOL AND METEOROLOGICAL PARAMETER ON LIGHTNING, CONVECTIVE RAIN OVER THE SOUTH/SOUTHEAST ASIA

DEVENDRAA SIINGH[1], P. RAMESH KUMAR[1], R. N. GHODPAGE[2]

[1]Indian Institute of Tropical Meteorology, Pune, India
[2]Indian Institute of Geomagnetism, Shivaji University Campus, Kolhapur, India-416004.
E mail : devendraasiingh@tropmet.res.in; devendraasiingh@gmail.com

Keywords: SOLAR VARIABILITY, THUNDER STORMS, MET PARAMETERS

INTRODUCTION

Firstly, Fritz (1878) correlated thunderstorm frequencies with the relative sunspot numbers using data collected at different stations in Europe and North America between 1755 and 1875 and showed a positive correlation at some stations. Later on, Brooks (1934) considering worldwide data reported a low correlation at mid – latitude and enhanced correlation towards the pole and the equator. Additionally, it was also reported that the correlation coefficient changed significantly over relatively short distances. The dependence of climate on various factors associated with lightning and precipitation has enhanced interest in the study of lightning and precipitation. Satellite data have provided global picture of lightning flash rate and precipitation (rainfall). The regional distributions for thunderstorm activity are ranked from the most active to the least active as: (1) Africa (2) South America (3) Southeast Asia. The ranking based on rainfall is (1) Southeast Asia, (2) South America, (3) Africa (Price, 2009; Siingh et al., 2008). Thus, the long term data display the opposite relationship between global lightning activity and rainfall. Studies showed that rainfall production and lightning activity have quite different dependencies on updraft speed.Weak to moderate updrafts arerequired for rainfall, whereas stronger and deeper uplift is necessary for lightning. In the present study, the dependence of lightning activity and convective rain in the Asian continent containing India, Pakistan, Bangladesh, Burma, Part of China and Islands in Bay of Bengal as depicted in Fig.1. have been examined.

DATA AND ANALYSIS

Area of our investigation for the study of the spatio – temporal variations of lightning activity and convective rain comprises of South/Southeast Asia (8 ^{0}N – 35 ^{0}N, 60 ^{0}E – 95 ^{0}E – Region 1 and 8 ^{0}N – 35 ^{0}N, 95 ^{0}E – 120 ^{0}E – Region 2) as shown in Fig.1. Monthly average –sunspot number, cosmic rays flux, A_p index, solar flux ($F_{10.7}$, cm) data taken from the website:
http://solarscience.msfc.nasa.gov/greenwch.shtml;
http://cro.izmiran.rssi.ru/bjng/main.html;http://www-app3.gfz-potsdam.de;
http://celestrak.com/SpaceData/SpaceWx-format.asp, are analyzed. For the cosmic rays flux data we have used data from the nearest location for neutron monitoring station at Beijing (39.08 ^{0}N, 116.26 ^{0}E, altitude 48 m), China, operated by the Institute of Physics, Beijing. The lightning data (number of flashes) derived from Lightning Imaging Sensors (LISs) aboard Tropical Rainfall Measuring Mission (TRMM) satellite have been used (Simpson, 1988). The monthly data available in the grid resolution of 5 deg × 5 deg for the period 1998 – 2010 were downloaded from the website (http://ghrc.msfc.nasa.gov) for the region of interest.The convective rain data is derived from the TRMM PR 3A25 data product with a spatial resolution of 0.5^0 x 0.5^0 at 2 km height. The data is

downloaded from the website www.daac.gsfc.nasa.gov.The meteorological parameters such as surface temperature, convective available potential energy (CAPE), OLR (Outgoing Long wave Radiation), convective cloud layer: total cloud cover, AOD, atmospheric columnar total ozone with 2.5 degree grid resolution from Climate Forecast System Reanalysis (CFSR) data developed by NOAA's National Center for Environmental Prediction (NCEF) (http://nomadl.ncep.noaa.gov/ncep-data/index.html) have been used.

LIGHTNING FLASH RATES, CONVECTIVE RAIN AND SOLAR PARAMETERS

The variation of sunspot number, A_p index, $F_{10.7}$ solar flux and cosmic rays which define solar activity is shown in Fig. 1b (upper panel) for the period 1989 – 2010 (sunspot cycles 22, 23). The variation of lightning flash rates with sunspot numbers for the geographical regions R_1 and R_2 are shown in Fig. 1b (lower panel). Note that lightning flashes are available for the period 1998- 2010. Lightning flashes for the Indian Peninsular region reported by Perieira Felix et al. (2010) are also shown in the same figure. Lightning flashes show almost an opposite behaviour to sunspot number variations.It is also observed that flash rates started increasing even when sunspot numbers remained almost maximum (during the period 2001 – 2003) and showed a secondary maxima during the period 2003 – 2006, when the sunspot number showed a decreasing trend.

LIGHTNING/CONVECTIVE RAIN VARIABILITY WITH METEOROLOGICAL PARAMETERS

Fig.2a shows the annual variation of the total number of lightning flashes, convective rain, average temperature anomaly, convective cloud layer: total cloud cover, CAPE, mean OLR, aerosol optical depth (AOD), atmospheric columnar total ozone of the region R_1 and R_2 during the period 1998 – 2010.The variation in CAPE follows temperature anomaly. The AOD in region R_1 is higher than in region R_2,except during the year 2005 when it is slightly smaller in region R_1 as compared to the region R_2. The higher values in the region R_1 may be due to the higher coverage area.The cloud cover in region R_2 is more than that in region R_1, but the same pattern is not usually followed by the convective rain, which is sometimes greater in the region R_2 and sometimes in the region R_1. The mean OLR and the atmospheric columnar total ozone in the region R_1 are larger than in region R_2. Cloud cover forbids the OLR. Hence smaller cloud cover in region R_1 is consistent with larger OLR. The seasonal variation based on the monthly averaged data of lightning flashes, convective rain, average temperature anomaly, total convective cloud cover, CAPE, mean OLR, AOD and atmospheric columnar total ozone of the regions R_1 and R_2 are shown in Fig. 2b. Interestingly the AOD in region R_1 shows maxima during the monsoon season, whereas intheregion R_2 it exhibits maxima in thepre-monsoon season. Cloud cover in both the regions exhibits maxima during the months of June to September, whereas during the same period in both the region mean outgoing long wave radiation shows minima. Out of all the parameters discussed in this figure, the variation in CAPE could clearly explain the trend of total lightning flash variation. The dependence of lightning on various parameters becomes clearer from Fig. 3. where we have tried to find out correlation between the total number of lightning flashes and different meteorological parameters. In both the regions lightning flashes are well correlated (correlation coefficient > 0.80) with temperature, CAPE and columnar ozone. In the region R_1, the correlation coefficient between total thenumber of flashes and cloud cover is ~ 0.46 whereas for the region R_2 it is ~ 0.7. In Fig. 3a, we had shown outgoing long wave radiation to be negatively correlated. The correlation coefficient for the region R_1 and R_2 comes out to be – 0.33 and – 0.6 respectively. An increase in the AOD leads to enhancement in lightning flashes in the region R_1 (correlation coefficient ~ 0.6). However, in the region R_2 similar

relation is not observed (correlation coefficient ~ 0.15). The depicts dependence of convective rain on the temperature anomaly, CAPE, cloud cover, OLR, AOD and columnar ozone concentration. Convective rain increases with an increase in temperature anomaly, CAPE, cloud cover, columnar ozone concentration. The data distribution in the region R_1 are less scattered as compared to the region R_2. As a result the derived correlation coefficient for the R_2 region is more as compared totheregion R_1. Convective precipitation decreases with mean OLR (Figure is not given for convective rain). It is interesting to note that as in the case of lightning, aerosols have much less control over convective rain in the region R_2 as compared to region R_1.

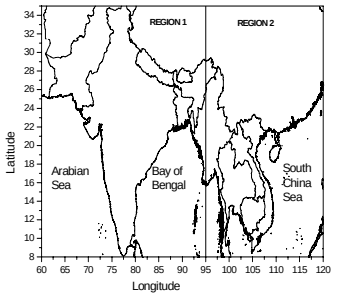

Fig. 1a

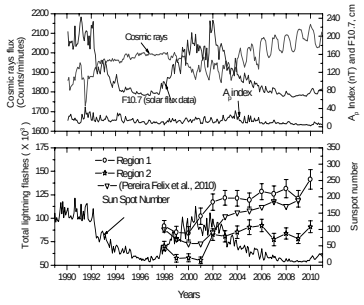

Fig.1b

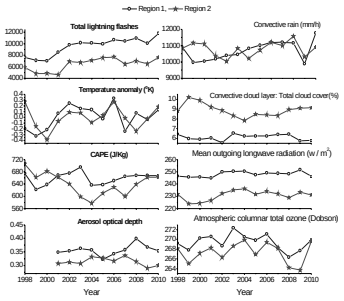

Fig. 2a

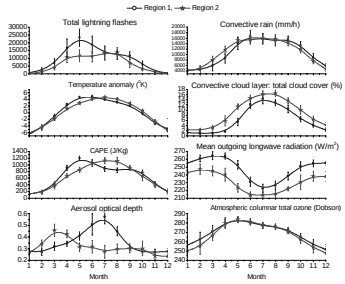

Fig. 2b

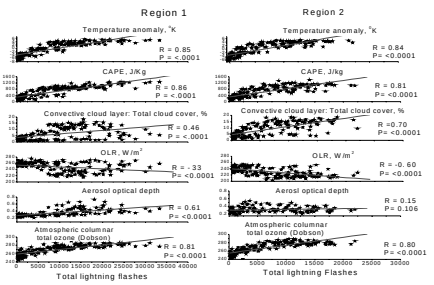

Fig. 3

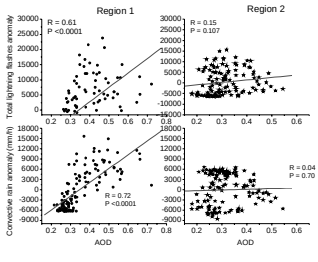

Fig.4

Fig. 1a. Map of South/Southeast Asia showing two regions (Region 1) and region 2. Fig. 1.b Yearly variation of cosmic rays flux, $F_{10.7}$ cm (solar radio flux) and A_p index for the 22, 23 solar cycles are shown (upper limit); yearly variation of sunspot number, lightning flash counts for regions R_1 and R_2 are shown. Lightning flash counts for the Indian Peninsular Region (India) are also shown in the same figure (lower limit). Fig. 2a. Annual variation of lightning flash counts, convective rain, temperature anomaly , Convective cloud layer: total cloud cover, CAPE, OLR, AOD and Atmospheric columnar total ozone for region 1 and 2 are given. Fig. 2b. Same as Fig. 5 but for seasonal variation Fig.3. Variations of lightning flash counts with metrological parameter for the region 1 and 2 are shown. Values of correlation coefficients and significance level of the parameter are also given in each panel. Fig.4. variations of lightning flash anomaly and convective rain anomaly with AOD. Values of correlation coefficients and significant level of the parameter are also given in each panel.

Fig.4 shows the correlations of convective rain anomaly and total number of lightning flash anomaly with AOD. Correlation coefficient is found to be greater than 0.6 with a very high significance level for region 1 but for the region 2 it is not showing the correlation.

SUMMARY AND CONCLUSION

Many studies showed that thunderstorms with more lightning are likely to produce more rain, i.e. lightning and rain fall are positively related. On the global scale, the opposite behavior has been observed, i.e. tropical continental centers of lightning and rain range is in the opposite order. The available lightning data (from 1998 to 2010) in both the regions showed similar annual variation and clearly showed negative correlation with sunspot numbers. Lightning flashes and convective rain in both (R_1 and R_2) the regions do not show significant correlation with solar activity parameters. However, these are well correlated with meteorological parameters such as the temperature variation, CAPE, cloud cover, aerosol optical depth and ozone. The correlation coefficient varied between 0.46 and 0.86, except for the region R_2 it came down to 0.15 for aerosol optical depth. The outgoing long wave radiation is negatively correlated with both lightning flashes and convective precipitation in both the regions R_1 and R_2. Good correlation (r = 0.68 and 0.81) is found between lightning flashes and convective rain in both the regions R_1 and R_2.

ACKNOWLEDGEMENTS

We acknowledge with thanks the NASA and NOAA for making the data available. DS, PRK are thankful to Prof. B.N. Goswami, for the kind support and encouragement.

REFERENCES

Brooks, C.E.P., (1934). *Q. J. Royal Met. Soc*.**60**, pp 153–165.

Fritz, H., (1878). Die wichtigsten periodischen Erscheinungender Meteorologie und Kosmologie. In: NatuurkundigeVerhandelingen van de Hollandsche Maatschappij derWetenschappen te Haarlem, Deel III, Haarlem.

Price, C., (2009). Will a drier climate result in more lightning?,*Atmos. Res*.**91**, pp 479-484.

Siingh, D. et al:, (2011).*Sur. Geophys*.**29**, pp 499–551.

COMPARATIVE STUDY OF WAVELET SPECTRA AND TREND IN AEROSOLS WITH THE VARIOUS PARAMETERS RELATED TO CLOUD OVER THE INDIAN REGION

S. S. DUGAM AND SATHY NAIR

Indian Institute of Tropical Meteorology, Pune-410008
Email:dugam@tropmet.res.in

Keywords: CLOUD CONDENSATION NUCLEI (CCN), CLOUD DROPLET SIZE (CDS), AEROSOL CONCENTRATIONS

INTRODUCTION

Aerosols have been studied for a long time by number of scientist but after 1990 it was recognized that the role of aerosols is an important in climate change study. The important role played by Asian aerosol on the seasonal, intraseasonal monsoon variability and Cloud- Aerosol interaction has been widely recognized recently.

Objective of paperis to see the effect of aerosols concentration on rainfall activity over Indian region and also its effect on precipitation rate and perceptible water in south west monsoon period (June-September) we used the linear trend analysis method so that to see what is trend in recent period. The comparative study of Morlet wavelet spectra of different cloud parameters such as cloud condensation nuclei, cloud droplet size and temperature are also carried out. The objective of doing the Morlet wavelet spectra is to see what will be the critical time range in cloud microphysical process for the formation of the cloud droplet within the cloud after injection of CCN particle for the precipitation enhancement within the cloud over the Indian region.

DATA AND DISCUSSIONS

In this paper, to see the effect of aerosols concentration on rainfall activity over Indian region the satellite derived monthly aerosols data over Indian region (5°N to 40°N and 50°E -100°E) have been analyzed from 1981 to 2002. Comparative study of the trend analysis has been carried out between aerosols concentrations and monsoon rainfall. It is found that in recent period there is decreasing trend in aerosols concentrations and in summer monsoon rainfall over west central Indian region. Probable reason may that the less aerosols concentrations may provide the lesser cloud condensation nuclei for the formation of rain producing clouds also because this region is more far away from sea shore it might get lesser sea salt for the formation of cloud in recent period due to weak of cross-equatorial flow. Similarly the comparative study of trends in precipitation rate and perceptible water in monsoon period over Indian region is also carried out. For the analysis precipitation rate and perceptible water data for the period from 1948-2011 in monsoons period June-September over Indian region is taken from the Department of commerce/National Oceanic Atmospheric Administration /NOAA research USA. From the analysis it is seen that the precipitation rate and perceptible water shows a decreasing trend over the Indian region from 1974 on words see figure 1 and 2.

The wavelet spectra analysis of time series of the Cloud Condensation Nuclei (CCN), Cloud Droplet Size (CDS) and temperature within the cloud over the Indian region is carried out. For the analysis, the data collected during the experiment (CAIPEX) Cloud Aerosol Interaction and Precipitation Enhancement Experiment conducted, by I.I.T.M. PUNE during the period 2009 to 2011 is used.

From the wavelet analysis it is seen that cloud drop size increases after injecting the CCN particles figure 3a and b and also same time it is observed that temperature drops suddenly (figure not given). This study may be useful for understanding the cloud dynamic of tropical cloud over the Indian region and also for cloud seeding experiment.

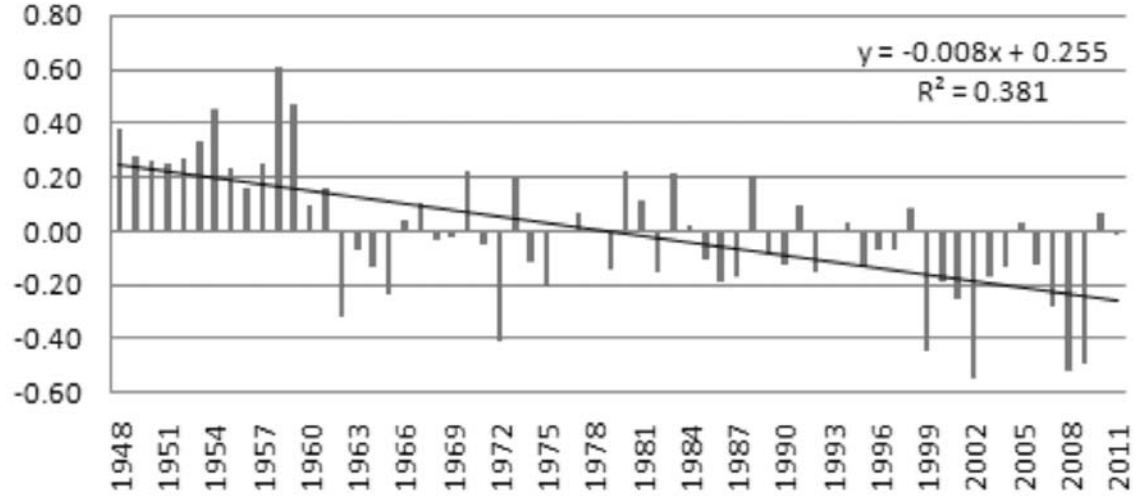

Figure 1 . Precipitation Rate over Indian Region in Monsoon Period (June- September)

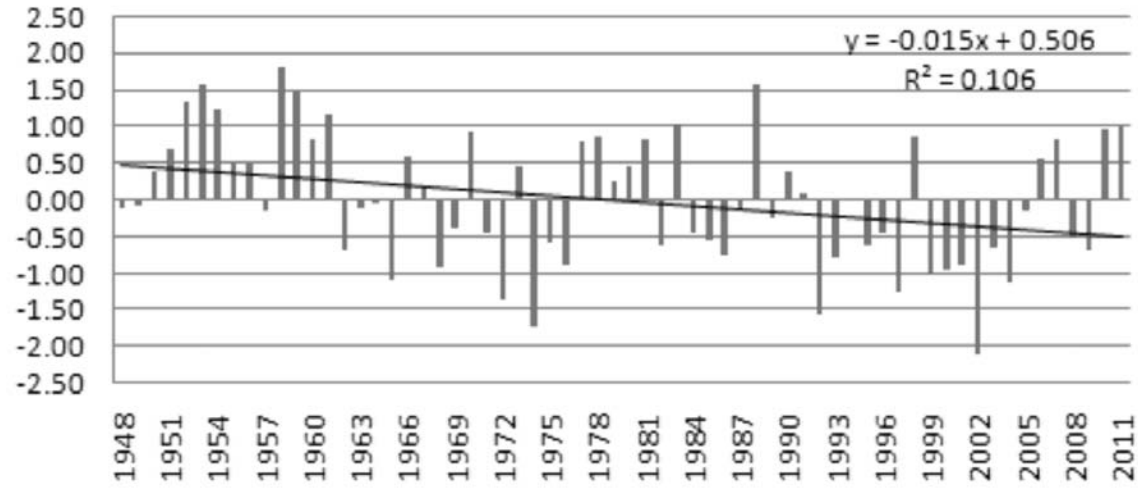

Figure 2. Perceptible water in monsoon period (June-September) from 1948-2011

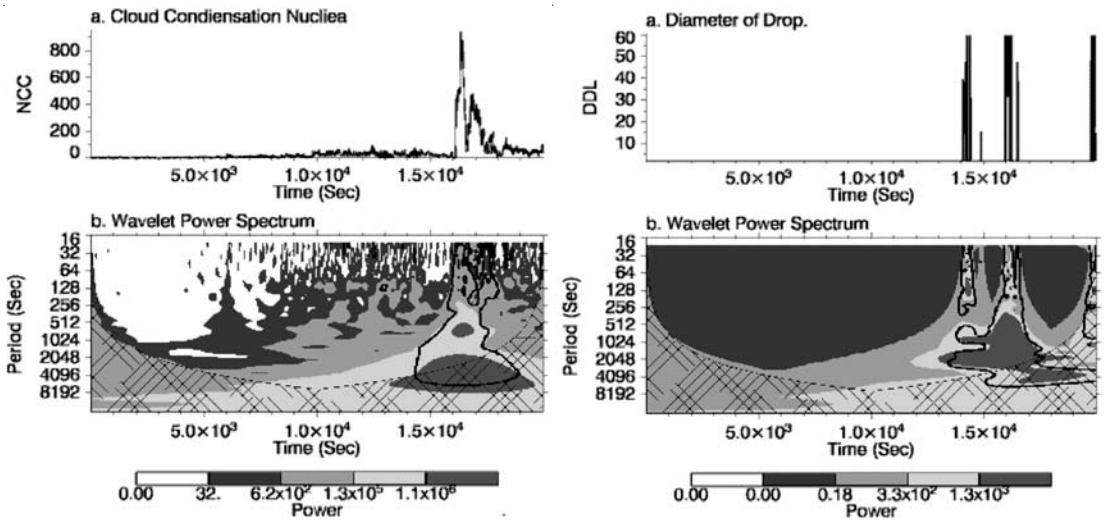

Figure 3a and b. Wavelet spectra of CCN and cloud drop diameter

CONCLUSIONS

1. It is found that in recent period there is decreasing trend in aerosols concentrations and decreasing trend in west central monsoon rainfall goes hand in hand.

2. From the wavelet analysis it is seen that cloud drop size increases within the time range of 2 $x10^4$ sec after injecting the CCN particles and also same time it is observed that temperature drops suddenly. This study may be useful for understanding the cloud dynamic of tropical cloud over the Indian region and also for cloud seeding experiment.

3. It is observed that there is a decreasing trend in precipitation rate and perceptible water in monsoon period from 1974 onwards.

ACKNOWLEDGMENT

The authors are grateful to Prof. B.N. Goswami Director, I.I.T.M. for providing necessary facilities for completing this study and to CAIPEX team for supplying the data and NOAA. And the Department of Science and Technology Government of India.

IMPACTS OF METEOROLOGY ON MASS AEROSOLS OF SOOT PARTICLE AND $PM_{2.5}$: YEAR LONG MONITORING OVER DELHI

TIWARI S.[1], BISHT D. S.[1] PASHA G.S.M[2], KUMAR R[3] AND SRIVASTAVA A. K.[1]

[1]Indian Institute of Tropical Meteorology (Branch), Prof Ramnath Vij Marg, New Delhi
[2]GhpusiaCollege of Engineering, Dept. of Civil Eng. Ramanagara, Karnataka
[3]ShardaUniversity, KnowledgePark –III, Greater Noida-201306

Keywords: MONSOON, BLACK CARBON (BC), METEOROLOGY, ATMOSPHERIC AEROSOL

INTRODUCTION

Highly absorbing capacity of solar radiation and reducing albedo of atmospheric aerosol called soot particles (black carbon) and fine particles ($PM_{2.5}$), play crucial role in climate and health, were monitored online in a year-long of 2011 at a mega urban city Delhi, situated in the northern part of India. Black carbon (BC) is an important constituent (90% in $PM_{2.5}$) of airborne fine particulate matter (PM) that is often emitted as product of incomplete combustion (Koelmans et al., 2006). The two most important BC sources are fossil fuel combustion and biomass burning (Penner et al., 1993; Cooke and Wilson, 1996). Due to above mentioned importance of BC and $PM_{2.5}$ (<2.5 ìm in aerodynamic diameter), monitoring of these aerosols were conducted over Delhi in the premises of Indian Institute of Tropical meteorology, near national Physical research laboratory, during January to December, 2011. Delhi, has more than 17 million inhabitants, is situated (28º 35' N; 77º 12' E) at an altitude of about 218 m above sea level. The measurement of BC mass concentrations were carried out by 7-λAethalometer (Model AE-31, Magee Scientific Company, Berkley, CA, USA) online monitor with temporal resolution of 5 minutes for the period from January to December, 2011.However, fine particle aerosol ($PM_{2.5}$) was measured by Thermo Andersen, Inc. Series FH 62 C14 (C14 BETA) instrument in five minute interval. The $PM_{2.5}$ cut-point was achieved with a 4 $Lmin^{-1}$, sharp-cut cyclone inlet (Kenny et al., 2000).

RESULTS AND DISCUSSION

Variations in daily mean mass concentrations of BC and fine particles (i.e. $PM_{2.5}$) from 01st January to 31st December, 2011 are shown in Fig. 1a and 1b. The annual averaged concentration of BC was observed to be about 7(±5) μg m^{-3} (median: 4.2μg m^{-3}), varied from 1 to 26 μg m^{-3} and displayed clear monsoon minima and post-monsoon and winter maxima, which follows the order of: winter > post-monsoon > summer > monsoon. BC concentrations in winter (10.8±6.4μg m^{-3}) and post-monsoon (9.4±5.4μg m^{-3}) were approximately three times higher than those during the summer (3.5±1.94 μg m^{-3}) and monsoon (2.8±1.5μg m^{-3}). The BC mass concentrations were found to be exceeded by ~37.5% of the days to the average during study period. Such high BC concentration would suggest that the air has been polluted by the anthropogenic activities. The great range of the daily BC variation was due to the variation of daily aerosols in Delhi, which would be in favor of the accumulation of BC aerosol produced in the surroundings and then transported in the local, regional, and even the long-range areas. The fine particles, i.e. $PM_{2.5}$, are responsible for most of the airborne particle threats to human health having respirable range (< 2.5 μm) at Delhi, which were also studied simultaneously along with BC (Fig. 1b). The annual mean concentration of $PM_{2.5}$ was observed to be about 123(±96) μg m^{-3} (median: 90.7 μg m^{-3}), varied from 20 to 540 μg m^{-3}. Though

the magnitude of $PM_{2.5}$ strongly differs with the magnitude of BC, both follows by and large similar trends. In diurnal study, it was seen that BC concentrations were peaked between 0800 and 1000 LST and again between 2100 and 2300 LST, corresponds to the morning and evening traffic combined with the ambient meteorological effect. The most commonly occurring BC concentrations were found to be < 5 μg m^{-3} during summer and monsoon. However, BC concentration occurred in highest concentrations (32%) segments from <5 to >10μg m^{-3} during the winter. BC concentration accounted for ~6% of the $PM_{2.5}$ mass, with a range of 1.0% and 14.3%, indicating the dominance of fine particles. A clear inverse relationship (r= -0.53) was observed between BC and wind speed over the station. A case study for source identification during winter indicated impact of burning during post monsoon and winter period. Mixed layer depths (MLDs) were shallower during post monsoon (379m) and winter (335m) as compared to summer (1023m) and monsoon (603m). Relation between visibility and BC were also studied and significant negative correlation (-0.81) was observed, having higher during post-monsoon (-0.85) and winter (-0.78) periods when the visibility was less than 3 km. However, relatively low correlation was during summer (-0.45) and monsoon (-0.54) periods when visibility was greater than 3mm. Results are well associated with the rapid growth of anthropogenic emissions and ambient meteorological conditions over the station.

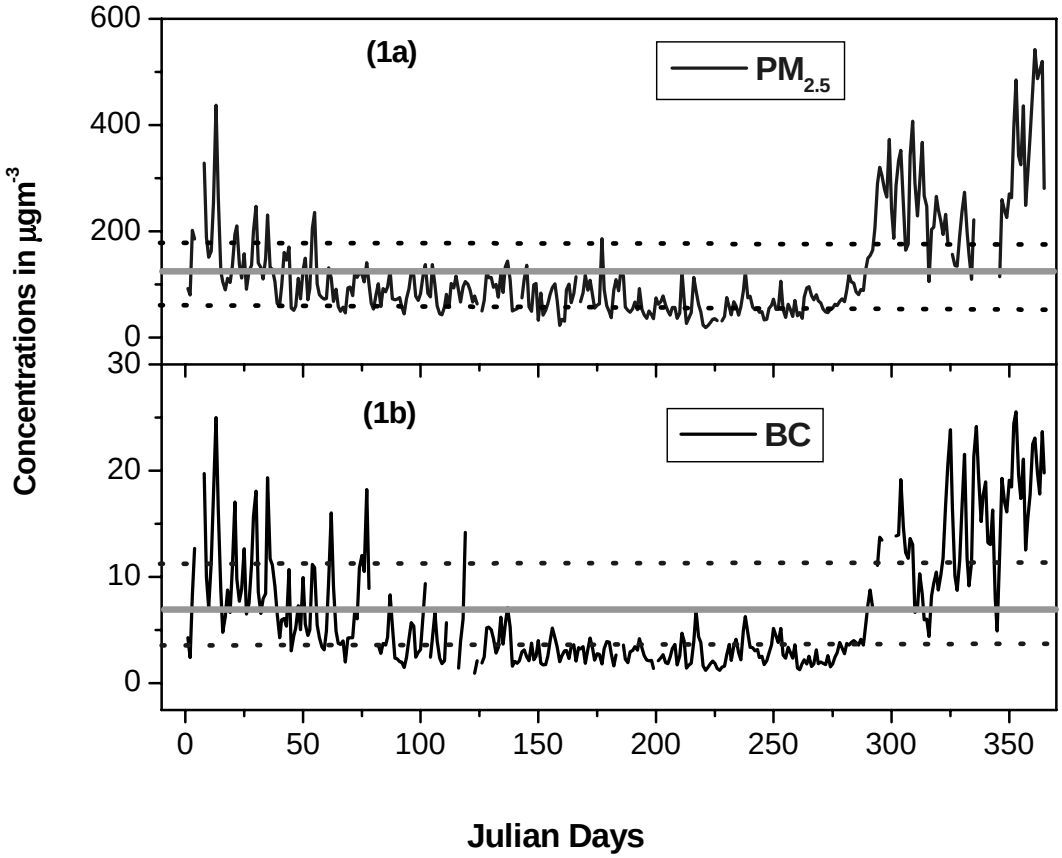

Figure 1. Daily (Julian days) mass concentrations of $PM_{2.5}$ (1a) and BC (2b) from 1st Jan. to 31st Dec.2011.

REFERENCES

Cooke,W.F., Liousse, C., Cachier, H., et al :, (1999). Construction of a 1°×1° fossil fuel data set for carbonaceous aerosol and implementation and radiative impact in the ECHAM4 model, *J. Geophys*. Res. **104 (D18**), pp 22137–22162.

Kenny, L.C., Gussman, R., Meyer, M. (2000). Development of a sharp-cut cyclone for ambient aerosol monitoring applications. *Aerosol Sci. Technol*.**32**, pp 338–358.

Koelmans, A.A., Jonker, Michiel T.O., Cornelissen, Gerard, Bucheli, Thomas D., Van Noort, Paul C.M., Gustafsson, Örjan (2006). Black carbon: the reverse of its dark side, *Chemosphere***63**, pp 365–377.

Penner, J.E., Eddleman, H., Novakov, T., (1993). Towards the development of a global inventory for black carbon emissions. *Atmos. Environ*. **27**, pp 1277–1295.

INFLUENCE OF AEROSOL ON THE CLOUD AND TROPOSPHERIC OZONE OVER THE INDO-GANGETIC PLAIN

S. D. PATIL, D. M. LAL, H. N. SINGH AND SACHIN D. GHUDE

Indian Institute of Tropical Meteorology, Pune
E-mail: patilsd@tropmet.res.in

Keywords: TROPOSPHERIC OZONE RESIDUAL, INDUSTRIAL ACTIVATES, LOW CLOUD COVER, HIGH CLOUD COVER

INTRODUCTION

The radioactively important properties of atmospheric aerosols (both direct and indirect) are determined at the most fundamental level by the chemical composition and size distribution of aerosol. The catalytic effect of aerosols on cloud microphysics is quite complex and their interaction may be influence or obscured by regional as well as local meteorological conditions and dynamics embedded thereon (Ten Hoeve et al. 2011; IPCC 1995). Large concentrations of human-made aerosols have been reported to both decrease and increase rainfall as a result of their radiative and CCN activities. With the advent of satellite measurements, it became possible to observe the larger picture of aerosol effects on clouds and precipitation. Urban and industrial air pollution plumes were observed to completely suppress the precipitation. Kaufman and Koren (2006) showed that an increase in cloud cover with an increase in the aerosol column concentration and vice-versa. Certain interactions between aerosols and clouds are also relatively well studied and understood (Spichtinger and Cziczo 2008). While depletion of stratospheric ozone is threatened, the enhancement in the level of tropospheric ozone has been reported by several researchers (Fishman et al., 2003; Ghude et al., 2009; Patil et al., 2009). Northern plain of India (Indo-Gangetic Plain (IGP)) is one of the most polluted regions in the world in terms of gasses and aerosol loading and shows distinct seasonal characteristics and mixing (Singh et al. 2004). The industrial growth, increasing usage of fossil fuel and other sources lead to massive load of aerosol and ozone precursors in the region (Ramanathan and Ramana, 2005; Tripathi et al., 2006; Ghude et al., 2011). In view of this, an attempt has been made in the present study to examine the influence of aerosol concentration on the cloud cover and tropospheric ozone over the IGP region during the period 1979-2010 for the pre-monsoon and summer monsoon seasons.

DATA AND ANALYSIS

Monthly mean Tropospheric Ozone Residual (TOR) data from the satellite measurements of Total Ozone Mapping Spectrometer/Solar Backscattered Ultraviolet (TOMS/SBUV, http://asd-www.larc.nasa.gov/TOR/TOR_Data_and_Images. html) provided by Fishman et al. (2003) and aerosol index (AI) data at 1.0°×1.25° latitude/longitude grid resolution from TOMS instrument aboard Earth Probe Satellite (EPS) are used in the present study for the period 1979–1992.The clouds (low cloud cover (LCC) and high cloud cover (HCC) in percentage) data at $2.5^{o}\times2.5^{o}$ latitude/longitude grid resolution from NCEP/NCAR reanalysis have also been used in the present study for the period 1979–1992. On account of unavailability of TOMS measurements between 1993 and 1996 and EP TOMS calibration problem from middle of the 2000s, we restrict our study to 1979–1992 period. We have also used recent data from 2005 to2010 for tropospheric ozone, AI and clouds over the IGP region.

RESULTS AND DISCUSSION

In order to see the correlation between TOR and AI (proxy for industrial activates), we have presented scatter plot of TOR and AI for pre-monsoon and monsoon seasons (Fig. 1a and b) respectively. In recent decades rapid growth of population and industries over the IGP region increases the aerosol loading. Significant positive correlation between TOR and AI has been observed during pre-monsoon (0.52, N=42) and monsoon (0.57, N=56) seasons respectively. Positive correlation between TOR and AI in this region imply that, because of increasing anthropogenic activities, significant increase in ozone precursor gasses occurred in this region. This eventually led to increasing ozone production during the study period. Thus, the quality of correlation between TOR and AI suggested that tropospheric ozone appeared to be influenced by the increased anthropogenic activities over the IGP region. During pre-monsoon (MAM) season, high cloud cover (R=0.25, P=0.387) shows increasing tendency with increasing trend of AI (R=0.63, P=0.0163) which is statistically significant whereas low cloud cover (R=-0.17, P=0.555) have negative trend. Increasing of AI over the region during this period may be due to transportation of dust by strong winds from northwestern deserts.

In summer monsoon season (JJAS), AI still showing the increasing trend (R=0.74, P=0.0026) during the study period, but high and low clouds have no trends (high cloud cover have slightly decreasing trend). During JJAS season, due to heavy precipitation though AI is significantly dropped, still residuals are remains, this might be due to manmade activities are continued and transported of dust particles is taken place over the region. Therefore, AI shows increasing tendency whereas low and high clouds have no trends. The cause for this, may be reduced the cloud drop size by enhancing the aerosol concentration (Fig. 2a, b and c) and increase the evaporation of the hydrometers. Thus, it can be concluded that the during pre-monsoon season, when aerosol loading is more, high cloud cover showincreasing trend and found to be positively correlated with the AI and low cloud cover show decreasing trend and found to be anti-correlated with the trend in AI.

The important role of humidity has also been explored in the present study. The IGP region is divided into six blocks to see their individual effect in greater depth. The effect of aerosol can be seen only at lower humidity area (Block No. 1) but as the humidity is increasing aerosol effect are decreasing (Fig. 3). This is the reason to increase the trend of HCC and decrease the trend of LCC with AI and these effects can be seen from Block No. 1-6.

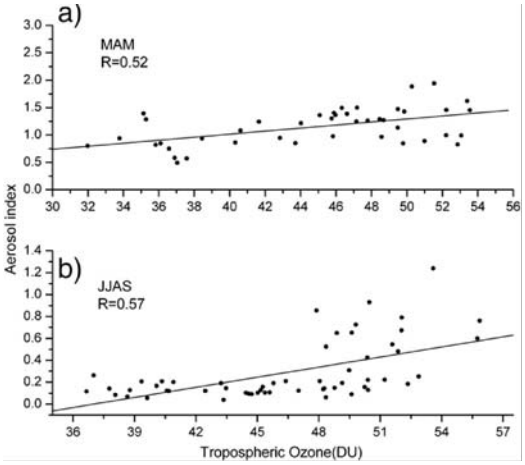

Figure 1. Scatter plot between monthly mean TOR and AI over the IGP region (a) pre-monsoon (MAM) and (b) monsoon (JJAS) seasons.

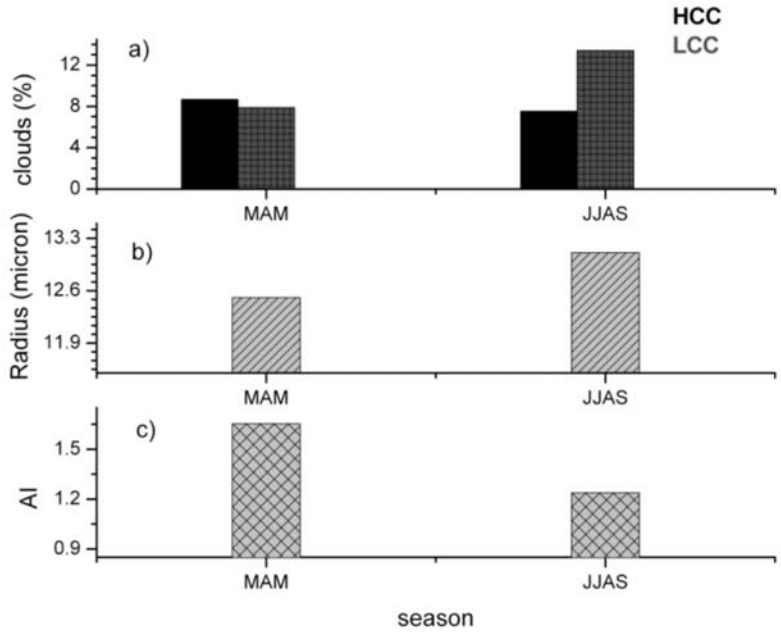

Figure 2. Variation in the (a) HCC (%) and LCC (%), (b) Cloud effective radius (micron) and (c) AI over the IGP region.

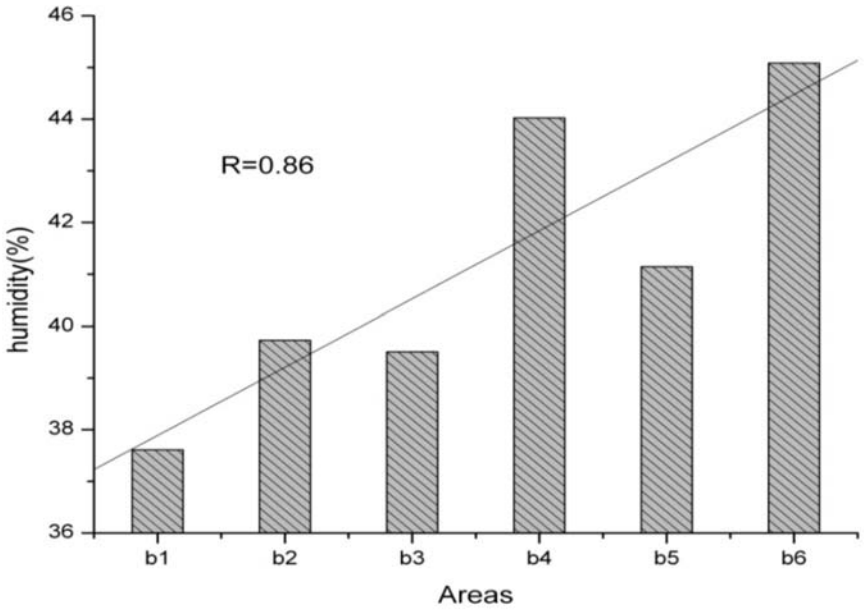

Figure 3. Average annual variation of humidity (%) over the six blocks of IGP region.

ACKNOWLEDGEMENTS

The authors are thankful to the Director, Indian Institute of Tropical Meteorology, Pune, for providing necessary facilities to carry out this research work and constant encouragement.

REFERENCES

Fishman et al. (2003). *Atmos. Chem. Phys*,.**3**, pp 893-907.

Ghude et al. (2009). *J. Atmos. Chem.*, **60**, pp 237-252.

Ghude et al. (2011). *Environ. Sci. Poll. Res.,***18**, pp 1442-1455.

IPCC (1995). Cambridge Uni. Press, New York, pp 339.

Kaufman and Koren (2006). *Science*,**313**, 655-658.

Patil et al. (2009). *Int. J. Rem. Sens.*, **30** (11), 2813-2826.

Ramanathan and Ramana (2005). *Pure App. Geophys.*, **162**, 1609-1626.

Spichtinger and Cziczo (2008). *Environ. Res. Lett.*, **3**, doi:10.1088/1748-9326/3/2/025002.

Singh et al. (2004). *J. Geophys. Res.*,**109**, D23206. doi:10.1029/2004JD004966.

Ten Hoeve et al. (2011). *Atmos. Chem. Phys.,***11**, 3021-3036.

Tripathi et al. (2006). *J. Geophys. Res.*,**111**, doi:10.1029/2006JD007278.

SEASONAL BEHAVIOUR OF ATMOSPHERIC AEROSOL OVER VARANASI LOCATED IN INDO-GANGETIC BASIN DURING 2011

S. TIWARI AND A. K. SINGH

Atmospheric Research Lab., Department of Physics, Banaras Hindu University, Varanasi-221005.
Email: pshanitiwari@gmail.com; abhay_s@rediffmail.com

Keywords: AEROSOL, AEROSOL OPTICAL DEPTH (AOD), INDO-GANGETIC BASIN (IGB)

INTRODUCTION

Atmospheric aerosol particles are tiny liquid or solid particles which are suspended into the atmosphere and injected into the atmosphere by natural as well as anthropogenic sources. Natural aerosols share 80% and play an important role in global scale climate through the modification of transmission of solar irradiance cloud nucleation and electrical properties of the atmosphere. Anthropogenic aerosols dominate on regional scale (Kaskaoutis et al., 2009). Aerosols play an important role in the Earth's atmospheric processes due to their direct and indirect effect (Dockery and Pope, 1994; Ranjan et al., 2007; Badrinath et al., 2008). The aerosols are not uniformly distributed over globe and its radiative forcing is strongly dependent on the geographical location on the Earth. The presence of aerosols particles control the cooling/heating effect on the Earth surface and in turn the warming and cooling of the atmosphere (Seinfeld, 2008).

Indian subcontinent and surrounding regions are rich sources of many kinds of aerosols of natural and anthropogenic origin such as mineral dust, soot, nitrates, sulphates and organic aerosols. This region has been the focus of investigations due to its potential impact on regional and global climate. Numerous measurements to investigate the optical properties and impact assessments have been reported from the Indian region in recent years (Satheesh et al., 2001; Ramachandran et al., 2008, Sharma et al., 2010). The Indo-Gangetic Basin (IGB) traversed by the Ganga river and its tributaries is one of the largest basins in the world, which is densely populated primarily due to the presence of numerous small and large rivers and fertile soil that make this region agriculturally highly productive. The topography of the IG basin from the west to east and variable meteorological conditions control the dynamic behaviour of atmospheric aerosols in both space and time and significant uncertainty in aerosol radiative forcing limits the performance of climate models.

EXPERIMENTAL OBSERVATION AND DATA ANALYSIS

In the present study, we analyzed aerosol data of complete one year during 2011 to study the seasonal behaviour of aerosol optical depth. For the study, we are using a MICROTOPS-II Sunphotometer (Solar Light Co, United States), with a Global Positioning System (GPS) receiver attached with the sunphotometer to provide information on the location, altitude and pressure. It provides us the Aerosol Optical Depth at 5 wavelengths about 380, 440, 500, 675 and 870 nm.

RESULTS AND DISCUSSIONS

Aerosol optical depth (AOD) is one of the most important optical properties of aerosols, which is directly related to the magnitude of attenuation of direct solar radiation by scattering and absorption processes (Ranjan et al., 2007) and calculated from the angstrom power law:

$$\tau = \beta\lambda^{-\alpha}$$

where λ is the wavelength in micrometer, is AOD, α is angstrom exponent and β is turbidity coefficient which is equal to columnar AOD at $\lambda = 1\mu m$. Apart from the aerosol optical depth there are two other parameters Angstrom exponent (α) and the turbidity coefficient (β) which are very important for the study of aerosol optical properties . Extensive analysis on the Angstrom exponent and its spectral variations have been made by Kaskaoutis et al. (2007) while Jacovides et al. (2005) have analyzed both α and β, even in different spectral bands.

The seasonal behaviour of atmospheric aerosol at different wavelength is shown in Figure 1. From this figure we observed that AOD value is higher in winter season than other seasons. This may be due to the biomass burning. From this figure we also conclude that higher wavelength have lower AOD and vice versa. The presence of high concentration of the fine-mode particles selectively enhances the irradiance scattering at lower wavelength and therefore, the AOD values are high at the shorter wavelengths. Likewise, the coarse-mode particles provide similar contributions to the AOD at relatively larger wavelengths.

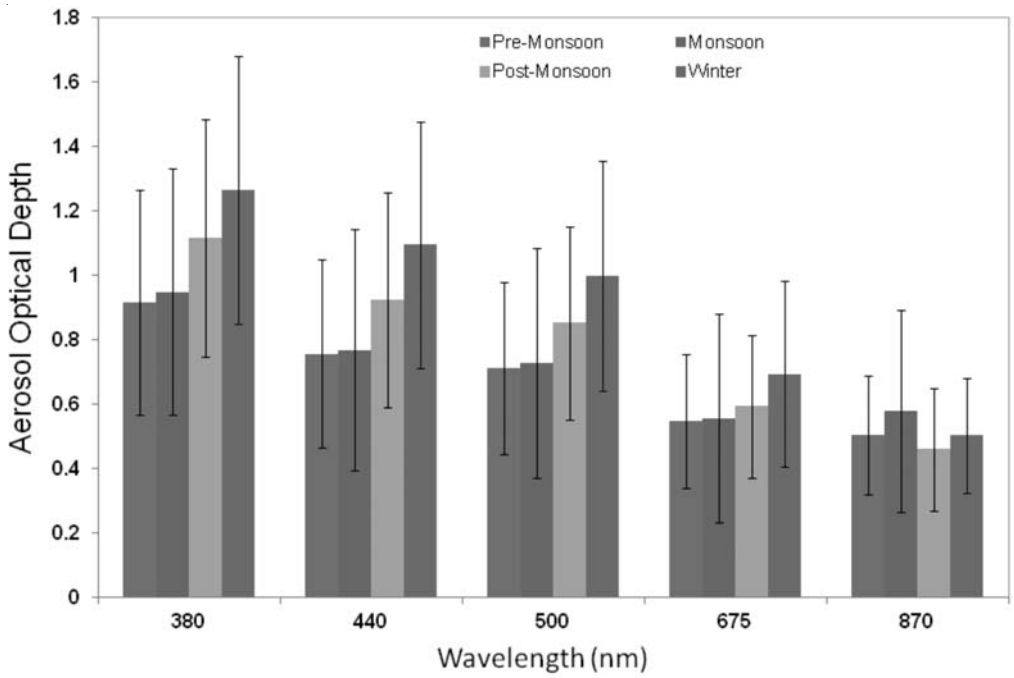

Figure 1. Seasonal behaviour of atmospheric aerosol at different wavelength observed at Varanasi during the year 2011.

The seasonal behaviour of angstrom exponent (α) and turbidity coefficient (β) is shown in Figure 2. From this figure we conclude that in winter season the value of α is higher than the other seasons which represents that in winter seasons the bigger size of aerosol particles that may be due to the burning of agricultural field products that generate plenty of biomass burning aerosol. In this figure we also see that in pre-monsoon season α value is relatively smaller with $\alpha < 1.0$ ($r \geq 0.5$ μm) which indicate the existence of bigger size of aerosol particles thatmay be due to the burning of agricultural field products that generate plenty of biomass burning aerosol and also due to dust aerosol coming from Thar desert and Sahara desert. On the other hand in winter season α value are higher $\alpha > 1.0$ ($r \leq 0.5$ μm) indicating that in winter small aerosols particle are dominant.

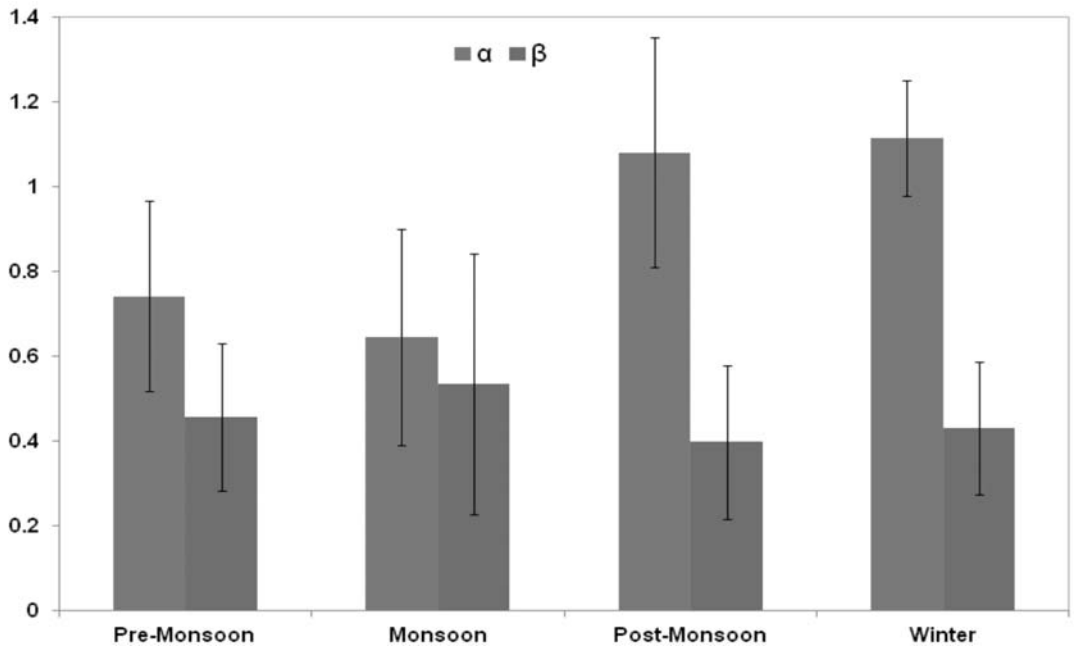

Figure 2. Seasonal behaviour of angstrom exponent (α) and turbidity coefficient (β) observed at Varanasi during the year 2011.

CONCLUSIONS

From the above study we observed the following conclusions:

1. IGB is the highest aerosol loaded region of India during 2011 due to its unique topography and different sources of anthropogenic aerosols.

2. The aerosol optical properties over Varanasi are found to show a large variation with a seasonal effect.

3. At shorter wavelengths AODs are higher while at longer wavelengths they are relatively lower attributing to the presence of fine to coarse particles.

4. The value of angstrom exponent varies from season to season which indicate that there are different type of aerosol particles are present. In pre-monsoon season coarse-mode aerosol particles are dominant while in winter fine-mode particles are dominant over Varanasi.

ACKNOWLEDGEMENT

The research work is financially supported by Indian Space Research Organization (ISRO), Bangalore under ISRO-SSPS Program to BHU.

REFERENCES

Badarinath, K.V.S., Kharol ,S.K., Prasad ,V.K., Sharma, A.R., Reddi, E.U.B., Kambezidis ,H.D., and Kaskaoutis ,D.G. (2008). Influence of natural and anthropogenic activities on UV Index variations—a study over tropical urban region using ground based observations and satellite data. *J Atmos. Chem*. **59,** pp 219–236.

Dockery, D.W. and Pope, C.A. (1994). Acute respiratory effects of particulate air pollution. *Annu Rev. Public Health***15,** pp 107-132.

Jacovides, C.P., Kaltsounides, N.A., Asimakopoulos, D.N. and Kaskaoutis, D.G. (2005). Spectral aerosol optical depth and angstrom parameters in the polluted Athens atmosphere. *Theor. Appl. Climatol.***81,** pp 161–167.

Kaskaoutis, D.G., Kambezidis, H.D., Hatzianastassiou, N., Kosmopoulos, P.G. and K.V.S. Badarinath, (2007). Aerosol climatology: On the discrimination of the aerosol types over four AERONET sites. *Atmos. Chem. Phys. Discuss.***7,** pp 6357– 6411.

Kaskaoutis, D.G., Badarinath,K.V.S., Kharol,S.K., Sharma,A.R. and Kambezidis, H.D. (2009). Variations in the aerosol optical properties and types over the tropical urban site of 468 Hyderabad, India. *J. Geophys. Res.* **114,** D22204. doi:10.1029/2009JD012423.

Ramachandran, Cherian, S. R. (2008). Regional and seasonal variations in aerosol optical characteristics and their frequency distributions over India during 2001-2005. *J. Geophys. Res.*,**113,** D08207, doi: 10.1029/2007JD008560.

Ranjan, R.R., Joshi, H.P., Iyer, K.N. (2007). Spectral variation of total column aerosol optical depth over Rajkot: a tropical semi-arid Indian station. *Aerosol Air Qual. Res***7(1),** pp 33–45.

Seinfeld, J. (2008). Black carbon and brown clouds, *Nature Geosciences*. **1,** pp 15 -16.

Sharma, A. R., Shailesh, K. K. , Badarinath, K. V. S. and Darshan, S. (2010). Impact of agriculture crop residue burning on atmospheric aerosol loading – a study over Punjab State, India, *Ann. Geophys.*,**28,** pp 367–379.

LONG TERM TRENDS IN THE PARTICULATE MATTER CONCENTRATIONS (PM_{10} AND $PM_{2.5}$) AT DIFFERENT LOCATIONS IN INDIA

ONKAR NATH VERMA[1], S NASEEMA BEEGUM[1], SANJEEV AGRAWAL[2], SACHCHIDANAND SINGH[1]

[1] Radio & Atmospheric Sciences Division, National Physical Laboratory, CSIR, New Delhi-110012
[2]Central Pollution Control Board, Parivesh Bhavan, East Arjun Nagar, New Delhi - 110 032
E mail: ssingh@nplindia.org

Keywords: AIR QUALITY, PM_{10} AND $PM_{2.5,}$ REPIRABLE, RESUSPENSIONS

INTRODUCTION

Air quality, the measure of the concentrations of gaseous pollutants and particulate matter, is one of the most important problems all over the world and has strong implications to human health, ecosystems as well as regional and global climate. The Particulate Matter (PM) is a complex mixture of extremely small particles and liquid droplets. One of the particulates, ~ 2.5 micrometers in diameter or even smaller that, generally pass through the throat and nose and enter the lungs is known as Respirable suspended particulate matter (RSPM or $PM_{2.5}$) and can affect the heart and lungs and cause serious health effects. The particle with diameter ~ 10 μm is called the suspended particulate matter (SPM or PM_{10}). The levels of these air pollutant concentrations are increasing rapidly in developing countries, leading to degradation of air quality and harmful effect on human health. The major anthropogenic sources of air pollutants are industrial emissions, domestic fuel burning, emission from the power plants and transportation activities.

In the present paper, we present the long-term trends and variations of pollutant concentrations of MP_{10} and RSPM, from distinct geographical locations in India, viz., the comparatively pristine western coastal station Goa, in the peninsular India, the urban location, Guwahati, in the north western India and four distinct sites in the megacity of Delhi (three residential (Janakpuri, Nizamuddin, Sirifort) and one industrial (Shahazada bagh)) in the Indo Gangetic Plain, based on continuous measurements for a period of ~22 years from 1987-2008. These are the stations under the National Ambient Air Quality Monitoring (NAAQM) network, established by the Central Pollution Control Board (CPCB) in collaboration with the State Pollution Control Board. So far no studies have been reported on such type on long term variations of air pollutants from geographically distinct environments.

RESULTS AND DISCUSSION

Monthly mean mass concentrations for a period of 22 years (1987-2008) have been used to examine the inter-annual variations and trends of each of the pollutant species. Fig.1(a) represents the pattern of long-term trends of SPM at the four sites in Delhi. Even though the concentration at the residential areas (>350 $\mu g/m^3$) are slightly lower than at the industrial area Shahzada Bagh (398 $\mu g/m^3$), these remains much higher than the prescribed NAAQS values, which is ~140 $\mu g/m^3$ in residential areas. Where as for the industrial areas, the values are within the permissible levels (NAAQS of 360$\mu g/m^3$). The figure shows large scatter of points with no significant trends in the pattern of SPM; whereas RSPM shows significant increasing trend for all the stations except Nizamuddin, where a decreasing trend is observed (Fig.1b). The estimated values of trends are found to be statistically

significant at 95% confidence levels. The climatological average values of RSPM at all the stations in Delhi are higher than that of the NAAQS values. The sources of the RSPM include, vehicles, natural dust, industries such as thermal power plants, sugar, cement, resuspension of dust, biomass burning etc. As coarser particles contribute more to the SPM concentrations, dust (either produced locally by the dust storms or construction activities related to urbanization) might be the main contributor. These results have been compared with that of other stations such as Guwahati and Vasco in Goa and the pattern is shown in Figure 2a and 2b. At both the stations of Goa and Guwahati, the concentrations of the pollutants were within the permissible levels. Unlike the pattern of trends obtained at the stations in Delhi, the SPM concentrations show an increasing trend at both the stations, where as for RSPM, Goa registered significant decreasing trend.

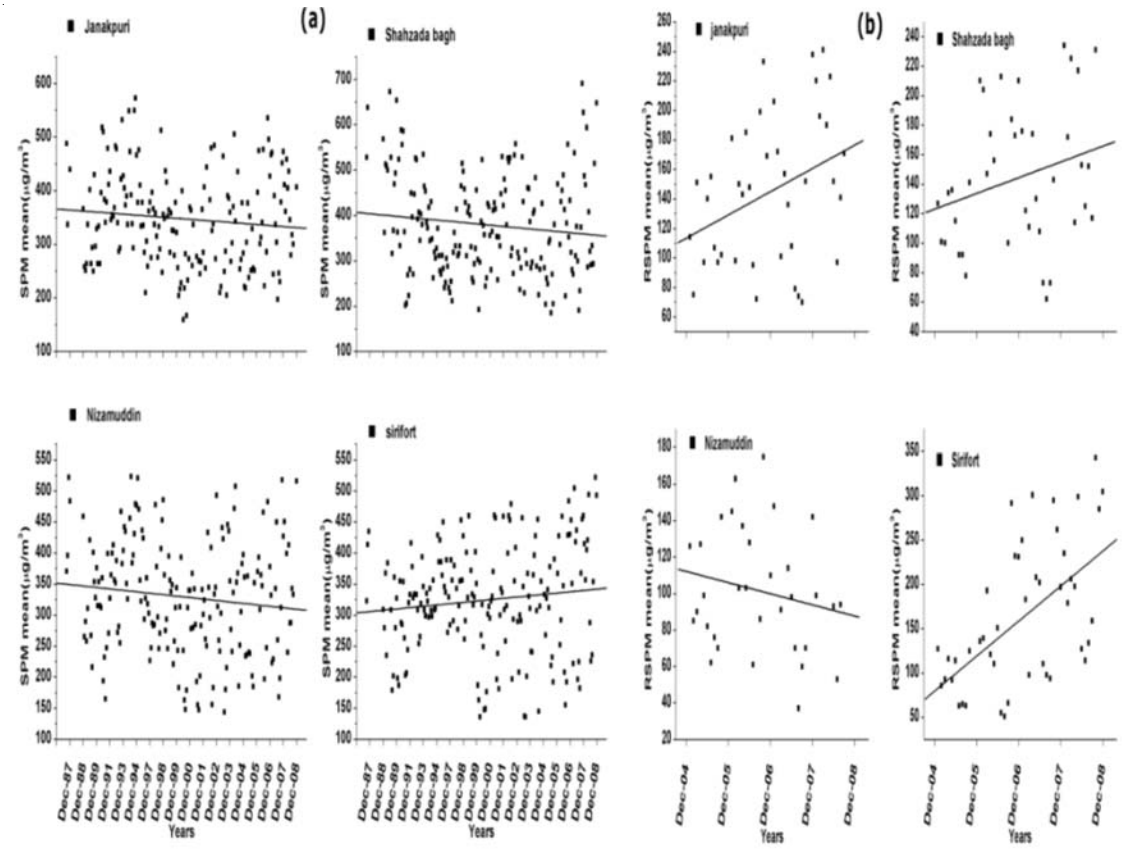

Figure1. Monthly mean mass concentrations of (a) SPM and (b) RSPM at four sites in Delhi. The black lines represent the trend.

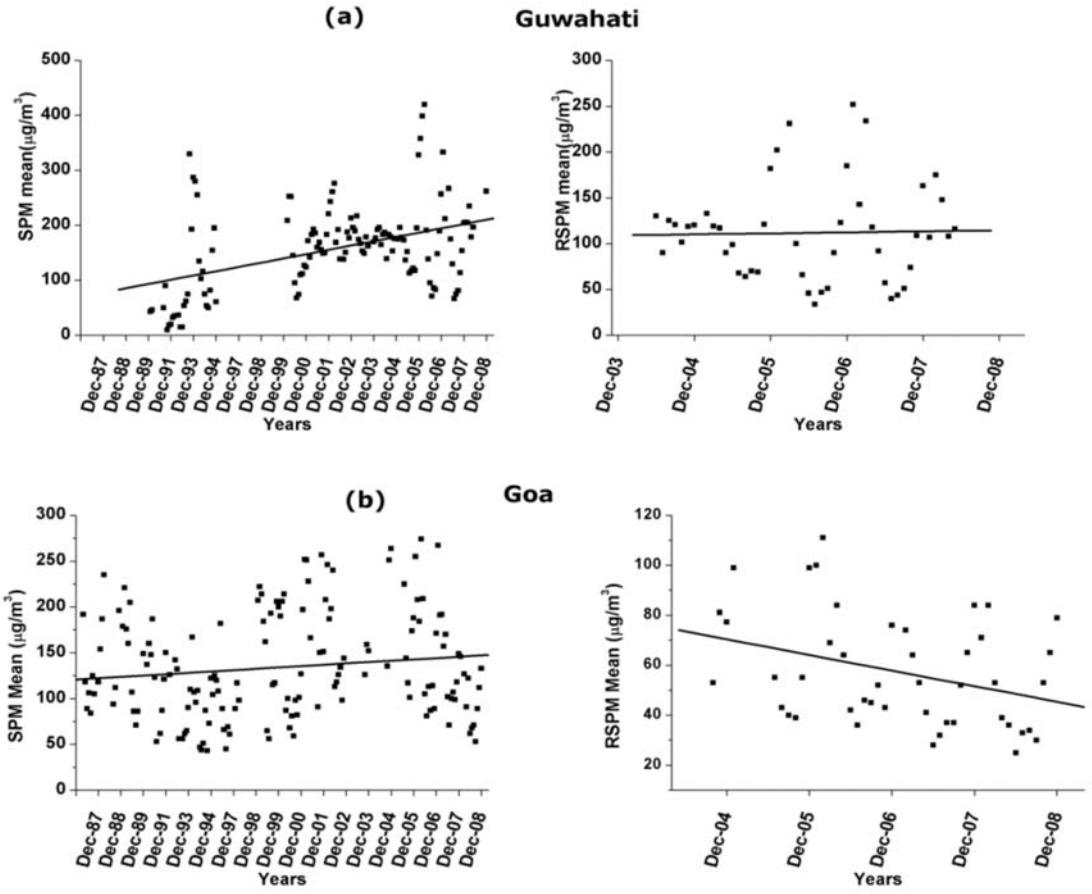

Figure2. Monthly mean mass concentrations of SPM and RSPM at (a) Guwahati and (b) Goa. The black lines represent the trend.

The data base is robust to generate the climatological variations. As such, the climatological mean seasonal variations of these species have been estimated for all the stations. For Delhi, the average concentrations were estimated by averaging the corresponding measurements at the four locations. The resulting bar-chart showing spatial pattern of the seasonal variations of SPM and RSPM are shown in Figure 3. Irrespective of the seasons, the highest values of the concentrations are observed at the urban centre Delhi for both SPM and RSPM. Seasonally, highest values of the pollutant concentrations are observed during winter (December to February) for Goa and Guwahati, where as for Delhi, post monsoon (October-November) season registered the highest values. The lowest concentrations are observed during monsoon (June to September) season for all the stations. The confinement of particles by the shallow boundary Layer added with reduced convections is responsible for the higher concentrations in winter. Towards pre-monsoon (March to May), the observed weak decrease in the concentrations was due to the efficient dispersal of the pollutants due to the well evolved boundary layer during the season. The sudden decrease in concentrations towards the monsoon season is due to the efficient removal of the pollutants due to enhanced rainfall. The concentrations again increase towards post monsoon seasons and the increase being higher at Delhi due to the high anthropogenic activities, such as burning of crackers associated with the festivals of Dushara and Diwali.

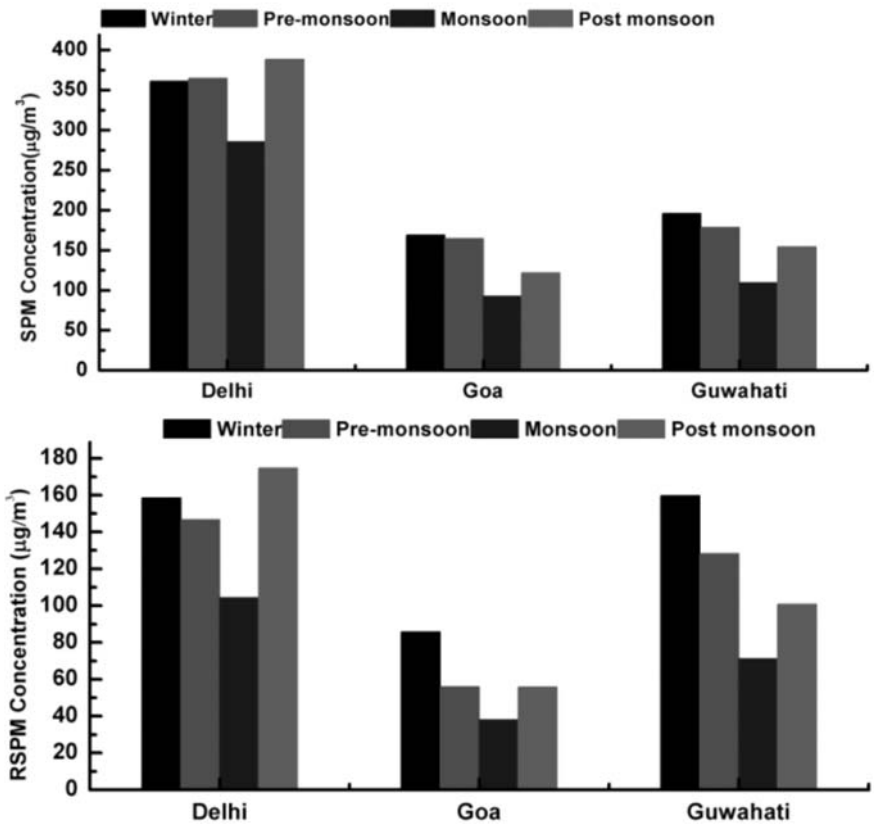

Figure.3: Climatogical mean seasonal variations of SPM and RSPM

CONCLUSIONS

Analysis of the long term measurements of particulate matter mass concentrations at four stations in Delhi, Goa and Guwahati for a period of 22 years (1987-2008) brought out certain interesting results. The analysis revealed that concentrations of the pollutants are significantly higher than that of the NAAQS prescribed values at all the sites in Delhi, whereas for Goa and Guwahati, these are within the permissible limits. Eventhough the concentrations of SPM remained more or less constant over the long-term, the RSPM concentrations were found to be increasing at Delhi, whereas at Goa and Guwahati, the pattern is quite different with an increasing trend for SPM.

THE SOUTH ASIAN WINTER HAZE AT A TROPICAL COASTAL STATION – VISAKHAPATNAM

MALLESWARA RAO BALLA[1,] & NIRANJAN KANDULA[2]

[1]Department of Engineering Physics, School of Technology, GITAM University (Hyderabad campus), Rudraram, Medak Dist., A.P. 502329, India
[2]Department of Physics, Andhra University, Visakhapatnam 530003, India
Email: mallesh@gitam.edu

Keywords: SOUTH ASIAN WINTER HAZE, SYNOPTIC METEOROLOGY, ATMOSPHERIC AEROSOL EFFECTS

INTRODUCTION

Visakhapatnam (17.7°N, 83.3°E) is a tropical coastal site on the east coast of India, with a moderate industrial/urban activity. It is an important network station of the Indian Space Research Organisation's Geosphere-Biosphere Program (ISRO-BGP). The station is identified as a key aerosol measurements site to study the characteristic features of urban aerosol superposed over the background maritime airmasses. In spite of the clean maritime airmass and awesome clear blue skies, the wintertime aerosol spectral optical depths obtained with ground-based multi-wavelength solar radiometers and size-segregated near surface aerosol mass concentrations obtained with in-situ samplers show unexpectedly higher values (Rao, 2009). The so called "city of destiny" has now appears to become a hotspot of public ill-health during wintertime. The culprit behind this environmental calamity has been recently explored to be the lower atmospheric polluted aerosol (haze) transported by the synoptic wind field from the regions of high population density in the northern hemisphere towards up to Visakhapatnam and its environs. Atmospheric remote sensing imageries obtained with Moderate Imaging Spectroradiometers (MODIS) onboard the satellites Terra and Aqua have revealed that the spread of this polluted aerosol is not only limited to this location and its surroundings, but to many parts of South Asia, Bay of Bengal and the adjoining tropical Indian Ocean. This regional level polluted haze plume is now known as the South Asian Winter Haze (SAWH), or the Asian Brown Cloud (ABC), the implications of which are not only limited to public health and environmental pollution on a local scale but have important consequences on climate, earth's radiation budget, and hydrological cycle on a regional and global scales. The purpose of this paper is to demonstrate the evolution and spread of this lower atmospheric regional haze, and to discuss some of its effects at Visakhapatnam.

CLIMATIC FEATURES OF VISAKHAPATNAM

Fig.1(a) shows the geographic location of Visakhapatnam, on the east coast of India, along with other useful information. This site is often called "the city of destiny". It is no exaggeration to say that no other place in the state of Andhra Pradesh (India) is as blessed with such scenic surroundings as Visakhapatnam. It is the only place on the east coast of India where the hill ranges (the Eastern Ghats) and the sea meet. Visakhapatnam and its environs present a soul-stirring panorama of golden beaches, lush green vegetation, and splendid monuments form a rich historical heritage. Its natural local climate owes its origin to the peculiar topography on the north and the south (hills), and the vast water body on the east (the Bay of Bengal) contributing to the interesting land and sea breeze circulations. The following is a brief description of the general climatic features of Visakhapatnam

based on climatic data obtained from the local meteorological observatories as well as from publications of the Indian Meteorological Department (IMD, Pune, India).

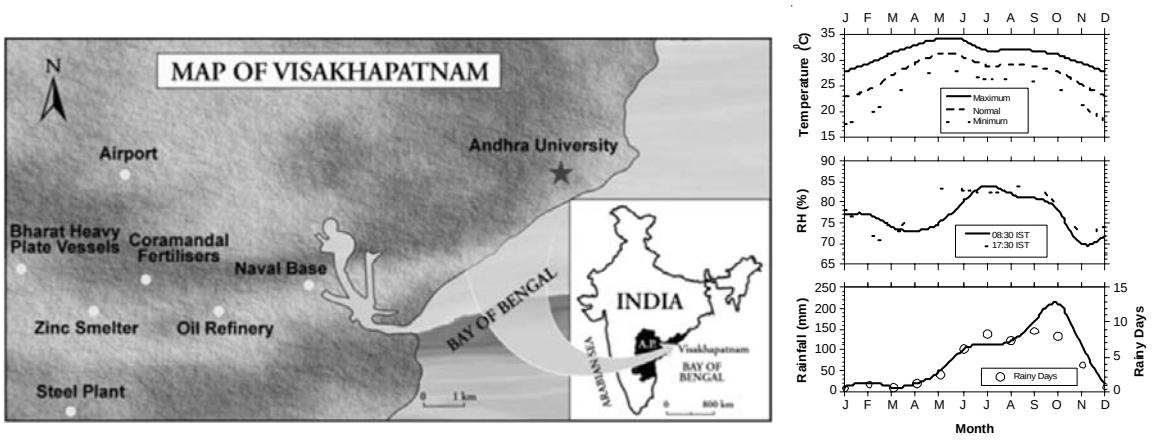

(a) (b)

Figure 1(a). Map showing the geographic location of Visakhapatnam. Star symbol locates the measurements station (Andhra University) (b) Climatic features of Temperature (top panel), RH (middle panel) and Rainfall (bottom panel) at Visakhapatnam.

Fig. 1(b) shows the climatic features of Temperature (top panel), Relative Humidity (RH, middle panel), and Rainfall (lower panel) at Visakhapatnam. The top panel shows the climatic monthly means of maximum, minimum and normal temperatures. The annual mean temperature varies from a minimum of 23.5°C to a maximum of 30.9°C. The mean maximum temperature is the highest (34°C) in the month of May and the mean minimum temperature is the lowest (17.3°C) in January. The minimum RH (~70%) is observed in the month of November and the maximum (~84%) is in the month of July. The annual rainfall is about 954 mm. 35% of the annual number of rainy days occurs during the southwest monsoon period. The maximum amount of rainfall (212.1 mm) in the month of October is an account of the cyclonic activity in the Bay of Bengal during the transition period.

The prevailed wind directions are easterly to northeasterly during post monsoon and the winter season while they are southwesterly during summer monsoon period. The monthly mean wind speeds remain below 4.4 ms^{-1} during winter monsoon, i.e., from November to February, but from March onwards a gradual increase is noticed till the maximum of 7.5 ms^{-1} during summer monsoon. Occasions with wind speeds exceeding 5.5 to 16.6 ms^{-1} are rare and may occur as gales during cyclonic period. The measurements site (Andhra University) is generally expected to have a clean maritime atmosphere during the winter and pre-monsoon periods due to the prevailed meteorological conditions (since positioned along upwind direction to the industrial belt and urban activity). However, the situation has drastically changed in recent times and the misfortune of health and environmental effects arrives on its way by what is known as the South Asian Winter Haze (SAWH).

THE SOUTH ASIAN WINTER HAZE AT VISAKHAPATNAM

The South Asia (which includes the Indian subcontinent as well as Sri Lanka and Maldives) is one of the most densely populated regions in the world, with present population densities of 100–500 persons/km^2. Several of the world's megacities that produce unacceptably high emissions of health

endangering gaseous and particulate matter are found in this region. The most visible impact of this air pollution is the haze (or aerosol), a brownish atmospheric layer that pervades many regions in South Asia. A satellite image of this regional haze plume spreading over the Indo-Gangetic Plains (IGP), which encompasses most populous northern and eastern parts of India, Pakistan, Southern Nepal and Bangladesh, is shown in Figure 2(a).

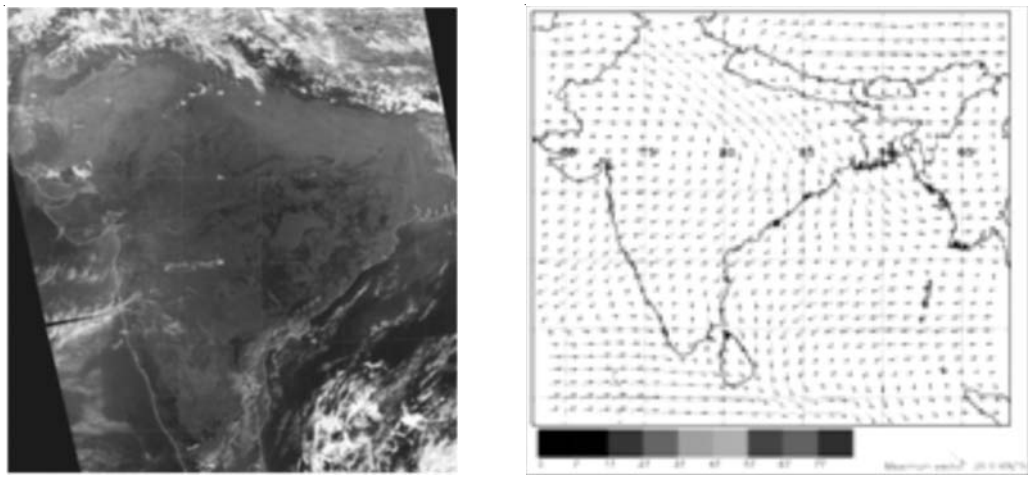

(a) (b)

Figure 2. (a) True Colorscene captured on 3rd December 2003 by MODIS onboard the satellite Aqua showing the haze plume (grayish tint near top-right corner) spreading over the Indo-Gangetic Plains (b) Map of 850-hPa wind field typically representing the Asian winter monsoon. Star symbol at the centre of the map locates Visakhapatnam on the east coast of India [Source: READY Web Server of NOAA Air Resource Laboratory].

The region is characterized by a tropical monsoon climate, an important feature of which is the seasonal alteration of atmospheric flow patterns associated with the monsoon. The dry northeast monsoon winds carry this anthropogenic haze thousands of kilometers south and southeastwards, and spread it over most of the continent, Bay of Bengal and the tropical Indian Ocean between 25 °N to about 5 °S (UNEP and C^4, 2002).

Visakhapatnam is also affected by this anthropogenic haze transported from IGP. The low-altitude synoptic wind field (please see Figure 2(b)) sets up in winter and pre-monsoon periods over this region is particularly favourable for the advection of this anthropogenic haze towards south up to Visakhapatnam and its environs. Accordingly, this polluted haze plume characterizes the airmass over Visakhapatnam and its environs during the dry winter monsoon period. The expected implications of this haze layer spreading over prevailed monsoon climate are not only limited to public health and environmental effects on a local scale but also have important consequences on climate, earth's radiation budget, agricultural productivity and the hydrological cycle on a regional scale (UNEP and C^4, 2002).

SOME EFFECTS OF THE SAWH AT VISAKHAPATNAM

1.Optical and environmental effects

- Atmospheric spectral optical depth data show unusually large spread in magnitude (~0.4 to 1.2 at 400 nm), which is very prominent at the shorter wavelengths side of the spectrum than the longer wavelengths side (Rao, 2009; Rao & Niranjan, 2012).

- The study of inter-channel multi-wavelength optical depth slope and the ratio of extinction efficiency factors revealed that the SAWH at Visakhapatnam is best represented by soot as the chief component with an effective radius of 0.169 μm (Rao, 2009). This result has significance regarding aerosol radiative forcing and radiative balance of the earth-atmosphere system.
- Near surface aerosol mass concentrations during the wintertime show higher values than the standard set by environmental agencies. Relative predominance of submicron-sized aerosol particles over the supermicron-sized particles, with a percentage share of 71.5% versus 28.5% to the total mass concentration has been observed during the wintertime at Visakhapatnam (Rao, 2009).
- Most of the aerosol loading during wintertime is due to PM10 and PM2.5 with percentage shares of 97% and 87.5%, respectively. Levels of PM10 as well as PM2.5 are above the standards set by Environmental Pollution Agency (EPA, USA) and National Ambient Air Quality Standards (NAAQS, India) (Rao, 2009).

2.Health effects

- The wintertime atmosphere at Visakhapatnam is becoming highly polluted and causes discomfort and ill health to its residents (Suneetha, 1999). The discomfort due to the haze ranges from coughing, burning of eyes, throat irritation, etc.; while the ill health is due to bronchitis, asthma, rheumatism, etc.
- The diseases identified to be more prevalent are malaria, viral and typhoid fevers, diarrhea, tuberculosis, pneumonia and other respiratory tract infections, viral hepatitis, skin diseases and allergies. Of these, malaria and viral fevers showed higher prevalence followed by respiratory tract infections (Suneetha, 1999).

DISCUSSION & CONCLUSIONS

It is quite unusual to expect such large spread in optical depths and higher mass concentrations, as mentioned in optical and environmental effects section above, during the winter season at Visakhapatnam due to the prevailing northeasterly wind and since the measurements location is in the upwind direction of the city's industrial activity (see Fig.1(a)). However, the observed variations can be consistently explained on the basis of prevailing synoptic airmass conditions at the measurements location once the low altitude synoptic wind field (Fig. 2(b)) and the wet removal activity during the season are considered. It is very clear that the wintertime airmasses over Visakhapatnam are largely influenced by the synoptic transport of polluted anthropogenic/urban aerosol from the continental areas of high population density in the northern hemisphere such as the IGP. It is also reported in several other studies that during the period of Asian winter monsoon the prevailing atmospheric circulation in the lower troposphere is primarily from the Northern Hemispheric continents to the Oceanic regions towards the south that is primarily driven by the different heating between land areas in the Indian subcontinent and the adjacent Ocean regions (S. K. Nair et al., 2003). These northeasterly winds from the Asian continent transport large amount of polluted airmass deep into the otherwise pristine locations (Rajeev et al., 2000, Nair, S. K., et al., 2003). Mean wind field at the 850 hPa (Fig. 2(b)) indicate that the winds carry the highly polluted airmass from the northern India into the Bay of Bengal and streamlines re-enter the peninsular India around 17-18^{o} N latitude responsible for the high aerosol optical depths in this region (Niranjan et al., 2005).

ACKNOWLEDGEMENTS

Acknowledgements are due to Indian Meteorology Department (Pune) for the provision of necessary meteorological data, National Aeronautics and Space Administration for the provision of MODIS Atmosphere Images (http://modis-atmos.gsfc.nasa.gov) and NOAA Air Resource Laboratory for the provision of READY web server (http://arl.noaa.gov/ready.html).

REFERENCES

Nair, S.K., Rajeev, K., and Parameswaran, K. (2003). Wintertime regional aerosol distribution and the influence of continental transport over the Indian Ocean, *J. Atmos. Solar Terr. Phys.***656**, pp 149–165.

Niranjan, K., Malleswara Rao ,B., Brahmanandam, P.S., Madhavan, B.L., Sreekanth, V. and Moorthy, K.K. (2005). Spatial characteristics of aerosol physical properties over the northeastern parts of peninsular India. *Annales Geophysicae***23**, pp 3219-3227.

Rajeev, K., Ramanathan ,V. and Meywerk M. (2000). Regional aerosol distribution and its long range transport over the Indian Ocean. *J. Geophys. Res.***105**, pp 2029– 2043.

Rao, B.M. (2009). *Remote Sensing the South Asian Winter Haze at Visakhapatnam using a ground-based Multi-wavelength Solar Radiometer.* Ph. D. thesis, Andhra University, Visakhapatnam, India.

Rao, B.M. and Niranjan K. (2012). Optical properties of the South Asian winter haze at a tropical coastal site in India. *Atmos. Environ.***54**, pp 449–455.

Suneetha, P. (1999). *Urban microclimatic study of Visakhapatnam, Andhra Pradesh, India.* Ph. D. Thesis (Geography), Andhra University, Visakhapatnam, India.

UNEP and C^4 (2002). *The Asian Brown Cloud: Climate and other Environmental Impacts,* (United Nations Environmental Programme, Nairobi, Kenya)

INFLUENCE OF METEOROLOGICAL CONDITIONS ON BULK AIRBORNE PARTICLES AND THEIR COMPOSITION OVER A COASTAL STATION IN GOA (INDIA)

KAMANA YADAV[1], RAJESH AGNIHOTRI[2], PRAKASH MEHRA[1], V.V.S.S. SARMA[3], S.G. KARAPURKAR[1], P. PRAVEEN[3] AND M. DILEEP KUMAR[1]

[1]National Institute of Oceanography, Dona Paula, Goa
[2]National Physical Laboratory, New Delhi 110012
[3]National Institute of Oceanography, Regional Center Vishakhapatnam

Keywords: TOTAL SUSPENDED PARTICULATE MATTER (TSPM), AIR TEMPERATURE, TOTAL NITROGEN, $\delta^{15}N$.

INTRODUCTION

Bulk aerosols particles (Total Suspended particulate matter; TSPM) in ambient air are multi-phase complex mixture of all airborne solids and low vapor pressure liquid particles having aerodynamic particle sizes 0.01-100 ìm or larger. These particles have relatively shorter life time in the troposphere (of the order of a few days) and are removed by dry/wet deposition. Despite their rapid removal these are considered important as these can potentially influence cloud properties, radiation budgets, regional air quality and precipitation patterns and also human health. In coastal environments aerosol particles are also important as their deposition supplies biologically important nutrients to coastal surface waters that promote surface biological productivity during lean periods. Carbonaceous fraction of aerosols may originate both from natural (mineral dust, eroded soil, biogenic components of plants such as pollens) as well as anthropogenic sources (burning of biomass-biofuel, industrial emissions, vehicular traffic, mining etc.). As Carbon (C) and Nitrogen (N) constitute bulk of carbonaceous fraction of aerosol mass detailed chemical and isotopic characterization of these two elements can greatly help in identifying dominant sources as well as secondary processes in aerosols during their long range transport (Agnihotri et al., 2011; Pavuluri et al., 2010). In view of multiple sources and continuous secondary processes aerosol chemical composition varies greatly both spatially and temporally, especially in relation to changing meteorological conditions.

Here we report our results on the observed temporal variability of physical (TSPM), chemical (TC and TN mass concentrations) and stable isotopic characteristics ($\delta^{13}C$ and $\delta^{15}N$) of bulk aerosol particles over a costal environment in Goa in tandem with contemporaneous meteorological parameters (e.g. air temperature, relative humidity, wind speed and wind direction) measured at the same site. Bulk aerosols over Goa show appreciable seasonal changes in their chemical and isotopic characteristics and conspicuous influence of carbonaceous material that mainly originated from biomass-biofuel burning occurring in northern parts of India during winter.

METHODOLOGY

Using high volume air sampler (APM 430; *Envirotech*) bulk aerosols were collected on pre-combusted and pre-desiccated tissue quartz filters from the roof (at 55.8 MASL) of National Institute of Oceanography Goa (15.46°N, 73.8°E). Samples were collected during monsoon (June to August), post- monsoon (October-November), and full winter (December to February) periods of 2011-12. A total of 43 TSP samples were analyzed for their chemical and isotopic characterization i.e. carbon and nitrogen mass concentrations (TC, TN) and their isotopic values ($\delta^{13}C$, $\delta^{15}N$) using an Elemental

Analyzer coupled to Isotope ratio mass-spectrometer (CF-IRMS), and following a modified methodology described in Agnihotri et al. (2011). Contemporaneous meteorological data were obtained using automated weather station installed at NIO (at 33.8 m MASL height), details of which are given in (Mehra et al., 2005).

RESULTS

Chemical and isotopic signatures of ambient aerosols over NIO, Goa were investigated. The average mass concentrations of TC, TN and TSPM (Figure 1) during monsoon were found to be 8.15±5, 1.34±0.8, 67.5±31 μg.m^{3}, respectively (n=7). In post monsoon period TC and TN mass concentrations show a substantial increase with 18.4±7.2, 3.16±2.3 μg.m^{3}, respectively (n=6), but TSP concentrations showed a marginal decrease with an average value of 57.7±35 μg.m^{3}. Aerosol samples collected at high temporal resolution (nearly weekly) during the winter of 2011-12 (a total of 30) show highest mass concentrations of TC, TN and TSPM with average values 29.1±9.5, 6.14±2.3, and 109.6±30 μg.m^{3}, respectively. As far as stable isotopes of C and N are concerned, overall, a narrow range (average: −22.8±2.7‰) of δ^{13}C of TC was observed compared to a wider range of δ^{15}N (average: 12.7±5.1‰) during entire sampling campaign. Significantly lower δ^{15}N of TN values were found (average: 3.0±0.5‰) during monsoon period as compared to those for post monsoon (average: 12.3±3.8‰) and winter periods (average: 14.2±3.8‰). Similarly coarse size (PM_{10}) aerosols over Mumbai (a nearby costal location of western India) were found to be significantly enriched in δ^{15}N of TN in winter compared to those in summer (averages: 22.8±1.4‰ and20.2±1.2‰ respectively) (Aggrawal et al., 2012).

In contrast, δ^{13}C of TC showed overlapping values during monsoon and post-monsoon periods (average: −23.1±2.8‰ and −23.6±1.9‰, respectively), compared to those during winter slightly enriched values (average: −22.6±2.9‰). This trend is in excellent agreement with winter and summer time aerosol signatures over Mumbai i.e. slight enrichment in δ^{13}C of TC during winter (average: "25.9±0.3 ‰) compare to summer ("26.5±0.3 ‰) (Aggrawal et al., 2012).

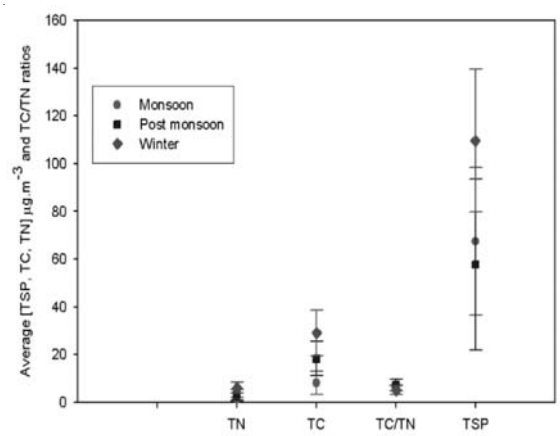

Figure 1.Average mass cocentrations of TC, TN and TSP (as shown by circular, square and diamond symbols) along with associated ranges observed (as shown vertical uncertainty bars) in ambient aerosols over Goa during monsoon, post monsoon and winter period of 2011-2012.

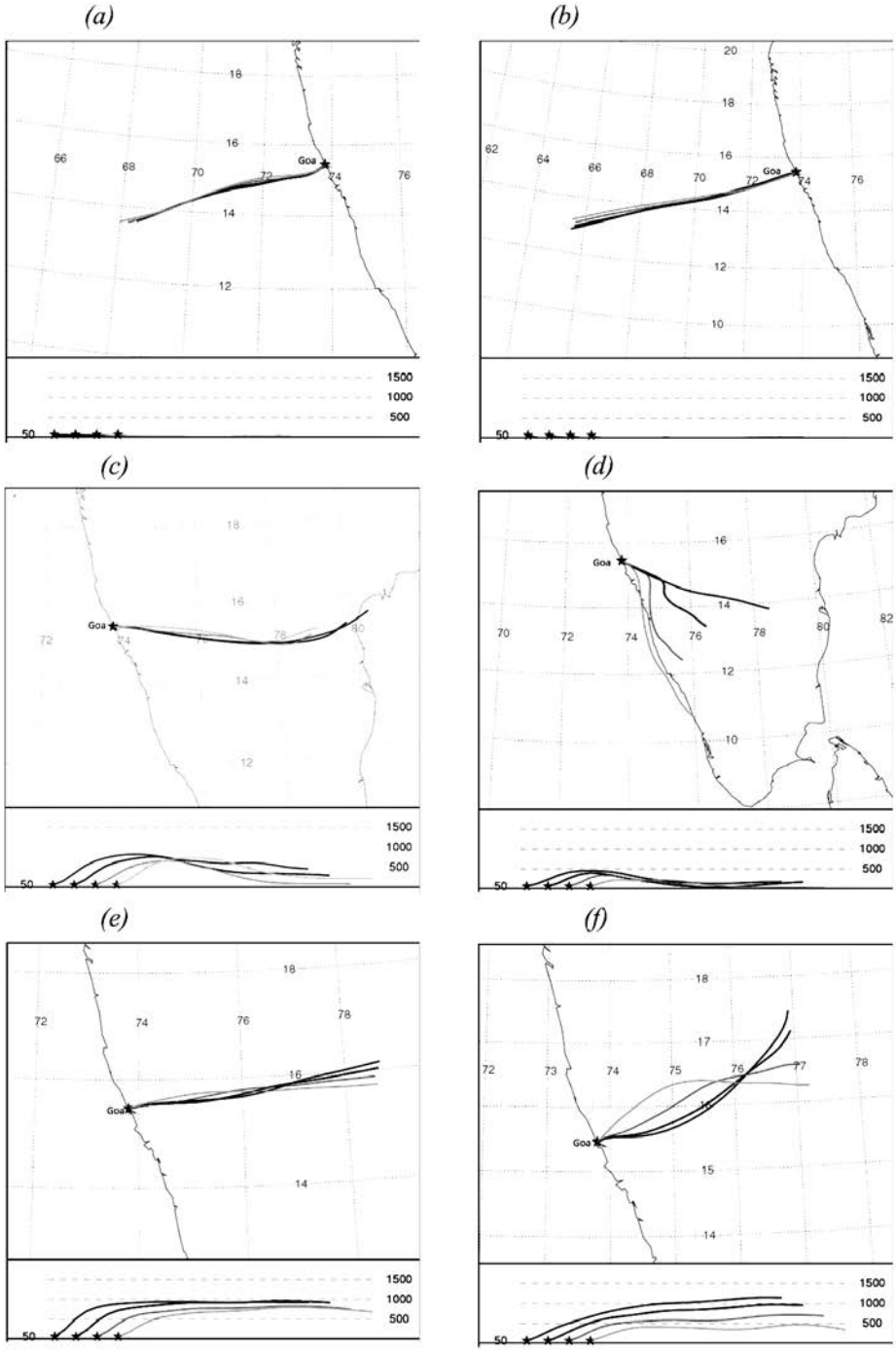

Figure 2. 7 day backward trajectories obtained using NOAA Hysplit Model at sampling location (15.46°N, 73.8°E) in Goa. (a) & (b) present air flow during monsoon (1 July & 9 August 2011, respectively), (c) & (d) for post monsoon 27 (October & 29 November 2011, respectively) and (e) & (f) for winter (15 December 2011& 16 January 2012 respectively).

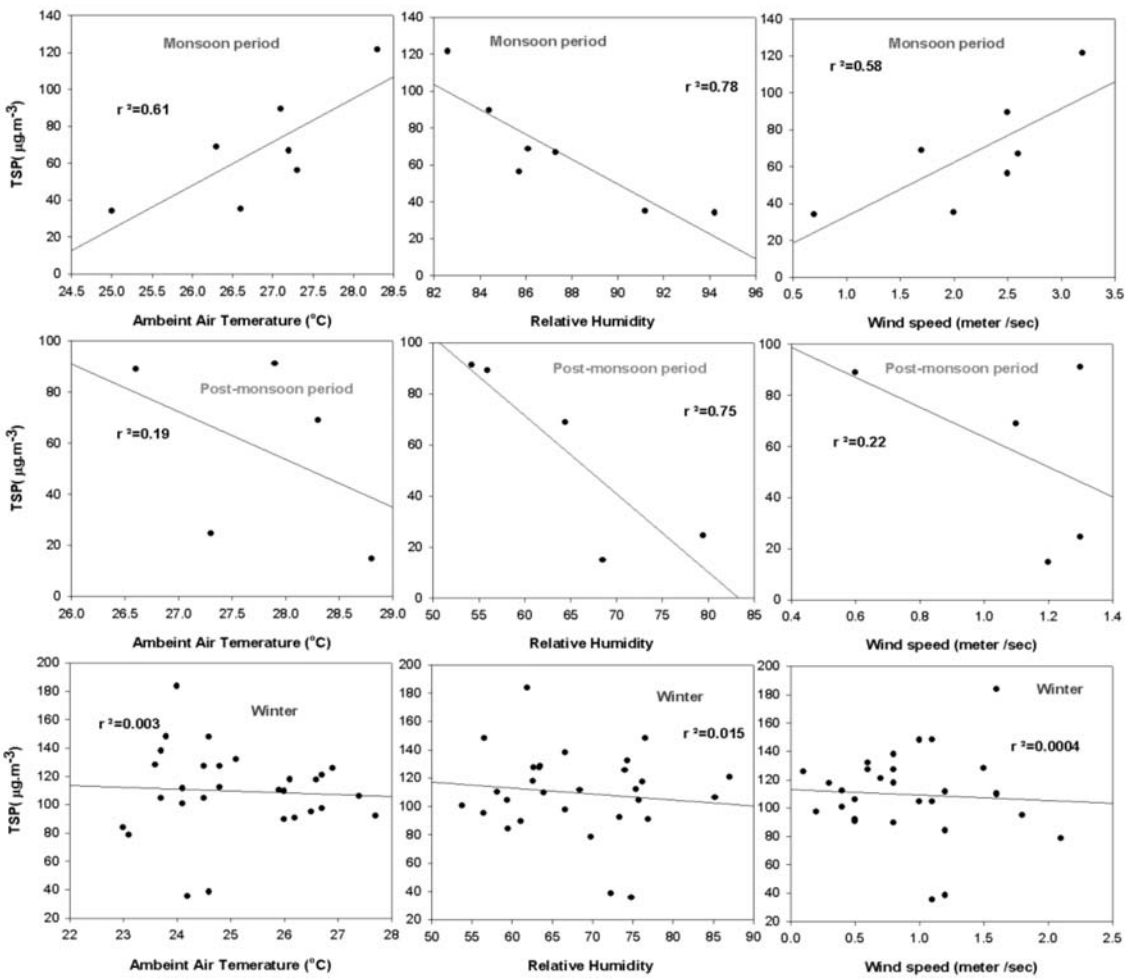

Figure 3.Covariance of ambient temperature, relative humidity and wind speed with measured TSP concentrations over Goa during monsoon period of 2011-2012.

Backward wind trajectories were obtained using NOAA Hysplit model (Fig. 2). It was found that during monsoon period prevailing winds were blowing from the west, west-northwest or west-southwest, whereas during post monsoon these were mainly originating from east or east-southeast. In contrast, during winter winds were found to originate mainly from north-northwest, north or west. Clear differences in wind directions over sampling site during different seasons (Fig. 2) appear to have a significant impact on the chemical composition of ambient aerosol over Goa. Significantly higher TSP, TC and TN mass concentrations, and high $\delta^{15}N$ (up to 26‰) found in bulk aerosols were due to carbonaceous material (that result from biomass-biofuel burning) transported by winds blowing from north in winter. It is important to mention that the higher $\delta^{15}N$ of aerosols during winter months is indicative of aging effect i.e. high degree of secondary processes in aerosol particles during the long range transport. Study of (Aggrawal et al. 2012) also supports dominant aging and in turn enhanced photolytic activity carbonaceous material in ambient aerosols during winter, as witnessed by enriched isotopic values of aerosols.

We also examined inter-relationships between chemical and isotopic characteristics of aerosols with ambient air temperature, wind speed and relative humidity. Noticeable meteorological influence on ambient aerosol mass concentrations (TSP) was obvious (Fig. 3) during different seasons. There appears to be an appreciable influence of local meteorological factors on ambient TSP concentrations during monsoon which seem to become weaker during post monsoon season. However, relative humidity still appears to be controlling ambient aerosol mass concentration during both monsoon and post- monsoon periods. During winter months, these meteorological parameters seem to have no influence on ambient TSP mass concentrations. Inter-relationships among chemcial and isotopic characteristis of atmopsheric bulk aerosols along with local meterological parameters are being further invesigated that will help us to better understand seasonal chnages in complex tropospehric chemisry in a typical costal environment.

CONCLUSIONS

Major outcome of the study is the observation of signficantly higher TSPM, TC and TN mass concentrations during winter compared to those duirng monsoon and post monsoon. Winds coming from north and north-northwwest appear to carry higher amounts of carbonacous material released by biomass –biofuel buring in northern parts of India. Stable isotopic ratios of C and N also support different origin as well as higher degree of secondary processing of ambient aerosol partciles duirng winter. Meterological factors such as air temperature, relative humidity and wind speed appear to influence aerosol mass concentrations during monsoon and to some extent post monsoon period. Winter aerossols over Goa do not appear showing any such local meterological influence.

REFERENCES

Agnihotri, R., Mandal, T.K., Karapurkar, S.G., Naja, M., Gadi, R., Nazeer, Y., Kumar, A., Saud, T., Saxena, M.(2011). Stable carbon and nitrogen isotopic composition of bulk aerosols over India and northern Indian Ocean, *Atmospheric Environment,* **45**, pp. 2828–2835.

Aggrawal, S.G., Kawamura, K., Umarji, G. S., Tachibana, E., Patil, R. S., Gupta, P.K.(2012). Organic and inorganic markers and stable C-, N-isotopic compositions of tropical coastal aerosols from megacity Mumbai: sources of organic aerosols and atmospheric processing, *Atmos. Chem. Phys. Discuss,* **12**, pp 20593–20630.

Mehra,P., Prabhudesai, R.G., Joseph, A., Vijay, K., Dabholkar, N., Prabudesai, S., Nagvekar, S. and Agarvadekar ,Y. (2005) Endurance and Stability of Some Surface Meteorological Sensors under Land- and Ship-Based Operating Environments. *Proceedings of the National Symposium on Ocean Electronics, SYMPOL-2005,* 15-16 December, 2005, pp 257-264.

Pavuluri, C.M., Kawamura, K., Tachibana, E., Swaminathan, T., (2010) Elevated nitrogen isotope ratios of tropical Indian aerosols from Chennai: implication for the origins of aerosol nitrogen in South and Southeast Asia. *Atmospheric Environment,* **44**, pp 3597-3604.

AEROSOL-CLOUD INTERACTIONS UNDER DIFFERENT ENVIRONMENTS

K. VIJAYAKUMAR[1] AND P.C.S. DEVARA[1]

[1]Indian Institute of Tropical Meteorology, Pune-411008, India
Email: devara@tropmet.res.in

Keywords: SPACE-TIME VARIATIONS, AEROSOL-CLOUD PARAMETERS, MODIS SATELLITE DATA, MULTI-ENVIRONMENTS

INTRODUCTION

The interactions between aerosol and cloud are complex because clouds and precipitation remove aerosols from atmosphere where aerosols may be produced and enhanced within clouds through chemical and physical processes. More information is needed on aerosol-induced cloud properties in various regions, particularly over the tropics where the convective and dynamical processes associated with high-altitude thunderstorms greatly affect the vertical distributions of aerosols and pre-cursor gases. Such observations also provide better understanding of coupling processes that exist between chemical, radiative, dynamical and biological phenomena in the earth's environment for model simulation studies of monsoon climate and air quality (Kamineni *et al.*, 2003).

DATA, RESULTS AND DISCUSSION

The MODIS (Terra AM-1) data for the period from 2000 to 2011 over some specific sites associated with different environments have been utilized in the present study. Fig.1 shows monthly mean AOD values over different environments during 200-2011. Higher AOD values are observed over urban regions compared to other environments considered in the study. Aerosol loading over the northernpart increased more than that over the southern part of India from 2000 to 2011. The southern India is characterized by more extensive vegetation cover and less human activities, resulting in steady increase in aerosol loading. While aerosol loading in the northern India might associate with human activities induced constructive soil, traffic dust, industrial emissions, agriculture crop and as well as dust storms (Sharma *et al.*, 2009), and those in the southern India might associate with natural emissions. Higher AOD values (>0.4) are found over areas with intense anthropogenic activity such as industrial regions.

Fig. 2 shows spatial correlation for AOD Vs. CF, CTP, CTT and WV for the period 2000-2011. MODIS shows an increase in the Cloud Fraction (CF) or cloud cover with increasing AOD in all areas. It is clear from the figure that some regions such as Sinhagad, Mumbai and Goa showed a strong positive correlation. It is important to mention that a marked increase in the correlation between CF with AOD in those regions with aerosols which are relatively hydrophobic, such as biomass and dust aerosols, indicating that meteorological factors are inuencing the relationship. But there is no such strong correlation observed over Island stations. CTP and CTT show strong positive correlation with AOD in high-altitude stations (such as Sinhagad and Nainital), other environments shows negative correlation.

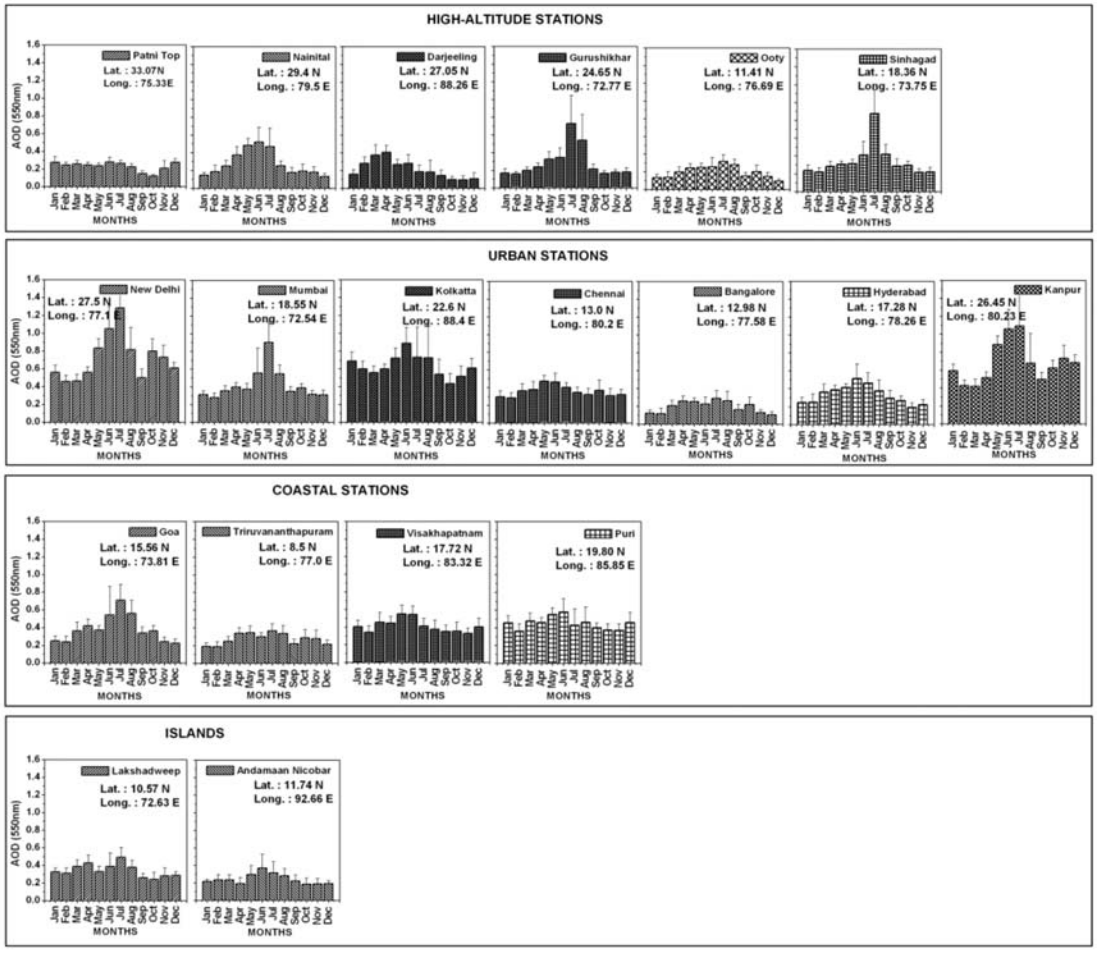

Figure 1.Monthly average AOD values at different environments during 2000-2011.

Rosenfeld and Lensky (1998) reported that CTP decreases with AOD, because the cloud effective radius increases with a decreasing CTP of convective clouds. This is supported by the CF increase with AOD and CTP decrease with CF. AOD and CF showed a strong positive correlation over some regions. But AOD and CTT, however, showed a negative correlation over the same region. Because of the CF–AOD relationship, co-variation of AOD with CTT due to large-scale meteorology might be ruled out as primary reason for the correlation found in MODIS data (Quass *et al.*, 2009). AOD versus WV shows positive correlation at high-altitude, urban and coastal stations. But Island station shows very strong negative correlation. The aerosol-cloud interaction in terms of cloud effective radius, and more details on such interactions over the environments considered in the present study will also be discussed. The relationships between cloud and aerosol properties are complicated, and there is potential for oversimplification to occur if large regions are averaged over. Based on this preliminary analysis, it is hard to identify and distinguish microphysical, seasonal, synoptic, humidity and retrieval related effects.

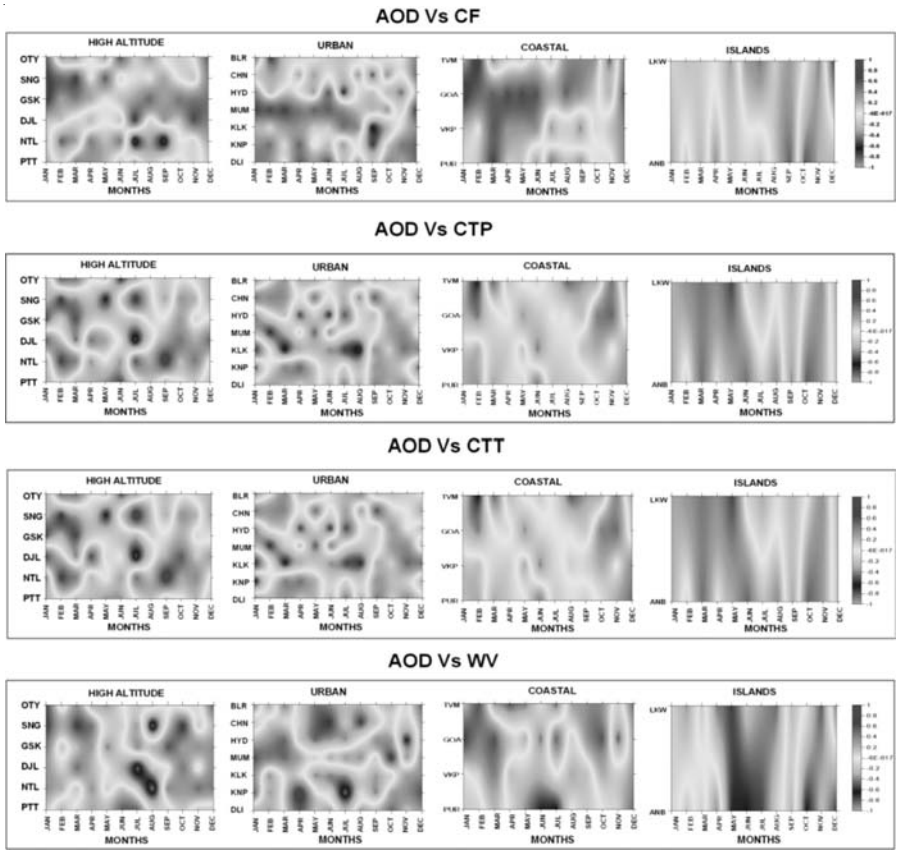

Figure 2.Spatial correlation between AOD versus CF, CTP, CTT and WV for the period 2000-2011.

ACKNOWLEDGEMENTS

This work is supported by the sponsored project, ISRO-GBP-ARFI Program of ISRO, Department of Space, Government of India. One of the authors (KV) acknowledges the financial support, in the form of Research Fellowship, from the ISRO-GBP-ARFI Project. The MODIS data used in this study were acquired as part of NASA's Earth Science Enterprise. Finally, we thank the Director, Indian Institute of Tropical Meteorology, Pune for infrastructure support.

REFERENCES

Kamineni, R., Krishnamurti, T. N., Ferrare, A.R., Ismail, S., Browell and Edward ,V.(2003).Impact of high resolution water vapor cross-sectional data on hurricane forecasting, *Geophysical Research letters,* **30**, 1234.

Rosenfeld, D. and Lensky, I.M. (1998). Satellite-based insights into precipitation formation processes in continental and maritime convective clouds, *Bulletin of the American Meteorological Society,* **79**, pp 2457–2476.

Sharma, A.R., Shailesh Kumar,K. and Badarinth, K.V.S. (2009). Satellite observations of unusual dust event over North-East India and its relation with meteorological conditions, *Journal of Atmospheric and Solar-Terrestrial Physics,* **71**, 2032–2039.

Quaas, J., Y. e tal.,(2009).Aerosol indirect effects - general circulation model intercomparison and evaluation with satellite data, *Atmospheric Chemistry and Physics,* **9**, 8697-8717.

ASSOCIATION BETWEEN AEROSOLS AND CLIMATE CHANGE

INDIRA SUDHIR JOSHI

Indian Institute of Tropical Meteorology
Dr.HomiBhabha Road, Pashan
Pune-411008, Maharastra India

Keywords: VOLCANIC AEROSOLS, MONSOON, CLIMATE CHANGE, RADIATION

INTRODUCTION

Volcanic activity could lead to the Climate changes directly by single and especially by multiple volcanic eruptions. Volcanic explosions introduce silicate dust particles and sulphur bearing gases into the stratosphere (Castleman et al., 1974; Pollack et al., 1976). Roback, (1983) has suggested a decrease of the direct solar beam by 20-30 percent for many months following thegreat volcanic eruptions. Maccracken and Luther, (1984) have shown that within a few months after the eruption of Elchichon, the zonal rain belt, i.e. the Inter tropical convergence zone(ITCZ), which was located just north of the equator, shifted southward and resulted in enhancement of precipitation by approximately 10 percent just south of the eruption zone. Sear et al., 1987 found that the induced temperature change appears more rapidly in Northern Hemisphere for major Northern Hemisphere Volcanoes. Other Climate regions which have been shown to be associated with volcanic aerosols include the Indian summer monsoon (Handler, 1986b; Mukherjee et al., 1987; Indira, 2011), the Sri Lankan monsoon, tree rings in the U.S. and South Africa. All the above studies have suggested the role of volcanic eruptions in modulating the Climate and weather.Keeping the above in view a study has been undertaken to examine the effect of volcanic aerosols on OLR and monsoon rainfall.

METHODS

In this study volcanic eruption of April 2010 (Iceland) effects on OLR (Outgoing Long wave Radiation) and Indian summer monsoon rain fall of 2010 studied. Information about the Volcano Eyjafjallajokull that erupted on 18th April 2010 was collected from Volcanic advisory from London (Information source Iceland MET Office). Satellite images of latitude-time diagrams of daily OLR (monsoon season) and monsoon rain fall figures for 2010 are collected from India Meteorological Department. Figure.1 shows the latitude –Time diagram of daily OLR (Monsoon Season) 2010. Figure .2 shows the figure of Monsoon 2010 produced by India Meteorological department.

CONCLUSIONS

Aerosols produced by the volcanic eruptions increased the outgoing long wave radiation from 25 N and above latitudes during 2010 (year of volcanic eruption). Following the volcanic eruption year an increase in OLR from 10 N onwards (2012) was observed. During 2010 and 2011 except in one or two places of NE India following the volcanic eruption an increase in Indian summer monsoon rainfall was observed.

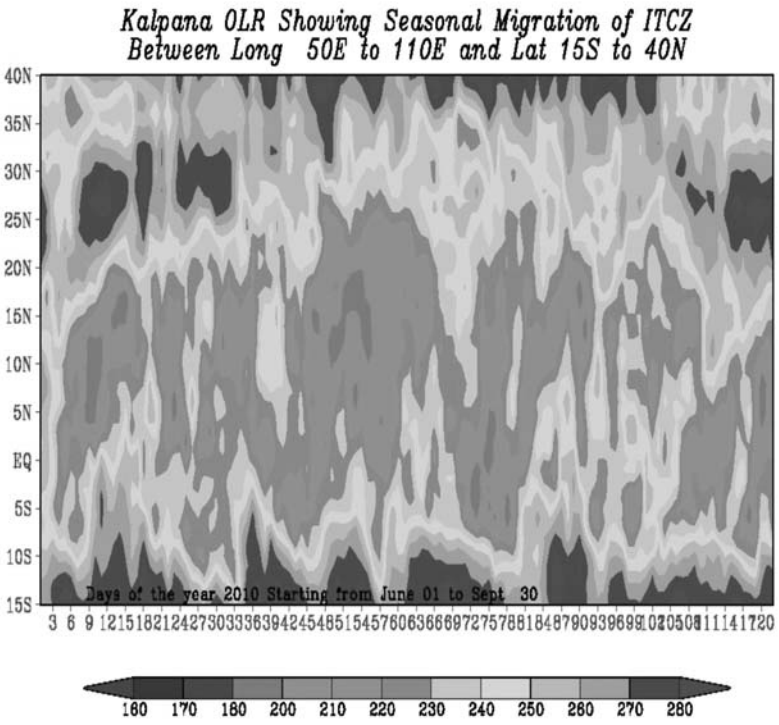

Figure.1: Satellite picture of out going long-wave radiation for 2010

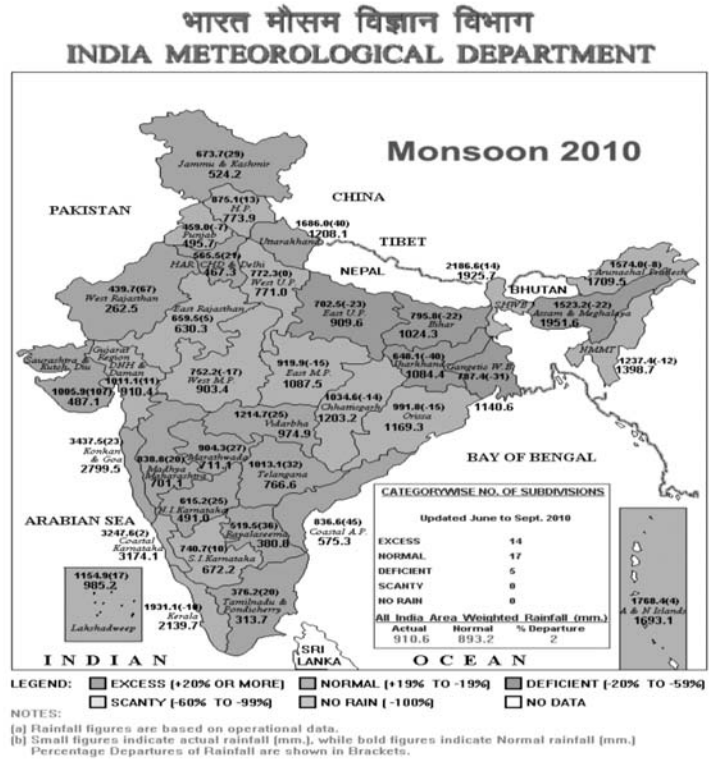

Figure.2 Indian summer Monsoon rainfall 2010

ACKNOWLEDGEMENTS

The author is thankful to Dr. P.C.S. Devara for his valuable suggestions while preparing the manuscript. The author expresses her deep sense of gratitude to the Director, Indian Institute of Tropical Meteorology, Pune for carrying out the research work and providing the facilities and infrastructure.

REFERENCES

Castleman, A. W. Mukelwititz, H.R., and Manow, B. (1974), isotopic studies of the sulphate component of the stratospheric aerosol layer, Tellus, 26, 222.

Handler, P. (1986b). Possible association between stratospheric aerosols and corn yields in the United States, *Agricult. Meteorol,* **35**, 205.

Indira, S. J. (2011). Effect of volcanic eruptions on stratosphere ozone and temperatures, *Res.J.Chem.Environ,* **15**, 530

Maccracken, M.C., and Luther, F.M. (1984), Preliminary estimate of the radiative and Climate effects of the elchichon eruption, Geophys. International, **23**, 385.

Mukherjee , B.K., Indira, K. and Dani, K.K. (1987), Low-latitude volcanic eruptions and their effects on Sri Lankan rainfall during NE monsoon, J. Climatol, **7**, 145.

Pollack. J. B., Toon, O.B., Summers, A Baldwin, B and Vancamp, W. (1976), Stratosphere aerosols and Climate change, J. Geophys. Res., **81**, 1071

Roback, A. (1983), The Mount St.Helens volcanicEruption of 18 May 1980, Nature, **310**, 373.

NUCLEAR AND RADIOACTIVE AEROSOLS

INVESTIGATION ON SODIUM AEROSOL CARBONATION PROCESS

[1]J. MISRA,[1] V. SUBRAMANIAN, [1]AMIT KUMAR, [1]R. BASKARAN,
[2]R. ANATHANARAYANAN, [2]P. SAHOO, AND [1]B. VENKATRAMAN

[1]Radiological Impact Assessment Section, RSD, EIRSG, IGCAR, Kalpakkam-603102
[2]Innovative Instrumentation Section, RTSD, EIRSG, IGCAR, Kalpakkam-603102

Keywords: SODIUM AEROSOL, FILTER PAPER SAMPLING SYSTEM

INTRODUCTION

In sodium cooled fast reactors (SFR), the leakages in the secondary sodium pipes leads to sodium fires, which are classified as Pool fire, Spray fires and Column fire. The hot sodium burns in air and gives rise to aerosols. The aerosols are mainly sodium oxide (Na_2O) or higher oxides of sodium (Na_2O_2 and NaO_2) depending upon the ratio of sodium to oxygen available during the onset of fire. Since these oxides are highly reactive, they are further converted to sodium hydroxide and sodium carbonate or sodium bi-carbonate upon reaction with water vapour and carbon dioxide present in the environment. The studies related to chemical characterization of sodium aerosols help in hazards evaluation of sodium fire incidences if any, occurring in SFR, and to the associated research facilities with respect to dispersion of sodium aerosols. Hence, a study has been initiated with collaboration of CEA, France, to quantify various chemical species of sodium aerosols with time for different relative humidity (RH %) and CO_2 conditions. This paper addresses the result of experimental runs on sodium aerosol carbonation process by varying relative humidity at 20%, 50%, 80% and 96% and keeping CO_2 content as per atmospheric condition.

MATERIALS AND METHODS

Experiments are being conducted in Aerosol Test Facility (ATF) (Baskaran *et al.*, 2004). Sodium aerosols are generated using a sodium combustion cell and fed into the aerosol chamber. The aerosol chamber is maintained at various RH% condition and keeping all atmospheric parameters same.

Manifolds for aerosol sampling

The sample collection for the carbonation studies is accomplished by Filter Paper Sampling System. The Filter paper sampling system has been designed, fabricated and integrated with aerosol chamber, which consists of two sampling heads which can be operated in quick succession. A photograph of the Filter Paper Sampling System is shown in Fig.1.

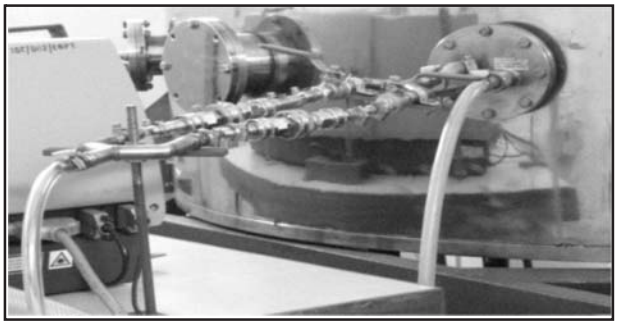

Figure1. Filter paper sampling system

It consists of two numbers of closed face type filter paper sample holder (25mm dia. filter paper) connected in parallel by using Y tubes. A ball valve is connected in each of the sampling line to regulate the flow through one sampling line at a time. A non-lubricant air displacement pump coupled with rotameter is used to control the sampling flow rate. Sampling is continued in quick succession by closing the valve on one line and opening the valve on the other line. Multiple filter paper sample holders are kept ready and it will be replaced immediately on the first line before the end of the sampling duration in the other line. The cumulative experimental error for the measurement of time, flow rate and mass of the filter paper is estimated to be ±10%.

Sampling Parameters

The experiments are conducted at an initial mass concentration of about 5 g/m^3. The value is arrived based on a hypothetical secondary loop leakage condition of PFBR viz. (i) the amount of leak (ii) the burning rate (40 $kg/h\text{-}m^2$), (iii) the release rate (50 g/s), (iv) GPM modeling to arrive ground level concentration (Punitha and Venkatesan, 2006).

In order to change the Relative Humidity content in the chamber, a system has been designed, fabricated in house and installed in the ATF. The chamber air is purged through Silica Gel rotor in order to dehumidify the chamber or purged through a water bath to make the chamber humid with a help of a 50 lpm oil free rotary pump. The online humidity meter indicates (certified with calibration) the relative humidity percentage inside the chamber. The RH% can be adjusted from 20% to 96% inside the chamber.

The experiments are conducted by keeping the chamber in the ambient atmospheric condition (pressure, temperature and CO_2 content).

Experimental

The experiments are conducted by keeping RH% at different conditions i.e. 20%, 50%, 80% and 96%. The sampling is started as soon as the aerosols are bottled-up in the aerosol chamber. The sampling duration is 100s at a flow rate of 10 lpm. The samples are immediately weighed, kept immersed in DM water and covered with parafilm (to prevent further reaction with atmosphere). After sampling, the sample solution is subjected to high resolution conductometric titration, developed in-house, to establish the presence of hydroxide, carbonate and bi-carbonate species present in the solution (Subramanian *et al.*, 2009).

RESULTS AND ANALYSIS

The results of the experiments showing relative concentration of hydroxide and carbonate species of sodium aerosols with different RH% are presented in Fig.2.

As stated in the introduction the main species are hydroxide and carbonate as (i) $Na_2O + H_2O \rightarrow 2NaOH$ and (ii) $Na_2O + CO_2 \rightarrow Na_2CO_3$. It is observed from Fig. 2(a) with 50%RH, the aerosols are initially formed as hydroxide and carbonate. Then the hydroxide is progressively converted to carbonate as per the reaction $2NaOH + CO_2 \rightarrow Na_2CO_3 + H_2$. The similar trend of formation with varying ratios of carbonate to hydroxide during the initial time of sampling is seen in all other cases of 80% RH, 96%RH and 20%RH.But in the cases of 80%RH and 96% RH, the hydroxide is progressively converted into carbonate as shown in Fig.2 (b) and Fig. 2 (c), but it is not so in 20%RH condition [Fig.2 (d)]. The major observation is: at 96%RH, all the hydroxide become carbonate in 900s, while it is getting converted in about 1300s at 80%RH and the conversion is slow

at 50% RH (there exist 20% of mole fraction remains to be converted at the end of 1200s). But at 20%RH the ratio of carbonate to hydroxide remains almost same even upto 1200s [Fig.2 (d)].

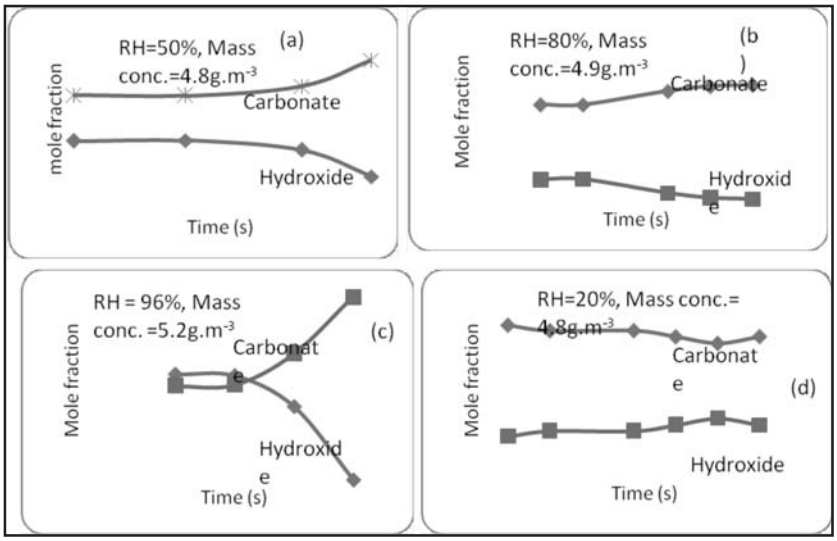

Figure 2. The relative concentration of hydroxide and carbonate content of sodium aerosols at various RH%

It is also observed in the case of RH=96%, formation of bi-carbonate species is seen after the complete conversion of hydroxide to carbonate beyond 900s during the sampling period of 1200s. The preliminary analysis of the result shows that when RH is at 20%, there exist unreacted oxides (yet to become hydroxide) is available during the entire sampling time for the conversion and it is progressively getting converted into hydroxide with time. This will be verified with determination of oxides in the sampling. But in all other cases complete conversion of species to carbonate is seen but the difference in the time could be due to difference in reaction rates.

SUMMARY

The experiments are conducted by varying RH% and keeping ambient atmospheric condition. The major species observed is carbonate. Though the formation of hydroxide is seen, but it is progressively converted into carbonate in a confined environment (aerosol chamber) for a given initial mass concentration of about 5 g/m^3 in about 1300s. Hence chemical toxicity due to hydroxide is reduced to great extent when time progresses. Further experiments will be conducted at lower RH% for understanding the chemical conversion process.

REFERENCES

Baskaran, R., Selvakumaran, T. S., and Subramanian, V. (2004). Aerosol Test Facility (ATF) for Fast Reactor Safety Studies, *Indian Journal of Pure and Applied Physics*, **42**, p.873

Punitha, G., and Venkatesan, R. (2006). Sodium Aerosol Dispersion Studies at Plant and Site Boundary, IGC/SG/SED/SSSS/DN/92102/3019/Rev. A.

Subramanian, V., Sahoo, P., Malathi, N., Ananthanarayanan, R., Baskaran, R. and Saha, B. (2009). Studies on chemical speciation of sodium aerosols produced in sodium fire, *Nuclear Technology*, **165**, p.257.

SODIUM AEROSOLS DISPERSION STUDIES IN OPEN ATMOSPHERE

V. SUBRAMANIAN[1], J. MISRA[1], AMIT KUMAR[1], R. BASKARAN[1], C.V. SRINIVAS[1]., R. ANANTHANARAYANAN[2],P. SAHOO[2], N. KRISHNAKUMAR[3],A. ASHOK KUMAR[3], S. CHANDRAMOULI[3], B. VENKATRAMAN[1] AND K.K. RAJAN[3]

[1]Radiological Impact Assessment Section, RSD, EIRSG, IGCAR, Kalpakkam-603102
[2]Innovative Instrumentation Section, RTSD, EIRSG, IGCAR, Kalpakkam-603102
[3]DD & SRD, FRTG, IGCAR, Kalpakkam-603102

Keywords: SODIUM AEROSOL, AEROSOL DISPERSION, FALLOUT LINE DENSITY

INTRODUCTION

In sodium cooled fast reactors (SFR), the leakages in the secondary sodium pipes leads to sodium fires. The hot sodium burns in air and gives rise to aerosols. Sodium aerosols released in the atmosphere are sodium monoxide (Na_2O) when sodium is in excess and peroxide (Na_2O_2) when oxygen is in excess. These oxide aerosols quickly react with water vapor to form sodium hydroxide (NaOH) and then sodium carbonate (Na_2CO_3) upon further reaction with carbon dioxide. Sodium hydroxide is highly corrosive and it is responsible for material damage and restricts the functionality of various devices in Steam Generator Building (SGB). The Threshold Limiting Value (TLV), for the atmospheric concentration of soda (NaOH) is $2mg.m^{-3}$ for humans. The aerosols that are released into the atmosphere will be carried away by the wind and get deposited along the ground in the downward direction. Hence, if sodium aerosols in hydroxide form and get in contact with humans, it is hazardous, but if it is in carbonate form, the concern is reduced to a great extent. So the quantity of sodium aerosols and quantitative information on chemical species presents in the aerosols in a given sodium fire event is important for the safety studies (Clough and Garland, 1971). Hence it is proposed to undertake the study on atmospheric dispersion of sodium aerosols. In this context a small scale fire of about 5 kg sodium is burnt in the sodium disposal area of Fast Reactor Technology Group (FRTG), and aerosol sampling was carried out upto the distance of 50m. Physical and chemical characteristics of sodium aerosols, sodium aerosol ground concentration and quantity of sodium aerosols deposited upto 50m distance were determined using suitable sampling instruments. All these results are presented in this paper.

MATERIALS AND METHODS

A small pool fire is created with 5kg of sodium in the fenced area (30m x 25m) of sodium disposal site of FRTG. The aerosols dispersed (ground level release) within the site upto 50m distance would be characterized by using various diagnostic equipments such as Filter paper sampling system, Low pressure impactor, High volume sampler and collection trays.

Measurement System

An open face filter paper sample holder (47mm diameter) and a non-lubricant rotary vane pump coupled with a rotameter (flow rate 20 lpm), comprise of Filter paper sampler. A known volume of air is made to pass through a filter and the particles suspended in the flow are filtered by the filter paper. The filter paper is weighed before and after sampling and mass of the aerosol deposited on the filter paper is determined. By knowing the volume of air drawn through the filter media, a typical mass concentration of the aerosols is estimated. Typical filters used in this study are made of glass

fiber filters. In this experiment, the filter papers are immediately kept immersed in DM water and covered with parafilm (to prevent further reaction with atmosphere). The sample solution is subjected to high resolution conductometric titration, developed in-house, to establish the presence of hydroxide, carbonate and bi-carbonate species present in the solution (Subramanian *et al.*, 2009).

High volume sampler is same as that of filter paper sampler discussed above but with the change in the flow rate. The flow rate through the high volume sampler is 500 lpm. This system is used to determine mass concentration. The mass-size distribution is measured using Low Pressure Impactor (LPI). The LPI consists of an eight stage ambient Andersen Sampler Mark II (M/s Andersen Inc. USA) to which a five-stage adopter assembly is attached, which functions as Low Pressure Impactor (LPI). The LPI operates at a flow rate of 2.8 lpm with a down pressure of 114 mm of Hg and determines the mass-size distribution between 0.08 – 35 mm (aerodynamic).The collection tray is a glass plate having area 8 cm^2 with tare weight of about 0.8g. These plates are placed near the samplers and fall out of sodium aerosols on the tray is determined gravimetrically.

Sampling

To begin with physical inspection of the site was carried-out. Meteorological parameters were ascertained and sodium burning location is fixed in the upwind direction of the field. The sampling stations are identified in the down wind direction and drawn along the arc of 30° conical sector at a distance of every 10m. A typical plan of the sodium burning point and sampling stations is shown in Fig.1.

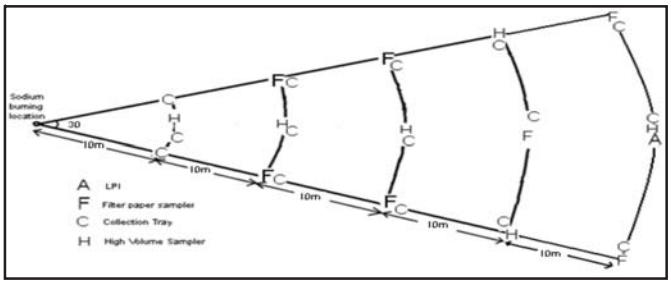

Figure 1. A schematic diagram showing layout of sampling stations and sodium burning.

The photographs of the sodium burning and sampling stations are shown in Fig. 2. The instruments are kept at 1 m height at all the locations. There are 7 custom built filter paper air samplers, 6 numbers of high volume air samplers, and one LPI were deployed for this experiment. The required AC power supply was drawn through power supply extension boards. 15 numbers of collection trays were placed in such a way that 3 numbers in each arc. Besides, 3 more trays were kept at 60m distance. The sampling was started as soon as the combustion started. It is observed that 5kg sodium burning last for 15-20 minutes. The sampling was terminated in 30 minutes.

Figure 2. Photographs of the sodium burning and sampling equipments deployed at various locations

Analysis

Fallout line density: The fall-out line density (Johnson *et al.*, 1979) is a measure of deposited aerosol line density along an arc. This is determined as average aerosol mass deposited per unit area (obtained from the collection tray) of a particular arc multiplied by the arc length.

Fall out line density (g/m) =M g/m^2 X arc length 'l' (m)

where, M is average aerosol mass deposited per unit area (g/m^2) on a glass plant in a particular arc and ' l' is arc length in m.

A graph is plotted between fall out line density and radial distance of the arc from the release point (centre). The area under the curve (integral) gives the total fall out of aerosol from the release point upto the arc distance or the mass of the aerosols deposited between any two points, for a given sodium fire.

Chemical speciation: Custom built filter paper sampler is made to run for one minute duration soon after the plume was set i.e., at 5 minutes later.

Mass Concentration and Mass-size distribution along with Mass Median Aerodynamic Diameter (MMAD) are determined as per the standard procedure.

Measurement of Meteorological Condition at the Experimental Site: An Ultra Sonic Anemometer was installed in the experimental site at 2m elevation at the middle of the fenced area to measure the wind and turbulence condition of the site. This instrument provides wind speed, wind direction and turbulence fluxes at a rate of 10 readings for every second. One week data of wind profile was analyzed and experiment is planned accordingly. Table 1 includes the metrological condition during the experiment. The experiment is conducted with stable atmosphere, humid and gentle wind in NW-N direction.

RESULTS AND DISCUSSION

Table 1 gives sodium burning characteristics like sodium aerosol release rate and sodium burning rate. It is observed that, the plume rises from the tray upto 3m height and get dispersed in the down wind direction. The vertical component of the plume touches the ground at about 20m from the tray. The results of the mass concentration measurements taken at 20m, 30m, 40m and 50m distance are shown in Fig. 3. It is observed from the figure that mass concentration decreases from 20m location to 50m location by four times i.e. 4.4 g/m^3 to 1.4 g/m^3. The deviation in the 30m location is due to presence of tree which hinders the dispersion of sodium aerosols. The mass of the aerosol deposited on the collection tray were weighed. The fall out line density is calculated for the arc drawn at 40m, 50m and 60m are plotted (Fig.4) and found to obey linear fit. (The mass of the aerosols collected below 40m are found below the detection level of the balance).It is calculated from the Fig.4, that, mass of the sodium aerosol deposited on the ground from 40 to 60m distance on the conical sector is estimated to be ~0.3 kg (area under the curve). The mass-size distribution at 50m distance is shown in Fig.5, which is multi-model with MMAD 1.73 ìm and 3.36 ìm.

The chemical species of sodium aerosols collected on the filter paper was determined as bi-carbonate in all the sampling locations (Table 1). It is ascertained that since the mass deposited is about 1 mg, hence the quantification of chemical species results only bi-carbonate‡, which is formed either in the filter paper or during analysis.

Atmospheric condition	Wind speed : 0.5 m/s,Wind direction : 270 – 290º,RH : 80 %
Quantity of sodium	4.972 kg
Duration of fire & Temperature	30 minute, ~ 700ºC
Sodium burning characteristics	Mass of sodium burnt : 1340 g Sodium aerosol release rate as Na_2O : 1.07 g/s Sodium burning rate : 13.25 kg/h-m^2

Table 1. Initial condition and sodium burning characteristics

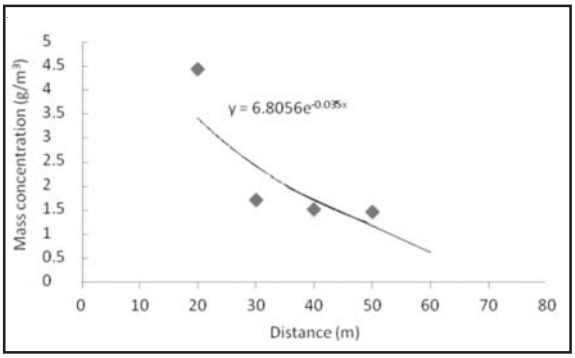

Figure 3. Aerosol mass conc. vs distance

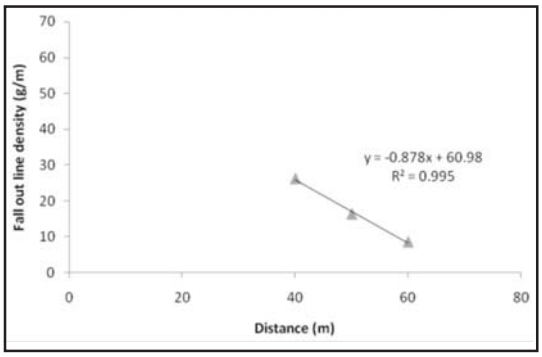

Figure 4. Fallout line density vs distance

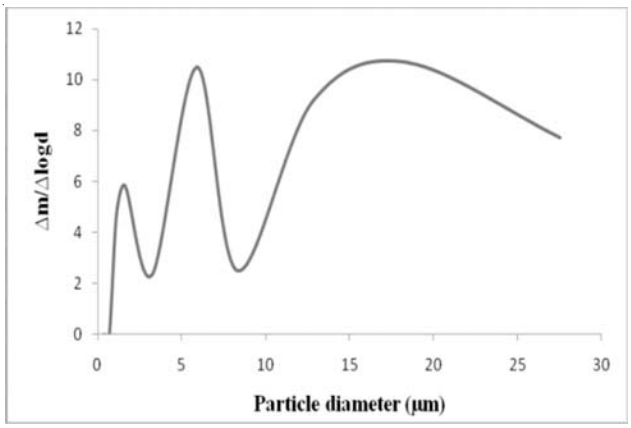

Figure 5. Mass-size distribution at 50m

SUMMARY

The hazard evaluation of secondary sodium fire is a major task in the safety analysis of SFR. The present study is very useful in this context. It is the beginning of the objective stated and it is a pilot experiment for the large fire and long range dispersion studies The experimental procedure and sampling/analysis techniques were standardized.

REFERENCES

Clough, W. S. and Garland, J.A. (1971). The behavior in the atmosphere of the aerosol from a sodium fire, *Journal of Nuclear Energy*, **25**, 425-435.

Johnson, R. P., Cuderjahn, C., Morewitz, H. A., Nelson, C. T. and Otter, J. (1979). Atmospheric fallout of sodium combustion aerosols, *Proceedings of Intl. meeting on Fast reactor safety Technology*, Aug 19, 1974, Seattle, Washington.

Subramanian, V., Sahoo, P., Malathi, N., Anathanarayanan, R., Baskaran, R. and Saha, B. (2009). Studies on Chemical Speciation of Sodium aerosols produced in Sodium fire, *Nuclear Technology*, **165**, 257.

FISSION PRODUCT AEROSOL TRANSPORT AND RETENTION STUDY FOR PHWR UNDER STATION BLACK OUT CONDITION

MAHENDER SINGH[1], B. CHATTERJEE, D. MUKHOPADHYAY and H. G. LELE

Reactor Safety Division, Bhabha Atomic Research Centre,
Mumbai-400085, India.
E mail: [1]mahender@barc.gov.in

Keywords: STATION BLACK OUT, PRIMARY HEAT TRANSPORT SYSTEM, FISSION PRODUCTS, AEROSOL RETENTION AND TRANSPORT

INTRODUCTION

A study has been carried out to analyse fission product (FP) aerosol transport and retention for PHWR under a severe accident condition like "Station Black Out (SBO)" without operator intervention. Large PHWR is a Pressure Tube type reactor having two loop systems. The Primary Heat Transport (PHT) system is having large amount of heat sinks available in Steam Generators, moderator system and calandria vault. Under the accident postulation, the available sink gets boiled off over a significant time during the postulated accident. Loss of heat sinks leads to fuel heat-up and failure of some of the coolant channels leading to blow-down of PHT system inventory into calandria vessel. Under the heat-up phase, fission product inventory gets released from fuel gap and matrix to coolant channels. The inventory mainly constitutes of volatile, semi volatile and refractory fission products. It is expected that volatile products like Cs, I, Ru undergo different chemical species formation which flows in the coolant channels and piping of Primary Heat Transport (PHT) system as an aerosol under severe accident condition. During course of time it gets retained in the long and colder sections of PHT piping and the non retained part gets released through break path.

Conditions of fission products released within PHT and their transport and retention within PHT, decides the fission products inventory in the containment and subsequently the release to the environment. Hence it is very important to carry out the estimation as it determines the accident source term. Before slumping of fuel channels into calandria vessel, PHT of the reactor acts as a filter (provide retention) for all fission products except fission gases Xe and Kr. The fission products may get deposited on wall or remain in the aerosol form or a combination of both. The situation is dictated by system pressure, temperature, and flow rate and wall temperature conditions. As observed in general, that deposition of aerosols within PHT system is governed by transport system geometry and system parameters. A detailed analysis has been carried out (i) to study the influence of feeder sizes on the FP retention within PHT system and (ii) to study the aerosol behavior at different locations of the PHT. The analysis is carried out with Accident Source Term Evaluation Code (ASTEC).

The code ASTEC (Dorsselaere *et al.*, 2005; Dorsselaere *et al.*, 2009) computes distribution for fission product aerosol species within PHT and their release into containment after breach in PHT system.

Calculation methodology (shown in fig. 1) as suggested by Gera *et al.*, (2010) is adopted for FP transport and retention.

METHODS

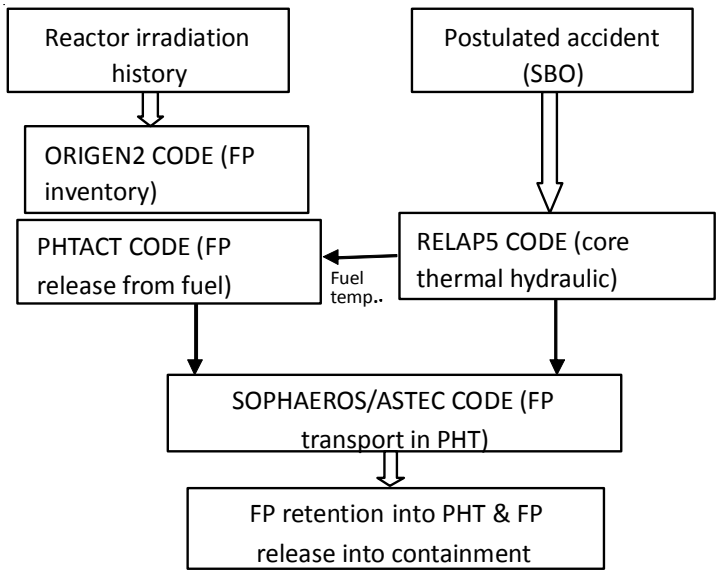

Figure 1. Block diagram showing adopted analysis methodology

Code requires boundary conditions like FP inventory, transient FP release from fuel, and time history of thermal hydraulic data like wall temperature, fluid temperature, fluid pressure, and junction fluid mass flow rate for each PHT volume. These boundary conditions are provided by various codes like ORIGEN2 code (Forschungszentrum, 1980) for FP inventory calculation, PHTACT code (Lele *et al.*, 2001) for FP release calculation, RELAP5 code (SCDAP/RELAP5 Development Team, 1995) for PHT thermal hydraulic data.

CONCLUSIONS

Influence of feeder size on retention: Reactor core consist of feeders with five classes of diameters and each feeder consisting of small horizontal and large vertical section. Due to complexity of modeling, feeders are modeled only as vertical section. Effect of feeder size on FP retention is summarized in table 1 below:

Diameter size(mm)	%FP retention				
Species	I	Cs	Te	Kr	Xe
49.3	62.46	56.78	56.25	0	0
59	62.46	56.78	56.25	0	0
73.4	63.88	56.78	56.25	0	0
85.4	64.1	57.9	56.8	0	0
%FP release to containment					
For all diameters	6.81	7.81	5.16	100	100

Table 1. Table showing effect of feeder size on FP retention and their release

It is observed that there is marginal increase in FP retention with increase in feeder size and FP release to containment remains unaffected. Retention variation up to (~8%) is observed within feeder pipes and major retention processes are turbulent diffusion, eddy impaction and bending impaction of FP aerosols.

FP Distribution in PHT Circuit: Major FP aerosol retention is found in reactor core channels with eddy impaction (~75%) and thermophoresis (~20%) as predominant retention processes. However analysis carried out by Gera et al. (2010) for a postulated scenario of Loss of Coolant Accident along with ECCS, shows thermophoresis and settling are major retention processes within reactor channels. This study implies that the processes of aerosols retention are dependent on specific scenario.

REFERENCES

Dorsselaere, J. P. V., Pignet,S., Seropian, C., Montanelli,T., Giordano, P., Jacq, F. and Scwhinges, B. (2005). Development and assessment of ASTEC code for severe accident simulation, (NURETH-11, Avignon, France).

Dorsselaere, J. P. V., Seropian, C., Chatelard, P., Jacq, F., Fleurot, J., Giordano, P. and Scwhinges, B. (2009).The ASTEC integral code for severe accident simulation, *Nuclear Technology* ,**165**, pp. 293–307.

Gera, B., Kumar, M., Thangamani, I., Prasad, H., Srivastava, A., Majumdar, P. , Dutta, A., Verma, V., Ganju, S., Chatterjee, B., Lele, H. G., Rao V.V.S.S. and Ghosh A. K. (2010). Estimation of Source Term and related consequences for some postulated severe accident scenarios of Indian PHWR**,** *Nuclear Engineering and Design,* **240 (10)**, pp. 3529-3538.

Forschungszentrum Karlsruhe GmbH, (1980).National Radiological Protection Board, (1995). PC COSYMA Version 2.0 Users Guide, EUR 16240 EN (NRPB-SR280). November, ORNL, 1980.ORIGEN-2, Isotope Generation and Depletion Code. ORNL TM-7175, July.

Lele, H.G., Mukhopadhyaya, D., Behera, G., Gupta, S.K., (2001). PHTACT—a computer code for estimation of fission product release and transport for pressurised heavy water reactor during accident conditions, (RSD/CSSS/SKG/2069/2001, Divisional Report, April).

The SCDAP/RELAP5 Development team (1995).SCDAP/RELAP5/MOD3.2 Code Manual. NUREG/CR-5535, INEL-95/0174.

MATHEMATICAL MODELLING OF AEROSOL SCRUBBING BY SPRAY SYSTEM IN NUCLEAR CONTAINMENT

I.THANGAMANI, VISHNU VERMA AND R.K.SINGH

Reactor Safety Division,
Bhabha Atomic Research Centre, Mumbai, India

Keywords: CONTAINMENT, SPRAY SYSTEM, AEROSOL SCRUBBING, AEROSOL TRANSPORT AND DEPOSITION

INTRODUCTION

The containment building of nuclear power plant is a leak tight concrete structure which houses reactor core and other associated systems and it acts as an ultimate barrier to the release of radioactivity to the atmosphere in case of severe accident. The containment is also employed with many Engineered Safety Features (ESFs) to mitigate the consequences of LOCA with safety system failure, during which high enthalpy steam and radioactive fission products will be discharged into the containment. In such conditions, the pressurized containment will be the source of activity release to the environment by way of leakage. Containment spray system is one of the engineered safety feature proposed to employ in future Indian containments as it assists in removing energy by way of condensation and scrubbing aerosols from containment atmosphere. Mathematical modelling of containment spray system was developed and incorporated in in-house containment thermal hydraulic code CONTRAN, which is capable of modelling aerosol deposition, decay and transport within containment compartments. The paper covers the modelling aspects of aerosol scrubbing through spray system and its effects on aerosol concentration in containment.

METHODOLOGY

In case of accident such as LOCA/MSLB, the water from sump is pumped into containment spray systems and it sprays the water into the containment atmosphere through spray nozzles. Water jet formation takes place at nozzle exit and it further breaks down into droplets of varying sizes and are ejected at varying angles and velocities. These droplets then move downwards and undergo heat and mass transfer with containment atmosphere and scrub aerosols.

Simplified modeling has been carried out for an array of falling droplets having same initial droplet size, temperature, velocity, angle and initial concentration of aerosol (Iodine). A spray droplet with initial concentration and temperature is projected with an initial velocity at an angle with respect to the vertical direction. As the droplet move down, depending upon the containment ambient conditions, the droplet may undergo condensation or evaporation in presence of non-condensable and at the same time the mass transfer of aerosol to droplets takes place through diffusion process.

The steam condensation over droplets or evaporation of droplets depends upon ambient temperature, partial pressure of steam and droplet velocity. The diffusive mass transfer of Iodine from containment atmosphere to spray droplets was calculated based on Iodine partition coefficient, droplet velocity, droplet Iodine concentration and concentration in containment atmosphere. The mass, energy, concentration of aerosol and velocity of droplets were calculated by solving mass, momentum and energy equations using Runge-Kutta fourth order method. Net mass, energy and quantity of aerosol transferred to droplets are evaluated for each time step in spray system subroutine and then it is

returned to CONTRAN code for solving the containment mass and energy equations for evaluating the new containment pressure, temperature and concentration of aerosol.

CONCLUSIONS

Mathematical model of containment spray system has been developed as subroutine and integrated to thermal hydraulic code CONTRAN. For a postulated 200% break LOCA with safety system failure, the containment pressure-temperature transients, aerosol concentration transients and leakage from containment were evaluated and the impact of containment spray system over aerosol scrubbing were studied.

COMPARISION OF RADON DECAY PRODCTS DEPOSITION ON SURFACES WITH THEIR SIMULATED DEPOSITION IN HUMAN RESPIRATORY TRACT

RAJESWARI P. ROUT, ROSALINE MISHRA, B. K. SAPRA, Y. S. MAYYA
Radiological Physics and Advisory Division,
Bhabha Atomic Research Centre, Mumbai-400094, India.

Keywords: RADON, HUMAN RESPIRATORY TRACT, SURFACE DEPOSITION, FRICTION VELOCITY

INTRODUCTION

The inhalation of radon (^{222}Rn) and its decay products contribute to a major fraction (55%) of the natural background radiation dose to humans (UNSCEAR, 2000). When air with radon and its decay products is inhaled, the short-lived decay products deposit in respiratory tract which may lead to the development of lung cancer. Recent epidemiological studies of indoor radon have provided strong evidence of lung cancer risk with respect to radon exposure (Darby *et al.*, 2005; Krewski *et al.*, 2005). Assessing radon exposure has been a complex issue as there is no direct method for measuring personal doses analogous to Thermo Luminescence Dosimeter (TLD) for gamma exposures. One of the direct methods may be evolved through a comparative study between particle deposition in human respiratory tract (HRT) and on detector surface.

The objective of the present study is to carry out a comparison between particle deposition rates in HRT and surface. An attempt has been made to mimic HRT deposition, through deposition of particles on a wire mesh capped surrogate surface. In order to achieve this goal, modeling of particle deposition on flat surfaces has been carried out using the friction velocity based models which take into account various available forms of eddy diffusivities on gas surface boundary layers. Study of HRT deposition has been done using ICRP respiratory tract deposition models for various particle size distributions. Comparison between surrogate surface deposition and HRT deposition has been worked out to achieve at an optimum wire-mesh combination that will approximately mimic the HRT deposition.

COMPARISION OF PARTICLE DEPOSITIONS IN HUMAN RESPIRATORY TRACT (HRT) AND ON SURROGATE SURFACES (SS)

DEPOSITION OF PARTICLES IN HRT

For calculation of particle deposition in HRT, the morphological model used in this study is the ICRP 66 (ICRP, 1994) HRT model. Deposition of particles occurs in all regions of the HRT, but with different efficiencies. Deposition efficiency is defined as the fraction of the number of particles deposited to the number of particles enters in a region of the respiratory tract and it depends on particle size, volumetric flow rate, average transit time and scaling factors.

A model calculation has been done for estimating particle deposition fractions in each region of the HRT using the empirical formulae given in ICRP 66 for an adult nose breather. The various deposition processes, namely diffusion, inertial impaction and gravitational sedimentation are considered in this calculation. The model describes the deposition of particles in a very wide range of diameters, from atomic dimensions up to about 1 μm. Then the total deposition fraction of particles in HRT was calculated taking the sum of particle depositions in all regions of the RT.

DEPOSITION OF PARTICLES ON SS

Deposition of particles on surfaces is an important mechanism of activity removal by plate-out. Surface deposition of particles is characterized by their deposition velocities (V_d) which is related to the surface deposition rate (λ_d) and the surface-to-volume ratio of the room (S/V), by the following equation:

$$V_d = \lambda_d / (S/V) \quad (1)$$

Where the deposition velocity V_d is the ratio of the time-averaged flux of particles (particles $m^{-2} h^1$) on the surface to its mean airborne concentration, C (particles m^{-3}).

For calculation of deposition velocity Lai-Nazaroff model (Lai and Nazaroff, 2000) and Zhao-Wu model (Zhao and Wu, 2006) were used in this study. The advantage of using these models is that only friction velocity (u*) is required as the input parameter which can be easily estimated from the turbulence generating parameters. Lai-Nazaroff model considers particle deposition by Brownian diffusion, turbulent diffusion and gravitational sedimentation where as turbophoresis is included as an additional deposition mechanism in Zhao-Wu model. It was observed that in the range 1 nm to 5 μm turbophoresis has negligible effect on particle deposition.

COMPARISION OF PARTICLE DEPOSITIONS IN HRT AND ON SS

A comparison between particle deposition rates (particles h^{-1}) in HRT and on SS was carried out to understand the similarity and difference between their particle deposition rates.

If $N_a(d)$ is number of particles in a room, q is the breathing rate in $m^3 h^{-1}$ and $\eta_D(d)$ is the deposition fraction of particles in the HRT, then HRT deposition rate is given by the following equation.

$$J_{lung} = \eta_D(d)\ q\ N_a(d) \quad (2)$$

Similarly if V_d is the deposition velocity of particles on a surface and A_s is the area of the surface on which deposition occurs, then the surface deposition rate is given by

$$J_{surface} = V_d\ N_a(d)\ A_s \quad (3)$$

Considering an adult nose breather in an indoor environment the value of q is taken as 0.75 $m^3 h^{-1}$ (BEIR VI, 1999). Fig. 1 shows comparison of particle deposition rates in HRT and on SS as a function of particle size in the range of 1 nm to 1 μm at u*=12 cm/s. It is observed that the total deposition of particles in the HRT has a V-shape curve with minima at about 0.3 μm. This is due to the importance of diffusion process for smaller particle sizes and inertial impaction and gravitational sedimentation for larger particle sizes.

It is also observed that the surface deposition rate has a V-shape with respect to particle size and the two curves show good agreement for larger particle sizes (greater than 0.07 μm) but deviate from each other as the particle size becomes smaller. This deviation is due to the unattached fraction of particles which deposit faster than the attached fractions (Porstendorfer, 1996) where as in case of RT, unattached fractions are removed in the upper part of HRT. Therefore the SS was capped with different combinations of wire meshes (50, 80, 100, 200, 635 types) for tailoring the unattached fractions so that the HRT and SS deposition curves will approach each other.

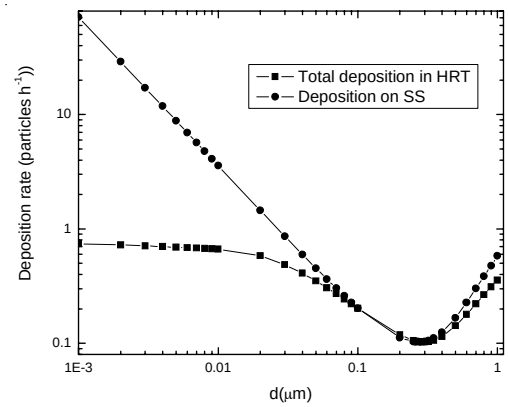

Figure 1. Comparison of deposition rates for lung and surface as a function of particle size in the range of 1 nm to 1 μm at u*=12 cm/s.

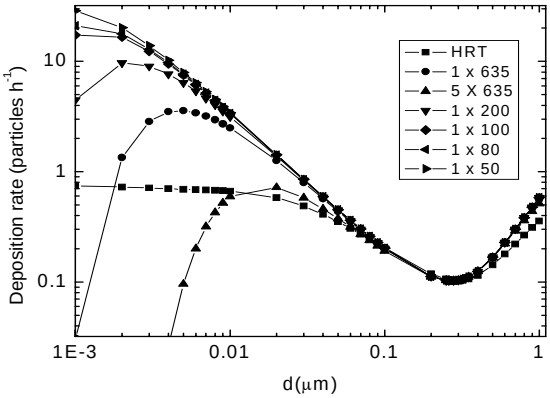

Figure 2. Comparison of RT and surface deposition rates with the use of different wire meshes at u*=12 cm/s.(Note: 5 x 635 means 5 number of 635 meshes stacked one above the other).

Fig. 2 shows comparison of particle deposition rates in HRT and SS capped with the use of different wire meshes at u*=12 cm/s. It is observed that, as the mesh becomes finer, the surface deposition curve approaches HRT deposition curve and for a combination of five 635 meshes stacked one above the other, they are in good agreement for particle size greater than 0.01 μm but for d < 0.01 μm, there is a sharp fall of the surface deposition rate.

CONCLUSION

The deposition in the HRT based on ICRP66 was calculated for an adult nose breather and a V-shape deposition curve was obtained for particle size 1 nm to 5 μm. The radon progeny deposition on surfaces was also calculated using two models, namely, Lai-Nazaroff and Zhao and Wu model for particle deposition in indoor environment. Interestingly, the results from both the models were same for particle size up to 5 μm, implies negligible contribution from the turbophoresis process. A similar V-shape deposition curve has also been obtained using these models for various particle sizes. It has been observed that the particle deposition in the lung is similar to that of the progeny deposition on the surface except at lower particle sizes. Therefore, wire-mesh capped detector surfaces were chosen to see whether the deposition on such surfaces matches with the particle deposition in the lung at smaller particle sizes. The deposition on the detector surface was calculated by transmission through various combinations of wire meshes. It was observed that deposition through a set of five 635 meshes kept parallel one above the other (at a u* of 12 cm/s and for particle size greater than 0.01 μm), matched well with deposition curve of particle deposition in the RT. This result would be used for mimicking lung deposition with a wire-mesh capped detector. However this requires series of experimental measurements for validation.

REFERENCES

BEIR VI (1999). Committee on Health Risks of Exposure to Radon National Research Council, National Academy Press, Washington.

Darby, S., Hill, D., Auvinen, A., Barros-Dios, J. M., Baysson, H., Bochicchio, F., Deo, H., Falk, R., Forastiere, F., Hakama, M., Heid, I. , Kreienbrock, L., Kreuzer, M., Lagarde, F., Makelainen, I.,

Muirhead, C., Oberaigner, W., Pershagen, G., Ruano-Ravina, A., Ruosteenoja, E., Rosario, A. S. R., Tirmarche, M., TomaBek, L., Whitley, E., Wichmann, Doll, H. E., R. (2005). Radon in homes and risk of lung cancer: collaborative analysis of individual data from 13 European case-control studies, *British Medical Journal*, **330**, 223.

International Commission on Radiological Protection (1994). Annals of the ICRP 24, *ICRP Publication 66*, Pergamon Press, Oxford.

Krewski, D., Lubin, J. H., Zielinski, J. M., Alavanja, M. (2005). Residential radon and risk of lung cancer: a combined analysis of 7 North American case-control studies, *Epidemiology*, **16**, 137.

Lai, A. C. K., Nazaroff, W. W. (2000). Modeling indoor particle deposition from turbulent flow onto smooth surfaces, *Journal of Aerosol Science*, **31**, 463.

Porstendorfer J. (1996). Radon: measurements related to dose, *Environment International*, **22**, 563.

UNSCEAR (2000). United Nations Scientific Committee on the Effects of Atomic Radiation. Report to General Assembly with Annexes, United Nations. Sources and Effects of Ionizing Radiation.

Zhao, B., Wu, J. (2006). Modeling particle deposition from fully developed turbulent flow in ventilation duct, *Atmospheric Environment*, **40**, 457.

A STUDY OF NANOPARTICLE DEPOSITION USING DEPOSITION BASED RADON/ THORON PROGENY SENSORS IN INDOOR AND OUTDOOR ENVIRONMENTS

R. MISHRA, R. PRAJITH, A.C.GOLE, R. P. ROUT, B. K. SAPRA, Y. S. MAYYA

Radiological Physics and Advisory Division,
Bhabha Atomic Research Centre, Mumbai-400094, India.

Keywords: DEPOSITION VELOCITY, RADON PROGENY, THORON PROGENY, ATTACHED FRACTION DEPOSITION VELOCITY

INTRODUCTION

The decay products of Radon and Thoron constitute a major part of the indoor aerosol and are the actual dose-givers through inhalation route. Among the several aspects of decay product behaviour, deposition on surfaces is of special significance because of its prominent role in activity removal by plate out and consequent occurrence of progeny disequilibrium with the parent gases. Due to their high diffusivities and ability to stick to surfaces, the freshly formed decay products soon attach to existing aerosol particles, thereby giving rise to a continuous activity size distribution. This distribution is broadly classified into two groups, namely, the fine/unattached fraction (~ 2 nm diameter) and the coarse/attached fraction (~100 nm). Deposition depends on the activity size distribution and the structure of turbulence at the air-surface interface. But, the radioactive nature of the decay products renders their detection far easier than non-radioactive particles and hence they provide excellent surrogates for understanding nano-particle deposition rates.

The experimental data available show large variations in the deposition velocity estimates of the progeny species (Bigu, 1985; Jacobi, 1972; Knutson, 1985; Morawska and Jamriska, 1996; Pörstendorfer, 1978; Scott, 1983). Although it is difficult to attribute specific reasons for this variability, it could in part be due to limitations of the measurement techniques and also due to uncontrolled variations in the environmental conditions. To improve measurement reliability, it is more prudent to carry out long term, time integrated measurements of deposition velocity using passive track detectors (Mishra and Mayya, 2008, Mishra *et al.*, 2009). So, in the present work, the effective and the aerosol-attached fraction deposition velocities measurements for both Radon and Thoron progenies are carried out in in indoor as well as outdoor environments.

MEASUREMENT TECHNIQUE

Passive direct Radon and Thoron progeny sensors (DRPS/DTPS) are absorber mounted Solid state nuclear track detectors (SSNTDs) which detect the alpha particle emitted from the deposited progeny atoms (Mishra *et al.*, 2008, 2009). DRPS and DTPS were used both in bare and wire-mesh capped mode to measure the total and coarse fraction deposited atom flux, from which the effective deposition and coarse fraction deposition velocities were estimated. The effective (V_e) and the coarse fraction (V_c) deposition velocities are defined as:

$$V_e = \frac{\text{Total atom deposition flux (atoms/cm}^2\text{/s) of progeny species on the sensor}}{\text{Total atom concentration (atoms/cm}^3\text{) in the atmosphere}}$$

$$V_c = \frac{\text{Coarse fraction atom deposition flux (atoms/cm}^2\text{/s) of progeny species on the sensor}}{\text{Coarse fraction atom concentration (atoms/cm}^3\text{) in the atmosphere}}$$

The total atom deposition flux was carried out by exposing the Direct Radon/Thoron Progeny sensors (DRPS/DTPS) in bare-mode (Mishra *et al.*, 2011) in the indoor and outdoor environments for a period of 90 days. The total atom concentration was obtained using filter-paper sampling for a period of 5 hours followed by alpha counting (Mishra *et al.*, 2009). The coarse fraction atom deposition flux was obtained by exposing DTPS/DRPS in wire-mesh capped mode (Mayya *et al.*, 2010). The coarse fraction atom concentration was obtained using wire-mesh and filter-paper sampling and counting the filter-paper by ZnS photomultiplier counter (efficiency 26%).

RESULTS

DEPOSITION VELOCITIES IN INDOOR ENVIRONMENT

The DRPS/DTPSs were deployed in bare-mode only in 15 houses and in bare mode+wire-mesh capped mode in 8 houses. The exposure continued for a period of 90 days, during which regular wire-mesh and filter paper sampling followed by alpha counting were carried out in these houses. At the end of exposure time, the detectors were retrieved, chemically processed and alpha track counting were carried out to estimate the deposited atom flux. The detectors in bare-mode yielded the total deposited atom flux, where as attached fraction deposited flux was obtained from the wire-mesh capped detectors. Fig. 1 shows the plot of deposited atom flux (both effective and attached fraction) versus the atom concentration in the respective rooms (both total as well as the attached fraction). The deposition velocity was obtained from the slope of the graph as indicated in the figure.

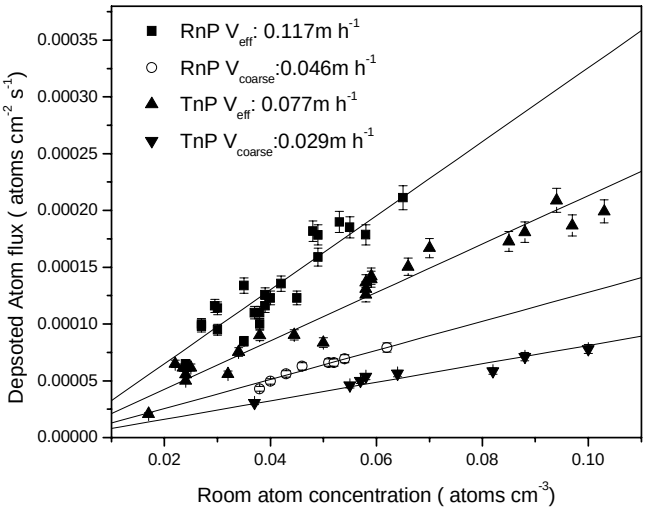

Figure 1. Deposited atom flux versus atom concentration in indoors.

DEPOSITION VELOCITIES IN OUTDOOR ENVIRONMENT

The DRPS/DTPSs were deployed in bare-mode only in 10 outdoor locations and in bare mode+wire-mesh capped mode in 8 outdoor locations. During 90 days exposure period, regular wire-mesh and filter paper sampling followed by alpha counting were carried out in these locations. At the end of exposure time, the detectors were chemically processed. The detectors in bare-mode and wire-mesh capped mode yielded the total and coarse fraction deposited atom flux respectively. Fig. 2 shows the plot of deposited atom flux (both effective and attached fraction) versus the atom concentration in the respective rooms (both total as well as the attached fraction). The deposition velocity was obtained from the slope of the graph as indicated in the figure.

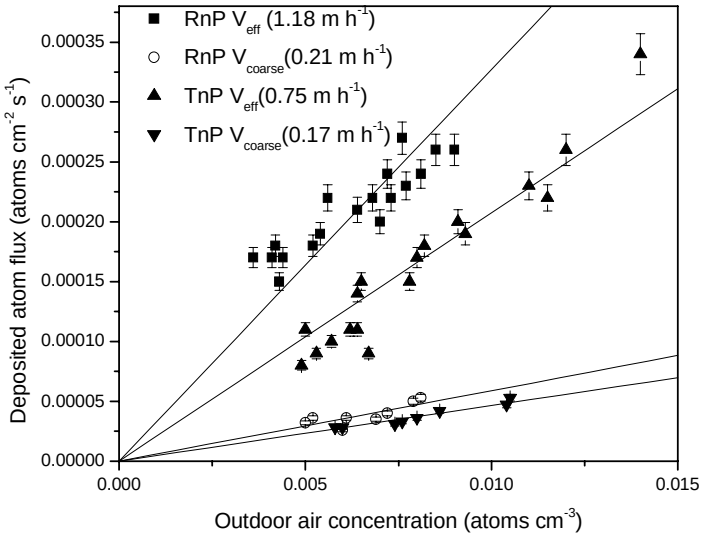

Figure 2. Deposited atom flux versus atom concentration outdoors.

CONCLUSION

The indoor and outdoor deposition velocities were measured using deposition based direct Radon and Thoron progeny sensors. The summary table of the deposition velocities is given in Table 1.

Indoor				**Outdoor**			
V_{eff} (m h^{-1})		V_{coarse}(m h^{-1})		V_{eff} (m h^{-1})		V_{coarse}(m h^{-1})	
RnP	TnP	RnP	TnP	RnP	TnP	RnP	TnP
0.117±0.015	0.077±0.012	0.046±0.002	0.029±0.002	1.18±0.19	0.75±0.1	0.21±0.03	0.17±0.01

Table 1. Summary values of the effective and coarse fraction deposition velocities of Radon and Thoron progeny in indoor and outdoor environments.

The ratio between outdoor to indoor effective deposition velocity was measured to be around 10 for both radon and thoron progeny, whereas the coarse fraction deposition velocity in the outdoor was found to be ~5 times higher than that measured indoor.

REFERENCES

Bigu, J. (1985). Radon daughter and thoron daughter deposition velocity and unattached fraction under laboratory controlled conditions and in underground uranium mines, *J. Aerosol Science*, **16 (2)**, pp. 157-165.

Jacobi, W. (1972). Activity and potential á-energy of ^{222}Rn and ^{220}Rn daughters in different air atmospheres, *Health Phys.*, **22**, pp. 441-450.

Knutson, E., George, A., Frey, J., Koh, B. (1983). Radon daughter plate-out, *Health Phys.*, **45**, pp. 445-452.

Mayya, Y. S., Mishra, Rosaline, Prajith, R., Sapra, B. K., Kushwaha, H. S. (2010). Wire-mesh capped deposition sensors: Novel passive tool for coarse fraction flux estimation of radon thoron progeny in indoor environments, *Science of the total environment*, **409 (2)**, pp. 378-383.

Mishra, Rosaline and Mayya, Y. S. (2008). Study of a deposition based Direct Thoron Progeny Sensor (DTPS) technique for estimating Equilibrium Equivalent Thoron Concentration (EETC) in indoor environment, *Radiation Measurements*, **43**, pp. 1408-1416.

Mishra, Rosaline, Mayya, Y. S., Kushwaha, H. S. (2009). Measurement of $^{220}Rn/^{222}Rn$ progeny deposition velocities on surfaces and their comparison with theoretical models, *Journal of Aerosol Science*, **40**, 1-15.

Morawska, L., Jamriska, M. (1996). Deposition of Radon progeny on indoor surfaces, *Journal of Aerosol Science* , **27 (2)**, 305-312.

Pörstendorfer, J., Wicke, A., Schraub, A. (1978). The influence of exhalation, ventilation and deposition processes upon their concentration of radon thoron and their decay products in room air, *Health Physics*, **34**, 465

Scott, A. G. (1983). Radon daughter deposition velocities estimated from field measurements, *Health Physics*, 45 **(2)**, 481-485.

EFFICACY OF UNIPOLAR IONIZERS ON ^{220}Rn PROGENY REMOVAL: STEADY SOURCE

PALLAVI A. KHANDARE, MANISH JOSHI, B. K. SAPRA, Y. S. MAYYA

Radiological Physics & Advisory Division
Bhabha Atomic Research Centre, Mumbai, India

Keywords: AEROSOL, THORON, PROGENY, IONIZER

INTRODUCTION

A significant fraction of the natural radiation exposure in humans results from the inhalation of the short lived, particulate decay products of ^{222}Rn (Radon) and ^{220}Rn (Thoron), which occur in free atmosphere and in higher concentrations in poorly ventilated rooms of buildings. Besides, radon/ thoron progenies pose a potential inhalation hazard in workplaces and confined areas such as thorium storage facilities. It is essential to control exposures to the workers engaged in day to day activities in these industries. In order to meet these requirements, considerable body of work has been carried out both in India and abroad on the various aspects pertaining to the behavior, measurement and hazard control of radon/thoron and their progenies.

The radon and thoron progeny aerosols in the atmosphere are generated in two steps: After the formation from the radon isotope by decay, the freshly generated radio-nuclides react very fast (< 1 s) with trace gases and air vapors, and become small particles, called clusters or "unattached" radio-nuclides with diameters ranging from 0.5 to 5 nm. Besides the cluster formation, these radio-nuclides attach to the existing aerosol particles within 1-100 s, forming the "attached" fraction of the radioactive aerosol of radon/thoron progeny. At the same time, the newly formed decay product clusters are positively charged (Postendorfer and Mercer, 1979) ^{218}Po (80-82 %) and ^{212}Pb (85-88 %). These ions become neutral by recombination with negative air ions and charge transfer processes involving NO, NO_2, H_2O vapors and other air impurities. As a result, the progeny atoms in the atmosphere exist both in charged and neutral state. Both attached and unattached fractions deposit in the human airways during inhalation and deliver alpha doses to the sensitive tissues. Deposition occurs by various mechanisms depending upon the cluster size and charge state of the decay products.

In view of the above, reduction of inhalation doses in radioactive workplaces can be greatly achieved by mitigating the concentration of progeny in these environments. While increased ventilation, filtration systems are large scale choices for reducing the concentrations, it may be of certain relevance if one can achieve reduction at local scales, i.e. specified work zones using non-intrusive techniques. In this context, it is worthwhile to examine this possibility by employing unipolar air ionizers. Corona discharge based unipolar ionizers have been commonly used for reducing aerosol particle concentrations in indoor environments. These ionizers generate ions which help in charging the particles in the room, and subsequently they are migrated to the walls, floors etc. due to space charge induced electric fields. Particle charging and electro-migration are the main mechanisms responsible for particle removal.

Several room studies and chamber experiments have been conducted in the past to examine the feasibility of particle reduction using ionizers. For example, Bohgard and Eklund (1998) studied the

effect of an ionizer on sub micron particles in indoor air. In a study by Sapra *et al.* (2011) the dependence of size on particle removal from air in the presence of ionizers was studied using the combustion particulates generated from mosquito repellent coils.

These studies have been extended to radon/thoron progeny as well. Bigu (1983) has investigated the effect of a negative ion generator and a mixing fan on the plate out of radon decay products in an experimental radon/thoron box. A substantial decrease was observed, when negative ion generator, fan or both were operated. In another study, Sheets and Thompson (1995) found that the activity concentrations of decay products decreased when the ionizer was switched ON, and increased when they were turned off again. Such studies have been extended to study the effect of ion generators in reducing the concentrations of radon/thoron progeny thus leading to lowered inhalation doses (Li and Hopke 1991, Hopke *et al.*, 1993). A study by Joshi *et al.*, (2010) demonstrates the feasibility of reducing the activity concentrations in room environments upto a factor of about 7. Even though, ionizer technique leads to increase in the unattached fraction, the total inhalation dose incurred is lowered with the use of ionizer. This study proves that for realistically achievable activity reduction ratios of about 3-5 with the employment of ionizers, the inhalation dose in workplace environments can be reduced by a factor of at least 4. In another study by Joshi *et al.*, (2011) particle and activity concentration has been compared for three experimental conditions (two for positive ions and one for negative) in an unoccupied room with elevated ^{220}Rn levels. The negative ionizer configuration provided a better concentration reduction factor of about 4.59 with the smallest characteristic depletion time of 13 min.

Although several experimental studies to show the effectiveness of ion generators in reducing particle concentrations, in general and radon/thoron progeny in particular, there are not many studies which model the possible mechanisms leading to this effect. A significant effort to quantify the phenomenon was carried out by Mayya *et al.* (2004). This model describes aerosol removal by unipolar ionizers by formulating a system of equations considering various processes responsible for this removal. These pertain to the space charge generated electric field, particle removal rates under the combined action of diffusion, gravitational sedimentation, external ventilation and electric fields. However, this model is limited to the realm of non radioactive particles and cannot be used to estimate the reduction of particulate radioactivity concentration in the presence of unipolar ionizers. To extend its scope for the latter case, the formation and decay equations of the progeny radionuclides need to be integrated into this model. The aim of this work is to validate this combined model with the experimental data.

THEORETICAL FORMULATION

Detailed modeling of the decay product behavior in the presence of the ionizer first requires the setting up of equations for the electric field, ion concentration and particle charging and depletion. These have been formulated earlier by Mayya *et al.* (2004). The important quantities of interest are being mentioned here. Under the assumption of spatially uniform ion and particle concentrations and a characteristic charge $q_c = q_c(t)$ per particle, the surface averaged electric field $E_S(t)$ at the depositing wall of surface area A of a room of volume V is given by:

$$E_S(t) = \frac{1}{A}\oiint_A \vec{E}.d\vec{A} = \frac{e}{\varepsilon_0}\left[n(t) + q_C(t)C(t)\right].\frac{V}{A} \qquad (1)$$

Where e is the elementary charge, e_0 is the permittivity of free-space, $n(t)$ is the ion concentration and $C(t)$ is the aerosol particle number concentration.

For the case wherein particles of charge q (0, ±1, ±2,…) are constantly introduced into the room at a steady volume-averaged rate of $S(q)$ per unit volume, with $C(q,t)$ as the concentration of particles with q charges at time t., the unipolar charging equation may be written as

$$\frac{\partial C(q,t)}{\partial t} = n(t)K(q-1)C(q-1,t) - \left[n(t)K(q) + \lambda_p(q,t) + \lambda_v\right]C(q,t) + S(q) = 0 \qquad (2)$$

After the ionizer is switched on, these particles are removed from air space at an instantaneous rate of (l_p+l_v) where $l_p=l_p(q,t)$ is the removal rate due to wall deposition and l_v is the ventilation rate. $K(q)$, the ion-particle attachment coefficient between the q-charged particles having the same sign of charge as the unipolar ions is given by (Mayya and Sapra, 2002).

The generalized particle removal rate in the presence of the ionizer, l_p(t) is given by:

$$\lambda_p(t) = \sum_{\sigma=-1}^{1} f_\sigma \left[\frac{\lambda_p^E(t) - \sigma\lambda_p^g}{1 - \exp\left\{-\left(\lambda_p^E(t) - \sigma\lambda_p^g\right)/\lambda_p^d\right\}}\right] \qquad (3)$$

The superscripts E, g and d refer to the removal rates due to electrical effects, gravitation and diffusion respectively. The symbol s =cos(q) where q is the angle between the surface normal and acceleration due to gravity.

^{220}Rn decays to give three important short-lived progeny species namely, ^{216}Po (ThA: 0.158 s), ^{212}Pb (ThB: 10.6 hr) and ^{212}Bi (ThC; 60.5 min). These may exist in both the fine (unattached) and coarse (attached) forms. The fine fraction may again be positively charged or neutral. To qualitatively understand the kinetics of the progeny in the presence of the ionizer, first consider the charged fraction of the first progeny species namely, Po^{216}. In the ionizer field, it undergoes motion in the direction opposite to the motion of negative ions. During the migration, the ^{216}Po ion may loose charge due to recombination with negative ions, or due to charge transfer to water vapour or trace gases. Its subsequent motion in the field occurs due to attachment to aerosol particles until it transforms to ^{212}Pb by radioactive decay. Similar processes would also occur with other progeny species. Quantitatively, the above mechanisms may be modeled as follows:

For an activity concentration a_0 of ^{220}Rn present in the room, the number concentrations for the fine fractions $N_{1,f}^{+}$ and $N_{1,f}^{0}$ (positively charged and neutral) and the coarse attached fraction $N_{1,c}$ of ^{216}Po (ThA) are presented below:

$$\frac{\partial}{\partial t}N_{1,f}^{+}(t) + \left(\lambda_1 + \lambda_v + \lambda_{1,f,w}^{+} + \lambda_{1,f,neut}^{+} + X(t)\right)N_{1,f}^{+}(t) - a_0 = 0 \qquad (4)$$

$$\frac{\partial}{\partial t}N_{1,f}^{z}(t) + \left(\lambda_1 + \lambda_v + \lambda_{1,f,w}^{z} + X(t)\right)N_{1,f}^{z}(t) - \lambda_{1,f,neut}^{+}N_{1,f}^{+}(t) = 0 \qquad (5)$$

$$\frac{\partial}{\partial t} N_{1,c}(t) + \left(\lambda_1 + \lambda_v + \lambda_c(t)\right) N_{1,c}(t) - X(t)\left(N^{+}_{1,f}(t) + N^{z}_{1,f}(t)\right) = 0 \qquad (6)$$

In the above, l_1 is the radioactive decay constant of ^{216}Po, l_v is the leak rate in the vessel, $\lambda^{0}_{1,f,w}, \lambda^{+}_{1,f,w}$ is the background wall deposition rate and ionizer enhanced deposition rate of fine fraction, l_c is the wall loss rate of coarse fraction, $\lambda^{+}_{1,f,neut}$ is the neutralization rate of charged fine fraction and $X(t)$ is the attachment rate to aerosols. Similar equations will hold for ThB and ThC.

EXPERIMENTAL DESCRIPTION

In order to study the behavior of progeny aerosols in the presence of ionizers in room sized environment, experiments were carried out in a room of volume 16 m^3. The schematic diagram of the experimental set up and instruments is shown in Fig. 1. 60 g of Thorium nitrate powder was used as source of ^{220}Rn, placed at the centre of the room at a distance of about 50 cm from the ground level. A small fan was kept operating in the room so as to homogenize the thoron concentration in the room. Online thoron monitor RAD7 was used to record the thoron concentration in the room. Five units of negative ion generators (NIG) were placed about 80 cm apart from the source and at the same level from the ground as the source. Particle number size measurements were recorded online using Scanning Mobility Particle Sizer (SMPS). The progeny concentrations were estimated using gross filter paper sampling @ 10 lpm, for the filter paper being counted for alpha activity. For the measurement of the fine fraction of the progeny in the room wire mesh sampling was carried out at regular intervals, again these screens and filter paper were counted for gross alpha counts.

Thorium nitrate powder source was kept open for 24 hours so as to get enough thoron and progeny concentrations in the room and was kept open throughout the experiment. After ascertaining steady concentrations of thoron as well as progeny in the room, ionizers were switched ON and the temporal variation in unattached fraction, progeny activity concentration and aerosol number concentrations were continuously monitored for 10-12 hours. The rises in activity and number concentration were also recorded after the ionizers were switched off.

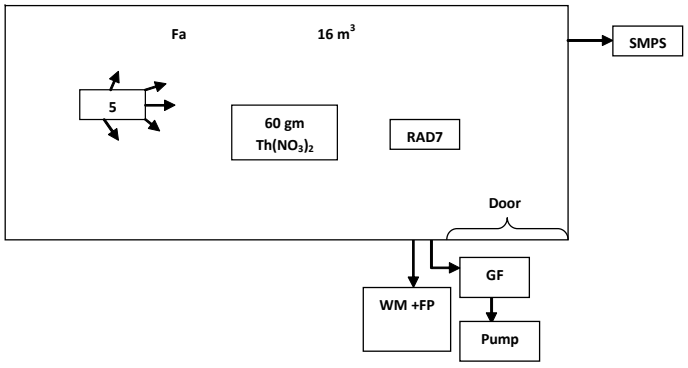

Figure 1.Schematic diagram for the experimental setup

RESULTS AND DISCUSSIONS

Steady ^{220}Rn concentration in the room as recorded by RAD7 was found to be about 1140±703 Bq/m^3. Progeny concentration in the room before ionizer on was found to be about 60 to 70 Bq/m^3. Reduction in progeny and aerosol number concentrations was observed after ionizer was switched on.

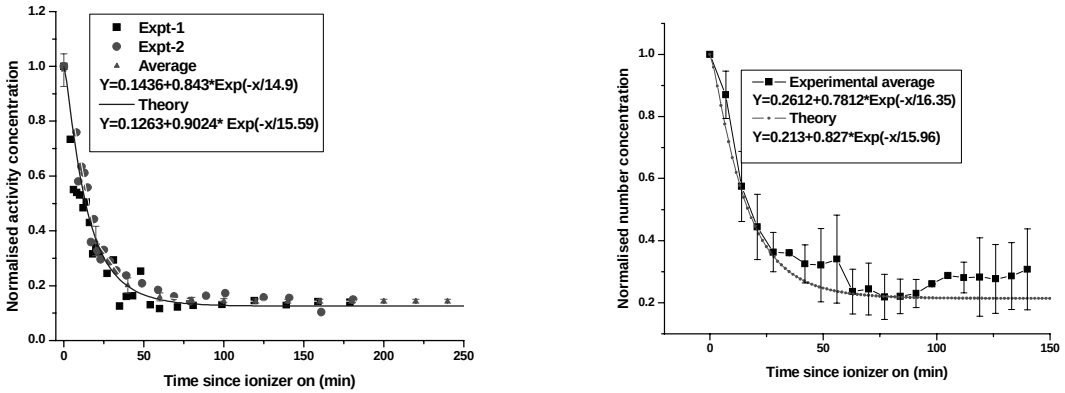

Figure 2. Comparison of experimental and theoretical curves of depletion in activity and aerosol number concentration sin the presence of ionizer

In case of steady source experiments, the progeny activity concentrations decreased by a factor of 7. The variation in activity concentration due to progeny was fitted to an exponential fit to obtain the mean progeny residence time in the room, which was found to be about 14.9 minutes (Fig. 2). The experimental results have been compared with the theory and a theory shows a close agreement with the experimental curve with a mean residence time of 15.59 minutes.

The variation in particle number concentration as recorded by SMPS showed the mean aerosol lifetime in the room to be 16.35 minutes which is matching with the theoretical value 15.96 minutes. The number particle size distributions in the room as recorded by SMPS before the operation of ionizer and in the presence of ionizer are shown in Fig. 3(a). It clearly depicts the lowered particle number concentration in all the size ranges with the use of ionizer. The particle number concentration reduction factor (CRF), which is defined as the ratio of steady particle number concentration without NIG to with NIG are plotted against varying particle sizes Fig. 3(b). CRF shows that the particle number concentration is greater than 1 for all the particle sizes, is maximum, about 7-8 times for sizes of 50-100 nm. Also, the comparison with the theoretically obtained values has been shown, which agree quite well with the experimental values for particles all greater than 30 nm. The discrepancy for the particles below 30 nm, could be due to the assumption of average characteristic charge on a particle used in the theory which may not be valid for very small particles.

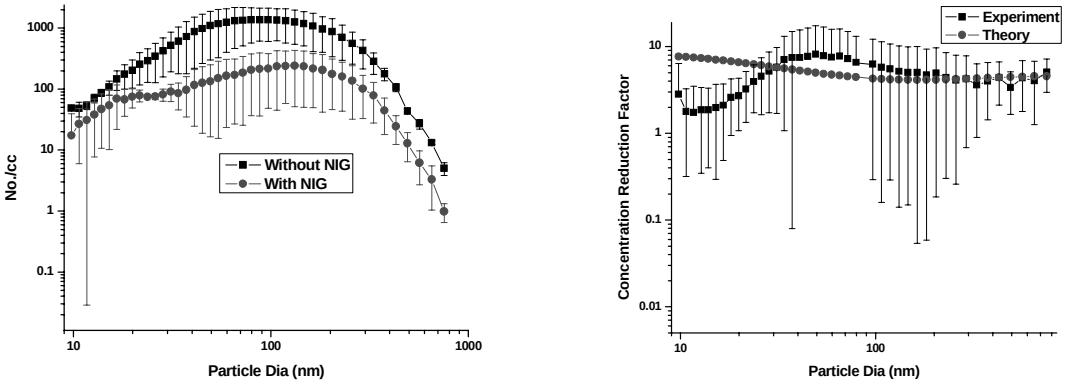

3(a) 3(b)

Fig. 3(a) Particle number size distributions without and with ionizer 3(b) Comparison between the particle number concentration reduction factors obtained experimentally and theoretically

The count median diameters (CMD) are found to be decreasing from 83.77 nm with a geometric standard deviation (GSD) of 2.06 to 56.33 nm with a GSD of 2.28. As is seen from the CRF curve ionizers are more effective for larger particle removal, hence the mean size gets shifted to lower size ranges in the presence of ionizers. The same could also be inferred from the unattached fraction measurements, as the fine fraction increases from about 1.4 % to 29.98 % due to ionizer action.

CONCLUSIONS

It could thus be concluded that the implication of ionizer technique leads to reduction in airborne activity concentration due to ^{220}Rn progeny. The problem could successfully be theoretically formulated and the experimental results are in fair agreement with the theoretically predicted ones. This study has a possible application in the thorium storage areas where airborne alpha activity levels due to progeny is very high and may pose significant inhalation hazard to the person entering. Ionizers are very effective, relatively cheaper and feasible option than the highly expensive and bulky ventilation and filtration systems to reduce the inhalation risk.

REFERENCES

Postendorfer, J. and Mercer, T.T. (1979). Influence of Electric charge and humidity upon the Diffusion Coefficient of radon decay Products, *Health Physics,* **37**, pp 191-199.

Bohgard, M., and Eklund, P. (1998). Effect of an ionizer on sub micron particles in indoor air, Journal *of Aerosol Science,* **29**, pp S1313-S1314.

Sapra, B. K., Kothalkar, P. S., Joshi, M., Khan, A., and Mayya, Y. S. (2011). Mitigating particulates emitted by mosquito coils using unipolar ionizers: Implications to the deposition in Human respiratory Tract system. Indoor and Built Environment, pp 1-13, DOI: 10.1177/1420326X11424769.

Bigu, J. (1983). On the effects of a negative ion generator and a mixing fan on the plate out of radon decay products in a radon box, Health *Physics,* **44(3)**, pp 259-266.

Sheets, R. W. and Thompson, C. C. (1995). Effects of negative ion generators on radon and thoron progeny concentrations in an occupied residence, *Journal Radioanalytical Nuclear Chemistry,***193(2)**, pp 301-308.

Li, C. C. and Hopke, P.K. (1991). Efficacy of air cleaning systems in controlling indoor radon decay product, *Health Physics,* **61**, pp 785-797.

Hopke, P. K., Montassier, N., and Wasiolek, P. (1993). Evaluation of the effectiveness of several air cleaners for reducing the hazard from indoor radon progeny, *Aerosol Science and Technology,* **19**, pp 268–278.

Joshi, M., Sapra, B. K., Khan, A., Kothalkar, P., and Mayya, Y. S. (2010). Thoron (^{220}Rn) decay products removal in poorly ventilated environments using unipolar ionizers: Dosimetric implications, *Science of Total Environment,* **408(23)**, pp 5701-5706.

Joshi, M., Sapra, B. K., Kothalkar, P. S, Khan A., Modi R., and Mayya Y. S. (2011), Implications of polarity of unipolar ionizers on reduction of effective dose attributable to thoron progeny, *Radiation Protection Dosimetry,* **145(2-3)**, pp 256-259.

Mayya, Y. S., Sapra, B. K., Khan A., Sunny F., (2004), Aerosol removal by unipolar ionization in indoor environments, *Journal of Aerosol Science,* **35**, pp 923-941.

Mayya, Y. S. and Sapra B. K. (2002). Kinetic derivation of the electro-migration equation for aerosol particle in the presence of bipolar charging, *Journal of Colloid & Interface Science,* **284**, pp 283-294.

SEASONAL VARIATION IN RADON PROGENY CONCENTRATION INSIDE A LABORATORY HAVING ONCE THROUGH VENTILATION

T. DAS, V.A.P. BARA, D.JAT AND P.SRINIVASAN

Radiation Safety System Division, Bhabha Atomic Research centre
Trombay, Mumbai-400085

Keywords: RADON DAUGHTER, MINIMUM DETECTABLE ACTIVITY, TRANSURANICS, GROSS ALPHA COUNTING

INTRODUCTION

Radon and its short-lived decay products in the atmosphere are the most important contributors to human exposure from natural sources. ^{222}Rn (Radon) and ^{220}Rn(Thoron) are the gaseous members of the naturally occurring Uranium and Thorium series which diffuses out of the earth into the air. The radioactive radon daughters, which are solids under ordinary conditions, attach themselves to the atmospheric dust. Atmospheric concentration of radioactivity from this source varies widely around the earth and is dependent on the local concentrations of Uranium and Thorium in the soil. The atmospheric concentrations of radon daughters also depend on the temperature profile of the atmosphere. Seasonal variation in the atmospheric concentration of radon is also observed. The radon progeny concentration is likely to be functions of a) Uranium and Thorium content of building material b) emanation rate from building material; c) rate of vertical mixing; d) rate of horizontal transport or advection and e) removal due to ventilation and settling.

The monitoring of radioactive aerosols in a plant or a laboratory is done by sampling the aerosol on a filter paper and estimating the activity deposited on the filter paper. The particulate matter will also contain naturally occurring short lived radioisotopes of Radon gas. The daughter products of radon being particulate in nature and alpha active they interfere with the detection of alpha emissions from transuranic isotopes. Even in the absence of long lived alpha emitters, the filter when analyzed immediately shows possible air-borne contamination. Therefore either radiochemistry is utilized to separate the anthropogenic activity from naturally occurring radioactive materials or the filter sample is allowed to decay sufficiently to make radon/thoron progeny contribution negligible. These methods take considerable time and hence immediate assessment of air-borne concentration of long-lived component in the filter sample is not possible.

In a spent fuel reprocessing plant and also in a plutonium fuel fabrication facility, prompt and timely detection of air-borne plutonium is not only an essential requirement for minimizing inhalation hazard, but also an aid in the investigation of the source causing it. Presence of short lived daughter products of ^{222}Rn and ^{220}Rn in air interferes with the prompt detection of airborne plutonium. Hence, to find out the transuranic concentration in air one has to subtract the concentration of naturally occurring radioisotopes from gross alpha emitter concentration. It is observed that this short lived activity concentration varies with temperature, wind speed, rainfall etc.

A low cost continuous air monitor based on gross alpha count can be developed if the variation in background count rate is known and incorporated in the design of the system. The minimum detectable activity by a system is given by

MDA= $\frac{2.71+4.6\sqrt{B}}{\varepsilon}$ (Hurtgen *et al.*, 2000).

Where, *B* is the background count rate due to Radon daughter products. e is the efficiency of the detector. In this paper, the seasonal variation of naturally occurring short lived isotope concentration is presented which implies the similar variation in Radon/Thoron concentration in the near surface atmosphere.

MATERIAL AND METHODS

Air samples were collected over a period of three years, from January 2009 to December 2011, on 38mm dia glass fiber filter papers amounting to 675 total air samples. The samples were taken inside an air conditioned, once through ventilated room having a ventilation rate of 10 air changes per hour. The temperature profile of the room as well as of outside the lab was recorded for the entire sampling period. The samples were collected for duration of 8 hrs (daytime) at a flow rate of 0.04 m^3/min. The samples were counted for gross alpha activity on a ZnS(Ag) based counting system. Efficiency of the counting system was measured throughout the sampling period and was found to be within 1.5 percentage points of 33%. The delay time from the flow switch off and time of actual counting varied from 5 to 8 minutes with an average time delay of 6 minutes. The filter samples were counted for duration of 1 min to obtain the gross alpha activity due to radon progeny in the filter paper.

Monthly averages of the radon progeny activity was calculated and was plotted against time for each individual year. The activity values were normalized with respect to the activity concentration of January month of respective year. Fig. 1 presents the seasonal variation of the radon progeny in ambient air. To correlate the variation with the temperature of the atmoshphere, the monthly average temperature variation was also noted and shown in Fig. 2.

RESULTS AND DISCUSSION

From Fig. 1, It was observed that the Radon daughter products concentration decreases as summer appears and it remains at its low till the end of monsoon and the again it increases during winter season. The short lived activity concentration in summer was in the range of 14% to 20 % of the concentration in winter.

Since air-conditioned air was being supplied to the laboratory, the temperature inside the laboratory did not vary much. It was outside weather condition which caused a variation in Radon daughter product concentration and was reflected in the air-sample taken from inside the Laboratory. From Fig. 2, one can also draw a conclusion that the Radon emanation from the building material was very less as compared to the outside radon contribution to the laboratory air.

CONCLUSION

The monthly variation in the levels of Radon and Thoron progeny concentration in a laboratory having once through ventilation system is presented. The variation was measured with respect to outdoor and indoor temperature and relative humidity. A seasonal variation in the activity with winter maximum and summer minimum is observed. This study provides a baseline data to interpret the gross alpha activity for its long lived component in the presence of short lived components. The study highlights the feasibility of developing continuous air monitor by gross alpha counting by incorporating the variation in the background count with respect to time.

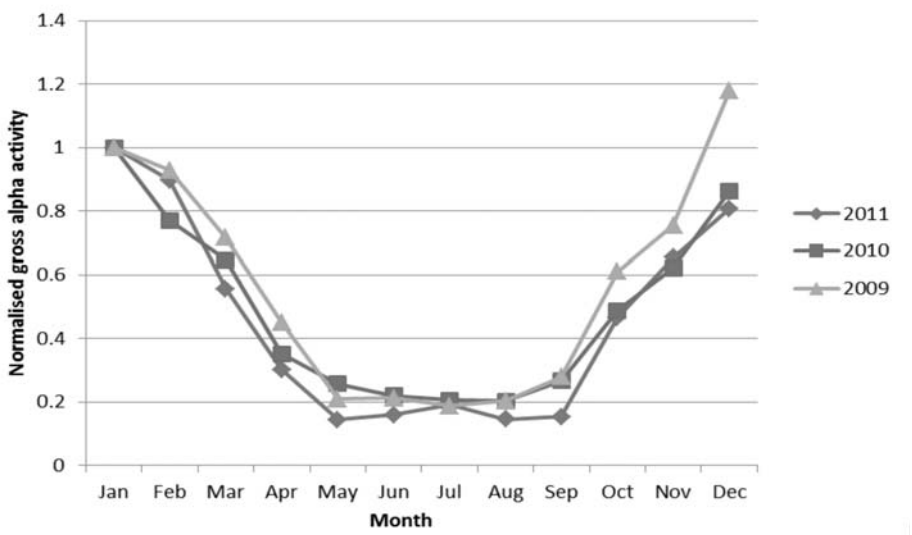

Figure 1. Monthly variation of short lived particulate activity concentration

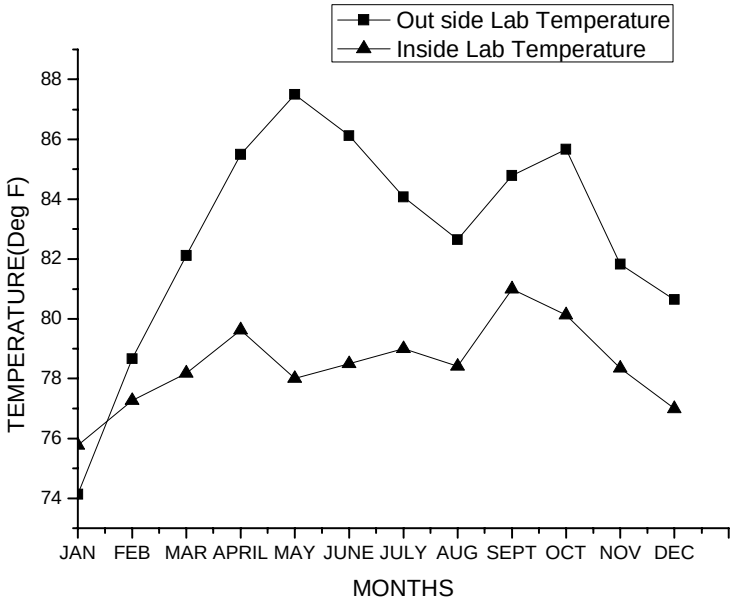

Figure 2. Monthly variation of temperature profile inside and out side the Laboratory atmosphere

ACKNOWLEDGMENT

The authors are thankful to Product Development Division staff at South Site, BARC for providing their help and suggestion for this study.

REFERENCES

Hurtgen C, Jerome S and Woods M (2000). Revisiting Curie-How low can we go?, *Applied radiation and Isotope*, **53**, 45-50.

STANDARDISATION OF SODIUM AEROSOLS CHARACTERISATION TECHNIQUE

AMITKUMAR, V. SUBRAMANIAN, J. MISRA, R. BASKARAN AND B. VENKATRAMAN

Radiological Safety Division, Electronics Instrumentation & Radiological Safety Group
Kalpakkam-603 102, INDIA

Keywords: SODIUM AEROSOL, SILVERINA

INTRODUCTION

In the normal operation of the fast reactors, evaporation of sodium from the hot sodium pool surface and subsequent condensation results in the formation of sodium aerosol within the cover gas space. These aerosols are pure sodium metal aerosols and they form as a mist near the pool surface and as height increases from the pool, condensation of vapour results in formation of larger sized aerosols. When sufficient concentration, these aerosols will participate in the radiative exchange within the cover gas space and modify the total heat transfer to the cooled roof structure by absorption and scattering mechanisms. Further, the mass transfer occurs due to deposition of sodium aerosols on the bottom surface of the roof plug and side wall, which may get affected when these droplets fall back to sodium pool surface. The sodium aerosols can also deposit in annular gap of rotating plug (Kumar *et al.*) .Thus, in order to predict the interaction of thermal radiation with an aerosol and mass transfer due to condensation of aerosols, it is necessary to know the aerosol concentration and droplet size distribution. It is also to be considered that sodium aerosol properties would get modify due to (i) temperature difference between the sodium pool surface and the bottom of the roof top plug and (ii) possible enhanced coagulation of sodium aerosols upon interaction with gamma radiation, resulting increase in sizes. Hence, it is proposed to carry out the experimental studies to characterize the size distribution and mass concentration of sodium aerosols in the cover gas region by adopting suitable procedures. The initial experiments are planned to be conducted in SILVERINA sodium loop facility at Fast Reactor Technology Group (FRTG) and fallowed by Fast Breeder Test Reactor (FBTR) under two conditions i.e. (i) when reactor is shut down and (ii) when reactor is operating. Before getting into the sampling system design, a suitable technique for the characterization of sodium aerosols has been adopted and qualified in Aerosol Test Facility (ATF) (Baskaran *et al.* 2004) .The challenge lies here is to aspire the sodium metal aerosols into the collector (without exposing them to the environment, because it will catch fire) and analyze them using off-line technique. In this context, the experimental procedure, sampling and analysis techniques for measurement of sodium aerosols were standardized. The sodium aerosols are generated in combustion cell and sampling was carried in ATF. The sodium aerosols size distribution & mass concentration were determined using suitable techniques and results are presented in this paper.

SAMPLING PROCEDURE

The schematic diagram of the sampling systems is shown in Fig.1. The fig. 1 also includes the photograph of the gas washing bottles trapped with sodium aerosols.

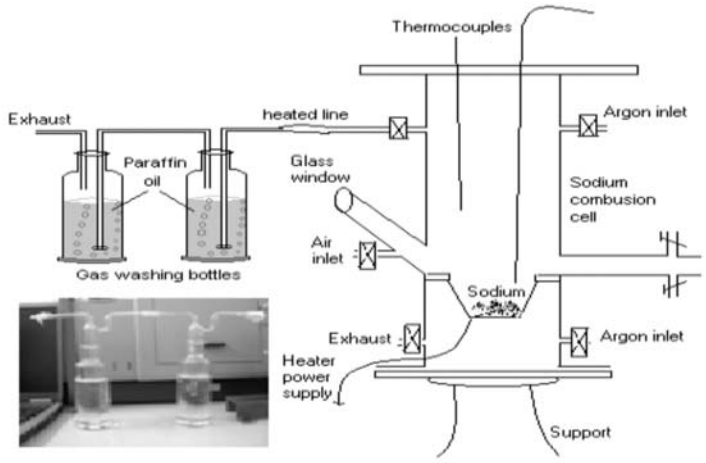

Figure 1. Schematic representation of sampling system

About 5g of sodium is heated in Argon environment, with the help of electrical Bunsen heater, up to 500°C. After attaining the temperature of 500°C, the vapour along with argon gas is made to bubble through a gas washing bottle filled with liquid paraffin oil (200ml) at a flow rate (f) of 2lpm and sampling time (t) for about 10 minute. The sodium aerosols condense in the liquid paraffin while argon escapes out. The 2nd bottle is used to trap the sodium aerosols if any, escaped from the first bottle. To prevent sodium aerosols condensation and solidification within the sampling tube the wall temperature of the sampling tube is maintained at the temperature (110°C) by externally wound wire heaters. Temperature of sampling tube is monitored by thermocouple and the current in heating coil is controlled by using Proportional Integral Derivative (PID) temperature controller.

AEROSOL DIAGNOSTICS TECHNIQUES

Technique for measuring sodium aerosols size distribution

The measurement of sodium aerosols size distribution is carried out by using Mastersizer(M/s Malvern Instruments, UK). The Mastersizer uses the principle of ensemble diffraction technique. The instrument is provided with a liquid flow cell and a powder spray unit and these units are useful for the measurement of particle size distribution in liquid and air medium respectively. The sampling liquid (dispersant) with suspended aerosols is made to circulate across the laser beam by using a liquid flow cell. Particles in the beam scatter light in all directions. By measuring the scattered light intensity spectrum at an angle 'θ' and obscuration of the laser beam by the aerosol and comparing this to a background measurement taken under identical conditions with no aerosol present, gives the particle size distribution. The Mastersizer measures the volume-size distribution of particles in the laden volume of liquid medium from 0.05 – 900 mm. Sodium aerosols trapped in the liquid parafin is made to circulate in the liquid flow cell and the volume-size distribution and its MMD of the sodium aerosols are determined.

Technique for measuring sodium aerosols mass concentration

The measurement of sodium aerosols mass concentration is carried out by conductivity method using the instrument conductometer (M/s Metrohm, 856 conductivity module, Switzerland). The instrument works on the principle of Ohm's law. The sampling probe consists of two plates which

would be immersed in a sample solution. Conductivity (G), the inverse of resistivity (R), is determined from the applied voltage and current values for various concentration of the solution. For this, known quantity of sodium in steps of 5mg is added into 100ml of demineralised (DM) water. The change in conductivity is measured using Metrohmconductometer (the conductivity of DM water is around 1μS/cm). Every addition of 5 mg of sodium produces change in conductivity. A graph is drawn with sodium mass versus conductivity and it is shown in Fig. 2, which fallows a linear fit.

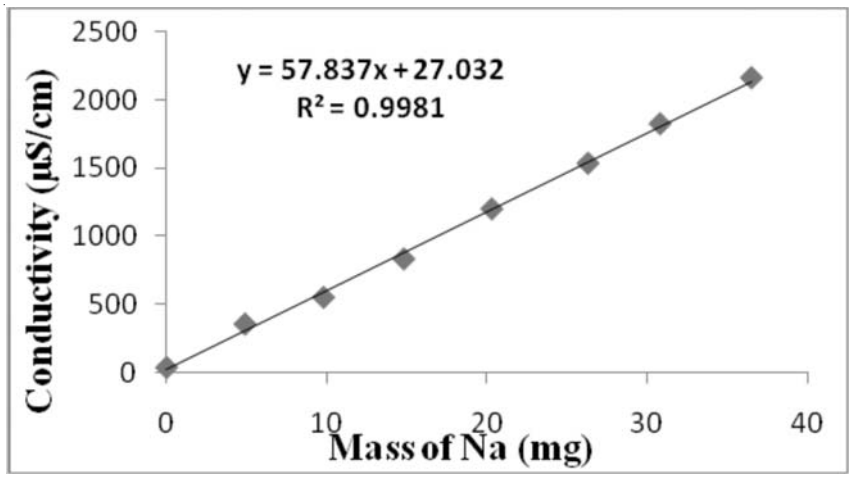

Figure 2. The conductivity versus Sodium mass graph

RESULT AND ANALYSIS

Sodium aerosols size distribution

The liquid paraffin from the two bottles was analyzed with the Master-sizer to determine the size distribution of trapped sodium aerosols. The volume size distribution of sodium aerosols is given in Fig. 3. It is observed from the Fig. 3, that the particles range in size from5.68 – 12.20 μm with Mass Median Diameter (MMD) at7.72 μm.

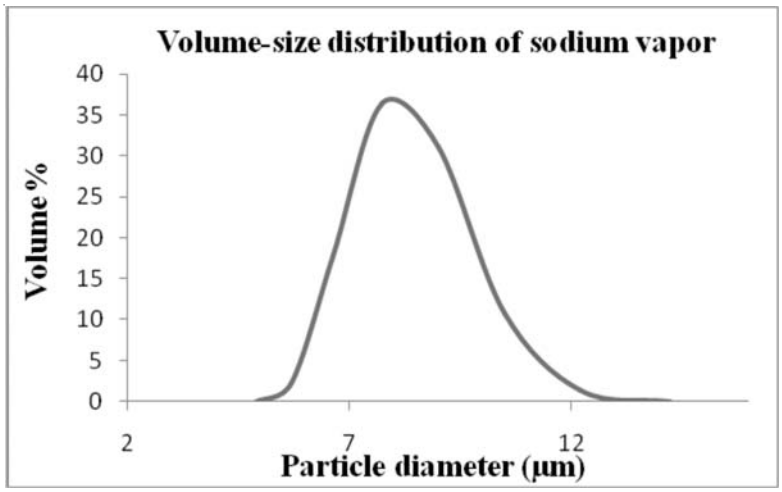

Figure 3. Volume – size distribution of sodium aerosols

Sodium aerosols concentration

The mass of sodium aerosols trapped in the liquid paraffin is measured by transferring them into a water medium (to become NaOH) and measuring the change in conductivity of the NaOH solution by using Metrohmconductometer. 200ml of liquid paraffin (trapped with sodium aerosols) is mixed with same amount of water (1:1 ratio) in a separating funnel to transfer the sodium into the water medium (to become NaOH). Out of 200ml solution, 100 ml solution is taken for the conductivity measurement. The conductivity of the 100ml solution is found to be 125μS/cm. Using the calibration graph the quantity of sodium in the paraffin is estimated and it is found to be 1.719 mg. After knowing the sodium mass, by adopting suitable corrections for the volume of the sample, the sodium aerosols mass concentration in combustion cell is calculated and it is found to be 0.173 g/m^3. It is observed that, in few trial experiments, the conductivity of the paraffin oil filled in the second bottle hardly show 2-5 μS/cm, for which the estimated sodium aerosol mass concentration is negligible. Hence, it is taken that for the sample concentration of about few mg/m^3, the first bottle is sufficient to have nearly 100% efficiency. However if the sample concentration exceeds upto few g/m^3, the concentration estimated from the second bottle will be added-up to estimate the actual concentration of the sample. The result obtained from the conductivity measurement is cross checked with conductometric titration (Subramanian *et al.* 2009) method. The same 100ml solution was analyzed and the sodium aerosols mass concentration in combustion cell is estimated to be 0.18 g.m^{-3}. It is observed that, the error associated with measurement of mass concentration between these two methods is estimated to be 5.5%.

SUMMARY

The experimental procedure and sampling/analysis techniques adopted for the measurement of sodium aerosols were standardized. The result obtained using this technique was evaluated by conventional chemical analysis, and it is proved to have good agreement. This technique will be used further characterization of sodium aerosols in cover gas region of SILVERINA sodium loop facility at Fast Reactor Technology Group (FRTG) and fallowed by Fast Breeder Test Reactor (FBTR).

As stated in our introduction, in order to conduct the experiment at SILVERINA sodium loop facility and FBTR, a sampling system along with special bottle arrangement is designed, fabricated, and installed (Kumar *et al.*).The photo graph of the sodium aerosols sampling system integrated with SILVERINA sodium loop facility is shown in fig.4.

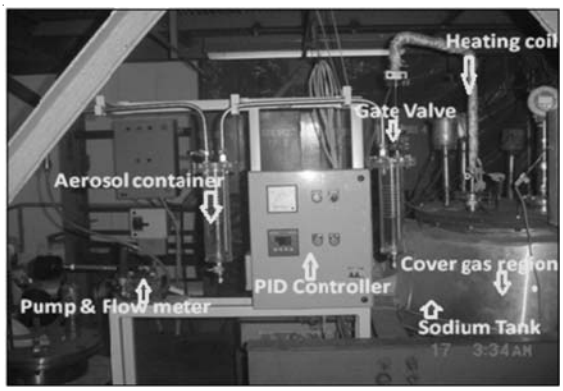

Figure 4. Photo graph of the sodium aerosols cover gas sampling system

Fig.4 shows Test Pot (TP) -1, sodium tank& cover gas region of SILVERINA loop and aerosol sampling system (gate valve, surface heater, PID controller, aerosol container, flow metre and pump). The experiments are being planned by drawing suitable operational procedures.

REFERENCES

Kumar, Amit, Subramanian, V., Baskaran, R., and Venkataraman, B. Review on sodium aerosol characteristics in cover gas region of SFR ,IGC/RSEG/RSD/RIAS/92614/GI/3018/REV-A.

Baskaran, R., Selvakumaran, T. S., Subramanian, V. (2004). Aerosol test facility for fast reactor safety studies, *Indian journal of pure & applied physics*, **42**, pp. 873-878.

Subramanian, V., Sahoo, P., Malathi, N., Anathanarayanan, R., Baskaran, R., Saha, B. (2009). Studies on Chemical Speciation of Sodium aerosols produced in Sodium fire, *Nuclear Technology*, **165**, pp.257.

Kumar, Amit, Krishnakumar S., Subramanian, V., Chandramouli S., Baskaran, R., Nashine, B. K., Venkataraman, B., Rajan, K. K. Sodium aerosols characterization in cover gas region of SILVIRINA loop",IGC/RSEG/RSD/RTAS/92614/EP/3019/REV-A.

RADIOACTIVE AEROSOLS AND RADON MEASUREMENTS AT NARL, GADANKI

KAMSALI NAGARAJA[1], K. CHARAN KUMAR[1], T. RAJENDRA PRASAD[2], T. NARAYANA RAO[2] AND M VENKATARATNAM[2]

[1]Department of Physics, Bangalore University, Bangalore 560 056
[2]National Atmospheric Research Laboratory, Department of Space, Gadanki – 517 502
Email: kamsalinagaraj@bub.ernet.in (Nagaraja)

Keywords: RADON, PROGENY, AEROSOLS, ALPHAGURARD.

INTRODUCTION

Natural radioactive aerosols form as a result of the decay of radon isotopes emitted from the soil surface into the atmosphere, as well as during the interaction of particles of cosmic radiation with the nuclei of atoms of elements that are components of the air. The radioactive atoms thus formed precipitate onto particles of nonradioactive atmospheric dust. In addition, dust containing radioactive isotopes of potassium, uranium, thoriumand is carried from soil surface into atmosphere by winds. Certain quantity of radioactive aerosols enteratmosphere with cosmic dust and meteorites. Artificial radioactive aerosols containing fission products and radioactive isotopes with induced radioactivity are formed within a certain radius from the explosion of a nuclear bomb, as well as in industrial or accidental radioactive emissions at atomic industry plants, in uranium mines, and in enrichment plants. Composition of radioactive aerosols depends on their origin and on atmospheric conditions.

The ultimate fate of radon is transformation through radioactive decay. Radon decays only by normal radioactive processes, that is, an atom of radon emits an alpha particle resulting in an atom of polonium, which itself undergoes radioactive decay to other radon progeny. In soil, radon is transported primarily by alpha recoil and mechanical flow of air and water in the soil. Alpha recoil is the process by which radon, when it is formed by radium emitting an alpha particle, actually recoils in the opposite direction from the path of particle ejection. If radon gets released into the pore spaces, its ultimate entry to ambient air is function of the soil porosity and meteorological factors. Once radon is released to ambient air, its dispersion is primarily determined by atmospheric stability, including vertical temperature gradients and effects of wind.

The radon gas is a scourge by nature. Not only the gas itself but also its progeny are radioactive. In addition, it uses its physical properties to spread like gases do and its progeny uses its physical properties to spread or attach like aerosols or dust do. The activity size distribution of the short-lived radon decay products is an important parameter for the estimation of radiation dose by inhalation, because the amount and the place of the inhaled activity in the lung depend primarily on particle size. The radon daughter aerosol in the atmosphere is generated in two steps, viz., the formation from the radon gas by decay, the freshly generated radionuclides, mostly positively charged, neutralize and become small particles, called clusters, by reaction with atmospheric trace gases and water vapour in air. Besides the cluster formation, these radionuclides attach to the existing aerosol particles in the atmosphere within a fraction of second, forming the radioactive aerosol of the radon progeny. The variation of activity concentration and the meteorological parameters are presented.

EXPERIMENTAL METHODOLOGY

The radon detector is based on a design-optimized pulse ionization chamber and in regular operation the measuring gas gets in diffusion mode via a large-surface glass fiber filter into the ionization chamber. For example, through the glass fiber filter only the gaseous Radon-222 may pass, while the radon progeny products are prevented to enter the ionization chamber. At the same time the filter protects the interior of the chamber from contamination of dusty particles. The cylindrical ionization chamber has an active volume of 0.56 L. Metallic interior of the cylinder has operated at a potential of 750 V and along longitudinal axis the stiff centre electrode is located which lies at zero potential. The center electrode is connected with the signal input of highly sensitive preamplifier unit and then signal of the preamplifier are transmitted to an electronic network for further digital processing.

Radon progeny are measured using AlphaPM and works on similar principles as active radon progeny monitors. That is, the aerosol-transported radon progenies are continuously absorbed by a small pump and intercepted on a special filter. Aerosol particles were captured, with retention efficiency more than 99%, on a glass micro-fiber filter by drawing the air through the filter with a suction pump. The alpha particles emitted by the filter's surface are counted by a detector unit. The counting results in total number of pulses that were continuously recorded. Based on the known flow volume and the total number of pulses registered during measurement cycle, progeny concentration is calculated.

These two instruments were coupled to get synchronized results and then fed to a memory module for data acquisition. AlphaGuard is also housed with sensors of meteorological variables such as temperature, relative humidity and pressure housed in the AlphaGuard give complete picture of variation of radon and its progeny and their variations because of change in weather. Observations were carried out at the campus of the National Atmospheric Research Laboratory (NARL) Gadanki (13.5%N, 79.2%E) isa rural tropical warm location in peninsular India,2 km north eastfrom main residential area with no major industrialactivities. The observations were made at a height of 1m in an open space far away from buildings. Monthly meantemperature during April was 29.1%C with maximumtemperature reaching as high as 41%C. The monthly meantemperature came down to 24.1%C during November.Monthly mean relative humidity (RH) was 60% during April, which decreased to a value of 47.5% during May and increased continuously thereafter. During October and November, mean RH was 77%. Gadanki region experiences both summer (Southwest) and winter (Northeast) monsoons. The maximum rainfall of 308 mm was recorded in November. Overall wind direction was southerly and southeasterly during April, westerly from Mayto September and northeasterly during October and November (Gadhavi and Jayaraman, 2010).

RESULTS AND DISCUSSIONS

Airborne concentrations of radon and its progeny vary from time-to-time, depending upon the meteorological conditions, such as temperature, relative humidity, wind speed, rainfall, etc. The atmospheric concentrations of ^{222}Rn and its progenies at the ground level are governed by its exhalation rate and atmospheric diffusion depending on meteorological parameters. The radon emanated from the earth's surface distribute in the atmosphere depending on the geological and meteorological parameters. As temperature inversion occurs in the atmosphere, radon concentration will vary accordingly and show diurnal variations (Nagaraja *et al.*, 2003). Therefore, the diurnal variation of radon in air is measured along with the ambient temperature and humidity.

The variations of radon, its progeny and all the meteorological variables during October 2011 to May 2012 at a height of 1m at above the earth's surface at NARL Gandnki are shown in Fig. 1. The statistical variations with their range of values, mean and median are tabulated in Table 1. The radon concentration varies from 4.5 to 30.3 Bq m^{-3} with a mean value of 13.4 Bq m^{-3}, showing significant variation by a factor of 7, and its frequency distribution is shown in Fig. 2. It can also observed that the radon concentration is maximum during the nighttime and starts to decrease after sunrise and reaches minimum during daytime and thereafter it increases. It is interesting to note that the concentration of radon varies proportionately with the relative humidity. This is due to the fact that as temperature increases, the humidity decreases resulting in the decrease of moisture content in the atmosphere and is shown in Fig. 3. This causes increased vertical mixing and raising of aerosols to the higher altitudes which results in lower concentrations at ground level. Decrease in temperature leads to enhancement of relative humidity as evident from Fig. 3, and as a result the vertical mixing and raising of aerosols to the higher altitude reduces. As a consequence, the aerosols to which radon and its progeny are attached will be present at higher concatenations at ground level air. This results in the increase of radon concentration in the ground level air.

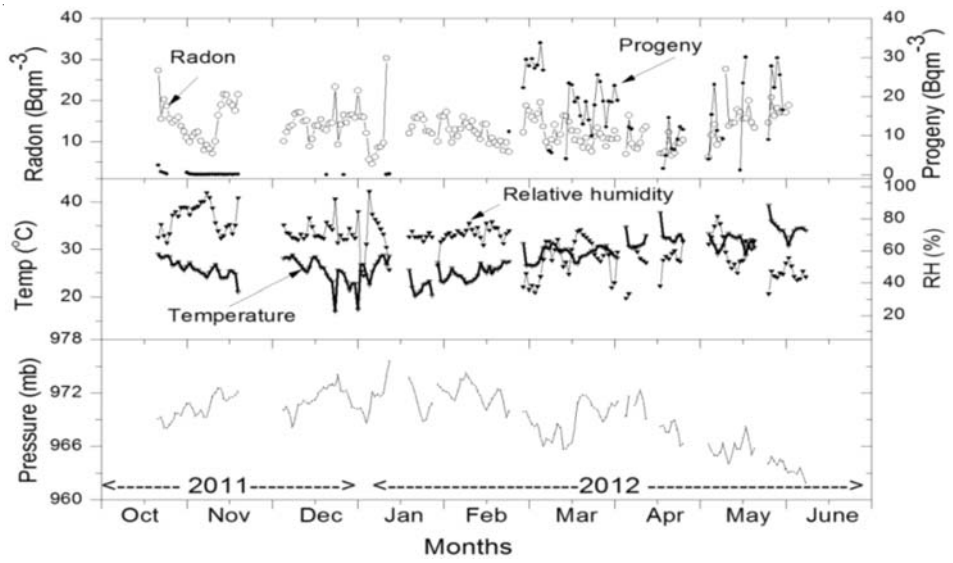

Figure 1.Continuous measurement of the concentrations of radon, its progeny and meteorological variables during October 2011 to May 2012 at a height of 1m at NARL Gandnki.

Diurnal variations in radon concentration are universally ascribed to variations in atmospheric stability (Hoppel *et al.*, 1986). Early morning atmospheric temperature inversions lead to an extremely stable atmosphere. This restricts the vertical turbulent mixing which leads to relatively higher near ground level radon concentrations. After sunrise, solar radiations warm the lower atmosphere, breaking up the inversion leading to a substantial decline in concentration. Concentrations remain low until late afternoon when radiant cooling of the surface leads to increase in atmospheric stability and a corresponding increase in radon concentration. It is also seen that the concentration of radon shows a positive correlation with the humidity and anti-correlation with ambient temperature indicating their incoherence. The relative humidity is usually associated with periods when wind speed is low and atmosphere is stable. The low winds and atmospheric stability are probably the most important factors resulting in increased concentration of radon.

The variation of radon progeny is also presented graphically in Fig. 1. It can be observed from the figure that the atmospheric concentration of progenies varies from 0.02 to 33.7 Bq m^{-3} showing significant variations. The trend observed is in consistence with the findings of Porstendorfer (1994) for the environment of Germany, and found that, the large variations of radon progenies in atmosphere during a single day are caused by changes in the eddy diffusivity in the boundary layer. The observed trend of diurnal variations at NARL is in consistence with the trends observed in the case variation of radon in atmospheric air elsewhere (Nagaraja *et al.*, 2003). The variation of in the radon progeny concentrations can also be attributed to the similar reasons as already discussed with radon variations. Because of the temperature inversion during early morning hours the radon gas and the aerosols are present in higher concentrations at ground level air, resulting in the higher concentration of radon progeny in air samples near the ground. As the ambient temperature increases, the convective current of the atmospheric air transports the radon gas and aerosols to the upper atmosphere. However, the continuous measurements are required to study in detail dynamics of the atmosphere; meteorological influences etc to get the clear picture of these variations. Present data does not give much information about the linkage between progeny variation due to the variation of temperature and/or pressure.

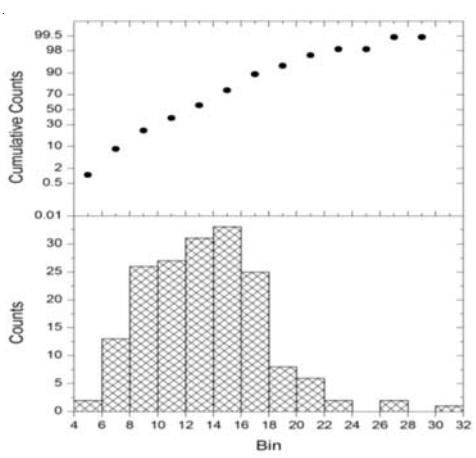

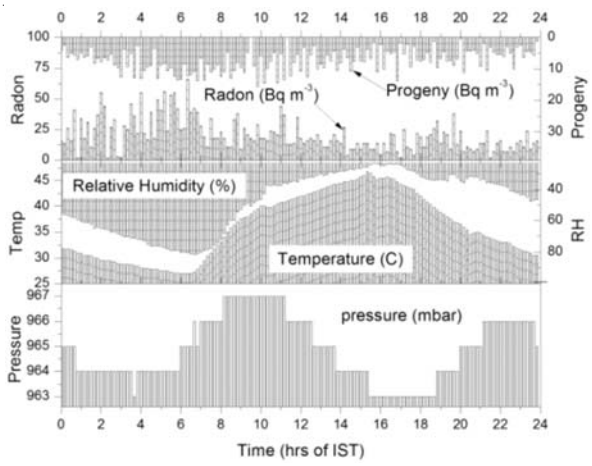

Figure 2. Freqency distribution of radon and Figure 3. Diurnal variations of radon, its progeny and meteorological parameters for a typical day on 19th May 2012 at NARL.

SUMMARY

In the atmosphere above the surface of the Earth the activity concentrations of radon and its progeny were measured using AlphaGuard PQ-2000PRO along with the meteorological parameters at a continental location, Gadanki, India. The concentrations show maxima in early morning hours when turbulence mixing is minimum; minima in the afternoon where turbulence mixing is maximum. The diurnal and seasonal variations in the concentrations of radon and its progeny are found to exhibit correlation with the relative humidity, and anti-correlation with the temperature.

ACKNOWLEDGEMENTS

Authors are thankful to the Director, National Atmospheric and Research Laboratory for the constant encouragement and extending all the facility to carry out the experiments at Gadanki.

REFERENCES

Gadhavi, H., Jayaraman, A. (2010). Absorbing aerosols: contribution of biomass burning and implications for radiative forcing, *Ann. Geophys.*, **28**, pp. 103–111.

Hoppel, W.A., Anderson, R.V., Willet, J.C., (1986). Atmospheric electricity in theplanetary boundary layer, *The Earth's Electrical Environment*, National Academy Press, Washington, DC, USA, pp. 149–165.

Nagaraja, K., Prasad, B. S. N., Madhava, M. S., Chandrashekara, M. S., Paramesh, L.,Sannappa, J., Pawar, S. D., Murugavel, P., Kamra, A. K., (2003). Radon and its short-lived progeny: variations near the ground, *Radiat. Meas.*, **36**, pp. 413–417.

Prasad, B. S. N., Nagaraja, K., Madhava, M. S., Chandrashekara, M. S., Paramesh, L., Madhava, M. S. (2005). Diurnal and seasonal variations of radioactivity and electrical conductivity near the surface for a continental location Mysore, India, *Atmos. Res.*, **76**, pp. 65 – 77.

Porstendorfer, J., Butterweck, G., Reineking, A. (1991). Diurnal variation of the concentrations of radon and its short-lived daughters in the atmosphere near the ground, *Atmos. Environ.*, **25**, pp. 709–713.

SIMULATION OF ^{220}RN AND ITS DECAY PRODUCTS DISTRIBUTION IN INDOOR AIR USING COMPUTATIONAL FLUID DYNAMICS SOFTWARE

T.K. AGARWAL, B.K. SAHOO, B.K. SAPRA, Y.S. MAYYA

Radiological Physics and Advisory Division,
Bhabha Atomic Research Centre, Mumbai, 400 094,
E mail : tarunphys@gmail.com

Keywords: THORON, DECAY PRODUCTS, RADIOACTIVE AEROSOLS, SIMULATION

INTRODUCTION

The decay of naturally occurring radioactive gases radon (^{222}Rn) and thoron (^{220}Rn) in the environment results in the formation of their particulate progeny. These attach to the ambient aerosols to form radioactive aerosols and contribute a major fraction (52 %) of the natural radiation dose to the humans. The dose level increases further in cases where technologically enhanced naturally occurring radioactive materials (TENORMs) are handled e.g. Uranium mines and Thorium facilities. In the past studies, focus was on assessment of doses due to ^{222}Rn and its decay products. ^{220}Rn and its decay products have been considered to be of low radiological significance and hence dose due to them was neglected. However, the significance of ^{220}Rn has been recognized in recent years with discovery of ^{220}Rn prone regions in India, China and Brazil as well as in occupational environment such as thorium fuel handling facilities. Also, Potential Alpha Energy Concentration (PAEC) of ^{220}Rn decay products being higher than that of ^{222}Rn decay products, the radiological risk due to the ^{220}Rn decay products is higher. However, considerable spatial in-homogeneity in ^{220}Rn distribution due to its short half life (55.6 s) makes it challenging to assess the representative ^{220}Rn dose in an environment.

MATERIAL AND METHOD

To develop the correct protocol for ^{220}Rn and its decay products dose assessment, it is first required to understand the spatial distribution of ^{220}Rn and their decay products in indoor air. In view of this, a numerical simulation using a Computational Fluid Dynamic (CFD) based Software has been attempted in the present study to understand ^{220}Rn and its decay products concentration distribution in a test chamber of dimension 0.8 x 0.8 x 0.8 m^3. CFD simulations were carried out in the chamber having inlet and outlet positioned at (0.25 m,0 m,0.40 m) and (0.55 m,0 m,0.40 m) along (x,y,z) axis respectively to study the distribution profile of ^{220}Rn and its decay product ^{212}Pb ($T_{1/2}$ ~10.6h) at the flow rate of 30 l min^{-1}. Fig. 1 shows the geometry of the test chamber and coordinates taken for the simulation.

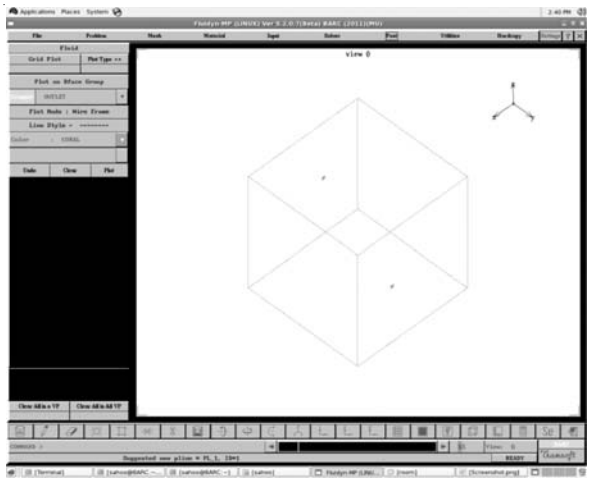

Figure 1. Geometry of the test chamber of dimensions 0.8 x 0.8 x 0.8 m^3 having inlet and outlet positioned at (0.25 m, 0 m, 0.40 m) and (0.55 m, 0 m, 0.40 m)

RESULTS AND DISCUSSION

Spatial distribution of ^{220}Rn and ^{212}Pb in horizontal plane (x-y plane) at the height of 0.60 m are shown in Fig. 2(a) and Fig. 2(b) respectively. As may be seen, distribution of ^{220}Rn concentration is not uniform but distribution of ^{212}Pb concentration tends to be homogenous. Owing to its short half life, ^{220}Rn migrates a very short distance from the source before it decays and hence mixing in indoor air is non-uniform even under turbulent ventilation conditions (Fig. 2(a)). Thus, the local ^{220}Rn concentrations can't be considered as the representative value inside a confined space and the dose estimation by measurements of ^{220}Rn is highly position dependent. On the contrary, ^{212}Pb distribution tends to be homogenous (as shown in the Fig. 2(b)) because of its long half life ($T_{½}$ ~10.6 h) which allows ^{212}Pb to diffuse over a long distance. It is for this reason that a dose assessment for ^{220}Rn must be based on the concentrations of the decay products (^{212}Pb).

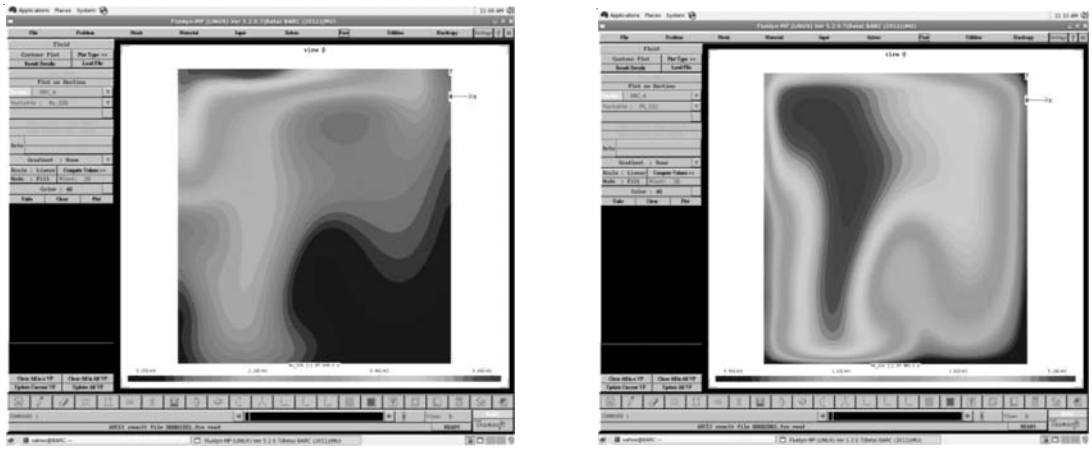

Fig 2 (a) **Fig 2 (b)**

Figure 2. Spatial profile of (a) ^{220}Rn and (b) ^{212} Pb atomic concentration respectively at the simulation time of 350 seconds.

Fig. 3 & Fig. 4 provide the transient variation of average volumetric activity concentration for ^{220}Rn and ^{212}Pb inside the chamber. From Fig. 3, it can be seen that ^{220}Rn attains saturation in about 350 seconds after the injection of ^{220}Rn in the chamber which is roughly equal to seven half life's of ^{220}Rn. On the contrary, ^{212}Po requires a long time to attain saturation (Fig. 4). This is expected since the two elements will not be in secular equilibrium. The numerical solution is found to be consistent with closed form analytical solution. Similarly, the results obtained from simulations were found in close agreement (within 10% deviation) with experimental observations indicating the validity of the numerical predictions.

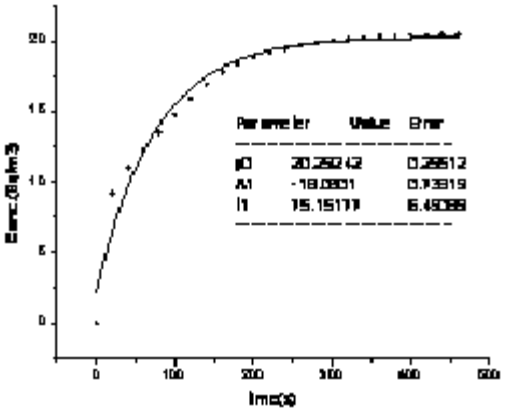

Figure 3. Transient variation of average volumetric activity concentration of ^{220}Rn

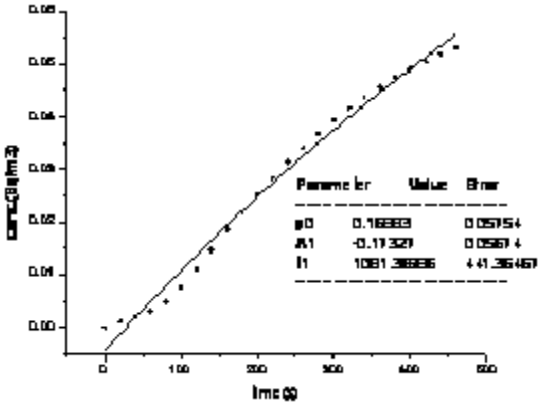

Figure 4. Transient variation of average volumetric activity concentration of ^{212}Po

CONCLUSION

The results of this work will be helpful in understanding distribution profile of radon, thoron and their decay products in indoor environments for better inhalation dosimetry as well as developing deployment criteria for dosimeters to get representative values in the indoor environment, especially in the context of ^{220}Rn.

GRAPHITE AEROSOL GENERATION UNDER ACCIDENT CONDITION IN HTR's

ARSHAD KHAN, MANISH JOSHI, B K SAPRA, S N TRIPATHI AND Y S MAYYA

Radiological Physics and Advisory Division
Bhabha Atomic Research Centre
Mumbai – 400 085, India

Keywords: GRAPHITE AEROSOLS, HIGH TEMPERATURE REACTORS, REACTOR ACCIDENT

INTRODUCTION

Nuclear aerosol particle generation, deposition and the assessment of its resuspension during a Design Basis Accident (DBA) in the primary circuit are a key issue in the development and certification of High Temperature Reactors (HTRs). Kissane (2009) and Moormann (2008) mentioned that dust arose due to friction between the graphite pebbles and oxidation of the graphite from impurities in the helium medium. The annual dust production for a 400 MWth pebble bed HTR was estimated to be 100 kg/yr.

There is a basic knowledge of the amount of graphite dust and its distribution in the HTR primary circuit during standard service but dust behaviour during a DBA is rather unknown. Reactor system code computations offer a general idea where the irradiated dust deposits during standard service. There is however a growing need of high quality experimental data in order to understand DBA related graphite dust generation and deposition characteristics and to further foster CFD code development in this field.

In Indian context BARC is developing High temperature reactor with the objective of providing energy to facilitate combined production of hydrogen, electricity, and drinking water. The reject and waste heat in the overall energy scheme will be utilised for electricity generation and desalination, respectively (Dulera and Sinha, 2008). A typical CHTR fuel bed consists of prismatic BeO moderator block with centrally located graphite fuel tube carrying fuel compacts. This reactor has been designed so as the graphite aerosol generation is averted even in case of reactor accident. But in case of DBA it is possible that graphite oxidation could generate aerosols. This paper presents measurements carried out to understand the graphite aerosol generation under high temperature.

METHOD

Experiments have been carried out in a programmable tubular furnace designed to attain maximum 1200° C temperature as shown in fig. 1. Furnace was connected to HEPA filter from one side and aerosol chamber on the other. Aerosol chamber was connected to the temperature sensor and aerosol monitor. The tube of the furnace have been checked for aerosol generation from the furnace construction material before starting of the experiments by passing the clean air and heating at 1000° C. Experiments have been planned in such a way that the graphite remains at a particular temperature for 15 min then again the temperature is increased. Temperature was monitored in the aerosol chambers so that the sample temperature does not cross 45°C as required by Aerodynamic particle Sizer (TSI APS 3321). APS measures the aerodynamic particle size from 0.5 mm to 20 mm in 50 size channels in 20 sec sampling interval based on time of flight aerodynamic sizing.

Experiment has been carried out by keeping a 20 mm dia, 10mm thick graphite block at the centre of the tubular furnace. The zero air was passed throughout the experiment to carry the generated aerosol in the aerosol chamber, from where it is sampled through APS.

Figure 1. Experimental set up

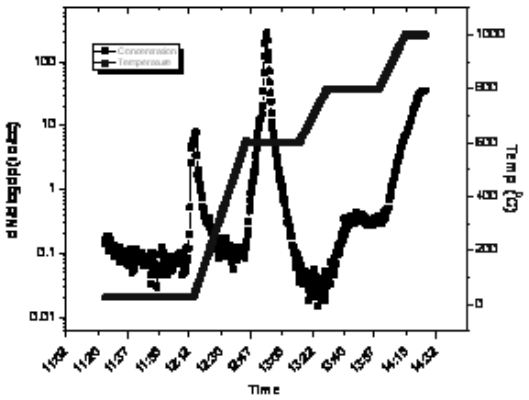

Figure 2. Variation of temperature and particle concentration with the time

CONCLUSIONS

As it is seen from the fig. 2 graphite generates copious amount of aerosols even in the lower temperature of 600 ^{o}C. Aerodynamic particle sizer showed a median size of 980 nm with GSD of 1.73 when the graphite is heated to 600 ^{o}C. This is excluding the particles which are below 0.5 mm. As the lower limit for the instrument is only 0.5 mm it will be interesting to see the particle size distribution in the size range below 0.5 mm.

REFERENCES:

Dulera, I. V., Sinha, R. K. (2008). High temperature reactors, *Journal of Nuclear Materials*, **383**, pp. 183–188.

Kissane, M. (2009). A review of radionuclide behaviour in the primary system of a very-high temperature reactor, *Nuclear Engineering and Design*, **239**, pp. 3076-3091.

Moormann, R. (2008). Fission Product Transport and Source Terms in HTRs: Experience from AVR Pebble Bed Reactor, *Science and Technology of Nuclear Installations*, 14.

PARTICLE SIZE CHARACTERIZATION AND DISTRIBUTION OF ^{226}Ra AND ^{228}Ra AS A FUNCTION OF DEPTH IN MARINE SEDIMENTS

AJAY KUMAR, RUPALI KARPE, SABYASACHI ROUT, MANISH K. MISHRA, V.M. JOSHI AND P.M. RAVI

Health Physics Division, Bhabha Atomic Research Centre, Trombay, Mumbai, India

Keywords : SEDIMENTS, RADIUM

INTRODUCTION

Sediments are complex heterogeneous materials that readily accumulate pollutants from water column and transport them to other parts of water system. These are considered as major repository of radionuclides released into water and serve as main potential source of uptake for water feeding biota. The sedimentation rate and the physicochemical nature of radionuclides are determined by the rate of deposition and accumulation in core sediments. Moreover, it also indicates the temporal variation and the impact of radionuclides released through fallout and discharges from nuclear installations. The main objective of this study is to see the impact of particle size on distribution of uranium and thorium as a function of depth core in marine sediment.

MATERIALS & METHODS

The core sediment samples were collected from two locations (CIRUS and PP) of Mumbai Harbor Bay at sea water depth about 1 m using a corer sampler and taken to a sediment depth of 48 cm with increment of 4 cm core fractions. The collected samples were dried at 110°C for 24 h, pulverized, homogenized and transferred to a known geometry of cylindrical acrylic container, weighed, sealed and kept for 30 days to allow for in-growth of radon gas in order to achieve secular equilibrium between ^{226}Ra, ^{214}Pb and ^{214}Bi in the ^{238}U decay chain and between ^{212}Pb, ^{208}Tl and ^{228}Ac in the ^{232}Th decay chain. After attaining the secular equilibrium, the activity of ^{226}Ra was determined using Gamma–ray spectrometry system by taking the average activity of two separate photo-peaks of two radon daughters: ^{214}Pb at 352 keV and ^{214}Bi at 609 keV and for ^{228}Ra, activity of its daughter nuclide ^{228}Ac having ã -ray transition line; at 911 keV was assumed. The particle size distribution as sand (>63 µm), silt (>2-<63 µm) and clay (<2 µm) of each core fractions was determined using a laser diffraction particle size analyzer.

RESULTS AND DISCUSSIONS

In general, the sediments were mainly composed of silt and clay. The mean % of sand, silt and clay in the study regions were ranged from ND-12%, 70.54-76.22% and 16.61-26.76% respectively. The mean of bulk density and porosity of sediments were determined to be 1.98g/cm^3 and 19.47% respectively. Generally, sand percentage was found to increase as core depth increases. Highest percentage of sand (12%) was observed at core fractions of 28-32 cm, while at the top fractions, the lowest percentage was observed. Silt and clay showed a corresponding opposite increasing and decreasing trend to each other with silt exhibiting three prominent peaks (~ 76%) in depth core fractions of 4-8 cm, 12-16 cm and 32-36 cm which corresponds to the lowest percentage of clay (~ 23%). The content of sand as well as silt & clay in terms of mean % age of both locations as a function of depth are depicted in Fig.1 and 2 respectively. The distribution of ^{226}Ra and ^{228}Ra in core

sediments as a function of depth showed a linear relationship with a strong degree of correlation coefficient of R = + 0.73 and R = + 0.85 as shown in Fig.3 and 4 respectively. The high trapping tendency of uranium and thorium in the silt-clay type of sediments may be due to high cation exchange capacity and large surface area while sandy type sediments have little ability to retain the metal ions.

CONCLUSIONS

The depth-wise distribution of radio-nuclides indicates the sedimentation rate. The accumulation on surface sediment and thereafter migration to bottom sediment is affected by physico-chemical processes. The uneven pattern of silt and clay distribution is attributed to dynamic nature of system under study. The accumulation of U and Th was highly influenced by sediment grain-size and organic matter content.

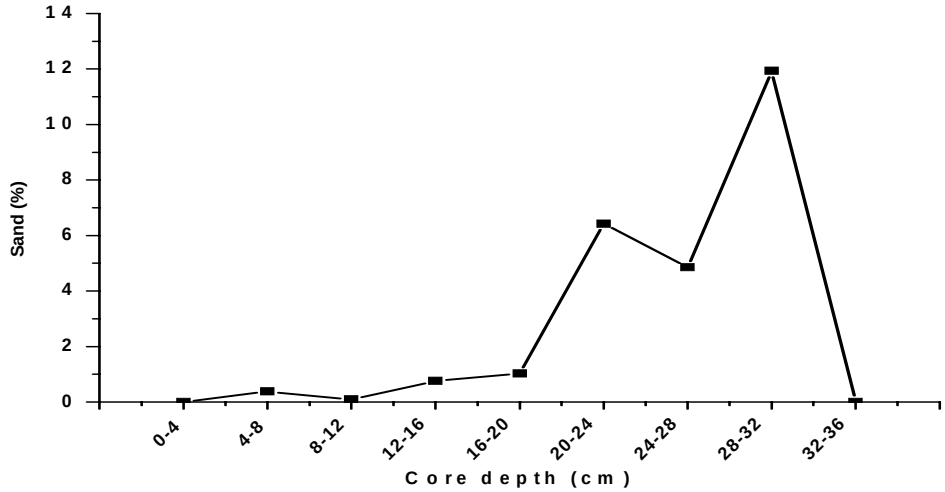

Figure 1. Content of sand as a function of depth

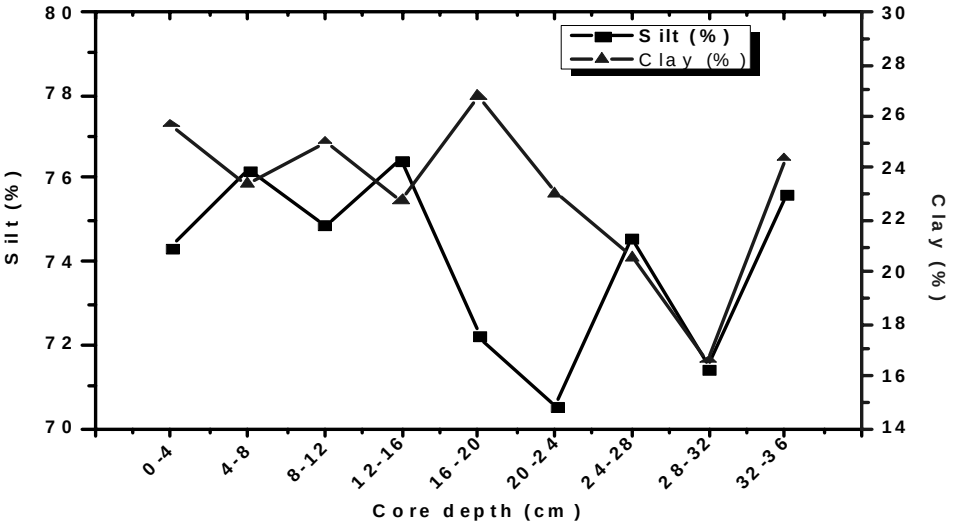

Figure 2. Content of silt and clay as a function of depth

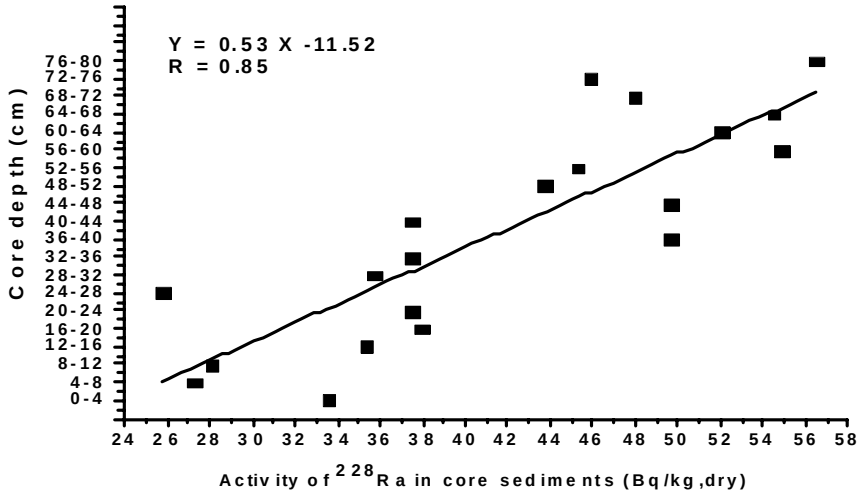

Figure 3. ^{226}Ra content as a function of depth

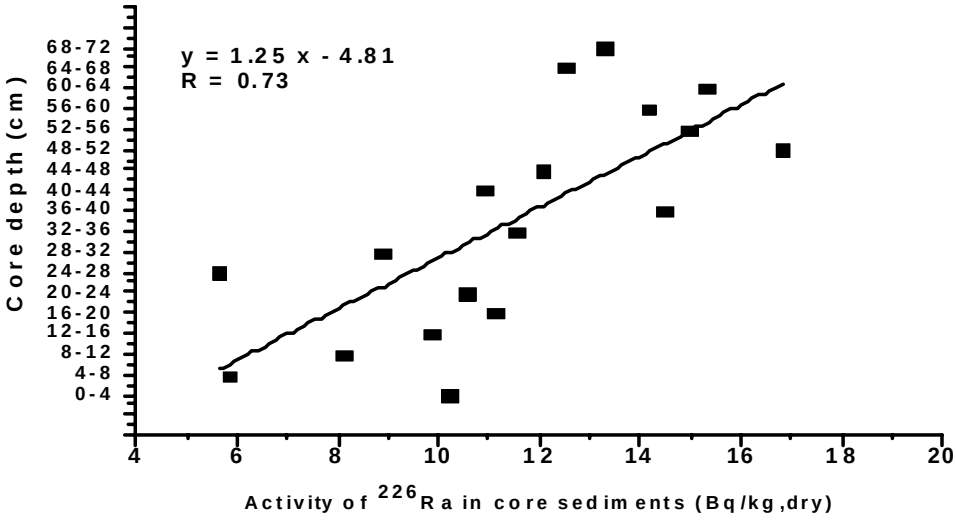

Figure 4. ^{228}Ra content as a function of depth

AEROSOLS IN HEALTH

AND

AGRICULTURE

ASSESSMENT OF BIO AEROSOLS IN ROOMS OF TERTIARY CARE HOSPITAL IN NEW DELHI, INDIA

P. TYAGI AND K. MUKHOPADHYAY

School of Environmental Sciences, Jawaharlal Nehru University, New Delhi-110067, India.

Keywords: BIOAEROSOLS, TERTIARY CARE HOSPITAL, COLONY FORMING UNITS, METHICILLIN RESISTANT STAPHYLOCOCCUS AUREUS

INTRODUCTION

Bacteria and Fungi are associated with aerosols and present in atmosphere for centuries (Fahlgren, *et al.,* 2010) and known as Bioaerosols. These bioaerosols may consist of live or dead, pathogenic or non pathogenic bacteria and fungi, viruses, bacterial and fungal endotoxins, pollens, plant fibresetc (Douwes, *et al.,* 2003). Bioaerosols contribute to about 5-34% of indoor air pollution (Srikanth, *et al.,* 2008). Major cause of hospital acquired infections (HAIs) or a nosocomial infection is indoor air pollution caused by the presence of infectious bioaerosols. Nosocomial infections in hospitals constitute major health problems for hospital staffs and patients particularly in view of the spreading of antibiotic resistance among bacteria. Though many of these nosocomial infections are associated person to person contact but airborne transmission has been proved important route for their spread. It has been calculated that airborne route is 10-20% responsible for endemic nosocomial infections (Fletcher *et al.,* 2004). *Staphylococcus aureus (S. aureus)* is a leading human nosocomial pathogen and emergence of its resistance is creating attention worldwide. Irrational and wide spread use of antibiotics in hospital settings is playing significant role in spreading microorganisms, especially which are resistant to antibiotics. Due to the outbreaks of multidrug and methicillin resistant *S. aureus* (MRSA), it has become critical to assess the airborne microflora of different areas of hospitals.

METHODS

In this preliminary work, our main attempt was to evaluate the levels of indoor airborne micro flora (bacteria and fungi) and airborne antibiotic resistant *S. aureus* in the tertiary care hospital of New Delhi, India. For this purpose, we used Anderson six stage sampler to collect bioaerosols samples at the important locations within the hospital (pediatric intensive care unit (ICU), gastrointestinal ICU, medicine outpatient department (OPD), orthopedics OPD, general surgery operation theater (OT), orthopedics OT, children ward, general ward, accident & emergency ward and emergency OT). Indoor air samples were collected for four months (November 2011, January, February and March, 2012) on selective media for bacteria and fungi. Bacterial and fungal colonies were counted and expressed as CFU/m^3. Bacteria were classified as gram positive and gram negative bacteria as standard procedure (Cappuccino & Sherman, 2011). *S. aureus* colonies developed on mannitol salt agar (MSA) (selective for *Staphylococcus sp.*) plates were identified by biochemical tests and agglutination kit. Antimicrobial susceptibility testing was done for identified *S. aureus* isolates against vancomycin and oxacillin (methicillin) to find out the methicillin resistant *S. aureus* (MRSA) and vancomycin resistant *S. aureus* (VRSA) according to the NCCLS 2009 procedure. They were further cross checked with the four antibiotics belonging to different classes of drugs (gentamicin, ciprofloxacin, rifampicin & tetracycline).

RESULTS & CONCLUSION

The maximum number of bacterial aerosols concentration was reported from accident and emergency ward (2417CFU/m^3) followed by medicine OPD (1759CFU/m^3) and orthopedics OPD (820CFU/m^3). The maximum number of fungal aerosols concentrations was reported from accident and emergency ward (2134 CFU/m^3) followed by medicine OPD (1491 CFU/m^3) and orthopedics OPD (269 CFU/m^3). The microbial load was lowest in general surgery OT (82 CFU/m^3) and gastrointestinal ICU (289 CFU/m^3). Gram-positive bacteria and fungi were obtained more in numbers than gram-negative bacteria. Respirablebioaerosols belonging to size range 0.65-4.7 µm (fungi & bacteria) were mainly contributed by accident & emergency and medicine OPD. Out of 292 colonies on MSA, 34 (11.6%) colonies on MSA plates were tested positive for *S. aureus*. Among 34 *S. aureus*, 18 isolates were found to be MRSA and none was resistant to vancomycin.. Further, it was found that all the reported MRSA were resistant to the gentamicin and ciprofloxacin but less resistant to tetracyclin and sensitive to rifampicin and present in 8 locations out of 10 sampling locations. This study indicates that bacterial and fungal bioaerosols including antibiotic resistant airborne *S. aureus* strains are commonly found and also in higher concentrations inside the critical areas of the hospital. The results of our study, in combination with other recent studies (Gandara, *et al.*, 2006 and Chambers, 2001) provide justification to further assess the health effects associated with potentially pathogenic airborne *S. aureus.* Lack of reported data in studying bacterial aerosols distribution in Indian hospital environments, provide enough reasons to intiate research in understanding the relationship between airborne concentrations of resistant *S. aureus*and HAIs. Present study is just the preliminary step towards the attainment of this aim.

ACKNOWLEDGEMENTS

This work was supported by Council of Scientific and Industrial Research (CSIR) to PT and Capacity Building Fund (CBF) provided by Jawaharlal Nehru University to KM. PT and KM thank Dr. A. Kapil, AIIMS, New Delhi for her help in Sample analysis.

REFERENCES

Cappuccino, J.G., Sherman, N. (eds) (2011). Microbiology- A laboratory manual (9th edition).Published by *Pearson Education,* Inc.

Chambers, H.F. (2001). The Changing Epidemiology of *Staphylococcus aureus.Emerg. Inf. Dis.*, **7(2)**, 178-182.

Douwes, J., Thorne, P., Pearce, N., Heederik, D. (2003).Bioaerosol Health Effects and Exposure Assessment: Progress and Prospects, *Ann Occup. Hyg.*,**47(3)**, 187-200.

Fahlgren, C., Hagstrom, A., Nilsson, D., Zweifel, U.L. (2010). Annual variations in the diversity and origin of airborne bacteria, *App. Env.Microbio*.,**76(9**), 3015-3025.

Fletcher, L.A., Noakes, C.J., Beggs, C.B., Sleigh, P.A. (2004). The importance of bioaerosols in hospital infections and the potential for control using germicidal ultraviolet radiation, Murcia, Spain. Aerobiology Research Group, School of Civil Engineering, University of Leeds.

Gandara, A., Mota, L.C., Flores, C., Perez, H.R., Green, C.F., Gibbs, S.G. (2006).Isolation of *Staphylococcus aureus* and antibiotic resistant *Staphylococcus aureus* from residential indoor bioaerosols. *Env. Health Pers.*, **114(12),** 1859-1864.

NCCLS(National Committee for Clinical Laboratory Standards) (2009). Methods for Dilution Antimicrobial Susceptibility Tests for Bacteria That Grow Aerobically- 8th Edition: Approved Standard M7-A5, 29(2), 1-65.

Srikanth, P., S. Sudharsanam and R. Steinberg (2008). Bio-aerosols in indoor environment: composition, health effects and analysis. *Ind J. Med. Microbio.*, **26(4),** 302-312.

DECADAL CHANGES IN FINE PARTICULATE MATTER ($PM_{2.5}$) OVER INDIA: IMPLICATIONS FOR HUMAN HEALTH

SAGNIK DEY[1], L. DI GIROLAMO[2], A. VAN DONKELAAR[3], S. N. TRIPATHI[4], T. GUPTA[4], MANJU MOHAN[1] AND AJIT SINGH[1]

[1]Centre for Atmospheric Sciences, Indian Institute of Technology Delhi, India
[2]Department of Atmospheric Sciences, University of Illinois at Urbana-Champaign, USA
[3]Department of Atmospheric and Oceanic Sciences, Dalhousie University, Halifax, Canada
[4]Department of Civil Engineering, Indian Institute of Technology Kanpur, UP, India
Email: sagnik@cas.iitd.ac.in

Keywords : FINE PARTICULATE MATTER, MISR, AEROSOL OPTICAL DEPTH

INTRODUCTION

The health impacts from short and long-term exposure to fine particulate matter ($PM_{2.5}$) are well established (Anenberg, *et al.*, 2010; Balakrishnan, *et al.*, 2002; Pope, *et al.*, 2009). Rapid increase in aerosols over India in the past decade has possible implications for health impacts. Epidemiological studies quantifying these impacts rely on long-term measurements of $PM_{2.5}$, which is lacking in the Indian subcontinent. Satellite data showed potential in filling this data gap (van Donkelaar, *et al.*, 2010). Here, Multiangle Imaging SpectroRadiometer (MISR)-retrieved columnar aerosol optical depth (AOD) has been converted to surface $PM_{2.5}$ (fine particulate matter with diameter less than 2.5 μm) utilizing a chemical transport model and spatio-temporal patterns of $PM_{2.5}$ over Indian subcontinent during the period 2000-2010 was examined. The decadal changes in $PM_{2.5}$ have been examined for possible health impacts.

METHODOLOGY

MISR level 2 (Version 22) aerosol products have been analyzed for the present work. MISR-AOD has previously been evaluated against AERONET in India (Dey and Di Girolamo, 2010), with a low bias increasing with an increase in AOD. Median AOD within $0.5^0 \times 0.5^0$ grids was calculated from level 2 pixels and multiplied by a climatological conversion factor η to estimate MISR-$PM_{2.5}$. ηvalues (ratio of $PM_{2.5}$ to columnar AOD) were obtained from GEOS-Chem model at MISR overpass time as function of all possible factors (e.g. meteorology, vertical distribution and emission) that may influence AOD (Van Donkelaar, *et al.*, 2010).

The method was evaluated against available daily in-situ measurements in Kanpur and Delhi. The low bias in MISR-$PM_{2.5}$ may have its roots in several places. For example, MISR-AOD is biased low in heavily polluted regions, while the model also underestimates AOD. The bias in MISR-concentration is much larger. Recent epidemiological studies argued about the nature of exposure-response function (Pope *et al.*, 2011; Brauer, *et al.*, 2012). $PM_{2.5}$ statistics presented here provide a first opportunity to estimate health risks across India covering a larger geographical region.

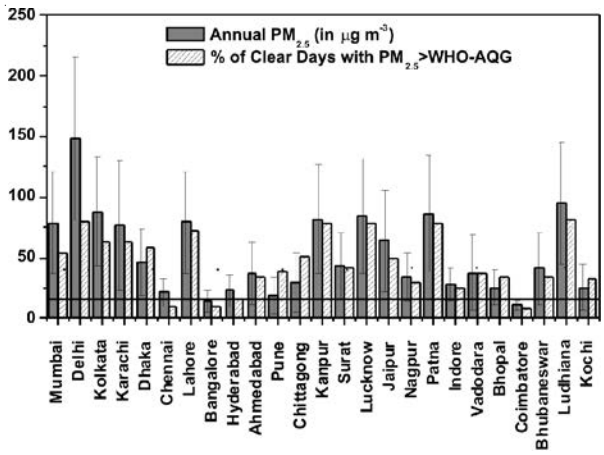

Figure 1. Mean annual $PM_{2.5}$ (error bars represent ±1 standard deviation, σ) and percentage of clear days in a year when daily $PM_{2.5}$ exceeds daily WHO Interim Target 3 (37.5 μg m^{-3}) over major urban centers over the Indian subcontinent as derived from MISR. The bold horizontal line and dotted horizontal line represent WHO (10 μg m^{-3}) and Indian (40 μg m^{-3}) annual standards for $PM_{2.5}$.

CONCLUSIONS

We presented the first statistics of $PM_{2.5}$ over the Indian subcontinent for an entire decade. Five hotspots are identified, where the $PM_{2.5}$ has increased by more than 15 μg m^{-3} over ten year period. The increase in these regions is larger than the WHO annual air quality threshold. 82% of the subcontinent's population is exposed to this enormous and persistent pollution level that covers both rural and urban areas. We recommend generating a national health database for carrying out cohort studies at these hotspots to establish exposure-response relation for local conditions.

ACKNOWLEDGEMENTS

SD acknowledges research grant from DST under contract IITD/IRD/RP02509. This research was partially supported by a grant from the Jet Propulsion Laboratory of the California Institute of Technology under contract 1260125. MISR aerosol data are distributed by the NASA Langley Research Atmospheric Science Data Center. SNT acknowledges research grant from MoES under Indo-UK Changing Water Cycle project. PIs of Kanpur AERONET site are acknowledged for their efforts in establishing and maintaining the operation of the instrument since the year 2001.

REFERENCES

Anenberg, S. C., Horowitz, L. W., Tong, D. Q., West, J. J. (2010). An estimate of the global burden of anthropogenic ozone and fine particulate matter on premature human mortality using atmospheric modeling, *Environ. Health Pers.,**118* **(9),** 1189-1195.

Balakrishnan, K., Sankar, S., Parikh, J., Padmavathi, R, Srividya, K, Venugopal, V., Prasad, S., Pandey, V. L. (2002). Daily average exposures to respirable particulate matter from combustion of biomass fuels in rural households of Southern India, *Environ. Health Pers*., **110 (11),** 1069-1075.

Brauer, M. *et al.* (2012).Exposure assessment for estimation of the global burden of disease attributable to outdoor air pollution, *Environ. Sci. Tech.,* **46,** 652-660.

Dey, S., Di Girolamo, L. (2010). A climatology of aerosol optical and microphysical properties from nine years (2000-2008) of Multiangle Imaging SpectroRadiometer (MISR) data over the Indian Subcontinent, *J. Geophys. Res*., **115,** D15204, doi:10.1029/2009JD013395.

Pope, C. A., Brook, R. D., Burnett, Dockery, D. W. (2011a). How is cardiovascular disease mortality risk affected by duration and intensity of fine particulate matter exposure? An integration of the epidemiologic evidence, *Air Qual. Atmos. Health,* **4,** 5-14.

Pope, C. A., Burnett, R. T., Krewski, D., Jerret, M., Shi, Y., Calle, E. E., Thun, M. J. (2009). Cardiovascular mortality and exposure to airborne fine particulate matter and cigarette smoke: shape of the exposure-response relationship, *Circulation,***120,** 941-948.

Van Donkelaar, A., Martin, R. V., Brauer, M., Kahn, R., Levy, R., Verduzco, Villenueve, P. J. (2010). Global estimates of ambient fine particulate matter concentrations from satellite-based aerosol optical depth: Development and application, *Environ. Health Pers.,* **118 (6)**, 847-855.

WHO (2006). Air quality guidelines: global update 2005. Geneva: World Health Organization. Available at http://www.euro.who.int.

A STUDY ON BIOLOGICAL CONSTITUENTS OF AEROSOL AT A SUBTROPICAL SITE IN INDIA

RANJIT KUMAR[1*], J.N. SRIVASTAVA[2], MAMTA[2], AND G.P. SATSANGI[2]

[1]Department of Chemistry, Technical College,
[2]Department of Botany, Faculty of Science
Dayalbagh Educational Institute (Deemed University)
Dayalbagh, Agra-5 (India).
E-mail: rkschem@rediffmail.com

Keywords: AEROSOL, BIOAEROSOL, BACTERIA, FUNGI, CONCENTRATION.

INTRODUCTION

Air pollution has worsened the health status of residents of the cities of both developed and developing countries. Research in the past decades confirms that outdoor air pollution contributes to morbidity and mortality. Aerosol plays significant role in health problems due to its biotic and abiotic constituents. Although the biological mechanisms are not fully understood, state of art epidemiological studies have found consistent and coherent association between air pollution and various health outcomes. Biotic constituent is less than one fifth of the total aerosol but causes severely and in the presence of chemical constituents its effects get exacerbated. Many numbers of diseases are caused by biological components viz. different microorganism, fungal spores, debris suspended in the atmosphere, hence estimation of biological constituents of aerosol is needed over an Indo-Gangetic plain which hosts 40% of the country total population.

METHODS

Aerosol sampling was carried out at Dayalbagh, Agra, suburban site in subtropical India. Aerosols samples were collected by Polltech High Volume Sampler (HVS) using Whatman glass fiber filter of diameter 47 mm for TSPM and PM_{10} and PTFE filter for $PM_{2.5}$. The aerosol mass loading was determined by dividing the difference in weight of the filters before and after sampling by total air volume.Biological analysis of filter was done by keeping it in desiccators.

Biological constituents of aerosol are determined by extraction of half part of filter (aerosol sample) in de-ionised water. Aqueous extract of filter was used for estimation of biological constituent: bacteria and fungi using culture techniques. Bacterial concentrations are determined using NAM media while fungal concentrations are determined using SDA media and concentration are reported as colony forming unit per cubic meter (CFU m^{-3}).

Parameters	Mean	Standard deviation	Range	
			Minimum	Maximum
Mass concentration				
TSPM	388.2	209.3	176.5	691.5
PM_{10}	180.8	80.7	41.8	245.2
$PM_{2.5}$	125.4	39.8	74.6	185.3
Total microbial counts				
TSPM	65.2	49.1	23.3	150.4
PM_{10}	34.5	34.9	10	95.2
$PM_{2.5}$	36.4	17.3	14.8	52.5
Fungal counts				
TSPM	52.5	47.6	16.7	132.7
PM_{10}	18.5	21.6	3.3	54.8
$PM_{2.5}$	21.3	16.7	3.7	46.7
Bacterial count				
TSPM	12.7	4.5	5.8	17.5
PM_{10}	16.3	13.7	6.7	40.4
$PM_{2.5}$	15.1	4	10.8	19.1

Table 1. Average, standard deviation and range of concentration (µg m^{-3}) of TSPM, PM_{10}, $PM_{2.5}$ and biological constituents (cfu/m^3)

CONCLUSIONS

The sampling was carried out at Dayalbagh, Agra a suburban site of subtropical India. The mean concentration: The concentration of TSPM, PM_{10} and $PM_{2.5}$ are 388.2 µg m^{-3}, 180.8 µg m^{-3} and 125.4 µg m^{-3}, respectively. The concentrations are higher than the standard value. Mean total microbial counts are 65.2 cfu m^{-3}, fungal spore counts are 52.3 cfu $m^{-3}$and bacterial spore counts are 12.7 cfu m^{-3}. These values are below the reported range 100-1000 cfu m^{-3} as present site is a suburban site and relatively clean site.

ACKNOWLEDGEMENT

This work is supported by Department of Science and Technology, Govt. of India, New Delhi

IMPACT OF VEHICULAR AND RAILWAY TRAFFIC ON AMBIENT AIR QUALITY: CASE STUDY KANPUR CITY 2011

D. SRIVASTAVA AND A. GOEL

Environmental Engineering and Management Program, Department of Civil Engineering,
Indian Institute of Technology Kanpur, Kanpur -208016, India
E mail : anubha@iitk.ac.in

Keywords: AEROSOL CHARACTERIZATION, VEHICULAR EMISSION, PM LEVELS, AMBIENT AIR QUALITY, RAILWAY LINE

INTRODUCTION

It is well known that $PM_{2.5}$ act as carrier of toxic substances (McEntee and Ogneva-Himmelberger, 2008), contain a high proportion of toxic metals and organic compound (Zhang and Qi, 2001), and aerodynamically it can penetrate deeper into the respiratory tract. Moreover, finer particles get deposited in the alveolar region of lung where they are retained for a long time which results in decreased lung function. Studies in Several Indian cities (Gupta et al,. 2010; Karar and Gupta, 2006)clearly show that presence of PM_{10} and especially $PM_{2.5}$ in ambient airresults in significant health problems related to respiratory system (Dockery and Pope 1994; Kawanaka 2009).

A study was undertaken for aerosol characterization in ambient air of Kanpur city (year 2011), which has seen more than doubling of vehicle registrations in past decade (CSE 2009) and is currently rated as the most polluted city in India (TheIndianExpress 2011). This presentation provides an overview of the air quality in the city and discusses results highlighting factors affecting levels observed in ambient environment. Physical and chemical properties of the particles have been analyzed to assess effects of finer Particulate Matter (PM) on human health. Results from this study can further facilitate control of anthropogenic sources of PM emissions (Braziewicz *et al.* 2004).

METHODS

Ambient air samples were collected at major traffic and railway line intersections in Kanpur City in both summer and winter of 2011. PM distribution on a size segregated basis (0.03µm – 20µm) during peak traffic hours of the day was determined using an Optical Particle Counter (OPC). PM samples were also chemically characterized for metals, ions (cations/anions) and WSOC (Water Soluble Organic Carbon) by using ICP OES (Inductively Coupled Plasma with Optical Emission Spectroscopy), Ion chromatograph(IC) and Total Organic analyzer(TOC).

RESULTS

PM_{10} levels at all sites were significantly higher than the permissible levels, Respirable PM content (range: 58.44µg m^{-3}- 141.22µg m^{-3}) was more than two times greater than the permissible levels (60µg m^{-3}, CPCB) at some railway line and traffic intersection (Fig. 1).

Factors influencing PM levels

Major factors influencing PM levels (PM_{10}, $PM_{2.5}$, and PM_{1}) in ambient air are vehicular traffic, and railway line. Influence of construction activity on coarse PM was observed by comparison of

samples collected during (summer) and post completion (winter) of a construction activity at a major traffic intersection (TIC1 in Fig.2); construction activity accounted for 70% of TSPM load. Results support the theory that coarse particles generated due to mechanical friction between railway tracks and train wheels is a possible source of PM.

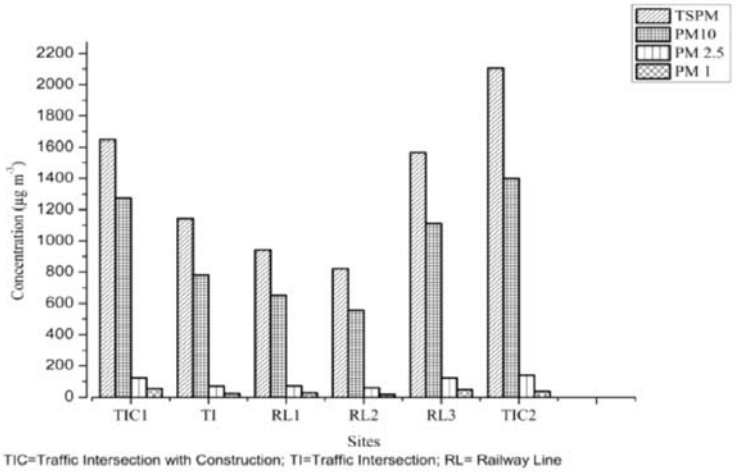

Figure 1. PM levels (TSPM, PM_{10}, $PM_{2.5}$ and PM_{1}) at all six sites in summer 2011.

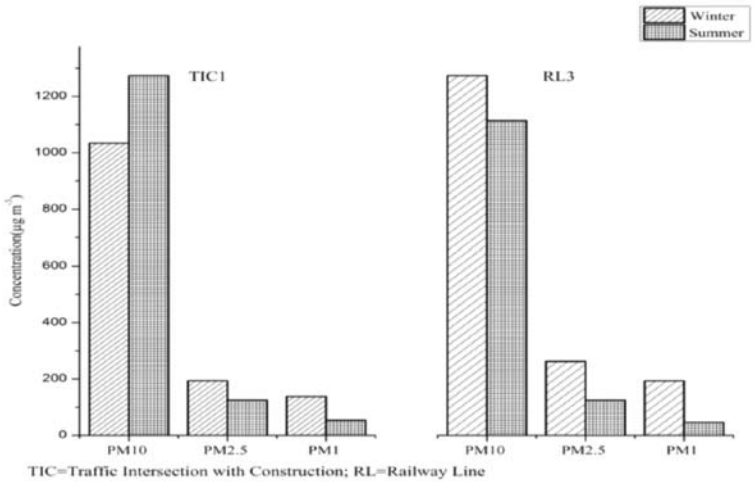

Figure 2. Seasonal variations of PM_{10}, $PM_{2.5}$ and PM_{1} at two sites.

Seasonal variations and proof of anthropogenic sources

Impact of weather change on PM size distribution (Fig. 2) and metal concentrations in ambient environment was also observed. All metals (n=11; Mn, Fe, Ni, Cu, Zn, Cd, Cr, Ca, Mg, Na and Pb were detected at all sites. Although the levels of Fe at traffic intersections were relatively consistent (Average: 92 ±12μg m^{-3}), it is interesting to note that the busiest railway intersection (RL3) showed the highest level (300μg m^{-3}). High K/Na ratio (range: 0.9 to 4.4) for all sites highlights anthropogenic sources.

CONCLUSIONS

Results from this study reveal that the city of Kanpur is reeling under high air pollution. More than doubling of vehicle registration numbers in the city during the past decade and continued growth in registration statistics accentuate the need for infrastructure development and stricter control measures. Observations revealing railway line as possible prominent source for high pollution level in the city warrant further investigation. With continued growth in economy and living standards leading to increased vehicular registration, implementation of mitigation strategies to control air pollution is inevitable and possibilities will be discussed.

REFERENCES

Braziewicz, J., Kownacka, L., Majewska, U., and Korman, A. (2004). Elemental concentrations in tropospheric and lower stratospheric air in a Northeastern region of Poland, *Atmos. Environ.***38**: 1989-1996.

CSE (2009). Air pollution on the rise in Kanpur. http:// www.cseindia.org/node/558. Accessed 17 December 2009.

Dockery, D. W. and Pope, C. A. (1994). Acute respiratory effects of particulate air pollution. *Annu. Rev. Public Health*. **15**, 107-132.

Gupta, I., Salunkhe, A., and Kumar, R. (2010). Modelling 10-year trends of PM10 and related toxic heavy metal concentrations in four cities in India. *J. Hazard. Mater.***179,** 1084-1095.

Karar, K., and Gupta, A. K. (2006). Seasonal variations and chemical characterization of ambient PM10 at residential and industrial sites of an urban region of Kolkata (Calcutta), India. *Atmospheric Research*. **81**, 36-53.

Kawanaka, Y. T. Y., Yun, S.J. and Sakamoto K. (2009). Size distributions of polycyclic aromatic hydrocarbons in the atmosphere and estimation of the contribution of ultrafine particles to their lung deposition. *Environ Sci Technol.* . **43**, 6851-6856.

McEntee, J. C., and Ogneva-Himmelberger, Y. (2008). Diesel particulate matter, lung cancer, and asthma incidences along major traffic corridors in MA, USA: A GIS analysis. *Health & Place*. *14*: 817-828.

TheIndianExpress. (2011). Kanpur second most polluted city, Lucknow fifth: WHO. Available at: *http:// www.indianexpress.com/news/kanpur-second-most-polluted-city-lucknow-fifth-who/ 852395/ Accessed 27 September 2011*.

Zhang, W. C. J. and Qi, Q. (2001). Advances on the biological effect indices for fine particles (PM2.5) in air. *Wei Sheng Yan Jiu*. **30**: 379-382.

BIOAEROSOL EXPOSURE IN DIFFERENT SECTIONS OF PRINTING PRESS AREA OF DELHI

BIPASHA GHOSH, HIMANSHU LAL, RAJESH KUSHWAHA, NABA HAZARIKA, ARUN SRIVASTAVAV, V.K. JAIN

School of Environmental Sciences, J.N.U.
New Delhi 110067, India

Keywords: BIOAEROSOL, PRINTING PRESS ENVIRONMENT, SOURCE IDENTIFICATION, ALLERGIC FUNGI, INDOOR AIR QUALITY

INTRODUCTION

Bioaerosols are defined as airborne particles consisting of living organisms such as microorganisms or originating from living organisms, such as metabolites, toxins or fragments of microorganisms. Bacterial cells and cellular fragments, fungal spores and by-products of microbial metabolism, present as particulate, liquid or volatile organic compounds may be components of bioaerosols (Stetzenbach, *et al.* 2004). In reference to manufacturing industries Crook (1995) demonstrated that printing works and textile mills, bacteria can contaminate humidifiers used to condition workplace air. Certain recent studies carried out by Zhu, *et al.* (2003) in offices and industrial units reveal positive impact of air conditioning system on growing indoor bioaerosol concentration by acting as a major pathway for bacteria transfer from outdoor to indoor. However, several studies done by Huang, *et al.* (2011) pertaining to the presence of ozone and their impact on indoor bioaerosol totally contradicts the possibility of finding high bioaerosol concentration. In India, few works related to bioaerosols have been done. Most of them have concentrated on the effect of pollen triggering allergic reactions. Aerobiological study carried out at different indoor environments such as food grain godowns, library building and bakery in Gwalior revealed the impact of bioaerosol on the organic materials stored and present there (Jain, 2002). In Delhi, the national capital, few studies related to aerobiological studies have been done. Some of these include, study of fungal spora in various part of Delhi region (Agarwal, *et al.*, 1969). Viable bioaerosol assessment carried out within the campus of JawaharLal Nehru University, New Delhi, identifies fungal bioaerosol associated with immunotoxic diseases such as sick building syndrome in respirable fractions (Srivastava, *et al.* 2011).

The present study has been undertaken with the following objectives

- To estimate concentration bioaerosols at various end-use locations of Printing Press area.
- To check the relationship between various meteorological parameters with bioaerosol concentration and to check the relation between indoor and outdoor bioaerosol concentration.
- To identify various fungal samples at their specific levels.

METHODOLOGY

The present study pertains to Delhi, the capital city of India. Sampling was carried out in different section of a Printing Press named Graphic lines (15 years old) situated in Industrial area of Naraina Phase II in West Delhi. Sampling was done in the outdoor as well as indoor in the three main sections of the Press namely office, printing area and store. Sampling was done with the help of a viable air sampler named Buck Bio-culture pump (Model B30120). Each air samples were taken at a flow rate of 40 lit/min for 1 minute. The sampling was carried out for three different fractions of

bioaerosols viz. fungi, gram positive and gram negative bacteria from July - October 2011. Three samples were taken from each site in each month.

For detection and enumeration of fungi and bacteria media were used on the collection plates. Potato dextrose agar (PDA), Eosin methylene blue agar media (EMB agar media) and Blood agar were used for counting of fungi, Gram negative bacteria and Gram positive bacteria respectively**.** In this study the bacterial plates were incubated at 30^0C to 37^0C for 48h for both Gram negative and Gram positive bacteria. Fungal plates were incubated at 28^0C for 3 days. The resultant colonies were reported as colony-forming units (CFU m^{-3}). Fungal isolates were mainly identified by the direct observation on the basis of spore and colony morphological features.

Bioaerosol concentration (cfu/m^3) = No. of colonies / Flow rate × Sampling Duration (minutes)

Microscopic examination and visual identification

Preserved stock cultures were sent to Plant Pathology Department, IARI, New Delhi for authentic identification of the fungal species upto their species level.

Statistical analysis (Regression) was carried out with the help of Microsoft Excel 2007.

CONCLUSIONS

From the present study the following conclusions can be drawn:

- Though temperature and relative humidity are important for microbial growth yet the R^2 values reveal that change in these environmental parameters did not impose any significant change in bioaerosol concentration at all the four sites. Other factors such as substratum (preferably dry), mechanical movements by wind and human may be the main reason for release of microbes in air.
- Store was found to contain maximum bioaerosol concentration due to water damped walls, piles of paper bundles and leftover paper cutting as well as their handling by the workers may primarily be attributed for fungal concentration. Occupancy and influx of outdoor air may be the main reasons for bacterial concentration. In the printing area due to release of ozone from printing machines, the bioaerosol concentration was found to be much less than expected. Bioaerosol concentration was found to be least in the office section due to cleanliness. Use of latest technologically based air conditioning system and absence of other ventilation system also play an important role in presence of less air microbes.
- From the present study it can be said that the indoor environment can become contaminated with particles that present different and sometimes more serious risks than those related to outdoor exposure, when their concentration exceed the recommended maximum limits. For all the four sites the total bioaerosol concentration was found to exceed 1000cfu/m^3, the standard set by the National Institute of Occupational Safety and Health (NIOSH) and American Conference of Governmental Industrial Hygienists (ACGIH).
- Round five fungal genera identified namely *Aspergillusflavus, Aspergillusniger, Chaetomium sp., Penicllium sp. and Curvularia sp.* were found in abundance in most of the sections of the printing area. Presence of *Aspergillus* sp. in maximum represents an allergic environment.*Aspergillusniger* is one of the most common causes of Otomycosis (fungal ear infection) which can cause pain, temporary hearing loss and in severe cases damage the ear

canal and tympanum membrane. *Aspergillusflavus* is the second most common agent of aspergillosis.

ACKNOWLEDGEMENTS

We take the opportunity to thank the director of the Graphic Lines Printing Press, New Delhi for providing opportunity to collect air samples within different sections of the printing area. We also thank Dr. Prameela Devi and Dr. NetaMathur of Indian Type Culture Collection (ITCC), Division of Mycology and Plant Pathology, Indian Agriculture Research Institute, New Delhi for authentic identification of fungal bioaerosolsupto their species level.

REFERENCES

Agarwal, M. K., Shivpuri, D. N., Mukherji, K. G. (1969). Studies on the allergenic fungal spores of the Delhi, India, metropolitan area: Botanical aspects (aeromycology), *Journal of Allergy*, **44**, pp. 193-203.

Crook, B. (1995). Airborne microorganisms in humidified textile mills and print works Biodeterioration and Biodegradation, Institute of Chemical Engineers Publications, Rugby, U.K . , **9**, pp. 328–333.

Huang, H., Lee, M., Tai, J. (2011).Controlling Indoor Bioaerosols using a Hybrid system of Ozone and catalysts, *Aerosol and Air quality Research*, pp. 1-10.

Jain, A. K. (2000). Survey of bioaerosol in different indoor working environments in central India, Earth and Environmental Science, **16**, pp. 221-225.

Srivastava, A., Singh, M., Jain, V. K. (2011). Identification and characterization of size-segregated bioaerosols at Jawaharlal Nehru University, New Delhi, *Nat Hazards*, **60**, pp. 485-499.

Stetzenbach, L. D., Buttner, M. P., Cruz, P. (2004). Detection and enumeration of airborne biocontaminants, Curr.Opin.Biotechno.,**15**, pp. 170-174.

Zhu, H., Phelan, P., Duan, T., Raupp, G., Fernando, H. J. S. (2003).Characterizations and relationships between outdoor and indoor bioaerosols in an office building, China, Particuology, pp. 119-123.

CHARACTERIZATION OF ATMOSPHERIC AEROSOLS FOR AN EVALUATION OF ENVIRONMENTAL PERFORMANE INDEX IN INDIA

P.V.N.NAIR[1] AND R.V.CHOWGULE[2]

[1]B-13, Basera, Deonar, Mumbai -400088, India
[2]Indian Institute of Environmental Medicine
Kasturba Hospital, Ward No.12
Sane GurujiMarg, Mumbai - 400011, India

Keywords :AEROSOLS IN HEALTH, AEROSOL CHARACTERIZATION

INTRODUCTION

India was ranked last in air quality and its effect on human health , in 2012, as per Environmental Performance Index (EPI), based on a worldwide study of 132 countries, conducted jointly by environmental research groups at the Yale and Columbia Universities, USA from 2002, in collaboration with World Economic Forum and European Union. India's overall ranking in EPI was 125 (Yale Center for Environmental Law & Policy, 2012) . EPI has been accepted worldwide. In India, the Planning Commission (PCI) and Ministry of Environment and Forests (MoEF), with the help of some NGOs have announced a proposal to evaluate and rank the environment in states in India on the basis of EPI (Planning Commission, 2011).

Atmospheric aerosols play a key role in environmental health. Their Characterization consistent with International standards is needed to be carried out systematically along with measurement of several other specified variables for a reliable evaluation of EPI. In this context, lack of suitable data, specially on aerosols at ground level is reported and satellite-based estimates are often substituted in the study. Hence, the current scenario in our country on characterization of atmospheric aerosols is examined and corrective measures are suggested, to ensure availability of suitable data consistent with the needed Quality Assurance and Quality Control (QA&QC) for a realistic assessment of EPI .

METHODS

There are several initiatives and action plans by Institutions such as MoEF, PCI, Ministry of Health & Family Welfare (MoH&FW) ,Central Pollution Control Board(CPCB) and National Environ. Engineering Research Institute (NEERI) at the Center, Pollution Control Boards in different States, Municipal Corporations such as Municipal Corporation of Greater Mumbai and NGOs. Indian Institute of Environmental Medicine (IIEM) has carried out sampling and analysis of air pollutants and correlated the data with respiratory health and asthma (Chowgule et al., 1998).

The published data are compared with data available from studies by different Institutions and used by the Yale and Columbia teams to estimate EPI. Further, work related to Bio-Aerosols in connection with specific conditions prevalent in India, such as solid waste pollution giving rise to air-borne bacteria and microorganisms is studied. Procedures that may be adopted so as to obtain better data are suggested so as to help in improving Environmental Quality in our Country.

CONCLUSIONS

While the good work already done is acknowledged, it is suggested that further effort needs to be undertaken, to enable compliance with International Standards. Apart from strict adherence to

QA-QC measures, measurements of PM2.5 and Ozone on a continuous (round-the-clock) basis and monitoring of Bio-aerosols are important, to support work in improving human health.

REFERENCES

Chowgule, R.V., Shetye, V.M., Parmar, J.R., Bhosale, A.M., Khandagale, M.R., Phalnitkar, S.V. *(*1998). Prevalence of respiratory symptoms,bronchialhyperreactivity, and asthma in a megacity—results ofthe European community respiratory health survey in Mumbai [Bombay], *Am J RespirCrit Care Med* **158,** 547–54.

Planning Commission (2011). Government of India, Mid-term Appraisal 11th Five Year Plan 2007-2012, Chapter 22, 453, Oxford University Press.

Rakesh Kumar and Abba Elizabeth Joseph (2006). Air Pollution Concentrations of PM2.5, PM10 & NO2 at Ambient and Kerbsite and Their Correlation in Metro-City, Mumbai, *Environmental Monitoring and Assessment,* **119,**191.

World Bank (2005). Ten Years of Managing Air Quality in India.

Yale Center for Environmental Law & Policy (2012). Yale University and Center for International Information Network, Columbia University, In collaboration with World Economic Forum and JRC, European Commission, EPI 2012, Full Report, 10.

RETRIEVAL OF VERTICAL PROFILES OF GHGS AND OTHER TROPOSPHERIC TRACE GASES OVER AN URBAN ENVIRONMENT OF INDIA (DELHI) USING A GROUND-BASED FTIR TECHNIQUE: PRELIMINARY RESULTS AND IMPLICATIONS TO AEROSOL FORMATION

S. K. MISHRA[1], B. BARRET[2], R. AGNIHOTRI[1], B.C. ARYA[1], A. KUMAR[1], V. KANAWADE[3]

[1]CSIR- National Physical Laboratory, New Delhi, 110012, India
[2]Laboratoire d'Aérologie, OMP, CNRS/Université de Toulouse, Toulouse, France
[3]Department of Civil Engineering, IITK, Kanpur, 208016

Keywords**:**FTIR, SOLAR ABSORPTION SPECTRA, GHGS, TRACE GASES, DELHI

INTRODUCTION

The understanding of the vertical distribution of tropospheric trace gases [e.g. ethane (C_2H_6), acetylene (C_2H_2), hydrogen cyanide (HCN), carbon monoxide (CO)] and GHGs [green house gases e.g**.** nitrous oxide(N_2O), methane (CH_4), and ozone (O_3)] over Delhi (a typical urban environment, India) is extremely limited. There is a dire necessity for such experimental observations to understand the tropospheric chemical processes where trace gases, GHGs and aerosols are key participants. CO, C_2H_6, and C_2H_2 are important tropospheric O_3 precursors. The changes in the concentrations of these tropospheric trace gases could affect the regional to global scale tropospheric O_3 budget while the major sink of tropospheric CO, C_2H_6, and C_2H_2 is their reaction with the hydroxyl radical (OH) (Logan et al., 1981, Singh and Zimmerman, 1992). C_2H_6 is the second most abundant organic trace gas in the background troposphere whichis roughly three orders of magnitude less abundant than methane. Owing to highly reactive nature, this is very important gas in the troposphere and it has more probability for forming highly complex intermediates (e.g., acetaldehyde, peroxyacetyl nitrate, and acetic acid), also the oxidation of ethane is important to tropospheric chemistry. Biomass burning is a significant source of tropospheric CO and HCN. CO, C_2H_6, C_2H_2, and HCN have been observed as biomass burning products in the field and laboratory fire experiments (Holzinger, *et al*., 1999). Combustion of fossil fuel and oxidation of CH_4 also provide an important source for tropospheric CO. Natural gas and automobile emissions are important sources which give rise to C_2H_6 and C_2H_2, respectively. Tropospheric lifetimes (global averages) of CO, C_2H_6, and C_2H_2 are ~2 months for both CO and C_2H_6 and ~1 month for C_2H_2 (Logan, *et al*., 1981). Owing to the relatively short tropospheric lifetimes, spatial and temporal variations in the concentrations of the above mentioned gases gives important signatures for their sources, sinks, and transport. HCN being a relatively inactive species, is assumed to be a potential tracer of biomass burning emission (Rinsland, *et al*., 2001). Among greenhouse gases, CH_4 is the second most important anthropogenic GHG which is the target gas of the Kyoto protocol. The global atmospheric concentration of CH_4 has been more than double since preindustrial times and reached 1774 ppb in 2005 (Forster, *et al*., 2007). In general, in tropics, a large uncertainty exists in retrieval of gas profiles by space borne observations (due to complexity of satellite retrieval algorithms) due to the scarcity of ground based measurements which can validate the satellite observations. This lead us to believe that there is an urgent need to measure the vertical distribution of aforementioned gases by ground-based Fourier Transform InfraRed (FTIR) spectrometer (FTIR), which could compliment to available space-borne instruments.

METHODS

The solar absorption spectra were recorded using a ground-based Fourier Transform InfraRed (FTIR) spectrometer with a resolution of 0.005 cm^{-1} at National Physical Laboratory (28°38'14''N, 77°10'25''E), Delhi, India from March to May, 2012. The profiles of tropospheric gases were retrieved from the FTIR solar spectra using the Atmosphit software developed at ULB (UniversitéLibre de Bruxelles).

CONCLUSIONS

In March, the retrieved volume mixing ratio (vmr) of $C_2H_6$was ~1.3 ppbv in the troposphere (Fig. 1), consistent with reported observations i.e. 1-2 ppbv from Japan (Zhao et al., 2002). The likely sources of C_2H_6 over Delhi may be biomass burning and natural gas emissions in the National Capital Region (NCR). Retrieval of CH_4 and N_2O yield vmr values of ~1800 and ~320 ppbv respectively, while Cape Rama Indian GAW station observed the similar vmr_s~1750-1900 and 324 ppbv respectively in 2010. On 15th May, the tropospheric HCN was retrieved to be ~200 pptv (vmr), which also agrees well with the reported vmr ~180-330 pptv by Zhao et al. (2002). Tropospheric HCN is a biomass burning tracer and its variability over Delhi is probably linked to the biomass burning activities in NCR. These results are indeed very encouraging and first of its kind using FTIR spectrometer in Delhi. This allows us to conduct a continuous monitoring of gaseous pollutants and GHG's in the troposphere over Delhi.

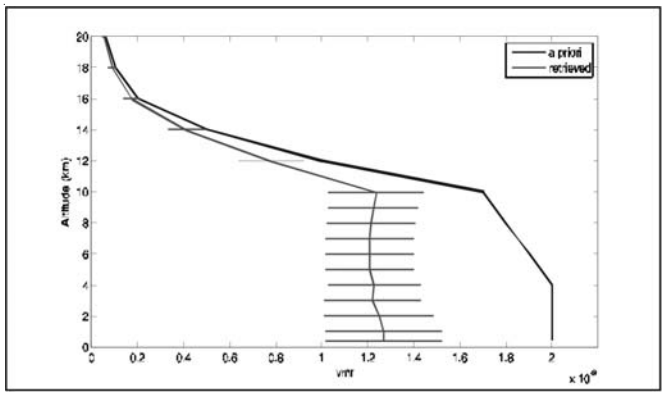

Figure 1. Vertical distribution of volume mixing ratio (vmr) of C_2H_6 (red colored line) with associated uncertainty, together with 'a priori' distribution of the same (blue colored line).

IMPLICATIONS TO AEROSOL-GAS INTERACTIONS AND SECONDARY AEROSOL FORMATION

Role of greenhouse and other trace gases in the formation of aerosols (specifically secondary aerosol formation) and their interaction with pre-existing primary aerosols is highly uncertain and thus remain an area of topical interest. For instance, formation of poly-cyclic aromatic hydrocarbons (PAH) gets facilitated in the atmosphere in presence of acetylene gas (C_2H_2) interacting with nano-scale crystalline mineral dust particles (Tian et al., 2012). Likewise, photolysis of gaseous volatile organic compounds (e.g. C_2H_6) may catalyze formation of peroxyacetyl nitrate (PAN), acting as NO_x reservoir, thereby, formation of secondary aerosols and enhancing tropospheric O_3 levels (Angelbratt et al., 2011). In addition, GHGs have been reported to enhance their warming potential by interacting with ambient pre-existing aerosols (Shindell et al., 2009). In aggregate, retrieved

vertical distribution of greenhouse and other aforementioned gases in tandem with information on physical and chemical characteristics of size segregated aerosols (especially rapidly modernizing and industrializing mega cities like Delhi) can greatly improve understanding of gas-aerosol interactions and associated secondary aerosol formations.

ACKNOWLEDGEMENTS

The authors are thankful to Director NPL, Prof. R. C. Budhani for his consistent support for the ongoing work. We also thank D. Hurtmans and P. Coheur from ULB for providing the Atmosphit retrieval software and the necessary support for using it.

REFERENCES

Angelbratt, J., Mellqvist, J., Simpson, D., Jonson, J.E., Blumenstock, T., Borsdorff, T., Duchatelet P., Forster F. et al. (2011). Carbon monoxide (CO) and ethane (C_2H_6) trends from ground-based solar FTIR measurements at six European stations, comparison and sensitivity analysis with the EMEP model.,*Atmos. Chem. Phys.*, **11**, pp. 9253–9269.

Ehhalt, D. H. (1992). Concentrations and distributions of atmospheric trace gases. *Ber.Bunsenges. Phys. Chem.*,**96**, pp. 229-240.

Forster, P. et al. (2007). Changes in atmospheric constituents and in radioactive forcing, in Climate Change 2007: The Physical Science Basis. Contribution of Working Group I to the Fourth Assessment Report of the Intergovernmental Panel on Climate Change, *Cambridge Univ. Press*, 825 Cambridge, New York

Holzinger, R., Warneke, C., Hansel, A., Jordan, A., and Lindinger, W. (1999).Biomass burning as a source of formaldehyde, acetaldehyde, methanol, acetone, acetonitrile, and hydrogen cyanide, *Geophys. Res. Lett.* **26,** pp. 1161–1164.

Kanakidou, M., Singh, H. B., Valentin, K. M. and Crutzen, P. J. (1991).A Two-dimensional study of ethane and propane oxidation in the troposphere, *J. Geophys. Res.*,**96**, pp.15,395-15,413.

Logan, J. A., Prather, M. J., Wofsy, S. C., and McElroy, M. B. (1981). Tropospheric chemistry: A global perspective, *J. Geophys. Res.*,**86**, pp. 7210–7254.

Rinsland, C. P., Goldman, A., Zander, R., and Mahieu,E. (2001).Enhanced tropospheric HCN columns above Kitt Peak during the 1982–1983 and 1997–1998 El Nin˜o warm phase, *J. Quant. Spectrosc.Radiat. Transfer*, **69**, pp. 3–8.

Shindell D.T., Faluvegi, G, Koch, D.M., Schmidt, G.A., Unger, N., Bauer, S.E.(2009). Improved attribution of climate forcing to emissions, *Science*, **326**, pp. 716–718.

Singh, H. B., and Zimmerman, P. B. (1992). Atmospheric distribution and sources of nonmethane hydrocarbons, in Gaseous Pollutants: Characterization and Cycling, edited by J. O. Nriagu, pp. 177–235, John Wiley, New York.

Tian, M. et al. (2012).Formation of polycyclic aromatic hydrocarbons from acetylene over nanosized olivine-type silicates, *Phys. Chem. Chem. Phys.*, **14**, pp. 6603–6610,

Zhao, Y., et al.(2002). Spectroscopic measurements of tropospheric CO, C_2H_6, C_2H_2, and HCN in northern Japan, *J. Geophys. Res.*, **107** (D18), 4343, doi:10.1029/2001JD000748.

NUMBER SIZE DISTRIBUTION OF ULTRA-FINE AEROSOLS GENERATED FROM BIOMASS BURNING

M. TIWARI, S.K. SAHU, P.Y. AJMAL, R.C. BHANGARE, G.G. PANDIT AND V.D. PURANIK

Environmental Assessment Division, Bhabha Atomic Research Center
Trombay, Mumbai-400085, India
e-mail: ggp@barc.gov.in

Keywords: COMBUSTION AEROSOL, BIOMASS, SMPS, GSD

INTRODUCTION

Particle size distribution (PSD) is an important characteristic of combustion aerosols for evaluating their health hazards. The health hazards associated with exposure to combustion aerosols depends on their size distribution for deposition in respiratory tract and toxic chemicals adsorbed on the aerosols. In present study, the number size distributions of aerosols generated from two commonly used household fuels in rural India namely firewood and dung cake were investigated using scanning mobility particle sizer (SMPS). More than half the world's population relies on solid fuels, including biomass fuels (wood, dung, agricultural residues) and coal, to meet their basic energy needs. Globally, indoor air pollution is responsible for approximately 1.5 million deaths annually (WHO, 2007). Combustion of fuels for cooking and warming the houses is the most dominant source of particulates in indoor environment. It is estimated that as many as 70% of households in developing countries use cooking fuels such as firewood, coal and dung cake with homemade traditional stoves (IEA, 2002). Particle size distribution is an important physical characteristic to evaluate how deep it can travel within and beyond the respiratory tract, which in turn is a necessity for assessment of health impacts (Hays, *et al*., 2002). Most of the studies reported in literature are confined to the mass size distribution of combustion aerosols (Raiyani, *et al*., 1993; Tiwari, *et al*., 2012) in micron range. Since primarily combustion generated particles predominate in the nanometer range, the physical characterization in this range is inevitable to estimate the actual consequent health impacts. The formation of biomass combustion aerosols in different mode (nucleation, Atkins and accumulation) was described. Important parameters of PSD such as total number concentration, geometric mean (GM) and geometric standard deviation (GSD) for tested fuels were evaluated and compared.

METHODS

Firewood and dung cake fuels were purchased locally. Samples were oven dried to reduce their moisture content at 60^0 C for one hour prior to experiment. The stoves used for dung cake and firewood were traditional stoves locally named as "chulha" which were made of clay with a U shaped front opening and cylindrical pot hole. The experimental setup for determination of particle size distributions of combustion aerosols is shown in Fig. 1.In this study, the Sequential Mobility Particle Sizer (DMA + CPC) of GRIMM, Germany, Series 5.400 was utilized for number size distributions of combustion generated aerosols. Sheath air (Particle free air) at ten times flow rate of sample inlet (3 lpm) also flow in differential mobility analyzer (DMA) to maintain the laminar flow in classifier. Only particles with an appropriate charge and size travel to the sample air outlet, entering the Condensation Particle Counter as a mono-disperse aerosol. According to the used DMA type, particles in the size range of 11.1 to 1083.3 nm (for the Vienna U-Type DMA) are

classified in 44 channels by scanning/stepping. Particles are classified with an according to their electrical mobility and their concentration is measured with a Condensation Particle Counter (CPC).

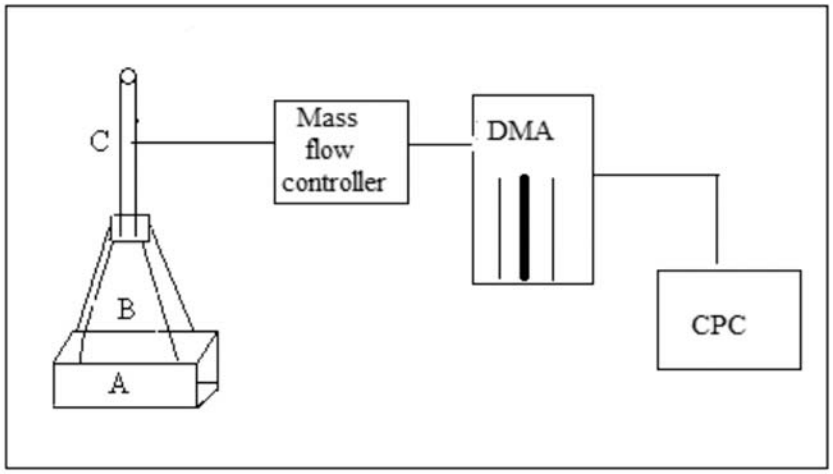

Figure 1. Experimental setup for particle size distributions of combustion aerosols part (A) of setup design to contains stove, part (B) was provide a space to combustion aerosol get cool and dilute prior to analysis while part (C) contain sampling point. DMA (differential mobility analyzer), CPC (Condensation particle counter).

RESULTS AND DISCUSSIONS

The number size distribution for firewood combustion generated aerosol was shown in Fig. 2. Experimental data shows average total number concentration of particles generated from combustion of firewood was found to be 4.9×10^7 #/cm^3. The geometrical mean (GM) for the distribution is calculated to be 123 nm, and the geometrical standard deviation (GSD) 1.78 indicates poly dispersed size distribution. Most of the particles were distributed in mobility size range 30nm to 120nm. Some particles were also found in micron size ranges near 1µm. The percentage contribution of accumulation mode particle concentration was found to be 58.6%, which was higher than nucleation (13.88%) and Aitken modes (27.52%).Higher number concentration of firewood generated aerosol in the accumulation mode was due to primary emission of particle in this size ranges, and also because of incomplete combustion of solid biomass.

The smoke emission from dung cake looks overwhelming due to visible smoke, which may be due to additional moisture content. The number size distribution of combustion aerosols generated from dung cake was shown in Figure 2. The average total number concentration was found to be 3.4×10^7 #/cm^3. The geometrical mean (GM) and the geometrical standard deviation (GSD) for the distribution was found to be 152 nm 1.89 respectively. The distribution obtained for dung cake generated aerosol was found to poly dispersive in nature. Particles were distributed all over the mobility size ranges 10 nm to 1000 nm. The number concentration found to be smaller, but consistently increasing from 10 to 40 nm and remains constant throughout 40 – 200 nm. The number concentration was found to be peaking over 200 – 400 nm mobility size range. The moisture content would have been responsible for the very high concentration of particle at 800 – 1000 nm mobility size range. The percentage contribution of accumulation mode particle concentration was found to be 73.96%, which is higher than other modes. In dung cake generated combustion aerosol the percentage contribution of nucleation and Aitken modes were found to be 10.56% and 15.48% respectively.

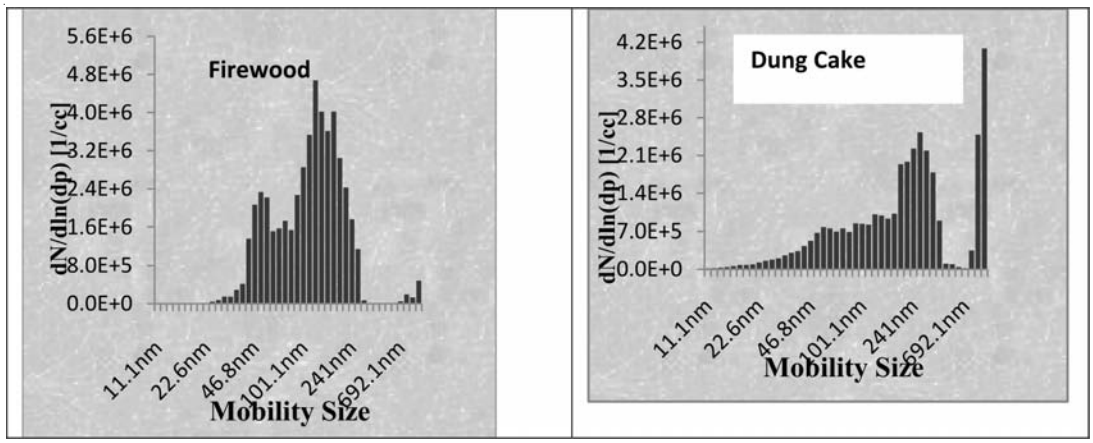

Figure 2. Number size distributions of combustion aerosols generated by firewood and dung cake.

CONCLUSIONS

For biomass fuels the number concentrations were of the order of 10^7#/cm^3. The geometric mean diameters were 123 nm and 152 nm for firewood and dung cake generated combustion aerosols respectively. Firewood and dung cake generated aerosol is found dominantly in accumulation mode because of solid matrix, incomplete combustion and higher moisture content which may leads to primary particle emission in accumulative mode size range. Those data can be used for health hazard calculations, like deposition of combustion aerosols in respiratory tract.

ACKNOWLEDGEMENT

Authors would like to acknowledge Dr. Y. S. Mayya, Head RP&AD, BARC for instrumental support and valuable suggestions.

REFERENCES

IEA (International Energy Agency) (2002). *World Energy Outlook*, Chapter 13, *Energy and Poverty.*

Hays, M. D., Geron, C. D., Linna, K. J. (2002).Speciation of gas-phase and fine particle emissions from burning of foliar fuels.*Environ. Sci. Technol*. **36**, pp. 2281–2295.

Raiyani, C. V., Shah, S. H., Desai, N. M., Venkaiah, K., Patel, J. S., Parikh, D. J., and Kashyap, S. K. (1993b). Characterisation and problems ofindoor air pollution due to cooking stove smoke. *Atmospheric Environment*.**27**(A), pp. 1643-1655.

Tiwari, M., Sahu S.K., Bhangare R.C., Ajmal P.Y., Pandit G. G. (2012). Estimation of polycyclic aromatic hydrocarbons associated with size segregated combustion aerosols generated from household fuels. *Microchemical Journal* doi:10.1016/j.microc.2012.05.008

WHO (World Health Organization) (2007). Indoor air pollution: national burden of disease estimates Geneva.

NUMBER CONCENTRATION AND PARTICLE SIZE DISTRIBUTION OF MAINSTREAM AND EXHALED CIGARETTE SMOKE

R.C. BHANGARE, S.K. SAHU, P.Y. AJMAL, M.TIWARI, G.G. PANDIT AND V.D. PURANIK

Environmental Assessment Division, Bhabha Atomic Research Centre, Trombay,
Mumbai – 400 085, India
e-mail: ggp@barc.gov.in

Keywords: PARTICLE SIZE DISTRIBUTION, MAINSTREAM CIGARETTE SMOKE, EXHALED CIGARETTE SMOKE, SMPS

INTRODUCTION

Tobacco smoke is a complex mixture of gaseous compounds and particulates. About 4800 identified gaseous and particulate bound compounds are found in cigarette smoke (Baker, 1999). In assessing the effects of cigarette smoke on smokers and nonsmokers, the particle size distribution of the generated aerosols is an important factor. During cigarette smoking there are two dominant pathways of exposure to smoke namely active smoking (the one who is smoking cigarette) and passive smoking (the person who is not smoking but is exposed to exhaled smoke of the active smoker). Retention of cigarette smoke in the respiratory tract is a key mechanism in exposure of smokers to smoke constituents and in understanding smoking-related diseases (Feng, *et al*., 2007). Particle size distribution is important to assess as the sizes of cigarette smoke particles govern the mechanism of absorption or retention of the same in body. After its generation the cigarette smoke may undergo various transformations, leading to changes in the particle size distribution at source and at target levels as Environmental Tobacco Smoke (ETS). While undergoing dispersion, the median tobacco smoke particle size can shrink as particle mass evaporates or it can grow as particles coagulate (Klepeis, *et al*., 2003).The mainstream smoke is directly concern of smoker, at the same time the exhaled and side stream ETS is responsible for passive smoking.

METHODS

Experimental set up

A study for cigarette smoke (mainstream and exhaled) analysis was carried on the popular and widely consumed brands in India. Cigarettes used for this experiment were conditioned in a humidified chamber at 65% ± 5% relative humidity (RH) at room temperature (24°C ± 3°C) for at least 24 h prior to smoking. The cigarettes were smoked under ambient laboratory conditions (45% ± 5 % RH, 24°C ± 3°C). The experimental setup is shown in Fig. 1. In the first set of experiment the puff volume was fixed to around 35 ml with a flow rate of 1 lpm and puff duration was kept for 2-3 seconds to know number concentration wise size distribution on puff after puff basis The second set of experiment was designed to reveal changes in particle size distribution after exhalation of the cigarette smoke also on puff by puff basis. Volunteers were asked to exhale the smoke in a specially designed mouthpiece that was opening at one end in a dilution chamber. Particle size distribution of exhaled cigarette smoke was measured directly collecting the smoke in dilution chamber.

In present study, the GRIMM made SMPS-C (Sequential Mobility Particle Sizer) Series 5.400 was used to measure particle size distributions.

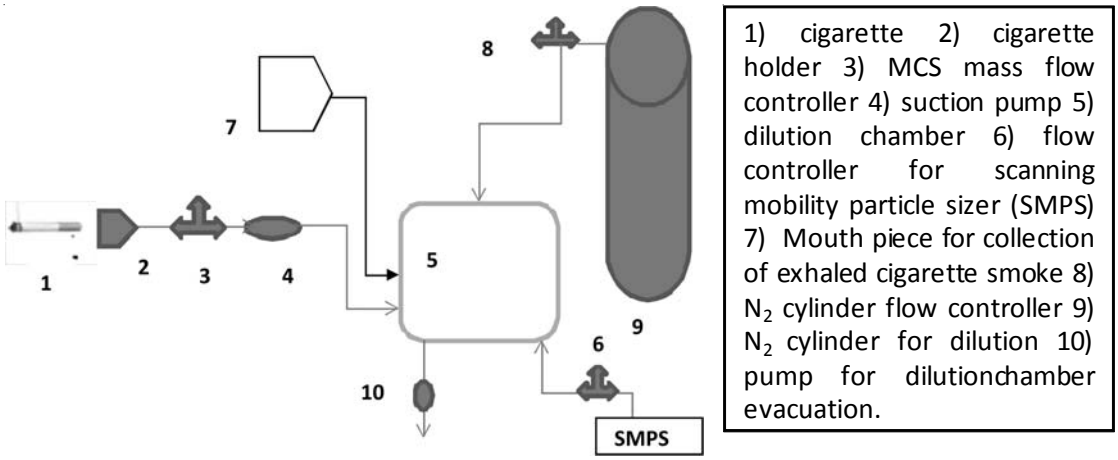

Figure 1. Mainstream cigarette smoke analysis setup.

RESULTS AND DISCUSSIONS

Particle size distribution for mainstream cigarette smoke

The measurement of number concentrations of size fractionated aerosols generated from cigarette smoke showed very slight variation in particle size distribution patterns with number of puffs. Total number concentration of cigarette smoke was of the order of 10^9 N/ml of air. This does not include the water associated with the smoke aerosol, or the volatile organic compounds lost due to evaporation. The particle size distribution of cigarette smoke with puff number is presented in Fig. 2. It was observed that all puffs generated particles in the mobility size range of 10 to 1082 nm and showed a lognormal distribution (positively skewed). It also was found that the cigarette smoke particles above 1.0 μm sizes were not contributing significantly to the total number concentration. Considering all the puffs it was found that the cigarette smoke particles mostly distributed to submicron size range i.e. 0.01-1μm which is in good agreement with an earlier published work (Chang, *et al*., 1985).

The particle size distribution of puff wise mainstream cigarette smoke revealed that there was no significant effect on distributions with puff number. The count median diameters (CMD) for initial four puffs were 193nm, 198nm, 194nm and 186nm. The geometric standard deviation (GSD) values for mainstream cigarette smoke were found in range of 1.42 to 1.46. This reveals that previous puff did not affect the distribution of particle concentration distribution of the next puff significantly. The physical factor of such distribution may arise due to various physiochemical conditions during puffing behavior. Though there wasn't much change in the particle size distribution during different puffs, the number concentration increased with increase in number of puff. As the number of puffs increased there was decrease in filtering capacity of cigarette due to lesser smoke residence time in cigarette and also rise in the temperature at filter end of cigarette. This effect in filtering capacity of cigarette tip and rise in the temperature close to filter end of cigarette alter the thermal or kinematic coagulation as the number of puff increased.

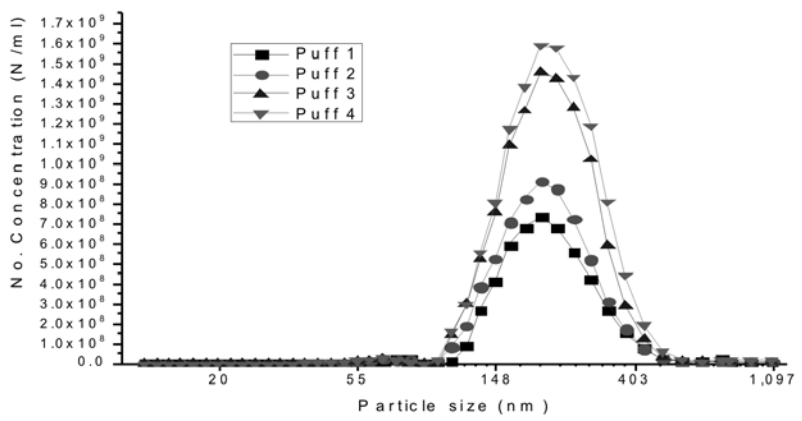

Figure 2. Mainstream cigarette smoke particle size distribution for initial four puffs, puff duration 2-3 second at flow rate of 1L/min

Particle size distribution for exhaled cigarette smoke

Exhaled cigarette smoke is major contributor to environmental tobacco smoke and ingredient of second hand (passive) smoking. The particle size distribution of exhaled cigarette smoke was also investigated. Exhaled puffs were passed in the dilution chamber and diluted to avoid instrument saturation. The particle size distribution is shown in Fig. 3.

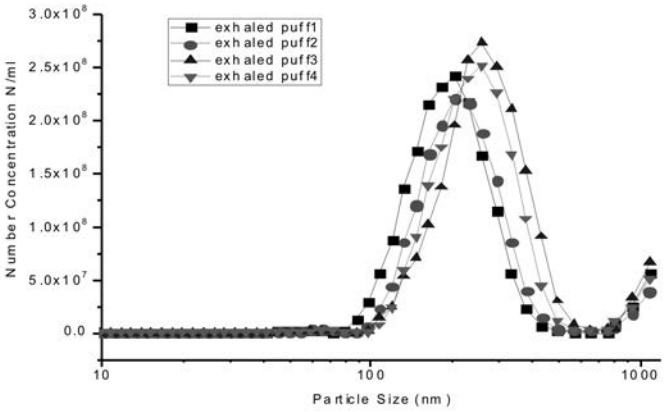

Figure 3. Particle size distribution of puff wise exhaled cigarette smoke measured with SMPS.

The number concentration for exhaled cigarette smoke was found in the range of 10^8 N/ml and didn't show much variation with different numbers of puffs. The count median diameter (CMD) for exhaled smoke was found to be in 0.23±0.05µm range while the geometrical standard deviation (GSD) was found to be in the range of 1.85 to 2.10. The ratio of mainstream smoke CMD to exhaled cigarette smoke (growth factor) was found to be 1.5 ± 0.3 which may vary person to person and also depends on smoking behaviour. Hygroscopic coagulation is dominant parameter for growth factor. In practice exhaled cigarette smoke goes into atmosphere and gets diluted while smoking in indoor environment it being a constituent of environmental tobacco smoke (ETS) may undergo deposition by normal respiration.

CONCLUSIONS

Size fractionated smoke particles emitted by cigarettes were measured under a variety of conditions. The values of CMD of the mainstream smoke for initial four consecutive puffs were found to be significantly consistent, which indicates that there was no significant effect on particle size distribution with increasing puff numbers. Exhaled cigarette smoke showed a growth factor of 1.5 ± 0.3 indicating the coagulation and hygroscopic growth of particles inside the respiratory system.

REFERENCES

Baker, R. R. (1999). Smoke chemistry. In: D. Layten Davis & Mark T. Nielsen. Eds. Tobacco Production, *Chemistry and Technology, Oxford: Blackwell Science Ltd*., pp. 398-439.

Chang, Pao, T., Peters, L. K., and Ueno, Y. (1985).Particle Size Distribution of Mainstream Cigarette Smoke Undergoing Dilution, *Aerosol Sci. Technol*.**4** (2), pp. 191-207.

Feng, S., Plunkett, S. E., Lam, K., Kapur, S., Muhammad, R., Jin, Y., Zimmermann, M., Mendes, P., Kinser, R., Roethig, H. J. (2007). A new method for estimating the retention of selected smoke constituents in the respiratory tract of smokers during cigarette smoking. *Inhal.Toxicol.*, **19**, pp. 169–179.

Klepeis, N. E., Apte, M. G., Gundel, L. A., Sextro, R. G. and William, W. (2003). Determining Size Specific Emission Factors for Environmental Tobacco Smoke Particles, *Aerosol Sci.Technol.* **37**(10), pp. 780-790.

SPATIAL DISTRIBUTION OF AEROSOL DIRECT RADIATIVE EFFECTS FROM CLIMATE MODEL AND COMPARISON AGAINST MEASUREMENT-BASED ESTIMATES OVER INDIA

S. VERMA

Department of Civil Engineering, Indian Institute of Technology Kharagpur,
Kharagpur-721302, India
Email: shubhaverm@gmail.com; shubha@iitkgp.ac.in

Keywords: AEROSOL RADIATIVE FORCING, GCM SIMULATIONS, SINGLE SCATTERING ALBEDO

INTRODUCTION

Human activities causing release of greenhouse gases and aerosols are the main drivers of climate change (Forster, *et al*., 2007). Radiative forcing of the surface-troposphere system is the change in net irradiance at the tropopause after allowing for stratospheric temperatures to readjust to radiative equilibrium but with surface and tropospheric temperatures and other state variables held fixed at the unperturbed values (Forster, *et al*., 2007). Anthropogenic aerosols alter the earth's energy balance by changing radiative fluxes both at the surface and at the top of the atmosphere (Bellouin, *et al*., 2005) and hence exert radiative forcing of climate. Aerosols reduce the solar radiation reaching the earth's surface by absorbing and scattering respectively the incoming solar radiation and hence cause negative radiative forcing at the surface. Additionally, aerosols such as black carbon absorb solar radiation resulting in a positive radiative forcing at the top-of-atmosphere (TOA). Since aerosol radiative forcing is related to the change in equilibrium temperature of the earth's surface, it is used as an index to understand potential climate response.

Change in the radiative flux due to aerosols is a function of the atmospheric loading of aerosols and the sign of radiative forcing at the TOA will depend upon the aerosol single scattering albedo as well as the albedo of underlying surface and the distribution of solar zenith angle, the balance between absorption and scattering being the key. On the other hand, the regional climate response to the variation (spatial and temporal) in aerosol radiative effects will depend on the intensity of radiative-convective coupling between the surface and the atmosphere which could be different during the different seasons over the tropical and non-tropical world regions. This could lead to climate response due to aerosols which could be different regionally and globally. In this context, it is necessary to examine the radiative effects due to aerosols on a regional basis. In the present study, we carry out an analysis of spatial distribution of aerosol radiative effects during the winter monsoon season from estimates of aerosol transport simulations in a climate model of the Laboratoire de MétéorologieDynamique (LMD). We further carry out a comparative study of climate model estimates against estimates of aerosol radiative forcing obtained from measurements data over India. The specific objectives of the study include the following: (i) evaluate aerosol single scattering albedo due to contribution to assess the relative importance of scattering or absorbing aerosols, (ii) analyse the spatial distribution of aerosol radiative effects from model simulations and compare them with those from measurement-based estimates over India.

METHODOLOGY

Aerosol transport simulations were carried out in the General Circulation Model (GCM) of Laboratoire de MétéorologieDynamique (LMD). The current version of the model includes all major tropospheric aerosol species namely sulfate, black carbon (BC), organic matter (OM), dust, and sea salt. Horizontal model winds were nudged to 6- hourly winds from ECMWF analyses with a relaxation time of 0.1 days. This ensured that the model transport is reasonably constrained by ECMWF meteorology while other dynamical and physical processes are driven by the model parameterizations. Assuming external mixing of aerosol species, aerosol optical properties (mass extinction coefficient, single scattering albedo (SSA), and asymmetry factor, g) were computed using Mie theory assuming prescribed lognormal size distributions and refractive indices. Radiative fluxes in the shortwave spectrum (0.25-4.00 μm) were computed every 2 h, at the top-of-atmosphere (TOA) and at the surface, with and without the presence of clouds, and with and without the presence of aerosols using a double radiation call at each time-step of the model integration. The clear-sky and all-sky direct aerosol radiative effects can then be estimated as the difference in radiative flux with and without aerosols.

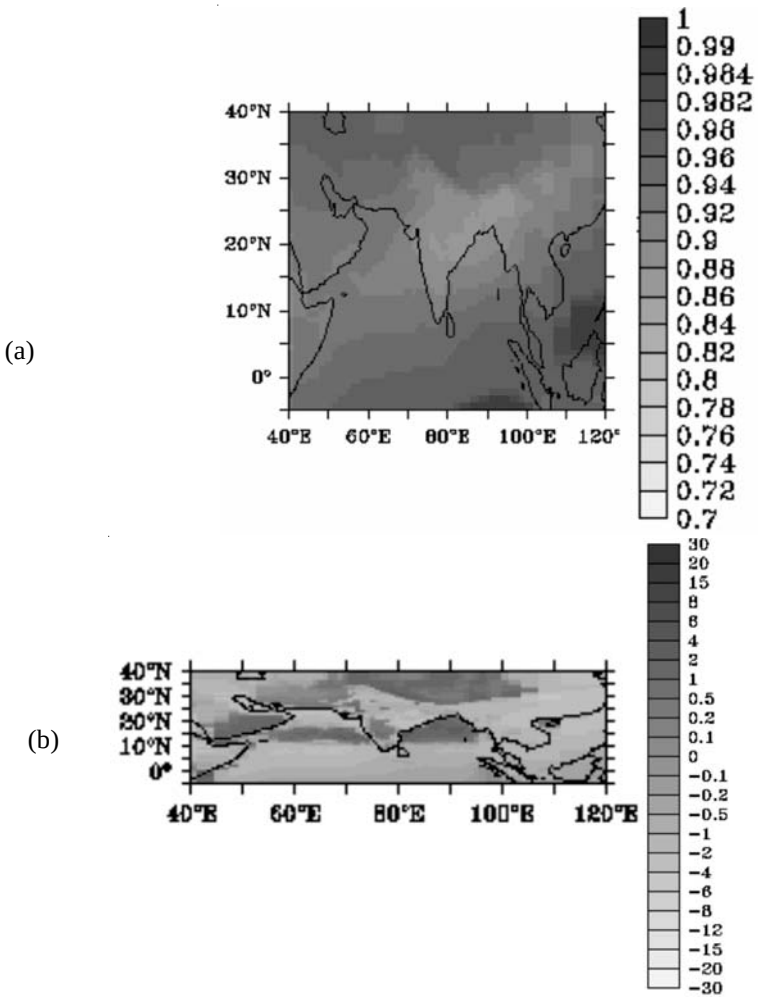

Figure1.(a) Spatial distribution of SSA, (b) Spatial distribution of aerosol radiative effects at TOA over Indian subcontinent and Ocean during winter monsoon.

In order to estimate aerosol radiative forcing from measurements data, aerosol optical properties obtained from ground- and satellite based observations are used to generate spectralvaluesofaerosolopticalproperties (aerosol optical depth, single scattering albedo, and asymmetry parameter) in 40 wavelength channels of shortwave spectrum (0.25-4 μm) to perform radiative transfer calculations. In order to perform radiative transfer calculations in the shortwave region, we have used the radiation code SBDART (Santa Barbara DISORT Atmospheric Radiative Transfer) (Ricchiazzi, *et al*., 1998). The shortwave aerosol radiative forcing calculations were performed using 65 atmospheric layers and eight radiation streams.

CONCLUSIONS

Model estimated mean aerosol single scattering albedo (SSA) as presented in Fig. 1a showed the presence of lower SSA values (0.86-0.9) over the Indian subcontinent compared to the adjoining oceanic regions of Arabian sea (AS) and Bay of Bengal (BoB) (0.88-0.94) and was in the range 0.94-0.98 over the region south to 10°N. The SSA estimated from the present study is found to be consistent with the SSA values inferred based on aerosol measurements on various platforms over the Indian Ocean and subcontinent. The spatial distribution of aerosol radiative effects estimated from the simulations at TOA is shown in Figure 1b. At the surface, aerosols lead to a decrease in the radiation over the Indian subcontinent by 10-15Wm^{-2} and over the adjoining oceanic regions by 4-10 Wm^{-2} with a maximum reduction (15 to 20 W m^{-2}) present along the east coast of India. The positive aerosol radiative effects of 0.5-1 Wm^{-2} at the TOA are seen over most of the parts of the AS, BoB, and parts of central India, with the values as high as 2-4 W m^{-2} over the BoB. It is interesting to see somewhat higher intensity of positive radiative effects at the TOA over the BoB than the AS, which is due to the presence of higher concentration of BC in correspondence with the lower values of SSA over the BoB than the AS. Within the atmosphere, aerosols trapped 8-15 W m^{-2} of solar radiation over the Indian subcontinent and ocean. Comparison of model estimated values against measurement-based estimates will be presented over India.

REFERENCES

Bellouin, N., Boucher O., Haywood J., and Reddy M. S. (2005). Global estimate of aerosol direct radiative forcing from satellite measurements, *Nature*, **438**, pp. 1138– 1141.

Forster, P., et al. (2007), Changes in atmospheric constituents and in radiative forcing, in Climate Change 2007: The Physical Science Basis. Contribution of Working Group I to the Fourth Assessment Report of the Intergovernmental Panel on Climate Change, edited by S. Solomon et al., Cambridge Univ. Press, New York.

Ricchiazzi, P.,Yang, S., Gautier, C., Sowle, D. (1998). SBDART, a research and teaching tool for plane-parallel radiative transfer in the earth's atmosphere. *Bull. Am. Meteorol. Soc.*, **79**, pp. 2101–2114.

AEROSOL SYNTHESIS OF COMPOSITE NANOPARTICLES FOR CONTROLLED DRUG RELEASE APPLICATIONS

PRANAV KUMAR ASTHANA, AMOL ASHOK PAWAR AND CHANDRA VENKATARAMAN

Department of Chemical Engineering
Indian Institute of Technology Bombay
Powai, Mumbai, Maharashtra - 400076, India

Keywords:NANOPARTICLE, NALM, TEM

BACKGROUND AND MOTIVATION

Composite nanoparticles for controlled drug release applications are particles containing one or more than one matrix material with one or more drugs or active agents. For example, anti-cancer applications have used functionalized lipid-polymer hybrid matrices containing docetaxel (Zhang and Zhang, 2010) or paclitaxel–gemcitabine drug conjugates encapsulated in a lipid-coated polymeric nanoparticle (Aryal, *et.al*, 2010). Use of composite nano-particles sometimes improves the stability of the matrix e.g. lipid nanoparticles composed of multiple matrix lipids exhibit reduced polymorphic transformations and prevents burst drug release (Muller, *et al*., 2000). Further, it may allow encapsulation of both hydrophilic and hydrophobic drugs e.g. lipid nanoparticles containing multiple anti-tubercular drugs (Pandey, *et al*., 2005). It has been suggested that the underlying microstructure of these composite particles influences multi-drug release rates (Seylor, *et al*., 2007). Use of layered nanoparticles, confining different active agents in different layers, allows customization of release profiles, as demonstrated in tri-layered composites for drug release application (Lee, *et al*., 2011).

Various techniques based on single and double emulsion evaporation and emulsion polymerization have so far been employed to prepare composite microparticles (Catarina et al., 2006). High speed stirring or ultrasonication used, result in high shear and thermal stresses allowing poor or little control over the microstructure or layering that evolve during nanoparticle formation(Hannele et al., 2003). Recently, aerosol synthesis has been used for drug nanoparticles with encapsulation (Eerikainen and Kauppinen, 2003; Lee, *et al*., 2011; Pawar, *et al*., 2012). An air-jet atomization based aerosol method was used to make stearic acid nanoparticles (NALM or nanoparticle aerosol lipid matrices) with controlled crystallinity and drug release rates (Pawar, *et al*., 2012). Co-axial electrospray atomization has been used to produce layered structures by atomizing liquid droplets containing layers of different materials (Lee, *et al*., 2011). However, air-jet atomization, a more widely used method with greater throughput, it yet to be explored for production of composite or layered nanoparticles. Control of droplet evaporation rate influenced formation of solid or shell structures (Bandyopadhyay, *et al*., 2012) in a computational model study, suggesting the possibility of layered structure formation during precipitation in an evaporating drop. This work attempts to produce layered nanoparticles using an air-jet atomization based aerosol method.

EXPERIMENTAL APPROACH

Low-temperature aerosol reactor method was used to synthesize composite nanoparticles composed of stearic acid (>95% pure; Sigma Aldrich; St. Louis, USA), matrix material and Isonizid (LupinPharamaceuticals Ltd., Pune, India), an anti-tubercular drug. It had been demonstrated that the initial drug-to-lipid mass ratio of the precursor solution was preserved during this aerosol reactor

method and control over particle size, crystallinity can be achieved (Pawar et al., 2012). To investigate aerosol processing conditions leading to layer formation, the matrix material and drug were selected based on their diffusion coefficients and solubility in the selected precursor solvent, ethanol (Table 1). Precursor solutions (1 and 10 mg/ml) containing drug: lipid (1:1 and 1: 2) were freshly prepared in ethanol (99.9, Merk chemicals (Pty) ltd. Gauteng, South Africa).

Solute	**Molecular weight**	**Solubility in ethanol mg/ml**	**Diffusivity (10^{-12}) m^2/s**
Stearic acid	284.48	29.8	7.5
Isoniazid	137.139	125	12

Table 1.Solubility and diffusivity of solutes in ethanol.

Experimental set-up used for synthesis of composite nanoparticles comprised of an indigenously designed aerosol reactor (Fig.1), collision-type air jet atomizer (Model 3076; TSI Inc. Particle Instruments, St. Paul, MO, USA), scanning mobility particle sizer (SMPS; Model 3936; TSI Inc. Particle Instruments). SMPS was equipped with a differential mobility analyzer (Long DMA, Model 3081; TSI Inc. Particle Instruments) and a condensation particle counter (CPC, Model 3075; TSI Inc. Particle Instruments). The precursor solution was fed into the atomizer using a syringe pump (PHD 2000; Harvard Apparatus, Holliston, MA, USA).

The real-time mobility based size distribution of composite NALM was measured using SMPS. Wet-electrostatic precipitator was used for direct collection of composite NALM into water. The mean hydrodynamic diameter of collected NALM was measured using dynamic light scattering instrument (Malvern: ZEN 1600 (Red)). Characterization of composite properties was done using transmission electron microscope (JEM-2100F.; JEOL; Japan).

Figure 1.Schematic of aerosol reactor for synthesis of composite nanoparticles containing stearic acid and Isoniazid.

Preliminary results

Mean mobility diameter of composite NALM synthesized in the aerosol reactor using precursor solutions with different concentration and ratio (Fig. 2) ranged 90-160 nm, with a reasonably narrow unimodal size distribution (geometric standard deviations (GSD) of 1.69-1.77; Table 2). The NALM suspension was not stable (polydispersity index 0.86-1.00), (Table 2). The presence of layers was observed (Fig. 2) with three different image intensities, lightest on the interior and darkest on the exterior of the particles imaged by TEM. This implies a gradation from lowest to higher

molecular weight compounds from interior to exterior. In this case the matrix, stearic acid has a higher molecular weight than the active agent, isoniazid, implying a core of isoniazid and shell of stearic acid. The paper will discuss control of aerosol processing conditions to obtain particles with desired layering properties.

Concentration	Lipid: drug	SMPS		DLS	
		Mean Mobility diameter(nm)	G Std. dev	Hydrodynamic Diameter(nm)	PI
1mg/ml	1:01	93.9 ± 0.17	1.77	1704±40	0.86
	2:01	98.9 ± 0.15	1.74	472 ±49	0.75
10mg/ml	1:01	149.3 ± 0.15	1.71	591±12	0.82
	2:01	156.6 ± 0.06	1.69	1096 ±18	1

Table 2. Measured particle properties mean mobility dia, hydrodynamic dia, polydispersity index.

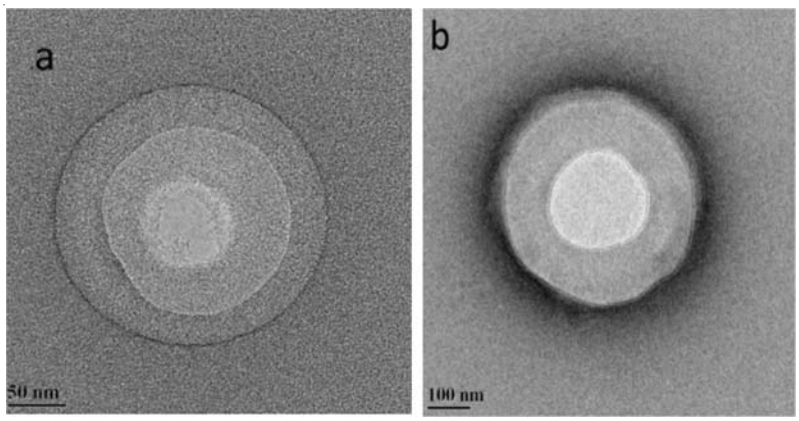

Figure 2. Composite NALM synthesized using stearic acid (lipid), isoniazid (drug), in ethanol as solvent. Precursor solution at total concentration of 10mg/ml exhibited layered structure in FEG-TEM imaging (Fig.2) - (a) lipid: drug 1:1 and (b)lipid: drug 2:1.

REFERENCES

Aryal, Che-Ming Jack Hu, Liangfang Zhang (2010). Combinatorial Drug Conjugation Enables Nanoparticle Dual-Drug Delivery, *small*, **13**, pp. 1442–1448.

Bandyopadhyay, A., Pawar, A.A., Venkataraman, C. and Mehra A. (2012). Aerosol synthesis of nanoparticles for drug delivery applications: modelling droplet evaporation and particle structure,Under review in *Aerosol Science & Technology*, Manuscript No. AST-MS—152

Catarina Pinto Reis, Ronald Neufeld J., Anto´nioRibeiro J., Francisco Veiga. Nanoencapsulation I. (2006). Methods for preparation of drug-loaded polymeric nanoparticles; Nanomedicine: Nanotechnology, *Biology and Medicine*, **2,** pp. 8– 21.

Eerikainen, H. and Kauppinen , E.I. (2003). Preparation of polymeric nanoparticles containing corticosteroid by a novel aerosol flow reactor method, *Int J Pharm*., **263**, pp. 69-83.

Hannele, Eerika¨inen, Wiwik Watanabe1, EskoKauppinen I., Petri Ahonen P. (2003).Aerosol flow reactor method for synthesis of drug nanoparticles, *European Journal of Pharmaceutics and Biopharmaceutics,* **55,** pp. 357–360.

Lee, Y.H., Bai, M.Y. and Chen, D.R. (2011). Multidrug encapsulation by coaxial tri-capillary electrospray, *Colloid Surface B.,* **82**, pp. 104-10.

Zhang, Li and zhang, Liangfang (2010). Lipid polymer hybrid nanoparticles: Synthesis, characterization and Applications, *Nano LIFE*, pp. 163-173.

Muller, R.H., Mader, K. and Gohla, S. (2000). Solid lipid nanoparticles (SLN) for controlled drug delivery - a review of the state of the art, *Eur. J. Pharm. Biopharm*., **50**, pp. 161-77.

Pandey, R., Sharm, S., Khuller, G.K. (2005). Oral solid lipid nanoparticle-based antitubercular chemotherapy, *Tuberculosis,* **85**, pp. 415-20.

Saylor, D.M., Kim, C.S., Patwardhan, D.V. and Warren J.A. (2007). Diffuse-interface theory for structure formation and release behavior in controlled drug release systems, *Acta. Biomate*r, **3**, pp. 851-64.

Pawar, A.A., Chen, D.R. and Venkataraman, C. (2012). Influence of precursor solvent properties on matrix crystallinity and drug release rates from nanoparticle aerosol lipid matrices, *International Journal of Pharmaceutics,* **430**, pp. 228-37.

INCIDENCE OF AIRBORNE POLLEN AT AHMEDNAGAR CITY (M.S.)

ABHIJIT A. KULKARNI[1], SACHIN D. RALEGANKAR[2]

[1]Department of Botany, Ahmednagar College, Ahmednagar (M.S.), India.
[2]Department of Physics, Ahmednagar College, Ahmednagar (M.S.), India.
E mail: sdralegankar@yahoo.co.uk

Keywords: POLLENS, HEALTH EFFECT, BIO PARTICLES

INTRODUCTION

Recent developments in aerobiology have once again affirmed the multidisciplinary character of this field, which benefits from the knowledge generated in applied microbiology, palynology, as well as atmospheric physics and chemistry. Another scientific field, which has emerged and fully developed through multidisciplinary interaction, is aerosol science. The physical principles of aerosol science contribute to one of the most important aspects of aerobiology: the measurement of airborne biological particles, such as pollen, fungi, and bacteria etc. (Grinshpun, *et al.*, 2004).

An aerobiology investigation was carried out at Ahmednagar city for the period of twelve consecutive months from June2011 to June 2012 by using Tilak continuous air sampler placed at different locations at Ahmednagar city. Quantitative fluctuations were affected by seasons and flowering patterns.

The present investigation was based on the prediction of time and intensity of pollen during various seasons which enable to alert sensitive individuals in this area. The role of pollen grain in causing allergy is well recognized. Certain pollen grains , if present in low concentration in air may be of allergenic significance as the pollen is responsible for allergenic reactions such as polinosis, bronchial asthma, allergic rhinitis , common cold, skin irritation/ itching, coughing etc. in susceptible individuals.

The present investigation was undertaken to quantify airborne pollen with their seasonal fluctuations to which an individuals is exposed in his day today life.

Ahmednagar (19^{o}N- Latitude; 74^{o}E- Longitude, 752 meter above mean sea level; rainfall 578.8mm). The vegetation spectrum in and around Ahmednagar is mostly of dry deciduous type, where most of the species exhibit xeromorphy. During summer this area is quite barren but at the advent of monsoon it is covered by small weeds and herbs, while shrubs and trees are thinly scattered.

MATERIAL AND METHODS

Airsampling was performed with volumetric spore traps (Tilak continuous air sampler). The volumetric Tilak air sampler is an electrically operated device. It consists of a clock motor having fixed a drum over it. Its rotation completes at the end of eighth day. The exhaust fan is fixed in the sampler which creates negative pressure by creating vacuum within the air tight apparatus. A volume of air enters the air sampler through orifice projecting tube at the rate of 5 L/min.As the air rushes in it impinges on the transparent cello tape of the rotating drum coated with a thin layer of petroleum jelly or Vaseline and thus entraps the bioparticles from the air. It gives seven days data of various components of air/unit volume/unit time. The slide thus obtained was observed under binocular microscope. Safranin was used as the stain for staining the pollen for making reference slides. Then the pollen was placed over the glass slide. Two to three drops of glycerin jelly containing safranin was placed over the pollen material and then cover slip would be mounted over the slide.

Identification of sample pollen grains was done by comparing them with the standard pollen in the reference collection. In general, the type and distribution of apparatus and various patterns of ornamentation of exine was the character employed for the identification of pollen. The technique proposed by Chitaley known as Chitaley technique was also used for preparing the slides, to understand the detailed morphology of pollen.

Vegetation of the area under survey is one of the most important considerations for the identification of airborne pollen grains. Pollen from the flowers of different genera has to be collected for preparing the reference slides. The flowering periods of different plants may be recorded for the easy identification of pollen grains.

RESULTS AND DISCUSSIONS

Altogether 17 pollen types were recorded as evident from table 1. Pollens of *Azadirachtaindica, Cassiauniflora, Lantana camara, Parkensonia aculeate, Partheniumhysterophorus* and pollen of family Poaceae appeared almost throughout the year. This indicated that there was no definite season for members of poaceae and other plant species mentioned above. Pollen of *Azadirachtaindica* (38.70%) was dominant in June. Pollen of members of Poaceae were maximum in number during June 2011 – Sept. 2011 (35.48 – 30.18%). *Prosopisjuliflora*pollen was abundantly present in air (26.10%) during July whereas pollen of *Samaniasaman*(30.97%), *Partheniumhysterophorus*(28.34%) were dominant during Aug. 2011 to Oct. 2011. (Table 1).(Tripathi, *et al.*, 2004, Kalra&Dumbrey, 1957). These patterns were represented in atmosphere throughout the year which may be due to their small size and light ornamentation which may have facilitated their suspension in air for long time. This clearly indicated that the above mentioned pollen incidences were dominant during monsoon season and the number of pollen belonging to these plant species decreased by the onset of winter and during summer.Airborne pollen reflected the vegetation of Ahmendagar. In the present investigation variation in pollen concentration was correlated with the flowering season of the plant species. The richness in variation in pollen concentration was observed through out the year with more or less similar trends in pollen concentration. Maximum number of pollen types were recorded in Nov. 2011 (17-types) followed by in Dec. 2011 and Jan 2012 (15-types each). Where as minimum number was recorded in Aug. 2011 (5- types).

This variation in number was correlated with the season and flowering in plants. With respect to pollen types it was observed that winter season (Nov 2011- Jan. 2012) was regarded as principle pollen season of Ahmednagar city, when maximum pollen types were recorded in year constituting approximately 57.94% of the annual catch. Second high pollen season was post winter and early spring season. 12 pollen types were recorded in Feb. 2012 followed by March 2012 (12- types each) as shown in table 2. (M. Sahney& S. Chaurasia, 2008)

Tree pollen like *Parkensoniaaculeata, Prosopisjuliflora,Feroniacitrulina* were abundantly present in air during winter (Nov. 2011 – Feb. 2012). During the present investigation it was observed that the concentration of pollen in air was highest during the month of Nov., and Dec. 2011 (21.85, 18.75%) followed by Jan (17.34%) and Feb. (8.98%) (Table 2). The total pollen load in air was minimum during June 2011 and the lowest was recorded during May 2012 (1.33%) Table 2. It was observed that maximum number of pollen grains were in air during the months of winter whereas lowest were present during April (3.64%) and May (1.33%). Average pollen density was recorded during the months of monsoon that is June (3.6%), July (4.35%) and Aug. (3.57%) Table 2.

Sr. No	Pollen Type	11-Jun	11-Jul	11-Aug	11-Sep	11-Oct	11-Nov	11-Dec	12-Jan	12-Feb	12-Mar	12-Apr	12-May
1	*Acacia nilotica*	--	8.1	13.08	7.52	1.08	5.94	4.81	3.84	3.86	1.98	--	--
2	*Albizialebeck*	--	--	--	--	14.67	3.59	3.13	2.94	3.08	--	--	--
3	*Argemonemaxicana*	--	1.8	--	5.64	--	10.95	11.08	9.27	12.35	11.25	8.6	--
4	*Azadirachtaindica*	38.7	18.91	--	9.1	9.78	4.66	7.94	7.01	1.93	10.59	11.82	--
5	*Callistemon lanceolatus*	--	--	--	--	--	5.56	4.6	4.29	3.08	--	--	--
6	*Cassia uniflora*	--	0.9	--	11.28	2.71	5.74	1.67	2.71	--	--	3.22	5.88
7	*Casuarinaequisetifolia*	--	--	--	--	--	9.84	10.66	10.63	10.42	17.88	--	--
8	*Eucalyptus globosus*	--	--	--	--	--	0.07	--	0.45	--	--	--	--
9	*Feriniacitrulina*	--	--	--	--	--	0.53	1.46	5.88	5.01	--	7.52	--
10	*Lantana camara*	--	--	7.63	5.66	1.08	5.74	8.99	11.08	14.28	14.56	15.05	--
11	*Parkensoniaaculeata*	3.28	--	--	--	--	8.43	8.78	11.53	18.14	25.16	26.88	32.55
12	*Partheniumhysterophorus*	8.6	9.9	28.34	22.64	4.89	7.18	8.15	5.65	1.15	1.98	--	2.94
13	*Peltophorumpterosperma*	--	0.9	--	--	21.19	3.23	12.76	13.22	5.01	8.6	--	--
14	Poaceae (grasses)	35.48	33.3	31.63	30.18	10.32	9.33	1.04	1.13	--	--	--	--
15	*Prosopisjuliflora*	--	26.1	18.53	16.98	3.26	8.79	5.85	1.8	--	3.97	--	8.82
16	*Samaniasaman*	4.3	--	--	--	30.97	--	7.11	8.59	10.03	11.92	26.86	32.35
17	*Tamarandusindica*	6.45	--	--	--	--	5.56	--	--	--	--	--	47.05

Table 1.Monthly record of pollen count during June 2011 to May 2012

Airborne pollen concentration not only differs from place to place and from year to year in a quantitative way but also with respect to their seasonal courses (Sinha*et al.*, 1971; Singh *et al.*, 1988). Besides the local vegetation spectrum and flowering patterns in the plants growing in and around also accounted for invariability of pollen incidences. From the observations it can be inferred that plants which bloom during June - August require comparatively lower temperature for their dehiscence and dissemination whereas species contributing airborne pollen during March require comparatively higher temperature.

CONCLUSIONS

Pollen of *Partheniumhysterophorus*, *Lantana camara*etc, was abundant during monsoon season which may affect the human health by certain allergic symptoms. Pollen incidences were minimum during April – June in almost all plants except few like *Argemonemaxicana*, which can be safe to the individuals sensitive to pollen allergy.

Sr	Pollen Type	11-Jun	11-Jul	11-Aug	11-Sep	11-Oct	11-Nov	11-Dec	12-Jan	12-Feb	12-Mar	12-Apr	12-May	TOTAL	%
1	*Acacia nilotica*	--	9	12	4	2	33	23	17	10	3	--	--	113	4.43
2	*Albizialebeck*	--	--	--	--	27	20	15	13	8	--	--	--	83	3.25
3	*Argemonemaxicana*	--	2	--	3	--	61	53	41	32	17	8	--	217	8.51
4	*Azadirachtaindica*	36	21	--	5	18	26	38	31	5	16	11	--	204	8
5	*Callistemon lanceolatus*	--	--	--	--	--	31	22	19	8	--	--	--	80	1.96
6	*Cassia uniflora*	3	1	--	6	5	32	8	12	--	--	3	2	72	2.82
7	*Casuarinaequisetifolia*	--	--	--	--	--	56	51	47	27	15	--	--	195	7.65
8	*Eucalyptus globosus*	--	--	--	--	--	1	--	2	--	--	--	--	3	0.11
9	*Feriniacitrulina*	--	--	--	--	--	2	7	26	13	--	7	--	55	2.17
10	*Lantana camara*	--	--	7	3	2	32	43	49	37	22	14	--	199	7.8
11	*Parkensoniaaculeata*	3	--	--	--	--	58	42	51	47	38	25	11	275	10.7
12	*Partheniumhysterophorus*	8	11	26	12	9	47	39	25	11	3	--	1	183	7.79
13	*Peltophorumpterosperma*	--	1	--	--	39	40	61	58	35	13	--	--	249	9.76
14	Poaceae (grasses)	33	37	29	16	19	18	14	5	--	--	--	--	171	4.59
15	*Prosopisiuliflora*	--	29	17	9	6	52	28	8	--	6	--	3	158	6.19
16	*Samaniasaman*	4	--	--	--	57	49	34	38	26	18	--	11	247	9.96
17	*Tamarandusindica*	6	--	--	--	--	25	--	--	--	--		16	47	1.96
	% MONTHLY	3.6	4.35	3.57	2.07	7.21	21.85	18.75	17.34	8.98	5.92	3.64	1.33	255	100%

Table 2.Average record of pollen count during June 2011 to May 2012

ACKNOWLEDGEMENT

Authors are thankful to UGC (WRO) for providing financial assistance to carry out this investigation. We are also thankful to Dr. R. J Barnabas, The Principal, Ahmednagar College, Ahmednagar for providing all the facilities and constant encouragement.

REFERENCES

Grinsphun, S. A. and Reponen, T. (2004). Sampling of biological particles from ambient environment: Physical principles, efficiency, and exposure assessment, *International Aerobiology Newsletter,***59**.

Sinha, U. K. and Johri, B. M. (1971). Pollution – A biological problem, *Sci. & Cult.,* **37**, pp. 69 – 73

Singh A. B., Singh, B. P, and Sharma, D. D. (1988). Influence of climatic factors on air borne pollen allergen, *Ind. Jr. Aerobiology,* **1(1),** pp.39 -44

Kalra S. L. &Dumbrey D. G. (1957). Aerobilogy of army medical campus poona, *Armed Forces Med. J. (India),***13**, pp. 3-16.

Tripathi D. M., Kale, M. K. *et al.* (2004). Atmospheric pollen and fungal spores at pune city, *Ind. J. Allergy Asthma, Immunol,***18(1),** pp.45-50.

Sahney, Manju and Chaurasia, Swati (2008). Seasonal variations of air borne pollen in Alahabad, India, *Ann. Agric. Environ. Med.,* **15**, pp. 287 – 293.

ROLE OF PARTICULATE PAHS AND METALS IN CONTAMINATION LEVELS OF LEAFY VEGETABLE GROWN IN SUBURBAN AREA OF DELHI

P.S. KHILLARE,DARPA SAURAV JYETHI AND SAYANTAN SARKAR

School of Environmental Sciences, Jawaharlal Nehru University, New Delhi
E mail: psk@mail.jnu.ac.in

INTRODUCTION

Chemical contamination of vegetables grown in the suburban areas is likely to affect a large fraction of the population. Vegetables grown in suburban areas tend to be contaminated by a multitude of pollutants and hence pose health risks upon consumption. Polycyclic aromatic hydrocarbons (PAHs) mainly found in particulate phase are products of incomplete combustion of fossil fuels and are a group of persistent organic pollutants (POPs). Some of them are highly carcinogenic and mutagenic. Exposure to high concentration of heavy metals is also known to pose deleterious health effects in humans. PAHs and metals are co-emitted from a number of sources such as, combustion of coal, oil and wood, refuse burning and emissions from motor vehicles and together can multiply the associated health risks upon exposure. The present paper discusses the impact of particulate-bound PAHs and heavy metals on the contamination levels of a leafy vegetable grown in a highly populated suburban area of Delhi.

MATERIALS AND METHODS

The site chosen for the present study was Mithapur, a sub-urban residential area with high population density and substantial vegetable cultivation, located ~2.5 km southeast of coal-fired Badarpur power plant (720 MW) and 5–7 km southeast of Okhla Industrial Area (phases I, II, and III). The heavy-traffic Delhi-Mathura Highway is at a distance of about 1.5 km from the site.

PM_{10} samples were collected on Whatman glass fiber filters GF/A (8" × 10") (pre-combusted at 450°C for 12 hours) once a week for a period of one year (December 2008–November 2009) using High–volume samplers (Respirable Dust Sampler, Bioanalytical Pvt. Ltd.). PM_{10} loads were determined gravimetrically by weighing the filters in a microbalance (Model AE163, Mettler, sensitivity 0.0001 g) after proper conditioning. Filters were stored in a refrigerator (4°C) until analysis. Six mature samples of spinach shoots (leafy vegetable) were collected in winter (January), summer (June) and monsoon (August) seasons of 2009. Vegetables were washed, dried, powdered and homogenized by grinding. Samples were then kept in sealed polythene bags at -20pC for further analysis. Metal extraction using a mixed acid solution was carried out using a microwave digestion system (Speedwave MWS–3+, Berghof, Germany). Metal analysis was carried out using a flame atomic absorption spectrometry system (Solaar M Series, Thermo Scientific) under optimized conditions. Metal recoveries were checked by spiking samples with standard solutions prior to extraction. PAHs were extracted using ultrasonication with toluene as solvent (Sonicator 3000, Misonix Inc., USA) and were subsequently concentrated by rotary evaporation (Büchirotavapor, Switzerland). This was followed by silica gel column clean up and final analysis using a HPLC system (Model 510, Waters, USA) equipped with a tunable absorbance UV detector (254 nm) and a PAH C18 column (4.6 mm×250 mm, particle size 5 µm, Waters). Quantification of PAHs was done by internal calibration method and their identification was carried out by comparing their retention times with those of authentic standards.

RESULTS AND DISCUSSIONS

Fig. 1 represents the annual mean concentration of $Ó_{16}$PAHs and metals (Cd, Cu, Fe, Mn, Cr and Zn) in PM_{10} and spinach shoots. Table 1 represents the correlation matrix for PAH and metal concentrations in PM_{10} and in spinach at the study site.Good correlations were observed between PM_{10} bound Cd (r=0.95, p<0.01), Cr (r=0.95, p<0.01) and Zn (r=0.97, p<0.01) concentrations and spinach levels of the same at the study site. Various anthropogenic sources such as vehicular tire wear, battery manufacture, pigments, metal plating and production, smelting industries, waste incineration, fossil fuel consumption, phosphate fertilizer, cement production, combustion exhaust, galvanized parts and railings, fuel and oil, brake linings and rubber tires contribute to the ambient PM_{10} levels of the above said metals. Industrial emissions possibly originating from the Okhla Industrial Area present upwind of the site, high traffic in nearby areas and proximity to a 720 MW coal fired power plant might add on the pollution load of the site.

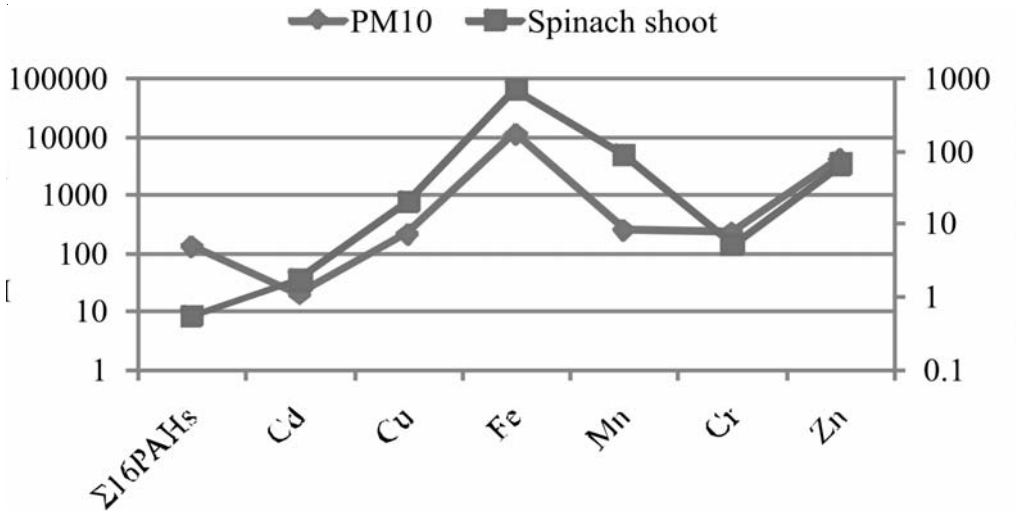

Figure 1. Mean concentration of PAHs and metals in PM_{10} and spinach shoots at Mithapur

Interestingly, Zn and Cd had extremely high enrichment factor (EF) values (between 100–1000) and were anomalously enriched in aerosol of the site. Cr had EF between 10-100 and was moderately enriched. This is in agreement with published literature as all the elements belonging to this group have a known crustal source in addition to various emission sources.

Negative correlations were observed for Cu (r=-0.73, p<0.01), Fe (r = -0.87, p<0.01) and Mn (r = -0.51, p<0.01) levels in spinach shoots with that in PM_{10}. Cu has partial crustal source whereas Fe and Mn have a predominant crustal source and are needed for plant growth. These are considered as micronutrients and are procured by plants from soil for their growth and development.

Moderate correlation (r = 0.73, p<0.01) was observed between spinach PAH levels and particulate-bound PAH levels. It is well known that air-leaf transfer and soil-root transfer are possible pathways for PAH contamination of vegetables. Air leaf transfer and particle deposition have been identified as the dominant contamination pathway by many studies. The presence of coal fired power plant in the vicinity, high traffic area and proximity to industrial area apart from being a source of particulate-bound PAHs, serves as an input source of PAH levels in the soil of study site.

	PM_{10} PAH	PM_{10} Cd	PM_{10} Cu	PM_{10} Fe	PM_{10} Mn	PM_{10} Cr	PM_{10} Zn	Spinach PAH	Spinach Cd	Spinach Cu	Spinach Fe	Spinach Mn	Spinach Cr	Spinach Zn
PM_{10} PAH	1													
PM_{10} Cd	**0.93**	1												
PM_{10} Cu	**0.89**	**0.95**	1											
PM_{10} Fe	-0.31	0.06	0.15	1										
PM_{10} Mn	-0.18	0.26	0.27	**0.91**	1									
PM_{10} Cr	**0.71**	**0.91**	**0.95**	**0.56**	*0.45*	1								
PM_{10} Zn	**0.92**	**0.98**	**0.98**	0.17	0.11	**0.93**	1							
Spinach-PAH	**0.73**	*0.44*	0.35	**-0.7**	**-0.87**	0.04	0.4	1						
Spinach-Cd	**0.97**	**0.95**	**0.92**	-0.14	-0.22	**0.76**	**0.94**	**0.68**	1					
Spinach-Cu	**-0.96**	**-0.8**	**-0.73**	**0.64**	**0.52**	*-0.48*	**-0.77**	**-0.89**	**-0.94**	1				
Spinach-Fe	-0.2	**-0.54**	**-0.62**	**-0.87**	**-0.62**	**-0.83**	**-0.57**	**0.52**	-0.27	-0.08	1			
Spinach-Mn	**0.98**	**0.83**	**0.77**	*-0.48*	**-0.51**	**0.54**	**0.81**	**0.86**	**0.96**	**-0.98**	0.03	1		
Spinach-Cr	**0.89**	**0.94**	**0.98**	0.27	0.18	**0.95**	**0.98**	0.34	**0.92**	**-0.72**	**-0.63**	**0.76**	1	
Spinach-Zn	**0.81**	**0.96**	**0.98**	0.32	0.37	**0.98**	**0.97**	0.19	**0.85**	**-0.62**	**-0.73**	**0.66**	**0.98**	1

Bold: Correlation significant at 99% confidence level; Italics: Correlation significant at 95% confidence level

Table 1. Correlation matrix for species (PAH and metal) concentrations in PM_{10} and in spinach at the study site

Diagnostic ratios of PAHs such as Anthracene/Phenanthrene+Anthracene and Benzo[a]anthracene/ Benzo[a]anthracene+Chrysene in particulate and spinach samples indicated towards combustion sources (Table 2). Further, ratios of Fluoranthene/Fluoranthene+Pyrene indicated towards coal and wood combustion in both particulate and spinach samples of the study site. The observation site can be considered valid because the site is located in downwind direction of a major coal fired power plant in Badarpur. Additionally, residential fuel use in the form of biomass and wood combustion in suburban areas of Delhi is also prevalent.

Ratio	Spinach shoots	PM_{10}	Source	Reference
Anth/Phen+Anth	0.37	0.52	Combustion (>0.1)	Budzinski et al. (1997)
B[a]A/B[a]A+Chry	0.84	0.56	Combustion (>0.35)	Yunker et al. (2002)
Flan/Flan+Pyr	0.63	0.59	Coal/wood combustion (>0.5)	Yunker et al. (2002)

Table 2. Diagnostic ratios of PAHs observed in spinach and PM_{10} at the study

CONCLUSIONS

Good correlation between particulate-bound Cd, Cr and Zn and spinach shoots grown at a suburban site in Delhi suggests of particulate deposition as the predominant contamination pathway. The correlation is also suggestive of similar sources of contamination. Metals with mostly crustal origin viz. Fe, Mn and Cu in spinach shoots negatively correlated with those of particulate-bound concentrations. Moderate correlation between particulate bound PAHs and spinach shoot PAHs suggests of alternate soil uptake pathway, which again is influenced by particulate deposition. Moreover, PAHs diagnostic ratios suggested combustion, especially coal and wood combustion as a chief source in both, PM_{10} and spinach grown in the site.

REFERENCES

Budzinsky, H., Jones, I., Bellocq, J., Pierard, C., &Garrigues, P. (1997). Evaluation of sediment contamination by polycyclic aromatic hydrocarbons in the Gironde estuary. Marine Chemistry, **58**, pp. 85–97.

Yunker, M. B., MacDonald, R. W., Vingarzan, R., Mitchell, R.H., Goyette, D., &Sylvestre, S. (2002). PAHs in the Fraser River basin: a critical appraisal of PAH ratios as indicators of PAH source and composition. Organic Geochemistry, **33**, pp. 489–515.

COLLECTION AND IDENTIFICATION OF BIO-AEROSOLS WITHIN AN ACADEMIC INSTITUTE

AVANTIKA AWASTHI[1], AMIT SINGH CHAUHAN[2], TARUN GUPTA[1,2]

[1]Environmental Engineering and Management Program and Department of [2]Civil Engineering,
Indian Institute of Technology Kanpur, Kanpur, UP
E mail: tarun@iitk.ac.in

INTRODUCTION

Ambient air contains a mixture of trace gases and particles which have been studied by many researchers mostly due to climatic and health impacts related to them. One of the salient components of these particles is attributed to living or dead organisms or their body part and is tagged in a broader category called Bio-aerosols. Bio-aerosols are particles of biological origin suspended in the air. In outdoor air, approximately 30 percent of all particles larger than 0.2 μm appear to be of biological origin.They generally range from approximately 0.02 to 100 micron in diameter, depending upon the type and source. Bio-aerosols can be classified on the basis of size, viability, infectivity, allergenicity, toxicity and pharmacological activity. Pollens, originating from plants are the largest in size with a typical size range of 10 to 100 microns; fungal spores are about0.5 to 30 micron in size, bacteria in the size range of 0.3 to 10 microns and viruses are the smallest and can be found in the size of 0.02 to 0.3 microns.

Once released, bio-aerosols may travel considerable distances due to atmospheric dispersion and may cause adverse health effects upon inhalation and their deposition at various places inside human respiratory system. The severity of effect typically depends upon their ability to survive and remain infectious in the environment as well as when inside our respiratory system. The survival or viability of bio-aerosols is referred to as their ability to replicate, whereas the infectivity of bio-aerosols is referred to as their ability to cause infection.

The present study is dealing with the collection and identification of bio-aerosols within an academic institute. For this purpose IIT Kanpur campus was selected. IIT Kanpur campus lies on the outskirts of the Kanpur city with a large variety of flora and fauna present within the campus. The air seems to be much cleaner and relatively less polluted within the campus compared to the main city. However, given the rich flora and fauna around the campus including various marshy barren lands, there are plenty of safe habitats for bio-aerosols.

OBJECTIVE

To collect and identify bio-aerosols present in the IIT Kanpur campus in different microenvironments during and immediately after the rainy season using indigenously developed bioaerosol samplers.

METHODOLOGY

Site selection

The IIT Kanpur campus is an academic institute with no industrial and commercial activities lying in the upwind direction about 15 km north of the main city. Currently sampling is going on at various indoor and outdoor microenvironments at different locations within the campus.

Sample Collection

Two impaction based bioaerosol samplers, designed for PM_{10} and PM_{1} cut-points and developed in our lab, using Agar (impregnated with various nutrient media) are being used cut size. The respective flow ratesare 10 lpm and 14 lpm, respectively, controlled by a rota-meter and calibrated using a mass flow meter. The impactors are indigenous developed in our lab at IIT Kanpur and have been tested both using artificially generated aerosols as well as ambient air. Quartz filters are being used as backup filter. Bioaerosol sampling is carried out for 4 h duration.

Microbiological Analysis

Each sample collected on the Agar base was divided into 4 sections. Out of these, two were directly analysed under the light microscope at $1000^{X}(100X10^{X})$, $400^{X}(40x10^{X})$, $200^{X}(20X10^{X})$ and $100^{X}(10x10^{X})$ resolution for particles, pollens and nonviable bio-aerosols for visual identification. The other two sections were both incubated for 24h and 48h for observing bacterial and fungal growth respectively, at 32^{0}C and 92 per cent RH. Further after incubation, these samples were studied under the light microscope using gram staining for bacteria and lactophenol cotton blue staining for fungi at 100^{x} and 40^{x} resolution for bacteria and fungi, respectively.

RESULTS

The preliminary results have shown prominence of eight different types of bacteria out of which two were identified as streptococcus and bacillus and some common fungal species.

CHARACTERISTICS OF FLUORESCENT BIOLOGICAL AEROSOL PARTICLES: NUMBER AND SIZE DISTRIBUTION MEASUREMENTS FROM A MARINE URBAN SITE IN SOUTHERN INDIA

E. V. SWATHY[1*], C. PÖHLKER[2], S. M. SHIVANAGENDRA[1], R. RAVIKRISHNA[3], R.S. VERMA[4], L. PHILIP[1], S. S. GUNTHE[1], J. A. HUFFMAN[5], AND U. PÖSCHL[2]

[1] EWRE Division, Dept. of Civil Engineering, Indian Institute of Technology Madras, Chennai -36, India

[2] Dept. of Biogeochemistry, Max Planck Institute for Chemistry, Mainz, Germany

[3] Dept. of Chemical Engineering, Indian Institute of Technology Madras, Chennai -36, India

Dept. of Biotechnology, Indian Institute of Technology Madras, Chennai -36, India

[5]University of Denver, Department of Chemistry and Biochemistry, Denver, CO, USA

Keywords: FLUORESCENT BIOLOGICAL AEROSOL PARTICLES (FBAP), SIZE DISTRIBUTION

INTRODUCTION

Biological aerosols particles are a very diverse group of biological materials and structures, including microorganisms, and fragments of animals and plants. Recently several investigations have suggested that biological aerosol particles can have a substantial influence on clouds and precipitation and thus may influence the hydrological cycle and climate at least on regional scales. Various fields of medical research are also concerned with biological aerosols as many pathogens use air for their dispersal. Biological particles have been linked to many different adverse health effects spanning from infectious deceases to acute toxic effects, allergies, asthma, and even cancer.

METHODS

Here we report the number concentration and size distribution of Fluorescent Biological Aerosol Particles (FBAP), which were obtained by deploying an Ultraviolet Aerodynamic Particle Sizer (UV-APS) for the first time in Indian subcontinent. Measurements were carried over the period of five months (November 2011 – March 2012) in Chennai (12.9876^{o}N, 80.2235^{o}E), a marine urban site located on the eastern coast in south Indian region.

RESULTS AND CONCLUSIONS

Analysis of five months of dataset showed that the mean number and mass concentration of coarse FBAP were 18.7 x 10^{-2} cm^{-3} and 1.47 µg m^{-3} respectively, which accounted for 8.28% of total particle number and 9.85% of total particle mass. The number concentration of FBAP also showed a varying trend over these 5 month measurements with maximum mean concentration in March (23.4 x 10^{-2} cm^{-3}) and minimum in January (12.2 x 10^{-2} cm^{-3}). It was also observed that the maximum number concentration was in the size range of 1 – 2 µm, which is somewhat different from the previous continental measurements, where maximum concentration was mostly observed in the size range of 3 – 4 µm (Huffman *et al.*, 2010;). Such a peak in size distribution of FBAP in the size range of 1 – 2 µm may indicate that the number concentration of FBAP might have been dominated by marine sources rather than common continental sources as evidenced by 48 hr back trajectory analysis. These indicate that during most measurements periods wind originated over the Bay of Bengal bringing clean marine air to the observational site. FBAP showed highest concentrations

during night time, with two prominent peaks at around midnight and early morning. The number concentration of FBAP exhibited a decreasing trend after rainfall. This may be due to wash out of biological aerosol particles during the rain. Additional details about these measurements will be presented.

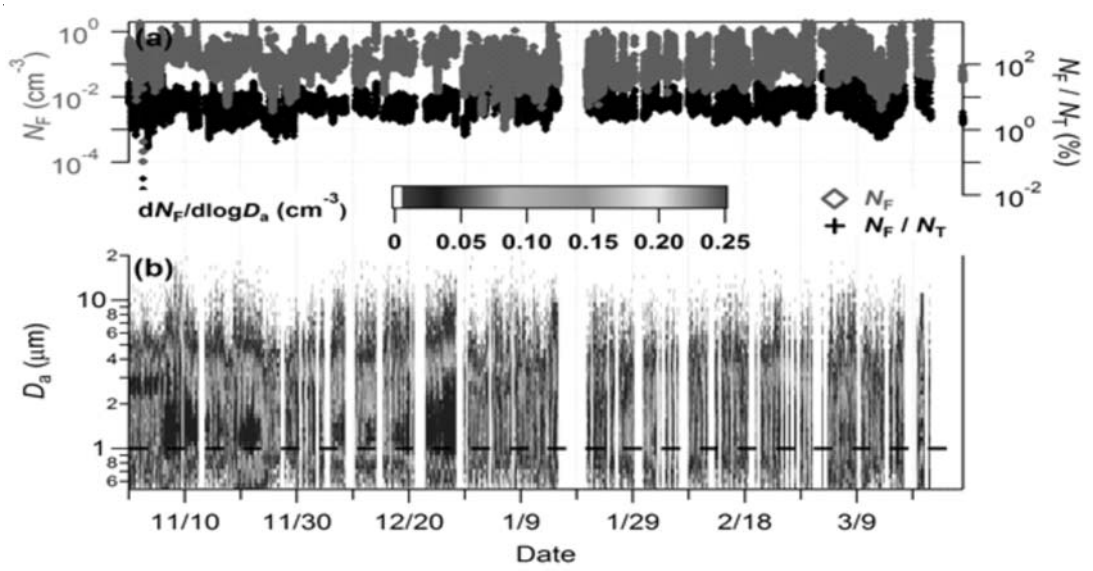

Figure 1. Enumerated Time series of Number Concentration of FBAP measured during the period of Nov 2011 – March 2012 at a coastal urban site of Chennai in India.

ACKNOWLEDGEMENTS

Authors would like to thank Prof. Swaminathan for useful suggestions and simulating discussions. SSG would like to thank support from new faculty seed grant from IC&SR, IIT Madras under project number CIE/11-12/560/NFSC/SAC.

REFERENCES

Deprés, *et al.*, (2012). Primary biological aerosol particles in the atmosphere: a review, *Tellus B.*

Huffman, *et al.* (2010).Fluorescent biological aerosol particle concentrations and size distribution measured with an UV-APS in central Europe, *ACP*.

S.M. Burrows, *et al.*(2009). Bacteria in the global atmosphere – Part 1: Review and synthesis of literature data for different ecosystems, *ACP*.

ADDRESSING CLIMATE CHANGE TO ENSURE SUSTAINABILITY: AGRICULTURAL GROWTH WITH MINIMAL HEALTH HAZARDS

A. GOEL

Department of Civil Eng. Environmental Engineering & Management Program,
Indian Institute of Technology Kanpur, Kanpur – 208 016, India

Keywords: AEROSOLS IN HEALTH AND AGRICULTURE,CLIMATE CHANGE, SUSTAINABLE AGRICULTURE, INHALATION EXPOSURE, SIZE SEGREGATED DISTRIBUTION

INTRODUCTION

Third Assessment Report of the IPCC (2001) concluded that climate change would hit the poorest countries severely in terms of reducing agricultural productivity. Briefly, one of the foremost impacts of climate change is food security. It can affect crop yield by impacting agricultural inputs such as water for irrigation, amounts of solar radiation that affect plant growth, as well as the prevalence of pests and new or changed insect/pest incidence. In South Asia losses of many regional staples, such as rice, millet and maize could top 10 per cent by 2030. Studies suggest that food production has to be increased to the tune of 300 mt by 2020 in order to feed India's ever-growing population, which is likely to reach 1.30 billion by the year 2020. Total food grain production has to be increased by 50 per cent by 2020 to meet the requirement. Major challenges facing agricultural sector include development of climate resistant crops, and combating new breeds of insects, which requires development of new agrochemicals including pesticides.

METHODS

Contaminated PM Health Effects

It is well known that many current use pesticides are carcinogens and rampant use of these chemicals has given rise to several short-term and long-term adverse effects. Other than ingestion through water and food, inhalation of pesticide contaminated particulates can be a major health risk. Research conducted in Europe on size distribution of particle-bound OCPs in the atmosphere (Chrysikou and Samara, 2009) supports this possibility. Results show strong accumulation in the submicron size fractions which as part of Respirable Particulate Matter (RSPM) reach human lungs. A similar study in Beijing, China (Wang *et al.*, 2008) revealed distinct concentrations variations in PM with different particle diameters.

Sustainable Agricultural Growth: Government Initiatives

Recognition of impact of 'Aerosols in Health and Agriculture' is a motivational force for government to set strategic framework to meet India's agriculture challenges.

This study provides an overview of Indian Government's response for addressing impact of climate change on the agricultural sector including steps taken to increase food production and ensure sustainable agricultural growth. National Mission for Sustainable Agriculture, (one of the eight missions included in National Action Plan on Climate Change (NAPCC)) launched by Government of India on June 30th 2008 is a step in this direction. The poster will also showcase occurrence of pesticides

in ambient PM and our understanding of the health effects caused by exposure to pesticides through inhalation.

CONCLUSIONS

Other than ingestion through water and food, inhalation of pesticide contaminated particulates can be a major health risk. These observations combined with current government initiatives highlight the need to examine the occurrence of pesticides – both in use and newer ones - on aerosols in agricultural regions. Mainly, insight in atmospheric phase distribution will aid in assessment of transport potential, fate and health risks posed by pesticides currently being developed.

REFERENCES

Chrysikou, L. P. and Samara, C. A. (2009). Seasonal variation of the size distribution of urban particulate matter and associated organic pollutants in the ambient air, Atmospheric*Environment*, **43(30)**,pp.4557-4569.

IPCC Third Assessment Report: Climate Change (2001).

National Action Plan on Climate Change (NAPCC) (2008).

Vision 2030. (2011).

Xiaofei, *et al.*, (2008). Organochlorine pesticides in particulate matter of Beijing, China, *J. Haz. Mat*., **155**, pp. 350–357

POLYCHLORINATED BIPHENYLS (PCBs) IN ENVIRONMENT: AN OVERVIEW UNDER INDIAN CONTEXT

K. UPADHYAY [1] AND A. GOEL[1]

[1]Environmental Engineering and Management Program, Department of Civil Engineering, Indian Institute of Technology Kanpur, Kanpur -208016, India
E mail: anubha@iitk.ac.in

Keywords: AEROSOL CHARACTERIZATION, INDIA, PCB, SOURCE DISTRIBUTION

INTRODUCTION

Polychlorinated biphenyls (PCBs), mixtures of chlorinated hydrocarbons, have been used extensively since 1929 mainly in industry as dielectrics in transformers and large capacitors, heat exchange fluids, and also as paint additives. In U.S. alone an estimated 1.1 billion pounds (498951200kg) of PCBs were produced between 1929 and 1977. They are persistent Organic Pollutants (POPs) and have been detected in almost all environmental compartments. PCBs are known to bio-magnify and bioaccumulate through the food chain and represent a potential threat to public health. Recognition of adverse health impacts has resulted in efforts to reduce their production and use; US officially banned production in 1979. Co-signatories of the Stockholm Convention (an international environmentaltreaty, effective from May 2004) agreed to outlaw nine of the dirty dozen chemicals which include PCBs. Despite prohibition on usage in most South East Asian Countries (banned in Indonesia since 1994) PCBs are still being detected in the environment and India is being considered as a major source.

METHODS

Today, main sources of PCBs to the environment include poorly maintained hazardous waste sites, and illegal or improper dumping of PCB e-wastes. India generates approximately 150 000 t/year of e- waste which is poorly managed. Total PCB levels in air (Ó28PCB: range: 120 to 1077 pg/m3, Table 1) at coastal and inland sites in India are higher than reported in other Asian countries (Zhang, *et al*., 2008). Concentration of PCBs in soils in National Capital Region (NCR) India was determined (Bhupander, *et al.,* 2012). Results revealed that soils from Uttar Pradesh had levels of PCBs comparatively higher than soils from Delhi and Haryana states. Although India emits more PCBs than other surrounding countries (Kang, *et al.,* 2009), only a few studies have been conducted within India (Bhupander, *et al.,* 2012; Zhang, *et al.,* 2008). Consequently information about the occurrence and behaviour of PCBs in Indian environment is very limited. This poster provides an overview of the information available about occurrence and source distribution of PCBs in India. The poster will also showcase initiatives by Indian government to phase out PCBs in India which includes participation in multimillion dollar project, part of Stockholm Convention, with United Nations Industrial Development Organisation (UNIDO).

			PCB28	PCB52	PCB153	PCB138	PCB180	ΣPCBs
Asia (China, Japan, South Korea, and Singapore)		**Range**						5-340
India	**Urban(n=9)**	**Range**	18-140	Jan-66	0.38-16	0.38-77	0.09-8	216-1077
		Avg ±SD	76 ± 43	31 ± 29	8±6	22±25	2±3	662 ± 257
	Rural(n=6)	**Range**	31-175	0.06-137	0.46-3	0.29-9	0.07-1	279- 805
		Avg ±SD	66 ± 55	27 ± 54	2±1	2±3	1±1	464 ± 190
	Wetland(n=3)	**Range**	Sep-47	23-Feb	17-Feb	9-Jan	BDL-15	120 - 320
		Avg ±SD	22 ± 22	9 ± 12	7 ±9	7±5	6 ±8	238 ± 104

n=number of samples

Table 1. PCB levels in air (pg/m3) along coastal areas of India (Urban, Rural, and Wetland locations; sources: Zhang, *et al*., 2008;Jaward, et al., 2005).

		Range	Mean	SE**
Study areas (n)*	Delhi (44)	<0.01-4.30	0.67	0.14
	Uttar Pradesh (30)	0.26-24.72	13.5	1.21
	Haryana (9)	<0.01-22.48	2.8	2.46
Dominant Congeners	PCB - 44	<0.01-9.38	1.58	0.27
	PCB - 49	<0.01-5.81	1.19	0.2
	PCB-151	<0.01-3.36	0.62	0.11
	PCB-74	<0.01-4.22	0.44	0.12

<0.01=below detection limit; *n=number of samples; **SE=SD/”n

Table2. PCB levels in Roadside Agricultural Soils India (ng/g) (from NCR: National Capital Region; source: Bhupander, *et al.,* 2012).

CONCLUSIONS

Investigations on public health implications of PCBs in the environment reveal that exposure to PCBs can lead to neuro developmental effects and lead to an alarming increase in cases of liver

cancer among people occupationally exposed to PCBs (Barry, *et al*., 2008). Even though initiatives by Indian government to phase out PCBs will help in reducing active sources to the environment, PCBs residuals will be around for a long time to come. Lack of information about their source distribution and size segregated distribution on ambient air particles hinders assessment of risk posed. Research needs to focus on aerosol characterization to assess occurrence in atmosphere, source distribution and transport of PCBs in the environment under Indian climatic conditions. Availability of such information will aid in development of risk remediation strategies. Need for an air quality study in the most densely populated region of the country which is also highly industrialized (namely the Indo-Gangetic Plain) is highlighted by the fact that positive correlation between PCBs in different environmental media and population density has been suggested (Güray, et al.,2011). Current research underway to bridge the gap between existing information and required knowledge in one of the densely populated major industrial locations in Indo – Gangetic plain, Kanpur, also home to one of the biggest Solid Waste Management facilities in the country, will also be presented.

REFERENCES

Barry, *et al.,* (2008). Public Health Implications Of Exposure to Polychlorinated Biphenyls (PCBs). *Agency for Toxic Substance and Disease Registry*, USA.

GüraySalihoglu*et al.,* (2011). Spatial and temporal distribution of polychlorinated biphenyl (PCB)concentrations in soils of an industrialized city in Turkey, *Journal of Environmental Management* , **92**, pp. 724-732.

Jaward, F. M., Zhang, G., Nam, J.J., Sweetman, A,.J., Obbard, J. P., Kobara, Y., Jones, K. C. (2005). Passive air sampling of polychlorinated biphenyls, organochlorine compounds, and polybrominateddiphenyl ethers across Asia, *Environ. Sci. Technol.*, **39(22)**, pp. 8638-45.

Kang, *et al.,* (2009). Atmospheric deposition of persistent organic pollutants to the East Rongbuk Glacier in the Himalaya , *Science of the Total Environment*, **408**, pp. 57–63.

Kumar, Bhupander, Verma, V. K., Singh, S. K., Kumar, Sanjay and Sharma, C. S. (2012). Occurrence of Congener Specific Polychlorinated Biphenyls in Soils from Roadside Agricultural Fields,*Asian Journal of Plant Science and Research* , **2 (3)**, pp. 299-305.

National Implementation Plan- Stockholm Convention on Persistent Organic Pollutants (April 2011). Ministry of Environment & Forests Government of India.

UNEP (2002). Regionally Based Assessment of Persistent Toxic Substances – South East Asia and South Pacific Regional Report, United nations Environment ProgrammeChemcials, Geneva, pp.125

Zhang, *et al.* (2008). Passive Atmospheric Sampling of Organochlorine Pesticides, Polychlorinated Biphenyls, and PolybrominatedDiphenyl Ethers in Urban, Rural, and Wetland Sites along the Coastal Length of India,*Environ. Sci. Technol., 42*,pp. 8218–8223.

INFLUENCE OF AEROSOLS ON AOT AND AGRICULTURE OVER MANDYA

KAMSALI NAGARAJA[1], H.T. ANANDA[2], L.A. SATHISH[3] AND L. PARAMESH[4]

[2] Department of Physics, Bangalore University, Bangalore 560 056
[2] Department of Physics, Government college (Autonomous), Mandya 571 401
[3] Department of Physics, Government Science College, Bangalore 560 001
[4] Department of studies in Physics, University of Mysore, Mysore 570 006
E mail: kamsalinagaraj@bub.ernet.in

Keywords: AEROSOLS, AGRICULTURE, CROP YIELD, RAINFALL, WEATHER, CLIMATE.

INTRODUCTION

India is having greater dependence of agriculture and the agricultural meteorology is concerned with the meteorological, hydrological, pedological and biological factors, has great demand both by the governmental and public sectors in the country. The major objective is to eluci-date these effects and to assist farmers in preparing themselves by applying this supportive knowl-edge and information in agrometeorological practices. Agricultural production is dependent on weather and climate that is influenced greatly by aerosols in the atmosphere. Despite the impressive advances in agricultural technology over the past century, the study has become essential because of chal-lenges to many forms of agricultural production posed by increasing weather change, associated extreme events and climate variability. Existence of aerosols have the control on energy budget through aerosol radiative forcing, alters the cloud properties and influence monsoon appreciably. These challenges have repercussions in terms of socio-economic conditions, particularly in India. The economic value of weather information prod-ucts is steadily increasing as a result of rising public awareness over the years. Vari-ous agrometeorological requirements such as agroclimatology for land-use planning and crop zonation, operational crop monitoring and agromete-orological practices based on output of crop growth simulation models, rainfall reliability statistics with respect to date of sowing and crop calendars, weather requirements for crops and input applications are essential for appropriate yield of the crop. Quantification by physical methods is the basis for research and to understand various processes that explain phenomena in detail, determines the growth, develop-ment and yield of plants in agriculture. When the extent of measure-ments is limited, agrometeorological indices are a first attempt to relate phenomena like drought or erosion empirically to such observations.An effort is made to study the influence of aerosols or climate in general and weather in particular on the agricultural products in terms of crop yield, temperature anomaly, rainfall trend etc. over Mandya in Karnataka. The results are discussed in detail.

Atmospheric aerosol is a major concern for climate prediction and public health, but records of global aerosol distributions have only become available in the last decade from dedicated satellite observations such as MODerate resolution Imaging Spectro-radiometer (MODIS) and the Multiangle Imaging Spectro Radiometer (MISR). The atmospheric aerosols have increased significantly in the last three decades due to population growth, energy demand, forest fires, industrial growth, changes in land use/land cover and anthropogenic activities. The effect of increasing atmospheric loading is being felt by people living in the region directly and indirectly locally and also globally. In this regard, an effort is made to study the influence of AOT on the weather and indirectly on agriculture.

METHODOLOGY

The aerosol optical thickness (AOT) data retrieved from MODIS sensors aboard the Terra and Aqua satellites from 2000 to 2010 were evaluated thoroughly for a station Mandya, Karnataka in India. The rainfall data and crop yield over the study station are used as primary tools for the analysis.

RESULTS AND DISCUSSIONS

The effect of aerosols on climate has an important role since they alter the radiation balance of the earth-atmosphere system considerable and reduce amount of solar radiation reaching the ground. The spatial and vertical distribution of aerosols and their absorptive and reflective properties also influence atmospheric circulation patterns, cloud formation and hydrological processes (Lawrence and Lelieveld, 2010). Therefore, monitoring the spatial distribution of aerosols and their properties is critical for climate research, and for validating the performance of dust models in higher-resolution mesoscale models.

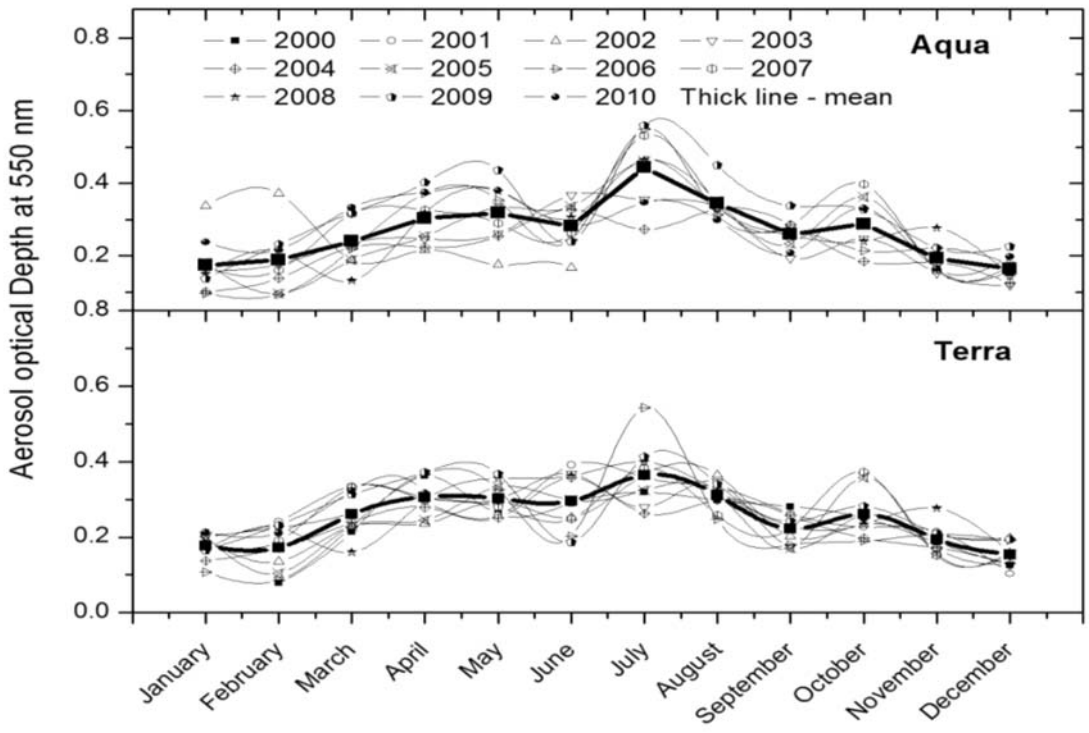

Figure 1.Monthly mean of AOT at 550 nm from Aqua/Terra from January 2000 to December 2010.

Fig. 1 shows the area-averaged time series of Aerosol optical depth at 550 nm from Terra/ Aqua for the duration from January 2000 to December 2010 for the region 75E-80E and 10N-15N. One can observe the maxima in AOTs in July and all the profiles show similar trend. The values show an increasing trend from January to July and then decrease till the end of the year, December. Monthly variations range from 0.165 to 0.443 with a mean of 0.267 ± 0.08 for Aqua, and from 0.154 to 0.365 with a mean of 0.25 ± 0.07 for Terra, respectively. The standard deviation does not exceed 0.1 in all the cases. Higher concentrations were observed during summer and monsoon seasons

compared to winter and post-monsoon seasons. The seasons were classified according the standard convention of India Meteorological Department (IMD), Government of India and considered as winter during January and February, summer from March through May, Monsoon from June through September and post-monsoon falls from October to December. The results obtained here show contradiction to the usually expected behaviour of decrease in AOT due to washout because of precipitation. The reason can be explained as; even though the reduction in AOTs exists in monsoon, the transportation of aerosols from other areas and local activities such as vehicular traffic, emissions from industries will lead to enhancement of AOTs (Vinoj*et al.*, 2004).

Potential role of aerosols in altering rainfall distribution of the greatest importance to large populations and to the poor, the Indian summer monsoon is the biggest source of freshwater resource. More than 70% of the annual precipitation over India occurs during the summer monsoon season (June-July-August-September). The subcontinent heats rapidly during the pre-monsoon months, while the Indian Ocean warming is relatively less compared to the landmass (Gautam*et al.*, 2009). The resulting meridional thermal contrast causes strong moisture-laden winds from the oceanic regions to the landmass leading to heavy rainfall during the monsoon period. Against the backdrop of increasing aerosol concentrations, recent studies have recognized the potential role of aerosols inducing changes in the monsoon circulation and rainfall over India (Sing et al., 2004).Fig. 2 shows the monthly mean rainfall over Mandya for the duration from 2007 to 2010 and showing much rainfall during monsoon period. However, fig. 2 shows the frequency distribution of occurrence of rainfall (in cm) over the past 100-years in Mandya, and ranges from 30.23 to 133.82 with a mean of 74.94. Mandya receives a good amount of rain throughout the year from April to December with its peak during May, September and October covering pre-monsoon, monsoon and post-monsoon.

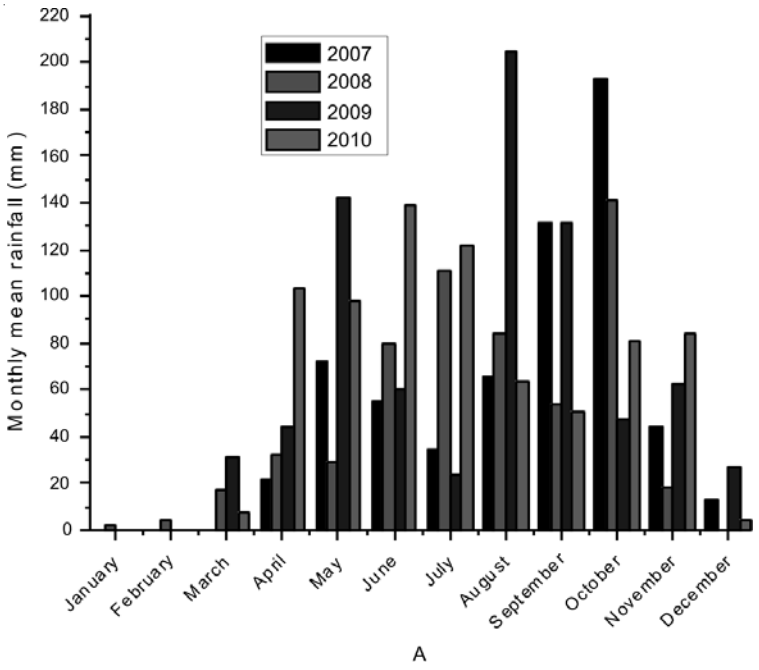

Figure 2.Monthly mean rainfall for the period 2007 to 2010.

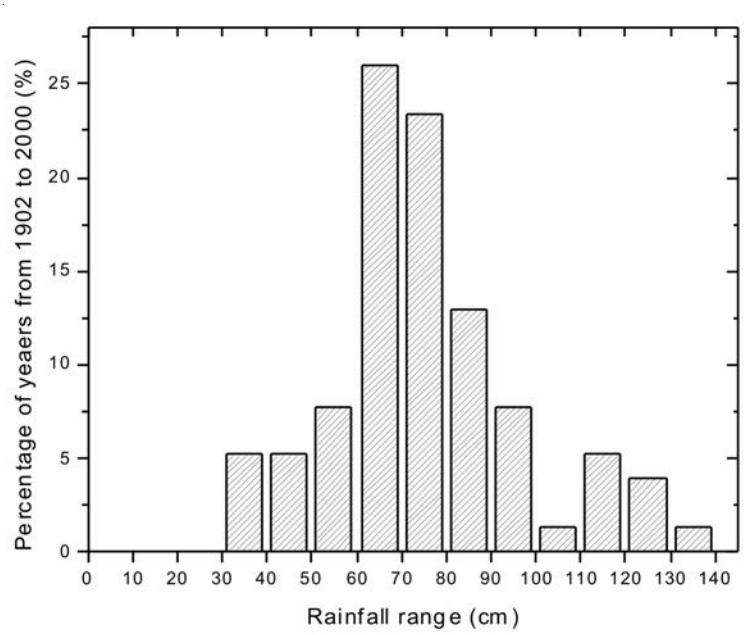

Figure 3.Frequency distribution of rainfall over Mandya for the duration of 1902 to 2000.

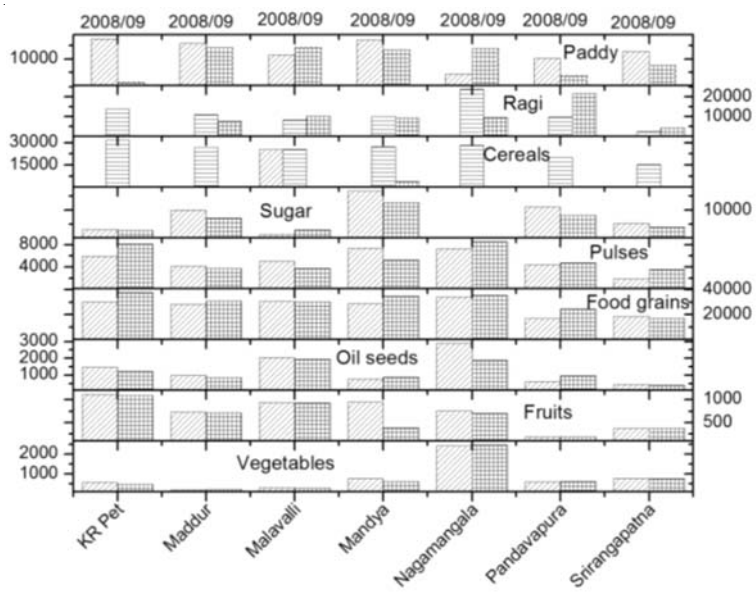

Figure 4. Different types of crops in Mandy district during 2008 and 2009.

Fig. 4 represents the crop yield through their cultivation over agricultural land (in terms of hectares) in different taluks of Mandya district in Karnataka state, India for the year 2008 and 2009. The rainfall and crop yield shows a positive correlation, however increase in AOT during monsoon period also has positive correlation with monsoon and has certainly a bearing on the agriculture. Further study is required with large amount of data and work is in progress.

REFERENCES

Gautam, R., Hsu, N. C., Lau, K. M. and Kafatos, M. (2009). Aerosol and rainfall variability over the Indian monsoon region: distributions, trends and coupling, *Ann. Geophys*, **27**, pp.3691–3703.

Lawrence, M. G. and Lelieveld, J. (2010). Atmospheric pollutant outflow from south Asia: a review, *Atmos. Chem. Phys. Discuss*, **10**, pp. 9463–9646.

Singh, R.P., Dey, Sagnik, Tripathi, S. N., and Tare, Vinod (2004). Variability of aerosol parameters over Kanpur, northern India, *J. Geophys.Res.*, **109.** D23206.

Vinoj, V., Satheesh, S. K., Babu, S. S., and Krishna Moorthy, K. (2004). Large aerosol optical depths observed at an urban location in southern India associated with rain-deficit summer monsoon season, *Annales. Geophysicae.*,**22**, pp.3073-3077.

INFLUENCE OF INDIAN FESTIVALS ON AIR QUALITY OVER PUNE

K. VIJAYAKUMAR[1], P.C.S. DEVARA[1], S.M. SONBAWNE[1], M. P. RAJU[1], P.D. SAFAI[1] AND P.S.P. RAO[1]

[1]Indian Institute of Tropical Meteorology, Pune-411008, India
E mail: devara@tropmet.res.in

Keywords : AEROSOL LOADING AND CHEMISTRY, INDIAN FESTIVALS, SOLAR RADIOMETER, ANGSTROM EXPONENT.

INTRODUCTION

Atmospheric aerosols are important from a perspective of ambient air pollution and health to humans and other biological receptors as well as for potential effects on local weather and global climate. As the aerosols are produced due to a wide range of global natural activities such as forest fires, dust storms and oceanic waves and also due to a large number of regional and local anthropogenic activities such as burning of fossil-fuel, industrial waste, automobiles, home furnaces, etc. On a global scale, the natural sources of aerosols are more important than the anthropogenic aerosols, but regionally anthropogenic aerosols are more important (Kaufman and Fraser, 1983; Ramanathan*et al*., 2001).

In this paper, we present Aerosol Optical Depth (AOD), Angstrom exponent, fine- and coarse-mode AODs, and chemical components observed during major Indian festivals such as 'Holi' and 'Diwali' periods using Sun-sky radiometer, MODIS satellite and chemical analysis. 'Holi' is one of the major Indian festivals, usually occurs in February/March. It is the most popular festivals in India. The origin of the traditional lighting of Holi is attributed by some to the burning of demonesses like Holika. Holi is also called 'The Festival of Colors', and people celebrate this festival by smearing each other with paint, and throwing colored powder and dye around in an atmosphere of great good humor. On the day of Holi, the firewood is arranged in a huge pile at a clearing in the locality. In the evening, the fire is lit. Thus, high concentrations of anthropogenic aerosols and metals are injected into the atmosphere due to colored powder and fireworks especially in urban regions (Vijayakumar and Devara, 2012). Another major Indian festival, namely, Diwali is also celebrated across the Indian Subcontinent in the span of a few days of October/November of each year. During this period, a large number of anthropogenic activities like bursting of firecrackers and sparkles, burning of bio-gases and residues of waste agricultural crop materials etc., take place over many places. Urban areas have been known to be a major source of particulate pollution, which is expected to continue to increase due to population growth, industrialization and energy use, especially in developing countries.

DATA

In this study, we have examined the daily AERONET data archived over Pune between 2004 and 2011 encompassing 'Holi' and 'Diwali' festival periods. We have also used daily MODIS AOD (550 nm) and fine-mode fraction data for the period 2004-2011 during the above festival periods.

RESULTS AND DISCUSSION

Ground-based Measurements

Fig. 1 shows day-to-day variations in mean AOD and Angstrom parameter over Pune during 'Holi' and 'Diwali' festival periods. It may be noted that in each figure, day number 6 is identified as festival day, 1-5 day number as pre-festival days and 7-11 as post-festival days during Holi/Diwali. During festival day, aerosol optical depth is observed to be greater in 'Holi' as compared to 'Diwali', which may be ascribed to dominance of fine-mode particles during the former. Both figures show that, pre-festival onwards, the aerosol concentration is slowly increasing over the experimental site. The Angstrom exponent shows lower values in 'Diwali' compared to 'Holi' festival day, indicating dominance of coarse-mode aerosols during 'Diwali' festival day (fig. 2).

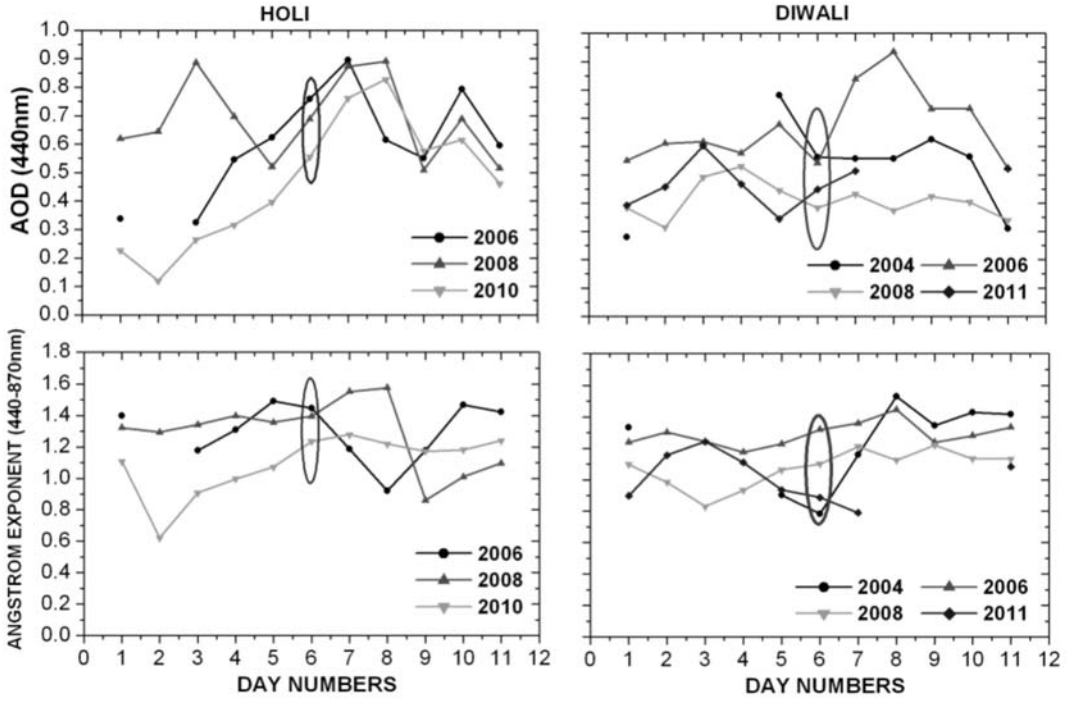

Figure1. Day-to-day variability in average values of AOD and Angstrom exponent from pre-festival to post-festival days over Pune during 2004-2011.

Fig. 2 shows daily average values of fine-mode, coarse-mode and fine-mode fraction at 500 nm over the experimental site during 2004-2011. From figure, during festival day, higher fine-mode AOD's were observed during 'Holi' day compared to 'Diwali' day. But higher coarse-mode aerosols are observed in Diwali period. The fine-mode fraction values show dramatically higher in 'Diwali' compared to 'Holi' festival period. During Diwali to Post-Diwali period, the fine-mode AOD, coarse-mode AOD, and fine- mode fraction values are found to slowly increasing, but in Holi to Post-Holi period, fine-mode AOD and fine-mode fraction values are found to decreasing and coarse-mode AOD values are increasing. Chemical analysis of the samples collected during the above festival periods also supports the inferred results related to the optical properties of aerosols.

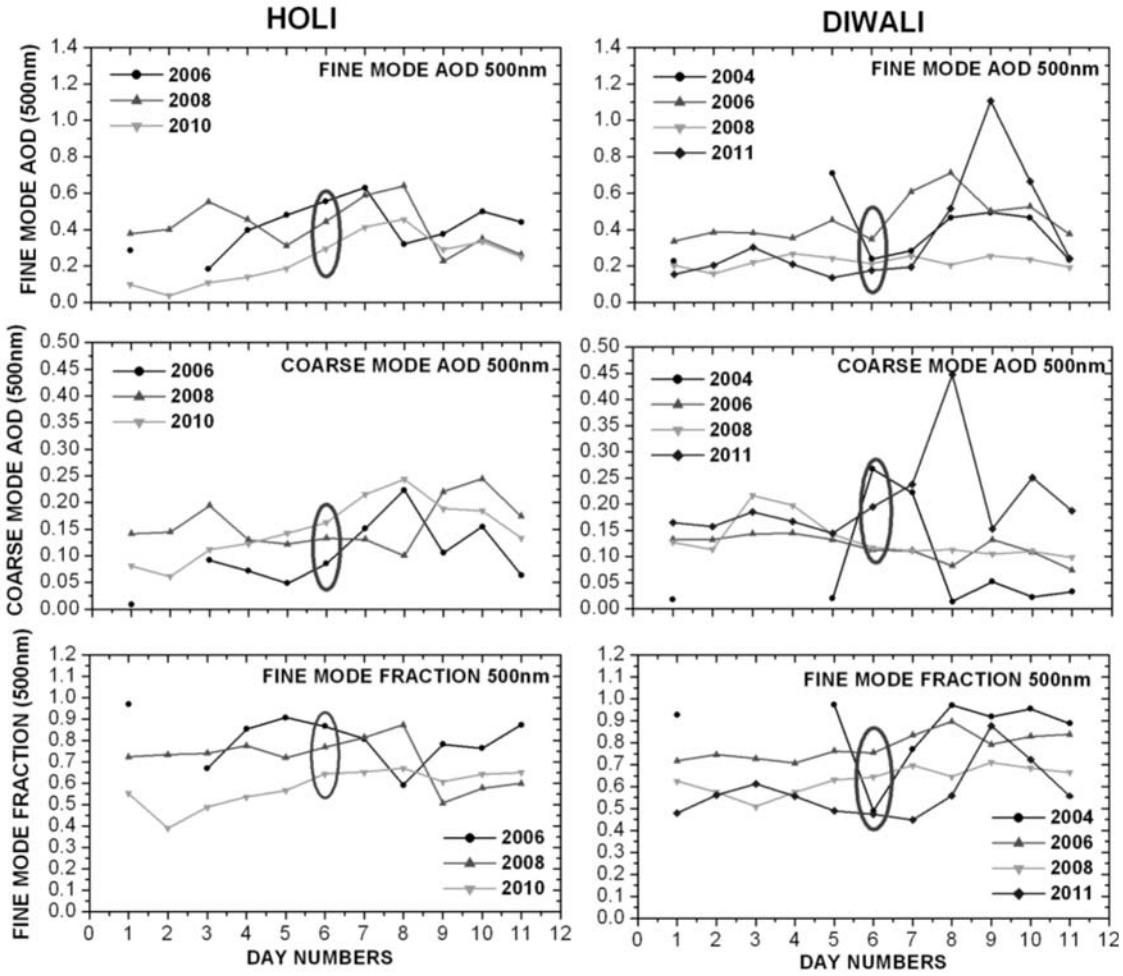

Figure 2.Day-to-day variability in average values of fine-mode AOD (500 nm), coarse-mode AOD (500nm), and fine-mode fraction (500nm) from pre-festival to post-festival days over Pune during 2004-2011.

Satellite Observations

Fig. 3 shows the daily MODIS values of AOD (550nm) and fine-mode fraction during Holi and Diwali festival periods. From figure, higher AOD values were observed during "Diwali' festival period compared to "Holi' festival. It is also evident from the figure that, pre-festival to festival period, the AOD values are slowly increasing. The fine-mode fraction shows higher values in 'Diwali' period compared to 'Holi' festival.

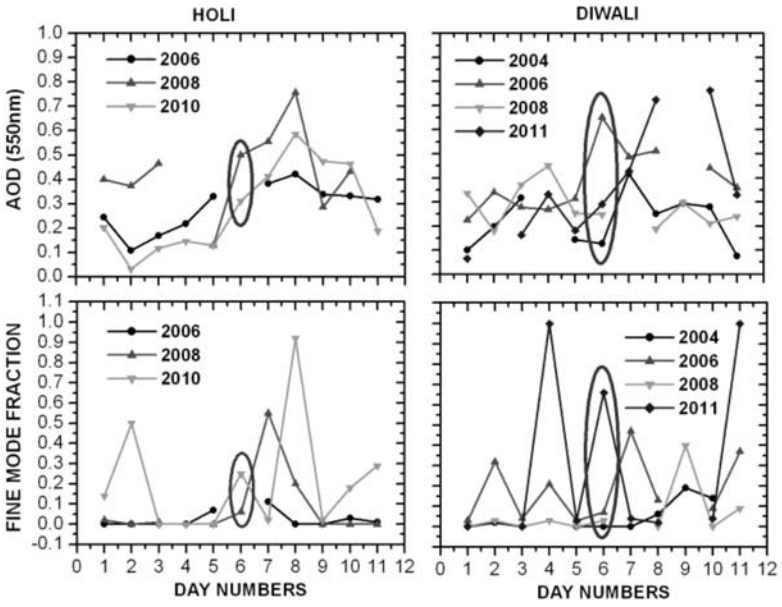

Figure 3. Daily values of AOD (550nm) and fine-mode fraction values from MODIS satellite data during 'Holi' and 'Diwali' festival periods.

ACKNOWLEDGEMENTS

This work was carried out as a part of ISRO-GBP-ARFI Program of ISRO, Department of Space, Government of India. One of the authors (KV) acknowledges the financial support, in the form of Research Fellowship, from the ISRO-GBP-ARFI Project. We are thankful to Brent Holben and his Group of AERONET, NASA; and MODIS science team for support. Thank are also due to Director IITM, Pune for encouragement and infrastructure support.

REFERENCES

Kaufman, Y. J. and Fraser, R. S. (1983). Light extinction by aerosols during summer air pollution, *Journal of Climate and Applied Meteorology*, **22**, pp. 1694-1725.

Ramanathan, V., Crutzen, P. J. and Lelievld, J. (2001). Indian Ocean Experiment: An integrated analysis of the climate forcing and effects of the great Indo-Asian haze, *Journal of Geophysical Research*,**106**, pp. 28371-28398.

Vijayakumar, K. and Devara, P. C. S. (2012). Variations in aerosol optical and microphysical properties during an Indian festival observed with space-borne and ground-based observations, *Atmosfera*, **25**, pp. 381-395.

CHARACTERIZATION AND SEASONAL VARIATION OF ATMOSPHERIC POLYCYCLIC AROMATIC HYDROCARBONS IN VISAKHAPATNAM, INDIA

[1]K.S. KULKARNI, [2]P.Y. AJMAL, [2]S. K. SAHU, [2]M. TIWARI, [2]G.G. PANDIT, [1]N. L. DAS, [2]V. D. PURANIK.

[1]Gitam Institute of Science, Department of chemistry, GITAM University, Visakhapatnam-530 045, India

[2]Environmental Assessment Division
Bhabha Atomic Research Centre
Trombay, Mumbai-400094
E mail: ggp@barc.gov.in

Keywords: PAH, SEASONAL VARIATION, MOLECULAR DIAGNOSTIC RATIOS.

INTRODUCTION

Polycyclic Aromatic Hydrocarbons (PAHs) are considered to be hazardous atmospheric contaminants due to their carcinogenic properties. They are present in both gaseous and particulate phases. They are mainly associated with particulate matter having aerodynamic diameter, ≤ µm which is one of the causes of respiratory and cardiac diseases (Lee, *et al.*, 2006).The main sources of PAHs are natural as well as anthropogenic especially vehicular exhaust, power generation and industrial activities. In addition, the contribution of tobacco smoke, emissions from cooking and other domestic activities is also significant. Meteorological conditions such as temperature and rainfall strongly affect PAHs concentrations in atmosphere. In recent years, many studies on PAHs associated with aerosols have been conducted in various cities of the world (Guo, *et al.*, 2003; Dallarosa, *et al.*, 2005; and India (Raiyani, *et al.*, 1993; Pandit, *et al.*,1996) which show that total PAHs concentrationsin Indian cities are about 2 to 3 times higher than those reported internationally.

This paper presents a study on US EPA listed 16 priority PAHs associated with respirable ambient aerosols collected from March 2010 to February 2011 at Visakhapatnam, Andhra Pradesh. The distribution and seasonal variations of PAHs were studied. Molecular diagnostic ratios were used for preliminary assessment of PAH sources. The study will help to set control measures considering the hazardous health impacts.

SAMPLE COLLECTION AND ANALYSIS

Visakhapatnam is the second largest city in the state of Andhra Pradesh and the only natural harbor on the eastern coast of India. In the present study, an industrial cum residential area "Parwada" was selected for monitoring of air quality. It is a Mandal including 17 villages with a dense population in Visakhapatnam district. The site is surrounded by various heavy industries such as National Thermal Power Plant (Simhadri), Vizag Steel Plant, Hindustan Petroleum Corporation Limited (HPCL), Hindustan zinc limited and Bharat Heavy Plates etc (Harji, *et al.*, 2010). About 150 Respirable Suspended Particulate Matter (PM_{10}) samples were collected during March 2010 to February 2011 using High Volume Sampler (HVS-430). It was installed on the roof of a house at about 5m height. Sample collection was carried out over a period of 24 h on glass fiber filters (Whatmann EPM 2000) at an average flow rate of 1.1 m^3 min^{-1}. The filters were extracted with n-hexane (E. Merck, HPLC grade) by ultrasonication for 1 h to ensure good recovery. The samples

were filtered and the extracts were concentrated to about 1 ml and then subjected to undergo cleanup process (Pandit, *et al.*, 1996).The PAHs containing fraction was concentrated and evaporated to dryness by passing nitrogen and stored in glass test tubes for further analysis. The characterization and quantification of PAHs were done by high performance liquid chromatograph (HPLC) system (Shimadzu LC-10AD) with UV–visible detector. The analyte recoveries were determined by spiking filter paper samples with PAHs standard mixture. The mean recovery varied from 80 to 97%. Quality control and assurance was maintained in every stage of analysis.

RESULTS AND DISCUSSION

Total PAHs concentration varied between 15.49 to 112.07 ng m^{-3} while the concentration of PM_{10} varied between 27.18 to 138.54 µg m^{-3}. The yearly average concentration of individual PAH (in ng m^{-3}) is listed in Table 1.There are high concentrations of low molecular weight PAHs i.e. Acenaphthylene, Fluorene, Acenaphthene and Phenanthrene. These are the characteristic PAHs found near thermal power plants. Earlier studies also show that lower molecular weight PAHs are the major contributors among the total PAHs in fly ash from pulverized coal power station (Sahu, *et al.,* 2009).The significantly higher level of Benzo[ghi]pyrene, and Phenanthrene were observed which are contributed by motor vehicle emissions (Smith and Harrison, 1998).The concentrations of Benzo(a)Pyrene, Benzo(a)Anthracene, Chrysene, Pyrene and Benzo(k)Fluoranthene which are potent carcinogenic and mutagenic were also found to be high. The Steel plant and diesel vehicle emissions are contributing to these PAHs. The sources of Fluoranthene, Phenanthrene and Indeno [1,2,3-cd]pyreneare incomplete combustion and pyrolysis of fuels (Yang, *et al.*, 1998).

PAHs	No. of rings	Min	Max	average
NAPH	2	0.15	8.42	2.64
ACY	3	0.21	50.26	13.46
FLUO	3	0.22	12.24	2.42
ACE+PHEN	3	0.39	47.1	7.57
ANTHRA	3	0.51	24.16	2.78
FLT	4	0.55	8.45	1.26
PYR	4	0.1	15.53	2.7
CHRY+BaA	4	0.52	5.77	1.25
BbF	5	0.03	4.69	1.25
BKF	5	0.51	15.85	2.47
PERY	5	0.22	7.71	0.93
BaP	5	0.54	9.54	1.81
InD	6	0.04	5.62	1.42
BghiP	6	0.36	37.27	6.04
Σ16PAHs		15.49	112.07	50.92

NAPH: Napthalene, ACY: Acenapthylene, FLUO: Flurene, ACE: Acenaphthene, PHEN: Phenantherene, ANTHRA:Anthracene, FLT: Fluoranthene, PYR: Pyrene, BaA: Benzo(a)Anthracene, CHRY: Chrysene, BbF: Benzo(b)fluoranthene, BkF: Benzo(k)fluoranthene, PERY: Perylene, BaP: Benzo(a) Pyrene, BghiP : Benzo(ghi)perylene , InP: Indeno (1,2,3-cd)pyrene. LMW PAH: NAPH, ACY, FLUO, ACE, PHEN, ANTHRA. HMW PAH: FLT, PYR, CHRY, BaA, BbF, BKF, PERY, BaP, InD, BghiP.

Table 1. Average concentrations of individual PAHs (in ng m^{-3}) during the year 2010-2011.

The seasonal variation studies showed that monthly average concentration of PM_{10} varied between 61.29 to 111.59 µg m^{-3} and that of PAHs varied between 32.14 to 77.81 ng m^{-3}. Fig. 1 shows the seasonal variation in concentrations of PAHs. The concentrations of PAHS are higher in winter season than summer. Both PM_{10} and Σ16PAHs follow similar seasonal trend. In summer, high temperature and enhanced photodecomposition of PAHs, leads to decrease in their concentration,

whereas in winter low wind speeds and low temperatures make the atmosphere stable which leads to more gas-to-particle conversion of PAHs which turns to higher concentration of PAHs. In monsoon, the PAHs are scavenged away by precipitation resulting in the least concentration of PAHs. (Guo, *et al.*,2003).

The diagnostic ratios method for PAHs source identification involves comparing ratios of pairs of the frequently found PAHs emissions. Molecular diagnostic ratios of PAHs observed in this study compared with corresponding source signatures from published literature showed that the ratio InP/(InP+BghiP) with its value of 0.19 is similar to the value reported for vehicle emission range. A value 0.23 for the ratio Ind/BghiP is reported for gasoline engine and the value 0.3 for the ratio BaP/BghiP is again reported for vehicular emission. (Carricia, *et al.*,1999). The value of ratio FLT/(FLT+PYR) is between 0.4-0.5 indicates fossil fuel combustion especially coal combustion. Further the BbF/BkF ratio with a value >0.5 may be attributed to diesel emissions (Park, *et al*., 2002). Thus vehicular emission especially gasoline and diesel vehicles and fossil fuel combustion are the major sources of PAHs in Visakhapatnam.

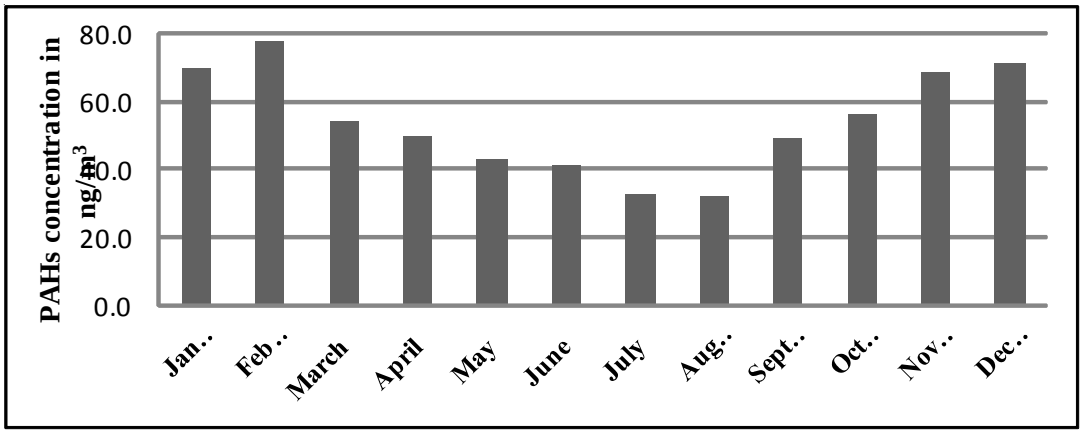

Figure 1. Annual trend of PAHs during year 2010-2011.

REFERENCES

Caricchia, A.M., Chiavarini, S., Pezza, M., (1999). Polycyclic aromatic hydrocarbons in the urban atmospheric particulate matter in the city of Naples (Italy), *Atmospheric Environment*, **33**, pp. 3731–3738.

Dallarosa, J. B., Monego, J. G., Teixeira, E. C., Stefans, J. L.,&Weigand, F. (2005). Polycyclic aromatic hydrocarbons in atmosphere particles in metropolitan area of Porto Alegre, Brazil, *Environment,* **39**, pp. 1609–1625.

Guo, H., Lee, S.C., Ho, K.F., Wang, M.X., Zou, S.C. (2003). Particle-associated polycyclic aromatic hydrocarbons in urban air of Hong Kong, *Atmospheric Environment*, **37**, pp. 5307-5317.

Harji R.R., Bhosle N.B., Garg A., Sawant S.S., Krishnamurthy V. (2010). Sources of organic matter and microbial community structure in the sediments of the Visakhapatnam harbour, east coast of India, *Chemical Geology*,**276**, pp. 309–317.

Lee, S.C., Cheng, Y., Ho, K.F., Cao, J.J., Louie, P.K.K., Chow, J.C. (2006). PM1.0 and PM2.5 characteristics in the roadside environment of Hong Kong, *Aerosol Science and Technology*, **40**, pp. 157-165.

Pandit, G. G., Sharma, S., Mohan Rao, A. M., Krishnamoorthy, T. M. (1996).Chromatographic methods for the estimation of Polycyclic Aromatic Hydrocarbons in atmospheric particulates.In proceedings of the 5th National Symposium on Environment, pp. 133–136.

Park, S.S., Kim Y.J., Kang, C.H., (2002). Atmospheric polycyclic aromatic hydrocarbons in Seoul, Korea, *Atmospheric Environment*, **36**, pp. 2917-2924.

Raiyani, C. V., Jani, J. P., Desai, N. M., Shaha, J. A., &Kashyap, S. K. (1993). Assessment of indoor exposure to polycyclic aromatic hydrocarbons for urban poor using various types of cooking fuel, *Indian Journal of Environment Protection*,**13(3)**, pp. 206-216.

Sahu, S. K., Bhangare, R. C., Ajmal, P.Y., Sharma, S., Pandit, G.G., Puranik, V.D. (2009). Characterization and quantification of persistent organic pollutants in fly ash from coal fueled thermal power stations in India, *Microchemical Journal*, **92**, pp. 92–96

Smith, D.J.T., Harrison, R.M. (1998). Polycyclic aromatic hydrocarbons in atmospheric particles. In: Harrison, R.M., Van Grieken, R. (Eds.), Atmospheric Particles. Wiley.

Yang, H. H., Lee, W. J., Chen, S. J., Lai, S. O. (1998). PAH emission from various industrial stacks, *Journal of Hazardous Materials*, **60**, pp. 159–174.

CHARACTERIZATION OF AIRBORNE BIOLOGICAL PARTICLES FROM WASTEWATER TREATMENT PLANTS IN MUMBAI

S. GANGAMMA

Centre for Environmental Science and Engineering,
Indian Institute of Technology Bombay, Mumbai-400 076
Department of Chemical Engineering,
National Institute of Technology Karnataka,
Surathkal-575 025

Key words: AIRBORNE BACTERIA. ENDOTOXIN. INFLAMMATORY RESPONSE. *EX VIVO*.

INTRODUCTION

Wastewater contains a variety of potentially pathogenic microorganisms and their toxic components. Several unit operations such as surface aeration, mechanical sludge removal and screening in treatment plants may cause aerosolization of these biological components into the air environment. Depending on the physical properties of these aerosolized biological particles and meteorological conditions, they are likely to be carried by the air currents and may reach significant distances. This in turn could expose the workers working in the immediate vicinity to these biological components and may also affect the downwind population. Bacteria are abundant and important class of the microorganism present in wastewater treatment plants (WWTPs) (Bauer, *et al*., 2002; Oppliger, *et al*., 2005). There is a scarcity of data on the characteristics of biological particles near WWTPs as well as similar sources in India. Particularly, the location of some of these plants in Mumbai also makes these studies relevant. The present study characterizes the airborne bacteria and elicits the influence of endotoxin on inflammatory induction in *ex vivo* whole bloodassay (WBA) across the six WWTPs in Mumbai.

MATERIALS AND METHODS

The monitoring of airborne biological particles was carried out at six municipal WWTPs of Municipal Corporation of Greater Mumbai (MCGM), Mumbai, India. The monitoring of bioaerosols in these sites was carried out in two different stages. During first phase, the samples (n=63) were collected with biosampler (SKC Inc., USA) in May-June 2009. The samples were collected on endotoxin free water (Lonza, India). PM-10 (particles with aerodynamic diameter smaller than 10ìm) samples (n=30) were collected with MiniVol samplers (Airmetrics, USA) during February - March 2011. The samples were collected on glass fiber filter paper (Whatmann, GF047). All filter samples were extracted into endotoxin free water for endotoxin analysis within two weeks after sampling.

In the laboratory, each biosampler sample was plated in triplicate onto tryptic soya agar (TSA) plates for determining the total culturable bacteria. The agar medium was prepared by using 40 g/L of TSA (Himedia, India) and supplemented with 0.5 g/L cycloheximide (S.D.fine Chemicals, India). A 100-250 µL aliquot was used for plating and uniform spreading was achieved with the help of Plate Master (Himedia, India). The plates were incubated at 37 ± 1°C for 2-5 days. The concentration of airborne bacteria was reported as CFU/m^3.

The biosampler and extracted PM-10 samples were analyzed for airborne endotoxin using kinetic limulus ambeocyte lysate (KQCL) assay (Lonza, India). The results were expressed in terms of Endotoxin unit (EU) and have potency of 13 (EU/ng). The assay was carried out according to manufacturer recommendations. All standards, samples, field blanks and endotoxin free water were analyzed in duplicate.

The individual colonies observed on TSA plates (from biosampler samples) were selected and isolated based on their morphology, including size, shape, color and surface properties. A total of 174 distinct colonies of bacteria were isolated from different plates. Samples were also plated on MacConkey and Eosin methylene blue (EMB) agar to isolate most of the bacterial species present in the samples. The bacterial colonies were identified up to species level using the Biolog Manual System-1(Biolog, Inc., Hayward, California). The classification and identification protocol was followed according to the manufacturer.

Twenty randomly selected extracted PM-10 samples were subjected for measurement of the tumor necrosis factor (TNF-á) induction in WBA. Venous blood was collected in EDTA coated vacutainer (BD bioscience, India) from six healthy donors under no medication. The 100µl of fresh whole blood was incubated with 100 µl of samples and 350 µl of 0.9% saline at 37°C for 18 hrs. The TNF-á concentration in the supernatant was measured with ELISA (Invitrogen, India) according to the manufacturer recommendation. All samples were analyzed in duplicate.

Non-parametric Mann-Whitney test was used for comparison of group means. All the analysis was carried out with 'R' version 2.13.1(R, 2011).

RESULTS AND DISCUSSION

In the WWTPs,the endotoxin concentration associated with PM-10 varied over the range of 0.22-2880 EUm^{-3}. The concentration variation in the plants is due to the operational variability, source water characteristics and due to the sampling conditions such as wind speed and sampling location. The concentration of endotoxin of field blanks was found to be below the detection limit of the assay. The average endotoxin concentration near source (404 EUm^{-3}) is found higher than the average endotoxin level at office area (89 EUm^{-3}) across all WWTPs ($p<0.002$). This indicates a significant reduction in the endotoxin concentration at office compared to the source (Fig.1). PM-10 concentration was found to be positively correlated with its endotoxin concentration ($p<0.001$) and may indicates increase of biological content of PM (endotoxin) with increase of particulate concentration. This correlation may indicate the existence of similar sources for PM and endotoxin. The concentrations observed in the current study and *in-vivo*/*in-vitro* studies (Ning, *et al*.,2000; Long, *et al*.,2001) indicate that endotoxin are likely to be an important parameter and may have significant health impacts.

The PM -10 induced TNF-α concentration varied over the range of 59-315 pg/ml. The average TNF-α concentration induced by PM-10 samples near source (223 pg/ml) is not significantly ($p<0.63$) different from the samples near office (200 pg/ml). Samples have not shown any significant differences among the treatment plant operations. TNF-á induced by the PM-10 samples has shown significant positive correlation ($p<0.001$) with logarithmic transformed endotoxin concentration of the sample.

Gram positive bacteria (GPB) were found to be predominantly present in all the biosampler samples across all WWTPs, with a percentage fractions vary from 67 to 90%. High levels of Gram negative bacterial (GNB) concentration in WWTPs are reported in literature. The presence and dominance

of different bacterial aerosols are highly dependent on the characteristics of wastewater, and the local climatic conditions. In GNB groups of bacteria, enterobacteriaceae group was more predominant (86-94%) in the WWTPs. More results about the characteristics of the airborne particulate matter will be discussed.

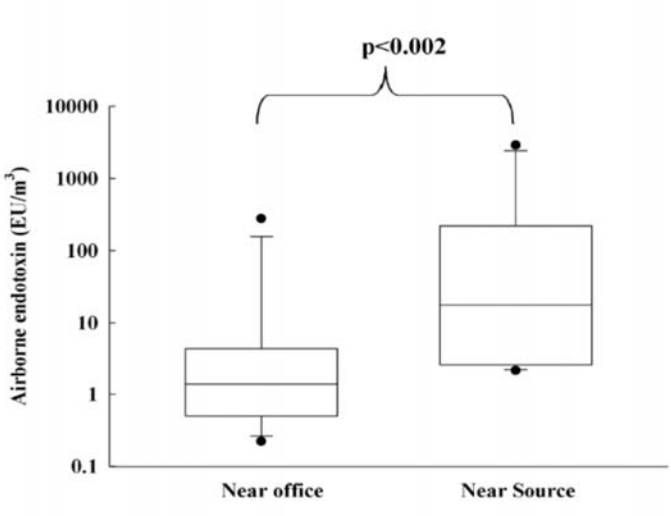

Figure 1. Concentration of airborne PM-10 associated endotoxin measured across WWTPs in Mumbai

ACKNOWLDGEMENTS

The author express sincere thanks to Department of Science and Technology, Govt. of India for providing financial support for carrying out this work (SR/S4/AS:283/2007, SR/FTP/ES-40/2008). Author thanks all officials of MCGM, Mumbai for extending facilities and cooperation. Author also express thank to Professor R.S. Patil and Professor SuparnaMukherji, IIT Bombay for providing laboratory facilities to carry out this work.

REFERENCES

Bauer, H., Fuerhacker, M., Zibuschka, F., Schmid, H. and H. Puxbaum (2002). Bacteria and fungi in aerosols generated by two different types of wastewater treatment plants, *Water Res.* , **36**, pp. 3965–70.

Long, C. M., Suh, H. H., Kobzik, L., Catalano, P. J., Ning, Y. Y. and P. Koutrakis (2001). A pilot investigation of the relative toxicity of indoor and outdoor fine particles: Invitro effects of endotoxin and other particulate properties, *Environ. Health Perspect.* , **109**, pp. 1019-1026.

Ning, Y., Imrich, A., Goldsmith, C.A., Qin, G. and L. Kobzik (2000). Alveolar macrophage cytokine production in response to air particles in vitro: Role of endotoxin, *J. Toxicol. Environ. Health*, **59**, pp. 165-180.

Oppliger, A., Hilfiker, S. and T. Vu Duc (2005). Influence of seasons and sampling strategy on assessment of bioaerosols in sewage treatment plants in Switzerland, *Ann. Occup. Hyg.* , **49**, pp. 393- 400.

R Development Core Team. R (2011). A language and environment for statistical computing. R Foundation for Statistical Computing, Vienna, Austria. ISBN 3-900051-07-0. Website; http://www.R-project.org/.

SPECIATION OF CHROMIUM IN AIR BORNE RESPIRATORY DUST PARTICULATE MATTER COLLECTED AROUND STAINLESS STEEL WELDING OPERATIONS

GARIMA SINGH[1], NISHITH GHOSH[1], R.K.SINGHAL[2], D. D. THORAT[3], S.K.KARAMCHANDANI[4],

S. SOUNDARARAJAN[1], AND D.N. SHARMA[1].

Radiation Safety Systems Division[1], Analytical Chemistry Division[2], Powder Metallurgy Division[3], Centre for Design and Manufacture[4]
Bhabha Atomic Research Centre, Trombay, Mumbai-400094
E mail: garima@barc.gov.in

Keywords: METAL AND OCCUPATIONAL EXPOSURE

INTRODUCTION

Chromium is a naturally occurring element found in the environment and can exist as Cr (III) and Cr (VI). While Cr (III) compounds are stable and relatively non toxic, Cr (VI) which is primarily produced by industrial processes is considered to be toxic in nature and can diffuse through cell membranes and oxidize biological molecules with toxic results. Cr (VI) is a proven carcinogen for human beings and life systems even at trace concentration levels. Therefore, determination of hexavalent chromium is of particular interest and there has been considerable effort within industry to assess the potential cancer risk to workers exposed to Cr (VI) in the workplace. Electric arc welding is a widely used industrial process for joining of metal components. The necessity and enormous economic value of such processes are well recognized. Even though welding is a critically important fabrication process underpinning industry in India and elsewhere, occupational exposure to welding fumes and gases continues to be an issue which has been of greater significance since the widespread introduction of welding in 1950. During this work, exposure of Cr (VI) to the workers involved in the stainless steel-304, 304 and 316 (SS) welding using SS electrode was determined. Introduction of chromium present in electrodes, welding wires, and base materials is in the form of Cr (0). However at high temperatures created during welding process, chromium in steel is oxidized to the hexavalent state Cr (VI) and it becomes airborne to which the workers may be exposed. The majority of the chromium found in welding fume is typically in the form of Cr (III) as Cr_2O_3 whereas a definite portion is oxidized to hexavalent chromium in the form of CrO_3.

MATERIAL AND METHODS

The Staplex ® Model TFIA series High Volume Air Samplers is used to collect the total suspended particulate matter (TSPM) at workshop for design and manufacture where SS welding operation was carried out on a regular basis. Air sampler has built-in rotameter for instantaneous flow reading. The sample is collected on filters through 0.5 μm pore size GF/A filter paper (Whatman Cat No 1820866) allowing a measurement of TSPM. Each sample is collected for ten minutes during which a flow rate of 500 LPM is maintained.

Sample processing

Each collected sample is air dried and kept in a dessicator for 24 hrs before weighing. For Total Chromium determination, the filter is digested with conc. HNO_3 along with a few drops of sulphuric

acid on a hot plate for 3- 4 hrs. When sample is near dryness, the chromium is extracted in 2% HNO_3 and before aspiring in ICP-OES, it is filtered through a 0.45 μm filter paper. For determination of Cr (VI), the sample is alkali digested (0.28 M $NaHCO_3$ and 0.5 M NaOH) and filtered through 0.45 μm filter paper. Cr (VI) in the filtered sample is analyzed by anodic striping voltammetry (Model PDV-6000 Plus, COGENT) using bare carbon working electrode and a patented electrolyte.

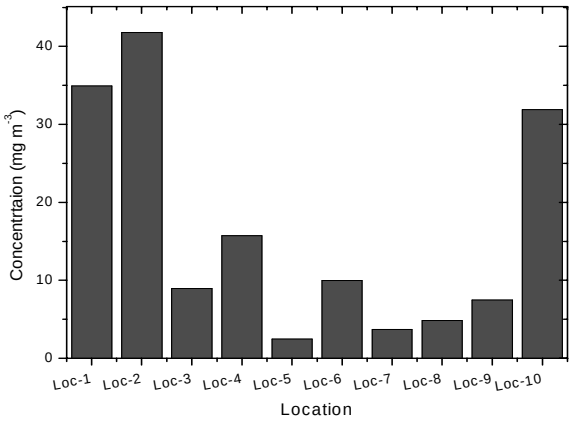

Figure 1. Particulate matter concentration at different locations

RESULTS AND DISCUSSION

The concentrations of particulate matter collected from different locations are shown in Fig. 1. The weight of TSPM is obtained by the difference in the weight of the filter paper before and after sampling. From this table it is clear that there is a wide variation in the concentration of TSPM i.e the values vary from 42 to 2.42 mg m^{-3}. It was observed that under the influence of welding fume extractor, TSPM values decrease by ten times.The concentration levels of Total Chromium and Cr (VI) in different samples are shown in Fig. 2. From this figure, it is clear that the airborne concentration of Cr (VI) increases with the amount of air particulates collected on the filter paper. The variation in percentage of Cr (VI) in total chromium is in the range of 20-30 % except some three locations where the percentage varies in the range of 70-90%. Locations having elevated level of Cr (VI) were within a close proximity (less than 2 meter) to the welding operation points. Detailed work is in progress to find out the reasons.

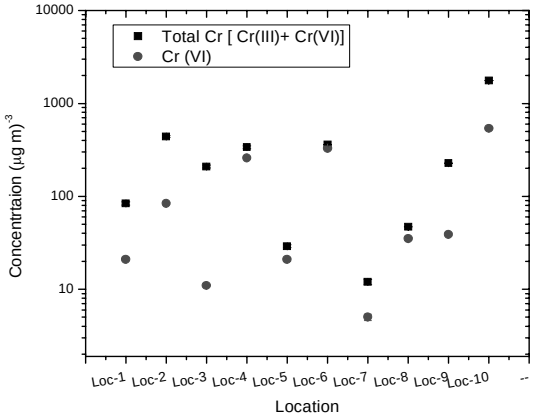

Figure 2. Chromium concentration

Kazantzis, (1972) describes excess lung cancers in occupational workers of chromium related industry, suggesting an association of Cr(VI) with human biological system, as it diffuses through cell membranes and oxidizes biological molecules with toxic results. The evidence relating to Cr(VI) exposure in welding fume has not yet demonstrated that it causes cancer in welders, but it is sensible to limit exposure during welding. American Conference of Governmental Industrial Hygienists (ACGIH) shows concern regarding exposure to Cr (VI) and specifies an occupational exposure limit (TLV-TWA) of 0.05 mg/m^3.

The experimental results of this study clearly indicates the advantage of using Gas Tungsten Arc Welding (GTAW) over the conventional Shielded Metal Arc Welding (SMAW) as the metal fumes were reduced by an order of magnitude in the former case. Metal fumes were also reduced by using filler metal. Filler metal is added manually to the front end of the weld pool and Argon is used as a shielding gas. Initial experimental results show a decrease of six times in metal fume concentration under these conditions.

CONCLUSIONS

There is much concern over control of exposure to Cr(VI) during SS welding. From this study, it is clearly indicated that the indoor welding operations must be carried out with welding fume extractor as there is a considerable decrease in the concentration of metal fumes with its use and also respiratory protection must be used by the workers.

REFERENCES

Dennis, J., et al. (2002). Ann. Occup. Hyg., **46 (1)**, pp. 33-42.

Kazantzis G. (1972). Chromium and nickel, Ann. Occup. Hyg., **15**, pp. 25–29.

AEROSOL RADIATIVE FORCING

SHORT WAVE RADIATIVE FORCING RESULTING FROM TEMPORAL CHARACTERISTICS OF AEROSOLS OVER KANNUR, A TROPICAL COASTAL LOCATION IN INDIA

PRASEED K.M[1, 3], NISHANTH T[2, 3], SATHEESH KUMAR M.K[2, 3]

[1]Department of Physics, Sir Syed College, Taliparamba, Kerala, India
[2]Department of Physics, Govt. Brennen College, Thalassery, Kerala, India 670 106
[3]Department of Atmospheric Science, Kannur University, Kerala, India- 670 567

INTRODUCTION

Among the various climate forcing agents like greenhouse gases, atmospheric aerosols are one of the decisive components in the atmosphere, contributing to climate change with maximum uncertainty (IPCC 2007). Asian monsoon region is prone to have high concentration of anthropogenic aerosols and is being influenced significantly to the regional climate through direct radiative forcing (Ramanathan, *et al.*, 2005). Various studies revealed that the concentration of aerosols has been increasing over Indian sub- continent and further analysis indicates that the Aerosol Optical Depth (AOD) over the northern part of India is much higher than that in the southern region (; Devara, *et al.*, 2005; Jayaraman, 2001; Moorthy, *et al.*, 2008; Satheesh and Moorthy, 2005,). Aerosol radiative forcing provides a scheme to quantify the contribution of aerosols in estimating the surface temperature modulated by the solar and terrestrial radiations (Charlson, *et al.* 1992). Since the distribution of aerosols is quite non- uniform over the globe, their radiative effect depends mainly on geographical location and time. Hence, the radiative forcing is a scale which indicates the extent to which it can impact a change in climate over a region. This work is essentially throws some light to the seasonal variations of AOD over Kannur, a tropical site confined between the coastal belt of the Arabian Sea and Western Ghats. The aerosol samples collected at this location have been chemically analyzed to formulate a simple aerosol model suited for this region. The aerosol radiative forcing has been estimated using SBDART and the heating rates are thus calculated.

OBSERVATION SITE AND GENERAL METEOROLOGY

The sampling site is at Kannur University Campus (KUC), (11.9^{o}N, 75.40^{o}E, 5m ASL) which is in the northern part of Kannur district. It is a rural area with no major industrial activity except for a few small scale industries. The air distance from the site to the sea shore is 4 km and that to the Western Ghats is 50 km. The most prominent meteorological feature of this region is the monsoon rain fall occurring in two spells during a year. The south west monsoon is active during the month June, July and August with heavy rain fall. The north east monsoon usually occurs in October-November is accompanied by thunder and lightning with moderate rain fall.

DATA AND METHODOLOGY

A hand held MICROTOPS II sun photometer (fitted with narrow-band interference filters) of Solar Light company, USA (2002) has been employed for the estimation AOD at discrete wavelengths 340nm, 440nm, 675nm, 870 nm and 1020nm. Subsequently, AODs were measured on all clear sky days from 09.00-17.00 hrs, IST, at 30 minutes interval, from January to December 2010. For a given spectral range, the variations of AOD (τ) follow Angstrom power law given by (Angstrom, 1961) as

$$\tau = \beta \lambda^{-\alpha}$$

where, λ is the wavelength in micrometer. Angstrom exponent α is a rough indicator of the size distribution of aerosols in the column. The Angstrom parameter α and turbidity factor β were retrieved by least square fit on a log -log scale plot of the observed AOD versus wavelength.

Aerosol samples less than PM_{10} were collected using a Respirable Dust High Volume sampler (ENVIROTECH, India Model APM 460 NL) from a height of 10m above the ground level, in the month of April, August and November, to account the aerosol loading during summer, monsoon and winter seasons. The instrument essentially collects aerosols on preconditioned glass microfiber filter. The sample laden substrates were later subjected to gravimetric analysis for the estimation of aerosol mass loading and chemical analysis for identifying and quantifying various chemical species. From the analysis of the results a simple aerosol model has been formulated by including 2% soot as well, to account for the vehicular emission.

The observed values of spectral AODs, along with estimated values of Single Scattering Albedo (SSA) and asymmetry factor 'g 'are incorporated into the SBDART (Ricchiazzi et al 1998) model and diurnally averaged, shortwave, clear sky radiative forcing at the surface(S) and the top of the atmosphere (TOA). They are estimated as

$$\mathbf{\Delta F}_{\mathbf{S,\,TOA}} = \mathbf{(fa\downarrow - fa\uparrow)}_{\mathbf{S,\,TOA}} - \mathbf{(fo\downarrow - fo\uparrow)}_{\mathbf{S,\,TOA}}$$

where fa↓ and fa↑ denotes the down welling and upwelling irradiance (in W m^{-2}) with aerosols and fo↓ and fo↑ denotes the respective quantities (in W m^{-2}) without aerosols. $\mathbf{(\Delta F_{TOA} - \Delta F_S)}$ gives "F_{atm}, the net atmospheric forcing. This energy gets converted into heat and thereby results in heating the atmosphere, which is a solid indicator of climatic impact of aerosols. The atmospheric heating rate have been calculated (Liou, 1980) as $\frac{\partial T}{\partial t} = \frac{g}{Cp}\frac{\Delta Fatm}{\Delta P}$ where $\partial T/\partial t$ is the heating rate, g is acceleration due to gravity, C_p is specific heat capacity at constant pressure and $\mathbf{\Delta}P$ is the change in atmospheric pressure.

RESULTS AND DISCUSSION

It is observed that the AODs are fairly high in summer, moderate in monsoon and low in post monsoon and winter seasons. Monthly variations of AOD during the period January 2010- December 2010 are depicted in fig. 1.

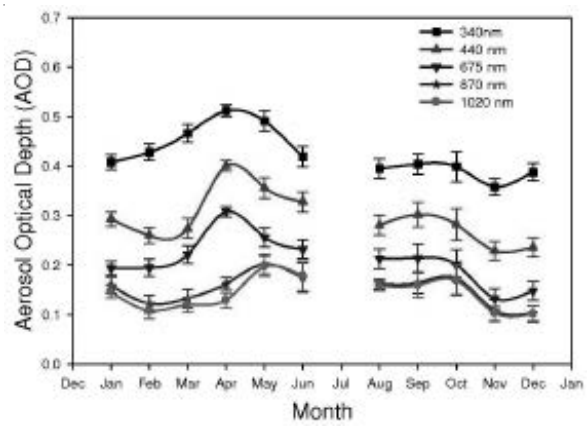

Figure 1. Monthly variation of AOD at Kannur

The low value of AOD in post monsoon and winter seasons may be due to the clear sky environment resulting of the settling of aerosols during heavy rain fall in monsoon. Further, in winter months, the atmospheric boundary layer is shallow which ensures a minimum mixing volume for the particle. During summer months, the boundary layer is relatively higher and hence pollutants have additional volume for scattering and absorption of solar radiation passing through it. The influence air mass movement from the western side of this of this location indicates a strong marine influence during pre-monsoon and monsoon seasons.

The average PM_{10} mass concentration was found to be 58±7 μg/m^3 in the month of April, 46±4 μg/m^3 in August and 38±3 μg/m^3 in the month of November. The chemical analysis of the samples revealed the presence of Cl, SO_4, NO_3.PO_4 and CO_3 as major anionic species. It was found that ions like Na, Cl, Ca, SO_4 and K which are mainly of oceanic origin showed a peak during monsoon and NO_3, PO_4 Fe, Al and trace elements exhibited a peak in summer. Seasonal variations of aerosol radiative forcing over Kannur is shown in fig. 2.

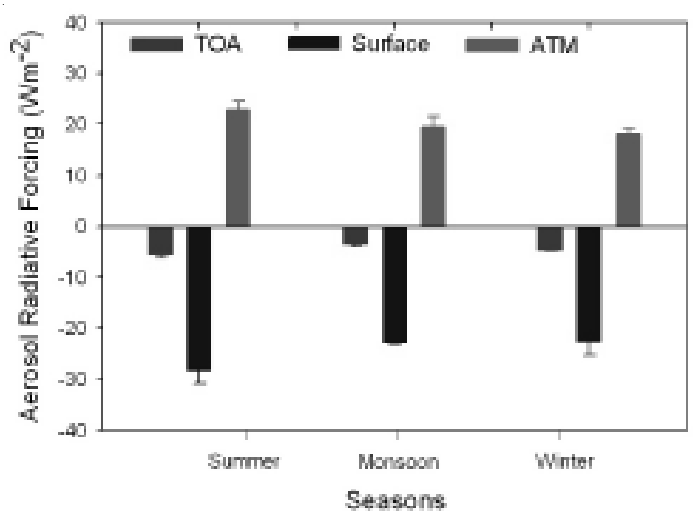

Figure 2. Variation of seasonal average direct aerosol radiation forcing over TOA, surface and in the atmosphere over Kannur

The highest value of atmospheric forcing (22.7±1.97) was observed in summer (March-May) and the lowest (18±0.24) in winter (Dec-Feb). During monsoon period (June-Nov), the corresponding value was found to be 19.37±2.18. The corresponding AOD values were found to be 0.29±0.03, 0.22±0.02 and 0.24±0.02 and á were 1.24±0.03, 1.12±0.03 and 0.79±0.15 respectively. The estimated heating rates are 0.63K/day, 0.49K/day and 0.55K/day which is essentially signifies the aerosol influence that modulates climate change. The significant difference between the TOA forcing and the surface forcing is due to the absorptive property of aerosols (Ramachandran, 2005).

ACKNOWLEDGEMENTS

The authors are indebted to the Kerala State council of Science, Technology and Environment (KSCSTE) for their financial support in the form of a project granted for the study of aerosols over this region.

REFERENCES

Ångström, A., (1961). Techniques of determining the turbidity of the atmosphere, *Tellus.* ,**13**, pp. 214-223.

Charlson, R.J., Schwartz, S.E., Hales, J.M., Coss, R.D., Coakley, J.A., Hansenand, J.E. Hoffmann, D.J., (1992). Climate forcing by anthropogenic aerosols, *Science*, **255**, pp. 423-43.

Devara, P.C.S., Saha, S.K., Raj, P.E., Sonbawne, S. M., Dani, K. K., Tiwari, Y. K., Mahesh Kumar, R. S., (2005). A four-year climatology of total column tropical urban aerosol, ozone and water vapor distributions over Pune, India, *Aerosol Air Qual. Res.* , **5**, pp. 103-114.

IPCC, Climate change (2007). The Physical Science basis, changes in atmospheric constituents and in radiative forcing.

Jayaraman, A., (2001).Aerosol radiation cloud interactions over the tropical Indian Ocean prior to the onset of the summer monsoon, *Current Science*, **81(11)**, pp. 1437-1445.

Liou, K. N. (1980). An Introduction to Atmospheric Radiation, Harcourt Brace Jovanovich, New York, 392.

AEROSOL OPTICAL AND RADIATIVE PROPERTIES DURING INTENSE DUST STORM OF MARCH 2012 : A 4-D CHARACTERIZATION

R. SRIVASTAVA AND S.M.BHANDARI

Indian Centre for Climate and Societal Impacts Research, Navrangpura, Ahmedabad
E mail: rohit.srivastava@iccsir.org

Keywords: MODIS, DUST STORM

INTRODUCTION

Dust storms are a catastrophic atmospheric phenomenon in which strong, violent winds pick up fine dust aerosol and silt from the ground, and transport these vertically up a few kms and horizontally to large distances and over large areas, making the air hazy and restricting the horizontal visibility to less than a km. The formation and evolution of dust storms are controlled by special climatic and surface conditions. Mineral dust in the atmosphere has terrestrial sources and represents an important process of land-atmosphere interaction. Dust also has an impact on the nutrient dynamics and biogeochemical cycling of ecosystems; and it has a major influence on soil characteristics, oceanic productivity, and air chemistry. Aerosols, including dust, are an active participants of the Earth's climate system and influence climate through their direct radiative effects of scattering and absorption of incoming solar radiation, and through indirect radiative effects via their influence on clouds microphysics (IPCC, 2007). In the present study, the four-dimensional (4-D) (horizontal, vertical and temporal) characterization of optical and radiative properties of aerosol over western Indian region during an intence dust storm that occurred during March 2012 are presented and discussed.

DATA ANALYSIS

The MODerate resolution Imaging Spectroradiometer (MODIS) sensor on board Terra and Aqua satellites, operating at an altitude of 705 km, measures reflected solar radiance and terrestrial emission in 36 channels in the wavelength range of 0.41 - 14.4 μm with horizontal resolutions varying between 0.25 and 1 km (Remer, *et al.*, 2008). The retrieval algorithm of MODIS follows a lookup table approach. In this approach, a small set of aerosol types, loadings and geometry are assumed to span the range of global aerosol conditions. The algorithm fits the measured spectral reflectance with the lookup table and theoretically retrieves the atmospheric scenario that produced the observed radiation field. MODIS retrieval algorithms have been continuously evaluated against in situ and/or other remote sensing data and periodically updated (Li, *et al.*, 2009; Remer, *et al.*, 2008). The retrieval uncertainty of MODIS derived AOD was found to be ±(0.05 + 0.15AOD) over land and ±(0.03 ± 0.05AOD) over ocean (Li, *et al.*, 2009; Remer, *et al.*, 2008). Level 2 MODIS Collection V005 daily 0.55 μm aerosol optical depth (AOD) at a horizontal resolution of 10 km X 10 km from Terra and Aqua are utilized in this study.

Monthly mean single scattering albedo (SSA) at 0.50 μm is obtained from Ozone Monitoring Instrument (OMI). OMI is a high resolution spectrograph which measures the top of the atmosphere upwelling radiance in ultraviolet and visible regions (0.27 - 0.50 μm) of solar spectrum. OMI Level 3 data at a latitude - longitude resolution of 1^0 X 1^0 are used in the present study. OMI AOD and SSA were validated with AERosol RObotic NETwork (AERONET) sunphotometer over several locations in Asia, Africa and South America (Torres et al., 2007). SSA obtained from AERONET

and OMI for carbonaceous aerosols was found to agree well resulting in a root mean square (RMS) difference of 0.03, while for desert dust aerosols the comparison yielded an RMS difference of 0.02 (Torres, *et al.*, 2007). SSA obtained at 0.388 μm is used to obtain SSA at 0.354 and 0.50 μm based on OMAERUV algorithm (Torres, *et al.*, 2007). However, this can increase the dependence of the algorithm on the assumed aerosol model which can lead to an uncertainty in the SSA at 0.50 μm.

Aerosol extinction vertical profiles are obtained from CALIPSO (Cloud-Aerosol Lidar and Infrared Pathfinder Satellite Observations) lidar measurements and used in this study. Cloud-Aerosol Lidar with Orthogonal Polarization (CALIOP) on board CALIPSO has been providing information on the vertical distribution of aerosols and clouds as well as on their optical properties on a global scale since June 2006 (Winker, *et al.*, 2007). In the present study, level 2 aerosol extinction profile data for 0.532 ì m available at a horizontal resolution of 5 km are obtained over the study region. The measurement uncertainty in CALIPSO derived aerosol extinction products are reported to be about 40% (http://wdc.dlr.de/sensors/calipso/).

RESULTS AND DISCUSSIONS

A super dust storm was observed over the Arabian peninsula on 19 March, 2012 and huge amount of dust was seen in different satellite observations. Fig. 1 shows MODIS Aqua image during the dust storm and the transport of dust aerosol within a day over western Indian region through the Arabian Sea. Mid-visible (0.55 μm) aerosol optical depth before the storm was 0.2 ± 0.08 and enhanced to 1.5 ± 0.9 after dust storm which is > 5 times higher over western India ($21^0 – 26^0$N and $69^0 – 74^0$E). The Ångström exponent was found to decrease from 0.62 to 0.54, which shows the dominance of super micron particles over the western Indian region. Similar changes were also observed during earlier dust storms.

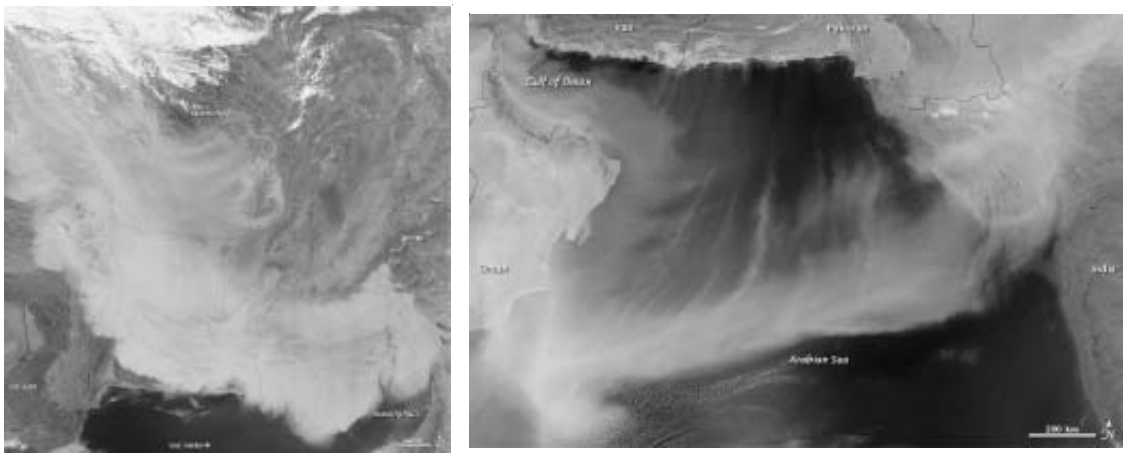

Figure 1. MODIS Aqua image on (a) 19 March, 2012 showing occurrence of dust storm in Arabian peninsula, (b) 20 March, 2012 showing transport of dust over western Indian region via the Arabian sea.

For example, an increase in AOD by greater than 50% and decrease in the Ångström exponent by 70–90% were observed after dust events over aerosol robotic network station Kanpur in Indo-Gangetic plain during May (Dey, *et al.*, 2004). Absorption aerosol optical depth (AAOD) at 0.5 μm from OMI shows higher values, while single scattering albedo exhibit the lower values after dust storm when compared to those during normal day.

The large increase in AOD and absorption during dust storm can be attributed to higher a positive atmospheric radiative forcing and can result in a higher heating. Enhancement in aerosol extinctions at the altitude of 1 - 2 km are observed in the vertical profile of aerosol obtained form CALIPSO (Fig. 2). The increase in aerosol extinction at higher altitude gives rise to enhancement in radiative heating rate (Srivastava and Ramachandran, 2012). The 4-D characterization of dust storm is very crucial while parameterizing the climate impacts of aerosols. The detailed results obtained on the characterization of aerosol optical and radiative properties during dust storm will be presented and discussed.

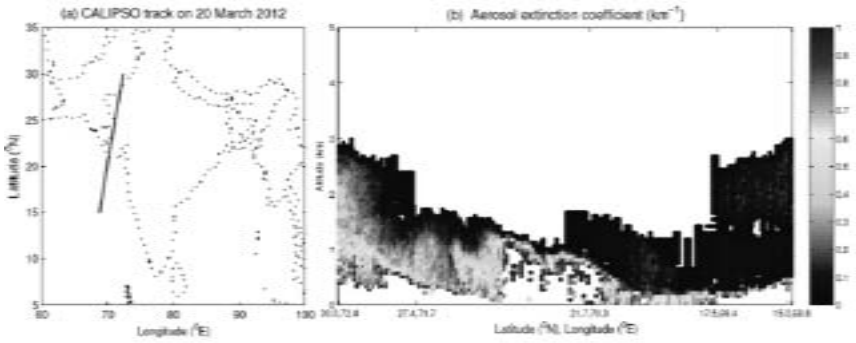

Figure 2. (a) CALIPSO pass over the western Indian region on 20 March, 2012 (b) Aerosol extinction coefficient (km^{-1}) along the CALIPSO pass.

ACKNOWLEDGEMENTS

MODIS images and AOD, AAOD, and SSA were downloaded from the GESDISC, NASA. CALIPSO data were obtained from the NASA Langley Research Center Atmospheric Science Data Center.

REFERENCES

Dey, S., Tripathi, S. N., Singh, R. P., and Holben, B. N. (2004). Influence of dust storms on the aerosol optical properties over the Indo-Gangetic basin, *J. Geophys. Res.*, **109**, D20211.

Intergovernmental Panel on Climate Change (IPCC) (2007). Summary for policymakers, in Climate Change 2007: The Physical Science Basis. Contribution of Working Group I to the Fourth Assessment Report of the Intergovernmental Panel on Climate Change, edited by S. Solomon *et al.*, Cambridge Univ. Press, New York, pp. 129-234,

Li, *et al.* (2009). Uncertainties in satellite remote sensing of aerosols and impact on monitoring its long-term trend: a review and perspective, *Ann. Geophys.*, **27**, pp. 2755—2770.

Remer, L. A., et al. (2008). Global aerosol climatology from MODIS satellite sensors, *J. Geophys. Res.*, **113**.

Srivastava, R, Ramachandran, S. (2012). The mixing state of aerosols over the Indo-Gangetic Plain and its impact on radiative forcing, *Q. J. R. Meteorol. Soc.*, doi:10.1002/qj.1958.

Torres, O., *et al.* (2007), Aerosols and surface UV products from Ozone Monitoring Instrument observations: An overview, *J. Geophys. Res.*, **112**.

Winker, D. M., Hunt, W. H. , McGill, M. J. (2007). Initial performance assessment of CALIOP, *Geophys. Res. Lett.*, **34**.

RADIATIVE FORCING DUE TO ELEVATED AEROSOL LAYER: EFFECT OF CLOUD REFLECTION

KISHORE REDDY[a*], Y. NAZEER AHAMMED[a] AND D.V.PHANI KUMAR[b]

[a]Dept of Physics, Yogi Vemana University, Kadapa – 516003
[b]Aryabhatta Research Institute of observational sciencES (ARIES), Nainital - 263129
E-mail: ikrphy2005@gmail.com

Key words: AEROSOL PROPERTIES, ELEVATED AEROSOL LAYER, RADIATION BUDGET.

INTRODUCTION

Atmospheric aerosols are very important in the global climate system as they modify global radiation budget: directly, by scattering and absorption of solar radiation coming to the earth surface; indirectly, by modifying the cloud micro physical properties such as albedo, precipitation and life time (Ackerman, *et al.,* 2000; Kim and Ramanathan, 2008). Due to the diverse aerosol type, short residence time and lack of information on vertical profiles of aerosols the direct and indirect effect of aerosol radiative forcing still remains a significant uncertainty for climate studies. During the measurement period it has been observed in many instants that the elevated aerosol layer present above and below the low level clouds. In the present paper it has been quantified the effect of cloud reflection in estimating the aerosol radiative forcing over the measurement site. In the clear sky conditions vertical profiles of aerosol is insensitive to the atmospheric radiative forcing (Podgorny, *et al.* 2001). But vertical profiles are very important as this distribution critically modifies the thermal structure and hence its stability with effect on cloud formation process (Satheesh, *et al.* 2008). Apart from this we need to have information of elevated aerosol layer as they can significantly reduce the incoming solar radiation lead changes in local boundary layer characteristics such as mixed later height and if these layers are present over the oceans leads changes in hydrological cycle. The current study is on observation of elevated aerosol layer and its contribution in radiative forcing calculations. The formation of the elevated aerosol layers in the atmosphere has great impact in radiative forcing as they potentially reduce the incoming solar radiation.

The elevated aerosol layers are found in northern India especially in Himalayan regions due to convective lifting of aerosols at distant sources and subsequent horizontal long range transport (Srivastava, *et al*. 2010, Kishore, *et al*. 2011). At the present measurement site (Manora Peak) we observed these elevated aerosol layers in all months (Hegde, *et al*. 2009). Further, Hegde, *et al*. 2009 have discussed in detailed about the seasonal variation of height, thickness and origin of this elevated aerosol layers over the Manora Peak. Srivastava, *et al*. 2010 and Kishore, *et al*. 2011 have also studied the effect of this elevated aerosol layers in the estimation of aerosol radiative forcing. Aerosol optical, physical and chemical properties are not the only determinants of aerosol radiative effects, but the altitude of the aerosol layer and the altitude and type of clouds are also important (Satheesh, et al., 2002). In the present study, we examine the role of altitude variation of reflecting cloud along with the elevated aerosol layers in changing the radiation budget.

METHOD

A portable Micro Pulse LIDAR (MPL) in a temperature and humidity controlled environment is used to study the vertical profile of aerosols at ARIES, Nainital. CIMEL sun-photometer attached

with AERONET has been used to obtain the AODs over the site. Other optical properties of aerosols and clouds have been estimated using OPAC model and all these input parameters have been incorporated in SBDART radiative transfer model to derive the radiation flux data. In the present paper we have studied radiative forcing in two extreme cases 1) aerosol layer is below the cloud layer and 2) aerosol layer is below the cloud layer.

RESULTS

Vertical profiles of aerosol measured using Micro Pulse LIDAR over the Manora Peak have been analyzed for the month of October, 2008. Fig. 1, shows the averaged vertical aerosol extinction coefficient profile derived from the LIDAR system during October, 2008.

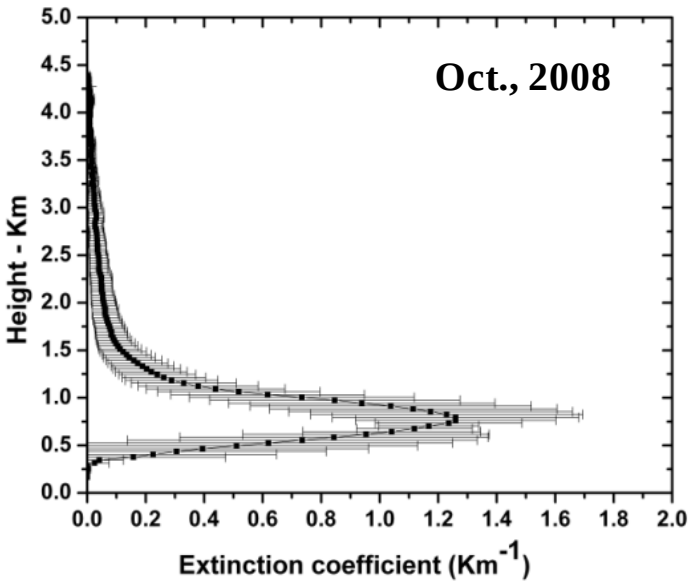

Figure 1. Monthly average vertical profile of aerosol extinction coefficient.

The extinction profile showed no variation from surface to near ~ 0.30 km. Extinction then increased with altitude with a mean extinction coefficient of about ~ 1.26 km^{-1} at ~ 0.80 km and finally showing continuous decrease until reaching the top of aerosol layer which is near ~ 3 to 4 Km altitude. This type of elevated aerosol layers can be attributed due to dry convective lifting of pollutants at distant sources and subsequent horizontal upper air long rang transport of aerosols. These types of aerosol layers are found very frequently over Manora Peak where as no such aerosol layer are observed over low altitude location such as Gadanki (Kishore, *et al.* 2011).

Aerosol optical properties derived from OPAC were incorporated in SBDART model (Ricchiazzi, *et al.,* 1998) to derive net fluxes in the spectral range 0.3 to 4.0 μm at surface and at top of the atmosphere. Tropical model atmospheric profiles of temperature, humidity and vegetation surface type reflectance were used in radiative transfer model. The radiative flux values obtained by using SBDART model for with and without aerosol cases have been used to estimate diurnally averaged aerosol radiative forcing at surface and top of the atmosphere.

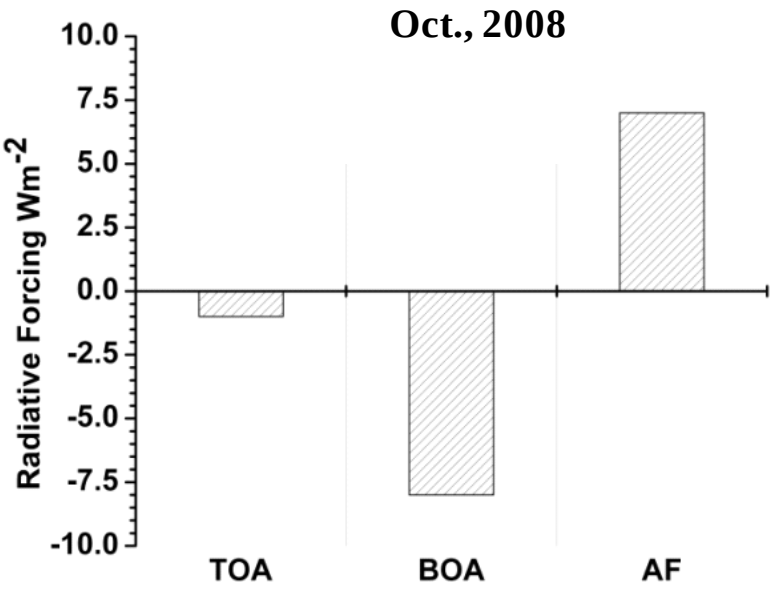

Figure 2. Radiative forcing due to aerosols.

We found that at the surface radiative forcing due to aerosol is ~ -8Wm^{-2} and radiative forcing at the top of the atmosphere is ~ -1 Wm^{-2} as shown in Fig. 2. Subsequently atmospheric radiative forcing due to aerosol over Manora Peak is +7 Wm^{-2}. This is the amount of radiation trapped in the aerosol layer leads the heating.

In many instants the aerosol layer is observed above and below low level clouds. To see the effect of cloud reflection in aerosol radiative forcing we will incorporate optical properties of cloud in to the vertical profiles of aerosol in two extreme conditions (Satheesh, *et al.*, 2002). In the first case the aerosol layer is below the cloud and in the second case aerosol layer above the cloud.

In the first case we assumed a status continental optically thin low level cloud which has optical depth of 3.5 and SSA 1.0 at 0.50 μm lies above the aerosol layer. It is also assumed that the thickness of the cloud layer is about 0.2 km and present at 2.5 km altitude. In the second case, we assumed an elevated aerosols layer, which lies above a thin layer of cloud. Again we assumed the properties of cloud and aerosol layer are same as in the first case. The cloud layer is below the aerosol layer at an altitude of 0.2 km.

CONCLUSIONS

Vertical profiles of aerosols are very important along with the properties of aerosols in order to estimate aerosol radiative forcing. When there are elevated aerosol layer in the atmosphere, the height of aerosol layer, and albedo of surface (ground reflectivity) are very important. The observed radiative forcing in the atmosphere over Manora Peak is about +7 Wm^{-2} due to aerosol layer.

If there are clouds in the atmosphere the height of cloud layer (either cloud is above the aerosol layer or below the layer) and type of cloud and microphysical properties of clouds are also important in order to estimate atmospheric radiation budget. If the cloud is above the aerosol layer most of the radiation will reflected back form cloud (depends on albedo), the available radiation to interact with

the aerosol layer is less implies less radiation budget in the atmosphere and if the cloud is below the aerosol layer, incoming radiation will interact with aerosol layer and after passing through the aerosol layer it gets reflected by cloud and reflected radiation will again interacts with aerosol layer in this case the radiation budget in the atmosphere is higher than the above case.

ACKNOWLEDGEMENTS

This work was carried out as a part of the ARFI and ABLN&C project under Indian Space Research Organization - Geosphere Biosphere Program. One of the authors is grateful to CSIR for awarding research fellowship. The authors are also thankful to the Director ARIES, Manora Peak, Nainital for their constant encouragement to undertake this work.

REFERENCES

Ackerman, A. S., Toon, O. B., Stevens, D. E., Heymsfield, A.J., Ramanathan, V., and Welton, E.J. (2000). Reduction of tropical cloudiness by soot, *Science,* **288** (5468), pp.1042-1047.

Hegde, P., Pant, P., Bhavani kumar, Y. (2009). An integrated analysis of lidar observations in association with optical properties of aerosols from a high altitude location in central Himalayas, *Atmospheric Science Letters,* **10,** pp. 48-57.

Kim, D., and Ramanthan, V. (2008). Solar radiation budget and radiative forcing due to aerosols and clouds, *J. Geophys Res.,* **113**, D02203.

Kishore, Reddy., Pant, P., Phani Kumar, D. V., Dumka, U. C., Bhavani kumar, Y., Singh, N., and Joshi, H. (2011). Radiative effects of elevated layer in Central Himalays, *International Journal of Remote Sensing*, **32**, pp. 9721-9734.

Pondgorny, I. A., and Ramanathan, V. (2001). A modeling study of the direct effect of aerosols over the tropical Indian Ocean, *Geophys. Res. Lett.*, **106**:D20, pp. 24,097-24,105.

Ricchiazzi, P., Yang, S., Gautier, C., and Sowle, D. (1998). SBDART: A research and teaching software tool for plane-parallel radiative transfer in the Earth's atmosphere, *Bull. Am. Meteorol. Soc.*, **79**, pp. 2101–2114.

Satheesh, S. K. (2002). Aerosol radiative forcing over land: effect of surface and cloud reflection, *Annales Geophysicae.,* **20**, pp. 2105-2109.

Satheesh, S. K., Moorthy, K. K., Babu, S. S., Vinoj, V., and Dutt, C.B.S. (2008). Climate implications of large warming by elevated aerosol over India. *Geophys. Res. Lett.,* **35**, L19809.

Srivastava, *et al.* (2010). Influence of south Asian dust storm on aerosol radiative forcing at high-altitude station in central Himalayas, *International Journal of Remote Sensing*, **32**, pp. 7827-7845.

AEROSOL OPTICAL PROPERTIES DERIVED FROM CHEMICAL COMPOSITION MEASURED AT MAHABUBNAGAR DURING CAIPEEX-IGOC: IMPLICATIONS TO THE DIRECT RADIATIVE FORCING

A. K. SRIVASTAVA[1], D. S. BISHT[1], S. TIWARI[1], K. K. DANI[2] and G. PANDITHURAI[2]

[1]Indian Institute of Tropical Meteorology (Branch), Prof Ramnath Vij Marg, New Delhi, India
[2]Indian Institute of Tropical Meteorology, Dr Homi Bhabha Road, Pashan, Pune, India
E mail: atul@tropmet.res.in

Keywords: AEROSOLS, CAIPEEX-IGOC, OPAC, OPTICAL PROPERTIES, RADIATIVE FORCING.

INTRODUCTION

Radiative forcing due to atmospheric aerosols is one of the largest sources of uncertainties in estimating climate perturbations due to large spatial variability of aerosols and the lack of an adequate database on their radiative properties (IPCC, 2007). Aerosol exerts direct radiative effects (DRE) through scattering and absorption of sunlight, but the magnitude and variability of its effect depends on the relative proportion of its anthropogenic and natural components, as they have distinct characteristics and size distributions (Kaufman, *et al.*, 2005). Although, there are numerous studies on the estimations of total aerosol DREs based on measured or modeled aerosol properties, these studies are sparse based on measured chemical composition of aerosols (Srivastava, *et al.*, 2012).

As a part of National experiment named as Cloud Aerosol Interaction and Precipitation Enhancement Experiment (CAIPEEX), an Integrated Ground Observational Campaign (IGOC) was conducted at Mahabubnagar- a tropical rural station in the southern peninsular India in Andhra Pradesh during the period from July to October 2011 to understand aerosol-cloud-climate interactions. Apart from other aerosol measurements, fine- ($PM_{2.5}$) and coarse- (PM_{10}) mode aerosol samples were collected through medium volume sampler on a filter based technique. These sampled filters were aimed to understand the mass loading of $PM_{2.5}$ and PM_{10} aerosol particles and for their chemical and carbonaceous aerosol analysis, which will be presented, in detailed, during the conference as a separate paper. However, in the present paper, the measured chemical compositions along with carbonaceous aerosols were used to understand detailed optical and radiative characteristics of aerosols over the station.

DATA AND METHODOLOGY

Aerosol samples were collected at a rural station at Mahabubnagar using a single stage aerosol sampler (Model: APM 550 from Envirotech Pvt. Ltd., India), with suitable impactors for PM_{10} and $PM_{2.5}$ during July to October 2011. These samples were analyzed for ionic species (mainly water-soluble) by Ion chromatograph and for carbonaceous aerosols such as elemental and organic carbon (EC and OC) with OC-EC analyzer. Daily variations in the measured mass concentrations of water-soluble and EC in $PM_{2.5}$ and PM_{10} aerosol samples are shown in Fig. 1a and 1b, respectively. A gradual increase in the magnitude of both the species from July to October indicates the monsoon effect (decreases with increasing month). As expected, the magnitude of water-soluble and EC was found to be relatively highly in PM_{10} as compared to $PM_{2.5}$.

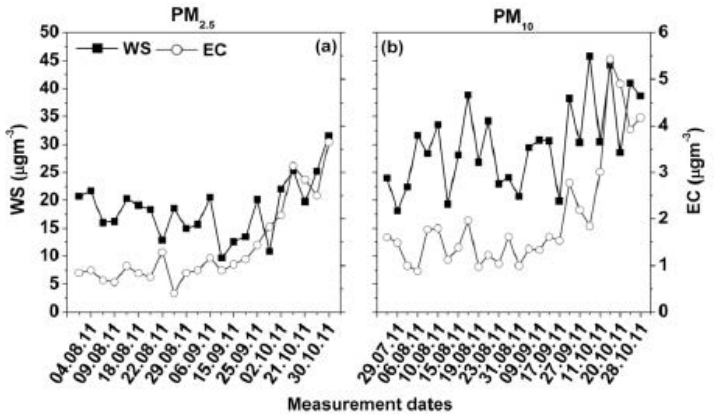

Figure 1. Daily variation of water-soluble (WS) and elemental carbon (EC) measured at Mahabubnagar in (a) $PM_{2.5}$ and (b) PM_{10} during the campaign period from July to October 2011.

To understand the possible implication of aerosols to the direct radiative forcing (DRF), the measured chemical composition of aerosols, as shown in Figure 1, along with the ambient meteorological condition of the station were used in an aerosol optical model to obtain crucial optical properties of aerosols (e.g. aerosol optical depth, single scattering albedo, asymmetric parameter etc). The model derived these optical parameters were verified with the available direct measured optical parameters and thus modeled aerosol data sets are assumed to be the representative of composite aerosols over the station.

The derived aerosol optical parameters were then used in a radiative transfer model along with the suitable surface albedo values for the station to estimate aerosol DRF at the top of the atmosphere and surface. The resultant atmospheric forcing was estimated with the difference between the TOA and surface forcing values. Further, atmospheric heating rates were also estimated over the station using resultant atmospheric forcing values.

ACKNOWLEDGEMENTS

The authors would like to thank Prof. B. N. Goswami, Director, IITM for his encouragement and support for conducting IGOC campaign under the CAIPEEX. Thanks are also owed to the others, participated and helped in collecting aerosol samples during the campaign.

REFERENCES

Intergovernmental Panel on Climate Change (IPCC) (2007). Climate Change 2007: The Physical Science Basis: Contribution of Working Group I to the Fourth Assessment Report of the Intergovernmental Panel on Climate Change, Chapter 2, 129.

Kaufman, *et al.*, (2005). Aerosol anthropogenic component estimated from satellite data, *Geophysical Research Letters* , **32**, L17804.

Srivastava, A. K., Singh, S., Tiwari, S. and Bisht, D. S. (2012). Contribution of anthropogenic aerosols in direct radiative forcing and atmospheric heating rate over Delhi in the Indo-Gangetic Basin, *Environmental Science and Pollution Research*, **19**, pp. 1144-1158.

LONG TERM STUDIES ON BLACK CARBON AEROSOLS OVER A TROPICAL URBAN STATION PUNE, INDIA

P.D.SAFAI, M.P. RAJU, P.S.P.RAO AND P.C.S. DEVARA.

Indian Institute of Tropical Meteorology, Pune (India)
E mail: pdsafai@tropmet.res.in

Keywords: BLACK CARBON AEROSOLS, TEMPORAL VARIATIONS

INTRODUCTION

Black Carbon (BC) aerosols are the product of different type of incomplete combustion processes. They are the strong absorbers of solar radiation with specific absorption cross section of 10 g/m^2. BC aerosols cause direct radiative forcing ranging from + 0.27 to + 0.54W/m^2 (IPCC, 2007). Various studies from different locations in India have reported surface BC levels. However, studies on long term trends in BC aerosols over any location are very scarce. For the formation of Climatology of BC aerosols over India, there is a need to obtain continuous observations for a longer period of time from different locations over the country. This paper describes the temporal variations of BC mass concentrations measured at Pune, an urban location in south western India during a period of 7 years i.e. 2005–2011. Also, the correlation between BC with fine and coarse particles as well as with anthropogenic aerosol components like non sea salt SO_4, NO_3, non sea salt K are discussed.

DETAILS ON SAMPLING LOCATION, METEOROLOGY AND INSTRUMENTATION

Pune ($18^0$32'N, $73^0$51'E, 559 m mean sea level altitude) is one of the rapidly growing cities in India in terms of industrial installations as well as vehicular population and urbanization. It is about 100 km inland on the west coast of India, on the leeward side of Western Ghats. Sampling was carried out on the terrace of the Indian Institute of Tropical Meteorology (IITM) building at about 12m above the ground at Pashan which is located about 10 km from the centre of Pune city. Continuous observations on BC aerosols were carried out by using an Aethalometer (Magee Sci., Inc., USA, Model AE-42) at 3 LPM flow rate and 5 minute interval. In order to account for Loading effect during filter tape advancement, correction algorithm employed Park et al. (2010) was used.

RESULTS AND DISCUSSION

TEMPORAL VARIATIONS OF BC OVER PUNE

Fig.1 indicates the mean monthly variation of BC for 7-year period. The monthly variation for BC showed similar trend in all these years with minimum concentrations observed during monsoon season and maximum during winter. The overall mean BC concentration at Pune was 3.55 ± 2.34 μg / m^3 over the 7 year period. Fig. 2 shows the season wise percentage variation of BC concentration from the annual mean. During summer season (March to May), mean BC concentration (2.66 ± 0.53 μg / m^3) was about 22 % less than the annual mean BC concentration. Similarly during monsoon season (June to September) mean BC concentration was lowest (1.28 ± 0.31μg / m^3) and was about 64 % less than the annual mean BC concentration. However, both post-monsoon (October and November, 5.08 ± 1.29 μg / m^3) and winter (December to February, 6.71 ± 1.31 μg / m^3) showed about 39 % and 78 % more BC concentrations respectively than the mean annual BC

concentration. This type of seasonal variation is attributed mainly to the prevailing local boundary layer conditions as well as certain man-made activities carried out in particular period of time (Dutkiewicz *et al.*, 2009; Latha and Badrinath, 2005). Fig. 3 shows the mean hourly variation of BC for the 7 yr period. There was a significant morning peak at about 0900 hrs whereas lowest concentrations were found during 14-16 hrs in the afternoon followed by another minor peak during late evening (20-23 hrs). The hourly variation of BC is linked with that of local boundary layer and vehicular density.

BC, TSP AND SIZE SEPARATED AEROSOLS

Total suspended particulates (TSP) were collected weekly/fortnightly at the same location, using high-volume air sampler on Whatman 41 filter papers. These samples were collected during all the months and the sampling period for each sample was about 8 h at the mean flow rate of 1 m^3/min. Heitzenberg, (1989) have reported about 5 % and 9 % of EC (elemental carbon synonymous to BC) to fine particle composition for non-urban continental and urban continental regions, respectively. Fig. 4 shows the mass fraction of BC to TSP during different months. It can be seen that mean annual mass fraction of BC to TSP was 2.9 %. However, during winter, it was maximum (5.6%) and during monsoon it was minimum (1.3%). Tripathi, *et al.* (2005) reported 7–15% of BC to total aerosol mass for Kanpur during December 2004.

The mean monthly BC concentrations were related with those of size separated particulate matter (PM) such as PM_{10}, $PM_{2.5}$ and $PM_{1.0}$. Data on PM was obtained from an aerosol spectrometer (GRIMM, Model 1.108). The carbonaceous component of fine PM is important because of its role in visibility reduction and radiative budget of the atmosphere (Malm and Day, 2000), their potential to influence many heterogeneous reactions involving atmospheric aerosols and trace gases (Lary, *et al.*, 1999), and the suspected health effects (Neuberger et al, 2004). On an annual basis, BC showed a good correlation with $PM_{1.0}$ i.e. fine particles ($r = 0.90$, $p < 0.0001$) whereas, it showed comparatively less good correlation with $PM_{10\text{-}1}$ i.e. coarse particles ($r = 0.35$, $p = 0.12$). However, as observed for TSP, there was significantly good correlation ($r = 0.81$, $p = 0.05$) between BC and coarse particles during monsoon and post-monsoon (June to Nov) and a very weak correlation ($r = 0.14$, $p = 0.80$) during winter and summer (Dec to May). The diurnal variation of BC and $PM_{1.0}$ was also similar (Fig. 5) indicating similar sources and formation mechanisms for them. Similar results have been reported by Baxla et al (2009). A comprehensive report on studies on PM in Europe (Putaud, *et al.*, 2002) has reported that BC contributes 5–10% to PM2.5 and somewhat less to PM10 at all the measurement sites, including the natural background sites however, its contribution increases to 15–20% at some of the kerbside sites. This implies that the BC particles occurred mainly in less than 1μm size. Therefore, the increased concentrations of BC during post-monsoon and winter (Oct to Feb) seasons at Pune are hazardous for the human health especially to the population suffering from respiratory and skin diseases. The most important thing is that the concentrations of fine particles like BC are more during morning and evening hours when the exposure of people to outdoor air is also more that is hazardous for human health.

BC AND OTHER CHEMICAL CONSTITUENTS OF AEROSOLS

Mean concentrations of chemical constituents of TSP collected over Pune during 2004-2009 were compared with the BC measurements carried out during the same period. BC showed a significant correlation with Nss SO_4 ($r = 0.84$, $p = 0.0006$), NO_3($r = 0.89$, $p = 0.001$), NH_4($r = 0.94$, $p < 0.0001$) and Nss K ($r = 0.91$, $p < 0.0001$). Also, it was correlated with Nss Ca ($r = 0.76$, $p = 0.004$) and Fe

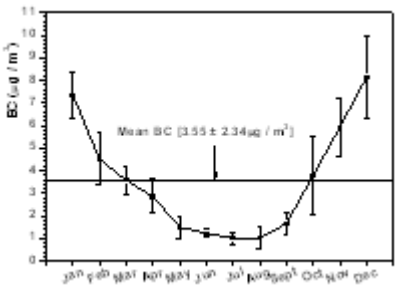

Figure 1. Mean monthly variation of BC during 2005-11 at Pune.

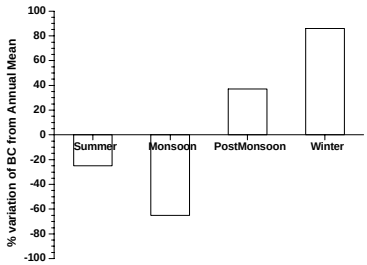

Figure 2. Month wise percentage variation of BC concentration from the annual mean

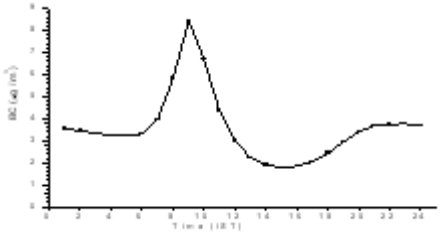

Figure 3. Mean annual hourly variation of BC at Pune.

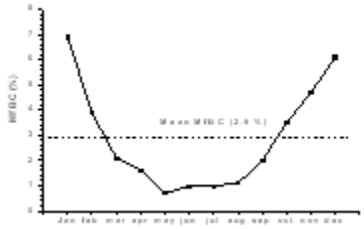

Figure 4. Mass fraction of BC to TSP during different months

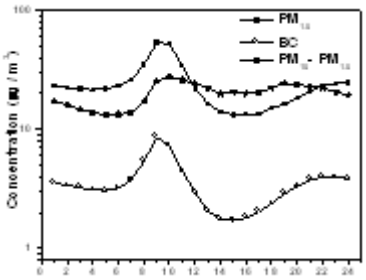

Figure 5. Diurnal variation of BC and $PM_{1.0}$ and $PM_{10-2.5}$ particles over Pune.

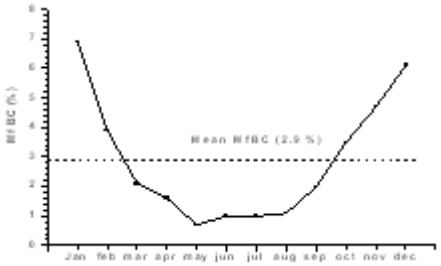

Figure 6. Variation of mean BC concentration with respect to aerosol components.

(r = 0.72, p = 0.009). The very good correlation of BC with Nss SO_4, NO_3, NH_4, NssK is not surprising as all of them are predominantly originated from combustion (fossil fuel or bio-mass burning) activities. A good correlation between Nss K and BC have been reported to be an indication of biomass burning source for both (Andreae, *et al*., 1998; Mao, *et al.*, 2011). The ratio of Nss K to BC is suggested to signify the nature of BC, whether it is from biomass burning or from fossil fuel burning. This ratio for different bio fuels has been quantified i.e. 0.21 ± 0.06 for wood fuels and 0.88 for herbaceous fuels (Hadley, 2008). At Pune, this ratio was found to be 0.032, 0.056 and 0.058 during October, December and February months whereas in May this ratio was < 0.01. This indicates some contribution of bio-fuel sources during post-monsoon and winter seasons but no contribution from these sources during summer and monsoon.

The mixing state of BC i.e. its combination with other chemical components is very crucial to decide its existence in atmosphere and also its role in radiative properties of aerosols (Bond, *et al.*, 2006). Freshly emitted BC is hydrophobic but as it ages and when it comes in contact with sulphate, organic carbon (OC), sea-salt; it becomes hydrophilic and can further act as condensation nuclei and get scavenged through precipitation. BC aerosols have been reported to play an important role in the formation of SO_4 by acting as a catalyst and thus enhancing the oxidation of SO_2 to SO_4. Also, it is reported that there is an enhancement in the HNO_3 formation rate in the presence of soot or BC aerosols (Chang, *et al.*, 1982; Disselkamp, *et al.* 2000). Therefore, BC is supposed to play an important role in the acidity of aerosols.

ACKNOWLEDGEMENTS

Authors are thankful to the Dr. B. N. Goswami, Director, Indian Institute of Tropical Meteorology, Pune for encouragement to undertake this work. Thanks are also due to the ISRO-GBP, Department of Space, Government of India for providing financial support to carry out these observations.

REFERENCES

Andreae, M.O., Andreae, T.W., Annegarn, H., Beer, J., Cachier, H., Canut, P.le., Elbert, W., Maenhaut, W., Salma, I., Wienhold, F.G., Zenke, T. (1998). Airborne studies of aerosol emissions from savanna fires in southern Africa: 2. Aerosol chemical composition, *J. Geophys. Res.* ,**103**, D24, pp. 32,119-32,128.

Baxla, S.P., Roy, A.A., Tarun Gupta., Tripathi, S.N., Bandyopadhyaya, R. (2009). Analysis of Diurnal and Seasonal Variation of Submicron Outdoor Aerosol Mass and Size Distribution in a Northern Indian City and Its Correlation to Black Carbon, *Aerosol and Air Quality Research* , **9**, pp. 458-469.

Bond, T. C., Habib, G., Bergstrom, R.W. (2006). Limitations in the enhancement of visible light absorption due to mixing state, *J. Geophys. Res.* , **111**, D20211.

Bond, T., Anderson, T., Campbell, D. (1999). Calibration and intercomparison of filter-based measurements of visible light absorption by aerosols, *Aerosol Science and Technology*, **30**, pp. 582–600.

Chang, S.G., Brodzinsky, R., Gundel, L.A., Novakov, T. (1982). Chemical and Catalytic Properties of Elemental Carbon, *Particulate Carbon Atmospheric Life Cycle*, 159-181.

Disselkamp, R.S., Carpenter, M.A., Cowin, J.P. (2000). A chamber investigation of nitric acid – soot aerosol chemistry at 298K, *J. Atmos. Chem.* **37**,pp. 113-123.

Dutkiewicz, V.A., Alvi, S., Ghauri, B.M., Choudhary, M.I., Husain, L. (2009). Black carbon aerosols in urban air in South Asia, *Atmospheric Environment* **43**, pp. 1737-1744.

Hadley, O.L. (2008). Black carbon transport and deposition to the California mountain snow pack, Ph. D. Thesis in Earth Sciences, University of California, San Diego, USA

Heintzenberg, J. (1989). Fine particles in the global troposphere A review, *Tellus* ,**41B**, pp. 149-160.

Lary, D. J., Shallcross, D. E., Toumi, R. (1999). Carbonaceous aerosols and their potential role in atmospheric chemistry, *J. Geophys.Res.,* **104**, pp. 15929–15940.

Latha, M. K., Badarinath, K.V.S., Reddy, M.P. (2005). Scavenging efficiency of rainfall on black carbon aerosols over an urban environment, *Atmospheric Science Letter*, 14801251.

Malm, W.C., Day, D.E. (2000). Optical properties of aerosols at Grand Canyon National Park, *Atmospheric Environment* , **34**, pp. 3373-3391.

Mao, Y.H., Li, Q.B., Zhang, L., Chen, Y., Randerson, J.T., Chen, D., Liou, K.N. (2011). Biomass burning contribution to black carbon in the Western United States Mountain Ranges, *Atmos. Chem. Phys.*, **11**, pp. 11253–11266.

Neuberger, M., Schimek, M., Horak Jr., F., Moshammer, H., Kundi, M., Frischer, T., Gomiscek, B., Puxbaum, H., Hauck, H., AUPHEP-Team. (2004). Acute effects of particulate matter on respiratory diseases, symptoms and functions, Epidemiological results of the Austrian Project on Health Effects of Particulate Matter (AUPHEP), *Atmospheric Environment* , **38**.

Park, S.S., Hansen, A.D.A., Sung.Y.Cho. (2010). Measurement of real time black carbon for investigating spot loading effects of Aethalometer data, *Atmospheric Environment* , **44(11)**, pp. 1449-1455.

Putaud, J.P. et al. (2002). A European Aerosol Phenomenology: physical and chemical characteristics of particulate matter at kerbside, urban, rural and background sites in Europe. Joint Research Centre, Ispry. Italy.

Tripathi, S. N., Day, S., Tare, V., Satheesh, S. K. (2005). Aerosol black carbon radiative forcing at an industrial city in northern India, *Geophysical Research Letters*, **32**.

SPECTRAL BEHAVIOR OF OPTICAL CHARACTERISTICS OF AEROSOLS OVER A COMPLEX MINING REGION

R LATHA[1], B S MURTHY[1], K LIPIKUMARI[2] , S JYOTSNA[2], S MANOJKUMAR[2] AND K PRADEEP[3]

[1]Indian Institute of Tropical Meteorology, Pashan, Pune - 411008, India
[2]Birla Institute of Technology, Dept. of Applied Mathematics, Mesra, Ranchi- 835215, India
[3]Center for Environmental Remote Sensing Chiba University, Chiba, Japan

Keywords: SPECTRAL VARIATION, COMPLEX AEROSOLS, BACK TRAJECTORY AND REFRACTIVE INDEX

INTRODUCTION

Aerosol optical spectral variations are studied over Ranchi in Jharkhand state a varied mining region of India (Fig. 1). Five wavelength viz. 400, 500, 675, 870 and 1020 nm, are used by the POM-1 type PREDE make sky-radiometer to derive the aerosol optical properties using the inversion algorithm "Skyrad-pack version 4.0/5.0" inverting measured sky radiances. Data presented is for the duration February 2011- January 2012. Aerosol optical depth (AOD) decreases with wavelength (Fig. 2) and exhibits maximum independence during monsoon while it is very much wavelength dependant during pre-monsoon period. Post monsoon and winter show the least variability about average AOD at all wavelengths. Being a complex mining region spectral variation of single scattering albedo (SSA) (Fig. 3), real and imaginary parts of refractive index (Fig. 4 & 5) are unique. SSA tends to be minimum (highly absorbing) in winter of all seasons; imaginary part of refractive index that closely connects to the absorption coefficient follows the same spectral behavior of SSA.

Figure 1. Mineral mining map of Jharkhand

However, the reduction of SSA in 870-1020nm wavelength range is anomalously sharp, not reported elsewhere though reports from China (Zheng, *et al.*, 2008) are indicative of this behavior. Influence

of humidity is seen in the real part of refractive index during monsoon to post monsoon as the graphs (Fig. 4) show almost parallel variation and their back trajectory tracks are also similar.

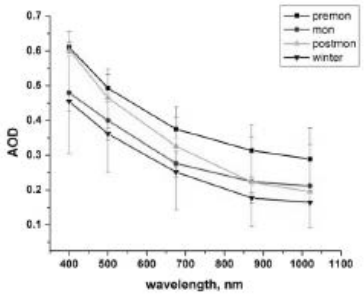

Figure 2. Seasonal spectral variation of AOD: Jan, Feb & Dec constitutes winter season, March – May, Pre-monsoon, June – September, monsoon and October & November Post monsoon

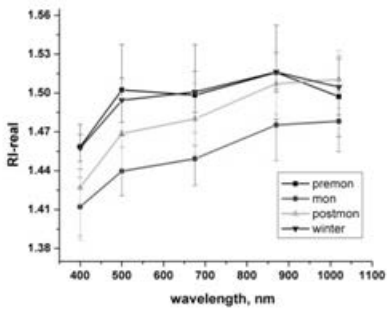

Figure 4. Same as Fig 2 but for RI-real

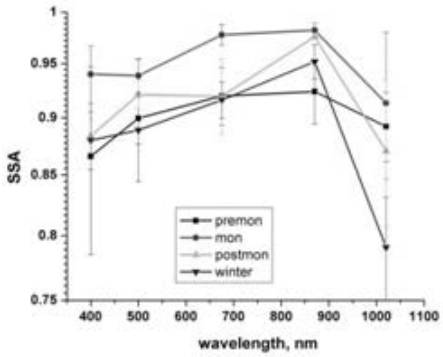

Figure 3. same as Fig 2 but for SSA

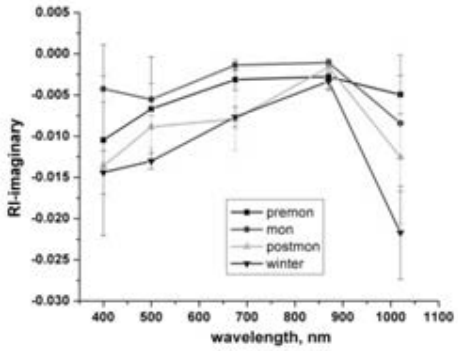

Figure 5. same as Fig 2 but for RI-imaginary

Peak beyond 1000 nm in monsoon (Fig. 6) and fine mode higher peak in post monsoon are expected to be the result of specific nature of particles present then having loaded with plentiful moisture available. Pre-monsoon period increase in dust –raising- wind is the cause behind peaking of coarse mode fraction. The lowest position of volume concentration curve of winter states the lower aerosol loading of the place compared to neighboring IGP stations. It also points to the minimum advection during the season which results in less AOD but increase in the absorbing nature.

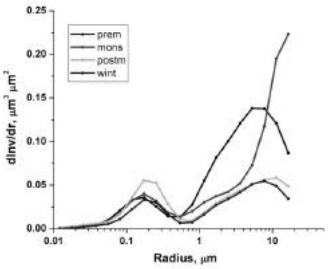

Figure 6. Seasonal volume size distribution

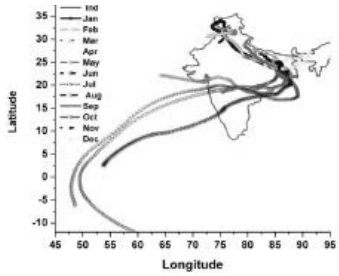

Figure 7. 8 day back trajectories of each month ending by 15th of each month

An attempt is made to investigate the type of aerosol resulting in such variations in spectral behavior. OPAC model (Hess, *et al.*, 1998) along with its data base is used to inspect the nature of aerosol. Considerable amount of BC/OC measurements were also made during this year at the station using AE-31 model Magee Scientific make aethalometer (Manojkumar, *et al.*, 2011) though for some months it is not available or a little is only available. Considering the observed parameter variations and back trajectories of onward wind to the station, (Fig. 7) a single group of OPAC aerosol types are not used altogether but in different combinations for different period. Observed BC was input in terms of number concentration (measured from 5 am to 5 pm) and other aerosol types were varied to closely match both observed AOD as well as SSA for the selected day, possible aerosol selection depending on the trajectory path. The results are shown in Fig. 8.

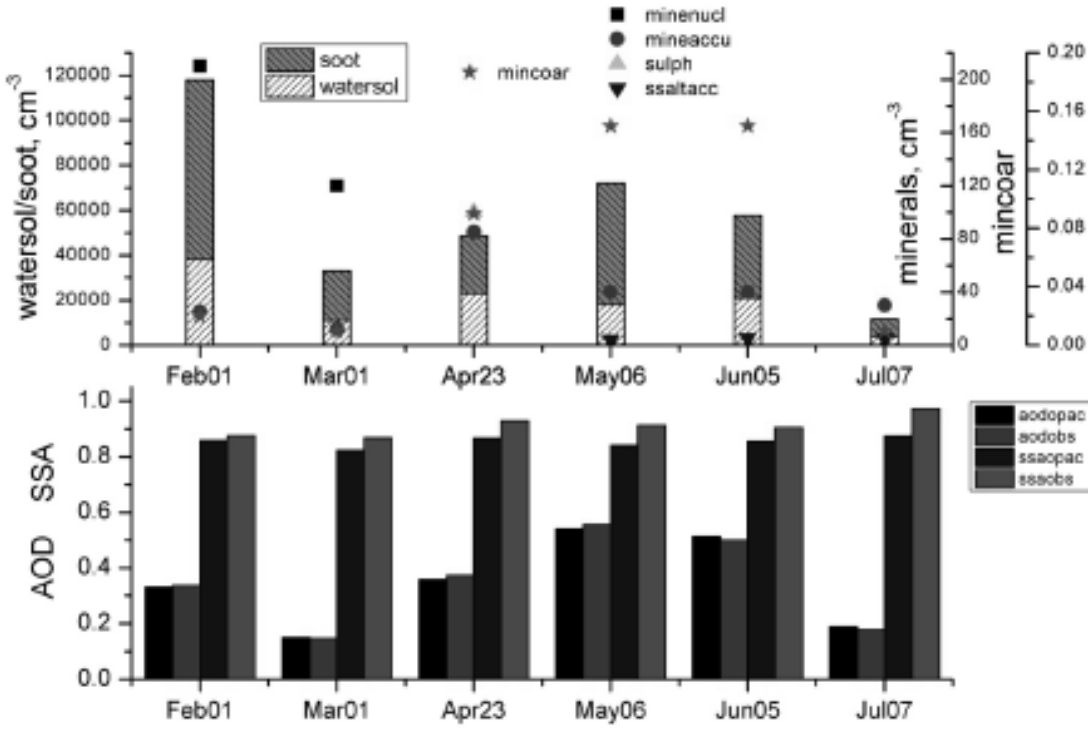

Figure 8. OPAC derived aerosol types constrained by observed BC, AOD and SSA

This shows the temporal variability and complexity of aerosol particles present at the station, however, a chemical analysis is very much necessary to assess the real composition and impact as OPAC enables only very limited options. A meteorological background of the observing station is provided through Fig. 9.

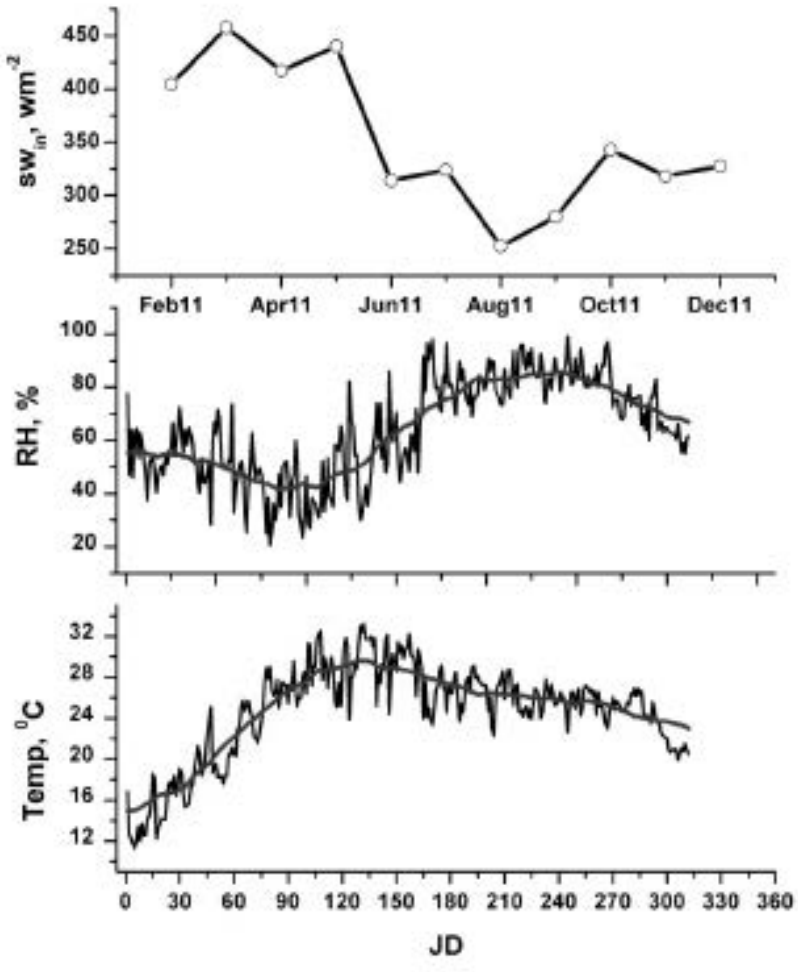

Figure 9. Meteorological background of the station, Ranchi

ACKNOWLEDGEMENT

Sincere efforts of Bodhnath, Technical assistant in collecting the met parameters and other help for procuring data are thankfully acknowledged. Prof. B N Goswami and Prof. N C Mahanthy are sincerely acknowledged as mentors to this effort.

REFERENCES

Hess, M., Koepke, P., Schultz, I. (1998). Optical properties of aerosols and clouds: The software package OPAC, *Bulletin of American Meteorological Society*, **79**, pp. 831–844.

Kumar, Manoj, Kumari, Lipi, Sureshbabu, S.and Mahanti, N. C. (2011). Aerosol properties over Ranchi measured from aethalometer, *Atmos. Climate. Sci.*, **1,** pp. 91-94.

Zheng, Youfei. Liu, Jianjun, Wu, Rongjun, Zhanqing Li, Wang, Biao,and Takamura Tamio. (2008). Seasonal statistical characteristics of aerosol optical properties at a site near a dust region in China, *J. Geophy. Res.*, **113**, D16205.

ON THE OPTICAL PROPERTIES AND RADIATIVE FORCING OF AEROSOLS OVER THE EASTERN END OF MONSOON TROUGH REGION, RANCHI

B S MURTHY[1], R LATHA[1], G PANDITHURAI[1], S JYOTSNA[2], K LIPIKUMARI[2] AND S MANOJ KUMAR[2]

[1]Indian Institute of Tropical Meteorology, Pashan, Pune - 411008, India
[2]Birla Institute of Technology, Dept. of Applied Mathematics, Mesra, Ranchi- 835215, India

Keywords: AEROSOL RADIATIVE FORCING, OPTICAL PROPERTIES, FINE FRACTION, ATMOSPHERIC ABSORPTION

INTRODUCTION

Optical properties of aerosols over Ranchi, eastern end of monsoon trough region highly populated with mines and where wind turns from north west through north and east to south west, are studied and reported for the first time on an annual scale for the year 2011. A 7 wavelength, POM1 type skyradiometer (Prede make) is used to measure sky radiances. Inversion software SKYRAD.PACK version 4.5/5.0 is used to derive optical properties. Radiative forcing is calculated using the widely used SBDART radiative transfer model (Ricchiazzi et al., 1998). A general increase in aerosol optical depth (AOD) is seen from December to June; however lower values are observed compared to the reports of other stations in the IGP plane (Dey, et al, 2004; Nair, et al., 2007; Srivastava, et al., 2012; Tripathi, et al, 2005 etc.) with an annual average of 0.43, lowest in August (0.245) and highest in June (0.56) (Fig. 1). Volume concentration in the fine mode remaining rather unchanged, single scattering albedo (SSA) diminishes indicating increase in absorption fraction peaking in March (Fig. 2). Imaginary part of refractive index is highest in winter season and the real part variation shows the effect of humidity (Fig.1). Angstrom exponent, alpha (400-1020nm) does not show much correlation with AOD but during winter months correlates positively (< 0.5), highest in January and negatively in monsoon months with highest value in August (Fig. 3) which is statistically not significant.

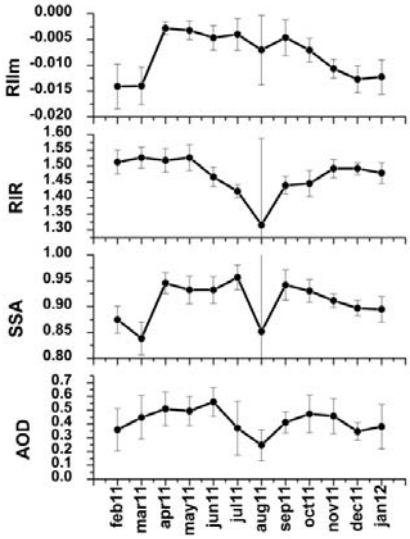

Figure 1. Monthly mean variation of aerosol optical parameters

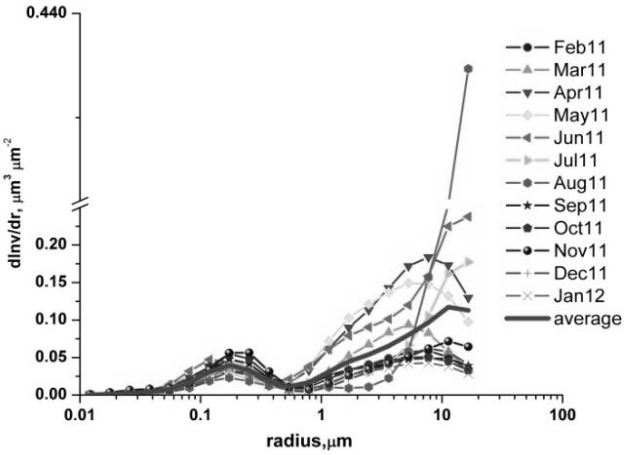

Figure 2. Monthly mean volume size distribution

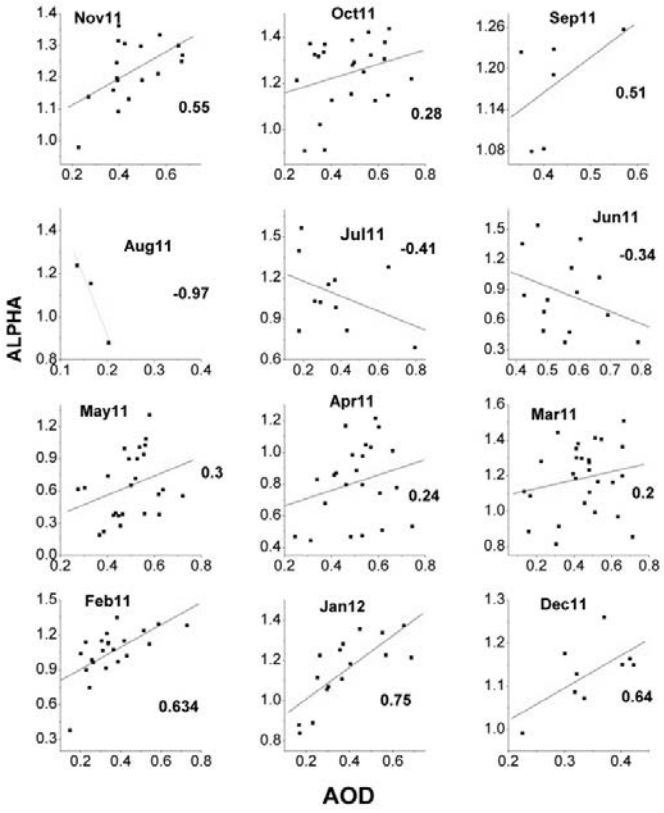

Figure 3. Scatter-plot and correlation coefficient for AOD vs alpha (400-1020 nm).

Surface radiative forcing (ARF_{bot}) is calculated for chosen best two clear sky days per month from February 2011- December 2011 on the basis of the lowest and highest AOD for the month. Typical days for each month are compared with observed radiation and it compares best in May, September,

October and February in that order (Fig. 4). AOD and ARF_{bot} show a good correlation of 0.899. Dissecting this result AOD is fragmented (Srivastava, *et al.*, 2012) into AOD- absorption (AAOD) and AOD-scattering (SAOD) and also to fine fraction (FF: cumulative AOD up to 500 nm) and coarse fraction (CF: AOD from 675-1020 nm); as per the notion that fine fraction contributes maximum to absorption. Though AAOD remains 10% or less than SAOD its contribution to ARF_{bot} is generally equal or more than the scattering part. A trend analysis of AAOD%, FF and available BC/OC (black/organic carbon) concentrations could not fetch any appreciable co-variation (Fig. 5). A linear fit of radiative forcing at the surface, top-of–the atmosphere and atmospheric absorption based on the 21 chosen days indicate that a 0.1 increase in AOD could result in an additional forcing/absorption of -8.52, -2.86 and 5.66 wm^{-2} at Ranchi (Fig. 6).

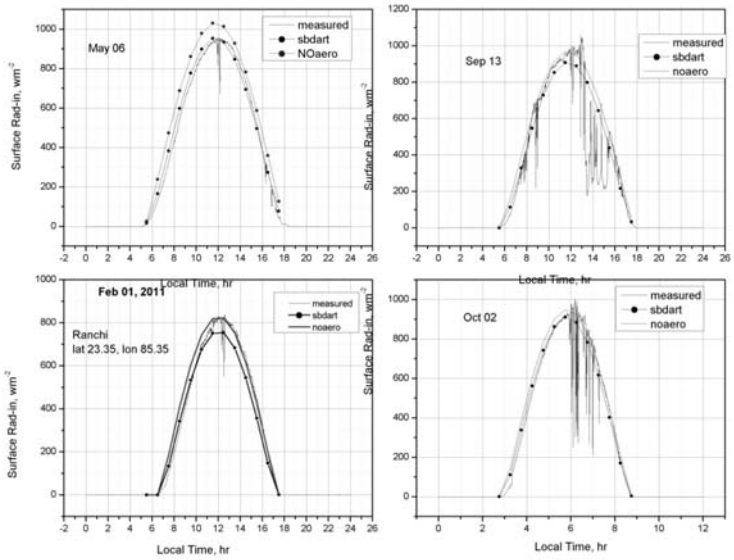

Figure 4. comparison of radiation observed vs SBDART (no aerosol and with aerosol)

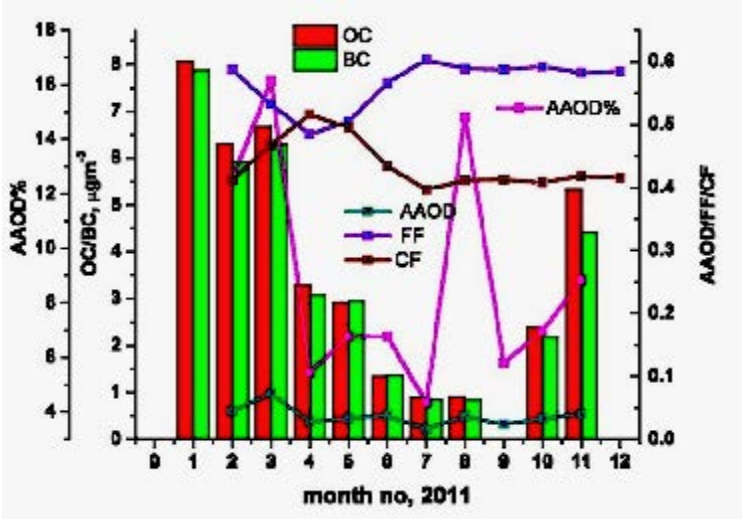

Figure 5. Co-variation of AAOD%, FF, CF, OC and BC.

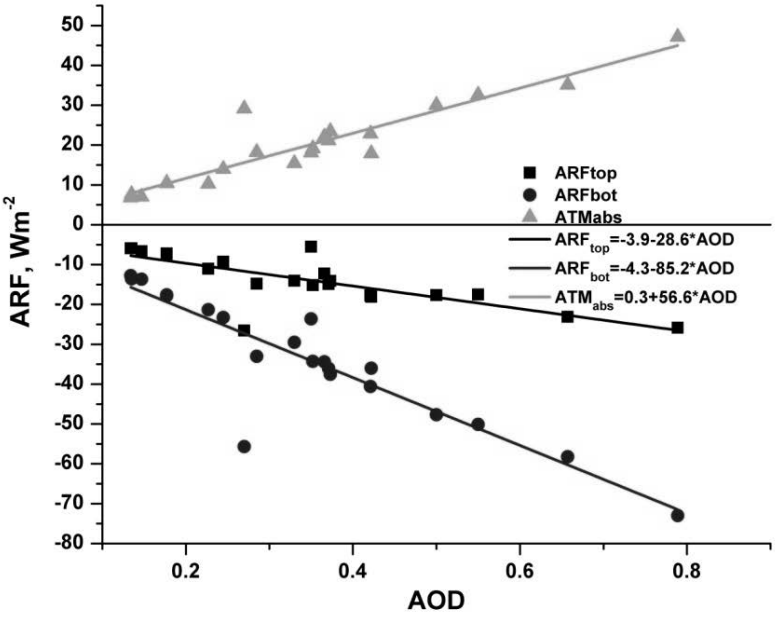

Figure 6. Radiative forcing efficiency, ARF top (TOA), bottom (surface) and atmospheric absorption.

ACKNOWLEDGEMENTS

Dipu and Sriwin of IITM are thankfully acknowledged for helping with the software installation. Prof. Mohanthy of BIT-Ranchi for his kind moral support and Director, IITM for all his support for execution of this work.

REFERENCES

Dey, S., Tripathi, S. N., Singh, R. P. (2004). Influence of dust storms on the aerosol optical properties over the Indo-Gangetic basin, *J. Geophy. Res.*, **109**, D20211.

Nair, V. S., Moorthy, K. K., Alappattu, D. P., *et al.*, (2007). Wintertime aerosol characteristics over the Indo-Gangetic Plain (IGP): Impacts of local boundary layer processes and long-range transport, Journal *of Geo-physical Research* ,**112**, D13205.

Tripathi, S. N., Dey, Sagnik, Chandel, A., Srivastva, S., Singh, R. P. and Holben, B. (2005). Comparison of MODIS and AERONET derived aerosol optical depth over the Ganga basin, India, *Ann. Geophys.* , **23**, pp. 1093-1101.

Ricchiazzi, P., Yang, S., Gautier, C., and Sowle, D. (1998). SBDART: a research and teaching software tool for plane-parallel radiative transfer in the Earth's atmosphere, *B. Am. Meteorol. Soc.*, **79**, pp. 2101– 2114.

Srivastava, A. K., Ram, K., Pant, P., Hegde, P. and Joshi, Hema. (2012). Black carbon aerosols over Manora Peak in the Indian Himalayan foothills: implications for climate forcing, *Environ. Res. Lett.* , **7**, 014002.

EFFECT OF PRECIPITATION ON BLACK CARBON AEROSOLS SCAVENGING

G. GOPALAKRISHNAN, P.D. SAFAI, M. P. RAJU, P. MURUGUEL, S. D. PAWAR and P.C. S. DEVARA

Indian Institute of Tropical Meteorology, Pune

Keywords: BLACK CARBON, ATHELOMETER

INTRODUCTION

The knowledge of concentration of Black carbon (BC) is important because of its high absorbing property and hence its possible role in radiative forcing (Ramanathan, *et al.*, 2001). During their lifetime of about one week, BC aerosols can be transported over long distances, and hence the role of BC in clouds and removal rate especially, on a regional scale is very important (Cape, *et al.*, 2012). Aerosols present in the atmosphere are removed by dry and wet scavenging processes. However, unlike other aerosol particles, BC is hydrophobic and therefore its removal by wet processes is comparatively weak. Very few works have been carried out to understand the wet scavenging of BC. Cape, *et al.,* (2012) suggest that the lifetime of BC is dependent on rainfall and have acknowledged that removal mechanism of BC from the atmosphere is different. Latha, *et al.*, (2005) have attempted to derive the scavengingcoefficient for black carbon aerosols based on Aethalometer measurements at Hyderabad. They found drastic reduction in black carbon aerosol loading during a rainy day compared to a normal day. However, their results are based on observations made for a short duration. Cooke, *et al*. (1997) have also reported an inverse relation between BC concentration and precipitation based on Mace Head observational data. Here, we report our observations of BC and rainfall made at Pune during the rainy season of 2009 and analyse the relationship between them in three different categories of rain (rainrate).

INSTRUMENTATION

Continuous observations of BC were carried out using an Athelometer (AE-42) at sampling flow rate of 3LPM and time base of 5 minutes. The BC data were corrected for the filter loading effect by using a method described by Park, *et al.*, (2012). Details of Aethalometer and BC measurement are described by Hansen, *et al.* (2003). The raindrop size distribution (RSD) is measured by an Optical Disdrometer. The disdrometer can measure raindrops in the size range of 0.5 to 20 mm diameter. From the RSD, we can estimate the rainfall intensity and amount of rainfall. Observations of BC and rainfall were carried out in the same location in IITM, Pune during the rainy season of 2009. Sampling of rainfall size distribution is done at 30 second interval. Rainfall intensities obtained at each distribution during a particular spell are averaged to get the rain intensity during that spell.

RESULTS

Observations of BC and raindrop size spectra were made on all rainy days of 2009 season. In the present study, we have included only the measurements made in July where we had 19 rainy days. We have divided our observations into three categories i) light rains: days with rains less than 5mm/ hr for short duration; ii) intermittent rains: days with intensity less than 10 mm/hr and iii) heavy rains: days with rain throughout the day. For simplicity, we have used 5-minutes averaged values of BC concentration and rainfall intensity in our analysis. Typical variation of BC with rain intensity is shown in Fig. 1.

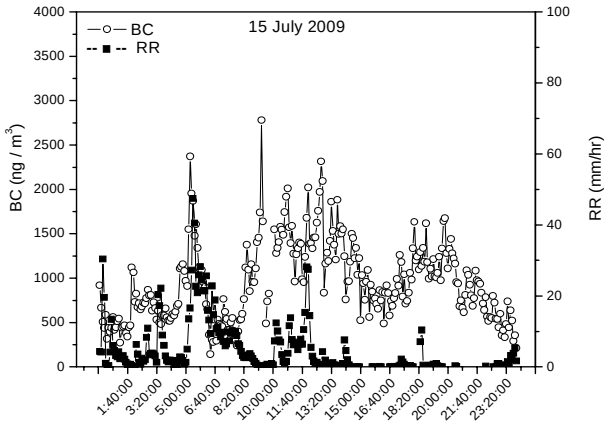

Figure1. Diurnal variation of BC and rain intensity on July 15, 2009.

It is observed that there is no one-to-one relation of BC concentration with rain intensity. During some spells of rain, concentrations of BC decreased with rain while during some other spells with same rain intensity; BC concentration increased. It is observed that generally rain with intensity less than 3mm/hr has no impact on the concentration of black carbon.

However, when we average all the days with rain mentioned in the three categories mentioned above, we get some clarity on the relationship between rain and BC. The diurnal variation of BC on rainy days as well as that on the back ground averaged variation for July month is shown in Fig. 2. As seen from this figure, we observe that there are two maxima for BC with one in morning at around 0700 hrs and another in the evening around 1900 hrs. The minima is observed at around 0300 hrs in early morning and there is another minima in BC concentration during daytime at around 13.30 hrs in the noon. However, all the three categories of rains seem to affect both the magnitude and diurnal pattern of BC. On days with light rain, we observe considerable increase in BC concentration and both daytime and night-time maxima occur one-to-two hours earlier than normal. Diurnal variation of BC during days with intermittent rains seems to follow the background variation. Further, it is worth to note here that there is no appreciable change in magnitude of BC concentration. However, on days with rain throughout the day and when rain intensity exceeds 20 mm/hr, we observe reduction in the concentration of BC. Further, there is a shift in the occurrence of maxima and we observe maxima one hour later than the normal occurrence.

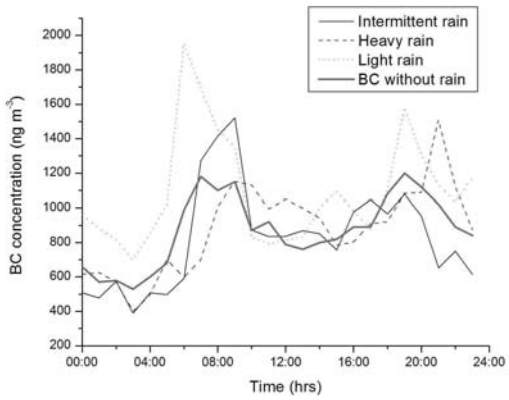

Figure 2. Average diurnal variation of BC on different types of rainy days. Typical background variation shown as bold line (BC without rain).

DISCUSSION

Latha, *et al*. (2005) have reported a drastic reduction in BC concentration on rainy day. Further, the BC concentration decreases with rain intensity. However, their observations are limited to rain intensity less than 15 mm/hr and for major duration the intensity is less than 5 mm/hr. Further, they have not observed any reduction during the daytime. However, our observations, averaged for many days, clearly show that during days with rain less than 5mm/hr, there is increase in BC concentration even during rains. However, there is some reduction in BC, when averaged for long duration, during heavy rains with intensity more than 20 mm/hr.

REFERENCES

Cape, J. N., Coyle, M. and Dumitrean, P. (2012). The atmospheric lifetime of black carbon, *Atmos. Environ*. **59**, 256.

Cooke, W. F., Jennings, S. G., Spain, T. G. (1997). Black carbon measurements at Mace Head, 1989–1996, *J. Geophys. Res.* , **102**, 25339.

Hansen ADA. (2003) Magee Scientific Aethalometer User's Guide, Magee Sci. (Berkeley, California, USA).

Latha, K. M., Badrinath, K. V. S. and Reddy, P. M. (2005). Scavenging efficiency of rainfall on black carbon aerosols over an urban environment, *Atmos. Sci. Lett*, **6**, 148.

Park, S.S., Hansen, A.D.A., Sung.Y.Cho. (2010). Measurement of real time black carbon for investigating spot loading effects of Aethalometer data, *Atmospheric Environment* , **44 (11)**, pp. 1449-1455.

Ramanathan, *et al.* (2001). Indian Ocean Experiment: An integrated assessment of the climate forcing and effects of the Great Indo-Asian Haze, *J Geophys Res.*, **106** (D22), pp. 28,371– 399.

INTER-COMPARISON AMONG THREE TECHNIQUES OF AEROSOL OPTICAL DEPTH OVER CENTRAL HIMALAYAS

U. C. DUMKA[1], MANISH NAJA[1], NARENDRA SINGH[1], RAMAN SOLANKI[1], D.V. PHANIKUMAR[1], P. PANT[1], RAM SAGAR[1], HEMA JOSHI[1], S. K. SATHEESH[2], K. KRISHNA MOORTHY[3] AND V R KOTAMARTHI[4]

[1]Aryabhatta Research Institute of Observational Sciences (ARIES), Nainital 263129, India
[2]Center for Atmospheric and Oceanic Sciences, India Institute of Observational Sciences, India
[3]Space Physics Laboratory, Vikaram Sarabhai Space Center, Trivandrum, India
[4]Argonne National Laboratory, USA

INTRODUCTION

The Indo-Gangetic Plain (IGP) region in Northern India is one of the most populated regions of the world and encompasses a variety of anthropogenic and biogenic source of aerosols and pollutants due to rapidly growing industrialization and expanding urbanization in recent years. Based on the satellite observations this region is considered to be most polluted regions in India. However, the ground based observations are very limited to verify the same. Based on the model study, the vertical lifting of pollutants from this region and the wide spread transport of aerosols and pollutants during the prevailing higher wind speed, hence influencing the radiation budget and thereby climate change over the wide region. In view of this the first Atmospheric Radiation Measurement mobile facility (AMF1) has been set-up at ARIES, Nainital (29.4^{o}N, 79.5^{o}E, 1958 m above mean sea level) under the Regional Aerosol Warming Experiment (RAWEX)-Ganges Valley Aerosol Experiment (GVAX) project. The observations of physical, optical and microphysical properties of atmospheric aerosols, radiation and meteorological parameters were made during June 2011-March 2012. The vertical profiling of meteorological parameters was also made using Radiosonde launches at 00, 06, 12, and 18 GMT on the regular basis. The vertical winds were measured using a wind profiler. A Doppler Lidar and ceilometer were also operational. Observations of the aerosol optical depth (AOD) were also carried out using different observational techniques like (MICROTOP Sun Photometer; CIMEL AERONET and MFRSR). The main goal of this study is to determine the level of agreement among these three different instruments in similar operational conditions.

EXPERIMENT DETAILS AND DATA BASE

The experimental site (29.4^{o}N, 79.5^{o}E) Manora Peak, Nainital is located in the lower part of central Himalayas at an altitude of ~1958 meter above mean sea level and hence is above the planetary boundary layer for most of the time (Pant *et al.*, 2006). The geographical location and topography of the observational site is shown in Fig. 1(a). The experimental data considered of spectral aerosol optical depth (AOD) estimated using three different instruments, five-channel hand held Microtops Sun photometer (MTOPS; Solar Light Co., USA), MFRSR (Multi-Filter Rotating Shadowband Radiometer) and Aerosol Robotic NETwork (AERONET). All three instruments, viz MTOPS, MFRSR and AERONET, used in the present study are ground-based passive remote sensing instruments which measure directly transmitted ground reaching solar flux as a function of wavelength. The common and unique features of all the instruments along with their specifications are given in Table 1. The raw data obtained from MFRSR are analyzed using the conventional Langley technique to deduce the columnar AOD; whereas MTOPS derived AOD is based on its internal calibration

coefficients. The instrument details, methods of data analysis, and error budget are described in earlier paper (Pant *et al.*, 2006 and cited therein; Dumka *et al.*, 2008). Estimates of AOD were made regularly on all the clear/partly clear days as part of the RAWEX-GVAX programme and data during the periods from June 2011 to March 2012 are used in the present study.

RESULTS AND DISCUSSION

Fig. 1 (b) shows time series of AOD at 500 nm derived from the MFRSR (τ_{MFRSR}), MTOPS (τ_{MTOPS}) and AERONET ($\tau_{AERONET}$) observations with the respective concurrent measurements. It is evident from the figures, that the MTOPS measured AODs follow the same trend with those derived from the other two instruments, except the MTOPS AODs are slightly higher than the MFRSR and AERONET. With a view to quantifying the association between AODs derived from MTOPS, MFRSR and AERONET instruments, the statistical parameters, viz mean bias difference (MBD), root mean square difference (RMSD) and absolute percentage difference (APD) are calculated using the following relations:

$$MBD = \frac{1}{\mathrm{N}}\left(\sum_{i}^{N}\left(X_i - MFRSR_i\right)\right); RMSD = \left[\frac{1}{\mathrm{N}}\sum_{i}^{N}\left(X_i - MFRSR_i\right)^2\right]^{1/2} \text{ and}$$

$$APD = \left(\left|\left(\mathrm{X_i} - MFRSR_i\right)\right| / MFRSR_i\right)*100$$

Where X_i represents the individual AOD at 500 nm retrieved from MTOPS and AERONET. The parameter MBD gives the information about the offset between two observations, whereas RMSD gives an idea about the non-systematic component of the differences in measurements, as it is very sensitive to the extreme values, while the APD tells us about the deviation in an observed quantity from the standard reference and which is useful to quantifying the deviation in a set of observations. Brief information on statistical comparison of MTOPS retrieved AOD with MFRSR and AERONET is given in table 2. In addition to this the correlation plots between MTOPS & MFRSR and MTOPS & AERONET is also shown in Fig. 1c and 1d.

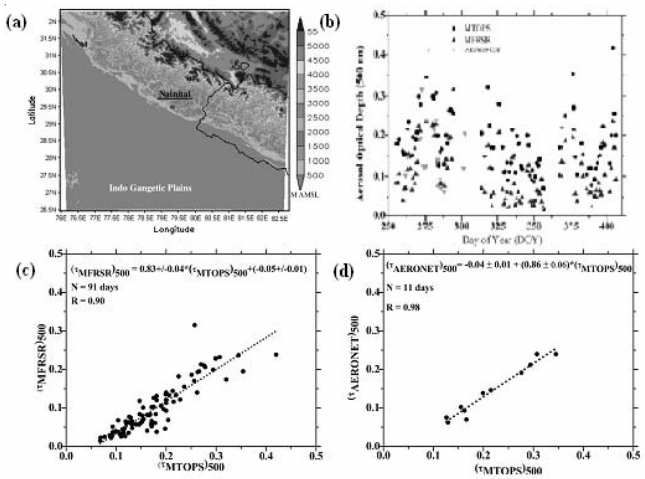

Figure 1. (a) The geographical location of the study area. Color code in the figure shows the altitudes in meters above the mean sea level. (b) Time series of aerosol optical depth at 500 nm using different instruments. (c) Inter-comparison of aerosol optical depth at 500 nm retrieved from MTOPS and MFRSR. (d) Inter-comparison of aerosol optical depth at 500 nm retrieved from MTOPS and AERONET. The dotted line in panel (c) and (d) represent the linear least square fit of the data.

Specification	MTOPS	MFRSR	AERONET
Measurement	Direct	Total, diffuse, direct	Direct
Operation	Hand Held, Sun	Automatic,	Automatic
No of Channels	5	6	8
Central wavelengths, nm	380, 440, 500, 675	415, 500, 615, 675	340, 380, 440, 500,
FWHM	10 nm	10 nm	10 nm
FOV	2.5^o	3.3^o	1.2^o

Table 1. Specification details of MTOPS, MFRSR and AERONET Sun Photometer.

Parameter	MFRSR	AERONET
Absolute percentage difference (APD) (%)	49.16	36.35
Root mean square difference (RMSD)	0.09	0.07
Mean bias difference (MBD)	-0.08	-0.07
Regression coefficient (R)	0.9	0.98

Table 2. Statistical comparison of MTOPS retrieved AOD with MFRSR and AERONET.

CONCLUSION

The AOD at 500 nm obtained from hand held Microtops Sun Photometer were inter-compared with the AOD obtained from MFRSR and AERONET Sun Photometer. MTOPS and MFRSR retrieved AODs well correlated with correlation coefficients of R ~0.90 and correlation coefficient is 0.98 between MTOPS and AERONET. The results obtained from these there instruments shows similar variations except the values obtained from MTOPS are little bit high.

ACKNOWLEDGEMENT

The author wishes to thank the technical staff of ARM for providing the valuable data. This study is carried out under the RAWEX-GVAX project in collaboration among Department of Energy, U.S., Indian Institute of science, Bangalore, Indian Space Research Organization and ARIES.

REFERENCES

Dumka, U. C. et al. (2008). JAMC.

Pant, *et al.*, *J. Geophys. Res.*, 111, D17206.

EFFECT OF AEROSOL OPTICAL DEPTH ON CLEARNESS INDEX DURING DIFFERENT SEASON OVER DELHI

T. BANO [1, 2,] S. SINGH [1] AND N.C. GUPTA [2]

1. Radio and Atmospheric Science Division, National Physical Laboratory, CSIR, New Delhi-110012, India.

2. University School of Environment Management, Guru Gobind Singh Indraprastha University, New Delhi, India

Key words: AOD, UV RADIATION, BROADBAND RADIATION, CLEARNESS INDEX (K_T)

INTRODUCTION

Aerosols particles suspended in the atmosphere influence the Earth's climate in a direct as well as indirect manner. Aerosol attenuates solar radiation through scattering and absorption (Charlson, *et al*., 1992). The ultraviolet (UV) and the broadband (or shortwave) radiation (that includes visible and near infrared) of the solar spectrum are of utmost importance to all life forms on earth. The variations in the UV and broad-band radiation flux become more complex to understand due to the presence of aerosols, clouds, water vapour and other gases in the atmosphere. The measurement of solar irradiance is however essential for studying the atmospheric phenomena, large-scale weather analysis and prediction, climate change studies etc. The clearness index (K_T) is a general indicator of all the extinction (scattering + absorption) occurring in the atmosphere due to clouds, aerosols, water vapour (Elhadidy, et al., 1990; Liu and Jordan, 1960). K_T, is the ratio of global to extraterrestrial radiation. A low value of K_T indicates lower global solar radiation at surface. K_T is very useful in characterizing the sky conditions over a particular location (Okogbue, *et al.*, 2002) and in estimating the diffuse radiation (Okogbue, *et al.*, 2009). It can also be used to analyze the effects of aerosols, water vapour and clouds on the radiation (Hu, *et al.*, 2007). In this study, we have estimated the clearness index at Delhi for two season summer and winter for the year (April 2010 to March 2011) and also studied the impact of aerosols on K_T.

METHODOLOGY

The data used in this study were collected at the National Physical Laboratory in New Delhi (28.38 °N, 77.10 °E, 235 m AMSL) during the time period 1st April to 30th June 2010 (summer season) and 1st October 2010 to 31st January 2011 (winter season). The database consists of hourly broadband global (G) and global UV (GUV) radiant fluxes measured on a horizontal plane. Broadband global radiant flux, G, (total bandwidth, 285–2800 nm) was measured using the Kipp & Zonen CMP-21 model pyranometer (Delft, The Netherlands). The GUV (total bandwidth, 280–400 nm) radiant flux was measured with the Kipp & Zonen CUV-4 model radiometer. All radiation values were recorded at 2-min intervals. The hourly values of solar radiation were integrated from the minute values. The daily (or monthly) clearness index (K_T) may be calculated using daily (or monthly) averaged global solar radiation measured on the horizontal surface (H) and the daily (or monthly) average extraterrestrial radiation (H_0) as $KT = H/H_0$ (A-Hinai and Al-Alawi, 1995; Angstrom, 1924; Duffie and Beckman, 1991; Page, 1961).Where the extraterrestrial H_0 radiation is estimated as (Iqbal, 1983; Ulgen and Hepbasli, 2002). For measuring aerosol optical depth (AOD), Microtops Sunphotometer – make Solar Light Company, USA, has been used. The instrument gives column

AOD at five wavelengths from UV to near infrared (340, 500, 675, 870 and 1020 nm). The AOD values were recorded nearly half an hour interval during the day time 09:00 to 17:00 h on cloud free days.

RESULTS AND DISCUSSIONS

In order to see the effect of AOD on K_T we have plotted the scatter plot for the daily clearness index variation with respect to the corresponding daily average AOD in fig. 1. The upper panel of figure represent the summer season with AOD 340nm and AOD 500nm respectively whereas the lower panel of figure shows the winter season representing again the two AOD at 340 and AOD at 500 nm. Regression analysis between K_T and AOD has been done. There is a very strong negative linear correlation between K_T and AOD for both the season. The coefficient of correlation (R) between K_T and AOD at 500nm during summer is -0.936 and coefficient of determination (R^2) is 0.876 which means about 88% of K_T values can be explained by the linear relationship between K_T and AOD. The AOD at 500 nm gives better picture than AOD at 340 nm because; it is directly related to the atmospheric turbidity levels. During summer, for every unit increase in AOD at 500 nm, K_T decreases by 0.07 and for AOD at 340 nm it is 0.05.

In the lower panel of fig. 1 variation of K_T for the corresponding variation in AOD at 340nm and AOD at 500nm for winter season have been presented. There is a direct effect of aerosols on K_T measurement over Delhi. During this season, negative linear correlation between K_T and the AOD at 500nm of the order -0.78 can be noticed. For every unit increase in AOD at 500 nm the average K_T is found to decrease by ~0.06.

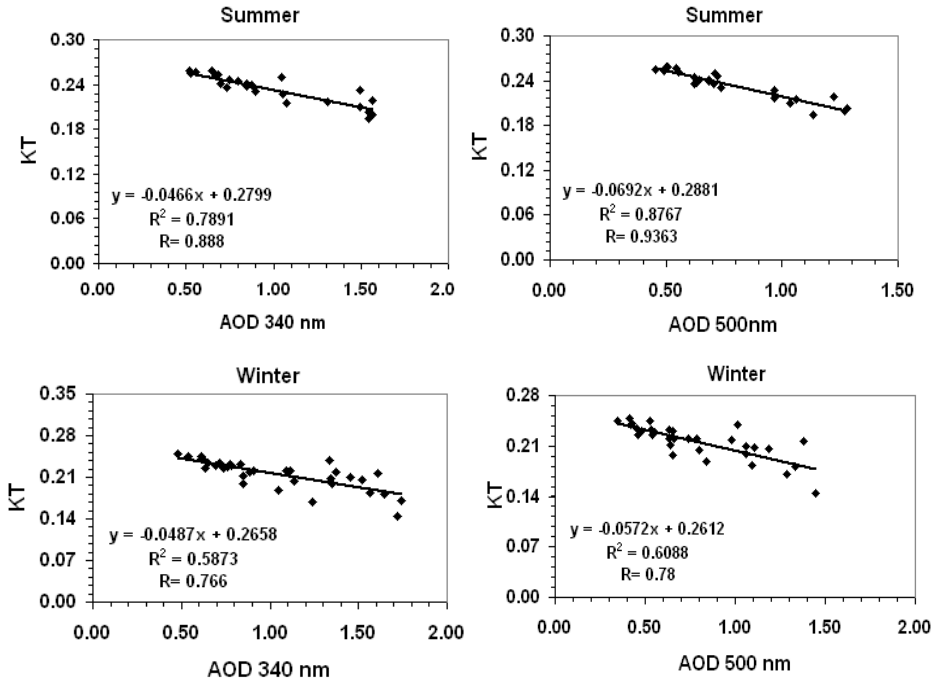

Figure1. Variation of Clearness index (K_T) with AOD at 340 nm and AOD at 500nm during clear sky conditions for summer and winter season over Delhi

CONCLUSIONS

The following conclusions may be drawn from the study over Delhi

- The strong anti- correlations with coefficient –0.93 have been observed for AOD at 500nm and K_T for summer season, whereas –0.78 have been observed during winter season indicating a decrease in K_T with increasing AOD
- Correlation is better in summer season as compared to winter months because in winter along with aerosols; fog also affects the K_T

AKNOWLEDGEMENT

The author Tarannum Bano is thankful to Council for Scientific and Industrial Research (CSIR) for her Research Associateship being provided during this work.

REFERENCES

Al-Aruri, S. D., Rasas, M., Al-Jamal, K., Shaban, N. (1998). An assessment of global ultraviolet solar radiation in the range 0.290–0.385 mm in Kuwait, *Solar Energy* , **41**, pp. 159–162.

Al-Hinai H. A., Al-Alawi, S. M. (1995). Typical solar radiation data for Oman, *Applied Energy*, *52*, pp. 153–163

Elhadidy, M. A., Abdel-Nabi, D.Y., Kruss, P. D. (1990). Ultraviolet solar radiation at Dhahran, Saudi Arabia, *Solar Energy* , **44(6)**, pp. 315–319.

Hu, B., Yuesi, W., Liu, G. (2007). Ultraviolet radiation spatio-temporal characteristics derived from the ground-based measurements taken in China, *Atmospheric Environment*, **41**, pp. 5707–5718.

Iqbal, M. (1983). *An Introduction to Solar Radiation*, Academic Press: New York, pp. 59–67.

Liu, B. Y. H., Jordan, R. C. (1960). The interrelationship and characteristic distribution of direct, diffuse and total solar radiation, *Solar Energy*, 4, pp. 1–19.

Page, J. K. (1961). The estimation of monthly mean values of daily total short wave radiation on vertical and inclined surfaces from sunshine records for latitudes 401N–401S, In *proceedings of the UN Conference on New Sources of Energy.* Rome, pp. 378–390.

Okogbue, E. C., Adedokun, J. A., Jegede, O. O. (2002). Fourier series analysis of daily global and diffuse Irradiation for Ile-Ife, Nigeria, *Journal of Applied Sciences*, **5(3)**, pp. 3034–3045.

Okogbue, E. C., Adedokunb, J. A., Holmgrenc, B. (2009). Review-hourly and daily clearness index and diffuse fraction at a tropical station, Ile-Ife, Nigeria, *International Journal of Climatology*, **29**, pp. 1035–1047.

Ulgen, K, Hepbasli, A. (2010). Prediction of solar radiation parameters through clearness index for Izmir, Turkey, *Energy Sources*, **24**, pp. 773–785.

INTER-COMPARISON STUDY BETWEEN SURFACE O_3, NO_x, AEROSOL AND BC CONCENTRATIONS OVER ANANTAPUR (INDIA)

A.P. LINGASWAMY[1], K. RAMA GOPAL[1*], R.R. REDDY[1], S.MD. ARAFATH[1], K. UMADEVI[1], S. PAVAN KUMARI[1], N. SIVAKUMAR REDDY[1], G. BALAKRISHNAIAH [1,2], B. SURESH KUMAR REDDY[1,3], K. RAGHAVENDRA KUMAR[1,4], Y. NAZEER AHAMMED [5]AND SHYAM LAL[6]

[1] Aerosol & Atmospheric Research Laboratory, Department of Physics, Sri Krishnadevaraya University, Anantapur 515 055, Andhra Pradesh, India

[2] Institute of Environmental Engineering, National Chiao Tung University, No. 1001, University Road, Hsinchu 300, Taiwan

[3] Institute of Low Temperature Science, Hokkaido University, Sapporo 060 0819, Japan

[4] School of Chemistry and Physics, University of KwaZulu-Natal, Westville Campus, Durban 4000, South Africa

[5] Atmospheric Science Laboratory, Department of Physics, Yogi Vemana University, Kadapa 516 003, Andhra Pradesh, India

[6] Space and Atmospheric Sciences Division, Physical Research Laboratory, Ahmedabad 380 009, Gujarat

E mail:krgverma@yahoo.com

Keywords: OZONE, BC, AEROSOLS, AIR POLLUTION MONITORING

INTRODUCTION

Ozone (O_3) is a natural compound present in different layers of atmosphere. In the troposphere, it is involved in several atmospheric physical and chemical processes. For instance, Tropospheric ozone is a major greenhouse gas in the troposphere and plays an important role in determining the oxidation capacity of the atmosphere as a photo chemical precursor of OH radicals (Brasseur, *et al.*, 1999). Its concentration in any given area is the result of the combination of formation, transport, destruction and deposition. Their sources include: (i) photochemical reactions involving its precursors (volatile organic compounds and nitrogen oxides) with natural or anthropogenic origin; (ii) downward transport from stratosphere; (iii) long-range transport (intercontinental) of ozone from distant pollutant sources (Reddy, *et al.*, 2011).

An abundance fraction of aerosols is part of the natural components of the Earth's atmosphere and harmful to human health and contributes to visibility degradation when present in high amounts (Leitao, *et al.*, 2010). Aerosols present in the atmosphere interact with radiation and affect the atmospheric trace gases. The change of aerosol concentration has an important impact on the surface ozone concentration and oxides of nitrogen. Li, *et al.* (2005) have been reported that the presence of black carbon aerosols resulted, decrease in ground level O_3 in the Houstan area. Reddy, *et al.* (2010) have been reported that there is a clear anti correlation existed between aerosol mass concentration and Surface O_3. Moreover high aerosol concentration can increase the NO_x concentration in Megacity Plumes in spring over the north western Pacific by reducing its photolytic loss (Tang, *et al.*, 2003).

Anantapur is a very dry continental rain shadow region of Andhra Pradesh in Southern India, is a non-industrialized, medium-sized city with a population of ~5 Lakhs inhabitants. Within 50 km radius,

this region is surrounded by a number of cement plants, lime kilns, slab polishing and brick making units. These industries, the national highways (NH 7 and NH 205) and the town area are situated in the north to southwest side of the sampling site. In this study mainly exposed that mean diurnal and monthly variations of surface O_3, NO_x along with total aerosol mass and black carbon mass (BC) for the total study period, January-July 2011. And also multi-regression analysis of Mt and BC with Surface O_3 was analyzed.

INSTRUMENTATION

Surface ozone was measured by using an analyzer (O_3 41M; Environment S.A, France) based on absorption of Ultraviolet (UV) radiation at 253.7 nm by ozone molecules. NO_X is measured continuously by using an ambient analyzer (model APNA-370, HORIBA, and Germany). The APNA-370 uses a combination of the dual cross flow modulation type chemiluminescence principle and the reference calculation method. For black carbon measurements, Magee Scientific Aethalometer (model AE-21) was used. The ten channel Quartz crystal microbalance impactor was used to measure total aerosol concentration. Ten wavelength Multi Wavelength Radiometer (MWR) was used to measure Aerosol Optical Depth (AOD) during the study period.

RESULT AND DISCUSSION

DIURNAL VARIATION OF SURFACE O_3, NO_X, AEROSOL (MT) AND BC MASS CONCENTRATIONS

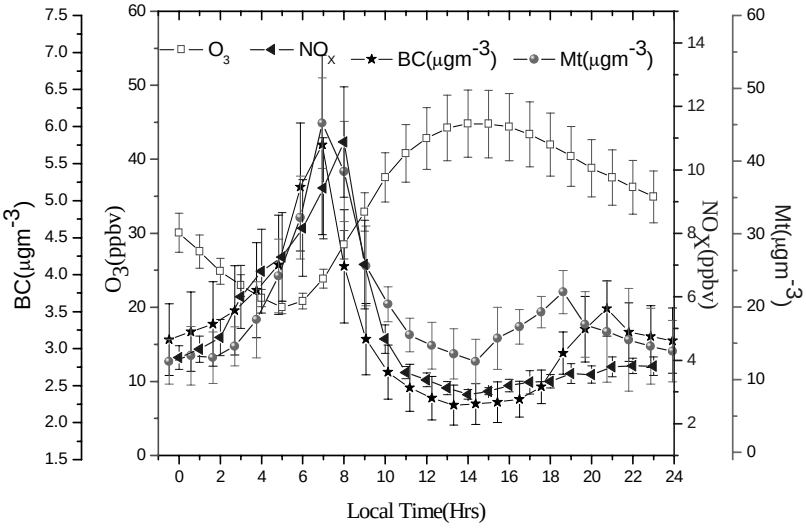

Figure 1. Mean diurnal variations of surface O_3, $NO_{X,}$ aerosol (Mt) and BC concentrations over Anantapur during study period January-December 2011.

The mean diurnal variations of surface O_3, NO_x, Aerosol (Mt) and BC concentrations were observed at measurement site during the study period are shown in Figure1. The vertical bars denote the $\pm 1\sigma$ standard deviation. The diurnal variation of surface O_3 shows a minimum at before sunrise and concur with solar radiation attain maximum at noon time and after gradually decreasing due to titration effect. And boundary layer also plays an important role on a diurnal scale of O_3 and its

precursors. Whereas NO_x has opposite trend to O_3 maximum values during morning and late evening hours and low values during noon hours. The surface aerosol (BC and aerosol) mass variations are same of NO_x variation and opposite to O_3 variations.

The diurnal variation of O_3 at this measurement site are characterized by high concentration during the day time and low concentration during the early morning hours and late evening hours for entire study period. The minimum O_3 concentration of about (19±1.6 ppbv) is noticed during the early morning around (08:00 hrs). From onwards O_3 concentration starts increasing and attains maximum value (45 ±2.6 ppbv) during (14:00-16:00 hrs). It decreases rapidly after peak until evening, maintains low values during night hours due to the absence of photolysis of NO_2 and continuous loss of O_3 by NO_X. Similar results are also shown in rural site Gadanki rural site in southern India (Naja and Lal, 2002). The maximum peak during the afternoon time mainly from oxidation of natural and anthropogenic emission of hydrocarbons, carbon monoxide (CO), methane (CH_4) by hydroxyl radical in the presence of NO_X and VOC (Seinfeld and Pandis, 1928).

The diurnal cycle of NO_X shows that maximum peak (11±0.9 ppbv) is present during early morning hours (08:00-09:00 hrs) and late evening hours (18:00-20:00 hrs) and minimum (2.1±0.2 ppbv) is present during afternoon time (16:00 hrs). The morning peak is higher in magnitude than the late evening peak. O_3 showed low values when NO_X had highest concentration during early morning hours. During early morning hours NO values are abruptly increase from motor vehicles and industrial activities. The newly emitted NO react with O_3 without solar radiation forms NO_2 and reducing O_3 concentration.

$$NO_2 + h\acute{\imath}' \rightarrow NO + O \quad (1)$$

$$O + O_2 + M' \rightarrow O_3 + M \quad (2)$$

$$O_3 + NO' \rightarrow NO_2 + O_2 \quad (3)$$

Where M represents a molecule (N_2 or O_2) absorbs excess vibrational energy and forms stable O_3. Surface ozone shows peak values when NO_X had the lowest concentration during after noon time. During this period, NO_X accumulations were not significant because of more NO_X photochemical consumption and increased dilution as the height of the boundary layer increases.

The diurnal variation of black carbon concentration (BC) and total aerosol concentration shows that maximum peak is present during early morning hours, due to biomass burning and vehicle emissions, after onwards slowly decreases and attains minimum values at (14:00-16:00 hrs). Furthermore attains another peak during (18:00 – 22:00 hrs), at this time increasing vehicle emissions and more stable atmospheric conditions are responsible for presence of second peak. During the afternoon period aerosols shows less concentration due to the boundary layer height should reach a maximum and additional venting of the boundary layer convection. The fig.1 clearly shows that O_3 had low values when aerosol concentration maximum. This strongly suggests that high aerosol concentration should show impact on trace gases budget. High aerosol concentration significantly affects chemical oxidation process, especially through photo-dissociation (Li, *et al.*, 2005). This generally happens at early morning hours, this characterized by windless condition and less stratified boundary layer. If an ozone molecule collides with an active site on the surface of carbon sample, one of its oxygen atoms gets adsorbed while the resultant oxygen molecule is liberated. The adsorbed oxygen atom can then combine with another adsorbed oxygen atom to form oxygen molecule. The reaction

causes ozone depletion in the atmosphere (Fendel, *et al.*, 1995). The authors are found that the O_3 concentration was very sensitive to aerosol loading over measurement site. Similar results are also shown in (Bian, *et al.*, 2007).

MULTI-REGRESSION ANALYSIS OF SURFACE O_3 WITH MT AND BC MASS CONCENTRATIONS

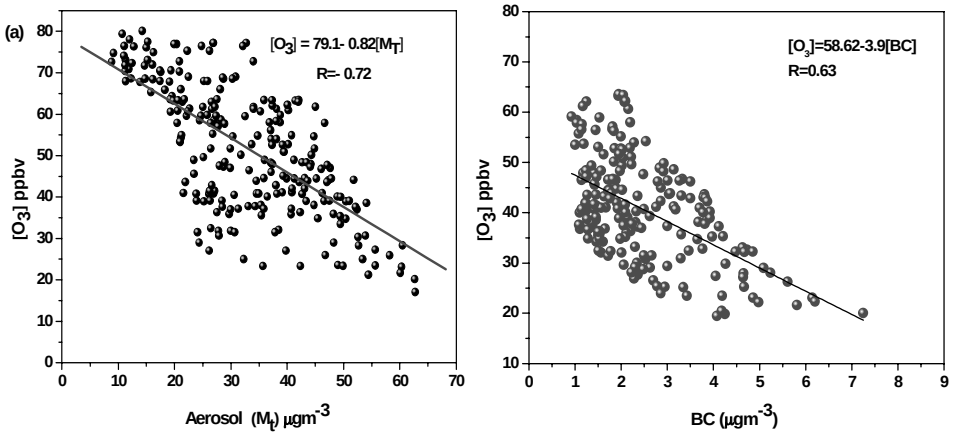

Figure 2. Multi-regression analysis of Surface O_3 with aerosol (Mt) and BC mass concentrations during study period

The authors have made an attempt to study the correlation among total aerosol concentration and black carbon aerosols with surface ozone (see Fig. 2). The results suggest an inverse relation among Mt and BC with surface ozone was found to be correlation coefficient (R) of 0.72, 0.63 res. The slope between the black carbon aerosols and surface ozone has been found to be – 3.9 suggesting that an increase of 1 $\mu g/m^3$ black carbon aerosol mass concentration causes a reduction of 3.9 $/m^3$ in surface ozone concentration. Moreover, it is clearly depicted from figure1 that that positive relation between aerosol concentration and oxides of nitrogen (NO_x). The results estimated that aerosols can increase the NO_x concentration by reducing the photolytic loss over the measurement site. Similar results are also shown in (Tang, *et al.*, 2003).

ACKNOWLEDGEMENTS

The authors wish to thank the Indian Space Research Organization (ISRO), Bangalore for carrying out this work through its Geosphere Biosphere Programme (GBP) under ARFI project. The authors are grateful to Dr. P.P.N. Rao, Program director, IGBP. One of the authors (RRR) wishes to express his thanks to UGC, New Delhi for providing UGC BSR Faculty Fellowship during which part of the was done.

REFERENCES

Bian, H., Han, S., Tie, X., Sun, M., Liu, A. (2007). Evidence of impacts of aerosols on surface ozone comentration in Tianjin, China, *Atmospheric Environment*, **41**, pp. 4672-4681.

Brasseur, G. P., Orlando, J. J., Tyndall, G. S. (1999). Atmospheric Chemistry and Global Change, Oxford Univ. Press, New York, **13**, pp. 465–486.

Fendel, W., Matter, D., Burtscher, H. and Schmidt-Ott, A. (1995). Interaction between Carbon or Iron Aerosol Particulates and Ozone, *Atmos. Environ.*, **29**, pp. 967–973.

Leitao, J., Richter, A., Vrekoussis, M., kokhanovsky, A., Zhang, Q.J., Beekmann, M., and Burrrows, J.P. (2010). On the improvement of NO2 sattellite retrievals – aerosol impact on the airmass factors, *Atmospheric Measurement Technique*, **3**, pp. 475-493.

Li, G., Zhang, R., Fan, J., Tie, X. (2005). Impact of black carbon aerosol on photolysis frequencies and ozone in the Houston area, *J. Geophys. Res.*, 110, D23206.

Naja, M. and Lal, S. (2002). Surface Ozone and Precursor Gases at Gadanki (13.5°N, 79.2°E), a Tropical Rural Site in India, *J. Geophys. Res.*, **107**, 4197.

Reddy, B.S.K., Kumar, K.R., Balakrishnaiah, G., Gopal, K.R., Reddy, R.R., Narasimhulu, K., Ahammed, Y.N., Reddy, L.S.S. and Lal, S. (2010). Observational Studies on the Variations in Surface Ozone Concentrations at Anantapur in Southern India, *Atmos. Res.* , **98**, pp. 125–139.

Reddy, B.S.K., Reddy, L.S.S., Cao, J.J., Kumar, K.R., Balakrishnaiah, G., Gopal, K.R., Reddy, R.R., Narasimhulu, K., Lal, S., and Ahammed, Y.N. (2011). Simultaneous measurements of surface ozone at two sites over the southern Asia: a comparative study, *Aerosol Air Qualit.*, **11**, pp. 895-902

AEROSOL RADIATIVE FORCING OVER THE INDO-GANGETIC BASIN DURING PRE-MONSOON SEASON (2010)

SARVAN KUMAR AND A. K. SINGH

Atmospheric Research Lab., Department of Physics
Banaras Hindu University, Varanasi-221005

Keywords: AEROSOLS, DUST STORMS, RADIATIVE FORCING, INDO-GANGETIC BASIN.

INTRODUCTION

The Indo-Gangetic Basin (IGB) is one of the largest river basins in the world; it suffers from the long range transport of mineral dust from the western arid and desert regions of Africa, Arabia, Pakistan and Rajasthan during the pre-monsoon season, (April–June). These dust storms influence the aerosol properties like, Aerosol Optical Depth (AOD), Single Scattering Albedo (SSA), Refractive Index (RI) and Aerosol Size Distribution (ASD) across the IGB (Prasad and Singh, 2007). The Kanpur AERONET (Aerosol Robotic Network) station data show pronounced effect on the aerosol optical properties and aerosol size distribution during major dust storm events over the IG plains that have significant effect on the Aerosol Radiative Forcing (ARF) (Prasad, *et al*., 2007).

The multi-band AOD, from AERONET, show clear changes in wavelength dependency over dust affected regions. The average surface forcing and the top of the atmosphere (TOA) forcing are found to change during dust events compared to the non-dusty clear-sky days. A strong correlation is found between AOD at 500 nm and the ARF. At surface, the correlation coefficient between AOD and ARF is found to be 0.68, in atmosphere is found to be 0.39 and at the TOA is found to be 0.70. The slope of the regression line gives the aerosol forcing efficiency at 500 nm at the surface, in atmosphere and the TOA, respectively. The ARF is found to increase with the advance of the dry season in aggregation with the gradual rise in AOD (at 500 nm) from April to June over the IG basin.

DATA AND METHODOLOGY

The ground monitoring of dusts is possible using ground-based CIMEL sky radiometer (Kanpur AERONET station) (Holben, et al., 1998) which is operational as of January 21, 2001 under a joint collaboration with the NASA and the Indian Institute of Technology Kanpur (IIT K). The aerosol optical properties data is available from the AERONET website (http://aeronet.gsfc.nasa.gov/) in three categories; the cloud contaminated (level 1.0), cloud screen (level 1.5) and the quality assured (2.0 level) (Prasad *et al.,* 2007). We have taken AERONET level 1.5 AOD and daily average values of Radiative Forcing data for major dust event days between April 19 and April 23, 2010. We have also used cloud screened level 1.5 Radiative Forcing monthly data for year 2010.

ARF DURING MAJOR DUST STORM EVENT (APRIL, 19-23, 2010)

The aerosol radiation forcing at the top of the atmosphere (TOA) and at the surface is defined as the difference in the net fluxes (down minus up) (solar plus long wave; in Wm^{-2}) with and without aerosol at the TOA and at the surface levels, respectively. The difference of the two gives the ARF in the whole atmosphere. The monthly average ARF variations at TOA, at the surface and in the atmosphere during the period from January 2010 to December 2010 are shown in Fig. 1. The ARF at

TOA, surface and in the atmosphere are found to be in the range of -12 to -31Wm^{-2}, -50 to -140Wm^{-2} and +28 to +128Wm^{-2}, respectively. The TOA and surface forcing for the pre-monsoon season (April, May and June) 2010 are (-13, - 140) Wm^{-2}, (-18, -126) and (-12, -133) Wm^{-2} respectively. Figure 2 shows the ARF and Forcing Efficiency during the pre-monsoon season of 2010.

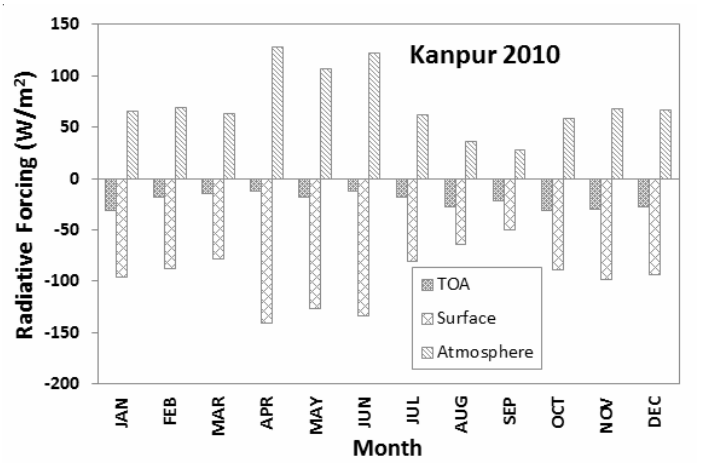

Figure 1. Monthly variation of Radiative forcing over Kanpur during 2010.

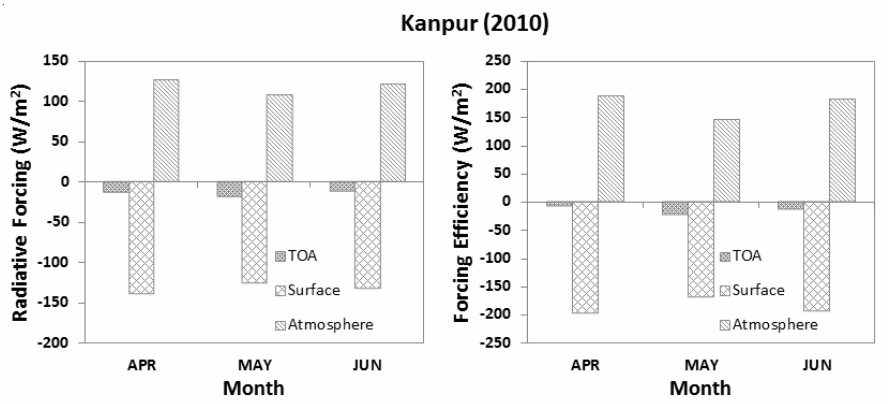

Figure 2. Radiative Forcing and Forcing Efficiency during pre-monsoon season 2010.

The ARF values are highest for April-June (Fig. 1) due to the dust storm activities in the Indo-Gangetic Basin. The ARF value is also high for November 2010; it could be attributed to anthropogenic emission. The AERONET ARF and Forcing efficiency values are shown in Table 1. A good correlation has been observed between AOD (at 500 nm) and ARF (Fig. 3).

AERONET Aerosol RadiativeForcing(W/m^2)				**AERONET Forcing**		
Month	**TOA**	**Surface**	**Atmosphere**	**TOA**	**Surface**	**Atmosphere**
APRIL	-13	-140	127	-9	-198	189
MAY	-18	-126	108	-24	-170	146
JUNE	-12	-133	121	-13	-195	182

Table 1. Monthly variation of ARF and Forcing Efficiency for Kanpur AERONET during pre-monsoon season 2010.

CONCLUSIONS

A large increase has been observed in ARF in IGB during dusty days compared to non-dusty days during pre-monsoon season (April–June), 2010. The average surface forcing and the TOA forcing are changing during dust event days as compared to the non-dusty days. The correlation have been found between AOD at the wavelength 500 nm and ARF (negative or cooling) at surface (R^2 = 0.68), at the TOA (R^2= 0.70) and (R^2 = 0.39) in the atmosphere. The aerosol forcing efficiency at the wavelength 500 nm is found to be-109 Wm^{-2}, -38 $Wm^{-2}$and +72Wm^{-2} at surface, TOA and in the Atmosphere respectively during dust storm period April 19-23, 2010 (Fig. 3) over the Kanpur.

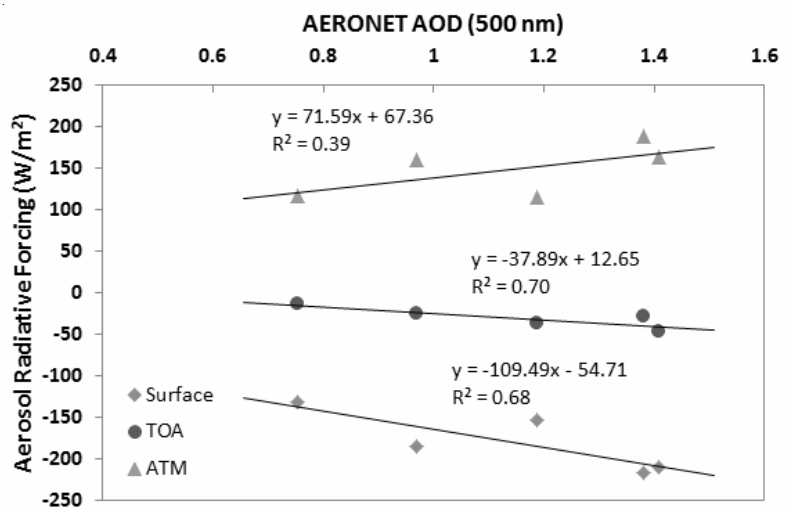

Figure 3. Correlation between AOD (500 nm) with ARF values at Surface, TOA and ATM. The slope of the regressions defines the radiative forcing efficiency.

ACKNOWLEDGEMENTS

The work is supported by the Indian Space Research Organization under ISRO-SSPS to BHU. We are thankful to Dr. Brent Holben (NASA) and Dr. Ramesh P. Singh, to initiate AERONET station at IIT Kanpur (http://aeronet.gsfc.nasa.gov). Mr. Sarvan Kumar is thankful to UGC for providing Rajiv Gandhi National Fellowship as a SRF.

REFERENCES

Holben, *et al.,* (1998). AERONET a federated instrument network and data archive for aerosol characterization, *Remote Sensing of Environment,* **66 (1)**, pp. 1–16.

Prasad, A. K., and Singh, R. P. (2007). Changes in aerosol parameters during major dust storm events (2001–2005) over the Indo-Gangetic Plains using AERONET and MODIS data, *J. Geophys. Res.*, **112**, D09208.

Prasad, A. K., Singh, S., Chauhan, S. S., Srivastava, M. K., Singh, R. P., and Singh, R. (2007). Aerosol radiative forcing over the Indo-Gangetic plains during major dust storms, *Atmospheric Environment,* **41(29)**, pp. 6289–6301.

AEROSOL SPECTRAL OPTICAL DEPTHS OF THE SOUTH ASIAN WINTER HAZE AT VISAKHAPATNAM

MALLESWARA RAO BALLA[1,]& NIRANJAN KANDULA[2]

[1]Department of Engineering Physics, School of Technology, GITAM University (Hyderabad campus), Rudraram, Medak Dist., A.P. 502329, India
[2]Department of Physics, Andhra University, Visakhapatnam530003, India
Email: mallesh@gitam.edu

Keywords: AEROSOL OPTICAL DEPTH, SOUTH ASIAN WINTER HAZE, SOLAR RADIOMETER, GROUND-BASED REMOTE SENSING

INTRODUCTION

Optical depth is a key parameter in atmospheric studies that characterizes the integrated extinction of solar radiation on its transittance through the atmosphere. Atmospheric columnar optical depth derived from spectral extinction measurements of direct solar flux by solar radiometers or sun photometers is due to various constituents of the atmosphere; among which aerosol optical depth (AOD) has been currently the largest factor of uncertainty in the earth-atmosphere radiative balance studies. AOD in the lower atmosphere particularly exhibits high spatial and temporal heterogeneity subject to the vicinity of aerosol sources, sinks and transportation processes. Information on spectral AOD at a geographic location of interest is essential for the assessment of aerosol effect on radiative budget of the earth-atmosphere system, accurate retrieval of aerosol properties from satellite remote sensors and the atmospheric correction of imageries in satellite remote sensing. Recent studies suggest that analysis of spectral AOD can provide important additional information on various aerosol types, and can be effectively utilized to discriminate their characteristics (see Rao, 2009 and the references therein).

Every year during the winter and pre-monsoon periods most of the Indian peninsula, Bay of Bengal and the Southern Indian Ocean are affected by a regional level transport of the lower atmospheric polluted anthropogenic aerosol, known as the South Asian winter haze (SAWH). Many researchers studied and reported AOD during SAWH, over sea and land (please see Rao, 2009 for a list of references). It is clear that the AOD discussed in these studies is a column integrated quantity over the whole atmosphere. However, since the SAWH is a lower atmospheric aerosol it is essential to isolate SAWH AOD from columnar AOD, and consequently their spectral distribution be obtained in order to have a true assessment of possible direct and indirect effects (Gautam, et al., 2007; Ramanathan, et al., 2001; UNEP and C4, 2002). Visakhapatnam (17.7°N, 83.3°E), a tropical coastal station in India, is also largely affected by the SAWH. Geographical location of the measurements location and its characteristic features, climatology of the meteorological parameters, and the presence of SAWH at Visakhapatnam are described in another article of the proceedings of this conference (i.e., Rao & Niranjan, 2012b).

The problem of retrieving SAWH AOD was addressed in our recent paper (Rao & Niranjan, 2012a), where a two component linear model was formulated based on the observed inter-channel correlations of atmospheric optical depths and airmass characteristics. The present work is concerned with estimation of spectral AODs of the SAWH at Visakhapatnam during two successive winter seasons that span over the years 2002, 2003 and 2004.Columnar spectral AODs at Visakhapatnam

are also obtained for the same period following the works of Moorthy, *et al.* (1997, 1999, 2001) and Niranjan, *et al.* (1997, 2004). The estimated spectral AODs of the SAWH are compared with the columnar spectral AODs and the results are discussed.

INSTRUMENT, DATA COLLECTION AND ANALYSIS

A Multi-wavelength Solar Radiometer (MWSR) was installed at Andhra University (Visakhapatnam) as a part of the ISRO-GBP project. The MWSR was designed and fabricated at Space Physics Laboratories of Vikram Sarabhai Space Centre (Thiruvanantapuram, India) following the principle of filter wheel radiometers (Shaw, *et al.*, 1973). The instrument makes spectral extinction measurements of ground reaching directly transmitted solar flux at 10 narrow wavelength bands (centered at 380, 400, 450, 500, 600, 650, 750, 850, 935 and 1025 nm) in the visible and near infrared spectrum. More details of the instrument, data acquisition and analysis of errors are found elsewhere in literature (Moorthy, *et al.*, 1997, 1999, 2001; Niranjan, *et al.*, 1997, 2004; Rao, 2009).A photograph of the instrument (optics unit of MWSR) installed on the roof of physics department building of Andhra University is shown in Fig. 1(a).

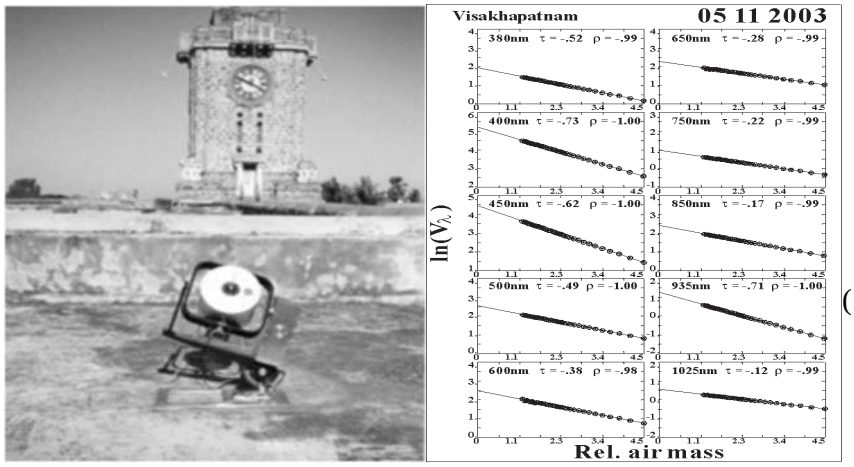

(a) (b)

Figure 1. (a) Photograph of MWSR system (optics unit) installed over the roof of physics department building of Andhra University at Visakhapatnam (b) Typical Langley plot obtained using the MWR data collected at Visakhapatnam

The raw data obtained using the MWSR has been analysed to obtain atmospheric columnar optical depth (τ_λ) at each wavelength following Langley plot technique (Shaw, 1983). The Langley plot obtained for a typical day is shown in Fig. 1(b). Aerosol spectral optical depths of the SAWH (τ_p^{SAWH}) at Visakhapatnam for two successive winter seasons during the years 2002, 2003 and 2004 are estimated following a two component linear model formulated by Rao and Niranjan, (2012a). The τ_p^{SAWH} values are obtained for 9 of the MWSR wavelengths. Optical depth data at the 380 nm filter is, however, discardeddue to degraded filter transmission. Columnar spectral aerosol optical depths (τ_p^{C}) at Visakhapatnam are also obtained for the same period following the works of Moorthy, *et al.* (1997, 1999, 2001) and Niranjan, *et al.* (1997, 2004). The time period of this dataset is purposefully selected since it is a volcanically quiescent period on record for the past 30 years and thus corresponds to a background state of the stratospheric aerosol (please see Deshler, *et al.*, 2003). This consideration makes the estimation of τ_p^{SAWH}somewhat less complicated.

RESULTS & DISCUSSION

Fig. 2 shows the scatter plots of the estimated values of τ_p^{SAWH} versus τ_p^{C} for three typical wavelengths of the MWSR: (a) 500 nm, (b) 750 nm and (c) 935 nm. The horizontal and vertical error bars represent the maximum systematic errors in the retrieved τ_p^{SAWH} and τ_p^{C}, respectively.The dotted line represents a relationship of 1:1 between τ_p^{SAWH} and τ_p^{C}. There is generally a good agreement between $\tau_p^{SAWH}$and τ_p^{C}at all the three wavelengths. The data show a large variability with a minimum of 0.0737 to a maximum of 0.6854 at different wavelengths. In the case of 500 nm channel the minimum and maximum values are of 0.1402 and 0.6854; where as in the case of 935 nm the minimum and maximum values are 0.0737 and 0.3602. Several other studies also have concluded to higher optical depths as the characteristic of SAWH (e.g., Satheesh, *et al.*, 1999; Rajeev, *et al.*, 2000, Ramanathan, *et al.*, 2001; Tahnk and Coakely, 2002; Rao, 2009; Rao & Niranjan, 2012a).

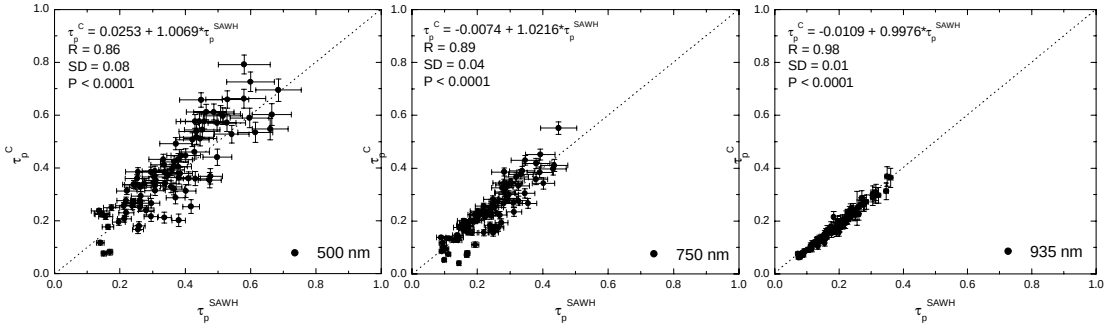

(a) (b) (c)

Figure 2. Scatter plots of the estimated values of τ_p^{SAWH} versus τ_p^{C} for three typical wavelengths of the MWSR: (a) 500 nm, (b) 750 nm and (c) 935 nm, along with the parameters of linear regression analysis.

A striking feature of these scatter plots is that the data appeared to be more scattered for shorter wavelengths, while it is less scattered for longer wavelengths.The distribution of data points is almost symmetrical about the dotted line (unity slope). Performing a linear regression analysis yielded the relations $\tau_p^{C} = 0.0252 + 1.0069 \times \tau_p^{SAWH}$, $\tau_p^{C} = -0.0074 + 1.0216 \times \tau_p^{SAWH}$ and $\tau_p^{C} = -0.0109 + 0.9976 \times \tau_p^{SAWH}$; with high correlation coefficients (R^2) of 0.86, 0.89 and 0.98; and standard deviations (*SD*) of 0.08, 0.04 and 0.01 at 500 nm, 750 nm and 935 nm, respectively. The ensemble averaged $\langle\tau_p^{C}\rangle$ at 500nm 750 nm and 935 nm are 0.387, 0.237 and 0.189, respectively, which are 7.79%, 1.87% and 1.4% higher than $\langle\tau_p^{SAWH}\rangle$ of 0.359, 0.235 and 0.177.The values indicate that the columnar AODs are only slightly higher than the SAWH AODs. The difference is prominent at shorter wavelengths but diminishes at longer wavelengths.The near unity slope in the regression line equations along with higher correlation coefficients and near zero y-intercept suggest that the columnar AOD is almost entirely due to the SAWH AOD at longer wavelengths, but may have additional components at shorter wavelengths. This may be due to the near background state of the stratospheric aerosolsas applicable to this dataset (please see Deshler, et al., 2003) and the relative abundance of smaller aerosol particles at higher atmospheric layers.

Fig. 3 shows the spectral distribution of monthly mean AOD for two successive South Asian winter seasons(a) 2002-2003 and (b) 2003-2004. Both the columnar AODs (open symbols) and the SAWH AODs (solid symbols) are plotted for the purpose of inter-comparison. Error bars are omitted for the readability of features.

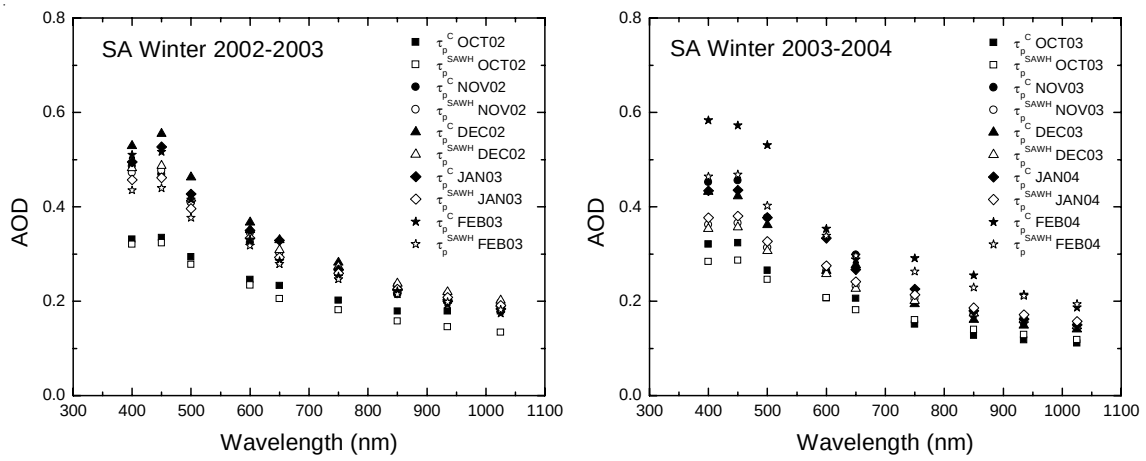

Figure3. The spectral distribution of monthly mean AOD for two successive South Asian winter seasons (a) 2002-2003 and (b) 2003-2004. The open symbols represent the SAWH AOD while the solid ones, the columnar AOD.

The data show monthly as well as inter-annual variations. During the winter season 2002-2003 the spectral AOD increases gradually from the month of October to December and then decreases slightly up till the end of the season in February 2003. During 2003-2004 the spectral AOD increases from the month of October to November and then decreases slightly in the month of December. It rises again and reaches its peak by the end of the season in February 2004. For both the winter seasons (i.e., during 2002-2003 as well as 2003-2004) the lowest values of spectral AOD were recorded during the month of October due to the effect of synoptic meteorology on the lower atmospheric aerosols. The highest rainfall received during the transition period of summer and winter monsoons (please see the climatic features of rainfall at Visakhapatnam in Rao & Niranjan, 2012b) effectively cleanses the atmosphere and lowers the AOD during the month of October since wet deposition is the most effective in removing aerosol mass from the lower atmosphere (Jaenicke, 1984). The abundance of haze at this location is primarily due to the advection of polluted aerosol from Indo-GangeticPlains by the synoptic wind field, driven by the differential heating between landmass and the adjacent oceanic water body of the Indian subcontinent (Rajeev, *et al.*, 2000; Nair, *et al.*, 2003, Rao, 2009; Rao & Niranjan, 2012a, 2012b).Thus, the observed variability in spectral AOD can be attributed to the loading and removal of SAWH at this location, and the effect of synoptic meteorology. Significant inter-annual variations of SAWH AOD are also possible due to excursion of Inter Tropical Convergence Zone along with large-scale vertical decent airmass over the peninsular India (Saha, et al., 2005).

CONCLUSIONS

1. This study retrieves and compares the aerosol spectral optical depths of the South Asian winter haze with that of the columnar aerosol optical depths obtained during two successive winter seasons at a tropical coastal station, Visakhapatnam.

2. There is generally a good agreement between the two at all wavelengths. The columnar AODs are only slightly higher than the SAWH AODs. The difference is prominent at shorter wavelengths but diminishes at the longer wavelengths side.

3. The large spread in SAWH AOD during the wintertime at this station can be explained on the basis of loading and removal of the haze, and the effect of synoptic meteorology.

REFERENCES

Deshler, T., Hervig, M. E., Hofmann, D. J., Rosen, J. M., and Liley, J. B. (2003). Thirty years of in situ stratospheric aerosol size distribution measurements from Laramie, Wyoming (41°N), using balloon-borne instruments, *J. Geophys. Res.*, **108(D5)**, 4167.

Gautam, R., Hsu, N. C., Kafatos, M., and Tsay, S.C. (2007). Influence of winter haze on fog/low cloud over the Indo-Gangetic plains, *J. Geophys. Res.*,**112**, D05207.

Jaenicke R. (1984). Physical aspects of atmospheric aerosol: *Aerosols and Their Climatic Effects*, (A. Deepak Publishing, USA)

Moorthy, K. K., Satheesh, S. K., and Murthy, B. V. K. (1997). Investigations of marine aerosols over the tropical Indian Ocean, *J. Geophys. Res.*, **102**, pp. 18827–18842.

Moorthy, *et al*. (1999). Aerosol Climatology over India, *ISRO-GBP Scientific Report: ISRO-GBP-SR-03-99*, ISRO, Bangalore, India.

Moorthy, K. K., Saha, A., Prasad, B. S. N., Niranjan, K., and Jhurry, D. (2001). Aerosol optical depths over peninsular India and adjoining oceans during the INDOEX CAMPAIGNS: spatial, temporal and spectral characteristics, *J. Geophys. Res.*, **106**, pp. 28539–28554.

Nair, S. K., Rajeev, K. and Parameswaran, K. (2003). Wintertime regional aerosol distribution and the influence of continental transport over the Indian Ocean, *J. Atmos. Solar Terr. Phys.*,**656**, pp. 149–165.

Niranjan, K., Ramesh Babu, Y., Satyanarayana, G.V. and Thulasiraman, S. (1997). Aerosol spectral optical depths and typical size distributions at a coastal urban location in India, Tellus, **49B**, pp. 439–446.

Niranjan, K., MalleswaraRao, B., Saha, A., and Murthy, K.S.R. (2004).Aerosol spectral optical depths and size characteristics at a coastal industrial location in India-effect of synoptic and mesoscale weather, *Ann. Geophys.*, **22**, pp. 1851–1860.

Rajeev K., Ramanathan, V. and Meywerk, M. (2000). Regional aerosol distribution and its long range transport over the Indian Ocean, *J. Geophys. Res.*,**105**, pp. 2029– 2043.

Ramanathan V., et al. (2001). The Indian Ocean Experiment: An integrated analysis of the climate forcing and effects of the great Indo-Asian haze, *J. Geophys. Res.*,**106**, pp. 28371–28398.

Rao B.M. (2009). Remote Sensing the South Asian Winter Haze at Visakhapatnam using a ground-based Multi-wavelength Solar Radiometer, Ph. D. thesis, Andhra University, Visakhapatnam, India.

Rao B.M. and Niranjan K. (2012a). Optical properties of the South Asian winter haze at a tropical coastal site in India, *Atmos. Environ.*,**54**, pp. 449–455.

Saha, A., Moorthy, K. K., and Niranjan, K. (2005). Interannual Variations of Aerosol Optical Depth over Coastal India: Relation to Synoptic Meteorology, *J. Appl. Meteorol.*, **44**, pp. 1066–1077.

Satheesh S.K., et al. (1999). A model for the natural and anthropogenic aerosols over the tropical Indian Ocean derived from Indian Ocean Experiment data, *J. Geophys. Res.*, **104**(D22), pp. 27421–27440.

Shaw, G.E., Peck, R.L., and Allen, G.R. (1973). A filter-wheel solar radiometer for atmospheric transmission studies, *Rev. Sci. Instrum.*,**44**, pp. 1772-1776.

Shaw G.E. (1983). Sun photometry, *Bull. Amer. Meteor. Soc.*,**64**, pp. 4–10.

Tahnk, W.R., and Coakley, J. A. Jr. (2002). Aerosol optical depths and direct radiative forcing for INDOEX derived from AVHRR: Observations. January–March, 1996–2000, *J. Geophys. Res.*, **107**(D19), 8010.

UNEP and C^4 (2002).*The Asian Brown Cloud: Climate and other Environmental Impacts*, (United Nations Environmental Programme, Nairobi, Kenya)

IMPACT OF INTENSE DUST STORM EVENT ON AEROSOL CHARACTERISTICS AND SURFACE RADIATIVE FORCING OVERALIBAG, WESTERN COAST OF INDIA

G.V. PAWAR[1], G. R. AHER1, PAWAN GUPTA[2], P. C. S. DEVARA[3],

[1]Physics Department, Nowrosjee Wadia College, Pune 411 001, India
[2]Universities Space Research Association, Columbia, MD 20771, USA
[3]Indian Institute of Tropical Meteorology, Pashan, Pune 411 008, India
Email: ganesh@physics.unipune.ac.in

Keywords: AEROSOL, AOD AND RADIATIVE FORCING

INTRODUCTION

Dust is one of the major types of tropospheric aerosol. A dust particle perturbs the radiation energy balance of the Earth-atmosphere system, and thus is considered to be a significant climate forcing factor. (Haywood and Boucher, 2000; Satheesh and Ramanathan, 2000). Dust storms also affect atmospheric heating and stability, tropical cyclone activity, chemical and biological ecosystem, as well as ambient air quality and human health.

Dust storms are a kind of natural disaster occurring most frequently over deserts and regions of dry soil, where particles are loosely bound to the surface (Slingo, et al., 2006). Dust aerosols get lifted into the air by the strong surface winds(> 5 ms^{-1}) and can swept thousands of kilometers downwind from the source region and represent an important process of land-atmosphere interaction. (Tegen, *et al.*, 1996; Ginoux, *et. al.*, 2001).Dust storms produced considerable reduction invisibility; reduce soil fertility in dust storm source areas, damage telecommunication and mechanical systems and cause air pollution.

On a global scale, dust contributes to about one quarter of aerosol optical depth (AOD) in the mid-visible wavelengths. Mineral dust is believed to play an important role in radiative forcing, with an estimated global TOA radiative forcing in the range -0.6 to 0.4 W/m^2 (IPCC, 2001). Remote sensing is an established method for the detection and mapping of dust events due to the high spatial variability of the dust plume characteristics along its transport (Badarinath, *et al.*, 2007).

In the present study, we have analysed for the first time the optical and physical properties of aerosols during the dust event that occurred over Alibag, Western coast of India, during March 21-22, 2012.

OBSERVATIONAL DATA AND SITE

Alibag ($18^0$65' N, $72^0$86' E, 0 amsl) is situated on the Western coast of India and on shore of Arabian Sea. Collocated measurements of aerosol optical depth (AOD)and Short Wave global solar flux in the spectral range 0.28-2.8 μm by employing MICROTOPS II sun photometer (at wavelengths 0.44, 0.5, 0.675, 0.870 and 1.020 μm) and Precision Spectral Pyranometer (PSP) respectively were carried at the IIG Alibag Magnetic Observatory. These were supplemented with concurrent meteorological observations and MODIS (Aqua and Terra) Level 2AOD values averaged over 30x30 km^2 box centered at station.

RESULTS AND DISCUSSIONS

IDENTIFICATION OF DUST EVENT

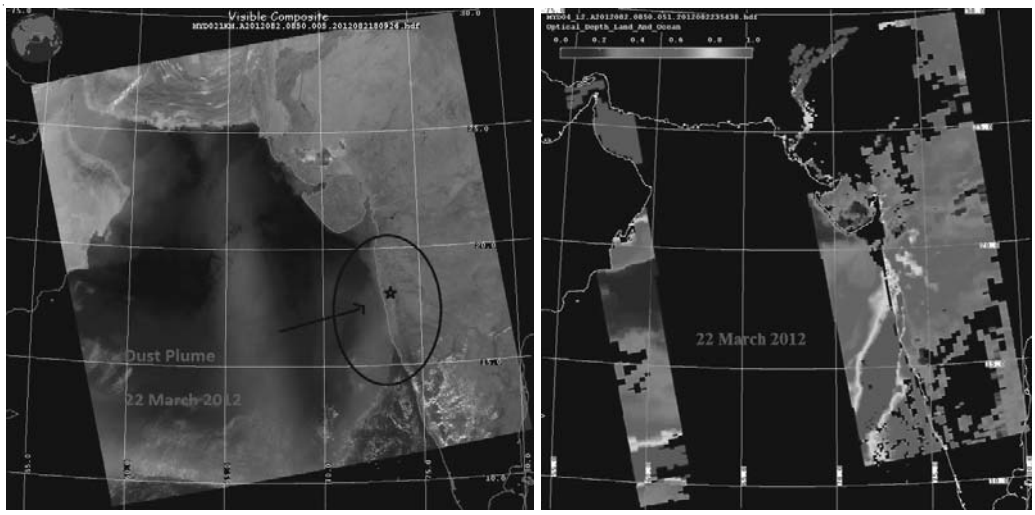

(a) ***(b)***

Figure. 1(a & b) Satellite image from Terra-MODIS sensor on March 22, 2012

Fig. 1(a) shows the True Color Composite/False Color Composite (FCC) of Terra/Aqua MODIS respectively for 22nd March 2012 covering the Western coast of India. An intense thick layer of dust/haze can be clearly seen from Fig. 1(a) over the observing site on. Several meteorologists have characterized ensuing dust activity as a "super sandstorm" whose effects are seen over Southeast Asia. Fig. 1(b) shows that the spatial distribution of Aqua-MODIS AOD_{550} over Western coast of India on 22nd March 2012. During this dust storm, values of AOD_{550}> 0.8 occur over the observing site, indicating presence of dust aerosols.

AEROSOL OPTICAL PROPERTIES AND SURFACE RADIATIVE FORCING

Day-to-day variation of AOD, surface radiative forcing (SRF) and Angstrom exponent obtained from ground based (Microtops) and Satellite (MODIS Terra and Aqua sensors)measurements is analyzed during the month of March. Results are shown in Fig. 2. From the figure, it is seen that both AOD on an average is about 0.45 for normal observing days. It rises considerably and becomes about 2.2 - 2.5 times its value on the days of the dust event i.e. on 21-22 March 2012 (Fig. 2a). The corresponding Angstrom exponent (AE)derived from the Angstrom empirical formula (AOD = â ë$^{-á}$) by evolving linear least square fit to the log-log plot of AOD against wavelength (ë in µm) is anti-correlated with AODs. Fig. 2e indicates that AE is about 0.39of the average value (1.16) on days before occurrence of dust event. Increase is more pronounced at longer wavelengths (ë > 0.675 µm). This indicates that on the days of dust, aerosol loading is much higher probably due to coarse-mode aerosols outnumbering fine-mode aerosols. Maghrabi, *et al.*, (2011) have analyzed the impact of the March 2009 dust event in Saudi Arabia on aerosol optical properties. They reported that AOD at 550nm increased from 0.396 to 1.71. The Angstrom exponent á rapidly decreased from 0.192 to -0.078. The mean AOD at 550 nm on the day of the storm was 0.953 higher than during the previous clear day, while á was -0.049in comparison with 0.323 during the previous day.

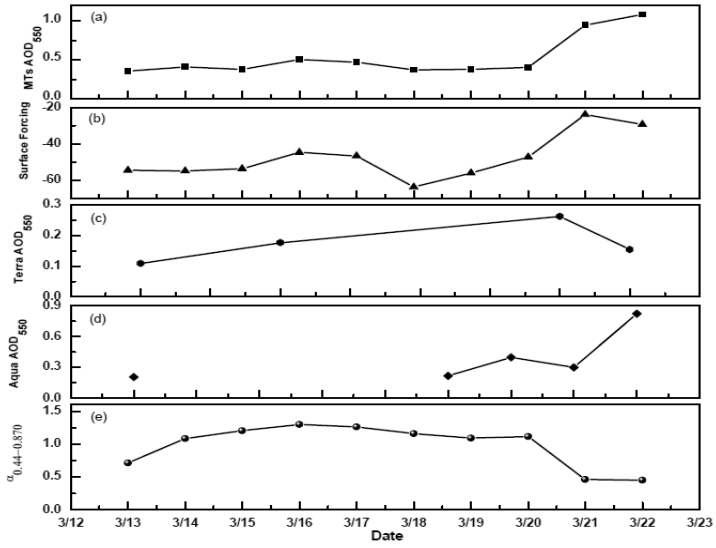

Figure 2 (a, b, c, d, e) Day-to-day variation of Microtops II sunphotometer AOD_{550}, Short wave aerosol direct radiative forcing, AOD_{550} from Terra and Aqua – MODIs sensors and Angstrom exponent ($\alpha_{0.44\text{-}0.870}$)

Fig. 2(b) also shows the day-to-day variation of surface radiative forcing (i.e. the change in short wave solar flux per unit 0.1 AOD). As the dust storm activity builds up, SRF shows two-fold rise as compared to its value during non-dust days and attains its maximum values of -23.9 W/m^2 and -29 W/m^2 on 21 March and 22 March, 2012 respectively. Thus, the dust event affects the radiative balance of the atmosphere.

CONCLUSIONS

The present study examines the effect of dust storm event on aerosol optical and radiative properties of atmospheric aerosols over Alibag. Significant increase in AODs values up to 1.13 has been observed during the dust storm event, with the pronounced increase at longer wavelengths. This indicates higher aerosol loading due to dominance of coarse-mode aerosols as compared to fine-mode aerosols. The results on Angstrom exponent variation and surface radiative forcing on these days also corroborate this finding. The Aqua-MODIS observations justify the dust transport over Alibag particularly on March 21-22, 2012.

ACKNOWLEDGEMENTS

The present study was supported and funded by the Indian Space Research Organization under the joint programme of ISRO. Authors also thank the Principal, Nowrosjee Wadia College, Pune and Dr. M. M. Andar, Secretary, Modern Education Society, Pune for support and encouragement.

REFERENCES

Badarinath, K.V.S., Kharol, S.K., Kaskaoutis, D.G., Kambezidis, H.D. (2007). Case study of dust storm over Hyderabad area, India: its impact on solar radiation using satellite data and ground measurements, *Science of the Total Environment*, **384**, 316.

Haywood, J. M., and Boucher, O. (2000). Estimates of the direct and indirect radiative forcing due to tropospheric aerosols: A review., *Review of Geophysics*, **38**, 513.

Intergovernmental Panel on Climate Change (2001). Climate Change 2001: The Scientific Basis. Contribution of Working Group 1 to the Third Assessment Report, (Cambridge Univ. Press, New York)

Maghrabi, A., Alharbi, B, Tapper, N. (2011). Impact of the March 2009 dust event in Saudi Arabia on aerosol optical Properties, Meteorological Parameters, Sky temperature and emissivity, S1352-2310(11)00112-9, 10.1016/j.atmosenv.2011.01.071.

Ginoux, P., Chin, M., Tegen I.,et al. (2001). Sources and distributions of dust aerosols simulated with the GOCART model, *Journal of Geophysical Research*,**106**, D17, pp. 20255–20273.

Satheesh, S.K. and Ramanathan, V. (2000). Large differences in tropical aerosol forcing at the top of the atmosphere and Earth's surface, *Nature* , **405**, 60.

Slingo, A., *et al.*, (2006). Observations of the impact of a major Saharan dust storm on the atmospheric radiation balance, *Geophysical Research Letters*, **33**, L24817.

Tegen, A., Lacis, A. and I. Fung I. (1996). The influence on climate forcing of mineral aerosols fromdisturbed soils, *Nature*, **380**, 6573, 419.

SEASONAL TREND OF AIRMASS BACKWARD WIND TRAJECTORIES AND ITS ASSOCIATION WITH AOD 550nm OVER WESTERN INDIAN THAR DESERT SITE

B. M. VYAS, MUKESH KUMAR VERMA AND ABHISHEK SAXENNA

Department of Physics, M. L. Sukhadia University, Udaipur – 313001 (Rajasthan) INDIA
E mail :bmvyas@yahoo.com

Keywords: ATMOSPHERIC AEROSOLS, ANTHROPOGENIC ACTIVITY, LONG RANGE TRANSPORT, AIR MASS BACKWARD WIND TRAJECTORY

INTRODUCTION

Although, the day to day and seasonal aerosols optical depth (AOT) variability has been associated with large number of sources and sinks mechanisms deal to anthropogenic as well as natural activities (Charlson, *et al.*, 1992). However, the contributions about such types of variability concerned to anthropogenic types of aerosols loading are quite dominant as compared to natural activities. It is due to rapid rise of present industrial growth, urbanization, production, and consumption of fossil and biomass fuel energy due primary need of human population growth in the present decades (Seinfeld and Pandis, 1998). In such numerous manmade and natural activities, aerosols sources and sinks are also possessing a wide range of complex varieties overseveral geographical region during different seasons, in which the role of long range transportation phenomena is very much pronounced and well dominated type of causes of variability of air pollutants over receptor side due transportation of the shortlived air pollutants from far reaching site(Moorthy, *et al*., 2003).Thus, advection of aerosols with air mass movement has identifiedas one of the major potential source to explain day-to-day and seasonal variability in aerosols loadings over observing site in recent years. Extensive studies over different parts of world have given the indication that the aerosols or air pollutants concentrations at any receptor site may be perturbed due advection of air mass from far away remote areas(Moorthy, *et al*., 2003; Nair, *et al*., 2007). In realizing this perspectives, main objective of this study is focused on study the effect of transportation of air pollutants during different air mass back ward trajectory (AMBWT) parameters on the aerosols loading characteristics in each season of period from 2009-2011 over Western Indian region located in central part of Thar Dessert tropical site i.e., Jaisalmer. (27° N, 70°E, 221m).

DATASETS AND METHODOLOGY

The basis of present work is collection of each day backward air mass trajectories concerned to observing site of Jaisalmer at 500m and 4 km during the entire three year period from 2009 to 2011. Such daily backward air mass trajectories for study period have been accessed from http://www.ready.noaa.gov/. (Draxler & Roliph, 2003).**READY(Real-time Environmental Applications and Display sYstem)** is a world-wide-web based system that has been developed for accessing meteorological data file and obtaining each trajectory and dispersion model file of particular selected duration on **ARL**'s **(Air Resources Laboratory)** web server. Each day estimated 72- hours isentropic AMBWT is used to compute the percentage occurrences of its originated directions, its corresponding originated height value for individual group direction and their percentages duration of its path on land and sea for all the days of AOD measurements concerned to observing site. In the this work, only eight source group of directions such as North (N), North-East (NE), East (E), South-East (SE), South (S), South–West (SW), West (W) and North-West (NW) from

the observing location are considered. After that for these individual group direction, its corresponding mean percentage occurrence, their average source height, percentage duration of its paths on sea and continents or land are computed for two height (500m and 4km) as well as every season for the selected period. In the present study, following seasonal groupings are made according to group of following months; Winter season includes the December to February, Pre- monsoon consider the March to June, Monsoon season covers the July to September and Post- Monsoon season includes the October and November.

The results of variation of average percentage occurrence of each group direction, their average originated height, percentage duration of its path on sea and continent and their average value of MODIS derived AOD 550nm and these standard errors in that days of seasons are plotted with respect to each group directions for Pre – monsoon & Monsoon as well as Post Monsoon & Winter season of height 500m (below the atmospheric boundary layer), and 4km (free tropospheric height) over Jaisalmer, separately, in Fig. 1(a-d) and 2(a-d),.

RESULTS AND DISCUSSIONS

(i) Pre Monsoon season

It is observed from Fig. 1(a,b) that during Pre Monsoon, average value of percentage occurrences of air mass wind coming from different originated direction groups towards the observing site have been found to be maximum range in 40 to 55 % in SW followed by NW order of 40% for the case of 500 m altitude case, whereas in case of 4 km altitude over measuring site, the such maximum percentage occurrencesvalues are observed in range from 45 to 75% from NW followed by SW direction ranging from 15 to 35%. It is very interesting to note at here that AOT values from .45 to .9 areobserved onlyindirection groups of like NE, SE,SW and NW. During such same direction groups, the source heights ranges of AMBWT of 500m and 4km are found to be varied from .5 to 3km and 4km to 8km, respectively. In same group directions, maximum percentage duration of path of air mass movement parcel is seen on both land and sea area for both trajectories cases.

(ii) Monsoon season

The mean percentage occurrences of originated direction groups of AMBWT in monsoon month have shown higher values in SW direction site case of 500m and NW & SE for the case of 4km above the observing site (Fig.1 c-d). The AOT valuesin range of .8 to 1.3 and .6 to 1.2 for both AMBWT cases areobserved only NE, SE, SW and NW direction groups.In such direction group of observed AOT value, it also displays the source height from .3 to 3 km and .5 to 5 km in case of 500m, and 4km with highest altitude in NW direction only, for both AMBWT cases. Furthermore, the duration of AMBWT is seen more on sea region specifically in SW direction than to the land in both trajectories.

(iii) Post Monsoon season

The average behavior of the some AMWBT' s parameters of 500m and 4km in post monsoon month with respect to specified direction groups are depicted for thestudy period in Fig 2(a,b). It is clear from the figures that the higher values of percentage occurrences of sources direction groups are found in SW, NE, NW & SE and NW, SW , SE sides from the receptor side at 500m and 4km altitude, respectively. It is also noticed at here that AOT value from .3 to .7 are also found in such direction groups where, the source heights of AMBWT of 500m and 4km are seen to changed between .5 to 2.5km and 2 to 6km, respectively. In the same directions sector, the duration

of path of AMBWT for both cases is found to retain only on the land except the SW direction, where trajectories paths are seen on both land and sea.

(iv) Winter season

Fig. 2(c,d) illustratethe variation of various AMWT's variables concerned to both cases with function of different direction groups for winter month of period 2009-11. It is evident at here that main source direction group isonly NE site for the 500m AMBWT case, while in case of 4km , such direction groups are NW and SW. The AOT values from .2 to .4 are observed in NE, SE, SW and NW for reaching air mass at 500m above the experimental site. However, in caseof 4km, the AOT's range is observed from .3 to .5 in NW, SW and SE . The aerosols are seen to advected from height values from 500m to 3km and .5 to 6km for AMBWT of 500m and 4km, respectively. During winter months, the maximum duration of path trajectories are observed only over land region.

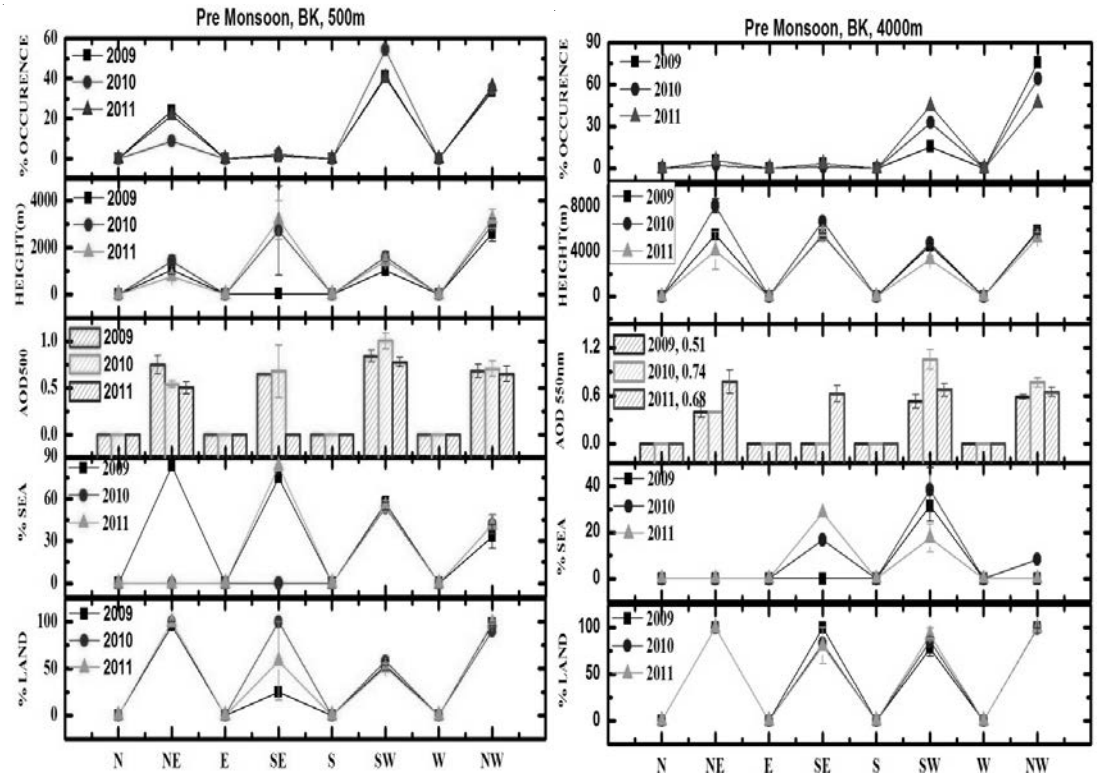

(a) (b)

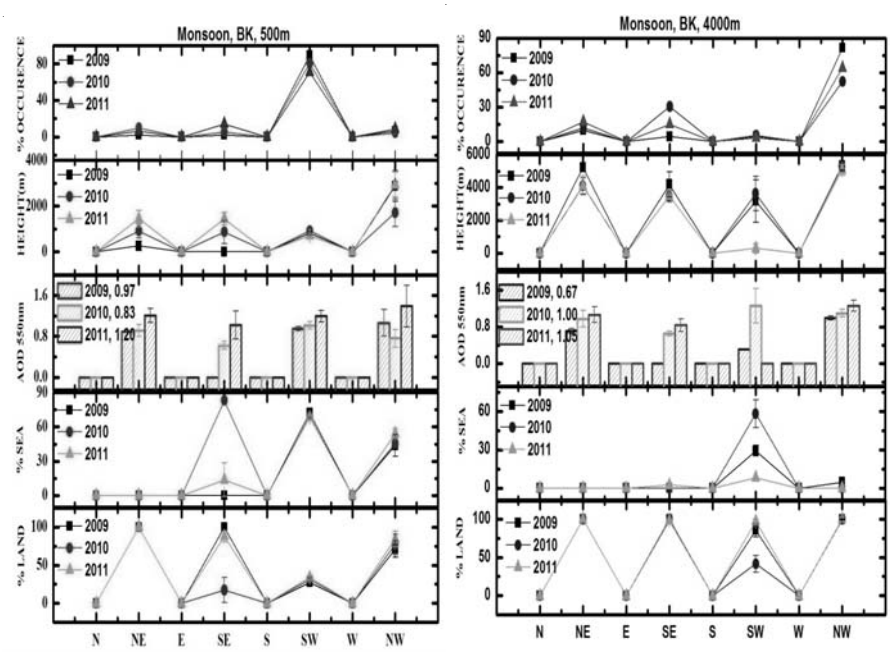

(c) (d))

Figure 1(a-d). Direction groups of air mass backward wind trajectories

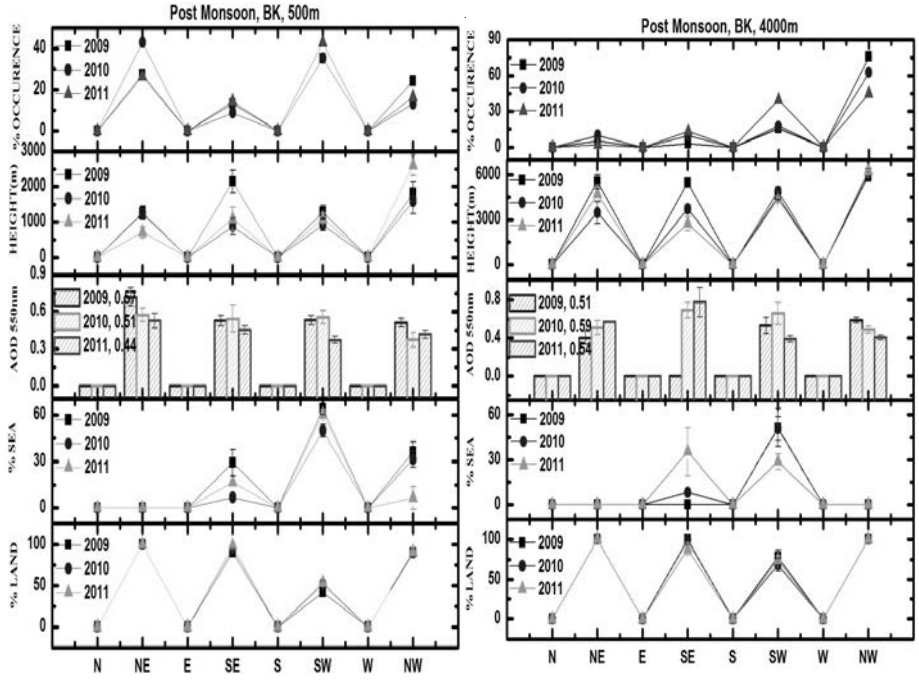

(a) (b)

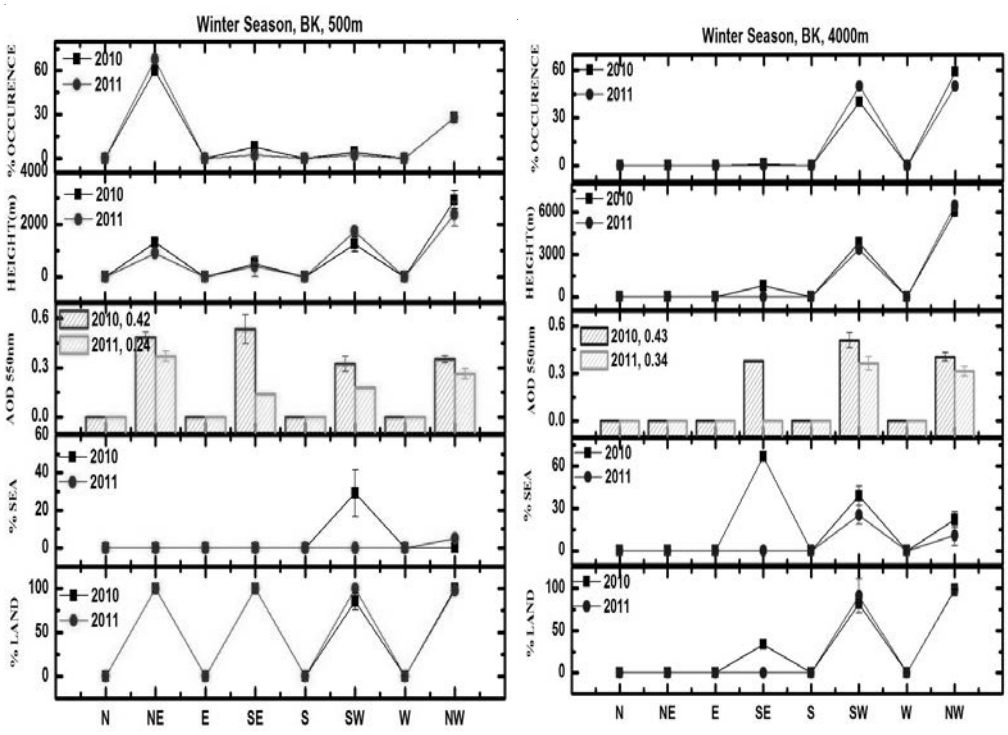

(c) (d)

Figure 2 (a-d). Direction groups of air mass backward wind trajectories

CONCLUSIONS

The maximum percentage occurrence of source direction groups of AMBWT over 500m at Jaisalmerare are seen in SW and NE directions during Monsoon and winter month, respectively. However, during Pre-monsoon and Post- Monsoon month's maximum values of occurrences are seen in SW and NE which show the mixed pattern observed in Monsoon and winter month. While in case of 4km of AMBWT, the most predominant direction sectors are NW and SW direction in all three season except in Monsoon month, it main direction groups are NW,SE and NE. The occurrences of AMBWT of 4 km have shown the highest values for NW direction group in all season. But, the highest occurrences' of AMBWT of 500m show in SW direction in all season except in winter season, it is primarily seen towards NE direction. The variation of AOD value in each season are not dependent only the maximum occurrence value for direction group, but, at the same, it also depend on source height,as well as duration of air mass trajectories on land or seas. The air mass coming from lower altitude and more on land area are portrayed the higher variation in AOT values for any particular season, even than value of percentage occurrence is very low in both cases like below the boundary layer and from the tropospheric height.

ACKNOWLEDGEMENT

The work was carried out under ARFI Research Project as a part of ISRO- GBP. Authors would like to express their sincere gratitude to Prof. K. Krishna Moorthy, Projector Director, ARFI, Director,

SPL, VSSC, and Dr S. Suresh Babu, Project Manager, ARFI, SPL, VSSC, Trivandruam for fruitful discussions.

REFERENCES

Charlson, *et al.* (1992). Climate forcing by anthropogenic aerosols, Science, **255,** pp. 423-430.

Seinfeld, J. H., Pandis, S. N. (1998). Atmospheric Chemistry and Physics, Wiley, Hoboken, N.J. 662.

Draxler, R. R., Rolph, G. D., (2003). HYSPLIT (Hybrid Single-Particle Lagrangian Integrated

Trajectory) Model access via NOAA ARL READY Website (http://www.arl.noaa.gov/

ready/ hysplit4.html), NOAA Air Resources Laboratory, Silver Spring, MD.

Moorthy, K. K., Babu, S. S. and Satheesh, S. K. (2003). Aerosol spectral optical depths over the Bay of Bengal: Role of transport, Geophys. Res.Lett., **30(5)**, 1249.

Nair, *et al*. (2007). Wintertime aerosol characteristics over the Indo-Gangetic Plain (IGP): Impacts of local boundary layer processes and long-range transport, *Journal of Geophysical Research,***112**, D13205.

SEASONAL VARIATION OF THE SURFACE AEROSOL RADIATIVE FORCING DERIVED FROM THE GROUND-BASED MEASUREMENTS AT DELHI

SACHCHIDANAND SINGH, S NASEEMA BEEGUM, SHAMBHUNATH

Radio & Atmospheric Sciences Division, National Physical Laboratory, CSIR,
New Delhi-110012
E mail: ssingh@nplindia.org

Keywords: AOD AND SCATTERING ALBEDO

INTRODUCTION

The effect of atmospheric aerosols on radiation balance of earth is well recognised now at local, regional and global levels. The aerosols are known to affect the climate directly by scattering and absorbing the solar and terrestrial radiation, and indirectly by affecting the lifetime and albedo of the clouds. Aerosols are also thought of modifying the precipitation. The radiative effects of aerosols, called the aerosol radiative forcing is measured in terms of W/m^2. Usually, the aerosol radiative forcing is estimated by measuring the aerosol optical properties and then using the same in the radiative transfer models.Generally, these radiative transfer models assume a certain vertical structure which can cause uncertainty in the radiative forcing estimations. Other sources of uncertainty in the ARF estimations arise from the estimation or measurements of aerosol properties like, single scattering albedo (SSA), asymmetry parameters, size distribution of aerosols and uncertainty in the surface albedo values. Instead, the aerosol radiative forcing estimated from the direct flux measurements may be more sensitive and accurate than the model estimates.

In the present case simultaneous measurements of surface irradiance and aerosol optical depth (AOD) during clear-sky conditions spanning over a year during April 2010 to March 2011 have been used to estimate the aerosol radiation forcing (ARF) at the surface.

RESULTS AND DISCUSSIONS

The ARF has been estimated for three different wavelength regions, shortwave (310-2800nm), UV (280-400nm) and Infra-Red (4.5 to 42 m). The surface flux was measured using the Kipp Zonen Pyranometers and the AOD was obtained using the microtop sunphotometer. In order to obtain the monthly ARF at the surface, the aerosol radiation forcing efficiency was first calculated and then multiplied with the average AOD. This method is commonly known as the differential method which is independent of model assumptions and small instrumental calibration errors.

Fig. 1 shows the average monthly aerosol optical depth measured during the observation period. The vertical bars indicate the 1σ standard deviation of the data from the average. It clearly shows that the AOD is generally very high at Delhi with minimum during September, which was the rain affected month and the maximum was during the month of November, which was the festival season affected by crackers etc. The pre-monsoon months also had high AOD values. These observations are in line with other previous AOD observed at Delhi.

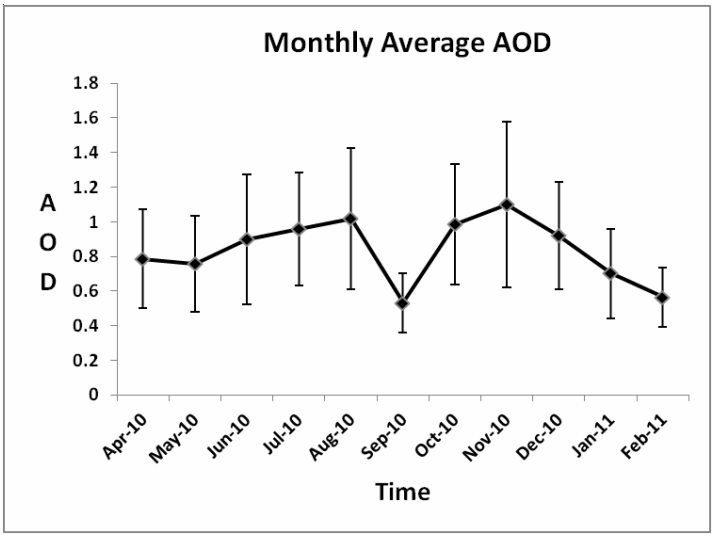

Figure 1. Monthly averaged AOD values as observed at Delhi during observation period. (Vertical bars denote standard deviations)

Fig. 2 (lower panel) shows the average monthly forcing efficiencies calculated in the shortwave wavelength range (310 - 2800nm). The preliminary investigation shows that the averagemonthly shortwave aerosol radiation forcing efficiency during the year is generally found to vary in the range -40 to -100 W/m^2 per unit AOD at 500nm.The calculated Radiative forcing efficiencies depicted strong seasonal variations.

The forcing efficiency when multiplied with the average aerosol optical depth gives rise to the observed aerosol forcing at the surface. The aerosol forcing at the surface varied in the range -38 W/m^2 to - 67W/m^2. It was maximum (most negative) during April which gradually decreased till November (least negative) and then again starts increasing.

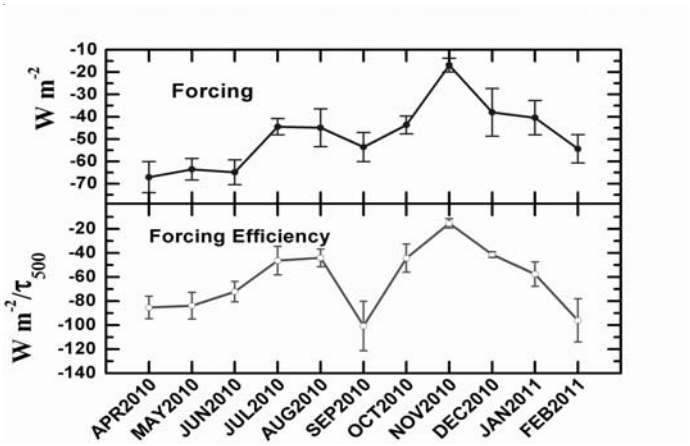

Figure 2. Average Forcing Efficiency and the monthly averaged surface aerosol radiative forcing in shortwave region at Delhi.

ATMOSPHERIC CIRCULATION AND AEROSOL RADIATIVE FORCING OVER INDIA: CURRENT STATUS

RAJ PAUL GULERIA, JAGDISH CHANDRA KUNIYAL* AND NAND LAL SHARMA

G.B. Pant Institute of Himalayan Environment and Development, Himachal Unit,
Mohal-Kullu 175 126, Himachal Pradesh, India
E-mail: jckuniyal@gmail.com, jckuniyal@rediffmail.com

Keywords: AEROSOL RADIATIVE FORCING

INTRODUCTION

Aerosols have great potential to bring the changes in the climatic conditions at regional and global scale. After IPCC report 1990 the studies of aerosol become most important among the space and atmospheric scientists of the globe. In this direction numerous efforts are taken by international and national agencies. Climate impact of aerosols remains uncertain despite concentrated efforts of global scientific community. This is mainly because of aerosols are not represented in climate models with adequate spatio-temporal heterogeneity. This is more so for India, with its large natural diversity, tropical nature, wide range of human activities, long coastline, vast semi-arid and arid regions. In late 1980's the major initiatives are taken in this direction under the Indian Space Research Organization Geosphere Biosphere program (ISRO-GBP). The Aerosol Radiative Forcing over India (ARFI) is the hallmark of ISRO-GBP under the umbrella of Space Physics Laboratory, Vikram Sarabhai Space Centre, Thiruvananthapuram as a lead centre. Under ARFI a number of Multi-wavelength Radiometer (MWR) installed and at present there are more than 30 MWR stations nationwide. The present study conducted over Mohal during April 2006 to March 2010 under ARFI, using MWR to characterize the radiative effect of aerosol in reducing the surface reaching solar radiation. Attempt is also made to document the seasonal variability in the surface aerosol radiative forcing (SARF) over Indian region (Fig. 1).

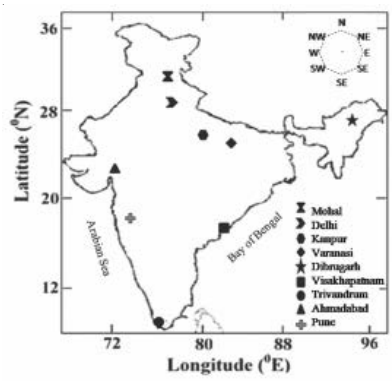

Figure 1. Seasonal variability in the surface aerosol radiative forcing (SARF) over Indian region

RESULTS AND DISCUSSIONS

Mohal (31.9°N, 77.12°E), located in the northwestern part of India, is a semi-urban continental site. During pre-monsoon (Pre-M) the predominant prevailing atmospheric circulation over Mohal is

generally northwesterly which shifts towards northeasterly during the monsoon (M). During post-monsoon (Post-M) and winter (W) the predominant prevailing atmospheric circulation over Mohal is westerly. The larger aerosol optical depth (AOD) and higher concentration of coarse mode aerosols in the Pre-M; smaller AOD and significant concentration of fine mode aerosols in Post-M are the main characteristics of the region. The SARF during Pre-M, M, Post-M and W are estimated to be –20.8 Wm^{-2}, –18.1 Wm^{-2}, –19.0 Wm^{-2},–19.8 Wm^{-2}, respectively.

Dibrugarh (27.3°N, 94.6°E), located in the northeast part of India, is a rural continental site. The predominant prevailing atmospheric circulation over Dibrugarh is generally northeasterly, which shifts towards easterly during the Pre-M and M (Gogoi, *et al.*, 2008). The larger AOD and higher concentration of coarse mode aerosols in the Pre-M; smaller AOD and significant concentration of fine mode aerosols in Post-M are the main characteristics of the region. The seasonal SARF during Pre-M, M, Post-M and W of the order of –37.1 Wm^{-2}, –33.7 Wm^{-2}, –12.5 Wm^{-2}, and –34.2 Wm^{-2}, respectively (Pathak, *et al.*, 2010).

Visakhapatnam (17.72°N, 83.32°E), located in the east coast of India, is an industrial site. During Pre-M period the predominant prevailing atmospheric circulation over Visakhapatnam is generally southwesterly, which transport marine aerosol from Arabian Sea into Bay of Bengal via Visakhapatnam. During W period the wind circulation is north-northeasterly, which transport continental airmass into Bay of Bengal via Visakhapatnam and therefore increase the possibility of anthropogenic aerosols (Niranjan, *et al.*, 2011). During Pre-M, M, Post-M and W the SARF are –16.8 Wm^{-2}, –9.9 Wm^{-2}, –2.81 Wm^{-2} and –35.78 Wm^{-2}, respectively (Sreekanth *et al.*, 2007).

Trivandrum (8.55°N, 76.96°E), located in the southern India, is a sparsely industrialized, semi-urban tropical coastal site. During W and Pre-M the prevailing atmospheric circulations in the lower troposphere is primarily from continental regions directed towards Arabian Sea, constitute continental airmass. Whereas during M and Post-M the prevailing wind circulation is almost reverse, directed from the Arabian Sea, constitute marine airmass (Pillai and Moorthy, 2004). The seasonal SARF during Pre-M, M, Post-M and W are reported –37.4 to –34.2 Wm^{-2}, –26.9 to –24.4 Wm^{-2}, –30.2 to –27.8 Wm^{-2} and –48.9 to –44.8 Wm^{-2}, respectively (Babu, *et al.*, 2007).

Pune (18.5°N, 73.8°E), is situated on the lee-side of the Western Ghats of India, is an urban environmental location (Bhawar and Devara, 2010). During Pre-M the prevailing winds are from the semi-arid region in the north-west of the site. Thus, the transport of soil dust from the semi-arid region is the major source of absorbing aerosols over Pune. During M season the prevailing wind circulation in the lower atmosphere is predominantly westerly, which is the source of marine aerosol. During Post-M north-westerly winds predominantly flow, which is the source of continental aerosols. Fair-weather conditions and light surface winds are the characteristics of the W season. The maximum value of SARF reported to be –27.9 Wm^{-2} during Pre-M while minimum –16.7 Wm^{-2} during W season (Bhawar and Devara, 2010).

Ahmadabad (23.03°N, 72.55°E), located in the western India, is a semiarid, industrial urban location. During Pre-M and M the prevailing winds are from Arabian Sea in the west-southwest of the site. During Post-M and W the winds are from continental India in the northwest and northeast of the site (Kedia and Ramachandran, 2011). Ganguly, *et al.* (2006) conducted the study on aerosol radiative forcing over Ahmadabad and report that during Pre-M, M, Post-M and W the SARF are –41.4 Wm^{-2}, –41 Wm^{-2}, –63 Wm^{-2} and –54 Wm^{-2}, respectively.

Delhi (28.63°N, 77.17°E), Kanpur (26.4°N, 80.4°E) and Varanasi (25.45°N, 83.03°E,) are the major cities located in the Indo-Gangetic Basin (IGB). During Pre-M period the predominant prevailing

atmospheric wind circulation over IGB is generally westerly to north-westerly, which shifts towards north-easterly during W. Kanpur located in the central part of IGB is one of the highly polluted mega cities in Asia. Significant higher surface forcing is reported by Sarkar, *et al*. (2006) during Pre-M (–70.97 Wm^{-2}) and W (–44.37 Wm^{-2}) in comparison to the western part i.e., Delhi and eastern part i.e., Varanasi. Over Delhi and Varanasi the SARF values during Pre-M are –67.18 Wm^{-2} and –46.36 Wm^{-2}, whereas during W –36.92 Wm^{-2} and –29.4 Wm^{-2}, respectively.

From the present analysis it conclude that during Pre-M the radiative effect of aerosol in cooling the earth's surface over the northwestern part of India, IGB and northeastern part of India is considerable higher as compared to other seasons, where coarse mode aerosols are accompanied with large fraction of desert aerosols. Over the southern and east coast part of India the radiative effect of aerosol in cooling the earth's surface is higher in W, where continental aerosols are accompanied with large fraction of anthropogenic aerosols. In western India the radiative effect of aerosol in cooling the earth's surface is noted to be higher in Post-M, where continental aerosols are accompanied with large fraction of anthropogenic aerosols. One of the main outcomes of the present discussion is that in the northern and eastern subcontinent of India the large reduction in surface reaching solar radiation is due to abundance of coarse mode aerosol loading with significant fraction of desert dust. In the western and southern subcontinent of India the large reduction in surface reaching solar radiation is mainly attributed to abundance of fine mode aerosols with significant fraction of anthropogenic aerosols.

ACKNOWLEDGEMENT

The authors are thankful to the Director, G.B. Pant Institute of Himalayan Environment and Development, Kosi-Katarmal, Almora (Uttarakhand) for providing facilities.

REFERENCES

Babu, S.S., Moorthy, K.K. and Satheesh, S.K. (2007). Temporal heterogeneity in aerosol characteristics and the resulting radiative impacts at a tropical coastal station - Part 2: direct short wave radiative forcing, *Ann. Geophys.* , **25**, 2309.

Bhawar, R.L. and Devara, P.C.S. (2010). Study of successive contrasting monsoons (2001-2002) in terms of aerosol variability over a tropical station Pune, India, *Atmos. Chem. Phys.* ,**10**, 29.

Ganguly, D., Jayaraman, A. and Gadhavi, H. (2006). Physical and optical properties of aerosols over an urban location in western India: seasonal variabilities, *J. Geophys. Res*., **111**, D24206.

Gogoi, M.M., Bhuyan, P.K. and Moorthy, K.K. (2008). Estimation of the effect of long-range transport on seasonal variation of aerosols over northeastern India, *Ann. Geophys.* ,**26**, 1365.

Kedia, S. and Ramachandran, S. (2011). Seasonal variations in aerosol characteristics over an urban location and a remote site in western India, *Atmos. Environ*., **45**, 2120.

Niranjan, K., Spandana, B., Devi, T.A., Sreekanth, V. and Madhavan, B.L. (2011). Measurements of aerosol intensive properties over Visakhapatnam, India for 2007, *Ann. Geophys*., **29**, 973.

Pathak, B., Kalita, G., Bhuyan, K., Bhuyan, P.K. and Moorthy, K.K. (2010). Aerosol temporal characteristics and its impact on shortwave radiative forcing at a location in the northeast of India, *J. Geophys. Res.*, **115**, D19204.

Pillai, P.S. and Moorthy, K. K. (2004). Size distribution of near-surface aerosols and its relation to the columnar aerosol optical depths, *Ann. Geophys*., **22**, 3347.

Sarkar, S., Chokngamwong, R., Cervone, G., Singh, R.P. and Kafatos, M. (2006). Variability of aerosol optical depth and aerosol forcing over India, *Adv. Space Res*., **37**, doi:10.1016/ j.asr.2005.09.043.

Sreekanth, V., Niranjan, K. and Madhavan, B.L. (2007). Radiative forcing of black carbon over eastern India, *Geophys. Res. Lett*., **34**, L17818.

SEASONAL VARIABILITY OF AEROSOL VERTICAL DISTRIBUTION OVER INDIA

GEORGE BASIL, PARUL SRIVASTAVA, SAGNIK DEY and P. AGARWAL

Centre for Atmospheric Sciences, Indian Institute of Technology Delhi

Keywords: AEROSOL VERTICAL DISTRIBUTION, SEASONAL VARIABILITY.

INTRODUCTION

Quantifying the effects of aerosols on the Earth's climate is one of the most challenging problems in atmospheric sciences. Aerosol-cloud interaction strongly depends on relative vertical distributions of aerosols and clouds (Chand, *et al.*, 2009). In India, where aerosol loading is very high, aerosol vertical distribution is not well-known due to lack of measurements. The present study analyzes CALIPSO data for six years during July 2006 to June 2012 in order to understand the seasonal variability of aerosol profiles over India to fill in this gap.

METHODS

The CALIPSO mission is dedicated to study the vertical distributions of clouds and aerosols in the atmosphere (Winker, *et al.*, 2009). CALIPSO is flying at 705 km in polar orbit with several other satellites forming a constellation called the A train.CALIPSO has operated since June 2006, measuring through its lidar CALIOP (Cloud Aerosol Lidar with Orthogonal Polarization), the total attenuated backscatter at 532 nm and 1064 nm, and the depolarization at 532 nm. With its vertical resolution of 60 m in the upper troposphere and 180 m in the stratosphere CALIPSO samples the atmosphere at global scale with an unprecedented resolution. Because of its near nadir view and the 16 day repeating cycle, a global view of aerosol can only be acquired by averaging the CALIOP cloud free profiles collected over a large period of time.

In this study, we calculate seasonal average cloud free aerosol extinction profiles and AOD over $5^0 \times 5^0$grids for robust statistics. The aerosol scale heights (H) for the region are calculated from the CALIPSO extinction profiles following Hayasaka, *et al.* (2007):

$$\int_0^H b_{ext} dz = (1 - e^{-1}) \times AOD = 0.63 \times AOD \quad (1).$$

Aerosol scale height is defined as the height above ground level below which 63% (i.e. the height up to which b_{ext} reduces by a factor of e) of total columnar extinction (i.e. AOD) is present.Although it does not represent the detailed vertical structure, it is a good approximation of the aerosol vertical distribution on regional and global scales, particularly for satellite retrievals, model simulations, and model-model and model-satellite inter-comparison (Yu, *et al.*, 2010). Note that the equation 1 is a parameterized expression of aerosol vertical distribution and does not follow exponential decay with increasing altitude. Analysis has been carried out for both day and night-time profiles.

The particulate depolarization ratio (PDR) profiles are analyzed to identify the occurrence of dust layers over India by using the threshold of 0.35 (Huang, *et al.*, 2008). The frequency of presence of dust in the atmosphere is calculated.

RESULTS

Fig. 1 shows the latitudinal cross section of extinction profile during day and night time over India.During the post-monsoon and winter seasons, scale heights are found to be lower than 1.25 km, suggesting the confinement of aerosols within boundary layer. During the pre-monsoon and monsoon seasons, elevated aerosol layers (spread up to 8-9 km altitude) are evident as the scale heights increase.The transport of dust across the Indian subcontinent during these seasons is supported by high PDR values with peak transport altitude at 4-5 km. The towering Himalayas form a barrier to the passage of dust storms, resulting in the accumulation of dusts, largely over the foothills of the Himalayas and the Indo- gangetic planes.

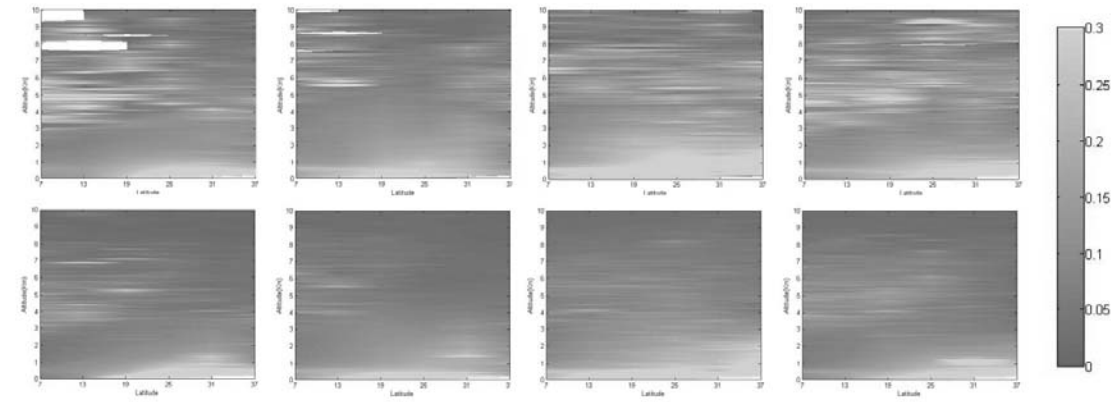

Figure 1. Latitudinal cross section ofExtinction Profile

Considerable difference is observed between AOD at daytime and nighttime. A case study over Delhi NCR is shown in Fig. 2, where in general, daytime AOD is found to be higher than night-time AOD in the post-monsoon to winter months and vice versa in the other two seasons. Previous studies (e.g. Singh, *et al.*, 2005; Srivastava, *et al.*, 2012) have considered standard tropical distribution of aerosols to calculate columnar optical properties from available chemical data. Sensitivity of AOD to scale height and thickness of aerosol layer has been carried out to understand the validity of such assumption. We found that AOD may be overestimated (for same composition) by as high as 40%, if the scale height is increased from 1 km to 2 km. These results provide benchmark statistics of aerosol vertical profiles that can be used to validate climate models and to improve estimations of aerosol forcing.

CONCLUSIONS

We have generated climatology of aerosol vertical distributions over India using six years of CALIPSO data. The seasonal variability shows thicker aerosol layer and larger scale heights in the pre-monsoon and monsoon seasons relative to the other two seasons. Significant difference in day and night-time profiles is observed in all seasons. Peak dust transport is observed to be at 4-5 km altitude during these two seasons. Sensitivity study shows that incorrect scale height and aerosol layer thickness can lead to significant error (as high as 40%) in estimated AOD, and hence in direct radiative forcing. These results may improve such estimates over India.

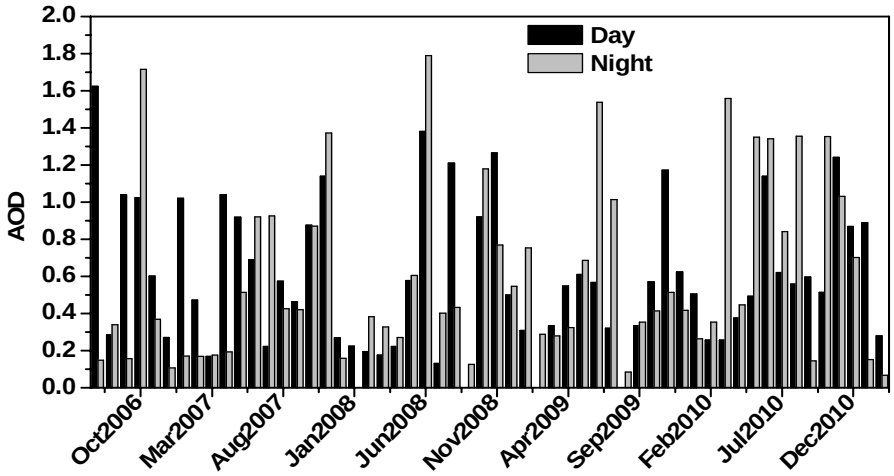

Figure 2. Mean monthly day and night-time AOD over Delhi during the study period

ACKNOWLEDGEMENTS

CALIPSO data are downloaded from Langley Atmospheric Science Data Centre. The work is partially supported by research grants from DST, Govt. of India under contract SR/FTP/ES-191/ 2010 through research project operational at IIT Delhi (IITD/IRD/RP02509).

REFERENCES

Hayasaka, T., Satake, S., Shimizu, A., Sugimoto, N., Matsui, I., Aoki, K., and Muraji, Y. (2007). Vertical distribution and optical properties of aerosols observed over Japan during the Atmospheric Brown Clouds-East Asia Regional Experiment 2005, *J. Geophys. Res.*, **112**, D22S35.

Jianping Huang, *et al.* (2008). Long-range transport and vertical structure of Asian dust from CALIPSO and surface measurements during PACDEX. ,*Journal of Geophysical Research*, **113**, D23212.

Singh, S., Nath, S., Kohli, R., and Singh, R. (2005). Aerosol over Delhi during pre-monsoon months: Characteristics and effect on surface radiative forcing, *Geophys. Res. Lett.*, **32**, L13808.

Yu, H. B., Chin, M., Winker, D. M., Omar, A. H., Liu, C. K. and Diehl, T. (2010). Global View of Aerosol Vertical Distributions from CALIPSO Lidar Measurements and GOCART Simulations: Regional and Seasonal Variations, *J. Geophys. Res.*, **115**, D00H30.

COLUMNAR AND SURFACE AEROSOL SINGLE SCATTERING ALBEDO OVER GADANKI AND THEIR IMPLICATION FOR AEROSOL RADIATIVE FORCING

V. RAVI KIRAN[1], HARISH GADHAVI[1], M. N. SAI SUMAN[1] AND A. JAYARAMAN[1]

[1]National Atmospheric Research Laboratory, Gadanki, 517 112 India
E-mail: varaharavi@gmail.com

INTRODUCTION

Aerosols scatter and absorb incoming solar radiation. Aerosol radiative forcing is defined as the difference in net flux with and without aerosol at any layer while keeping all other parameters constant. Flux without aerosol is obtained by radiative transfer models, whereas flux with aerosol can be obtained by radiance measurements or by radiative transfer model simulations. In the later case simulations requires aerosol optical properties such as aerosol optical depth, single scattering albedo and asymmetry parameter. It is understood that single scattering albedo (SSA) over an atmospheric column is often different from that of near-surface because of atmospheric dynamics and transportation of aerosols. However, researchers often rely only on near surface SSA observations to estimate aerosol radiative forcing, which may or may not be correct. In this article we discuss, difference between observed columnar and surface SSA and their implication for radiative forcing estimates.

DATA & METHODOLOGY

A climate observatory named ICON established at Gadanki campus of National Atmospheric Research Laboratory (NARL) aims at providing long-term and comprehensive data for aerosol and trace-gases properties. Observations of surface SSA are carried out since October 2008 using nephelometer and aethalometer. Scattering coefficient measured using is corrected for truncation error and non-lambertian-diffuser error by following an empirical relation (Anderson, *et al.*, 1998). Aethalometer measured attenuation coefficient of light is accounted for multiple scattering and shadowing effects (Weingartner, *et al.*, 2003) to ensure the derived absorption coefficient is error free. Observations of direct and diffuse radiation were carried out using Sky radiometer since April 2008. The software package SKYRAD.pack is used in retrieval of columnar SSA (Nakajima, *et al.*, 1996). One of the aerosol optical parameter namely asymmetry parameter is obtained from OPAC (Hess, *et al.*, 1998) by constraining the iterations of model till both the measured and observed AOD, SSA spectra approximately coincide with each other. Finally, aerosol radiative forcing at TOA as well as at surface is estimated using radiative transfer model SBDART (Ricchiazzi, *et al.*, 1983). The model is run separately with columnar and surface SSA values, while keeping all other parameters unaltered.

RESULTS

Fig. 1 shows scatter plot between surface and columnar SSA for year 2009. Majority of columnar SSA values are higher than surface SSA values. Seasonal variation of surface and columnar SSA over Gadanki is shown in Fig. 2. Both SSA's are found to be distinct in all the seasons except during post-monsoon, where the difference is low (~2% of columnar SSA). Implication's of SSA for aerosol radiative forcing will be discussed during the presentation.

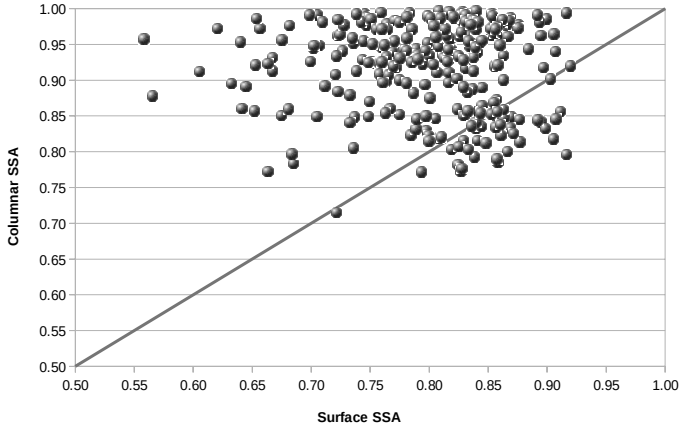

Figure 1. Comparison between surface and columnar aerosol single scattering albedo measured during the year 2009. Straight line represents the 1:1 line.

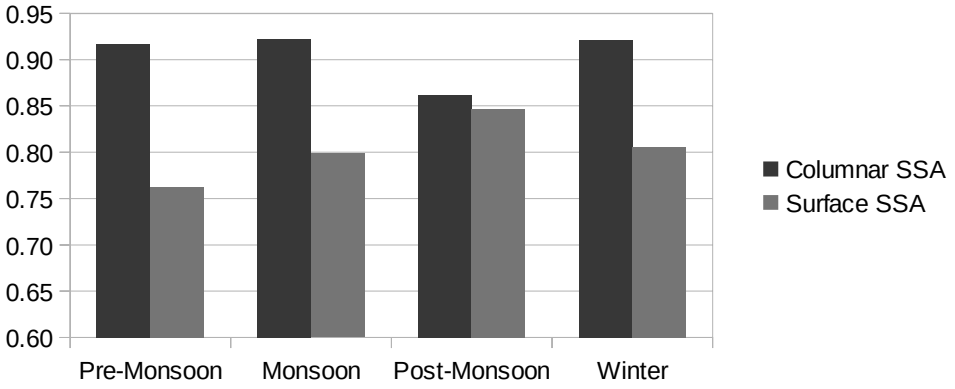

Figure 2. Seasonal variation of Aethalometer and Nephelometer measured SSA and columnar SSA over Gadanki.

REFERENCES

Anderson, T. L., & Ogren, J. A. (1998). Determining Aerosol Radiative Properties Using the TSI 3563 Integrating Nephelometer, *Aerosol Science and Technology* , **29 (1)**, pp. 57–69.

Hess, M., Koepke, P., & Schult, I. (1998). Optical Properties of Aerosols and Clouds: The Software Package OPAC, *Bulletin of American Meteorological Society*, pp. 831–844.

Nakajima, T., Tonna, G., Rao, R., Boi, P., Kaufman, Y., & Holben, B. (1996). Use of sky brightness measurements from ground for remote sensing of particulate polydispersions, *Applied optics*, **35(15)**, pp. 2672–86.

Ricchiazzi, P., Yang, S., Gautier, C., & Sowle, D. (1983). SBDART: A Research and Teaching Software Tool for Plane-Parallel Radiative Transfer in the Earth ' s Atmosphere, pp. 2101–2114.

Weingartner, E., Saathoff, H., Schnaiter, M., Streit, N., Bitnar, B., & Baltensperger, U. (2003). Absorption of light by soot particles: determination of the absorption coefficient by means of aethalometers, *Journal of Aerosol Science*, **34 (10)**, 1445–1463.

CONTRIBUTION OF BLACK CARBON TO THE COMPOSITE AEROSOL RADIATIVE FORCING IN AN URBAN ATMOSPHERE IN EAST INDIA

SHANTANU KUMAR PANI[1], SHUBHA VERMA[1, 2] and SOUMENDRA BHANJA[3]

[1]Center for Oceans, Rivers, Atmosphere and Land Sciences
[2]Department of Civil Engineering
[3]Department of Geology and Geophysics
Indian Institute of Technology Kharagpur
Kharagpur, West Bengal, 721302

Keywords: BLACK CARBON, RADIATIVE FORCING, KOLKATA.

INTRODUCTION

Anthropogenic aerosols influence the climate system directly by scattering and absorbing sunlight (Coakley, *et al.,* 1983) and indirectly by altering the radiative properties and lifetime of clouds (Twomey, 1977). Black carbon (BC) aerosols are an important constituent of atmospheric aerosols, which absorb solar radiation from visible to infrared spectrum and cause atmospheric heating. On the global scale, atmospheric warming due to BC aerosols constitutes about 55% of carbon-dioxide forcing (Ramanathan and Carmichael, 2008). BC aerosols are emitted directly into the atmosphere mostly by incomplete combustion processes such as fossil fuel combustion; biomass combustion (Goldberg, 1985). However, continuous and near-real-time measurements of BC are needed to examine the temporal evolution of BC required to assess realistically the shortwave radiative impacts of BC on climate. Southeast Asia is one of the largest sources of BC aerosols on a global scale (Menon, *et al.*, 2002). To understand the radiative effects of BC aerosols over Indo Gangetic Plain (IGP) region of Southeast Asia, several monitoring studies in various locations have been carried out over the past decade. The characteristic variation and radiative effects of winter BC over Kolkata has been already reported in Verma, *et al.*, (2012). However, there is a lack of reported data on BC aerosols at a specific urban agglomeration, near a mega city, Kolkata, eastern Ganges Delta region in east India. Hence an attempt has been made to estimate the seasonal variation in contribution of black carbon to the composite aerosol radiative forcing over this site.

INSTRUMENTATIONS

Measurements were carried out at the campus of the Indian Institute of Technology Kharagpur Extension Centre (22.57ºN, 88.42ºE), which is on the outskirts of Kolkata city in east India. Observations were carried out on the rooftop of a building, about 12 m above ground level. Continuous and near-real-time measurements of BC mass concentration were carried out using an Aethalometer (model AE-42, Magee scientific, USA) operated at 3 litres per minute (LPM) at an average time of 5 minutes interval. BC mass concentration is measured from the attenuation of light transmitted through the sample collected on a quartz filter paper, which is proportional to the amount of BC loading (Hansen, *et al.*, 1984). Observation at 0.88 ìm wavelength is considered standard for BC measurement because BC is the principal absorber of light at this wavelength (other aerosol components have negligible absorption) (Hansen, *et al.*, 1984). Complementary data on ambient

total aerosol mass concentration were obtained from simultaneous measurements using Grimm aerosol spectrometer (Model 1.108, Grimm Aerosol Technik, Germany) at 5-minute intervals giving particle concentration in the size range 0.23-20 ìm, grouping them in 16 different size bins using light scattering technology (http://www.grimm-aerosol.com). Measurements of aerosol optical depth (AOD), are measured using a handheld Sun photometer Microtops-II at 0.38, 0.44, 0.5, 0.675, 0.87 and 1.02 µm and the accuracy of measurement is ± 2% (Leckner, 1978).

METHODOLOGY

The composite aerosol optical properties (AOD, SSA, Assymetry) were estimated by using aerosol mass concentrations, Mie theory and Optical Properties of Aerosols and Clouds (OPAC) data base, as per Hess, *et al.*, (1998). The observed values of BC and total aerosol mass were used in our urban aerosol model and the concentrations of other components were adjusted (constrained by observed BC mass fraction). This iterative procedure was continued such that estimated spectral optical depths and Angstrom exponent are consistent with the observations. This procedure is described in earlier studies (Babu, *et al.*, 2002; Tripathi, *et al.*, 2005). The model derived AOD and Angstrom exponent were found to match closely with our observed values at mid visible wavelength 0.5 µm. BC number density derived from the BC mass concentration was used in OPAC to calculate the optical properties solely due to BC. Modeled spectral aerosol optical properties for composite aerosol (Insoluble, water soluble, BC, Mineral accumulation and Mineral coarse mode) in the shortwave range 0.25 - 0.4 µm were used as inputs in SBDART for the estimation of radiative transfer.

RESULTS AND DISCUSSIONS

Radiative forcing for both composite and solely due to BC aerosols was estimated as explained above. Fig. 1 shows the monthly composite (a) and BC aerosols (b) averaged values of shortwave clear days aerosol radiative forcing due to BC at surface level, and top of the atmosphere over the Kolkata during the study period. The monthly estimated composite aerosol radiative surface forcing (Fig. 1a) is in the range of -36 to -67 Wm^{-2} at the surface and -2 to -12 Wm^{-2} at TOA. Similarly the monthly estimated aerosol radiative surface forcing due to BC (Fig. 1b) is in the range of -11 to -18 Wm^{-2} at the surface and +0.2 to +1.1 Wm^{-2} at TOA. The negative forcing values estimated at the surface imply a net cooling effect over the region. On analysis of the seasonal mean, the composite aerosol surface forcing is highest in summer (-59 Wm^{-2}) and the lowest in winter (-39 Wm^{-2}). The composite and BC aerosol atmospheric radiative forcing is shown in fig. 2. The difference between the TOA and surface gives the composite atmospheric forcing (ATM), which indicates the net atmospheric absorption are +29, +31, +44 and +55 Wm^{-2} during winter (November and December), NE-Monsoon (January and February), T-summer (March) and summer (April and May) respectively. Similarly the BC induced atmospheric forcing values were found to be +13, +17, +16, +14 respectively during winter, NE-Monsoon, T-summer and summer. However, the highest BC surface forcing was observed during NE-monsoon than in summer. The forcing solely due to BC during NE-monsoon was found to be -16 Wm^{-2} and +0.97 Wm^{-2} at the surface and at TOA respectively.

SUMMARY

he atmospheric forcing derived for composite aerosols were found to be are +29, +31, +44, +55 Wm^{-2} and for BC aerosols were found to be +13, +17, +16, +14 respectively during winter, NE-Monsoon, T-summer and summer respectively. Our study suggests that, BC atmospheric shortwave radiative forcing over Kolkata is 56% of the composite aerosol atmospheric forcing.

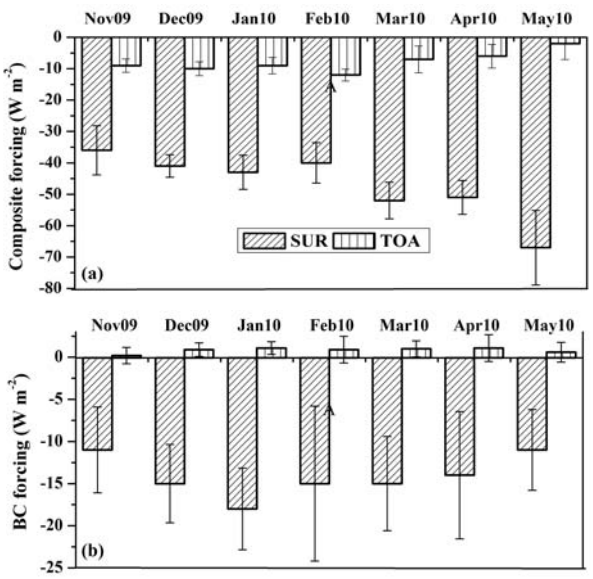

Figure 1. Shortwave aerososl radiative forcing estimated at the surface and at the TOA for (a) composite aerosol; and (b) BC aerosols.

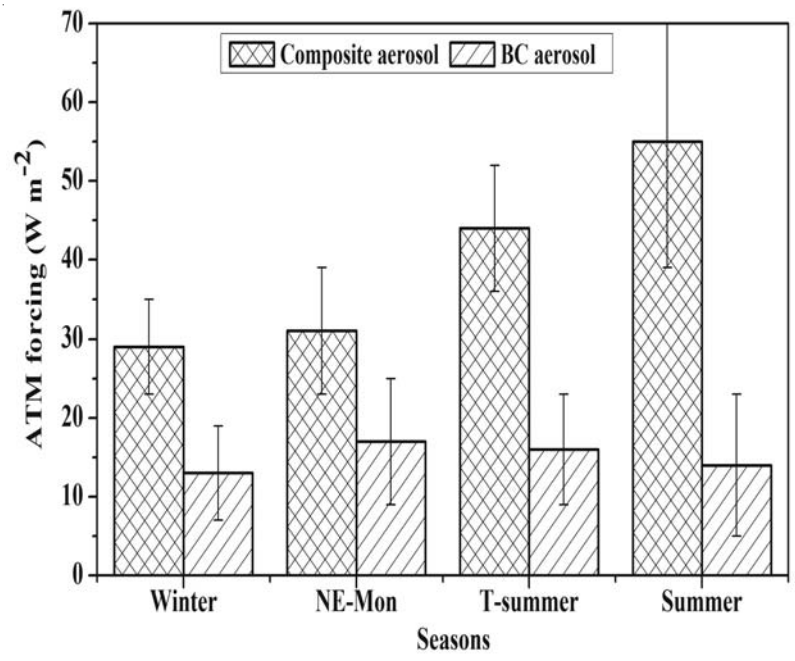

Figure 2. Seasonal averages of shortwave atmospheric forcing for composite and BC aerosols.

REFERENCES

Babu, S. S. and Moorthy, K. K. (2002). Aerosol black carbon over a tropical coastal station in India, *Geophys. Res. Lett.* ,**29 (23)**, 2098.

Coakley, J. Jr., Cess, R. and Yurevich, F. (1983). The effect of tropospheric aerosols on the earth's radiation budget: A parameterization for climate models, *J. Atmos. Sci*., 40, pp. 116-138.

Goldberg, E.D. (1985). Black Carbon in the Environment: Properties and Distribution (*John Wiley & Sons*. New York).

Hansen, A. D. A., Rosen, H. and Novakov, T. (1984). The aethalometer: An instrument for the realtime measurements of optical absorption by aerosol particles, *Sci. Total Environ.* , **36**, pp. 191–196.

Hess, M., Koepke, P. and Schult, I. (1998). Optical properties of aerosols and clouds: The software package OPAC, *Bull. Am. Meteorol. Soc.*, **79**, pp. 831–844.

Leckner, B. (1978). The spectral distribution of solar radiation at the earth's surface — elements of a model, *Sol. Energy*, **20(2)**, pp. 143–150.

Menon, S., Hansen, J., Nazarenko, L. and Luo, Y. (2002). Climate effects of black carbon aerosols in China and India, *Science*, **297**, pp. 2250–2253.

Ramanathan, V. and Carmichael, G. (2008). Global and regional climate changes due to black carbon, *Nature Geoscience*. **1**, pp. 221–227.

Tripathi, S.N., Dey, S. and Tare, V. (2005). Aerosol black carbon radiative forcing at an industrial city in northern India, *Geophys. Res. Lett*. **32**, L08802.

Twomey, S. (1977). The influence of pollution on the shortwave albedo of clouds, *J. Atmos. Sci.*, **34**, pp. 1149-1152.

Verma, S., Pani, S.K. and Bhanja, S.N. (2012). Sources and Radiative Effects of Wintertime Black Carbon Aerosols in an Urban Atmosphere in east India, *Chemosphere*. (in press).

WINTERTIME VARIABILITY OF AEROSOL PROPERTIES OVER AN URBAN LOCATION IN EAST INDIA: IMPLICATIONS FOR SHORTWAVE AEROSOL RADIATIVE FORCING

S. N. BHANJA[a], S. K. PANI[b] AND S. VERMA[c]

[a]Department of Geology and Geophysics, Indian Institute of Technology Kharagpur, Kharagpur-721302, India.
[b]Center for Oceans, Rivers, Atmosphere and Land sciences, Indian Institute of Technology Kharagpur, Kharagpur-721302, India.
[c]Department of Civil Engineering, Indian Institute of Technology Kharagpur, Kharagpur-721302, India.

Keywords: AEROSOL OPTICAL DEPTH, AEROSOL RADIATIVE FORCING.

INTRODUCTION

Aerosols alter global radiative budget, directly in the process of scattering and absorption of solar radiation and indirectly in the process of influencing cloud formation, modifying cloud life time, cloud condensation nuclei formation and regulating cloud droplet number (Penner, *et al.*, 2001). Aerosol exerts surface cooling which may have masked as much as half of the global warming attributed to the recent rapid rise of greenhouse gases (Forster, *et al.*, 2007). Large uncertainties still persist in quantifying the magnitude of aerosol radiative forcing due to their short residence times and large heterogeneity in their properties with spatial and temporal variation (Forster, *et al.*, 2007).

The Indo-Gangetic basin (IGB) situated in the northern part of India (comprising of ~ 21% Indian land area). IGB is a very densely populated region (supporting ~ 40% Indian population). Numerous anthropogenic activities are increasing at a faster rate with intensification of winter. As a result, IGB became a regional hotspot in the Global air pollution scenario (Ramanathan and Carmichael, 2008). Rasch, *et al.* (2001) found that anthropogenic aerosols are transported to the INDOEX region through three main entry points: a strong near surface south-ward flow near Mumbai; a deeper plume flowing south and east of Kolkata and a westward flow originating from south-east Asia and entering the Bay of Bengal. They also found that, very strong outflow occurs through Kolkata/Bangladesh region than Mumbai region in the lower altitude. In this context, characterization of aerosols and quantitative estimation of aerosol radiative forcing at this potentially important region will have valuable impact on studies related to regional as well as in global radiative budget.

METHODS

We carried out measurements of aerosol optical depth using a handheld multichannel Microtops II Sunphotometer (Solar Light Co., USA) at the campus of Indian Institute of Technology Kharagpur Extension Centre (22.57æ%N, 88.42æ%E) in Kolkata from November 2009 to February 2010. The sunphotometer was operated at 5 different wavelength channels (0.34, 0.44, 0.50, 0.87 and 1.02 ì m) and AOD measurements are carried out at an interval of 2 hours during daytime (08:00-16:00 local time). Measurements were repeated for at least three times and the one with the lowest AOD has been used in analysis. High AOD (>1.0) values are screened out as they are most likely originating from cloud contamination. We have used Mie theory to generate optical properties of aerosol. Combination of aerosol components such as insoluble, water soluble, soot and minerals (coarse and

accumulation) is used here to generate aerosol optical properties in the entire short wavelength range (0.25 to 4 ì m). Estimated spectral values of aerosol optical properties, including aerosol optical depth, aerosol single scattering albedo, and asymmetry parameter for each day of measurement are incorporated in a Discrete Ordinate Radiative Transfer model [Santa Barbara DISORT Atmospheric Radiative Transfer (SBDART)] (Ricchiazzi, *et al.*, 1998) to estimate short-wave clear-sky aerosol radiative forcing at surface, atmosphere, and the top of the atmosphere (TOA).

CONCLUSIONS

Monthly mean AOD at 0.5 μm and angstrom exponent (α) are found to be 0.68 to 0.82 and 1.14 to 1.32 respectively with their highest value being 0.82 and 1.32 respectively in December. Mean AOD in December is slightly higher than the AOD reported at Kanpur (0.77±0.29; December, 2004) (Tripathi, *et al.*, 2005), and lower than the mean AOD reported at Delhi (0.91±0.48; December, 2004) (Ganguly, *et al.*, 2006). On comparing the mean AOD spectra (Fig. 1), it is seen that AOD and its standard deviation are higher at shorter wavelength channels (0.34, 0.44 and 0.5 μm) and they decrease rapidly towards longer wavelength channels (0.87 and 1.02 ìm). AODs at shorter wavelengths are more sensitive to changes in smaller particles, while those at longer wavelengths to changes in coarser particles. The spectral variation of monthly mean AOD thus reveals relatively higher contribution from finer particles than coarser ones to columnar aerosol loading during the entire study period. Seasonal mean AOD and á are found to be 0.75 and 1.23 respectively. Analysis of spectral AOD and á indicates predominant contribution of submicron particles to total columnar loading during the entire study period. Relatively higher fraction of submicron particles arising from anthropogenic activities is observed in December than in other months. Surface forcing values are found to vary from -21.8 wm^{-2} to -51.9 wm^{-2} (Fig. 2). The atmospheric heating rate is found to vary from 0.4 to 1.3 K/day with a seasonal mean of 0.84 ± 0.2 K/day. Estimation of large values of atmospheric forcing and atmospheric heating rate on mid-winter months (December and January) reveal a net increase in atmospheric heating as aerosol concentration increased in the mid-winter months, inducing formation of wintertime haze and wintertime inversion layer which hamper atmospheric dispersion of aerosols over the region.

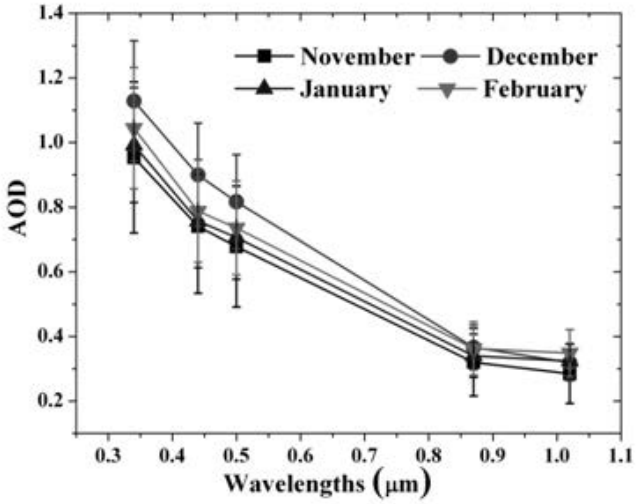

Figure 1. Spectral dependency of monthly mean AOD obtained from sunphotometer measurements.

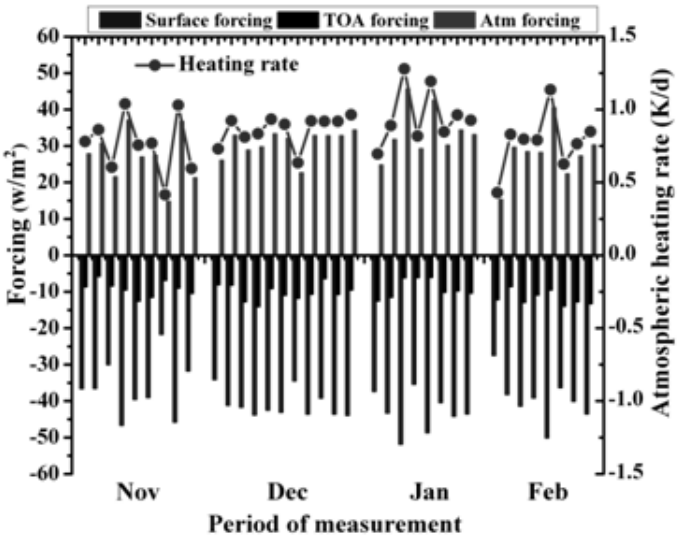

Figure 2. Shortwave direct aerosol radiative forcing (0.25 to 4.00 ì m) at the surface, top of the atmosphere and in the atmosphere and atmospheric heating rate.

REFERENCES

Forster, P. (2007). Changes in atmospheric constituents and in radiative forcing, In: Climate Change 2007: The Physical Science Basis. Contribution of Working Group I to the Fourth Assessment Report of the Intergovernmental Panel on Climate Change, edited by Solomon, S., D. Qin, M. Manning, Z. Chen, M. Marquis, K.B. Averyt, M.Tignor and H.L. Miller, (Cambridge University Press), pp. 186-217.

Ganguly, D., Jayaraman, A., Rajesh, T. A., and Gadhavi, H. (2006). Wintertime aerosol properties during foggy and nonfoggy days over urban center Delhi and their implications for shortwave radiative forcing, *J. Geophys. Res.* , **111**.

Penner, J., Hegg, D. and Leaitch R. (2001). Unraveling the role of aerosols in climate in climate change. *Environ. Sci. Technol.* ,**35**, pp. 332A–340A.

Ramanathan, V. and Carmichael, G. (2008). Global and regional climate changes due to black carbon, *Nature Geoscience*, 1, pp. 221-227.

Rasch, P. J., Collins, W. D. and Eaton, B. E. (2001). Understanding the Indian Ocean Experiment (INDOEX) aerosol distributions with an aerosol assimilation, *J. Geophys. Res*., **106**, pp. 7337-7355.

Ricchiazzi, P., Yang, S., Gautier, C. and Sowle, D. (1998). SBDART, a research and teaching tool for plane-parallel radiative transfer in the earth's atmosphere, *Bull. Am. Meteorol. Soc*.,**79**, pp. 2101–2114.

Tripathi, S. N., Dey, S., Tare ,V., Satheesh, S. K., Lal, S. and Venkataramani, S. (2005). Enhanced layer of black carbon in a north Indian industrial city, *Geophys. Res. Lett.* , **32**, L12802.

EFFECT OF AEROSOL ON UV RADIATION FLUX UNDER CLEAR SKY CONDITION

ONKAR NATH VERMA, SANJEEV KUMAR, S NASEEMA BEEGUM,

SACHCHIDANAND SINGH

Radio & Atmospheric Sciences Division, National Physical Laboratory, CSIR,
New Delhi-110012
E mail: ssingh@nplindia.org

INTRODUCTION

Many studies on atmospheric aerosols have been done to understand its effects on shortwave and UV solar flux. Aerosols are suspension of fine solid particles or liquid droplets in a gaseous medium. The high value of aerosol decreases the radiation flux reaching the earth surface. If the aerosol is mostly scattering (SSA = 0.95) then surface measurement shows lower radiation level. On the other hand, if the aerosol is highly absorbing (SSA = 0.60) the reduction persists at all altitudes. Wide-ranging ground based measurements, satellite estimates, and model calculation have been done to analyze the UV irradiance particularly in the UV region (280nm-400nm). Here we represent the effect of aerosol on UV radiation done from National Physical Laboratory, New Delhi. The measurements were taken by using broadband UV radiometer CUV-4 for Feb 2011. The measurement of aerosol optical depth (AOD) at the site during the experiment was 0.46 at 550 nm. The observations show typical daytime variation of total UV irradiance as a function of time. These observations are compared with the model calculations done using the tropospheric ultra violet radiation model (TUV) and show nearly good conformity. The TUV model predicted surface irradiances to within ±3% for high sun and ±10% for low sun.

OBSERVATIONS AND METHODOLOGY

The observations were carried out using broadband UV radiometer CUV4. It contains high quality dome and diffuser give optimized directional response and an optical filter provides sensitivity to combined UV-A and UV-B. The photodiode generates a voltage output linearly proportional to UV intensity. The tropospheric ultraviolet visible radiation model (TUV) developed by Sasha Madronich and is suitable for obtaining UV irradiances. The model derived irradiance has been compared with the UV irradiance measurements. The major input parameters required to run this model is column ozone in Dobson unit (DU), aerosol optical depth at 550 nm, and surface albedo, apart from other parameters such as location, altitude etc. The aerosol optical depth at 550 nm for model was calculated from the formula

$$\tau_{550} = \tau_{500}(500/550)^{\alpha}$$

Where τ_{500} is the measured AOD at 500 nm and α is the Angstrom coefficient.

RESULTS AND DISCUSSIONS

We have used UV observation data for the month Feb 2011. For the present paper we have chosen only cloud free clear sky day data of 2nd Feb 2011. The observed irradiance data was obtained for

every two minutes time interval, but for comparison with model values we have chosen hourly data only. Fig. 1 shows the measured solar irradiance values in W m^{-2} nm^{-1}. The red dots represents model value of irradiances whereas black squares are observed value of irradiances. The observed and the model values show nearly similar characteristic features. The model values are slightly lower than that of the observed one. The percentage error between observed and model value is ~7%. Since there is no incident solar radiation during the night, due to infrared radiation loss, the flux shows negative values, which are adjusted for the daytime measurements. The irradiances go to maximum values at 13:00 hours. The maximum observed and model irradiances are 0.28 W m^{-2} $nm^{-1}$and 0.26 W m^{-2} nm^{-1} at 13:00 hours respectively on 2 Feb 2011.

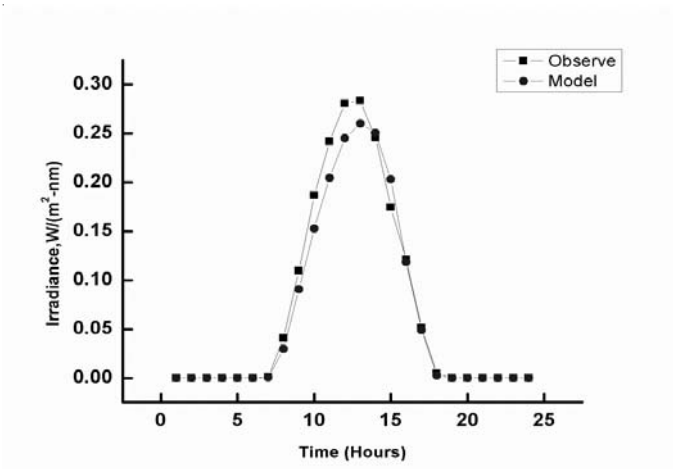

Figure 1. Comparison of observed and modeled UV flux at Delhi during Feb 2, 2011

Figure 2(a) shows variation of maximum flux with variation in single scattering albedo (SSA). Maximum flux vs SSA has positive slope which is nearly 0.037 W/m^2 for every 0.1 increase in SSA. This means on increasing SSA the flux will also increase. The flux was calculated by varying only SSA and keeping all other parameters fixed with value for fixed AOD 0.46. Figure 2(b), on the other hand, shows the variation of maximum flux with aerosol optical depth (AOD). Maximum flux vs AOD has negative slope, nearly equal to -0.018 W/m^2 for every 0.1 increase in AOD. The column ozone value and surface albedo for 2nd Feb are 290 DU and 0.3 respectively.

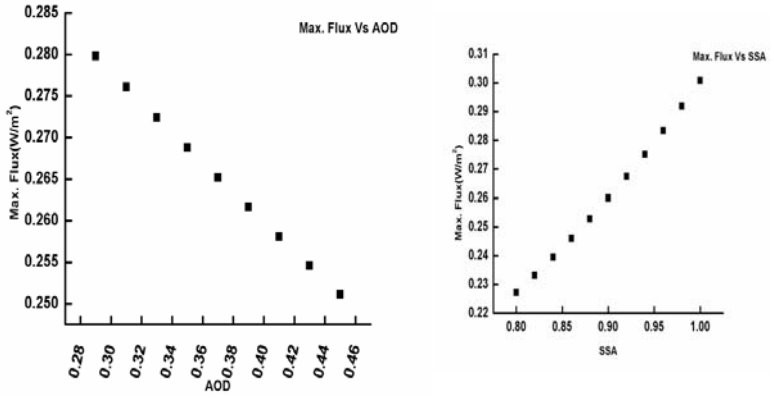

Figure 2: (a) Max. Flux Vs SSA (b) Max. Flux Vs AOD

CONCLUSIONS

On the basis of measurements made at NPL, New Delhi for 2nd Feb 2011, we wave presented a short analysis of the clear sky direct solar UV irradiance at 280 nm-400 nm. The maximum absolute irradiances at local noon observed was 0.28 W m^{-2} nm^{-1} whereas for model it was 0.26 W m^{-2} nm^{-1}.The entire daytime clear sky direct solar UV irradiance measurements were compared with the TUV radiation model on 2nd Feb 2011. The input data included the column ozone values and aerosol optical depths at the site of observation. The best fit between the model and the observation was obtained at 550 nm of AOD. The value of AOD at 550 nm on 2nd Feb 2011 was 0.46 which is slightly high due to the fine dust aerosols in the atmosphere. High value of aerosol is also responsible for large deviation in the value of irradiance obtained through model calculation. The model value compare well with the observed one in the region.

TEMPORAL FEATURES OF ANGSTROM PARAMETERS AS A FUNCTION OF METEROLOGICAL PARAMETERS IN THE KULLU VALLEY OF THE NORTH WEST HIMALAYAN REGION, INDIA

N. L. SHARMA[1], J. C. KUNIYAL[2], R. P. GULERIA[2].

[1]Department of Physics, Govt. Postgraduate College, Kullu 175 101, Himachal Pradesh, India
[2]G.B. Pant Institute of Himalayan Environment & Development, Himachal Unit, Mohal-Kullu, 175 126, Himachal Pradesh, India
E-mail : nlsharmakullu@hotmail.com

Keywords: ANGSTROM PARAMETERS, TURBIDITY, METEOROLOGICAL PARAMETERS, CORRELATION

INTRODUCTION

In atmosphere, there are aerosol particles of different sizes, ranging from few nanometers to hundreds of micrometer (Junge, 1963).These atmospheric aerosols play a major role in earth radiation budget and climate forcing (Charlson, *et al.,* 1992). The Aerosol optical depth (AOD) is an important parameter in radiometry.The spectral dependence of AOD gives an idea about concentration of fine, coarse and total particles in atmosphereand is suitably expressed by the Ångström relation (Angstrom, 1961).The two constants in this relation; one called Ångström wavelength exponent 'α', and other is called Ångström turbidity coefficient 'β' which together are referred as Ångström parameters. The first indicates relative abundance of fine to coarse particles while second gives the information about concentration of particles of all sizes i.e. turbidity in atmosphere (Tomasi, *et al.,* 1999). The long term trend of these parameters and their correlation with meteorological parameters give an idea about sources of particles of different sizes in different seasons and in relation to climatic conditions at a place.In this communication, we present temporal features and meteorological correlations of these parameters with Angstrom parameters in the Kullu valley during three seasonal years spanning from April 2006 to March 2009 for clear, hazy and partially clear days.

EXPERIMENTAL SITE AND METHODOLOGY

The Kullu valley is an important tourist destination of the western Himalayas. It is a bowl shaped valley endowed with rugged mountainous region mostly on eastern side and evergreen forests mostly on western side (Sharma, *et al.,* 2011a).On the basis of meteorological parameters for long periods, the climate of this valley consist of four local seasons(Sharma, *et al.,* 2011b); summer (April to June), monsoon (July to September), autumn (October and November) and winter (December to March).Observations of reduced intensity of solar radiation for calculation ofAerosol optical depths (AODs)which were used to evaluate Angstrom parameters were carried out at Mohal (31.90^0N, 77.11^0E, 1154m amsl), 5 km south to a famous tourist spot and district headquarters-Kullu in Himachal Pradesh state of India, using Multi-wavelength Radiometer (MWR).These AOD valuesare used to compute Angstrom Parameters ('α' and 'β') throughÅngströmrelation (Angstrom, 1961) as

$$\tau_{p\lambda} = \beta\lambda^{-\alpha} \qquad (1)$$

$$\ln \tau_{p\lambda} = \ln \beta - \alpha ln\, \lambda \qquad (2)$$

The graph between log of AOD values and log of corresponding wavelength gives α and 'β'; a method used by many researchers (Schuster, *et al.*, 2006). Also, the correlation between 'α', 'β' and corresponding mean value of meteorological parameters at our site, was estimated using student's 't' distribution formula (Goyal and Sharma, 1963)

$$t = \frac{r\sqrt{n-2}}{\sqrt{1-r^2}} \qquad (3)$$

Where 'r' is correlation coefficient, n = number of data points. These 't' values are used to find probability Ps of correlation outside the region of significance in two tailed co t- Table.

RESULTS & CONCLUSIONS

The time series of variations of FN and AN values 'α' and 'β' for all 204 clear days of three years study period are shown in Fig. 1.

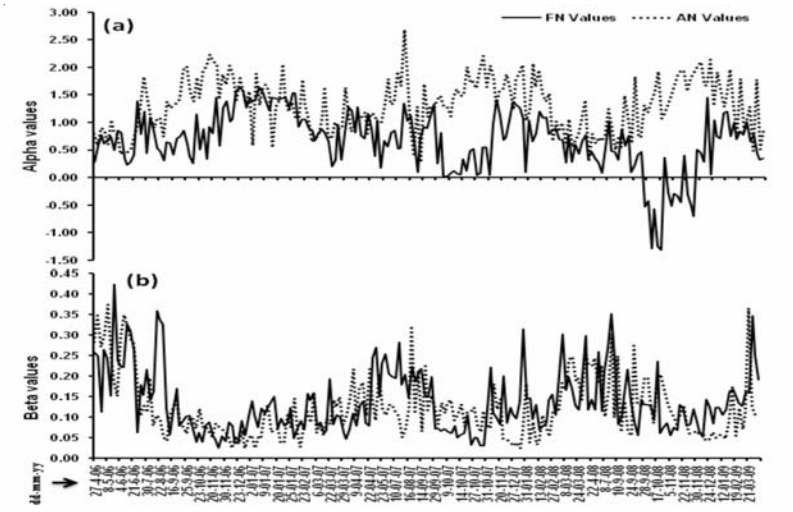

Figure1. Day wise variations in FN and AN values of 'α' and 'β' during clear sky days

The panel (a) which depicts diurnal variations of 'α' clearly indicates that afternoon values of 'α' is more than forenoon values during most of clear days of three years study period. It suggests that concentration of fine particles increases from morning till evening due to increasing anthropogenic activities. The afternoon values of fine particles are more in monsoon and much more in autumn.The panel (b) which shows the daily variations of 'β' also indicates that 'β' is mostly more during AN parts of the days. It shows that turbidity also increases during afternoon parts of the clear measurement days due to increasing natural and anthropogenic activities.The increase in AN values of 'β' is mostly small indicating that coarse particulate matter increase by small amount in our region than fine particles. Similar trend are seen for hazy and partially clear days.

The seasonal variations of FN and AN values of 'α' and 'β' during clear as well as hazy days for all the three years of study period are shown in Fig 2.The panel (a) which shows the seasonal variations of 'á' indicates that in all seasons AN values are more than FN values. The difference is

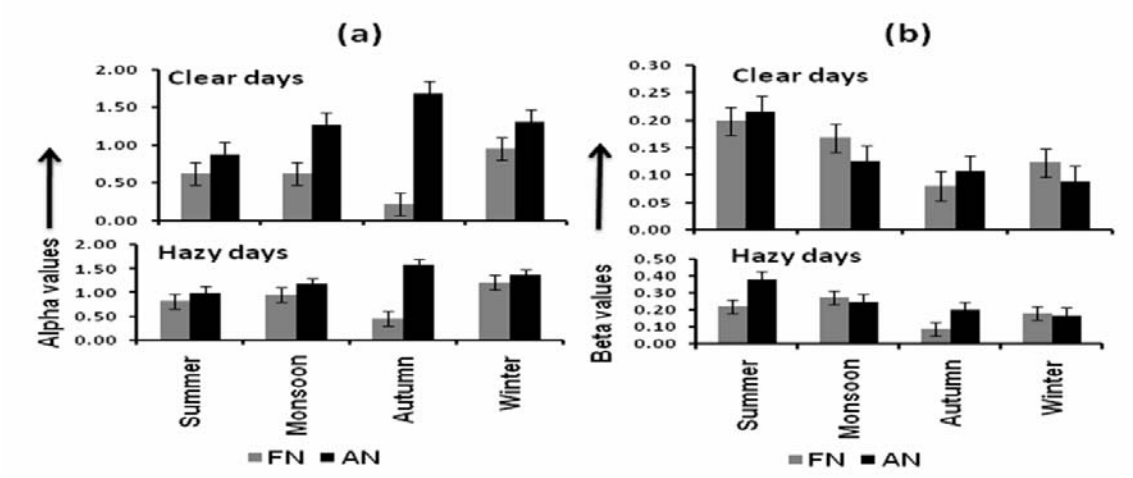

Figure 2. Seasonal variations in FN andAN values of 'α' and 'β' during clear and hazy sky days

high in monsoon and considerably higher in autumn season probably due to evaporation of fog moisture on fine particles byFigure 2. Seasonal variations in FN andAN values of 'α' and 'β' during clear and hazy sky days afternoon hours in monsoon and International Kullu Dussehra festival in autumn (Guleria, *et al.* 2011). The difference on clear days is more comparedto hazy days in all seasons indicating that fine mode fraction of aerosols are more produced on clear days than on hazy days possibly due to more photoelectric effect aiding more gas to particle conversion. The three years average value of 'α' during FN and AN parts of clear days is 0.63±0.19 and 1.31±0.03, while on hazy days its value is 0.81±0.14 and 1.27±0.03 respectively. On average, the values of 'β' during FN and AN parts of clear days for three years came out to be 0.14±0.003 and 0.12±0.004, while during hazy days these values are 0.18±0.01 and 0.26±0.04 respectively.

Dependence of 'α' and 'β' on meteorological parameters gives an important insight into production and abundance of fine and coarse mode fraction of aerosols in relation to climatic conditions. The year wise correlation of 'α' and 'β' with corresponding meteorological parameters is shown in Table 1. These results show that 'α' has negative correlation, while 'β' has positive correlation with temperature during almost all parts of all type of sampling days for the all the three years. Similarly with wind speed, 'α' has negative correlation while 'β' has positive correlation during most parts of all type of sampling days during all the three years. With wind direction, 'α' has a weak positive correlation for most part of all types of sampling days during all the three years while 'β' has weak negative correlation during most parts of all types of days. The table also shows that with humidity, 'α' has mostly negative correlation during most of the parts of all types of sampling days during three years with few exceptions, while 'β' mostly has positive correlation with humidity during most of the parts of all types of days.

(a) Correlation between alpha and meteorological parameters

Met. parameters		Clear days			Hazy days			Partially clear days		
		2006-07	2007-08	2008-09	2006-07	2007-08	2008-09	2006-07	2007-08	2008-09
Temperature	FN	-	-0.1562	0.0128	-	-	0.2581	-	-	0.080
	AN	-	-0.1687	-	-	-	-			
	ME	-	-0.0781	-	-	-	-			
Wind speed	FN	-	-0.0533	0.3249	-	0.096	0.1127	-	-	-
	AN	-	-0.2416	-	-	-	-			
	ME	-	-0.2792	-	-	-	-			
Wind direction	FN	0.263	-0.0342	0.3078	-	0.388	-	0.168	-	0.187
	AN	-	-0.3201	-	0.189	0.360	0.2561			
	ME	0.253	-0.3809	-	0.241	0.514	-			
Humidity	FN	-	-0.0017	-	-	0.249	0.1998	0.570	-	-
	AN	0.307	0.2402	-	0.201	-	-			
	ME	0.114	0.0448	-	-	-	-			

(b) Correlation between beta and meteorological parameters

Met. parameters		Clear days			Hazy days			Partially clear days		
		2006-07	2007-08	2008-09	2006-07	2007-08	2008-09	2006-07	2007-08	2008-09
Temperature	FN	0.767	0.4290	0.6697	0.599	0.554	0.3963	0.576	0.723	0.744
	AN	0.727	0.5943	0.8173	0.745	0.491	0.6509			
	MEA	0.766	0.5835	0.7785	0.708	0.508	0.5883			
Wind speed	FN	0.665	0.5526	0.2805	0.628	0.597	0.4787	0.651	-	0.022
	AN	0.217	0.5152	-	0.536	0.519	0.0718			
	MEA	0.437	0.5287	0.3474	0.512	0.499	0.2115			
Wind direction	FN	-	-0.0930	-	0.185	-	0.2205	0.024	-	0.129
	AN	0.024	-0.2029	0.2647	-	-	0.0410			
	MEA	-	-0.2344	0.0945	-	-	0.5603			
Humidity	FN	0.088	0.4815	0.6455	0.149	0.792	0.1353	0.218	0.474	0.609
	AN	-	0.1098	-	-	0.251	-			
	MEA	0.128	0.3980	0.3562	0.048	0.714	-			

Table 1. Intra-annual correlation of alpha and beta with meteorological parameters

REFERENCES

Angstrom, A. (1961). Technique of determining turbidity of the atmosphere, *Tellus*, **13**, pp. 214-223.

Charlson, R. J., Schwartz, S. E., Hale,s J. M., Cess, R. D., Coakley, J. A., Hansen, J. E., and Hoffman, D. J. (1992).Climate forcing by anthropogenic aerosols, *Science,* **225**, pp. 423-430

Goyal, J. K. and Sharma, J. N. (1963). Mathematical Statistics. Krishna Prakashan Mandir, Meerut (India), pp. 378-476.

Guleria, *et al.* (2011). The assessment of aerosol optical properties over Mohal in the northwestern Indian Himalayas using satellite and ground based measurements and an influence of aerosol transport on aerosol radiative forcing, *Meteo. Atmos. Phys.* **113** (3,4), pp. 153-169.

Junge, C.E. (1963). *Air chemistry and radioactivity*, academic press Inc, New York, USA, pp.11 208.

Schuster, G. L., Dubovik, O., and Holben, B. N. (2006). Angstrom exponent and bimodal aerosol size distributions, *J. Geophys. Res.*, **111**, D07207.

Sharma, N. L., Kuniyal, J. C., Singh, M., Sharma, M. and Guleria, R. P. (2011). Characteristics of Aerosol optical depth and Angstrom parameters over Mohal in the Kullu Valley of Northwest Himalayan region, India, *ActaGeophys.*, **59 (2)**, pp. 334-360.

Sharma, *et al.* (2012). Three years aerosol meteorology derived from ground based sun radiometry over Mohal in the Kullu valley of Northwest Himalayan region, India, *Journal of Atmospheric and Solar Terrestrial Physics* (Elsevier), **77**, pp. 26-39.

Tomasi, C., Prodi, F., Sentimenti, M., and Cesari, G. (1983). Multi wavelength sun photometers for accurate measurements of atmospheric extinction in the visible and near-IR spectral range, *Appl. Opt.*, **22**, pp. 622–630.

RADIATIVE FORCING DUE TO ATMOSPHERIC AEROSOLS AT KADAPA, ANDHRA PRADESH

C. VISWANATH VACHASPATI, G. RESHMA BEGAM, KISHORE REDDY AND Y. NAZEER AHAMMED

Atmospheric Science Laboratory, Department of Physics, Yogi Vemana University, Kadapa.
E mail:ynahammed@gmail.com

Keywords: OPTICAL PROPERTIES OF AEROSOLS, SEMI-ARID REGION, RADIATIVE FORCING

INTRODUCTION

Aerosols have a direct radiative forcing because they scatter and absorb solar and infrared radiation in the atmosphere. Aerosols also alter the formation and precipitation efficiency of liquid water, ice and mixed-phase clouds, thereby causing an indirect radiative forcing associated with these changes in cloud properties.

The quantification of aerosol radiative forcing is more complex than the quantification of radiative forcing by greenhouse gases because aerosol mass and particle number concentrations are highly variable in space and time (IPCC, 2001; Yoon and Kim, 2006). Quantifying and assessing the climatic impact of atmospheric aerosols require knowledge of their physical, chemical, optical, and radiative properties, as well as of their spatial and temporal variability (Huebert et al., 2003; Penner et al., 1994; Yoon et al., 2005). Important parameters are size distribution, change in size with relative humidity, complex refractive index, and solubility of aerosol particles. Estimating radiative forcing also requires an ability to distinguish natural and anthropogenic aerosols.

In this paper, we present results of aerosol optical and radiative forcing studies, performed using aerosol chemical, physical, and optical measurements at Kadapa in the month of December, 2011 together with an aerosol optical model (OPAC) and a radiative transfer model (SBDART).

OBSERVATIONAL SITE AND METHODOLOGY

Kadapa is situated in the central part of Andhra Pradesh is located 8 km south of the penna river and is surrounded by the Nallamala and the Palakonda hill on three sides. Kadapa is located at 14.47 °N and 78.82 E at an elevation of about 138 meters. Kadapa has a tropical climate and the weather conditions are generally hot. HYSPLIT model, 5-day back-trajectory analysis revealed pathway cluster for advection of aerosols in the month of December 2011 from northeast side.

Regional atmospheric aerosol optical properties like spectral variation of optical depth along with Water Vapor have been measured using Microtops II: Sun-photometer since January, 2011 and also continuous observation on Black Carbon (BC) aerosols have been carried out by using an Aethalometer (Magee Sci. Inc., USA, Model AE-42-7) since April, 2011 at Yogi Vemana University, Kadapa

RESULTS AND CONCLUSIONS

Actual implications of the measured aerosol properties in terms their potential capability to perturb the radiative balance of the Earth-atmosphere system can be quantified only from model estimates of aerosol radiative forcing. Major aerosol parameters required for the estimation of radiative forcing due to aerosol include spectral values of aerosol optical depth, single-scattering albedo and asymmetry factor. In the absence of data on aerosol composition, we used the Optical Properties of Aerosols and Clouds (OPAC) model developed by Hess, *et al.* (1998), to make estimates of aerosol components which possibly contributed toward the measured properties of aerosols over Kadapa. Single-Scattering Albedo (SSA), which indicates the relative contribution of scattering and absorption to the total extinction by aerosols, is an important input to the radiative forcing calculation. SSA and Asymmetry parameter (g) values derived for each observational day. The mean SSA for the composite aerosol comes out to be 0.94 ± 0.01, whereas the corresponding value for g is 0.7 ± 0.01.

Finally, the radiation code Santa Barbara DISORT Atmospheric Radiative Transfer (SBDART), developed by Ricchiazzi et al. [1998], has been used to perform radiative transfer calculations in the shortwave (SW, 0.25–4.0 mm) region. Calculations of diurnally averaged radiative forcing for the surface and top of the atmosphere has been carried using SBDART model. Fig. 1 shows the average values of SW aerosol radiative forcing at the surface level and TOA computed separately for individual days in the month of December 2011 over Kadapa. Over the period of our study, we find a large negative forcing at the surface level in the range of -67.5 to -73.9 W/m^2, while forcing at the TOA varied between -11.7 and -15.8 W/m^2. The difference of forcing values at the surface and TOA is known as atmospheric forcing, and it represents the energy trapped within the atmosphere by aerosols and results in heating of the atmosphere.

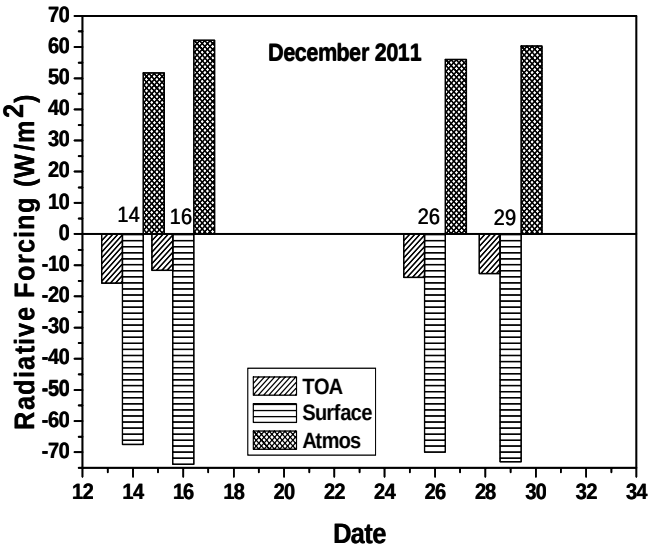

Figure 1. Day averaged variation of simulated aerosol radiative forcing (ARF) over TOA, surface and in the atmosphere during the month of December 2011 at Kadapa

ACKNOWLEDGMENT

Authors are thankful to ISRO - GBP for their financial assistance in the form of Research project under ARFI Network stations. G. Reshma Begam is also thankful to DST for awarding JRF under INSPIRE Programme.

REFERENCES

Hess, M., Koepke, P., Schult, I. (1998). Optical properties of aerosols and clouds: The software package OPAC, *Bulletin of the American Meteorological Society*, **79**, pp. 831–844.

Huebert, B.J., *et al.* (2003). An overview of ACE-Asia: strategies for quantifying the relationships between Asian aerosols and their climatic impacts, *Journal of Geophysical Research*, **108 (D23)**, 8633.

Intergovernmental Panel on Climate Change (IPCC), 2001. Climate Change 2001. In: Houghton, J.T., et al. (Eds.). Cambridge University Press, New York.

Penner, J.E., et al. (1994). Quantifying and minimizing uncertainty of climate forcing by anthropogenic aerosols, *Bulletin of the American Meteorological Society*, 75, pp. 375–400.

Ricchiazzi, P., Yang, S., Gautier, C., Sowle, D. (1998). SBDART: A research and teaching software tool for plane-parallel radiative transfer in the earth's atmosphere. *Bull. Am. Meteorol. Soc.*,**79**, pp. 2101–2114.

Yoon, S.-C., Won, J.-G., Omar, A.H., Kim, S.-W., Sohn, B.-J. (2005). Estimation of the radiative forcing by key aerosol types in worldwide locations using a column model and AERONET data, *Atmospheric Environment*, **39**, pp. 6620–6630.

Yoon, S.-C., Kim, J. (2006). Influences of relative humidity on aerosol optical properties and aerosol radiative forcing during ACE-Asia, *Atmospheric Environment*, **40 (23)**, pp. 4328–4338.